



A Platform for the Discovery of New Lincosamide Antibiotics

Permanent link

<http://nrs.harvard.edu/urn-3:HUL.InstRepos:40050042>

Terms of Use

This article was downloaded from Harvard University's DASH repository, and is made available under the terms and conditions applicable to Other Posted Material, as set forth at <http://nrs.harvard.edu/urn-3:HUL.InstRepos:dash.current.terms-of-use#LAA>

Share Your Story

The Harvard community has made this article openly available.
Please share how this access benefits you. [Submit a story](#).

[Accessibility](#)

HARVARD UNIVERSITY
Graduate School of Arts and Sciences



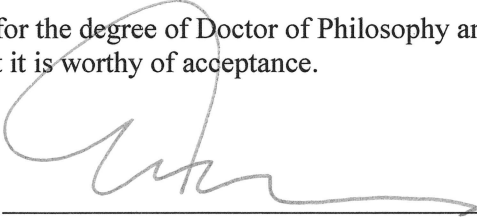
DISSERTATION ACCEPTANCE CERTIFICATE

The undersigned, appointed by the
Department of Chemistry & Chemical Biology
have examined a dissertation entitled:

A Platform for the Discovery of New Lincosamide Antibiotics

presented by : Matthew J. Mitcheltree

candidate for the degree of Doctor of Philosophy and hereby
certify that it is worthy of acceptance.

Signature 

Typed name: Professor Andrew Myers

Signature 

Typed name: Professor Eric Jacobsen

Signature 

Typed name: Professor Christina Woo

Date: 2 May 2018

A Platform for the Discovery of New Lincosamide Antibiotics

A dissertation presented by

Matthew J. Mitcheltree

to

The Department of Chemistry and Chemical Biology

in partial fulfillment of the requirements

for the degree of

Doctor of Philosophy

in the subject of

Chemistry

Harvard University

Cambridge, Massachusetts

May 2018

© 2018 – Matthew J. Mitcheltree

All rights reserved

A Platform for the Discovery of New Lincosamide Antibiotics

Abstract

This dissertation presents a flexible synthetic approach to the lincosamide antibiotics, developed with the aim of rejuvenating an underexploited class to combat multidrug-resistant bacterial pathogens. The only clinically relevant lincosamide, clindamycin (**1.3**), has been in continuous clinical use for nearly half a century, though its utility is limited by a narrow spectrum of action and a liability to promote life-threatening *C. difficile* infections. Prior campaigns to address these concerns have relied largely upon semi-synthetic approaches, owing in part to the lack of practical synthetic routes to the two molecular hemispheres – a “northern” aminooctose and a “southern” cyclic amino acid – that constitute the class. Exploiting the lincosamides’ natural modularity, I developed synthetic routes to both moieties, enabling diversification at strategic sites identified by analysis of X-ray crystal structures of canonical lincosamides bound to the bacterial ribosome, as well as by existing structure–activity relationship (SAR) data.

Three synthetic routes are exhibited in this dissertation, beginning with the preparation of β -oxygenated prolines as rationally designed variants of clindamycin’s southern half. In this work, a novel annulation of pseudoephedrine glycinamide (**2.3**) is described, marrying prior methods developed in the Myers laboratory for *C,N*-bis-alkylation and aldolization of chiral glycine equivalents. This chemical innovation led to the discovery of a bicyclic southern-half scaffold amenable to further optimization, displaying particular promise in our search for candidates with improved *in vitro* antimicrobial activity and diminished risk for colitis relative to clindamycin.

Also presented are two independent routes to the northern-half component. In the first, a pivotal nitroaldol coupling enabled the component-based synthesis of methylthiolincosamine (**1.11**) from non-carbohydrate building blocks **3.28** and **3.29**. Adaptation of this route permitted the synthesis and evaluation of 41 lincosamides bearing modifications to the strategic positions C1 and C6, offering actionable insights into the SAR of this residue. Consequently, a second-generation synthesis to northern-half variants was developed, enabling more expedient exploration of this hemisphere, and facilitating the synthesis of clindamycin (**1.3**) in 4 steps from the versatile *N*-*tert*-butanesulfinimine intermediate **4.10**. Through building-block exchange and adaptation of the routes described here, I have prepared 92 novel lincosamides as part of a growing library of >330 candidates our team has evaluated to date. Most of these are active antibiotics, and some, we hope, hold the potential to impact those aims of efficacy and safety identified at the outset of our work.

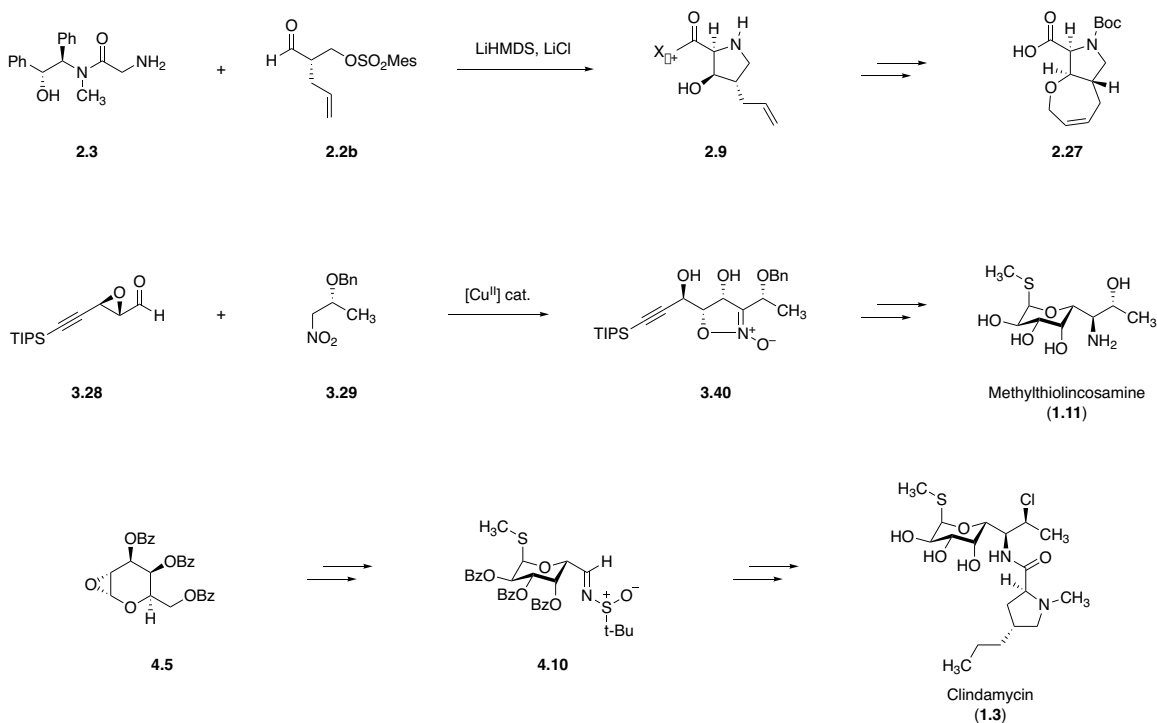


Table of Contents

Abstract	iii
Table of Contents	v
Acknowledgements	viii
List of Abbreviations	xi
Chapter 1. Introduction	1
Chemical synthesis and antibiotic discovery	2
Introduction to the lincosamides	5
Mechanism of action	8
Mechanisms of resistance	14
Clinical utility and limitations	22
The structure–activity relationship of the lincosamides	25
A fully synthetic approach to the lincosamide antibiotics	43
Chapter 2. Southern-half variants bearing 3' oxygenation	47
Introduction	48
Annulation of pseudoephedrine glycinamide by aldol–cyclization	50
Synthesis and evaluation of 3'-hydroxy and 3'-alkoxy lincosamide analogs	54
Oxazolidinone–lincosamide hybrid antibiotics	58
Discovery of a novel oxepinoproline southern-half scaffold	63

Oxepinoprolinamide analogs bearing 7-arylthio substitution	71
Secondary screening of active oxepinoprolinamides	76
Summary and conclusion	80
Experimental section	82
Chapter 3. A nitroaldol-based route to methylthiolincosamine	189
Introduction	190
Original retrosynthesis and discovery of a nitroaldol–cyclization reaction	194
A fully synthetic route to methylthiolincosamine	199
<i>C</i> -Glycosidic lincosamide analogs	203
8-Norlincomycin and its derivatives	215
Summary and conclusion	222
Experimental section	223
Chapter 4. A sulfinimine-based route to methylthiolincosamine variants	421
Introduction	422
Synthesis of 6-modified propylhygramides by a sulfinimine-based route	423
Design and synthesis of C6-modified azepanamides by the same strategy	429
Synthesis of clindamycin by radical hydrochlorination of a 6-vinyl lincosamide precursor	436
Summary and conclusion	438
Experimental section	439

Appendix A. Catalog of X-ray crystal structures	543
Appendix B. Catalog of synthetic lincosamide structures	578
Appendix C. Minimum inhibitory concentrations of synthetic lincosamides	598
Appendix D. Secondary <i>in vitro</i> profiling of FSA-213064	607
Appendix E. Catalog of spectra	617

Acknowledgements

When in 2012 my undergraduate advisor, Prof. Seth Herzon, expressed that I could find no better match in a doctoral advisor than with Prof. Andrew Myers, I couldn't have known how right he was. It is with great pride and an even greater debt of gratitude that I may count Prof. Myers among those mentors who have shaped my thinking – both scientific and otherwise – very much for the better. Over the five years that I have studied under him, Prof. Myers has entrusted me with an abundance of enriching opportunities to grow as a young scientist and has steadfastly conveyed invaluable lessons in scientific research and leadership, which I hope may form the basis of a long, productive, and fulfilling career in chemistry to follow.

My earlier mentors deserve equal recognition for their selfless labor to instill in me those skills that were most essential to my success in graduate school. These include Profs. Seth Herzon and Christina Woo, who above all else impressed upon me the merits of truly committed chemical research – I'll not forget Prof. Herzon's maxim to "grab the bull by the horns," nor Prof. Woo's less quotable but equally enduring lesson that one's work can be both joy and solace. I am grateful to Dr. Ian Bell for introducing me to the world of medicinal chemistry, a vocation for which I didn't have a name before I had lived it; and perhaps most of all I am grateful to Drs. Shyam Srinivas and Steve Huang, whose irrational investment in an eager high schooler helped a new scientist take root. Beyond voicing my gratitude for these advisors and others, I can only hope to one day pay such a valuable gift forward.

The work that is presented in this thesis constitutes only a small portion of a collaborative effort, performed by a team of colleagues and friends with whom I've had the good fortune of working. Ioana Moga's keen scholarship of chemical literature has more than once impacted the project through the design of enabling routes and the uncovering of important SAR, while

Katherine Silvestre, endowed with an enviable work ethic and an undeniable love for chemistry, has made pivotal discoveries through difficult sequences that would make less devoted chemists shiver. It would be difficult to overstate the outsize impact that Dr. Amarnath Pisipati has had on the project, and on me personally, through his marvelous blend of collegiality, deep expertise, and commitment to scientific integrity. Lastly, Jack Stevenson, whom I'm lucky to call both a mentee and a friend, deserves recognition not only for his contributions to the work presented here, but also for his reciprocal lessons in *la gourmandise*, imparted over nights of cooking numerous enough to almost outstrip my vivid memories of each dish we made.

In many respects, the lincosamide team encompasses a broader cast of contributors than those listed above. Our laboratory administrator, Tracey Schaal, is among them, for her partnership in grant writing and logistics, without which the project would have foundered before it even began. Likewise, the collated insights of Barry Wohl, Dr. Su Chiang, Dr. Vivian Berlin, Irit Ben-Chelouche, and Dr. Thomas Dougherty substantially shaped the strategic priorities of our project. Drs. Michael Gilmore and François Lebreton deserve our thanks for their continued support, which has taken the form of illuminating discussions, generous access to bacterial strains, and genetic-sequencing labor. William Weiss, Dr. Dean Shinabarger, Dr. Chris Pillar, and Prof. Michael Cameron are likewise gratefully acknowledged for their biological-profiling work, and Dr. Hardwin O'Dowd deserves thanks for sharing his personal experience with lincosamide research in the early days of our program. Prof. Eric Jacobsen, who has served on my committee from the beginning, also deserves special recognition for his unwavering personal support, tough questions, and open office door, all of which I've been fortunate to profit from.

I have been the grateful recipient of financial support through the National Science Foundation's Graduate Research Fellowship Program, and am indebted to the Blavatnik

Biomedical Accelerator, the Gustavus and Louise Pfeiffer Research Foundation, and Alistair and Celine Mactaggart for supporting the research which formed the basis of my graduate studies.

It's a lovely thing to take stock of those friendships that have sustained me since I moved to Boston. Dr. Robin Sussman and Prof. Ian Seiple were among my first friends and mentors here, who readily folded me into the social fabric of the department. It's no secret that those I share meals with are closest of all, and I've been delighted to spend some thousand-plus lunches (and some dinners, too!) with the likes of Dr. Ziyang Zhang, Dr. Jon Mortison, Dr. Fan Liu, Jack Stevenson, and Ethan Magno, whose minds have enriched my life both in and out of lab through their shared virtues of brilliant wit, compassion, and depth of character. The Myers laboratory has no monopoly on such people, either – I find myself particularly grateful for the companionship of Jeff Bessen, Greg Certo, Dr. Nick Calandra, Charlie Margarit, Dr. Anna Klöckner, and Clara Messina, scientists all; but first and foremost, dear friends. And among the many I've met in Boston's artistic orbit, Chando Ao, Yve Yang, and Eric Lee deserve special recognition as some of my closest companions – although they've since moved away, it's to them that I owe the feeling that Boston can be a place where all my facets find expression.

Finally, I owe an ineffable and continuously compounding debt of gratitude to my parents, Pat and Hal Mitcheltree, to whose efforts all of my accomplishments may be attributed. From science journal subscriptions, to summer camps, to trips to the dollar store and Radio Shack, they have kindled my decades-long love affair with science from the start and have presented me with more opportunities to grow than I can count.

List of Abbreviations

A	adenosine
Å	ångstrom
<i>A. baumannii</i>	<i>Acinetobacter baumannii</i>
Ac	acetyl
Bn	benzyl
Boc	<i>tert</i> -butoxycarbonyl
BSTFA	<i>N,O</i> -bis(trimethylsilyl)trifluoroacetamide
Bu	butyl
Bz	benzoyl
C	cytosine
°C	degrees Celsius
CAM	cerium ammonium molybdate
calc'd	calculated
CDAD	<i>Clostridium difficile</i> -associated diarrhea
<i>C. difficile</i>	<i>Clostridium difficile</i>
cLogD	calculated decimal logarithm of distribution coefficient
d	day
Da	dalton
DABCO	1,4,-diazabicyclo[2.2.2]octane
DBU	1,8-diazabicyclo[5.4.0.]undec-7-ene
DCE	1,2-dichloroethane
DCM	dichloromethane

DEAD	diethyl azodicarboxylate
DET	diethyl tartrate
DIAD	diisopropyl azodicarboxylate
DIBAL-H	diisobutylaluminum hydride
DMAP	4-dimethylaminopyridine
DMDO	dimethyldioxirane
DMF	<i>N,N</i> -dimethylformamide
DMP	Dess–Martin periodinane
DMS	dimethyl sulfide
DMSO	dimethyl sulfoxide
dr	diastereomeric ratio
<i>D. radiodurans</i>	<i>Deinococcus radiodurans</i>
<i>E. coli</i>	<i>Escherichia coli</i>
<i>E. faecalis</i>	<i>Enterococcus faecalis</i>
EDC	1-ethyl-3-(3-dimethylaminopropyl)carbodiimide
ee	enantiomeric excess
equiv	molar equivalent
<i>erm</i>	erythromycin ribosome methyltransferase gene
ESI	electrospray ionization
Et	ethyl
FIA	flow injection analysis
FSA	fully synthetic antibiotic
FTIR	Fourier-transform infrared spectroscopy

g	gram
G	guanosine
Grubbs II	second-generation Grubbs catalyst
h	hour
h ν	irradiation with visible or ultraviolet light
HATU	1-[bis(dimethylamino)methylene]-1 <i>H</i> -1,2,3-triazolo[4,5- <i>b</i>]pyridinium 3-oxide hexafluorophosphate
<i>H. influenzae</i>	<i>Haemophilus influenzae</i>
<i>H. marismortui</i>	<i>Haloarcula marismortui</i>
HMDS	hexamethyldisilazane, hexamethyldisilazide
HPLC	high-pressure liquid chromatography
HRMS	high-resolution mass spectrometry
Hz	hertz
<i>i</i>	iso
imid.	imidazole
<i>J</i>	coupling constant
<i>K. pneumoniae</i>	<i>Klebsiella pneumoniae</i>
L	liter
LCMS	liquid chromatography–mass spectrometry
M	molar
m	meter
<i>m</i>	mass
<i>mef</i>	macrolide efflux gene

Mes	mesityl (2,4,6-trimethylphenyl)
MIC	minimum inhibitory concentration
min	minute
MLS _B	macrolide, lincosamide, and streptogramin B
mol	mole
MRSA	methicillin-resistant <i>Staphylococcus aureus</i>
MS	mass spectrometry, or molecular sieves
Ms	methanesulfonyl
<i>msr</i>	macrolide–streptogramin resistance gene
MW	molecular weight
<i>n</i>	normal
NMR	nuclear magnetic resonance spectroscopy
NT	not tested
PAA	<i>p</i> -anisaldehyde
<i>P. acnes</i>	<i>Propionibacterium acnes</i>
<i>P. aeruginosa</i>	<i>Pseudomonas aeruginosa</i>
<i>P. berghei</i>	<i>Plasmodium berghei</i>
PET	peptide exit tunnel
<i>P. falciparum</i>	<i>Plasmodium falciparum</i>
Ph	phenyl
pH	decimal negative logarithm of proton activity
pK _a	decimal negative logarithm of acid dissociation constant
pK _a '	decimal negative logarithm of conjugate-acid dissociation constant

PMA	phosphomolybdic acid
ppm	parts per million
Pr	propyl
PTC	peptidyltransferase center
PTFE	polytetrafluoroethylene
<i>P. vulgaris</i>	<i>Proteus vulgaris</i>
Pyr	pyridine
<i>R</i>	rectus (Cahn–Ingold–Prelog system)
<i>rac</i>	racemic
R_f	retention factor
R_t	retention time
RNA	ribonucleic acid
<i>S</i>	sinister (Cahn–Ingold–Prelog system)
s	second
<i>s</i>	secondary
<i>S. aureus</i>	<i>Staphylococcus aureus</i>
<i>S. epidermidis</i>	<i>Staphylococcus epidermidis</i>
<i>S. pneumoniae</i>	<i>Streptococcus pneumoniae</i>
<i>S. pyogenes</i>	<i>Streptococcus pyogenes</i>
<i>S. schottmeulleri</i>	<i>Salmonella schottmeulleri</i>
Su	succinimidyl
T	thymidine
<i>t</i>	tertiary

TBAF	tetra- <i>n</i> -butylammonium fluoride
TBDPS	<i>tert</i> -butyldiphenylsilyl
TBS	<i>tert</i> -butyldimethylsilyl
Teoc	2-(trimethylsilyl)ethoxycarbonyl
Tf	trifluoromethanesulfonyl
TFE	2,2,2-trifluoroethanol
<i>T. gondii</i>	<i>Toxoplasma gondii</i>
THF	tetrahydrofuran
TIPS	triisopropylsilyl
TLC	thin-layer chromatography
TMP	2,2,6,6-tetramethylpiperidide
TMS	trimethylsilyl
Ts	<i>p</i> -toluenesulfonyl
U	uridine
UV	ultraviolet
<i>z</i>	charge
δ	chemical shift, in parts per million

Chapter 1. Introduction

Chemical synthesis and antibiotic discovery

That the academic tradition of complex-molecule synthesis may directly serve the pragmatic aims of human medicine has been demonstrated perhaps no more consistently than in the case of antibiotics discovery.¹ Many antibiotics – indeed, most of those used in the clinic today – present unique and formidable challenges to the classically trained chemist, making the endeavor of synthesizing them a rewarding scholarly pursuit in its own right. At the same time, a rare near-convergence of evolutionary incentives exists between those microbial producers of natural antibiotics and the humans who would use them to treat disease – these fruits of ancient industry are, after all, endowed with the ability to kill those same organisms that would do humans harm. A near-convergence, but not a perfect one, as one important parameter was missing among the evolutionary pressures that forged biosynthetic machineries within producing organisms: the suitability of these products for direct administration to humans. In response to this particular problem, chemists have reliably intervened, marshalling the tactics and strategies of chemical synthesis to transform molecules of promise into those of practical use. Thus, the histories of today’s antibiotics largely trace the same arc as countless other medicinal chemistry campaigns, but for the fact that those critical early-stage tasks of “target validation” and “lead discovery” were in fact performed by countless generations of microbes, struggling for dominance in anonymous patches of soil.

Natural products are excellent starting points for the development of medicines, as the contemporary armamentarium against bacterial pathogens can attest – since the discovery of penicillin in 1928, nearly all antibiotics introduced to the clinic have represented structural classes

¹ For a review of the role of chemical synthesis in antibiotics discovery, see: Wright, P. M.; Seiple, I. B.; Myers, A. G. *Angew. Chem. Int. Ed.* **2014**, *53*, 8840–8869.

with naturally occurring embodiments. Time and again, chemical approaches have proven well suited to address the pharmacokinetic, pharmacodynamic, and toxicological liabilities of natural products, delivering derivatives with improved biological activity and diminished side-effect profiles. Likewise, the inevitable emergence of antibiotic resistance to a diverse host of structural classes has been met successfully with chemical innovations to overcome resistance without abandoning the classes altogether – this decades-long molecular arms race is illustrated by the β -lactams, for example, where no fewer than 4 generations of penicillins (and no fewer than 5 generations of cephalosporins) have undergone development to counteract new forms of resistance.

Owing to an historical reliance on semisynthetic strategies, however, this latter point regarding the suitability of existing classes to keep pace with rising resistance is challenged. When complex fermentation products serve as physical – rather than conceptual – starting points for antibiotics discovery, the chemical space available for exploration can be substantially limited. Not only do increasingly lengthy and costly routes become necessary in order to continue the exploration of a class once the “low-hanging fruit” has been picked, but indeed the very complexity of the starting material fundamentally limits the nature of modifications that can be performed practically (if at all). The 16-step, linear synthesis of the ketolide clinical candidate solithromycin from erythromycin,² or the 7-step synthesis of the aminoglycoside candidate plazomicin (proceeding in 0.16% overall yield) from sisomicin³ stand as stark examples of the costs incurred by a reliance on semisynthesis to advance the frontiers of anti-infective medicine.

² Fernandes, P. B. Methods for treating gastrointestinal disease. WO patent 2010/048599 A1, April 29, 2010.

³ Aggen, J. B.; Armstrong, E. S.; Goldblum, A. A.; Dozzo, P.; Linsell, M. S.; Gliedt, M. J.; Hildebrandt, D. J.; Feeney, L. A.; Kubo, A.; Matias, R. D.; Lopez, S.; Gomez, M.; Wlasichuk, K. B.; Diokno, R.; Miller, G. H.; Moser, H. E. *Antimicrob. Agents Chemother.* **2010**, *54*, 4636–4642.

Fully synthetic approaches have emerged as promising alternatives to semisynthesis, fueled by steady progress in the capabilities of modern organic chemistry, as well as by programmatic endorsement by researchers in the field, including my doctoral advisor, Professor Andrew G. Myers. Prior to my own graduate studies, his laboratory had demonstrated the viability of this approach applied toward the discovery of new members of the tetracycline⁴ and macrolide⁵ classes. This work was in turn preceded by other notable examples of fully synthetic antibiotic-discovery campaigns, leading most notably to the development of novel β -lactam,⁶ quinolone, and oxazolidinone antibiotics.⁷ These approaches hinge on the synthesis of clinically validated antibiotic scaffolds from simple commercial chemicals, ideally assembled by convergent sequences that enable the generation of orders of magnitude more structural diversity within a given class, through simple substitution of the building blocks that feed into such platforms. The realization of such an approach applied toward the lincosamide family of antibiotics forms the subject of this dissertation.

⁴ (a) Liu, F.; Myers, A. G. *Curr. Opin. Chem. Biol.* **2016**, *32*, 48–57. (b) Sun, C.; Wang, Q.; Brubaker, J. D.; Wright, P. M.; Lerner, C. D.; Noson, K.; Charest, M.; Siegel, D. R.; Wang, Y.-M.; Myers, A. G. *J. Am. Chem. Soc.* **2008**, *130*, 17913–17927. (c) Charest, M. G.; Lerner, C. D.; Brubaker, J. D.; Siegel, D. R.; Myers, A. G. *Science* **2005**, *308*, 395–398.

⁵ Seiple, I. B.; Zhang, Z.; Jakubek, P.; Langlois-Mercier, A.; Wright, P. M.; Hog, D. T.; Yabu, K.; Allu, S. R.; Fukuzaki, T.; Carlsen, P. N.; Kitamura, Y.; Zhou, X.; Condakes, M. L.; Szczypiński, F. T.; Green, W. D.; Myers, A. G. *Nature* **2016**, *533*, 338–345.

⁶ Page, M. G. P. Beta-Lactam Antibiotics. In *Antibiotic Discovery and Development*; Dougherty, T. J.; Pucci, M. J., Eds.; Springer: New York, 2012; pp 79–117.

⁷ Notably, the oxazolidinones represent a rare historical example of an antibiotic class uncovered not through natural-product isolation, but through phenotypic screening of a corporate library. The origin of the quinolone class is similar, if less transparently documented: (a) Gregory, W. A.; Brittelli, D. R.; Wang, C.-L. J.; Wuonola, M. A.; McRipley, R. J.; Eustice, D. C.; Eberly, V. S.; Bartholomew, P. T.; Slee, A. M.; Forbes, M. *J. Med. Chem.* **1989**, *32*, 1673–1681. (b) Bisacchi, G. S. *J. Med. Chem.* **2015**, *58*, 4874–4882.

Introduction to the lincosamides

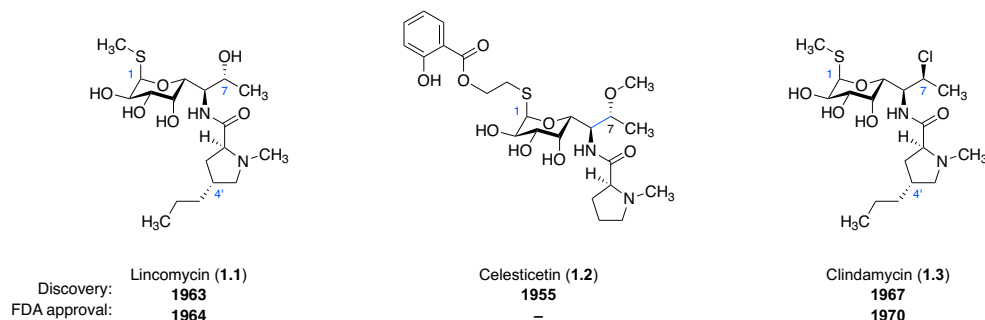


Figure 1.1. Examples of lincosamide antibiotics.

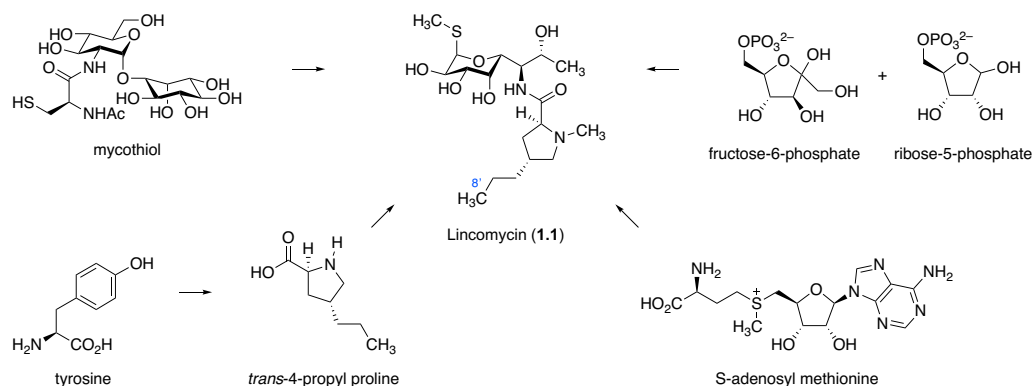
The lincosamides are a class of molecules typified by an unusual carbohydrate–alkaloid framework linking a northern thiooctose residue to a southern cyclic amino acid via a central amide bond. They take their name from their prototypical member, lincomycin (**1.1**), which researchers at The Upjohn Company recovered from the soil microbe *Streptomyces lincolnensis* var. *lincolnensis* found growing in Gering, Nebraska, some 400 miles from Lincoln.⁸ As early as 1955, celesticetin (**1.2**) – another natural product isolated from the related organism *Streptomyces caelestis* – had been known, but it wasn't until a team of Upjohn scientists rigorously established the structure of lincomycin in 1964 that the familial identity of these two antibiotic substances was cemented.⁹ That same year, lincomycin was approved for human use by the U.S. Food and Drug Administration (FDA), followed six years later by its semisynthetic derivative clindamycin (**1.3**).¹⁰

⁸ (a) Mason, D. J.; Dietz, A.; DeBoer, C. *Antimicrob. Agents Chemother.* **1963**, 554–559. (b) Magerlein, B. J. *Adv. Appl. Microbiol.* **1971**, 14, 185–229.

⁹ (a) Hoeksema, H.; Bannister, B.; Birkenmeyer, R. D.; Kagan, F.; Magerlein, B. J.; MacKellar, F. A.; Schroeder, W.; Slomp, G.; Herr, R. R. *J. Am. Chem. Soc.* **1964**, 86, 4223–4224. (b) Hoeksema, H. *J. Am. Chem. Soc.* **1964**, 86, 4224–4225. (c) Herr, R. R.; Slomp, G. *J. Am. Chem. Soc.* **1967**, 89, 2444–2447. (d) Schroeder, W.; Bannister, B.; Hoeksema, H. *J. Am. Chem. Soc.* **1967**, 89, 2448–2453. (e) Hoeksema, H. *J. Am. Chem. Soc.* **1967**, 90, 755–757.

¹⁰ (a) U. S. Food and Drug Administration. Drugs@FDA: FDA Approved Drug Products, Lincocin Hydrochloride (Lincomycin Hydrochloride), NDA #050316. <https://www.accessdata.fda.gov/scripts/cder/daf/index.cfm?event=overview.process&ApplNo=050316> (accessed 7 March, 2018). (b) U. S. Food and Drug Administration. Drugs@FDA: FDA Approved Drug Products, Cleocin Hydrochloride (Clindamycin Hydrochloride), NDA #050162.

The striking fact that no new lincosamides have entered clinical use since 1970 has prompted some experts to dub them an underexploited family within today's armamentarium.¹¹



Scheme 1.1. The biosynthetic precursors of lincomycin.

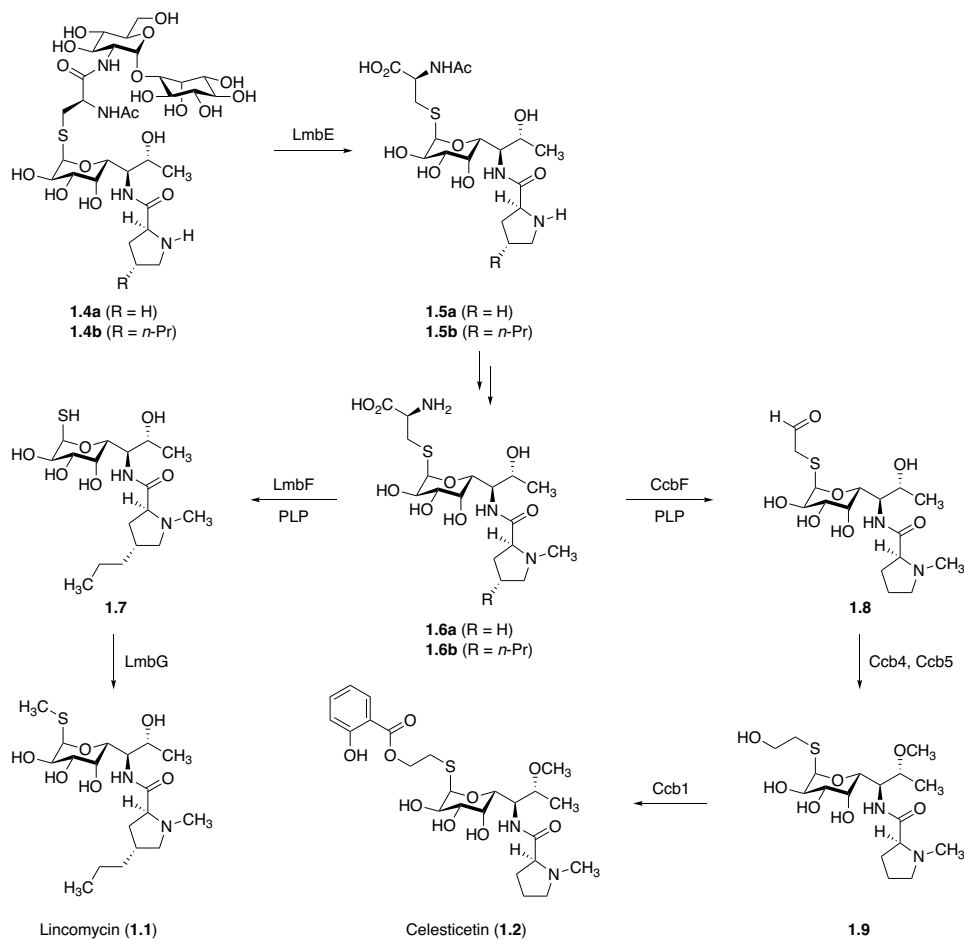
Inquiries into the biosynthesis of the lincosamides – motivated by these molecules' clinical utility as much as by their peculiar structures – have afforded a number of valuable insights, with implications for the discovery of new members of the class. Early stable-isotope feeding studies performed by Upjohn's fermentation research and development team established the provenance of all carbon atoms within lincomycin (Scheme 1.1).¹² The northern-half octose arises through transaldolase-catalyzed C₃–C₅ carbohydrate fragment coupling, they found; while the propylhygric acid motif derives from L-tyrosine, through extradiol oxidative cleavage of its downstream metabolite, L-dihydroxyphenylalanine (L-DOPA). Three remaining carbons within lincomycin were traced to S-adenosyl methionine, namely the *S*-methyl and *N*-methyl groups, as

<https://www.accessdata.fda.gov/scripts/cder/daf/index.cfm?event=overview.process&ApplNo=050162> (accessed 7 March, 2018).

¹¹ O'Dowd, H.; Erwin, A. L.; Lewis, J. G. Lincosamide Antibacterials. In *Natural Products in Medicinal Chemistry*; Hanessian, S., Ed.; Wiley-VCH Verlag GmbH & Co. KGaA, Weinheim, Germany, 2014.

¹² (a) Brahme, N. M.; Gonzales, J. E.; Rolls, J. P.; Hessler, E. J.; Mizensak, S.; Hurley, L. H. *J. Am. Chem. Soc.* **1984**, *106*, 7873–7878. (b) Brahme, N. M.; Gonzales, J. E.; Mizensak, S.; Rolls, J.; Hessler, E.; Hurley, L. H. *J. Am. Chem. Soc.* **1984**, *106*, 7878–7883.

well as the C8' methyl terminus of the *n*-propyl chain. The origin of the sulfur atom, however, remained a mystery until 2015, when Wen Liu and coworkers demonstrated the dual involvement of ergothioneine and mycothiol in the installation of the anomeric substituent of naturally occurring lincosamides. Differential processing of cysteinyl-*S*-glycoside intermediates (**1.6a/b**) was found to underlie the variation in sulfur appendages observed between lincomycin and celesticetin (Scheme 1.2) – an insight that enabled the preparation of a library of *S*-alkyl analogs, including lincomycin–celesticetin hybrid analogs, through engineered biosynthesis (*vide infra*).



Scheme 1.2. Selected enzymes involved in the biosynthetic processing of *S*-glycosidic intermediates *en route* to lincomycin and celesticetin.

Mechanism of action

Lincosamide antibiotics target the bacterial ribosome, blocking protein synthesis by interfering with the proper positioning of aminoacyl-tRNA within the ribosomal A site. Unlike several other important ribosome-targeting antibiotics,¹³ the lincosamides do not interfere with the action of eukaryotic ribosomes, whether cytosolic or mitochondrial;¹⁴ and in the case of the eukaryotic parasite *T. gondii*, clindamycin's target is in fact the ribosome of the apicoplast, an organelle believed to have descended from secondary endosymbiosis of an alga.¹⁵ The lincosamide ribosomal binding site overlaps with those of other widely used antibiotic classes including the phenicols, oxazolidinones, mutulins, and macrolides (Figure 1.2) – all of which occupy an axis extending from the catalytically active peptidyltransferase center (PTC) through the proximal end of the nascent peptide exit tunnel (PET), although subtle differences in structure and relative positioning cause these classes to diverge with respect to the details of their action.¹⁶ Consequential to their activity as protein-synthesis inhibitors, the lincosamides are bacteriostatic, meaning that exposure to these antibiotics does not directly lead to cell death. This has its advantages, as lincosamides effectively suppress toxin production even at sub-inhibitory concentrations and do not cause lytic release of bacterial cell contents, differentiating them from other classes such as the

¹³ The tetracycline antibiotics modulate the activity of human cytosolic ribosomes, with potential therapeutic applications, for example, whereas aminoglycoside ototoxicity is believed to arise in part from human mitoribosome inhibition. See: (a) Mortison, J. D.; Schenone, M.; Myers, J. A.; Zhang, Z.; Chen, L.; Ciarlo, C.; Comer, E.; Natchiar, S. K.; Carr, S. A.; Klaholz, B. P.; Myers, A. G. **2018** [pre-print], bioRxiv doi: 10.1101/256230. (b) Hobbie, S. N.; Akshay, S.; Kalapala, S. K.; Bruell, C. M.; Shcherbakov, D.; Böttger, E. C. *Proc. Nat. Acad. Sci. U. S. A.* **2008**, *105*, 20888–20893.

¹⁴ Böttger, E. C.; Springer, B.; Prammananan, T.; Kidan, Y.; Sander, P. *EMBO Rep.* **2001**, *2*, 318–323.

¹⁵ Camps, M.; Arrizabalaga, G.; Boothroyd, J. *Mol. Microbiol.* **2002**, *43*, 1309–1318.

¹⁶ Wilson, D. N. *Crit. Rev. Biochem. Mol. Bio.* **2009**, *44*, 393–433.

β -lactams in applications such as the treatment of toxic shock syndrome and necrotizing infections.¹⁷

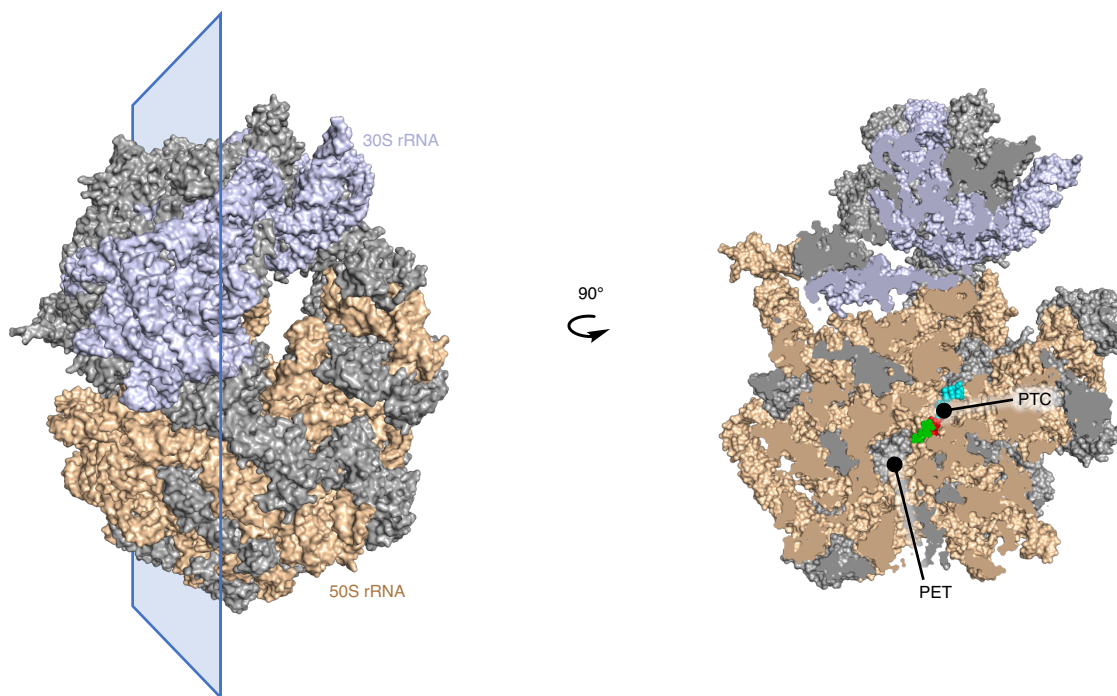


Figure 1.2. Gross structure and cross-section of the 70S bacterial ribosome, showing the binding site of clindamycin (red) relative to antibiotics targeting the PTC (CC-puromycin, cyan) and PET (azithromycin, green). Color code: 30S rRNA, cornflower; 50S rRNA, wheat; ribosomal proteins, gray. Compiled from PDB entries 4V7V, 3CD6, and 1YHQ.

X-ray crystallographic studies of lincosamides bound to the ribosomes or ribosomal subunits of no fewer than four distinct bacterial species have illuminated with atomic precision the means by which these antibiotics engage their cellular target. In 2001, Ada Yonath, François Franceschi, and co-workers published the first such report, wherein clindamycin was studied in complex with the 50S large ribosomal subunit of the extremophilic eubacterium *D. radiodurans*.¹⁸

¹⁷ Smieja, M. *Can. J. Infect. Dis.* **1998**, *9*, 22–28.

¹⁸ Schlünzen, F.; Zarivach, R.; Harms, J.; Bashan, A.; Tocilj, A.; Albrecht, R.; Yonath, A.; Franceschi, F. *Nature* **2001**, *413*, 814–821.

This study validated earlier chemical footprinting work¹⁹ that had proposed a lincosamide binding site within the peptide exit tunnel (PET), bridging the peptidyltransferase center (PTC) and the canonical macrolide binding site (Figure 1.3A). This co-crystal structure defined the binding pose of clindamycin as roughly longitudinal to the PET, whereby the thiooctose moiety, overlapping with the macrolides' desosamine binding site, resides downstream of the propylhygric acid subunit. Upon comparison with the apo structure, it was found that lincosamide binding involves displacement of a divalent magnesium ion by the pyrrolidine ring, whose positive charge under physiological pH likely compensates for the loss of this A-site scaffolding element.²⁰ In addition to this important electrostatic interaction, Yonath's work also identified an extensive hydrogen-bonding network involving all three pyranose hydroxyls and the central amide group, which together anchor clindamycin to the PET surface, and thus drive molecular recognition between drug and target.

In 2005, a team of researchers at Yale University led by Thomas Steitz (who would later share the 2009 Nobel Prize in Chemistry with Ada Yonath and Venkatraman Ramakrishnan for his work on ribosomal structure and function) reported the co-crystal structure of clindamycin bound to a large ribosomal subunit of another extremophile – the Archaeon *H. marismortui* – and observed some striking differences compared to the *D. radiodurans* structure.²¹ The *H. marismortui* ribosomal subunit used in Steitz's study contained the mutation G2099A, introduced

¹⁹ (a) Douthwaite, S. *Nucleic Acids Res.* **1992**, *20*, 4717–4720. (b) Hansen, L. H.; Mauvas, P.; Douthwaite, S. *Mol. Microbiol.* **1999**, *31*, 623–631.

²⁰ A similar phenomenon is believed to drive the affinity of aminoglycoside antibiotics for their polynucleic acid targets. Accordingly, displacement of magnesium ions with basic amines has served as a successful design strategy in several medicinal chemistry campaigns. For a review, see: Meanwell, N. A. *Bioorg. Med. Chem. Lett.* **2017**, *27*, 5355–5372.

²¹ Tu, D.; Blaha, G.; Moore, P. B.; Steitz, T. A. *Cell* **2005**, *121*, 257–270.

in order to more closely resemble the native structure of the eubacterial ribosome, particularly in light of the fact that mutations to this position (A2058 in *E. coli*; this numbering system is used hereafter) are known to confer resistance to many PET-targeting antibiotics, including the lincosamides. In this system, the binding pose adopted by clindamycin's northern half coincides closely with the *D. radiodurans* structure, but the propylhygric acid moiety is rotated nearly 180° around the C6–N bond. (Figure 1.3B) The *s-trans* conformation Steitz and co-workers observed more closely recapitulates ribosome-free structures of clindamycin solved by single-crystal X-ray diffraction, and in the *H. marismortui* co-crystal structure places the *n*-propyl terminus in the same A-site cleft occupied by CC-puromycin, indicating that clindamycin acts primarily by blocking proper positioning of A-site aminoacyl-tRNA.

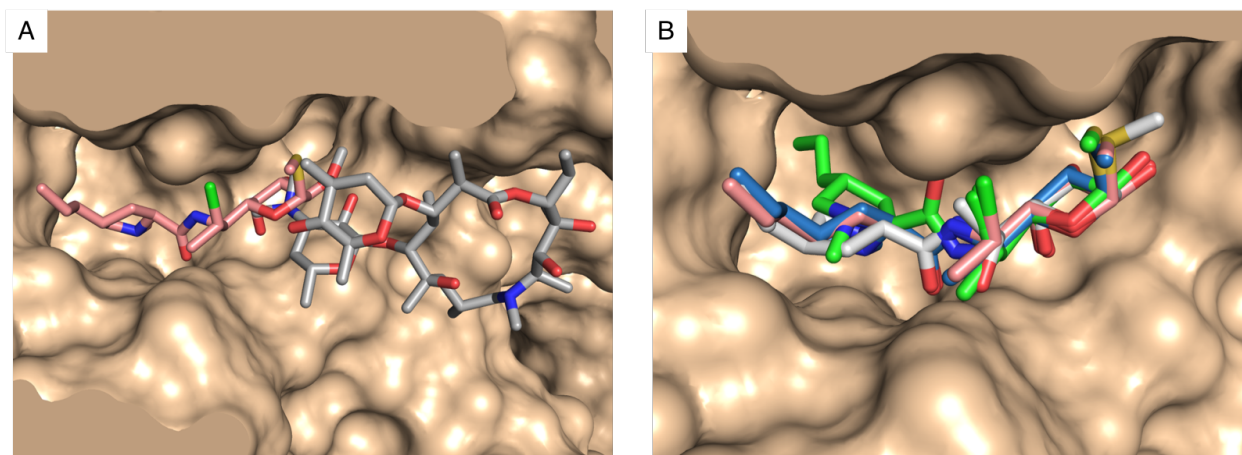


Figure 1.3. The lincosamides bind the neck of the PET, adjacent to the PTC. (A) Clindamycin (salmon, PDB: 1YJN) binds upstream of azithromycin (gray, PDB: 1M1K) within the PET, its thiooctose moiety overlapping with the desosamine residue of the macrolides. (B) Overlay ribosome-bound lincosamide structures reveals an anomalous 180° rotation of the propyl subunit in the first reported structure. *D. radiodurans* 50S–clindamycin (green, PDB: 1JZX); *H. marismortui* 50S–clindamycin (salmon, PDB: 1YJN); *E. coli* 70S–clindamycin (blue, PDB: 4V7V); *S. aureus* 50S–lincomycin (gray, PDB: 5HKV).

Two additional studies using ribosomes from clinically germane bacterial pathogens would later bolster this revised binding pose (Figure 1.3B), and together with earlier reports would enable

the coalescence of a useful model to describe mechanisms of lincosamide action and resistance. The first of these, led by Professors Alexander Mankin and Jamie Cate, afforded the co-crystal structure of clindamycin bound to the 70S ribosome of the Gram-negative bacillus *E. coli*.²² This report reinforced the role of the *n*-propyl chain in obstructing the A site, and identified key differences (relative to *H. marismortui*) in *E. coli* ribosomal structure, particularly in the region abutting clindamycin's southern half. Likewise, in 2017, Yonath and co-workers reported the structures of the *S. aureus* 50S ribosomal subunit in complex with both lincomycin and a semisynthetic analog termed RB02 (**1.10**),²³ in which the aminoacyl moiety of the natural product is replaced by a neutral *p*-nitrobenzamide group (Figure 1.4). Lacking a basic amine in its southern half, RB02 binds the ribosome in an analogous fashion to lincomycin, but lacks the ability to compensate electrostatically for the displacement of a structural magnesium ion: Accordingly, in an *in vitro* *S. aureus* ribosomal translation assay, RB02 is roughly 600-fold less potent than lincomycin ($IC_{50} = 19.2 \pm 1.1 \mu\text{g/mL}$, versus $0.030 \pm 0.002 \mu\text{g/mL}$), and only 10–20-fold more potent than methylthiolincosamine (MTL, **1.11**, $IC_{50} \sim 300 \mu\text{g/mL}$), the aminooctose portion of lincomycin lacking a southern half altogether.

²² Dunkle, J. A.; Xiong, L.; Mankin, A. S.; Cate, J. H. D. *Proc. Nat. Acad. Sci. U. S. A.* **2010**, *107*, 17152–17157.

²³ Matzov, D.; Eyal, Z.; Benhamou, R. I.; Shalev-Benami, M.; Halfon, Y.; Krupkin, M.; Zimmerman, E.; Rozenberg, H.; Bashan, A.; Fridman, M.; Yonath, A. *Nucleic Acids Res.* **2017**, *45*, 10284–10292.

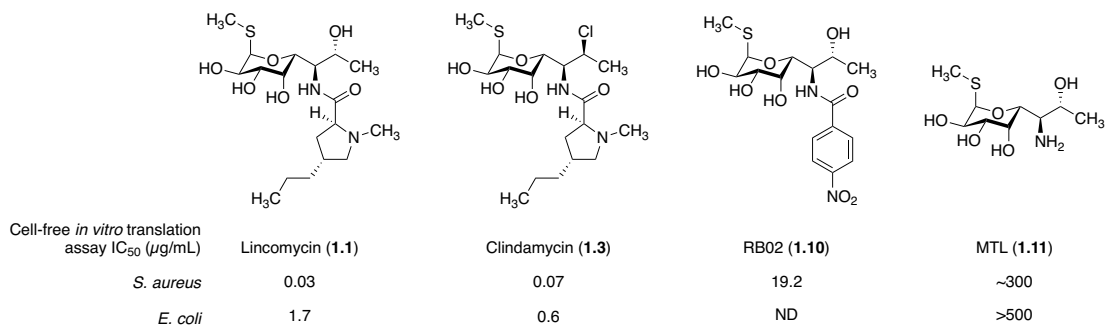


Figure 1.4. In-vitro activities of clindamycin, lincomycin, and simplified analogs in cell-free translation-inhibition assays using ribosomes from *S. aureus* and *E. coli*. Adapted from Reference 23.

Taken together, these studies suggest three orthogonal driving forces, conserved among all species studied, forming the basis for lincosamide affinity for the ribosome: (1) a well-ordered hydrogen-bond network involving the substituents of C2–C6, providing molecular recognition between ligand and target; (2) an electrostatic interaction between an aminium ion in the southern half and the phosphodiester backbone of A-site rRNA, compensating for the displacement of a structural magnesium ion upon lincosamide binding; and (3) hydrophobic interactions between the A-site residues A2451 and C2452, leading to favorable desolvation of lipophilic appendages on the southern half (Figure 1.5).

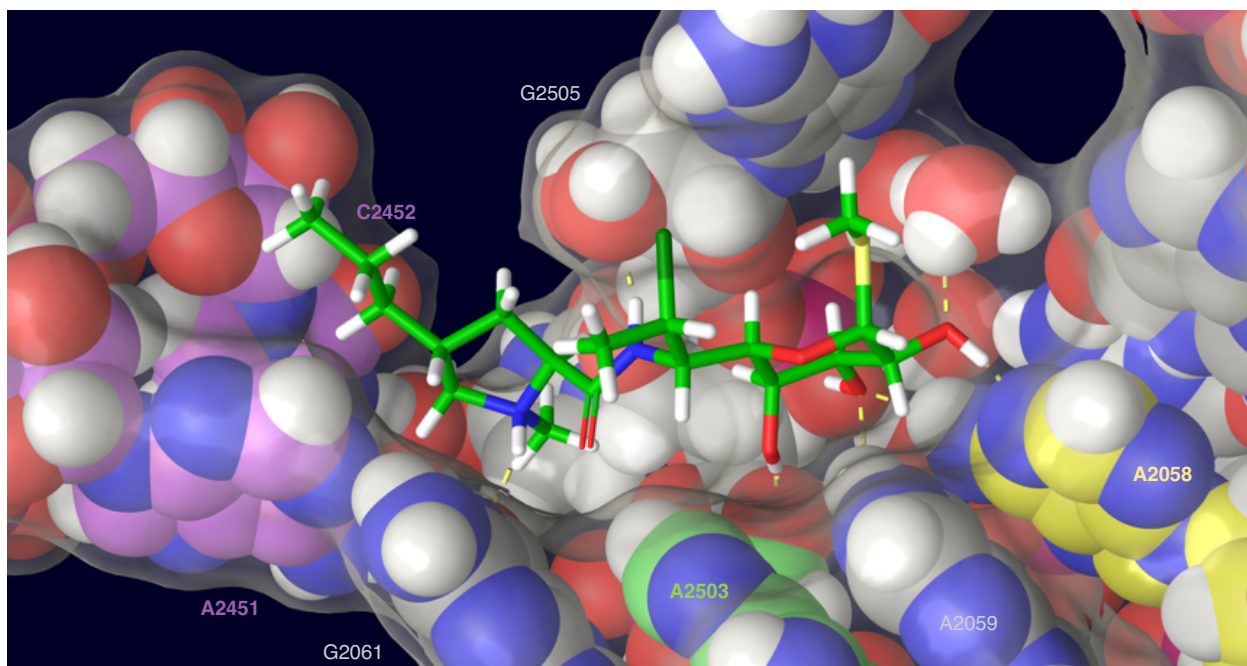


Figure 1.5. Detailed depiction of the lincosamide ribosomal binding site. The hydrophobic faces of residues A2451 and C2452 (lilac) form an interaction with the aliphatic southern-half motif of clindamycin (green), while a network of hydrogen bonds (yellow dashed lines) anchors the thiooctose moiety. Residues A2058 (yellow) and A2503 (light green) are highlighted – mutation or modification of these nucleotides confers resistance to lincosamides. Model constructed from PDB entry 1YJN.²¹

Mechanisms of resistance

Within the lincomycin biosynthetic gene cluster of *S. lincolnensis* can be found two resistance determinants, whose orthogonal actions to protect the producing organism appear to anticipate common forms of lincosamide resistance encountered in the clinic.²⁴ The first of these putative genes, *lmrA*, is believed to encode a proton-dependent transport protein, based on the predicted presence of 12 transmembrane domains, and close sequence homology with known multidrug efflux proteins such as the Mmr protein from the producing organism of methylenomycin (*Streptomyces caelicolor*) and the QacA multidrug transporter from *S. aureus*.

²⁴ Zhang, H.-Z.; Schmidt, H.; Piepersberg, W. *Mol. Microbiol.* **1992**, *6*, 2147–2157.

The other, *lmrB*, likewise shows similarity to ribosome methyltransferase genes whose products are known to perform N⁶ mono- or dimethylation of A2058 in rRNA – a residue identified both by chemical footprinting^{19a} and ribosome X-ray crystallography^{18,21–23} as essential for proper targeting by the lincosamides. Surprisingly, while bearing close correspondence with genes known to produce multidrug-resistant phenotypes, *lmrA* and *lmrB* do not confer resistance to lincomycin's close relatives clindamycin and celesticetin.²⁴

Mirroring the strategies used by the producing organism to evade the action of lincomycin, the most commonly encountered forms of lincosamide resistance in the clinic are driven by target modification and drug efflux. Post-transcriptional modification of 23S rRNA accounts for the majority of acquired resistance encountered today, most commonly occurring through acquisition of transferrable elements encoding members of the erythromycin resistance methyltransferase (Erm) family of enzymes, of which over 40 have been discovered so far.²⁵ Members of this family operate in an S-adenosyl methionine–dependent fashion to dimethylate N⁶ of A2058 (Figure 1.6), analogously to the purported action of LmrB, and confer cross-resistance to macrolides, lincosamides, and streptogramin B – a multidrug-resistance phenotype commonly abbreviated as MLS_B, which may be inducible (iErm) or constitutive (cErm).²⁶ Since the discovery of the first Erm proteins in the years following the introduction of erythromycin to the clinic, members of this family have been found in a wide array of common pathogens, including *S. aureus*, *S. pneumoniae*, *S. pyogenes*, *E. faecalis*, *C. difficile*, and *E. coli*. The rising prevalence of *erm* genes, found particularly among hospital-acquired infections, accordingly threatens to curtail the clinical utility

²⁵ (a) Leclercq, R. *Clin. Infect. Dis.* **2002**, *34*, 482–492. (b) Roberts, M. C.; Sutcliffe, J.; Courvalin, P.; Jensen, L. B.; Rood, J.; Seppala, H. *Antimicrob. Agents Chemother.* **1999**, *43*, 2823–2830.

²⁶ Courvalin, P.; Ounissi, H.; Arthur, M. *J. Antimicrob. Chemother.* **1985**, *16* (Suppl A), 91–100.

of contemporary macrolides and lincosamides, prompting the U.S. Centers for Disease Control and Prevention to call for action against MLS_B-resistant streptococcal infections specifically in their widely circulated 2013 Threat Report.²⁷

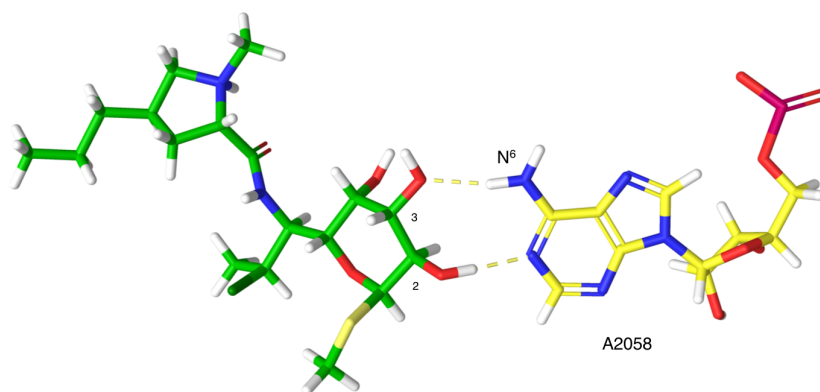


Figure 1.6. Pseudo-base pairing interaction of clindamycin with rRNA residue A2058. Erm-mediated N⁶ methylation confers cross-resistance to macrolide, lincosamide, and streptogramin A antibiotics.²¹

Erm-mediated ribosome methylation forms the basis of the now-famous D test for inducible MLS_B resistance, first reported by Griffith and coworkers in 1965 (Figure 1.7).²⁸ In this solid agar susceptibility test, a D-shaped zone of inhibition forms around lincosamide-loaded disks if an erythromycin disk is placed nearby. Subsequent studies of this so-called “erythromycin antagonizability” would later show that inducible expression of *erm* genes is controlled through a translation-attenuation mechanism, wherein ribosomal binding of macrolide antibiotics causes sequence-specific translation arrest at leader open reading frames; global mRNA rearrangement

²⁷ Centers for Disease Control and Prevention. *Antibiotic resistance threats in the United States, 2013*. <http://www.cdc.gov/drugresistance/threat-report/2013>. Accessed March 6, 2018.

²⁸ (a) Griffith, L. J.; Ostrander, W. E.; Mullins, C. G.; Beswick, D. E. *Science* **1965**, *147*, 746–747. (b) Weisblum, B.; Demohn V. *J. Bacteriol.* **1969**, *98*, 447–452. (c) Leclercq, R. Macrolides, Lincosamides, and Streptogramins. In *Antibiogram*; Courvalin, P.; Leclercq, R.; Rice, L. B., Eds.; Eska Publishing: Portland, OR, 2010; pp 305–326.

leading to displacement of a stem-loop structure that otherwise sequesters the Shine-Dalgarno sequence of the methyltransferase-encoding mRNA; and consequent translation of the Erm protein. Importantly, because lincosamides bind upstream of the macrolides within the PET and thus typically arrest translation at the initiation codon²⁹ (versus the ninth or tenth codon in the case of erythromycin),³⁰ they are able to elude detection by this common ribo-regulatory apparatus – a key advantage of the class.

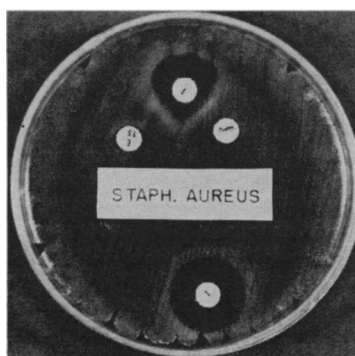


Figure 1.7. D test for inducible MLS_B resistance in *S. aureus*. Erythromycin disks (labeled “E,” right and left) produce a diminished zone of inhibition surrounding lincomycin (“L,” top and bottom) disks placed nearby. From Griffith, L. J.; Ostrander, W. E.; Mulins, C. G.; Beswick, D. E. *Science* **1965**, *147*, 746–747. Reprinted with permission from AAAS.

Another increasingly common mode of resistance is driven by post-transcriptional modification of rRNA at a site approximately 8 Å upstream of A2058 at the neck of the PET, giving rise to phenicol, lincosamide, oxazolidinone, pleuromutilin, and streptogramin A (PhLOPS_A) cross-resistance. The gene responsible for this phenotype, *cfr* (chloramphenicol-florfenicol resistance), was discovered in 2000 by a team surveilling florfenicol resistance among

²⁹ Marks, J.; Kannan, K.; Roncase, E. J.; Klepacki, D.; Kefi, A.; Orelle, C.; Vásquez-Laslop, N.; Mankin, A. S. *Proc. Nat. Acad. Sci. U. S. A.* **2016**, *113*, 12150–12155.

³⁰ Gupta, P.; Liu, B.; Klepacki, D.; Gupta, V.; Schulten, K.; Mankin, A. S.; Vásquez-Laslop, N. *Nat. Chem. Biol.* **2016**, *12*, 153–158.

staphylococcal veterinary isolates in Germany.³¹ Homologous to the housekeeping ribosome methyltransferase RlmN, which methylates C2 of the A-site residue A2503 (and does not substantially impact antibiotic susceptibility), Cfr instead methylates the C8 position of this same rRNA residue, altering the local structure of PET floor, and sterically blocking molecular recognition between PhLOPS_A drugs and their target (cf. Figure 1.5).³² Importantly, *cfr* has been shown to carry only a small associated fitness cost upon expression, is almost always found on plasmids or together with insertion sequences, and readily undergoes horizontal transfer between pathogenic hosts,³³ all with clear epidemiologic consequences. While current estimates indicate that *cfr* is not particularly widespread, recent reports of *cfr*-mediated multidrug-resistant *S. aureus*, *E. faecalis*, and *S. epidermidis* outbreaks³⁴ present further evidence of rising resistance to clinical standbys like clindamycin.

In addition to post-transcriptional modification of the ribosome, mutations to rRNA primary structure are known to confer lincosamide resistance as well. Indeed, some of the first known lincosamide-resistant strains of *S. aureus*, obtained deliberately through repeated passage on lincomycin- or clindamycin-treated growth media,³⁵ are believed to have arisen through

³¹ Schwarz, S.; Werckenthin, C.; Kehrenberg, C. *Antimicrob. Agents Chemother.* **2000**, *44*, 2530–2533.

³² (a) Long, K. S.; Poehlsgaard, J.; Kehrenberg, C.; Schwarz, S.; Vester, B. *Antimicrob. Agents Chemother.* **2006**, *50*, 2500–2505. (b) Toh, S.-M.; Xiong, L.; Bae, T.; Mankin, A. S. *RNA* **2008**, *14*, 98–106.

³³ (a) LaMarre, J. M.; Locke, J. B.; Shaw, K. J.; Mankin, A. S. *Antimicrob. Agents Chemother.* **2011**, *55*, 3714–3719. (b) Kehrenberg, C.; Aarestrup, F. M.; Schwarz, S. *Antimicrob. Agents Chemother.* **2007**, *51*, 483–487.

³⁴ (a) Diaz, L.; Kiratisin, P.; Mendes, R. E.; Panesso, D.; Singh, K. V.; Arias, C. A. *Antimicrob. Agents Chemother.* **2012**, *56*, 3917–3922. (b) Morales, G.; Picazo, J. J.; Baos, E.; Candel, F. J.; Arribi, A.; Peláez, B.; Andrade, R.; de la Torre, M. A.; Fereres, J.; Sánchez-García, M. *Clin. Infect. Dis.* **2010**, *50*, 821–825. (c) Baos, E.; Candel, F. J.; Merino, P.; Pena, I.; Picazo, J. J. *Diagnost. Microbiol. Infect. Dis.* **2013**, *76*, 325–329. (d) O’Connor, C.; Powell, J.; Finnegan, C.; O’Gorman, A.; Barrett, S.; Hopkins, K. L.; Pichon, B.; Hill, R.; Power, L.; Woodford, N.; Coffey, J. C.; Kearns, A.; O’Connell, N. H.; Dunne, C. P. *J. Hosp. Infect.* **2015**, *90*, 316–321.

³⁵ Benner, E. J.; Adams, A. P., Jr. *Antimicrob. Agents Chemother.* **1969**, *9*, 100–103.

accumulated mutations in 23S rRNA sequence.¹¹ While point mutations such as A2058G are known to produce MLS_B resistance phenotypes – in the case of clindamycin, by disrupting the pseudo-base-paired interaction normally formed between the C2,C3-diol motif of clindamycin and A2058 (Figure 1.6) – this mechanism of resistance is not commonly encountered in most pathogenic bacteria, which carry multiple copies of ribosomal DNA.³⁶ One notable exception is that of *T. pallidum*, the organism that causes syphilis, which harbors only two copies of the rRNA gene:³⁷ In 2015, a survey of *T. pallidum* clinical isolates (n = 109) in Shanghai revealed a staggering 95.4% prevalence of the A2058G mutation in both copies of the 23S rRNA gene, explaining high rates of treatment failure with azithromycin, a macrolide antibiotic.³⁸ Similarly, prolonged topical administration of clindamycin for the treatment of acne vulgaris is believed to partially underlie an increase in MLS_B-resistant *P. acnes*, many isolates of which harbor the A2058G ribosomal mutation.³⁹

Bacteria expressing lincosamide-modifying enzymes have also been reported, although the clinical significance of drug modification–based resistance is not well known. All of the lincosamide-modifying enzymes reported to date function as adenylyltransferases and fall into two main groups based on sequence similarity with other nucleotidyltransferase families. The first group, typically found in staphylococci, comprise LinA and its relatives LnuC and LnuD; these enzymes are homologous to ANT(2'')-1a, an enzyme known to function similarly in the

³⁶ The presence of multiple rRNA gene copies in most bacteria explains why high-level resistance is slow to develop in these organisms, as point mutations to target genes rarely rescue organisms from the action of an antibiotic. For a review of this so-called “multiple-target hypothesis,” see: Silver, L. *Nature Rev. Drug Discov.* **2007**, *6*, 41–55.

³⁷ Fukunaga, M.; Okuzako, N.; Mifuchi, I.; Arimitsu, Y.; Seki, M. *Microbiol. Immunol.* **1992**, *36*, 161–167.

³⁸ Lu, H.; Li, K.; Gong, W.; Yan, L.; Gu, X.; Chai, Z.; Guan, Z.; Zhou, P. *Emerg. Microbes Infect.* **2015**, *4*, e10; doi:10.1038/emi.2015.10.

³⁹ Nakase, K.; Okamoto, Y.; Aoki, S.; Noguchi, N. *J. Dermatol.* **2018**, *45*, 340–343.

nucleotidylative deactivation of aminoglycoside antibiotics.⁴⁰ The second, including LinB and LnuF, appear to derive instead from bacterial DNA polymerase, and are observed in enterococci (Figure 1.8).⁴¹ Intriguingly, while LinB selectively modifies the 3-hydroxyl group of both clindamycin and lincomycin, LinA shows more pronounced substrate sensitivity, producing upon exposure to lincomycin the corresponding 3-(5'-adenylate), whereas clindamycin is modified at the 4-position.⁴² As with the enzymes responsible for target modification-mediated resistance, these drug-inactivating enzymes are often encoded on transmissible elements.¹¹

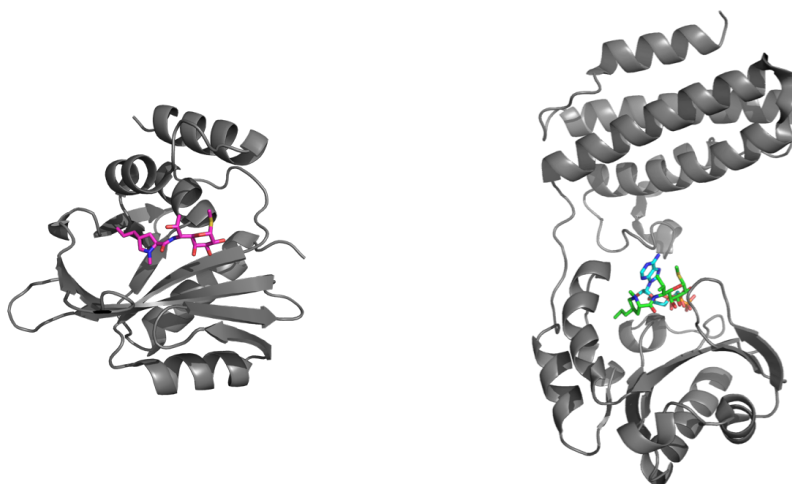


Figure 1.8. Structures of lincosamide adenylyltransferases solved by X-ray crystallography. Left: LinA in complex with lincomycin (magenta; PDB: 4WH5). Right: LinB bound to clindamycin (green) and an ATP mimetic (cyan; PDB: 3JZ0).

While no lincosamide-specific efflux pumps have been well characterized (besides perhaps LmrA, the transporter protein encoded in the lincomycin biosynthetic gene cluster), nonspecific drug efflux nonetheless represents a major driver of lincosamide resistance. In Gram-negative

⁴⁰ Petinaki, E.; Guerin-Fauble, V.; Pichereau, V.; Villers, C.; Achard, A.; Malbruny, B.; Leclercq, R. *Antimicrob. Agents Chemother.* **2008**, *52*, 626–630.

⁴¹ Morar, M.; Bhullar, K.; Hughes, D. W.; Junop, M.; Wright, G. D. *Structure* **2009**, *17*, 1649–1659.

⁴² Brisson-Noël, A.; Delrieu, P.; Samain, D.; Courvalin, P. *J. Biol. Chem.* **1988**, *263*, 15880–15887.

organisms particularly, chromosomally encoded multidrug transporters such as the AcrAB-TolC complex in *E. coli* confer intrinsic resistance to lincosamides, as evidenced by a ≥ 16 -fold increase in susceptibility to clindamycin upon deletion of the *tolC* gene (encoding the outer-membrane portion of the AcrAB-TolC pump assembly) in otherwise isogenic *E. coli* strains. This intrinsic resistance represents a general challenge to the class, as even next-generation lincosamides effective against cErm-expressing Gram-positive pathogens display extensive efflux from Gram-negative organisms.

Indeed, even in some Gram-positive organisms, including strains of staphylococcal species typically susceptible to lincosamides, ATP-binding cassette (ABC) transporters conferring lincosamide resistance have been identified.⁴³ More recently, in work showcasing a newly developed method for high-throughput ribo-regulator discovery, Israeli and French researchers uncovered a lincomycin-dependent regulatory apparatus operating in *L. monocytogenes*, which controls expression of an ABC transporter-type resistance determinant.⁴⁴ This ribo-regulator, *lmo0919*, specifically senses translational stalling of lincomycin-bound ribosomes on a 9-base upstream open reading frame, leading to reorganization of a downstream mRNA termination structure and consequent translation of the downstream ABC transporter gene. This attenuation-based regulatory system closely recalls the canonical mechanism underlying the iErm phenotype, demonstrating that while the lincosamides arrest translation at an earlier stage than macrolides, ribosomal detection – and consequent expression of multidrug-resistance determinants – is possible for both classes.

⁴³ Novotna, G.; Janata J. *Antimicrob. Agents Chemother.* **2006**, *50*, 4070–4076.

⁴⁴ Dar, D.; Shamir, M.; Mellin, J. R.; Koutero, M.; Stern-Ginossar, N.; Cossart, P.; Sorek, R. *Science* **2016**, *352*, aad9822.

Clinical utility and limitations

Clindamycin, which replaced lincomycin as the only clinically relevant member of the lincosamide class upon FDA approval in 1970, has been in continuous use for nearly half a century. Listed as an essential medicine by the World Health Organization, clindamycin's quarterly unit sales have doubled over a 12-year period,⁴⁵ tracking with the growing rate of antibiotic use.⁴⁶ The lincosamides have a spectrum of activity similar to the macrolides, typically limited to Gram-positive cocci such as *S. aureus*, *S. pneumoniae*, and *S. pyogenes*;⁴⁷ some Gram-positive bacilli such as *L. monocytogenes* and *B. anthracis*; and select Gram-negative bacteria such as *N. gonorrhoeae* and *B. fragilis*. As such, clindamycin (Cleocin, Pfizer) is commonly prescribed to patients allergic to β -lactams or macrolides (or in pediatric cases, where tetracycline administration is inappropriate) for the treatment of staphylococcal or streptococcal infections, where its mechanism of action has the added benefit of suppressing bacterial exotoxin production.¹⁷ Owing to its excellent distribution into bones and joints upon systemic administration, clindamycin is also recommended for the treatment of osteomyelitis.⁴⁸ Likewise, its oral bioavailability, excellent staphylococcal activity, and inability to trigger iErm have made clindamycin part of the standard

⁴⁵ Wohl, B. Blavatnik Fellow, Harvard University, Cambridge, MA. Personal communication based on analysis of wholesaler data from IMS Health, September 2016.

⁴⁶ Baggs, J.; Fridkin, S. K.; Pollack, L. A.; Srinivasan, A.; Jernigan, J. A. *JAMA Intern. Med.* **2016**, doi:10.1001/jamainternmed.2016.5651.

⁴⁷ *E. faecalis* presents a noteworthy exception. Intrinsic resistance to clindamycin is observed in this organism, a common cause of urinary tract infections, owing to a conserved gene (*lsa*) encoding a putative ABC transporter protein. See: Kristich, C. J.; Rice, L. B.; Arias, C. A. Enterococcal Infection – Treatment and Antibiotic Resistance. In *Enterococci: From Commensals to Leading Causes of Drug-Resistant Infection*; Gilmore, M. S.; Clewell, D. B.; Ike, Y.; Shankar, N., Eds.; [Online] Massachusetts Eye and Ear Infirmary: Boston, MA, 2014 (accessed 7 March, 2018).

⁴⁸ (a) Nicholas, P.; Meyers, B. R.; Levy, R. N.; Hirschman, S. Z. *Antimicrob. Agents Chemother.* **1975**, *8*, 220–221. (b) Summersgill, J. T.; Schupp, L. G.; Raff, M. J. *Antimicrob. Agents Chemother.* **1982**, *21*, 601–603. (c) Darley, E. S. R.; MacGowan, A. P.; *J. Antimicrob. Chemother.* **2004**, *53*, 928–935. (d) Zeller, V.; Dzeing-Ella, A.; Kitzis, M.-D.; Ziza, J.-M.; Mamoudy, P.; Desplaces, N. *Antimicrob. Agents Chemother.* **2010**, *54*, 88–92.

of care in methicillin-resistant *S. aureus* (MRSA) infections. In a troubling development perhaps deriving directly from this success, however, up to 50% of MRSA isolates in some settings now display clindamycin resistance.⁴⁹ Interestingly, owing to its activity against the eukaryotic pathogen *P. falciparum*, clindamycin has also found limited use as an antimalarial agent, typically as a component of combination therapies.⁵⁰

Topical formulations of clindamycin have been developed as well, primarily for the treatment bacterial infections of the skin and mucosa. One such indication is acne vulgaris, for which more than 866,000 total prescriptions (amounting to \$442 million in sales) are filled annually.⁵¹ Formulated as the corresponding 2-phosphoester prodrug in combination with tretinoin (Ziana, Valeant) or benzoyl peroxide (Acanya and Onexton, Valeant), clindamycin nominally targets the Gram-positive bacillus *P. acnes*, though destruction of other constituents of the skin flora almost certainly occurs as well. Likewise, intravaginal delivery of clindamycin-2-phosphate (Clindesse, Perrigo) is indicated for the treatment of bacterial vaginosis.⁵²

The greatest liability associated with the use of clindamycin is its tendency to promote intestinal infections by the opportunistic pathogen *C. difficile*, leading to potentially life-threatening colitis.⁵³ This risk of *C. difficile*-associated diarrhea (CDAD) is significantly higher

⁴⁹ Liu, C.; Bayer, A.; Cosgrove, S. E.; Daum, R. S.; Fridkin, S. K.; Gorwitz, R. J.; Kaplan, S. L.; Karchmer, A. W.; Levine, D. P.; Murray, B. E.; Rybak, M. J.; Talan, D. A.; Chambers, H. F. *Clin. Infect. Dis.* **2011**, *52*, e18–55.

⁵⁰ (a) Lell, B.; Kremsner, P. G. *Antimicrob. Agents Chemother.* **2002**, *46*, 2315–2320. (b) Kremsner, P. G. *J. Antimicrob. Chemother.* **1990**, *25*, 9–14.

⁵¹ Foamix Pharmaceuticals. Changing the Face of Dermatology, January 2017. <http://phx.corporate-ir.net/External.File?t=1&item=VHlwZT0yYFBhcmVudEIEPTUyNDYwNzR8Q2hpbGRJRD02NTY1ODk=> (accessed 7 March, 2018).

⁵² Livengood, C. H., III; Thomason, J. L.; Hill, G. B. *Obstetrics and Gynecology* **1990**, *76*, 118–123.

⁵³ For early reports and etiological studies of lincomycin- and clindamycin-associated colitis see: (a) Ecker, J. A.; Williams, R. G.; McKittrick, J. E.; Failing, R. M. *Am. J. Gastroenterol.* **1970**, *54*, 214–228. (b) Anonymous. *British*

for clindamycin than for other common antibiotics,⁵⁴ and appears to arise through clindamycin's particular spectrum of action against commensal anaerobes that make up the colonic flora. Indeed, so pronounced is this hazard that clindamycin bears an FDA-mandated boxed warning for CDAD, and concerns of similar risks have hampered the discovery and development of new lincosamides to replace clindamycin.¹¹ Recent work led by Dr. Eric Pamer of Memorial Sloan Kettering Cancer Center traced the phenomenon of antibiotic-associated diarrhea down to the destruction of the obligate anaerobe *Clostridium scindens*, a metabolically active constituent of the gut microbiome and close relative of *C. difficile*, which acts to produce secondary bile acids conferring host resistance to *C. difficile* infection (CDI).⁵⁵ While compelling, these findings describe only one of what is likely to be a compendium of operative mechanisms by which antibiotic treatment leads to *C. difficile* overgrowth – other studies have noted, for example, that antibiotics with little reported effect on anaerobic flora nonetheless can promote pseudomembranous colitis;⁵⁴ and no confident consensus exists yet to map the spectrum of action of an antibiotic to its associated CDAD risk.

The continued use of clindamycin despite limitations in antibacterial spectrum of action, associated CDAD risk, and rising resistance strongly suggests that the lincosamide class represents an historically underexploited class of antibiotics. Indeed, no new members have been introduced to the clinic in nearly 50 years – a discovery void that extends for longer than that of virtually any other class. Accordingly, an unmet medical need for novel lincosamides addressing one or more

Medical Journal **1974**, *4*, 65–66. (c) Onderdonk, A. B.; Brodasky, T. F.; Bannister, B. *J. Antimicrob. Chemother.* **1981**, *8*, 383–393.

⁵⁴ Although all antibiotics carry some risk of CDAD, clindamycin, third-generation cephalosporins, penicillins, and some fluoroquinolones are traditionally considered among the most problematic. See: Owens, R. C., Jr.; Donskey, C. J.; Gaynes, R. P.; Loo, V. G.; Muto, C. A. *Clin. Infect. Dis.* **2008**, *46* (Suppl 1), S19–31.

⁵⁵ Buffie, C. G.; Bucci, V.; Stein, R. R.; McKenney, P. T.; Ling, L.; Gobourne, A.; No, D.; Liu, H.; Kinnebrew, M.; Viale, A.; Littman, E.; van den Brink, M. R. M.; Jenq, R. R.; Taur, Y.; Sander, C.; Cross, J.; Toussaint, N. C.; Xavier, J. B.; Pamer, E. G. *Nature* **2015**, *517*, 205–208.

of the current shortcomings facing the class has prompted several lincosamide discovery campaigns to take on the challenge. These efforts and their findings are discussed in the section that follows.

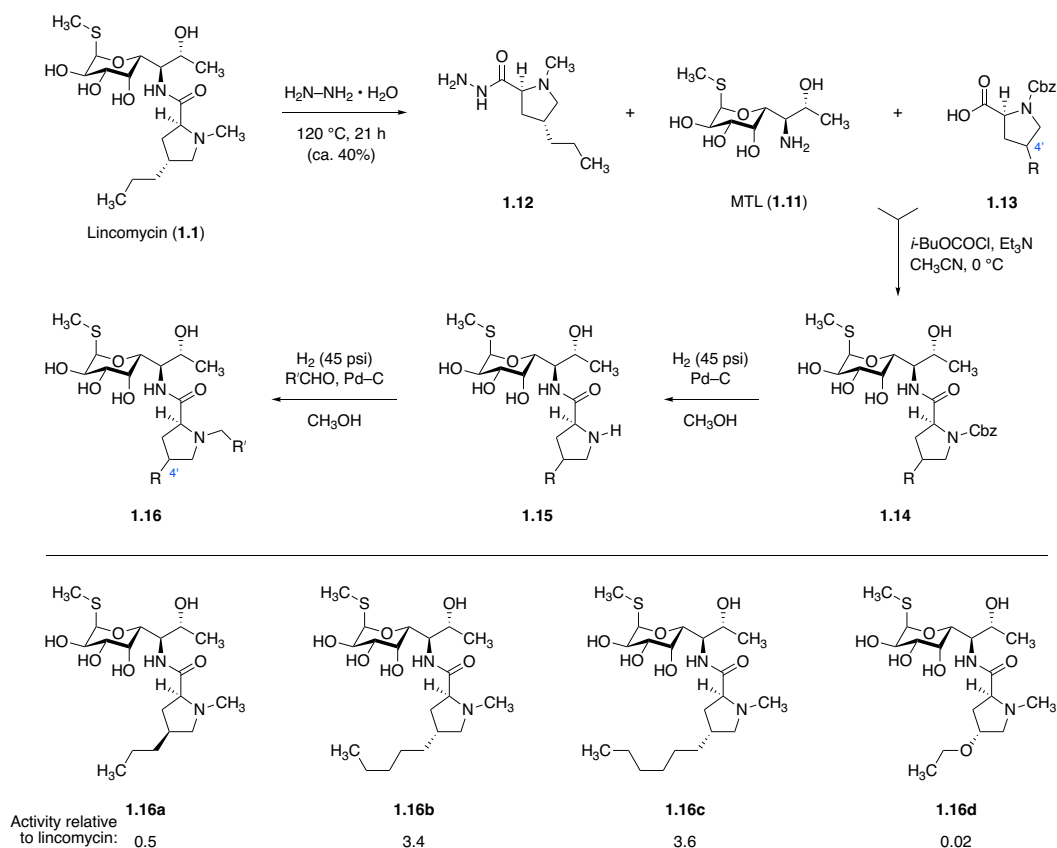
The structure–activity relationship of the lincosamides

Many of the most impactful insights into the structure–activity relationship (SAR) of the lincosamides were made in the first two decades following their discovery. Using a hydrazinolytic method to separate lincomycin into its constituent propylhygric acid and methylthiolincosamine (MTL, **1.11**) fragments – a transformation that figured prominently in the team’s earlier work to solve the structure of the natural product – scientists at Upjohn performed independent modification of both molecular hemispheres, leading to pivotal discoveries that would prove general over subsequent decades of lincosamide research (Scheme 1.3). The earliest such reports described modifications to the 4′ position of the cyclic amino acid motif, whereby the native 2′,4′-*trans* relationship native to the natural product proved favorable to the *cis* alternative (**1.16a**). More importantly, a survey of linear alkyl substituents at the 4′ position was performed, establishing that increased lipophilicity at this position is beneficial for activity. *n*-Pentyl and *n*-hexyl substitutions were shown to be ideal, conferring a 3- to 5-fold improvement in potency against the Gram-positive bacterium *S. lutea*⁵⁶ (a result that would be reproduced through mutasynthetic studies as late as 2010),⁵⁷ whereas isosteric replacement of the 6′ methylene carbon of lincomycin with an oxygen atom, affording 4′-depropyl-4′-ethoxylincomycin (**1.16d**), nearly abolished all

⁵⁶ Magerlein, B. J.; Birkenmeyer, R. D.; Kagan, F. J. *Med. Chem.* **1967**, *10*, 355–359

⁵⁷ Ulanova, D.; Novotná, J.; Smutná, Y.; Kameník, Z.; Gažák, R.; Šulc, M.; Sedmera, P.; Kadlčík, S.; Plháčková, K.; Janata, J. *Antimicrob. Agents Chemother.* **2010**, *54*, 927–930.

antimicrobial activity.⁵⁸ In light of contemporary crystallographic understanding of how lincomycin binds its target, these findings come into clearer focus: Site-specific inclusion of lipophilic functionality at the tail portion of lincosamides likely drives target engagement directly through favorable interactions with the hydrophobic cleft comprising A2451 and C2452.



Scheme 1.3. Early studies at Upjohn focused on C4' and N-alkyl derivatization of the southern half using hydrazinolysis to generate the northern-half MTL residue from lincomycin. Relative activities were measured against the test organism *S. lutea*.⁵⁶

In concert with this survey of 4'-alkyl modifications, changes to the aminosugar component were also explored. These studies would cement the role of the pyranose hydroxyls (positions 2–4) as a “conserved” motif necessary for activity and would identify the 7 position as a strategic

⁵⁸ Magerlein, B. J. *J. Med. Chem.* **1967**, *10*, 1161–1163.

site by which several properties could be favorably influenced. In a series of transactions from Brian Bannister in the 1970s, modifications to the core of MTL were detailed,⁵⁹ including the evaluation of 2-*O*-methylincomycin (**1.17**), 2-deoxyincomycin (**1.18**), 4-epilincomycin (**1.19**), and a group of 2,3-di-*epi*-3-substituted derivatives (**1.21**) arising through Fürst–Plattner attack of an intermediate 2,3-anhydrolincosamide, **1.20**. Each of these semisynthetic analogs was devoid of activity, as might be expected given the key role that the pyranose hydroxyls play in establishing a hydrogen-bond network with the ribosome. Indeed, in an early example of SAR deconvolution in the class, the enzymatic activity of isolated ribosomes was measured in the presence of 2-deoxyincomycin (**1.18**): No significant inhibition of amino acid incorporation was observed, proving that poor target engagement, rather than cell penetration, was to blame for the lack of biological activity.

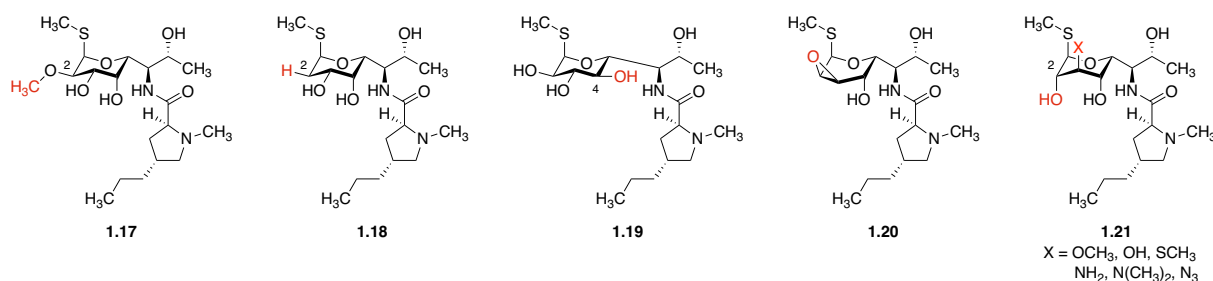


Figure 1.9. Northern-half variants bearing changes to the C1–C4 substituents (Upjohn).⁵⁹

Within their first reports of analogs bearing southern-half modifications, Barney Magerlein, Robert Birkenmeyer, and Fred Kagan of Upjohn noted that 7-deoxychlorination of lincomycin and its 4' analogs potentiated the *in vitro* activities of the resulting antibiotics.⁵⁸ What's more, it was shown that in an animal model of infection with *S. aureus*, orally dosed 7-

⁵⁹ (a) Bannister, B. *J. Chem. Soc. Perkin Trans. 1* **1972**, 3025–3030. (b) Bannister, B. *J. Chem. Soc. Perkin Trans. 1* **1972**, 3031–3036. (c) Bannister, B. *J. Chem. Soc. Perkin Trans. 1* **1973**, 1676–1682. (d) Bannister, B. *J. Chem. Soc. Perkin Trans. 1* **1974**, 360–369.

deoxychlorinated analogs were substantially more efficacious. Among these analogs was 7-deoxy-7-chloro lincomycin – clindamycin (**1.3**) – whose 7(*S*) stereochemistry would later be established by Magerlein and Kagan in 1969.⁶⁰ This single-atom substitution, achieved industrially in a single semisynthetic step through the action of a Vilsmeier reagent on lincomycin,⁶¹ had far-reaching consequences: Relative to the parent compound, clindamycin was found to have superior human oral bioavailability; improved potency *in vitro*; and, for the first time within the class, anti-malarial activity, including against strains of chloroquine- and quinine-resistant *P. berghei*. What's more, modifications to the C7 position had dramatic effects on Gram-negative activity, with 7(*S*)-halo substitution providing ≥ 4 -fold diminution in minimum inhibitory concentrations (MICs) measured against *E. coli*, *P. vulgaris*, and *S. schottmeulleri* (Figure 1.10). Together with the observation that the preferred stereochemical configuration at C7 was dependent upon its chemical substitution, these results offered compelling evidence that targeted modifications to this position could deliver lincosamides with substantially improved properties.⁶²

⁶⁰ Magerlein, B. J.; Kagan, F. *J. Med. Chem.* **1969**, *12*, 780–784.

⁶¹ (a) Livingston, D. A. Synthesis of 7-halo-7-deoxylincomycins. U.S. Patent 4,568,741, February 4, 1986. (b) Zhou, X.-D.; Guo, Q.-H.; Han, F.-Z.; Long, D.-B. Industrial production method for clindamycin or salts thereof. China Patent 101,333,234, June 13, 2012.

⁶² Birkenmeyer, R. D.; Kagan, F. *J. Med. Chem.* **1970**, *13*, 616–619.

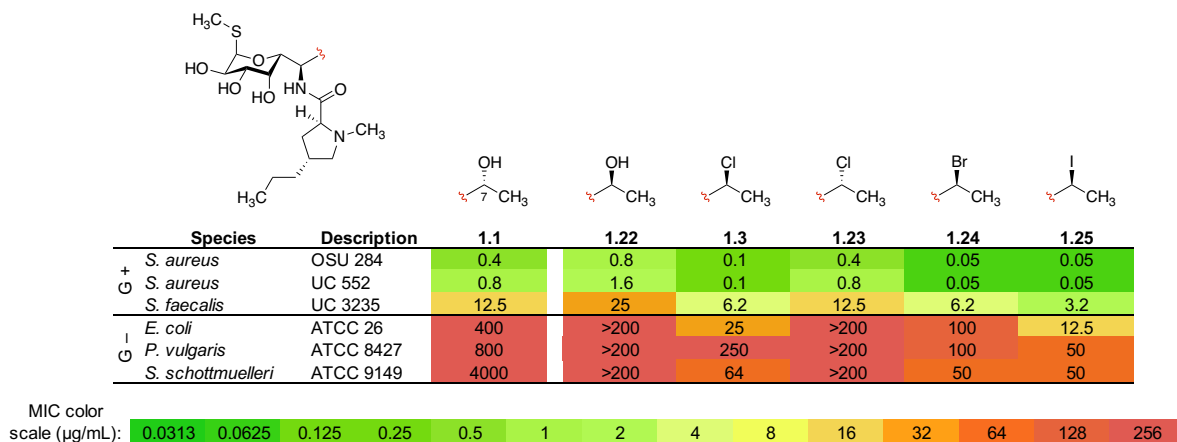


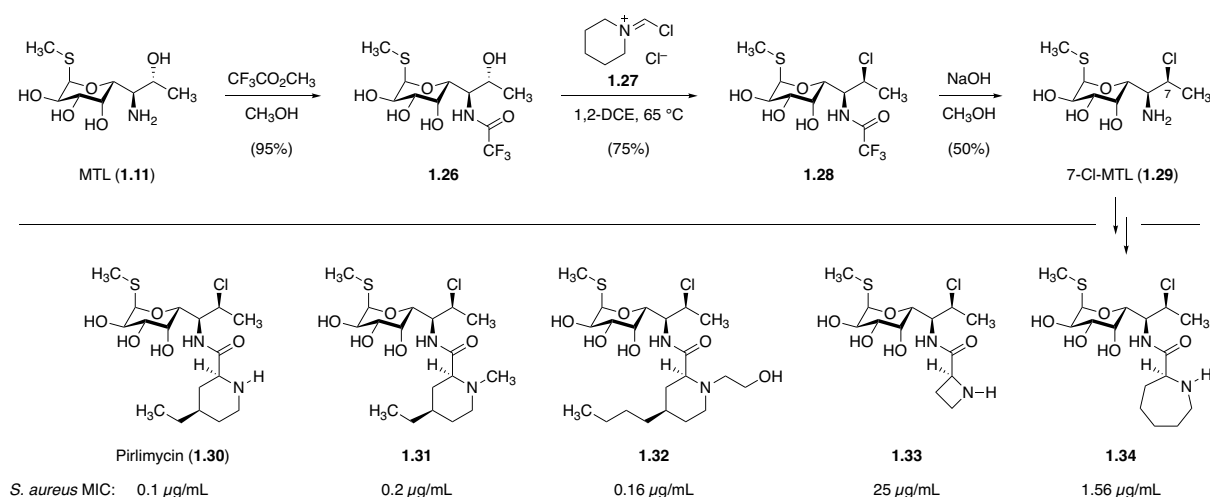
Figure 1.10. Minimum inhibitory concentrations ($\mu\text{g/mL}$) of selected C7-modified lincomycin derivatives against a panel of three Gram-positive (G+) and three Gram-negative (G-) bacterial strains. Adapted from Reference 62 (Upjohn).

Following the commercial launch of clindamycin, efforts at Upjohn focused once again on the southern half, where azetidino-, piperidino-, and azepano-based scaffolds (together with acyclic amino acids) were evaluated. From this work emerged pirlimycin (**1.30**), a second-generation lincosamide unifying the 7(*S*)-chloro methylthiolincosamine fragment of clindamycin (7-Cl-MTL, **1.29**) with *cis*-4-ethyl-L-pipecolic acid (Scheme 1.4). While roughly equipotent to clindamycin in *in vitro* susceptibility assays, pirlimycin featured reduced median protective doses (ED_{50} 's) in murine models of *S. aureus*, *S. pneumoniae*, *B. fragilis*, and *P. berghei* infection.⁶³ Low acute toxicity, high oral bioavailability, and remarkable pharmacokinetic/pharmacodynamic (PK/PD) properties conspired to distinguish pirlimycin from clindamycin, which over the course of the intervening decade had cemented the lincosamides' place in medicine. Pirlimycin displayed excellent metabolic stability⁶⁴ and increased serum drug exposure over time – particularly valuable characteristics in light of the fact that the key PK/PD driver of lincosamide efficacy is the duration

⁶³ Birkenmeyer, R. D.; Kroll, S. J.; Lewis, C.; Stern, K. F.; Zurenko, G. E. *J. Med. Chem.* **1984**, *27*, 216–223.

⁶⁴ When urine was collected from rats and fractionated based on antimicrobial activity, only unmodified drug was recovered. This stands in contrast to clindamycin, which afforded four distinct antimicrobially active fractions.

of time that serum drug concentration exceeds the MIC ($T > MIC$).⁶⁵ Despite these promising attributes, however, pirlimycin was ultimately diverted into veterinary medicine as concerns ostensibly mounted over the CDI liability that had come to be associated with the class.^{11,66} The story of pirlimycin thus serves to illustrate the central importance of PK/PD and safety considerations – independent of antimicrobial activity – for their role in the successful development of new members of the class.



Scheme 1.4. Synthesis of lincosamide analogs bearing 4-, 6-, and 7-membered southern halves proceeded through the intermediacy of the semisynthetic intermediate 7-Cl-MTL (Upjohn). Routes to 7-Cl-MTL are described in References 60 and 68.

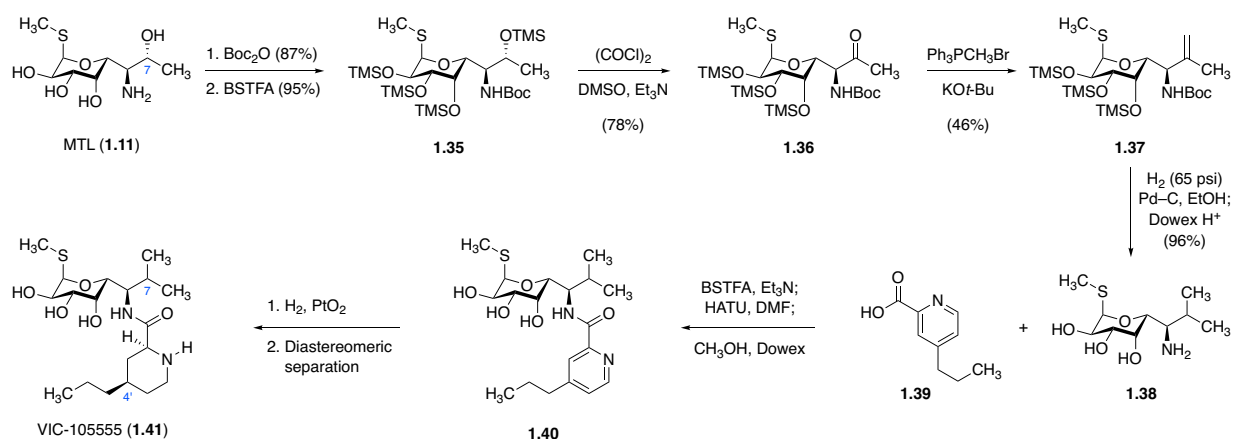
Following a merger of Upjohn and Pharmacia in 1995 and subsequent acquisition of the resulting company in 2003, Pfizer acquired the rights to market clindamycin and pirlimycin;⁶⁷

⁶⁵ The literature is not consistent on this topic, particularly pertaining to whether clindamycin's clinical efficacy is driven instead by the 24-hour AUC/MIC ratio. While clindamycin features a negligible post-antibiotic effect (favoring the $T > MIC$ model), lincosamides with prolonged persistent effects could be expected to depend less on dosing frequency, and thus transition to a regime better described by the 24-h AUC/MIC determinant. See: (a) Vogelmann, B.; Gudmundsson, S.; Leggett, J.; Turnidge, J.; Ebert, S.; Craig, W. A. *J. Infect. Dis.* **1988**, *158*, 831–847. (b) Craig, W. A. *Clin. Infect. Dis.* **2001**, *33* (Suppl 3), S233–S237. (c) Craig, W. A.; Kiem, S.; Andes, D. R. *Free drug 24-hr AUC/MIC is the PK/PD target that correlates with in vivo efficacy of macrolides, azalides, ketolides, and clindamycin*, abstr. A-1264. Abstr. Intersci. Conf. Antimicrob. Agents Chemother.: San Diego, CA, 2002.

⁶⁶ Thornsberry, C.; Marler, J. K.; Watts, J. L.; Yancey, R. J., Jr. *Antimicrob. Agents Chemother.* **1993**, *37*, 1122–1126.

⁶⁷ Whereas clindamycin (Cleocin) continues to be sold by Pfizer, pirlimycin (Pirsue) is instead marketed by Zoetis, Inc., a veterinary spin-off incorporated in 2014. See: Zoetis Inc. Pfizer Provides Update on Animal Health Strategic

meanwhile, in the early 2000s, scientists at Vicuron Pharmaceuticals began their own lincosamide discovery campaign.^{11,68} This work initially hinged on the replacement of Upjohn's invention, the 7-chloro group, with a methyl isostere – a “patent-busting” strategy that allowed Vicuron to identify an early lead, VIC-105555 (**1.41**, Scheme 1.5). This compound, which bears a striking resemblance to pirlimycin, featured a similar spectrum of activity, together with improved PK parameters that would come to typify the pipecolamides (Table 1.1). Compared to clindamycin, VIC-105555 displayed longer serum half-life in all four animals studied and was more orally bioavailable in higher-order animals (dog and monkey), with important implications toward projected clinical efficacy.



Scheme 1.5. Synthesis of VIC-105555 employing a formal C7-deoxymethylation sequence (Vicuron).¹¹

Alternatives Review Process. Press release, June 7, 2014. <https://www.zoetis.com/news-and-media/pfizer-provides-update-on-animal-health-strategic-alternatives-review-process.aspx> (accessed 10 March 2018).

⁶⁸ Lewis, J. G.; Anandan, S. K.; O'Dowd, H.; Gordeev, M. F.; Li, L. Lincomycin derivatives possessing antibacterial activity. US Patent 7,361,743 B2, April 22, 2008.

Table 1.1. Comparison of pharmacokinetic parameters measured for clindamycin and VIC-105555 in four animals. Adapted from Reference 11. IV = intravenous; PO = oral.

Species	Clindamycin (1.3)				VIC-105555 (1.41)				
	Mouse	Rat	Dog	Monkey	Mouse	Rat	Dog	Monkey	
IV	Dose (mg/kg)	2	2	2	2	2	2	2	
	C _{max} (mg/L)	0.49	0.69	2.77	1.28	0.52	0.51	1.15	1.74
	T _½ (h)	0.24	1.1	3.52	10.8	2.84	3.72	16.5	14.4
	AUC (mg h/L)	0.14	0.53	7.94	1.42	0.49	0.81	1.89	2.1
PO	Dose (mg/kg)	8	8	10	10	8	8	10	10
	C _{max} (mg/L)	0.105	0.277	5.13	0.382	0.015	0.015	1.07	1.03
	T _{max} (h)	0.25	0.33	0.37	0.75	2	0.83	0.37	1
	Bioavailability	7%	23%	43%	10%	3%	2%	76%	48%

With VIC-105555 advancing through preclinical evaluation as a benchmark compound, the Vicuron team shifted their attention to the northern half, where C1-modified variants of this lead compound were sought. Toward this end, a route to lincosamine originally reported by Dondoni and co-workers⁶⁹ was adapted to install the desired C6-isopropyl substituent. With subsequent activation of the anomeric position, a number of *O*-, *S*-, and *C*-glycosides were prepared, and the resulting aminosugars were paired with previously optimized pyrrolidine- and piperidine-based southern fragments (Figure 1.11).

⁶⁹ Dondoni, A.; Franco, S.; Merchan, F.; Merino, P.; Tejero, T. *Synlett* **1993**, 78–80.

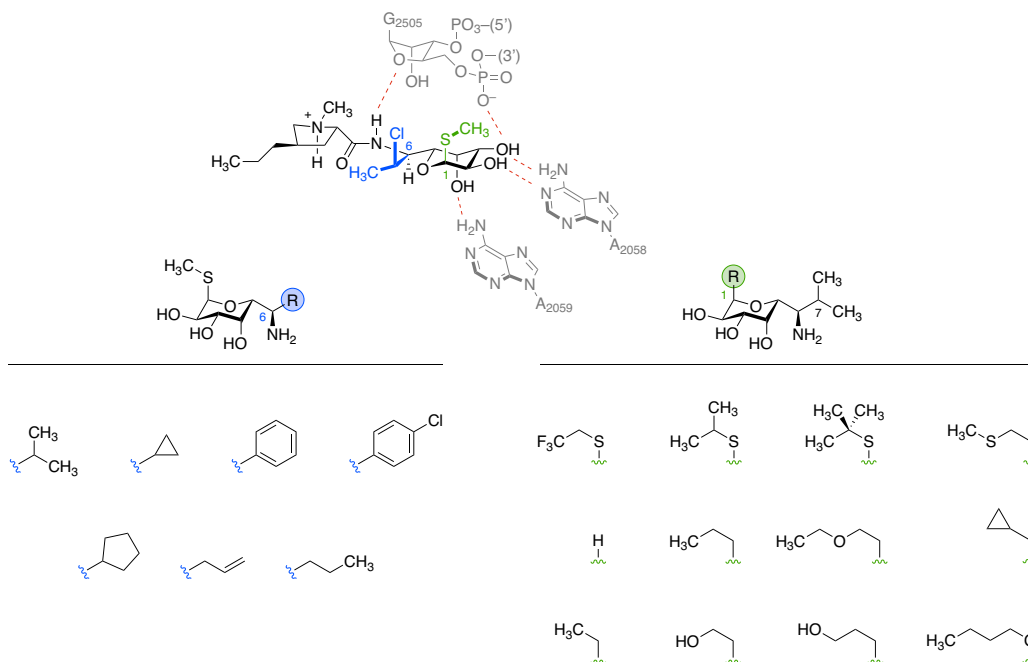
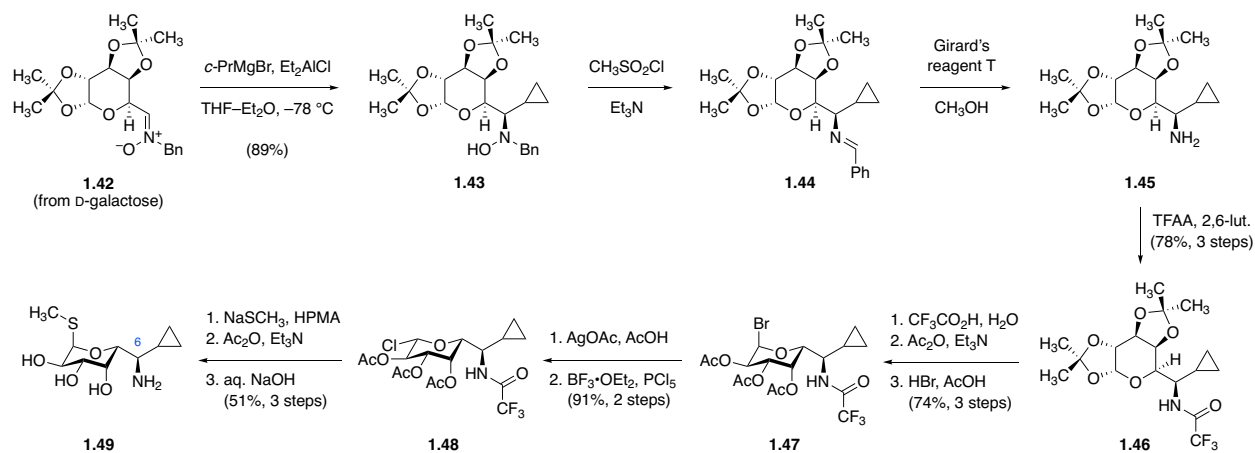


Figure 1.11. Northern-half variants pursued by Vicuron. While generally well tolerated, none of these modifications conferred substantial gains in activity.^{11,68}

This route was readily adapted to enable similar exploration of the C6 position, another site of the lincosamide scaffold that Vicuron scientists had identified as a high priority, based on analysis of available crystallographic data and prior SAR on the related C7 position. By engaging nitrene intermediate **1.42** with various Grignard reagents (in the presence of diethylaluminum chloride, in order to impart diastereoselectivity, Scheme 1.6), a small library of C6-modified lincosamides were prepared as well (Figure 1.11).⁷⁰ As was found in the case of those C1 variants the team explored, modifications to C6 were generally well tolerated, but did not provide any tractable improvements in activity or spectrum of action.

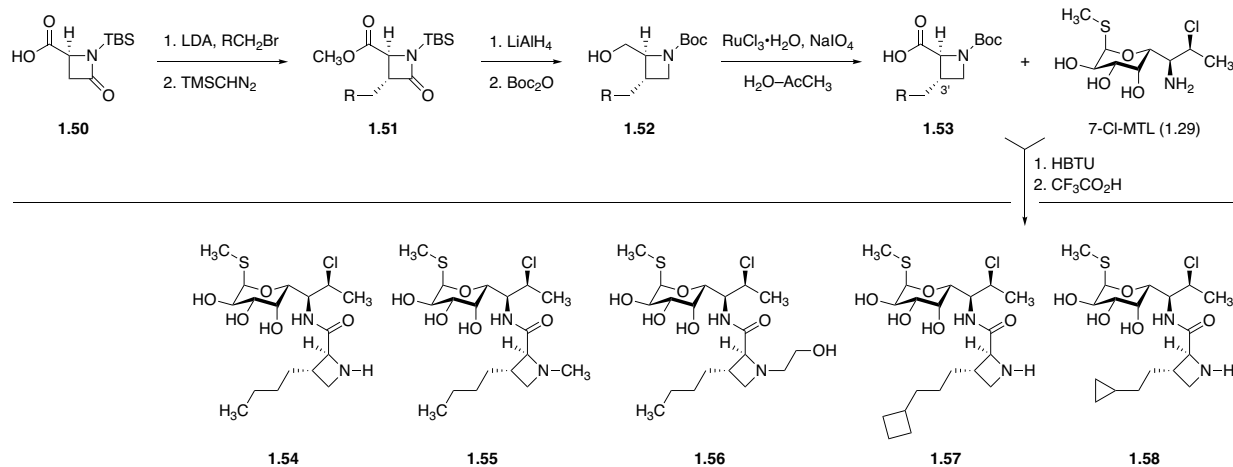
⁷⁰ O'Dowd, H.; Lewis, J. G.; Gordeev, M. F. *Tetrahedron Lett.* **2008**, *49*, 2979–2981.



Scheme 1.6. Synthesis of a C6-modified northern-half component through adaptation of a route to lincosamine (Vicuron).⁷⁰ HMPA = hexamethylphosphoramide; TFAA = trifluoroacetic anhydride; 2,6-lut. = 2,6-lutidine.

Thorough exploration of southern-half scaffolds was met with more encouraging results. While Upjohn had investigated azetidines and azepanes as early as 1982, these examples did not feature substitution of the heterocyclic ring. Identifying these scaffolds as comparatively underexplored, the Vicuron team performed a survey of 3'-alkylazetidine and 5'-alkylazepane analogs. From the azetidine series, a *trans*-3'-*n*-butyl compound (**1.54**, Figure 1.12) emerged, featuring superior inhibition of *E. coli* ribosomal activity in a cell-free transcription/translation assay ($\text{IC}_{50} = 0.36$ nm, versus 2.70 nm for clindamycin) and offering a roughly 2-fold improvement in *in vivo* efficacy in a murine septicemia model, dosed either orally (PO) or intravenously (IV).⁷¹ However, the *in vitro* potency, spectrum of action, and PK profile of **1.54** were similar to clindamycin, rendering it unlikely to outperform VIC-105555 (**1.41**) in projected clinical trials.¹¹

⁷¹ O'Dowd, H.; Lewis, J. G.; Trias, J.; Asano, R.; Blais, J.; Lopez, S. L.; Park, C. K.; Wu, C.; Wang, W.; Gordeev, M. F. *Bioorg. Med. Chem. Lett.* **2008**, *18*, 2645–2648.



	Species	Description	Clindamycin	1.54	1.55	1.56	1.57	1.58
MIC ranges (µg/mL)	<i>S. aureus</i>	n = 3	0.125–0.25	0.06	1	0.5	0.03	0.25
	<i>S. aureus</i>	MLS _B	>8	>8	>4	>8	>4	>4
	<i>S. pneumoniae</i>	n = 1	0.06	0.06	0.125	0.125	0.016	0.125
	<i>E. faecium</i>	n = 2	0.125–4	0.125–1	1–>4	0.25–4	0.06–0.25	0.125–1
	<i>E. faecalis</i>	n = 2	0.25–8	0.125–8	2–>4	0.5–>8	0.06–0.5	0.25–>4
	<i>B. fragilis</i>	n = 2	0.06–1	0.125–2	0.125–2	0.5–>8	0.25	0.25
Ribosome inhibition	<i>E. coli</i> TT IC ₅₀ (µM)		2.70	0.36	-	-	2.44	7.80
	<i>In vivo</i> efficacy							
		IV ED ₅₀ (mg/kg)	2.8	1.1	-	-	3.0	3.0
		PO ED ₅₀ (mg/kg)	19.9	10.8	-	-	-	-

Figure 1.12. Synthesis of 3'-alkyl azetidine analogs and their corresponding *in vitro* and *in vivo* data (Vicuron).⁷¹ HBTU = (2-(1H-benzotriazol-1-yl)-1,1,3,3-tetramethyluronium hexafluorophosphate; TT = transcription/translation.

The real breakthrough for Vicuron came upon the discovery of *cis*-5'-substituted azepane analogs, which demonstrated an unexpectedly broadened spectrum of action against both enterococci and Gram-negative pathogens like *H. influenzae* and *E. coli*. These analogs were prepared by a flexible sequence employing ring-closing metathesis to forge the 7-membered ring, which enabled preliminary exploration of the 5' substituent (Figure 1.13), and ultimately prompted the development of a second-generation route employing a ring-expanding Beckmann rearrangement to provide the desired 2',5'-*cis* stereochemistry.⁷² These chemical innovations led to the discovery that subtle perturbations to the azepane 5' substituent altered the spectrum of

⁷² Wishka, D. G.; Bédard, M.; Brighty, K. E.; Buzon, R. A.; Farley, K. A.; Fichtner, M. W.; Kauffman, G. S.; Kooistra, J.; Lewis, J. G.; O'Dowd, H.; Samardjiev, I. J.; Samas, B.; Yalamanchi, G.; Noe, M. C. *J. Org. Chem.* **2011**, *76*, 1937–1940.

action of the resulting lincosamides, particularly against the normally commensal gut anaerobe *B. fragilis*. This led researchers to believe that precise installation of polar functionality at this position could be used to influence the anaerobic spectrum of activity, offering a possible handle by which to control the CDAD liability of resulting antibiotics. Despite these promising advances, parallel programs in Vicuron's pipeline – most notably, the clinical evaluation of dalbavancin, a lipoglycopeptide antibiotic, for the treatment of bloodstream and skin and soft tissue infections caused by Gram-positive bacteria – prompted Pfizer to acquire the company in 2005; the lincosamide program was terminated shortly thereafter.

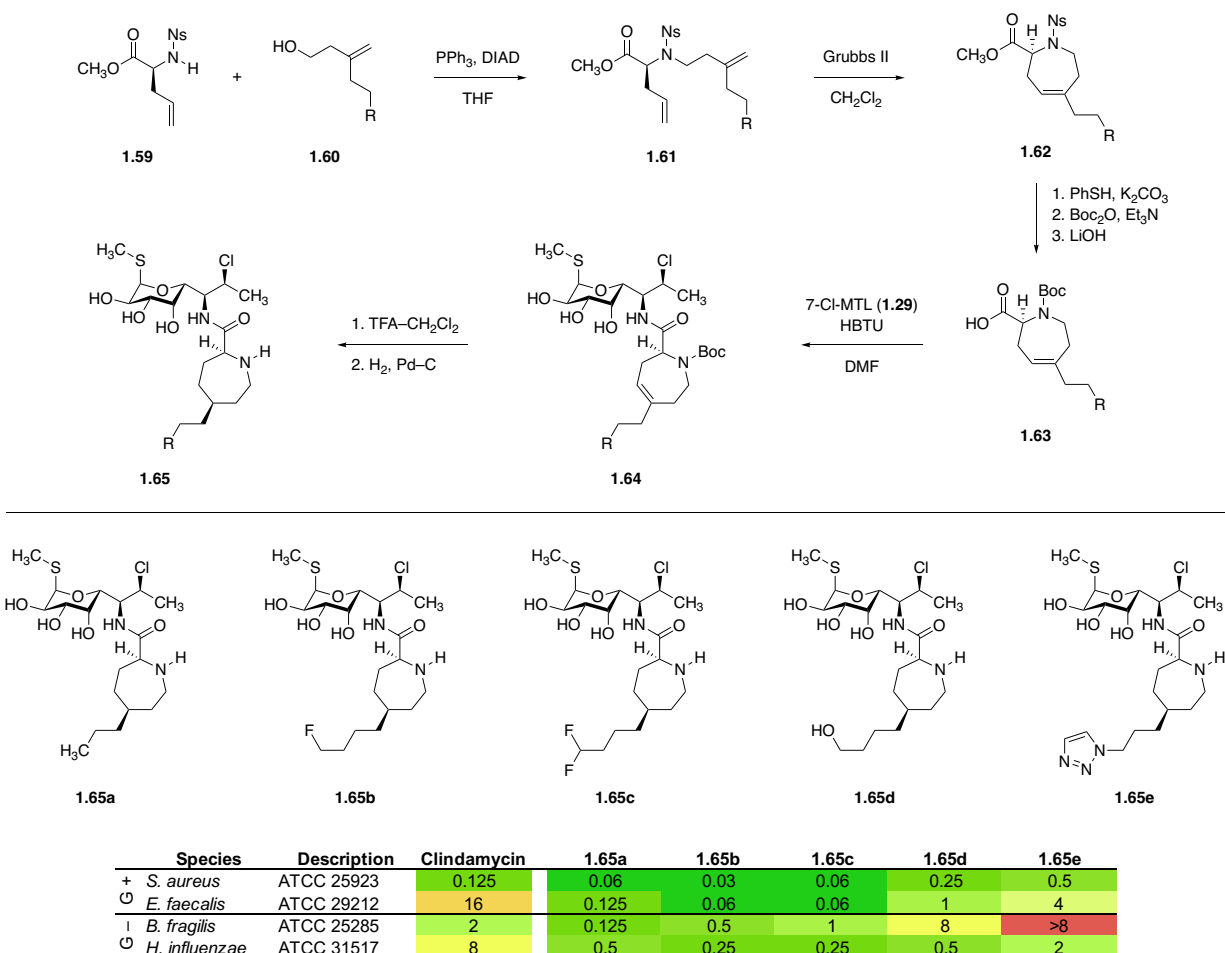
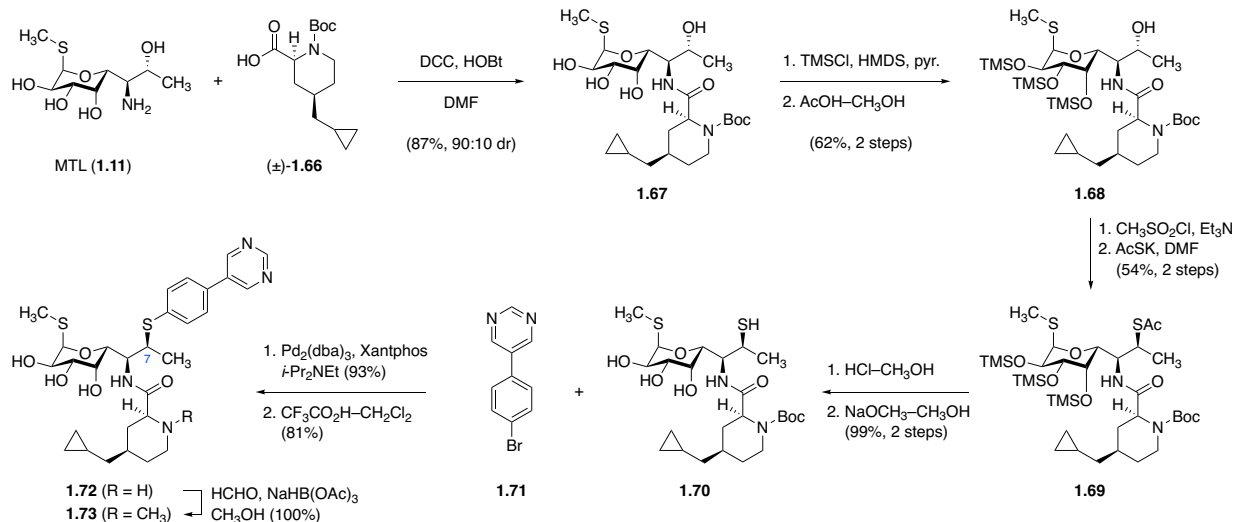


Figure 1.13. 5'-Substituted azepanes discovered by Vicuron demonstrate an expanded spectrum of activity and feature tunable potency against anaerobic species such as *B. fragilis*.¹¹ DIAD = diisopropyl azodicarboxylate; Ns = 2-nitrobenzenesulfonyl.

Most recently, researchers under the leadership of Dr. Keiichi Ajito of Japan's Meiji Seika Pharma Co. have revisited the C7 position, achieving dramatic gains in activity against multidrug-resistant Gram-positive streptococci through semisynthetic modification.⁷³ The team's focus on streptococci is unusual from a Western perspective, where recent antibiotics discovery efforts have centered around Gram-negative species and ESKAPE pathogens (*E. faecium*, *K. pneumoniae*, *A. baumannii*, *P. aeruginosa*, and *Enterobacter spp.*); however the staggeringly high incidence of drug-resistant pneumococcal disease in East Asia, where the MLS_B phenotype is found in up to 96% of clinical isolates, undoubtedly influenced the team's objectives with the project.⁷⁴

⁷³ (a) Umemura, E.; Wakiyama, Y.; Kumura, K.; Ueda, K.; Masaki, S.; Watanabe, T.; Yamamoto, M.; Hirai, Y.; Fushimi, H.; Yoshida, T.; Ajito, K. *J. Antibiot.* **2013**, *66*, 195–198. (b) Wakiyama, Y.; Kumura, K.; Umemura, E.; Ueda, K.; Masaki, S.; Kumura, M.; Fushimi, H.; Ajito, K. *J. Antibiot.* **2016**, *69*, 368–380. (c) Kumura, K.; Wakiyama, Y.; Ueda, K.; Umemura, E.; Watanabe, T.; Shitara, E.; Fushimi, H.; Yoshida, T.; Ajito, K. *J. Antibiot.* **2016**, *69*, 440–445. (d) Wakiyama, Y.; Kumura, K.; Umemura, E.; Masaki, S.; Ueda, K.; Watanabe, T.; Yamamoto, M.; Hirai, Y.; Ajito, K. *J. Antibiot.* **2016**, *69*, 428–439. (e) Wakiyama, Y.; Kumura, K.; Umemura, E.; Masaki, S.; Ueda, K.; Sato, Y.; Watanabe, T.; Hirai, Y.; Ajito, K. *J. Antibiot.* **2017**, *70*, 52–64. (f) Kumura, K.; Wakiyama, Y.; Ueda, K.; Umemura, E.; Watanabe, T.; Kumura, M.; Yoshida, T.; Ajito, K. *J. Antibiot.* **2017**, *70*, 655–663. (g) Wakiyama, Y.; Kumura, K.; Umemura, E.; Ueda, K.; Watanabe, T.; Yamada, K.; Okutomi, T.; Ajito, K. *J. Antibiot.* **2017**, *70*, 888–906. (h) Kumura, K.; Wakiyama, Y.; Ueda, K.; Umemura, E.; Hirai, Y.; Yamada, K.; Ajito, K. *J. Antibiot.* **2017**, *70*, 1112–1121. (i) Kumura, K.; Wakiyama, Y.; Ueda, K.; Umemura, E.; Watanabe, T.; Yamamoto, M.; Yoshida, T.; Ajito, K. *J. Antibiot.* **2018**, *71*, 104–112. (j) Wakiyama, Y.; Kumura, K.; Umemura, E.; Masaki, S.; Ueda, K.; Sato, Y.; Hirai, Y.; Hayashi, Y.; Ajito, K. *J. Antibiot.* **2018**, *71*, 298–317. (k) Umemura, E.; Kumura, K.; Masaki, S.; Ueda, K.; Wakiyama, Y.; Sato, Y.; Yamamoto, M.; Ajito, K.; Watanabe, T.; Kaji, C. Lincosamide Derivatives and Antimicrobial Agents Comprising the Same as Active Ingredient. U. S. Patent 7,867,980 B2, January 11, 2011.

⁷⁴ (a) Cheng, A. C.; Jenney, A. W. *Pneumonia* **2016**, *8*, doi:10.1186/s41479-016-0010-1. (b) Song, J. H.; Jung, S. I.; Ko, K. S.; Kim, N. Y.; Son, J. S.; Chang, H. H.; Ki, H. K.; Oh, W. S.; Suh, J. Y.; Peck, K. R.; Lee, N. Y.; Yang, Y.; Lu, Q.; Chongthaleong, A.; Chiu, C.-H.; Lalitha, M. K.; Perera, J.; Yee, T. T.; Kumarasinghe, G.; Jamal, F.; Kamarulzaman, A.; Parasakthi, N.; Van, P. H.; Carlos, C.; So, T.; Ng, T. K.; Shibl, A. *Antimicrob. Agents. Chemother.* **2004**, *48*, 2101–2107. (c) Zhang, B.; Gertz, R. E., Jr.; Liu, Z.; Li, Z.; Fu, W.; Beall, B. *J. Med. Microbiol.* **2012**, *61*, 42–48.



Scheme 1.7. Synthesis of a C7-arenesulfide derivative effective against MLS_B-resistant Gram-positive organisms (Meiji Seika).^{73j} DCC = *N,N*-dicyclohexylcarbodiimide; HOBT = *N*-hydroxybenzotriazole; dba = dibenzylideneacetone.

Relying on S_N2 displacement chemistry to install 7(*S*)-arenyl (or azetidyl) sulfide appendages in combination with previously reported southern halves, the team identified two lead compounds (**1.72** and **1.73**, Scheme 1.7), selected for their excellent *in vitro* activities against *S. pneumoniae* (MIC₉₀'s ≤ 0.25 μg/mL, n = 60), *S. pyogenes*, *H. influenzae*, and *Mycoplasma pneumoniae*. These leads both bear a 4-(5-pyrimidinyl)phenyl side chain identified through extensive optimization of this residue and differ only in the *N*-methylation pattern of the pipercolamide southern half. In a mouse model of pneumonia using *S. pneumoniae* harboring both macrolide efflux pump (*mef*) and *erm* genes, a 3-log reduction in colony forming units (CFUs) recovered from lung tissue was observed upon subcutaneous dosing with **1.72** (a ca. 2-log reduction was seen in the case of the *N*-methylated congener, **1.73**). In the course of their work, Meiji Seika scientists identified a number of other potent antibiotics bearing 7-thio substitution, including propylhygramides **1.75** and **1.76**, and morpholino derivatives **1.77** and **1.78** (Figure 1.14), further reinforcing the strategic value of C7 modification. These breakthroughs come with

an important caveat, however, as questions of oral bioavailability and first-pass metabolism of the sulfur-rich analogs generated through this semisynthetic approach presently remain unaddressed.

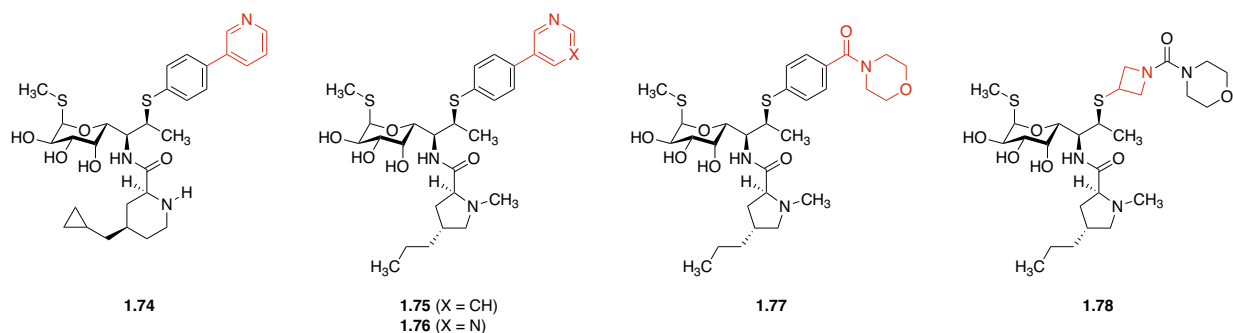


Figure 1.14. Structures of 7-thio-modified lincosamides discovered by Meiji Seika Pharma Co, displaying improved activity against Gram-positive MLS_B -resistant organisms.

In addition to these industrial programs, academic research groups have probed selected aspects of lincosamide SAR as well. In one particularly impressive example of early structure-based drug design, a team led by Stephen Hanessian of the University of Montreal (in collaboration with Upjohn) designed and synthesized “quantamycin” (**1.79**), a hybrid nucleoside–lincosamide compound based on an early working hypothesis of lincomycin’s binding mode with the ribosome (Figure 1.15).⁷⁵ This amounted to the replacement of the α -methylthio substituent of the northern fragment with a β -C-glycosidic linkage in order to fuse a pseudo-adenosyl motif to the pyranose ring of lincomycin – a structural change that required a sequence of >18 semisynthetic steps to realize (Scheme 1.8). Intriguingly, while quantamycin displayed no antibacterial activity, it did demonstrate moderate ribosomal binding ability in competition experiments with ^{14}C -labeled lincomycin – a puzzling result given contemporary understanding of lincomycin’s binding orientation (cf. Figure 1.3A), which is the reverse of that which formed the basis of quantamycin’s design.

⁷⁵ Hanessian, S.; Sato, K.; Liak, T. J.; Danh, N.; Dixit, D. *J. Am. Chem. Soc.* **1984**, *106*, 6114–6115.

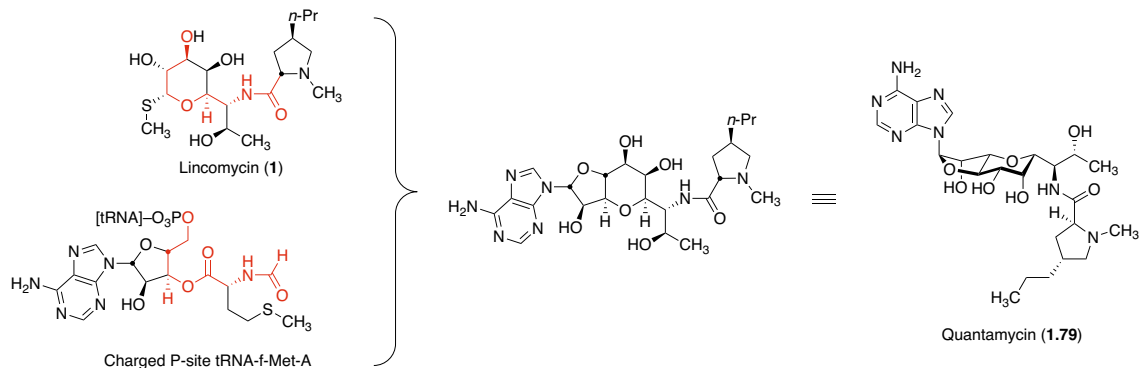
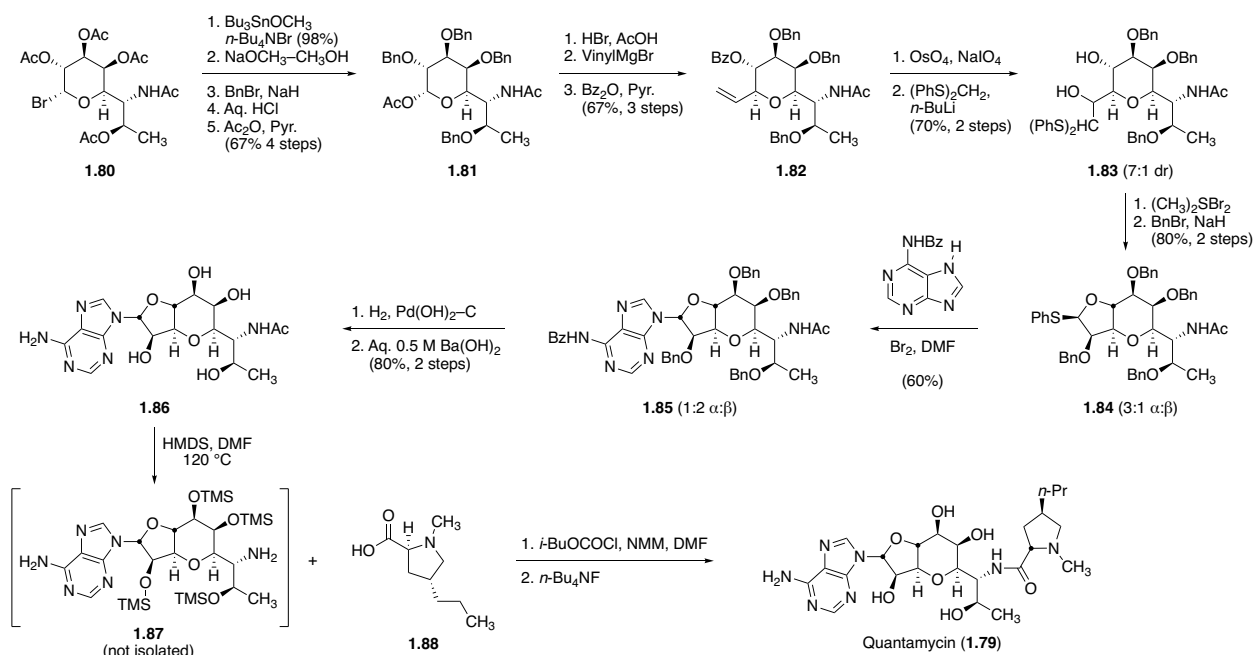


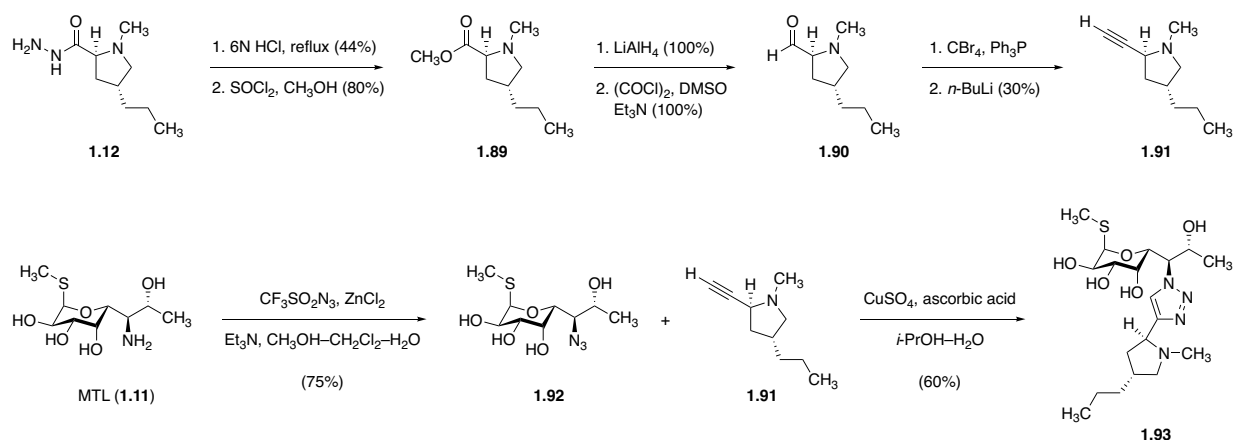
Figure 1.15. Structural analogy between the charged P-site amino acyl-tRNA residue (tRNA-f-Met-A) and lincomycin led to the design of quantamycin by Hanessian and co-workers.⁷⁵



Scheme 1.8. Synthesis of quantamycin via sequential C- and N-glycosylation. NMM = N-methylmorpholine.⁷⁵

Two studies published by Andrea Vasella and his co-workers at ETH Zurich serve to reinforce the model of lincosamide target engagement that emerged in the post-crystallographic period. In the first, replacement of the central amide linkage of lincomycin with a bioisosteric

1,2,3-triazolyl motif was explored (Scheme 1.9).^{76,77} Hydrazinolysis of lincomycin, followed by transformation of the two subunits to a corresponding azide–alkyne pair allowed the preparation of **1.93** by copper-catalyzed cycloaddition. This analog possessed no detectible antimicrobial activity, as might be expected in light of the hydrogen bond–donor role that the native amide group plays in its interaction with the 4' oxygen atom of G2505 (Figure 1.5). The second study, by contrast, targeted the C1 position, which does not directly interface with the PEC in X-ray co-crystal structures. Vasella and co-workers' semisynthetic preparation of C1-arylthio, alkylthio, and C1-disubstituted thioglycoside analogs (e.g., **1.94a–e**, **1.95a–e**) served to reinforce Vicuron's findings that that modifications to this site are often well tolerated; however, just as before, no substantial improvements in antibiotic activity were realized (Figure 1.16).⁷⁸



Scheme 1.9. Vasella and co-workers' synthesis of a lincomycin derivative possessing a bioisosteric 1,2,3-triazole in place of the native amide.⁷⁶

⁷⁶ Collin, M.-P.; Hobbie, S. N.; Böttger, E. C.; Vasella, A. *Helv. Chim. Acta* **2008**, *91*, 1838–1848.

⁷⁷ For a discussion of the 1,2,3-triazole group as an amide bioisostere, see: Kolb, H. C.; Sharpless, K. B. *Drug Discov. Today* **2003**, *8*, 1128–1137.

⁷⁸ Collin, M.-P.; Hobbie, S. N.; Böttger, E. C.; Vasella, A. *Helv. Chim. Acta* **2009**, *92*, 230–266.

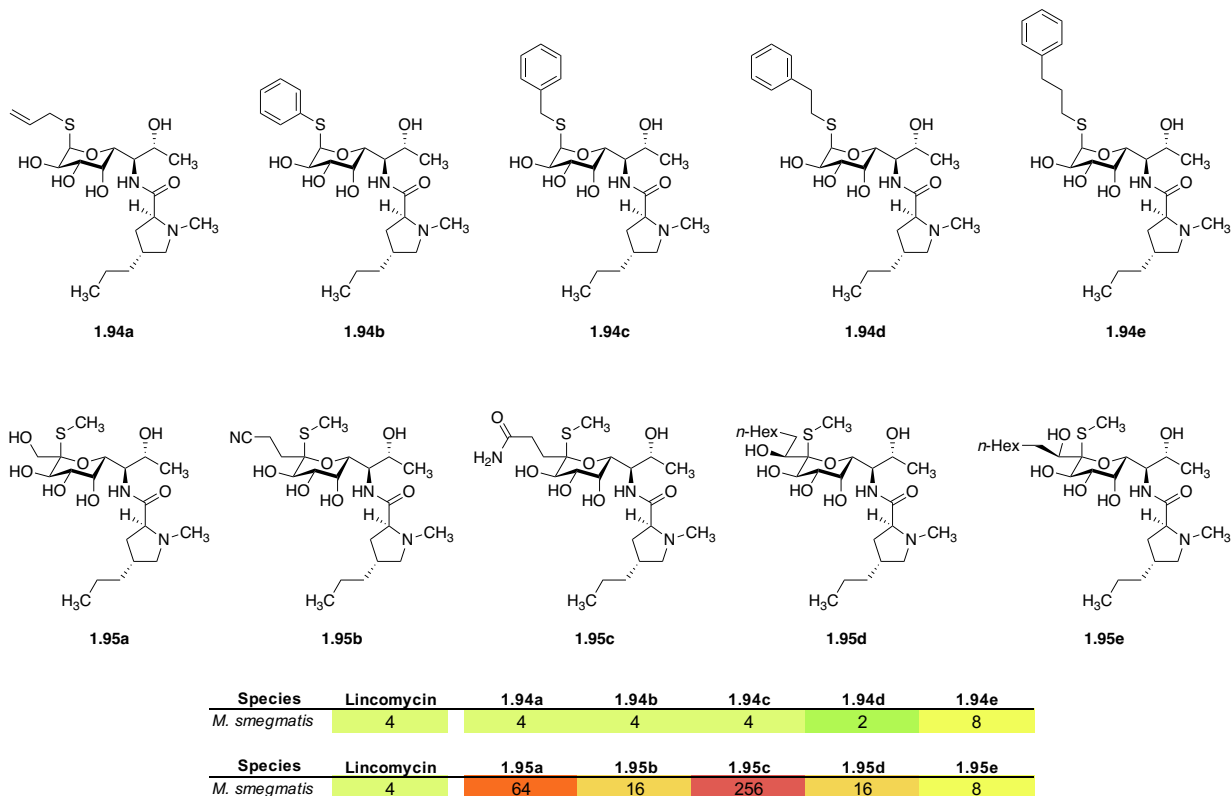


Figure 1.16. Minimum inhibitory concentrations ($\mu\text{g/mL}$) of selected analogs bearing C1 modifications, introduced semisynthetically by Andrea Vasella and co-workers.⁷⁸

The recent discovery of “odcelin” (**1.96**, Figure 1.17), a hybrid antibiotic uniting the C1 substituent of celesticetin with the C6 (propylhygramide) and C7 (hydroxyl) substituents of lincomycin, represents an exception, albeit minor, to this rule. This non-natural lincosamide was prepared alongside a small library of other lincomycin–celesticetin chimeras through *in vitro* processing of cysteinyl *S*-glycoside **1.6b** by appropriate recombinant enzymes obtained from the celesticetin biosynthetic pathway. Compared to lincomycin, odcelin proved moderately more active in a disk-diffusion assay against the Gram-positive organism *Kocuria rhizophila*,⁷⁹ signaling that modification of the C1 substituent in concert with certain C6 and C7 appendages can indeed afford antibiotics with superior activity compared to their 1- α -methylthio congeners.

⁷⁹ Kadlcik, S.; Kamenik, Z.; Vasek, D.; Nedved, M.; Janata, J. *Chem. Sci.* **2017**, *8*, 3349–3355.

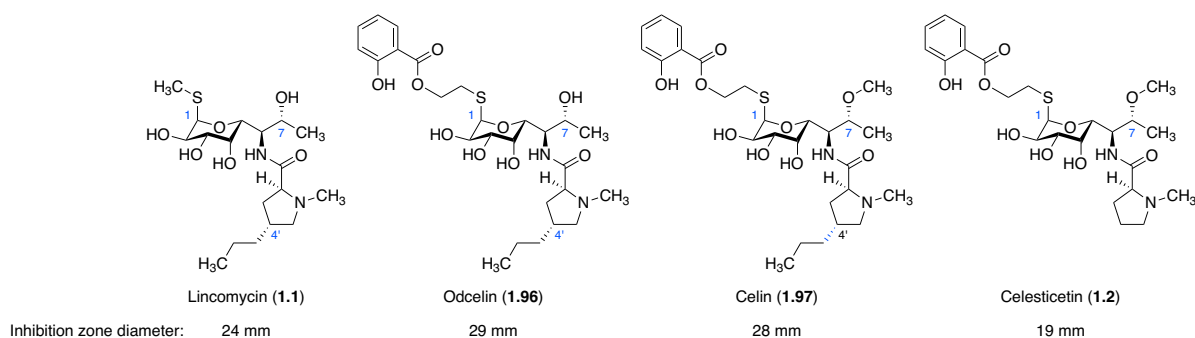


Figure 1.17. Structural characteristics and antimicrobial activities (disk diffusion assay against *K. rhizophila*) of natural and bio-engineered lincosamides, demonstrating additive effects of selected C1, C7, and C4' modifications.⁷⁹

Taken together, the body of research surrounding the lincosamide class suggests strongly that through continued chemical innovation, the discovery of improved alternatives to clindamycin is possible, particularly if considerations of PK/PD and CDAD-related safety are taken into account. These prior efforts have identified powerful new southern-half scaffolds that provide gains in PK/PD performance, potency, and spectrum of activity; and likewise have demonstrated that modifications to key positions in the northern hemisphere can favorably impact these same parameters. Nonetheless, the lincosamides remain underexplored relative to other families of similar clinical utility, owing in part to a lack of practical and flexible synthetic routes for the discovery of new members of the class.

A fully synthetic approach to the lincosamide antibiotics

In 2013, upon joining the Myers laboratory, I began work on a program for the discovery of new lincosamides as part of the research group's ongoing efforts to develop fully synthetic platforms toward clinically validated antibiotic classes. I was later joined on this project by two graduate researchers, Katherine Silvestre and Ioana Moga; Jack Stevenson, an undergraduate student; and Dr. Amarnath Pisipati, a post-doctoral microbiologist. Together, our cross-disciplinary team was tasked with establishing and implementing new chemical routes to the

lincosamides' key pharmacophores with the ultimate goal of identifying candidates with potential for clinical development.

My work, which forms the subject of this dissertation, sought to identify practical chemical routes to both hemispheres of the lincosamide antibiotics, enabling specifically the exploration of novel β -oxygenated proline scaffolds in the south, as well as northern-half variants bearing modification to C1 and C6. Such modifications were targeted based on careful analysis of prior SAR, as well as X-ray crystallographic analysis; and in some cases required the development of new chemistry. The chemical enablements and synthetic strategies that emerged from this work in turn led to the discovery of unprecedented scaffolds, including an oxepinoproline construct demonstrating particular promise in *in vitro* microbiological susceptibility experiments, and provided valuable insight into those structural elements within the northern half that contribute favorably to the activity of the antibiotic class. Each of the routes described here was devised so as to facilitate modifications brought about through building-block exchange and the incorporation of diversifiable elements – a tactic whose utility had been demonstrated before by our group in the synthesis of other ribosome-targeting antibiotics by fully synthetic means.

The second chapter of this dissertation describes my development of an aldol-based annulation reaction of pseudoephedrine glycinamide to provide β -hydroxyproline derivatives, their incorporation into synthetic lincosamide candidates, and subsequent studies leading to the discovery of the aforementioned oxepinoprolinamide series. The third and fourth chapters present the analogous development of routes to the aminosugar component – the former illustrating the suitability of nitroaldol logic to assemble the heteroatom-rich stereochemical array present within this glycoside in a *de novo* sense, while the latter provides a concise, component-based synthesis of northern-half variants bearing modifications to the acyclic portions of this moiety.

The aim of this work was to enable chemical modifications to the lincosamides whose consequences directly address those aspects of the class that have hampered their more widespread development and clinical implementation. Namely, we sought to identify antibiotics with (1) increased activity against MLS_B-resistant pathogens, (2) a diminished projected CDAD liability, and (3) an expanded spectrum of action against Gram-negative organisms. Through the combined efforts of the lincosamide team, >330 novel candidates have been prepared and subjected to antimicrobial evaluation, leading to the identification of several series of particular promise, and enabling the coalescence of a more complete picture of lincosamide SAR. Importantly, many of these analogs would be difficult or impossible to produce by traditional semisynthesis, engineered biosynthesis, or previously reported fully synthetic routes; and as such we hope this work may form the basis for the discovery of new antibiotic candidates with potential to meet those challenges facing the clinic today.

Page intentionally left blank

Chapter 2. Southern-half variants bearing 3' oxygenation

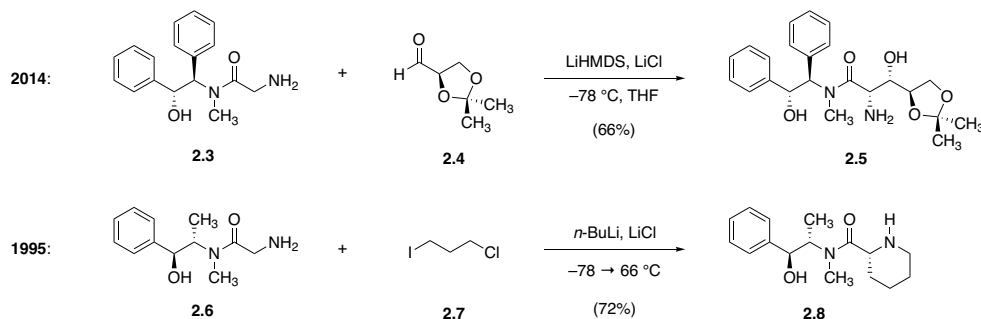
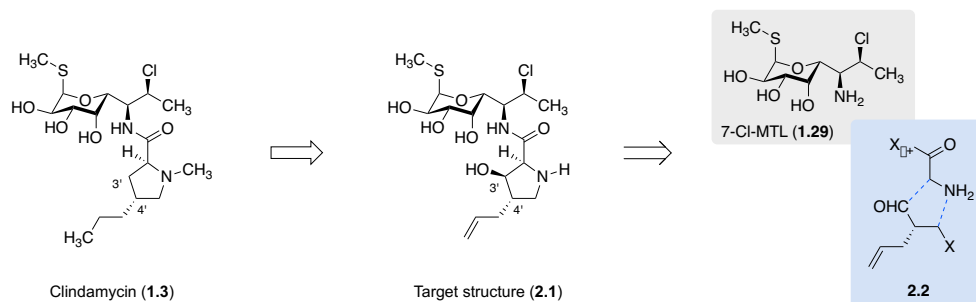
Introduction

My earliest goal in the lincosamide project involved incorporation of a hydroxyl group at the 3' position of clindamycin's proline motif, stereochemically disposed *cis* to the adjacent 2'-carboxamide group (Scheme 2.1). This particular modification was targeted for a number of reasons, not least of which was that our laboratory had recently reported a practical method for direct *syn* addition of pseudoephedrine glycinamide (**2.3**),⁸⁰ a chiral glycine equivalent, to aldehyde and ketone substrates, affording β -hydroxy- α -amino acid motifs in high yield and diastereomeric purity.⁸¹ This transformation, discovered by Dr. Ian Seiple and improved substantially with respect to scope and practicality by Jaron Mercer, Dr. Robin Sussman, and Dr. Ziyang Zhang, had proven indispensable in its application toward the synthesis of new macrolide antibiotics, and – it was hoped – could be of similar utility in the context of other antibiotic classes. Paired with an earlier discovery from the Myers laboratory demonstrating that sequential *C*- and *N*-alkylation of the closely related pseudoephedrine glycinamide (**2.6**) could forge cyclic amino acid motifs such as pipercolamide **2.8**,⁸² we expected that the desired β -hydroxy proline could be prepared from a suitable coupling partner (**2.2**) containing an aldehyde as one of its two electrophilic foci. Anticipating that modification of the 4' appendage might be sought, we targeted a more readily diversifiable allyl group at this position (rather than the native *n*-propyl chain).

⁸⁰ Morales, M. R.; Mellem, K. T.; Myers, A. G. *Angew. Chem. Int. Ed.* **2012**, *51*, 4568–4571.

⁸¹ Seiple, I. B.; Mercer, J. A. M.; Sussman, R. J.; Zhang, Z.; Myers, A. G. *Angew. Chem. Int. Ed.* **2014**, *53*, 4642–4647.

⁸² (a) Myers, A. G.; Gleason, J. L.; Yoon, T. *J. Am. Chem. Soc.* **1995**, *117*, 8488–8489. (b) Myers, A. G.; Gleason, J. L.; Yoon, T.; Kung, D. W. *J. Am. Chem. Soc.* **1997**, *119*, 656–673.



Scheme 2.1. Target structure and retrosynthesis, drawing on earlier results from the Myers laboratory demonstrating amino acid synthesis by bis-alkylation and aldolization of chiral glycine equivalents.

Analysis of clindamycin–ribosome X-ray co-crystal structures encouragingly indicated that the 3'*R* configuration in target structure **2.1** was likely preferable to the epimeric alternative. The *pro-R* hydrogen atom of clindamycin's 3' position, unlike its geminal counterpart, does not directly engage the surface of the binding pocket, and extends along a vector that transverses the neck of the PET. Further, early docking studies indicated that 3'*R* hydroxylation might increase ribosome affinity through hydrogen bonding with the adjacent 2'-hydroxyl group of G2505 (Figure 2.1). Our motivation to hydroxylate this position of clindamycin additionally arose from the observation that, particularly within a given class, polarity often correlates positively with Gram-

negative activity,⁸³ and, as such modifications had not been pursued before, 3'-hydroxylated lincosamides would represent novel composition of matter.

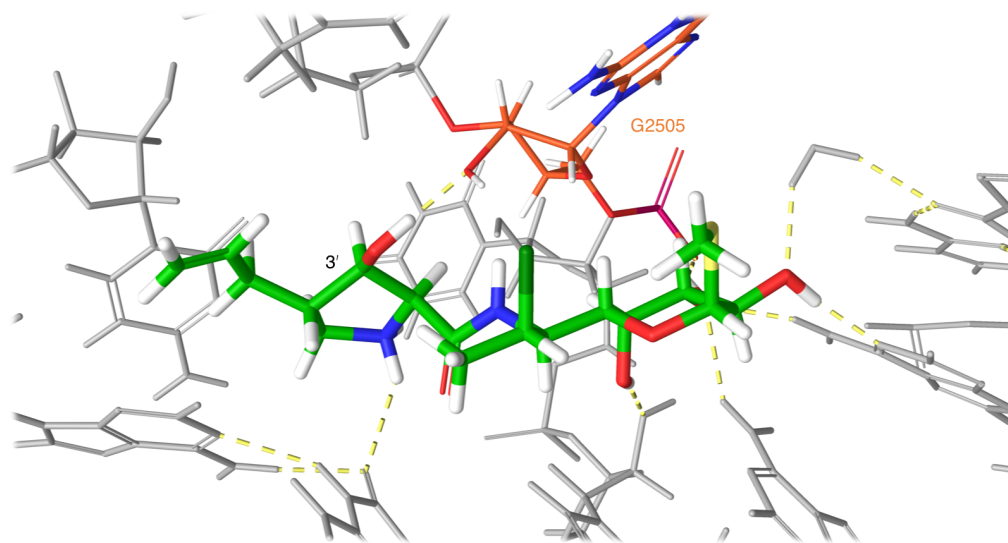


Figure 2.1. Computed structure 3'-hydroxylated lincosamide **2.1** (green) docked to the bacterial ribosome, illustrating the potential for hydrogen bonding to the 2'-hydroxyl group of G2505 (orange). Docking and visualization performed using Schrödinger Suite 2017, using a grid generated from PDB entry 1YJN.

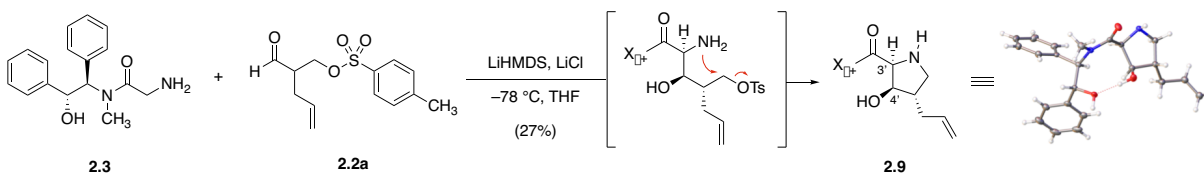
Annulation of pseudoephedrine glycinamide by aldol-cyclization

In order to test the hypothesis that sequential aldolization and cyclization of a bis-electrophilic building block could indeed form the desired β -hydroxyproline nucleus, I first prepared aldehyde **2.2a** in racemic form.⁸⁴ When introduced to a slight molar excess of the lithium enolate generated upon exposure of glycinamide **2.3** to lithium hexamethyldisilazide (in the presence of excess lithium chloride), complete consumption of electrophile was observed within 5 minutes at -78 °C. After aqueous workup, a complex mixture of products was separated by flash-

⁸³ For a widely circulated review on the unique physicochemical space occupied by antibacterial drugs, see: O'Shea, R.; Moser, H. E. *J. Med. Chem.* **2008**, *51*, 2871–2878.

⁸⁴ Prepared by monotosylation of 2-allyl-1,3-propanediol, followed by oxidation with Dess–Martin periodinane; data not shown.

column chromatography. Among them, the desired 3'*R*,4'*S* annulation product **2.9** (lincomycin numbering) was obtained, and was successfully crystallized, thus permitting unambiguous structural assignment (Scheme 2.2). It is notable that while the yield of this product was low, its successful preparation, purification, and crystallographic characterization were established in a single experiment, highlighting the practicality and robustness of the pseudoephedrine chiral-auxiliary platform.⁸⁰

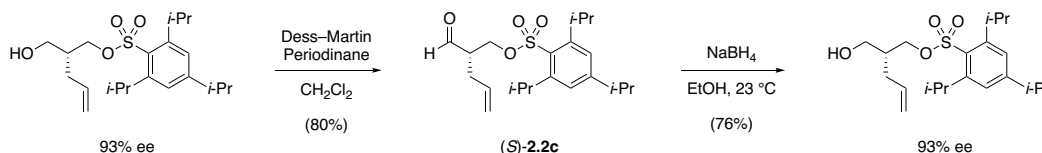


Scheme 2.2. Synthesis of the desired β -hydroxyproline nucleus via a novel aldol–cyclization reaction.

With this proof of principle in hand, I then sought to increase the yield of prolinamide **2.9** empirically, through modulation of key reaction parameters (Table 2.1). The most obvious of these was the optical purity of the bis-electrophilic substrate – unexpectedly, preparation of aldehyde (*S*)-**2.2a** in optically active form (93% ee by Mosher analysis of the precursor alcohol⁸⁵) and subsection of this enantiomerically enriched building block to the same reaction conditions did not immediately lead to increased yield of **2.9** (Entry 2).⁸⁶ Indeed, when tosyloxy aldehyde **2.2a** was used, yields were often variable, and sensitive both to reaction scale and concentration effects;

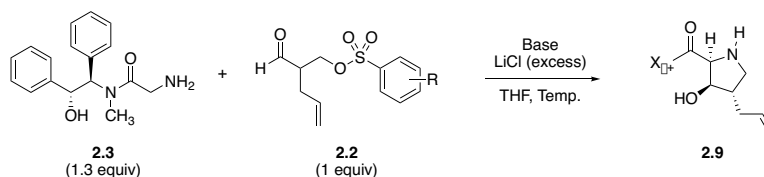
⁸⁵ Yoshii, Y.; Otsu, T.; Hosokawa, N.; Takasu, K.; Okano, K.; Tokuyama, H. *Chem. Commun.* **2015**, *51*, 1070–1073.

⁸⁶ Racemization of the aldehyde substrate prior to its introduction in the annulation reaction has been ruled out in the case of **2.2c**. Reduction of this aldehyde with sodium borohydride produces the corresponding alcohol with optical purity identical to that of its synthetic precursor:



nonetheless, even for this capricious substrate, dilution of the reaction mixture by half (from 130 mM to 67 mM with respect to (*S*)-**2.2a**) reliably led to increased yields (Entry 3).

Table 2.1. Optimization of the glycinamide annulation reaction.



Entry	Substrate	Substrate ee	Base	Temp. (°C)	[2.2] (mM)	Scale (mmol)	Yield 2.9
1	2.2a	0%	LiHMDS	-78	130	0.77	27%
2	2.2a	93%	LiHMDS	-78	130	3.8	27%
3	2.2a	93%	LiHMDS	-78	67	0.37	48%
4	2.2b	93%	LiHMDS	-78	67	0.36	73%
5	2.2b	93%	LiHMDS	-78	67	3.2	50%
6	2.2b	93%	LiHMDS	-90	67	10.1	64%
7	2.2c	93%	LiHMDS	-90	67	4.1	64%
8	2.2c	93%	LiTMP	-90	67	0.53	66%

It is believed that base-induced decomposition of β -(arenesulfonyl)oxyaldehyde starting material via an E1cB mechanism principally accounts for the mass balance when optically pure electrophile is used in the reaction. Based on this hypothesis, I probed the effects of structural changes to the arenesulfonate leaving group on reaction efficiency (Figure 2.2). 2,4,6-Trimethylbenzenesulfonate and 2,4,6-triisopropylbenzenesulfonate analogs of (*S*)-**2.2a** were prepared on the basis that increased steric bulk at the *ortho* positions might disfavor base-promoted elimination pathways and might increase steric differentiation of competing aldol transition state assemblies, leading to higher observed diastereomeric ratios. Indeed, both (*S*)-**2.2b** and (*S*)-**2.2c** provided improved yields in the annulation reaction (Table 2.1, entries 4–8), thus supporting the

hypothesis that steric perturbation of the leaving group could suppress non-productive consumption of electrophile under the reaction conditions. It should be noted that solutions of triisopropylbenzene derivative (*S*)-**2.2c** had a tendency to crystallize upon cooling; for this reason mesitylenesulfonate (*S*)-**2.2b** was selected for subsequent scale-up of this preliminarily optimized coupling reaction.

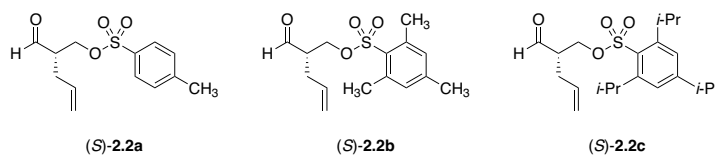
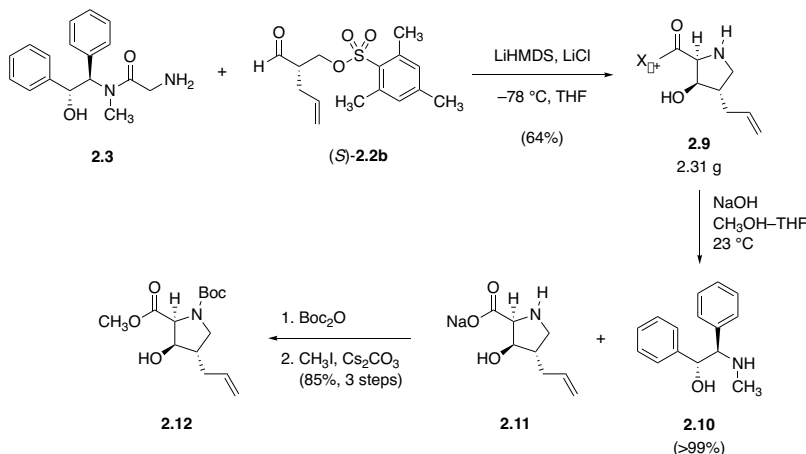


Figure 2.2. Electrophilic substrates evaluated in the pseudoephedrine glycinamide annulation reaction.

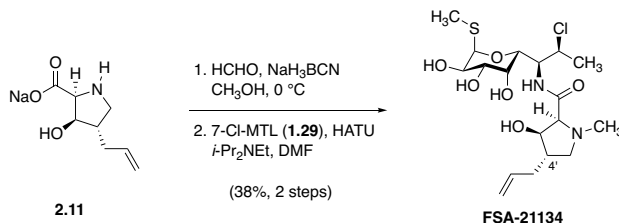
This novel annulation reaction was reliably scaled to provide up to 2.45 grams of **2.9** in a single batch, without significant deterioration in yield. In order to remove the chiral auxiliary from this product and suitably protect the resulting amino acid, a three-step telescoped sequence was developed. First, (*R,R*)-pseudoephedrine (**2.10**) was liberated under the action of sodium hydroxide (1 molar equivalent) in a tetrahydrofuran–methanol mixture. Consistent with our group’s earlier findings, this reaction proceeded under much milder conditions than those required to hydrolyze pseudoephedrine amides lacking β -hydroxyl groups – an observation ascribed to hydrogen bonding between the amide carbonyl and the β -hydroxy substituent, facilitating *N*→*O* acyl transfer.⁸¹ Pseudoephedrine auxiliary was recovered at this stage by partitioning the reaction mixture between water and dichloromethane; separation and concentration of the two phases afforded **2.10** in >99% yield, alongside the desired proline derivative as its corresponding sodium salt (**2.11**). Sequential protections of the amine and carboxylate functional groups within this material were then performed to provide *N*-Boc-amino methyl ester **2.12** in 85% overall yield.



Scheme 2.3. Scalable synthesis of a diversifiable β -hydroxyproline derivative.

Synthesis and evaluation of 3'-hydroxy and 3'-alkoxy lincosamide analogs

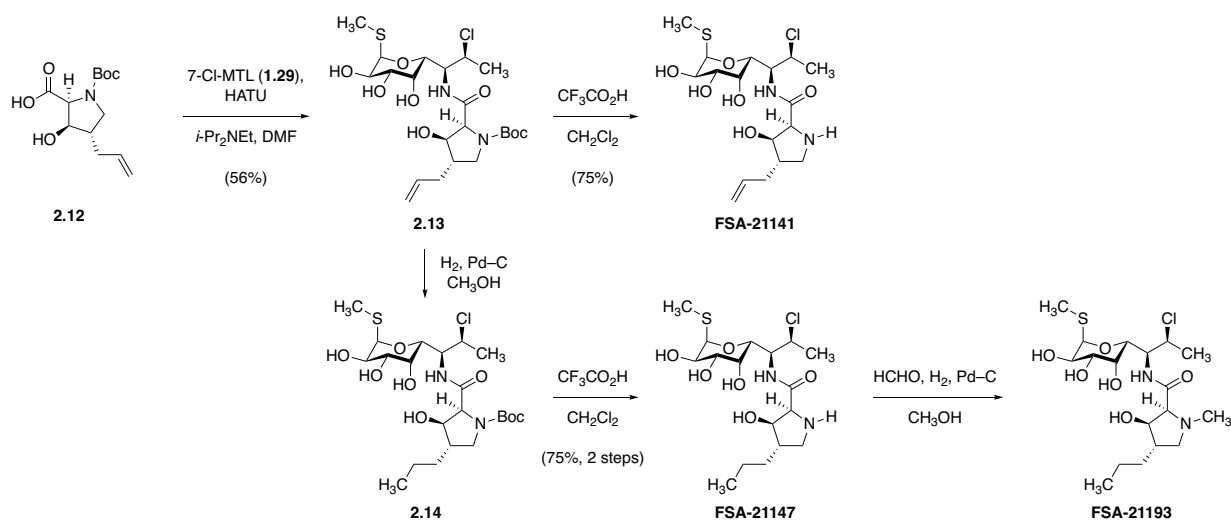
With this sequence established, I prepared a series of novel lincosamides in order to test the original hypothesis that 3'*R* hydroxylation of clindamycin would improve its antibiotic activity. I first prepared 3'-hydroxy-4'-depropyl-4'-allylclindamycin (**FSA-21141**)⁸⁷ through a sequence involving *N*-methylation of proline **2.11** by reductive amination, followed by coupling of the resulting hygric acid derivative with 7-Cl-MTL (**1.29**) under standard amide bond-forming conditions (HATU, diisopropylethylamine, *N,N*-dimethylformamide, 23 °C).



Scheme 2.4. Synthesis of **FSA-21134**.

⁸⁷ According to Myers laboratory convention, FSA (fully synthetic antibiotic) codes are assigned to all candidate compounds which undergo *in vitro* antimicrobial evaluation. For a description of how these code numbers are formulated, and for a list of structure-activity data of all lincosamide FSAs prepared to date, see Appendices B and C.

N-Desmethyl variants of this analog were prepared by coupling the crude carboxylic acid **2.12** obtained upon *N*-Boc protection of **2.11** (*vide supra*) with 7-Cl-MTL (**1.29**) in the same fashion (Scheme 2.5). Deprotection of the resulting *N*-Boc-protected lincosamide **2.13** under standard conditions (trifluoroacetic acid–dichloromethane, 23 °C) provided **FSA-21141**, while hydrogenation of **2.13** followed by analogous deprotection provided the saturated analog **FSA-21147**. Reductive amination of this analog provided the original target compound, 3'-hydroxycyclindamycin (**FSA-21193**).



Scheme 2.5. Synthesis of 3'-hydroxycyclindamycin (**FSA-21193**) and related analogs.

In vitro microbiological susceptibility testing of these analogs against a panel of Gram-positive and Gram-negative organisms displaying a range of resistance phenotypes was performed in collaboration with William Weiss at the UNT Health Science Center (Figure 2.3). None of these analogs displayed superior activity relative to clindamycin, though valuable observations emerged nonetheless. In particular, *N*-desmethyl-3'-hydroxycyclindamycin (**FSA-21147**) was equipotent to clindamycin in some Gram-positive organisms (*S. pneumoniae*, *S. pyogenes*, and *E. faecalis*), while wild-type *S. aureus* displayed a 256-fold shift in MIC – an early example of a trend that further experimentation would bear out regarding the sensitivity of *S. aureus* to the polarity and

N-methylation state of proline-based lincosamides (prolinamides). Notably, despite similarities in Gram-positive potency and spectra of activity, all 3'-hydroxylated lincosamides demonstrated poor Gram-negative activity.

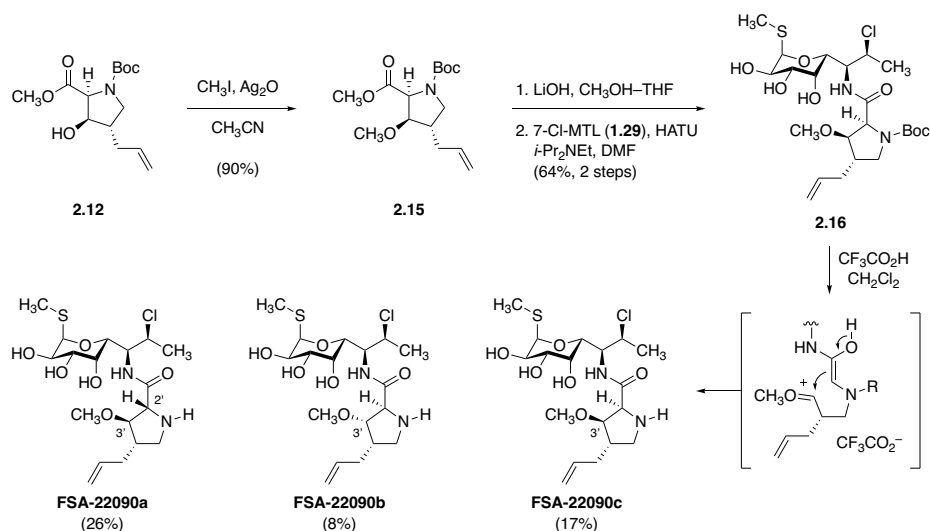
Species	Description	Clinda	21141	21134	21147	21193
Gram +	<i>S. aureus</i> ATCC 29213	0.25	4	8	16	8
	<i>S. aureus</i> BAA-1556; USA 300	>32	>32	>32	>32	>32
	<i>S. aureus</i> UNT96; USA100	>32	>32	>32	>32	>32
	<i>S. aureus</i> UNT-146; ErmA	>32	>32	>32	>32	>32
	<i>S. aureus</i> UNT-120; USA 600; GISA	>32	>32	>32	>32	>32
	<i>S. pneumoniae</i> ATCC 49619	0.12	0.0625	0.5	<0.0313	0.5
	<i>S. pneumoniae</i> UNT-038; MefA	≤0.0313	<0.0313	0.25	<0.0313	0.5
	<i>S. pneumoniae</i> UNT-039; MefA	≤0.0313	<0.0313	0.0625	<0.0313	0.25
	<i>S. pneumoniae</i> TP 1579; ErmB+Tet(M,O)	≤0.0313	<0.0313	0.125	<0.0313	0.5
	<i>S. pneumoniae</i> TP 1537; ErmB+MefA	>32	>32	>32	>32	>32
	<i>S. pyogenes</i> ATCC 19615	0.06	0.0625	0.25	<0.0313	0.25
	<i>S. pneumoniae</i> UNT-014; MacRes	≤0.0313	0.125	1	0.0625	0.5
	<i>E. faecalis</i> ATCC 29212	16	32	>32	16	>32
	<i>E. faecalis</i> UNT-039; VRE	>32	>32	>32	>32	>32
Gram -	<i>K. pneumoniae</i> ATCC 10031	8	>32	>32	>32	>32
	<i>E. coli</i> ATCC 25922	>64	>32	>32	>32	>32
	<i>P. aeruginosa</i> ATCC 27853	>64	>32	>32	>32	>32
	<i>H. influenzae</i> ATCC 49247	16	>32	>32	>32	>32
	<i>H. influenzae</i> UNT	2	>32	>32	8	>32
	<i>A. baumannii</i> ATCC 19606	64	>32	>32	>32	>32

Figure 2.3. Minimum inhibitory concentrations ($\mu\text{g/mL}$) of selected 3'-hydroxy prolinamides against a panel of standard and clinically derived bacterial strains. MIC data by William Weiss.

Reasoning that 3'-hydroxylation might diminish cell permeability, I targeted *O*-methylated analogs of **FSA-21141** and **FSA-21193** in order to evaluate whether masking the hydrogen bond-donor ability of the 3'-hydroxy substituent could improve activity (Scheme 2.6).⁸⁸ Toward this end, alcohol **2.12** was treated with methyl iodide and silver(I) oxide as a mild base, effecting methylation with no detectable elimination of the β substituent. The resulting ester, **2.15**, was saponified with methanolic lithium hydroxide, and the acid thus obtained was coupled with 7-Cl-MTL (**1.29**) to form the protected lincosamide intermediate **2.16** in 64% yield after flash-column

⁸⁸ Lipinski, C. A.; Lombardo, F.; Dominy, B. W.; Feeny, P. J. *Adv. Drug Deliv. Rev.* **1997**, *23*, 3–25.

chromatography. Subjection of this material to acidic conditions for the removal of the *N*-Boc protecting group resulted in an unexpected scrambling of stereochemistry at C2' and C3' in a process likely involving retroaldol-type fragmentation of the pyrrolidine ring followed by re-closure, giving rise to a mixture of three separable and independently characterized isomers, **FSA-22090a–c**. At this point it is not known whether this putative retroaldol fragmentation occurs before or after the *N*-Boc group is removed.

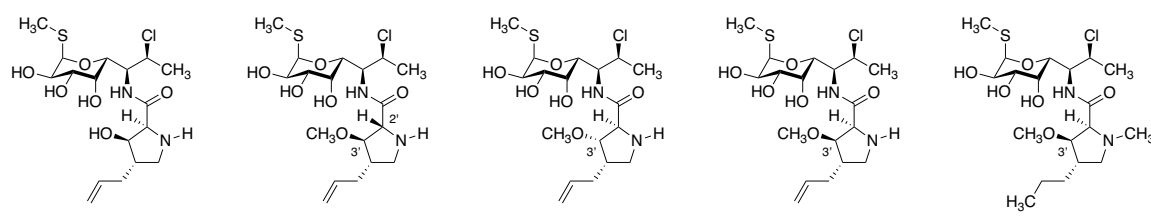


Scheme 2.6. Synthesis of 3'-methoxy analogs, and proposed mechanism for acid-induced stereochemical scrambling. R = Boc or H.

Figure 2.4 shows the results of 3'-*O*-methylation on antimicrobial activity. Direct comparison of **FSA-21147** with its congener **FSA-22090c** reveals a global diminution in potency upon *O*-methylation, with the exception of wild-type *S. aureus* activity, which does not show significant change,⁸⁹ consistent with the observation that lipophilicity and *S. aureus* activity are generally positively correlated. Likewise, (3'*R*)-methoxyclindamycin (**FSA-23005**, prepared by sequential *N*-methylation and hydrogenation of **FSA-22090c** by the methods described above)

⁸⁹ A twofold difference in MIC is considered within the typical margin of error for broth microdilution susceptibility assays.

demonstrates a ≥ 128 -fold increase in MIC relative to clindamycin, further reinforcing the deleterious effect of proline β -oxygenation on biological activity. While discouraging, these data did offer one additional, important insight: The unexpected stereochemical scrambling observed upon deprotection of **2.16** enabled independent evaluation of both 3'-methoxy epimers **FSA-22090b/c**. The ≥ 64 -fold difference in relative potencies lent support to our earlier supposition that 2',3'-*cis* diastereomeric configurations would be better suited for ribosomal binding, and thus would offer superior biological activity.



Species	Description	Clinda	21141	22090a	22090b	22090c	23005
<i>S. aureus</i>	ATCC 29213	0.25	4	>32	>32	8	32
<i>S. aureus</i>	BAA-1556; USA 300	>32	>32	>32	>32	>32	>32
<i>S. pneumoniae</i>	ATCC 49619	0.12	0.0625	16	16	0.25	8
<i>S. pneumoniae</i>	UNT-038; MefA	≤ 0.0313	< 0.0313	16	16	0.125	8
<i>S. pneumoniae</i>	UNT-039; MefA	≤ 0.0313	< 0.0313	32	16	0.5	16
<i>S. pneumoniae</i>	TP 1579; ErmB+Tet(M,O)	≤ 0.0313	< 0.0313	16	16	0.125	16
<i>S. pneumoniae</i>	TP 1537; ErmB+MefA	>32	>32	>32	>32	>32	>32
<i>S. pyogenes</i>	ATCC 19615	0.06	0.0625	32	32	0.5	16
<i>S. pyogenes</i>	UNT-014; MacRes	≤ 0.0313	0.125	>32	>32	1	16
<i>E. faecalis</i>	ATCC 29212	16	32	>32	>32	>32	>32
<i>E. faecalis</i>	UNT-039; VRE	>32	>32	>32	>32	>32	>32
<i>K. pneumoniae</i>	ATCC 10031	8	>32	>32	>32	>32	>32
<i>E. coli</i>	ATCC 25922	>64	>32	>32	>32	>32	>32
<i>P. aeruginosa</i>	ATCC 27853	>64	>32	>32	>32	>32	>32
<i>H. influenzae</i>	ATCC 49247	16	>32	>32	>32	>32	>32
<i>A. baumannii</i>	ATCC 19606	64	>32	>32	>32	>32	>32

Figure 2.4. Minimum inhibitory concentrations ($\mu\text{g/mL}$) of 3'-methoxy analogs alongside comparators. MIC data by William Weiss.

Oxazolidinone–lincosamide hybrid antibiotics

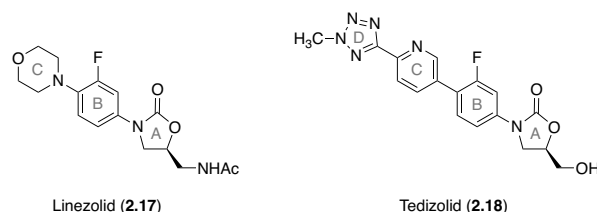


Figure 2.5. Examples of oxazolidinone antibiotics

Oxazolidinone antibiotics such as linezolid (**2.17**) and tedizolid (**2.18**) bind the PTC of the bacterial ribosome, their A and B rings overlapping with the propylhygric acid moiety of clindamycin. As Figure 2.6 demonstrates, the *n*-propyl terminus of clindamycin nearly coincides with the proximal atom of the oxazolidinone C ring (the nitrogen atom of the morpholine ring, in the case of linezolid), suggesting that synergistic gains in activity might be realized if the AB-ring system of these oxazolidinones were replaced with an appropriate lincosamide-based scaffold.⁹⁰ I therefore sought to prepare analogs bearing an ethylene linker between the pyrrolidine ring of clindamycin and the C rings of linezolid and tedizolid.

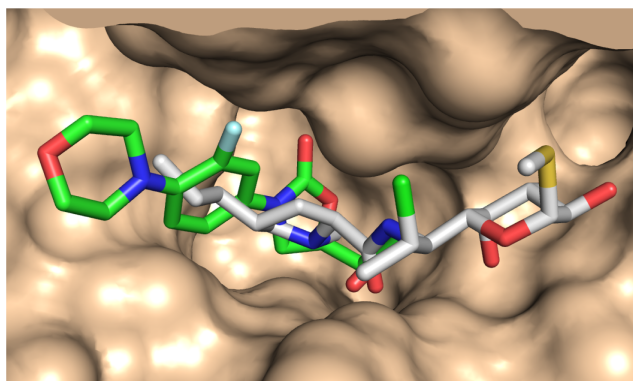
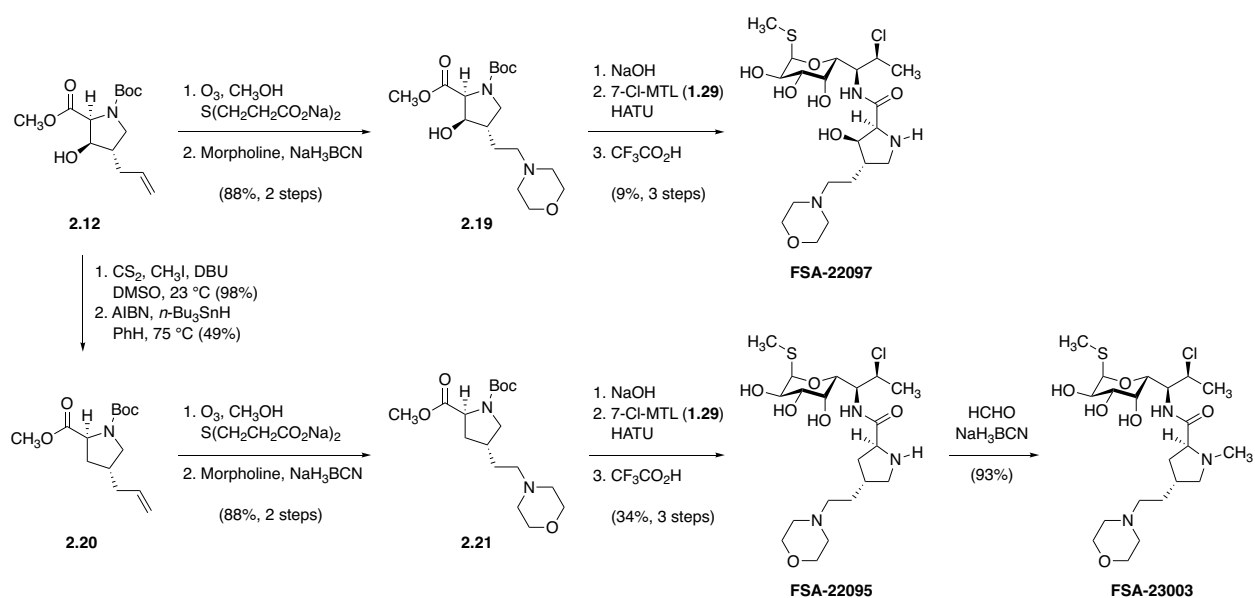


Figure 2.6. Overlay of the X-ray crystal structures of clindamycin (gray; PDB: 1YJN) and linezolid (**2.17**, green; PDB: 3CPW) shows close correspondence between the *n*-propyl terminus of the former and the C(D)-ring system of the oxazolidinones.

⁹⁰ This structure-based, chimeric design strategy has been employed with some success in the past, most notably by Melinta Therapeutics (formerly Rib-X Pharmaceuticals): (a) Wang, D.; Sutcliffe, J. A.; Oyelere, A. K.; McConnell, T. S.; Ippolito, J. A.; Abelson, J. N.; Springer, D. M.; Salvino, J. M.; Lou, R.; Goldberg, J. A.; Farmer, J. J.; Duffy, E.; Bhattacharjee, A. Bifunctional Heterocyclic Compounds and Methods of Making the Same. U. S. Patent 7,091,196 B2, August 15, 2006. (b) Zhou, J.; Bhattacharjee, A.; Chen, S.; Chen, Y.; Duffy, E.; Farmer, J.; Goldberg, J.; Hanselmann, R.; Ippolito, J. A.; Lou, R.; Orbin, A.; Oyelere, A.; Salvino, J.; Springer, D.; Tran, J.; Wang, D.; Wu, Y.; Johnson, G. *Bioorg. Med. Chem. Lett.* **2008**, *18*, 6179–6183. (c) Long, D.; Marquess, D. G. *Future Med. Chem.* **2009**, *1*, 1037–1050

In the former case, this was readily accomplished by ozonolysis of the allyl group within **2.12**, reductive workup with sodium thiodipropionate,⁹¹ and reductive amination of the resulting aldehyde with morpholine. This sequence provided **2.19**, which was transformed into hybrid analog **FSA-22097** by the standard saponification–coupling sequence described earlier. To enable more direct comparison of these bifunctional analogs with their parent compounds, deoxygenation of the 3' position of hydroxyproline **2.12** was performed using Barton's process; conversion of the resulting product, **2.20**, to linezolid–clindamycin hybrid analogs **FSA-22095** and **FSA-23003** was then performed analogously to the sequence used to prepare the corresponding 3'-hydroxy chimera.



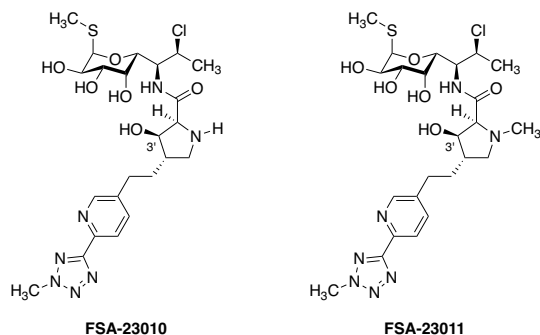
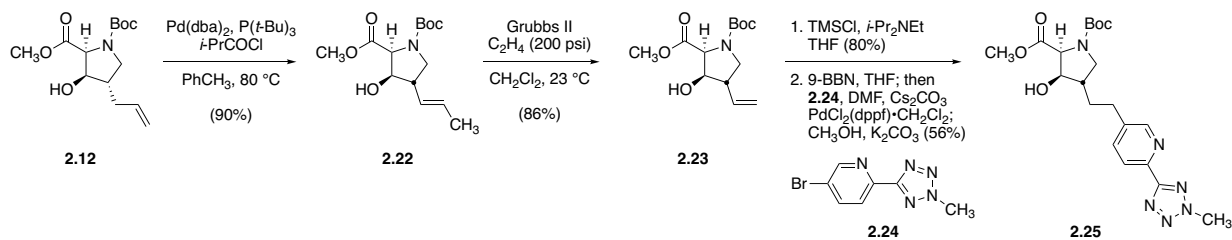
Scheme 2.7. Synthesis of linezolid–clindamycin hybrid analogs.

The synthesis of a tedizolid–lincosamide hybrid analog was less straightforward, as it was necessary to shorten the three-carbon allyl group present in **2.12** to a suitable two-carbon linker.

⁹¹ Use of this dibasic sulfide reagent in place of dimethyl sulfide dramatically reduced the formation of undesired dimethyl acetal by-product in this case. See: Appell, R. B.; Tomlinson, I. A.; Hill, I. *Synth. Commun.* **1995**, *25*, 3589–3595.

This was ultimately achieved using an isomerization–ethenolysis route conceived by my co-worker at the time, Dr. Daniel Hog. In the first step of this sequence, I found that the terminal olefin of **2.12** was transformed to its internal isomer under the catalytic action of a bulky palladium(II)-hydride species, formed *in situ* from palladium bis(dibenzylideneacetone), tri-*tert*-butylphosphine, and isobutyryl chloride according to a method developed by Professor Troels Skrydstrup and co-workers.⁹² This reaction proceeded reliably in good yield, and with good (albeit inconsequential) selectivity for the *E* product isomer. Ruthenium-catalyzed ethenolysis of this internal olefin was then performed, providing γ -vinyl proline **2.23** in 88% yield. Following protection of this suitably truncated intermediate as the corresponding trimethylsilyl ether, a tandem hydroboration–B-alkyl Suzuki coupling with bromopyridine **2.24** was finally performed, providing the chimeric southern-half fragment **2.25**. This intermediate was converted to tedizolid–lincosamide hybrid analogs **FSA-23010** and **FSA-23011** using the same saponification, coupling, and *N*-methylation methods described earlier.

⁹² Gauthier, D.; Lindhardt, A. T.; Olsen, E. P. K.; Overgaard, J.; Skrydstrup, T. *J. Am. Chem. Soc.* **2010**, *132*, 7998–8009.



Scheme 2.8. Synthesis of a 3'-hydroxy tedizolid-clindamycin hybrid analog.

These hybrid analogs did not perform favorably to clindamycin in *in vitro* susceptibility screening (Figure 2.7). Morpholino analogs belonging to the linezolid-clindamycin hybrid series displayed virtually no antimicrobial activity, particularly in the case of 3'-hydroxylated example **FSA-22097**. Tedizolid-based analogs **FSA-23010** and **FSA-23011** performed marginally better against clindamycin-susceptible *S. aureus* and streptococcal strains, but nonetheless were ≥ 32 -fold less active than clindamycin. One possible explanation for the failure of these analogs to display activities surpassing those of their parent compounds may be that the C4' ethylene bridge used to link the two chimeric hemispheres may have provided insufficient rigidity, improper spacing, or poor alignment of the oxazolidinone fragments, such that the heterocyclic ring system could not recapitulate the ribosomal binding pose normally adopted by the oxazolidinones. A series of additional tedizolid-clindamycin hybrid analogs featuring saturated and unsaturated three-carbon linkers were prepared using analogous procedures in order to test this hypothesis; these compounds likewise failed to demonstrate substantial activity (see Appendices B and C).

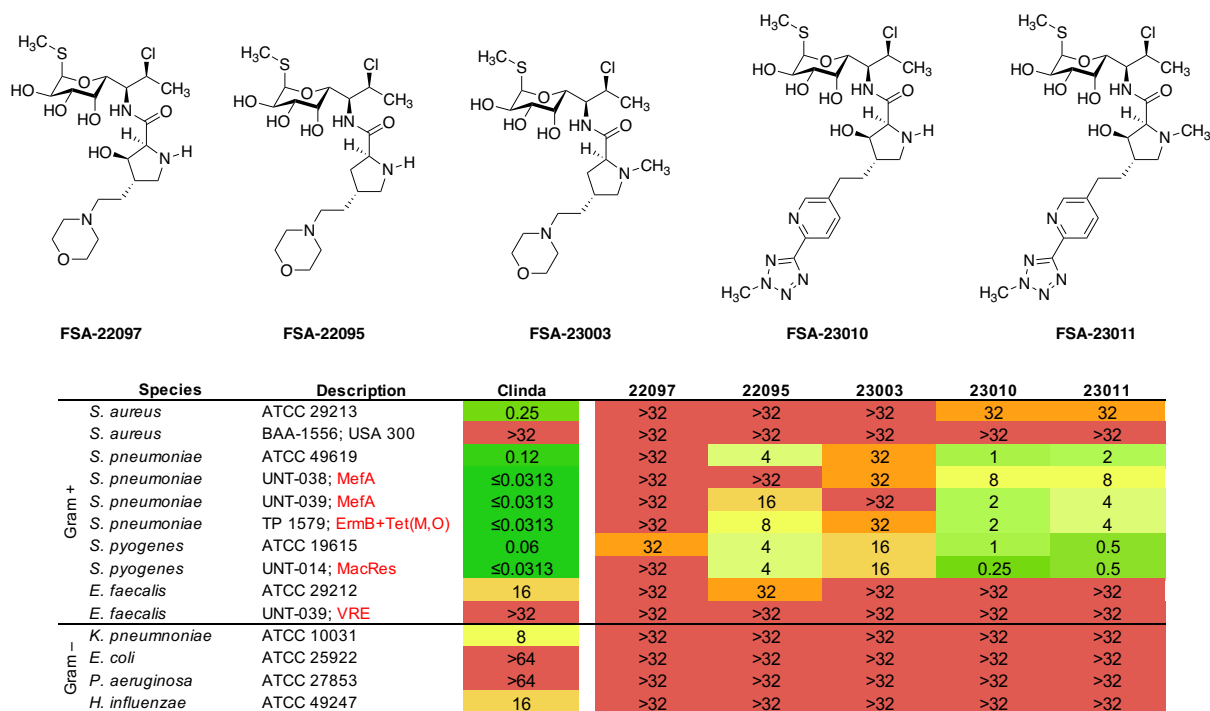
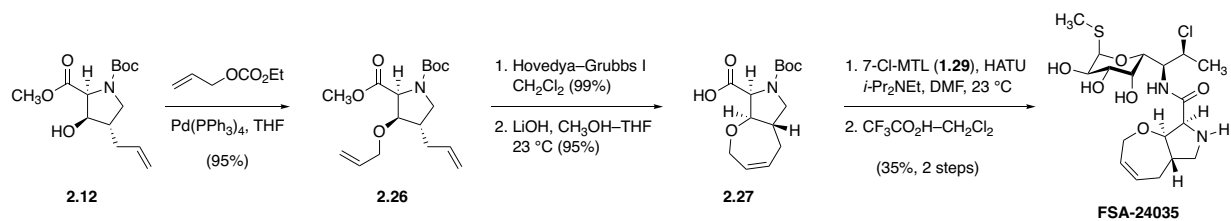


Figure 2.7. Minimum inhibitory concentrations of selected oxazolidinone–lincosamide hybrid analogs. MIC data by William Weiss.

Discovery of a novel oxepinoproline southern-half scaffold

An important breakthrough in the project came when a novel bicyclic southern-half scaffold was discovered, following the realization that the β and γ substituents of **2.1**, which had been modified independently before, could be connected to produce a rigid structure with potential for further structural diversification. Accordingly, I developed an *O*-allylation–ring-closing metathesis sequence to generate oxepinoproline **2.27** efficiently from **2.12** (Scheme 2.9). This enabled the preparation of **FSA-24035**, an early example of a oxepinoproline-based lincosamide, whose energy-minimized structure closely corresponds to the conformation that clindamycin adopts when bound to the bacterial ribosome (Figure 2.8).²¹



Scheme 2.9. Synthesis of oxepinoprolinamide analog **FSA-24035**.

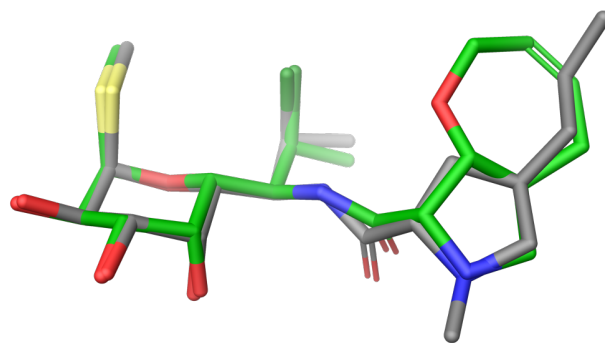
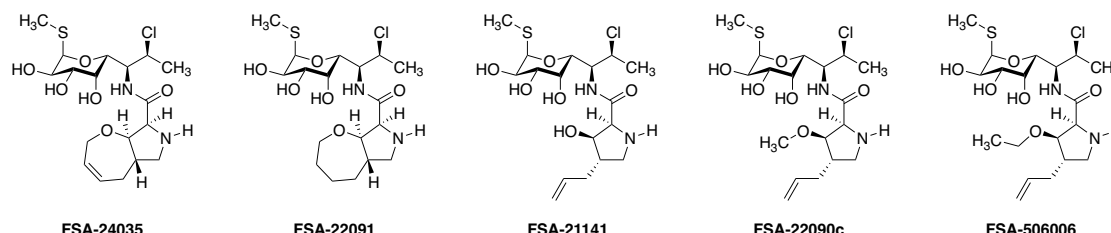


Figure 2.8. Overlay of the energy-minimized structure of **FSA-24035** (green) with the structure of clindamycin bound to the bacterial ribosome (PDB entry 1YJN).

The antimicrobial activities of **FSA-24035** and its saturated derivative **FSA-22091** are listed in Figure 2.9. For the first time, equipotency to clindamycin against Gram-positive organisms had been achieved with a 3'-oxygenated prolinamide; even more encouragingly, against strains of the Gram-negative species *K. pneumoniae* and *H. influenzae*, **FSA-24035** and **FSA-22091** displayed moderate improvements in activity, signaling that further exploration of this novel southern-half scaffold might provide broader potency against Gram-negative organisms. Compared to acyclic 3'-hydroxy, 3'-methoxy, and 3'-ethoxy derivatives (the last of which, **FSA-506006**, was prepared by my colleague Katherine Silvestre), oxepinoprolinamides display

substantially improved activity, supporting the claim that structural rigidification underlies these compounds' superior performance.⁹³



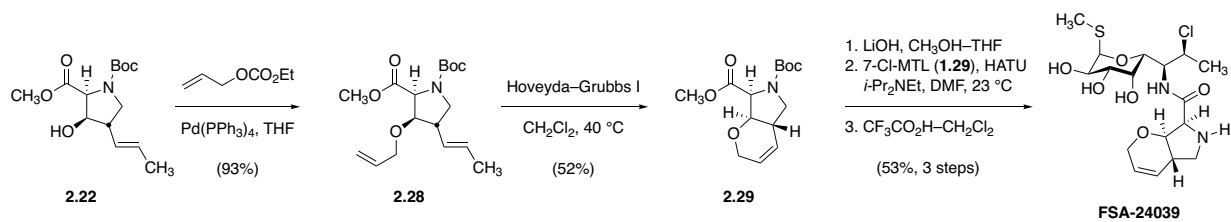
Species	Description	Clinda	24035	22091	21141	22090c	506006
Gram +	<i>S. aureus</i> ATCC 29213	0.25	0.12	0.125	4	8	>32
	<i>S. aureus</i> BAA-1556; USA 300	>32	>32	>32	>32	>32	NT
	<i>S. aureus</i> UNT-146; ErmA	>32	>32	>32	>32	>32	NT
	<i>S. pneumoniae</i> ATCC 49619	0.12	≤0.06	<0.0313	0.0625	0.25	16
	<i>S. pneumoniae</i> MMX 3028 cErnB	>64	64	NT	NT	NT	>32
	<i>S. pneumoniae</i> UNT-038; MefA	≤0.0313	≤0.0313	<0.0313	<0.0313	0.125	NT
	<i>S. pneumoniae</i> UNT-039; MefA	≤0.0313	≤0.0313	<0.0313	<0.0313	0.5	NT
	<i>S. pneumoniae</i> TP 1579; ErnB+Tet(M,O)	≤0.0313	≤0.0313	<0.0313	<0.0313	0.125	NT
	<i>S. pneumoniae</i> TP 1537; ErnB+MefA	>32	32	32	>32	>32	NT
	<i>S. pyogenes</i> ATCC 19615	0.06	≤0.0313	<0.0313	0.0625	0.5	16
	<i>S. pyogenes</i> MMX 946; MLS_B	>64	16	NT	NT	NT	>32
	<i>S. pyogenes</i> UNT-014; MacRes	≤0.0313	≤0.0313	<0.0313	0.125	1	NT
	<i>E. faecalis</i> ATCC 29212	16	16	>32	32	>32	>32
	<i>E. faecalis</i> UNT-039; VRE	>32	>32	>32	>32	>32	NT
	Gram -	<i>K. pneumoniae</i> ATCC 10031	8	>64	8	>32	>32
<i>K. pneumoniae</i> IHMA 658692; KPC-2		>32	32	>32	>32	>32	NT
<i>E. coli</i> ATCC 25922		>64	>64	32	>32	>32	>32
<i>E. coli</i> GUEST131; NDM-1		>32	>32	>32	>32	>32	NT
<i>P. aeruginosa</i> ATCC 27853		>64	>64	>32	>32	>32	>32
<i>H. influenzae</i> ATCC 49247		16	1	8	>32	>32	16

Figure 2.9. Minimum inhibitory concentrations ($\mu\text{g/mL}$) of selected analogs bearing 3' oxygenation. MIC data by William Weiss, Micromyx LLC, and Dr. Amarnath Pisipati. NT = not tested; KPC = *K. pneumoniae* carbapenemase; NDM-1 = New Delhi metallo- β -lactamase 1.

Following up on this discovery, I prepared a number of bicyclic derivatives to probe the SAR of this novel scaffold. In addition to oxepine saturation and *N*-methylation, I also performed formal ring contraction of the 7-membered ring present in **FSA-24035** (Scheme 2.10). This was achieved by *O*-allylation of the olefin-migration product **2.22** prepared earlier *en route* to

⁹³ Conformational constraint is among the design principles used most widely in drug discovery. In the context of antibiotics specifically, it bears mentioning that in a widely circulated publication by Professor Paul Hergenrother and co-workers, conformational rigidity (as measured by the number of rotatable bonds) was identified among those molecular attributes most reliably predicting Gram-negative activity. **FSA-24035** possesses five rotatable bonds, the maximum recommended number; clindamycin has seven. See: (a) Richter, M. F.; Drown, B. S.; Riley, A. P.; Garcia, A.; Shirai, T.; Svec, R. L.; Hergenrother, P. J. *Nature* **2017**, *545*, 299–304. (b) Zheng, Y.; Tice, C. M.; Sing, S. B. *Bioorg. Med. Chem. Lett.* **2017**, *27*, 2825–2837. (c) Fang, Z.; Song, Y.; Zhan, P.; Zhang, Q.; Liu, X. *Future Med. Chem.* **2014**, *6*, 885–901.

oxazolidinone–lincosamide hybrid analogs, followed by ring-closing metathesis as before. This sequence furnished the 5,6-*trans*-fused bicycle **2.29**, albeit in lesser yield than was observed for the 5,7-fused system – a potential indication of relative strain energies within the two related scaffolds. As in the oxepinoprolinamide series, both saturated (**FSA-24041**) and unsaturated (**FSA-24039**) manifestations of this 5,6-bicyclic scaffold were investigated.



Scheme 2.10. Synthesis of **FSA-24039**, an analog bearing a *trans*-5,6-fused bicyclic southern half.

Valuable insights can be gained through careful analysis of the *in vitro* antimicrobial activities of lincosamides bearing simple, unsubstituted bicyclic southern halves (Figure 2.10).⁹⁴ While both 5,6- and 5,7-bicycles impart comparable activity against clindamycin-susceptible Gram-positive organisms for example, the latter scaffold was substantially more active against Gram-negative species. Methylation of the pyrrolidine nitrogen atom likewise had negligible effects on most organisms, but *S. aureus* (ATCC 29213) proved uniquely sensitive to this modification: *N*-methylated analog **FSA-24040** demonstrated ≥ 4 -fold greater potency against this strain compared to its *N*-desmethyl congener. Analogously, the enterococcal pathogen *E. faecalis* demonstrated an intriguing sensitivity toward oxepine saturation, as against this organism **FSA-22091** was ≥ 4 -fold less potent compared to its Δ^7 relative **FSA-24035**. Perhaps most importantly, however, was the substantial impact on the anaerobic spectrum of activity that this new scaffold

⁹⁴ While *trans*-fused oxepinoprolinamides are shown here, my colleague Katherine Silvestre synthesized both 3',4'-*cis* isomers of **FSA-24035**. These analogs (**FSA-504059** and **FSA-507051**) were substantially less potent (see Appendices B and C).

displayed – whereas clindamycin potently inhibits the growth of the normally commensal gut anaerobe *B. fragilis* and is only moderately active against the opportunistic pathogen *C. difficile*, **FSA-24035** showed a complete reversal in these relative activities. This trend would prove general among oxepinoprolinamides and signaled to us that this novel scaffold may hold promise to overcome the CDAD liability that dogged prior lincosamide discovery campaigns.¹¹

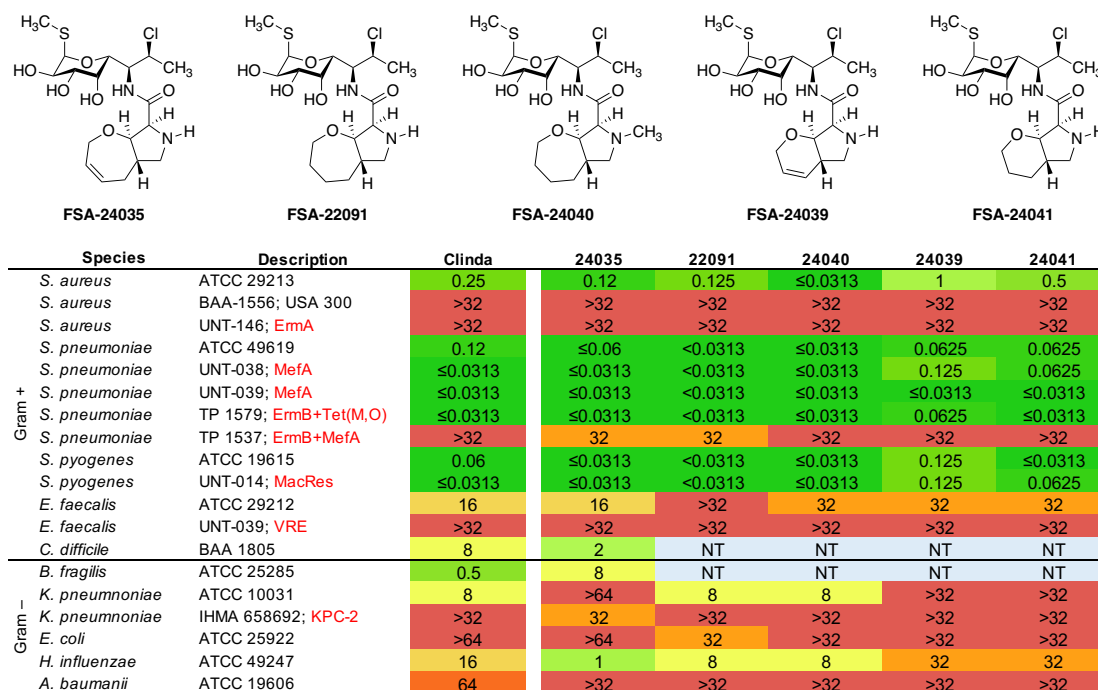


Figure 2.10. Minimum inhibitory concentrations ($\mu\text{g/mL}$) of analogs bearing unsubstituted bicyclic southern halves. MIC data by William Weiss and Micromyx, LLC.

The results emerging from this promising new scaffold led me to develop a means by which to functionalize it, so as to further explore its potential. Structural overlay of **FSA-24035** with clindamycin bound to the bacterial ribosome revealed close shape complementarity between much of the oxepane ring and the ribosomal surface – a phenomenon that likely underlies the effectiveness of the scaffold, but which limits the opportunities available for modification, given that most perturbations would likely disrupt this close structural correspondence (Figure 2.11). One position on the oxepine ring, however, did not appear to interact directly with the ribosome,

and thus presented an appealing site for derivatization. This position, C7', abuts the “hydrophobic wedge” comprising residues A2451 and C2452, and projects toward the PTC from the neck of the PET, presenting an appealing vector along which to build.

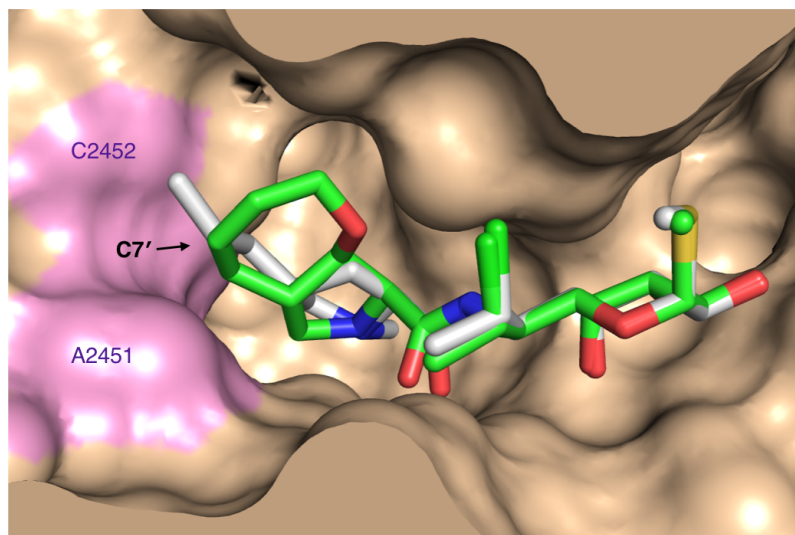
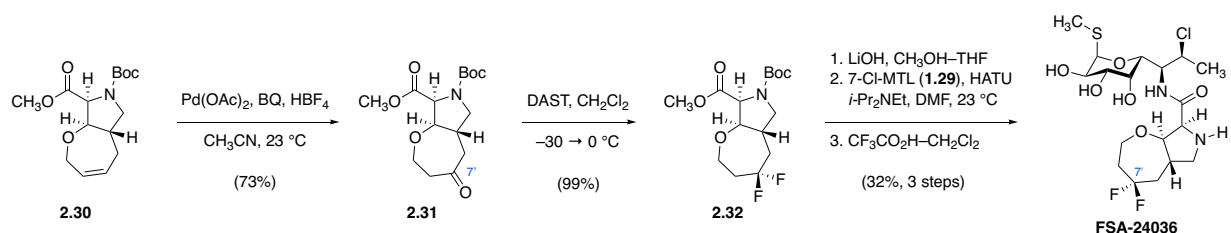


Figure 2.11. Overlay of energy-minimized structure of **FSA-24035** (green) with the X-ray co-crystal structure of clindamycin (gray) bound to the bacterial ribosome (PDB: 1YJN) identifies C7' as a strategic site for modification of the oxepinoprolinamide scaffold. The hydrophobic pocket formed by PTC residues A2451 and C2452 is highlighted in rose.

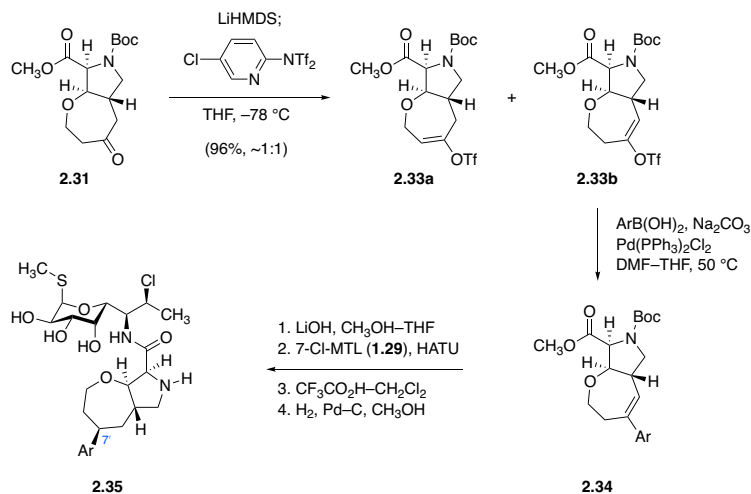
I reasoned that within oxepinoproline **2.30**, the 7' position could be functionalized regioselectively via Wacker oxidation, owing to the σ -withdrawing effect of the oxygen atom embedded within the 7-membered ring, which acts to make C8' (the olefinic position proximal to this oxygen atom) comparatively less electron-rich. Application of an oxidation method originally reported by Morandi, Wickens, and Grubbs (palladium(II) acetate, tetrafluoroboric acid, benzoquinone, water–acetonitrile, 23 °C)⁹⁵ achieved the desired transformation, providing ketone **2.31** in 80% yield as a single regioisomer. This intermediate underwent exceptionally efficient

⁹⁵ Morandi, B.; Wickens, Z. K.; Grubbs, R. H. *Angew. Chem. Int. Ed.* **2013**, *52*, 9751–9754.

deoxydifluorination under the action of diethylaminosulfur trifluoride,⁹⁶ affording *C7'*-gem-difluoro analog **FSA-24036** following typical saponification, aminosugar coupling, and *N*-Boc deprotection. Likewise, my colleague Katherine Silvestre identified a sequence for *C7'* arylation relying on chemoselective enolization of **2.31** with lithium hexamethyldisilazide, trapping of the resulting enolates with Comins' reagent, and subjecting of the resulting vinyl triflate regioisomers to palladium-catalyzed Suzuki cross-coupling with arylboronic acids (Scheme 2.12).



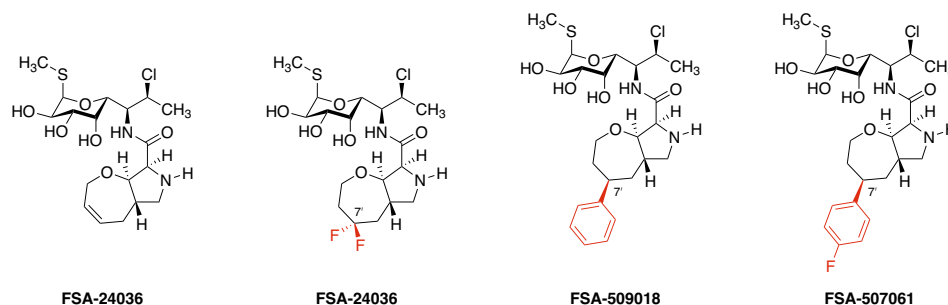
Scheme 2.11. Regioselective *C7'* functionalization by Wacker oxidation, and synthesis of 7'-difluoro oxepanoprolinamide analog **FSA-24036** by deoxydifluorination. BQ = benzoquinone; DAST = diethylaminosulfur(IV) trifluoride.



Scheme 2.12. Synthesis of *C7'*-aryl oxepanoprolinamide analogs via an enolization-triflation-Suzuki coupling sequence (Katherine Silvestre). Ar = arenyl.

⁹⁶ Rye, C. S.; Withers, S. G. *J. Am. Chem. Soc.* **2002**, *124*, 9756–9767.

Oxepanoprolinamides bearing C7' modifications are among the most potent antibiotics to emerge from our lincosamide program to date (Figure 2.12). Notably, lipophilic substitution at C7' confers considerable gains in potency against *E. faecalis*, against which clindamycin is not typically effective: C7'-gem-difluoro analog **FSA-24036** and C7'-aryl analogs such as **FSA-509018** (designed and prepared by Katherine Silvestre) are 2- to >256-fold more potent against this species compared both to clindamycin and to unsubstituted oxepinoprolinamides. What's more, C7'-arylated analogs display remarkable potency against clinically derived strains of *S. pneumoniae* and *S. pyogenes* constitutively expressing *erm* methyltransferase genes, as well as measurable activity against similarly MLS_B-resistant strains of *S. aureus* and *E. faecalis*. In cases where MICs against a trio of genetically matched *E. coli* strains (wild-type, ATCC-25922; efflux pump knockout mutant, Δ TolC; and outer-membrane permeabilized LptD mutant) were measured, it appears that both low outer-membrane permeability and ABC transporter-dependent efflux are to blame for these analogs' lack of activity in Gram-negative organisms.



		Clinda	24035	24036	509018	507061	
Gram +	S. aureus	ATCC 29213	0.25	0.12	0.25	≤0.06	0.12
	S. aureus	BAA 977; iErmA	0.25	0.25	0.5	0.25	0.25
	S. aureus	MP-549; USA 300; MsrA	0.125	0.5	NT	0.25	0.125
	S. aureus	Micromyx USA 300	0.25	0.12	0.12	NT	≤0.06
	S. aureus	MMX 3035; cErmA	>64	>64	>64	>64	64
	S. pneumoniae	ATCC 49619	0.12	≤0.06	≤0.06	≤0.06	≤0.06
	S. pneumoniae	MMX 3028 cErmB	>64	64	64	16	4
	S. pneumoniae	MMX 3031 cMefA	0.06	≤0.06	≤0.06	0.125	≤0.06
	S. pyogenes	ATCC 19615	0.06	≤0.0313	≤0.0313	≤0.06	≤0.06
	S. pyogenes	MMX 946; cErmB	>64	16	4	>64	4
	E. faecalis	ATCC 29212	16	16	4	≤0.06	≤0.06
	E. faecalis	MMX 847; cErmB	>64	>64	>64	>64	32
	C. difficile	BAA 1805	8	2	2	NT	2
C. difficile	ATCC 700057	8	NT	NT	32	8	
Gram -	B. fragilis	ATCC 25285	0.5	8	4	32	64
	K. pneumoniae	ATCC 10031	8	>64	16	16	16
	E. coli	ATCC 25922	>64	>64	>64	64	64
	E. coli	MP-9 ΔTolC	8	8	NT	16	4
	E. coli	LptD mutant	2	NT	NT	16	8
	P. aeruginosa	ATCC 27853	>64	>64	>64	NT	>64
	H. influenzae	ATCC 49247	16	1	4	16	4
	H. influenzae	MMX 565 ΔAcrB	4	0.5	1	NT	0.25
	A. baumannii	ATCC 19606	64	>32	>32	>64	>64

Figure 2.12. Minimum inhibitory concentrations ($\mu\text{g/mL}$) of selected C7'-modified oxepanoprolinamides, including C7'-aryl analogs designed and prepared by Katherine Silvestre. MIC data by Micromyx, LLC and Dr. Amarnath Pisipati.

Oxepinoprolinamide analogs bearing 7-arylthio substitution

In a series of communications to the *Journal of Antibiotics* beginning in 2013, Meiji Seika chemists described novel lincosamides discovered through semisynthetic modification of lincomycin, including propylhygramides **2.36** and **2.37**; and pipecolamides **1.72** and **1.74** (Figure 2.13).⁷³ These analogs displayed potent *in vitro* growth inhibition of Gram-positive bacteria expressing the MLS_B phenotype, owing to the installation of biarylsulfide appendages to C7 of the northern half. Based on docking studies performed by Meiji Seika,^{73d} these side chains are believed to engage in additional contacts with domain V of the bacterial ribosome in a manner analogous –

though not identical – to the purported action of biaryl side-chain motifs in the ketolides telithromycin and solithromycin (which in some cases engage domain-II rRNA residues).^{22,97}

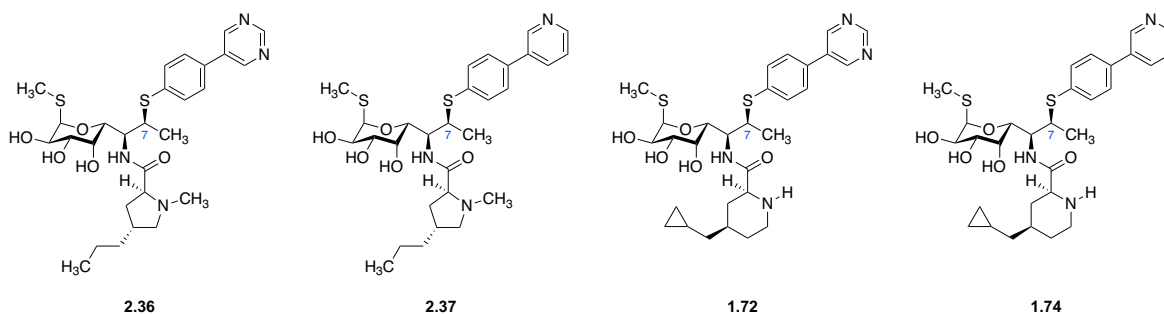
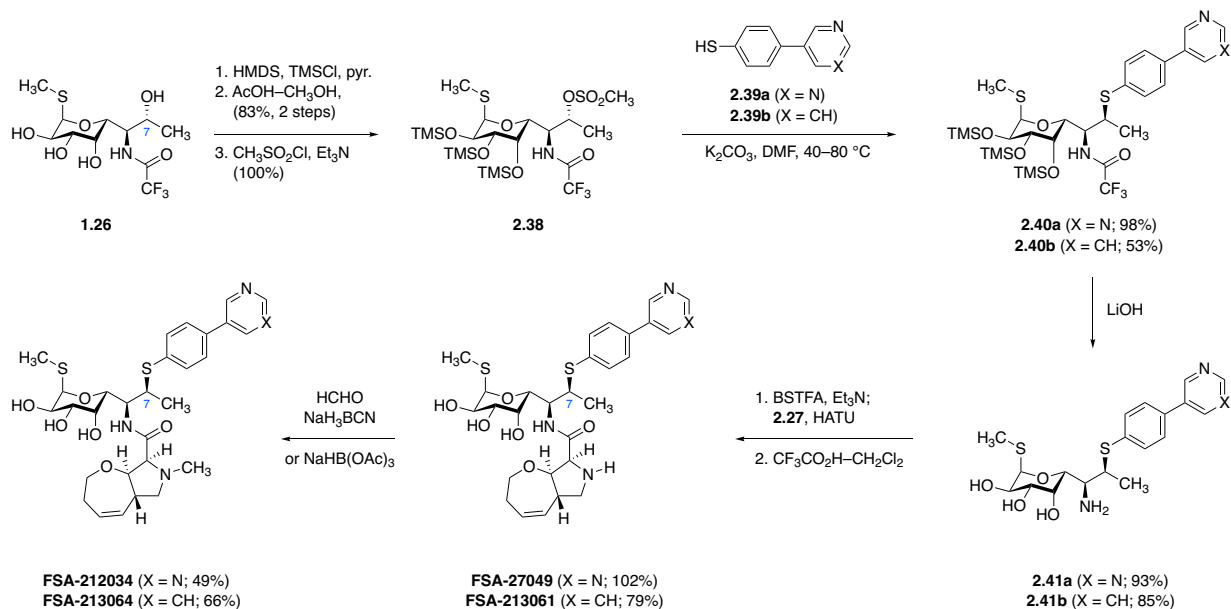


Figure 2.13. Semisynthetic lincomycin derivatives bearing 7-biarylthio side chains discovered by Meiji Seika Pharma Co., Ltd.

The success of the oxepinopropine southern-half scaffold, paired with its close structural correspondence with the propylproline moiety present in **2.36** and **2.37**, prompted me to pursue oxepinoprolinamide analogs bearing the same C7-arenesulfide appendages. Accordingly, I prepared the corresponding 7-modified aminosugars via manipulation of semisynthetic MTL trifluoroacetamide **1.26** (Scheme 2.13). Adapting procedures originally reported by Meiji Seika, global silylation, regioselective 7-desilylation, and mesylation of the resulting alcohol were performed. Stereospecific substitution of **2.38** with appropriate arenethiolate nucleophiles and global deprotection (desilylation and trifluoroacetamide cleavage; lithium hydroxide, methanol–tetrahydrofuran, 23–40 °C) provided MTL derivatives **2.41a** and **2.41b**. *In situ* O-silylation of these aminosugars with *N,O*-bis(trimethylsilyl)trifluoroacetamide and coupling of the protected intermediates with oxepinopropine **2.27** was performed using conditions originally reported by the Vicuron team.⁶⁸ Following global deprotection and optional *N*-methylation using standard

⁹⁷ (a) Douthwaite, S.; Champney, W. S. *J. Antimicrob. Chemother.* **2001**, *48* (Suppl 2), 1–8. (b) Lonks, J. R.; Goldmann, D. A. *Clin. Infect. Dis.* **2005**, *40*, 1657–1664.

methods,⁹⁸ C7-modified analogs **FSA-27049**, **FSA-212034**, **FSA-213061**, and **FSA-213064** were obtained.

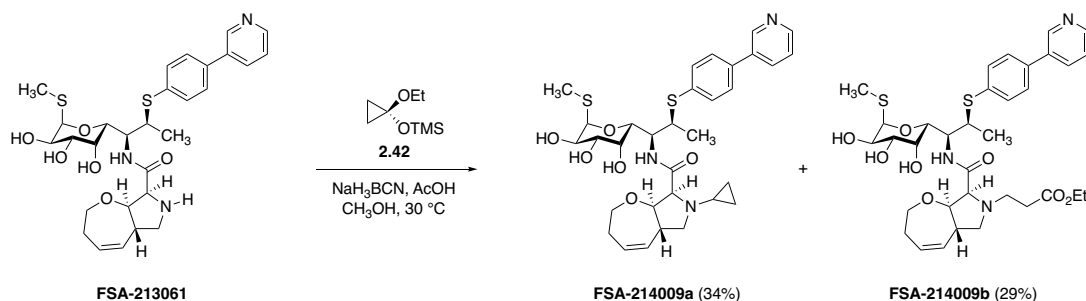


Scheme 2.13. Synthesis of 7-arylthio oxepinoprolinamide analogs by semisynthetic modification of MTL derivative **1.26**.

As part of an ongoing effort to improve the Gram-negative activity of our lincosamide candidates, I sought to modulate the basicity of the oxepinoprolinamide nucleus through alternative *N*-alkyl substitution. This work was motivated by an evolving hypothesis in our lab that ribosome-targeting antibiotics bearing moderately basic amino groups ($pK_a' \sim 6-8$), by virtue of their ability to adopt both charged and uncharged states under physiologically relevant conditions, are better able to transverse both the inner and outer membranes of Gram-negative bacteria so as to engage their intracellular target. Indeed, steric hindrance and σ -withdrawal by the adjacent carboxamide already imbue the amino group of lincomycin with a relatively low pK_a' of 7.5,^{9a} and β -oxygenation within the pyrrolidinoxepine scaffold is expected to further depress this value

⁹⁸ When sodium cyanoborohydride was used in the *N*-methylation of **FSA-27049**, undesired reduction of the pyrimidine ring was observed; use of sodium triacetoxyborohydride avoided this.

through σ -withdrawing effects (**FSA-24035** calculated $pK_a' = 6.9$).⁹⁹ Nevertheless, introduction of an *N*-cyclopropyl group was targeted in order to lower amine basicity further still, while imposing minimal steric demands.¹⁰⁰ Treatment of **FSA-213061** with [(1-ethoxycyclopropyl)oxy]-trimethylsilane (**2.42**) and sodium cyanoborohydride provided the desired *N*-cyclopropylamine analog **FSA-214009a**, together with an unexpected by-product, ethyl propionate derivative **FSA-214009b** (Scheme 2.14). The later was structurally identified thanks to the insight of my colleague Ioana Moga and is believed to have arisen through *in situ* generation of ethyl acrylate by aerobic fragmentation of **2.42**.



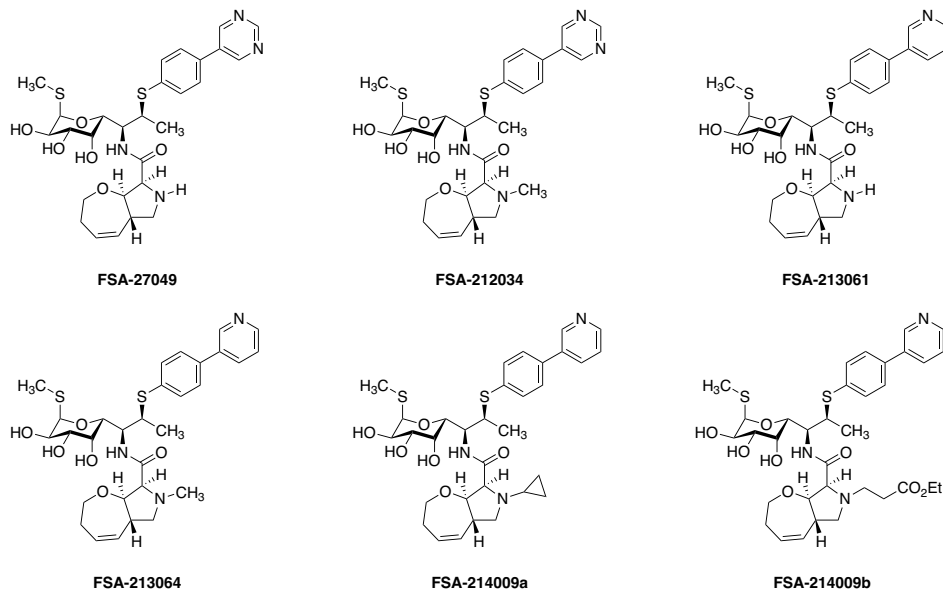
Scheme 2.14. Synthesis of *N*-cyclopropanated analog **FSA-214009a** and an unexpected by-product arising by oxidative cleavage of the cyclopropanation reagent.

Figure 2.14 lists the antimicrobial activities of these *C7*-modified oxepinoprolinamide analogs relative to clindamycin (**1.3**) and Meiji Seika biarylsulfide **2.37**. Notably, whereas clindamycin and **FSA-24035** – a matched pair of lincosamides differing only in southern-half architecture – displayed nearly identical Gram-positive activities (Figure 2.10), propylhygramide **2.37** was far more potent than the matched oxepinoprolinamide **FSA-213064**, illustrating that modifications to the northern and southern hemispheres are not necessarily additive.

⁹⁹ Calculated by density functional theory with empirical correction using Schrödinger's Jaguar pK_a prediction software, following molecular-dynamics conformational searching with the OPLS3 force field.

¹⁰⁰ Gillaspay, M. L.; Lefker, B. A.; Hada, W. A.; Hoover, D. J. *Tetrahedron Lett.* **1995**, *36*, 7399–7402.

Complementary to this observation, C7-arylthio oxepinoprolinamides showed a scaffold-specific reversal in anaerobic spectrum of action relative to the propylhygramides (clindamycin and **2.37**), with important implications for the design of lincosamides with diminished CDAD risk. While no clear trends emerged to distinguish pyrimidine- and pyridine-based 7-arylthio decoration, *N*-methylation in both series had a pronounced effect on *S. aureus* activity, with methylation conferring a roughly 4-fold gain in potency against a clinically derived strain of *S. aureus* constitutively expressing an *ermA* resistance gene. Other *N*-alkyl substituents, such as those found in **FSA-214009a** and **FSA-214009b**, abolished nearly all activity even against clindamycin-susceptible strains.



	Species	Description	Clinda	2.37	27049	212034	213061	213064	214009a	214009b
Gram ⁺	<i>S. aureus</i>	ATCC 29213	0.25	≤0.06	1	0.25	0.25	0.25	64	≥64
	<i>S. aureus</i>	BAA 977; iErmA	0.25	≤0.125	2	0.25	0.25	0.25	NT	NT
	<i>S. aureus</i>	MP-549; USA 300; MsrA	0.125	NT	0.25	0.5	0.5	0.25	NT	NT
	<i>S. aureus</i>	MMX 3035; cErmA	>64	2	>64	32	64	16	NT	NT
	<i>S. pneumoniae</i>	ATCC 49619	0.12	≤0.06	≤0.06	≤0.06	≤0.06	≤0.125	4	32
	<i>S. pneumoniae</i>	MMX 3028; cErmB	>64	0.5	32	4	8	8	NT	NT
	<i>S. pneumoniae</i>	MMX 3031; cMefA	0.06	≤0.06	≤0.06	≤0.06	0.125	0.125	NT	NT
	<i>S. pyogenes</i>	ATCC 19615	0.06	≤0.06	≤0.06	≤0.06	≤0.06	≤0.125	4	8
	<i>S. pyogenes</i>	MMX 946; cErmB	>64	0.25	2	2	4	2	NT	NT
	<i>E. faecalis</i>	ATCC 29212	16	1	64	16	16	32	>64	>64
Gram ⁻	<i>E. faecalis</i>	MMX 847; cErmB	>64	4	>64	>64	>64	>64	NT	NT
	<i>C. difficile</i>	BAA 1805	8	0.06	1	0.5	NT	NT	NT	NT
	<i>C. difficile</i>	ATCC 700057	8	NT	0.5	NT	4	0.5	NT	NT
	<i>B. fragilis</i>	ATCC 25285	0.5	≤0.06	>64	1	32	1	NT	NT
	<i>K. pneumoniae</i>	ATCC 10031	8	NT	64	64	32	64	NT	NT
	<i>E. coli</i>	ATCC 25922	>64	>64	>64	>64	>64	>64	>64	>64
	<i>E. coli</i>	MP-9 ΔToIC	8	4	32	16	8	8	NT	NT
	<i>E. coli</i>	LptD mutant	2	NT	32	NT	8	4	NT	NT
	<i>P. aeruginosa</i>	ATCC 27853	>64	>64	>64	>64	NT	>64	NT	NT
	<i>H. influenzae</i>	ATCC 49247	16	2	32	4	32	2	NT	NT
<i>H. influenzae</i>	MMX 565 ΔAcrB	4	≤0.06	0.5	≤0.06	NT	NT	NT	NT	
<i>A. baumannii</i>	ATCC 19606	64	NT	>64	NT	>64	NT	NT	NT	

Figure 2.14. Minimum inhibitory concentrations ($\mu\text{g/mL}$) of C7-modified oxepinoprolinamide analogs. MIC data by Micromyx, LLC and Dr. Amarnath Pisipati.

Secondary screening of active oxepinoprolinamides

As 7-arylthio oxepinoprolinamide analogs displayed activity against clindamycin-resistant pathogens and featured a reversed anaerobic spectrum of activity, a number of follow-up experiments were performed in order to probe other key parameters related to the developability of these antibiotics. A post-doctoral researcher on the team, Dr. Amarnath Pisipati, found that pyridine-based analogs **FSA-213061** and **FSA-213064** did not lyse human red blood cells at

concentrations up to 200 μM – a gratifying result in light of the fact that Meiji Seika researchers had observed hemolytic activity from the closely related pipicolamide analog **1.74**.^{73j} Accordingly, Dr. Pisipati found that **FSA-213061** was non-toxic to human cells, displaying no detectable growth inhibition of A549 lung adenocarcinoma cells at a concentrations up to 200 μM . These results provided evidence that the antibiotic activities of these novel compounds could be attributed to improved engagement with the bacterial ribosome, rather than to a distinct and non-selective mechanism of action.¹⁰¹

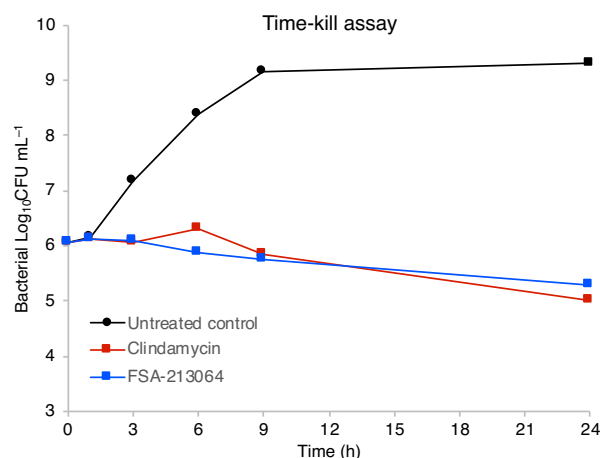


Figure 2.15. Time-kill kinetics of clindamycin and **FSA-213064** versus *S. aureus* ATCC 29213, demonstrating the bacteriostatic effects of both antibiotics at $4 \times \text{MIC}$ (1 $\mu\text{g}/\text{mL}$). Experiment was designed and performed by Dr. Amarnath Pisipati.

Secondary *in vitro* microbiological profiling conducted by Dr. Pisipati on **FSA-213064** illuminated the pharmacodynamic basis for this candidate’s improved activity.¹⁰² Namely, while **FSA-213064** demonstrated identical (bacteriostatic)¹⁰³ time-kill kinetics to clindamycin against *S.*

¹⁰¹ The latter was observed in some cases where overly lipophilic southern-half fragments were investigated. These compounds were hemolytic and cytotoxic owing to their action as surfactants, rather than protein-synthesis inhibitors.

¹⁰² For experimental details, refer to Appendix D.

¹⁰³ An antibiotic is deemed bactericidal versus bacteriostatic if, following 18–24 h exposure of cultured bacteria to antibiotic at $4 \times \text{MIC}$, a $\geq 1,000$ -fold (≥ 3 -log) reduction in colony-forming units is observed. See: Clinical and

aureus ATCC 29213 (against which both antibiotics display the same MIC = 0.25 µg/mL; Figure 2.15), the former induced a post-antibiotic effect (PAE) nearly twice that of clindamycin (3.65 h, versus 1.85 h, following antibiotic exposure at 4 × MIC for 1 hour), offering evidence of increased persisting effects (Figure 2.16A). What's more, the post-antibiotic sub-MIC effect (PA-SME) of **FSA-213064** represented a dramatic improvement over the comparator (Figure 2.16B). In this experiment, an inoculum of *S. aureus* ATCC 29213 containing ~ 1 × 10⁶ colony-forming units (CFUs) per milliliter of broth was exposed to 4 × MIC (1 µg/mL) of either clindamycin or **FSA-213064** for 1 hour; the inoculum was then diluted 1000-fold (to ~1 × 10³ CFU/mL), and was supplemented with antibiotic at concentrations of either 0.25 × MIC or 0.5 × MIC. Bacterial counts were taken periodically for a duration of 30 hours, revealing that while clindamycin exhibited a bacteriostatic effect under both sub-MIC regimes, only after 24 hours at 0.5 × MIC did clindamycin achieve a reduction of bacterial counts below the limit of detection (1 × 10² CFU/mL). Regrowth of clindamycin-treated bacteria was observed by the 30-hour time point. By contrast, **FSA-213064** achieved functional elimination of bacterial counts within 6 hours at 0.5 × MIC (within 9 hours at 0.25 × MIC), and these counts remained below the limit of detection for the duration of the experiment. The superior performance of **FSA-213064** indicated that this candidate, or others like it, could likely demonstrate better efficacy compared to the contemporary clinical standard, clindamycin. We are hopeful that further screening of oxepinoprolinamides with potent *in vitro* activity profiles in animal infection models may further validate the potential of this scaffold.

Laboratory Standards Institute. *Methods for Determining Bactericidal Activity of Antimicrobial Agents; Approved Guideline. LCCLS Document M26-A*. NCCLS, Wayne, PA, 1999.

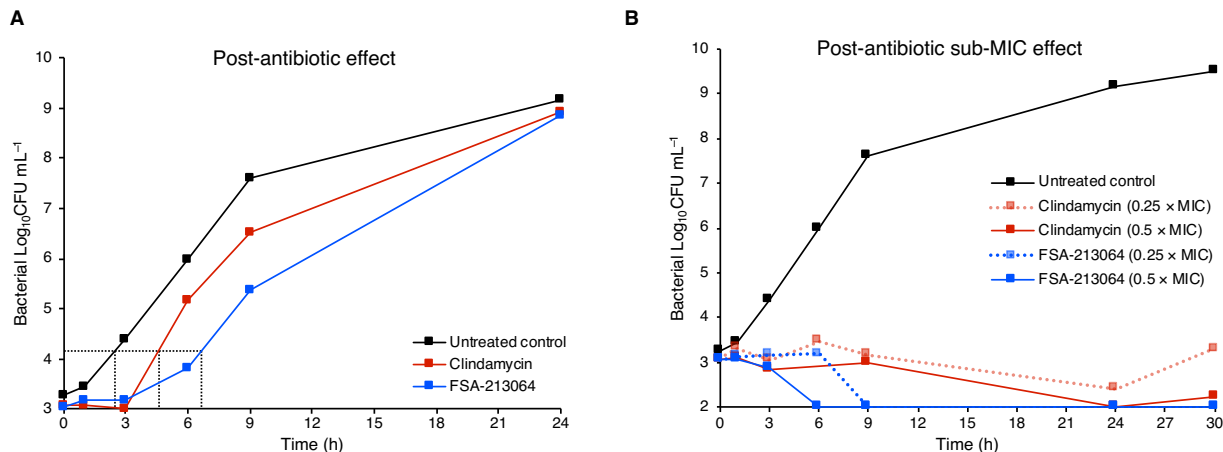


Figure 2.16. Post-antibiotic effect profiling of **FSA-213064** reveals a prolonged PAE compared to clindamycin (A), as well as more rapid and durable clearance in PA-SME experiments. Experiments were designed and performed by Dr. Amarnath Pisipati.

Consequently, and with an eye toward *in vivo* evaluation of these compounds, we aimed to study the microsomal stability of oxepinoprolinamide analogs, as we had concerns that sulfur(II)-rich embodiments bearing 7-arylthio substitution might not be well tolerated from the metabolic point of view. A preliminary pharmacokinetic assessment of representative lincosamides was therefore undertaken in collaboration with Professor Michael Cameron of the Scripps Research Institute in Jupiter, Florida. The *in vitro* human liver microsomal stabilities of **FSA-213061**, **FSA-213064**, **FSA-507061**, and **FSA-509018** were measured alongside those of clindamycin (**1.3**) and **2.37** as experimental controls. As Figure 2.17 illustrates, among the 7-chloro-substituted lincosamides, **FSA-507061** ($T_{1/2} = 20$ minutes) and **FSA-509018** ($T_{1/2} = 22$ minutes) – representatives of a series of 7'-arylated oxepanoprolinamides pioneered by my teammate Katherine Silvestre – demonstrated a nearly twofold enhancement in stability relative to clindamycin (**1.3**, $T_{1/2} = 13$ minutes). Conversely, 7-arylthio oxepinoprolinamides **FSA-213061** and **FSA-213064** demonstrated low chemical resilience, with the latter *N*-methylated analog undergoing particularly rapid degradation ($T_{1/2}$'s = 7 and 3 minutes, respectively). Importantly,

these data strongly suggested that the 7-arylthio group present in these molecules – rather than the oxepinoproline motif – was directly responsible for this metabolic instability, as propylhygramide **2.37** ($T_{1/2} = 3$ minutes) was degraded at the same rate as its oxepinoprolinamide counterpart, **FSA-213064**. Thus, while the low microsomal stability of 7-arylthio analogs counterbalances their high antimicrobial potency, these pharmacokinetic data were broadly encouraging, as they implicated factors other than the bicyclic southern-half motif, and thus cleared the way for further optimization of the 7'-aryl-oxepanoprolinamide series.

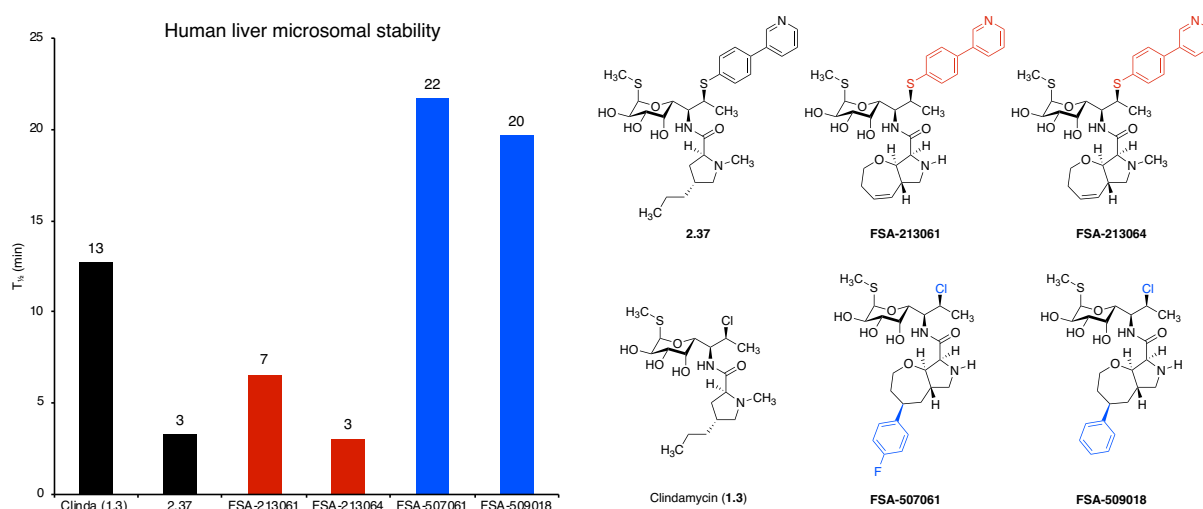


Figure 2.17. Human liver microsomal stability data for selected lincosamide analogs, demonstrating that 7-arylthio substitution leads to rapid metabolism, whereas oxepanoprolinamides bearing 7-chloro substitution in the north show increased resilience relative to clindamycin. Data by Prof. Michael Cameron.

Summary and conclusion

In this chapter, I described my efforts to prepare 3'-oxygenated lincosamide analogs via the development of a novel pseudoephenamine glycinamide annulation reaction involving sequential aldol-cyclization with a bis-electrophilic coupling partner. The product of this transformation (**2.9**) enabled me to probe the SAR of the 3' position of clindamycin for the first time, as well as to synthesize and evaluate novel oxazolidinone-lincosamide hybrid antibiotics.

Through elaboration of this key β -hydroxy- γ -allyl proline derivative, I uncovered a novel bicyclic scaffold and developed a means by which to functionalize it regioselectively, clearing the way for the discovery of some of the most potent lincosamides to emerge from our research program to date.

Taken together, the experiments described in this chapter indicate that this oxepinoproline scaffold represents a promising new avenue for lincosamide discovery. Two distinct series emerging from this work – 7-arylthio oxepinoprolinamides and 7-chloro-7'-aryl oxepanoprolinamides – have demonstrated remarkable gains against Gram-positive bacteria, including MLS_B-resistant strains. The bicyclic amino acid motif underpinning these analogs appears to be intrinsically stable toward hepatic metabolism, and in many cases substantially alters the anaerobic spectrum of activity of those lincosamides which incorporate it. These properties have the potential to directly impact several of clindamycin's major shortcomings, namely its propensity to promote opportunistic bowel infections, its relatively short serum elimination half-life (2.4 hours in adults, dominated by hepatic metabolism),¹⁰⁴ and the global emergence of MLS_B resistance.

¹⁰⁴ Cleocin HCl [package insert]. Pharmacia & Upjohn Co., Division of Pfizer Inc., New York, NY; Revised July 2016.

Experimental section

General Experimental Procedures. All reactions were performed in oven- or flame-dried round-bottomed or modified Schlenk flasks fitted with rubber septa under a positive pressure of argon (dried by passage through a column of Drierite calcium sulfate desiccant), unless otherwise noted. Air- and moisture-sensitive liquids and solutions were transferred via syringe or stainless-steel cannula. When necessary (so noted), solutions were deoxygenated by three cycles of freezing (liquid nitrogen), evacuation, and thawing under static vacuum. Organic solutions were concentrated by rotary evaporation (house vacuum, ~60 Torr) at 23–30 °C. Flash-column chromatography was performed as described by Still et al.,¹⁰⁵ employing silica gel (60-Å pore size, 230–400 mesh, Agela Technologies, Chicago, IL; or RediSep silica cartridges, Teledyne Isco, Lincoln, NE). Analytical thin-layer chromatography (TLC) was performed using glass plates pre-coated with silica gel (0.25 mm, 60-Å pore size, 230–400 mesh, Merck KGA) impregnated with a fluorescent indicator (254 nm). In special cases (so noted), analytical TLC was performed with aminopropyl-modified silica gel (NH₂ silica gel, 60-Å pore size, Wako Chemicals USA) impregnated with a fluorescent indicator (254 nm). TLC plates were visualized by exposure to ultraviolet light (UV) and/or exposure to iodine vapor (I₂), basic aqueous potassium permanganate solution (KMnO₄), acidic ethanolic *para*-anisaldehyde solution (PAA), acidic aqueous ceric ammonium molybdate solution (CAM), or ethanolic solution of phosphomolybdic acid (PMA) followed by brief heating on a hot plate as needed (~200 °C, ≤15 s).¹⁰⁶ In some cases, reaction

¹⁰⁵ Still, W. C.; Khan, M.; Mitra, A. *J. Org. Chem.* **1978**, *43*, 2923–2925.

¹⁰⁶ Sanford, M. TLC stains. umich.edu/~mssgroup/docs/TLCStains.pdf (accessed April 14, 2018).

monitoring was carried out by analytical liquid chromatography–mass spectrometry (LCMS), or by flow-injection analysis–high-resolution mass spectrometry (FIA-HRMS).

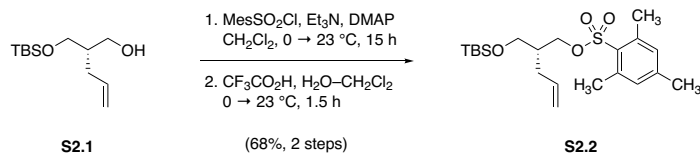
Materials. Commercial reagents and solvents were used as received, unless mentioned otherwise. Dichloromethane, diethyl ether, tetrahydrofuran, 1,4-dioxane, *N,N*-dimethylformamide, toluene, and benzene were purified by passage through Al₂O₃ under argon, according to the method of Pangborn and co-workers.¹⁰⁷ 7-Chloro-methylthiolincosamine (MTL, **1.29**) was prepared as described by Lewis and co-workers.⁶⁸ Mesitylenesulfonyl chloride, trifluoroacetic acid, Dess–Martin periodinane, hexamethyldisilazane, di-*tert*-butyl dicarbonate, and HATU were purchased from Oakwood Products, Inc. (Estill, SC, USA). 4-(*tert*-Butylthio)phenylboronic acid was purchased from Alchem Pharmtech, Inc. (Monmouth Junction, NJ, USA). Ethylene gas (ultra-high purity) was purchased from Airgas (Radnor, PA, USA). Allyl ethyl carbonate was purchased from TCI America (Portland, OR, USA). All other chemicals and reagents were purchased from Sigma-Aldrich Corporation (Natick, MA, USA).

Instrumentation. Proton nuclear magnetic resonance (¹H NMR) spectra and carbon nuclear magnetic resonance (¹³C NMR) spectra were recorded on Varian Mercury 400 (400 MHz/100 MHz), Varian Inova 500 (500 MHz/125 MHz), or Varian Inova 600 (600 MHz/150 MHz) NMR spectrometers at 23 °C. Proton chemical shifts are expressed in parts per million (ppm, δ scale) and are referenced to residual protium in the NMR solvent (CHCl₃, δ 7.26; CHD₃OD, δ 3.31;

¹⁰⁷ Pangborn, A. B.; Giardello, M. A.; Grubbs, R. H.; Rosen, R. K.; Timmers, F. J. *Organometallics* **1996**, *15*, 1518–1520.

C₆H₅D, δ 7.16). Carbon chemical shifts are expressed as parts per million (ppm, δ scale) and are referenced to the carbon resonance of the NMR solvent (CDCl₃, δ 77.2; CD₃OD, δ 49.0; C₆D₆, δ 128.1). Data are reported as follows: Chemical shift, multiplicity (s = singlet, d = doublet, t = triplet, q = quartet, qn = quintet, dd = doublet of doublets, td = triplet of doublets, ABq = AB quartet, m = multiplet, br = broad, app = apparent), integration, and coupling constant (*J*) in Hertz (Hz). Infrared transmittance (IR) spectra were obtained using a Bruker ALPHA FTIR spectrophotometer referenced to a polystyrene standard. Data are represented as follows: Frequency of absorption (cm⁻¹), and intensity (s = strong, m = medium, br = broad). Melting points were determined using a Thomas Scientific capillary melting point apparatus. High-resolution mass spectrometry (including FIA-HRMS reaction monitoring) was performed at the Harvard University Mass Spectrometry Facility using a Bruker micrOTOF-QII mass spectrometer. X-ray crystallographic analysis was performed at the Harvard University X-Ray Crystallographic Laboratory by Dr. Shao-Liang Zheng. High-performance liquid chromatography–mass spectrometry (LCMS) was performed using an Agilent Technologies 1260-series analytical HPLC system in tandem with an Agilent Technologies 6120 Quadrupole mass spectrometer; a Zorbax Eclipse Plus reverse-phase C₁₈ column (2.1 × 50 mm, 1.8 μ m pore size, 600 bar rating; Agilent Technologies, Santa Clara, CA) was employed as stationary phase. LCMS samples were eluted at a flow rate of 650 μ L/min, beginning with 5% acetonitrile–water containing 0.1% formic acid, grading linearly to 100% acetonitrile containing 0.1% formic acid over 3 minutes, followed by 100% acetonitrile containing 0.1% formic acid for 2 minutes (5 minutes total run time).

For clarity, intermediates that have not been assigned numbers in the preceding text are numbered sequentially in the following section, beginning with **S2.1**.



Sulfonate ester S2.2.

A magnetically stirred solution of (–)-**S2.1** (15.0 g, 65.1 mmol, 1 equiv)⁸⁵ in dichloromethane (325 mL) was cooled to 0 °C before it was treated sequentially with triethylamine (11.8 mL, 85.0 mmol, 1.3 equiv), 4-(dimethylamino)pyridine (795 mg, 6.51 mmol, 0.100 equiv), and 2,4,6-trimethylbenzenesulfonyl chloride (17.1 g, 78.0 mmol, 1.20 equiv). The mixture was stirred at 0 °C for 15 min before the ice-water cooling bath was removed, and the mixture was allowed to warm to 23 °C overnight. After 15 h, TLC analysis (20% ethyl acetate–hexanes, KMnO₄) showed that no starting material remained. The mixture was poured into a separatory funnel containing water, and the mixture was shaken vigorously. The layers were separated, and the aqueous layer was extracted with ether (4 × 300 mL). The combined organic phases were then washed with saturated aqueous sodium bicarbonate solution (200 mL), dried over sodium sulfate, filtered, and concentrated to give *tert*-butyldimethylsilyl mesitylenesulfonate ester intermediate as a milky yellow oil.

This crude residue was transferred to a 2000-mL round-bottomed flask, where it was dissolved in dichloromethane (650 mL). Water (7.20 mL) was added, and the mixture was chilled to 0 °C before trifluoroacetic acid (36.0 mL) was introduced. The mixture was stirred at 0 °C for 15 minutes before the ice-water cooling bath was removed and the mixture was allowed to warm to 23 °C. After 1.5 h, TLC (20% ethyl acetate–hexanes, UV+KMnO₄) showed that no *tert*-butyldimethylsilyl ether intermediate remained. The mixture was diluted with toluene (250 mL), and the diluted mixture was concentrated in vacuo. The residue thus obtained was purified by

flash-column chromatography (1.0 kg silica gel, eluting with 20% diethyl ether–hexanes, grading to 50% diethyl ether–hexanes) to furnish the product as a colorless oil (13.3 g, 68%, 2 steps).

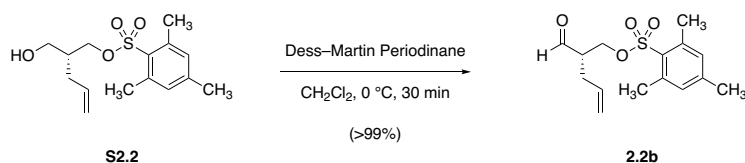
$R_f = 0.28$ (30% ethyl acetate–hexanes, UV+KMnO₄).

¹H NMR (500 MHz, CDCl₃) δ 6.98 (s, 2H), 5.70 (ddt, $J = 17.4, 9.8, 7.2$ Hz, 1H), 5.05–5.01 (m, 2H), 4.05 (dd, $J = 9.9, 4.7$ Hz, 1H), 3.97 (dd, $J = 9.9, 5.8$ Hz, 1H), 3.67 (dd, $J = 11.2, 4.8$ Hz, 1H), 3.60 (dd, $J = 11.1, 6.5$ Hz, 1H), 2.63 (s, 6H), 2.32 (s, 3H), 2.15–2.06 (m, 2H), 1.97–1.89 (m, 1H).

¹³C NMR (126 MHz, CDCl₃) δ 143.5, 140.0, 135.2, 131.9, 130.6, 117.6, 68.9, 61.9, 40.4, 32.1, 22.8, 21.2.

FTIR (neat, cm⁻¹): 3420 (br), 2940 (w), 1604 (2), 1351 (m), 1190 (m), 1173 (s), 1036 (m), 966 (m), 814 (m), 664 (m).

HRMS (ESI+, m/z): [M+H]⁺ calc'd for C₁₅H₂₂O₄S, 299.1312; found 299.1322.



Aldehyde 2.2b.

A magnetically stirred solution of alcohol **S2.2** (3.00 g, 10.1 mmol, 1 equiv) in dichloromethane (50.3 mL) was cooled to 0 °C in an ice-water bath before Dess–Martin periodinane (4.26 g, 10.1 mmol, 1.00 equiv) was added in one portion. After stirring for 5 min at 0 °C, the cooling bath was removed, and the mixture was allowed to warm to 23 °C. After 30 min, TLC analysis (40% ethyl acetate–hexanes, UV+KMnO₄) indicated that no starting material remained. Saturated aqueous sodium bicarbonate (25 mL) was added, and the mixture was stirred at 23 °C for 3 min before aqueous sodium thiosulfate solution (4.0 M, 25 mL) was added. The resulting mixture was stirred vigorously at 23 °C for 30 min before it was transferred to a separatory funnel, where the layers were separated. The aqueous phase was extracted with dichloromethane (2 × 20 mL), and the combined organic layers were washed sequentially with fresh saturated aqueous sodium bicarbonate solution (20 mL) and saturated aqueous sodium chloride solution (20 mL). The washed organic solution was then dried over sodium sulfate, filtered, and concentrated to provide the product as a cloudy oil (3.01 g, 101%). This material analytically pure and was suitable for use without further processing.

$R_f = 0.54$ (40% ethyl acetate–hexanes, UV+KMnO₄).

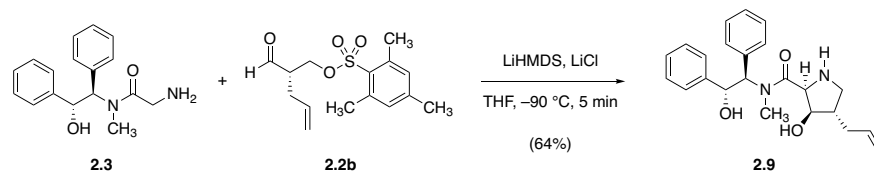
¹H NMR (600 MHz, CDCl₃) δ 9.63 (d, $J = 1.0$ Hz, 1H), 6.98 (s, 2H), 5.67 (ddt, $J = 17.2, 10.3, 7.0$ Hz, 1H), 5.10–5.06 (m, 2H), 4.20 (dd, $J = 10.2, 6.0$ Hz, 1H), 4.16 (dd, $J = 10.2, 5.0$ Hz,

1H), 2.76–2.71 (m, 1H), 2.59 (s, 6H), 2.49 (dtt, 14.6, 6.6, 1.4 Hz, 1H), 2.34–2.29 (m, 1H),
2.31 (s, 3H).

¹³C NMR (151 MHz, CDCl₃) δ 200.5, 143.7, 140.1, 133.1, 131.9, 130.2, 118.9, 66.1, 50.2, 29.9,
22.7, 21.2.

FTIR (neat, cm⁻¹): 1727 (m), 1604 (w), 1355 (s), 1190 (s), 1175 (s), 977 (m), 929 (m), 807 (m),
663 (m).

HRMS (ESI+, *m/z*): [M+Na]⁺ calc'd for C₁₅H₂₀O₄S, 319.0975; found 319.0971.



Pseudoephedrine β -hydroxyprolinamide **2.9**.

An oven-dried 500-mL round-bottomed flask was charged with a magnetic stir bar and anhydrous lithium chloride (6.23 g, 147 mmol, 15.6 equiv). The vessel was then evacuated (0.1 mmHg), heated with a gentle flame for 2 min in order to drive off any residual moisture from the lithium chloride, and allowed to cool to room temperature before it was back-filled with argon. Next, (*R,R*)-pseudoephedrine glycinamide (**2.3**, 3.48 g, 12.3 mmol, 1.30 equiv) and tetrahydrofuran (131 mL) were added, and the mixture was stirred for 5 min at $23\text{ }^{\circ}\text{C}$, until all pseudoephedrine glycinamide had dissolved (lithium chloride does not completely dissolve). The mixture was then chilled to $-78\text{ }^{\circ}\text{C}$ in a dry ice–acetone bath, and a freshly prepared solution of lithium hexamethyldisilazide (1.00 M in tetrahydrofuran, 23.6 mL, 23.6 mmol, 2.50 equiv) was added dropwise over a period of 3–4 min. The resulting yellow mixture was stirred at $-78\text{ }^{\circ}\text{C}$ for 5 min before it was warmed to $0\text{ }^{\circ}\text{C}$ for a period of 30 min. The glycinamide enolate solution was then chilled to $-90\text{ }^{\circ}\text{C}$ in an acetone bath cooled with liquid nitrogen, and a solution of aldehyde **2.2b** (2.79 g, 9.42 mmol, 1 equiv) in tetrahydrofuran (10.1 mL) was added via cannula over 2 min. After stirring at $-90\text{ }^{\circ}\text{C}$ for 5 min following complete addition of the electrophile, the reaction was quenched with the addition of half-saturated aqueous ammonium chloride solution (1.00 mL), causing the vibrant yellow color to darken to orange-yellow. The cooling bath was removed, and the mixture was warmed to $23\text{ }^{\circ}\text{C}$ before the mixture was transferred to a separatory funnel containing half-saturated aqueous ammonium chloride solution (200 mL) and ethyl acetate (200 mL). The layers were shaken, then separated, and the aqueous phase was extracted with additional

portions of ethyl acetate (3×100 mL). The combined organic extracts were washed with saturated sodium chloride solution, dried over sodium sulfate, filtered, and concentrated to provide a foaming straw-colored solid, which was purified by flash-column chromatography (330 g silica gel, eluting with 1% ammonium hydroxide–3% methanol–dichloromethane initially, grading to 1% ammonium hydroxide–4% methanol–dichloromethane) to provide the product as a snow-white, foaming solid (2.31 g, 64%), along with recovered pseudoephedrine glycinate (1.28 g).

Crystals suitable for single-crystal X-ray diffraction analysis were prepared as follows: In a 1-mL glass sample vial, pure **2.9** (10 mg) was deposited, and this material was dissolved in a minimal quantity of methanol. A drop of benzene was added to this solution, and the vial was partially sealed with a screw cap, leaving the cap slightly ajar so as to allow slow evaporation of solvent. After several days of standing at 23 °C, needle-shaped crystals had formed (see Appendix A for X-ray crystal structure data).

Melting point: 135–137 °C.

$R_f = 0.21$ (1% ammonium hydroxide–10% methanol–dichloromethane, UV+PMA).

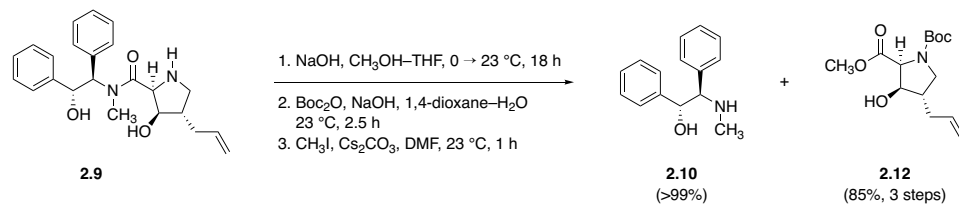
^1H NMR (52:48 mixture of rotamers, asterisks [*] denote minor rotameric signals that could be resolved, 600 MHz, CD_3OD) δ 7.40–7.32 (m, 4H), 7.24–7.12 (m, 6H), 5.93 (ddt, $J = 17.0, 10.2, 6.9$ Hz, 1H), 5.90 (d, $J = 8.5$ Hz, 1H),* 5.81 (ddt, $J = 16.9, 10.2, 6.7$ Hz, 1H),* 5.46 (d, $J = 8.7$ Hz, 1H),* 5.45 (d, $J = 10.1$ Hz, 1H), 5.19 (d, $J = 10.3$ Hz, 1H), 5.18 (app dq, $J = 17.0, 1.7$ Hz, 1H), 5.10 (ddt, $J = 10.4, 2.2, 1.1$ Hz, 1H),* 5.07 (app dq, $J = 16.9, 1.5$ Hz, 1H), 5.01 (ddt, $J = 10.2, 2.0, 1.1$ Hz, 1H), 4.62 (dd, $J = 5.8, 4.0$ Hz, 1H),* 4.36 (d, $J = 5.8$ Hz, 1H),* 4.18 (dd, $J = 6.2, 3.7$ Hz, 1H), 4.04 (d, $J = 6.1$ Hz, 1H), 3.36 (dd, $J = 11.6, 7.3$

Hz, 1H), 3.30 (dd, $J = 12.9, 6.5$ Hz, 1H),* 3.08 (s, 3H), 3.06 (s, 3H),* 2.48 (dd, $J = 11.6, 8.2$ Hz, 1H), 2.43 (dd, $J = 11.4, 6.6$ Hz, 1H), 2.42–2.37 (m, 1H),* 2.30–2.25 (m, 2H), 2.17 (app pd, $J = 74, 3.9$ Hz, 1H),* 2.08–2.03 (m, 2H).

^{13}C NMR (52:48 mixture of rotamers, asterisks [*] denote rotameric signals that could be resolved, 126 MHz, CD_3OD) δ 172.6, 171.2,* 143.3,* 142.5, 138.6,* 138.0, 137.7, 137.3,* 130.3, 129.9, 129.6,* 129.4, 129.2 ($2 \times \text{C}$),* 129.1 ($2 \times \text{C}$), 128.6 ($2 \times \text{C}$), 128.6,* 128.3, 116.7,* 116.6, 79.0,* 78.3, 73.3, 72.6,* 66.9,* 65.9, 64.3,50.8,* , 50.1, 49.9, 49.9,* 37.2,* 36.9, 32.1,* 29.0.

FTIR (neat, cm^{-1}): 3292 (br), 2930 (w), 1639 (s), 1453 (m), 1394 (m), 1087 (m), 1062 (m), 699 (m).

HRMS (ESI+, m/z): $[\text{M}+\text{H}]^+$ calc'd for $\text{C}_{23}\text{H}_{28}\text{N}_2\text{O}_3$, 381.2173; found 381.2182.



Auxiliary cleavage and synthesis of protected proline **2.12**.

A magnetically stirred solution of hydroxyprolinamide **2.9** (2.31 g, 6.07 mmol, 1 equiv) in 50% v/v methanol–tetrahydrofuran (30.4 mL) was chilled to 0 °C before aqueous sodium hydroxide solution (1.00 M, 6.19 mL, 6.19 mmol, 1.02 equiv) was added dropwise. The cooling bath was then removed, and the mixture was allowed to warm to 23 °C overnight. After 18 h, LCMS analysis showed that not all starting material had been consumed (estimated 80% conversion), and the mixture was heated to 40 °C for 5 h to drive the reaction to completion. Once it was confirmed that no starting material remained, the reaction mixture was concentrated in vacuo to give a tan-colored sludge, which was re-dissolved in water (100 mL). In order to recover the chiral auxiliary, this aqueous mixture was extracted with dichloromethane (4 × 25 mL), and the combined dichloromethane extracts were dried over sodium sulfate, filtered, and concentrated to provide analytically pure (*R,R*)-pseudoephedrine (**2.10**, 1.31 g, 95%).⁵ The aqueous mixture was concentrated separately, and residual water was removed by azeotropic distillation from methanol in vacuo. This provided the sodium pyrrolidinecarboxylate salt as a dull brown solid (1.21 g, 103%).

A portion of this this crude residue (0.900 g, 4.66 mmol) was transferred to a 200-mL round-bottomed flask, where it was dissolved in 50% v/v 1,4-dioxane–water (38.8 mL). Aqueous sodium hydroxide (1.00 M, 6.99 mL, 6.99 mmol, 1.50 equiv) and di-*tert*-butyl dicarbonate (2.16 mL, 9.32 mmol, 2.00 equiv) were added, and the mixture was stirred at 23 °C. After 2.5 h, LCMS analysis showed that *N*-Boc protection was complete, and the mixture was diluted with water (100

mL). The diluted mixture was washed with ether (3×30 mL) in order to remove excess di-*tert*-butyl dicarbonate before the washed aqueous solution was chilled to 0 °C. The aqueous solution was acidified to pH = 2 with the dropwise addition of 1N aqueous hydrogen chloride solution, and the acidified mixture was extracted with ethyl acetate (4×25 mL) to recover *N*-Boc-protected amino acid as a white solid.

This material was finally transferred to a 100-mL round-bottomed flask, where it was dissolved in *N,N*-dimethylformamide (17.2 mL). Cesium carbonate (1.59 g, 4.88 mmol, 1.05 equiv) was added in one portion, followed by methyl iodide (348 μ L, 5.57 mmol, 1.20 equiv), which was added dropwise at 23 °C. After 1 h of stirring, LCMS analysis showed that methylation of the starting material was complete, and the mixture was diluted with ethyl acetate (50 mL), causing a white precipitate to form. This suspension was transferred to a separatory funnel containing saturated aqueous sodium bicarbonate solution (50 mL), and the layers were shaken. The layers were then separated, the aqueous phase was extracted with additional ethyl acetate (3×20 mL), and the combined organic layers were washed with saturated aqueous sodium chloride (2×20 mL). The washed organic solution was then dried over sodium sulfate, filtered, and concentrated to provide a viscous oil, which was purified by flash-column chromatography (80 g silica gel, eluting with 30% ethyl acetate–hexanes initially, grading to 40% ethyl acetate–hexanes) to furnish *N*-Boc-protected hydroxyproline methyl ester **2.12** as a colorless, highly viscous oil (1.29 g, 97%, 2 steps).

$R_f = 0.30$ (40% ethyl acetate–hexanes, KMnO_4).

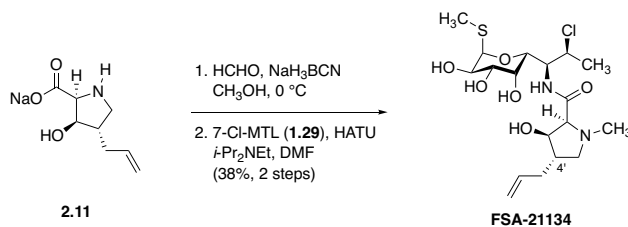
^1H NMR (60:40 mixture of rotamers, asterisks [*] denote minor rotameric signals that could be resolved, 600 MHz, CDCl_3) δ 5.80 (ddt, $J = 16.9, 10.0, 7.34$ Hz, 1H), 5.11 (d, $J = 17.0$ Hz,

1H), 5.06 (d, $J = 10.2$ Hz, 1H), 4.46 (d, $J = 7.8$ Hz, 1H),* 4.38 (d, $J = 7.5$ Hz, 1H), 4.18 (app dtd, $J = 12.9, 7.5, 4.9$ Hz, 1H), 3.79 (dd, $J = 10.9, 7.5$ Hz, 1H), 3.77 (s, 3H),* 3.76 (s, 3H), 3.72 (dd, $J = 10.8, 7.7$ Hz, 1H),* 3.07 (dd, $J = 10.7, 7.6$ Hz, 1H), 3.04 (dd, $J = 8.6, 2.5$ Hz, 1H),* 2.39–2.30 (m, 2H), 2.25–2.15 (m, 1H), 2.13–2.06 (m, 1H), 1.45 (s, 9H)* 1.40 (s, 9H).

^{13}C NMR (60:40 mixture of rotamers, asterisks [*] denote minor rotameric signals that could be resolved, 126 MHz, CDCl_3) δ 171.3, 171.2,* 154.4,* 153.9, 135.6,* 135.5, 117.0, 116.9,* 80.4, 80.3,* 75.8, 75.0,* 63.5, 62.9,* 52.2,* 52.0, 49.2,* 48.7, 35.1, 28.4,* 28.3.

IR (neat, cm^{-1}): 3439 (br), 2977 (m), 1749 (m), 1701 (s), 1677 (s), 1402 (s), 1368 (m), 1207 (m), 1177 (s), 915 (w).

HRMS (ESI+, m/z): $[\text{M}+\text{Na}]^+$ calc'd for $\text{C}_{14}\text{H}_{23}\text{NO}_5$, 308.1468; found 308.1476.



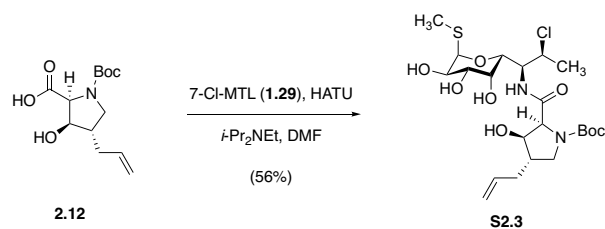
Synthetic lincosamide FSA-21134.

To a solution of sodium carboxylate **2.11** (10.8 mg, 52.1 μmol , 1 equiv) in *N,N*-dimethylformamide (522 μL) was added HATU (21.8 mg, 57.4 μmol , 1.10 equiv) at 23 $^{\circ}\text{C}$. After stirring the resulting colorless solution for 10 min, 7-Cl-MTL (**1.29**, 21.3 mg, 78.3 μmol , 1.50 equiv) was added. After the resulting yellow solution was stirred for 20 min, diisopropylethylamine (22.8 μL , 131 μmol , 2.50 equiv) was added. After 1 h, LCMS analysis indicated that coupling was complete, and the mixture was concentrated to dryness in vacuo. The residue was purified by flash-column chromatography (10 g silica gel, eluting with 1% ammonium hydroxide–5% methanol–dichloromethane initially, grading to 1% ammonium hydroxide–10% methanol–dichloromethane) to provide **FSAS-21134** as a colorless film (9.7 mg, 42%).

R_f = 0.22 (1% ammonium hydroxide–10% methanol–dichloromethane, PMA).

^1H NMR (600 MHz, CD_3OD) δ 5.84 (ddt, J = 16.9, 10.1, 6.8 Hz, 1H), 5.30 (d, J = 5.6 Hz, 1H), 5.10 (dq, J = 16.8, 1.6 Hz, 1H), 5.03 (dq, J = 10.2, 1.4 Hz, 1H), 4.64 (qd, J = 6.8, 1.5 Hz, 1H), 4.42 (dd, J = 9.5, 0.7 Hz, 1H), 4.20–4.16 (m, 2H), 4.07 (dd, J = 10.2, 5.6 Hz, 1H), 4.03 (d, J = 3.8 Hz, 1H), 3.58 (dd, J = 10.2, 3.4 Hz, 1H), 3.38 (br, 1H), 3.21 (br, 1H), 2.46 (br, 3H), 2.38–2.34 (m, 1H), 2.21–2.16 (m, 1H), 2.14 (s, 3H), 2.12–2.09 (m, 1H), 1.50 (d, J = 6.8 Hz, 3H).

HRMS (ESI+, m/z): $[\text{M}+\text{H}]^+$ calc'd for $\text{C}_{18}\text{H}_{31}\text{ClN}_2\text{O}_6\text{S}$, 439.1664; found 439.1667.



Protected lincosamide S2.3.

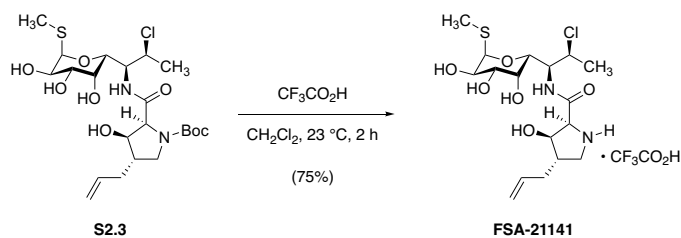
In a 25-mL round-bottomed flask, hydroxyproline **2.12** (36.5 mg, 135 μmol , 1 equiv) was dissolved in *N,N*-dimethylformamide (673 μL). To this solution was added HATU (56.3 mg, 148 μmol , 1.10 equiv); the resulting solution was stirred for 10 min at 23 $^{\circ}\text{C}$ before 7-Cl-MTL (**1.29**, 54.8 mg, 202 μmol , 1.50 equiv) was added as well. After 20 min, diisopropylethylamine (58.7 μL , 336 μmol , 2.50 equiv) was finally added, which caused the solution to gradually attain a canary-yellow color. After 3 h of stirring at 23 $^{\circ}\text{C}$, LCMS analysis indicated that the reaction was complete, and the mixture was partitioned between saturated aqueous sodium chloride solution (8 mL) and ethyl acetate (10 mL). The layers were shaken, then separated, and the aqueous layer was extracted with fresh portions of ethyl acetate (2×10 mL). The combined organic extracts were dried over sodium sulfate, filtered, and concentrated. The crude product mixture was then purified by flash-column chromatography (6 g silica gel, eluting with 10% methanol–dichloromethane) to provide the product as a white solid (39.5 mg, 56%).

$R_f = 0.15$ (10% methanol–dichloromethane, PMA).

^1H NMR (complex rotameric mixture, asterisks [*] denotes rotameric signals that could be resolved, 500 MHz, CDCl_3) δ 5.83 (ddt, $J = 17.0, 9.6, 7.0$ Hz, 1H), 5.29 (d, $J = 5.6$ Hz, 1H), 5.09 (dt, $J = 17.2, 1.9$ Hz, 1H), 5.04 (dd, $J = 10.3, 2.0$ Hz, 1H), 4.64–4.56 (m, 1H), 4.50–4.46 (m, 1H),* 4.42 (br d, $J = 9.9$ Hz, 1H), 4.35 (br d, $J = 7.3$ Hz, 1H),* 4.24 (br d, J

= 9.8 Hz, 1H), 4.19 (br d, $J = 9.8$ Hz, 1H),* 4.15 (app t, $J = 7.4$ Hz, 1H), 4.10–4.05 (m, 2H), 3.96–3.91 (m, 1H),* 3.74–3.64 (m, 1H), 3.59–3.57 (m, 1H), 3.13–3.10 (m, 1H), 2.45–2.28 (m, 2H), 2.15 (s, 3H),* 2.14 (s, 3H), 2.00–1.94 (m, 1H), 1.59–1.53 (m, 3H), 1.47 (s, 9H).

MS (ESI⁻, m/z): [M-H]⁻ calc'd for C₂₂H₃₇ClN₂O₈S, 523.2; found 523.2.

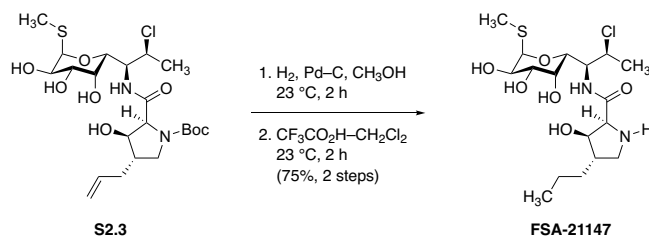


Synthetic lincosamide FSA-21141.

In a 4-mL glass vial fitted with a magnetic stir bar, *N*-Boc-protected lincosamide **S2.3** (15.5 mg, 29.5 μmol , 1 equiv) was dissolved in 20% v/v trifluoroacetic acid–dichloromethane (600 μL) at 23 $^\circ\text{C}$. After stirring at 23 $^\circ\text{C}$ for 2 h, LCMS analysis indicated that *N*-Boc removal was complete. The mixture was diluted with toluene (1 mL) and the diluted mixture was concentrated to dryness in vacuo. The dried residue was triturated with dichloromethane ($2 \times 1\text{ mL}$) to provide **FSA-21141** \cdot $\text{CF}_3\text{CO}_2\text{H}$ (11.9 mg, 75%) as a white solid.

^1H NMR (600 MHz, CD_3OD) δ 5.85 (ddt, $J = 17.2, 10.3, 6.8\text{ Hz}$, 1H), 5.31 (d, $J = 5.7\text{ Hz}$, 1H), 4.18 (app dq, $J = 17.1, 1.6\text{ Hz}$, 1H), 5.15 (ddt, $J = 10.2, 2.0, 1.2\text{ Hz}$, 1H), 4.59–4.55 (m, 2H), 4.46 (dd, $J = 5.1, 2.8\text{ Hz}$, 1H), 4.41 (d, $J = 5.1\text{ Hz}$, 1H), 4.30 (dd, $J = 10.0, 1.2\text{ Hz}$, 1H), 4.10 (dd, $J = 10.2, 5.7\text{ Hz}$, 1H), 3.85 (dd, $J = 3.4, 1.2\text{ Hz}$, 1H), 3.68 (dd, $J = 11.9, 7.3\text{ Hz}$, 1H), 3.59 (dd, $J = 10.2, 3.3\text{ Hz}$, 1H), 3.08 (dd, $J = 11.8, 4.8\text{ Hz}$, 1H), 2.46–2.41 (m, 1H), 2.32–2.28 (m, 1H), 2.15 (s, 3H), 2.15–2.09 (m, 1H), 1.53 (d, $J = 6.8\text{ Hz}$, 3H).

HRMS (ESI+, m/z): $[\text{M}+\text{H}]^+$ calc'd for $\text{C}_{17}\text{H}_{29}\text{ClN}_2\text{O}_6\text{S}$, 425.1508; found 425.1517.



Synthetic lincosamide FSA-21147

In a 4-mL glass vial fitted with a magnetic stir bar, olefin **S2.3** (11.1 mg, 21.1 mg, 1 equiv) was dissolved in methanol (420 μL). To this solution was added palladium on carbon (10% w/w, 5 mg), and hydrogen gas was bubbled through the resulting black suspension. After 5 min, bubbling was discontinued, and the mixture was stirred rapidly (700 rpm) under 1 atm of hydrogen gas (supplied by a balloon). After 2 h, LCMS analysis indicated that hydrogenation was complete, and the mixture was filtered through a pad of Celite to remove the heterogeneous catalyst. The filter cake was rinsed with fresh portions of methanol ($3 \times 1 \text{ mL}$), and the filtrate was concentrated to give 4'-*n*-propyl *N*-Boc-protected lincosamide intermediate.

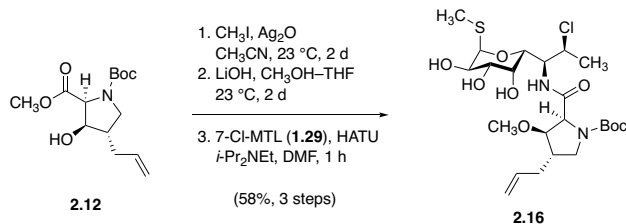
This intermediate was transferred to a clean 4-mL glass vial, where it was dissolved in 20% v/v trifluoroacetic acid–dichloromethane (500 μL). The resulting solution was stirred at 23 $^\circ\text{C}$ for 2 h, at which point LCMS analysis indicated that *N*-Boc removal was complete. Toluene (1 mL) was added, and the diluted mixture was concentrated to dryness in vacuo. The dried residue was purified by flash-column chromatography (6 g silica gel, eluting with 1% ammonium hydroxide–8% methanol–dichloromethane) to provide the product as a colorless film (6.8 mg, 75%, 2 steps).

^1H NMR (500 MHz, CD_3OD) δ 5.29 (d, $J = 5.6 \text{ Hz}$, 1H), 4.62 (qd, $J = 6.7, 1.6 \text{ Hz}$, 1H), 4.38 (dd, $J = 10.0, 1.6 \text{ Hz}$, 1H), 4.20–4.17 (m, 2H), 4.08 (dd, $J = 10.2, 5.6 \text{ Hz}$, 1H), 3.95 (dd, $J = 3.5, 1.1 \text{ Hz}$, 1H), 3.86 (d, $J = 5.6 \text{ Hz}$, 1H), 3.57 (dd, $J = 10.2, 3.4 \text{ Hz}$, 1H), 2.69 (dd, $J = 10.8,$

4.7 Hz, 1H), 2.14 (s, 3H), 2.07–2.01 (m, 1H), 1.49 (d, $J = 6.8$ Hz, 3H), 1.43–1.37 (m, 3H),
1.30–1.24 (m, 2H), 0.96 (t, $J = 7.1$ Hz, 3H).

^{13}C NMR (126 MHz, CD_3OD) δ 175.0, 89.6, 79.0, 71.8, 71.1, 69.6 (2 \times C), 66.3, 59.2, 54.3, 50.8,
35.1, 22.8, 22.1, 14.5, 13.3.

HRMS (ESI+, m/z): $[\text{M}+\text{H}]^+$ calc'd for $\text{C}_{17}\text{H}_{31}\text{ClN}_2\text{O}_6\text{S}$, 426.2; found 426.2.

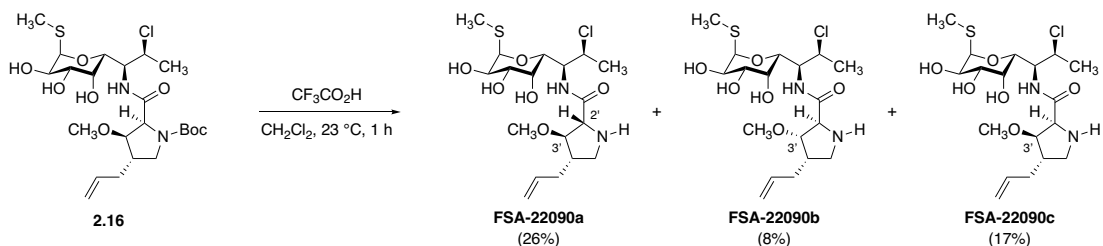


Protected lincosamide **2.16**.

In a 4-mL glass vial fitted with a magnetic stir bar, hydroxyproline **2.12** (50.0 mg, 175 μmol , 1 equiv) was dissolved in acetonitrile (1.46 mL). To this solution, silver(I) oxide (207 mg, 894 μmol , 5.10 equiv) and iodomethane (112 μL , 1.79 mmol, 10.2 equiv) were added sequentially; the reaction vial was then capped with a PTFE-lined screw cap and was shielded from light with aluminum foil. After 2 d of stirring at 23 °C, TLC analysis (50% ethyl acetate–hexanes, KMnO_4) demonstrated that all starting material had been consumed. The mixture was filtered through a 0.2- μm PTFE filter in order to remove all insoluble silver salts, and the filtrate was concentrated in vacuo to provide *O*-methylated intermediate (47.3 mg, 158 μmol , 90%).

This material was transferred to a clean 4-mL glass vial, where it was dissolved in 50% v/v methanol–tetrahydrofuran (786 μL). Aqueous lithium hydroxide solution (1.00 M, 157 μL , 157 μmol , 1.00 equiv) was then added at 23 °C, and the mixture was stirred for 2 d, until LCMS analysis indicated that saponification was complete. The reaction mixture was then diluted with water (3 mL), cooled to 0 °C, and acidified to pH = 2 with the addition of aqueous hydrogen chloride solution (1N). The acidified solution was extracted with ethyl acetate (4 \times 3 mL), and the combined organic extracts were dried over sodium sulfate. The dried organic product solution was then filtered, and the filtrate was concentrated to provide carboxylic acid intermediate (46.8 mg, 104%).

This material was transferred to a 2–5 mL glass microwave vial fitted with a magnetic stir bar, where it was dissolved in *N,N*-dimethylformamide (820 μ L). To this solution, HATU (68.6 mg, 180 μ mol, 1.10 equiv) was added, followed by 7-Cl-MTL (**1.29**, 66.9 mg, 246 μ mol, 1.50 equiv) 10 minutes later. Finally, diisopropylethylamine (71.6 μ L, 410 μ mol, 2.50 equiv) was added to the canary-yellow solution, and the mixture was stirred for 1 h, at which point LCMS analysis indicated that the amide coupling reaction was complete. The mixture was concentrated in vacuo, and the dried residue was purified by flash-column chromatography (10 g silica gel, eluting with dichloromethane initially, grading to 5% methanol–dichloromethane) to provide *N*-Boc lincosamide product (R_f = 0.50, 10% methanol–dichloromethane, PMA) as a white solid (54.4 mg, 58%, 3 steps). This material was carried forward through *N*-Boc removal without further purification or characterization.



Synthetic lincosamides FSA-22090a, FSA-22090b, and FSA-22090c.

In a 2–5 mL glass microwave vial fitted with a magnetic stir bar, **2.16** (54.0 mg, 100 μmol , 1 equiv) was dissolved in 10% v/v trifluoroacetic acid–dichloromethane (1.10 mL) at 23 $^\circ\text{C}$. After stirring for 1 h, LCMS analysis indicated that *N*-Boc removal was complete, and that several diastereomeric products had been formed. Toluene (1 mL) was added, and the mixture was concentrated to dryness in vacuo. The residue thus obtained was purified by preparative HPLC on a Waters SunFire prep C₁₈ column (5 μm , 250 \times 19 mm; eluting with 0.1% trifluoroacetic acid–water initially, grading to 0.1% trifluoroacetic acid–40% acetonitrile–water over 40 min, with a flow rate of 15 mL/min; monitored by UV absorbance at 210 nm) to provide in order of elution, the diastereomeric products **FSA-22090a** \cdot CF₃CO₂H (14.6 mg, 26%), **FSA-22090b** \cdot CF₃CO₂H (4.6 mg, 8%), and **FSA-22090c** \cdot CF₃CO₂H (9.6 mg, 17%) as white solids. The relative C2' and C3' configurations were established by 1D nuclear Overhauser effect ¹H-NMR analysis (data not shown).

FSA-22090a \cdot CF₃CO₂H:

¹H NMR (600 MHz, CD₃OD) δ 5.82 (dddd, $J = 17.2, 10.1, 7.3, 6.4$ Hz, 1H), 5.31 (d, $J = 5.6$ Hz, 1H), 5.18 (app dq, $J = 17.5, 1.6$ Hz, 1H), 5.12 (app dq, $J = 10.0, 1.1$ Hz, 1H), 4.59–4.56 (m, 2H), 4.40 (dd, $J = 9.7, 1.4$ Hz, 1H), 4.31 (d, $J = 3.4$ Hz, 1H), 4.09 (dd, $J = 10.1, 5.6$ Hz, 1H), 3.91 (app t, $J = 3.4$ Hz, 1H), 3.82 (dd, $J = 1.4$ Hz, 1H), 3.61 (dd, $J = 10.2, 3.3$ Hz,

1H), 3.56 (dd, $J = 11.7, 7.8$ Hz, 1H), 3.47 (s, 3H), 3.33–3.31 (m, 1H), 2.55–2.37 (m, 1H), 2.34 (app dtt, $J = 14.2, 6.3, 1.4$ Hz, 1H), 2.22–2.17 (m, 1H), 2.16 (s, 3H).

^{13}C NMR (126 MHz, CD_3OD) δ 168.4, 136.2, 118.2, 89.8, 89.0, 72.1, 70.3, 70.1, 69.4, 66.3, 59.2, 58.2, 55.1, 50.3, 44.1, 35.9, 23.1, 13.5.

FTIR (neat, cm^{-1}): 3339 (br), 1673 (s), 1542 (w), 1201 (s), 1135 (s).

HRMS (ESI+, m/z): $[\text{M}+\text{Na}]^+$ calc'd for $\text{C}_{18}\text{H}_{31}\text{ClN}_2\text{O}_6\text{S}$, 461.1484; found 461.1487.

FSA-22090b • $\text{CF}_3\text{CO}_2\text{H}$:

^1H NMR (600 MHz, CD_3OD) δ 5.85 (ddt, $J = 17.1, 10.2, 6.9$ Hz, 1H), 5.30 (d, $J = 5.6$ Hz, 1H), 5.14 (app dq, $J = 17.4, 1.5$ Hz, 1H), 5.08 (app dq, $J = 10.2, 1.8$ Hz, 1H), 4.58–4.56 (m, 2H), 4.40 (d, $J = 10.5$ Hz, 1H), 4.08 (dd, $J = 10.1, 5.6$ Hz, 1H), 4.01 (d, $J = 3.8$ Hz, 1H), 3.74 (dd, $J = 3.2, 1.4$ Hz, 1H), 3.61 (dd, $J = 10.2, 3.3$ Hz, 1H), 3.57 (dd, $J = 11.1, 8.6$ Hz, 1H), 3.52 (s, 3H), 3.06 (app t, $J = 11.0$ Hz, 1H), 2.50–2.44 (m, 1H), 2.40–2.36 (m, 1H), 2.25–2.20 (m, 1H), 2.16 (s, 3H), 1.49 (d, $J = 6.8$ Hz, 3H).

FTIR (neat, cm^{-1}): 3339 (br), 1672 (s), 1201 (s), 1137 (s).

HRMS (ESI+, m/z): $[\text{M}+\text{H}]^+$ calc'd for $\text{C}_{18}\text{H}_{31}\text{ClN}_2\text{O}_6\text{S}$, 439.1664; found 439.1680.

FSA-22090c • $\text{CF}_3\text{CO}_2\text{H}$:

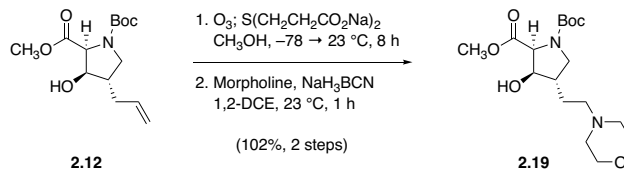
^1H NMR (600 MHz, CD_3OD) δ 5.85 (ddt, $J = 17.1, 10.2, 6.9$ Hz, 1H), 5.30 (d, $J = 5.6$ Hz, 1H), 5.14 (app dq, $J = 17.4, 1.6$ Hz, 1H), 5.08 (dd, $J = 10.2, 1.8$ Hz, 1H), 4.58–4.56 (m, 2H), 4.40 (d, $J = 10.5$ Hz, 1H), 4.08 (dd, $J = 10.1, 5.6$ Hz, 1H), 4.01 (d, $J = 3.8$ Hz, 1H), 3.74 (dd, $J = 3.2, 1.4$ Hz, 1H), 3.61 (dd, $J = 10.2, 3.3$ Hz, 1H), 3.57 (dd, $J = 11.1, 8.6$ Hz, 1H),

3.52 (s, 3H), 3.06 (app t, $J = 11.0$ Hz, 1H), 2.50–2.44 (m, 1H), 2.40–2.36 (m, 1H), 2.25–2.20 (m, 1H), 2.16 (s, 3H), 1.49 (d, $J = 6.7$ Hz, 3H).

^{13}C NMR (126 MHz, CD_3OD) δ 166.1, 135.8, 118.7, 89.8, 85.2, 72.2, 70.4, 69.7, 69.5, 64.8, 59.5, 57.6, 54.5, 43.2, 36.4, 22.7, 13.4.

FTIR (neat, cm^{-1}): 3331 (br), 1674 (s), 1201 (s), 1134 (m).

HRMS (ESI+, m/z): $[\text{M}+\text{H}]^+$ calc'd for $\text{C}_{18}\text{H}_{31}\text{ClN}_2\text{O}_6\text{S}$, 439.1664; found 439.1682.



Morpholino compound 2.19.

In a 25-mL round-bottomed flask fitted with a magnetic stir bar, a solution of olefin **2.12** (40.0 mg, 140 μmol , 1 equiv) in methanol (4.67 mL) was chilled to $-78\text{ }^\circ\text{C}$ in a dry ice–acetone cooling bath. Through this solution, an ozone–dioxygen gas mixture from an ozone generator was bubbled for approximately 5 minutes, until the reaction solution attained a persistent ultramarine coloration. Nitrogen was then bubbled through the mixture for 5 minutes in order to sparge the solution of residual ozone before sodium thiodipropionate (62.3 mg, 280 μmol , 2.00 equiv) was added at $-78\text{ }^\circ\text{C}$. The mixture was then removed from the cooling bath, and the mixture was allowed to warm to $23\text{ }^\circ\text{C}$ gradually. After 8 h, LCMS analysis indicated that no trioxolane intermediate remained, and the mixture was diluted with saturated aqueous sodium bicarbonate solution (20 mL). The resulting mixture was extracted with dichloromethane ($3 \times 15\text{ mL}$), and the combined organic extracts were washed with saturated aqueous sodium chloride solution (15 mL). The organic product solution was then dried over sodium sulfate, filtered, and concentrated to provide crude aldehyde as a colorless oil. This material was carried forward without further purification.

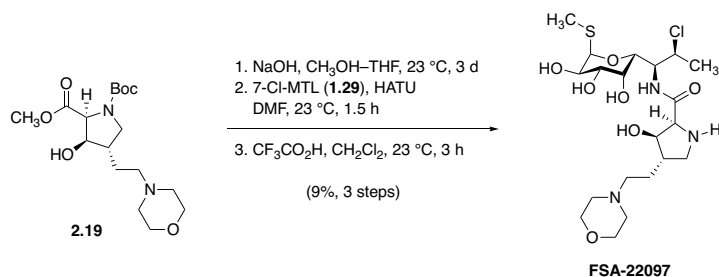
This crude aldehyde observed by ozonolytic cleavage was transferred to a 10-mL round-bottomed flask, where it was dissolved in 1,2-dichloroethane (679 μL). To this solution, morpholine (35.5 μL , 407 μmol , 3.00 equiv) was added, followed by sodium cyanoborohydride (17.1 mg, 271 μmol , 2.00 equiv). After stirring for 1 h, LCMS analysis indicated that no aldehyde remained. The mixture was directly subjected to flash-column chromatography (6 g silica gel,

eluting with 1% ammonium hydroxide–5% methanol–dichloromethane) to provide the product as a white, foaming solid (51.3 mg, 104%, 2 steps).

$R_f = 0.50$ (1% ammonium hydroxide–10% methanol–dichloromethane, KMnO_4).

^1H NMR (55:45 rotameric mixture, asterisk [*] denotes minor rotameric signals that could be resolved, 600 MHz, CDCl_3) δ 4.50 (d, $J = 8.1$ Hz, 1H),* 4.41 (d, $J = 8.2$ Hz, 1H), 3.96 (ddd, $J = 9.7, 8.1, 3.1$ Hz, 1H), 3.92 (dd, $J = 12.8, 3.6$ Hz, 1H), 3.83 (dd, $J = 10.7, 8.5$ Hz, 1H),* 3.77 (s, 3H),* 3.76 (s, 3H), 3.74–7.71 (m, 2H), 3.69–3.65 (m, 2H), 3.14 (app dd, $J = 13.5, 2.2$ Hz, 1H), 2.83–3.76 (m, 1H), 2.64 (br, 2H), 2.56–2.51 (m, 2H), 2.43–2.34 (m, 3H), 1.73–1.55 (m, 2H), 1.42 (s, 9H),* 1.38 (s, 9H).

MS (ESI+, m/z): $[\text{M}+\text{H}]^+$ calc'd for $\text{C}_{17}\text{H}_{30}\text{N}_2\text{O}_6$, 359.2; found 359.2.



Synthetic lincosamide FSA-22097.

To a solution of ester **2.19** (50 mg, 140 μ mol, 1 equiv) in 50% v/v methanol–tetrahydrofuran (700 μ L), an aqueous solution of sodium hydroxide (1.0 M, 140 μ L, 140 μ mol, 1.0 equiv) was added. The mixture was then warmed to 40 °C in a pre-heated oil bath. The mixture was stirred at that temperature for 3 d, at which point LCMS analysis indicated that saponification was complete. The mixture was concentrated in vacuo to afford crude sodium carboxylate salt, which was used in the next transformation without purification.

This material was transferred to a 2–5 mL glass microwave vial, where it was dissolved in *N,N*-dimethylformamide (530 μ L). To this solution was added HATU (45 mg, 0.12 mmol, 1.1 equiv) at 23 °C, followed by 7-Cl-MTL (**1.29**, 43 mg, 0.16 mmol, 1.5 equiv) 10 min later. The resulting yellow suspension was stirred for 1.5 h, at which point the amide coupling reaction was judged to be complete by LCMS analysis. The mixture was concentrated in vacuo, and the residue was purified by flash-column chromatography (6 g silica gel, eluting with dichloromethane initially, grading to 1% ammonium hydroxide–10% methanol–dichloromethane) to provide *N*-Boc-protected lincosamide product (R_f = 0.31, 1% ammonium hydroxide–10% methanol–dichloromethane, PMA) as a white film (18 mg, 28%, 2 steps). Owing to significant rotamerism, this product was not characterized at this point, but was instead advanced through *N*-Boc removal.

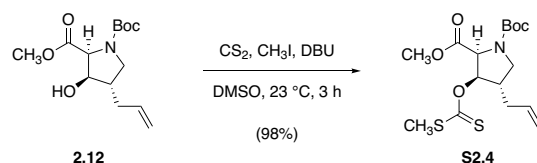
Accordingly, the *N*-Boc lincosamide intermediate (18 mg, 30 μ mol, 1 equiv) was dissolved in 10% v/v trifluoroacetic acid–dichloromethane (300 μ L) at 23 °C. After 3 h, LCMS analysis indicated that *N*-Boc removal was complete, and toluene (1 mL) was added. The diluted mixture was concentrated in vacuo, and the dried residue was purified by preparative HPLC on a Waters SunFire prep C₁₈ column (5 μ m, 250 \times 19 mm; eluting with 0.1% trifluoroacetic acid–water initially, grading to 0.1% trifluoroacetic acid–20% acetonitrile–water over 40 min, with a flow rate of 15 mL/min; monitored by UV absorbance at 210 nm) to provide **FSA-22097** • 2 CF₃CO₂H as a white solid (9.5 mg, 44%).

¹H NMR (500 MHz, CD₃OD) δ 5.31 (d, *J* = 5.7 Hz, 1H), 4.60–4.55 (m, 2H), 4.48 (d, *J* = 2.9 Hz, 1H), 4.30 (d, *J* = 10.0 Hz, 1H), 4.10 (dd, *J* = 10.3, 5.6 Hz, 1H), 4.06 (br, 2H), 3.86 (d, *J* = 3.3 Hz, 1H), 3.80 (br, 2H), 3.73 (dd, *J* = 11.8, 7.5 Hz, 1H), 3.59 (dd, *J* = 10.2, 3.3 Hz, 1H), 3.50 (br, 2H), 3.28 (dd, *J* = 10.7, 5.2 Hz, 1H), 3.23 (dd, *J* = 12.6, 5.1 Hz, 1H), .16 (br, 2H), 3.13 (dd, *J* = 11.9, 6.8 Hz, 1H), 2.37–2.30 (m, 1H), 2.16 (s, 3H), 2.04–1.97 (m, 1H), 1.93–1.86 (m, 1H), 1.53 (d, *J* = 6.8 Hz, 3H).

¹³C NMR (126 MHz, CD₃OD) δ 167.2, 152.2 (q, *J* = 36.3 Hz), 117.7 (q, *J* = 290.7 Hz), 89.8, 76.2, 72.1, 70.7, 69.8, 69.6, 65.0, 64.1, 59.2, 56.4, 54.8, 44.9, 25.9, 22.7, 13.5. Four carbon signals were not well resolved: Two trifluoroacetate carbon signals were partially obscured by coupling to ¹⁹F nuclei, and two signals from the morpholine ring were not observed due to peak broadening.

FTIR (neat, cm⁻¹): 3355 (br), 1673 (s), 1200 (s), 1134 (m).

HRMS (ESI+, *m/z*): [M+H]⁺ calc'd for C₂₀H₃₆ClN₃O₇S, 287.5613; found 287.5696.



Xanthate ester S2.4.

Methyl xanthate formation was performed following the procedure described by Bartley and Coward.¹⁰⁸ To a solution of hydroxyproline **2.12** (50.0 mg, 175 μmol , 1 equiv) in dimethyl sulfoxide (350 μL) were added 1,8-diazabicyclo[5.4.0]undec-7-ene (29.1 μL , 193 μmol , 1.10 equiv) and carbon disulfide (69.7 μL , 1.16 mmol, 6.60 equiv) at 23 $^\circ\text{C}$. Upon addition of carbon disulfide, the reaction solution immediately changed from colorless to auburn-colored. After 75 min of stirring at 23 $^\circ\text{C}$, methyl iodide (21.9 μL , 350 μmol , 2.00 equiv) was added, causing the auburn color to change to canary yellow. After 1.5 h, LCMS analysis indicated that methyl xanthate formation was complete. The reaction mixture was diluted with ethyl acetate (30 mL), and the diluted organic solution was washed with water (3×10 mL). The combined aqueous washes were extracted with a fresh portion of ethyl acetate (15 mL), and the combined organic layers were washed with saturated aqueous sodium chloride solution (10 mL). The organic product solution was then dried over sodium sulfate, filtered, and concentrated to provide analytically pure product as a yellow, viscous oil (64.5 mg, 98%).

R_f = 0.67 (30% ethyl acetate–hexanes, UV+KMnO₄).

¹H NMR (60:40 rotameric mixture, asterisk [*] denotes minor rotameric signals that could be resolved, 500 MHz, CDCl₃) δ 5.91–5.86 (m, 1H), 5.73 (ddt, $J = 17.1, 10.2, 7.0$ Hz, 1H),

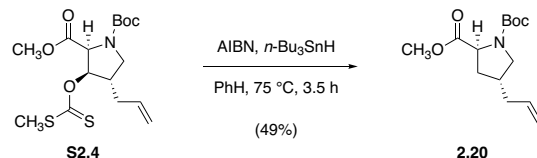
¹⁰⁸ Bartley, D. M.; Coward, J. K. *J. Org. Chem.* **2006**, *71*, 372–374.

5.08–5.02 (m, 2H), 4.75 (d, $J = 7.5$ Hz, 1H),* 4.65 (d, $J = 7.5$ Hz, 1H), 3.81 (dd, $J = 10.8$, 8.0 Hz, 1H), 3.75–3.71 (m, 1H),* 3.70 (s, 3H), 3.15 (dd, $J = 10.5$, 8.1 Hz, 1H), 2.75–2.69 (m, 1H), 2.54 (s, 3H), 2.31–2.26 (m, 1H), 2.14–2.06 (m, 1H), 1.44 (s, 9H),* 1.38 (s, 9H).

^{13}C NMR (60:40 rotameric mixture, asterisk [*] denotes minor rotameric signals that could be resolved, 126 MHz, CDCl_3) δ 215.3, 215.2,* 169.7, 169.5,* 154.2,* 153.5, 134.5,* 134.4, 117.6, 117.6,* 83.5, 82.9,* 80.7, 80.6,* 60.2, 59.8,*52.4,* 52.3, 48.6,* 48.1, 41.2,* 40.4, 34.7, 28.5,* 28.3, 19.3.

FTIR (neat, cm^{-1}): 1749 (m), 1699 (s), 1393 (s), 1366 (m), 1175 (s), 1144 (s), 1065 (s).

HRMS (ESI+, m/z): $[\text{M}+\text{H}]^+$ calc'd for $\text{C}_{16}\text{H}_{25}\text{NO}_5\text{S}_2$, 376.1247; found 376.1247.



Proline derivative 2.20.

Barton reduction was performed according to the method reported by Robbins, Wilson, and Hansske.¹⁰⁹ In a 2–5 mL glass microwave vial, a solution of methyl xanthate **S2.4** (64.5 mg, 172 μmol , 1 equiv), 2,2'-azobis(2-methylpropionitrile) (5.64 mg, 34.3 μmol , 0.200 equiv), and tri-*n*-butylstannane (69.3 μL , 258 μmol , 1.50 equiv) in toluene (4.29 mL) was sparged of molecular oxygen by bubbling argon through it for 10 min. The mixture was then heated to 75 $^\circ\text{C}$ in a pre-heated oil bath; over the course of 30 min, the yellow color of the reaction mixture gradually dissipated as starting material was consumed. After 3.5 h, TLC analysis (30% ethyl acetate–hexanes, UV+PMA) revealed that no starting material remained. The mixture was allowed to cool to ambient temperature before it was concentrated in vacuo. The crude residue was purified by flash-column chromatography (4 g silica gel, eluting with hexanes initially, grading to 40% ethyl acetate–hexanes) to provide the product as a colorless oil (22.8 mg, 49%).

R_f = 0.41 (30% ethyl acetate–hexanes, PMA).

¹H NMR (60:40 rotameric mixture, asterisk [*] denotes minor rotameric signals that could be resolved, 500 MHz, CDCl₃) δ 5.73 (dddd, J = 18.5, 10.1, 7.6, 6.3 Hz, 1H), 5.05–4.99 (m, 2H), 4.35 (dd, J = 9.0, 2.5 Hz, 1H),* 4.25 (dd, J = 8.9, 3.0 Hz, 1H), 3.73–3.69 (m, 1H), 3.71 (s, 3H),* 3.70 (s, 3H), 3.64 (dd, J = 10.4, 7.6 Hz, 1H),* 3.04 (dd, J = 10.6, 8.1 Hz,

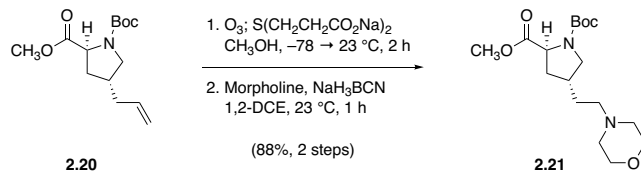
¹⁰⁹ Robbins, M. J.; Wilson, J. S.; Hansske, F. *J. Am. Chem. Soc.* **1983**, *105*, 4059–4065.

1H), 2.97 (dd, $J = 10.4, 8.4$ Hz, 1H),* 2.41–2.31 (m, 1H), 2.15–2.03 (m, 3H), 1.92–1.80 (m, 1H), 1.44 (s, 9H),* 1.39 (s, 9H).

^{13}C NMR (60:40 rotameric mixture, asterisk [*] denotes minor rotameric signals that could be resolved, 126 MHz, CDCl_3) δ 173.7, 173.5,* 154.5,* 153.8, 136.0,* 135.9, 116.7, 116.6,* 80.0, 59.1, 58.8,* 52.2,* 52.1, 51.7,* 51.4, 37.3, 37.2, 37.1,* 36.2,* 36.2, 35.5,* 28.6,* 28.4.

FTIR (neat, cm^{-1}): 2976 (w), 1749 (m), 1699 (s), 1395 (s), 1366 (m), 1161 (m), 1120 (m).

HRMS (ESI+, m/z): $[\text{M}+\text{H}]^+$ calc'd for $\text{C}_{14}\text{H}_{23}\text{NO}_4$, 270.1700; found 270.1704.



Morpholino compound 2.21.

A solution of olefin **2.20** (22.8 mg, 84.7 μmol , 1 equiv) in methanol (2.82 mL) was cooled to $-78\text{ }^{\circ}\text{C}$ in a dry ice–acetone bath before an ozone–dioxygen mixture from an ozone generator was bubbled through it. Ozone addition was continued until the reaction mixture attained a persistent ultramarine color, at which point nitrogen gas was bubbled through the mixture for 5 min in order to sparge it of excess oxidant. Sodium thiodipropionate (37.6 mg, 169 μmol , 2.00 equiv) was added at $-78\text{ }^{\circ}\text{C}$, the cooling bath was removed, and the mixture was allowed to warm to $23\text{ }^{\circ}\text{C}$ with stirring. Reductive consumption of the trioxolane intermediate was monitored by LCMS, and after 2 h, the reaction was complete. The mixture was diluted with saturated aqueous sodium bicarbonate solution (15 mL), and the resulting mixture was extracted with dichloromethane ($3 \times 10\text{ mL}$). The combined extracts were dried over sodium sulfate, filtered, and concentrated to provide crude aldehyde intermediate as a colorless oil.

This material was transferred to a 2–5 mL glass microwave vial fitted with a magnetic stir bar, where it was dissolved in 1,2-dichloroethane (424 μL). Morpholine (22.1 μL , 254 μmol , 3.00 equiv) was added to this mixture, followed by sodium cyanoborohydride (10.7 mg, 169 μmol , 2.00 equiv) at $23\text{ }^{\circ}\text{C}$. After 1 h of stirring, LCMS analysis indicated that no aldehyde remained, and the mixture was concentrated in vacuo. Purification of the resulting residue by flash-column chromatography (6 g silica gel, eluting with 1% ammonium hydroxide–7% methanol–dichloromethane) provided the product as a colorless film (25.4 mg, 88%, 2 steps).

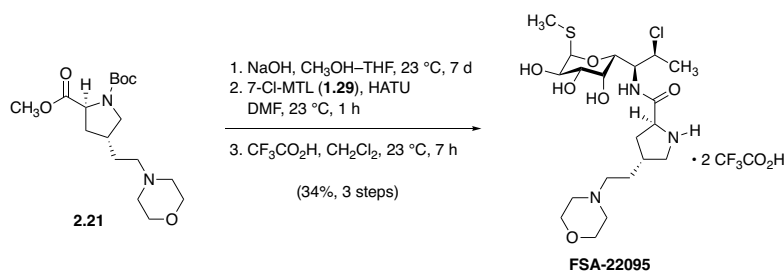
$R_f = 0.36$ (1% ammonium hydroxide–10% methanol–dichloromethane, KMnO_4).

^1H NMR (60:40 rotameric mixture, asterisk [*] denotes minor rotameric signals that could be resolved, 600 MHz, CDCl_3) δ 4.35 (ddd, $J = 9.1, 4.4, 2.0$ Hz, 1H),* 4.25 (ddd, $J = 9.1, 3.9, 2.5$ Hz, 1H), 3.93 (dd, $J = 12.8, 3.5$ Hz, 1H),* 3.78–3.74 (m, 1H), 3.70 (s, 3H), 3.69–3.67 (m, 3H), 3.64 (app t, $J = 6.5$ Hz, 1H), 3.15 (d, $J = 13.3$ Hz, 1H),* 3.03–2.91 (m, 1H), 2.82 (dddd, $J = 13.8, 11.8, 10.6, 3.7$ Hz, 1H),* 2.45–2.36 (m, 3H), 2.32–2.27 (m, 2H), 2.13–2.06 (m, 1H), 1.93–1.78 (m, 2H), 1.62 (app q, $J = 6.8$ Hz, 2H),* 1.54 (app q, $J = 7.5$ Hz, 2H), 1.44 (s, 9H),* 1.38 (s, 9H).

^{13}C NMR (60:40 rotameric mixture, asterisk [*] denotes minor rotameric signals that could be resolved, 126 MHz, CDCl_3) δ 173.7, 173.5,* 154.5,* 153.5, 80.1, 67.1, 65.2,* 61.5,* 61.4, 59.1,* 59.1, 58.8,* 58.8, 57.6,* 57.6, 52.3,* 52.2, 52.2,* 52.1, 51.7, 50.9, 36.8, 36.0, 35.9,* 35.0, 34.6,* 33.7,* 30.1,* 30.1, 28.6,* 28.6.

FTIR (neat, cm^{-1}): 2952 (w), 1748 (m), 1698 (s), 1400 (s), 1366 (m), 1163 (m), 1118 (s).

HRMS (ESI+, m/z): $[\text{M}+\text{H}]^+$ calc'd for $\text{C}_{17}\text{H}_{30}\text{N}_2\text{O}_5$, 343.2227; found 343.2233.



Synthetic lincosamide FSA-22095.

To a solution of methyl ester **2.21** (25.4 mg, 74.2 μmol, 1 equiv) in 50% v/v methanol–tetrahydrofuran (370 μL) was added an aqueous solution of sodium hydroxide (1.00 M, 74.2 μL, 74.2 μmol, 1.00 equiv) at 23 °C. The mixture was heated to 40 °C in a pre-heated oil bath, and stirring was continued for 7 d. At this point, LCMS analysis showed that saponification was complete, and the mixture was concentrated to dryness in vacuo.

This crude sodium carboxylate salt was transferred to a 2–5 mL glass microwave vial fitted with a magnetic stir bar, where it was dissolved in *N,N*-dimethylformamide (371 μL). To this solution was added HATU (31.0 mg, 132 μmol, 1.10 equiv) at 23 °C, followed 10 minutes later by 7-Cl-MTL (**1.29**, 30.2 mg, 111 μmol, 1.50 equiv). The resulting yellow suspension was stirred at 23 °C for 1 h, at which point LCMS analysis indicated that amide coupling was complete. The mixture was concentrated in vacuo, and the crude residue was purified by flash-column chromatography (6 g silica gel, eluting with dichloromethane initially, grading to 1% ammonium hydroxide–8% methanol–dichloromethane) to provide *N*-Boc protected morpholino lincosamide intermediate ($R_f = 0.30$, 1% ammonium hydroxide–10% methanol–dichloromethane, PMA) as a colorless film (21.1 mg). Owing to substantial rotamerism, the material was subjected to *N*-Boc removal prior to characterization.

Accordingly, this *N*-Boc–protected intermediate was dissolved in 10% v/v trifluoroacetic acid–dichloromethane (300 μL) at 23 °C. After 7 h, LCMS analysis indicated that *N*-Boc removal

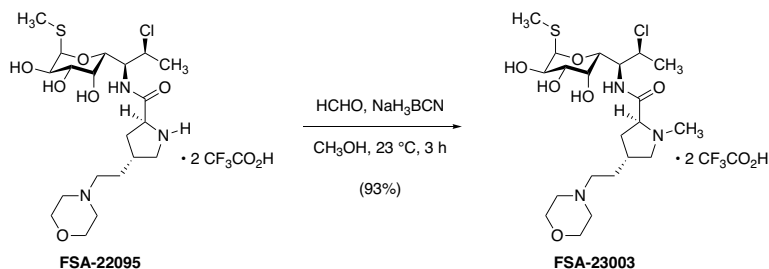
was complete, and toluene (1 mL) was added. The diluted mixture was concentrated, and the dried residue was purified by preparative HPLC on a Waters SunFire prep C₁₈ column (5 μm, 250 × 19 mm; eluting with 0.1% trifluoroacetic acid–water initially, grading to 0.1% trifluoroacetic acid–50% acetonitrile–water over 40 min; monitored by UV absorbance at 210 nm) to provide **FSA-22095** • 2 CF₃CO₂H as a white powder (18.0 mg, 34%, 3 steps).

¹H NMR (500 MHz, CD₃OD) δ 8.52 (d, *J* = 9.4 Hz, amide NH), 5.31 (d, *J* = 5.6 Hz, 1H), 4.60–4.51 (m, 3H), 4.31 (dd, *J* = 10.0, 1.3 Hz, 1H), 4.09 (dd, *J* = 10.2, 5.6 Hz, 1H), 4.04 (br, 2H), 3.84 (dd, *J* = 3.4, 1.2 Hz, 1H), 3.80–3.76 (m, 2H), 3.67 (dd, *J* = 11.5, 7.3 Hz, 1H), 3.59 (dd, *J* = 10.2, 3.3 Hz, 1H), 3.50 (br d, *J* = 11.5 Hz, 2H), 3.27–3.11 (m, 4H), 3.07 (dd, *J* = 11.6, 8.8 Hz, 1H), 2.44–2.36 (m, 1H), 2.34–2.23 (m, 2H), 2.15 (s, 3H), 1.96 (app q, *J* = 8.0 Hz, 2H), 1.45 (d, *J* = 6.8 Hz, 3H).

¹³C NMR (126 MHz, CD₃OD) δ 170.4, 89.8, 72.1, 70.5, 69.7, 69.5, 60.6, 59.1, 56.5, 54.6, 53.2, 51.4, 37.0, 36.2, 27.1, 23.2, 13.4. Two trifluoroacetate carbon signals were not observed due to coupling to ¹⁹F nuclei.

FTIR (neat, cm⁻¹): 3372 (br), 1672 (s), 1463 (w), 1201 (s), 1132 (m).

HRMS (ESI+, *m/z*): [M+H]⁺ calc'd for C₂₀H₃₆ClN₃O₆S, 482.2086; found 482.2089.



Synthetic lincosamide FSA-23003.

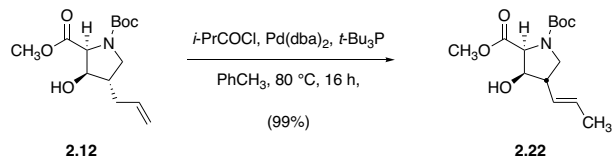
In a 4-mL glass vial fitted with a stir bar, **FSA-22095** • 2 CF₃CO₂H (8.0 mg, 11 μmol, 1 equiv) was dissolved in methanol (100 μL). To this solution was added an aqueous solution of formaldehyde (37% w/w, 1.7 μL, 23 μmol, 2.0 equiv), followed by sodium cyanoborohydride (1.4 mg, 23 μmol, 2.0 equiv) at 23 °C. After 3 h, LCMS analysis showed that *N*-methylation was complete. The mixture was concentrated to dryness in vacuo, and the crude residue was purified by preparative HPLC on a Waters SunFire prep C₁₈ column (5 μm, 19 × 250 mm; eluting with 0.1% trifluoroacetic acid–water initially, grading to 0.1% trifluoroacetic acid–30% acetonitrile–water over 30 min, with a flow rate of 15 mL/min; monitored by UV absorbance at 210 nm) to provide **FSA-23003** • 2 CF₃CO₂H as a white solid (7.6 mg, 93%).

¹H NMR (600 MHz, CD₃OD) δ 5.31 (d, *J* = 5.6 Hz, 1H), 4.60–4.56 (m, 2H), 4.34 (dd, *J* = 9.9, 1.3 Hz, 1H), 4.29 (dd, *J* = 9.4, 6.7 Hz, 1H), 4.10 (dd, *J* = 10.2, 5.6 Hz, 1H), 4.06 (br d, *J* = 11.1 Hz, 2H), 3.86 (dd, *J* = 11.2, 6.6 Hz, 1H), 3.82 (dd, *J* = 3.2, 1.3 Hz, 1H), 3.81–3.75 (m, 2H), 3.59 (dd, *J* = 10.2, 3.3 Hz, 1H), 3.50 (br, 2H), 3.25–3.09 (m, 4H), 3.04 (app t, *J* = 10.6 Hz, 1H), 2.98 (s, 3H), 2.47–2.39 (m, 1H), 2.34–2.30 (m, 1H), 2.15 (s, 3H), 2.00 (app dtd, *J* = 11.0, 6.6, 4.3 Hz, 1H), 1.45 (d, *J* = 6.8 Hz, 3H).

¹³C NMR (126 MHz, CD₃OD) δ 168.9, 162.0 (q, *J* = 36.6 Hz), 117.6 (q, *J* = 290.8 Hz), 89.9, 72.2, 70.3, 69.7, 69.5, 69.3, 65.0, 61.3, 59.1, 56.3, 54.6, 53.2, 41.0, 36.2, 35.5, 27.6, 23.2, 13.5.

FTIR (neat, cm^{-1}): 3323 (br), 1674 (s), 1201 (s), 1129 (m).

HRMS (ESI+, m/z): $[\text{M}+\text{H}]^+$ calc'd for $\text{C}_{21}\text{H}_{38}\text{ClN}_3\text{O}_6\text{S}$, 496.2243; found 496.2262.



Disubstituted olefin **2.22**.

Conditions for selective olefin migration were adapted from the report of Gauthier and co-workers.⁶ In a 5–10 mL glass microwave vial, olefin **2.12** (450 mg, 1.58 mmol, 1 equiv) and bis(dibenzylideneacetone)palladium(0) (27.2 mg, 47.3 μmol , 0.0300 equiv) were dissolved in toluene. Argon gas was bubbled through this solution for 5 min in order to sparge it of any dissolved dioxygen, and to the degassed solution were then added tri-*tert*-butylphosphine solution (1.0 M in toluene, 47 μL , 47 μmol , 0.030 equiv) and isobutyryl chloride solution (0.473 M in toluene, 100 μL , 47.3 μmol , 0.0300 equiv) sequentially at 23 $^\circ\text{C}$. The vial was sealed, and the reaction mixture was heated to 80 $^\circ\text{C}$ in a pre-heated oil bath. Upon heating, the burgundy-colored solution changed to straw-yellow. Progress was monitored by aliquot NMR: Approximately 50- μL portions of the reaction solution were periodically removed by syringe, diluted with chloroform-*d*, and analyzed by ^1H NMR. After 16 h, no starting material was observed, and the reaction was judged to be complete. The mixture was cooled to 23 $^\circ\text{C}$, the cooled solution was concentrated in vacuo, and the residue was purified by flash-column chromatography (24 g silica gel, eluting with 30% ethyl acetate–hexanes initially, grading to 40% ethyl acetate–hexanes) to provide the product as a colorless oil (447 mg, 99%).

$R_f = 0.23$ (30% ethyl acetate–hexanes, KMnO_4).

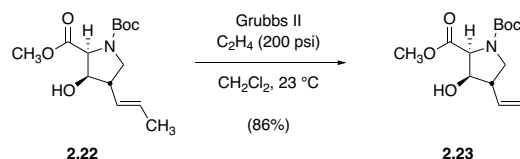
^1H NMR (60:40 mixture of rotamers, asterisk [*] denotes minor rotamer signals that could be resolved, 500 MHz, CDCl_3) δ 5.60 (dq, $J = 13.2, 6.4$ Hz, 1H), 5.26 (dd, $J = 15.2, 8.0$ Hz,

1H), 4.40 (d, $J = 7.7$ Hz, 1H),* 4.32 (d, $J = 7.7$ Hz, 1H), 4.13 (app t, $J = 8.5$ Hz, 1H), 3.76–3.67 (m, 4H), 3.07 (ddd, $J = 11.8, 9.6, 2.8$ Hz, 1H), 3.01 (dd, $J = 14.3, 4.3$ Hz, 1H), 2.88–2.77 (m, 1H), 1.64 (d, $J = 6.5$ Hz, 3H), 1.40 (s, 9H),* 1.35 (s, 9H).

¹³C NMR (60:40 mixture of rotamers, asterisk [*] denotes minor rotamer signals that could be resolved, 126 MHz, CDCl₃) δ 171.3, 154.8,* 153.8, 129.3, 129.2,* 128.2,* 128.1, 80.4, 80.3,* 75.9, 75.1,* 63.0, 62.4,* 52.2,* 52.0, 49.2,* 48.6, 47.4,* 46.7, 28.4,* 28.3, 18.1.

FTIR (neat, cm⁻¹): 3435 (br), 2976 (m), 1748 (m), 1700 (s), 1677 (s), 1396 (s), 1367 (s), 1206 (s), 1176 (s), 1137 (m).

HRMS (ESI+, m/z): [M+H]⁺ calc'd for C₁₄H₂₃NO₅, 286.1649; found 286.1654.



Vinyl compound 2.23.

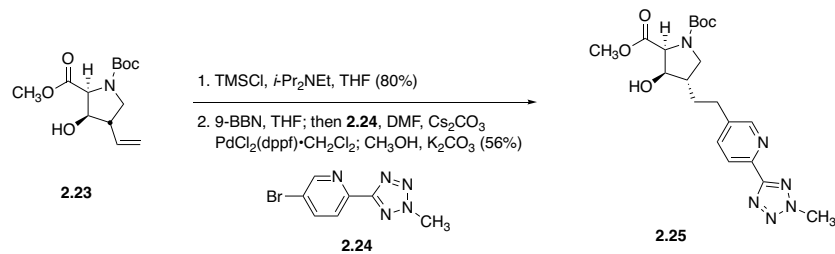
In a 100-mL round-bottomed flask fitted with a magnetic stir bar, olefin **2.22** (180 mg, 631 μmol , 1 equiv) was dissolved in dichloromethane (63.1 mL). To this solution was added dichloro[1,3-bis(2,4,6-trimethylphenyl)-2-imidazolidinylidene](benzylidene)(tricyclohexylphosphine)ruthenium(II) (second-generation Grubbs catalyst, 10.7 mg, 12.6 μmol , 0.0200 equiv). Ethylene gas was bubbled through the mauve-taupe colored solution at 23 $^\circ\text{C}$ for 10 min before bubbling was discontinued and the then-brown solution was stirred vigorously (700 rpm) under 1 atm of ethylene gas overnight. After 1 d, LCMS analysis showed $\sim 80\%$ conversion of the starting material to product. In order to drive the reaction to completion, an additional portion of ruthenium catalyst (10.7 mg, 12.6 μmol , 0.0200 equiv) was added, and the mixture was placed in a Parr pressure reactor. The sealed reactor was charged with ethylene gas (200 psi, 99.9%),¹¹⁰ and the mixture was stirred at 23 $^\circ\text{C}$ for 1 d. After this period, LCMS analysis showed complete disappearance of starting material. The mixture was concentrated in vacuo, and the residue obtained was purified by flash-column chromatography (12 g silica gel, eluting with 30% ethyl acetate–hexanes initially, grading to 40% ethyl acetate–hexanes) to provide γ -vinylproline product as a brown oil (148 mg, 86%).

¹¹⁰ High-purity ethylene is necessary for ethenolysis, as acetylene (a common impurity in commercial ethylene) is known to poison metathesis catalysts. See: Marx, V. M.; Sullivan, A. H.; Melaimi, M.; Virgil, S. C.; Keitz, B. K.; Weinberger, D. S.; Bertrand, G.; Grubbs, R. H. *Angew. Chem. Int. Ed.* **2015**, *54*, 1919–1923.

$R_f = 0.19$ (40% ethyl acetate–hexanes, KMnO_4).

^1H NMR (55:45 rotameric mixture, asterisk [*] denotes minor rotameric signals that could be resolved, 400 MHz, CDCl_3) δ 5.68 (dddd, $J = 17.8, 10.1, 7.6, 2.4$ Hz, 1H), 5.19 (app ddt, $J = 17.3, 3.0, 1.3$ Hz, 1H), 5.13 (app dq, $J = 10.4, 1.2$ Hz, 1H), 4.42 (d, $J = 7.7$ Hz, 1H),* 4.35 (d, $J = 7.7$ Hz, 1H), 4.24–4.18 (m, 1H), 3.79 (dd, $J = 10.9, 8.1$ Hz, 1H), 3.73 (s, 3H),* 3.72 (s, 3H), 3.18–3.07 (m, 2H), 2.94–2.83 (m, 1H), 1.41 (s, 9H),* 1.36 (s, 9H).

MS (ESI+, m/z): $[\text{M}+\text{Na}]^+$ calc'd for $\text{C}_{13}\text{H}_{21}\text{NO}_5$, 294.1; found 294.2.



Heterobiaryl compound **2.25**.

In a 25-mL round-bottomed flask fitted with a magnetic stir bar, a solution of β -hydroxy- γ -vinylproline **2.23** (147 mg, 542 μ mol, 1 equiv) and diisopropylethylamine (142 μ L, 813 μ mol, 1.50 equiv) in tetrahydrofuran (2.71 mL) was chilled to 0 °C. To this cooled solution was then added chlorotrimethylsilane (83.0 μ L, 650 μ mol, 1.20 equiv); the mixture was stirred at 0 °C for 5 min before the ice-water cooling bath was removed, and the mixture was allowed to warm to 23 °C. After 2 h, the mixture was diluted with ethyl acetate (25 mL), and the diluted organic solution was washed with saturated aqueous sodium chloride solution (3 \times 10 mL). The organic layer was then dried over sodium sulfate, filtered, and concentrated to provide *O*-trimethylsilylated intermediate as a light brown oil (150 mg, 434 μ mol, 80%), which was suitable for use in the subsequent transformation without further purification.

This silylated intermediate was transferred to a 25-mL round-bottomed flask fitted with a magnetic stir bar, where it was dried by azeotropic removal of benzene. The dried material was dissolved in tetrahydrofuran (450 μ L), and the resulting solution was chilled to 0 °C in an ice-water bath. A solution of 9-borabicyclo(3.3.1)nonane in tetrahydrofuran (0.50 M, 3.5 mL, 1.7 mmol, 4.0 equiv) was then added, the cooling bath was removed, and the reaction mixture was allowed to warm to 23 °C gradually. After 1 h, aliquot ¹H-NMR analysis (CDCl₃) showed complete disappearance of the olefin signals corresponding to the starting material. *N,N*-Dimethylformamide (3.15 mL), cesium carbonate (283 mg, 868 μ mol, 2.00 equiv), 5-bromo-2-(2-

methyl-2H-tetrazol-5-yl)pyridine (**2.24**, 208 mg, 868 μmol , 2.00 equiv), and [1,1'-bis(diphenylphosphino)ferrocene]dichloropalladium(II)-dichloromethane complex (7.08 mg, 8.68 μmol , 0.0200 equiv) were added sequentially. The resulting mixture was heated to 50 $^{\circ}\text{C}$, and after 1 h, LCMS analysis indicated that B-alkyl Suzuki coupling was complete. The mixture was diluted with ethyl acetate (50 mL), and the diluted mixture was washed with saturated aqueous sodium bicarbonate solution (10 mL). The washed organic solution was then dried over sodium sulfate, filtered, and concentrated. In order to remove the trimethylsilyl protecting group, the residue was re-dissolved in methanol (3.00 mL), and potassium carbonate (30.0 mg, 217 μmol , 0.500 equiv) was added. After stirring at 23 $^{\circ}\text{C}$ for 1 h, LCMS analysis indicated that desilylation was complete. The mixture was filtered to remove undissolved salts, and the filtrate was concentrated. The crude residue was purified by flash-column chromatography (6 g silica gel, eluting with 0.1% ammonium hydroxide-1% methanol-dichloromethane initially, grading to 0.4% ammonium hydroxide-4% methanol-dichloromethane) to provide the product as an off-white, foaming solid (105 mg, 56%).

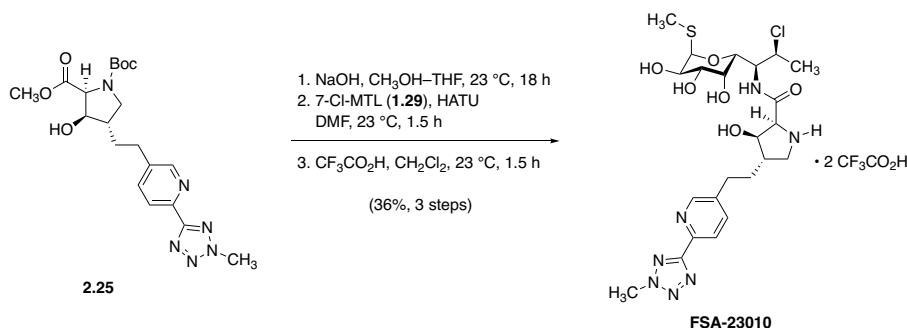
R_f = 0.45 (1% ammonium hydroxide-10% methanol-dichloromethane, UV).

¹H NMR (60:40 rotameric mixture, asterisk [*] denotes minor rotameric signals that could be resolved, 600 MHz, CDCl₃) δ 8.55 (dd, *J* = 8.2, 2.2 Hz, 1H), 8.10 (dd, *J* = 7.9, 6.3 Hz, 1H), 7.65 (ddd, 10.3, 7.9, 2.3 Hz, 1H), 4.42 (d, *J* = 7.9 Hz, 1H), * 4.40 (s, 3H), 4.36 (d, *J* = 7.8 Hz, 1H), 4.24-4.18 (m, 1H), 3.87 (dd, *J* = 10.7, 8.1 Hz, 1H), 3.77 (dd, *J* = 10.5, 8.2 Hz, 1H), * 3.71 (s, 3H), 3.58 (br, 1H), * 3.51 (br, 1H), 3.03 (dd, *J* = 10.7, 9.0 Hz, 1H), 2.98 (app t, *J* = 9.9 Hz, 1H), * 2.79-2.69 (m, 2H), 2.40-2.28 (m, 1H), 2.04-1.96 (m, 1H), 1.63-1.57 (m, 1H), 1.41 (s, 9H), * 1.37 (s, 9H).

^{13}C NMR (60:40 rotameric mixture, asterisk [*] denotes minor rotameric signals that could be resolved, 126 MHz, CDCl_3) δ 171.2, 164.9, 154.3,* 153.8, 150.2, 144.6, 138.8,* 138.8, 137.0, 136.9,* 122.2, 80.5, 76.3, 75.5,* 63.5, 62.9,* 52.2,* 52.1, 49.6,* 49.0, 43.3,* 42.7, 39.7, 32.8,* 32.8, 31.3, 28.4,* 28.3.

FTIR (neat, cm^{-1}): 3392 (br), 2949 (w), 1744 (m), 1695 (s), 1396 (s), 1367 (m), 1208 (m), 1177 (m), 729 (m).

HRMS (ESI+, m/z): $[\text{M}+\text{H}]^+$ calc'd for $\text{C}_{20}\text{H}_{28}\text{N}_6\text{O}_5$, 433.2194; found 433.2209.



Synthetic lincosamide FSA-23010.

In a 2–5 mL glass microwave vial fitted with a magnetic stir bar, a solution of methyl ester **2.25** (105 mg, 242 μ mol, 1 equiv) in 50% v/v methanol–tetrahydrofuran (1.21 mL) was treated with an aqueous solution of sodium hydroxide (1.00 M, 254 μ L, 254 μ mol, 1.05 equiv) at 23 °C. The mixture was stirred at 23 °C for 18 h, during which time the mixture changed from a light straw-colored solution to an off-white, thick paste. LCMS analysis at this point indicated that saponification was complete; the mixture was concentrated to dryness, and residual water was removed by azeotropic removal of benzene.

A portion of this crude sodium carboxylate salt (50.0 mg, 114 μ mol, 1 equiv) was suspended in *N,N*-dimethylformamide (568 μ L), and to this suspension was added HATU (47.5 mg, 125 μ mol, 1.10 equiv) whereupon a canary-yellow homogeneous solution was formed. After stirring for 5 min at 23 °C, 7-Cl-MTL (**1.29**, 46.3 mg, 170 μ mol, 1.50 equiv) was added. After 1.5 h of stirring, LCMS analysis indicated that the reaction was complete. The reaction mixture was loaded directly onto a silica gel column (6 g, equilibrated with dichloromethane). This column was eluted with dichloromethane initially, grading to 1% ammonium hydroxide–10% methanol–dichloromethane, to provide the *N*-Boc protected product as a white solid (R_f = 0.31, 1% ammonium hydroxide–10% methanol–dichloromethane, UV+PMA; 30.4 mg, 40%). This material was subjected to *N*-Boc removal prior to full characterization.

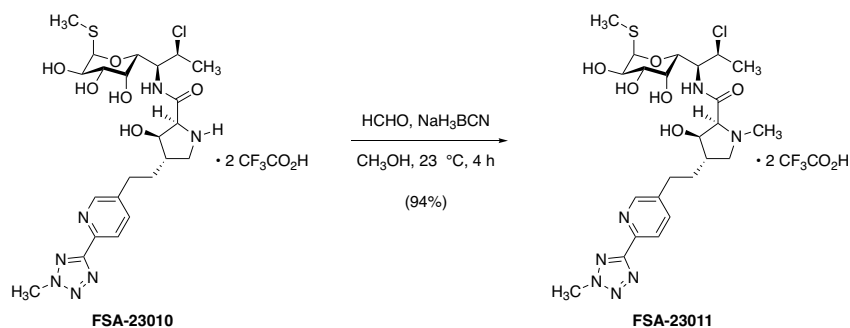
In a 2–5 mL glass microwave vial, *N*-Boc protected intermediate (30.4 mg, 45.2 μmol , 1 equiv) was dissolved in 20% v/v trifluoroacetic acid–dichloromethane (600 μL) at 23 °C. After 1.5 h of stirring at 23 °C, LCMS analysis indicated that no starting material remained. The reaction solution was diluted with toluene (1 mL), and the diluted mixture was concentrated in vacuo. The crude residue was purified by preparative HPLC on a Waters SunFire prep C_{18} column (5 μm , 250 \times 19 mm; eluting with 0.1% trifluoroacetic acid–water initially, grading to 0.1% trifluoroacetic acid–50% acetonitrile–water over 40 min, with a flow rate of 15 mL/min; monitored by UV absorbance at 254 nm) to provide **FSA-23010** • 2 $\text{CF}_3\text{CO}_2\text{H}$ as a fine, snow-white powder (32.7 mg, 90%).

^1H NMR (600 MHz, CD_3OD) δ 8.64 (d, J = 2.3 Hz, 1H), 8.33 (d, J = 9.6 Hz, 1H, amide NH), 8.23 (d, J = 8.0 Hz, 1H), 8.04 (dd, J = 8.2, 2.2 Hz, 1H), 5.31 (d, J = 5.6 Hz, 1H), 4.57–4.54 (m, 3H), 4.50 (d, J = 1H), 4.48 (s, 3H), 4.29 (app dt, J = 10.0, 1.3 Hz, 1H), 4.10 (dd, J = 10.2, 5.6 Hz, 1H), 3.91 (dd, J = 3.4, 1.2 Hz, 1H), 3.75 (dd, J = 11.8, 7.3 Hz, 1H), 3.58 (dd, J = 10.2, 3.4 Hz, 1H), 3.18 (dd, J = 11.8, 5.2 Hz, 1H), 2.89 (t, J = 8.0 Hz, 2H), 2.42–2.37 (m, 1H), 2.14 (s, 3H), 1.95–1.89 (m, 1H), 1.81–1.74 (m, 1H), 1.53 (d, J = 6.8 Hz, 3H).

^{13}C NMR (126 MHz, CD_3OD) δ 167.3, 164.6, 161.0 (q, J = 37.9 Hz), 149.9, 144.7, 141.0, 140.5, 123.9, 117.1 (q, J = 288.4 Hz), 89.7, 76.4, 72.1, 70.7, 69.7, 69.6, 64.8, 59.2, 54.7, 47.8, 40.2, 33.3, 31.6, 22.7.

FTIR (neat, cm^{-1}): 3333 (br), 1674 (s), 1201 (m), 1133 (m).

HRMS (ESI+, m/z): $[\text{M}+\text{H}]^+$ calc'd for $\text{C}_{23}\text{H}_{34}\text{ClN}_7\text{O}_6\text{S}$, 572.2053; found 572.2065.



Synthetic lincosamide FSA-23011.

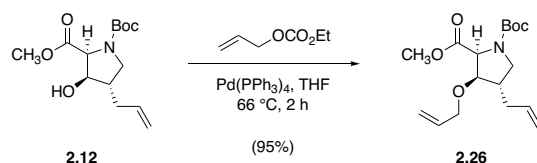
In a 4-mL glass vial fitted with a magnetic stir bar, **FSA-23010** • 2 CF₃CO₂H (6.6 mg, 8.3 μmol, 1 equiv) was dissolved in methanol (100 μL). Aqueous formaldehyde solution (37% w/w, 1.8 μL, 25 μmol, 3.0 equiv) was added, followed by sodium cyanoborohydride (1.6 mg, 25 μmol, 3.0 equiv) at 23 °C. After 4 h, LCMS analysis of the reaction mixture revealed that N-methylation was complete, and the mixture was concentrated to dryness in vacuo. The crude residue was purified by preparative HPLC on a Waters SunFire prep C₁₈ column (5 μm, 250 × 19 mm; eluting with 0.1% trifluoroacetic acid–water initially, grading to 0.1% trifluoroacetic acid–40% acetonitrile–water over 40 min, with a flow rate of 15 mL/min; monitored by UV absorbance at 254 nm) to provide **FSA-23011** • 2 CF₃CO₂H as a white solid (6.3 mg, 94%).

¹H NMR (600 MHz, CD₃OD) δ 8.62 (d, *J* = 2.2 Hz, 1H), 8.21 (d, *J* = 8.1 Hz, 1H), 7.98 (dd, *J* = 8.1, 2.2 Hz, 1H), 5.31 (d, *J* = 5.7 Hz, 1H), 4.62–4.54 (m, 3H), 4.33 (dd, *J* = 10.0, 1.3 Hz, 1H), 4.29 (d, *J* = 6.1 Hz, 1H), 4.11 (dd, *J* = 10.2, 5.7 Hz, 1H), 3.96 (dd, *J* = 11.7, 7.7 Hz, 1H), 3.84 (dd, *J* = 3.3, 1.3 Hz, 1H), 3.59 (dd, *J* = 10.2, 3.3 Hz, 1H), 3.00 (dd, *J* = 11.8, 8.5 Hz, 1H), 2.97 (s, 3H), 2.88 (t, *J* = 8.0 Hz, 2H), 2.36–2.31 (m, 1H), 2.16 (s, 3H), 2.05–1.98 (m, 1H), 1.90–1.84 (m, 1H), 1.54 (d, *J* = 6.9 Hz, 3H).

^{13}C NMR (126 MHz, CD_3OD) δ 165.9, 165.0, 161.0 (q, $J = 36.0$ Hz), 150.4, 145.3, 140.6, 139.7, 123.8, 117.2 (q, $J = 288.5$ Hz), 89.9, 76.8, 73.7, 72.2, 70.6, 69.8, 69.5, 59.7, 59.4, 54.6, 47.7, 41.5, 40.2, 33.9, 31.6, 22.7, 13.5.

FTIR (neat, cm^{-1}): 3344 (br), 1673 (s), 1202 (s), 1135 (m).

HRMS (ESI+, m/z): $[\text{M}+\text{H}]^+$ calc'd for $\text{C}_{23}\text{H}_{36}\text{ClN}_7\text{O}_6\text{S}$, 586.2209; found 586.2222.



Diene 2.26.

In a 50-mL round-bottomed flask containing a magnetic stir bar, alcohol **2.12** (500 mg, 1.75 mmol, 1 equiv) and allyl ethyl carbonate (461 μL , 3.50 mmol, 2.00 equiv) were dissolved in tetrahydrofuran (8.75 mL), and the flask was fitted with a reflux condenser. In a separate pear-shaped flask, tetrakis(triphenylphosphine)palladium(0) (51.0 g, 44.2 μmol , 0.0250 equiv) was dissolved in tetrahydrofuran (8.75 mL). The precatalyst solution was then added via cannula to the flask containing the starting materials, the apparatus was shielded from light with aluminum foil, and the reaction mixture was heated to reflux in a pre-heated oil bath (75 $^\circ\text{C}$ bath temperature). Over 30 min, the reaction mixture changed color from very faint yellow to sunset orange. After 2 h, TLC analysis showed that no starting material remained. The mixture was cooled to 23 $^\circ\text{C}$ before it was passed through a plug of silica gel. Upon exposure to silica gel, the reaction mixture attained a cherry-red color. The filter pad was rinsed with *tert*-butyl methyl ether (2 \times 15 mL), and the combined filtrates were concentrated to give a yellow residue. This crude product was purified by flash-column chromatography (30 g silica gel, eluting with hexanes initially, grading to 10% ethyl acetate–hexanes) to furnish the product as a faint yellow viscous oil (539 mg, 95%).

$R_f = 0.58$ (30% ethyl acetate–hexanes, KMnO_4).

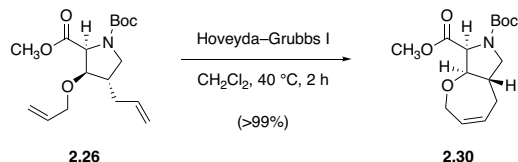
$^1\text{H NMR}$ (60:40 mixture of rotamers, asterisks [*] denote minor rotameric signals that could be resolved, 500 MHz, CDCl_3) δ 5.85 (ddt, $J = 17.0, 10.3, 5.8$ Hz, 1H), 5.80–5.71 (m, 1H), 5.27 (app dq, $J = 17.2, 1.4$ Hz, 1H), 5.19 (ddt, $J = 10.3, 2.8, 1.4$ Hz, 1H), 5.08–5.00 (m,

2H), 4.56 (d, $J = 7.5$ Hz, 1H),* 4.47 (d, $J = 7.5$ Hz, 1H), 4.16 (dddt, $J = 12.4, 8.3, 5.4, 1.5$ Hz, 1H), 3.99 (ddt, $J = 12.5, 6.1, 1.3$ Hz, 1H), 3.82 (ddd, $J = 16.2, 8.9, 7.6$ Hz, 1H), 3.80–3.75 (m, 1H), 3.73 (s, 3H),* 3.72 (s, 3H), 3.70 (dd, $J = 10.2, 7.8$ Hz, 1H), 2.97 (td, $J = 11.0, 9.0$ Hz, 1H), 2.50–2.41 (m, 1H), 2.40–2.34 (m, 1H), 2.05–1.97 (m, 1H), 1.44 (s, 9H),* 1.39 (s, 9H).

^{13}C NMR (60:40 mixture of rotamers, asterisks [*] denote minor rotameric signals that could be resolved, 126 MHz, CDCl_3) δ 170.9, 154.5,* 153.9, 135.6,* 135.4, 134.2, 117.9, 116.9, 116.8,* 82.4, 81.6,* 80.3, 72.1, 61.8, 61.0,* 52.2,* 52.0, 48.9,* 48.4, 41.5,* 40.9, 35.1,* 35.0, 28.5,* 28.4.

FTIR (neat, cm^{-1}): 2930 (w), 1749 (m), 1703 (s), 1396 (s), 1367 (m), 1179 (m), 1146 (m), 917 (w).

HRMS (ESI+, m/z): $[\text{M}+\text{H}]^+$ calc'd for $\text{C}_{17}\text{H}_{27}\text{NO}_5$, 326.1962; found 326.1969.



Oxepinoproline 2.30.

In a 100-mL round-bottomed flask to which a reflux condenser had been affixed, a solution of diene **2.12** (539 mg, 1.66 mmol, 1 equiv) and dichloro(2-isopropoxyphenylmethylene)(tricyclohexylphosphine)ruthenium(II) (first-generation Hoveyda-Grubbs catalyst, 50.0 mg, 83.3 μmol , 0.0500 equiv) in dichloromethane (33.1 mL) was heated to reflux in a pre-heated oil bath (55 $^\circ\text{C}$ bath temperature). After 2 h, TLC analysis (30% ethyl acetate-hexanes, KMnO_4) showed that no starting material remained. The mixture was cooled to 23 $^\circ\text{C}$ before it was concentrated to dryness to give a thick brown oil. This crude residue was purified by flash-column chromatography (30 g silica gel, eluting with hexanes first, grading to 20% ethyl acetate-hexanes) to provide the product as a leather-brown oil (499 mg, 101%).

$R_f = 0.39$ (30% ethyl acetate-hexanes, KMnO_4).

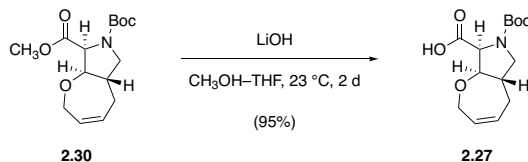
^1H NMR (60:40 mixture of rotamers, asterisks [*] denote minor rotameric signals that could be resolved, 500 MHz, CDCl_3) δ 5.86–5.80 (m, 1H), 5.75–5.69 (m, 1H), 4.53 (d, $J = 8.3$ Hz, 1H),* 4.44 (d, $J = 8.3$ Hz, 1H), 4.32 (dd, $J = 6.3, 1.2$ Hz, 1H),* 4.29 (dd, $J = 6.2, 1.3$ Hz, 1H), 4.09–4.03 (m, 1H), 3.93–3.88 (m, 1H), 3.88–3.86 (m, 1H),* 3.83–3.78 (m, 1H), 3.76 (s, 3H),* 3.74 (s, 3H), 2.91 (app td, $J = 10.6, 4.0$ Hz, 1H), 2.55–2.41 (m, 2H), 2.04–1.96 (m, 1H), 1.44 (s, 9H),* 1.40 (s, 9H).

^{13}C NMR (60:40 mixture of rotamers, asterisks [*] denote minor rotameric signals that could be resolved, 126 MHz, CDCl_3) δ 171.2,* 171.0, 154.1,* 153.7, 130.2, 130.1,* 130.0, 86.6,

85.9,* 80.4, 80.4,* 68.6, 62.5, 61.9,* 52.3,* 52.1, 50.0,* 49.4, 41.6,* 40.9, 31.1,* 31.0,
28.5,* 28.4.

FTIR (neat, cm^{-1}): 2976 (w), 1749 (s), 1703 (s), 1396 (s), 1209 (m), 1174 (m), 1127 (m).

HRMS (ESI+, m/z): $[\text{M}+\text{Na}]^+$ calc'd for $\text{C}_{15}\text{H}_{23}\text{NO}_5$, 320.1468; found 320.1477.



Carboxylic acid **2.27**.

To a magnetically stirred solution of methyl ester **2.30** (73 mg, 0.25 mmol, 1 equiv) in 50% v/v methanol–tetrahydrofuran (1.2 mL) was added aqueous lithium hydroxide solution (1.0 M, 270 μL , 0.27 mmol, 1.1 equiv) at 23 $^\circ\text{C}$. After stirring at ambient temperature for 2 d, LCMS analysis showed that saponification was complete. The reaction mixture was diluted with water (2 mL), and the diluted solution was chilled to 0 $^\circ\text{C}$ before being acidified to pH = 2 with the dropwise addition of 1N aqueous hydrogen chloride solution. The acidified aqueous mixture was extracted with ethyl acetate (5 \times 2 mL), and the combined extracts were dried over sodium sulfate. The dried solution was filtered, and the filtrate was concentrated to provide carboxylic acid saponification product as a dull white solid (66 mg, 95%).

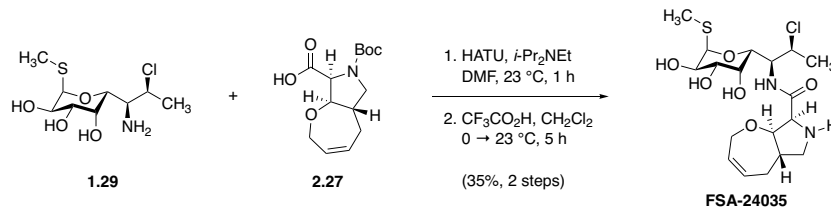
^1H NMR (70:30 mixture of rotamers, asterisks [*] denote minor rotameric signals that could be resolved, 600 MHz, CDCl_3) δ 10.93 (br, 1H), 5.82 (app dtt, J = 13.6, 8.1, 2.7 Hz, 1H), 5.72 (app ddt, J = 11.9, 5.9, 2.9 Hz, 1H), 4.52 (d, J = 8.3 Hz, 1H),* 4.43 (d, J = 8.3 Hz, 1H), 4.31 (ddd, J = 15.1, 8.6, 6.2 Hz, 1H), 4.06 (app dq, J = 15.7, 3.0 Hz, 1H), 3.93 (app td, J = 9.9, 8.2 Hz, 1H), 3.86 (dd, J = 10.7, 8.3 Hz, 1H), 3.77 (dd, J = 10.5, 8.5 Hz, 1H),* 2.91 (app td, J = 10.6, 1.5 Hz, 1H), 2.51–2.40 (m, 2H), 1.99 (ddd, J = 17.0, 11.3, 2.9 Hz, 1H), 1.43 (s, 9H),* 1.39 (s, 9H).

^{13}C NMR (70:30 mixture of rotamers, asterisks [*] denote minor rotameric signals that could be resolved, 151 MHz, CDCl_3) δ 176.1, 175.5,* 154.2,* 153.7, 130.2, 130.1,* 130.0,* 129.9,

86.4, 85.7,* 80.9, 80.5,* 68.6, 68.5,* 62.3, 61.7,* 49.9,* 49.3, 41.6,* 40.9, 31.0,* 30.9,
28.5,* 28.3.

FTIR (neat, cm^{-1}): 2975 (m), 1745 (m), 1721 (s), 1698 (s), 1395 (s), 1368 (s), 1248 (m), 1171 (s),
1127 (s), 912 (m), 730 (m).

HRMS (ESI+, m/z): $[\text{M}+\text{Na}]^+$ calc'd for $\text{C}_{14}\text{H}_{21}\text{NO}_5$, 306.1312; found 306.1298.



Synthetic lincosamide FSA-24035.

In a 2–5 mL glass microwave vial, carboxylic acid **2.27** (66 mg, 0.23 mmol, 1 equiv) was dried by azeotropic removal of benzene. The dried starting material was then dissolved in *N,N*-dimethylformamide (1.2 mL), and HATU (98 mg, 0.26 mmol, 1.1 equiv) was added at 23 °C. After stirring this mixture for 10 min, 7-chloro-methylthiolincosamine (**1.29**, 96 mg, 0.35 mmol, 1.5 equiv) was added next, and the resulting light cream-yellow suspension was stirred at ambient temperature for 20 min. Finally, *N,N*-diisopropylethylamine (100 μL, 0.59 mmol, 2.5 equiv) was added dropwise. After stirring an additional 1 h, LCMS analysis indicated that no carboxylic acid or activated-ester intermediate remained, and the reaction mixture was concentrated to dryness in vacuo. The residue was purified by flash-column chromatography (12 g silica gel, eluting with dichloromethane initially, grading to 5% methanol–dichloromethane). Fractions containing product were identified by TLC ($R_f = 0.34$, 5% methanol–dichloromethane, PMA); these fractions were pooled and concentrated to provide *N*-Boc–protected product as a white film (100 mg, 79%). Due to substantial amide and carbamate rotamerism observed in the ¹H-NMR spectrum, this material was carried forward through *N*-Boc deprotection prior to full characterization.

The *N*-Boc–protected lincosamide was finally dissolved in dichloromethane (1.4 mL), and dimethyl sulfide (140 μL) was added. This solution was chilled to 0 °C, whereupon trifluoroacetic acid (140 μL) was added dropwise. The mixture was allowed to warm gradually to 23 °C over 5 h, at which point LCMS analysis showed that Boc removal was complete. The reaction mixture was consequently diluted with toluene (2 mL), and the diluted mixture was concentrated in vacuo.

The residue was purified by flash-column chromatography (10 g silica gel, eluting with 1% ammonium hydroxide–5% methanol–dichloromethane initially, grading to 1% ammonium hydroxide–10% methanol–dichloromethane) to provide **FSA-24035** as a white solid (35 mg, 35%, 2 steps).

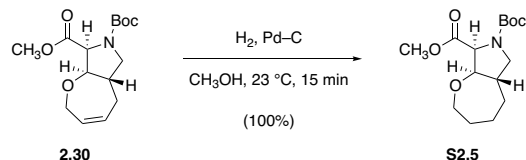
$R_f = 0.22$ (1% ammonium hydroxide–10% methanol–dichloromethane, CAM).

$^1\text{H NMR}$ (600 MHz, CD_3OD) δ 5.84 (ddt, $J = 12.5, 7.3, 2.7$ Hz, 1H), 5.71 (ddt, $J = 12.1, 6.0, 2.9$ Hz, 1H), 5.30 (d, $J = 5.7$ Hz, 1H), 4.59 (qd, $J = 6.8, 1.6$ Hz, 1H), 4.42 (dd, $J = 10.1, 1.6$ Hz, 1H), 4.31 (dd, $J = 15.9, 6.0$ Hz, 1H), 4.19 (dd, $J = 10.0, 1.2$ Hz, 1H), 4.12–4.04 (m, 3H), 3.96 (app t, $J = 9.0$ Hz, 1H), 3.89 (dd, $J = 3.4, 1.2$ Hz, 1H), 3.56 (dd, $J = 10.2, 3.4$ Hz, 1H), 3.28 (dd, $J = 10.3, 7.1$ Hz, 1H), 2.60 (app t, $J = 10.8$ Hz, 1H), 2.47 (ddd, $J = 16.6, 7.4, 3.2$ Hz, 1H), 2.14 (s, 3H), 2.10–2.04 (m, 1H), 2.02–1.97 (m, 1H), 1.50 (d, $J = 6.8$ Hz, 3H).

$^{13}\text{C NMR}$ (126 MHz, CD_3OD) δ 174.3, 130.8, 89.6, 88.7, 71.9, 71.1, 69.7, 69.6, 69.1, 63.4, 59.2, 54.4, 50.6, 45.4, 31.3, 22.6, 13.3. Only one vinyl signal is observed, due to coincidence of the two vinyl resonances, as confirmed by HSQC.

FTIR (neat, cm^{-1}): 3345 (br), 2919 (m), 1659 (s), 1524 (m), 1442 (m), 1256 (m), 1141 (m), 1082 (s), 1053 (s), 845 (m).

HRMS (ESI+, m/z): $[\text{M}+\text{H}]^+$ calc'd for $\text{C}_{18}\text{H}_{29}\text{ClN}_2\text{O}_6\text{S}$, 437.1508; found 437.1503.



Oxepanoproline S2.5.

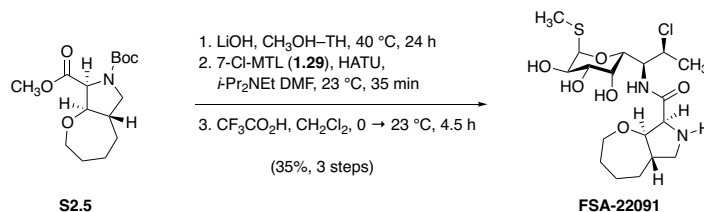
To a magnetically stirred solution of pyrrolidinooxepine **2.30** (12 mg, 40 μmol , 1 equiv) in methanol (3.0 mL) was added palladium on carbon (10% w/w, 2.1 mg). Hydrogen gas was bubbled through this mixture at 23 $^\circ\text{C}$ for 15 min, at which point LCMS analysis indicated that hydrogenation was complete. The black suspension was filtered through a pad of Celite in order to remove the heterogeneous catalyst, and the filter cake was rinsed with fresh portions of methanol (3×1 mL). The filtrate was concentrated to provide oxepanoproline product as a colorless film (12 mg, 100%).

^1H NMR (60:40 mixture of rotamers, asterisks [*] denote minor rotameric signals that could be resolved, 500 MHz, CDCl_3) δ 4.45 (d, $J = 8.2$ Hz, 1H),* 4.36 (d, $J = 8.3$ Hz, 1H), 4.08–4.03 (m, 1H), 3.87 (d, $J = 8.6$ Hz, 1H), 3.84 (d, $J = 3.85$ Hz, 1H),* 3.81–3.75 (m, 3H), 3.75 (s, 3H),* 3.73 (s, 3H), 2.88 (app td, $J = 10.6, 2.0$ Hz, 1H), 2.60–2.44 (m, 1H), 2.00–1.91 (m, 1H), 1.86–1.79 (m, 2H), 1.77–1.70 (m, 1H), 1.63–1.51 (m, 2H), 1.43 (s, 9H),* 1.39 (s, 9H), 1.25–1.16 (m, 2H),

^{13}C NMR (60:40 mixture of rotamers, asterisks [*] denote minor rotameric signals that could be resolved, 126 MHz, CDCl_3) δ 171.8,* 171.5, 154.1,* 153.6, 81.8, 81.1,* 80.2, 80.2,* 70.1, 70.0,* 62.6, 62.0,* 52.2,* 52.0, 50.7,* 50.0, 42.8,* 42.1, 30.6,* 30.5, 28.5,* 28.4, 25.7,* 25.7.

FTIR (neat, cm^{-1}): 2930 (m), 1749 (m), 1703 (s), 1401 (s), 1205 (m), 1177 (m), 1131 (m).

HRMS (ESI+, m/z): [M+Na] calc'd for C₁₅H₂₅NO₅, 322.1625; found 322.1637.



Synthetic lincosamide FSA-22091.

To a magnetically stirred solution of methyl ester **S2.5** (12 mg, 40 μmol, 1 equiv) in 50% v/v methanol–tetrahydrofuran (200 μL) was added aqueous lithium hydroxide solution (1.0 M, 40 μL, 40 μmol, 1.0 equiv) at 23 °C. The mixture was then heated to 40 °C with stirring, and LCMS analysis after 7 h indicated that saponification was not complete. Consequently, an additional portion of aqueous lithium hydroxide solution (1.0 M, 40 μL, 40 μmol, 1.0 equiv) was added, and stirring was maintained at 40 °C for an additional 17 h. At this point, LCMS analysis indicated that no methyl ester remained. The mixture was diluted with water (2 mL), and the resulting solution was chilled to 0 °C. The ice-cold mixture was acidified to pH = 2 with the addition of 1N aqueous hydrogen chloride solution, and the acidified mixture was extracted with ethyl acetate (5 × 2 mL). The combined organic extracts were dried over sodium sulfate, filtered, and concentrated to provide carboxylic acid intermediate as a white powder.

This residue was transferred to a 2–5 mL glass microwave vial, where it was dissolved in *N,N*-dimethylformamide (210 μL). To this solution, HATU (18 mg, 46 μmol, 1.1 equiv) was added, and the mixture was stirred at 23 °C for 10 min. Next, 7-chloro-methylthiolincosamine (**1.29**, 17 mg, 63 μmol, 1.5 equiv) was added; the resulting light-yellow suspension was stirred for 20 min before *N,N*-diisopropylamine (18 μL, 0.11 mmol, 2.5 equiv) was finally added, causing a canary yellow solution to form. After 35 min, LCMS analysis showed that no carboxylic acid or activated-ester intermediate remained, and the reaction mixture was concentrated in vacuo. The residue was purified by flash-column chromatography (4 g silica gel, eluting with dichloromethane

initially, grading to 5% methanol–dichloromethane). Fractions containing *N*-Boc–protected coupled product were identified by TLC ($R_f = 0.41$, 10% methanol–dichloromethane, PMA). These fractions were pooled and concentrated to provide *N*-Boc–protected lincosamide as a white film.

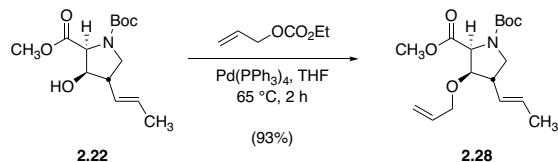
This residue was finally dissolved in dichloromethane (300 μ L). The resulting solution was chilled to 0 °C before trifluoroacetic acid (30 μ L) was added; the mixture was stirred at 0 °C for 4.5 h, at which point LCMS analysis showed that Boc removal was complete. The solution was diluted with toluene (5 mL), and the diluted mixture was concentrated in vacuo. The residue was purified by flash-column chromatography (4 g silica gel, eluting with 1% ammonium hydroxide–5% methanol–dichloromethane initially, grading to 1% ammonium hydroxide–10% methanol–dichloromethane) to provide **FSA-22091** as a white solid (6.1 mg, 35%, 3 steps).

$R_f = 0.27$ (1% ammonium hydroxide–10% methanol–dichloromethane, PMA).

$^1\text{H NMR}$ (600 MHz, CD_3OD) δ 5.30 (d, $J = 5.6$ Hz, 1H), 4.60 (qd, $J = 6.8, 1.6$ Hz, 1H), 4.41 (dd, $J = 10.1, 1.6$ Hz, 1H), 4.20 (dd, $J = 10.0, 0.8$ Hz, 1H), 4.12 (app t, $J = 9.1$ Hz, 1H), 4.08 (dd, $J = 10.2, 5.6$ Hz, 1H), 3.95 (d, $J = 9.0$ Hz, 1H), 3.91 (dd, $J = 3.5, 1.1$ Hz, 1H), 3.87 (ddd, $J = 11.8, 7.6, 4.2$ Hz, 1H), 3.76 (ddd, $J = 11.7, 5.7, 3.9$ Hz, 1H), 3.57 (dd, $J = 10.2, 3.4$ Hz, 1H), 3.26 (dd, $J = 10.2, 7.2$ Hz, 1H), 2.56 (dd, $J = 11.2, 10.3$ Hz, 1H), 2.19–2.12 (m, 1H), 2.14 (s, 3H), 1.94 (app dq, $J = 13.4, 5.2$ Hz, 1H), 1.90–1.76 (m, 3H), 1.67 (app ddt, $J = 17.5, 8.7, 5.5$ Hz, 1H), 1.51 (d, $J = 6.8$ Hz, 3H), 1.26 (dddd, $J = 14.0, 11.4, 9.0, 5.3$ Hz, 1H).

$^{13}\text{C NMR}$ (126 MHz, CD_3OD) δ 174.7, 89.6, 84.1, 71.9, 71.2 (2 \times C), 69.7, 69.6, 63.9, 59.2, 54.4, 51.3, 46.7, 30.2, 29.9, 27.1, 22.6, 13.3.

HRMS (ESI+, m/z): $[M+H]^+$ calc'd for $C_{18}H_{31}ClN_2O_6S$, 439.1664; found 439.1678.

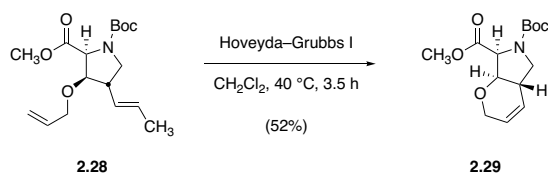


Diene **2.28**.

In a 2–5 mL glass microwave vial, alcohol **2.22** (17 mg, 60 μmol , 1 equiv) and allyl ethyl carbonate (16 μL , 120 μmol , 2.0 equiv) were dried together by azeotropic removal of benzene. A separate 4-mL glass vial was charged with tetrakis(triphenylphosphine)palladium(0) (1.7 mg, 1.4 μmol , 0.025 equiv), and this precatalyst was dissolved in tetrahydrofuran (600 μL). The precatalyst solution was added to the reaction vial containing the starting materials via cannula, and the reaction vial was sealed. The mixture was heated to $65\text{ }^\circ\text{C}$ in a pre-heated oil bath. After 2 h, TLC analysis (30% ethyl acetate–hexanes, UV+ KMnO_4) showed that etherification was complete, and the mixture was cooled to $23\text{ }^\circ\text{C}$ before it was concentrated to dryness in vacuo. The crude residue was then purified by flash-column chromatography (4 g silica gel, eluting with 10% ethyl acetate–hexanes) to provide the product as a colorless oil (18 mg, 93%).

$R_f = 0.60$ (30% ethyl acetate–hexanes, KMnO_4).

^1H NMR (60:40 mixture of rotamers, asterisks [*] denote minor rotameric signals that could be resolved, 600 MHz, CDCl_3) δ 5.87–5.79 (m, 1H), 5.65–5.58 (m, 1H), 5.31–5.27 (m, 1H), 5.26 (dq, $J = 17.2, 1.6\text{ Hz}$, 1H), 5.18 (ddq, $J = 10.5, 3.0, 1.4\text{ Hz}$, 1H), 4.55 (d, $J = 7.6\text{ Hz}$, 1H),* 4.45 (d, $J = 7.6\text{ Hz}$, 1H), 4.17–4.12 (m, 1H), 4.05–4.02 (m, 1H), 3.87 (ddd, $J = 10.8, 9.1, 7.6\text{ Hz}$, 1H), 3.76–3.71 (m, 1H), 3.74 (s, 3H),* 3.73 (s, 3H), 3.09–3.04 (m, 1H), 3.02–2.92 (m, 1H), 1.68 (dd, $J = 6.7, 1.8\text{ Hz}$, 1H), 1.44 (s, 9H),* 1.40 (s, 9H).



Bicyclic compound 2.29.

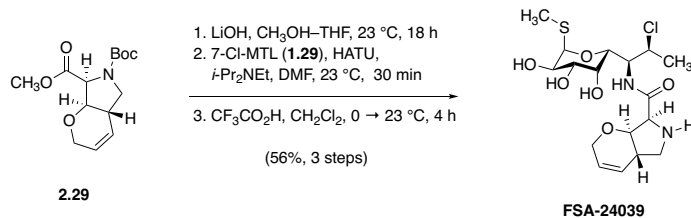
In a 10-mL round-bottomed flask fused to a reflux condenser, diene **2.28** (18 mg, 55 μmol , 1 equiv) and dichloro(2-isopropoxyphenylmethylene)(tricyclohexylphosphine)ruthenium(II) (first-generation Hoveyda–Grubbs catalyst, 1.6 mg, 2.8 μmol , 0.050 equiv) were dissolved in dichloromethane (1.1 mL). The resulting solution was heated to reflux in a pre-heated oil bath (55 $^\circ\text{C}$ bath temperature), and after 3.5 h, TLC analysis (30% ethyl acetate–hexanes, KMnO_4) indicated that no starting material remained. The mixture was concentrated to dryness, and the residue was purified by flash-column chromatography (4 g silica gel, eluting with 20% ethyl acetate–hexanes) to furnish the product as a colorless oil (8.2 mg, 52%).

$R_f = 0.42$ (30% ethyl acetate–hexanes, KMnO_4).

^1H NMR (60:40 mixture of rotamers, asterisks [*] denote minor rotameric signals that could be resolved, 600 MHz, CDCl_3) δ 5.99 (app dq, $J = 10.1, 2.1$ Hz, 1H), 5.95 (app dq, $J = 10.0, 2.2$ Hz, 1H),* 5.69–5.66 (m, 1H), 4.49 (d, $J = 7.9$ Hz, 1H),* 4.41–4.39 (m, 2H), 3.92–3.89 (m, 1H), 3.83–3.79 (m, 1H), 3.78 (s, 3H),* 3.77 (s, 3H), 2.92–2.86 (m, 1H), 1.46 (s, 9H),* 1.41 (s, 9H).

^{13}C NMR (60:40 mixture of rotamers, asterisk [*] denotes minor rotamer signals that could be resolved, 126 MHz, CDCl_3) δ 170.8, 153.9, 153.7,* 127.5,* 127.4, 125.0, 124.9,* 80.6, 80.5,* 78.8, 78.3,* 68.5, 68.4,* 59.7, 59.1,* 52.5,* 52.3, 46.8,* 45.9, 37.2,* 36.6, 28.5,* 28.4.

HRMS (ESI+, m/z): $[M+Na]^+$ calc'd for $C_{14}H_{21}NO_5$, 306.1312; found 306.1319



Synthetic lincosamide FSA-24039.

A magnetically stirred solution of methyl ester **2.29** (45 mg, 0.16 mmol, 1 equiv) in 50% v/v methanol–tetrahydrofuran (790 μ L) was treated with aqueous lithium hydroxide solution (1.0 M, 190 μ L, 190 μ mol, 1.2 equiv) at 23 °C. After stirring for 18 h at ambient temperature, LCMS analysis indicated that saponification was complete. The reaction mixture was consequently diluted with water (3 mL), the diluted solution was chilled to 0 °C, and the cooled mixture was acidified to pH = 2 with the addition of 1N aqueous hydrogen chloride solution. The acidified mixture was then extracted with ethyl acetate (5 \times 2 mL), and the combined extracts were dried over sodium sulfate. The dried organic product solution was filtered, and the filtrate was concentrated to afford carboxylic acid saponification product as a white solid.

This residue was then transferred to a 2–5 mL glass microwave vial, where it was dried by azeotropic removal of benzene. The dried carboxylic acid was dissolved in *N,N*-dimethylformamide (930 μ L), and the solution was treated with HATU (78 mg, 0.20 mmol, 1.1 equiv). The colorless solution was stirred at 23 °C for 10 min before 7-chloromethylthiolincosamine (**1.29**, 76 mg, 0.28 mmol, 1.5 equiv) was added. A light cream-yellow suspension formed, and this mixture was stirred at 23 °C for 20 min before *N,N*-diisopropylethylamine (81 μ L, 0.46 mmol, 2.5 equiv) was added dropwise. After 30 min of additional stirring at 23 °C, LCMS analysis showed no trace of carboxylic acid or activated-ester intermediate. The mixture was concentrated in vacuo, and the dried residue was purified by flash-

column chromatography (4 g silica gel, eluting with dichloromethane initially, grading to 5% methanol–dichloromethane). Fractions containing the coupled, *N*-Boc–protected product were identified by TLC ($R_f = 0.50$, 10% methanol–dichloromethane, PMA); these fractions were pooled and concentrated to provide *N*-Boc–protected lincosamide as a white film.

Finally, this residue was dissolved in dichloromethane (1.6 mL), and the solution was chilled to 0 °C. Dimethyl sulfide (120 μ L) and trifluoroacetic acid (200 μ L) were added sequentially, and then the mixture was allowed to warm to 23 °C gradually over 4 h. At this point, LCMS analysis showed that Boc removal was complete. The reaction mixture was diluted with toluene (3 mL), and the diluted mixture was concentrated in vacuo. The residue was then redissolved in methanol (1.5 mL), the solution was chilled to 0 °C, and Amberlyst A26 ion-exchange resin (hydroxide form, 500 mg) was added. The mixture was stirred at 0 °C for 30 min before the beads were filtered off, and the filtrate was concentrated. The residue obtained was then purified by flash-column chromatography (4 g silica gel, eluting with 1% ammonium hydroxide–5% methanol–dichloromethane initially, grading to 1% ammonium hydroxide–10% methanol–dichloromethane) to provide **FSA-24039** as a white powder (38 mg, 56%, 3 steps).

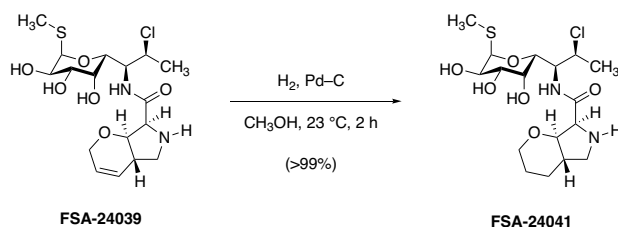
$R_f = 0.13$ (1% ammonium hydroxide–10% methanol–dichloromethane, PMA).

$^1\text{H NMR}$ (500 MHz, CD_3OD) δ 6.01 (app dq, $J = 10.1, 2.1$ Hz, 1H), 5.74 (app dq, $J = 10.1, 2.5$ Hz, 1H), 5.29 (d, $J = 5.7$ Hz, 1H), 4.60 (qd, $J = 6.8, 1.6$ Hz, 1H), 4.44–4.41 (m, 3H), 4.19 (dd, $J = 10.0, 1.1$ Hz, 1H), 4.08 (dd, $J = 10.2, 5.6$ Hz, 1H), 3.92 (d, $J = 8.5$ Hz, 1H), 3.84–3.80 (m, 2H), 3.56 (dd, $J = 10.2, 3.4$ Hz, 1H), 3.25 (dd, $J = 8.9, 6.5$ Hz, 1H), 2.58 (dd, $J = 12.2, 8.9$ Hz, 1H), 2.52 (br, 1H), 2.15 (s, 3H), 1.49 (d, $J = 6.8$ Hz, 3H).

^{13}C NMR (126 MHz, CD_3OD) δ 174.5, 128.8, 126.2, 111.4, 89.7, 81.6, 72.0, 71.1, 69.7, 69.6, 59.2, 59.0, 54.4, 46.4, 39.5, 22.6, 13.4.

FTIR (neat, cm^{-1}): 3348 (br), 2923 (m), 1660 (s), 1450 (m), 1389 (m), 1090 (s), 1056 (s), 987 (s), 845 (m).

HRMS (ESI+, m/z): $[\text{M}+\text{H}]^+$ calc'd for $\text{C}_{17}\text{H}_{27}\text{ClN}_2\text{O}_6\text{S}$, 423.1351; found 423.1344.

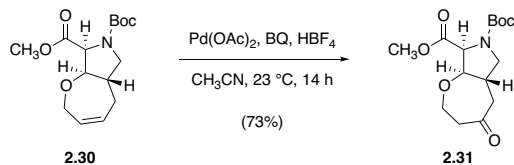


Synthetic lincosamide FSA-24041.

In a 2–5 mL glass microwave vial, **FSA-24039** (6.7 mg, 16 μmol , 1 equiv) was dissolved in methanol (160 μL). To this solution was added palladium on carbon (10% w/w, 1.0 mg), and the headspace of the reaction vial was replaced with hydrogen gas supplied by a balloon. After stirring for 2 h at 23 $^\circ\text{C}$, LCMS analysis showed that hydrogenation was complete, and the mixture was filtered through a pad of Celite to remove the heterogeneous catalyst. The filtrate was concentrated to provide the product as a white film (7.0 mg, 104%).

^1H NMR (400 MHz, CD_3OD) δ 5.29 (d, $J = 5.6$ Hz, 1H), 4.60 (qd, $J = 6.5, 1.4$ Hz, 1H), 4.42 (dd, $J = 9.8, 1.4$ Hz, 1H), 4.18 (d, $J = 10.4$ Hz, 1H), 4.11–4.06 (m, 2H), 3.89 (d, $J = 8.7$ Hz, 1H), 3.85 (d, $J = 3.3$ Hz, 1H), 3.59–3.47 (m, 3H), 3.14 (dd, $J = 9.7, 6.7$ Hz, 1H), 2.54 (dd, $J = 11.5, 9.7$ Hz, 1H), 2.14 (s, 3H), 2.06–2.03 (m, 1H), 1.75–1.67 (m, 1H), 1.65–1.58 (m, 2H), 1.50 (d, $J = 6.8$ Hz, 3H), 1.40–1.32 (m, 1H).

MS (ESI+, m/z): $[\text{M}+\text{H}]^+$ calc'd for $\text{C}_{17}\text{H}_{29}\text{ClN}_2\text{O}_6\text{S}$, 425.2; found 425.2.



Bicyclic ketone 2.31.

Conditions for regioselective olefin Wacker oxidation were adapted from the report of Morandi, Wickens, and Grubbs.⁹⁵ In a 25-mL round-bottomed flask, oxepinoproline **2.30** (169 mg, 568 μmol , 1 equiv), palladium acetate (6.38 mg, 28.4 μmol , 0.0500 equiv), and 1,4-benzoquinone (61.0 mg, 568 μmol , 1.00 equiv) were dissolved in acetonitrile (2.49 mL). To this solution were then added water (349 μL) and aqueous tetrafluoroboric acid solution (48% w/w, 102 μL , 784 μmol , 1.38 equiv). The reaction mixture was stirred at 23 $^\circ\text{C}$, and after 14 h, TLC analysis (30% ethyl acetate–hexanes, KMnO_4) indicated that no starting material remained. The mixture was diluted with saturated aqueous sodium chloride solution (10 mL), and the diluted mixture was extracted with dichloromethane (3×5 mL). The combined organic extracts were dried over sodium sulfate, filtered, and concentrated. The crude residue thus obtained was subjected to flash-column chromatography (12 g silica gel, eluting with 40% ethyl acetate–hexanes) to provide the product as a pale-yellow oil (131 mg, 73%).

$R_f = 0.40$ (60% ethyl acetate–hexanes, CAM).

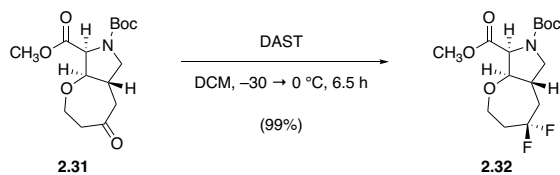
$^1\text{H NMR}$ (60:40 mixture of rotamers, asterisks [*] denote minor rotameric signals that could be resolved, 500 MHz, CDCl_3) δ 4.53 (d, $J = 8.3$, 1H),* 4.45 (d, $J = 8.4$ Hz, 1H), 4.12–4.08 (m, 1H), 3.95–3.89 (m, 2H), 3.84 (dd, $J = 10.4$, 8.3 Hz, 1H),* 3.74 (s, 3H),* 3.73 (s, 3H), 3.65 (app t, $J = 12.2$ Hz, 1H),* 3.66 (app t, $J = 12.1$ Hz, 1H), 2.95–2.89 (m, 2H), 2.86–2.69

(m, 2H), 2.55 (dd, $J = 15.7, 4.7$ Hz, 1H), 2.41 (dd, $J = 17.8, 12.0$ Hz, 1H), 1.41 (s, 9H),*
1.37 (s, 9H).

^{13}C NMR (60:40 mixture of rotamers, asterisks [*] denote minor rotameric signals that could be resolved, 126 MHz, CDCl_3) δ 209.1,* 209.0, 171.0,* 170.8, 153.8,* 153.3, 86.2, 85.6,* 80.7, 66.5, 66.5,* 62.2, 61.7,* 52.4,* 52.2, 49.8,* 49.2, 47.8, 44.6,* 44.5, 37.6,* 36.8, 28.4,* 28.3.

FTIR (neat, cm^{-1}): 2975 (w), 1745 (m), 1694 (s), 1400 (s), 1366 (s), 1247 (m), 1208 (s), 1174 (s), 1138 (s), 1123 (s), 1101 (s).731 (m).

HRMS (ESI+, m/z): $[\text{M}+\text{H}]^+$ calc'd for $\text{C}_{15}\text{H}_{23}\text{NO}_6$, 314.1598; found 314.1599.



Difluoro compound 2.32.

In a 2–5 mL glass microwave vial, a solution of ketone **2.31** (20 mg, 64 μ mol, 1 equiv) in dichloromethane (430 mL) pre-chilled to -30 $^{\circ}$ C was treated with diethylaminosulfur trifluoride (DAST, 51 μ L, 0.38 mmol, 6.0 equiv), added dropwise over 30 s. The cooling bath was removed, and the reaction mixture was then allowed to warm to 23 $^{\circ}$ C. After 2.5 h, TLC analysis (60% ethyl acetate–hexanes, CAM) indicated that some starting material remained, so the mixture was chilled to 0 $^{\circ}$ C, an additional portion of DAST (42 μ L, 0.32 mmol, 5.0 equiv) was added dropwise, and the mixture was then re-warmed to 23 $^{\circ}$ C as before. The reaction was judged to be complete by TLC analysis 4 h after this second addition of deoxyfluorinating reagent. The reaction mixture was cooled to -5 $^{\circ}$ C, and methanol (200 μ L) was added to quench excess DAST. The quenched mixture was stirred at -5 $^{\circ}$ C for 1 min and was then diluted with dichloromethane (15 mL). The diluted mixture was washed with saturated aqueous sodium bicarbonate solution (5 mL), the organic phase was dried over sodium sulfate, the dried solution was filtered, and the filtrate was concentrated to give a crude residue. This residue was subjected to flash-column chromatography (4 g silica gel, eluting with 20% ethyl acetate–hexanes initially, grading to 40% ethyl acetate–hexanes) to provide the product as a colorless film, 21 mg, 99%).

$R_f = 0.71$ (50% ethyl acetate–hexanes, CAM).

^1H NMR (55:45 mixture of rotamers, asterisks [*] denote minor rotameric signals that could be resolved, 500 MHz, CDCl_3) δ 4.50 (d, $J = 8.1$ Hz, 1H),* 4.41 (d, $J = 8.2$ Hz, 1H), 4.08–

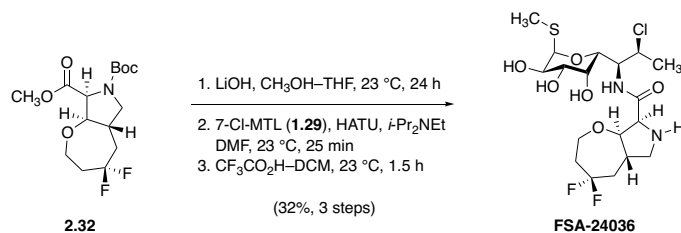
4.03 (m, 1H), 3.99–3.94 (m, 1H), 3.92 (dd, $J = 10.6, 8.5$ Hz, 1H), 3.85 (dd, $J = 10.5, 8.4$ Hz, 1H),* 3.80–3.78 (m, 1H),* 3.76 (s, 3H), 3.75 (s, 3H), 3.73–3.70 (m, 1H), 2.95–2.89 (m, 1H), 2.81–2.68 (m, 1H), 2.51–2.41 (m, 1H), 2.39–2.27 (m, 1H), 2.00 (app dtd, $J = 22.3, 14.6, 11.8$ Hz, 1H), 1.44 (s, 9H),* 1.40 (s, 9H).

^{13}C NMR (55:45 mixture of rotamers, asterisks [*] denote minor rotameric signals that could be resolved, 500 MHz, CDCl_3) δ 171.2,* 171.0, 153.8,* 153.4, 124.5 (t, $J = 241.9$ Hz), 83.9, 83.3,* 80.7, 63.7 (dd, $J = 9.3, 4.6$ Hz), 62.5, 62.0,* 52.4,* 52.2, 49.8,* 49.2, 39.9 (app t, $J = 26.0$ Hz), 39.6 (td, $J = 28.1, 4.6$ Hz),* 36.3 (dd, $J = 9.1, 3.8$ Hz),* 35.62 (dd, $J = 8.9, 3.8$ Hz), 28.5,* 28.4.

^{19}F NMR (471 MHz, CDCl_3) δ -82.55 (app dtd, $J = 247.5, 12.4, 8.4, 4.2$ Hz, 1F), -84.96 (dddd, $J = 247.5, 21.8, 17.5, 8.2, 5.3$ Hz, 1F).

FTIR (neat, cm^{-1}): 2975 (w), 1749 (s), 1702 (s), 1404 (s), 1368 (m), 1210 (m), 1179 (m), 1135 (s), 1112 (s), 1059 (m).

HRMS (ESI+, m/z): $[\text{M}+\text{Na}]^+$ calc'd for $\text{C}_{15}\text{H}_{23}\text{F}_2\text{NO}_5$, 358.1437; found 358.1447.



Synthetic lincosamide FSA-24036.

To a solution of methyl ester **2.32** (21 mg, 63 μ mol, 1 equiv) in 50% v/v methanol–tetrahydrofuran (310 μ L) was added aqueous lithium hydroxide solution (1.0 M, 75 μ L, 75 μ mol, 1.2 equiv) at 23 °C. After 24 h, LCMS analysis showed that saponification was complete; the reaction mixture was diluted with water (4 mL), was chilled to 0 °C, and was acidified to pH = 2 by the dropwise addition of aqueous hydrogen chloride solution (1.0 N). The acidified solution was then extracted with ethyl acetate (4 \times 3 mL). The combined extracts were dried over sodium sulfate, filtered, and concentrated to provide carboxylic acid intermediate as a white powder (17 mg, 53 μ mol).

This crude carboxylic acid was then transferred to a 2–5 mL glass microwave vial, where it was dissolved in *N,N*-dimethylformamide (270 μ L). To this solution was added HATU (22 mg, 58 μ mol, 1.1 equiv). The mixture was stirred at 23 °C for 10 min before 7-chloromethylthiolincosamine (**1.29**, 22 mg, 79 μ mol, 1.5 equiv)⁷ was added, causing a light cream-yellow suspension to form. This mixture was stirred for 20 min, during which time it gradually became a homogeneous solution. At this point, *N,N*-diisopropylethylamine (23 μ L, 0.13 mmol, 2.5 equiv) was added, causing the mixture to attain a vibrant yellow color. After 25 min of additional stirring, LCMS analysis indicated no trace of carboxylic acid or activated-ester intermediate. The mixture was loaded directly onto a column silica gel (4 g), where it was purified by flash chromatography (eluting with dichloromethane initially, grading to 5% methanol–

dichloromethane). Fractions containing the Boc-protected coupling product were identified by TLC ($R_f = 0.44$, 10% methanol–dichloromethane, PMA), pooled, and concentrated to afford a white solid residue.

Finally, this residue was transferred to a clean 2–5 mL glass microwave vial, where it was dissolved in dichloromethane (450 μL). Dimethyl sulfide (44 μL) and trifluoroacetic acid (45 μL) were added, and the mixture was stirred at 23 °C for 1.5 h, whereupon LCMS analysis showed that Boc removal was complete. The mixture was concentrated under a stream of argon, and the residue was purified by flash-column chromatography (4 g silica gel, eluting with 1% ammonium hydroxide–5% methanol–dichloromethane initially, grading to 1% ammonium hydroxide–10% methanol–dichloromethane) to provide **FSA-24036** as a white film (9.6 mg, 32%, 3 steps).

$R_f = 0.23$ (1% ammonium hydroxide–10% methanol–dichloromethane, PMA).

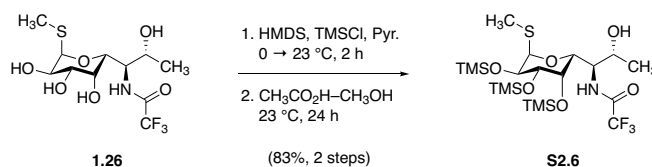
^1H NMR (500 MHz, CD_3OD) δ 5.30 (d, $J = 5.6$ Hz, 1H), 4.59 (qd, $J = 6.8, 1.7$ Hz, 1H), 4.42 (dd, $J = 10.0, 1.6$ Hz, 1H), 4.20 (dd, $J = 10.0, 1.1$ Hz, 1H), 4.12 (app td, $J = 9.0, 1.3$ Hz, 1H), 4.08 (dd, $J = 10.2, 5.6$ Hz, 1H), 4.01 (d, $J = 8.9$ Hz, 1H), 3.97 (app ddt, $J = 7.2, 3.9, 1.9$ Hz, 1H), 3.89 (dd, $J = 3.5, 1.2$ Hz, 1H), 3.79–3.75 (m, 1H), 3.57 (dd, $J = 10.2, 3.4$ Hz, 1H), 3.30 (dd, $J = 10.2, 7.1$ Hz, 1H), 2.59 (app t, $J = 10.6$ Hz, 1H), 2.47–2.28 (m, 4H), 2.14 (s, 3H), 2.03 (app dt, $J = 20.0, 14.9, 11.7$ Hz, 1H), 1.50 (d, $J = 6.8$ Hz, 3H).

^{13}C NMR (126 MHz, CD_3OD) δ 174.3, 126.2 (t, $J = 241.4$ Hz), 89.6, 86.0, 71.9, 71.1, 69.7, 69.6, 64.6 (dd, $J = 9.2, 4.9$ Hz), 64.1, 59.1, 54.4, 50.7, 40.4 (app t, $J = 25.5$ Hz), 40.2 (dd, $J = 8.2, 4.6$ Hz), 39.7 (app t, $J = 27.7$ Hz), 22.7, 13.3.

^{19}F NMR (471 MHz, CD_3OD) δ –83.40 (app dqd, $J = 246.9, 6.9, 3.7$ Hz, 1F), –85.69 (app ddq, $J = 247.1, 11.6, 5.4$ Hz, 1F).

FTIR (neat, cm^{-1}): 3345 (br), 2929 (m), 1658 (s), 1525 (m), 1442 (m), 1262 (m), 1136 (s), 1082 (s), 1082 (s), 1055 (s), 984 (m), 859 (w).

HRMS (ESI+, m/z): $[\text{M}+\text{H}]^+$ calc'd for $\text{C}_{18}\text{H}_{29}\text{ClF}_2\text{N}_2\text{O}_6\text{S}$, 475.1476; found 475.1462.



Alcohol S2.6.

Conditions for sequential persilylation–regioselective desilylation were adapted from the procedure reported by Ajito and co-workers.^{73b} In a 25-mL round-bottomed flask, *N*-trifluoroacetyl methylthiolincosamine (**1.26**, 400 mg, 1.15 mmol, 1 equiv)⁶⁸ was dissolved in pyridine 1.91 mL, and this solution was chilled to 0 °C. Hexamethyldisilazane (607 μL, 2.90 mmol, 2.53 equiv) and chlorotrimethylsilane (840 μL, 6.57 mmol, 5.74 equiv) were then added sequentially, dropwise. Addition of chlorotrimethylsilane caused the formation of a white precipitate. The mixture was warmed to 23 °C and was stirred at that temperature for 2 h before it was concentrated to dryness in vacuo. To the dried, white solid residue were added hexanes (7 mL) and water (7 mL), and the mixture was stirred until both phases were clear and all solids were dissolved. The mixture was then transferred into a separatory funnel containing an additional portion of hexanes (20 mL); the layers were shaken, then separated. The organic phase was then washed with a fresh portion of water (10 mL), dried over sodium sulfate, filtered, and concentrated to provide tetrakis-*O*-trimethylsilylated intermediate as a white solid.

This residue was dissolved in methanol (850 μL), and 80% v/v acetic acid–water (141 μL) was added to this solution at 23 °C. After 24 h of stirring, TLC demonstrated complete consumption of tetrakis-*O*-trimethylsilyl intermediate ($R_f = 0.66$, 20% ethyl acetate–hexanes, CAM). The mixture was neutralized with the addition of saturated aqueous sodium bicarbonate solution (400 μL). After gas evolution ceased, the neutralized solution was transferred to a separatory funnel containing hexanes (25 mL) and water (10 mL). The layers were shaken, then

separated; the organic phase was washed with a fresh portion of saturated aqueous sodium bicarbonate solution (10 mL), water (10 mL), and saturated aqueous sodium chloride solution (10 mL). The organic layer was then dried over sodium sulfate, filtered, and concentrated to provide the product as a foaming white, amorphous solid (535 mg, 83%, 2 steps).

$R_f = 0.34$ (20% ethyl acetate–hexanes, CAM).

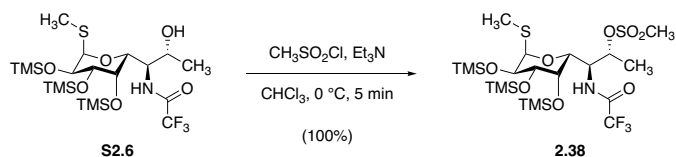
$^1\text{H NMR}$ (500 MHz, CDCl_3) δ 7.64 (d, $J = 8.3$ Hz, 1H), 5.18 (d, $J = 5.3$ Hz, 1H), 4.35 (dd, $J = 6.1$, 1.2 Hz, 1H), 4.18–4.14 (m, 2H), 4.06 (dd, $J = 9.5$, 5.3 Hz, 1H), 3.90–3.84 (m, 1H), 3.71 (dd, $J = 9.5$, 2.7 Hz, 1H), 2.15 (br, 1H), 2.00 (s, 3H), 1.26 (d, $J = 6.4$ Hz, 3H), 0.19 (s, 9H), 0.14 (s, 18H).

$^{13}\text{C NMR}$ (126 MHz, CDCl_3) δ 156.9 (q, $J = 37.0$ Hz), 115.1 (q, $J = 287.6$ Hz), 87.0, 72.8, 71.2, 67.8, 67.3, 67.0, 55.9, 19.7, 11.8, 0.0, -0.4 , -0.6 .

$^{19}\text{F NMR}$ (471 MHz, CDCl_3) δ -75.5 (s, 3F).

FTIR (neat, cm^{-1}): 2958 (w), 1714 (m), 1537 (w), 1250 (m), 1167 (m), 1135 (m), 1068 (m), 891 (s), 835 (s), 732 (s).

HRMS (ESI+, m/z): $[\text{M}+\text{H}]^+$ calc'd for $\text{C}_{20}\text{H}_{42}\text{F}_3\text{NO}_6\text{SSi}_3$, 566.2065; found 566.2082.



Methanesulfonate ester **2.38**.

To a magnetically stirred, ice-cold solution of alcohol **S2.6** (399 mg, 705 μ mol, 1 equiv) and triethylamine (246 μ L, 1.76 mmol, 2.50 equiv) in chloroform (2.20 mL) was added methanesulfonyl chloride (110 μ L, 1.41 mmol, 2.00 equiv) dropwise. After stirring for 5 min at 0 $^{\circ}$ C, TLC analysis (15% diethyl ether–dichloromethane, CAM) showed complete consumption of starting material. The reaction mixture was diluted with dichloromethane (7 mL), and saturated aqueous sodium bicarbonate solution (7 mL) was added to destroy any residual methanesulfonyl chloride. The biphasic mixture was stirred at 23 $^{\circ}$ C for 5 min before the layers were separated. The aqueous phase was extracted with dichloromethane (2×15 mL), and the combined organic extracts were dried over sodium sulfate. The dried solution was filtered and concentrated to provide methanesulfonate ester product as a bright white, amorphous solid (456 mg, 100%).

R_f = 0.74 (15% diethyl ether–dichloromethane, CAM).

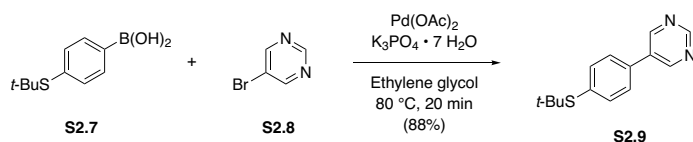
^1H NMR (500 MHz, CDCl_3) δ 7.51 (d, J = 8.8 Hz, 1H), 5.15 (d, J = 5.4 Hz, 1H), 4.92 (app p, J = 6.3 Hz, 1H), 4.48 (app dt, J = 68.4, 6.5 Hz, 1H), 4.25 (d, J = 7.2 Hz, 1H), 4.08–4.05 (m, 2H), 3.63 (dd, J = 9.6, 2.5 Hz, 1H), 3.04 (s, 3H), 2.02 (s, 3H), 1.45 (d, J = 6.5 Hz, 3H), 0.16 (s, 9H), 0.13 (s, 9H), 0.12 (s, 9H).

^{13}C NMR (126 MHz, CDCl_3) δ 157.7 (q, J = 37.3 Hz), 115.9 (q, J = 287.7 Hz), 88.4, 72.7, 72.0, 68.5, 67.8, 53.6, 39.0, 17.6, 13.3, 0.8, 0.5, 0.3.

^{19}F NMR (376 MHz, CDCl_3) δ -75.6 (s, 3F).

FTIR (neat, cm^{-1}): 3337 (w), 2958 (w), 1732 (m), 1331 (m), 1168 (m), 1143 (m), 1070 (m), 893 (s), 835 (s), 730 (s).

HRMS (ESI+, m/z): $[\text{M}+\text{Na}]^+$ calc'd for $\text{C}_{21}\text{H}_{44}\text{F}_3\text{NO}_8\text{S}_2\text{Si}_3$, 666.1660; found 666.1673.



***tert*-Butanesulfide S2.9.**

Ligand-free Suzuki coupling was performed according to the method of Liu, Han, Song, and Qiu.¹¹¹ Taking no special precautions to exclude air or moisture, a 25-mL round-bottomed flask was charged with a magnetic stir bar, 5-bromopyrimidine (**S2.7**, 180 mg, 1.13 mmol, 1 equiv), 4-(*tert*-butylthio)phenylboronic acid (**S2.8**, 357 mg, 1.70 mmol, 1.50 equiv), potassium phosphate heptahydrate (766 mg, 2.26 mmol, 2.00 equiv), palladium(II) acetate (12.7 mg, 0.0566 mmol, 0.0500 equiv), and ethylene glycol (8.71 mL). The heterogeneous, light-yellow mixture was heated to 80 °C with stirring in a pre-heated oil bath. After 20 min, the mixture had become a dark gray suspension, and LCMS analysis indicated that no 5-bromopyrimidine remained. The mixture was cooled to room temperature before it was poured into a separatory funnel containing saturated aqueous sodium chloride solution (25 mL). This mixture was then extracted with diethyl ether (3 × 15 mL). In order to remove excess boronic acid coupling partner, the combined organic extracts were washed with 1N aqueous sodium hydroxide solution (2 × 10 mL), and saturated sodium chloride solution (10 mL). The dried organic solution was dried over sodium sulfate, filtered, and concentrated to give off-white milky oil, which was purified by flash-column chromatography (12 g silica gel, eluting with 20% diethyl ether–hexanes initially, grading to 45% diethyl ether–hexanes) to furnish the product as a white crystalline solid (244 mg, 88%).

¹¹¹ Liu, C.; Han, N.; Song, X.; Qiu, J. *Eur. J. Org. Chem.* **2010**, 5548–5551.

Melting point: 64–66 °C.

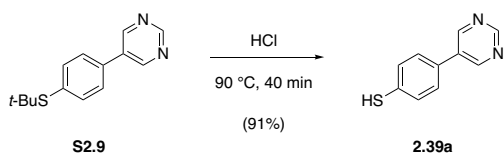
$R_f = 0.23$ (50% ethyl acetate–hexanes, UV).

$^1\text{H NMR}$ (600 MHz, CDCl_3) δ 9.12 (s, 1H), 8.88 (s, 2H), 7.60–7.57 (m, 2H), 7.48–7.45 (m, 2H),
1.23 (s, 9H).

$^{13}\text{C NMR}$ (151 MHz, CDCl_3) δ 157.6, 154.8, 154.7, 138.2, 134.4, 134.1, 133.5, 126.8, 46.3, 30.9.

FTIR (neat, cm^{-1}): 2964 (m) 1563 (s), 1417 (s), 1383 (m), 1354 (m), 1191 (m), 1167 (m), 999
(m), 836 (s), 719 (s), 561 (s).

HRMS (ESI+, m/z): $[\text{M}+\text{H}]^+$ calc'd for $\text{C}_{14}\text{H}_{16}\text{N}_2\text{S}$, 245.1107; found 245.1117.



Biaryl thiol **2.39a**.

Conditions for the acid-promoted cleavage of the *tert*-butyl blocking group were adapted from the report of Clavier and co-workers.¹¹² In a 100-mL round-bottomed flask, concentrated hydrochloric acid (35% w/v, 40.9 mL) was added to *tert*-butane sulfide **S2.9** (500 mg, 2.05 mmol, 1 equiv). The headspace of the flask was flushed with argon, and the mixture was heated to 90 °C. Upon heating, the mixture became a vibrant yellow, homogeneous solution, and gas bubbling was noted. After 40 min, the bubbling had subsided, and LCMS analysis indicated that the reaction was complete. The mixture was cooled to 23 °C and was then transferred to a 250-mL round-bottomed flask, where it was chilled to 0 °C. A steady stream of nitrogen was maintained over the mixture in order to minimize oxidative dimerization of the thiol product. A solution of 6N aqueous sodium hydroxide solution (ca. 60 mL) was added to neutralize excess hydrochloric acid; when all the acid was neutralized, a persistent precipitate had formed. The mixture was diluted with 1M sodium phosphate buffer solution (pH 7.0, 50 mL), and the resulting neutral solution was extracted with ethyl acetate (3 × 25 mL). The combined organic extracts were dried over sodium sulfate, filtered, and concentrated to give a faint gray crystalline solid. This crude product was purified by flash-column chromatography (12 g silica gel, eluting with 30% ethyl acetate–dichloromethane initially, grading to 50% ethyl acetate–dichloromethane) to furnish the product as a gleaming white crystalline solid (352 mg, 91%).

¹¹² Clavier, S.; Rist, Ø.; Hansen, S.; Gerlach, L.-O. Högberg, T.; Bergman, J. *Org. Biomol. Chem.* **2003**, *1*, 4248–4253.

Melting point: 98–100 °C.

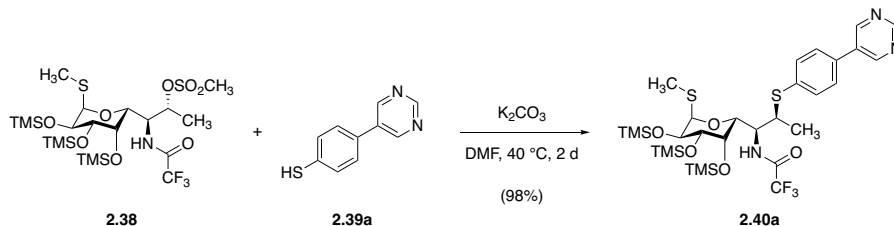
R_f = 0.30 (30% ethyl acetate–hexanes, UV).

^1H NMR (500 MHz, CDCl_3) δ 9.19 (s, 1H), 8.92 (s, 2H), 7.46 (d, J = 8.5 Hz, 2H), 7.41 (d, J = 8.5 Hz, 2H), 3.57 (s, 1H).

^{13}C NMR (126 MHz, CDCl_3) δ 157.6, 154.7, 133.7, 133.1, 131.6, 130.1, 127.7.

FTIR (neat, cm^{-1}): 2419 (br), 1598 (m), 1564 (m), 1415 (s), 1398 (m), 1103 (s), 1001 (m), 821 (s), 726 (m).

HRMS (ESI+, m/z): $[\text{M}+\text{H}]^+$ calc'd for $\text{C}_{10}\text{H}_8\text{N}_2\text{S}$, 189.0481; found 189.0482.



Biaryl sulfide **2.40a**.

In a 0.5–2 mL conical glass microwave vial fitted with a magnetic stir bar, methanesulfonate ester **2.38** (75 mg, 0.12 mmol, 1 equiv) and 4-(pyrimidin-5-yl)benzenethiol (**2.39a**, 66 mg, 0.35 mmol, 3.0 equiv) were mixed, and these starting materials were dried together by azeotropic removal of benzene. The dried mixture was then dissolved in *N,N*-dimethylformamide (290 μ L), and potassium carbonate (19 mg, 0.14 mmol, 1.2 equiv) was added to the solution, causing a vibrant canary yellow color to evolve. The vial was sealed, and the mixture was heated to 40 $^{\circ}$ C for 2 d, at which point TLC analysis (40% ethyl acetate–hexanes, UV+CAM) showed that no electrophile remained. The mixture was diluted with ethyl acetate (30 mL), and the diluted mixture was washed sequentially with saturated aqueous sodium bicarbonate solution (15 mL) and saturated aqueous sodium chloride solution (15 mL). The washed organic solution was then dried over sodium sulfate, filtered, and concentrated to give a colorless oil. This residue was subjected to flash-column chromatography (12 g silica gel, eluting with 10% ethyl acetate–hexanes initially, grading to 30% ethyl acetate–hexanes) to furnish the product as a colorless, viscous oil (84 mg, 98%).

R_f = 0.34 (40% ethyl acetate–hexanes, UV+CAM).

^1H NMR (500 MHz, CDCl_3) δ 9.21 (s, 1H), 8.93 (s, 3H), 7.53 (app d, J = 0.9 Hz, 4H), 6.93 (d, J = 9.6 Hz, 1H), 5.21 (d, J = 5.5 Hz, 1H), 4.62 (ddd, J = 9.6, 8.4, 3.8 Hz, 1H), 4.34 (d, J =

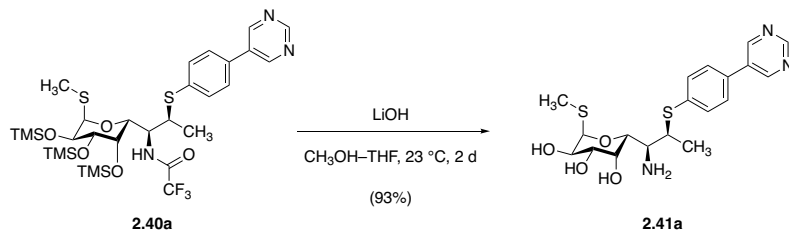
8.4 Hz, 1H), 4.11 (dd, $J = 9.6, 5.4$ Hz, 1H), 3.92 (dd, $J = 2.7, 1.0$ Hz, 1H), 3.85 (qd, $J = 7.0, 3.9$ Hz, 1H), 3.67 (dd, $J = 9.6, 2.6$ Hz, 1H), 1.97 (s, 3H), 1.33 (d, $J = 7.0$ Hz, 3H), 0.17 (s, 9H), 0.14 (s, 9H), 0.13 (s, 9H).

^{13}C NMR (126 MHz, CDCl_3) δ 157.8, 157.4 (q, $J = 37.2$ Hz), 154.8, 135.0, 133.6, 133.2, 132.5, 127.7, 116.0 (q, $J = 288.2$ Hz), 89.2, 72.7, 72.5, 69.4, 68.7, 54.1, 43.2, 19.3, 13.4, 0.8, 0.6, 0.3.

^{19}F NMR (471 MHz, CDCl_3) δ -75.47 (s, 3F).

FTIR (neat, cm^{-1}): 1729 (m), 1414 (m), 1170 (m), 1135 (m), 888 (s), 834 (s), 727 (s).

HRMS (ESI+, m/z): $[\text{M}+\text{H}]^+$ calc'd for $\text{C}_{30}\text{H}_{48}\text{F}_3\text{N}_3\text{O}_5\text{S}_2\text{Si}_3$, 736.2368; found 736.2399.



Aminotriol **2.41a**.

In a 2–5 mL glass microwave vial, trifluoroacetamide **2.40a** (107 mg, 145 μ mol, 1 equiv) was dissolved in 50% v/v tetrahydrofuran–methanol (1.45 mL). To this solution was added lithium hydroxide (17.4 mg, 727 μ mol, 5.00 equiv) at 23 °C; immediately, the colorless solution attained a canary yellow color. After 2 d, LCMS analysis indicated that global *O*-desilylation and trifluoroacetamide hydrolysis were complete; the reaction mixture was concentrated directly under a stream of nitrogen. The residue was purified by flash-column chromatography (4 g silica gel, eluting with 1% ammonium hydroxide–7% methanol–dichloromethane initially, grading to 0.1% ammonium hydroxide–10% methanol–dichloromethane) to provide the product as a white powder (57.0 mg, 93%).

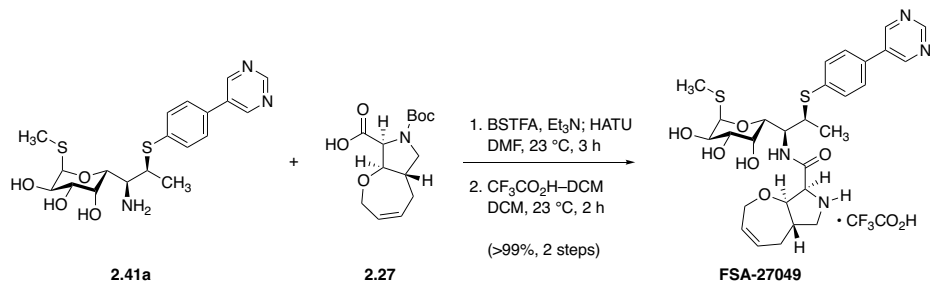
R_f = 0.34 (1% ammonium hydroxide–10% methanol–dichloromethane, I₂).

¹H NMR (600 MHz, CD₃OD) δ 9.12 (s, 1H), 9.07 (s, 2H), 7.68 (d, J = 8.4 Hz, 2H), 7.55 (d, J = 8.4 Hz, 1H), 5.24 (d, J = 5.5 Hz, 1H), 4.11 (dd, J = 3.4, 1.2 Hz, 1H), 4.09 (dd, J = 10.2, 5.5 Hz, 1H), 3.83 (qd, J = 7.0, 2.8 Hz, 1H), 3.61 (dd, J = 10.2, 3.4 Hz, 1H), 3.30 (dd, J = 8.6, 2.9 Hz, 1H), 1.89 (s, 3H), 1.51 (d, J = 6.9 Hz, 3H).

¹³C NMR (126 MHz, CD₃OD) δ 157.8, 155.8, 139.1, 135.3, 132.8, 131.7, 128.6, 89.9, 72.5, 72.2, 70.1, 69.6, 56.7, 45.5, 20.5, 13.6.

FTIR (neat, cm⁻¹): 3347 (br), 2920 (m), 1567 (m), 1417 (s), 1092 (s), 1052 (m), 819 (m), 722 (m).

HRMS (ESI+, m/z): $[M+H]^+$ calc'd for $C_{19}H_{25}N_3O_4S_2$, 424.1359; found 424.1369.



Synthetic lincosamide FSA-27049.

To an ice-cold solution of aminotriol **2.41a** (41.7 mg, 98.5 μmol , 1 equiv) and triethylamine (43.9 μL , 315 μmol , 3.20 equiv) in *N,N*-dimethylformamide (281 μL) was added *N,O*-bis(trimethylsilyl)trifluoroacetamide (39.6 μL , 148 μmol , 1.50 equiv). The mixture was then warmed to 23 $^{\circ}\text{C}$ and was stirred for 1 h at this temperature to ensure complete *O*-silylation. Carboxylic acid **2.27** (30.7 mg, 108 μmol , 1.10 equiv) and HATU (48.7 mg, 128 μmol , 1.30 equiv) were then added, and the mixture was stirred at 23 $^{\circ}\text{C}$. After 3 h, the reaction mixture was diluted with ethyl acetate (35 mL), and the diluted mixture was washed sequentially with 10% w/v aqueous citric acid solution (2×10 mL), water (10 mL), half-saturated aqueous sodium bicarbonate solution (2×10 mL), and saturated aqueous sodium chloride solution (10 mL). The washed organic phase was then dried over sodium sulfate, filtered, and concentrated.

The crude, coupled residue was then transferred to a 25-mL round-bottomed flask, where it was dissolved in dichloromethane (4.02 mL). Water (80.0 μL), dimethyl sulfide (80.0 μL), and trifluoroacetic acid (803 μL) were then added, and the resulting solution was stirred at 23 $^{\circ}\text{C}$ for 2 h, at which point LCMS analysis indicated that Boc removal was complete. The mixture was diluted with toluene (5 mL), and the diluted mixture was concentrated in vacuo. The residue was subjected to preparative HPLC on a Waters SunFire Prep C₁₈ column (5 μm , 250 \times 19 mm; eluting with 0.1% trifluoroacetic acid–10% acetonitrile–water initially, grading to 0.1% trifluoroacetic acid–40% acetonitrile–water over 40 min, with a flow rate of 15 mL/min; monitored by UV

absorbance at 254 nm) to provide **FSA-27049** • CF₃CO₂H as a white solid (70.1 mg, 102%, 2 steps).

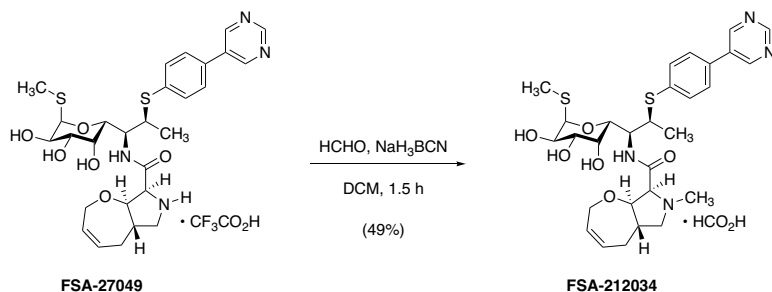
¹H NMR (600 MHz, CD₃OD) δ 9.15 (s, 1H), 9.10 (s, 2H), 8.33 (d, *J* = 9.9 Hz, 1H), 7.69 (d, *J* = 8.4 Hz, 2H), 7.53 (d, *J* = 8.4 Hz, 2H), 5.85 (app ddt, *J* = 12.5, 7.3, 2.6 Hz, 1H), 5.76 (app ddt, *J* = 12.2, 5.9, 2.9 Hz, 1H), 5.28 (d, *J* = 5.6 Hz, 1H), 4.71 (app td, *J* = 9.9, 2.3 Hz, 1H), 4.64 (d, *J* = 9.1 Hz, 1H), 4.47 (dd, *J* = 10.0, 1.2 Hz, 1H), 4.22–4.19 (m, 2H), 4.11 (dd, *J* = 10.3, 5.6 Hz, 1H), 3.94–3.92 (m, 2H), 3.67 (dd, *J* = 11.4, 7.4 Hz, 1H), 3.59 (dd, *J* = 10.3, 3.3 Hz, 1H), 3.03 (dd, *J* = 12.5, 11.4 Hz, 1H), 2.55 (ddd, *J* = 16.7, 7.4, 3.5 Hz, 1H), 2.26 (app dddd, *J* = 16.3, 12.5, 7.5, 3.5 Hz, 1H), 2.14–2.08 (m, 1H), 1.86 (s, 3H), 1.44 (d, *J* = 6.9 Hz, 3H).

¹³C NMR (126 MHz, CD₃OD) δ 167.4, 167.3, 157.7, 155.8, 139.4, 132.6, 131.2, 131.0, 129.9, 128.6, 90.3, 85.7, 72.1, 70.8, 70.0, 69.5, 69.4, 61.8, 55.0, 54.9, 45.0, 43.8, 30.0, 20.4, 13.9.

Trifluoroacetate carbons were not resolved due to ¹⁹F coupling.

FTIR (neat, cm⁻¹): 3367 (br), 1673 (s), 1417 (m), 1202 (s), 1140 (s), 1094 (m), 1052 (w), 722 (m).

HRMS (ESI+, *m/z*): [M+H]⁺ calc'd for C₂₈H₃₆N₄O₆S₂, 589.2149; found 589.2169.



Synthetic lincosamide FSA-212034.

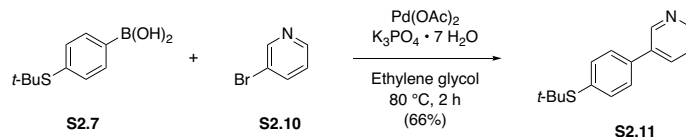
In a 1-mL glass vial fitted with a magnetic stir bar and PTFE-lined screw cap, **FSA-27049** • CF₃CO₂H (5.5 mg, 7.8 μmol, 1 equiv) was dissolved in dichloromethane (78 μL). Formalin (1.2 μL, 16 μmol, 2.0 equiv) was then added by micropipette, followed by sodium triacetoxyborohydride (3.3 mg, 16 μmol, 2.0 equiv) at 23 °C. After stirring for 1 h, an additional portion for formalin (1.2 μL, 16 μmol, 2.0 equiv) was added; 1 h later, additional sodium triacetoxyborohydride (3.3 mg, 16 μmol, 2.0 equiv) was added. LCMS analysis 15 min later indicated that no starting material remained. Excess sodium triacetoxyborohydride solution was quenched with the addition of saturated aqueous sodium bicarbonate solution (1 drop) before the mixture was concentrated to dryness in vacuo. The residue was subjected to preparative HPLC on a Waters SunFire Prep C₁₈ column (5 μm, 250 × 19 mm; eluting with 0.1% formic acid–2% acetonitrile–water initially, grading to 0.1% formic acid–30% acetonitrile–water over 40 min, with a flow rate of 20 mL/min; monitored by UV absorbance at 254 nm) to provide **FSA-212034** • HCO₂H as a colorless film (2.3 mg, 49%).

¹H NMR (600 MHz, CD₃OD) δ 9.13 (s, 1H), 9.08 (s, 2H), 8.24 (s, 2H), 7.72 (d, *J* = 7.7 Hz, 2H), 7.59 (d, *J* = 7.8 Hz, 2H), 5.81 (app ddt, *J* = 9.5, 6.2, 3.7 Hz, 1H), 5.63 (app ddt, *J* = 12.4, 5.6, 2.8 Hz, 1H), 5.27 (d, *J* = 5.5 Hz, 1H), 4.54 (dd, *J* = 10.0, 2.2 Hz, 1H), 4.37–4.33 (m,

2H), 4.14–4.03 (m, 4H), 3.96 (qd, $J = 7.4, 2.2$ Hz, 1H), 3.55 (dd, $J = 10.3, 3.5$ Hz, 1H), 3.53 (d, $J = 10.2$ Hz, 1H), 3.29 (dd, $J = 8.8, 6.0$ Hz, 1H), 2.52–2.47 (m, 1H), 2.50 (s, 3H), 2.41 (app t, $J = 10.6$ Hz, 1H), 2.29 (app tdd, $J = 14.4, 10.6, 4.9$ Hz, 1H), 2.05 (app t, $J = 14.4$ Hz, 1H), 1.95 (s, 3H).

FTIR (neat, cm^{-1}): 3362 (br), 1658 (m), 1595 (s), 1518 (m), 1416 (m), 1349 (m), 1141 (m), 1093 (s), 1054 (m).

HRMS (ESI+, m/z): $[\text{M}+\text{H}]^+$ calc'd for $\text{C}_{29}\text{H}_{38}\text{N}_4\text{O}_6\text{S}_2$, 603.2306; found 603.2319.



***tert*-Butane sulfide S2.11.**

Ligand-free Suzuki coupling was performed according to the method of Liu, Han, Song, and Qiu.¹¹¹ Taking no special precautions to exclude air or moisture, a 300-mL round-bottomed flask was charged with a magnetic stir bar, (4-(*tert*-butylthio)phenyl)boronic acid (**S2.7**, 4.79 g, 22.8 mmol, 1.20 equiv), potassium phosphate heptahydrate (12.9 g, 38.0 mmol, 2.00 equiv), palladium(II) acetate (43.0 mg, 0.190 mmol, 0.0100 equiv), and ethylene glycol (146 mL). 3-Bromopyridine (**S2.10**, 1.83 mL, 19.0 mmol, 1 equiv) was added last, stirring was initiated, and the reaction mixture was heated to 80 °C (open to the atmosphere) in a pre-heated oil bath. Within 30 min, the suspension had clarified, forming an amber-brown homogeneous solution; and after 1 h, the mixture became a light tan, turbid suspension. After 2 h of stirring at 80 °C, TLC analysis (60% ethyl acetate–hexanes, UV) showed that no starting material remained. The mixture was cooled to 23 °C and was then poured into a separatory funnel containing saturated aqueous sodium chloride solution (250 mL). The aqueous suspension was extracted with diethyl ether (4 × 50 mL), and the combined organic extracts were washed with a fresh portion of saturated aqueous sodium chloride solution (50 mL). The washed organic product solution was then dried over sodium sulfate, filtered, and concentrated to give a milky, light yellow oil that was purified by flash-column chromatography (120 g silica gel, eluting with 10% ethyl acetate–hexanes initially, grading to 40% ethyl acetate–hexanes) to provide the product as a brilliant white, fluffy powder (3.04 g, 66%).

Melting point: 55–57 °C.

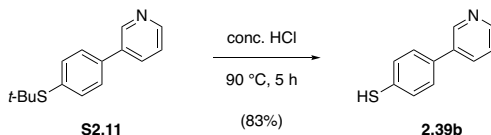
$R_f = 0.37$ (60% ethyl acetate–hexanes, UV).

$^1\text{H NMR}$ (600 MHz, CDCl_3) δ 8.86 (d, $J = 1.7$ Hz, 1H), 8.61 (dd, $J = 4.7, 1.6$ Hz, 1H), 7.88 (ddd, $J = 7.9, 2.4, 1.6$ Hz, 1H), 7.64 (d, $J = 8.3$ Hz, 2H), 7.55 (d, $J = 8.2$ Hz, 2H), 7.38 (ddd, $J = 7.8, 4.8, 0.9$ Hz, 1H), 1.33 (s, 9H).

$^{13}\text{C NMR}$ (100 MHz, CDCl_3) δ 148.9, 148.4, 138.2 ($2 \times \text{C}$), 136.0, 134.4, 133.0, 127.2, 123.7, 46.4, 31.1.

FTIR (neat, cm^{-1}): 2960 (s), 1573 (w), 1471 (s), 1363 (s), 1168 (m), 1001 (m), 800 (s), 711 (s), 561 (m).

HRMS (ESI+, m/z): $[\text{M}+\text{H}]^+$ calc'd for $\text{C}_{15}\text{H}_{17}\text{NS}$, 244.1154; found 244.1167.



Biaryl thiol **2.39b**.

In a 500-mL round-bottomed flask containing a magnetic stir bar, *tert*-butanesulfide **S2.11** (3.00 g, 12.3 mmol, 1 equiv) and concentrated hydrochloric acid (38% w/w in water, 123 mL) were combined. The headspace was flushed with argon, and the mixture was heated to 90 °C with constant stirring; the starting material gradually dissolved upon warming. After 5 h, LCMS analysis showed that no starting material remained, and the reaction mixture was cooled to 0 °C. The chilled solution was basified with the careful addition of aqueous 6N sodium hydroxide solution, until pH = 8 was achieved. The aqueous mixture was then extracted with diethyl ether (4 × 75 mL), the combined extracts were dried over sodium sulfate, the dried solution was filtered, and the filtrate was concentrated to give a colorless oil. This crude residue was finally purified by flash-column chromatography (80 g silica gel, eluting with 20% ethyl acetate–hexanes initially, grading to 60% ethyl acetate–hexanes) to provide arenethiol product as a light yellow solid (1.92 g, 83%).

Melting point: 42–44 °C.

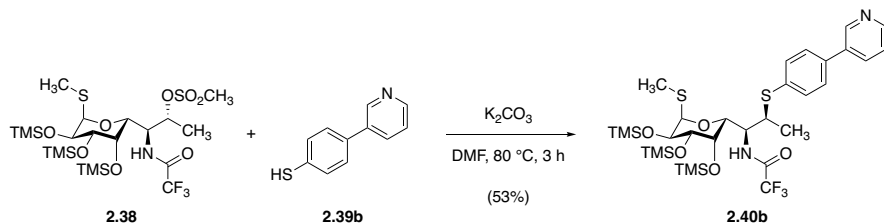
R_f = 0.23 (60% ethyl acetate–hexanes, UV).

$^1\text{H NMR}$ (600 MHz, CDCl_3) δ 8.79 (d, J = 2.4 Hz, 1H), 8.56 (dd, J = 4.8, 1.6 Hz, 1H), 7.79 (dt, J = 7.9, 2.0 Hz, 1H), 7.42 (d, J = 8.3 Hz, 2H), 7.34 (d, J = 8.3 Hz, 2H), 7.32 (dd, J = 7.9, 4.9 Hz, 1H), 3.55 (s, 1H).

$^{13}\text{C NMR}$ (100 MHz, CDCl_3) δ 148.5, 148.0, 135.8, 135.1, 134.0, 131.4, 129.8, 127.7, 123.6.

FTIR (neat, cm^{-1}): 3027 (m), 2398 (br), 1903 (w), 1597 (m), 1468 (s), 1423 (m), 1393 (m), 1185 (m), 1103 (s), 1000 (s), 794 (s), 708 (s), 547 (s).

HRMS (ESI+, m/z): $[\text{M}+\text{H}]^+$ calc'd for $\text{C}_{11}\text{H}_9\text{NS}$, 188.0528; found 188.0526.



Biaryl sulfide **2.40b**.

In a 5–10 mL glass microwave vial, methanesulfonate ester **2.38** (0.400 g, 0.621 μ mol, 1 equiv) and arenethiol **2.39b** (233 mg, 1.24 mmol, 2.00 equiv) were dried together by azeotropic removal of benzene. The dried mixture was then dissolved in *N,N*-dimethylformamide, and potassium carbonate was added. The vial was sealed, and the mixture was heated to 80 °C in a preheated oil bath. After 3 h, TLC analysis (30% ethyl acetate–hexanes, UV+CAM) showed complete consumption of starting material, and the mixture was diluted with ethyl acetate (30 mL). The diluted mixture was washed successively with saturated aqueous sodium bicarbonate solution (15 mL) and saturated aqueous sodium chloride solution (15 mL). The washed organic solution was then dried over sodium sulfate, filtered, and concentrated to give a colorless oil. This residue was purified by flash-column chromatography (40 g silica gel, eluting with 15% ethyl acetate–hexanes initially, grading to 50% ethyl acetate–hexanes) to provide the product as a bright white, crystalline solid (242 mg, 53%).

Melting point: 134–135 °C.

^1H NMR (500 MHz, CDCl_3) δ 8.83 (dd, $J = 2.4, 0.8$ Hz, 1H), 8.60 (dd, $J = 4.8, 1.6$ Hz, 1H), 7.84 (ddd, $J = 7.9, 2.3, 1.7$ Hz, 1H), 7.51 (ABq, $\Delta\delta_{\text{AB}} = 0.01$, $J_{\text{AB}} = 8.7$ Hz, 4H), 7.36 (ddd, $J = 7.9, 4.9, 0.9$ Hz, 1H), 7.02 (d, $J = 9.6$ Hz, 1H), 5.22 (d, $J = 5.4$ Hz, 1H), 4.62 (app td, $J = 9.0, 3.7$ Hz, 1H), 4.36 (d, $J = 8.4$ Hz, 1H), 4.12 (dd, $J = 9.6, 5.4$ Hz, 1H), 3.92 (d, $J = 2.6$

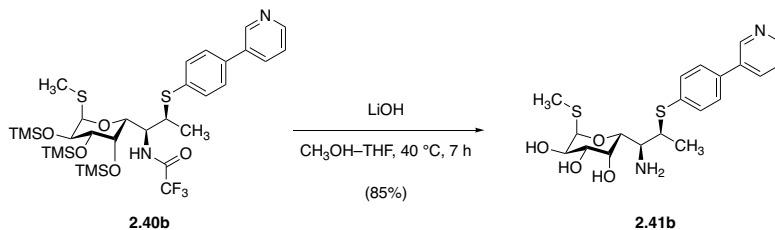
Hz, 1H), 3.83 (qd, $J = 7.0, 3.7$ Hz, 1H), 3.67 (dd, $J = 9.6, 2.6$ Hz, 1H), 2.00 (s, 3H), 1.33 (d, $J = 7.0$ Hz, 3H), 0.17 (s, 9H), 0.14 (s, 9H), 0.14 (s, 9H).

^{13}C NMR (126 MHz, CDCl_3) δ 148.9, 148.2, 137.1, 135.8, 134.3, 133.4, 132.7, 127.9, 123.8, 89.2, 72.7, 72.5, 69.5, 68.7, 54.1, 43.4, 19.4, 13.5, 0.8, 0.6, 0.4. Trifluoroacetamide carbons were not resolved due to ^{19}F nuclear coupling.

^{19}F NMR (471 MHz, CDCl_3) δ -75.46 (s, 3F).

FTIR (neat, cm^{-1}): 1729 (m), 1559 (w), 1250 (m), 1168 (s), 1139 (s), 972 (m), 888 (s), 835 (s).

HRMS (ESI+, m/z): $[\text{M}+\text{H}]^+$ calc'd for $\text{C}_{31}\text{H}_{50}\text{F}_3\text{N}_2\text{O}_6\text{S}_2\text{Si}_3$, 735.2416; found 735.2398.



Aminotriol **2.41b**.

In a 5–10 mL glass microwave vial fitted with a magnetic stir bar, a solution of trifluoroacetamide **2.40b** (240 mg, 326 μ mol, 1 equiv) in methanol (2.00 mL) was treated with aqueous sodium hydroxide solution (1.00 M, 2.61 mL, 2.61 mmol, 8.00 equiv) at 23 °C. A white, frothy mixture resulted as the trimethylsilyl ether groups were rapidly solvolyzed; the mixture was heated to 40 °C, and after 7 h of stirring at that temperature, cleavage of the trifluoroacetamide was complete as well, as indicated by LCMS. The white pasty mixture was chilled to 0 °C before it was subjected to vacuum filtration; the collected solids were washed with ice-cold water (2 \times 2 mL) and were dried under high vacuum (0.1 mmHg) to provide the product as a brilliant white, crystalline solid (118 mg, 85%).

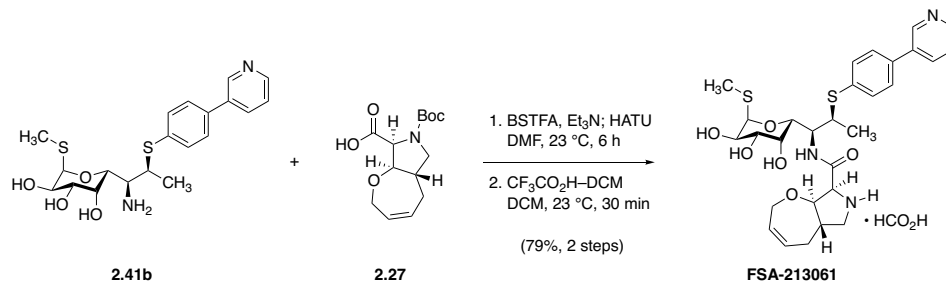
Melting point: 157–160 °C.

¹H NMR (500 MHz, CD₃OD) δ 8.80 (d, J = 2.3 Hz, 1H), 8.51 (dd, J = 4.9, 1.5 Hz, 1H), 8.09 (dt, J = 7.9, 1.9 Hz, 1H), 7.62 (d, J = 8.4 Hz, 2H), 7.52 (d, J = 8.1 Hz, 2H), 7.51 (dd, J = 7.9, 4.9 Hz, 1H), 5.23 (d, J = 5.6 Hz, 1H), 4.26 (d, J = 9.1 Hz, 1H), 4.11 (d, J = 2.7 Hz, 1H), 4.09 (dd, J = 10.3, 5.6 Hz, 1H), 3.81 (qd, J = 6.9, 2.3 Hz, 1H), 3.61 (dd, J = 10.2, 3.4 Hz, 1H), 3.28 (dd, J = 9.0, 2.5 Hz, 1H), 1.90 (s, 3H), 1.50 (d, J = 7.0 Hz, 3H).

¹³C NMR (100 MHz, CD₃OD) δ 148.7, 148.1, 138.1, 137.9, 136.3, 136.2, 131.8, 128.6, 125.5, 89.9, 72.8, 72.2, 70.1, 69.7, 56.7, 45.9, 20.7, 13.7.

FTIR (neat, cm^{-1}): 3346 (br), 1641 (m), 1596 (m), 1472 (m), 1338 (m), 1093 (s), 1054 (m), 802 (m).

HRMS (ESI+, m/z): $[\text{M}+\text{H}]^+$ calc'd for $\text{C}_{20}\text{H}_{26}\text{N}_2\text{O}_4\text{S}_2$, 423.1407; found 423.1417.



Synthetic lincosamide FSA-213061.

In a 4-mL glass vial fitted with a magnetic stir bar and a PTFE-lined screw cap, a solution of aminotriol **2.41b** (40 mg, 95 μmol , 1 equiv) and triethylamine (42 μL , 0.30 mmol, 3.20 equiv) in *N,N*-dimethylformamide (270 μL) was cooled to 0 $^{\circ}\text{C}$. To this chilled solution was added *N,O*-bis(trimethylsilyl)trifluoroacetamide (38 μL , 0.14 mmol, 1.5 equiv); the mixture was then warmed to 23 $^{\circ}\text{C}$ and stirred for 1 h to ensure complete *O*-silylation. Carboxylic acid **2.27** (30 mg, 0.10 mmol, 1.1 equiv) and HATU (47 g, 0.12 mmol, 1.3 equiv) were added next, and the mixture was stirred at 23 $^{\circ}\text{C}$ for 6 h, until LCMS indicated complete consumption of aminotriol starting material and its (oligo)trimethylsilylated congeners. The mixture was diluted with ethyl acetate (10 mL), and the diluted mixture was washed with saturated aqueous sodium chloride solution (2×5 mL). The washed organic solution was dried over sodium sulfate, filtered, and concentrated; residual *N,N*-dimethylformamide was removed by repeated concentration of the residue from 10% v/v methanol–toluene (2×5 mL).

The dried residue was then dissolved in dichloromethane (900 μL). Water (20 μL) and dimethyl sulfide (20 μL) were added, followed by trifluoroacetic acid (300 μL); the resulting solution was stirred at 23 $^{\circ}\text{C}$ for 30 min, at which point LCMS analysis indicated that Boc removal was complete. The mixture was diluted with toluene (2 mL), and the diluted mixture was concentrated to dryness in vacuo. The residue was subjected to preparative HPLC on a Waters SunFire Prep C_{18} column (5 μm , 250 \times 19 mm; eluting with 0.1% formic acid–5% acetonitrile–

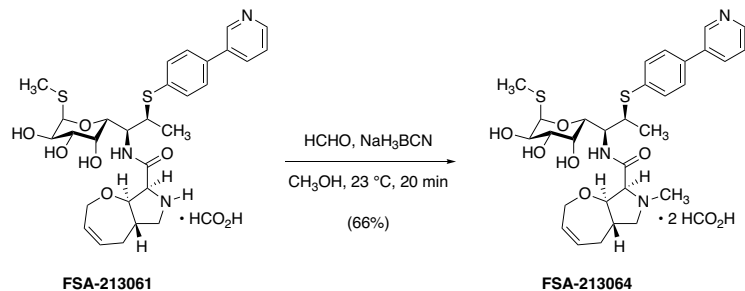
water initially, grading to 0.1% formic acid–40% acetonitrile–water over 40 min, with a flow rate of 15 mL/min; monitored by UV absorbance at 280 nm) to provide **FSA-213061** • HCO₂H as a white solid (48 mg, 79%).

¹H NMR (500 MHz, CD₃OD) δ 8.79 (s, 1H), 8.51 (d, *J* = 4.8 Hz, 1H), 8.37 (br, 1H), 8.07 (d, *J* = 8.0 Hz, 1H), 7.61 (d, *J* = 8.3 Hz, 2H), 7.50 (d, *J* = 8.1 Hz, 2H), 5.83 (dd, *J* = 12.5, 7.0 Hz, 1H), 5.75 (ddd, *J* = 12.5, 6.0, 2.8 Hz, 1H), 5.30 (d, *J* = 5.6 Hz, 1H), 4.70 (d, *J* = 10.0 Hz, 1H), 4.64 (d, *J* = 6.9 Hz, 1H), 4.48 (d, *J* = 10.1 Hz, 1H), 4.38 (dd, *J* = 16.0, 5.8 Hz, 1H), 4.21–4.17 (m, 2H), 4.12 (dd, *J* = 10.2, 5.5 Hz, 1H), 3.95 (d, *J* = 3.3 Hz, 1H), 3.89 (qd, *J* = 7.1, 1.9 Hz, 1H), 3.66 (dd, *J* = 11.4, 7.6 Hz, 1H), 3.61 (dd, *J* = 10.3, 3.2 Hz, 1H), 3.02 (app t, *J* = 11.2 Hz, 1H), 2.53 (ddd, *J* = 17.0, 7.4, 3.4 Hz, 1H), 2.31–2.22 (m, 1H), 2.10 (app t, *J* = 13.7 Hz, 1H), 1.88 (s, 3H), 1.43 (d, *J* = 6.9 Hz, 3H).

¹³C NMR (100 MHz, CD₃OD) δ 168.0, 148.7, 148.0, 138.0, 137.7, 136.2, 131.3, 131.1, 130.0, 128.7, 125.5, 90.3, 85.9, 72.1, 70.8, 70.0, 69.5, 69.3, 61.8, 54.9, 45.3, 43.9, 30.1, 20.5, 13.9.

FTIR (neat, cm⁻¹): 1677 (s), 1592 (s), 1470 (m), 1376 (m), 1348 (m), 1141 (m), 1094 (m), 1054 (m), 802 (m).

HRMS (ESI+, *m/z*): [M+H]⁺ calc'd for C₂₉H₃₇N₃O₆S₂, 588.2197; found 588.2193.



Synthetic lincosamide FSA-213064.

To a solution of **FSA-213061** • HCO₂H (15 mg, 24 μmol, 1 equiv) in methanol (470 μL) was added formalin (3.5 μL, 47 μmol, 2.0 equiv). After stirring the resulting solution for 5 min at 23 °C, sodium cyanoborohydride (4.5 mg, 71 μmol, 3.0 equiv) was added. After 20 min, LCMS analysis indicated that no starting material remained. The reaction mixture was directly subjected to preparative HPLC on a Waters SunFire Prep C₁₈ column (5 μm, 250 × 19 mm; eluting with 0.1% formic acid–5% acetonitrile–water initially, grading to 0.1% formic acid–40% acetonitrile–water over 25 min, with a flow rate of 15 mL/min; monitored by UV absorbance at 280 nm) to provide **FSA-213064** • 2 HCO₂H as a white solid (11 mg, 66%).

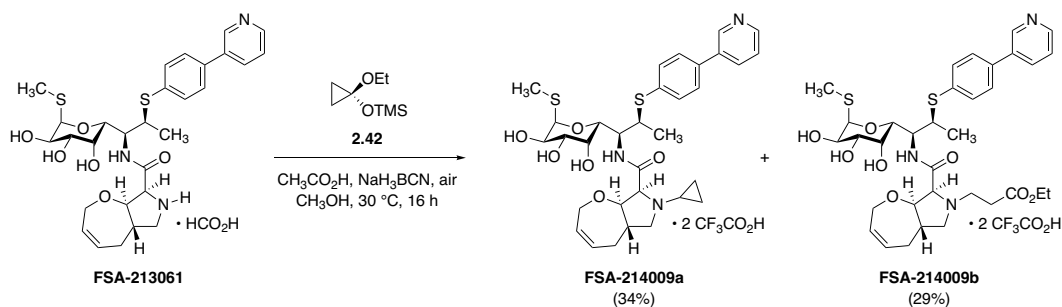
¹H NMR (600 MHz, CD₃OD) δ 8.81 (s, 1H), 8.52 (d, *J* = 4.6 Hz, 1H), 8.18 (s, 2H), 8.10 (app dq, *J* = 8.0, 1.7 Hz, 1H), 7.66 (d, *J* = 8.3 Hz, 2H), 7.56 (d, *J* = 8.1 Hz, 2H), 7.53 (dd, *J* = 7.9, 4.9 Hz, 1H), 5.83–5.79 (m, 1H), 5.67–5.63 (m, 1H), 5.27 (d, *J* = 5.6 Hz, 1H), 4.58 (app dt, *J* = 10.0, 1.9 Hz, 1H), 4.41 (d, *J* = 10.0 Hz, 1H), 4.36 (dd, *J* = 16.4, 5.7 Hz, 1H), 4.16–4.11 (m, 2H), 4.10 (ddd, *J* = 10.3, 5.6, 0.9 Hz, 1H), 4.00 (dd, *J* = 3.3, 1.6 Hz, 1H), 3.92 (qt, *J* = 6.9, 1.8 Hz, 1H), 3.74 (d, *J* = 9.9 Hz, 1H), 3.57 (ddd, *J* = 10.2, 3.4, 1.4 Hz, 1H), 3.39 (dd, *J* = 9.2, 6.4 Hz, 1H), 2.60 (s, 3H), 2.56 (dd, *J* = 12.1, 10.8 Hz, 1H), 2.50 (ddd, *J* = 17.2,

7.2, 3.7 Hz, 1H), 2.29 (app dtdd, $J = 14.9, 12.0, 6.1, 2.6$ Hz, 1H), 2.06 (app t, $J = 14.2$ Hz, 1H), 1.95 (s, 3H), 1.41 (d, $J = 6.9$ Hz, 3H).

^{13}C NMR (126 MHz, CD_3OD) δ 170.0, 165.6, 148.9, 148.1, 137.7, 136.9, 136.8, 136.3, 132.4, 130.5, 129.5, 128.7, 125.6, 90.3, 86.2, 72.6, 71.9, 71.2, 70.0, 69.6, 59.1, 54.7, 47.2, 45.0, 41.5, 30.6, 20.6, 13.9.

FTIR (neat, cm^{-1}): 3342 (br), 2919 (m), 2328 (m), 1677 (s), 1591 (m), 1471 (m), 1143 (s), 1094 (s), 1053 (s), 803 (s).

HRMS (ESI+, m/z): $[\text{M}+\text{H}]^+$ calc'd for $\text{C}_{30}\text{H}_{39}\text{N}_3\text{O}_6\text{S}_2$, 602.2353; found 602.2353.



Synthetic lincosamides FSA-214009a and FSA-214009b.

A 1-mL glass vial was charged sequentially with pyrrolidine hydroformate salt **FSA-213061** • HCO₂H (8.5 mg, 0.013 mmol, 1 equiv), methanol (150 μL), activated powdered 4Å molecular sieves (10 mg), acetic acid (7.7 μL, 0.13 mmol, 10 equiv), and (1-ethoxycyclopropoxy)trimethylsilane (**2.42**, 16 μL, 0.080 mmol, 6.0 equiv). The vial, originally open to air, was sealed, and the resulting white suspension was stirred at 23 °C for 10 min. Sodium cyanoborohydride (3.8 mg, 0.060 mmol, 4.5 equiv) was then added, the vial was re-sealed, and the mixture was heated at 30 °C for 16 h. At this point LCMS analysis indicated complete consumption of starting material, with concomitant formation of *N*-cyclopropanated product **FSA-214009a** and ester **FSA-214009b** (ca. 2:1 mixture), the latter likely arising through the generation of ethyl acrylate in situ via aerobic ring-opening fragmentation of (1-ethoxycyclopropoxy)trimethylsilane or a derivative thereof. The reaction mixture was diluted with dichloromethane (2 mL), and saturated aqueous sodium bicarbonate solution (2 mL) was added. The mixture was agitated, and the layers were separated. The aqueous phase was extracted with additional dichloromethane (3 × 2 mL), and the combined organic extracts were dried over sodium sulfate. The dried product solution was filtered, and the filtrate was concentrated to afford a colorless film. This residue was purified by preparative HPLC on a Waters SunFire Prep C₁₈ column (5 μm, 250 × 19 mm; eluting with 0.1% trifluoroacetic acid–10% acetonitrile–water, grading to 0.1% trifluoroacetic acid–40%

acetonitrile–water over 40 min, with a flow rate of 15 mL/min; monitored by UV absorbance at 280 nm; **FSA-214009a** $R_t = 18.3$ min, **FSA-214009b** $R_t = 21.5$ min) to provide **FSA-214009a** • 2 $\text{CF}_3\text{CO}_2\text{H}$ (3.9 mg, 34%) and **FSA-214009b** • 2 $\text{CF}_3\text{CO}_2\text{H}$ (3.5 mg, 29%).

FSA-214009a • 2 $\text{CF}_3\text{CO}_2\text{H}$:

^1H NMR (600 MHz, CD_3OD) δ 9.07 (br, 1H), 8.73 (br, 1H), 8.70–8.26 (m, 1H), 8.00–7.93 (m, 1H), 7.74 (d, $J = 8.4$ Hz, 2H), 7.55 (d, $J = 8.5$ Hz, 2H), 5.86–5.80 (m, 1H), 5.73–5.68 (m, 1H), 5.27 (d, $J = 5.7$ Hz, 1H), 4.75 (dd, $J = 10.1, 2.2$ Hz, 1H), 4.65–4.61 (m, 1H), 4.49 (d, $J = 10.2$ Hz, 1H), 4.38–4.30 (m, 2H), 4.22 (dd, $J = 16.0, 1.9$ Hz, 1H), 4.12 (dd, $J = 10.2, 5.6$ Hz, 1H), 3.98 (qd, $J = 7.0, 2.2$ Hz, 1H), 3.88 (dd, $J = 3.1, 1.0$ Hz, 1H), 3.75 (dd, $J = 10.8, 6.3$ Hz, 1H), 3.59 (dd, $J = 10.2, 3.3$ Hz, 1H), 3.21 (app t, $J = 11.3$ Hz, 1H), 2.90 (br, 1H), 2.55 (ddd, $J = 17.0, 7.3, 3.5$ Hz, 1H), 2.29 (br, 1H), 2.14 (app t, $J = 14.6$ Hz, 1H), 1.87 (s, 3H), 1.46 (d, $J = 6.9$ Hz, 3H), 1.13–1.09 (m, 1H), 1.05–1.01 (m, 1H), 0.93–0.87 (m, 2H).

HRMS (ESI+, m/z): $[\text{M}+\text{H}]^+$ calc'd for $\text{C}_{32}\text{H}_{41}\text{N}_3\text{O}_6\text{S}_2$, 628.2510; found 628.2509.

FSA-214009b • 2 $\text{CF}_3\text{CO}_2\text{H}$:

^1H NMR (500 MHz, CD_3OD) δ 9.04 (s, 1H), 8.71 (d, $J = 5.4$, 1H), 8.63 (d, $J = 8.1$ Hz, 1H), 7.94 (dd, $J = 8.2, 5.4$ Hz, 1H), 7.73 (d, $J = 8.4$ Hz, 2H), 7.55 (dd, $J = 8.5$ Hz, 2H), 5.86–5.81 (m, 1H), 5.76–5.71 (m, 1H), 5.26 (d, $J = 5.6$ Hz, 1H), 4.74 (dd, $J = 10.0, 2.3$ Hz, 1H), 4.51 (dd, $J = 10.0, 4.0$ Hz, 2H), 4.40 (dd, $J = 16.3, 5.7$ Hz, 1H), 4.31 (app t, $J = 9.4$ Hz, 1H), 4.27–4.19 (m, 3H), 4.10 (dd, $J = 10.2, 5.6$ Hz, 1H), 3.96 (qd, $J = 7.3, 2.6$ Hz, 1H), 3.91 (d, $J = 2.5$ Hz, 1H), 3.81 (dd, $J = 10.8, 6.3$ Hz, 1H), 3.59 (dd, $J = 10.2, 3.3$ Hz, 1H), 3.55–3.49 (m,

2H), 3.08 (app t, $J = 12.0$ Hz, 1H), 2.83 (t, $J = 7.2$ Hz, 2H), 2.56 (ddd, $J = 16.5, 6.7, 3.2$ Hz, 1H), 2.35–2.25 (br, 1H), 2.13 (app t, $J = 14.0$ Hz, 1H), 1.85 (s, 3H), 1.48 (d, $J = 7.0$ Hz, 3H), 1.29 (t, $J = 7.1$ Hz, 3H).

HRMS (ESI+, m/z): $[M+H]^+$ calc'd for $C_{34}H_{45}N_3O_8S_2$, 688.2721; found 688.2724.

Chapter 3. A nitroaldol-based route to methylthiolincosamine

Introduction

Methylthiolincosamine (MTL, **1.11**) is the 6-aminooctose residue that makes up the northern half of the natural product lincomycin (**1.1**). As described in Chapter 1, X-ray crystallographic studies, prior SAR, and *in vitro* ribosome-inhibition assays together identify this moiety as essential for the lincosamides' action, its galactopyranosyl core forming the structural basis for ribosomal recognition. Consequently, early semisynthetic work identified the C2–C4 triol motif as inviolate, with deletion, epimerization, and deoxyamination of these hydroxyl groups resulting in near-total ablation of antibacterial activity.⁵⁹ By contrast, modifications to the more exposed positions C1 and C7 have historically produced lincosamide candidates of particular promise (Figure 3.1). Most notable of these, of course, is clindamycin (**1.3**), whose 7-chloro substitution provided breakthrough gains in ribosomal engagement, spectrum of action, in-cell and *in vivo* potency, and PK/PD parameter space. Lincosamide candidates subsequently discovered and advanced through preclinical evaluation have all featured some form of C7 modification, including Vicuron's methyl variant VIC-105555 (**1.41**) and Meiji Seika's biarylthio lead **1.72**. Perhaps owing to the comparative difficulty of introducing modifications to C1 semisynthetically, examples of anomeric substitution are sparer, though existing reports clearly identify this position as a potential handle by which to modulate key parameters without negatively impacting activity.

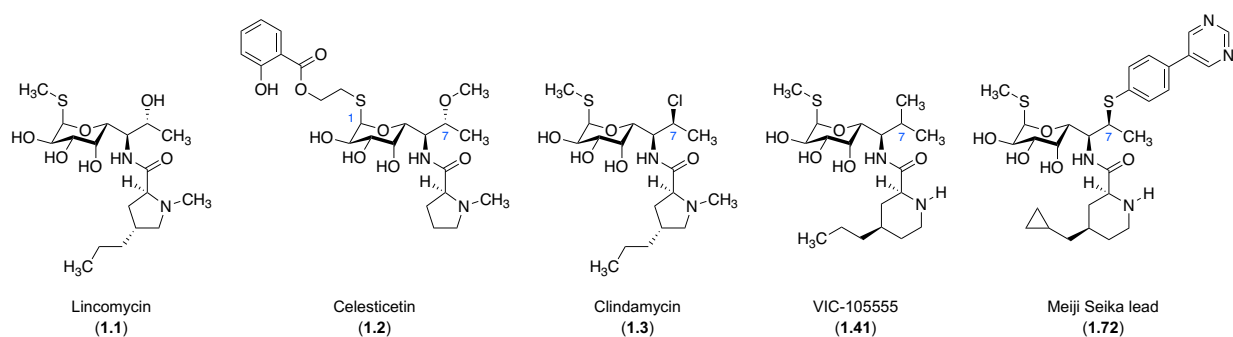
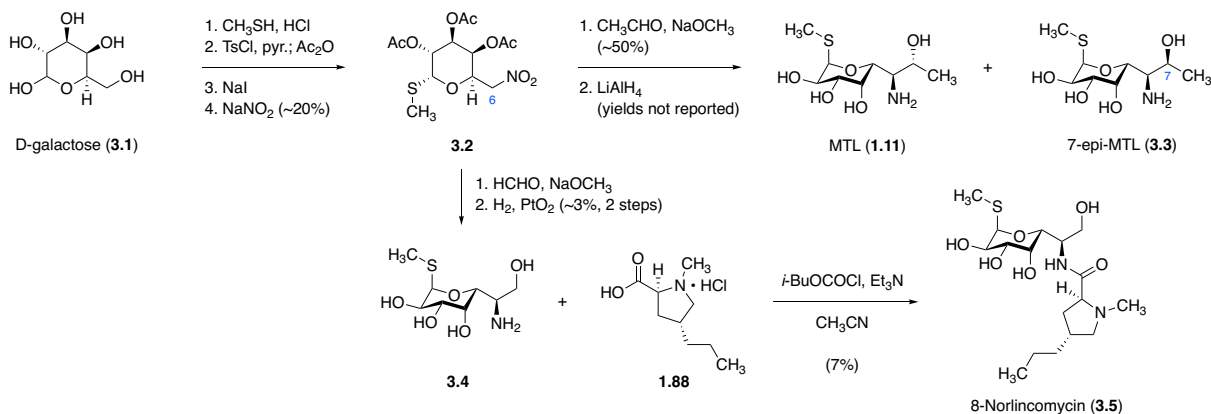


Figure 3.1. Examples of lincosamides bearing modifications to the northern-half component.

Since the discovery and structural characterization of lincomycin in the mid-1960s, a number of syntheses of methylthiolincosamine and its derivatives have been reported.¹¹³ Barney Magerlein of The Upjohn Company described the first such synthesis in 1970, an exceptionally concise if low-yielding sequence beginning with D-galactose (**3.1**, Scheme 3.1).¹¹⁴ Following condensation with methanethiol, site-selective functionalization of the C6-hydroxyl group, and nitroaldol coupling with acetaldehyde, MTL (**1.11**) and its 7-epi congener (**3.3**) were prepared in six steps. Notably, this sequence enabled Magerlein and Bannister to deploy the same 6-nitrosugar intermediate **3.2** toward the synthesis of 8-norlincomycin (**3.5**) in one of the earliest examples of lincosamide discovery employing a fully synthetic route to the northern-half component.¹¹⁵

Magerlein (1970):



Scheme 3.1. The first reported synthesis of methylthiolincosamine, developed by Barney Magerlein at Upjohn. This route enabled the preparation of 8-norlincomycin, an early example of a lincosamide candidate possessing a fully synthetic northern-half subunit.

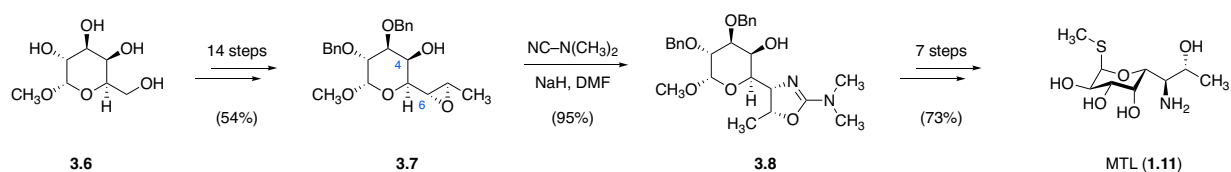
¹¹³ For a detailed review, see: Golebiowski, A.; Jurczak, J. Total synthesis of lincomycin and related chemistry, in *Recent Progress in the Chemical Synthesis of Antibiotics*; Lukacs, G.; Ohno, M., Eds. Springer-Verlag, Berlin, 1990; pp 365–385.

¹¹⁴ Magerlein, B. J. *Tetrahedron Lett.* **1970**, *1*, 33–36.

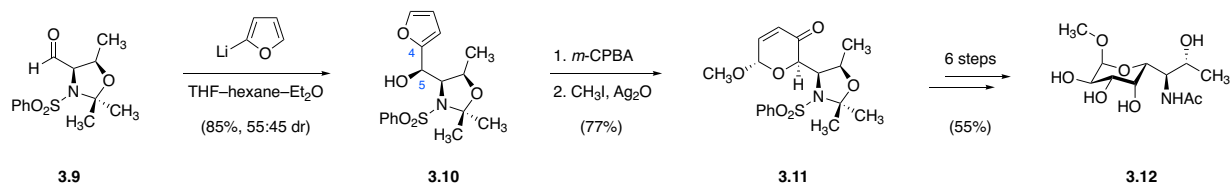
¹¹⁵ Bannister, B.; Magerlein, B. J. Lincomycin analogs and process. U.S. Patent 3,705,889, December 12, 1972.

Other syntheses of lincomycin's northern half include Knapp and Kukkola's 22-step synthesis of MTL (**1.11**) from methyl α -D-galactopyranoside (**3.6**), employing as a key step the regioselective opening of epoxide **3.7** with *N,N*-dimethylcyanamide, directed by the C4-hydroxyl substituent which was left deliberately unprotected (Scheme 3.2). Meanwhile, two syntheses from the groups of Professors Osman Achmatowicz and Samuel Danishefsky, while failing to produce the *S*-glycoside, nonetheless demonstrated that lincosamine could be prepared from non-carbohydrate precursors, showcasing each group's flagship methods for *de novo* saccharide synthesis. In the first case, Szechner and Achmatowicz targeted the central C4–C5 bond of the octose framework, developing a stereoselective addition of 2-furyllithium to D-*allo*-threonine derivative **3.9** that provided a 55:45 diastereomeric mixture of alcohols favoring the desired C5 epimer **3.10** under extensively optimized conditions. Achmatowicz rearrangement and subsequent manipulation of the resulting 3-pyrone ultimately furnished *N*-acetyl methyl α -lincosamine (**3.12**). Larson and Danishefsky developed a similarly convergent construction of the C4–C5 bond through a hetero-Diels–Alder coupling of diene **3.13** and crotonaldehyde under Lewis-acid catalysis. After a sequence of 15 steps, peracetylated methyl β -lincosaminide (\pm)-**3.17** was produced.

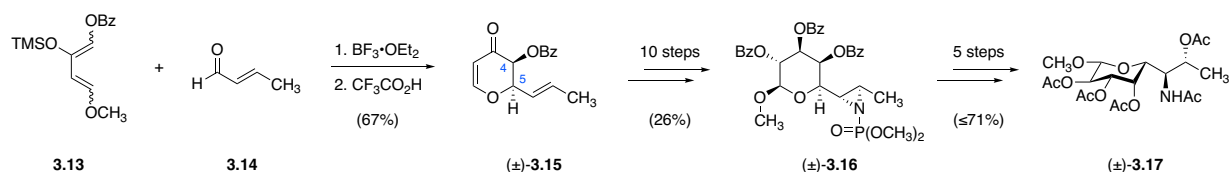
Knapp and Kukkola (1990):



Szechner and Achmatowicz (1992):

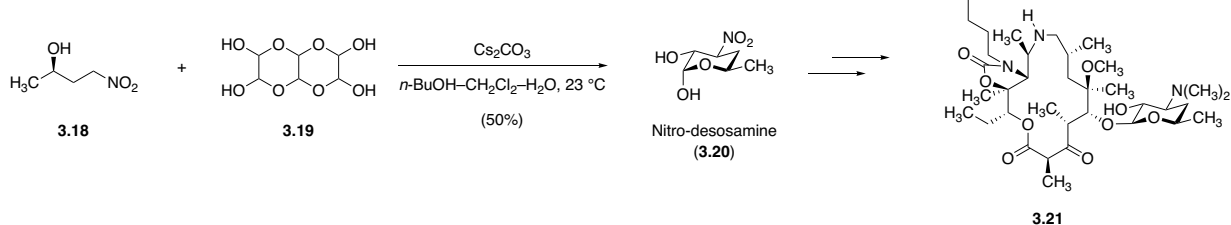


Larson and Danishefsky (1983):

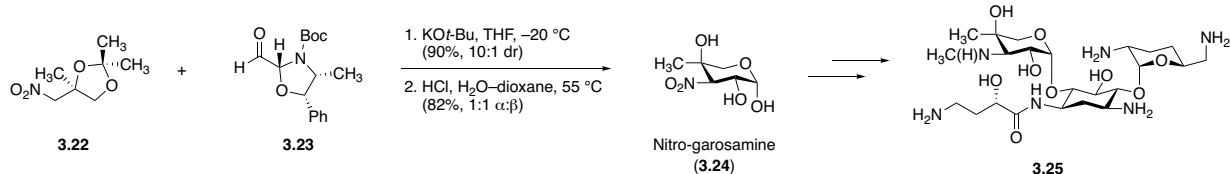


Scheme 3.2. Other notable routes to methylthiolincosamine and its derivatives.

Dr. Ziyang Zhang:



Dr. Fan Liu:



Scheme 3.3. My colleagues' successful development of nitroaldol couplings *en route* to the macrolide and aminoglycoside antibiotics served as inspiration for the development of a new synthetic route to methylthiolincosamine.

Owing to the limitations of these and other published routes to MTL and its derivatives, we sought to develop a practical, scalable, component-based route to the aminosugar moiety of the lincosamide antibiotics, alongside C1- and C6-variants thereof. At the same time, Professor Myers

and I desired to demonstrate the general viability of nitroaldol (Henry) coupling reactions applied toward the stereoselective construction of aminosugar motifs, complementary to ongoing work by my then graduate-student colleagues Dr. Ziyang Zhang and Dr. Fan Liu (Scheme 3.3). Specifically, in 2015, Dr. Zhang had demonstrated that the pyranosyl skeleton of D-desosamine – the essential aminosugar motif of the macrolide antibiotics, whose ribosomal binding site overlaps with that of the lincosamides’ northern half – could be constructed in a single step from (*R*)-nitro alcohol **3.18** and glyoxal trimer dihydrate (**3.19**).¹¹⁶ Likewise, contemporaneously with my own work on methylthiolincosamine, Dr. Liu had begun developing a synthesis of garosamine that would come to rely upon stereoselective nitroaldol coupling of **3.22** and the chiral glyoxal equivalent **3.23**; the resulting nitrogarosamine (**3.24**) was ultimately incorporated into Dr. Liu’s broader platform for aminoglycoside synthesis.¹¹⁷ Inspired by these successes, Professor Myers and I envisioned that a suitably flexible synthesis of the lincosamides’ northern half might similarly be enabled through application – or development – of appropriate nitroaldol chemistry.

Original retrosynthesis and discovery of a nitroaldol–cyclization reaction

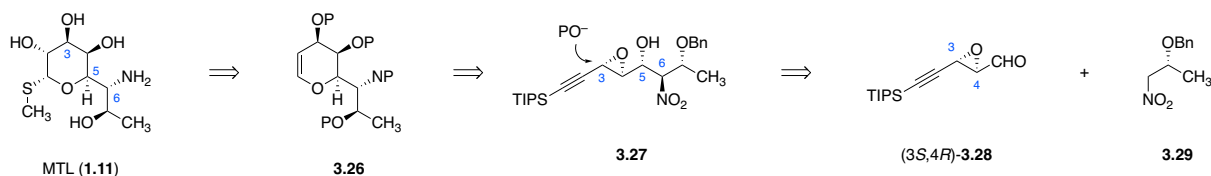
My original retrosynthesis of MTL (**1.11**) targeted the glycal **3.26** as a strategic intermediate, as I expected that the epoxide derived from it (a 1,2-anhydrosugar, or “Brigl’s anhydride”) might serve as a particularly flexible intermediate for the stereoselective synthesis of α -disposed *S*- and *C*-glycosidic MTL variants (Scheme 3.4).¹¹⁸ Reasoning that glycal **3.26** in turn

¹¹⁶ (a) Zhang, Z.; Fukuzaki, T.; Myers, A. G. *Angew. Chem. Int. Ed.* **2016**, *55*, 523–527. (b) Zhang, Z. A platform for the synthesis of new macrolide antibiotics. Ph.D. Dissertation, Harvard University, 2016.

¹¹⁷ Liu, F. Development of a component-based synthesis for the discovery of new aminoglycoside antibiotics, and diastereoselective Michael–Claisen cyclizations en route to 5-oxatetracyclines. Ph.D. Dissertation, Harvard University, 2017.

¹¹⁸ For a review of glycals as powerful intermediates in complex carbohydrate synthesis, see: Danishefsky, S. J.; Bilodeau, M. T. *Angew. Chem. Int. Ed.* **1996**, *35*, 1380–1419.

might be synthesized from a suitably protected alkynol by transition metal-catalyzed cycloisomerization, I arrived at **3.27** as a potentially tractable synthetic intermediate displaying the full retron for an *anti*-selective nitroaldol coupling of epoxyaldehyde (3*S*,4*R*)-**3.28** (lincomycin numbering) and nitropropanol derivative **3.29**.

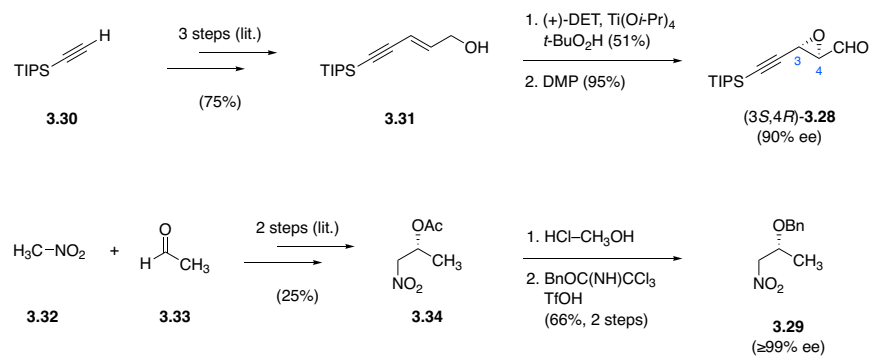


Scheme 3.4. Our initial retrosynthesis of MTL.

Each of these building blocks was readily prepared in enantiopure form by a sequence of four or five steps beginning from commercial chemicals (Scheme 3.5). In the case of epoxyaldehyde (3*S*,4*R*)-**3.28**, triisopropylethynylsilane (**3.30**) was first transformed to the allylic alcohol **3.31** by a known sequence;¹¹⁹ this alcohol was then subjected to Sharpless asymmetric epoxidation and Dess–Martin oxidation to provide the desired product in modest yield and 90% ee (Mosher ester analysis). Likewise, Henry coupling of nitromethane and acetaldehyde, followed by enzymatic resolution of the resulting racemic alcohol provided (*R*)-nitropropanol derivative **3.34**.¹²⁰ Methanolysis of this intermediate, followed by acid-promoted benzoylation of the resulting alcohol provided **3.29**, whose enantiopurity was brought to $\geq 99\%$ ee (HPLC analysis) upon repeated recrystallization from ethyl acetate–hexanes.

¹¹⁹ (a) Robles, O.; McDonald, F. E. *Org. Lett.* **2008**, *10*, 1811–1814. (b) Sohn, S. S.; Rosen, E. L.; Bode, J. W. *J. Am. Chem. Soc.* **2004**, *126*, 14370–14371. (c) Candy, M.; Tomas, L.; Parat, S.; Heran, V.; Bienaymé, H.; Pons, J.-M.; Bressy, C. *Chem. Eur. J.* **2012**, *18*, 14267–14271.

¹²⁰ Kitayama, T. *Tetrahedron* **1996**, *52*, 6139–6148.

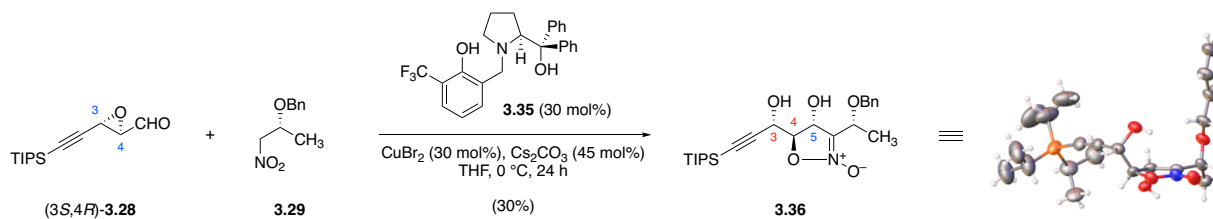


Scheme 3.5. Scalable synthesis of chiral building blocks.

With these building blocks in hand, I then investigated their proposed coupling to form nitroaldol adduct **3.27**. Under a host of conditions commonly used for such transformations (e.g., potassium *tert*-butoxide–tetrahydrofuran, potassium carbonate–methanol, potassium fluoride–isopropanol, silica gel), complex mixtures of products were formed, the isolation and characterization of which was complicated by the inherent instability of these nitroaldol adducts to silica-gel chromatography (data not shown). However, in an early experiment meant to probe whether catalyst control could impart the desired C5–C6 *anti* configuration in the nitroaldol coupling, a prolinol-ligated copper(II) system first reported by Zhiyong Wang and coworkers was investigated (Scheme 3.6).¹²¹ In this reaction, an unexpected product isomeric with the desired Henry adduct formed, and was ultimately isolated in 30% yield. One- and two-dimensional TLC analysis revealed that this product was more polar than the nitroaldol adducts observed in prior experiments and was stable toward silica gel chromatography. What’s more, this product was crystalline, enabling its unequivocal structural assignment as the isoxazoline *N*-oxide **3.36** by X-ray diffraction analysis. In retrospect, cyclization of the intermediate Henry adduct (which, incidentally, was formed with the desired C5 stereochemistry) might have been expected, as Paolo

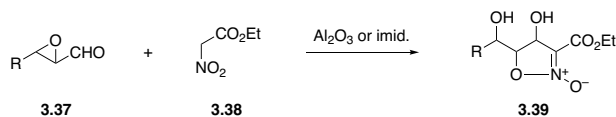
¹²¹ Xu, K.; Lai, G.; Zha, Z.; Pan, S.; Chen, H.; Wang, Z. *Chem. Eur. J.* **2012**, *18*, 12357–12362.

Righi and coworkers have described the highly analogous reaction of ethyl nitroacetate (**3.38**) with epoxyaldehydes promoted by alumina or imidazole (Table 3.1).¹²²



Scheme 3.6. Unexpected formation of a cyclic Henry adduct.

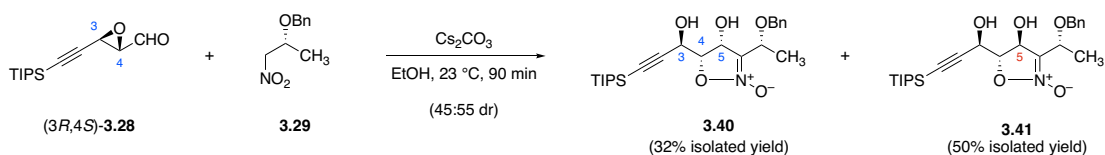
Table 3.1. Selected examples of alumina- and imidazole-promoted nitroaldol–cyclization couplings reported by Paolo Righi and coworkers.¹²²



Epoxyaldehyde	Conditions	Major product	Yield	dr
	Al_2O_3		99	60:40
	Al_2O_3		75	60:40
	Al_2O_3		47	95:5
	Al_2O_3		65	80:20
	Imid.		62	56:44

¹²² (a) Rosini, G.; Galarini, R.; Marotta, E.; Righi, P. *J. Org. Chem.* **1990**, *55*, 781–783. (b) Marotta, E.; Micheloni, L. M.; Scardovi, N.; Righi, P. *Org. Lett.* **2001**, *3*, 727–729.

While unanticipated, this result was a turning point in the development of a route to MTL. Namely, the spontaneous cyclization of nitroaldol addition products presented a number of key advantages: In addition to imparting configurational stability toward silica-gel chromatography, the cyclic architecture of isoxazoline *N*-oxides could be expected to provide an added element of stereocontrol in subsequent transformations – particularly in the establishment of the C1 and C6 stereocenters in downstream glycosylation and C=N bond reduction, respectively. The *N*-*O* linkage between the C4 and C6 substituents provided an attractive, atom-economical protecting group strategy; and the nature of the cascade reaction reduced the original problem of double diastereocontrol in nitroaldol addition to a more manageable challenge of rendering the key step diastereoselective with respect to C5 only.



Scheme 3.7. Probing the innate stereoselectivity of the nitroaldol–cyclization reaction.

As it happened, the (3*S*,4*S*) configuration (lincomycin numbering) of **3.28** was opposite of what would be desired – a problem easily addressed through the preparation of the enantiomeric epoxyaldehyde building block, (3*R*,4*S*)-**3.28**.¹²³ Coupling of this building block with **3.29** under the action of ethanolic cesium carbonate at ambient temperature furnished a mixture of C5-epimeric isoxazoline *N*-oxide products **3.40** and **3.41** (Scheme 3.7), providing the first evidence that the C3–C5 stereotriad present in MTL could be established in a single step; and that, while

¹²³ Compared to the synthesis of the (3*S*,4*R*) enantiomer depicted in Scheme 3.5, improvements in yield and reliability of the Sharpless asymmetric epoxidation reaction were realized *en route* to (3*R*,4*S*)-**3.28** through the use of Aldrich pre-powdered 4Å molecular sieves (versus manually crushed pellets). See the Experimental Section that follows for details.

unfavorable toward the formation of the desired diastereomer, the innate stereoselectivity of this coupling was modest and thus might succumb to catalyst control.

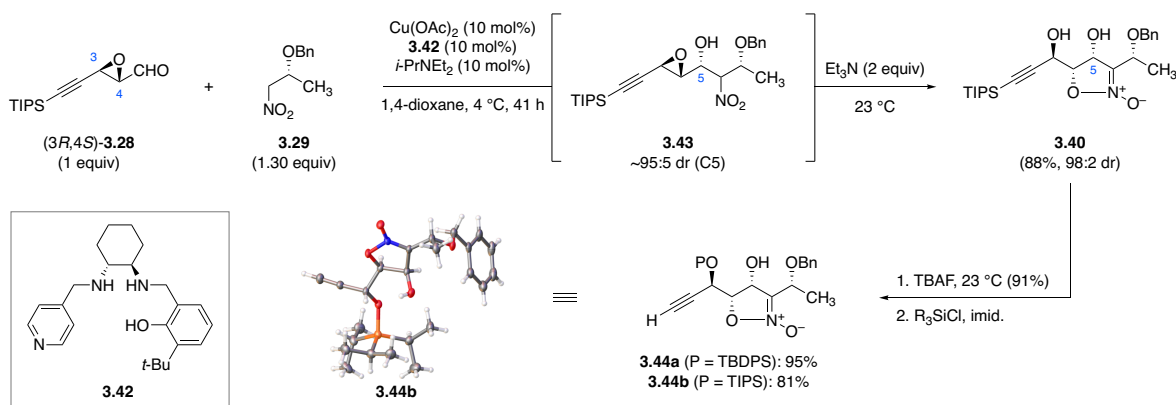
A fully synthetic route to methylthiolincosamine

In order to overcome the substrate bias of the nitroaldol–cyclization coupling described above, I evaluated a small number of asymmetric catalysts in detail, prioritizing those catalysts which could be prepared readily from commercial materials, and monitoring the diastereoselectivity of the initial nitroaldol addition by aliquot ¹H-NMR analysis. A copper(II) system employing cyclohexanediamine-based ligand **3.42** demonstrated particular promise (Scheme 3.8), imparting ~95:5 dr at C5 when addition of **3.29** to (3R,4S)-**3.28** was conducted at 4 °C (an inconsequential mixture of C6 epimers was observed as well, dr ~85:15).¹²⁴ When cesium carbonate (50 mol%) was added to the reaction mixture in order to induce cyclization, however, the C5 stereochemical purity of the isoxazoline *N*-oxide product was degraded to ≤73:27, very likely through base-promoted retro-nitroaldol fragmentation of **3.43**. By contrast, use of the milder, homogeneous base triethylamine (2.00 equiv) effected smooth conversion of linear intermediate **3.43** to the desired product with no observable epimerization at C5. These optimized conditions were readily and reliably scaled to produce up to 16.4 g of **3.40** in 88% isolated yield and 98:2 dr.¹²⁵ Tetra-*n*-butylammonium fluoride–promoted desilylation and regioselective protection of the sterically less encumbered C3-hydroxyl group of **3.40** then afforded products of type **3.44**. As it

¹²⁴ (a) Chougnet, A.; Zhang, G.; Liu, K.; Häussinger, D.; Kägi, A.; Allmendinger, T.; Woggon, W.-D. *Adv. Synth. Catal.* **2011**, 353, 1797–1806. (b) Zhang, G.; Yashima, E.; Woggon, W.-D. *Adv. Synth. Catal.* **2009**, 351, 1255–1262.

¹²⁵ The marginal observed increase in dr at C5 upon triethylamine-promoted cyclization may arise either from C5-epimeric linear intermediates displaying differing rates of cyclization, or more simply from limitations in the precision of ¹H-NMR measurements used to determine these ratios.

happened, the triisopropylsilyl ether **3.44b** was crystalline, enabling unequivocal confirmation of the assigned structure by X-ray diffraction analysis.



Scheme 3.8. Optimized conditions for nitroaldol–cyclization, relying on a cyclohexanediamine–copper(II) catalyst system to impart high diastereoselectivity.

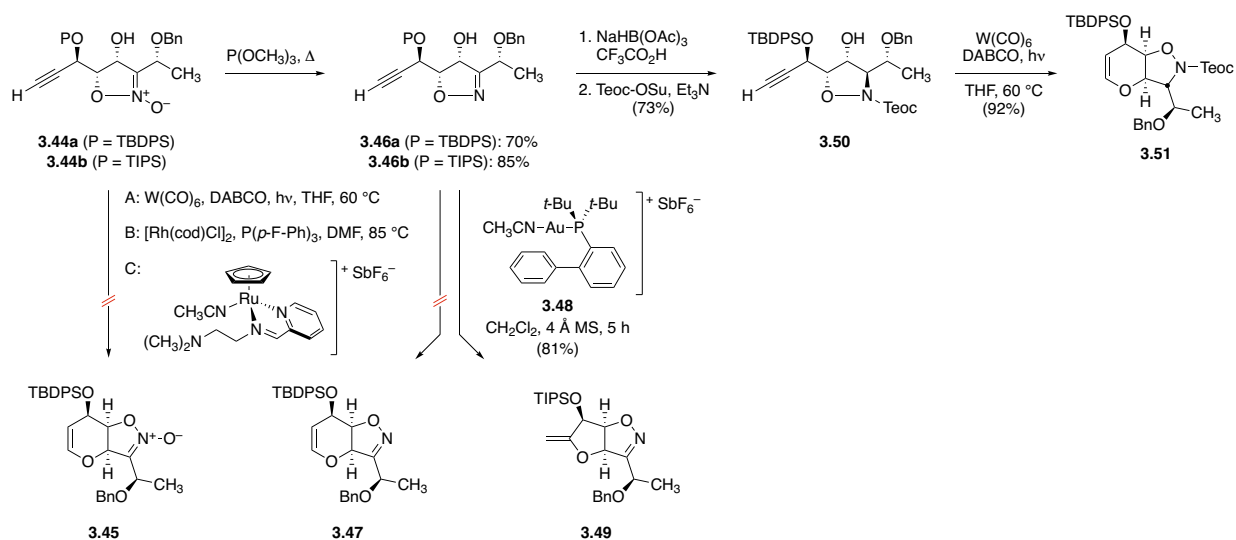
With the C3–C5 stereotriad of the target thus established, I then sought to transform alkynols **3.44** to the corresponding glycals by transition metal–catalyzed cycloisomerization (Scheme 3.9). However, application of tungsten(0),¹²⁶ rhodium(I),¹²⁷ and ruthenium(II)¹²⁸ conditions reported for *endo*-selective cycloisomerization failed both with these substrates and their *N*-deoxygenated derivatives **3.46**, likely owing to catalyst poisoning by the strongly metallophilic nature of these heterocyclic compounds. Notably, gold(I)-catalyzed cycloisomerization of isoxazoline **3.46b** proceeded smoothly; however, HSQC-NMR analysis revealed that the product of this transformation resulted from undesired 5-*exo* cyclization, as can

¹²⁶ (a) McDonald, F. E.; Reddy, K. S.; Díaz, Y. *J. Am. Chem. Soc.* **2000**, *122*, 4304–4309. (b) Koo, B.-S.; McDonald, F. E. *Org. Lett.* **2007**, *9*, 1737–1740. (c) Wipf, P.; Graham, T. H. *J. Org. Chem.* **2003**, *68*, 8798–8807.

¹²⁷ (a) Trost, B. M.; Rhee, Y. H. *J. Am. Chem. Soc.* **2003**, *125*, 7482–7483. (b) Codelli, J. A.; Puchlopek, A. L. A.; Reisman, S. E. *J. Am. Chem. Soc.* **2012**, *134*, 1930–1933.

¹²⁸ (a) Trost, B. M.; Rhee, Y. H. *J. Am. Chem. Soc.* **2002**, *124*, 2528–2533. (b) Trost, B. M.; Rhee, Y. H. *Org. Lett.* **2004**, *6*, 4311–4313. (c) Zeng, M.; Li, L.; Herzon, S. B. *J. Am. Chem. Soc.* **2014**, *136*, 7058–7067. (d) Zeng, M.; Herzon, S. B. *J. Org. Chem.* **2015**, *80*, 8604–8618.

be expected for gold(I) catalyst systems.¹²⁹ The desired cycloisomerization was ultimately realized after C5-hydroxyl-directed reduction of isoxazoline **3.46a** with sodium triacetoxyborohydride and trifluoroacetic acid (under these acidic conditions, trisopropylsilyl derivative **3.46b** underwent competitive desilylation),¹³⁰ followed by protection of the resulting isoxazolidine as its corresponding 2-(trimethylsilyl)ethoxycarbonyl (Teoc) derivative, **3.50**. This sequence, in addition to establishing the desired C6 stereochemistry, also served to mask the metallophilic nitrogen atom of the heterocyclic nucleus, enabling the smooth conversion of **3.50** to glycal **3.51** using tungsten(0)-catalyzed cycloisomerization conditions originally developed by Frank McDonald and coworkers.^{126a,b}



Scheme 3.9. Successive reduction events furnish an alkynol substrate suitably protected for tungsten-catalyzed cycloisomerization.

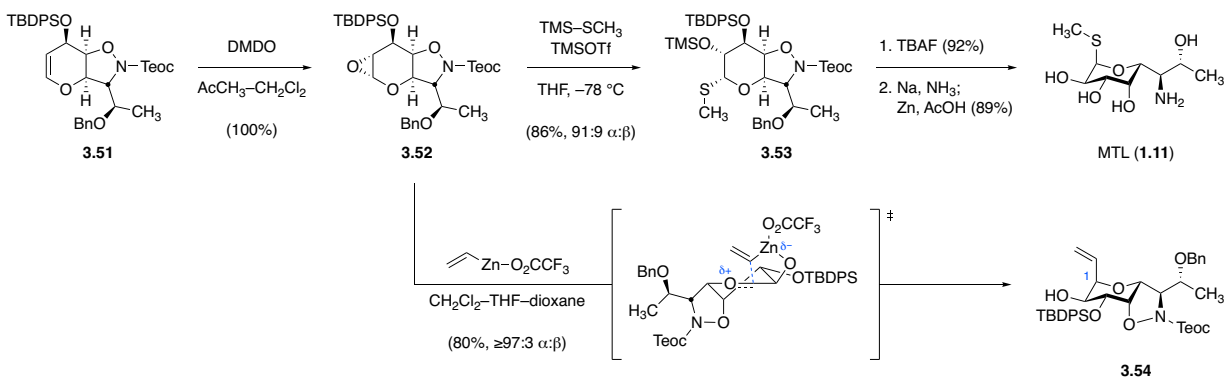
¹²⁹ Dorel, R.; Echavarren, A. M. *Chem. Rev.* **2015**, *115*, 9028–9072.

¹³⁰ Use of less acidic additives resulted in little to no conversion of the isoxazoline substrate. The pK_a' of 3-methylisoxazoline is 0.55 ± 0.10 , while the pK_a of trifluoroacetic acid is 0.23, consistent with a mechanistic model requiring substrate protonation for C=N bond reduction. See: (a) Bauder, C. *Org. Biomol. Chem.* **2008**, *6*, 2952–2960. (b) Grünanger, P.; Vita-Finzi, P.; Dowling, J. E. Isoxazoles. In *Chemistry of Heterocyclic Compounds*; Wiley: New York, 1991; Vol. 49.

This route to glycal **3.51** enabled the preparation of methylthiolincosamine (**1.11**) as anticipated in our original retrosynthesis (Scheme 3.10). Owing to the steric bulk of the adjacent C3-*tert*-butyldiphenylsilyloxy substituent, as well as the rigid bicyclic structure afforded by the connection of the C4 and C6 heteroatom substituents of **3.51**, epoxidation of this glycal with dimethyldioxirane (prepared as a solution in acetone according to the protocol of Murray and Singh)¹³¹ proceeded with perfect facial selectivity, providing Brigl's anhydride **3.52** in quantitative yield. Engagement of this glycosyl donor with trimethyl(methylthio)silane under the action of trimethylsilyl trifluoromethanesulfonate provided the desired *cis*- α -S-glycoside **3.53** in 86% yield and 91:9 dr.¹³² A brief deprotection sequence involving global desilylation followed by 7-*O*-denzylation under dissolving-metal conditions and *N*-*O* bond cleavage with zinc in aqueous acetic acid (the latter two steps may be performed sequentially in the same flask) then furnished MTL (**1.11**) in 82% overall yield from **3.53**. This synthetic material was spectroscopically identical to an authentic sample prepared by basic hydrolysis of lincomycin (see Experimental Section), or by established methods.^{9d}

¹³¹ Murray, R. W.; Singh, M. *Org. Synth.* **1997**, *74*, 91.

¹³² Anomeric selectivity was highly dependent on solvent choice, and participation of ethereal solvents is believed to underlie the high α selectivities observed. When *tert*-butyl methyl ether was used, for example, ~90:10 α : β selectivity was observed, while β -*O*-methyl glycoside – arising through putative loss of *tert*-butyl cation from a transient sugar-solvent oxonium adduct – was isolated as a by-product.



Scheme 3.10. Synthesis of methylthiolincosamine and a C-glycoside derivative proceeding through the intermediacy of a key 1,2-anhydrosugar.

Of course, the development of such a route was not motivated by a desire to prepare MTL (1.11) itself, as this particular aminosugar can be obtained much more economically by chemical degradation of lincomycin – instead, it was our hope that access to epoxide 3.52 might enable the preparation of a host of C1 derivatives not easily accessed by semisynthetic means. Toward this end, I found that stereospecific vinylation of 3.52 could be achieved under the action of vinylzinc trifluoroacetate (prepared *in situ* by the treatment of divinylzinc with trifluoroacetic acid), an ambiphilic reagent which serves both to activate the glycosyl donor as well as to deliver its vinyl group to the same face of the putative nascent oxocarbenium, providing α -vinyl C-glycoside 3.54 in 80% yield as a single diastereomer.¹³³ The C1-modified lincosamides whose synthesis and antimicrobial evaluation were enabled by this chemical sequence form the basis of the section that follows.

C-Glycosidic lincosamide analogs

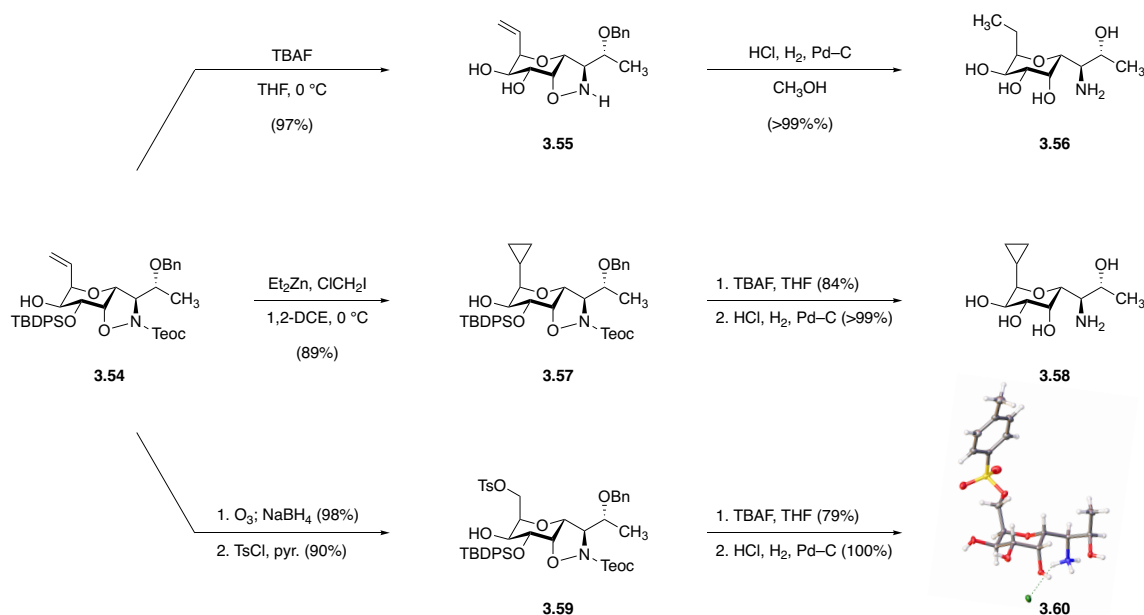
In humans, cytochrome P450 3A (CYP3A)-mediated metabolism of clindamycin to the corresponding inactive sulfoxide is a major route of drug metabolism, contributing substantially

¹³³ Xue, S.; Han, K.-Z.; He, L.; Guo, Q.-X.; *Synlett* **2003**, 870–872.

to the short *in vivo* half-life of the drug ($T_{1/2} = 2.4$ h).¹³⁴ Accordingly, we reasoned that replacement of the sulfur atom of clindamycin with a carbon-based isosteric equivalent might block this route of metabolism. Our interest in preparing C-glycoside lincosamide analogs also stemmed from the fact that while such substitutions were reported to be well tolerated in *in vitro* susceptibility screening (see Chapter 1), precious little SAR data beyond these qualitative assessments were available. Analysis of the X-ray co-crystal structure of clindamycin bound to the bacterial ribosome suggested that the C1 appendage presented an appealing vector along which to build; therefore, we aimed to incorporate a suitably diversifiable group at this position, so as to prepare a library of analogs to test the hypothesis that appropriately decorated C1 variants might feature improved *in vitro* activity and metabolic stability relative to clindamycin.

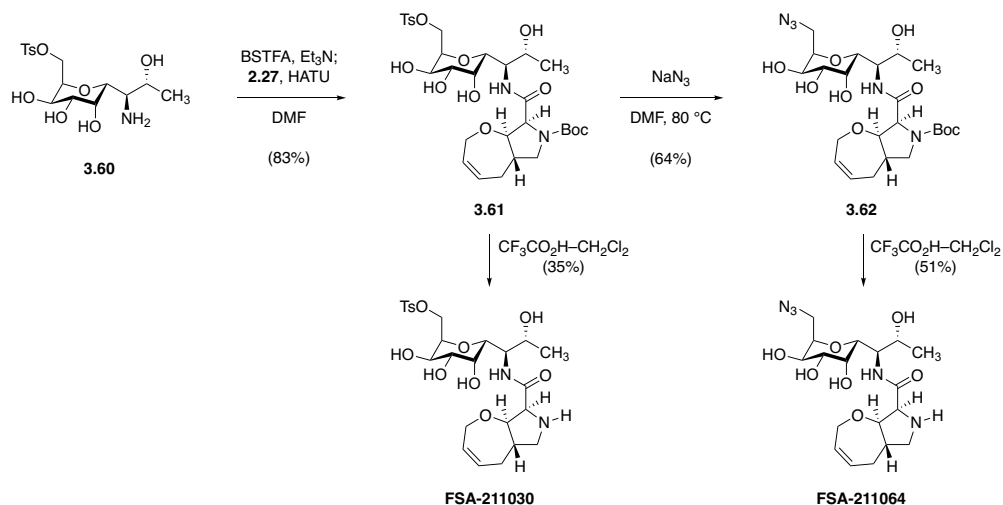
Using vinyl glycoside **3.54** as a starting point, I prepared two isosteric variants of MTL replacing the methylthio group of the natural product with ethyl (**3.56**) and cyclopropyl (**3.58**) groups (Scheme 3.11). Because these compounds lacked the sulfur(II) atom of the natural embodiment, 7-*O*-debenzylation and *N*-*O* bond cleavage (e.g. **3.55** → **3.56**) could be achieved without the use of dissolving-metal conditions; however, the addition of hydrochloric acid was necessary in order to prevent poisoning of the palladium catalyst by the basic nitrogen atom of the isoxazolidine starting materials. In addition to these simple bioisosteric MTL variants, I also prepared the (tosyloxy)methyl analog **3.60** (the structure of which was confirmed by single-crystal X-ray diffraction analysis) through regioselective sulfonylation of the primary alcohol obtained after ozonolysis and reductive workup of **3.54**.

¹³⁴ (a) Brodasky, T. F.; Lewis, C.; Eble, T. E. *Eur. J. Drug Metab. Pharmacokinet.* **1977**, *2*, 149–156. (b) Wynalda, M. A.; Hutzler, J. M.; Koets, M. D.; Podoll, T.; Wienkers, L. C. *Drug Metab. Dispos.* **2003**, *31*, 878–887.



Scheme 3.11. Synthesis of *C*-glycoside northern-half variants.

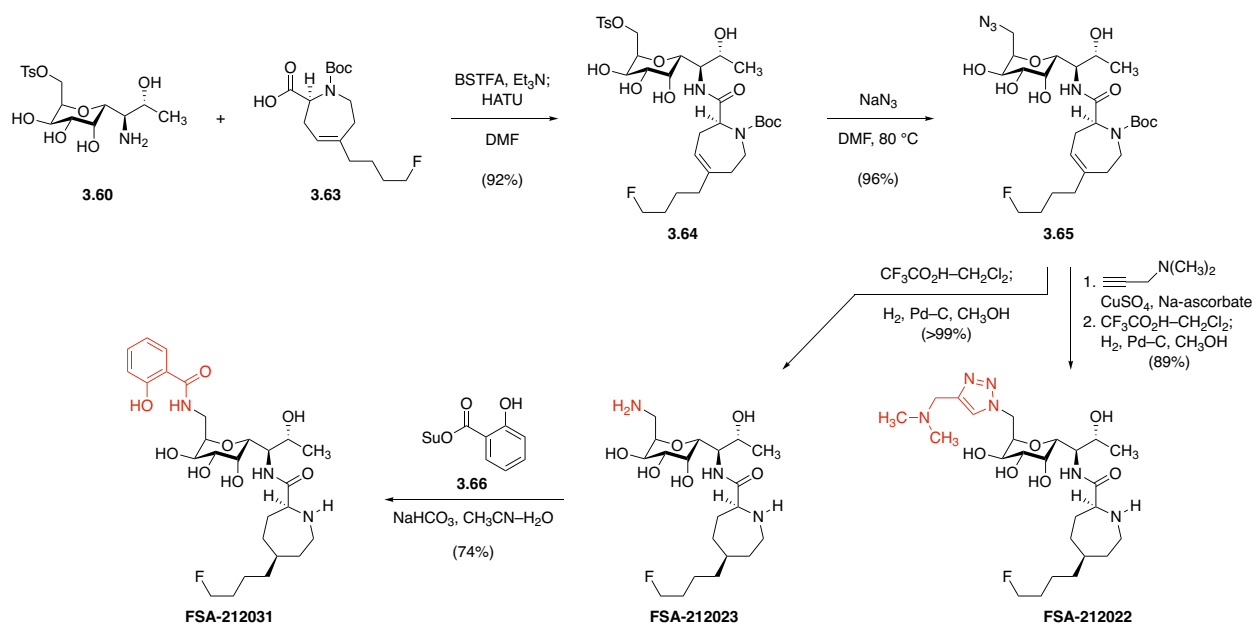
This (tosyloxy)methyl *C*-glycoside provided the opportunity to install a highly flexible azido group following coupling of **3.60** with various southern-half scaffolds (Scheme 3.12). For example, union of **3.60** with oxepinoproline **2.27** provided the *N*-Boc protected lincosamide **3.61**, which I elaborated to the corresponding antibiotic candidate **FSA-211030**. Alternatively, treatment with sodium azide transformed this same intermediate C1 derivative to **3.62** in modest yield. Removal of the *N*-Boc group from **3.62** likewise provided **FSA-211064**, which together with **FSA-211030** constituted one of the earliest examples of a fully synthetic lincosamide analog to emerge from our research program.



Scheme 3.12. Synthesis of selected oxepinoproline-based C1-(tosyloxy)methyl and -azidomethyl lincosamide analogs.

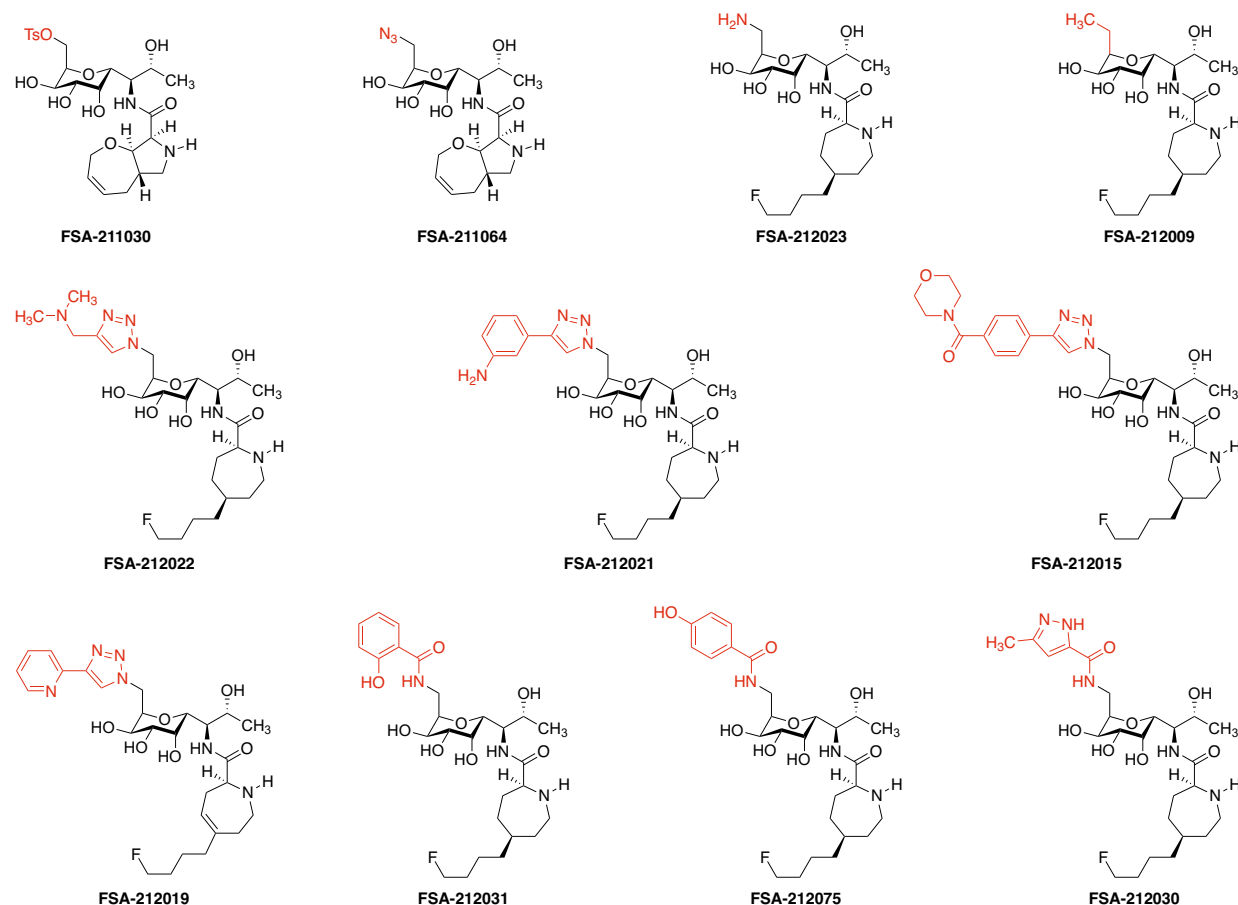
I also pursued C1-modified analogs incorporating the 5'-fluorobutyl azepane scaffold discovered by Vicuron, using an analogous sequence (Scheme 3.13). Here, coupling of **3.60** with azepine **3.63**,⁶⁸ followed by S_N2 substitution produced the flexible azidomethyl intermediate **3.64**. This compound provided access to a host of triazole-based analogs through a short sequence involving copper(II)-catalyzed azide-alkyne cycloaddition, *N*-Boc deprotection, and stereoselective azepine hydrogenation. Omitting the Huisgen cycloaddition step instead afforded the aminomethyl analog **FSA-212023**, which underwent regioselective *N*-acylation with various *N*-hydroxysuccinimidyl esters (e.g., **3.66**) in a sodium bicarbonate-buffered mixed solvent system of acetonitrile and water.¹³⁵

¹³⁵ Abdu-Allah, H. H. M.; Tamanaka, T.; Yu, J.; Zhuoyuan, L.; Sadagopan, M.; Adachi, T.; Tsubata, T.; Kelm, S.; Ishida, H.; Kiso, M. *J. Med. Chem.* **2008**, *51*, 6665–6681.



Scheme 3.13. Synthesis of selected azepane-based C1-modified lincosamide analogs

Figure 3.2 lists the antimicrobial activities of C1-modified oxepinoproline- and azepane-based lincosamides bearing 7-hydroxy substitution prepared by the methods described above. All such analogs displayed substantially diminished activity against both Gram-positive and Gram-negative species relative to clindamycin, with the partial exception of C1-ethyl azepinyl analog **FSA-212009**, which displayed equal potency to clindamycin against *E. faecalis* and *H. influenzae*. This modest potency can be attributed largely to the southern-half residue, however, which is known to confer improved activity against these two species. Paired comparison with *S*-glycoside analogs was not possible for these examples, all of which featured 7-hydroxy decoration. The modest potency of some *C*-glycoside analogs such as **FSA-212009** nonetheless supplied evidence that certain C1 modifications did not abolish all antimicrobial activity, and thus encouraged further exploration of the anomeric position in tandem with established C7 modifications.

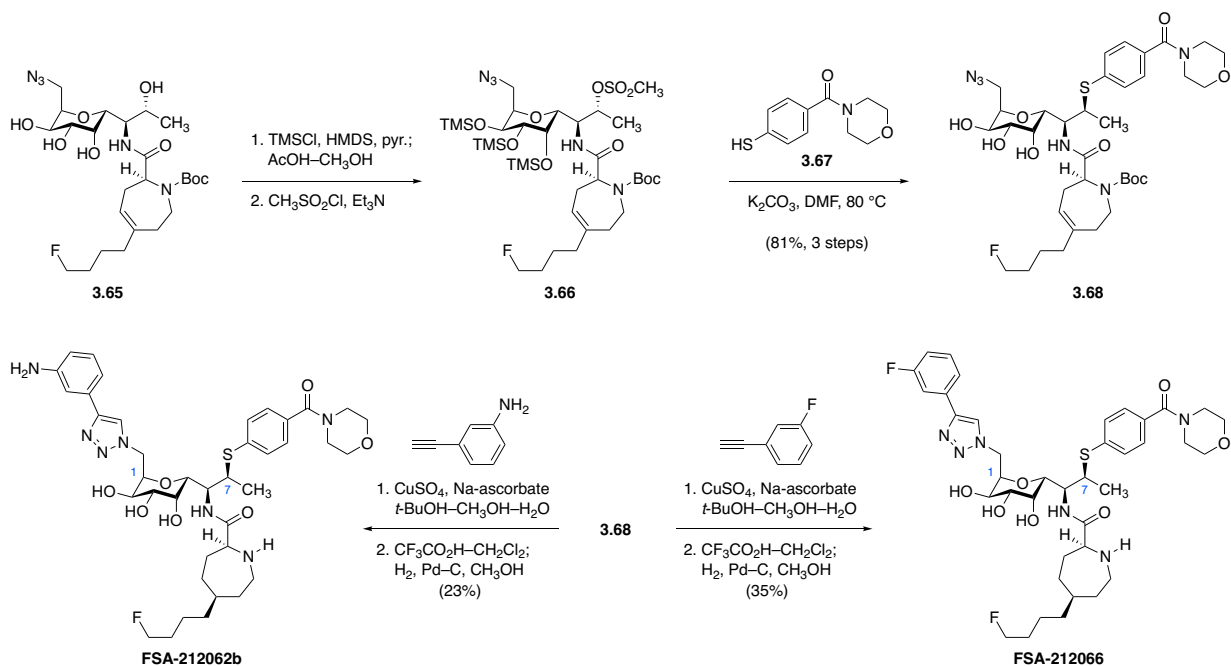


	Species	Description	Clinda	211030	211064	212023	212009	212022	212021	212015	212019	212031	212075	212030
Gram +	<i>S. aureus</i>	ATCC 29213	0.25	>64	>64	>64	16	>64	64	>64	>64	>64	>64	>64
	<i>S. aureus</i>	Micromyx USA 300	0.25	>64	>64	>64	16	>64	64	>64	>64	64	64	>64
	<i>S. pneumoniae</i>	ATCC 49619	0.12	32	16	>64	1	64	64	>64	>64	16	32	32
	<i>S. pneumoniae</i>	MMX 3031 cMefA	0.06	32	16	64	0.5	32	16	>64	>64	8	8	16
	<i>S. pyogenes</i>	ATCC 19615	0.06	1	4	32	0.25	32	4	16	>64	1	2	16
	<i>E. faecalis</i>	ATCC 29212	16	>64	>64	>64	16	>64	>64	>64	>64	>64	>64	>64
Gram -	<i>B. fragilis</i>	ATCC 25285	0.5	>64	>64	64	16	>64	>64	>64	>64	>64	>64	>64
	<i>E. coli</i>	ATCC 25922	>64	>64	>64	>64	>64	>64	>64	>64	>64	>64	>64	>64
	<i>P. aeruginosa</i>	ATCC 27853	>64	>64	>64	>64	>64	>64	>64	>64	>64	>64	>64	>64
	<i>H. influenzae</i>	ATCC 49247	16	>64	>64	>64	16	>64	>64	>64	>64	>64	>64	>64

Figure 3.2. Minimum inhibitory concentrations ($\mu\text{g/mL}$) of 7-hydroxy C-glycoside analogs. Data by Micromyx, LLC and Dr. Amarnath Pisipati.

Consequently, I investigated C1-modified lincosamides bearing a 7-arylthio substituent first discovered by Meiji Seika researchers, in order to evaluate whether C1, C7, and southern-half scaffold modifications were additive in this case. Taking the protected azepinamide **3.65** as a starting point, I performed global silylation, regioselective desilylation of the 7-hydroxy group, and mesylation of the same, following procedures originally described by the Meiji Seika team

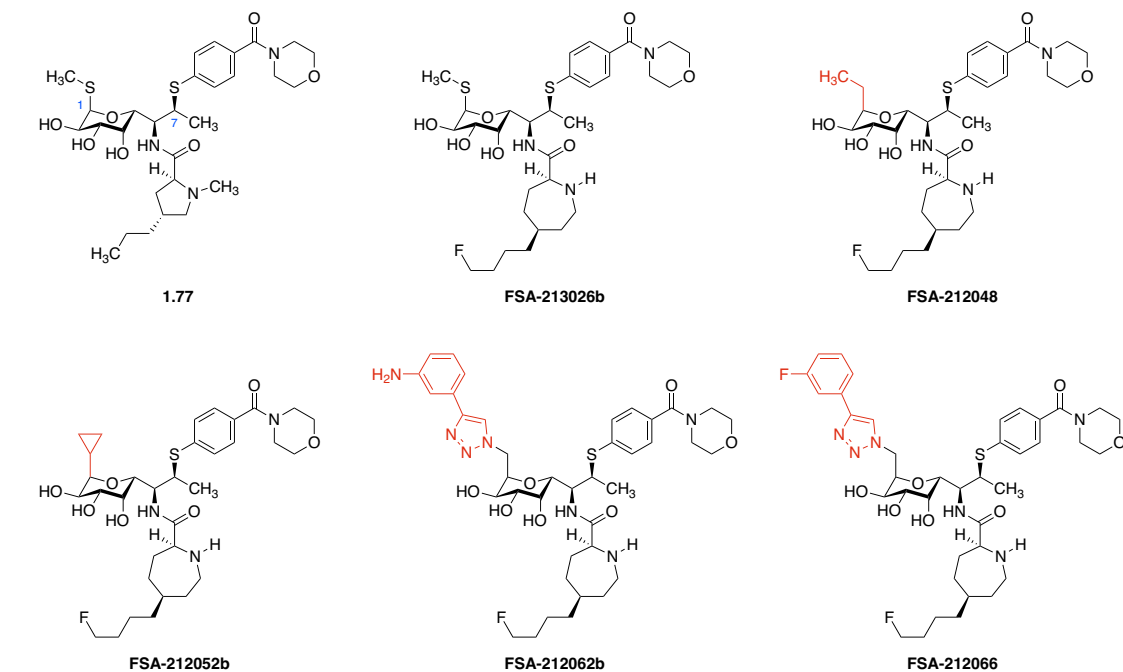
(Scheme 3.14).^{73b} Displacement of the resulting methanesulfonate ester with arenethiol **3.67** thus provided **3.68**, which I paired with ethynylbenzene derivatives in copper(II)-catalyzed click reactions to provide analogs **FSA-212062b** and **FSA-212066**. The C1-cyclopropyl derivative **FSA-212052b** and *S*-methyl glycoside **FSA-213026b** (Figure 3.3) were prepared in an analogous fashion from **3.56** and MTL (**1.11**) respectively (see Experimental Section for details).



Scheme 3.14. Synthesis of *C*-glycoside azepanamide analogs bearing 7-arylthio substitution.

As Figure 3.3 shows, the *in vitro* antimicrobial activities of these 7-arylthio *C*-glycoside analogs were considerably greater than their 7-hydroxy counterparts. Comparison of C1-ethyl (**FSA-212048**) and C1-cyclopropyl (**FSA-212052b**) analogs revealed that the former was generally more effective as a bioisosteric replacement of the native thiomethyl group. Indeed, against lincosamide-susceptible strains of *S. aureus*, C1-ethyl analog **FSA-212041** demonstrated 2–4-fold greater potency compared the matched *S*-glycoside counterpart **FSA-213026b**, possibly owing to the greater lipophilicity of the *C*-glycoside. However, the most striking observation to emerge from this series was that, against *H. influenzae* and MLS_B -resistant Gram-positive

organisms, the propylthioamide scaffold present in Meiji Seika's candidate **1.77** provided superior activity compared to the corresponding azepanamides, demonstrating that modifications to the northern and southern hemispheres of the lincosamide family are not necessarily additive.



	Species	Description	Clindamycin	1.77	213026b	212048	212052b	212062b	212066	
Gram +	<i>S. aureus</i>	ATCC 29213	0.25	0.5	8	2	8	32	8	
	<i>S. aureus</i>	BAA 977; iErmA	0.25	0.5	4	2	8	64	16	
	<i>S. aureus</i>	Micromyx USA 300	0.25	0.25	4	2	4	32	8	
	<i>S. aureus</i>	MMX 3035; cErmA	>64	32	>64	>64	>64	>64	>64	
	<i>S. pneumoniae</i>	ATCC 49619	0.12	≤0.06	0.12	≤0.06	0.12	2	0.5	
	<i>S. pneumoniae</i>	MMX 3028 cErmB	>64	4	8	32	16	64	16	
	<i>S. pneumoniae</i>	MMX 3031 cMefA	0.06	≤0.06	≤0.06	≤0.06	0.12	4	0.25	
	<i>S. pyogenes</i>	ATCC 19615	0.06	≤0.06	≤0.06	≤0.06	≤0.06	4	0.12	
	<i>S. pyogenes</i>	MMX 946; cErmB	>64	2	2	8	4	32	4	
	<i>E. faecalis</i>	ATCC 29212	16	8	2	2	4	32	16	
	<i>E. faecalis</i>	MMX 847; cErmB	>64	64	>64	>64	>64	>64	>64	
	<i>C. difficile</i>	BAA 1805	8	0.25	0.25	0.5	1	64	8	
	Gram -	<i>B. fragilis</i>	ATCC 25285	0.5	4	>64	>64	>64	>64	>64
		<i>E. coli</i>	ATCC 25922	>64	>64	>64	>64	>64	>64	>64
<i>E. coli</i>		MMX 0121 ΔTolC	4	1	8	8	16	64	16	
<i>P. aeruginosa</i>		ATCC 27853	>64	>64	>64	>64	>64	>64	>64	
<i>H. influenzae</i>		ATCC 49247	16	8	64	64	>64	>64	64	
<i>H. influenzae</i>		MMX 565 ΔAcrB	4	≤0.06	0.25	0.25	1	2	0.5	

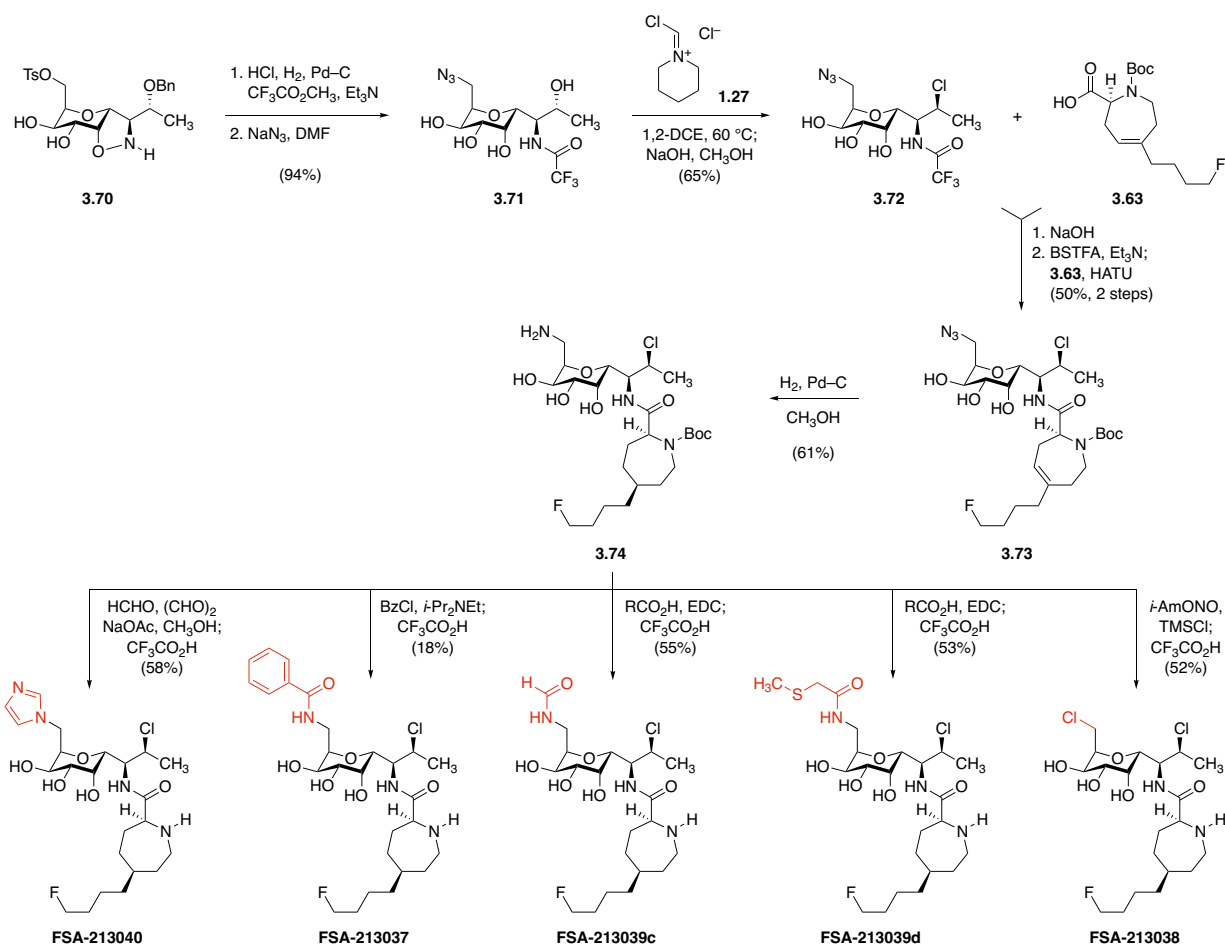
Figure 3.3. Minimum inhibitory concentrations ($\mu\text{g/mL}$) of 7-arylthio lincosamide analogs bearing different C1 modifications, compared to prolinamide analogs clindamycin and **1.77**. Data by Micromyx, LLC.

These earlier findings led me to target C-glycoside azepanamides bearing simple 7-chloro substitution, so as to gauge whether improvements to the antimicrobial activity or projected

pharmacokinetic profile of Vicuron's 7-chloro azepanamide **1.65b** could be realized (Scheme 3.15). Toward this end, I performed hydrogenolysis of (tosyloxy)methyl intermediate **3.70**, capped the newly formed 6-amino group as its corresponding trifluoroacetamide,¹³⁶ and conducted S_N2 displacement of the toluenesulfonate ester with sodium azide. The resulting product, **3.71**, smoothly underwent regioselective 7-deoxychlorination under the action of Vilsmeier reagent **1.27**, providing **3.72** in 65% yield. Cleavage of the *N*-trifluoroacetyl group with sodium hydroxide, coupling of the resulting amine to azepine **3.63**, and catalytic hydrogenation then provided **3.74** in roughly 30% overall yield. By design, this 1-aminomethyl compound was ripe for late-stage diversification: I found that condensation with formalin and glyoxal provided the imidazole derivative **FSA-213040**; acylation gave **FSA-213037** and **FSA-213039c-d**; and, in a striking transformation conceived by Professor Myers, diazotization with nitrosyl chloride (generated *in situ* by the action of chlorotrimethylsilane on isoamyl nitrite)¹³⁷ provided the 1-chloromethyl analog **FSA-213038**.

¹³⁶ In early work from The Upjohn Company, trifluoroacetylation of this amino group was found to facilitate subsequent 7-deoxychlorination. See Reference 60.

¹³⁷ Weiß, R.; Wagner, K.-G. *Chem. Ber.* **1984**, *117*, 1973–1976.

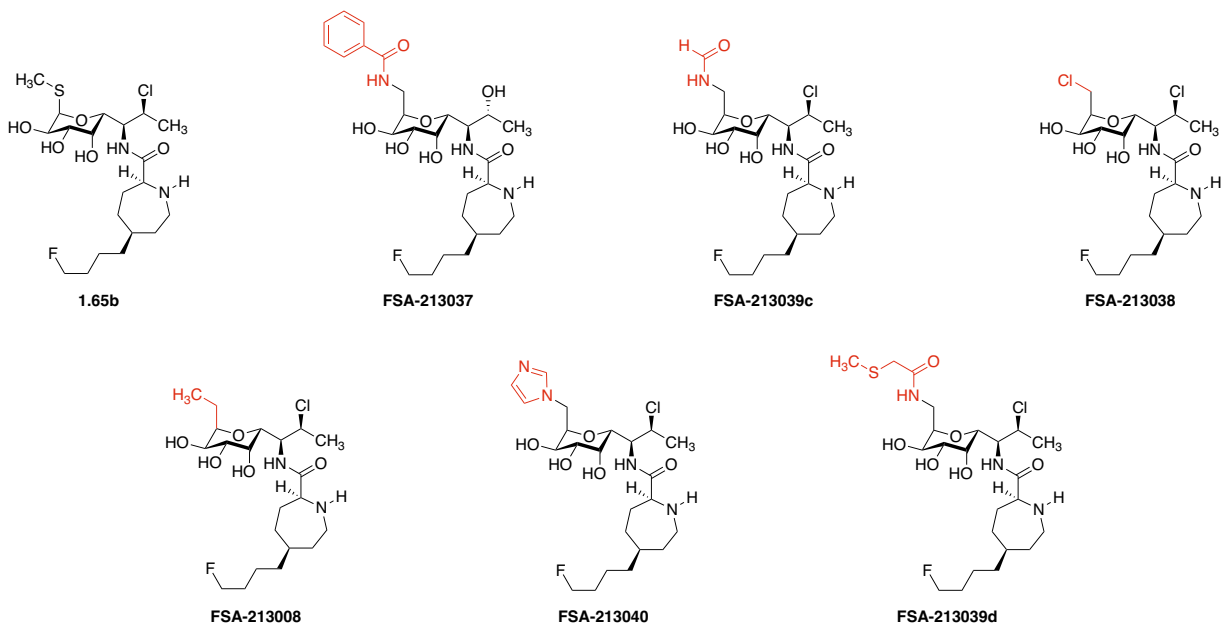


Scheme 3.15. Synthesis of *C*-glycoside azepanamide analogs bearing 7-chloro substitution.

As observed in earlier cases, these *C*-glycosides were less potent than their thiomethyl counterpart, **1.65b** (Figure 3.4). Indeed, 7-chloro-substituted azepanamides seemed particularly sensitive to C1 modification, with ablation of nearly all antimicrobial activity occurring even for the modestly substituted formamidomethyl and chloromethyl analogs **FSA-213039c** and **FSA-213038**. In the case of C1-ethyl substitution,¹³⁸ this effect was less pronounced, with **FSA-213008** displaying roughly 4–16-fold less potency against Gram-negative species and MLS_B resistant

¹³⁸ **FSA-213008** was prepared from **3.56** by a sequence analogous to the one presented in Scheme 3.15 – see Experimental Section for details.

strains of *S. pneumoniae* and *S. pyogenes*. In fact, this drop in potency was modest enough for **FSA-213008** to still feature greater activity against all strains compared to clindamycin.



	Species	Description	Clinda	1.65b	213008	213037	213040	213039c	213039d	213038
Gram +	<i>S. aureus</i>	ATCC 29213	0.25	≤0.06	≤0.06	16	>64	>64	>64	16
	<i>S. aureus</i>	BAA 977; iEmA	0.25	≤0.06	≤0.06	NT	>64	>64	>64	4
	<i>S. aureus</i>	Micromyx USA 300	0.25	≤0.06	≤0.06	NT	64	>64	>64	2
	<i>S. aureus</i>	MMX 3035; cEmA	>64	64	>64	NT	>64	>64	>64	>64
	<i>S. pneumoniae</i>	ATCC 49619	0.12	≤0.06	≤0.06	0.5	8	8	2	1
	<i>S. pneumoniae</i>	MMX 3028; cEmB	>64	8	64	NT	>64	>64	>64	>64
	<i>S. pneumoniae</i>	MMX 3031; cMefA	0.06	≤0.06	≤0.06	NT	8	16	4	1
	<i>S. pyogenes</i>	ATCC 19615	0.06	≤0.06	≤0.06	1	4	8	2	4
	<i>S. pyogenes</i>	MMX 946; cEmB	>64	4	64	NT	>64	>64	>64	>64
	<i>E. faecalis</i>	ATCC 29212	16	≤0.06	≤0.06	64	>64	>64	>64	32
	<i>E. faecalis</i>	MMX 847; cEmB	>64	64	>64	NT	>64	>64	>64	>64
	<i>C. difficile</i>	BAA 1805	8	≤0.06	0.5	NT	>64	64	32	16
Gram -	<i>B. fragilis</i>	ATCC 25285	0.5	0.25	0.25	NT	64	>64	64	8
	<i>K. pneumoniae</i>	ATCC 10031	8	0.5	1	NT	NT	NT	NT	NT
	<i>E. coli</i>	ATCC 25922	>64	4	32	NT	>64	>64	>64	>64
	<i>E. coli</i>	MMX 0120 parent strain	>64	8	>64	>64	>64	>64	>64	>64
	<i>E. coli</i>	MMX 0121 ΔTolC	4	0.25	2	NT	>64	>64	>64	>64
	<i>E. coli</i>	LptD mutant	2	4	16	NT	NT	NT	NT	NT
	<i>P. aeruginosa</i>	ATCC 27853	>64	>64	>64	NT	>64	>64	>64	>64
	<i>P. aeruginosa</i>	MMX 3475 Mex parent	>64	>64	>64	NT	>64	>64	>64	>64
	<i>P. aeruginosa</i>	MMX 3476 ΔMex	>64	8	64	NT	>64	>64	>64	>64
	<i>H. influenzae</i>	ATCC 49247	16	0.25	1	NT	>64	>64	>64	>64
	<i>H. influenzae</i>	MMX 565 ΔAcB	4	≤0.06	0.12	NT	64	>64	32	>64

Figure 3.4. Minimum inhibitory concentrations ($\mu\text{g}/\text{mL}$) of C-glycoside analogs bearing 7-chloro substitution. Data by Micromyx, LLC and Dr. Amarnath Pisipati.

Thus while **FSA-213008** was not as potent as **1.65b**, its lack of a metabolically labile thiomethyl appendage suggested that this C-glycoside might feature improved metabolic stability – and thus superior projected *in vivo* efficacy – compared to the Vicuron compound. Surprisingly,

this hypothesis was not supported by *in vitro* human liver microsomal stability profiling, conducted in collaboration with Professor Michael Cameron of the Scripps Research Institute. These data instead showed that while **FSA-218008** is more stable than clindamycin toward microsomal degradation ($T_{1/2}$'s = 13 min and 19 min, respectively), *S*-glycoside **1.65b** demonstrated the highest metabolic stability of any lincosamide tested, with an assay half-life of 35 minutes. Together these findings suggest that southern-half architecture likely exerts a strong influence on the metabolic susceptibility of the northern-half thioacetal group, and that subtle considerations of stereoelectronics or lipophilicity may underlie the observed difference in chemical resilience of **1.65b** and **FSA-213008**.

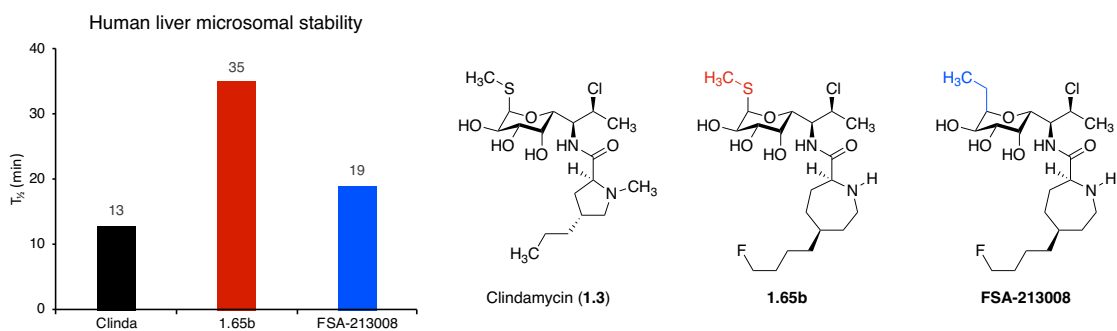


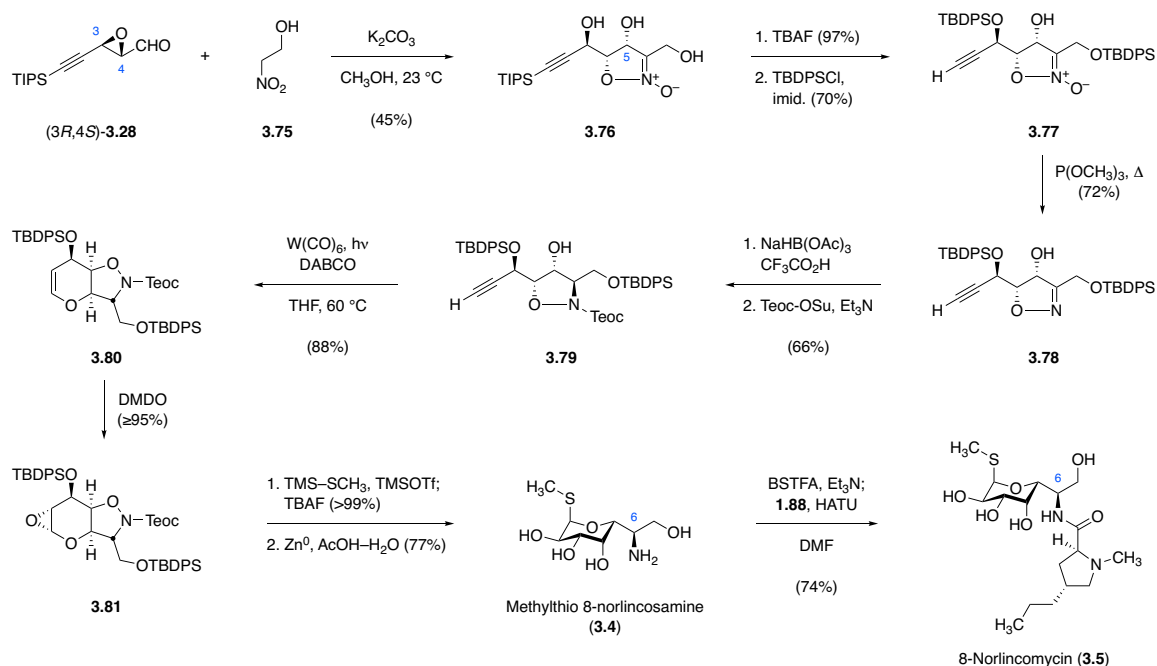
Figure 3.5. Metabolic stability of *S*- and *C*-glycoside-based lincosamides. Data by Prof. Michael Cameron.

The disappointing performance of various carbon-based C1 substituents relative to the thiomethyl group native to typical lincosamides might be understood in a number of ways. For one, exchange of S for CH₂ at the anomeric position involves removal of a σ -withdrawing substituent that likely acts via the anomeric effect to stabilize the ⁴C₁ chair conformer necessary for ribosomal binding; in addition, the same slight σ -withdrawal afforded by the thioacetal scaffold may acidify the C2-hydroxyl group, enhancing its hydrogen-bond-donor ability and thus strengthening the corresponding interaction with N¹ of A2058 (cf. Figure 1.6). The close contact

between the sulfur atom of clindamycin and the π face of G2505 in published X-ray co-crystal structures (Figure 1.5) also suggests that dispersion forces may play a role in binding, with the implication that substitution of the sulfur atom with a less polarizable methylene group might weaken the resulting Van der Waals interaction.

8-Norlincomycin and its derivatives

In addition to enabling the preparation of C1-modified analogs, this newly developed route to MTL permitted the preparation of variants bearing modifications to C6 as well. Through exchange of the nitroalkane coupling partner involved in the key nitroaldol–cyclization coupling reaction, we reasoned, lincosamide analogs that would be difficult or impossible to prepare by semisynthetic means could be prepared readily. In particular, we sought to incorporate a diversifiable element at the C6 position that could be unmasked at a late stage so as to enable the examination of a host of substitution patterns in a step-economical fashion. 6-Hydroxymethyl substitution was particularly appealing for this reason, as we expected incorporation of a primary alcohol at this strategic position would provide the most opportunity for derivatization.



Scheme 3.16. Synthesis of 8-norlincomycin by building-block exchange.

My teammate Jack Stevenson originally investigated the coupling of (3*R*,4*S*)-**3.28** with 2-(benzyloxy)nitroethane under the same conditions developed for the optimized synthesis of **3.4** (cf. Scheme 3.8). Unexpectedly, whereas nitropropanol derivative **3.29** underwent smooth nitroaldol addition to the epoxyaldehyde electrophile, its desmethyl congener instead underwent β elimination to form benzyl alcohol and nitroethylene under these conditions (not shown). Ultimately, Mr. Stevenson identified a sequence involving the coupling of (3*R*,4*S*)-**3.28** and nitroethanol (**3.75**) under the action of methanolic potassium carbonate, proceeding with modest diastereoselectivity (62:38 dr, favoring the desired C5 epimer) to provide **3.76** in 45% yield after isolation by column chromatography (Scheme 3.16). I advanced this product through alkynyl deprotection and regioselective bis-silylation to furnish **3.77**. The same conditions described above for sequential reduction, isoxazolidine protection, cycloisomerization, and glycal epoxidation afforded Brigl's anhydride **3.81**, which underwent efficient coupling with trimethyl(methylthio)silane to give the corresponding *S*-glycoside. Global desilylation could be

performed as part of the workup of this thioglycosylation reaction, and treatment of the resulting isoxazolidine with zinc powder in aqueous acetic acid furnished methylthio 8-norlincosamine (**3.4**). This sequence proceeded in ~10% overall yield from (3*R*,4*S*)-**3.28**, and permitted the synthesis of 8-norlincomycin by a slightly lengthier but perhaps more practical route than the one originally reported by Upjohn (7 steps, 0.042% yield, Scheme 3.1).

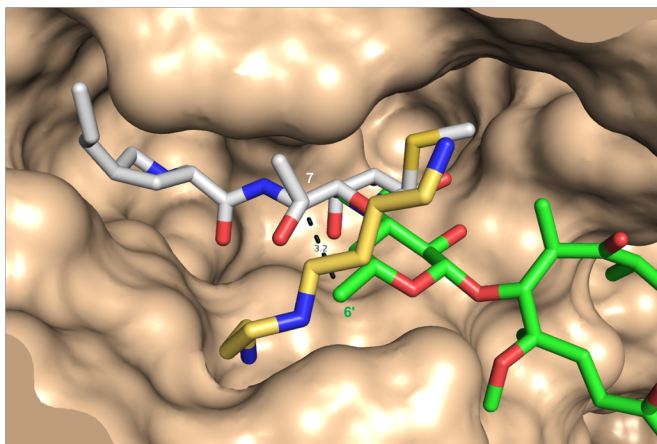
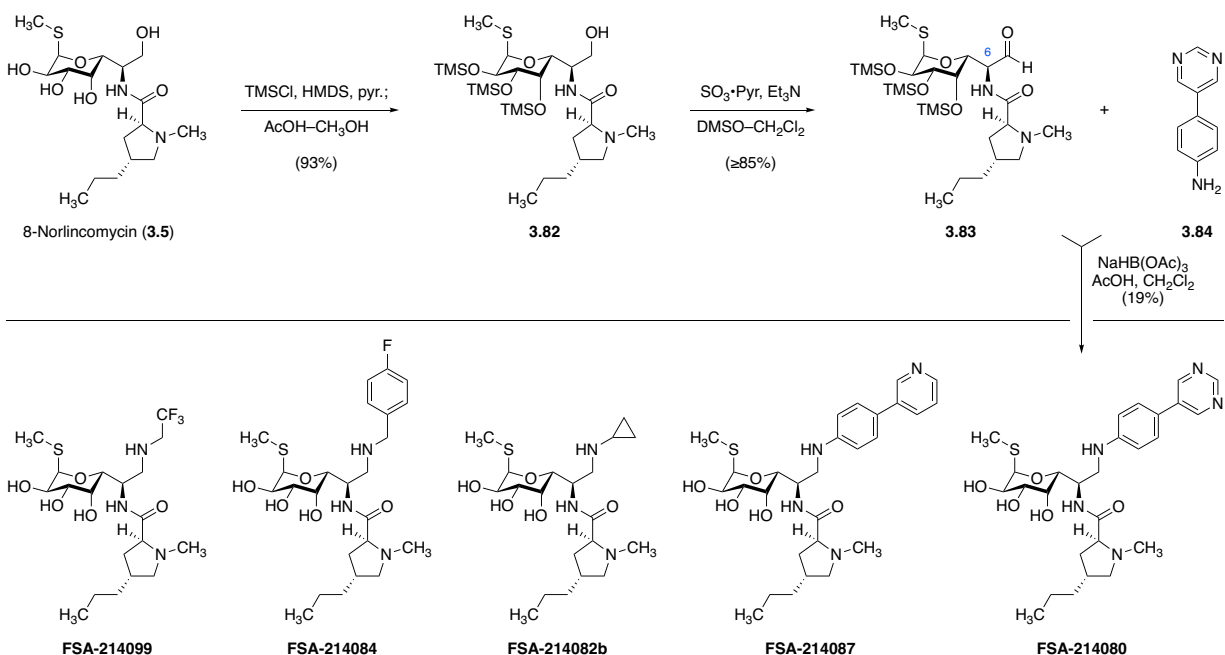


Figure 3.6. Rationale for the synthesis of 7-amino lincosamide analogs. Overlay of lincomycin (gray) and telithromycin (green) bound to the bacterial ribosome shows a close correspondence (3.2 Å) of lincomycin's C7 position with C6' of the macrolide scaffold. In the foreground, a molecule of spermidine that co-crystallized with lincomycin and the *S. aureus* 50S ribosomal subunit is depicted (gold). Compiled from PDB entries 5HKV and 1P9X.

One of the primary motivations for synthesizing 6-hydroxymethyl analogs such as 8-norlincomycin was the observation that the C7 position of clindamycin closely overlaps with C6' of the macrolide antibiotics in overlaid ribosome–antibiotic co-crystal structures (Figure 3.6). Ongoing work in the Myers laboratory spearheaded by my colleague Dr. Ziyang Zhang had identified desosamine C6'-amino derivatization as a high priority within the macrolide project,^{116b,139} and a contemporaneous publication from Ada Yonath's group described the

¹³⁹ (a) Myers, A. G.; Seiple, I. B.; Zhang, Z. Macrolides with modified desosamine sugars and uses thereof. WO 154591 A1, September 29, 2016. (b) Myers, A. G.; Zhang, Z. Synthesis of desosamines. WO 154533 A1, September 29, 2016.

crystallization of the *S. aureus* 50S ribosomal subunit with lincomycin and spermidine (a polyamine component of the crystallization buffer) bound in close proximity.²³ We therefore hypothesized that 7-amino derivatization of lincosamides would be well tolerated, and might afford gains in activity against target organisms including Gram-negative species. Accordingly, I prepared the selectively protected aminotetraol **3.82**, which was converted to corresponding aldehyde (with minimal epimerization at C6) by Parikh–Doering oxidation (Scheme 3.17). This aldehyde underwent smooth reductive amination with a variety of amines, chosen for their relatively low pK_a ' values and – in the case of **FSA-214087** and **FSA-214080**, for example – their structural homology to the biaryl side chains pioneered by Meiji Seika. In some cases, significant epimerization of the C6 stereocenter occurred, and separable mixtures of aminated products were obtained; empirically, it was found that such epimerization could be minimized through the use of 2,2,2-trifluoroethanol as solvent.



Scheme 3.17. Synthesis of 6-aminomethyl propylhygramide analogs.

Species	Description	Clinda	214080	214087	215009	215010	214082b	214099	214084	214088	214083b	
Gram+	<i>S. aureus</i>	ATCC 29213	0.25	>64	32	64	>64	>64	64	>64	>64	>64
	<i>S. pneumoniae</i>	ATCC 49619	0.12	>64	8	64	64	>64	16	>64	>64	>64
	<i>S. pyogenes</i>	ATCC 19615	0.06	>64	8	32	64	>64	32	>64	>64	>64
	<i>E. faecalis</i>	ATCC 29212	16	>64	>64	>64	>64	>64	>64	>64	>64	>64
Gram-	<i>E. coli</i>	ATCC 25922	>64	>64	>64	>64	>64	>64	>64	>64	>64	>64
	<i>E. coli</i>	MP-9 ΔToIC	8	NT	>64	NT	>64	NT	NT	NT	NT	NT

Figure 3.7. Minimum inhibitory concentrations ($\mu\text{g/mL}$) of selected 6-aminomethyl propylhygramide analogs. Data by Dr. Amarnath Pisipati.

As Figure 3.7 illustrates, 6-aminomethyl propylhygramide analogs demonstrated virtually no antibacterial activity, even against clindamycin-susceptible Gram-positive control strains. Trifluoroethylamino compound **FSA-214099** and pyridylaniline analog **FSA-214087** displayed marginal activity in some organisms, but attempts to optimize the latter scaffold through alkylation of the secondary amino group (as in **FSA-215009** and **FSA-215010**) only further reduced activity. These results were discouraging, as we had hoped that installation of a second basic amine within the lincosamide scaffold might increase activity particularly against Gram-negative species; together with a series of semisynthetic 7-deoxyaminolincomycin analogs I prepared,¹⁴⁰ these data

¹⁴⁰ The chemical structures and antibacterial activities of these semisynthetic derivatives are tabulated in Appendices B and C, respectively. For the details of their preparation, see: Mitcheltree, M. J.; Myers, A. G. Lincosamide antibiotics and uses thereof. Patent application in preparation, 2018.

offered compelling evidence that the 7 position of the lincosamide scaffold was not the ideal site on which to focus these efforts.

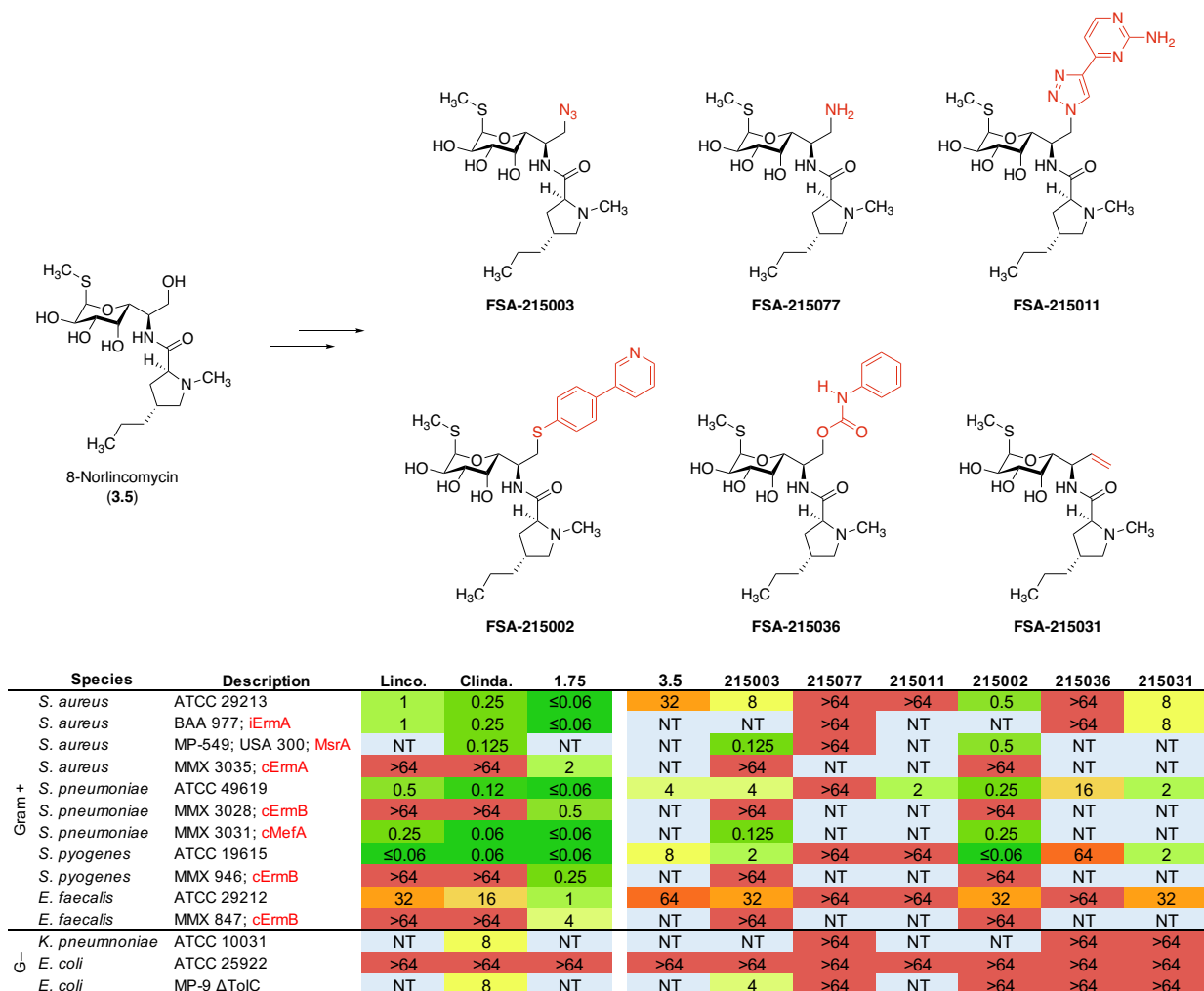


Figure 3.8. Generalized synthesis and minimum inhibitory concentrations ($\mu\text{g/mL}$) of additional 7-desmethyl lincomycin derivatives enabled by a route to 8-norlincomycin. See Experimental Section for synthetic details. Data by Micromyx, LLC and Dr. Amarnath Pisipati.

The synthetic flexibility of the 6-hydroxymethyl substituent within 8-norlincomycin enabled the installation of other targeted modifications as well (Figure 3.8). For example, activation of alcohol **3.82** as the corresponding methanesulfonate ester, and $\text{S}_{\text{N}}2$ displacement with sodium azide provided azidomethyl analog **FSA-215003**, which in turn provided access to the primary amine **FSA-215077** and triazolyl candidate **FSA-215011**. Likewise, Mitsunobu chemistry

could be used to activate this same hydroxymethyl group to install a (pyridyl)phenylthio side chain, providing **FSA-215002** as the 7-desmethyl congener of Meiji Seika's potent antibiotic **1.75**. Carbamate **FSA-215036** was prepared by straightforward coupling of **3.82** with phenyl isocyanate; and Wittig olefination of **3.83** produced the 6-vinyl analog **FSA-215031**.

The collated antimicrobial activities of these 8-norlincomycin derivatives point to an unexpectedly pronounced role that the C8 methyl group plays in driving the potency of naturally occurring and semisynthetic lincosamides. For example, 8-norlincomycin (**3.5**) itself displays up to ≥ 128 -fold less potency than its 7-methylated congener, lincomycin (**1.1**); while deletion of the 7-methyl group in Meiji Seika's candidate **1.75** delivers **FSA-215002**, which demonstrates no activity against MLS_B-resistant strains. Intriguingly, while azidomethyl analog **FSA-215003** displayed markedly diminished activity against Gram-positive strains relative to lincomycin and clindamycin, its activity against a strain of *E. coli* lacking a functioning efflux pump system (MP-9; Δ TolC) was not significantly different from that of clindamycin, signaling that differences in permeability or efflux of these compounds may partially explain their diminished activity. The magnitude of this 7-desmethyl effect was surprising, given that this group does not directly engage the ribosome, based on available X-ray evidence; but similarly striking phenomena appear commonly enough within drug discovery as to have been somewhat mythologized.¹⁴¹ In the present case, the “magic methyl” effect is likely to arise through a degree of conformational control that the C8 methyl group introduces within the acyclic portion of the lincosamides' northern hemisphere – a hypothesis that would ultimately form the basis for the development of a second-generation route to northern-half variants, the subject of the final chapter of this dissertation.

¹⁴¹ For reviews of the “magic methyl” effect, see: (a) Schönherr, H.; Cernak, T. *Angew. Chem. Int. Ed.* **2013**, *52*, 12256–12267. (b) Berreiro, E. J.; Kümmerle, A. E.; Fraga, C. A. M. *Chem. Rev.* **2011**, *111*, 5215–5246.

Summary and conclusion

In this chapter, I described my efforts to develop and apply a novel synthetic route to the northern-half component of lincosamide antibiotics relying on nitroaldol chemistry to forge the central C5–C6 carbon–carbon bond of methylthiolincosamine (MTL, **1.11**). In the course of this work, I identified an unexpected isoxazoline *N*-oxide product arising through spontaneous cyclization of a nitroaldol adduct, and developed conditions to render this transformation reproducible, scalable, and highly diastereoselective. By targeting a pivotal 1,2-anhydrosugar intermediate, I prepared both the *S*-glycoside MTL itself, alongside a host of *C*-glycosidic variants. The *C*-glycoside-based antibiotics to emerge from this series uniformly demonstrated weaker antibiotic activity compared to their thiomethyl counterparts, and, unexpectedly, replacement of the thiomethyl group within Vicuron’s azepanamide candidate **1.65b** with an isosteric ethyl group (**FSA-213008**) did not render the resulting lincosamide more resilient toward microsomal degradation.

This route was adapted to prepare a variant of MTL lacking the C8 methyl group, and subsequent elaboration to 8-norlincomycin provided a useful intermediate by which to probe the effects of C8-methyl deletion and 6-aminomethyl substitution. What emerged from these studies was an increased appreciation for the subtle, yet pronounced, effects that conformational control within the northern-half residue exerts on the antimicrobial properties of lincosamide analogs. These structural insights would inform subsequent analog design, and ultimately prompted the development of a new route to MTL, discussed in the chapter that follows.

Experimental section

General Experimental Procedures. All reactions were performed in oven- or flame-dried round-bottomed or modified Schlenk flasks fitted with rubber septa under a positive pressure of argon (dried by passage through a column of Drierite calcium sulfate desiccant), unless otherwise noted. Air- and moisture-sensitive liquids and solutions were transferred via syringe or stainless-steel cannula. When necessary (so noted), solutions were deoxygenated by three cycles of freezing (liquid nitrogen), evacuation, and thawing under static vacuum. Organic solutions were concentrated by rotary evaporation (house vacuum, ~60 Torr) at 23–30 °C. Flash-column chromatography was performed as described by Still et al.,¹⁰⁵ employing silica gel (60-Å pore size, 230–400 mesh, Agela Technologies, Chicago, IL; or RediSep silica cartridges, Teledyne Isco, Lincoln, NE). Analytical thin-layer chromatography (TLC) was performed using glass plates pre-coated with silica gel (0.25 mm, 60-Å pore size, 230–400 mesh, Merck KGA) impregnated with a fluorescent indicator (254 nm). In special cases (so noted), analytical TLC was performed with aminopropyl-modified silica gel (NH₂ silica gel, 60-Å pore size, Wako Chemicals USA) impregnated with a fluorescent indicator (254 nm). TLC plates were visualized by exposure to ultraviolet light (UV) and/or exposure to iodine vapor (I₂), basic aqueous potassium permanganate solution (KMnO₄), acidic ethanolic *para*-anisaldehyde solution (PAA), acidic aqueous ceric ammonium molybdate solution (CAM), or ethanolic solution of phosphomolybdic acid (PMA) followed by brief heating on a hot plate as needed (~200 °C, ≤15 s).¹⁰⁶ In some cases, reaction monitoring was carried out by analytical liquid chromatography–mass spectrometry (LCMS), or by flow-injection analysis–high-resolution mass spectrometry (FIA-HRMS).

Materials. Commercial reagents and solvents were used as received, unless mentioned otherwise. Dichloromethane, diethyl ether, tetrahydrofuran, 1,4-dioxane, *N,N*-dimethylformamide, toluene, and benzene were purified by passage through Al₂O₃ under argon, according to the method of Pangborn et al.¹⁰⁷ 5'-(4-Fluorobutyl)azepine acid **3.63** and 1-(chloromethylene)piperidine-1-ium chloride (Vilsmeier reagent **1.26**) were prepared according to Lewis and co-workers.⁶⁸ *Trans*-4-*n*-propyl-L-hygric acid hydrochloride (**1.88**) was prepared from lincomycin according to Herr and Slomp.^{9c} Ethynyltriisopropylsilane, triethylphosphonoacetate, 1,8-diazabicyclo[4.5.0]undec-7-ene, (-)-diethyl-D-tartrate, *tert*-butylchlorodiphenylsilane, chlorotriisopropylsilane, imidazole, trimethyl phosphite, sodium triacetoxyborohydride, trifluoroacetic acid, 1-[2-(trimethylsilyl)ethoxycarbonyloxy]pyrrolidin-2,5-dione (Teoc-OSu), Oxone monopersulfate compound, hexamethyldisilazane, methyl trifluoroacetate, HATU, and 2,4,6-trimethylbenzenesulfonyl chloride were purchased from Oakwood Products, Inc. (Estill, SC, USA). Anhydrous cupric acetate, tungsten hexacarbonyl (99%, <0.3% molybdenum), and palladium hydroxide on carbon (20% w/w) were purchased from Strem Chemicals, Inc. (Newburyport, MA, USA). 4-(*tert*-Butylthio)phenylboronic acid was purchased from Alchem Pharmtech, Inc. (Monmouth Junction, NJ, USA). (4-Ethynylphenyl)(morpholine)methanone (**S3.9**) was purchased from Ark Pharm, Inc. (Arlington Heights, IL, USA). 4-(Pyrimidin-5-yl)aniline (**3.84**) was purchased from Enamine, Ltd. (Monmouth, Jct., NJ, USA). 4-Pyridin-3-ylaniline (**S3.23**) was purchased from Maybridge Chemical Company (Altrincham, UK). 4-Ethynylpyrimidin-2-amine was prepared by Dr. Ziyang Zhang, according to literature procedures.¹⁴² (4-Mercaptophenyl)(morpholino)methanone (**3.67**) was prepared according to

¹⁴² Tibiletti, F.; Simonetti, M.; Nicholas, K. M.; Palmisano, G.; Parravicini, M.; Imbesi, F.; Tollari, S.; Penoni, A. *Tetrahedron* **2010**, *66*, 1280–1288.

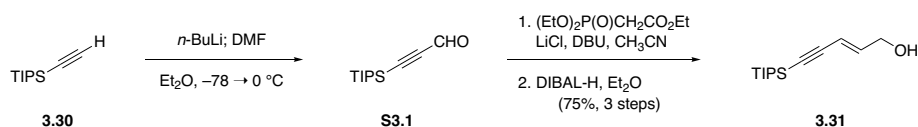
published procedures.¹⁴³ All other chemicals and reagents were purchased from Sigma-Aldrich Corporation (Natick, MA, USA).

Instrumentation. Proton nuclear magnetic resonance (¹H NMR) spectra and carbon nuclear magnetic resonance (¹³C NMR) spectra were recorded on Varian Mercury 400 (400 MHz/100 MHz), Varian Inova 500 (500 MHz/125 MHz), or Varian Inova 600 (600 MHz/150 MHz) NMR spectrometers at 23 °C. Proton chemical shifts are expressed in parts per million (ppm, δ scale) and are referenced to residual protium in the NMR solvent (CHCl₃, δ 7.26; CHD₃OD, δ 3.31; C₆H₅D, δ 7.16). Carbon chemical shifts are expressed as parts per million (ppm, δ scale) and are referenced to the carbon resonance of the NMR solvent (CDCl₃, δ 77.2; CD₃OD, δ 49.0; C₆D₆, δ 128.1). Data are reported as follows: Chemical shift, multiplicity (s = singlet, d = doublet, t = triplet, q = quartet, qn = quintet, dd = doublet of doublets, td = triplet of doublets, ABq = AB quartet, m = multiplet, br = broad, app = apparent), integration, and coupling constant (*J*) in Hertz (Hz). Infrared transmittance (IR) spectra were obtained using a Bruker ALPHA FTIR spectrophotometer referenced to a polystyrene standard. Data are represented as follows: Frequency of absorption (cm⁻¹), and intensity (s = strong, m = medium, br = broad). Melting points were determined using a Thomas Scientific capillary melting point apparatus. High-resolution mass spectrometry (including FIA-HRMS reaction monitoring) was performed at the Harvard University Mass Spectrometry Facility using a Bruker micrOTOF-QII mass spectrometer. X-ray crystallographic analysis was performed at the Harvard University X-Ray Crystallographic Laboratory by Dr. Shao-Liang Zheng. High-performance liquid chromatography–mass

¹⁴³ Ahlmark, M.; Din, B. D.; Kauppala, M.; Luiro, A.; Pajunen, T.; Pystynen, J.; Tiainen, E.; Vaismaa, M.; Messinger, J. Preparation of 2-substituted 4,5-dihydroxyisophthalonitriles and their analogs as inhibitors of catechol-*O*-methyltransferase for the treatment of Parkinson's disease. WO Patent 2013175053A1, May 23, 2013.

spectrometry (LCMS) was performed using an Agilent Technologies 1260-series analytical HPLC system in tandem with an Agilent Technologies 6120 Quadrupole mass spectrometer; a Zorbax Eclipse Plus reverse-phase C₁₈ column (2.1 × 50 mm, 1.8 μm pore size, 600 bar rating; Agilent Technologies, Santa Clara, CA) was employed as stationary phase. LCMS samples were eluted at a flow rate of 650 μL/min, beginning with 5% acetonitrile–water containing 0.1% formic acid, grading linearly to 100% acetonitrile containing 0.1% formic acid over 3 minutes, followed by 100% acetonitrile containing 0.1% formic acid for 2 minutes (5 minutes total run time).

For clarity, intermediates that have not been assigned numbers in the preceding text are numbered sequentially in this section, beginning with **S3.1**.



Enynol 3.31.

Formylation of ethynyltriisopropylsilane was performed according to the procedure reported by Robles and McDonald.^{119a} To a solution of ethynyltriisopropylsilane (**3.30**, 20.0 g, 110 mmol, 1 equiv) in diethyl ether (100 mL) was added *n*-butyllithium solution (2.12 M in hexane, 51.7 mL, 110 mmol, 1.00 equiv) slowly by cannula at 0 °C over approximately 15 min. The resulting solution was stirred at 0 °C for an additional 40 min. This lithium acetylide solution was then transferred via cannula over a period of 5–10 min to a 500-mL round-bottomed flask containing a mixture of *N,N*-dimethylformamide (25.5 mL, 329 mmol, 3.00 equiv) and diethyl ether (100 mL) chilled to -78 °C. A white suspension formed. The reaction mixture was stirred at -78 °C for 1 h before warming to 0 °C, at which temperature the mixture became homogeneous. After 1 h of stirring at 0 °C, the mixture was transferred to an ice-cold aqueous sulfuric acid solution (5% v/v, 250 mL). The resulting biphasic mixture was stirred at 0 °C for 1 h, and then the layers were separated. The aqueous phase was extracted with diethyl ether (3 × 150 mL), and the combined organic extracts were washed with saturated aqueous sodium chloride solution (150 mL). The washed organic solution was dried over sodium sulfate, the dried solution was filtered, and the filtrate was concentrated to give 3-(triisopropylsilyl)propionaldehyde (**2**) as a colorless oil that was used in the next step without further purification. The ¹H NMR data matched literature values.^{119a}

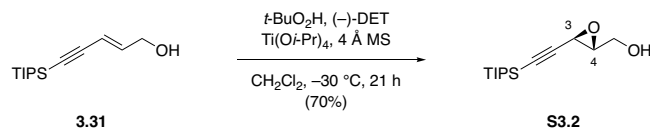
Horner–Wadsworth–Emmons olefination of the crude ynol formed in the preceding formylation reaction was performed according to the procedure reported by Bode and co-workers.^{119b} An oven-dried 2-L round-bottomed flask was charged with lithium chloride (5.60 g,

132 mmol, 1.20 equiv), and the apparatus was flame-dried. Once cooled, the flask was charged with a magnetic stir bar and acetonitrile (1.3 L), and the resulting suspension was stirred at 23 °C for 10 min (lithium chloride does not fully dissolve). 3-(Triisopropylsilyl)propionaldehyde (**S3.1**, theoretically 110 mmol, 1 equiv) and triethyl phosphonoacetate (22.5 mL, 112 mmol, 1.02 equiv) were then added sequentially. 1,8-Diazabicyclo[5.4.0]undec-7-ene (DBU, 16.6 mL, 110 mmol, 1.00 equiv) was added dropwise over 5 min, causing the mixture to warm to approximately 40 °C with concomitant transformation of the originally colorless reaction solution to an opaque, off-white suspension. Progress was monitored by TLC (20% dichloromethane–hexanes, UV+PAA); after 10 min, the reaction was judged to be complete. The mixture was concentrated by rotary evaporation to a volume of approximately 300 mL, and the concentrated mixture was transferred to a separatory funnel containing saturated aqueous ammonium chloride solution (400 mL) and diethyl ether (300 mL). The mixture was shaken, and the layers were separated. The aqueous phase was extracted with diethyl ether (3 × 300 mL); the combined organic layers were then washed sequentially with water (250 mL) and saturated aqueous sodium chloride solution (250 mL). The washed organic solution was dried over sodium sulfate, the dried solution was filtered, and the filtrate was concentrated to give ethyl (*E*)-5-(triisopropylsilyl)pent-2-en-4-ynoate as a colorless oil that was used in the next step without further purification. The ¹H NMR data matched literature values.^{119b}

Reduction of the crude ester formed in the preceding Horner–Wadsworth–Emmons olefination reaction was performed according to the procedure reported by Bressy and co-workers.^{119c} To a rapidly stirred solution of crude ethyl (*E*)-5-(triisopropylsilyl)pent-2-en-4-ynoate (theoretically 110 mmol, 1 equiv) in diethyl ether (220 mL) was added diisobutyl aluminum hydride (1.0 M solution in hexane, 243 mL, 2.2 equiv) by cannula at –78 °C. The mixture was

stirred at $-78\text{ }^{\circ}\text{C}$ for 1 h, then at $0\text{ }^{\circ}\text{C}$ for 1.5 h. The reaction mixture was then transferred by wide-bore cannula to a 2-L round-bottomed flask containing a rapidly stirred aqueous Rochelle salt solution (potassium sodium tartrate, 0.80 M, 410 mL, 328 mmol, 3.0 equiv) pre-chilled to $0\text{ }^{\circ}\text{C}$. A cloudy slurry formed immediately upon aqueous quenching of the reaction mixture; after approximately 3 min of stirring at $0\text{ }^{\circ}\text{C}$, this suspension thickened to form a gel. Gas evolution was then observed, followed by gradual collapse of the gel to form a cloudy, light yellow emulsion. The mixture was stirred at $23\text{ }^{\circ}\text{C}$ overnight under an atmosphere of nitrogen gas, during which time the emulsion separated into a biphasic mixture. The layers were separated at the end of this period, and the aqueous phase was extracted with diethyl ether ($3 \times 200\text{ mL}$). The combined organic layers were then washed with saturated aqueous sodium chloride solution (200 mL), and the washed organic product solution was dried over sodium sulfate. The dried solution was filtered, and the filtrate was concentrated to give a light yellow oil. This residue was purified by flash-column chromatography (500 g silica gel, eluting with 5% ethyl acetate–hexanes initially, grading to 10% ethyl acetate–hexanes) to afford allylic alcohol **3** as a colorless oil (19.7 g, 75%, 3 steps). The ^1H NMR data matched literature values.¹⁴⁴

¹⁴⁴ Cho, J.; Lee, Y. M.; Kim, D.; Kim, S. *J. Org. Chem.* **2009**, *74*, 3900–3904.

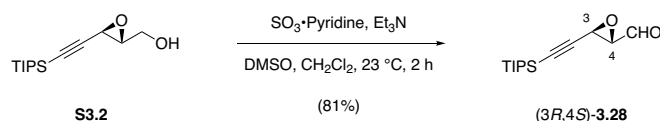


Propargylic epoxide S3.2.

Sharpless asymmetric epoxidation was performed according to a procedure adapted from the report of Kim and co-workers.¹⁴⁴ A 1-L, 2-necked round-bottomed flask was oven-dried. Once cooled, the flask was charged with a magnetic stir bar and powdered 4-Å molecular sieves (20.0 g, Sigma-Aldrich, activated by heating overnight in a vacuum drying oven [200 °C, ~70 Torr]). A thermocouple probe was fitted to one neck of the flask, while the other neck was sealed with a rubber septum. Dichloromethane (229 mL) was added, and the resulting slurry was cooled to –30 °C in a CryoCool bath. (–)-Diethyl-D-tartrate (7.21 mL, 41.9 mmol, 0.500 equiv) was added. Titanium(IV) isopropoxide (9.83 mL, 33.6 mmol, 0.400 equiv) was then added dropwise over 2 min, causing the internal temperature to rise to –26 °C briefly. The resulting mixture was stirred at –30 °C for 20 min, after which time a solution of allylic alcohol **3.31** (20.0 g, 84.0 mmol, 1 equiv) in dichloromethane (295 mL) was added slowly by cannula over 10 min. The mixture was incubated at –30 °C for 30 min. *tert*-Butylhydroperoxide solution (TBHP, ~5.5 M solution in decane, 30.5 mL, 170 mmol, 2.0 equiv) was finally added at a rate of 2.0 mL/min with a syringe pump, such that the internal temperature of the mixture did not rise above –28 °C. Stirring was maintained at –30 °C following the addition of TBHP, and progress was monitored by TLC (10% ethyl acetate–dichloromethane, UV+PAA). After 21 h, the reaction was judged to be complete. A solution comprising iron(II) sulfate heptahydrate (27 g, 97 mmol, 1.2 equiv), DL-tartaric acid (62 g, 0.41 mol, 4.9 equiv), and water (517 mL) was added to the reaction mixture, and the resulting biphasic mixture was stirred at 0 °C for 10 min at a moderate stir rate (350 rpm) The mixture was then transferred to a separatory funnel where the layers were separated. The aqueous phase was

extracted with diethyl ether (3×300 mL), and the combined organic layers were washed with saturated aqueous sodium chloride solution (2×200 mL). The washed organic solution was dried over sodium sulfate, the dried solution was filtered, and the filtrate was concentrated to give a slightly cloudy colorless oil. This residue was purified by flash-column chromatography (800 g silica gel, eluting with 5% ethyl acetate–hexanes initially, grading to 15% ethyl acetate–hexanes) to give epoxyalcohol product as a colorless, viscous oil (14.9 g, 70%). The ^1H NMR data matched reported values.¹⁴⁴

The enantiomeric excess was determined by conversion to the corresponding Mosher esters. In this procedure, a solution of epoxyalcohol **S3.2** (10 mg, 39 μmol , 1 equiv) in 4:1 dichloromethane–pyridine (200 μL) was treated with (*R*)-3,3,3-trifluoro-2-methoxy-2-phenylpropanoyl chloride (8.8 μL , 47 μmol , 1.2 equiv) at 23 °C. The mixture was stirred at 23 °C for 30 min, at which point TLC analysis (50% ethyl acetate–hexanes, UV+KMnO₄) indicated complete consumption of starting material. The reaction mixture was concentrated, and the crude residue was subjected to ^1H NMR analysis (600 MHz, CDCl₃). Integration of the major methylene resonance at δ 4.60 (dd, $J = 12.3, 3.2$ Hz, 1H) relative to its minor diastereomeric counterpart at δ 4.66 (dd, $J = 12.5, 3.0$ Hz, 1H, derived from undesired (*2S,3S*)-product enantiomer) demonstrated an enantiomeric ratio of 94:6 (88% ee). Use of the enantiomeric (*S*)-Mosher acyl chloride reagent gave the same result.



Epoxyaldehyde (3R,4S)-2.38.

A solution of epoxyalcohol **S3.2** (14.9 g, 58.6 mmol, 1 equiv) in dichloromethane (468 mL) and anhydrous dimethyl sulfoxide (117 mL) was treated with triethylamine (65.3 mL, 468 mmol, 8.00 equiv). Sulfur trioxide–pyridine complex (37.3 g, 234 mmol, 4.00 equiv) was then added in three portions over 15 min at 23 °C. The resulting salmon-pink solution was stirred at 23 °C, and after 2 h, TLC analysis (30% ethyl acetate–hexanes, PAA) indicated complete consumption of starting material. The reaction mixture was transferred to a separatory funnel containing 1.2 L of 0.5 M copper(II) sulfate solution. The layers were shaken, then separated, and the aqueous phase was extracted with dichloromethane (3 × 300 mL). The combined organic layers were then washed with saturated aqueous sodium chloride solution (200 mL), and the washed organic product solution was dried over sodium sulfate. The dried solution was filtered, and the filtrate was concentrated to give a brown oil. This residue was purified by flash-column chromatography (600 g silica gel, eluting with 5% ethyl acetate–hexanes initially, grading to 10% ethyl acetate–hexanes) to afford the product as a colorless oil (12.0 g, 81%).

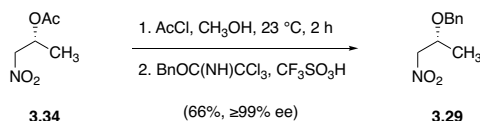
$R_f = 0.57$ (40% ethyl acetate–hexanes, KMnO_4).

$^1\text{H NMR}$ (500 MHz, CDCl_3): δ 9.02 (d, $J = 6.1$ Hz, 1H), 3.69 (d, $J = 1.8$ Hz, 1H), 3.54 (dd, $J = 6.1, 1.8$ Hz, 1H), 1.07 (s, 21H).

$^{13}\text{C NMR}$ (100 MHz, CDCl_3): δ 196.3, 99.9, 88.9, 60.5, 44.2, 18.6, 11.2.

FTIR (neat, cm^{-1}): 2944 (s), 2866 (s), 1733 (s), 1463 (m), 1411 (m), 1046 (m), 883 (m), 833 (m), 667 (m).

HRMS (ESI+, m/z): $[M+H]^+$ calc'd for $C_{14}H_{24}O_2Si$, 252.1542; found 252.1540.



Nitro compound 3.29.

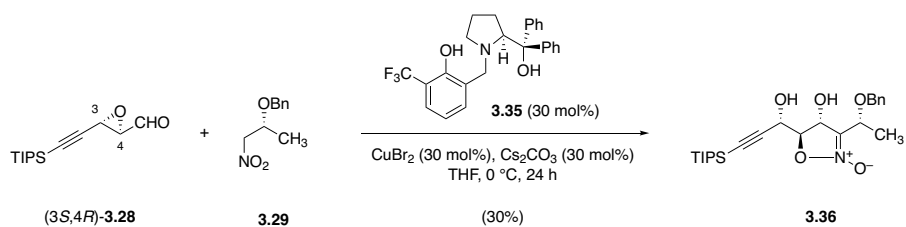
Acetyl chloride (123 mL, 1.73 mol, 12.8 equiv) was added dropwise over 15 min to a solution of (*R*)-1-nitropropan-2-yl acetate (**3.34**, 20.0 g, 136 mmol, 1 equiv)¹⁴⁵ in methanol (1.23 L) at 0 °C. Following the addition of acetyl chloride, the mixture was allowed to warm to 23 °C; progress was monitored by TLC (40% ethyl acetate–hexanes, KMnO₄). After 2 h, complete consumption of starting material was noted, and the mixture was concentrated by rotary evaporation to obtain (*R*)-1-nitropropan-2-ol as a faint yellow oil. Residual methanol present in the crude product was removed azeotropic removal of benzene. The crude product thus obtained was used in the next step without further purification.

To a solution of (*R*)-1-nitropropan-2-ol (theoretically 136 mmol) in 1:2 dichloromethane–hexane (412 mL) was added benzyl 2,2,2-trichloroacetimidate (30.5 mL, 163 mmol, 1.20 equiv). Trifluoromethanesulfonic acid (1.21 mL, 13.6 mmol, 0.100 equiv) was then added dropwise over 30 min at 23 °C, causing a white precipitate to appear. After 5 h, TLC analysis (20% ethyl acetate–hexanes, UV+KMnO₄) indicated that all starting material had been consumed. The reaction mixture was filtered through a pad of Celite to remove the trichloroacetamide precipitate, and the filter pad was washed with hexanes (2 × 50 mL). The filtrate was concentrated to give a muddy brown slurry, which was purified by two sequential recrystallizations from 1% ethyl acetate–hexanes (200 mL) to give benzyl ether product as a brilliant white, fluffy powder (17.4 g, 66%, 2

¹⁴⁵ Kitayama, T. *Tetrahedron* **1996**, 52, 6139–6148.

steps). The ^1H NMR and melting-point data matched reported values.¹⁴⁶ Enantiomeric excess was determined to be $\geq 99\%$ by chiral HPLC analysis using a chiral stationary-phase AD-H column using 2% isopropanol–hexanes as eluent at a flow rate of 1.0 mL/min, with detection at 300 nm. Major enantiomer $R_t = 14.7$ min, minor enantiomer $R_t = 11.7$ min.

¹⁴⁶ Bartoli, G.; Marcantoni, E.; Petrini, M. *J. Chem. Soc. Chem. Commun.* **1991**, 793–794.



Isoxazoline *N*-oxide **3.36**.

A 4-mL glass vial was charged with a magnetic stir bar, nitro compound **3.29** (64 mg, 0.33 mmol, 1.7 equiv), copper(II) bromide (13 mg, 59 μmol , 0.30 equiv), cesium carbonate (29mg, 89 μmol , 0.45 equiv), and prolinol ligand **3.35** (25 mg, 59 μmol , 0.30 equiv).¹²¹ This mixture was suspended in tetrahydrofuran (800 μL), the vial was sealed with a PTFE-lined screw cap, and the mixture was stirred at 23 $^\circ\text{C}$ for 4 h; over this time, the mixture changed from dark black to cerulean blue. The mixture was then chilled to 0 $^\circ\text{C}$ before a solution of epoxyaldehyde (3*S*,4*R*)-**3.28** (50 mg, 0.20 mmol, 1 equiv) in tetrahydrofuran (100 μL) was added. The mixture was warmed to 4 $^\circ\text{C}$, and it was stirred at this temperature for 24 h, until TLC analysis (30% ethyl acetate–hexanes) showed complete consumption of aldehyde starting material. The mixture was neutralized with the addition of saturated aqueous ammonium chloride solution (1.0 mL). This mixture was then extracted with ethyl acetate (3 \times 2 mL); the combined organic extracts were dried over sodium sulfate, filtered, and concentrated to provide a dark green-black oil. This crude mixture was purified by flash-column chromatography (12 g silica gel, eluting with 10% ethyl acetate–hexanes initially, grading to 35% ethyl acetate–hexanes) to provide the product as a white, crystalline solid (26 mg, 30%).

Crystals suitable for X-ray diffraction analysis were prepared by dissolving the product (20 mg) in dichloromethane (1 mL). This solution was passed through a cotton plug to remove any insoluble impurities, and the filtrate was collected in a 1-mL glass vial. This vial was placed within

a 20-mL glass vial into which hexanes (~5 mL) had been introduced. The large vial was capped, and the assembly was allowed to stand at 23 °C; after 1 d, the hexanes in the large vial was removed by pipette, and fresh portion of hexanes (~5 mL) was introduced. The cap to the large vial was left slightly ajar to allow slow evaporation of solvent, and after 4 d of standing, needle-shaped crystals had formed. See Appendix A for X-ray crystal structure data.

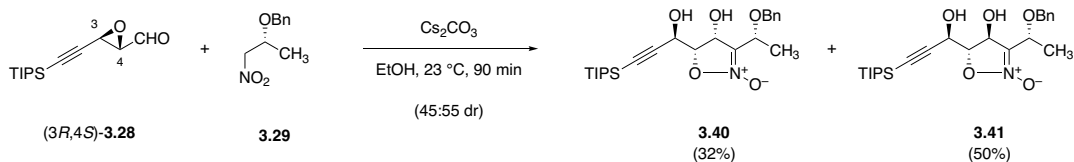
$R_f = 0.32$ (30% ethyl acetate–hexanes, UV+KMnO₄).

¹H NMR (500 MHz, CDCl₃) δ 7.35–7.29 (m, 5H), 5.60 (d, $J = 2.5$ Hz, 1H), 4.67 (d, $J = 3.0$ Hz, 1H), 4.60 (q, $J = 6.7$ Hz, 1H), 4.57 (d, $J = 11.2$ Hz, 1H), 4.45–4.43 (m, 2H), 1.52 (d, $J = 6.7$ Hz, 3H), 1.08 (s, 21H).

¹³C NMR (126 MHz, CDCl₃) δ 137.3, 128.7, 128.3, 128.2, 119.6, 102.2, 89.9, 84.6, 75.2, 72.1, 70.3, 62.6, 19.1, 18.7, 11.2.

FTIR (neat, cm⁻¹): 3386 (br), 2865 (m), 1636 (s), 1462 (m), 1366 (m), 1209 (m), 1088 (s), 882 (s), 676 (s).

HRMS (ESI+, m/z): [M+Na]⁺ calc'd for C₂₄H₃₇NO₅Si, 470.2333; found 470.2321.



Non-diastereoselective synthesis of isoxazoline *N*-oxides **3.40** and **3.41**.

In a 20-mL glass vial fitted with a magnetic stir bar, nitro compound **3.29** (914 mg, 4.68 mmol, 1.20 equiv) was added to a solution of epoxyaldehyde (3*R*,4*S*)-**3.28** (985 mg, 3.90 mmol, 1 equiv) in ethanol (200 proof, 7.80 mL). The mixture was stirred at 23 °C for 5–10 min, until the nitro compound was fully dissolved, before cesium carbonate (254 mg, 780 μmol, 0.200 equiv) was added in a single portion. The mixture immediately turned canary yellow in color. Progress was monitored by ¹H-NMR analysis; after 90 min, an aliquot of the reaction mixture was concentrated, re-dissolved in CDCl₃ and analyzed by ¹H-NMR, revealing that no epoxy aldehyde starting material remained, and that cyclization of the intermediate nitroaldol adducts was complete. The stir bar was removed, and the reaction mixture was concentrated directly in vacuo to provide a viscous, yellow oil. This was purified by flash-column chromatography (80 g silica gel, eluting with 5% ethyl acetate–hexanes initially, grading to 20% ethyl acetate–hexanes) to furnish, in order of elution, the undesired C5 epimer **3.41** (866 mg, 50%) and the desired C5 epimer **3.40** (560 mg, 32%) as colorless oils.

3.40:

$R_f = 0.61$ (50% ethyl acetate–hexanes, UV+KMnO₄).

¹H NMR (600 MHz, CDCl₃): δ 7.37–7.29 (m, 5H), 5.14 (app t, $J = 6.9$ Hz, 1H), 4.77 (app t, $J = 5.4$ Hz, 1H), 4.66 (d, $J = 12.1$ Hz, 1H), 4.63 (q, $J = 6.7$ Hz, 1H), 4.43 (d, $J = 12.2$ Hz, 1H),

3.92 (dd, $J = 6.7, 5.6$ Hz, 1H), 3.60 (d, $J = 7.2$ Hz, 1H), 3.35 (d, $J = 5.8$ Hz, 1H), 1.49 (d, $J = 6.7$ Hz, 3H), 1.09 (br s, 21H).

^{13}C NMR (150 MHz, CDCl_3) δ 162.6, 138.0, 128.7, 128.4, 127.9, 119.6, 103.2, 89.6, 79.4, 77.4, 77.2, 76.9, 74.7, 72.8, 70.8, 60.4, 19.1, 18.7, 11.2.

FTIR: 3380 (br), 2942 (s), 2865 (s), 1630 (s), 1463 (m), 1381 (m), 1083 (s), 883 (s), 678 (s).

HRMS (ESI+, m/z): $[\text{M}+\text{H}]^+$ calc'd for $\text{C}_{24}\text{H}_{37}\text{NO}_5\text{Si}$, 448.2514; found 448.2529.

3.41:

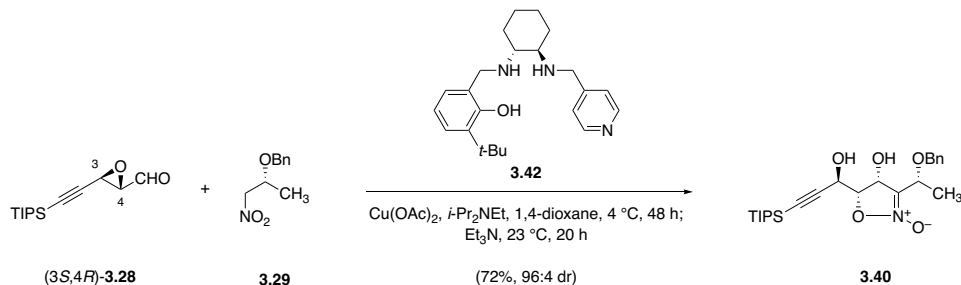
$R_f = 0.67$ (50% ethyl acetate–hexanes, UV+ KMnO_4).

^1H NMR (500 MHz, CDCl_3) δ 7.38–7.29 (m, 5H), 5.47 (dd, $J = 3.6, 2.5$ Hz, 1H), 4.72–4.68 (m, 2H), 4.63 (d, $J = 11.5$ Hz, 1H), 4.59 (d, $J = 11.5$ Hz, 1H), 4.47 (app t, $J = 2.7$ Hz, 1H), 2.85 (d, $J = 5.5$ Hz, 1H), 2.83 (d, $J = 3.7$ Hz, 1H), 1.45 (d, $J = 6.6$ Hz, 3H), 1.08 (s, 21H).

^{13}C NMR (126 MHz, CDCl_3) δ 137.3, 128.8, 128.3, 128.2, 117.9, 102.0, 90.0, 84.1, 74.5, 72.0, 70.0, 63.0, 18.7, 17.7, 11.1.

FTIR (neat, cm^{-1}): 3395 (br), 2943 (s), 2866 (s), 1630 (s), 1463 (m), 1213 (m), 1089 (s), 833 (s).

HRMS (ESI+, m/z): $[\text{M}+\text{H}]^+$ calc'd for $\text{C}_{24}\text{H}_{37}\text{NO}_5\text{Si}$, 448.2514; found 448.2502.

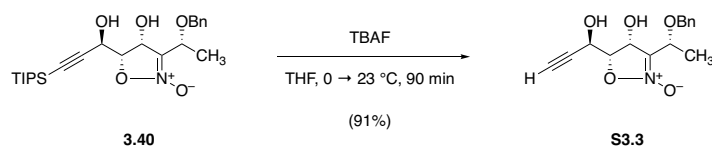


Diastereoselective synthesis of isoxazoline *N*-oxide **3.40**.

To a mixture of (*R,R*)-diaminocyclohexane ligand **3.42** (1.75 g, 47.5 mmol, 0.0100 equiv),¹²⁴ and anhydrous copper(II) acetate (863 mg, 4.75 mmol, 0.0100 equiv) was added 1,4-dioxane (47.5 mL mL). The resulting dark forest-green solution was stirred at 23 °C for 30 min before *N,N*-diisopropylethylamine (830 μL , 4.75 mmol, 0.0100 equiv) was added. The catalyst mixture was then stirred an additional 10 min at 23 °C before cooling to 5–10 °C in an ice-water bath. Nitropropane **3.29** (12.1 g, 61.8 mmol, 1.30 equiv) was added in one portion, followed by the epoxyldehyde (*3S,4R*)-**3.28** (12.0 g, 47.5 mmol, 1 equiv), which was added by cannula transfer (transfer was quantitated with 2 \times 2 mL 1,4-dioxane rinses). The mixture was then transferred to a 4 °C cold-room, where constant stirring was maintained at that temperature.¹⁴⁷ Progress was monitored by NMR as follows: Aliquots of the reaction mixture (ca. 50 μL) were diluted with ethyl acetate (2 mL), and the diluted samples were washed with saturated aqueous ammonium chloride solution (1 mL). The washed samples were then dried by passage through a short plug of sodium sulfate (1 \times 2 cm), and the dried filtrate was concentrated. The green-brown residue thus obtained was analyzed by ¹H NMR (CDCl_3), where consumption of epoxyldehyde was gauged relative to the triisopropylsilyl signal (δ 1.15–1.00, 21H). After 48 h at 4 °C,

¹⁴⁷ Although the melting point of pure 1,4-dioxane is 12 °C, freezing point depression prevents the solidification of the reaction mixture at these temperatures.

conversion of aldehyde had reached $\geq 95\%$, and triethylamine (13.3 mL, 95.0 mmol, 2.00 equiv) was added to induce cyclization. The mixture was warmed to 23 °C and stirred for 20 h, whereupon aliquot NMR analysis (as above) showed the absence of epoxide methine resonances (ca. δ 3.45, 3.30), with concomitant formation of isoxazoline *N*-oxide products as a 98:2 diastereomeric mixture. The product mixture was poured into a separatory funnel containing 175 mL saturated aqueous ammonium chloride solution, and the resulting mixture was extracted with ethyl acetate (3×150 mL). The combined organic extracts were washed with saturated aqueous sodium chloride solution (50 mL), and the washed organic phase was dried over sodium sulfate. The dried product solution was filtered, and the filtrate was concentrated to afford crude product as a dark brown oil. This residue was purified by flash-column chromatography (2.0 kg silica; eluting 10% ethyl acetate–hexanes initially, grading to 30% ethyl acetate–hexanes) to afford the isoxazoline *N*-oxide product an amber-brown, viscous oil (16.4 g, 77%).



Propargylic alcohol S3.3.

A solution of tetrabutylammonium fluoride (1.0 M in tetrahydrofuran, 88 mL, 88 mmol, 2.5 equiv) was added via cannula over 5 min to a solution of alkynyl silane **3.40** (15.8 g, 35.3 mmol, 1 equiv) in tetrahydrofuran (118 mL) at 0 °C. The mixture was then warmed to 23 °C, and after 90 min of stirring at this temperature, TLC analysis (50% ethyl acetate–hexanes, UV+KMnO₄) indicated full conversion of starting material. The product solution was then poured into a separatory funnel containing 350 mL of water to which 35 mL of saturated aqueous sodium chloride solution had been added. The resulting biphasic mixture was extracted with ethyl acetate (3 × 150 mL). The organic layers were combined, and the organic solution was washed with saturated aqueous sodium chloride solution (100 mL). The washed product solution was dried over sodium sulfate, and the dried solution was filtered. The filtrate was concentrated to afford crude product as a light amber oil. This residue was purified by flash-column chromatography (500 g silica; eluting 35% ethyl acetate–hexanes initially, grading to 50% ethyl acetate–hexanes) to provide the product as a sand-colored, powdery solid (9.38 g, 91%).

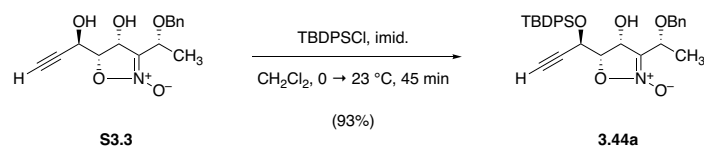
$R_f = 0.45$ (60% ethyl acetate–hexanes, UV+KMnO₄).

¹H NMR (600 MHz, CDCl₃): δ 7.37–7.29 (m, 5H), 5.22 (d, $J = 6.7$ Hz, 1H), 4.77 (dd, $J = 6.3, 2.3$ Hz, 1H), 4.61 (q, $J = 6.7$ Hz, 1H), 4.60 (d, $J = 12.2$ Hz, 1H), 4.45 (d, $J = 12.1$ Hz, 1H), 4.06 (app t, $J = 6.5$ Hz, 1H), 4.03 (br s, 1H), 2.59 (d, $J = 2.2$ Hz, 1H), 1.48 (d, $J = 6.7$ Hz, 3H).

^{13}C NMR (125 MHz, CDCl_3): δ 137.6, 128.7, 128.4, 127.9, 120.0, 80.3, 79.3, 75.7, 73.9, 72.6, 70.5, 59.2, 18.9.

FTIR (neat, cm^{-1}): 3373 (br), 3284 (m), 1628 (s), 1377 (m), 1085 (s), 1046 (m), 699 (m).

HRMS (ESI+, m/z): $[\text{M}+\text{Na}]^+$ calc'd for $\text{C}_{15}\text{H}_{17}\text{NO}_5$, 314.0999; found 314.1009.



***tert*-Butyldiphenylsilyl ether 3.44a.**

A mixture of diol **S3.3** (9.38 g, 32.2 mmol, 1 equiv) and imidazole (6.58 g, 97.0 mmol, 3.00 equiv) was dissolved in dichloromethane (161 mL), and the resulting solution was cooled to 0 °C. *tert*-Butyl(chloro)diphenylsilane (12.4 mL, 48.3 mmol, 1.50 equiv) was then added in one portion, and the solution was warmed to 23 °C. Within 2–5 min of addition of the silyl chloride, a precipitate formed, imparting a cloudy appearance to the reaction mixture. Progress was monitored by TLC (60% ethyl acetate–hexanes, UV+KMnO₄), and after 45 min, full consumption of starting material was observed. The reaction mixture was quenched with the addition of 150 mL saturated aqueous sodium bicarbonate solution, and the mixture was stirred rapidly at 23 °C for 10 min. The biphasic mixture was then extracted with dichloromethane (3 × 50 mL), and the combined organic extracts were washed with brine (50 mL). The organic solution was then dried over sodium sulfate, and the dried solution was filtered. The filtrate was concentrated to give a peach-colored oil, which was purified by flash-column chromatography (700 g silica; eluting with hexanes initially, grading to 25% ethyl acetate–hexanes) to provide the product as a colorless, highly viscous oil (15.8 g, 93%).

R_f = 0.49 (30% ethyl acetate–hexanes, UV+KMnO₄).

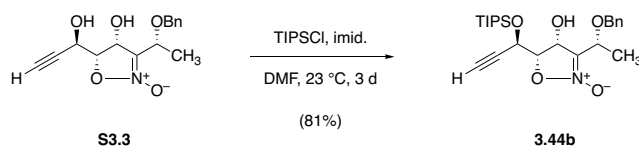
¹H NMR (500 MHz, CDCl₃): δ 7.75–7.68 (m, 4H), 7.49–7.44 (m, 2H), 7.43–7.28 (m, 9H), 5.17 (app t, J = 7.6 Hz, 1H), 4.72 (dd, J = 4.6, 2.2 Hz, 1H), 4.66 (q, J = 6.8 Hz, 1H), 4.64 (d, J

= 12.2 Hz, 1H), 4.46 (d, $J = 12.1$ Hz, 1H), 4.02 (dd, $J = 6.9, 4.7$ Hz, 1H), 3.59 (d, $J = 8.3$ Hz, 1H), 2.45 (d, $J = 2.3$ Hz, 1H), 1.50 (d, $J = 6.8$ Hz, 3H), 1.09 (s, 9H).

^{13}C NMR (125 MHz, CDCl_3): δ 138.1, 136.2, 136.1, 132.0, 131.4, 130.6, 130.4, 128.6, 128.2 (2 \times C), 127.9, 127.8, 118.9, 79.4, 78.9, 76.7, 74.6, 72.6, 70.7, 61.7, 26.9, 19.4, 19.2.

FTIR (neat, cm^{-1}): 3367 (br), 2932 (m), 2858 (m), 1632 (s), 1428 (m), 1112 (s), 1087 (s), 701 (s).

HRMS (ESI+, m/z): $[\text{M}+\text{Na}]^+$ calc'd for $\text{C}_{31}\text{H}_{35}\text{NO}_5\text{Si}$, 552.2177; found 552.2177.



Triisopropylsilyl ether **3.44b**.

To a solution of diol **S3.3** (329 mg, 1.13 mmol, 1 equiv) and imidazole (615 mg, 9.04 mmol, 8.00 equiv) in dimethylformamide (11.3 mL) was added triisopropylchlorosilane (718 μL , 3.39 mmol, 3.00 equiv) in one portion at 23 $^\circ\text{C}$. Reaction progress was monitored by TLC (80% ethyl acetate–hexanes, UV+KMnO₄). After 3 d, full consumption of starting material was observed, and water (25 mL) was added. The resulting mixture was extracted with diethyl ether (3 \times 25 mL), and the combined organic extracts were washed with saturated aqueous sodium chloride solution (25 mL). The washed organic solution was dried over sodium sulfate, the dried solution was filtered, and the filtrate was concentrated. The residue was purified by flash-column chromatography (24 g silica; eluting 5% ethyl acetate–hexanes, grading to 20% ethyl acetate–hexanes) to obtain the product as a bright white, crystalline solid (407 mg, 81%).

Crystals of **3.44b** suitable for X-ray analysis were prepared as follows: A 1-mL vial was charged with 20 mg of **3.44b**, and a minimum quantity of benzene (ca. 50 μL) was added to dissolve this material. The sample vial was then placed inside a larger, 20-mL scintillation vial filled with ca. 5 mL of hexanes, and the large vial was sealed with a screw cap. Slow diffusion of hexane into the solution of **3.44b** in benzene occurred over several days at 23 $^\circ\text{C}$, resulting in the growth of long, needle-shaped crystals. See Appendix A for X-ray crystal structure data.

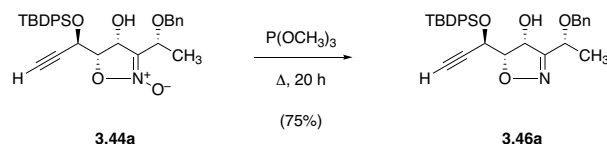
$R_f = 0.56$ (30% ethyl acetate–hexanes, UV+KMnO₄).

^1H NMR (600 MHz, CDCl_3) δ 7.38–7.28 (m, 5H), 5.21 (dd, $J = 8.1, 7.2$ Hz, 1H), 4.92 (dd, $J = 4.3, 2.3$ Hz, 1H), 4.65 (q, $J = 6.8$ Hz, 1H), 4.64 (d, $J = 12.2$ Hz, 1H), 4.45 (d, $J = 12.2$ Hz, 1H), 4.08 (d, $J = 8.2$ Hz, 1H), 4.04 (dd, $J = 7.2, 4.3$ Hz, 1H), 2.61 (d, $J = 2.2$ Hz, 1H), 1.50 (d, $J = 6.8$ Hz, 3H), 1.22–1.15 (m, 3H), 1.09 (app dd, $J = 7.4, 5.4$ Hz, 18H).

^{13}C NMR (151 MHz, CDCl_3) δ 140.2, 130.6, 130.2, 129.9, 120.9, 81.8, 80.6, 78.4, 76.9, 74.5, 72.7, 63.6, 21.1, 20.0, 19.9, 14.2.

FTIR (neat, cm^{-1}): 3345 (m), 3260 (m), 2939 (m), 2865 (m), 1639 (s), 1202 (m), 1115 (s), 873 (m), 816 (m), 733 (s).

HRMS (ESI+, m/z): $[\text{M}+\text{H}]^+$ calc'd for $\text{C}_{24}\text{H}_{37}\text{NO}_5\text{Si}$, 448.2514; found 448.2516.



Isoxazoline 3.46a.

The procedure for isoxazoline *N*-oxide deoxygenation was adapted from the report of Marotta and coworkers.^{122b} A 500-mL round-bottomed flask was charged with isoxazoline *N*-oxide **3.44a** (15.7 g, 29.6 mmol), and this substrate was dried by azeotropic removal of benzene. Once dried, the starting material was dissolved in trimethyl phosphite (119 mL; CAUTION: Trimethyl phosphite is a highly malodorous, volatile substance – all operations up to and including the aqueous acid quench should be carried out in a well-ventilated fume hood), and the flask was sealed. The mixture was heated to 100 °C in a pre-heated oil bath for 20 h, at which point TLC analysis (30% ethyl acetate–hexanes, UV+PAA) indicated full consumption of starting material. The solution was cooled to 23 °C, and the cooled product solution was transferred to a 2-L round-bottomed flask containing 500 mL of diethyl ether. The product solution was cooled to 5 °C in an ice-water bath, and the chilled mixture was treated very carefully with 1N aqueous hydrochloric acid solution (100 mL, added in 1-mL portions over 30 minutes). Care was taken not to allow the internal temperature of the mixture rise above 15 °C during the acidification procedure. The acidified mixture was transferred to a separatory funnel, where the layers were separated. The organic layer was washed with 1N aqueous hydrochloric acid solution (2 × 75 mL). The combined aqueous washes were extracted with fresh portions of diethyl ether (2 × 75 mL). The combined organic phases were then washed sequentially with half-saturated aqueous sodium chloride solution (50 mL), and saturated aqueous sodium chloride solution (50 mL). The organic layer was then dried over sodium sulfate, the dried solution was filtered, and the filtrate was concentrated to afford crude product as a light yellow oil. The crude material was purified by flash-column

chromatography (700 g silica; eluting with 5% ethyl acetate–hexanes initially, grading to 25% ethyl acetate–hexanes) to provide the product as a light peach-colored, highly viscous oil (11.5 g, 75%).

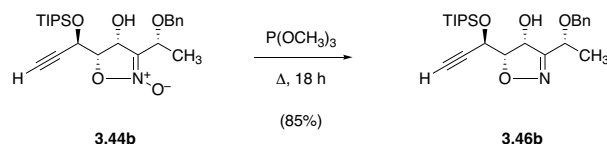
$R_f = 0.56$ (30% ethyl acetate–hexanes, UV+PAA).

$^1\text{H NMR}$ (600 MHz, CDCl_3): δ 7.79–7.76 (m, 4H), 7.50–7.46 (m, 2H), 7.44–7.41 (m, 4H), 7.37–7.34 (m, 4H), 7.32–7.29 (m, 1H), 5.28 (app t, $J = 8.3$ Hz, 1H), 4.88 (dd, $J = 4.0, 2.3$ Hz, 1H), 4.58 (q, $J = 6.8$ Hz, 1H), 4.56 (d, $J = 12.3$ Hz, 1H), 4.53 (d, $J = 12.0$ Hz, 1H), 4.23 (d, $J = 8.2, 4.0$ Hz, 1H), 4.15 (d, $J = 8.6$ Hz, 1H), 2.48 (d, $J = 2.3$ Hz, 1H), 1.59 (d, $J = 6.8$ Hz, 3H), 1.10 (s, 9H).

$^{13}\text{C NMR}$ (150 MHz, CDCl_3): δ 161.3, 137.5, 136.3, 136.2, 132.1, 131.3, 130.5, 130.2, 128.5, 128.0, 127.9, 127.7, 83.4, 80.1, 76.0, 71.2, 70.9, 62.6, 26.9, 20.0, 19.4.

FTIR (neat, cm^{-1}): 3471 (br), 2932 (m), 2858 (m), 1428 (m), 1086 (s), 907 (m), 608 (s).

HRMS (ESI+, m/z): $[\text{M}+\text{H}]^+$ calc'd for $\text{C}_{31}\text{H}_{35}\text{NO}_4\text{Si}$, 514.2408; found 514.2424.



Isoxazoline **3.46b**.

In a 2–5 mL glass microwave vial fitted with a magnetic stir bar, isoxazoline *N*-oxide **3.44b** (200 mg, 447 μmol , 1 equiv) was dissolved in trimethyl phosphite (1.79 mL). The vial was sealed before the mixture was heated to 100 $^{\circ}\text{C}$ in a pre-heated oil bath. After this mixture was stirred at this temperature for 18 h, TLC analysis (30% ethyl acetate–hexanes, UV+PAA) revealed that no starting material remained. The mixture was consequently cooled to 23 $^{\circ}\text{C}$ and was diluted with diethyl ether (50 mL). The diluted product solution was washed sequentially with aqueous hydrogen chloride solution (1N, 3 \times 15 mL), water (15 mL), and saturated aqueous sodium chloride solution (15 mL). The organic product solution was then dried over sodium sulfate, filtered, and concentrated to provide a yellow-tinged crusty solid residue. This material was purified by flash-column chromatography (12 g silica gel, eluting with hexanes initially, grading to 10% ethyl acetate–hexanes) to provide isoxazoline product as a light yellow, crystalline solid (164 mg, 85%).

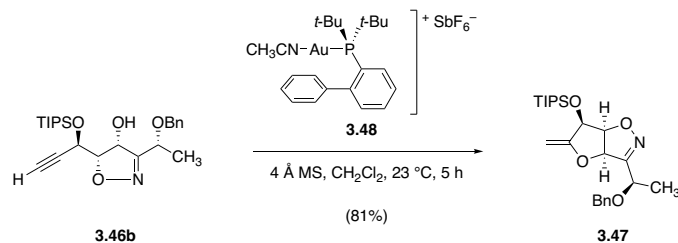
$R_f = 0.41$ (20% ethyl acetate–hexanes, KMnO_4).

$^1\text{H NMR}$ (600 MHz, CDCl_3) δ 7.34–7.33 (m, 4H), 7.30–7.27 (m, 1H), 5.29 (app t, $J = 8.5$ Hz, 1H), 5.05 (dd, $J = 3.5, 2.3$ Hz, 1H), 4.55–4.48 (m, 3H), 4.43 (d, $J = 8.7$ Hz, 1H), 4.26 (dd, $J = 8.4, 3.5$ Hz, 1H), 2.61 (d, $J = 2.3$ Hz, 1H), 1.55 (d, $J = 6.8$ Hz, 3H), 1.22–1.16 (m, 1H), 1.11–1.09 (m, 18H).

^{13}C NMR (151 MHz, CDCl_3) δ 161.2, 138.1, 128.6, 128.0, 127.9, 83.1, 80.7, 77.6, 75.6, 71.2, 70.9, 62.6, 20.0, 18.0, 12.1.

FTIR (neat, cm^{-1}): 2944 (m), 2867 (s), 1463 (m), 1096 (s), 883 (s)

HRMS (ESI+, m/z): $[\text{M}+\text{Na}]^+$ calc'd for $\text{C}_{24}\text{H}_{37}\text{NO}_4\text{Si}$, 454.2384; found 454.454.2392.



Exo-methylene compound **3.47**.

In a 4-mL glass vial fitted with a magnetic stir bar, a solution of alkyne **3.46b** (15 mg, 35 μmol , 1 equiv) in dichloromethane (700 μL) was treated with freshly activated, powered 4-Å molecular sieves. To this suspension was then added (acetonitrile)[(2-biphenyl)di-tert-butylphosphine]gold(I) hexafluoroantimonate (**3.48**, 2.7 mg, 3.5 μmol , 0.10 equiv) at 23 °C. After 5 h of stirring at this temperature, TLC analysis (30% ethyl acetate–hexanes) indicated that no starting material remained, and triethylamine (200 μL) was added to quench the Lewis-acid catalyst. The reaction mixture was then diluted with dichloromethane (10 mL), and the diluted mixture was filtered through a cotton plug in order to remove the molecular sieve powder. The filtrate was concentrated, and the residue was purified by flash-column chromatography (4 g silica gel, eluting with hexanes initially, grading to 10% ethyl acetate–hexanes) to provide the product as a colorless oil (12 mg, 81%).

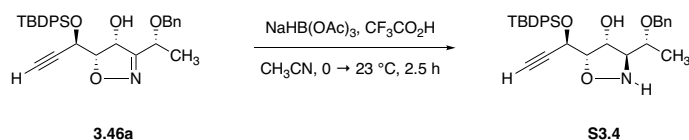
$R_f = 0.73$ (30% ethyl acetate–hexanes, KMnO_4).

^1H NMR (500 MHz, CDCl_3) δ 7.36–7.27 (m, 5H), 5.44 (d, $J = 5.9$ Hz, 1H), 4.85 (app dt, $J = 5.3$ Hz, 1H), 4.60–4.45 (m, 5H), 4.35 (app t, $J = 2.0$ Hz, 1H), 1.50 (d, $J = 6.7$ Hz, 3H), 1.23–1.16 (m, 3H), 1.14–1.12 (m, 18H).

^{13}C NMR (126 MHz, CDCl_3) δ 159.4, 157.8, 138.0, 128.6, 128.2, 127.9, 85.7, 85.2, 81.7, 73.0, 71.3, 70.3, 19.8, 18.0, 12.4.

FTIR (neat, cm^{-1}): 2943 (m), 2866 (s), 1686 (m), 1455 (m), 1168 (s), 1086 (m), 1006 (m), 883 (m).

HRMS (ESI+, m/z): $[\text{M}+\text{H}]^+$ calc'd for $\text{C}_{24}\text{H}_{37}\text{NO}_4\text{Si}$, 432.2565; found 432.2579



Isoxazolidine S3.4.

The procedure for isoxazoline reduction was adapted from the report of Bauder.^{130a} A mixture of isoxazoline **3.46a** (11.4 g, 22.1 mmol, 1 equiv) and sodium triacetoxyborohydride (23.4 g, 110 mmol, 5.00 equiv) was suspended in anhydrous acetonitrile (184 mL). The resulting milky-white suspension was cooled to 0 °C in an ice-water bath with constant stirring, and to the cooled suspension was added trifluoroacetic acid (170 mL, 2.21 mol, 100 equiv) over 10 min via an oven-dried pressure-equalizing addition funnel. Addition of trifluoroacetic acid caused the suspension to resolve into a colorless solution; following this addition, the ice-water bath was removed, and the reaction solution was allowed to warm to 23 °C. Progress was monitored by TLC (30% ethyl acetate–hexanes, UV+PAA), and after 2.5 h, starting material was fully consumed. The mixture was cooled to 0 °C, and was then transferred via cannula to a stirred, ice-cold mixture of dichloromethane (300 mL) and 2N aqueous sodium hydroxide solution (1.10 L, 2.21 mol). The resulting biphasic mixture was stirred rapidly for 10 min. Additional sodium hydroxide solution was added as necessary, until the aqueous phase attained pH > 8. The mixture was then transferred to a separatory funnel, and the layers were separated. The aqueous layer was extracted with dichloromethane (3 × 300 mL), and the combined organic extracts were washed with brine (300 mL). The washed organic layer was dried over sodium sulfate, the dried solution was filtered, and the filtrate was concentrated to afford crude isoxazolidine product as a colorless oil. This material was used in the next step without further purification.

For characterization purposes, a small quantity (ca. 25 mg) of crude residue was purified by HPLC (eluting with 0.1% trifluoroacetic acid–25% acetonitrile–water, grading to 0.1%

trifluoroacetic acid–95% acetonitrile–water over 45 min, with a flow rate of 15 mL/min; monitored by UV absorbance at 254 nm; product $R_t = 33.5$ min). The trifluoroacetic acid salt thus obtained (**S3.4** • $\text{CF}_3\text{CO}_2\text{H}$) exhibited the following spectral properties:

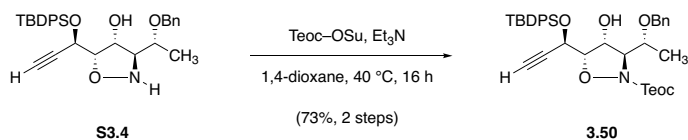
^1H NMR (600 MHz, CDCl_3) δ 7.76–7.69 (m, 4H), 7.48–7.43 (m, 2H), 7.42–7.28 (m, 9H), 4.91 (dd, $J = 5.1, 2.8$ Hz, 1H), 4.74 (dd, $J = 4.9, 2.2$ Hz, 1H), 4.66 (d, $J = 11.5$ Hz, 1H), 4.40 (d, $J = 11.6$ Hz, 1H), 3.98 (app t, $J = 5.0$ Hz, 1H), 3.81 (m, 1H), 3.51 (app t, $J = 3.3$ Hz, 1H), 2.40 (d, $J = 2.2$ Hz, 1H), 1.39 (d, $J = 6.2$ Hz, 3H), 1.09 (s, 9H).

^{13}C NMR (126 MHz, CDCl_3): δ 137.6, 136.2, 136.1, 132.2, 131.7, 130.5, 130.3, 128.8, 128.2, 128.1, 128.0, 127.7, 86.1, 80.4, 76.1, 75.4, 73.9, 70.9, 70.7, 62.1, 26.9, 19.4, 16.7.

Trifluoroacetate carbons were not resolved due to ^{19}F nuclear coupling.

FTIR (neat, cm^{-1}): 3302 (br), 2932 (m), 2859 (m), 1671 (s), 1428 (m), 1199 (m), 1113 (s), 701 (s).

HRMS (ESI+, m/z): $[\text{M}+\text{Na}]^+$ calc'd for $\text{C}_{31}\text{H}_{37}\text{NO}_4\text{Si}$, 538.2384; found 538.2385.



Alkynol 3.50.

A 200-mL round-bottomed flask was charged with isoxazolidine **S3.4** (crude product from the preceding directed reduction step, theoretically 22.1 mmol). The starting material was dissolved in 1,4-dioxane (55 mL) and to the resulting solution, triethylamine (15.4 mL, 110 mmol, 5.00 equiv) and *N*-[2-(trimethylsilyl)ethoxycarbonyloxy]succinimide (Teoc-OSu, 8.59 g, 33.1 mmol, 1.50 equiv) were added sequentially. The reaction mixture was heated to 40 °C, and consumption of starting material was monitored by LCMS. After 16 h, the reaction was judged to be complete. The reaction mixture was then diluted in 450 mL of ethyl acetate, and the diluted product solution was washed with saturated aqueous ammonium chloride solution (3 × 50 mL). The combined aqueous washes were extracted with a portion of fresh ethyl acetate (100 mL), and the combined organic layers were then washed with saturated aqueous sodium chloride solution (50 mL). The washed organic product solution was dried over sodium sulfate, the dried solution was filtered, and the filtrate was concentrated to give a viscous orange oil. This material was purified by flash-column chromatography (1.00 kg silica gel, eluting with 5% ethyl acetate–hexanes initially, grading to 20% ethyl acetate–hexanes) to provide the product as a highly viscous, colorless oil (10.6 g, 73%, 2 steps).

$R_f = 0.43$ (20% ethyl acetate–hexanes, UV+KMnO₄).

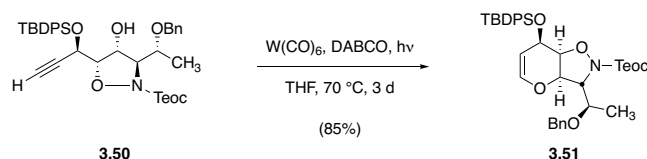
¹H NMR (600 MHz, CDCl₃): δ 7.78–7.74 (m, 4H), 7.48–7.44 (m, 2H), 7.42–7.36 (m, 4H), 7.35–7.27 (m, 5H), 4.90 (app t, *J* = 3.8 Hz, 1H), 4.79 (dd, *J* = 6.2, 2.2 Hz, 1H), 4.67 (d, *J* = 11.8

Hz, 1H), 4.48 (d, J = 11.8 Hz, 1H), 4.25–4.12 (m, 4H), 3.65 (app p, J = 6.3 Hz, 1H), 3.31 (d, J = 3.9 Hz, 1H), 2.36 (d, J = 2.2 Hz, 1H), 1.33 (d, J = 6.2 Hz, 3H), 1.10 (s, 9H), 1.05–0.94 (m, 2H), 0.04 (s, 9H).

^{13}C NMR (125 MHz, CDCl_3): δ 158.2, 138.3, 136.3, 136.0, 130.3, 130.2, 128.5, 127.9 (2 \times C), 127.8, 127.6, 83.9, 81.2, 75.7, 74.7, 74.1, 73.5, 71.4, 64.9, 62.1, 26.9, 19.4, 17.7, 17.0, 1.4.

FTIR (neat, cm^{-1}): 3463 (br), 2954 (m), 2858 (m), 1702 (m), 1325 (m), 1112 (s), 1064 (s), 838 (s), 700 (s).

HRMS (ESI+, m/z): $[\text{M}+\text{H}]^+$ calc'd for $\text{C}_{37}\text{H}_{49}\text{NO}_6\text{Si}_2$, 660.3171; found 660.3161.



Glycal **3.51**.

The procedure for tungsten-catalyzed cycloisomerization was adapted from the reports of McDonald and Koo.^{126b} In a 200-mL round-bottomed flask, alkynol **3.50** (4.17 g, 6.32 mmol, 1 equiv) was dried by azeotropic removal of benzene under vacuum. The flask was back-filled with argon, and tungsten hexacarbonyl (556 mg, 1.58 mmol, 0.250 equiv),¹⁴⁸ 1,4-diazabicyclo[2.2.2]octane (DABCO, 1.42 g, 12.6 mmol, 2.00 equiv), and degassed, anhydrous tetrahydrofuran (63.2 mL) were then added sequentially (CAUTION: Tungsten hexacarbonyl is a volatile source of metal and of carbon monoxide. Manipulations of this reagent should be conducted within a well-ventilated fume hood.). The flask was fitted with an oven-dried reflux condenser, and the apparatus was transferred to a pre-heated oil bath ($70\text{ }^\circ\text{C}$) positioned inside a photochemistry safety cabinet. A positive pressure of dry argon was maintained via tubing connected to an argon-filled balloon placed outside of the lightbox. The reaction mixture was refluxed with constant UV irradiation from an adjacent 200-Watt mercury-vapor bulb filtered through a water-cooled Pyrex glass jacket (CAUTION: Exposure to high-intensity UV light can cause irreversible vision loss – never open the safety cabinet when the UV lamp is on.). Progress was monitored by TLC (20% ethyl acetate–hexanes, UV+ $KMnO_4$). After 3 d, full consumption of the alkynol substrate was achieved, and the crude product mixture was concentrated under a stream of dry nitrogen. The canary-yellow residue was purified by flash-column chromatography (eluting

¹⁴⁸ Tungsten hexacarbonyl purchased from Strem (99%, <0.3% molybdenum) gave moderately higher yields than precatalyst purchased from Sigma-Aldrich (97%), likely due to the presence of molybdenum hexacarbonyl as a major impurity in the latter sample.

with hexanes initially, grading to 20% ethyl acetate–hexanes) to provide the product as a viscous, colorless oil (3.53 g, 85%).

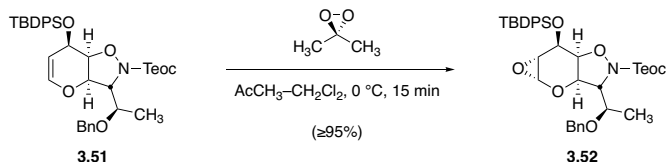
$R_f = 0.65$ (20% ethyl acetate–hexanes, UV+KMnO₄)

¹H NMR (500 MHz, CDCl₃): 7.77–7.74 (m, 2H), 7.70–7.67 (m, 2H), 7.44–7.38 (m, 2H), 7.37–7.31 (m, 4H), 7.27–7.23 (m, 3H), 7.22–7.19 (m, 2H), 6.10 (dd, $J = 6.4, 2.3$ Hz, 1H), 4.67 (app dt, $J = 6.5, 1.9$ Hz, 1H), 4.62 (d, $J = 2.9$ Hz, 1H), 4.56–4.51 (m, 2H), 4.36 (d, $J = 11.7$ Hz, 1H), 4.36–4.31 (m, 1H), 4.24 (td, $J = 10.4, 6.9$ Hz, 1H), 4.20 (app dt, $J = 4.6, 2.3$ Hz, 1H), 4.10 (d, $J = 5.1$ Hz, 1H), 3.72 (app p, $J = 6.2$ Hz, 1H), 1.27 (d, $J = 6.4$ Hz, 3H), 1.08 (s, 9H), 0.07 (s, 9H).

¹³C NMR (125 MHz, CDCl₃): δ 157.1, 141.8, 138.2, 136.0 (2 \times C), 133.8, 133.6, 129.9 (2 \times C), 128.5, 127.9, 127.8 (3 \times C), 102.0, 77.5, 77.3, 73.6, 72.4, 71.9, 64.8, 63.0, 27.0, 19.4, 17.8, 17.2, 1.2.

FTIR (neat, cm⁻¹): 2954 (m), 2858 (m), 1703 (m), 1328 (m), 1112 (s), 1066 (s), 838 (m), 702 (s).

HRMS (ESI+, m/z): [M+H]⁺ calc'd for C₃₇H₄₉NO₆Si₂, 660.3171; found 660.3164.



Brigl's anhydride **3.52**.

A solution of dimethyldioxirane in acetone was prepared, and its concentration was assayed according to the procedure of Murray and Singh.¹³¹ A solution of glycal **3.51** (1.45 g, 2.20 μmol, 1 equiv) in dichloromethane (22.0 mL) was cooled to 0 °C, whereupon dimethyldioxirane solution (0.0997 M, 26.4 mL, 2.64 μmol, 1.20 equiv) was added dropwise over 1 min. The reaction mixture was stirred at 0 °C for 15 min, at which point TLC analysis (20% ethyl acetate–hexanes, UV+PAA) indicated full consumption of starting material. The mixture was then concentrated under a stream of dry argon, and the residue was dried by azeotropic removal of benzene to afford glycal epoxide as a colorless oil that was suitable for use without further purification (quantitative yield, ≥95% purity by NMR).

$R_f = 0.56$ (NH₂ silica gel,¹⁴⁹ 2% methanol–20% ethyl acetate–hexanes, UV+CAM).

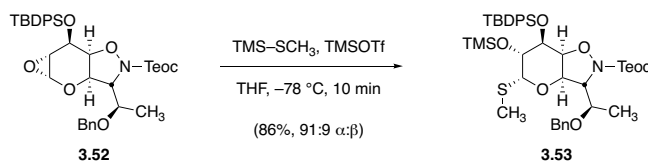
¹H NMR (500 MHz, C₆D₆) δ 7.89–7.83 (m, 2H), 7.77–7.71 (m, 2H), 7.21–7.09 (m, 7H), 7.08–7.00 (m, 4H), 4.66 (dd, $J = 2.6, 1.0$ Hz, 1H), 4.42 (d, $J = 5.1$ Hz, 1H), 4.34–4.21 (m, 4H), 4.21 (d, $J = 11.8$ Hz, 1H), 4.12–4.08 (m, 1H), 4.05 (d, $J = 11.8$ Hz, 1H), 3.56 (app p, $J = 6.2$ Hz, 1H), 2.97–2.92 (m, 1H), 1.19 (d, $J = 0.7$ Hz, 9H), 0.95 (d, $J = 6.4$ Hz, 3H), 0.91 (ddd, $J = 9.4, 6.7, 3.9$ Hz, 2H), –0.11 (d, $J = 0.7$ Hz, 9H).

¹⁴⁹ Note: The acid-sensitive product is unstable toward chromatography using standard silica gel.

^{13}C NMR (125 MHz, C_6D_6) δ 157.95, 138.78, 136.31, 136.13, 133.68, 133.47, 130.36, 130.34, 128.59, 128.35, 128.31, 128.25, 128.20, 128.06, 127.87, 127.75, 77.12, 74.25, 74.12, 73.79, 73.33, 71.60, 67.08, 64.65, 51.67, 27.12, 19.63, 17.74, 16.79, -1.45.

FTIR (neat, cm^{-1}): 2953 (m), 2858 (m), 1703 (m), 1249 (m), 1112 (s), 837 (s), 701 (s).

HRMS (ESI+, m/z): $[\text{M}+\text{H}]^+$ calc'd for $\text{C}_{37}\text{H}_{49}\text{NO}_7\text{Si}_2$, 676.3120; found 676.3118.



Thioglycoside **3.53**.

A 10-mL round-bottomed flask was charged with a magnetic stir bar and glycol epoxide **3.52** (103 mg, 152 μmol, 1 equiv). This starting material was dried by azeotropic removal of benzene before it was dissolved in tetrahydrofuran (760 μL). The solution was chilled to -78 °C before trimethyl(methylthio)silane (65.7 μL, 456 μmol, 3.00 equiv) was added. Trimethylsilyl trifluoromethanesulfonate (5.49 μL, 30.4 μmol, 0.200 equiv) was then added dropwise at -78 °C, and stirring was maintained at that temperature. Progress was monitored by TLC (NH₂ silica gel, 2% methanol–20% ethyl acetate–hexanes, UV+CAM), and after 10 min, the reaction was judged to be complete. The mixture was neutralized with the addition of 5% v/v triethylamine–dichloromethane (500 μL), and the quenched reaction mixture was concentrated in vacuo. Crude ¹H-NMR analysis revealed a 91:9 mixture of anomers; this mixture was subjected to flash-column chromatography (12 g silica gel, eluting with hexanes initially, grading to 20% ethyl acetate–hexanes) to provide the product as a colorless oil (105 mg, 86%).

R_f = 0.40 (20% ethyl acetate–hexanes, UV+PMA).

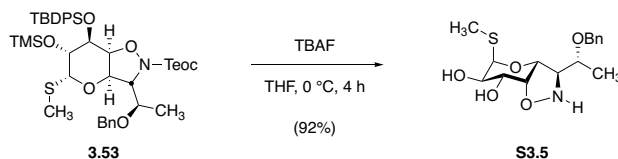
¹H NMR (500 MHz, CDCl₃) δ 7.88–7.86 (m, 2H), 7.82–7.80 (m, 2H), 7.44–7.34 (m, 6H), 7.27–7.22 (m, 3 H), 7.13–7.11 (m, 2H), 5.08 (d, *J* = 4.9 Hz, 1H), 4.52 (d, *J* = 2.2 Hz, 1H), 4.42 (d, *J* = 11.8 Hz, 1H), 4.41 (dd, *J* = 9.1, 5.1 Hz), 4.33 (app t, *J* = 8.5 Hz, 2H), 4.19 (dd, *J* = 9.5, 3.8 Hz, 1H), 4.17 (d, *J* = 11.6 Hz, 1H), 4.02 (d, *J* = 6.6 Hz, 1H), 3.70 (dd, *J* = 3.8, 2.3

Hz, 1H), 3.31 (app p, $J = 6.2$ Hz, 1H), 1.97 (s, 3H), 1.21 (d, $J = 6.2$ Hz, 3H), 1.11 (s, 9H), 0.20 (s, 9H), 0.11 (s, 9H).

^{13}C NMR (126 MHz, CDCl_3) δ 158.2, 138.0, 136.2, 136.1, 134.5, 133.3, 129.8, 129.6, 128.4, 127.7 ($2 \times \text{C}$), 127.6, 127.5, 87.3, 79.6, 73.3, 73.1, 71.6 ($2 \times \text{C}$), 70.2, 69.8, 64.7, 27.1, 19.4, 17.8, 17.2, 12.7, 0.4, -1.3.

IR (neat, cm^{-1}): 1703 (m), 1325 (m), 1105 (m), 1063 (m), 837 (s), 731 (s), 699 (s).

HRMS (ESI+, m/z): $[\text{M}+\text{Na}]^+$ calc'd for $\text{C}_{41}\text{H}_{61}\text{NO}_7\text{SSi}_3$, 818.3369; found 818.3356.



Isoxazolidine diol **S3.5**.

To a stirred solution of thioglycoside **3.53** (104 mg, 131 μmol , 1 equiv) in tetrahydrofuran (1.87 mL) was added tetrabutylammonium fluoride solution (1.0 M in tetrahydrofuran, 650 μL , 650 μmol , 5.0 equiv) at 0 °C. Progress was monitored by flow-injection analysis mass spectrometry, which showed rapid (<20 min) cleavage of the trimethylsilyl and (trimethylsilyl)ethoxycarbonyl groups; the *tert*-butyldiphenylsilyl group was removed more slowly. After 4 h at 0 °C, the reaction was judged to be complete, and the mixture was quenched with the addition of saturated aqueous sodium bicarbonate solution (10 mL). The resulting mixture was extracted with ethyl acetate (3×10 mL), and the combined extracts were washed with saturated aqueous sodium chloride solution (10 mL). Before it was discarded, the sodium chloride solution was extracted with fresh portions of ethyl acetate (2×5 mL), and the combined organic extracts were dried over sodium sulfate. The dried product solution was filtered, and the filtrate was concentrated to give a colorless oil. The crude isoxazolidine was purified by flash-column chromatography (10 g silica gel, eluting initially with 0.2% ammonium hydroxide–2% methanol–dichloromethane, grading to 0.3% ammonium hydroxide–3% methanol–dichloromethane in one step) to provide the product as a white solid (40.9 mg, 92%).

Owing to nitrogen inversion that occurred on the NMR time scale, the free-base form of this isoxazolidine featured ^1H -NMR peak broadening, as indicated below. For characterization purposes, a portion of this free-base (ca. 12 mg) was purified by HPLC-MS on a Waters SunFire prep C_{18} column (5 μm , 250×19 mm; eluting with 0.1% trifluoroacetic acid–10% acetonitrile–

water initially, grading to 0.1% trifluoroacetic acid–80% acetonitrile–water over 30 min, with a flow rate of 15 mL/min; monitored by UV absorbance at 254 nm and by ESI+ selected ion monitoring [$m/z = 342$]; $R_t = 14.8$ min) to provide the product as the corresponding hydrotrifluoroacetate salt, which featured sharper NMR peaks.

$R_f = 0.31$ (free base, 1% ammonium hydroxide–10% methanol–dichloromethane, UV+PAA).

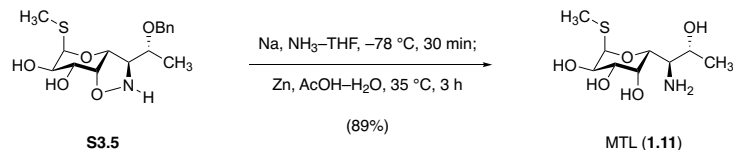
^1H NMR (free base, 600 MHz, CDCl_3) δ 7.37–7.35 (m, 2H), 7.32–7.28 (m, 2H), 5.24 (d, $J = 4.9$ Hz, 1H), 4.87 (br, 1H), 4.66 (d, $J = 11.7$ Hz, 1H), 4.35 (d, $J = 11.6$ Hz, 1H), 4.11 (br, 1H), 3.95 (br, 1H), 3.91 (dd, $J = 4.4, 2.8$ Hz, 1H), 3.55 (br, 1H), 3.36 (br, 1H), 3.17 (br, 1H), 3.03 (br, 1H), 2.15 (s, 3H), 1.32 (d, $J = 6.2$ Hz, 3H).

^1H NMR (hydrotrifluoroacetate salt, 500 MHz, CD_3OD) δ 7.38–7.34 (m, 4H), 7.31–7.29 (m, 1H), 5.26 (d, $J = 5.0$ Hz, 1H), 5.06 (d, $J = 2.2$ Hz, 1H), 4.69 (d, $J = 11.1$ Hz, 1H), 4.56 (dd, $J = 4.1, 2.3$ Hz, 1H), 4.49 (d, $J = 11.1$ Hz, 1H), 4.09 (dd, $J = 10.0, 5.0$ Hz, 1H), 3.99–3.97 (m, 2H), 3.93 (dd, $J = 9.9, 4.0$ Hz, 1H), 2.12 (s, 3H), 1.39 (d, $J = 5.8$ Hz, 3H).

^{13}C NMR (hydrotrifluoroacetate salt, 126 MHz, CD_3OD) δ 139.1, 129.5, 128.9 ($2 \times \text{C}$), 88.8, 85.6, 75.0, 73.1, 72.8, 72.1, 69.0, 68.7, 16.6, 13.1.

FTIR (neat, cm^{-1}): 3317 (br, w), 1668 (s), 1433 (w), 1197 (s), 1142 (s), 1093 (s), 699 (m).

HRMS (ESI+, m/z): $[\text{M}+\text{H}]^+$ calc'd for $\text{C}_{16}\text{H}_{23}\text{NO}_5\text{S}$, 342.1370; found 342.1365.



Completion of the synthesis of methylthiolincosamine (1.11).

A flame-dried 2–5 mL glass microwave reaction vial was fitted with a magnetic stir bar and was sealed with a rubber septum. The septum was pierced with a 20-gauge needle to supply dry argon gas, and a second needle was used to vent the apparatus; under a steady stream of argon to exclude air and moisture, the empty apparatus was chilled to $-78\text{ }^\circ\text{C}$. The chilled flask was then slowly charged with anhydrous ammonia gas (supplied via a 22-gauge needle). After approximately 2 mL of liquid ammonia was condensed in this fashion, the needle supplying ammonia gas was removed, and a small piece of sodium metal (approximately 1 mm^3) was added. The mixture attained a deep blue color, and was stirred at $-78\text{ }^\circ\text{C}$ for 5 min. After this time, a solution of isoxazolidine **S3.5** (40.0 mg, $117\text{ }\mu\text{mol}$, 1 equiv) in tetrahydrofuran ($500\text{ }\mu\text{L}$) was introduced dropwise via syringe. During this addition, the blue coloration of the reaction mixture disappeared, signaling that the initial portion of sodium metal was fully consumed; additional 1-mm^3 pieces of sodium were added until a deep-blue color persisted. The mixture was then stirred at $-78\text{ }^\circ\text{C}$ for 30 min, until LCMS analysis indicated that *O*-debenzylation was complete (*N*-*O* bond cleavage stalls in the course of this reaction, leaving a roughly 50:50 mixture of fully reduced product and *O*-debenzylated isoxazolidine intermediate even after prolonged exposure to dissolving-metal conditions). Solid ammonium chloride was added portionwise in order to quench excess reductant, until a colorless mixture was obtained; the apparatus was then allowed to warm to $23\text{ }^\circ\text{C}$ in order to allow the ammonia co-solvent to evaporate. The mixture was then dried in vacuo to provide a white solid residue.

This residue was re-dissolved in 50% v/v acetic acid–water (1.0 mL), zinc powder (30.6 mg, 469 μ mol, 4.00 equiv) was added, and the mixture was heated to 35 °C with stirring, in order to quantitate *N*–*O* bond cleavage of intermediate isoxazolidine compound. After 3 h, LCMS analysis revealed that no isoxazolidine remained, and the mixture was filtered through a pad of Celite in order to remove any residual zinc metal. The filtrate was concentrated, and residual acetic acid and water were removed by repeated azeotropic concentration from 50% v/v methanol–toluene. The dried residue, containing the aminotetraol as its hydroacetate salt, along with zinc acetate and ammonium acetate, was dissolved in methanol (5.0 mL), and Amberlyst A26 ion-exchange resin (hydroxide form, 1.0 g) was added. The mixture was stirred at 23 °C for 1 h before the ion-exchange beads were removed by filtration. The filtrate was concentrated to provide crude product in its free-base form; and this residue was purified by flash-column chromatography (4.0 g silica gel, eluting with 1% ammonium hydroxide–10% methanol–dichloromethane initially, grading to 10% ammonium hydroxide–40% methanol–dichloromethane) to provide the product as a brilliant white solid (26.4 mg, 89%).

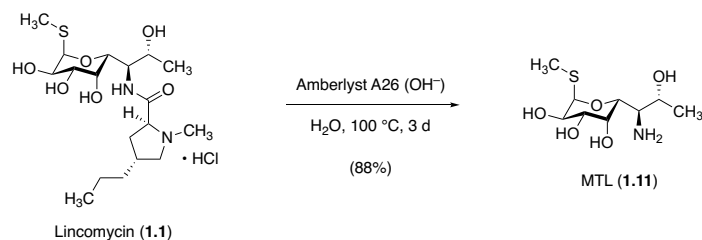
$R_f = 0.42$ (10% ammonium hydroxide–40% methanol–dichloromethane, PAA).

$^1\text{H NMR}$ (500 MHz, D_2O) δ 5.17 (d, $J = 5.8$ Hz, 1H), 3.97–3.93 (m, 3H), 3.82 (d, $J = 9.6$ Hz, 1H), 3.50 (dd, $J = 10.4, 3.3$ Hz, 1H), 3.01 (dd, $J = 9.6, 3.6$ Hz, 1H), 1.97 (s, 3H), 0.99 (d, $J = 6.4$ Hz, 3H).

$^{13}\text{C NMR}$ (126 MHz, D_2O) δ 88.0, 71.3, 70.4, 68.3, 67.7, 67.1, 53.6, 14.2, 12.9.

FTIR (neat, cm^{-1}): 3280 (br), 2904 (m), 1385 (m), 1076 (m), 1041 (s), 866 (m).

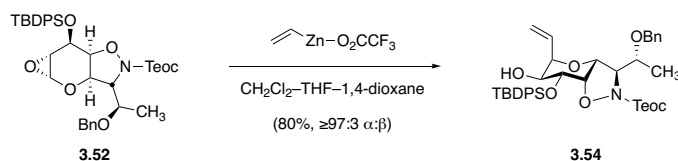
HRMS (ESI+, m/z): $[\text{M}+\text{H}]^+$ calc'd for $\text{C}_9\text{H}_{19}\text{NO}_5\text{S}$, 254.1057; found 254.1055.



Semisynthetic preparation of methylthiolincosamine (**1.11**).

Based on the original report of Schroeder, Banniser, and Hoeksema,^{9d} an improved procedure for the preparation of methylthiolincosamine (**1.11**) from lincomycin (**1.1**) avoiding the use of hydrazine, a hazardous reagent, was developed. In a 250-mL round-bottomed flask, lincomycin hydrochloride (1.58 g, 3.57 mmol, 1 equiv), Amberlyst A26 ion-exchange resin (hydroxide form, 15.8 g), and water (71.3 mL) were combined. The flask was fitted with a reflux condenser, and the mixture was heated to reflux for 3 d, at which point LCMS analysis indicated that hydrolysis was complete. The mixture was allowed to cool to ambient temperature before the ion-exchange beads were removed by filtration. The filtrate was concentrated directly to afford pure methylthiolincosamine (MTL, **1.11**) free base as a brilliant white solid (795 mg, 88%).

The TLC R_f , $^1\text{H-NMR}$, $^{13}\text{C-NMR}$, and HRMS data were identical to those of the synthetic sample prepared by the route described above.



Vinyl glycoside **3.54**.

An oven-dried 100-mL round-bottom flask was charged with a stir bar and divinylzinc solution (0.15 M solution in tetrahydrofuran–dioxane, 21.7 mL, 3.3 mmol, 2.3 equiv; prepared according to the method of Brubaker and Myers;¹⁵⁰ titrated according to the method of Krasovskiy and Knochel¹⁵¹). This solution was chilled to 0 °C, and trifluoroacetic acid (250 μL , 3.3 mmol, 2.3 equiv) was then added dropwise. The resulting solution was stirred for 30 min at 0 °C prior to use.

In a separate 100-mL round-bottom flask, epoxide **3.52** (954 mg, 1.41 mmol, 1 equiv) was dried by azeotropic removal of benzene. The dried epoxide was dissolved in anhydrous dichloromethane (14.1 mL), and the resulting solution was chilled to 0 °C. This epoxide solution was then transferred by cannula to the flask containing freshly prepared vinylzinc trifluoroacetate, also at 0 °C. The resulting solution was stirred at 0 °C for 4 h, at which point TLC analysis (NH_2 silica gel, 20% ethyl acetate–hexanes + 2% methanol, UV+CAM) indicated full consumption of epoxide starting material. The reaction was quenched with the addition of 35 mL of saturated aqueous ammonium chloride solution, and the resulting biphasic mixture was stirred for 10 min. The layers were then separated, and the aqueous phase was extracted with dichloromethane (3 \times 20 mL). The combined organic extracts were washed with saturated aqueous sodium chloride solution, and the washed organic product solution was dried over sodium sulfate. The dried solution was filtered, and the filtrate was concentrated to afford crude product as a faint yellow

¹⁵⁰ Brubaker, J. D.; Myers, A. G. *Org. Lett.* **2007**, *9*, 3523–3525.

¹⁵¹ Krasovskiy, A.; Knochel, P. *Synthesis* **2006**, 890–891.

oil. The product was purified by flash-column chromatography (40 g silica, eluting with 5% ethyl acetate–hexanes initially, grading to 20% ethyl acetate–hexanes) to provide the product a colorless oil (846 mg, 1.20 mmol, 85%).

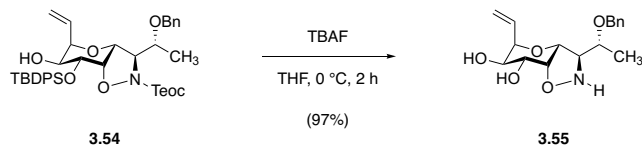
$R_f = 0.47$ (20% ethyl acetate–hexanes, UV+KMnO₄).

¹H NMR (600 MHz, C₆D₆) δ 7.96–7.94 (m, 2H), 7.83–7.79 (m, 2H), 7.22–7.19 (m, 2H), 7.18–7.16 (m, 1H), 7.15–7.11 (m, 4H), 7.07–7.00 (m, 4H). 5.74 (ddd, $J = 17.6, 11.0, 4.1$ Hz, 1H), 5.20 (app dt, $J = 17.6, 2.1$ Hz, 1H), 4.95 (app dt, $J = 11.1, 2.1$ Hz, 1H), 4.57 (app dt, $J = 9.7, 5.0$ Hz, 1H), 4.53 (d, $J = 2.4$ Hz, 1H), 4.50 (app ddt, $J = 6.1, 4.3, 2.2$ Hz, 1H), 4.40 (d, $J = 5.4$ Hz, 1H), 4.33 (app td, $J = 10.3, 6.5$ Hz, 1H), 4.30–4.25 (m, 2H), 4.23 (app t, $J = 3.0$ Hz, 1H), 4.09 (d, $J = 11.8$ Hz, 1H), 4.01 (dd, $J = 9.7, 3.6$ Hz, 1H), 3.60 (app qn, $J = 6.2$ Hz, 1H), 1.71 (d, $J = 4.2$ Hz, 1H), 1.18 (s, 9H), 1.07 (d, $J = 6.3$ Hz, 3H), 0.97–0.91 (m, 2H), –0.09 (s, 9H).

¹³C NMR (126 MHz, CDCl₃) δ 157.9, 138.1, 136.2, 135.8, 133.5, 133.3, 130.8, 130.1, 128.5, 128.0, 127.9, 127.8, 127.8, 119.2, 80.2, 76.3, 74.6, 73.2, 72.5, 71.7, 71.1, 68.7, 64.8, 27.1, 19.5, 17.7, 17.3, –1.2. Overlap of a single pair of phenyl carbon resonances accounts for the observation of only 11 unique phenyl-derived signals.

FTIR (neat, cm⁻¹): 3473 (br), 2953 (m), 2931 (m), 2895 (m), 2858 (m), 1702 (m), 1427 (m), 1250 (m), 1112 (s), 1082 (s), 838 (m), 702 (s).

HRMS (ESI+, m/z): [M+H]⁺ calc'd for C₃₉H₅₃NO₇Si₂, 704.3433; found 704.3418



Isoxazolidine diol **3.55**.

In a 10-mL round-bottomed flask, isoxazolidine **3.54** (150 mg, 213 μmol , 1 equiv) was dissolved in tetrahydrofuran (2.13 mL). The resulting solution was chilled to 0 °C before it was treated with tetra-*n*-butylammonium fluoride solution (1.0 M in tetrahydrofuran, 640 μL , 3.0 equiv). While cleavage of the 2-(trimethylsilyl)ethyl carbamoyl protecting group is rapid, the *tert*-butyldiphenylsilyl ether group is less labile – after 2 h of stirring at 0 °C, LCMS analysis showed that global desilylation was complete, and the reaction mixture was treated with saturated aqueous sodium bicarbonate solution (2 mL) and saturated aqueous sodium chloride solution (5 mL). This mixture was extracted with dichloromethane (3×10 mL), and the combined extracts were dried directly over sodium sulfate. The dried solution was then filtered, the filtrate was concentrated, and the crude residue was purified by flash-column chromatography (12 g silica gel, eluting with dichloromethane initially, grading to 10% methanol–dichloromethane) to furnish isoxazolidine diol product as a viscous, colorless oil (66.4 mg, 97%).

In its free-base form, this product displayed substantial ^1H - and ^{13}C -NMR peak broadening, likely owing to a nitrogen inversion process occurring on the NMR timescale. Thus, for NMR characterization purposes, the product was converted to its hydrochloride-salt form by treating an ice-cold solution of free base (61 mg, 190 μmol , 1 equiv) in methanol (5.0 mL) with hydrogen chloride solution (4.0 M in 1,4-dioxane, 190 μL , 760 μmol , 4.0 equiv). The mixture was then concentrated *in vacuo* to provide the hydrochloride salt **3.55** • HCl as a white solid.

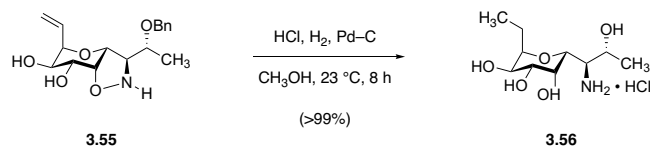
$R_f = 0.40$ (free base, 10% methanol–dichloromethane, I_2).

^1H NMR (hydrochloride salt, 500 MHz, CD_3OD) δ 7.39–7.33 (m, 4H), 7.30–7.27 (m, 1H), 6.09 (ddd, $J = 17.4, 10.8, 5.2$ Hz, 1H), 5.43 (app dt, $J = 17.4, 1.9$ Hz, 1H), 5.40 (app dt, $J = 10.1, 1.8$ Hz, 1H), 5.01 (dd, $J = 3.4, 2.1$ Hz, 1H), 4.71–4.70 (m, 1H), 4.67 (d, $J = 11.1$ Hz, 1H), 4.57–4.55 (m, 1H), 4.53 (d, $J = 11.1$ Hz, 1H), 4.14 (app t, $J = 2.5$ Hz, 1H), 4.09 (qd, $J = 6.2, 3.0$ Hz, 1H), 3.96–3.95 (m, 2H), 1.40 (d, $J = 6.3$ Hz, 3H).

^{13}C NMR (hydrochloride salt, 126 MHz, CD_3OD) δ 139.1, 132.7, 129.4, 128.8 ($2 \times \text{C}$), 119.8, 84.1, 76.8, 75.3, 72.5, 72.0, 71.4, 69.2, 68.5, 16.1.

FTIR (hydrochloride salt, neat, cm^{-1}): 3390 (br), 2895 (m), 1454 (m), 1087 (s), 698 (s).

HRMS (ESI+, m/z): $[\text{M}+\text{H}]^+$ calc'd for $\text{C}_{17}\text{H}_{23}\text{NO}_5$, 322.1649; found 322.1658.



Aminotetraol **3.56**.

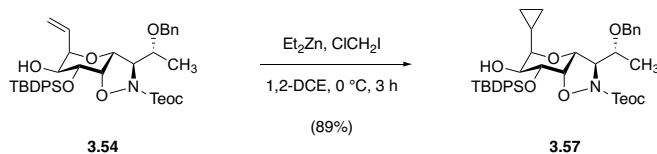
In a 10-mL round-bottomed flask, isoxazolidine **3.55** (67.6 mg, 0.189 mmol, 1 equiv) was dissolved in methanol (1.00 mL), and the solution was treated with hydrogen chloride solution (4.0 M in 1,4-dioxane, 190 μL , 4.0 equiv). The mixture was then concentrated to dryness to provide the hydrochloride salt of the starting material; this salt was dissolved in methanol (1.89 mL), and the solution was treated with palladium on carbon (10% w/w, 20 mg). The headspace of the flask was replaced with hydrogen gas, and the black suspension was stirred at 23 $^\circ\text{C}$ for 8 h, whereupon LCMS analysis revealed that olefin saturation, isoxazolidine hydrogenation, and debenzoylation were all complete. The mixture was filtered through a pad of Celite to remove the catalyst, and the filter cake was washed with fresh methanol ($3 \times 1\text{ mL}$). The filtrate was concentrated to afford **3.56** $\cdot\text{HCl}$ as a white foaming solid (54.3 mg, 106%).

^1H NMR (600 MHz, CD_3OD) δ 4.20 (app t, $J = 2.9\text{ Hz}$, 1H), 4.13 (app p, $J = 6.2\text{ Hz}$, 1H), 3.94–3.91 (m, 2H), 3.87 (td, $J = 7.0, 4.6\text{ Hz}$, 1H), 3.77 (dd, $J = 8.2, 3.1\text{ Hz}$, 1H), 3.63 (app t, $J = 6.4\text{ Hz}$, 1H), 1.64 (app p, $J = 7.3\text{ Hz}$, 2H), 1.29 (d, $J = 6.4\text{ Hz}$, 3H), 0.96 (t, $J = 7.3\text{ Hz}$, 3H).

^{13}C NMR (126 MHz, CD_3OD) δ 77.2, 71.5, 69.9, 69.7, 68.7, 65.5, 58.5, 19.7, 18.7, 10.9.

FTIR (neat, cm^{-1}): 3333 (br), 2968 (m), 2936 (m), 1503 (m), 1070 (s).

HRMS (ESI+, m/z): $[\text{M}+\text{H}]^+$ calc'd for $\text{C}_{10}\text{H}_{21}\text{NO}_5$, 236.1492; found 236.1488.



Cyclopropyl glycoside **3.57**.

Cyclopropanation was performed using the method described by Denmark and Edwards.¹⁵² In a 2–5 mL glass microwave vial fitted with a magnetic stir bar, a solution of diethylzinc (43.9 μL , 0.426 mmol, 3.00 equiv) in 1,2-dichloroethane (800 μL) was chilled to 0 $^\circ\text{C}$. Chloriodomethane (61.9 μL , 0.852 mmol, 6.00 equiv) was then added dropwise to this solution, and the mixture was aged at 0 $^\circ\text{C}$ for 5 min before a solution of olefin **3.54** (100 mg, 0.142 mmol, 1 equiv) in 1,2-dichloroethane (100 μL) was added by cannula. The reaction mixture was stirred at 0 $^\circ\text{C}$ for 3 h, whereupon TLC analysis (30% ethyl acetate–hexanes, UV+CAM) showed complete consumption of starting material. Excess Simmons–Smith reagent was quenched with the addition of saturated aqueous ammonium chloride solution (2 mL), and the resulting biphasic mixture was extracted with dichloromethane (3×10 mL). The combined organic extracts were washed with saturated aqueous sodium chloride solution (10 mL), dried over sodium sulfate, filtered, and concentrated. The residue thus obtained was purified by flash-column chromatography (12 g silica gel, eluting with 20% ethyl acetate–hexanes initially, grading to 50% ethyl acetate–hexanes) to furnish the product as a colorless oil (90.9 mg, 89%).

$R_f = 0.64$ (30% ethyl acetate–hexanes, UV+CAM).

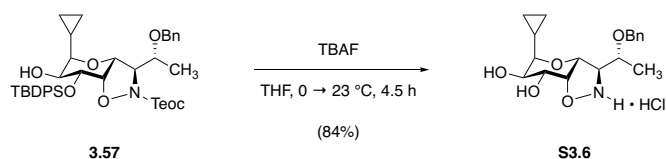
¹⁵² Denmark, S. E.; Edwards, J. P. *J. Org. Chem.* **1991**, *56*, 6974–6981.

^1H NMR (600 MHz, CDCl_3) δ 7.83–7.81 (m, 2H), 7.72–7.71 (m, 2H), 7.44–7.40 (m, 2H), 7.38–7.34 (m, 4H), 7.22–7.21 (m, 3H), 7.16–7.14 (m, 2H), 4.51 (d, $J = 11.5$ Hz, 1H), 4.41 (d, $J = 2.0$ Hz, 1H), 4.31 (d, $J = 11.7$ Hz, 1H), 4.30–4.26 (m, 2H), 4.20 (app dtd, $J = 7.6, 5.0, 2.5$ Hz, 1H), 4.02–4.00 (m, 2H), 3.95 (d, $J = 5.3$ Hz, 1H), 3.62 (app p, $J = 6.2$ Hz, 1H), 3.03 (dd, $J = 9.6, 5.4$ Hz, 1H), 1.75 (d, $J = 4.8$ Hz, 1H), 1.25 (d, $J = 6.3$ Hz, 3H), 1.11 (s, 9H), 1.09–1.06 (m, 2H), 0.61–0.52 (m, 2H), 0.40 (tt, $J = 9.7, 3.9$ Hz, 1H), 0.25 (ddt, $J = 16.1, 9.2, 4.6$ Hz, 2H), 0.08 (s, 9H).

^{13}C NMR (126 MHz, CDCl_3) δ 157.6, 138.2, 136.3, 135.9, 133.7, 133.5, 130.0, 128.5, 128.0, 127.8, 81.5, 79.9, 75.1, 73.4, 72.2, 71.9, 71.7, 70.2, 64.7, 27.1, 19.6, 17.7, 17.3, 7.4, 4.9, 1.7, –1.2. Overlapping pairs of phenyl carbon resonances are believed to account for the observation of only 9 unique phenyl-derived signals.

FTIR (neat, cm^{-1}): 2953 (m), 2931 (m), 2857 (m), 1698 (m), 1428 (m), 1333 (m), 1250 (m), 1113 (s), 1081 (s), 839 (m), 702 (s).

HRMS (ESI+, m/z): $[\text{M}+\text{H}]^+$ calc'd for $\text{C}_{40}\text{H}_{55}\text{NO}_7\text{Si}_2$, 718.3590; found 718.3569.



Isoxazolidine diol S3.6.

To an ice-cold solution of **3.57** (88 mg, 0.12 mmol, 1 equiv) in tetrahydrofuran (1.2 mL) was added tetra-*n*-butylammonium fluoride solution (1.0 M in tetrahydrofuran, 370 μ L, 370 μ mol, 3.0 equiv). The mixture was warmed to 23 °C, and desilylation was monitored by LCMS. While cleavage of the (trimethylsilyl)ethyl carbamate group was rapid (~30 min), the *tert*-butyldiphenylsilyl ether linkage underwent more sluggish deprotection. After 4.5 h, the reaction was complete, and the mixture was diluted with saturated aqueous sodium bicarbonate solution. The mixture was then extracted with dichloromethane (4 \times 10 mL), the combined extracts were dried over sodium sulfate, the dried solution was filtered, and the filtrate was concentrated. This crude residue was purified by flash-column chromatography (4 g silica gel, eluting with dichloromethane initially, grading to 10% methanol–dichloromethane) to furnish the product in its free-base form. This material was then converted to its hydrochloride salt by dissolving it in methanol (3 mL), treating the resulting solution with hydrogen chloride solution (4.0 M in 1,4-dioxane, 120 μ L, 0.49 mmol, 4.0 equiv), and concentrating the acidified solution to dryness. This gave the product (**S3.6** • HCl, 39 mg, 84%) as a light sand-colored solid.

R_f = 0.37 (free base, 10% methanol–dichloromethane, I_2).

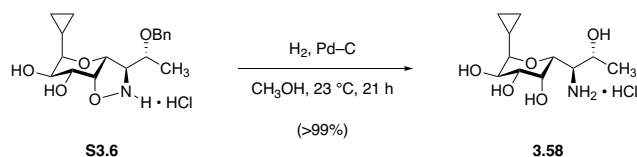
^1H NMR (hydrochloride salt, 600 MHz, CDCl_3) δ 7.40 (d, J = 7.0 Hz, 2H), 7.35 (t, J = 7.5 Hz, 2H), 7.28 (t, J = 7.3 Hz, 1H), 5.05 (app t, J = 3.7 Hz, 1H), 4.74 (app t, J = 4.1 Hz, 1H), 4.68 (d, J = 11.1 Hz, 1H), 4.55 (d, J = 11.2 Hz, 1H), 4.17 (dd, J = 7.7, 4.1 Hz, 1H), 4.11–

4.07 (m, 2H), 3.88 (dd, $J = 7.7, 3.7$ Hz, 1H), 3.14 (dd, $J = 9.8, 3.7$ Hz, 1H), 1.41 (d, $J = 6.0$ Hz, 1H), 1.15 (app tp, $J = 8.6, 4.6$ Hz, 1H), 0.65 (app tt, $J = 8.3, 4.3$ Hz, 1H), 0.58 (app tt, $J = 9.1, 4.1$ Hz, 1H), 0.36–0.28 (m, 2H).

^{13}C NMR (hydrochloride salt, 100 MHz, CDCl_3) δ 139.2, 129.4, 128.8, 128.7, 82.2, 80.2, 75.6, 72.2, 71.9, 70.4, 69.2, 68.8, 15.9, 9.6, 4.7, 3.0.

FTIR (hydrochloride salt, neat, cm^{-1}): 3347 (br), 2932 (w), 1454 (w), 1339 (w), 1127 (m), 1085 (s), 1026 (m), 677 (m).

HRMS (ESI+, m/z): $[\text{M}+\text{H}]^+$ calc'd for $\text{C}_{18}\text{H}_{25}\text{NO}_5$, 336.1805; found 336.1820.



Aminotetraol 3.58.

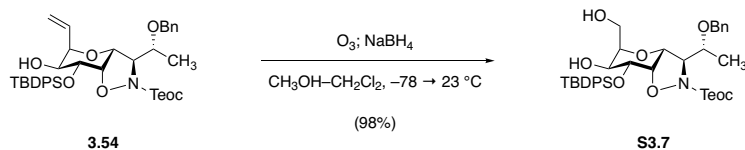
A 2–5 mL glass microwave vial was charged with a magnetic stir bar, isoxazolidine salt **S3.6** • HCl (38 mg, 0.10 mmol, 1 equiv), methanol (1.0 mL) and palladium on carbon (10% w/w, 11 mg). The headspace above the reaction mixture was flushed with hydrogen gas, and the mixture was stirred at 23 °C under a balloonful of hydrogen gas. After 21 h, LCMS analysis indicated that isoxazolidine hydrogenolysis and *O*-debenzylation were complete; the mixture was filtered through a Celite pad, and the filter cake was rinsed with methanol (3 × 1 mL). The filtrate was concentrated to afford analytically pure product as a white solid (32 mg, 111%).

¹H NMR (600 MHz, CD₃OD) δ 4.18 (app t, *J* = 2.3 Hz, 1H), 4.12 (app p, *J* = 6.3 Hz, 1H), 4.06 (dd, *J* = 7.4, 2.4 Hz, 1H), 3.96 (dd, *J* = 8.7, 5.0 Hz, 1H), 3.89 (dd, *J* = 8.7, 3.2 Hz, 1H), 3.55 (app t, *J* = 6.4 Hz, 1H), 3.11 (dd, *J* = 9.9, 5.0 Hz, 1H), 1.29 (d, *J* = 6.4 Hz, 3H), 1.15 (app ddq, *J* = 12.9, 9.3, 4.8 Hz, 1H), 0.71 (tdd, *J* = 8.5, 5.9, 4.4 Hz, 1H), 0.53 (app tt, *J* = 9.1, 5.3 Hz, 1H), 0.35 (dq, *J* = 9.7, 4.8 Hz, 1H), 0.29 (dq, *J* = 9.6, 4.9 Hz, 1H).

¹³C NMR (100 MHz, CD₃OD) δ 82.0, 71.9, 70.5, 69.9 (2 × C), 65.6, 58.2, 18.4, 93, 5.9, 2.6.

FTIR (neat, cm⁻¹): 3350 (br), 2925 (m), 1620 (w), 1510 (m), 1094 (s), 1072 (s), 1002 (m).

HRMS (ESI+, *m/z*): [M+H]⁺ calc'd for C₁₁H₂₁NO₅, 248.1492; found 248.1498.



Hydroxymethyl glycoside S3.7.

A solution of **3.54** (654 mg, 0.929 mmol, 1 equiv) in 50% v/v dichloromethane–methanol (18.6 mL) was chilled to $-78 \text{ }^\circ\text{C}$. A mixture of ozone and dioxygen from an ozone generator was bubbled gently through the reaction solution, until an azure color appeared and persisted for 15 seconds, signaling saturation of the solution with ozone gas with concomitant disappearance of starting material. Ozone bubbling was then discontinued, and nitrogen gas was bubbled through the solution for 5 minutes in order to flush the solution of residual ozone. The resulting colorless solution was treated with sodium borohydride (351 mg, 9.29 mmol, 10.0 equiv) at $-78 \text{ }^\circ\text{C}$, and the mixture was subsequently allowed to warm to $23 \text{ }^\circ\text{C}$ with constant stirring (Note: gas evolution occurs upon warming, and the reaction flask should be adequately vented to avoid overpressurization). After stirring for 1 h at $23 \text{ }^\circ\text{C}$, the mixture was carefully treated with 30 mL of half-saturated aqueous sodium chloride solution (Caution: gas evolution!). The resulting mixture was stirred for 5 minutes, or until gas evolution ceased; and the mixture was then extracted with ethyl acetate ($3 \times 20 \text{ mL}$). The combined organic extracts were washed with saturated aqueous sodium chloride solution, the washed solution was dried over sodium sulfate, and the dried solution was concentrated to afford the product as a brilliant white solid (644 mg, 98%). This material was suitable for use without further purification.

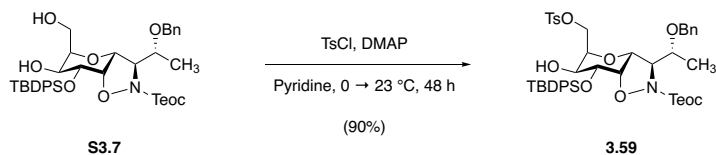
$R_f = 0.34$ (40% ethyl acetate–hexanes, UV+CAM).

^1H NMR (500 MHz, CDCl_3) δ 7.78–7.75 (m, 2H), 7.69–7.66 (m, 2H), 7.46–7.41 (m, 2H), 7.40–7.35 (m, 4H), 7.25–7.22 (m, 3H), 7.17–7.13 (m, 2H), 4.51 (d, $J = 11.6$ Hz, 1H), 4.39 (d, $J = 3.1$ Hz, 1H), 4.35–4.26 (m, 4H), 4.03 (t, $J = 3.3$ Hz, 1H), 4.00 (app q, $J = 5.9$ Hz, 1H), 3.95 (d, $J = 5.2$ Hz, 1H), 3.92 (dd, $J = 8.8, 3.3$ Hz, 1H), 3.67 (dd, $J = 11.9, 4.7$ Hz, 1H), 3.61 (app tt, $J = 11.8, 6.7$ Hz, 2H), 2.06 (s, 1H), 1.89 (s, 1H), 1.24 (d, $J = 6.4$ Hz, 3H), 1.09 (s, 9H), 1.07 (m, 2H), 0.08 (s, 9H).

^{13}C NMR (126 MHz, CDCl_3) δ 157.4, 138.1, 136.2, 135.8, 133.4, 133.1, 130.2, 130.2, 128.5, 128.1, 128.0, 127.9, 127.9, 79.6, 76.2, 75.4, 73.2, 72.0, 71.9, 71.8, 70.2, 64.9, 59.9, 27.1, 19.5, 17.7, 17.3, –1.2.

FTIR (neat, cm^{-1}): 3452 (br), 2953 (m), 2933 (m), 2857 (m), 1703 (m), 1428 (m), 1250 (m), 1112 (s), 1085 (m), 359 (m), 838 (m), 702 (s).

HRMS (ESI+, m/z): $[\text{M}+\text{H}]^+$ calc'd for $\text{C}_{38}\text{H}_{53}\text{NO}_8\text{Si}_2$, 708.3382; found 708.3366.



***para*-Toluenesulfonate ester 3.59.**

A flame-dried 25-mL round-bottomed flask was charged with diol **S3.7** (1.05 g, 1.48 mmol, 1 equiv), and this starting material was dried by azeotropic removal of benzene. Anhydrous pyridine (5.0 mL) was then added, and the resulting solution was chilled to 0 °C. Solid *p*-toluenesulfonyl chloride (481 mg, 2.52 mmol, 1.70 equiv) was added to the ice-cold solution, causing a golden yellow color to evolve. 4-Dimethylaminopyridine (DMAP, 9.1 mg, 74 μmol, 0.050 equiv) was then added, and the resulting solution was stirred at 0 °C for 5 minutes; the cooling bath was then removed, and the mixture was allowed to warm to 23 °C with constant stirring. The golden color dissipated within 30 minutes, leaving a colorless solution. Progress was monitored by TLC (60% ethyl acetate–hexanes, UV+CAM), and after 48 h, the reaction was judged to be complete. The mixture was concentrated *in vacuo*, and the residue was purified by flash-column chromatography (80 g silica, eluting with 10% ethyl acetate–hexanes initially, grading to 30% ethyl acetate–hexanes) to give the product as a white foaming solid (1.15 g, 90%).

$R_f = 0.49$ (30% ethyl acetate–hexanes, UV+CAM).

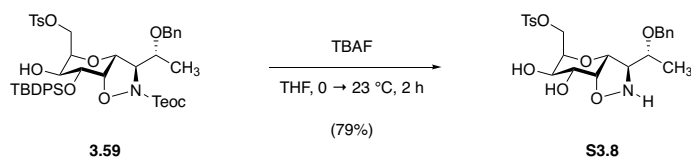
$^1\text{H NMR}$ (500 MHz, CDCl_3) δ 7.75–7.72 (m, 2H), 7.68–7.64 (m, 4H), 7.46–7.41 (m, 2H), 7.39–7.34 (m, 4H), 7.26–7.22 (m, 3H), 7.19–7.16 (m, 2H), 4.51 (d, $J = 11.7$ Hz, 1H), 4.44 (d, $J = 2.8$ Hz, 1H), 4.30 (d, $J = 11.8$ Hz, 1H), 4.28–4.24 (m, 3H), 4.10–4.00 (m, 3H), 3.96 (t, $J = 3.2$ Hz, 1H), 3.93 (d, $J = 5.4$ Hz, 1H), 3.83 (dd, $J = 9.2, 3.4$ Hz, 1H), 3.57 (app p, $J = 6.2$

Hz, 1H), 2.41 (s, 3H), 1.86 (d, $J = 3.7$ Hz, 1H), 1.22 (d, $J = 6.3$ Hz, 3H), 1.07 (s, 9H), 1.07–1.03 (m, 2H), 0.07 (s, 9H).

^{13}C NMR (126 MHz, CDCl_3) δ 157.5, 144.9, 138.2, 136.1, 135.7, 133.4, 133.0, 132.9, 130.2, 129.9, 128.5, 128.2, 128.0, 127.9, 127.8, 79.4, 77.4, 77.2, 76.9, 76.0, 73.9, 73.0, 72.2, 71.7, 71.5, 68.5, 66.0, 64.8, 27.0, 21.8, 19.5, 17.7, 17.1, –1.3, –1.5.

FTIR (neat, cm^{-1}): 2954 (m), 2931 (m), 2896 (m), 2858 (m), 1707 (m), 1362 (m), 1177 (s), 1098 (s), 837 (s), 703 (s).

HRMS (ESI+, m/z): $[\text{M}+\text{Na}]^+$ calc'd for $\text{C}_{45}\text{H}_{59}\text{NO}_{10}\text{SSi}_2$, 884.3290; found 884.3262.



Isoxazolidine diol **S3.8**.

In a 100-mL round-bottomed flask, a solution of carbamate **3.59** (1.15 g, 1.34 mmol, 1 equiv) in tetrahydrofuran (13.4 mL) was chilled to 0 °C was treated with tetrabutylammonium fluoride (1.0 M solution in tetrahydrofuran, 4.0 mL, 4.0 mmol, 3.0 equiv). Following the addition of TBAF, the ice-water cooling bath was removed, and the reaction solution was allowed to warm to 23 °C. Progress was monitored by LCMS; cleavage of the (trimethylsilyl)ethyl carbamate was observed within 15 minutes, while cleavage of the *tert*-butyldiphenylsilyl ether was comparatively slower. After 2 hours, the reaction was judged to be complete, and 20 mL of saturated aqueous sodium bicarbonate solution was added. The resulting mixture was extracted with dichloromethane (4 × 15 mL), and the combined organic layers were dried over sodium sulfate. The dried product solution was filtered, and the filtrate was concentrated to afford a colorless oil. This material was purified by flash-column chromatography (40 g silica, eluting with 1% methanol–dichloromethane initially, grading to 10% methanol–dichloromethane) to give the product as a white foaming solid (508 mg, 79%).

R_f = 0.52 (10% methanol–dichloromethane, UV+CAM).

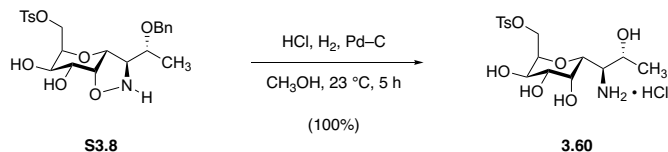
¹H NMR (600 MHz, CDCl₃) δ 7.76 (d, J = 8.3 Hz, 2H), 7.34–7.30 (m, 2H), 7.29–7.25 (m, 5H), 4.70 (dd, J = 4.1, 2.1 Hz, 1H), 4.61 (d, J = 11.6 Hz, 1H), 4.32 (d, J = 11.7 Hz, 1H), 4.26–4.21 (m, 2H), 4.18 (app dt, J = 6.9, 5.0 Hz, 1H), 3.97 (dd, J = 8.4, 5.3 Hz, 1H), 3.88 (app

t, $J = 4.0$ Hz, 1H), 3.79 (dd, $J = 8.4, 3.8$ Hz, 1H), 3.57 (br s, 1H), 3.23 (dd, $J = 3.9, 2.1$ Hz, 1H), 2.39 (s, 3H), 1.27 (d, $J = 6.3$ Hz, 3H).

^{13}C NMR (126 MHz, CDCl_3) δ 144.9, 138.0, 132.9, 130.0, 128.6, 128.0, 128.0, 127.8, 81.7 (br), 78.4, 72.9, 71.9, 70.9, 70.6, 70.1, 69.1, 67.2, 21.7, 16.9.

FTIR (neat, cm^{-1}): 3378 (br), 2929 (w), 1453 (w), 1356 (m), 1174 (s), 1071 (s), 974 (m), 732 (s).

HRMS (ESI+, m/z): $[\text{M}+\text{H}]^+$ calc'd for $\text{C}_{23}\text{H}_{29}\text{NO}_8\text{S}$, 480.1687; found 480.1711.



Aminotetraol **3.60**.

In a 25-mL round-bottomed flask, a solution of isoxazolidine **S3.8** (368 mg, 767 μmol , 1 equiv) in methanol (8.00 mL) was cooled to 0 $^\circ\text{C}$ and was treated with hydrogen chloride solution (4.0 M in 1,4-dioxane, 770 μL , 3.1 mmol, 4.0 equiv). This solution was immediately concentrated to dryness, and the white residue obtained was re-dissolved in fresh methanol (7.67 mL). This solution was treated with palladium on carbon (10 wt%, 82.0 mg), the headspace of the flask was flushed with nitrogen gas, and the apparatus was fitted with a 3-way stopcock to which one arm was affixed to a high-vacuum line, and the other was affixed to a hydrogen gas-filled balloon. The headspace of the flask was replaced by briefly evacuating, then back-filling the flask with hydrogen gas using the stopcock (3 evacuation–backfill cycles), and the black suspension was stirred at 23 $^\circ\text{C}$ under 1 atm of hydrogen gas. After 5 h, LCMS analysis indicated that isoxazolidine ring and benzyl ether hydrogenolysis were complete, and the headspace of the flask was flushed with nitrogen gas. The reaction mixture was filtered through a Celite pad, and the filter cake was rinsed with methanol (2×3 mL). The filtrate was concentrated to give the product as a dull white crystalline solid (327 mg, 100%). This material was suitable for use in subsequent transformations without further purification.

Crystals suitable for X-ray analysis were prepared as follows: In a 1-mL glass sample vial, **3.60** \cdot HCl (3 mg) was deposited, and this material was dissolved in approximately 200 μL of 190-proof ethanol. The vial containing the ethanolic solution was then placed inside a 20-mL scintillation vial containing approximately 3 mL of acetonitrile. The large vial was capped, and

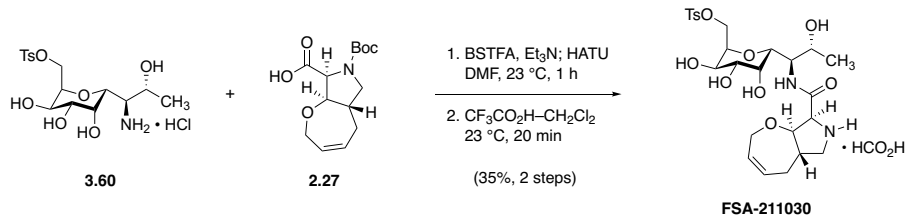
the assembly was allowed to stand undisturbed at 23 °C. After 2 days, needle-shaped crystals of sufficient size for X-ray analysis had formed (see Appendix A for X-ray crystal structure data).

^1H NMR (600 MHz, CD_3OD) δ 7.80 (d, $J = 8.0$ Hz, 2H), 7.46 (d, $J = 8.0$ Hz, 2H), 4.35 (dd, $J = 11.7, 9.6$ Hz, 1H), 4.24–4.21 (m, 2H), 4.18 (app s, 1H), 4.09 (app p, $J = 6.3$ Hz, 1H), 3.99 (dd, $J = 7.1, 2.8$ Hz, 1H), 3.95 (dd, $J = 8.3, 5.0$ Hz, 1H), 3.66 (dd, $J = 8.3, 3.0$ Hz, 1H), 3.56 (app t, $J = 6.4$ Hz, 1H), 2.46 (s, 3H), 1.26 (d, $J = 6.4$ Hz, 3H).

^{13}C NMR (126 MHz, CD_3OD) δ 146.7, 134.3, 131.2, 129.0, 74.0, 71.7, 69.8, 69.5, 68.7, 68.1, 65.5, 58.1, 21.6, 18.7.

FTIR (neat, cm^{-1}): 3345 (br), 2927 (br), 1598 (w), 1495 (w), 1356 (m), 1190(m), 1175 (s), 1080 (s), 976 (m), 554 (m).

HRMS (ESI+, m/z): $[\text{M}+\text{Na}]^+$ calc'd for $\text{C}_{16}\text{H}_{25}\text{NO}_8\text{S}$, 414.1193; found 414.1203.



Synthetic lincosamide FSA-211030.

To a solution of aminotetraol **3.60** • HCl (9.7 mg, 23 μ mol, 1 equiv) and triethylamine (13 μ L, 95 μ mol, 4.2 equiv) in *N,N*-dimethylformamide (110 μ L) was added *N,O*-bis(trimethylsilyl)trifluoroacetamide (12 μ L, 45 μ mol, 2.0 equiv). The mixture was stirred at 23 °C for 1 h in order to ensure complete *O*-silylation. Carboxylic acid **2.27** (7.1 mg, 25 μ mol, 1.1 equiv) and HATU (11 mg, 29 μ mol, 1.3 equiv) were then added sequentially, the vial was sealed, and the mixture was stirred at 23 °C for 1 h, at which point LCMS analysis showed complete consumption of aminotetraol starting material and its (oligo)trimethylsilylated congeners. The reaction mixture was diluted with ethyl acetate (15 mL), and this diluted solution was washed sequentially with 10% w/v aqueous citric acid solution (5 mL), water (5 mL), half-saturated aqueous sodium bicarbonate solution (5 mL), and saturated aqueous sodium chloride solution (5 mL). The washed organic solution was dried over sodium sulfate, filtered, and concentrated to provide crude (oligo)trimethylsilylated, *N*-Boc-protected coupled intermediate.

This residue was dissolved in dichloromethane (1.1 mL); and water (25 μ L), dimethyl sulfide (25 μ L), and trifluoroacetic acid (370 μ L) were added. The mixture was stirred at 23 °C for 20 min, whereupon LCMS analysis showed that Boc removal was complete. The mixture was diluted with toluene (2 mL), and the diluted mixture was concentrated to provide a light tan solid residue that was finally subjected to preparative HPLC on a Waters SunFire Prep C₁₈ column (5 μ m, 250 \times 19 mm; eluting with 0.1% formic acid–10% acetonitrile–water initially, grading to 0.1%

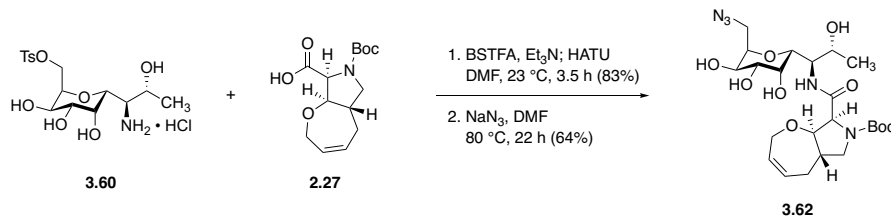
formic acid–50% acetonitrile–water over 40 min, with a flow rate of 15 mL/min; monitored by UV absorbance at 254 nm) to provide **FSA-211030** • HCO₂H as a white solid (4.8 mg, 35%).

¹H NMR (600 MHz, CD₃OD) δ 8.28 (br, 1H), 7.82 (d, *J* = 8.4 Hz, 2H), 7.46 (d, *J* = 8.0 Hz, 2H), 5.88 (app ddt, *J* = 12.5, 7.5, 2.6 Hz, 1H), 5.79 (app ddt, *J* = 12.2, 6.1, 3.0 Hz, 1H), 4.52 (d, *J* = 8.8 Hz, 1H), 4.39 (dd, *J* = 11.6, 10.1 Hz, 1H), 4.33 (dd, *J* = 15.8, 6.1 Hz, 1H), 4.23–4.21 (m, 3H), 4.18–4.13 (m, 2H), 4.00–3.94 (m, 3H), 3.80 (d, *J* = 7.1 Hz, 1H), 3.63 (dd, *J* = 11.4, 7.5 Hz, 1H), 3.49 (dd, *J* = 9.9, 3.2 Hz, 1H), 2.96 (app t, *J* = 11.8 Hz, 1H), 2.54 (ddd, *J* = 16.7, 7.6, 3.3 Hz, 1H), 2.46 (s, 3H), 2.21 (app qd, *J* = 13.1, 11.4, 7.3 Hz, 1H), 2.12–2.06 (m, 1H), 1.20 (d, *J* = 6.4 Hz, 3H).

¹³C NMR (126 MHz, CD₃OD) δ 167.3, 146.7, 134.1, 131.2, 131.0, 130.5, 129.1, 86.3, 76.0, 72.5, 72.3, 70.5, 69.3, 68.6, 68.1, 66.9, 61.8, 57.3, 43.0, 30.1, 21.6, 19.5. One methine carbon is believed to be obfuscated by the solvent signal, and consequently is not observed.

FTIR (neat, cm⁻¹): 3399 (br), 1676 (s), 1360 (m), 1202 (m), 1176 (s), 1133 (m), 1079 (m), 973 (m).

HRMS (ESI+, *m/z*): [M+H] calc'd for C₂₅H₃₆N₂O₁₀S, 557.2163; found 557.2181.



Protected lincosamide 3.62.

In a 4-mL glass vial fitted with a magnetic stir bar and a silicone septum screw cap, an ice-cold suspension of aminosugar salt **3.60** • HCl (35.7 mg, 83.5 μmol, 1 equiv) and triethylamine (48.8 μL, 0.350 mmol, 4.20 equiv) in *N,N*-dimethylformamide (417 μL) was treated with *N,O*-bis(trimethylsilyl)trifluoroacetamide (44.7 μL, 0.167 mmol, 2.00 equiv). A colorless solution formed immediately, and this mixture was warmed to 23 °C to stir for 1 h so as to ensure complete *O*-silylation. Next, carboxylic acid **2.27** (26.0 mg, 91.8 μmol, 1.10 equiv) and HATU (41.2 mg, 0.108 mmol, 1.30 equiv) were added, and the resulting yellow solution was stirred at 23 °C for 3.5 h, at which point LCMS analysis showed complete consumption of aminotetraol starting material and its (oligo)trimethylsilylated congeners. The reaction mixture was consequently diluted with ethyl acetate (30 mL), and the diluted solution was washed sequentially with aqueous citric acid solution (10% w/v, 2 × 10 mL), saturated aqueous sodium chloride solution (10 mL), half-saturated aqueous sodium bicarbonate solution (10 mL), and a fresh portion of saturated aqueous sodium chloride solution (10 mL). The washed organic layer was dried over sodium sulfate, filtered, and concentrated. The residue, containing (oligo)trimethylsilylated coupled product congeners, was dissolved in 50% v/v acetic acid–methanol (2.00 mL). The solution was heated to 40 °C for 4 h, at which point LCMS analysis showed that global desilylation was complete. The mixture was diluted with toluene, and the diluted mixture was concentrated in vacuo. The residue thus obtained was purified by flash-column chromatography (12 g silica gel, eluting with 1% methanol–dichloromethane initially, grading to 10% methanol–dichloromethane), and fractions containing

N-Boc-protected coupled product were identified by TLC ($R_f = 0.41$ (10% methanol–dichloromethane, UV+CAM). These fractions were pooled and concentrated to provide coupled, *N*-Boc protected product as a colorless solid (45.4 mg, 83%). Due to substantial amide and carbamate rotamerism observed in the ^1H -NMR spectrum, this material was carried forward through $\text{S}_{\text{N}}2$ displacement with sodium azide prior to full characterization.

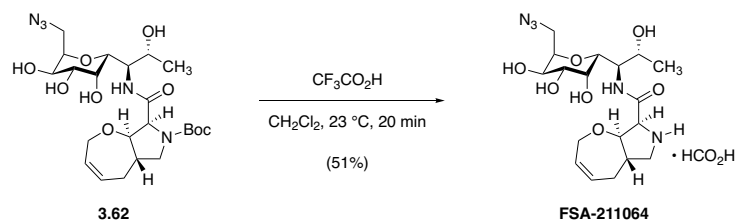
A portion of this *N*-Boc-protected *p*-toluenesulfonate ester intermediate (33 mg, 50 μmol , 1 equiv) was introduced to a 0.5–2 mL conical glass microwave vial. A magnetic stir bar, sodium azide (33 mg, 0.50 mmol, 10 equiv), and *N,N*-dimethylformamide (250 μL) were then added. The vial was sealed, stirring was initiated, and the reaction mixture was heated to 80 $^\circ\text{C}$ in a pre-heated oil bath. After 22 h, LCMS analysis indicated that no starting material remained. The reaction mixture was diluted with saturated aqueous sodium chloride solution (10 mL) and the mixture was extracted with ethyl acetate (3×5 mL). The combined organic extracts were dried over sodium sulfate, filtered, and concentrated; the residue thus obtained was subjected to flash-column chromatography (4 g silica gel, eluting with dichloromethane initially, grading to 10% methanol–dichloromethane) to provide the product as a white solid (17 mg, 64%).

^1H NMR (1:1 mixture of rotamers, asterisk [*] denotes rotameric signals that could be resolved, 500 MHz, CD_3OD) δ 5.91–5.84 (m, 1H), 5.80–5.73 (m, 1H), 4.43 (app t, $J = 8.0$ Hz, 1H), 4.31 (d, $J = 6.1$ Hz, 1H), 4.28 (d, $J = 6.1$ Hz, 1H),* 4.25–4.08 (m, 3H), 4.04–3.95 (m, 4H), 3.80–3.65 (m, 3H), 3.58–3.49 (m, 2H), 2.94 (app q, $J = 10.9$ Hz, 1H), 2.50–2.39 (m, 2H), 2.08 (app q, $J = 14.7, 13.8$ Hz, 1H), 1.46 (s, 9H), 1.45 (s, 9H),* 1.25 (d, $J = 6.0$ Hz, 3H), 1.22 (d, $J = 6.2$ Hz, 3H).

^{13}C NMR (1:1 mixture of rotamers, asterisk [*] denotes rotameric signals that could be resolved, 126 MHz, CD_3OD) δ 172.9, 172.8,* 156.0, 155.8,* 131.7, 131.5,* 131.1, 131.0,* 87.4, 86.9,* 82.0, 81.6,* 77.0, 76.8,* 73.2, 71.9,* 71.9, 71.8,* 70.6, 70.2,* 69.2, 69.0,* 69.0, 68.8,* 68.7, 64.2, 64.0,* 56.6, 55.6,* 51.0, 50.4,* 47.6, 47.4,* 42.6, 41.4,* 31.6, 31.5,* 19.5, 18.7.*

FTIR (neat, cm^{-1}): 3433 (br), 2100 (s), 1672 (s), 1452 (m), 1414 (s), 1368 (m), 1171 (m), 1126 (m), 1074 (m),

HRMS (ESI+, m/z): $[\text{M}+\text{H}]^+$ calc'd for $\text{C}_{23}\text{H}_{37}\text{N}_5\text{O}_9$, 528.2664; found 528.2680.



Synthetic lincosamide FSA-211064.

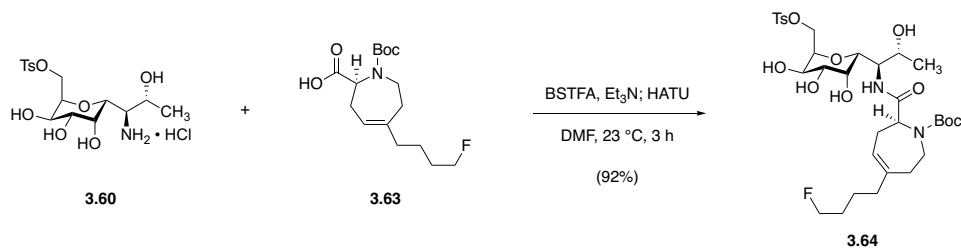
In a 4-mL glass vial, *tert*-butyl carbamate **3.62** (6.1 mg, 12 μ mol, 1 equiv) was dissolved in dichloromethane (170 μ L). Water (3.7 μ L), dimethyl sulfide (3.7 μ L), and trifluoroacetic acid (170 μ L) were then added sequentially, and the reaction mixture was stirred at 23 $^{\circ}$ C for 20 min, whereupon LCMS analysis showed that Boc removal was complete. The reaction mixture was diluted with toluene (1 mL), and the diluted mixture was concentrated to dryness in vacuo. The residue was then purified by preparative HPLC on a Waters SunFire Prep C₁₈ column (5 μ m, 250 \times 19 mm; eluting with 0.1% formic acid–5% acetonitrile–water initially, grading to 0.1% formic acid–50% acetonitrile–water over 40 min, with a flow rate of 15 mL/min; monitored by UV absorbance at 210 nm) to furnish **FSA-211064** \cdot HCO₂H as a white solid (2.8 mg, 51%).

¹H NMR (600 MHz, CD₃OD) δ 5.87 (app ddt, $J = 12.5, 7.4, 2.5$ Hz, 1H), 5.77 (app ddt, $J = 12.3, 6.1, 3.0$ Hz, 1H), 4.41 (d, $J = 8.7$ Hz, 1H), 4.33 (dd, $J = 15.8, 6.2$ Hz, 1H), 4.28 (app t, $J = 7.1$ Hz, 1H), 4.18–4.10 (m, 3H), 4.03–3.97 (m, 3H), 3.86 (d, $J = 7.6$ Hz, 1H), 3.70 (dd, $J = 13.8, 10.5$ Hz, 1H), 3.58–3.55 (m, 2H), 3.49 (dd, $J = 13.9, 3.0$ Hz, 1H), 2.90 (app t, $J = 11.6$ Hz, 1H), 2.53 (ddd, $J = 16.6, 7.5, 3.2$ Hz, 1H), 2.19 (app p, $J = 10.4$ Hz, 1H), 2.07 (app td, $J = 14.1, 12.3, 3.1$ Hz, 1H), 1.23 (d, $J = 6.3$ Hz, 3H).

^{13}C NMR (126 MHz, CD_3OD) δ 168.6, 130.9, 130.7, 86.8, 77.2, 71.9, 71.7, 70.5, 69.3, 68.8, 68.6, 62.1, 56.9, 47.4, 43.4, 30.4, 19.3. One methine carbon is believed to be obfuscated by the solvent signal, and consequently is not observed.

FTIR (neat, cm^{-1}): 3432 (br), 2090 (s), 1671 (m), 1590 (s), 1350 (m), 1067 (m).

HRMS (ESI+, m/z): $[\text{M}+\text{H}]^+$ calc'd for $\text{C}_{18}\text{H}_{29}\text{N}_5\text{O}_7$, 428.2140; found 428.2154.



Protected lincosamide **3.64**.

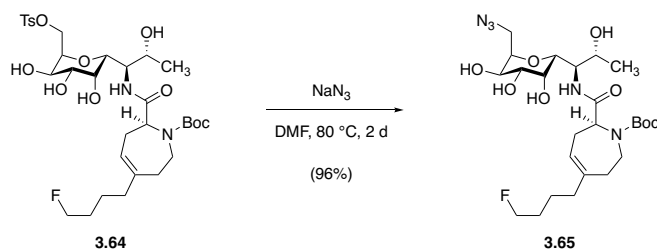
In a 2–5 mL glass microwave vial, an ice-cold solution of aminotetraol **3.50** • HCl (249 mg, 0.582 mmol, 1 equiv) in *N,N*-dimethylformamide (2.91 mL) was treated sequentially with triethylamine (341 μ L, 2.44 mmol, 4.20 equiv) and *N,O*-bis(trimethylsilyl)trifluoroacetamide (312 μ L, 1.15 mmol, 2.00 equiv). The mixture was warmed to 23 °C and was stirred at this temperature for 1 h to ensure complete *O*-silylation before a solution of azepine acid **3.63** (202 mg, 0.640 mmol, 1.10 equiv) in *N,N*-dimethylformamide (1.50 mL) was added by cannula. The mixture was then treated with HATU (288 mg, 0.756 mmol, 1.30 equiv), causing the cloudy mixture to attain a golden yellow color. After stirring at 23 °C for 3 h, the reaction mixture was diluted with ethyl acetate (50 mL). The diluted organic solution was washed sequentially with 15-mL portions of 10% w/v aqueous citric acid solution, saturated aqueous sodium bicarbonate solution, and saturated sodium chloride solution; the washed solution was dried over sodium sulfate, filtered, and concentrated. This residue was then re-dissolved in 50% v/v acetic acid–methanol, and this solution was stirred at 40 °C overnight. The mixture was then diluted with toluene (20 mL), and the diluted mixture was concentrated to dryness to provide a faint rose-brown oil. This crude product was purified by flash-column chromatography (48 g silica gel, eluting with dichloromethane initially, grading to 10% methanol–dichloromethane) to furnish the product as a white foaming solid (369 mg, 92%).

$R_f = 0.56$ (10% methanol–dichloromethane, I_2).

$^1\text{H NMR}$ (1:1 mixture of rotamers, asterisk [*] denotes rotameric peaks that could be resolved; 500 MHz, CDCl_3) δ 7.81 (d, $J = 8.1$ Hz, 2H), 7.45 (d, $J = 8.1$ Hz, 2H), 5.48 (br s, 1H), 4.50–4.32 (m, 4H), 4.26 (dd, $J = 11.3, 2.7$ Hz, 1H), 4.18 (ddd, $J = 9.4, 6.6, 2.7$ Hz, 1H), 4.10–3.95 (m, 3H) 3.94–3.70 (m, 3H), 3.65 (app t, $J = 12.9$ Hz, 1H), 3.47 (dd, $J = 10.1, 3.3$ Hz, 1H), 2.72 (app q, $J = 14.4$ Hz, 1H), 2.46 (s, 3H), 2.46–2.40 (br, 2H), 2.32 (br, 1H), 2.28 (br, 1H),* 1.99 (br, 2H), 1.65–1.59 (m, 2H), 1.53–1.48 (m, 2H), 1.47 (s, 9H), 1.44 (s, 9H),* 1.20 (d, $J = 6.3$ Hz, 3H), 1.15 (d, $J = 6.3$ Hz, 3H).*

FTIR (neat, cm^{-1}): 3388 (br), 2972 (m), 2933 (m), 1663 (s), 1453 (m), 1407 (m), 1366 (m), 1175 (s), 1080 (m), 973 (m), 554 (m).

HRMS (ESI+, m/z): $[\text{M}+\text{H}]^+$ calc'd for $\text{C}_{32}\text{H}_{49}\text{FN}_2\text{O}_{11}\text{S}$, 689.3114; found 689.3135.



Protected lincosamide **3.65**.

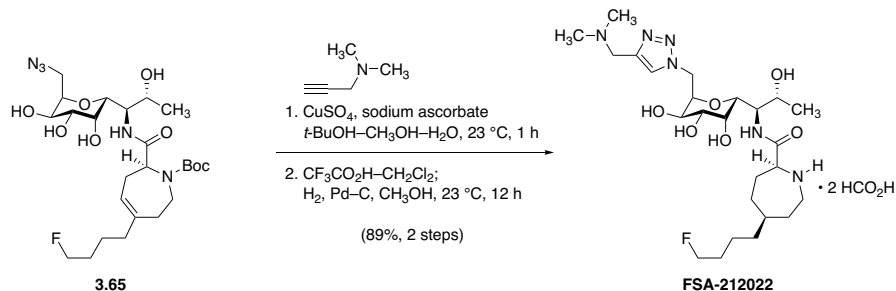
A 0.5–2 mL conical glass microwave vial was charged with a magnetic stir bar, *p*-toluenesulfonate ester **3.64** (150 mg, 0.218 mmol, 1 equiv), sodium azide (142 mg, 2.18 mmol, 10.0 equiv), and *N,N*-dimethylformamide (1.09 mL). The vial was sealed, and the mixture was heated to 80 °C in a pre-heated oil bath. After 2 d of stirring at elevated temperature, LCMS analysis of the reaction mixture showed that no starting material remained. The mixture was cooled to room temperature and was then partitioned between ethyl acetate (15 mL) and saturated aqueous sodium chloride solution (15 mL). The layers were shaken, then separated. The aqueous phase was extracted with additional ethyl acetate (2 × 10 mL), and the combined organic extracts were dried over sodium sulfate. The dried product solution was then filtered, and the filtrate was concentrated to give a crude residue that was subjected to flash-column chromatography (12 g silica gel, eluting with dichloromethane initially, grading to 10% methanol–dichloromethane) to furnish the product as a white powder (116 mg, 96%).

R_f = 0.41 (10% methanol–dichloromethane, I_2 or CAM).

^1H NMR (60:40 mixture of rotamers, asterisk [*] denotes minor rotameric peaks that could be resolved; 500 MHz, CD_3OD) δ 5.48 (br s, 1H), 4.50–4.43 (m, 2H), 4.38–4.35 (m, 1H), 4.18–4.99 (m, 4H), 3.98–3.93 (, 1H), 3.89–3.80 (m, 2H), 3.73–3.64 (m, 2H), 3.56 (d, J = 9.9 Hz, 1H), 3.46 (dd, J = 13.5, 3.1 Hz, 1H), 3.41 (dd, J = 13.8, 3.0 Hz, 1H),* 2.73 (app q,

$J = 10.8$ Hz, 1H), 2.50–2.28 (m, 2H), 2.34 (br, 1H), 2.30 (br, 1H),* 2.00 (br, 2H), 1.68–1.57 (m, 2H), 1.53–1.49(m, 2H), 1.48 (s, 9H), 1.45 (s, 9H),* 1.22 (d, $J = 6.4$ Hz, 3H),* 1.20 (d, $J = 6.5$ Hz, 3H).

MS (ESI+, m/z): $[M+H-N_2]^+$ calc'd for $C_{25}H_{42}FN_5O_8$, 532.3; found 532.3.



Synthetic lincosamide FSA-212022.

In a 1-mL glass fitted with a magnetic stir bar, azide **3.65** (11.6 mg, 20.8 μmol , 1 equiv) was dissolved in 2:2:1 *tert*-butanol–methanol–water (138 μL). To this solution were then added 3-dimethylamino-1-propyne (4.48 μL , 41.0 μmol , 2.00 equiv), aqueous sodium ascorbate solution (0.100 M, 41.5 μL , 4.15 μmol , 0.200 equiv), and aqueous cupric sulfate solution (0.100 M, 10.4 μL , 1.04 μmol , 0.0500 equiv). This mixture was stirred at 23 °C for 1 h, by which time LCMS analysis showed that no starting material remained. The reaction mixture was diluted with 50% v/v saturated aqueous sodium bicarbonate solution–saturated aqueous sodium chloride solution, and this diluted mixture was extracted with dichloromethane (3 \times 3 mL). The combined organic extracts were dried over sodium sulfate, filtered, and concentrated.

This residue was transferred to a 4-mL glass vial, where it was re-dissolved in 33% v/v trifluoroacetic acid–dichloromethane (600 μL). After 1 h of stirring at 23 °C, LCMS analysis showed that Boc removal was complete; the mixture was diluted with toluene (1 mL), and the diluted mixture was concentrated to dryness. This residue was then dissolved in methanol (300 μL), the solution was treated with palladium on carbon (10% w/w, 7.00 mg), and the headspace above the reaction mixture was replaced with hydrogen gas. The black suspension was stirred at 23 °C under hydrogen gas (1 atm) for 12 h, whereupon LCMS analysis showed that azepine hydrogenation was complete. The mixture was filtered through a Celite pad to remove the

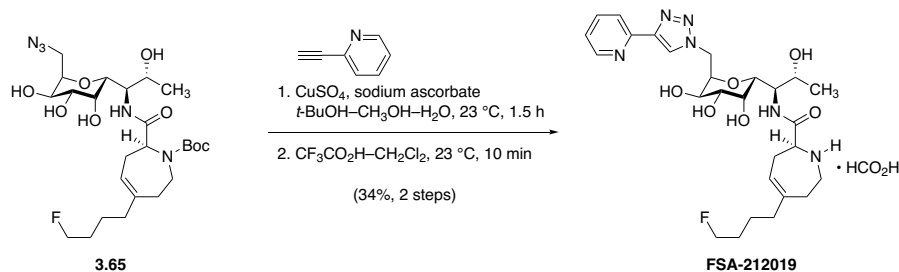
heterogeneous catalyst, and the filter cake was rinsed with methanol (3×1 mL). The filtrate was concentrated to give a colorless oil, which was purified by preparative HPLC on a Waters SunFire Prep C₁₈ column (5 μ m, 250 \times 19 mm; eluting with 0.1% formic acid–2% acetonitrile–water initially, grading to 0.1% formic acid–20% acetonitrile–water over 30 min, with a flow rate of 15 mL/min; monitored by UV absorbance at 210 nm) to provide the product (**FSA-212022** • HCO₂H, 11.8 mg, 89%, 2 steps) as a brilliant white solid.

¹H NMR (600 MHz, CD₃OD) δ 8.37 (br, 1H), 8.26 (s, 1H), 4.90 (app t, $J = 12.7$ Hz, 1H), 4.75 (d, $J = 14.4$ Hz, 1H), 4.50–4.47 (m, 1H), 4.43–4.39 (m, 2H), 4.41 (dt, $J = 47.5, 6.0$ Hz, 2H), 4.14–4.08 (m, 3H), 4.05–4.02 (m, 2H), 3.78 (app p, $J = 6.1$ Hz, 1H), 3.71 (d, $J = 9.6$ Hz, 1H), 3.43 (d, $J = 9.3$ Hz, 1H), 3.13 (app t, $J = 12.4$ Hz, 1H), 2.86 (s, 6H), 2.21–2.10 (m, 2H), 2.00 (d, $J = 15.2$ Hz, 1H), 1.93–1.88 (m, 1H), 1.71–1.62 (m, 3H), 1.57 (app q, $J = 11.3$ Hz, 1H), 1.46–1.37 (m, 3H), 1.35–1.31 (m, 2H), 1.08 (d, $J = 6.2$ Hz, 3H).

¹³C NMR (126 MHz, CD₃OD) δ 171.3, 138.6, 128.2, 84.7 (d, $J = 163.7$ Hz), 77.4, 72.1, 71.9, 70.5, 68.7, 68.2, 60.7, 56.8, 52.6, 47.2, 45.9, 43.1, 38.7, 37.4, 33.1, 31.6 (d, $J = 19.6$ Hz), 30.6, 28.7, 23.8 (d, $J = 5.1$ Hz), 19.5.

FTIR (neat, cm⁻¹): 3385 (br), 1675 (s), 1583 (w), 1202 (s), 1134 (m), 1085 (w), 722 (w).

HRMS (ESI+, m/z): [M+H]⁺ calc'd for C₂₅H₄₅FN₆O₆, 545.3457; found 545.3468.



Synthetic lincosamide FSA-212019.

In a 1-mL glass fitted with a magnetic stir bar, azide **3.65** (11.6 mg, 20.8 μmol , 1 equiv) was dissolved in 2:2:1 *tert*-butanol–methanol–water (138 μL). To this solution were then added 2-ethynylpyridine (4.16 μL , 41.5 μmol , 2.00 equiv), aqueous sodium ascorbate solution (0.100 M, 41.5 μL , 4.15 μmol , 0.200 equiv), and aqueous cupric sulfate solution (0.100 M, 10.4 μL , 1.04 μmol , 0.0500 equiv). This mixture was stirred at 23 $^{\circ}\text{C}$ for 1.5 h, by which time LCMS analysis showed that no starting material remained. The reaction mixture was diluted with 50% v/v saturated aqueous sodium bicarbonate solution–saturated aqueous sodium chloride solution, and this diluted mixture was extracted with dichloromethane (3 \times 3 mL). The combined organic extracts were dried over sodium sulfate, filtered, and concentrated to give a colorless oil.

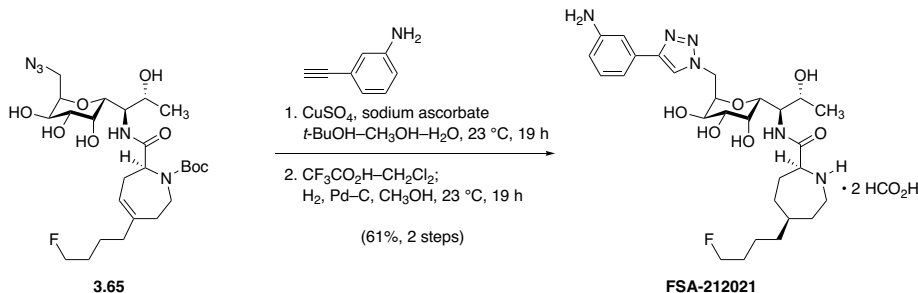
This residue was transferred to a 4-mL glass vial, where it was re-dissolved in 33% v/v trifluoroacetic acid–dichloromethane (600 μL). After 10 min of stirring at 23 $^{\circ}\text{C}$, LCMS analysis showed that Boc removal was complete; the mixture was diluted with toluene (1 mL), and the diluted mixture was concentrated to dryness. This residue was purified by preparative HPLC on a Waters SunFire Prep C₁₈ column (5 μm , 250 \times 19 mm; eluting with 0.1% formic acid–2% acetonitrile–water initially, grading to 0.1% formic acid–20% acetonitrile–water over 30 min, with a flow rate of 15 mL/min; monitored by UV absorbance at 210 nm) to provide the product (**FSA-212019** \cdot HCO₂H, 4.5 mg, 34%, 2 steps) as a brilliant white solid.

^1H NMR (600 MHz, CD_3OD) δ 8.59 (d, $J = 4.9$ Hz, 1H), 8.47 (s, 1H), 8.28 (br, 2H), 8.06 (d, $J = 7.9$ Hz, 1H), 7.92 (td, $J = 7.8, 1.7$ Hz, 1H), 7.38 (dd, $J = 7.0, 5.4$ Hz, 1H), 5.67 (app t, $J = 1$ Hz, 1H), 4.92 (dd, $J = 14.9, 11.3$ Hz, 1H), 4.78 (dd, $J = 14.9, 3.0$ Hz, 1H), 4.54 (ddd, $J = 11.3, 6.3, 2.9$ Hz, 1H), 4.43 (dt, $J = 47.5, 6.0$ Hz, 2H), 4.16 (dd, $J = 9.8, 6.3$, 1H), 4.09–4.05 (m, 3H), 4.00 (dd, $J = 9.1, 3.1$ Hz, 1H), 3.83 (app p, $J = 6.3$ Hz, 1H), 3.72 (dd, $J = 9.8, 3.1$ Hz, 1H), 3.44 (ddd, $J = 13.4, 7.5, 1.9$ Hz, 1H), 3.16 (dd, $J = 12.4, 9.6$ Hz, 1H), 2.69–2.62 (m, 2H), 2.57 (dd, $J = 17.3, 10.0$ Hz, 1H), 2.46 (dd, $J = 17.0, 7.1$ Hz, 1H), 2.12 (app t, $J = 7.5$ Hz, 2H), 1.72–1.64 (m, 2H), 1.56–1.51 (m, 2H), 1.09 (d, $J = 6.4$ Hz, 3H).

^{13}C NMR (126 MHz, CD_3OD) δ 170.4, 166.8, 151.1, 150.5, 148.8, 145.2, 138.9, 124.6, 124.5, 122.8, 121.6, 84.6 (163.7 Hz), 77.6, 72.1, 72.0, 70.9, 68.8, 67.6, 60.3, 57.4, 47.1, 45.1, 39.7, 31.1 (d, $J = 19.6$ Hz), 30.3, 29.9, 24.4 (d, $J = 5.0$ Hz), 19.6.

FTIR (neat, cm^{-1}): 3298 (br), 1673 (s), 1598 (s), 1572 (s), 1424 (m), 1202 (m), 1086 (m), 1067 (m), 787 (m).

HRMS (ESI+, m/z): $[\text{M}+\text{H}]^+$ calc'd for $\text{C}_{27}\text{H}_{39}\text{FN}_6\text{O}_6$, 563.3; found 563.3.



Synthetic lincosamide FSA-212021.

In a 1-mL glass fitted with a magnetic stir bar, azide **3.65** (11.6 mg, 20.8 μmol , 1 equiv) was dissolved in 2:2:1 *tert*-butanol–methanol–water (138 μL). To this solution were then added 3-ethynylaniline (4.76 μL , 41.5 μmol , 2.00 equiv), aqueous sodium ascorbate solution (0.100 M, 41.5 μL , 4.15 μmol , 0.200 equiv), and aqueous cupric sulfate solution (0.100 M, 10.4 μL , 1.04 μmol , 0.0500 equiv). This mixture was stirred at 23 °C for 1.5 h, by which time LCMS analysis showed that no starting material remained. The reaction mixture was diluted with 50% v/v saturated aqueous sodium bicarbonate solution–saturated aqueous sodium chloride solution, and this diluted mixture was extracted with dichloromethane (3 \times 3 mL). The combined organic extracts were dried over sodium sulfate, filtered, and concentrated to give a colorless oil.

This residue was transferred to a 4-mL glass vial, where it was re-dissolved in 33% v/v trifluoroacetic acid–dichloromethane (600 μL). After 10 min of stirring at 23 °C, LCMS analysis showed that Boc removal was complete; the mixture was diluted with toluene (1 mL), and the diluted mixture was concentrated to dryness. This residue was then dissolved in methanol (300 μL), the solution was treated with palladium on carbon (10% w/w, 7.00 mg), and the headspace above the reaction mixture was replaced with hydrogen gas. The black suspension was stirred at 23 °C under hydrogen gas (1 atm) for 19 h, whereupon LCMS analysis showed that azepine hydrogenation was complete. The mixture was filtered through a Celite pad to remove the

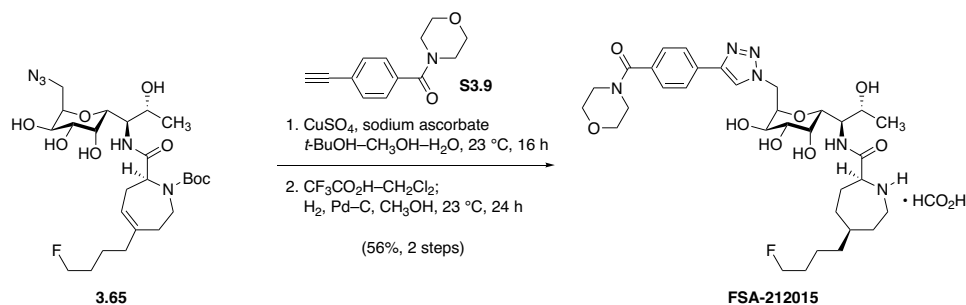
heterogeneous catalyst, and the filter cake was rinsed with methanol (3×1 mL). The filtrate was concentrated to give a colorless oil, which was purified by preparative HPLC on a Waters SunFire Prep C₁₈ column (5 μ m, 250 \times 19 mm; eluting with 0.1% formic acid–2% acetonitrile–water initially, grading to 0.1% formic acid–30% acetonitrile–water over 30 min, with a flow rate of 20 mL/min; monitored by UV absorbance at 210 nm) to provide the product (**FSA-212021** • HCO₂H, 7.3 mg, 61%, 2 steps) as a brilliant white solid.

¹H NMR (600 MHz, CD₃OD) δ 8.28 (s, 1H), 8.19 (br, 2H), 7.19–7.13 (m, 3H), 6.72 (dd, $J = 7.7$, 2.1 Hz, 1H), 4.89–4.87 (m, 2H), 4.73 (dd, $J = 14.9$, 2.9 Hz, 1H), 4.52–4.49 (m, 1H), 4.41 (dt, $J = 47.5$, 6.0 Hz, 2H), 4.17–4.11 (m, 3H), 4.05–4.04 (m, 2H), 3.83 (app p, $J = 6.2$ Hz, 1H), 3.72 (dd, $J = 9.9$, 3.2 Hz, 1H), 3.42 (dd, $J = 13.4$, 5.6 Hz, 1H), 3.14 (app t, $J = 12.7$ Hz, 1H), 2.19–2.08 (m, 2H), 2.00 (d, $J = 14.8$ Hz, 1H), 1.91 (app ddt, $J = 16.1$, 8.4, 4.2 Hz, 1H), 1.71–1.62 (m, 3H), 1.57 (app q, $J = 11.5$ Hz, 1H), 1.45–1.38 (m, 3H), 1.35–1.31 (m, 2H), 1.09 (d, $J = 6.2$ Hz, 3H).

¹³C NMR (126 MHz, CD₃OD) δ 171.1, 165.7, 149.5, 149.2, 132.3, 130.7, 122.6, 116.7, 116.6, 113.5, 84.7 (d, $J = 163.6$ Hz), 77.5, 72.0, 71.9, 70.7, 68.6, 67.8, 60.7, 57.1, 46.8, 45.9, 38.7, 37.4, 33.0, 31.6 (d, $J = 19.7$ Hz), 30.7, 28.7, 23.8 (d, $J = 5.1$ Hz), 19.4.

FTIR (neat, cm⁻¹): 3322 (br), 2935 (m), 1675 (s), 1590 (s), 1459 (m), 1202 (m), 1132 (m), 1083 (m), 1067 (m).

HRMS (ESI+, m/z): [M+2H]²⁺ calc'd for C₂₈H₄₃FN₆O₆, 290.1687; found 290.1693.



Synthetic lincosamide FSA-212015.

In a 1-mL glass fitted with a magnetic stir bar, azide **3.65** (14.3 mg, 25.6 μmol , 1 equiv) was dissolved in 2:2:1 *tert*-butanol–methanol–water (170 μL). To this solution were then added (4-ethynylphenyl)(morpholino)methanone (**S3.9**, 11.0 mg, 51.1 μmol , 2.00 equiv), aqueous sodium ascorbate solution (0.100 M, 51.1 μL , 5.11 μmol , 0.200 equiv), and aqueous cupric sulfate solution (0.100 M, 12.8 μL , 1.28 μmol , 0.0500 equiv). This mixture was stirred at 23 °C for 16 h, by which time LCMS analysis showed that no starting material remained. The reaction mixture was diluted with 50% v/v saturated aqueous sodium bicarbonate solution–saturated aqueous sodium chloride solution, and this diluted mixture was extracted with dichloromethane (3 \times 3 mL). The combined organic extracts were dried over sodium sulfate, filtered, and concentrated to give a colorless oil.

This residue was transferred to a 4-mL glass vial, where it was re-dissolved in 33% v/v trifluoroacetic acid–dichloromethane (600 μL). After 10 min of stirring at 23 °C, LCMS analysis showed that Boc removal was complete; the mixture was diluted with toluene (1 mL), and the diluted mixture was concentrated to dryness. This residue was then dissolved in methanol (300 μL), the solution was treated with palladium on carbon (10% w/w, 10.0 mg), and the headspace above the reaction mixture was replaced with hydrogen gas. The black suspension was stirred at 23 °C under hydrogen gas (1 atm) for 24 h, whereupon LCMS analysis showed that azepine

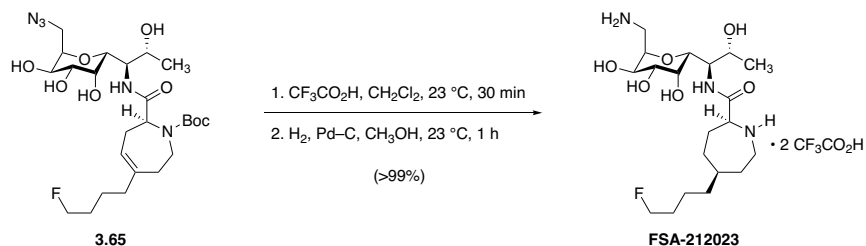
hydrogenation was complete. The mixture was filtered through a Celite pad to remove the heterogeneous catalyst, and the filter cake was rinsed with methanol (3×1 mL). The filtrate was concentrated to give a colorless oil, which was purified by preparative HPLC on a Waters SunFire Prep C₁₈ column (5 μ m, 250 \times 19 mm; eluting with 0.1% formic acid–2% acetonitrile–water initially, grading to 0.1% formic acid–40% acetonitrile–water over 30 min, with a flow rate of 15 mL/min; monitored by UV absorbance at 280 nm) to provide the product (**FSA-212015** • HCO₂H, 9.6 mg, 56%, 2 steps) as a brilliant white solid.

¹H NMR (600 MHz, CD₃OD) δ 8.49 (s, 1H), 8.29 (br, 1H), 7.95 (d, $J = 8.2$ Hz, 2H), 7.53 (d, $J = 8.2$ Hz, 2H), 4.90 (dd, $J = 14.9, 11.4$ Hz, 1H), 4.77 (dd, $J = 15.0, 2.9$ Hz, 1H), 4.51 (ddd, $J = 11.4, 6.4, 2.9$ Hz, 1H), 4.41 (dt, $J = 47.5, 6.0$ Hz, 2H), 4.18–4.11 (m, 3H), 4.06–4.05 (m, 2H), 3.85–3.47 (m, 10H), 3.41 (ddd, $J = 13.9, 5.8, 2.4$ Hz, 1H), 3.14 (app t, $J = 12.4$ Hz, 1H), 2.18 (app ddt, $J = 16.5, 8.4, 4.1$ Hz, 1H), 2.11 (app dtd, $J = 15.6, 7.6, 3.7$ Hz, 1H), 2.00 (app dt, $J = 15.7, 4.1$ Hz, 1H), 1.91 (app ddt, $J = 14.9, 8.0, 4.1$ Hz, 1H), 1.71–1.62 (m, 3H), 1.56 (app dtd, $J = 15.3, 11.1, 2.3$ Hz, 1H), 1.46–1.38 (m, 3H), 1.36–1.32 (m, 2H), 1.09 (d, $J = 6.4$ Hz, 3H).

¹³C NMR (126 MHz, CD₃OD) δ 170.7, 169.8, 165.6, 146.6, 134.7, 132.3, 127.6, 125.4, 122.0, 83.3 (d, $J = 163.2$ Hz), 76.1, 70.6, 69.3, 67.2, 66.4, 59.3, 55.7, 45.5, 44.6, 37.3, 36.0, 31.7, 30.2 (d, $J = 19.6$ Hz), 39.3, 27.3, 22.5 (d, $J = 5.0$ Hz), 18.1.

FTIR (neat, cm⁻¹): 3358 (br), 2936 (m), 1672 (m), 1601 (s), 1459 (m), 1438 (m), 1280 (m), 1114 (m), 1068 (m).

HRMS (ESI+, m/z): [M+H]⁺ calc'd for C₃₃H₄₉FN₆O₈, 677.3669; found 677.3683.



Synthetic lincosamide FSA-212023.

In a 4-mL glass vial, at 23 °C, trifluoroacetic acid (100 μL) was added to a suspension of azide **3.65** (50 mg, 89 μmol , 1 equiv) in dichloromethane (200 μL). After stirring for 30 min, LCMS analysis showed that Boc removal was complete, and the mixture was diluted with toluene (1 mL). The diluted mixture was concentrated to dryness, and the residue was re-dissolved in methanol (500 μL). This solution was treated with palladium on carbon (10% w/w, 25 mg), the headspace of the vial was replaced with hydrogen gas, and the black suspension was stirred under hydrogen gas (1 atm) at 23 °C. After 1 h, LCMS analysis showed that azepine hydrogenation was complete, and the mixture was filtered through a Celite pad to remove heterogeneous catalyst. The filter cake was rinsed with methanol (3×1 mL), and the filtrate was concentrated to give the product as a colorless oil (61 mg, 103%).

An analytically pure sample was prepared by subjecting a small quantity of crude product (~6 mg) to preparative HPLC on a Waters SunFire Prep C₁₈ column (5 μm , 250 \times 19 mm; eluting with 0.1% formic acid–2% acetonitrile–water initially, grading to 0.1% formic acid–25% acetonitrile–water over 30 min, with a flow rate of 15 mL/min; monitored by UV absorbance at 280 nm) to provide the product (**FSA-212023** • HCO₂H) as a brilliant white solid.

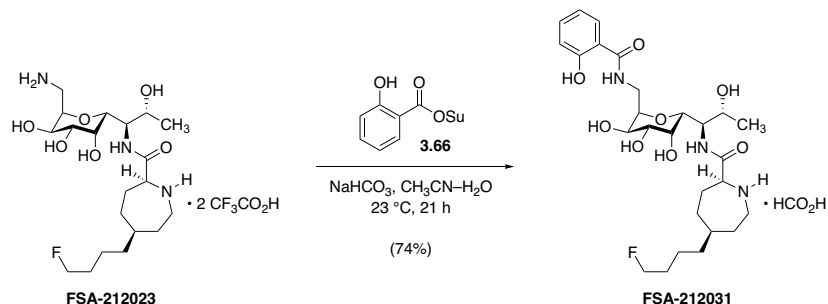
¹H NMR (hydroformate salt, 600 MHz, CD₃OD) δ 8.51 (br, 2H), 4.42 (dt, $J = 47.6, 6.0$ Hz, 2H), 4.26–4.24 (m, 1H), 4.10 (dd, $J = 7.7, 4.4$ Hz, 1H), 4.07 (dd, $J = 9.4, 6.5$ Hz, 1H), 4.01 (br,

1H), 3.96–3.92 (m, 2H), 3.86 (d, $J = 8.2$ Hz, 1H), 3.57 (d, $J = 8.6$ Hz, 1H), 3.39–3.33 (m, 2H), 3.24 (dd, $J = 13.4, 4.0$ Hz, 1H), 3.08 (app t, $J = 12.3$ Hz, 1H), 2.17–2.09 (m, 2H), 1.99 (d, $J = 15.0$ Hz, 1H), 1.90–1.86 (m, 1H), 1.71–1.61 (m, 3H), 1.55 (app q, $J = 11.5$ Hz, 1H), 1.46–1.38 (m, 3H), 1.36–1.32 (m, 2H), 1.30 (d, $J = 6.5$ Hz, 3H).

^{13}C NMR (hydroformate salt, 126 MHz, CD_3OD) δ 171.9, 169.8, 84.7 (d, $J = 163.8$ Hz), 74.1, 72.0, 71.5, 70.8, 70.1, 68.6, 60.6, 55.6, 45.6, 39.1, 37.4, 36.8, 33.8, 31.6 (d, $J = 19.7$ Hz), 30.6, 28.8, 23.9 (d, $J = 5.0$ Hz), 22.1.

FTIR (hydroformate salt, neat, cm^{-1}): 3246 (br), 2936 (m), 1670 (m), 1585 (s), 1377 (w), 1348 (m), 1078 (m).

HRMS (ESI+, m/z): $[\text{M}+\text{H}]^+$ calc'd for $\text{C}_{20}\text{H}_{38}\text{FN}_3\text{O}_6$, 436.2817; found 436.2830.



Synthetic lincosamide FSA-212031.

In a 16 × 100 mm glass test tube, diamine **FSA-212023** • 2 CF₃CO₂H (12 mg, 18 μmol, 1 equiv) was dissolved in water (300 μL). A solution of 2,5-dioxopyrrolidin-1-yl 2-hydroxybenzoate (**3.66**, 4.7 mg, 20 μmol, 1.1 equiv)¹⁵³ in acetonitrile (1.5 mL) was added, and the mixture was basified with the addition of saturated aqueous sodium bicarbonate solution (~20 μL), until pH 8–9 was achieved. After 1 h, LCMS showed the reaction had stalled due to acidification of the reaction mixture; additional sodium bicarbonate solution was added to re-establish pH 8–9. After 20 h of additional stirring, LCMS showed that no starting material remained. The mixture was concentrated to dryness, and the residue was purified by preparative HPLC on a Waters SunFire Prep C₁₈ column (5 μm, 250 × 19 mm; eluting with 0.1% formic acid–2% acetonitrile–water initially, grading to 0.1% formic acid–30% acetonitrile–water over 30 min, with a flow rate of 15 mL/min; monitored by UV absorbance at 254 nm) to provide **FSA-212031** • HCO₂H as an eggshell-white powder (8.0 mg, 74%).

¹H NMR (500 MHz, CD₃OD) δ 8.44 (br, 1H), 7.82 (d, *J* = 7.8 Hz, 1H), 7.38 (t, *J* = 7.7 Hz, 1H), 6.91 (d, *J* = 8.8 Hz, 1H), 4.41 (dt, *J* = 47.6, 6.0 Hz, 2H), 4.26–4.20 (m, 2H), 4.08 (dd, *J* =

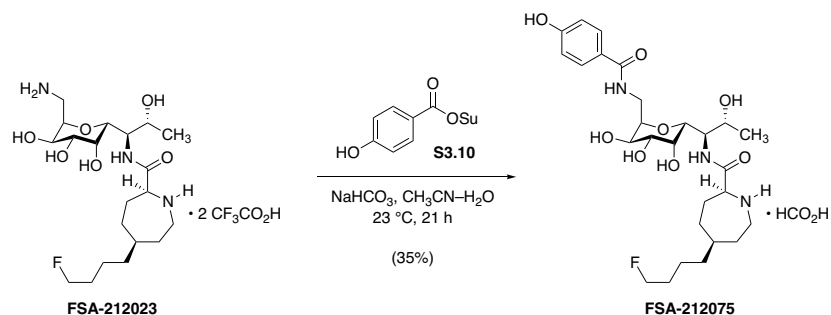
¹⁵³ Zhou, L.-S.; Yang, K.-W.; Feng, L.; Xiao, J.-M.; Liu, C.-C.; Zhang, Y.-L.; Crowder, M. W. *Bioorg. Med. Chem. Lett.* **2013**, *23*, 949–954.

10.0, 6.4 Hz, 1H), 4.05–4.00 (m, 2H), 3.94 (d, $J = 3.1$ Hz, 1H), 3.91–3.84 (m, 2H), 3.69 (dd, $J = 11.0, 3.5$ Hz, 1H), 3.67 (dd, $J = 6.3, 3.3$ Hz, 1H), 3.40 (dd, $J = 13.6, 4.7$ Hz, 1H), 3.09 (app t, $J = 12.4$ Hz, 1H), 2.20–2.08 (m, 2H), 2.00–1.97 (m, 1H), 1.88 (ddd, $J = 15.2, 8.1, 3.9$ Hz, 1H), 1.71–1.52 (m, 4H), 1.46–1.37 (m, 3H), 1.35–1.30 (m, 2H), 1.10 (d, $J = 6.4$ Hz, 3H).

^{13}C NMR (126 MHz, CD_3OD) δ 171.6, 170.8, 168.9, 160.7, 134.7, 129.4, 120.2, 118.3, 117.3, 84.7 (d, $J = 163.7$), 76.8, 71.8 ($2 \times \text{C}$), 70.6, 68.9, 68.6, 60.6, 56.2, 45.8, 38.9, 37.4, 35.6, 33.3, 31.6 (d, $J = 19.7$ Hz), 30.6, 28.8, 23.9 (d, $J = 5.0$ Hz), 19.1.

FTIR (neat, cm^{-1}): 3309 (br), 2935 (m), 1672 (m), 1634 (m), 1591 (s), 1376 (m), 1347 (m), 1077 (m), 757 (m).

HRMS (ESI+, m/z): $[\text{M}+\text{H}]^+$ calc'd for $\text{C}_{27}\text{H}_{42}\text{FN}_3\text{O}_8$, 556.3029; found 556.3054.



Synthetic lincosamide FSA-212075.

A 12 × 75 mm glass test tube was charged with a magnetic stir bar, diamine **FSA-212023** • 2 CF₃CO₂H (15 mg, 23 μmol), and water (377 μL). A solution of 2,5-dihydroxybenzoate (**S3.10**, 5.9 mg, 25 μmol, 1.1 equiv)¹⁵⁴ in acetonitrile (1.9 mL) was added next. Finally, the pH of the mixture was adjusted to pH 8–9 with the addition of aqueous sodium bicarbonate solution (1.1 M, 40 μL, 44 μmol, 1.9 equiv). After 21 h of stirring at 23 °C, LCMS analysis showed that no starting material remained. The mixture was concentrated to dryness, and the residue was subjected to preparative HPLC on a Waters SunFire Prep C₁₈ column (5 μm, 250 × 19 mm; eluting with 0.1% formic acid–5% acetonitrile–water initially, grading to 0.1% formic acid–30% acetonitrile–water over 30 min, with a flow rate of 15 mL/min; monitored by UV absorbance at 254 nm) to provide **FSA-212075** • HCO₂H as a brilliant white solid (4.7 mg, 35%).

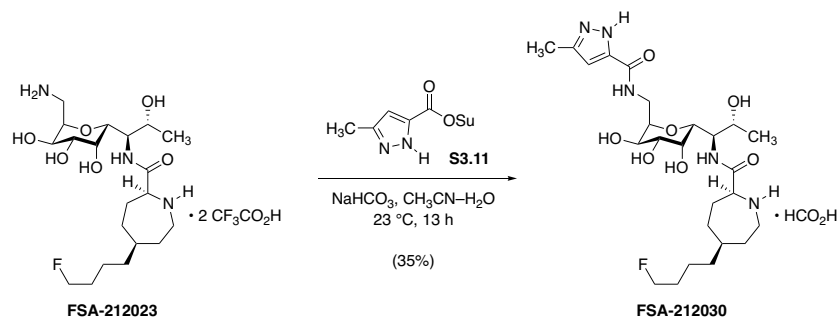
¹H NMR (600 MHz, CD₃OD) δ 8.46 (br, 1H), 7.73 (d, *J* = 8.7 Hz, 2H), 6.83 (d, *J* = 8.8 Hz, 2H), 4.41 (dt, *J* = 47.5, 6.0 Hz, 2H), 4.22 (ddd, *J* = 11.3, 6.4, 3.5 Hz, 1H), 4.17 (dd, *J* = 8.3, 5.0 Hz, 1H), 4.06 (d, *J* = 10.0, 6.4 Hz, 1H), 4.01 (dd, *J* = 6.0, 4.8 Hz, 1H), 3.95 (qd, *J* = 6.5, 1.5 Hz), 3.92–3.88 (m, 3H), 3.66 (dd, *J* = 10.0, 3.2 Hz, 1H), 3.59 (dd, *J* = 14.6, 3.6 Hz,

¹⁵⁴ Barré, A.; Tîntaş, M.-L.; Alix, F.; Gembus, V.; Papamicaël, C.; Levacher, V. *J. Org. Chem.* **2015**, *80*, 6537–6544.

1H), 3.40 (ddd, $J = 13.8, 5.6, 1.9$ Hz, 1H), 3.08 (app t, $J = 12.3$ Hz, 1H), 2.19–2.08 (m, 2H), 2.00–1.97 (m, 1H), 1.88 (app ddt, $J = 15.5, 8.4, 4.1$ Hz, 1H), 1.71–1.52 (m, 4H), 1.45–1.38 (m, 3H), 1.37–1.31 (m, 2H), 1.10 (d, $J = 6.5$ Hz, 3H).

FTIR (neat, cm^{-1}): 3271 (br), 2934 (m), 1671 (m), 1607 (s), 1580 (s), 1448 (s), 1348 (m), 1281 (m), 1077 (m), 743 (m).

HRMS (ESI+, m/z): $[\text{M}+\text{H}]^+$ calc'd for $\text{C}_{27}\text{H}_{42}\text{FN}_3\text{O}_8$, 556.3038; found 556.3036.



Synthetic lincosamide FSA-212030.

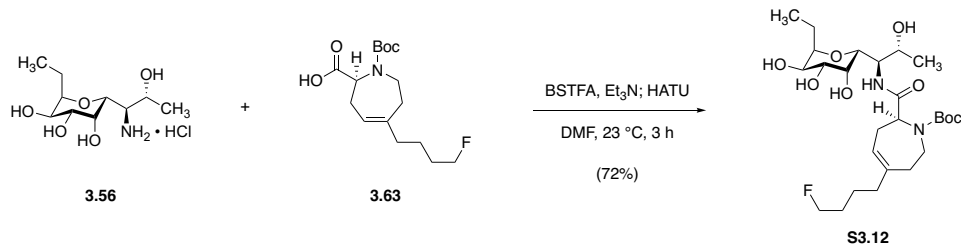
In a 16 × 100 mm glass test tube, diamine **FSA-212023** • 2 CF₃CO₂H (12 mg, 18 μmol, 1 equiv) was dissolved in water (300 μL). A solution of 2,5-dioxopyrrolidin-1-yl 3-methyl-1H-pyrazole-5-carboxylate (**S3.11**, 4.4 mg, 20 μmol, 1.1 equiv) in acetonitrile (1.5 mL) was added, and the mixture was basified with the addition of saturated aqueous sodium bicarbonate solution (~20 μL), until pH 8–9 was achieved. After 13 h of stirring at 23 °C, LCMS analysis indicated that no starting material remained. The mixture was concentrated to dryness, and the residue was subjected to preparative HPLC on a Waters SunFire Prep C₁₈ column (5 μm, 250 × 19 mm; eluting with 0.1% formic acid–2% acetonitrile–water initially, grading to 0.1% formic acid–30% acetonitrile–water over 30 min, with a flow rate of 15 mL/min; monitored by UV absorbance at 254 nm) to provide **FSA-212030** • HCO₂H as a white solid (3.7 mg, 35%).

¹H NMR (500 MHz, CD₃OD) δ 8.44 (br, 1H), 6.50 (s, 1H), 4.42 (dt, *J* = 47.6, 6.0 Hz, 2H), 4.23–4.17 (m, 1H), 4.12 (app t, *J* = 6.4 Hz, 1H), 4.08 (dd, *J* = 9.7, 6.7 Hz, 1H), 4.04–4.02 (m, 2H), 3.94–3.87 (m, 3H), 3.66 (d, *J* = 9.9 Hz, 1H), 3.55 (d, *J* = 14.6 Hz, 1H), 3.44 (dd, *J* = 14.0, 5.5 Hz, 1H), 3.14 (app t, *J* = 12.5 Hz, 1H), 2.32 (s, 3H), 2.16–2.07 (m, 2H), 2.02 (dd, *J* = 13.1, 5.0 Hz, 1H), 1.91–1.83 (m, 1H), 1.72–1.67 (m, 1H), 1.67–1.54 (m, 3H), 1.48–1.39 (m, 3H), 1.37–1.32 (m, 2H), 1.11 (d, *J* = 6.4 Hz, 3H).

^{13}C NMR (100 MHz, CD_3OD) δ 171.4, 169.0, 165.1, 147.4, 142.6, 105.1, 84.7 (d, $J = 163.6$ Hz),
77.1, 72.5, 71.9, 70.9, 68.9, 67.8, 60.7, 57.0, 45.7, 39.0, 37.3, 35.2, 33.3, 31.6 (d, $J = 19.8$
Hz), 30.5, 28.7, 23.9 (d, $J = 5.1$ Hz), 19.5, 10.7.

FTIR (neat, cm^{-1}): 3267 (br), 2931 (m), 1639 (s), 1582 (s), 1420 (m), 1346 (w), 1078 (m).

HRMS (ESI+, m/z): $[\text{M}+\text{Na}]^+$ calc'd for $\text{C}_{25}\text{H}_{42}\text{FN}_5\text{O}_7$, 566.2960; found 566.2975.



Protected lincosamide S3.12.

In a 4-mL glass vial fitted with a magnetic stir bar, aminotetraol **3.56** • HCl (54 mg, 0.20 mmol, 1 equiv) was dissolved in *N,N*-dimethylformamide (990 μ L), and triethylamine (120 μ L, 0.84 mmol, 4.2 equiv) was added. The mixture was chilled to 0 °C before *N,O*-bis(trimethylsilyl)trifluoroacetamide (110 μ L, 0.40 mmol, 2.0 equiv) was added; the mixture was then warmed to 23 °C and was stirred for 1 h to ensure complete *O*-silylation. This mixture was then transferred by cannula to a separate 4-mL glass vial containing azepine acid **3.63** (70 mg, 0.22 mmol, 1.1 equiv) that had been dried by azeotropic removal of benzene, and HATU (98 mg, 0.26 mmol, 1.3 equiv) was added. The resulting yellow solution was stirred at 23 °C for 3 h. The reaction mixture was then diluted with ethyl acetate (15 mL), and this solution was washed sequentially with 10-mL portions of 10% w/v aqueous citric acid solution, saturated aqueous sodium bicarbonate solution, and saturated aqueous sodium chloride solution. The washed organic solution was then dried over sodium sulfate, filtered, and concentrated. The residue was re-dissolved in 50% v/v acetic acid–methanol, and the resulting solution was stirred at 40 °C overnight in order to remove pendant trimethylsilyl groups from the coupled product. The mixture was then concentrated, and the crude residue was purified by flash-column chromatography (12 g silica gel, eluting with dichloromethane initially, grading to 10% methanol–dichloromethane) to provide the product as a white solid (76 mg, 72%).

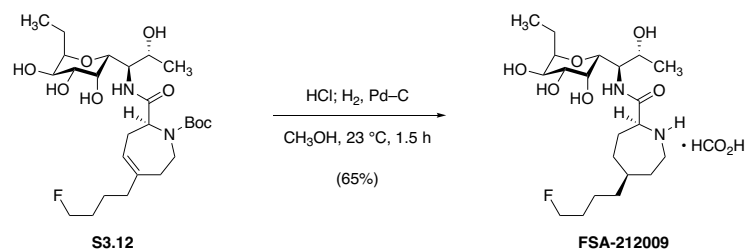
$R_f = 0.32$ (10% methanol–dichloromethane, I_2).

^1H NMR (1:1 ratio of rotamers, asterisk [*] denotes rotamer peaks that could be resolved; 600 MHz, CD_3OD) δ 8.07 (d, $J = 8.9$ Hz, 1H), 7.90 (d, $J = 9.3$ Hz, 1H),* 5.49 (d, $J = 6.2$ Hz, 1H), 5.46 (d, $J = 6.2$ Hz, 1H),* 4.49–4.42 (m, 2H), 4.36 (q, $J = 6.1$ Hz, 1H), 4.07–4.01 (m, 1H), 4.01–3.95 (m, 2H), 3.94–3.92 (m, 1H), 3.87–3.80 (m, 3H), 3.71 (d, $J = 7.5$ Hz, 1H),* 3.67 (ddd, $J = 15.3, 11.7, 3.9$ Hz, 1H), 3.59–3.56 (m, 1H), 2.77–2.69 (m, 1H), 2.50–2.38 (m, 2H), 2.34–2.32 (m, 1H), 2.01–1.97 (m, 2H), 1.67–1.59 (m, 4H), 1.53–1.49 (m, 2H), 1.48 (s, 9H), 1.45 (s, 9H),* 1.21 (d, $J = 6.3$ Hz, 3H), 1.18 (d, $J = 6.3$ Hz, 3H),* 0.96 (t, $J = 7.5$ Hz, 3H), 0.95 (t, $J = 7.5$ Hz, 3H).

^{13}C NMR (1:1 ratio of rotamers, asterisk [*] denotes rotamer peaks that could be resolved; 126 MHz, CD_3OD) δ 175.4, 175.3,* 157.7, 157.1,* 142.7, 142.5,* 120.4, 120.2,* 84.7 (d, $J = 163.8$ Hz) 82.0, 81.7,* 79.9, 79.8,* 71.5, 71.4,* 71.1, 70.9,* 70.6, 69.6, 69.5,* 68.9, 68.8,* 63.5, 62.6,* 57.8, 56.8,* 41.8, 41.2,* 39.5, 39.3,* 34.9, 34.2,* 31.0 (d, $J = 19.9$ Hz), 30.9 (d, $J = 19.9$ Hz),* 28.8, 28.7, 28.3,* 24.8 (d, $J = 4.8$ Hz), 24.6 (d, $J = 4.8$ Hz),* 20.7, 19.6,* 17.6, 11.0, 10.9.*

FTIR (neat, cm^{-1}): 3397 (br), 2970 (m), 2935 (m), 1655 (s), 1453 (m), 1410 (s), 1368 (m), 1165 (s), 1080 (s).

HRMS (ESI+, m/z): $[\text{M}+\text{H}]^+$ calc'd for $\text{C}_{26}\text{H}_{45}\text{FN}_2\text{O}_8$, 533.3233; found 533.3256.



Synthetic lincosamide FSA-212009.

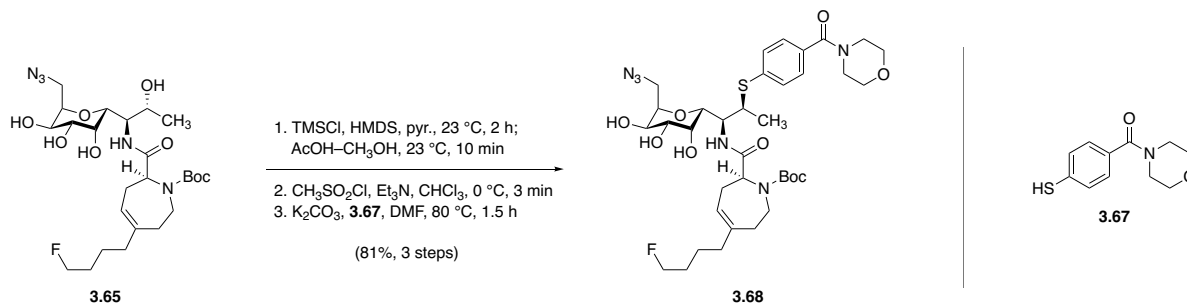
A 4-mL glass vial was charged with hydrogen chloride solution (4.0 M in 1,4-dioxane, 750 μ L), and this solution was chilled to 0 $^{\circ}$ C in an ice-water bath. Azepine **S3.12** (20 mg, 38 μ mol, 1 equiv) was then added, the cooling bath was removed, and the resulting solution was stirred at 23 $^{\circ}$ C for 35 min, whereupon LCMS analysis showed that Boc removal was complete. The mixture was diluted with toluene (1 mL), and the mixture was concentrated *in vacuo*. Residual dioxane was removed by re-concentration from 50% v/v methanol–toluene. The dried residue was then re-dissolved in methanol (1.0 mL), and the solution was treated with palladium on carbon (10% w/w, 10 mg). Hydrogen gas was bubbled through the black suspension for 5 min, and then the mixture was stirred under hydrogen gas (1 atm) at 23 $^{\circ}$ C for 1.5 h, whereupon LCMS analysis showed that olefin hydrogenation was complete. The reaction mixture was filtered through a pad of Celite, the filter cake was rinsed with fresh methanol (2×5 mL), and the filtrate was concentrated to give a colorless film. This residue was purified by preparative HPLC on a Waters SunFire Prep C₁₈ column (5 μ m, 250 \times 19 mm; eluting with 0.1% formic acid–2% acetonitrile–water initially, grading to 0.1% formic acid–50% acetonitrile–water over 40 min, with a flow rate of 15 mL/min; monitored by UV absorbance at 210 nm) to provide the product (**FSA-212009** \cdot HCO₂H, 12 mg, 65%) as a white solid.

^1H NMR (600 MHz, CD_3OD) δ 8.43 (s, 1H), 4.42 (dt, $J = 47.5, 6.0$ Hz, 2H), 4.23 (dd, $J = 8.5, 5.7$ Hz, 4.09–4.05 (m, 2H), 3.96 (dd, $J = 10.0, 6.2$ Hz, 1H), 3.90 (d, $J = 3.1$ Hz, 1H), 3.83 (ddd, $J = 11.3, 6.2, 3.3$ Hz, 1H), 3.64 (d, $J = 8.4$ Hz, 1H), 3.57 (dd, $J = 10.1, 3.1$ Hz, 1H), 3.42 (ddd, $J = 13.7, 6.0, 2.1$ Hz, 1H), 3.11 (app t, $J = 12.4$ Hz, 1H), 2.21–2.11 (m, 2H), 2.00 (app dt, $J = 15.3, 3.9$ Hz, 1H), 1.90 (app ddt, $J = 15.4, 8.1, 4.0$ Hz, 1H), 1.71–1.54 (m, 6H), 1.54–1.46 (m, 3H), 1.36–1.32 (m, 2H), 1.17 (d, $J = 6.3$ Hz, 3H), 0.96 (t, $J = 7.4$ Hz, 3H).

^{13}C NMR (126 MHz, CD_3OD) δ 171.7, 168.8, 84.7 (d, $J = 163.6$ Hz), 80.1, 71.6, 70.8, 70.7, 69.5, 68.1, 60.7, 56.5, 45.8, 38.9, 37.4, 33.3, 31.6 (d, $J = 19.6$ Hz), 30.6, 28.8, 23.8 (d, $J = 5.0$ Hz), 18.6, 17.5, 11.1.

FTIR (neat, cm^{-1}): 3281 (br), 2935 (m), 1670 (m), 1589 (s), 1346 (m), 1080 (s).

HRMS (ESI+, m/z): $[\text{M}+\text{H}]^+$ calc'd for $\text{C}_{32}\text{H}_{39}\text{FN}_2\text{O}_6$, 435.2865; found 435.2884.



Protected lincosamide **3.68**.

In a 2–5 mL glass microwave vial, an ice-cold solution of tetraol **3.65** (64.5 mg, 115 μmol, 1 equiv) in pyridine (192 μL) was treated sequentially with hexamethyldisilazane (139 μL, 662 μmol, 5.74 equiv) and chlorotrimethylsilane (37.3 μL, 292 μmol, 2.53 equiv). The resulting milky white suspension was warmed to 23 °C, and after 2 h of stirring at this temperature, the mixture was concentrated to dryness. The dried residue was partitioned between water (10 mL) and 20% v/v ethyl acetate hexanes (20 mL), the layers were shaken vigorously until both were clear, and then the layers were separated. The organic phase was washed with a fresh portion of water (10 mL), dried over sodium sulfate, filtered, and concentrated to provide 2,3,4,7-tetrakis-*O*-trimethylsilylated intermediate ($R_f = 0.52$, 20% ethyl acetate–hexanes, CAM). This material was then re-dissolved in methanol (500 μL), and 80% v/v acetic acid–water (75 μL) was added. After stirring for 10 min at 23 °C, TLC analysis showed that no tetrasilylated intermediate remained; the mixture was neutralized with the addition of saturated aqueous sodium bicarbonate solution (150 μL). The basified mixture was partitioned between water (10 mL) and 20% v/v ethyl acetate–hexanes (20 mL), and the layers were shaken vigorously before they were separated. The organic phase was then washed with a fresh portion of water (10 mL), dried over sodium sulfate, filtered, and concentrated to afford 2,3,4-tris-*O*-trimethylsilylated intermediate as a white foaming solid (85.7 mg, 96%).

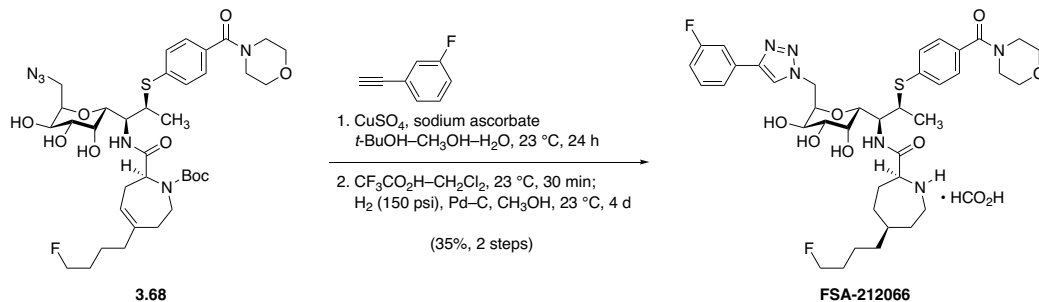
A portion of this intermediate (56.1 mg, 72.3 μmol , 1 equiv) was transferred to a clean 2–5 mL glass microwave vial, where it was dissolved with chloroform (241 μL). This solution was chilled to 0 $^{\circ}\text{C}$, and was treated sequentially with triethylamine (25.2 μL , 181 μmol , 2.50 equiv) and methanesulfonyl chloride (11.3 μL , 145 μmol , 2.00 equiv). After 3 min of stirring at 0 $^{\circ}\text{C}$, TLC analysis (40% ethyl acetate–hexanes) showed complete consumption of 7-hydroxy intermediate. The reaction mixture was diluted with dichloromethane (5 mL), and the diluted solution was washed with saturated aqueous sodium bicarbonate solution (2×2 mL). The washed product solution was then dried over sodium sulfate, filtered, and concentrated to give 7-*O*-methanesulfonyl ester intermediate as a colorless oil (67.6 mg, 109%).

Finally, in a 0.2–0.5 mL glass vial fitted with a magnetic stir bar and PTFE-lined screw cap, this 7-*O*-methanesulfonyl ester intermediate, (4-mercaptophenyl)(morpholino)methanone (**3.67**, 35.0 mg, 157 μmol , 2.00 equiv) and potassium carbonate (32.5 mg, 235 μmol , 3.00 equiv) were dissolved in *N,N*-dimethylformamide (196 μL). The vial was sealed, and the contents were heated with stirring to 80 $^{\circ}\text{C}$ for 90 min, at which point TLC analysis (40% ethyl acetate–hexanes, UV+PAA) showed that no sulfonate ester electrophile remained. The mixture was cooled to 23 $^{\circ}\text{C}$ and was diluted with ethyl acetate (5 mL); this diluted solution was washed with water (2×1 mL), and the washed solution was concentrated. The residue was re-dissolved in 50% v/v acetic acid–methanol, and the resulting solution was stirred at 40 $^{\circ}\text{C}$ overnight in order to effect global desilylation. The desilylated product mixture was concentrated to dryness and was purified by flash-column chromatography (12 g silica gel, eluting with dichloromethane initially, grading to 10% methanol–dichloromethane) to provide arenesulfide **3.68** as a brilliant white solid (46.5 mg, 81% overall).

$R_f = 0.26$ (10% methanol–dichloromethane, UV+CAM).

$^1\text{H NMR}$ (600 MHz, CDCl_3) δ 7.51 (d, $J = 8.4$ Hz, 2H), 7.35 (d, $J = 8.2$ Hz, 2H), 6.73 (d, $J = 9.1$ Hz, 1H), 5.43 (app t, $J = 6.7$ Hz, 1H), 4.53 (dd, $J = 11.3, 4.2$ Hz, 1H), 4.43 (dt, $J = 47.3, 6.0$ Hz, 2H), 4.26–2.33 (m, 1H), 4.17 (app td, $J = 9.6, 2.2$ Hz, 1H), 4.11–4.07 (1H), 4.04 (dd, $J = 9.7, 6.5$ Hz, 1H), 3.85–3.56 (m, 12H), 3.52 (dd, $J = 9.6, 3.7$ Hz, 1H), 3.48–3.39 (m, 1H),

MS (ESI+, m/z): $[\text{M}+\text{H}-\text{Boc}]^+$ calc'd for $\text{C}_{36}\text{H}_{53}\text{FN}_6\text{O}_9\text{S}$, 665.4; found 665.4.



Synthetic lincosamide FSA-212066.

In a 1-mL glass vial fitted with a magnetic stir bar and a PTFE-lined screw cap, azide **3.68** (12.9 mg, 16.9 μmol , 1 equiv) was dissolved in 2:2:1 v/v/v *tert*-butanol–methanol–water (112 μL). To this solution were then added 1-ethynyl-3-fluorobenzene (3.93 μL , 3.38 μmol , 2.00 equiv), aqueous sodium ascorbate solution (0.100 M, 33.7 μL , 3.37 μmol , 0.200 equiv), and aqueous cupric sulfate solution (0.100 M, 8.43 μL , 0.843 mmol, 0.0500 equiv) at 23 °C. Upon addition of copper catalyst, the mixture attained a fluorescent lemon-yellow color. The reaction was shielded from light using aluminum foil, and after stirring for 24 h, LCMS analysis showed that no starting material remained. Saturated aqueous sodium bicarbonate solution (1 mL) and saturated aqueous sodium chloride solution (1 mL) were added, and the diluted mixture was extracted with dichloromethane (3×2 mL). The combined extracts were dried over sodium sulfate, filtered, and concentrated to give a light yellow-green foaming solid.

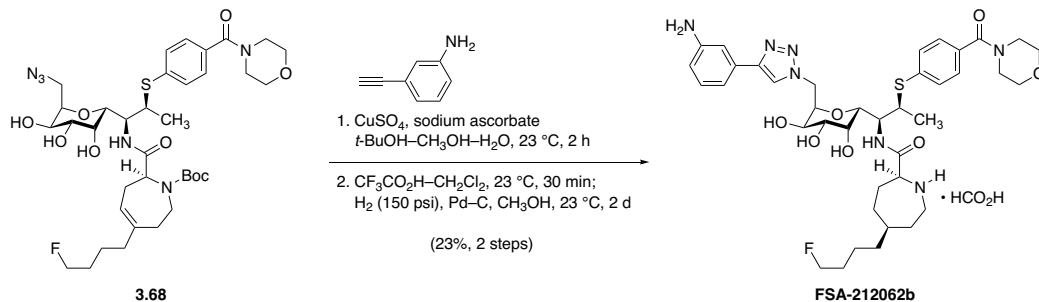
This residue was then transferred to a 4-mL glass vial, where it was dissolved in 33% v/v trifluoroacetic acid–dichloromethane (300 μL). After stirring at 23 °C for 30 min, LCMS analysis showed that Boc removal was complete, and the mixture was concentrated to dryness. The residue was then dissolved in methanol (300 μL), palladium on carbon (10% w/w, 20.0 mg) was added, and the vial was transferred to a Parr stainless-steel high-pressure reaction flask, where 150 psi of hydrogen gas pressure was applied. After stirring for 4 d, the pressure reactor was carefully

depressurized, and the reaction mixture was filtered through a pad of Celite to remove the heterogeneous catalyst. The filter cake was rinsed with methanol (3×1 mL), the filtrate was concentrated, and the residue thus obtained was subjected to preparative HPLC on a Waters SunFire Prep C₁₈ column (5 μ m, 250 \times 19 mm; eluting with 0.1% formic acid–5% acetonitrile–water initially, grading to 0.1% formic acid–50% acetonitrile–water over 30 min, with a flow rate of 15 mL/min; monitored by UV absorbance at 280 nm) to provide **FSA-212066** • HCO₂H as a white solid (4.9 mg, 35%, 2 steps).

¹H NMR (600 MHz, CD₃OD) δ 8.41 (br, 1H), 7.52 (d, $J = 7.8$ Hz, 1H), 7.47 (d, $J = 10.0$ Hz, 1H), 7.40 (td, $J = 8.0, 5.8$ Hz, 1H), 7.25 (d, $J = 7.9$ Hz, 2H), 7.17 (d, $J = 7.9$ Hz, 2H), 7.06 (td, $J = 8.5, 2.6$ Hz, 1H), 4.80 (dd, $J = 14.9, 10.7$ Hz, 1H), 4.74–4.69 (m, 2H), 4.53 (dd, $J = 9.5, 3.0$ Hz, 1H), 4.41 (dt, $J = 47.6, 5.8$ Hz, 2H), 4.12 (dd, $J = 8.9, 5.5$ Hz, 1H), 4.09–4.04 (m, 2H), 4.01–3.97 (br, 1H), 3.78–3.59 (br, 6H), 3.56 (dd, $J = 6.9, 3.1$ Hz, 1H), 3.42 (dd, $J = 14.1, 5.5$ Hz, 1H), 3.11 (app t, $J = 12.6$ Hz, 1H), 2.22–2.11 (m, 2H), 2.05–1.98 (m, 1H), 1.92–1.87 (m, 1H), 1.70–1.62 (m, 3H), 1.60–1.52 (m, 1H), 1.47–1.37 (m, 3H), 1.36–1.31 (m, 2H), 1.11 (d, $J = 6.8$ Hz, 3H).

FTIR (neat, cm⁻¹): 3335 (br), 2932 (m), 1677 (m), 1618 (s), 1590 (s), 1434 (m), 1280 (m), 1113 (m), 1086 (m).

HRMS (ESI+, m/z): [M+H]⁺ calc'd for C₃₉H₅₂F₂N₆O₇S, 787.3659; found 787.3648.



Synthetic lincosamide FSA-212062b.

In a 1-mL glass vial fitted with a magnetic stir bar and a PTFE-lined screw cap, azide **3.68** (12.5 mg, 16.3 μmol , 1 equiv) was dissolved in 2:2:1 v/v/v *tert*-butanol–methanol–water (109 μL). To this solution were then added 3-ethynylaniline (3.68 μL , 3.27 μmol , 2.00 equiv), aqueous sodium ascorbate solution (0.100 M, 32.7 μL , 3.27 μmol , 0.200 equiv), and aqueous cupric sulfate solution (0.100 M, 8.17 μL , 0.817 mmol, 0.0500 equiv) at 23 °C. Upon addition of copper catalyst, the mixture attained a golden yellow color. The reaction was shielded from light using aluminum foil, and after stirring for 2 h, LCMS analysis showed that no starting material remained. Saturated aqueous sodium bicarbonate solution (1 mL) and saturated aqueous sodium chloride solution (1 mL) were added, and the diluted mixture was extracted with dichloromethane (3×2 mL). The combined extracts were dried over sodium sulfate, filtered, and concentrated to give a light brown foaming solid.

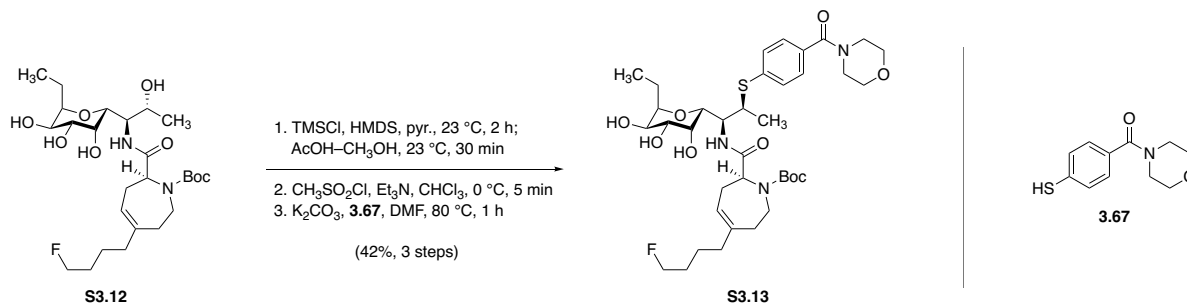
This residue was then transferred to a 4-mL glass vial, where it was dissolved in 33% v/v trifluoroacetic acid–dichloromethane (300 μL). After stirring at 23 °C for 30 min, LCMS analysis showed that Boc removal was complete, and the mixture was concentrated to dryness. The residue was then dissolved in methanol (300 μL), palladium on carbon (10% w/w, 15.0 mg) was added, and the vial was transferred to a Parr stainless-steel high-pressure reaction flask, where 150 psi of hydrogen gas pressure was applied. After stirring for 2 d, the pressure reactor was carefully

depressurized, and the reaction mixture was filtered through a pad of Celite to remove the heterogeneous catalyst. The filter cake was rinsed with methanol (3×1 mL), the filtrate was concentrated, and the residue thus obtained was subjected to preparative HPLC on a Waters SunFire Prep C₁₈ column (5 μ m, 250 \times 19 mm; eluting with 0.1% formic acid–5% acetonitrile–water initially, grading to 0.1% formic acid–50% acetonitrile–water over 40 min, with a flow rate of 15 mL/min; monitored by UV absorbance at 280 nm) to provide **FSA-212062b** • HCO₂H as a white solid (3.3 mg, 23%, 2 steps).

¹H NMR (600 MHz, CD₃OD) δ 8.43 (s, 1H), 7.65 (d, $J = 8.6$ Hz, 1H), 7.47 (t, $J = 7.9$ Hz, 1H), 7.45–7.44 (m, 1H), 7.22 (d, $J = 7.9$ Hz, 1H), 7.11 (d, $J = 8.4$ Hz, 2H), 7.08 (d, $J = 8.2$ Hz, 2H), 4.84–4.81 (m, 1H), 4.74 (dd, $J = 14.4, 2.3$ Hz, 1H), 4.61 (dd, $J = 9.7, 2.7$ Hz, 1H), 4.40 (dt, $J = 47.6, 6.0$ Hz, 2H), 4.17 (dd, $J = 9.3, 5.7$ Hz, 1H), 4.11 (dd, $J = 6.8, 4.1$ Hz, 1H), 3.96–3.95 (m, 1H), 3.80–3.68 (m, 4H), 3.64–3.59 (m, 1H), 3.59–3.53 (m, 1H), 3.44 (ddd, $J = 14.0, 5.9, 2.6$ Hz, 1H), 3.38–3.33 (m, 1H), 3.14 (app t, $J = 12.3$ Hz, 1H), 2.26–2.13 (m, 2H), 2.03–1.99 (m, 1H), 1.92 (app td, $J = 10.4, 9.4, 4.6$ Hz, 1H), 1.70–1.61 (m, 3H), 1.59–1.53 (m, 1H), 1.46–1.36 (m, 3H), 1.34–1.29 (m, 2H), 1.08 (d, $J = 6.8$ Hz, 3H).

FTIR (neat, cm⁻¹): 3388 (br), 2930 (m), 1672 (s), 1609 (m), 1463 (m), 1438 (m), 1202 (s), 1136 (m).

HRMS (ESI+, m/z): [M+H]⁺ calc'd for C₃₉H₅₂FN₇O₇S, 784.3862; found 784.3855.



Protected lincosamide **S3.13**.

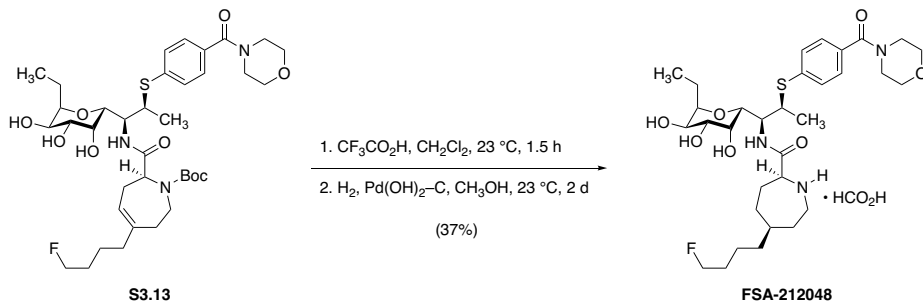
In a 1-mL glass vial, an ice-cold solution of tetraol **S3.12** (15 mg, 28 μ mol, 1 equiv) in pyridine (100 μ L) was treated with hexamethyldisilazane (15 μ L, 71 μ mol, 2.5 equiv) and chlorotrimethylsilane (21 μ L, 0.16 mmol, 5.7 equiv). A white suspension of pyridinium hydrochloride formed upon addition of chlorotrimethylsilane. The mixture was then warmed to 23 °C and was stirred at that temperature for 2 h before it was concentrated to dryness. The dried residue was partitioned between hexanes (10 mL) and water (10 mL), and the layers were shaken until both were clear. The layers were separated, and the organic layer was concentrated. The dried residue was re-dissolved in methanol (500 μ L), and 80% v/v acetic acid–water (75 μ L) was added at 23 °C. This mixture was stirred for 30 min, at which point TLC analysis showed that no tetrasilylated intermediate (R_f = 0.65, 20% ethyl acetate–hexanes, CAM) remained. The mixture was basified with the addition of saturated aqueous sodium bicarbonate solution (200 μ L), and the mixture was then concentrated to dryness. The residue was partitioned between water (10 mL) and 50% v/v ethyl acetate–hexanes (10 mL). The layers were shaken vigorously before they were separated. The organic layer was washed with a fresh portion of water (10 mL) and was then dried over sodium sulfate. The dried product solution was concentrated to provide 2,3,4-tris-*O*-trimethylsilylated intermediate (18 mg, 23 μ mol).

This intermediate was transferred to a 1-mL glass vial, where it was dried by azeotropic removal of benzene before it was dissolved in chloroform (100 μ L). This solution was chilled to 0 $^{\circ}$ C, and was then treated with triethylamine (7.9 μ L, 57 μ mol, 2.5 equiv) and methanesulfonyl chloride (3.5 μ L, 45 μ mol, 2.0 equiv). After 5 min of stirring at 0 $^{\circ}$ C, TLC analysis showed that no alcohol starting material remained (alcohol R_f = 0.24, methanesulfonate ester R_f = 0.63; 20% diethyl ether–dichloromethane, CAM). The mixture was diluted with dichloromethane (2 mL), and the diluted solution was washed with saturated aqueous sodium bicarbonate solution (1 mL). The washed organic solution was then dried over sodium sulfate, filtered, and concentrated to give 2,3,4-tris-*O*-trimethylsilyl-7-*O*-methanesulfonyl intermediate as a colorless oil (19 mg, 23 μ mol).

Finally, in a 0.2–0.5 mL glass microwave vial, this material was dried by azeotropic removal of benzene. To the dried residue were added (4-mercaptophenyl)(morpholino)methanone (**3.67**, 10 mg, 46 μ mol, 2.0 equiv), potassium carbonate (9.5 mg, 69 μ mol, 3.0 equiv) and *N,N*-dimethylformamide (57 μ L). The vial was sealed, and the mixture was heated to 80 $^{\circ}$ C for 1 h. The thick gel that formed was then cooled to 23 $^{\circ}$ C before it was diluted with dichloromethane. Trifluoroacetic acid (200 μ L) was added next; after 10 min of stirring at 23 $^{\circ}$ C, LCMS analysis showed that all three trimethylsilyl groups had been removed successfully, while the Boc group remained in place. The mixture was concentrated to dryness, and the dried residue was subjected to preparative HPLC on a Waters SunFire Prep C₁₈ column (5 μ m, 250 \times 19 mm; eluting with 0.1% formic acid–10% acetonitrile–water initially, grading to 0.1% formic acid–60% acetonitrile–water over 35 min, with a flow rate of 15 mL/min; monitored by UV absorbance at 280 nm) to provide the product as a colorless film (8.8 mg, 52%, 3 steps).

¹H NMR (60:40 mixture of rotamers, asterisk [*] denotes minor rotamer peaks that could be resolved; 500 MHz, CD₃OD) δ 7.70 (d, *J* = 9.6 Hz, 1H), 7.62 (d, *J* = 9.3 Hz, 1H), * 7.46 (d, *J* = 8.4 Hz, 2H), 7.39 (d, *J* = 8.4 Hz, 2H), 5.50 (br app s, 1H), 4.59 (dd, *J* = 11.0, 3.4 Hz, 1H), * 4.51 (dd, *J* = 11.9, 4.1 Hz, 1H), 4.46–4.42 (m, 2H), 4.37–4.35 (m, 1H), 4.05–3.93 (m, 2H), 3.91–3.78 (m, 5H), 3.76–3.60 (m, 6H), 3.59–3.40 (m, 3H), 2.82–2.74 (m, 1H), 2.49–2.39 (m, 2H), 2.35–2.32 (m, 1H), 2.01 (app t, *J* = 7.4 Hz, 2H), 1.69–1.56 (m, 4H), 1.55–1.51 (m, 2H), 1.49 (s, 9H), 1.47 (s, 9H), * 1.34 (d, *J* = 6.7 Hz, 3H), 0.80 (t, *J* = 7.4 Hz, 3H).

HRMS (ESI+, *m/z*): [M+H]⁺ calc'd for C₃₇H₅₆FN₃O₉S, 638.3270; found 638.3258.



Synthetic lincosamide FSA-212048.

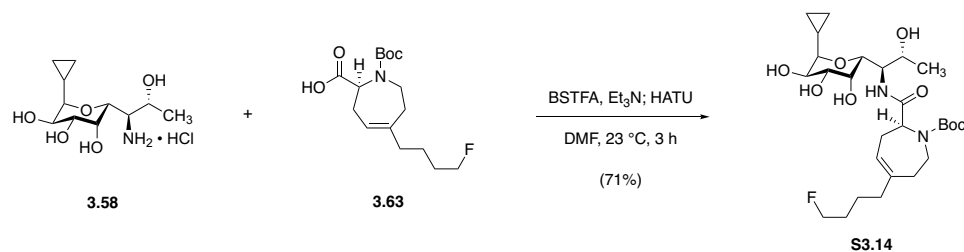
In a 4-mL glass vial fitted with a stir bar, azepine **S3.13** (8.8 mg, 12 μmol) was dissolved in 33% v/v trifluoroacetic acid–dichloromethane (300 μL). After 1.5 h, LCMS analysis showed that Boc removal was complete, and the mixture was diluted with toluene (500 μL). The diluted mixture was concentrated to dryness. The residue was re-dissolved in methanol (500 μL), and the solution was treated with palladium hydroxide on carbon (20% w/w, 8.0 mg). The black suspension was stirred under hydrogen gas (1 atm) at 23 $^\circ\text{C}$ for 2 d, at which point LCMS analysis showed that azepine hydrogenation was complete. The mixture was filtered through a Celite pad, and the filter cake was rinsed with methanol (3 \times 1 mL). The filtrate was concentrated to give a colorless film, which was purified by preparative HPLC on a Waters SunFire Prep C₁₈ column (5 μm , 250 \times 19 mm; eluting with 0.1% formic acid–10% acetonitrile–water initially, grading to 0.1% formic acid–60% acetonitrile–water over 30 min, with a flow rate of 15 mL/min; monitored by UV absorbance at 280 nm) to provide the product (**FSA-212048** \cdot HCO₂H, 3.0 mg, 37%) as a white solid.

¹H NMR (600 MHz, CD₃OD) δ 8.46 (br, 1H), 7.44 (dd, J = 8.4, 1.3 Hz, 2H), 7.38 (dd, J = 8.3, 1.3 Hz, 2H), 4.57 (d, J = 9.4 Hz, 1H), 4.41 (dtd, J = 47.6, 6.1, 1.3 Hz, 2H), 4.05–3.99 (m, 2H), 3.96 (dd, J = 10.1, 6.0 Hz, 1H), 3.87 (d, J = 9.8 Hz, 1H), 3.85–3.80 (m, 2H), 3.78–3.60 (m,

6H), 3.57 (dd, $J = 10.2, 3.1$ Hz, 1H), 3.55–3.39 (m, 3H), 3.12 (app t, $J = 12.6$ Hz, 1H), 2.25–2.14 (m, 2H), 2.05–1.98 (m, 1H), 1.93 (app td, $J = 11.0, 6.8$ Hz, 1H), 1.71–1.61 (m, 4H), 1.59–1.53 (2H), 1.47–1.40 (m, 3H), 1.35 (d, $J = 6.7$ Hz, 3H), 1.35–1.32 (m, 2H), 0.97 (t, $J = 7.3$ Hz, 3H).

FTIR (neat, cm^{-1}): 3333 (br), 2965 (m), 2933 (m), 1677 (s), 1595 (s), 1435 (m), 1280 (m), 1114 (m), 1084 (m).

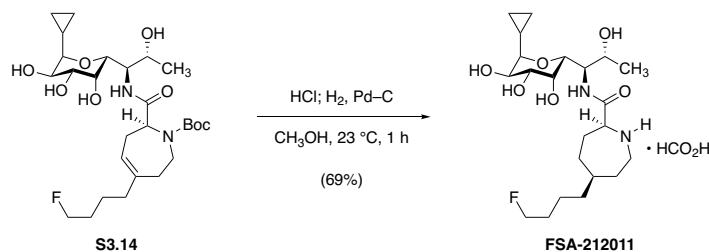
HRMS (ESI+, m/z): $[\text{M}+\text{H}]^+$ calc'd for $\text{C}_{32}\text{H}_{50}\text{FN}_3\text{O}_7\text{S}$, 640.3426; found 640.3435.



Protected lincosamide S3.14.

In a 4-mL glass vial fitted with a magnetic stir bar and silicone septum screw cap, an ice-cold solution of aminotetraol hydrochloride salt **3.58** • HCl (32 mg, 0.11 mmol) and triethylamine (66 μ L, 0.47 mmol, 4.2 equiv) in *N,N*-dimethylformamide (564 μ L) was treated with *N,O*-bis(trimethylsilyl)trifluoroacetamide (61 μ L, 0.23 mmol, 2.0 equiv). The mixture was warmed to 23 $^\circ$ C and was stirred at that temperature for 1 h to ensure complete *O*-silylation before it was transferred via cannula to a separate 4-mL glass vial (fitted with a magnetic stir bar and silicone septum screw cap) containing azepine acid **3.63** (39 mg, 0.12 mmol, 1.1 equiv). The resulting mixture was then treated with HATU (56 mg, 0.15 mmol, 1.3 equiv), and the yellow solution was stirred at 23 $^\circ$ C. After 3 h, this solution was diluted with ethyl acetate (20 mL), and the organic solution was washed sequentially with 10-mL portions of 10% w/v aqueous citric acid solution, saturated aqueous sodium bicarbonate solution, and saturated aqueous sodium chloride solution. The washed organic product solution was then dried over sodium sulfate, filtered, and concentrated to give a residue that was re-dissolved in 50% v/v acetic acid–methanol (4 mL). This solution was stirred at 40 $^\circ$ C overnight to effect global desilylation, the desilylated mixture was diluted with toluene (4 mL), and the diluted mixture was concentrated to dryness *in vacuo*. The residue thus obtained was purified by flash-column chromatography (12 g silica gel, eluting with dichloromethane initially, grading to 10% methanol–dichloromethane) to provide the product as a white solid (44 mg, 71%).

^1H NMR (60:40 mixture of rotamers, asterisk [*] denotes minor rotamer signals that could be resolved, 600 MHz, CD_3OD) δ 7.97 (d, $J = 8.9$ Hz, 1H), * 7.83 (d, $J = 9.3$ Hz, 1H), 5.50–5.46 (m, 1H), 4.48 (dd, $J = 12.3, 4.5$ Hz, 1H), 4.40 (app dq, $J = 47.5, 6.3$ Hz, 2H), 4.12–4.07 (m, 1H), 4.07–4.02 (m, 1H), 4.01–4.91 (m, 3H), 3.88 (d, $J = 8.1$ Hz, 1H), 3.86–3.80 (m, 1H), 3.78–3.74 (m, 1H), 3.71–3.64 (m, 1H), 3.07 (dd, $J = 9.8, 6.8$ Hz, 1H), 2.74 (app q, $J = 15.5$ Hz, 1H), 2.49–2.37 (m, 2H), 2.32 (br s, 1H), 2.29 (br s, 1H), * 1.99 (app q, $J = 7.2$ Hz, 1H), 1.67–1.57 (m, 2H), 1.52–1.48 (m, 2H), 1.48 (s, 9H), 1.45 (s, 9H), * 1.22 (d, $J = 6.3$ Hz, 3H), 1.19 (d, $J = 6.4$ Hz, 3H), * 1.15–1.09 (m, 1H), 0.74 (tdd, $J = 8.5, 6.0, 4.4$ Hz, 1H), 0.50 (tq, $J = 9.2, 4.9$ Hz, 1H), 0.37 (dq, $J = 9.8, 4.9$ Hz, 1H), 0.27 (dq, $J = 10.0, 5.1$ Hz, 1H).



Synthetic lincosamide FSA-212011.

In a 4-mL glass vial fitted with a magnetic stir bar and PTFE-lined screw cap, azepine **S3.14** (10 mg, 18 μmol , 1 equiv) was dissolved in hydrogen chloride solution (4.0 M in 1,4-dioxane, 370 μL). After 15 min of stirring at 23 $^\circ\text{C}$, a white precipitate had formed, and LCMS analysis showed that Boc removal was complete. Toluene (1 mL) was added, and the mixture was concentrated to dryness. The residue was then re-dissolved in methanol (500 μL), and palladium on carbon (10% w/w, 5.0 mg) was added. The headspace above the mixture was replaced with hydrogen gas, and the mixture was stirred under a balloonful of hydrogen gas at 23 $^\circ\text{C}$. After 1 h, LCMS analysis indicated that azepine hydrogenation was complete, and the mixture was filtered through a Celite pad to remove the heterogeneous catalyst. The filter cake was rinsed with methanol ($3 \times 1\text{ mL}$), and the filtrate was concentrated. This residue was purified by preparative HPLC on a Waters SunFire Prep C₁₈ column (5 μm , 250 \times 19 mm; eluting with 0.1% formic acid–2% acetonitrile–water initially, grading to 0.1% formic acid–40% acetonitrile–water over 40 min, with a flow rate of 15 mL/min; monitored by UV absorbance at 210 nm) to provide **FSA-212011** $\cdot \text{HCO}_2\text{H}$ as a white solid (6.2 mg, 69%).

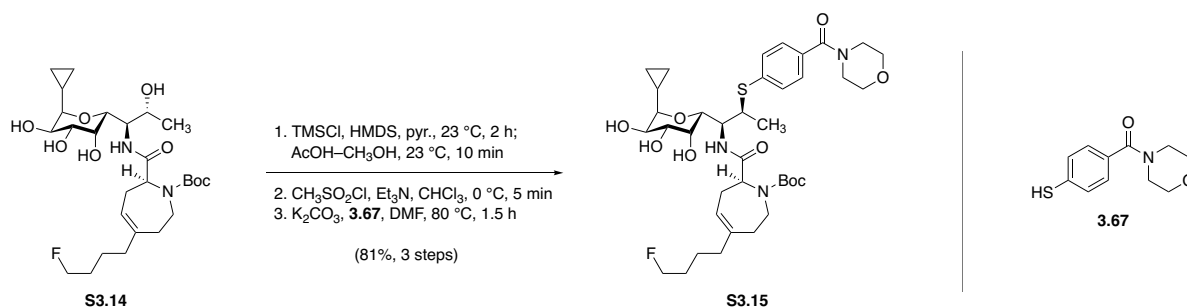
^1H NMR (600 MHz, CD_3OD) δ 8.39 (s, 1H), 4.42 (dt, $J = 47.6, 6.0$ Hz, 2H), 4.28 (dd, $J = 9.1, 5.1$ Hz, 1H), 4.12 (app p, $J = 6.3$ Hz, 1H), 4.08 (br, 1H), 3.97 (dd, $J = 9.9, 6.1$ Hz, 1H), 3.90 (br, 1H), 3.80–3.74 (m, 2H), 3.43 (dd, $J = 12.1, 4.3$ Hz, 1H), 3.12 (app t, $J = 12.5$ Hz, 1H),

3.06 (dd, $J = 10.1, 6.1$ Hz, 1H), 2.22–2.13 (m, 2H), 2.00 (d, $J = 14.5$ Hz, 1H), 1.93–1.88 (m, 1H), 1.72–1.55 (m, 4H), 1.55–1.47 (m, 3H), 1.36–1.32 (m, 2H), 1.20 (d, $J = 6.4$ Hz, 3H), 1.17–1.10 (m, 1H), 0.75 (tt, $J = 8.4, 4.9$ Hz, 1H), 0.51 (tt, $J = 8.7, 4.8$ Hz, 1H), 0.38 (dq, $J = 9.8, 4.8$ Hz, 1H), 0.25 (dq, $J = 9.6, 4.7$ Hz, 1H).

^{13}C NMR (126 MHz, CD_3OD) δ 171.8, 168.3, 84.7 (d, $J = 163.7$ Hz), 84.2, 72.4, 72.1, 70.6, 70.3, 67.8, 60.7, 55.7, 45.7, 38.9, 37.4, 33.2, 31.6 (d, $J = 19.6$ Hz), 30.6, 28.8, 23.9 (d, $J = 5.1$ Hz), 17.7, 8.6, 7.1, 2.0.

FTIR (neat, cm^{-1}): 3244 (br), 2936 (m), 1677 (m), 1660 (m), 1590 (s), 1462 (m), 1383 (m), 1345 (m), 1101 (m), 1076 (m), 1044 (m).

HRMS (ESI+, m/z): $[\text{M}+\text{H}]^+$ calc'd for $\text{C}_{22}\text{H}_{39}\text{FN}_2\text{O}_6$, 447.2865; found 447.2871.



Protected lincosamide S3.15.

In a 1-mL glass vial fitted with a magnetic stir bar, an ice-cold solution of tetraol **S3.14** (20.3 mg, 37.3 μ mol, 1 equiv) in pyridine (62.1 μ L) was treated sequentially with hexamethyldisilazane (44.8 μ L, 214 μ mol, 5.74 equiv) and chlorotrimethylsilane (12.1 μ L, 94.3 μ mol, 2.53 equiv). The cooling bath was then removed, and the milky white suspension was stirred at 23 °C for 2 h before it was concentrated to dryness. The dried residue was partitioned between water (10 mL) and 50% v/v ethyl acetate–hexanes (10 mL); the biphasic mixture was shaken vigorously until the layers were clear, and then the layers were separated. The organic layer was washed with a fresh portion of water (5 mL). The washed organic solution was dried over sodium sulfate, filtered, and concentrated to give 2,3,4,7-tetrakis-*O*-trimethylsilylated intermediate as a colorless oil. This material was dissolved in methanol (500 μ L), and 80% v/v acetic acid–water (75 μ L) was added. Desilylation was monitored by TLC, and after 1.5 h, complete disappearance of starting material (R_f = 0.50, 20% ethyl acetate–hexanes, CAM) was observed. The mixture was neutralized with the addition of saturated aqueous sodium bicarbonate solution (200 μ L), and the basified mixture was concentrated to dryness. The dried residue was partitioned between water (10 mL) and 50% diethyl ether–hexanes (10 mL), the biphasic mixture was agitated, and the layers were separated. The organic product solution was then washed with a fresh portion of water (5

mL), dried over sodium sulfate, filtered, and concentrated to give 2,3,4,-tris-*O*-trimethylsilylated intermediate as a colorless oil.

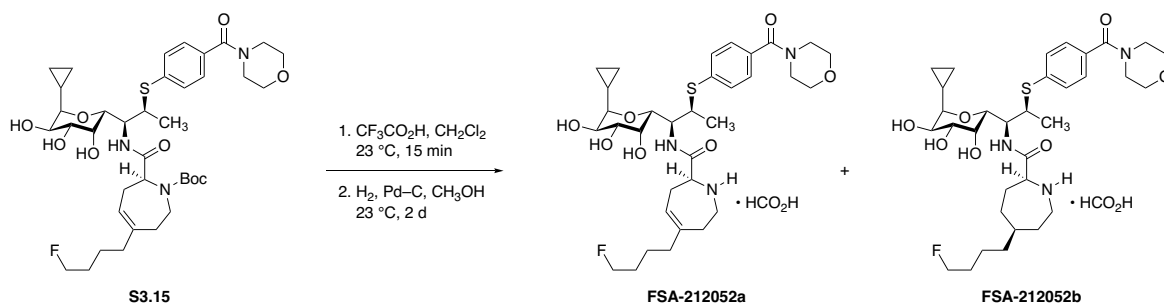
This material was transferred to a clean 1-mL glass vial containing a magnetic stir bar, where it was dissolved in chloroform (123 μ L). The solution was chilled to 0 °C before triethylamine (12.8 μ L, 92.0 μ mol, 2.50 equiv) and methanesulfonyl chloride (5.73 μ L, 73.6 μ mol, 2.00 equiv) were added sequentially by micropipette. After 5 min of stirring at 0 °C, TLC analysis (40% ethyl acetate–hexanes, CAM) indicated that no 2,3,4,-tris-*O*-trimethylsilylated intermediate remained. The reaction mixture was diluted with dichloromethane (5 mL), and the mixture was washed with saturated aqueous sodium bicarbonate solution (2 \times 2 mL). The washed product solution was then dried over sodium sulfate, filtered, and concentrated to give 2,3,4,-tris-*O*-trimethylsilyl-7-*O*-methanesulfonyl intermediate as a foaming, off-white solid.

Finally, in a 1-mL glass vial, methanesulfonate ester intermediate (25.6 mg, 30.5 μ mol, 1 equiv), (4-mercaptophenyl)(morpholino)methanone (**3.67**, 13.6 mg, 61.0 μ mol, 2.00 equiv), and potassium carbonate (12.7 mg, 91.5 μ mol, 3.00 equiv) were suspended in *N,N*-dimethylformamide (76.0 μ L). This mixture was heated to 80 °C for 1.5 h, whereupon TLC analysis (40% ethyl acetate–hexanes, UV+PAA) showed that no sulfonate ester intermediate remained. The reaction mixture was diluted with ethyl acetate (5 mL), the diluted solution was washed with water (2 \times 1 mL), and the washed solution was concentrated. The residue was re-dissolved in 50% v/v acetic acid–methanol (2 mL), and the resulting solution was stirred at 40 °C overnight in order to effect global desilylation. The desilylated product mixture was concentrated to dryness, and the dried residue was subjected to flash-column chromatography (4 g silica gel, eluting with dichloromethane initially, grading to 10% methanol–dichloromethane) to furnish the product as a colorless oil (18.2 mg, 69% overall).

$R_f = 0.26$ (10% methanol–dichloromethane, UV+PAA).

$^1\text{H NMR}$ (500 MHz, CDCl_3) δ 7.44 (d, $J = 8.4$ Hz, 2H), 7.37 (d, $J = 8.3$ Hz, 2H), 6.68 (d, $J = 9.2$ Hz, 1H), 5.44 (app t, $J = 6.8$ Hz, 1H), 4.55 (dd, $J = 11.5, 3.5$ Hz, 1H), 4.43 (dt, $J = 47.3, 6.0$ Hz, 2H), 4.19 (app td, $J = 9.6, 2.2$ Hz, 1H), 4.14–4.07 (m, 1H), 4.01 (dd, $J = 9.6, 6.0$ Hz, 1H), 3.88–3.77 (m, 3H), 3.76–3.76 (m, 7H), 3.20 (dd, $J = 9.6, 6.2$ Hz, 1H), 2.81–2.77 (br, 1H), 2.76–2.49 (br, 1H), 2.48–2.35 (br, 1H), 2.34–2.26 (m, 1H), 2.02–1.95 (m, 2H), 1.70–1.59 (m, 2H), 1.54–1.41 (m, 11H), 1.29–1.23 (m, 3H), 1.03–0.96 (br, 1H), 0.74–0.67 (br, 1H), 0.42–0.28 (br, 2H), 0.26–0.15 (br, 1H).

MS (ESI+, m/z): $[\text{M}+\text{H}]^+$ calc'd for $\text{C}_{38}\text{H}_{56}\text{FN}_3\text{O}_9\text{S}$, 750.4; found 750.4.



Synthetic lincosamides FSA-212052a and FSA-212052b.

In a 4-mL glass vial fitted with a magnetic stir bar and silicone septum screw-cap, azepine **S3.15** (18.2 mg, 24.3 μmol , 1 equiv) was dissolved in 33% v/v trifluoroacetic acid–dichloromethane (450 μL), and the resulting solution was stirred at 23 $^\circ\text{C}$. After 15 min, LCMS analysis indicated that Boc removal was complete; toluene (1 mL) was added, and the mixture was concentrated to dryness. The residue was then re-dissolved in methanol (500 μL), palladium on carbon (10% w/w, 20 mg) was added, the headspace above the reaction mixture was replaced with hydrogen gas, and the mixture was stirred at 23 $^\circ\text{C}$ under a balloonful of hydrogen gas. After 2 d, LCMS showed that azepine hydrogenation was $\sim 75\%$ complete, and the mixture was filtered through a Celite pad to remove the heterogeneous catalyst. The filter cake was rinsed with methanol (3×1 mL), and the filtrate was concentrated to give a colorless oil. This residue was purified by preparative HPLC on a Waters SunFire Prep C_{18} column (5 μm , 250×19 mm; eluting with 0.1% formic acid–10% acetonitrile–water initially, grading to 0.1% formic acid–50% acetonitrile–water over 30 min, with a flow rate of 15 mL/min; monitored by UV absorbance at 254 nm) to provide **FSA-212052a** $\cdot \text{HCO}_2\text{H}$ (3.3 mg, 20%) and **FSA-212052b** $\cdot \text{HCO}_2\text{H}$ (6.9 mg, 41%) as white solids.

FSA-212052a • HCO₂H:

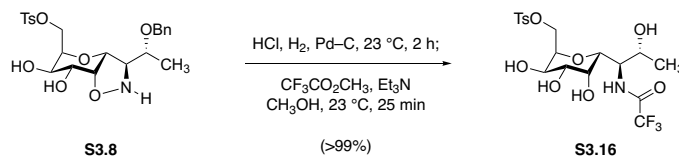
¹H NMR (600 MHz, CD₃OD) δ 8.26 (s, 1H), 7.48 (d, *J* = 8.4 Hz, 2H), 7.40 (d, *J* = 8.4 Hz, 2H), 5.73 (app t, *J* = 6.4 Hz, 1H), 4.53 (dd, *J* = 9.9, 2.3 Hz, 1H), 4.42 (dt, *J* = 47.5, 5.9 Hz, 2H), 4.11 (dd, *J* = 9.9, 1.2 Hz, 1H), 4.01 (qd, *J* = 7.5, 2.8 Hz, 1H), 3.98–3.95 (m, 2H), 3.86 (d, *J* = 3.6 Hz, 1H), 3.80–3.69 (br, 4H), 3.76 (dd, *J* = 10.0, 3.4 Hz, 1H), 3.67–3.59 (br, 2H), 3.48 (ddd, *J* = 13.5, 7.4, 2.2 Hz, 2H), 2.78–2.69 (m, 2H), 2.62–2.57 (m, 2H), 2.48–2.44 (m, 2H), 2.13 (app t, *J* = 7.7 Hz, 1H), 1.72–1.64 (m, 2H), 1.59–1.53 (m, 2H), 1.37 (d, *J* = 7.0 Hz, 3H), 1.10–1.04 (m, 1H), 0.62 (tdd, *J* = 8.5, 6.2, 4.6 Hz, 1H), 0.28 (qd, *J* = 10.0, 4.8 Hz, 1H), 0.13–0.08 (m, 1H), 0.04 (ddt, *J* = 9.2, 6.3, 4.7 Hz, 1H).

MS (ESI+, *m/z*): [M+H]⁺ calc'd for C₃₃H₄₈FN₃O₇S, 650.3; found 650.4.

FSA-212052b • HCO₂H:

¹H NMR (600 MHz, CD₃OD) δ 8.38 (br, 1H), 7.47 (d, *J* = 8.4 Hz, 2H), 7.40 (d, *J* = 8.3 Hz, 2H), 4.54 (dd, *J* = 9.8, 2.3 Hz, 1H), 4.42 (dt, *J* = 47.5, 6.0 Hz, 2H), 4.12–4.08 (m, 2H), 4.00 (qd, *J* = 6.8, 2.2 Hz, 1H), 3.97 (dd, *J* = 10.1, 6.1 Hz, 1H), 3.88 (d, *J* = 3.3 Hz, 1H), 3.77 (dd, *J* = 10.2, 3.3 Hz, 1H), 3.76–3.69 (br, 4H), 3.68–3.60 (br, 2H), 3.57–3.48 (br, 2H), 3.45 (dd, *J* = 13.5, 4.3 Hz, 1H), 3.14 (app t, *J* = 12.6 Hz, 3.06 (dd, *J* = 10.1, 6.1 Hz, 1H), 2.27–2.16 (m, 2H), 2.06–2.00 (m, 1H), 1.96–1.91 (m, 1H), 1.72–1.55 (m, 4H), 1.48–1.41 (m, 3H), 1.38 (d, *J* = 6.9 Hz, 3H), 1.37–1.33 (m, 2H), 1.07 (tdd, *J* = 12.9, 6.6, 4.0 Hz, 1H), 0.64–0.59 (m, 1H), 0.28 (dq, *J* = 9.5, 4.8 Hz, 1H), 0.10 (tt, *J* = 8.5, 5.1 Hz, 1H), 0.04 (ddd, *J* = 11.0, 9.3, 5.1 Hz, 1H).

HRMS (ESI+, *m/z*): [M+H]⁺ calc'd for C₃₃H₅₀FN₃O₇S, 652.3426; found 652.3443.



***N*-Trifluoroacetamido tetraol S3.16.**

A 50-mL round-bottomed flask was charged with isoxazolidine **S3.8** (508 mg, 1.06 mmol, 1 equiv). Methanol (10.6 mL) was added, the resulting solution was chilled to 0 °C, and the stirred solution was treated with hydrogen chloride (1.06 mL, 4 M solution in dioxane, 4.24 mmol, 4.00 equiv). The mixture was then concentrated *in vacuo* to remove methanol, dioxane, and excess hydrogen chloride; and the dried residue (**S3.8** • HCl) was re-dissolved in methanol (10.6 mL). To this solution was added 10% w/w palladium on carbon (113 mg). The reaction flask was fitted with a 3-way stopcock to which a hydrogen-filled balloon had been affixed. The headspace in the flask was replaced with hydrogen gas by three evacuation–backfilling cycles, and the black reaction mixture was stirred at 23 °C. After 2 h, LCMS analysis indicated that isoxazolidine hydrogenolysis and *O*-debenzylation were complete. At this point, triethylamine (738 μL, 5.30 mmol, 5.00 equiv) and methyl trifluoroacetate (533 μL, 5.30 mmol, 5.00 equiv) were added sequentially. After an additional 25 min, LCMS analysis demonstrated complete conversion of the primary amine intermediate to the corresponding trifluoroacetamide. The reaction mixture was filtered through a pad of Celite to remove catalyst, and the filtrate was concentrated to give product alongside triethylamine hydrochloride. In order to remove the latter, the crude residue was suspended in ethyl acetate (30 mL), and the organic solution was washed with saturated aqueous sodium chloride solution (3 × 10 mL). The combined aqueous washes were extracted with ethyl acetate (2 × 10 mL), and these extracts were washed with a fresh portion of saturated aqueous sodium chloride solution (10 mL). The combined organic layers were dried over sodium sulfate,

the dried solution was filtered, and the filtrate was concentrated to give the product as a white solid (529 mg, 102%). This material was sufficiently pure ($\geq 90\%$, based on ^1H NMR analysis) for use without further purification. An analytically pure sample (~ 25 mg) was prepared by flash-column chromatography (4.5 g silica gel, eluting with 3% methanol–dichloromethane initially, grading to 10% methanol–dichloromethane).

$R_f = 0.27$ (10% methanol–dichloromethane, UV+PMA).

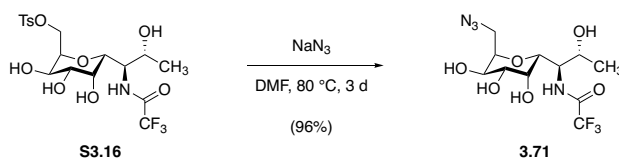
^1H NMR (600 MHz, CD_3OD) δ 7.81 (d, $J = 8.4$ Hz, 2H), 7.45 (d, $J = 8.1$ Hz, 2H), 4.41 (dd, $J = 11.4, 9.6$ Hz, 1H), 4.28 (dd, $J = 11.4, 2.8$ Hz, 1H), 4.21 (q, $J = 7.1$ Hz, 1H), 4.18 (ddd, $J = 9.5, 7.0, 2.9$ Hz, 1H), 3.98–3.95 (m, 2H), 3.87 (dd, $J = 7.2, 1.4$ Hz, 1H), 3.48 (dd, $J = 10.1, 3.2$ Hz, 1H), 2.46 (s, 3H), 1.15 (d, $J = 6.4$ Hz, 3H).

^{13}C NMR (100 MHz, CD_3OD) δ 146.6, 134.3, 131.2, 129.0, 76.1, 72.0, 70.9, 70.5, 68.2, 68.1, 66.6, 57.1, 21.6, 19.1. Trifluoroacetamide carbons were not resolved due to ^{19}F nuclear coupling.

^{19}F NMR (376 MHz, CD_3OD) δ -77.44 (s, 3F).

FTIR (neat, cm^{-1}): 3381 (br), 2519 (br), 1710 (s), 1353 (m), 1175 (s), 1080 (m), 973 (m).

HRMS (ESI+, m/z): $[\text{M}+\text{H}]^+$ calc'd for $\text{C}_{18}\text{H}_{24}\text{F}_3\text{NO}_9\text{S}$, 488.1197; found 488.1192.



Azidomethyl glycoside **3.71**.

An oven-dried 20-mL microwave vial was charged with a stir bar and **S3.16** (400 mg, 821 μmol , 1 equiv), and this material was dried by azeotropic removal of benzene. Sodium azide (533 mg, 8.21 mmol, 10.0 equiv) and anhydrous *N,N*-dimethylformamide (4.10 mL) were then added, and the vial was sealed. The mixture was heated to 80 $^\circ\text{C}$ with rapid stirring. After 3 days, LCMS analysis indicated complete consumption of starting material; at this time the mixture was cooled, and the cooled reaction mixture was diluted with water (5 mL) and saturated aqueous sodium chloride solution (35 mL). This mixture was extracted with ethyl acetate (4 \times 20 mL). The combined organic extracts were dried over sodium sulfate, the dried product solution was filtered, and the filtrate was concentrated to give a light brown oil. In order to remove residual *N,N*-dimethylformamide, the crude residue was concentrated repeatedly from 10% methanol–toluene, affording **3.71** as a dull brown solid (281 mg, 96%). This material could be used in subsequent steps without further purification; an analytically pure sample (\sim 20 mg) was prepared by flash-column chromatography (10 g silica gel, eluting with 5% methanol–dichloromethane initially, grading to 10% methanol–dichloromethane), affording a brilliant white crystalline solid.

Melting point: 140–143 $^\circ\text{C}$.

R_f = 0.12 (10% methanol–dichloromethane, PMA).

^1H NMR (600 MHz, CD_3OD) δ 4.26 (app t, $J = 6.9$ Hz, 1H), 4.18 (ddd, $J = 10.1, 6.5, 3.1$ Hz, 1H), 4.05–3.97 (m, 4H), 3.71 (dd, $J = 13.8, 10.5$ Hz, 1H), 3.56 (dd, $J = 9.9, 3.3$ Hz, 1H), 3.45 (dd, $J = 13.8, 3.1$ Hz 1H), 1.19 (d, $J = 6.4$ Hz, 3H).

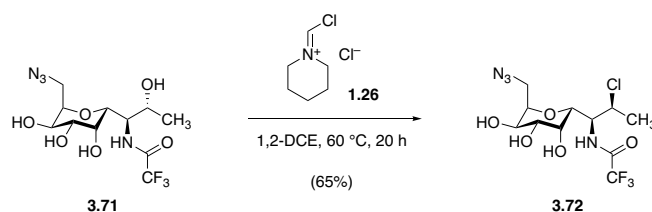
^{13}C NMR (100 MHz, CD_3OD) δ 77.3, 71.8, 70.8, 70.3, 68.6, 68.2, 57.5, 47.3, 19.4.

Trifluoroacetamide carbons were not resolved due to ^{19}F nuclear coupling.

^{19}F NMR (471 MHz, CD_3OD) δ -77.56 (s, 3F).

FTIR (neat, cm^{-1}): 3319 (br), 2933 (w), 2105 (s), 1710 (s), 1556 (m), 1282 (m), 1214 (s), 1183 (s), 1159 (s), 1073 (s).

HRMS (ESI+, m/z): $[\text{M}+\text{H}]^+$ calc'd for $\text{C}_{11}\text{H}_{17}\text{F}_3\text{N}_4\text{O}_6$, 359.1173; found 359.1180.



Chloro compound 3.72.

A flame-dried 20-mL microwave vial was charged with azidotetraol **3.71** (250 mg, 698 μmol , 1 equiv), and this starting material was dried by azeotropic removal of benzene. The dried residue was suspended in 1,2-dichloroethane (11.6 mL), and the resulting suspension was cooled to 0 $^\circ\text{C}$. Chloromethylenepipiridinium chloride (704 mg, 4.19 mmol, 6.00 equiv) was added in one portion, and the mixture was stirred rapidly at 0 $^\circ\text{C}$. After 15 min, the originally light yellow suspension had clarified, forming a yellow homogeneous solution. The reaction mixture was then heated to 60 $^\circ\text{C}$, and over the course of 2 h the solution attained an intense sunset orange color. After 20 h, LCMS analysis indicated that deoxychlorination was complete (evidenced by the disappearance of starting material and its mono- and di-formylated congeners; ESI- m/z = 357, 385, and 413, respectively). The reaction mixture was cooled to 23 $^\circ\text{C}$, and the cooled solution was transferred by cannula to a rapidly stirred, ice-cold sodium hydroxide solution (8.38 mL, 0.5 M, 4.19 mmol, 6.00 equiv). In order to saponify the formyl esters formed upon workup, the biphasic mixture was treated with additional 0.5 M sodium hydroxide solution until the aqueous phase achieved pH = 11; the mixture was then warmed to 23 $^\circ\text{C}$ with constant vigorous stirring, and additional sodium hydroxide solution was added periodically to maintain pH = 11. After 24 h, deformylation was complete by LCMS analysis. The mixture was transferred to a separatory funnel, and the layers were separated. The aqueous phase was then treated with solid sodium chloride until saturation was achieved, and the resulting aqueous solution was extracted with dichloromethane (5×7 mL). The combined organic layers were dried over sodium sulfate, the

dried solution was filtered, and the filtrate was concentrated to give a brown oil. This residue was purified by flash-column chromatography (12 g silica, eluting with dichloromethane initially, grading to 8% methanol–dichloromethane) to give the product as a brilliant white solid (170 mg, 65%).

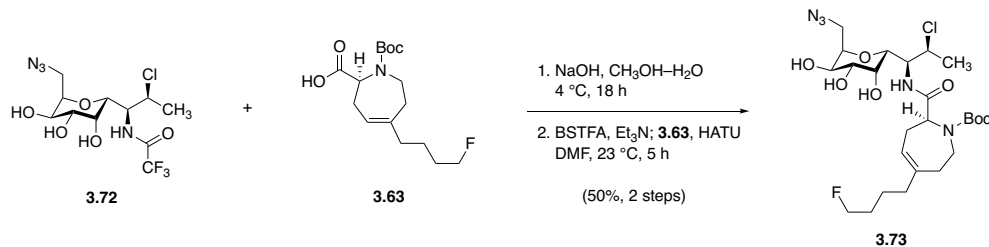
$R_f = 0.23$ (10% methanol–dichloromethane PMA).

$^1\text{H NMR}$ (600 MHz, CD_3OD) δ 4.64 (qd, $J = 6.8, 1.9$ Hz, 1H), 4.51 (dd, $J = 9.6, 1.8$ Hz, 1H), 4.15 (ddd, $J = 9.6, 6.5, 3.1$ Hz, 1H), 4.01 (dd, $J = 9.9, 6.6$ Hz, 1H), 3.97 (dd, $J = 9.5, 1.4$ Hz, 1H), 3.82 (dd, $J = 3.3, 1.3$ Hz, 1H), 3.66 (dd, $J = 13.8, 9.4$ Hz, 1H), 3.60 (dd, $J = 13.8, 3.2$ Hz, 1H), 3.53 (dd, $J = 9.9, 3.2$ Hz, 1H), 1.44 (d, $J = 6.8$ Hz, 3H).

$^{13}\text{C NMR}$ (126 MHz, CD_3OD) δ 159.3 (q, $J = 37.4$ Hz), 117.5 (q, $J = 286.8$ Hz), 77.1, 72.2, 71.3, 69.5, 68.6, 58.8, 55.1, 47.5, 22.8.

FTIR (neat, cm^{-1}): 3384 (br), 2106 (s), 1716 (s), 1545 (m), 1289 (m), 1217 (s), 1176 (s), 1165 (s), 1078 (s).

HRMS (ESI⁻, m/z): $[\text{M}-\text{H}]^-$ calc'd for $\text{C}_{11}\text{H}_{16}\text{ClF}_3\text{N}_4\text{O}_5$, 375.0689; found 375.0692.



Protected lincosamide **3.73**.

In a 10-mL round-bottomed flask, trifluoroacetamide **3.72** (170 mg, 451 μ mol, 1 equiv) was dissolved in a minimal quantity of methanol (500 μ L). This solution was chilled to 0 °C before it was treated with ice-cold aqueous sodium hydroxide solution (1.00 M, 2.26 mL, 2.26 mmol, 5.0 equiv). The mixture was stirred at 4 °C for 18 h, at which point LCMS analysis showed that no starting material remained. The mixture was acidified with the addition of aqueous hydrogen chloride solution (1.0 M), until the pH < 2 was attained. The acidified mixture was then concentrated to dryness to give a light yellow residue comprising deacylated product, sodium chloride, and sodium trifluoroacetate. This mixture was suspended in ethanol (190 proof, 5 mL), and the suspension was filtered. The solids were rinsed with fresh ethanol (190 proof, 2 \times 2 mL), and the combined filtrates were concentrated. This residue was then re-dissolved in methanol (10 mL), the solution was cooled to 0 °C, and the mixture was treated with Amberlyst A26 resin (hydroxide form, 2.0 g). After stirring for 1 h at 0 °C, the ion-exchange beads were removed by filtration, and the filtrate was concentrated to provide aminotriol intermediate (132 mg, 104%).

A portion of this crude aminotriol (100 mg, 360 μ mol, 1 equiv) transferred to a 2–5 mL glass microwave vial containing a magnetic stir bar, where it was dissolved in *N,N*-dimethylformamide (1.78 mL). This solution was chilled to 0 °C, triethylamine (169 μ L, 1.21 mmol, 3.40 equiv) and *N,O*-bis(trimethylsilyl)trifluoroacetamide (143 μ L, 534 μ mol, 1.50 equiv) were added, and the mixture was warmed immediately back to 23 °C. After 1 h of stirring at this

temperature, the mixture was transferred via cannula to a separate 4-mL glass vial (fitted with a magnetic stir bar and silicone septum screw cap) containing azepine acid **3.63** (135 mg, 427 μmol , 1.20 equiv). The mixture was then treated with HATU (176 mg, 463 μmol , 1.30 equiv), causing the dull brown solution to turn the color of chartreuse. After 5 h, the mixture was diluted with ethyl acetate (40 mL), and the diluted solution was washed sequentially with 10% w/v aqueous citric acid solution (2×10 mL), saturated aqueous sodium bicarbonate solution (2×10 mL), and saturated aqueous sodium chloride solution (10 mL). The product solution was then dried over sodium sulfate, filtered, and concentrated; the residue obtained was re-dissolved in 50% v/v acetic acid–methanol (8 mL), and the resulting solution was stirred at 40 °C overnight in order to effect global desilylation. The mixture was then diluted with toluene (10 mL) and the diluted solution was concentrated. The dried residue was purified by flash-column chromatography (24 g silica gel, eluting with dichloromethane initially, grading to 10% methanol–dichloromethane) to provide the product as white solid (98.2 mg, 50%, 2 steps).

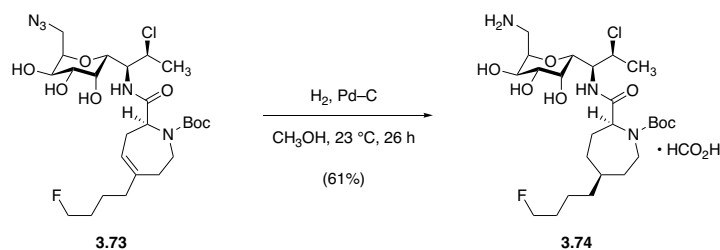
$R_f = 0.16$ (10% methanol–dichloromethane, PMA)

$^1\text{H NMR}$ (600 MHz, CD_3OD) δ 5.53–5.48 (m, 1H), 4.70–4.63 (m, 1H), 4.53 (dd, $J = 12.0, 4.1$ Hz, 1H), 4.41 (dt, $J = 47.5, 5.9$ Hz, 2H), 4.30 (d, $J = 9.5$ Hz, 1H), 4.14 (ddd, $J = 9.6, 6.7, 3.2$ Hz, 1H), 4.03–3.98 (m, 1H), 3.90–3.85 (m, 1H), 3.83 (dd, $J = 4.8, 3.8$ Hz, 1H), 3.80–3.73 (m, 2H), 3.67–3.57 (m, 2H), 3.54 (dd, $J = 10.0, 3.2$ Hz, 1H), 2.83–2.74 (m, 1H), 2.51–2.38 (m, 2H), 2.34–2.30 (d, $J = 17.8$ Hz, 1H), 2.01 (app t, $J = 7.6$ Hz, 2H), 1.69–1.58 (m, 2H), 1.54–1.44 (m, 14H).

^{13}C NMR (126 MHz, CD_3OD) δ 175.9, 157.8, 142.8, 120.2, 111.4, 84.7 (d, $J = 163.8$ Hz), 81.9, 77.2, 72.5, 72.1, 69.6, 68.9, 62.9, 59.4, 54.4, 47.7, 41.8, 39.5, 35.4, 31.0 (d, $J = 19.8$ Hz), 28.8, 24.8 (d, $J = 4.3$ Hz), 22.8.

FTIR (neat, cm^{-1}): 3395 (br), 2972 (m), 2935 (m), 2101 (s), 1663 (s), 1445 (m), 1413 (m), 1393 (m), 1368 (m), 1253 (m), 1163 (s), 1084 (m).

HRMS (ESI+, m/z): $[\text{M}+\text{H}]^+$ calc'd for $\text{C}_{25}\text{H}_{41}\text{ClFN}_5\text{O}_7$, 578.2751; found 578.2738.



Aminomethyl protected lincosamide **3.74**.

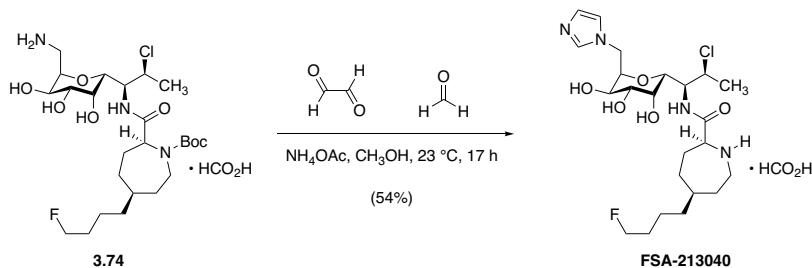
To a 1-dram vial containing azidotriol **3.73** (40.0 mg, 69.0 μmol , 1 equiv) was added methanol (690 μL) and 10% palladium on carbon (4.0 mg). The vial was fitted with a rubber septum and the headspace above the reaction mixture was flushed with hydrogen gas. The black heterogeneous reaction mixture was stirred at 23 $^{\circ}\text{C}$ under an atmosphere of hydrogen gas supplied by a balloon. After 26 h, complete consumption of starting material was noted by LCMS analysis, and the reaction mixture was filtered through a pad of Celite (1 \times 1 cm) to remove catalyst. The filter pad was rinsed with methanol (3 \times 2 mL), and the filtrate was concentrated to give a colorless oil. The residue was purified by preparative HPLC on a Waters SunFire Prep C₁₈ column (5 μm , 250 \times 19 mm; eluting with 0.1% formic acid–5% acetonitrile–water initially, grading to 0.1% formic acid–25% acetonitrile–water over 10 min, then grading to 0.1% formic acid–55% acetonitrile–water over the next 30 min, with a flow rate of 15 mL/min; monitored by UV absorbance at 210 nm) to provide the product as a brilliant white solid (25.4 mg, 61%).

¹H NMR (65:35 mixture of rotamers, asterisk [*] denotes minor rotamer peaks that could be resolved, 500 MHz, CD₃OD) δ 8.49 (br, 1H), 4.73 (q, $J = 6.5$ Hz, 1H), 4.51 (dd, $J = 12.6$, 5.8 Hz, 1H),* 4.47–4.35 (m, 4H). 4.22 (app dq, $J = 6.1$, 4.2 Hz, 1H), 4.08 (dd, $J = 9.4$, 6.4 Hz, 1H),* 4.05 (dd, $J = 9.5$, 6.3 Hz, 1H), 3.97–3.86 (m, 2H), 3.68 (d, $J = 9.5$ Hz, 1H), 3.66 (d, $J = 9.7$ Hz, 1H),* 3.54 (dd, $J = 9.5$, 3.2 Hz, 1H), 3.36 (app dt, $J = 13.5$, 4.1 Hz, 1H),

3.21 (ddd, $J = 13.3, 9.0, 3.1$ Hz, 1H), 3.11 (dd, $J = 15.1, 11.7$ Hz, 1H), 3.05 (dd, $J = 14.7, 12.0$ Hz, 1H),* 2.37–2.25 (m, 1H), 1.99–1.95 (m, 1H), 1.88–1.60 (m, 4H), 1.48 (s, 9H), 1.46–1.37 (m, 3H), 1.31–1.26 (m, 2H), 1.21–1.07 (m, 2H).

FTIR (neat, cm^{-1}): 3269 (br), 2967 (m), 2929 (m), 1655 (s), 1586 (s), 1406 (m), 1395 (m), 1367 (m), 1347 (m), 1248 (m), 1161 (s), 1082 (m), 776 (w).

HRMS (ESI+, m/z): $[\text{M}+\text{H}]^+$ calc'd for $\text{C}_{25}\text{H}_{45}\text{ClFN}_3\text{O}_7$, 554.3003; found 554.3005.



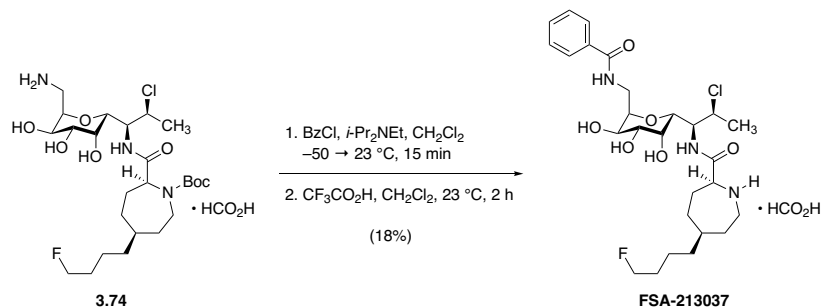
Synthetic lincosamide FSA-213040.

To a 1-mL vial, aminotriol **3.74** (5.0 mg, 9.02 μmol , 1 equiv), methanol (180 μL), ammonium acetate (2.1 mg, 27 μmol , 3.0 equiv), glyoxal (40% w/w aqueous solution, 3.9 μL , 27 μmol , 3.0 equiv), and formalin (37% w/w, 2.0 μL , 27 μmol , 3.0 equiv) were added sequentially. The mixture was stirred at $23\text{ }^\circ\text{C}$. After 3 h, additional glyoxal (3.9 μL , 3.0 equiv) and formalin (2.0 μL , 3.0 equiv) were added. After an additional 14 h, no starting material remained by LCMS, and the mixture was diluted with benzene (300 μL). The mixture was concentrated, and the dried residue was re-dissolved in 33% trifluoroacetic acid–dichloromethane (200 μL). After 30 min of stirring at $23\text{ }^\circ\text{C}$, LCMS analysis indicated that Boc removal was complete. Toluene (500 μL) was added, and the mixture was concentrated. The dried residue was purified by preparative HPLC on a Waters SunFire Prep C_{18} column (5 μm , $250 \times 19\text{ mm}$; eluting with 0.1% formic acid–5% acetonitrile–water initially, grading to 1% formic acid–50% acetonitrile–water over 40 min, with a flow rate of 15 mL/min; monitored by UV absorbance at 210 nm) to afford **FSA-213040** $\cdot\text{HCO}_2\text{H}$ as a white solid (2.9 mg, 54%).

^1H NMR (600 MHz, CD_3OD) δ 8.78 (s, 1H), 8.10 (br, 1H), 7.65 (s, 1H), 7.51 (s, 1H), 4.66–4.52 (m, 3H), 4.47–4.44 (m, 1H), 4.43 (dd, $J = 47.2, 6.0\text{ Hz}$, 2H), 4.25 (app q, $J = 6.6\text{ Hz}$, 1H), 4.14 (dd, $J = 9.7, 6.3\text{ Hz}$, 1H), 4.10–4.05 (m, 1H), 3.92–3.89 (m, 1H), 3.84 (d, $J = 9.6\text{ Hz}$, 1H), 3.67 (dd, $J = 9.9, 3.0\text{ Hz}$, 1H), 3.38 (ddd, $J = 14.3, 6.2, 3.3\text{ Hz}$, 1H), 2.33 (dd, $J = 14.8,$

6.3 Hz, 1H), 2.09–2.02 (m, 2H), 1.92 (app q, $J = 12.2$ Hz, 1H), 1.74–1.53 (m, 4H), 1.50–1.38 (m, 5H), 1.37 (d, $J = 7.0$ Hz, 3H). One methylene proton corresponding to the ζ position of the azepane is obfuscated by CHD₂OD signal.

HRMS (ESI+, m/z): [M+H]⁺ calc'd for C₂₃H₃₈ClFN₄O₅, 505.2588; found 505.2590.



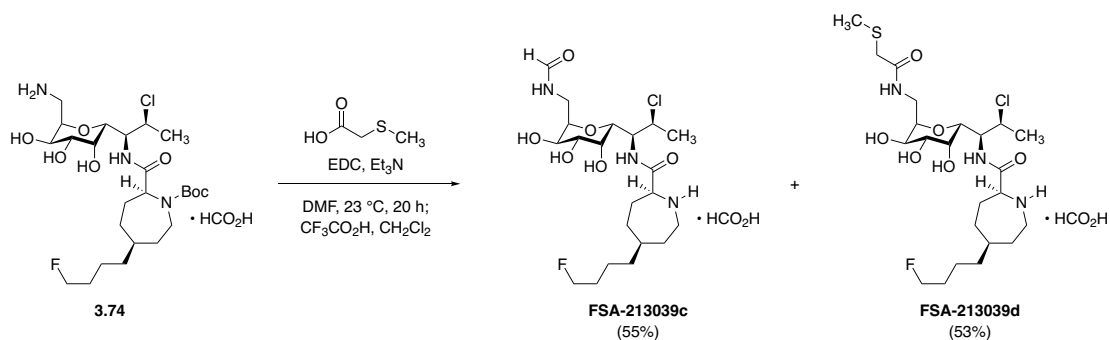
Synthetic lincosamide FSA-213037.

A solution of aminotriol **3.74** (5.0 mg, 8.3 μ mol, 1 equiv) and *N,N*-diisopropylethylamine (7.3 μ L, 42 μ mol, 5.0 equiv) in dichloromethane (83 μ L) was chilled to -50 °C. Benzoyl chloride (1.1 μ L, 9.2 μ mol, 1.1 equiv) was then added, causing a light white suspension to form. After 15 min, excess benzoyl chloride was quenched with the addition of methanol (50 μ L), the cooling bath was removed, and the mixture was concentrated to dryness. The residue was then re-dissolved in 33% v/v trifluoroacetic acid–dichloromethane (600 μ L), and the resulting solution was stirred at 23 °C for 2 h. After this time, toluene (1 mL) was added, and the diluted mixture was concentrated *in vacuo*. The residue was purified by preparative HPLC on a Waters SunFire Prep C₁₈ column (5 μ m, 250 \times 19 mm; eluting with 0.1% formic acid–5% acetonitrile–water initially, grading to 0.1% formic acid–25% acetonitrile–water over 10 min, then grading to 0.1% formic acid–55% acetonitrile–water over the next 25 min, with a flow rate of 15 mL/min; monitored by UV absorbance at 254 nm) to provide the product as a white solid (0.9 mg, 18%).

¹H NMR (600 MHz, CD₃OD) δ 8.29 (br, 1H), 7.83 (d, *J* = 7.2 Hz, 2H), 7.54 (t, *J* = 7.4 Hz, 1H), 7.46 (t, *J* = 7.6 Hz, 2H), 4.66 (q, *J* = 6.8 Hz, 1H), 4.49–4.48 (m, 1H), 4.42 (dt, *J* = 47.4, 6.0 Hz, 2H), 4.33 (ddd, *J* = 10.5, 6.4, 4.1 Hz, 1H), 4.07 (dd, *J* = 9.9, 6.3 Hz, 1H), 3.99 (dd, *J* = 11.5, 3.0 Hz, 1H), 3.84–3.71 (m, 4H), 3.68 (dd, *J* = 9.9, 3.3 Hz, 1H), 2.34–2.30 (m, 1H),

2.09–2.02 (m, 2H), 1.91 (app q, $J = 12.3$ Hz, 1H), 1.72–1.65 (m, 2H), 1.63–1.58 (m, 1H), 1.57–1.51 (m, 1H), 1.49–1.42 (m, 2H), 1.39 (d, $J = 7.0$ Hz, 3H), 1.39–1.35 (m, 3H). Two proton signals were not observed: Both are believed to be obfuscated by the CHD₂OD signal.

HRMS (ESI+, m/z): [M+H]⁺ calc'd for C₂₇H₄₁ClFN₃O₆, 558.2741; found 558.2754.



Synthetic lincosamides **FSA-213039c** and **FSA-213039d**.

A 1-mL vial was charged sequentially with aminotriol **3.74** (5.0 mg, 8.3 μ mol, 1 equiv), *N,N*-dimethylformamide (83 μ L), triethylamine (3.5 μ L, 25 μ mol, 3.0 equiv), and 2-(methylthio)acetic acid (1.1 μ L, 10 μ mol, 1.2 equiv). *N*-(3-Dimethylaminopropyl)-*N'*-ethylcarbodiimide hydrochloride (EDC, 1.8 mg, 9.2 μ mol, 1.1 equiv) was then added. The resulting solution was stirred at 23 °C for 1 h, at which time additional triethylamine (6.0 μ L, 43 μ mol, 5.2 equiv) and 2-(methylthio)acetic acid (1.1 μ L, 10 μ mol, 1.2 equiv) were added. After 19 h, LCMS analysis showed no starting material remained. Methanol (200 μ L) and toluene (200 μ L) were added, and the resulting solution was concentrated to dryness. The residue was then re-dissolved in 33% trifluoroacetic acid–dichloromethane (200 μ L), and after 30 min of stirring at 23 °C, LCMS analysis indicated that Boc removal was complete. Toluene (300 μ L) was added, and the resulting solution was concentrated to dryness. The crude residue was purified by preparative HPLC on a Waters SunFire Prep C₁₈ column (5 μ m 250 \times 19 mm, eluting with 0.1% formic acid–5% acetonitrile–water, grading to 0.1% formic acid–50% acetonitrile–water over 30 min, with a flow rate of 15 mL/min; monitored by UV absorbance at 210 nm) to afford **FSA-213039c** \cdot HCO₂H (2.4 mg, 55%) and **FSA-213039d** \cdot HCO₂H (2.6 mg, 53%) as white solids.

FSA-213039c • HCO₂H:

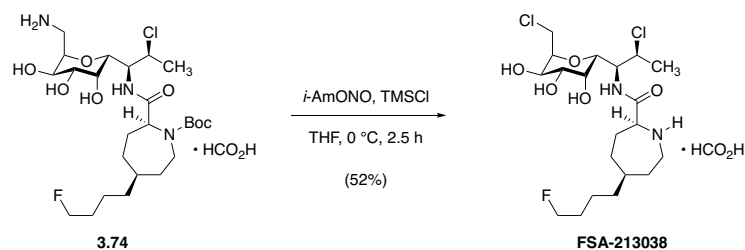
¹H NMR (600 MHz, CD₃OD) δ 8.08 (s, 1H), 4.71 (qd, *J* = 6.8, 1.8 Hz, 1H), 4.44 (dd, *J* = 9.6, 1.8 Hz, 1H), 4.43 (dd, *J* = 47.6, 6.0 Hz, 2H), 4.16 (ddd, *J* = 10.7, 6.5, 4.2 Hz, 1H), 4.05–4.00 (m, 2H), 3.81 (dd, *J* = 3.4, 1.2 Hz, 1H), 3.66 (d, *J* = 9.6 Hz, 1H), 3.63–3.53 (m, 3H), 3.37 (ddd, *J* = 14.0, 6.3, 3.4 Hz, 1H), 2.33 (ddt, *J* = 15.4, 6.8, 2.6 Hz, 1H), 2.10–2.03 (m, 2H), 1.93 (dtd, *J* = 15.4, 11.6, 2.0 Hz, 1H), 1.73–1.52 (m, 4H), 1.50–1.45 (m, 2H), 1.44 (d, *J* = 6.9 Hz, 3H), 1.42–1.35 (m, 3H). One methylene proton corresponding to the ζ position of the azepane is obfuscated by CHD₂OD signal.

HRMS (ESI+, *m/z*): [M+H]⁺ calc'd for C₂₁H₃₇ClFN₃O₆, 482.2428; found 482.2438.

FSA-213039d • HCO₂H:

¹H NMR (600 MHz, CD₃OD) δ 4.70 (q, *J* = 6.3 Hz, 1H), 4.47–4.43 (m, 1H), 4.42 (dd, *J* = 47.4, 5.9 Hz, 2H), 4.17 (ddd, *J* = 10.5, 6.4, 4.0 Hz, 1H), 4.06–3.99 (m, 2H), 3.82 (d, *J* = 3.3 Hz, 1H), 3.70 (d, *J* = 9.6 Hz, 1H), 3.65–3.53 (m, 3H), 3.37 (ddd, *J* = 13.9, 6.3, 3.2 Hz, 1H), 3.20 (app q, *J* = 15.1 Hz, 2H), 2.37–2.30 (m, 1H), 2.15 (s, 3H), 2.09–2.02 (m, 2H), 1.93 (app q, *J* = 12.6 Hz, 1H), 1.74–1.53 (m, 4H), 1.50–1.45 (m, 2H), 1.44 (d, *J* = 6.9 Hz, 3H), 1.43–1.34 (m, 3H). One methylene proton corresponding to the ζ position of the azepane is obfuscated by CHD₂OD signal.

HRMS (ESI+, *m/z*): [M+H]⁺ calc'd for C₂₃H₄₁ClFN₃O₆S, 542.2461; found 542.2451.



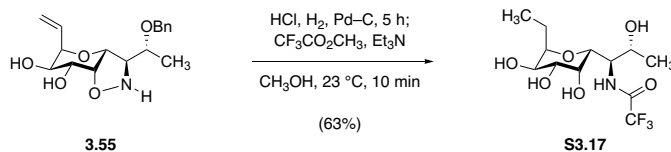
Synthetic lincosamide FSA-213038.

A nitrosyl chloride solution (1.08 M) was prepared according to the method described by Weiß and Wagner:¹³⁷ A solution of isoamyl nitrite (501 μL , 3.73 mmol) in tetrahydrofuran (2.50 mL) was cooled to 0 $^{\circ}\text{C}$ and was treated with chlorotrimethylsilane (475 μL , 3.73 mmol). The resulting solution was stirred at 0 $^{\circ}\text{C}$ for 1.5 h prior to use.

In a 1-mL vial, aminotriol **3.74** (5.0 mg, 9.0 μmol) was dried by azeotropic removal of benzene. The dried starting material was then dissolved in tetrahydrofuran (100 μL), and the resulting solution was cooled to 0 $^{\circ}\text{C}$ with stirring. Nitrosyl chloride solution (1.08 M, 100 μL , 108 μmol , 12.0 equiv) was then added, and the resulting solution was stirred at 0 $^{\circ}\text{C}$. After 2.5 h, LCMS analysis indicated no starting material remained; the reaction mixture was concentrated under a stream of nitrogen. The dried residue was re-dissolved in 33% trifluoroacetic acid–dichloromethane, and the resulting solution was stirred at 23 $^{\circ}\text{C}$ for 30 min, at which point LCMS analysis indicated that Boc removal was complete. Toluene (1 mL) was added, and the resulting mixture was concentrated to dryness. The residue was purified by preparative HPLC on a Waters SunFire Prep C₁₈ column (5 μm , 250 \times 19 mm; eluting with 1% formic acid–5% acetonitrile–water initially, grading to 0.1% formic acid–50% acetonitrile–water over 40 min, with a flow rate of 15 mL/min; monitored by UV absorbance at 210 nm) to afford **FSA-213038** \cdot HCO₂H as a white solid (2.2 mg, 52%).

^1H NMR (600 MHz, CD_3OD) δ 4.69 (q, $J = 7.0$ Hz, 1H), 4.43 (dt, $J = 47.5, 6.0$ Hz, 2H), 4.40 (m, 1H), 4.17 (app dt, $J = 8.9, 5.8$ Hz, 1H), 4.03 (dd, $J = 10.0, 6.5$ Hz, 1H), 4.00 (dd, $J = 10.1, 2.6$ Hz, 1H), 3.85 (m, 2.0 H), 3.81 (d, $J = 3.2$ Hz, 1H), 3.76 (d, $J = 9.7$ Hz, 1H), 3.54 (d, $J = 10.0, 3.2$ Hz, 1H), 3.36 (ddd, $J = 14.0, 6.2, 3.1$ Hz, 1H), 2.32 (m, 1H), 2.04 (m, 2H), 1.93 (m, 1H), 1.73–1.52 (m, 4H), 1.49–1.45 (m, 2H), 1.44 (d, $J = 6.9$ Hz, 3H), 1.42–1.36 (m, 3H). One methylene proton corresponding to the ζ position of the azepane is obfuscated by CHD_2OD signal.

HRMS (ESI+, m/z): $[\text{M}+\text{H}]^+$ calc'd for $\text{C}_{20}\text{H}_{35}\text{Cl}_2\text{FN}_2\text{O}_5$, 473.1980; found 473.1983.



Tetraol S3.17.

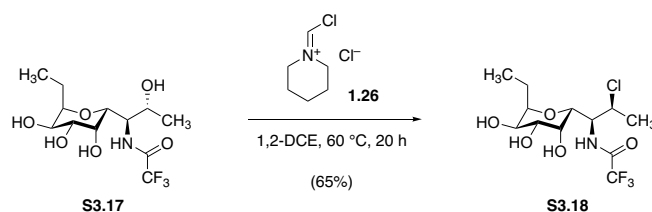
In a 10-mL glass microwave vial, an ice-cold solution of isoxazolidine **3.55** (66 mg, 0.21 mmol, 1 equiv) in methanol (2.1 mL) was treated with hydrogen chloride solution (4.0 M in 1,4-dioxane, 210 μL , 0.82 mmol, 4.0 equiv). This mixture was immediately concentrated to dryness to provide the hydrochloride salt of the starting material, which was re-dissolved in methanol (2.1 mL). This solution was then treated with palladium on carbon (10% w/w, 22 mg), the headspace of the reaction flask was replaced with hydrogen gas, and the black suspension was stirred under hydrogen gas (1 atm) at 23 $^\circ\text{C}$ for 5 h, at which point LCMS analysis indicated that olefin saturation, isoxazolidine hydrogenolysis, and debenzylation were all complete. Consequently, triethylamine (140 μL , 1.0 mmol, 5.0 equiv) was added to basify the reaction mixture, and methyl trifluoroacetate (100 μL , 1.0 mmol, 5.0 equiv) was added to protect the primary amine that had been generated in the hydrogenolytic operation. After 10 min of stirring at 23 $^\circ\text{C}$, LCMS analysis indicated that trifluoroacetylation was complete, and the mixture was filtered through a pad of Celite to remove the heterogeneous catalyst. The filter cake was rinsed with methanol ($3 \times 1\text{ mL}$), and the filtrate was concentrated *in vacuo* to give a white solid containing crude product contaminated with triethylamine hydrochloride. The latter was removed as follows: The crude product mixture was partitioned between ethyl acetate (15 mL) and saturated aqueous sodium chloride solution (15 mL). The layers were shaken, then separated; and the organic layer was washed with a fresh portion of saturated aqueous sodium chloride solution. These combined aqueous washes were then themselves extracted with fresh ethyl acetate ($2 \times 10\text{ mL}$), and the combined organic extracts (35 mL in total) were dried over sodium sulfate. The dried product

solution was filtered, and the filtrate was concentrated to give pure trifluoroacetamide as a white solid (43 mg, 63%).

^1H NMR (500 MHz, CD_3OD) δ 4.20 (app t, $J = 7.0$ Hz, 1H), 4.10 (qd, $J = 7.1, 1.7$ Hz, 1H), 4.01–3.96 (m, 2H), 3.88–3.82 (m, 2H), 1.70–1.60 (m, 2H), 1.17 (dd, $J = 6.4, 1.7$ Hz, 3H), 0.96 (t, $J = 6.8$ Hz, 3H).

^{19}F NMR (471 MHz, CD_3OD) δ -77.51 (s, 3F).

MS (ESI⁻, m/z): $[\text{M}-\text{H}]^-$ calc'd for $\text{C}_{12}\text{H}_{20}\text{F}_3\text{NO}_6$, 330.1; found 330.1.



Chloro compound S3.18.

In a 2–5 mL glass microwave vial, an ice-cold heterogeneous mixture of tetraol **S3.17** (44 mg, 0.13 mmol, 1 equiv) and 1,2-dichloroethane (2.2 mL) was treated with 1-(chloromethylene)piperidin-1-ium chloride (130 mg, 0.80 mmol, 6.0 equiv). The vial was sealed, and the mixture was stirred at 0 °C for 15 min, during which time the originally light-yellow suspension clarified to form a light-yellow solution. The mixture was then heated to 60 °C for 21 h, at which point LCMS analysis showed that deoxychlorination was complete, as evidenced by the disappearance of (oligo)formylated starting material congeners (ESI⁻, [M–H]⁻ m/z = 358, 386, 414). The mixture was chilled to 0 °C, and excess Vilsmeier reagent was quenched with the addition of aqueous sodium hydroxide solution (0.50 M, 1.60 mL, 0.80 mmol, 6.0 equiv). The resulting aqueous layer was still acidic, so additional sodium hydroxide solution (0.50 M) was added to achieve (and maintain) pH ~10. The biphasic mixture was warmed to 23 °C with rapid stirring, and saponification of pendant formyl groups was monitored by LCMS. After 18 h, deformylation was complete. The layers were separated, and the aqueous phase was then treated with sodium chloride to the point of saturation, in order to diminish the product's solubility. The resulting aqueous mixture was then extracted with dichloromethane (5 × 2 mL), until no product could be detected in the aqueous phase by LCMS. The combined organic extracts were dried over sodium sulfate, the dried solution was filtered, and the filtrate was concentrated. The crude residue thus obtained was purified by flash-column chromatography (4 g silica gel, eluting with

dichloromethane initially, grading to 7% methanol–dichloromethane) to provide the product as a white solid (30 mg, 65%).

$R_f = 0.31$ (10% methanol–dichloromethane, CAM).

$^1\text{H NMR}$ (500 MHz, CD_3OD) δ 4.63 (qd, $J = 6.9, 1.7$ Hz, 1H), 4.50 (dd, $J = 9.8, 1.6$ Hz, 1H), 3.97 (dd, $J = 10.1, 6.3$ Hz, 1H), 3.87–3.83 (m, 2H), 3.77 (dd, $J = 3.3, 1.3$ Hz, 1H), 3.56 (dd, $J = 10.2, 3.3$ Hz, 1H), 1.73–1.62 (m, 2H), 1.44 (d, $J = 6.9$ Hz, 3H), 1.02 (t, $J = 7.4$ Hz, 3H).

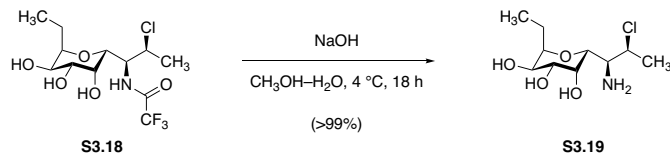
$^{13}\text{C NMR}$ (126 MHz, CD_3OD) δ 80.5, 71.9, 70.0, 69.9, 69.5, 58.9, 55.3, 23.1, 17.5, 11.2.

Trifluoroacetamide carbons were not resolved due to ^{19}F nuclear coupling.

$^{19}\text{F NMR}$ (471 MHz, CD_3OD) δ –76.74 (s, 3F).

FTIR (neat, cm^{-1}): 3365 (br), 2938 (w), 1712 (s), 1545 (w), 1212 (m), 1160 (s), 1079 (s), 963 (m).

HRMS (ESI+, m/z): $[\text{M}+\text{H}]^+$ calc'd for $\text{C}_{12}\text{H}_{19}\text{ClF}_3\text{NO}_5$, 350.0977; found 350.0981.



Aminotriol **S3.19**.

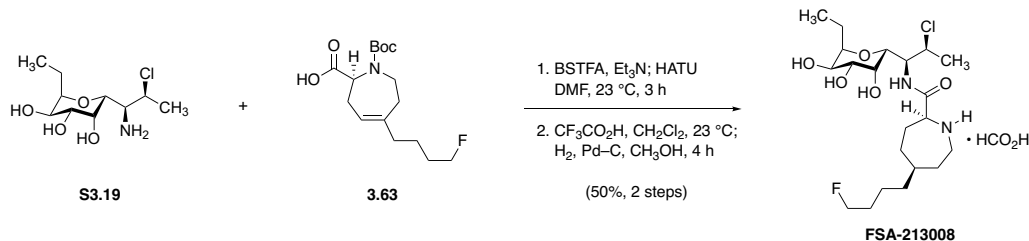
In a 4-mL glass vial, trifluoroacetamide **S3.18** (30 mg, 86 μmol , 1 equiv) was dissolved in methanol (50 μL). To this solution was then added ice-cold aqueous sodium hydroxide solution (1.0 M, 450 μL). Vigorous stirring was maintained, and the mixture was held at 4 $^\circ\text{C}$ for 18 h, at which point LCMS analysis indicated that no starting material remained. The mixture was diluted with 400 μL of ice-cold water, and the white suspension was filtered. This filter cake was washed with 300 μL of ice-cold water before being dried *in vacuo* to provide a crop of pure crystalline product (13 mg, 60%). The filtrate, containing additional aminotriol product, was acidified with the addition of aqueous hydrogen chloride solution (1.0 M, 500 μL) before it was concentrated to dryness to provide crude product as its hydrochloride salt, contaminated with sodium chloride. This solid was suspended in ethanol (190 proof, 1.0 mL), and the supernatant (containing **S3.19** • HCl) was transferred to a vial containing Amberlyst A26 resin (hydroxide form, 300 mg). This mixture was stirred at 0 $^\circ\text{C}$ for 30 min before the ion-exchange beads were removed by filtration. The filtrate was concentrated to provide additional product (11 mg, estimated 80% pure by ^1H NMR, ~40%).

^1H NMR (500 MHz, CD_3OD) δ 4.62 (q, $J = 6.7$ Hz, 1H), 4.08 (app t, $J = 2.6$ Hz, 1H), 3.91 (dd, $J = 9.4, 5.7$ Hz, 1H), 3.78 (app q, $J = 6.8$ Hz, 1H), 3.63 (dd, $J = 9.4, 3.4$ Hz, 1H), 3.48 (dd, $J = 9.3, 1.9$ Hz, 1H), 3.10 (d, $J = 9.2$ Hz, 1H), 1.63 (app p, $J = 7.4$ Hz, 2H), 1.56 (d, $J = 6.9$ Hz, 3H), 0.99 (t, $J = 7.4$ Hz, 3H).

^{13}C NMR (100 MHz, CD_3OD) δ 79.0, 72.9, 72.1, 70.2, 69.9, 61.0, 56.5, 22.7, 18.3, 11.1.

FTIR (neat, cm^{-1}): 3300 (br), 2929 (w), 2464 (w), 1620 (w), 1076 (s), 963 (m).

HRMS (ESI+, m/z): $[\text{M}+\text{H}]^+$ calc'd for $\text{C}_{10}\text{H}_{20}\text{ClNO}_4$, 254.1154; found 254.1154.



Synthetic lincosamide FSA-213008.

A solution of aminotriol **S3.19** (12.9 mg, 51.0 μmol , 1 equiv) in *N,N*-dimethylformamide (254 μL) was treated sequentially with triethylamine (22.7 μL , 163 μmol , 3.20 equiv) and *N,O*-bis(trimethylsilyl)trifluoroacetamide (20.5 μL , 76.0 μmol , 1.50 equiv) at 23 °C. The mixture was stirred for 1 h to ensure complete *O*-silylation before a solution of azepine acid **3.63** (17.6 mg, 56.0 μmol , 1.10 equiv) in *N,N*-dimethylformamide (200 μL) was added. The reaction mixture was then treated with HATU (25.1 mg, 66.0 μmol , 1.30 equiv), and the lemon-yellow mixture was stirred at 23 °C for 3 h. After this time, the reaction mixture was diluted with ethyl acetate (20 mL) and the diluted organic solution was washed sequentially with 10-mL portions of 10% w/v aqueous citric acid solution, saturated aqueous sodium bicarbonate solution, and saturated aqueous sodium chloride solution. The washed organic layer was then dried over sodium sulfate, filtered, and concentrated. The dried residue was transferred to a 4-mL glass vial, where it was re-dissolved in 33% v/v trifluoroacetic acid–dichloromethane (300 μL). Deprotection was monitored by LCMS, and after 15 min global trimethylsilyl and Boc removal was complete. The mixture was concentrated to dryness, and the residue was re-dissolved in methanol (300 mL). Palladium on carbon (10% w/w, 20 mg) was added, the headspace above the black suspension was replaced with hydrogen gas, and the mixture was stirred at 23 °C for 4 h, resulting in complete hydrogenation of the azepine, as indicated by LCMS. The mixture was filtered through a pad of Celite to remove the heterogeneous catalyst, and the filter cake was rinsed with methanol (3×1 mL). The filtrate

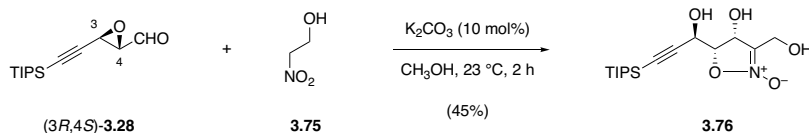
was concentrated to give a brown film, which was subjected to preparative HPLC-MS on a Waters SunFire Prep C₁₈ column (5 μm, 250 × 19 mm; eluting with 0.1% formic acid–5% acetonitrile–water initially, grading to 0.1% formic acid–40% acetonitrile–water over 40 min, with a flow rate of 15 mL/min; monitored by UV absorbance at 210 nm and ESI+ selected ion monitoring [*m/z* = 453]) to provide the product (**FSA-213008** • HCO₂H, 3.0 mg, 50%, 2 steps) as a white solid.

¹H NMR (600 MHz, CD₃OD) δ 8.42 (s, 1H), 4.64 (q, *J* = 6.8 Hz, 1H), 4.42 (dt, *J* = 47.5, 6.0 Hz, 2H), 4.41 (d, *J* = 9.7 Hz, 1H), 4.10 (app t, *J* = 5.6 Hz, 1H), 3.96 (dd, *J* = 10.1, 6.3 Hz, 1H), 3.85 (ddd, *J* = 10.1, 6.2, 3.2 Hz, 1H), 3.80 (app s, 1H), 3.68 (d, *J* = 9.7 Hz, 1H), 3.57 (dd, *J* = 10.3, 3.0 Hz, 1H), 3.44 (dd, *J* = 13.3, 4.5 Hz, 1H), 3.13 (app t, *J* = 12.5 Hz, 1H), 2.25–2.14 (m, 2H), 2.02 (br d, *J* = 14.9 Hz, 1H), 1.94 (ddd, *J* = 14.8, 8.2, 4.0 Hz, 1H), 1.72–1.61 (m, 5H), 1.61–1.53 (m, 1H), 1.47–1.42 (m, 3H), 1.44 (d, *J* = 6.7 Hz, 3H), 1.37–1.33 (m, 2H), 1.02 (t, *J* = 7.3 Hz, 3H).

¹³C NMR (126 MHz, CD₃OD) δ 171.6, 84.7 (d, *J* = 163.7 Hz), 80.4, 71.8, 70.6, 69.9, 69.6, 60.5, 59.3, 55.0, 45.6, 38.9, 37.4, 33.3, 31.6 (d, *J* = 19.6 Hz), 30.7, 29.1, 23.8 (d, *J* = 5.1 Hz, 1H), 23.2, 17.4, 11.2.

FTIR (neat, cm⁻¹): 3266 (br), 2934 (m), 1672 (m), 1590 (s), 1459 (m), 1378 (m), 1346 (m), 1084 (m).

HRMS (ESI+, *m/z*): [M+H]⁺ calc'd for C₂₁H₃₈ClFN₂O₅, 453.2526; found 453.2526.



Isoxazoline *N*-oxide **3.76**.

In a 100-mL round-bottomed flask, epoxyaldehyde (3*R*,4*S*)-**3.28** (4.93 g, 19.5 mmol, 1 equiv) was dissolved in methanol (39.1 mL). To this solution were added nitroethanol (2.80 mL, 39.1 mmol, 2.0 equiv) and potassium carbonate (270 mg, 1.95 mmol, 0.100 equiv). After stirring for 2 h at 23 °C, TLC analysis (60% ethyl acetate–hexanes, CAM) showed complete consumption of epoxyaldehyde starting material, as well as the disappearance of intermediate, linear, mid-polar nitroaldol adducts (R_f 's 0.63–0.77, 60% ethyl acetate–hexanes, CAM). The mixture was concentrated *in vacuo*, and crude $^1\text{H-NMR}$ analysis of the residue revealed a 62:38 diastereomeric ratio favoring the desired C5 epimer. This crude mixture was subjected to flash-column chromatographic separation (700 g silica gel, eluting with 50% ethyl acetate–hexanes initially, grading to 80% ethyl acetate–hexanes) to afford isoxazoline *N*-oxide product as a brilliant white powder (3.00 g, 45%).

Melting point: 55–57 °C.

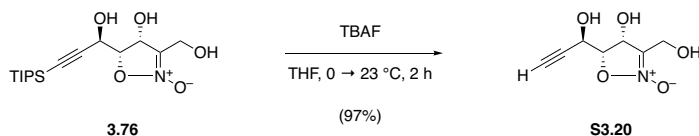
R_f = 0.38 (ethyl acetate, CAM).

$^1\text{H NMR}$ (500 MHz, CDCl_3) δ 5.51 (app t, J = 6.9 Hz, 1H), 4.89 (dd, J = 6.6, 5.0 Hz, 1H), 4.67 (dd, J = 7.4, 5.0 Hz, 1H), 4.56–4.53 (m, 2H), 3.42 (d, J = 6.6 Hz, 1H), 2.97 (d, J = 6.7 Hz, 1H), 2.42 (t, J = 6.3 Hz, 1H), 1.09–1.08 (m, 21H).

$^{13}\text{C NMR}$ (126 MHz, CDCl_3) δ 118.7, 103.0, 89.8, 79.7, 74.8, 60.6, 55.2, 18.7, 11.2.

FTIR (neat, cm^{-1}): 3357 (br), 2942 (s), 2865 (s), 1639 (s), 1463 (m), 1014 (s), 883 (s), 677 (s).

HRMS (ESI+, m/z): $[M+H]^+$ calc'd for $C_{16}H_{29}NO_5Si$, 366.1707; found 366.1703.



Triol S3.20.

To a solution of isoxazoline *N*-oxide **3.76** (4.70 g, 13.7 mmol, 1 equiv) in tetrahydrofuran (137 mL) was added tetrabutylammonium fluoride solution (1.0 M in tetrahydrofuran, 32.8 mL, 32.8 mmol, 2.40 equiv) dropwise at 0 °C. The resulting colorless solution was immediately warmed to 23 °C, and after 2 h of stirring at that temperature, TLC analysis (5% methanol–ethyl acetate, CAM) indicated complete consumption of starting material. The mixture was loaded directly onto a column of silica gel (500 g) pre-equilibrated with ethyl acetate. The product was eluted with 5% methanol–ethyl acetate, and product-containing fractions were pooled. The pooled fractions were concentrated to give the product as a buff white solid (221 mg, 97%).

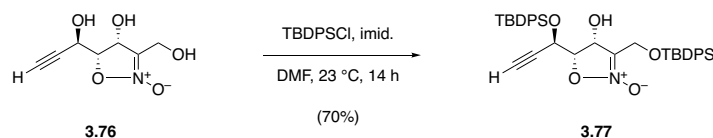
R_f = 0.32 (5% methanol–ethyl acetate, CAM).

$^1\text{H NMR}$ (500 MHz, CD_3OD) δ 5.25 (d, J = 6.3 Hz, 1H), 4.73 (dd, J = 8.1, 2.2 Hz, 1H), 4.45 (dd, J = 6.3, 8.1 Hz, 1H), 4.43 (d, J = 14.6 Hz, 1H), 4.33 (d, J = 14.1 Hz, 1H), 2.91 (d, J = 2.2 Hz, 1H).

$^{13}\text{C NMR}$ (126 MHz, CD_3OD) δ 120.8, 82.9, 81.9, 75.4, 75.4, 73.5, 73.5, 58.8, 55.1.

FTIR (neat, cm^{-1}): 3279 (br), 2933 (w), 1639 (s), 1293 (m), 1092 (m), 1044 (m), 1019 (m).

HRMS (ESI+, m/z): $[\text{M}+\text{H}]^+$ calc'd for $\text{C}_7\text{H}_9\text{NO}_5$, 210.0373; found 210.0370.



Bis-silyl ether 3.77.

To a solution of triol **3.76** (2.35 g, 12.6 mmol, 1 equiv) and imidazole (4.27 g, 62.8 mmol, 8.00 equiv) in *N,N*-dimethylformamide (62.8 mL) was added *tert*-butyl(chloro)diphenylsilane (7.26 mL, 28.3 mmol, 4.00 equiv) dropwise at 0 °C. The mixture was then warmed to 23 °C. Silylation of the primary alcohol was fast (generally complete within 5 min), while silylation of the propargylic alcohol was substantially slower – after 14 h of stirring at 23 °C, TLC analysis (60% ethyl acetate–hexanes, UV+KMnO₄) showed complete consumption of the mono-silylated intermediate ($R_f = 0.61$). Excess chlorosilane reagent was quenched with the addition of saturated aqueous ammonium chloride (100 mL), and the resulting mixture was stirred rapidly at 23 °C for 10 min. The mixture was then extracted with 20% ethyl acetate–hexanes (4 × 100 mL); the organic extracts were then combined, washed with saturated aqueous sodium chloride solution (100 mL), dried over sodium sulfate, filtered, and concentrated to give a light golden-amber oil. This residue was purified by flash-column chromatography (500 g silica gel, eluting with hexanes initially, grading to 20% ethyl acetate–hexanes) to provide the product as a white, foaming, amorphous solid (5.87 g, 70%).

$R_f = 0.39$ (20% ethyl acetate–hexanes, UV+KMnO₄).

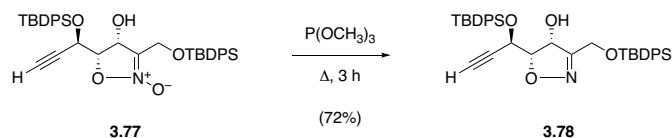
¹H NMR (500 MHz, CDCl₃) δ 7.80–7.78 (m, 2H), 7.76–7.71 (m, 6H), 7.51–7.46 (m, 4H), 7.45–7.40 (m, 8H), 5.34 (app t, $J = 7.7$ Hz, 1H), 4.81 (dd, $J = 5.1, 2.3$ Hz, 1H), 4.64 (d, $J = 13.7$

Hz, 1H), 4.57 (d, $J = 13.8$ Hz, 1H), 4.46 (dd, $J = 7.2, 5.1$ Hz, 1H), 3.38 (d, $J = 8.1$ Hz, 1H), 2.47 (d, $J = 2.3$ Hz, 1H), 1.12 (s, 18 H).

^{13}C NMR (126 MHz, CDCl_3) δ 136.2, 136.0, 135.6 (2 \times C), 132.6, 132.5, 132.1, 131.6, 130.5, 130.3, 130.2 (2 \times C), 128.1 (2 \times C), 128.0, 127.7, 116.9, 79.8, 79.2, 76.5, 74.3, 61.8, 57.0, 26.9 (2 \times C), 19.4, 19.3.

FTIR (neat, cm^{-1}): 2931 (w), 2858 (w), 1644 (m), 1427 (m), 1105 (s), 1082 (s), 699 (s).

HRMS (ESI+, m/z): $[\text{M}+\text{H}]^+$ calc'd for $\text{C}_{39}\text{H}_{45}\text{NO}_5\text{Si}_2$, 664.2909; found 664.2900.



Isoxazoline 3.78.

In a 100-mL round-bottomed flask, isoxazoline *N*-oxide **3.77** (2.50 g, 3.77 mmol, 1 equiv) was dried by azeotropic removal of benzene. The dried starting material was then dissolved in trimethyl phosphite (15.1 mL), the flask was fitted with an oven-dried reflux condenser, and the reaction solution was heated to 100 °C in a pre-heated oil bath. After 3 h, TLC analysis (20% ethyl acetate–hexanes, PAA) showed complete consumption of starting material. The mixture was cooled to 0 °C and diluted in diethyl ether (200 mL); the organic product solution was then washed sequentially with 0.1 M aqueous HCl solution (2 × 40 mL) and saturated aqueous sodium chloride solution (50 mL). The washed organic solution was dried over sodium sulfate, filtered, and concentrated to give a light yellow foaming solid. This residue was purified by flash-column chromatography (220 g silica gel, eluting with hexanes initially, grading to 20% ethyl acetate–hexanes) to provide the product as a white, foaming, amorphous solid (1.76 g, 72%).

$R_f = 0.47$ (20% ethyl acetate–hexanes, UV+KMnO₄)

¹H NMR (600 MHz, CDCl₃) δ 7.78–7.76 (m, 2H), 7.74–7.71 (m, 4H), 7.70–7.68 (m, 2H), 7.48–7.44 (m, 4H), 7.42–7.39 (m, 8H), 5.43 (app t, $J = 8.8$ Hz, 1H), 4.85 (dd, $J = 4.0, 2.4$ Hz, 1H), 4.60 (d, $J = 13.1$ Hz, 1H), 4.56 (d, $J = 12.9$ Hz, 1H), 4.39 (dd, $J = 8.5, 3.9$ Hz, 1H), 3.90 (d, $J = 9.0$ Hz, 1H), 2.48 (d, $J = 2.3$ Hz, 1H), 1.08 (s, 9H), 1.06 (s, 9H).

^{13}C NMR (126 MHz, CDCl_3) δ 159.9, 136.3 (2 \times C), 135.8, 135.7, 132.8 (2 \times C), 132.2, 131.5, 130.5, 130.2, 130.1 (2 \times C), 128.0, 128.0 (3 \times C), 127.7, 83.1, 80.4, 77.2, 76.0, 63.0, 57.5, 26.9 (2 \times C), 19.4 (2 \times C).

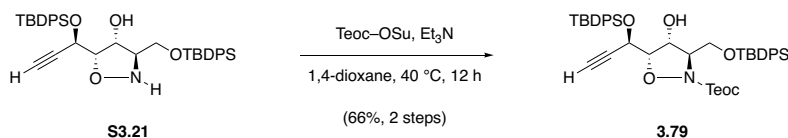
HRMS (ESI+, m/z): $[\text{M}+\text{H}]^+$ calc'd for $\text{C}_{39}\text{H}_{45}\text{NO}_4\text{Si}_2$, 648.2960; found 648.2957.

^1H NMR (500 MHz, CDCl_3) δ 7.80–7.72 (m, 4H), 7.67–7.61 (m, 4H), 7.50–7.36 (m, 12H), 4.90 (dd, $J = 5.3, 2.9$ Hz, 1H), 4.77 (dd, $J = 4.8, 2.2$ Hz, 1H), 3.94–3.88 (m, 2H), 3.71 (dd, $J = 11.0, 5.6$ Hz, 1H), 3.43 (dt, $J = 6.4, 3.6$ Hz, 1H), 2.44 (d, $J = 2.2$ Hz, 1H), 1.11 (s, 9H), 1.08 (s, 9H).

^{13}C NMR (126 MHz, CDCl_3) δ 136.3, 136.1, 135.7, 135.6, 132.9 ($2 \times \text{C}$), 132.3, 132.0, 130.4, 130.3, 130.1 ($2 \times \text{C}$), 128.0 ($3 \times \text{C}$), 127.8, 127.7, 81.1, 77.7, 75.8, 70.9, 63.1, 61.0, 27.0 ($2 \times \text{C}$), 19.4 ($2 \times \text{C}$).

FTIR (neat, cm^{-1}): 3288 (w), 2931 (m), 2858 (m), 1428 (m), 1112 (s), 701 (s).

HRMS (ESI+, m/z): $[\text{M}+\text{H}]^+$ calc'd for $\text{C}_{39}\text{H}_{47}\text{NO}_4\text{Si}_2$, 650.3116; found 650.3119.



Carbamate S3.79.

A solution of isoxazolidine **S3.21** (theoretically 3.09 mmol, 1 equiv) and *N*-[2-(trimethylsilyl)ethoxycarbonyloxy]succinimide (Teoc-OSu, 1.20 mg, 4.64 mmol, 1.50 equiv) in 1,4-dioxane (7.73 mL) was treated with triethylamine (2.15 mL, 15.5 mmol, 5.00 equiv) at 23 °C, and the resulting solution was warmed to 40 °C. After 12 h of stirring at this temperature, LCMS analysis showed full consumption of starting material, and the reaction mixture was diluted with ethyl acetate (200 mL). The resulting product solution was washed sequentially with saturated aqueous ammonium chloride solution (2 × 40 mL) and saturated sodium chloride solution (40 mL). The washed solution was then dried over sodium sulfate, filtered, and concentrated to provide a foaming, gummy oil. This crude residue was purified by flash-column chromatography (120 g silica gel, eluting with hexanes initially, grading to 15% ethyl acetate–hexanes) to furnish the product as a crispy white amorphous solid (1.61 g, 66%, 2 steps).

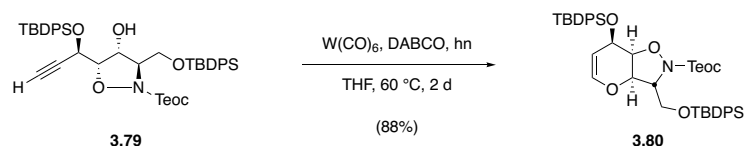
$R_f = 0.48$ (20% ethyl acetate–hexanes, UV+KMnO₄).

¹H NMR (500 MHz, CDCl₃) δ 7.83–7.80 (m, 4H), 7.71–7.67 (m, 4H), 7.51–7.38 (m, 8H), 4.96 (app t, $J = 3.8$ Hz, 1H), 4.87 (dd, $J = 5.6, 2.3$ Hz, 1H), 4.34 (dd, $J = 6.6, 4.1$ Hz, 1H), 4.27 (dd, $J = 5.6, 3.6$ Hz), 4.26–4.14 (m, 2H), 3.90 (dd, $J = 10.8, 4.1$ Hz, 1H), 3.73 (dd, $J = 10.8, 6.6$ Hz, 1H), 3.61 (d, $J = 3.8$ Hz, 1H), 2.42 (d, $J = 2.2$ Hz, 1H), 1.14 (s, 9H), 1.10 (s, 9H), 1.02–0.98 (m, 1H), 0.93–0.89 (m, 1H), 0.06 (s, 9H).

^{13}C NMR (126 MHz, CDCl_3) δ 157.1, 136.3, 136.1, 135.7 (2 \times C), 133.0 (2 \times C), 132.3, 131.9, 130.3, 130.2, 130.0, 129.9, 128.0, 127.9 (2 \times C), 127.7, 83.2, 80.8, 75.9, 70.2, 64.8, 62.9, 62.1, 26.9 (2 \times C), 19.4 (2 \times C), 17.7, -1.4.

IR (neat, cm^{-1}): 2954 (2), 2858 (w), 1702 (w), 1427 (m), 1104 (s), 837 (m), 731 (s), 699 (s).

HRMS (ESI+, m/z): $[\text{M}+\text{H}]^+$ calc'd for $\text{C}_{45}\text{H}_{59}\text{NO}_6\text{Si}_3$, 794.3723; found 794.3720.



Glycal **3.80**.

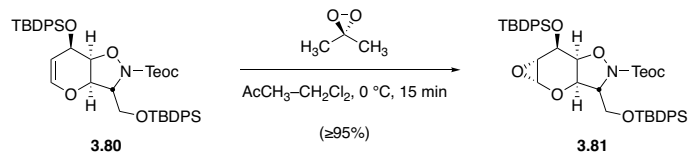
In a 100-mL borosilicate glass microwave reaction vial, alkyne **3.79** (1.60 g, 2.02 mmol, 1 equiv) was dried by azeotropic removal of benzene. To the dried starting material was added tungsten hexacarbonyl (177 mg, 0.504 mmol, 0.250 equiv) and 1,4-diazabicyclo[2.2.2]octane (452 mg, 4.03 mmol, 2.00 equiv). CAUTION: Tungsten hexacarbonyl is a volatile source of metal and of carbon monoxide. Manipulations of this reagent should be conducted within a well-ventilated fume hood. The vial was flushed with dry argon gas, and then anhydrous, degassed tetrahydrofuran (20.2 mL) was added at $23\text{ }^\circ\text{C}$. The resulting colorless solution attained a vibrant fluorescent yellow color within 3 minutes. The vial was sealed and was transferred to a pre-heated oil bath ($60\text{ }^\circ\text{C}$) positioned inside a photochemistry safety cabinet. The reaction mixture was heated with constant UV irradiation from an adjacent 200-Watt mercury-vapor bulb filtered through a water-cooled Pyrex glass jacket (CAUTION: Exposure to high-intensity UV light can cause irreversible vision loss – never open the safety cabinet when the UV lamp is on). Progress was monitored by TLC (20% ethyl acetate–hexanes, UV+KMnO₄). After 2 d, full consumption of alkyne substrate was achieved, and the crude product mixture was concentrated to dryness *in vacuo*. The goldenrod, oily residue was purified by flash-column chromatography (120 g silica gel, eluting with hexanes initially, grading to 15% ethyl acetate–hexanes) to provide the product as a viscous, colorless oil (1.40 g, 88%).

^1H NMR (500 MHz, C_6D_6) δ 7.93–7.91 (m, 2H), 7.88–7.85 (m, 2H), 7.70–7.65 (m, 4H), 7.28–7.18 (m, 12H), 5.98 (dd, $J = 6.5, 2.2$ Hz, 1H), 4.69 (app dt, $J = 6.5, 1.9$ Hz, 1H), 4.64 (dd, $J = 7.0, 4.1$ Hz, 1H), 4.61 (app dt, $J = 4.4, 2.1$ Hz), 4.32–4.26 (m, 2H), 4.24–4.17 (m, 2H), 3.85 (dd, $J = 10.9, 4.1$ Hz, 1H), 3.69 (dd, $J = 10.8, 7.0$ Hz, 1H), 1.22 (s, 9H), 1.10 (s, 9H), 0.91 (t, $J = 8.3$ Hz, 2H), -0.07 (s, 9H).

^{13}C NMR (126 MHz, C_6D_6) δ 157.3, 142.0, 136.3 ($2 \times \text{C}$), 136.0 ($2 \times \text{C}$), 134.2 ($2 \times \text{C}$), 133.5, 133.4, 130.2 ($4 \times \text{C}$), 128.4, 128.2 ($2 \times \text{C}$), 128.1, 102.1, 78.9, 76.9, 69.3, 64.5, 63.6, 63.3, 27.1 ($2 \times \text{C}$), 19.6, 19.4, 17.7, -1.4 .

IR (neat, cm^{-1}): 2954 (m), 2931 (m), 2857 (m), 1702 (m), 1427 (m), 1111 (s), 1066 (s), 837 (m), 701 (s).

HRMS (ESI+, m/z): $[\text{M}+\text{H}]^+$ calc'd for $\text{C}_{45}\text{H}_{59}\text{NO}_6\text{Si}_3$, 794.3723; found 794.3696.



Brigl's anhydride **3.81**.

A solution of dimethyldioxirane in acetone was prepared, and its concentration was assayed according to the procedures of Murray and Singh.¹³¹ A solution of glycal **3.80** (920 mg, 1.16 mmol, 1 equiv) in dichloromethane (11.6 μL) was cooled to 0 $^\circ\text{C}$, whereupon dimethyldioxirane solution (0.0775 M, 17.9 mL, 1.39 μmol , 1.20 equiv) was added dropwise over 3 min. The reaction mixture was stirred at 0 $^\circ\text{C}$ for 15 min, at which point TLC analysis (NH_2 silica gel, 20% ethyl acetate–hexanes, UV+PAA) indicated full consumption of starting material. The mixture was then concentrated under a stream of dry argon, and the residue was dried by azeotropic removal of benzene to afford Brigl's anhydride product as a colorless oil that was suitable for use without further purification (quantitative yield, $\geq 95\%$ purity by NMR).

$R_f = 0.63$ (NH_2 silica gel, 20% ethyl acetate–hexanes + 2% methanol, UV+CAM).

$^1\text{H NMR}$ (500 MHz, C_6D_6) δ 7.89–7.86 (m, 2H), 7.80–7.76 (m, 2H), 7.65–7.59 (m, 4H), 7.22–7.13 (m, 12H), 4.65 (app dt, $J = 2.3, 1.1$ Hz, 1H), 4.61 (dd, $J = 7.1, 4.3$ Hz, 1H), 4.31 (d, $J = 5.1$ Hz, 1H), 4.28–4.17 (m, 2H), 4.12 (d, $J = 2.0$, 1H), 3.88 (d, $J = 4.9$ Hz, 1H), 3.74 (dd, $J = 10.9, 4.3$ Hz, 1H), 3.53 (dd, $J = 10.8, 7.2$ Hz, 1H), 2.94 (app t, $J = 1.1$ Hz, 1H), 1.19 (s, 9H), 1.04 (s, 9H), 0.88 (t, $J = 8.3$ Hz, 2H), -0.11 (s, 9H).

$^{13}\text{C NMR}$ (126 MHz, C_6D_6) δ 157.2, 136.2, 136.1, 135.9 (2 \times C), 133.4 (2 \times C), 133.3, 133.2, 130.3 (2 \times C), 130.1, 128.3, 128.2, 128.1, 77.1, 74.7, 73.2, 69.4, 66.9, 64.5, 63.3, 51.6, 27.0, 19.6, 19.3, 17.6, -1.5 . Two phenyl carbons are not observed: One is believed to be

obfuscated by the solvent signal, and the other is believed to coincide with another resonance (δ 130.1).

IR (neat, cm^{-1}): 2954 (m), 2931 (m), 2858 (m), 1703 (m), 1427 (m), 1249 (m), 1111 (s), 822 (s), 700 (s).

HRMS (ESI+, m/z): $[\text{M}+\text{H}]^+$ calc'd for $\text{C}_{45}\text{H}_{59}\text{NO}_7\text{Si}_3$, 810.3672; found 810.3667.

over 18 min; monitored by UV absorbance at 210 nm; product $R_t = 8.75$ min) to give the trifluoroacetic acid salt of **S3.22** • $\text{CF}_3\text{CO}_2\text{H}$ in pure form.

$R_f = 0.06$ (free base, 10% methanol–ethyl acetate, PAA).

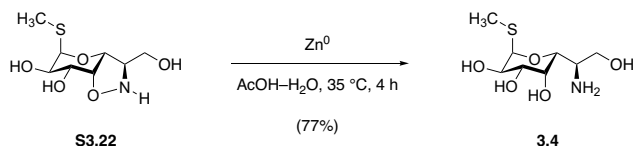
^1H NMR (hydrotrifluoroacetate salt, 500 MHz, CD_3OD) δ 5.27 (d, $J = 5.0$ Hz, 1H), 4.98 (d, $J = 2.0$ Hz, 1H), 4.71 (dd, $J = 3.8, 2.1$ Hz, 1H), 4.12 (dd, $J = 10.1, 5.1$ Hz, 1H), 4.10 (app t, $J = 5.5$ Hz, 1H), 3.99 (dd, $J = 10.0, 3.8$ Hz, 1H), 3.87 (dd, $J = 12.0, 4.8$ Hz, 1H), 3.83 (dd, $J = 12.0, 6.0$ Hz, 1H), 2.14 (s, 3H).

^{13}C NMR (hydrotrifluoroacetate salt, 100 MHz, CD_3OD) δ 89.0, 85.4, 76.1, 70.1, 69.0, 68.6, 59.0, 13.1.

^{19}F NMR (hydrotrifluoroacetate salt, 471 MHz, CD_3OD) δ -77.3 (s, 3F).

IR (hydrotrifluoroacetate salt, neat, cm^{-1}): 3349 (br), 1672 (s), 1434 (w), 1199 (s), 1139 (m), 1095 (m), 1051 (m).

HRMS (ESI+, m/z): $[\text{M}+\text{H}]^+$ calc'd for $\text{C}_8\text{H}_{15}\text{NO}_5\text{S}$ 238.0744; found 238.0739.



Aminotetraol 3.4.

To a solution of isoxazolidine triol **S3.22** (234 mg, 986 μmol , 1 equiv) in 50% v/v acetic acid–water (9.86 mL) was added activated zinc powder (258 mg, 3.94 mmol, 4.00 equiv). The mixture was heated to 35 °C with stirring, and after 4 h, LCMS showed complete conversion of starting material to aminotetraol product. The mixture was cooled before it was filtered through a Celite pad. The filter cake was washed with methanol (3 \times 5 mL), and the combined filtrates were concentrated to dryness. Residual acetic acid was removed by repeated concentration from 50% v/v methanol–toluene. Once dried, the crude residue, containing the hydroacetate salt of the desired product as well as zinc acetate as a major impurity, was dissolved in methanol (20 mL) and was treated with Amberlyst A26 resin (hydroxide form, 4.00 g). After stirring the mixture at 23 °C for 1 h, the ion-exchange beads were removed by filtration, and the filtrate was concentrated to give a white solid. This crude residue was finally purified by flash-column chromatography (25 silica gel, eluting with 1% ammonium hydroxide–10% methanol–dichloromethane initially, grading to 10% ammonium hydroxide–40% methanol–dichloromethane) to provide methylthio-8-norlincosamine as a white solid (182 mg, 77%).

$R_f = 0.30$ (10% ammonium hydroxide–40% methanol–dichloromethane, ninhydrin).¹⁵⁵

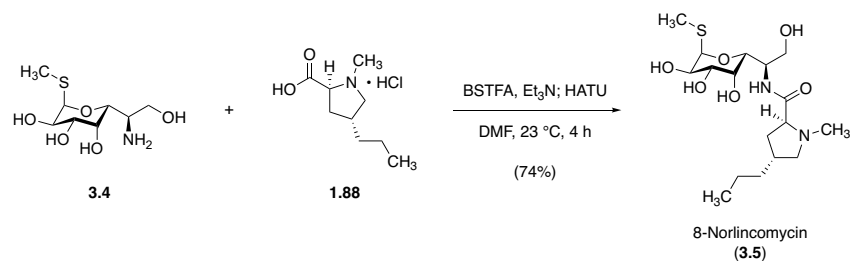
¹⁵⁵ Note: Prior to staining with ninhydrin, TLC plates must be heated thoroughly (~200 °C, 30 s) to drive off residual ammonia, which interferes with proper staining.

^1H NMR (400 MHz, D_2O) δ 5.17 (d, $J = 5.7$ Hz, 1H), 3.95–3.92 (m, 2H), 3.84 (d, $J = 9.2$ Hz, 1H), 3.63 (dd, $J = 11.0, 2.5$ Hz, 1H), 3.54 (dd, $J = 10.2, 2.9$ Hz, 1H), 3.38 (dd, $J = 11.2, 6.1$ Hz, 1H), 2.91 (ddd, $J = 9.0, 6.1, 3.2$ Hz, 1H), 1.92 (s, 3H).

^{13}C NMR (100 MHz, D_2O) 87.0, 70.5, 70.3, 68.2, 67.8, 63.0, 50.6, 12.0.

FTIR (neat, cm^{-1}): 2939 (s), 2865 (m), 1711 (s), 1464 (m), 1434 (m), 1125 (m), 1036 (m), 756 (s).

HRMS (ESI+, m/z): $[\text{M}+\text{H}]^+$ calc'd for $\text{C}_8\text{H}_{17}\text{NO}_5\text{S}$, 240.0900; found 240.0899.



8-Norlincomycin (3.5).

In a 2–5 mL glass microwave vial fitted with a magnetic stir bar, methylthio-8-norlincosamine (**3.4**, 100 mg, 418 μ mol, 1 equiv) was dissolved in *N,N*-dimethylformamide (2.09 mL). Triethylamine (262 μ L, 1.88 mmol, 4.50 equiv) and *N,O*-bis(trimethylsilyl)trifluoroacetamide (224 μ L, 836 μ mol, 2.00 equiv) were added next, and the solution was stirred at 23 °C for 1 h to ensure complete *O*-silylation. After this period, *trans*-4-*n*-propyl-L-hygric acid hydrochloride (**1.88**) (104 mg, 501 μ mol, 1.20 equiv) and HATU (222 mg, 585 μ mol, 1.40 equiv) were added, causing the reaction mixture to attain a canary yellow hue. Following 4 h of stirring at 23 °C, LCMS analysis showed complete conversion of aminotetraol starting material and its (oligo)silylated congeners to amide products. The reaction mixture was consequently diluted with ethyl acetate (25 mL) and the diluted solution was washed with saturated aqueous sodium bicarbonate solution (10 mL). The aqueous layer was extracted with ethyl acetate (3 \times 10 mL), and the combined organic layers were then washed with saturated aqueous sodium chloride solution (15 mL). The washed organic solution was dried over sodium sulfate, filtered, and concentrated; and the residue thus obtained was re-dissolved in 50% v/v methanol–acetic acid. This colorless solution was stirred at 40 °C for 24 h to ensure complete desilylation before it was concentrated to dryness *in vacuo*. Residual acetic acid was removed by repeated concentration of the mixture from 50% v/v methanol–toluene. Once thoroughly dried, the crude residue was treated with methanol (10 mL) and Amberlyst A26 resin (hydroxide form, 2.00 g). The resulting mixture

was stirred at 23 °C for 1 h before the ion-exchange beads were removed by filtration and the filtrate was concentrated. This light amber-colored oily residue was purified by flash-column chromatography (18 g silica gel, eluting with 0.5% ammonium hydroxide–5% methanol–dichloromethane initially; grading to 1% ammonium hydroxide–10% methanol–dichloromethane) to furnish 8-norlincomycin (**3.5**) as a light yellow, foaming solid (121 mg, 74%).

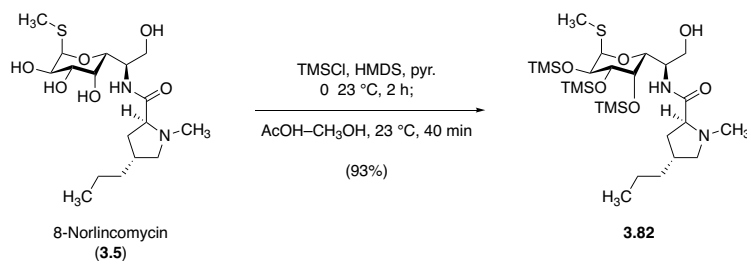
$R_f = 0.23$ (1% ammonium hydroxide–10% methanol–dichloromethane, PMA or I₂).

¹H NMR (500 MHz, CD₃OD) δ 5.29 (d, $J = 5.6$ Hz, 1H), 4.17 (d, $J = 8.9$ Hz, 1H), 4.12–4.08 (m, 2H), 3.78 (app dt, $J = 6.6, 5.1$ Hz, 2H), 3.72 (dd, $J = 10.7, 4.2$ Hz, 1H), 3.63 (dd, $J = 10.1, 3.4$ Hz, 1H), 3.21 (dd, $J = 8.7, 6.0$ Hz, 1H), 2.95 (dd, $J = 10.6, 4.8$ Hz, 1H), 2.37 (s, 3H), 2.19–2.15 (m, 1H), 2.08 (s, 3H), 2.05 (dd, $J = 10.1, 8.8$ Hz, 1H), 1.99 (ddd, $J = 13.0, 8.2, 4.8$ Hz, 1H), 1.84 (app dt, $J = 12.9, 10.3$ Hz, 1H), 1.36–1.31 (m, 4H), 0.92 (t, $J = 6.5$ Hz, 3H).

¹³C NMR (126 MHz, CD₃OD) δ 178.2, 89.0, 71.9, 70.4, 69.8 (2 \times C), 69.5, 63.8, 61.5, 51.9, 41.9, 38.9, 38.6, 37.0, 22.6, 14.6, 12.8.

FTIR (neat, cm⁻¹): 3333 (br), 2920 (s), 2787 (m), 1644 (s), 1525 (s), 1080 (s).

HRMS (ESI+, m/z): [M+H]⁺ calc'd for C₁₇H₃₂N₂O₆S, 393.2054; found 393.2050.



Alcohol 3.82.

In a 2–5 mL glass microwave vial, an ice-cold solution of 8-norlincomycin (**3.5**, 90.0 mg, 229 μmol , 1 equiv) in pyridine (382 μL) was treated sequentially with hexamethyldisilazane (121 μL , 578 μmol , 2.52 equiv) and chlorotrimethylsilane (168 μL , 1.31 mmol, 5.72 equiv). Following the addition of these reagents, the mixture was warmed to 23 $^\circ\text{C}$, and stirring was maintained for 2 h. The mixture was then concentrated to dryness *in vacuo*, and the residue was partitioned between hexanes (10 mL) and water (10 mL). The layers were separated, and the aqueous phase was extracted with additional hexanes (3×5 mL). The combined organic extracts were then dried over sodium sulfate, the dried solution was filtered, and the filtrate was concentrated to afford crude, persilylated 8-norlincomycin as a brilliant white solid. This material was then suspended in methanol (887 μL), and 80% v/v acetic acid–water (133 μL) was added to the suspension, causing the mixture to become a homogeneous, colorless solution. Desilylation was monitored by TLC (40% ethyl acetate–hexanes, CAM; persilylated intermediate $R_f = 0.64$; alcohol product $R_f = 0.16$), and after 40 min of stirring at 23 $^\circ\text{C}$, the reaction was judged to be complete. The reaction mixture was transferred to a separatory funnel containing hexanes (10 mL) and saturated aqueous sodium bicarbonate solution (10 mL). The mixture was shaken vigorously, and the layers were separated. The aqueous layer was extracted with fresh hexanes (3×5 mL), and the combined organic extracts were washed with saturated aqueous sodium chloride solution (10 mL). The washed organic

solution was then dried over sodium sulfate, filtered, and concentrated to provide 2,3,4-tris-*O*-trimethylsilyl-8-norlincomycin as a white, foaming, amorphous solid (115 mg, 93%).

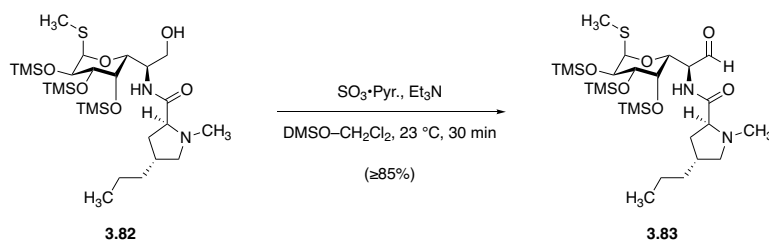
$R_f = 0.16$ (40% ethyl acetate–hexanes, CAM).

$^1\text{H NMR}$ (600 MHz, CDCl_3) δ 7.73 (d, $J = 8.8$ Hz, 1H), 5.22 (d, $J = 5.6$ Hz, 1H), 4.17–4.11 (m, 3H), 3.92 (br d, $J = 11.0$ Hz, 1H), 3.81 (d, $J = 2.6$ Hz, 1H), 3.70 (br d, $J = 10.8$ Hz, 1H), 3.66 (dd, $J = 9.4, 2.6$ Hz, 1H), 3.16–3.12 (m, 1H), 2.94 (dd, $J = 10.8, 4.2$ Hz, 1H), 2.57 (br, 1H), 2.34 (s, 3H), 2.07 (s, 3H), 2.04–2.02 (m, 2H), 1.97–1.93 (m, 1H), 1.85–1.80 (m, 1H), 1.30–1.24 (m, 4H), 0.87 (t, $J = 6.7$ Hz, 3H), 0.17 (s, 9H), 0.12 (s, 9H), 0.11 (s, 9H).

$^{13}\text{C NMR}$ (126 MHz, CDCl_3) δ 174.8, 88.3, 72.6 ($2 \times \text{C}$), 70.9, 69.0, 68.9, 62.9, 62.8, 50.0, 42.0, 38.3, 37.8, 35.8, 21.7, 14.4, 12.7, 0.9, 0.5, 0.3.

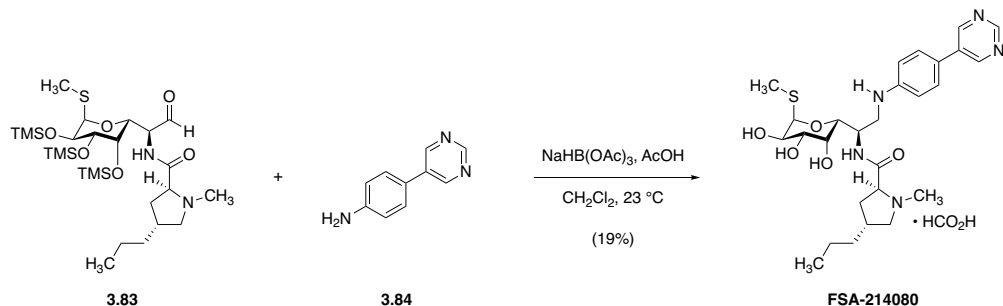
FTIR (neat, cm^{-1}): 2957 (m), 1659 (m), 1518 (m), 1250 (m), 1132 (m), 1070 (m), 893 (s), 839 (s).

HRMS (ESI+, m/z): $[\text{M}+\text{H}]^+$ calc'd for $\text{C}_{26}\text{H}_{56}\text{N}_2\text{O}_6\text{SSi}_3$, 609.3240; found 609.3259.



Aldehyde 3.83.

To a solution of 2,3,4-tris-*O*-trimethylsilyl-8-norlincomycin (**3.82**, 50 mg, 82 μmol , 1 equiv) in dichloromethane (660 μL) and dimethyl sulfoxide (160 μL) were added triethylamine (92 μL , 660 μmol , 8.0 equiv) and sulfur trioxide–pyridine complex (52 mg, 330 μmol , 4.0 equiv) at 23 $^\circ\text{C}$. After 15 min, TLC analysis (10% methanol–dichloromethane, PAA) showed that reaction progress had stalled, and additional portions of triethylamine (92 μL , 660 μmol , 8.0 equiv) and sulfur trioxide–pyridine complex (52 mg, 330 μmol , 4.0 equiv) were added. After an additional 15 min of stirring at 23 $^\circ\text{C}$, TLC analysis showed the reaction was complete. The mixture was diluted with dichloromethane (10 mL), and the diluted solution was transferred to a separatory funnel containing saturated aqueous sodium bicarbonate solution (10 mL). The layers were shaken vigorously, then separated, and the aqueous phase was extracted with fresh portions of dichloromethane (3 \times 5 mL). The combined organic extracts were then washed with saturated aqueous sodium chloride solution (10 mL) before being dried over sodium sulfate, filtered, and concentrated to provide crude aldehyde **3.83** as a dull white solid. This material was unstable toward column chromatography, and thus an analytically pure sample could not be obtained; instead, purity of $\geq 85\%$ was assumed based on crude ^1H NMR analysis (CDCl_3), and this material was used directly in subsequent transformations whereafter 2-step yields were determined.



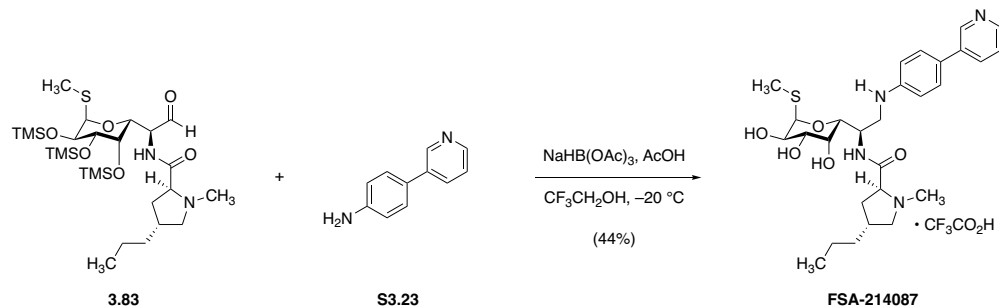
Synthetic lincosamide FSA-214080.

To a solution of aldehyde **3.83** (theoretically 9.7 mg, 16 mmol, 1 equiv) in dichloromethane (400 mL) were added 4-(pyrimidin-5-yl)aniline (**3.84**, 6.9 mg, 40 μmol , 2.5 equiv) and acetic acid (9.2 μL , 160 μmol , 10 equiv) at 23 $^\circ\text{C}$. After 15 min of stirring, the mixture was then treated with sodium triacetoxyborohydride (6.8 mg, 32 μmol , 2.0 equiv), and 2 h later, LCMS analysis showed complete consumption of aldehyde starting material and imine intermediate. The reaction mixture was concentrated under a stream of nitrogen, and the residue was re-suspended in 50% v/v methanol–1N aqueous hydrogen chloride solution (1.0 mL). The resulting canary yellow suspension was stirred at 23 $^\circ\text{C}$ for 5 min, whereupon LCMS analysis showed global desilylation was complete. The mixture was filtered through a 0.2- μm PTFE filter, and the filtrate was concentrated. The crude residue was subjected to purification by preparative HPLC on a Waters SunFire Prep C₁₈ column (5 μm , 250 \times 19 mm; eluting with 0.1% formic acid–5% acetonitrile–water, grading to 0.1% formic acid–40% acetonitrile–water over 40 min, with a flow rate of 15 mL/min; monitored by UV absorbance at 280 nm; R_t = 15.8 min) to provide (pyrimidyl)aniline analog **FSA-214080** • HCO₂H as a white solid (1.9 mg, 19%, 2 steps).

¹H (600 MHz, CD₃OD) δ 8.98 (s, 1H), 8.96 (s, 2H), 8.44 (br s, 1H), 7.51 (d, J = 8.7 Hz, 2H), 6.83 (d, J = 8.7 Hz, 2H), 5.31 (d, J = 5.6 Hz, 1H), 4.44 (app q, J = 6.5 Hz, 1H), 4.32 (dd, J =

6.4, 1.3 Hz, 1H), 4.12 (dd, $J = 10.2, 5.6$ Hz, 1H), 3.94 (dd, $J = 3.4, 1.3$ Hz, 1H), 3.64 (dd, $J = 10.1, 3.4$ Hz, 1H), 3.49 (dd, $J = 13.7, 5.2$ Hz, 1H), 3.40 (dd, $J = 13.6, 7.5$ Hz, 1H), 3.25 (app t, $J = 7.7$ Hz, 1H), 3.22–3.17 (m, 1H), 2.45 (s, 3H), 2.23–2.18 (m, 1H), 2.12 (s, 3H), 2.01–1.96 (m, 1H), 1.94–1.89 (m, 1H), 1.84–1.78 (m, 1H), 1.29–1.16 (m, 4H), 0.80 (t, $J = 7.1$ Hz, 3H).

HRMS (ESI+, m/z): $[M+H]^+$ calc'd for $C_{27}H_{39}N_5O_5S$, 546.2745; found 546.2753.

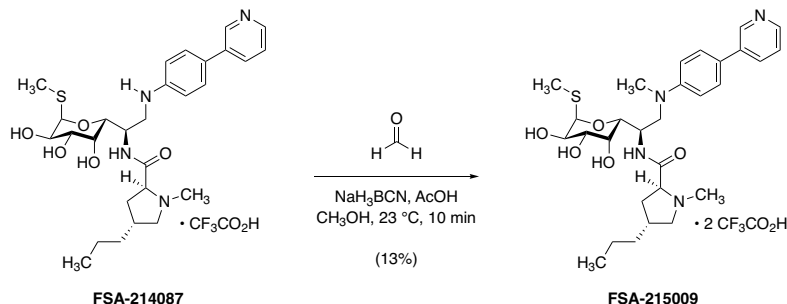


Synthetic lincosamide FSA-214087.

A 4-mL glass vial fitted with a PTFE-lined screw cap was charged with a magnetic stir bar, aldehyde **3.83** (theoretically 10 mg, 16 μmol , 1 equiv), 2,2,2-trifluoroethanol (330 μL), and powdered, activated 4 \AA molecular sieves (10 mg). The suspension was chilled to $-20\text{ }^\circ\text{C}$ in an acetone bath, whereupon acetic acid (5.7 μL , 99 μmol , 6.0 equiv) was added. 4-(Pyridin-3-yl)aniline (**S3.23**, 8.4 mg, 49 μmol , 3.0 equiv) was added next, causing the mixture to turn tennis-ball yellow; and the mixture was stirred at $-20\text{ }^\circ\text{C}$ for 15 min before the mixture was treated with sodium triacetoxyborohydride (10 mg, 49 μmol , 3.0 equiv). After 30 min, LCMS analysis showed complete consumption of aldehyde starting material and imine intermediate. The mixture was warmed to $23\text{ }^\circ\text{C}$ and was concentrated to dryness before being re-suspended in 50% v/v methanol–1N aqueous hydrogen chloride solution. After 5 min of stirring at $23\text{ }^\circ\text{C}$, LCMS analysis showed that global desilylation was complete, and the yellow mixture was filtered through a 0.2- μm PTFE filter. The filtrate was concentrated, and the crude residue was purified by preparative HPLC on a Waters SunFire Prep C_{18} column (5 μm , $250 \times 19\text{ mm}$; eluting with 0.1% trifluoroacetic acid–water, grading to 0.1% trifluoroacetic acid–50% acetonitrile–water over 40 min, with a flow rate of 15 mL/min; monitored by UV absorbance at 280 nm; $R_t = 22.2\text{ min}$) to provide (pyridyl)aniline analog **FSA-214087** \cdot $\text{CF}_3\text{CO}_2\text{H}$ as a white solid (5.6 mg, 44%, 2 steps).

^1H (500 MHz, CD_3OD) δ 9.03 (d, $J = 2.1$ Hz, 1H), 8.77 (ddd, $J = 8.4, 2.3, 1.3$ Hz, 1H), 8.62 (dd, $J = 5.6, 1.1$ Hz, 1H), 8.03 (dd, $J = 8.3, 5.6$ Hz, 1H), 7.63 (d, $J = 8.7$ Hz, 2H), 6.82 (d, $J = 8.7$ Hz, 2H), 5.35 (d, $J = 5.6$ Hz, 1H), 4.50 (app td, $J = 9.1, 3.9$ Hz, 1H), 4.25 (d, $J = 8.9$ Hz, 1H), 4.16–4.11 (m, 2H), 3.91 (dd, $J = 3.3, 1.1$ Hz, 1H), 3.72–3.66 (m, 2H), 3.62 (dd, $J = 10.1, 3.3$ Hz, 1H), 3.37 (dd, $J = 14.1, 9.3$ Hz, 1H), 2.91 (s, 3H), 2.83 (app t, $J = 11.0$ Hz, 1H), 2.23–2.16 (m, 1H), 2.09 (s, 3H), 2.09–2.00 (m, 2H), 1.43–1.30 (m, 2H), 1.27–1.19 (m, 2H), 0.84 (t, $J = 7.2$ Hz, 3H).

HRMS (ESI+, m/z): $[\text{M}+2\text{H}]^{2+}$ calc'd for $\text{C}_{28}\text{H}_{40}\text{N}_4\text{O}_5\text{S}$, 273.1432; found 273.1432.



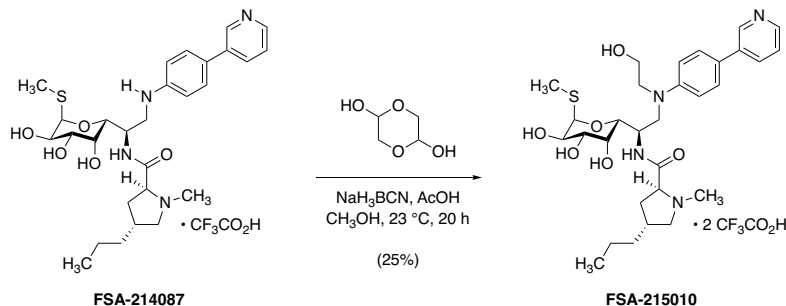
Synthetic lincosamide FSA-215009.

In a 4-mL glass vial fitted with a PTFE-lined screw cap and a magnetic stir bar, aniline **FSA-214087** (22 mg, 41 μ mol, 1 equiv) was dissolved in methanol (820 μ L) to which a spatula tipful of bromocresol green pH indicator had been added. The pH of the solution was adjusted to reach pH 4–5 (indicated by a forest green color) by addition of acetic acid. Formalin (92 μ L, 1.2 mmol, 30 equiv) and sodium cyanoborohydride (13 mg, 210 μ mol, 5.0 equiv) were then added, and the mixture was stirred at 23 °C for 10 min, whereupon LCMS analysis showed that the reaction was complete. The mixture was passed through a 0.2- μ m PTFE filter, the filtrate was concentrated, and the crude residue was purified by preparative HPLC-MS on a Waters SunFire Prep C₁₈ column (5 μ m, 250 \times 19 mm; eluting with 0.1% trifluoroacetic acid–water, grading to 0.1% trifluoroacetic acid–35% acetonitrile–water over 40 min, with a flow rate of 15 mL/min; monitored by UV absorbance at 280 nm and ESI+ selected ion monitoring [m/z = 280]; R_t = 29.2 min) to provide (pyridyl)aniline analog **FSA-215009** • 2 CF₃CO₂H as a white solid (4.1 mg, 13%)

¹H (600 MHz, CD₃OD) δ 9.06 (d, J = 2.2 Hz, 1H), 8.77 (ddd, J = 8.3, 2.3, 1.3 Hz, 1H), 8.62 (d, J = 5.4 Hz, 1H), 8.02 (dd, J = 8.3, 5.6, 1H), 7.71 (d, J = 9.1 Hz, 2H), 6.94 (d, J = 9.0 Hz, 2H), 5.35 (d, J = 5.7 Hz, 1H), 4.72 (app td, J = 8.6, 5.9 Hz, 1H), 4.26 (dd, J = 9.1, 1.5 Hz, 1H), 4.14 (dd, J = 10.1, 5.6 Hz, 1H), 3.99 (dd, J = 10.3, 6.1 Hz, 1H), 3.90 (dd, J = 3.4, 1.3

Hz, 1H), 3.76–7.74 (m, 2H), 3.63–3.59 (m, 2H), 3.05 (s, 3H), 2.85 (s, 3H), 2.72 (app t, $J = 11.1$ Hz, 1H), 2.14 (s, 3H), 1.96–1.90 (m, 1H), 1.76 (dt, $J = 13.4, 9.8$ Hz, 1H), 1.49 (ddd, $J = 13.9, 8.5, 6.1$ Hz, 1H), 1.24 (ddd, $J = 15.7, 8.2, 5.9$ Hz, 1H), 1.16–1.10 (m, 1H), 1.08–1.01 (m, 2H), 0.68 (t, $J = 7.3$ Hz, 3H).

HRMS (ESI+, m/z): $[M+2H]^{2+}$ calc'd for $C_{29}H_{42}N_4O_5S$, 280.1511; found 280.1514.



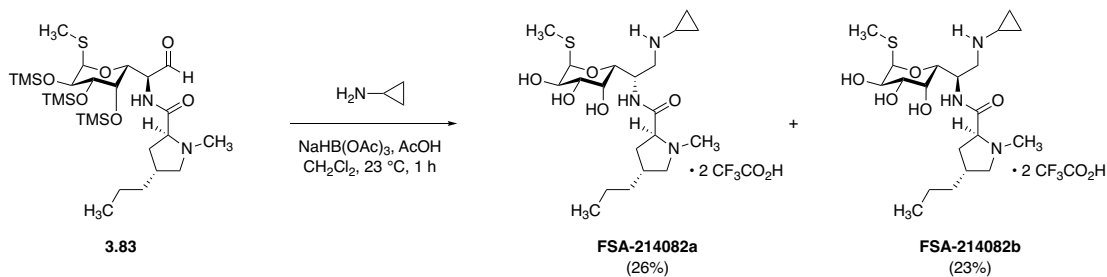
Synthetic lincosamide FSA-215010.

In a 4-mL glass vial fitted with a PTFE-lined screw cap and a magnetic stir bar, aniline **FSA-214087** (22 mg, 41 μ mol, 1 equiv) was dissolved in methanol (820 μ L) to which a spatula tipful of bromocresol green pH indicator had been added. The pH of the solution was adjusted to reach pH 4–5 (indicated by a forest green color) by addition of acetic acid. Glycolaldehyde dimer (74 mg, 0.62 mmol, 15 equiv) and sodium cyanoborohydride (13 mg, 0.21 mmol, 5.0 equiv) were then added, and the mixture was stirred at 23 °C for 20 h, whereupon LCMS analysis indicated that the reaction was complete. The mixture was passed through a 0.2- μ m PTFE filter, the filtrate was concentrated, and the crude residue was purified by preparative HPLC on a Waters SunFire Prep C₁₈ column (5 μ m, 250 \times 19 mm; eluting with 0.1% trifluoroacetic acid–water, grading to 0.1% trifluoroacetic acid–35% acetonitrile–water over 40 min, with a flow rate of 15 mL/min; monitored by UV absorbance at 280 nm; R_t = 26.0 min) to provide ethanolamine analog **FSA-215010** • 2 CF₃CO₂H as a white solid (8.3 mg, 25%).

¹H (600 MHz, CD₃OD) δ 9.08 (d, *J* = 2.1 Hz, 1H), 8.81 (ddd, *J* = 8.4, 2.3, 1.3 Hz, 1H), 8.64 (app dt, *J* = 5.6, 1.1 Hz, 1H), 8.05 (ddd, *J* = 8.4, 5.6, 0.7 Hz, 1H), 7.71 (d, *J* = 9.0, 2H), 6.99 (d, *J* = 9.1 Hz, 2H), 5.36 (d, *J* = 5.7 Hz, 1H), 4.71 (ddd, *J* = 10.9, 8.9, 3.5 Hz, 1H), 4.26 (d, *J* = 9.2 Hz, 1H), 4.14 (dd, *J* = 10.1, 5.6 Hz, 1H), 4.04 (dd, *J* = 10.1, 6.2 Hz, 1H), 3.90 (d, *J* =

3.2 Hz, 2H), 3.79–3.72 (m, 3H), 3.65–3.60 (m, 3H), 3.59–3.55 (m, 1H), 2.86 (s, 3H), 2.75 (app t, $J = 11.1$ Hz, 1H), 2.14 (s, 3H), 2.02–1.96 (m, 1H), 1.84 (dt, $J = 13.4, 9.6$ Hz, 1H), 1.58 (ddd, $J = 13.0, 8.6, 6.3$ Hz, 1H), 1.32–1.26 (m, 1H), 1.20–1.14 (m, 1H), 1.12–1.07 (m, 2H), 0.72 (t, $J = 7.3$ Hz, 3H).

HRMS (ESI+, m/z): $[M+2H]^{2+}$ calc'd for $C_{30}H_{44}N_4O_6$, 295.1564; found 295.1561.



Synthetic lincosamides **FSA-214082a** and **FSA-214082b**.

In a 4-mL glass vial fitted with a PTFE-lined screw cap and a magnetic stir bar, aldehyde **3.83** (theoretically 10 mg, 16 μmol , 1 equiv), dichloromethane (410 μL), acetic acid (9.4 μL , 0.17 mmol, 10 equiv) and cyclopropylamine (2.9 μL , 41 μmol , 2.5 equiv) were combined. This mixture was stirred for 15 min at 23 $^\circ\text{C}$ before sodium triacetoxyborohydride (7.0 mg, 33 μmol , 2.0 equiv) was added. After 1 h, LCMS analysis showed that the reaction was complete. The mixture was concentrated to dryness, and the residue was re-suspended in 50% v/v methanol–1N aqueous hydrogen chloride solution (1.0 mL). After 15 min, LCMS showed that global desilylation was complete, and the mixture was passed through a 0.2- μm PTFE filter. The filtrate was concentrated, and the crude residue was purified by preparative HPLC on a Waters SunFire Prep C₁₈ column (5 μm , 250 \times 19 mm; eluting with 0.1% trifluoroacetic acid–water, grading to 0.1% trifluoroacetic acid–40% acetonitrile–water over 40 min, with a flow rate of 15 mL/min; monitored by UV absorbance at 210 nm; **FSA-214082a** R_t = 22.4 min, **FSA-214082b** R_t = 23.7 min) to provide cyclopropylamine analogs **FSA-214082a** \cdot 2 CF₃CO₂H (2.3 mg, 26%, 2 steps) and **FSA-214082b** \cdot 2 CF₃CO₂H (2.1 mg, 23%, 2 steps) as white solids.

FSA-214082a • 2 CF₃CO₂H:

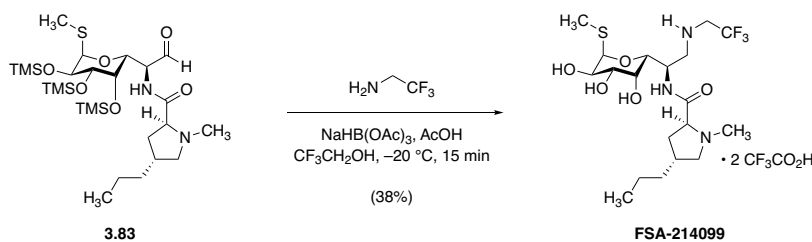
¹H NMR (600 MHz, CD₃OD) δ 5.30 (d, *J* = 5.5 Hz, 1H), 4.69 (ddd, *J* = 9.8, 5.7, 3.7 Hz, 1H), 4.24–4.18 (m, 2H), 4.10 (dd, *J* = 10.1, 5.5 Hz, 1H), 3.93 (dd, *J* = 3.4, 1.4 Hz, 1H), 3.76 (dd, *J* = 10.8, 6.3 Hz, 1H), 3.61 (dd, *J* = 10.0, 3.3 Hz, 1H), 3.50 (dd, *J* = 13.0, 3.7 Hz, 1H), 3.36 (dd, *J* = 13.0, 10.4 Hz, 1H), 2.98–2.94 (m, 4H), 2.91–2.83 (m, 2H), 2.37–2.29 (m, 2H), 2.26–2.19 (m, 1H), 2.11 (s, 3H), 1.51–1.44 (m, 2H), 1.40–1.33 (m, 2H), 0.97–0.90 (m, 8H).

HRMS (ESI+, *m/z*): [M+H]⁺ calc'd for C₂₀H₃₇N₃O₅S, 432.2527; found 432.2516.

FSA-214082b • 2 CF₃CO₂H:

¹H NMR (600 MHz, CD₃OD) δ 5.34 (d, *J* = 5.6 Hz, 1H), 4.52 (app td, *J* = 7.7, 4.9 Hz, 1H), 4.31 (dd, *J* = 7.3, 1.3 Hz, 1H), 4.19 (dd, *J* = 10.3, 6.5 Hz, 1H), 4.10 (dd, *J* = 10.1, 5.6 Hz, 1H), 3.89 (dd, *J* = 3.4, 1.3 Hz, 1H), 3.76 (dd, *J* = 11.0, 6.7 Hz, 1H), 3.60–3.59 (m, 1H), 3.59–3.58 (m, 1H), 3.40 (dd, *J* = 13.0, 8.0 Hz, 1H), 2.94 (s, 3H), 2.90 (app t, *J* = 10.9 Hz, 1H), 2.82 (app tt, *J* = 7.3, 4.4 Hz, 1H), 2.40–2.31 (m, 2H), 2.25–2.19 (m, 1H), 2.12 (s, 3H), 1.51–1.46 (m, 2H), 1.40–1.35 (m, 2H), 0.96 (t, *J* = 7.3 Hz, 3H), 0.93–0.92 (m, 4H).

HRMS (ESI+, *m/z*): [M+H]⁺ calc'd for C₂₀H₃₇N₃O₅S, 432.2527; found 432.2519.



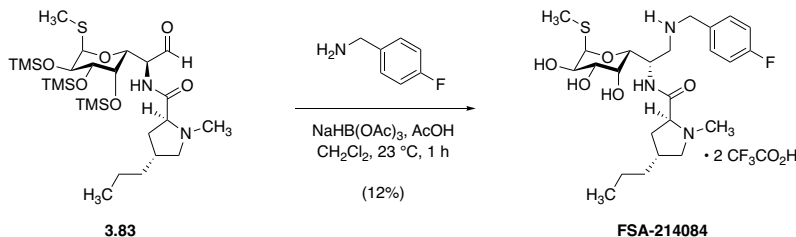
Synthetic lincosamide FSA-214099.

A 4-mL glass vial fitted with a PTFE-lined screw cap was charged with a magnetic stir bar, aldehyde **3.83** (theoretically 20 mg, 33 μmol , 1 equiv), 2,2,2-trifluoroethanol (660 μL), and powdered, activated 4 \AA molecular sieves (20 mg). The suspension was chilled to $-20\text{ }^\circ\text{C}$ in an acetone bath, whereupon acetic acid (11 μL , 0.20 μmol , 6.0 equiv) was added. 2,2,2-Trifluoroethan-1-amine (7.8 μL , 99 μmol , 3.0 equiv) was added next, and the mixture was stirred at $-20\text{ }^\circ\text{C}$ for 15 min before the mixture was treated with sodium triacetoxyborohydride (21 mg, 99 μmol , 3.0 equiv). After 1 h, LCMS analysis showed complete consumption of aldehyde starting material and imine intermediate. The mixture was concentrated to dryness, and the residue was re-suspended in 50% v/v methanol–1N aqueous hydrogen chloride solution (1.0 mL). After 15 min of stirring at $23\text{ }^\circ\text{C}$, LCMS analysis demonstrated that global desilylation was complete, and the mixture was filtered through a 0.2- μm PTFE filter. The filtrate was concentrated, and the crude residue was purified by preparative HPLC-MS on a Waters SunFire Prep C₁₈ column (5 μm , 250 \times 19 mm; eluting with 0.1% trifluoroacetic acid–water, grading to 0.1% trifluoroacetic acid–40% acetonitrile–water over 40 min, with a flow rate of 15 mL/min; monitored by UV absorbance at 210 nm and ESI+ selected ion monitoring [$m/z = 474$]; $R_t = 20.7$ min) to provide trifluoroethylamine analog **FSA-214099** $\cdot 2\text{ CF}_3\text{CO}_2\text{H}$ as a white solid (8.8 mg, 38%, 2 steps).

^1H NMR (500 MHz, CD_3OD) δ 5.31 (d, $J = 5.6$ Hz, 1H), 4.42 (td, $J = 8.0, 4.5$ Hz, 1H), 4.23 (dd, $J = 7.8, 1.2$ Hz, 1H), 4.19 (dd, $J = 10.2, 6.0$ Hz, 1H), 4.10 (dd, $J = 10.1, 5.6$ Hz, 1H), 3.89 (dd, $J = 3.4, 1.2$ Hz, 1H), 3.76 (dd, $J = 11.0, 6.6$ Hz, 1H), 3.74–3.64 (m, 2H), 3.58 (dd, $J = 10.1, 3.3$ Hz, 1H), 3.39 (dd, $J = 12.7, 4.5$ Hz, 1H), 3.15 (dd, $J = 12.7, 8.2$ Hz, 1H), 2.89 (app t, $J = 10.7$ Hz, 1H), 2.40–2.30 (m, 2H), 2.26–2.19 (m, 1H), 1.51–1.45 (m, 2H), 1.41–1.32 (m, 2H), 0.95 (t, $J = 7.3$ Hz, 3H).

$^{19}\text{F}\{^1\text{H}\}$ NMR (471 MHz, CD_3OD) δ -71.30 (s, 3F), -77.18 (s, 6F).

HRMS (ESI+, m/z): $[\text{M}+\text{H}]^+$ calc'd for $\text{C}_{19}\text{H}_{34}\text{F}_3\text{N}_3\text{O}_5\text{S}$, 474.2244; found 474.2252.



Synthetic lincosamide FSA-214084.

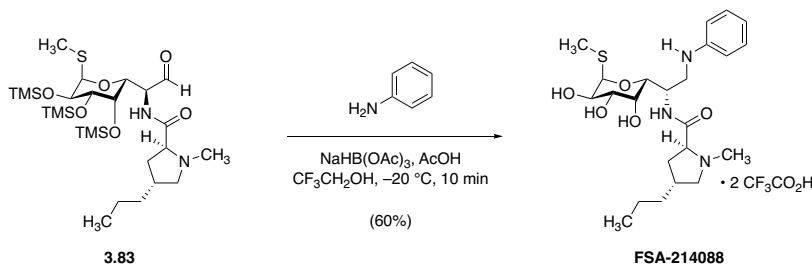
In a 4-mL glass vial fitted with a PTFE-lined screw cap and a magnetic stir bar, aldehyde **3.83** (theoretically 10 mg, 16 μmol , 1 equiv), dichloromethane (410 μL), acetic acid (9.4 μL , 0.17 mmol, 10 equiv) and 4-fluorobenzylamine (4.7 μL , 41 μmol , 2.5 equiv) were combined. This mixture was stirred for 15 min at 23 $^{\circ}\text{C}$ before sodium triacetoxyborohydride (7.0 mg, 33 μmol , 2.0 equiv) was added. After 1 h, LCMS analysis showed that the reaction was complete. The mixture was concentrated to dryness, and the residue was re-suspended in 50% v/v methanol–1N aqueous hydrogen chloride solution (1.0 mL). After 15 min, LCMS showed that global desilylation was complete, and the mixture was passed through a 0.2- μm PTFE filter. The filtrate was concentrated, and the crude residue was purified by preparative HPLC on a Waters SunFire Prep C_{18} column (5 μm , 250 \times 19 mm; eluting with 0.1% formic acid–water, grading to 0.1% formic acid–40% acetonitrile–water over 40 min, with a flow rate of 15 mL/min; monitored by UV absorbance at 210 nm; $R_t = 13.5$ min) to provide 4-fluorobenzylamine analog **FSA-214084** as a white solid (1.0 mg, 12%, 2 steps).

^1H NMR (500 MHz, CD_3OD) δ 7.58 (dd, $J = 8.6, 5.3$ Hz, 2H), 7.20 (app t, $J = 8.7$ Hz, 2H), 5.28 (d, $J = 5.6$ Hz, 1H), 4.44 (app td, $J = 8.3, 4.8$ Hz, 4.34–4.30 (m, 3H), 4.28–4.24 (m, 1H), 4.08 (dd, $J = 10.1, 5.6$ Hz, 1H), 3.87 (d, $J = 2.9$ Hz, 1H), 3.76 (dd, $J = 11.0, 6.6$ Hz, 1H), 3.57 (dd, $J = 10.1, 3.2$ Hz, 1H), 3.43 (dd, $J = 13.1, 4.8$ Hz, 1H), 2.96 (s, 3H), 2.91 (app t, J

= 10.8 Hz, 1H), 2.41–2.35 (m, 1H), 2.33–2.29 (m, 2H), 2.01 (s, 3H), 1.52–1.48 (m, 2H),
1.41–1.35 (m, 2H), 0.96 (t, $J = 7.3$ Hz, 3H).

$^{19}\text{F}\{^1\text{H}\}$ NMR (471 MHz, CD_3OD) δ –113.45 (s, 1F).

HRMS (ESI+, m/z): $[\text{M}+\text{H}]^+$ calc'd for $\text{C}_{24}\text{H}_{38}\text{FN}_3\text{O}_5\text{S}$, 500.2589; found 500.2577.



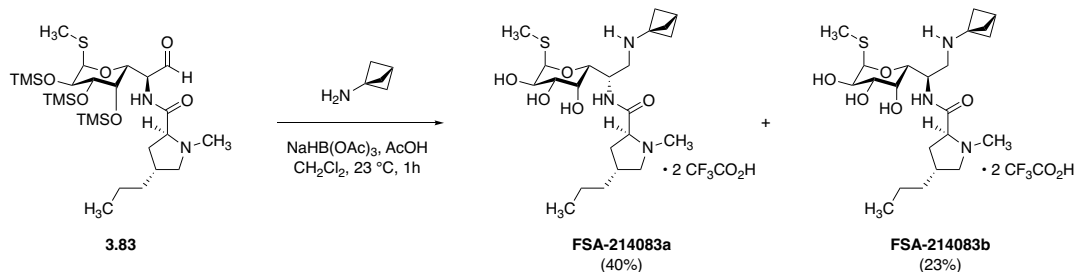
Synthetic lincosamide FSA-214088.

A 4-mL glass vial fitted with a PTFE-lined screw cap was charged with a magnetic stir bar, aldehyde **3.83** (theoretically 10 mg, 16 μmol , 1 equiv), 2,2,2-trifluoroethanol (330 μL), and powdered, activated 4 \AA molecular sieves (10 mg). The suspension was chilled to $-20\text{ }^\circ\text{C}$ in an acetone bath, whereupon acetic acid (5.7 μL , 0.10 μmol , 6.0 equiv) was added. Aniline (4.5 μL , 49 μmol , 3.0 equiv) was added next, and the mixture was stirred at $-20\text{ }^\circ\text{C}$ for 15 min before the mixture was treated with sodium triacetoxyborohydride (10 mg, 49 μmol , 3.0 equiv). After 10 min, LCMS analysis showed complete consumption of aldehyde starting material and imine intermediate. The mixture was concentrated to dryness, and the residue was re-suspended in 50% v/v methanol–1N aqueous hydrogen chloride solution (1.0 mL). After 15 min of stirring at $23\text{ }^\circ\text{C}$, LCMS analysis demonstrated that global desilylation was complete, and the mixture was filtered through a 0.2- μm PTFE filter. The filtrate was concentrated, and the crude residue was purified by preparative HPLC-MS on a Waters SunFire Prep C_{18} column (5 μm , $250 \times 19\text{ mm}$; eluting with 0.1% trifluoroacetic acid–water, grading to 0.1% trifluoroacetic acid–50% acetonitrile–water over 40 min, with a flow rate of 15 mL/min; monitored by UV absorbance at 254 nm; $R_t = 28.3\text{ min}$) to provide aniline analog **FSA-214088** $\cdot 2\text{ CF}_3\text{CO}_2\text{H}$ as a white solid (5.7 mg, 60%, 2 steps).

$^1\text{H NMR}$ (600 MHz, CD_3OD) δ 7.17–7.14 (m, 2H), 6.79–6.71 (m, 3H), 5.33 (d, $J = 5.7\text{ Hz}$, 1H), 4.47 (app td, $J = 8.8, 4.2\text{ Hz}$, 1H), 4.23 (d, $J = 8.6\text{ Hz}$, 1H), 4.14–4.09 (m, 2H), 3.89 (d, J

= 2.6 Hz, 1H), 3.71 (dd, $J = 10.8, 6.9$ Hz, 1H), 3.64–3.59 (m, 2H), 3.35 (dd, $J = 13.7, 8.9$ Hz, 1H), 2.90 (s, 3H), 2.82 (app t, $J = 11.1$ Hz, 1H), 2.23–2.18 (m, 1H), 2.09 (s, 3H), 2.05–1.97 (m, 2H), 1.43–1.35 (m, 2H), 1.33–1.28 (m, 2H), 0.93 (t, $J = 7.3$ Hz, 3H).

HRMS (ESI+, m/z): $[M+H]^+$ calc'd for $C_{23}H_{37}N_3O_5S$, 468.2527; found 468.2538.



Synthetic lincosamides **FSA-214083a** and **FSA-214083b**.

In a 4-mL glass vial fitted with a PTFE-lined screw cap and a magnetic stir bar, aldehyde **3.83** (theoretically 10 mg, 16 μ mol, 1 equiv), dichloromethane (410 μ L), acetic acid (9.4 μ L, 0.17 mmol, 10 equiv) and bicyclo[1.1.1]pentan-1-amine hydrochloride (4.9 mg, 41 μ mol, 2.5 equiv) were combined. This mixture was stirred for 15 min at 23 °C before sodium triacetoxyborohydride (7.0 mg, 33 μ mol, 2.0 equiv) was added. After 1 h, LCMS analysis showed that the reaction was complete. The mixture was concentrated to dryness, and the residue was re-suspended in 50% v/v methanol–1N aqueous hydrogen chloride solution (1.0 mL). After 15 min, LCMS showed that global desilylation was complete, and the mixture was passed through a 0.2- μ m PTFE filter. The filtrate was concentrated, and the crude residue was purified by preparative HPLC on a Waters SunFire Prep C₁₈ column (5 μ m, 250 \times 19 mm; eluting with 0.1% trifluoroacetic acid–water, grading to 0.1% trifluoroacetic acid–40% acetonitrile–water over 40 min, with a flow rate of 15 mL/min; monitored by UV absorbance at 210 nm; **FSA-214083a** R_t = 27.1 min; **FSA-214083b** R_t = 29.4 min) to provide propellamine analogs **FSA-214083a** \cdot 2 CF₃CO₂H (3.8 mg, 40%, 2 steps) and **FSA-214083b** \cdot 2 CF₃CO₂H (2.2 mg, 23%, 2 steps) as white solids.

FSA-214083a • 2 CF₃CO₂H:

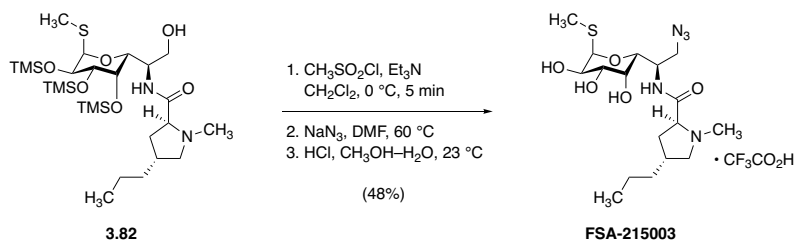
¹H NMR (600 MHz, CD₃OD) δ 5.29 (d, *J* = 5.5 Hz, 1H), 4.63 (ddd, *J* = 10.2, 6.1, 3.8 Hz, 1H), 4.22 (dd, *J* = 10.3, 5.0 Hz, 1H), 4.20 (dd, *J* = 6.1, 1.5 Hz, 1H), 3.93 (dd, *J* = 3.4, 1.5 Hz, 1H), 3.76 (ddd, *J* = 7.5, 5.8, 3.2 Hz, 1H), 3.61 (dd, *J* = 10.0, 3.3 Hz, 1H), 3.35 (dd, *J* = 12.9, 3.8 Hz, 1H), 3.20 (dd, *J* = 12.8, 10.4 Hz, 1H), 2.95 (s, 3H), 2.89 (app t, *J* = 10.6 Hz, 1H), 2.73 (s, 1H), 2.34–2.29 (m, 2H), 2.23–2.21 (m, 1H), 2.14 (s, 6H), 2.10 (s, 3H), 1.49–1.44 (m, 2H), 1.38–1.33 (m, 2H), 0.95 (t, *J* = 7.3 Hz, 3H).

HRMS (ESI+, *m/z*): [M+H]⁺ calc'd for C₂₂H₃₉N₃O₅S, 458.2683; found 458.2676.

FSA-214083b • 2 CF₃CO₂H:

¹H NMR (600 MHz, CD₃OD) δ 5.34 (d, *J* = 5.6 Hz, 1H), 4.46 (app td, *J* = 7.5, 5.2 Hz, 1H), 4.30 (dd, *J* = 7.0, 1.3 Hz, 1H), 4.18 (dd, *J* = 10.3, 6.5 Hz, 1H), 4.10 (dd, *J* = 10.1, 5.6 Hz, 1H), 3.89 (dd, *J* = 3.3, 1.3 Hz, 1H), 3.76 (dd, *J* = 10.9, 6.7 Hz, 1H), 3.59 (dd, *J* = 10.1, 3.2 Hz, 1H), 3.44 (dd, *J* = 12.9, 5.2 Hz, 1H), 3.21 (dd, *J* = 12.9, 7.8 Hz, 1H), 2.94 (s, 3H), 2.90 (app t, *J* = 10.8 Hz, 1H), 2.74 (s, 1H), 2.39–2.31 (m, 2H), 2.24–2.22 (m, 1H), 2.14 (s, 6H), 2.11 (s, 3H), 1.51–1.46 (m, 2H), 1.40–1.35 (m, 2H), 0.96 (t, *J* = 7.3 Hz, 3H).

HRMS (ESI+, *m/z*): [M+H]⁺ calc'd for C₂₂H₃₉N₃O₅S, 458.2683; found 458.2676.



Synthetic lincosamide FSA-215003.

In a 1-mL glass vial fitted with a magnetic stir bar and a PTFE-lined screw cap, 2,3,4-tris-*O*-trimethylsilyl-8-norlincomycin (**3.82**, 20 mg, 33 μmol , 1 equiv) was dissolved in chloroform (160 μL). Triethylamine (11 μL , 82 μmol , 2.5 equiv) was added, the vial was sealed, and the solution was chilled to 0 °C. Methanesulfonyl chloride (5.1 μL , 66 μmol , 2.0 equiv) was then added, the vial re-sealed, and the mixture stirred at 0 °C for 5 min, whereupon TLC analysis (10% methanol–dichloromethane, PAA) revealed that all of the starting material had been consumed. The reaction mixture was diluted with dichloromethane (1 mL), and the diluted mixture was transferred to a separatory funnel containing hexanes (10 mL) and saturated aqueous sodium bicarbonate solution (10 mL). The biphasic mixture was shaken vigorously for 1 min before the layers were separated; the aqueous layer was extracted with fresh hexanes (2 \times 5 mL), and the combined organic extracts were washed with saturated aqueous sodium chloride solution (5 mL). The washed organic solution was dried over sodium sulfate, filtered, and concentrated to give crude methanesulfonate ester intermediate as a white solid. This material was transferred to a 4-mL glass vial and was dried by azeotropic removal of benzene before sodium azide (21 mg, 330 μmol , 10 equiv) and *N,N*-dimethylformamide (330 μL) were added. The vial was sealed with a PTFE-lined screw cap, and the reaction mixture was heated to 60 °C in a pre-heated oil bath. After 18 h, LCMS analysis showed that all the intermediate sulfonate ester had been consumed, and the product mixture was transferred to a separatory funnel containing 50% v/v saturated aqueous

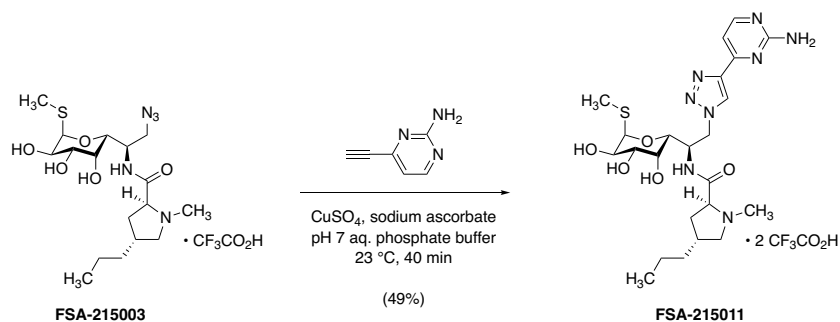
sodium bicarbonate solution–saturated aqueous sodium chloride solution (10 mL). This mixture was then extracted with ethyl acetate (4 × 5 mL), the combined organic extracts were dried over sodium sulfate, the dried product solution was filtered, and the filtrate was concentrated. The residue thus obtained was then re-dissolved in 50% v/v methanol–1N aqueous hydrogen chloride solution; after 30 min of stirring this mixture, LCMS analysis showed that global desilylation was complete, and the mixture was passed through a 0.2- μ m PTFE filter. The filtrate was concentrated, and the crude residue was subjected to preparative HPLC on a Waters SunFire Prep C₁₈ column (5 μ m, 250 × 19 mm; eluting with 0.1% trifluoroacetic acid–water, grading to 0.1% trifluoroacetic acid–40% acetonitrile–water over 40 min, with a flow rate of 15 mL/min; monitored by UV absorbance at 210 nm; R_t = 28.6 min) to provide azide analog **FSA-215003** • CF₃CO₂H as a white solid (8.4 mg, 48%).

¹H NMR (600 MHz, CD₃OD) δ 5.29 (d, *J* = 5.7 Hz, 1H), 4.42 (ddd, *J* = 9.3, 5.8, 3.3 Hz, 1H), 4.22 (dd, *J* = 9.5, 1.3 Hz, 1H), 4.18 (dd, *J* = 9.7, 6.6 Hz, 1H), 4.09 (dd, *J* = 10.2, 5.6 Hz, 1H), 3.85 (dd, *J* = 3.4, 1.3 Hz, 1H), 3.77 (dd, *J* = 11.1, 6.8 Hz, 1H), 3.69 (dd, *J* = 12.7, 3.4 Hz, 1H), 3.59 (dd, *J* = 10.2, 3.3 Hz, 1H), 3.53 (dd, *J* = 12.7, 5.9 Hz, 1H), 2.94 (s, 3H), 2.89 (app t, *J* = 11.0 Hz, 1H), 2.39–2.32 (m, 1H), 2.29–2.24 (m, 2H), 2.10 (s, 3H), 1.52–1.45 (m, 2H), 1.39–1.34 (m, 2H), 0.95 (t, *J* = 7.3 Hz, 3H).

¹³C NMR (100 MHz, CD₃OD) δ 169.0, 89.5, 72.0, 69.9, 69.8, 69.6, 69.4, 62.3, 52.7, 50.8, 41.1, 38.0, 36.4, 35.7, 22.1, 14.2, 13.1.

FTIR (neat, cm⁻¹): 3367 (br), 2927 (w), 2105 (s), 1671 (s), 1453 (m), 1202 (s), 1136 (m).

HRMS (ESI+, *m/z*): [M+H]⁺ calc'd for C₁₇H₃₁N₅O₅S, 418.2119; found 418.2132.



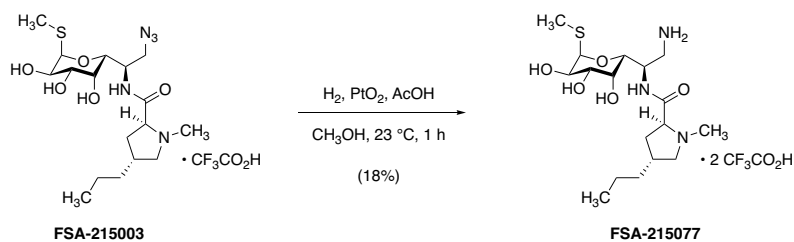
Synthetic lincosamide FSA-215011.

To a stirred suspension containing azide **FSA-215003** • CF₃CO₂H (6.3 mg, 12 μmol, 1 equiv), 4-ethynylpyrimidin-2-amine (4.2 mg, 35 μmol, 3.0 equiv), freshly prepared aqueous sodium ascorbate solution (0.10 M, 24 μL, 2.4 μmol, 0.20 equiv), and 0.10 M sodium phosphate buffer (120 μL), aqueous cupric sulfate solution (0.10 M, 5.9 μL, 0.59 μmol, 0.050 equiv) was added by micropipette at 23 °C. The originally white suspension immediately attained a vibrant sunset orange color. After 40 min of stirring, LCMS analysis indicated that no starting material remained. The crude reaction mixture was directly subjected to preparative HPLC on a Waters SunFire Prep C₁₈ column (5 μm, 250 × 19 mm; eluting with 0.1% trifluoroacetic acid–water, grading to 0.1% trifluoroacetic acid–50% acetonitrile–water over 40 min, with a flow rate of 15 mL/min; monitored by UV absorbance at 254 nm; R_t = 19.0 min) to provide triazole analog **FSA-215011** • 2 CF₃CO₂H as a white solid (4.4 mg, 49%).

¹H NMR (600 MHz, CD₃OD) δ 8.78 (s, 1H), 8.34 (d, *J* = 6.3 Hz, 1H), 7.52 (d, *J* = 6.3 Hz, 1H), 5.38 (d, *J* = 5.6 Hz, 1H), 5.03 (dd, *J* = 14.0, 3.5 Hz, 1H), 4.79 (app td, *J* = 10.0, 3.4 Hz, 1H), 4.63 (dd, *J* = 14.0, 10.2 Hz, 1H), 4.31 (dd, *J* = 9.1, 1.5 Hz, 1H), 4.15 (dd, *J* = 10.2, 5.6 Hz, 1H), 4.07 (dd, *J* = 9.7, 5.0 Hz, 1H), 3.91 (dd, *J* = 3.3, 1.3 Hz, 1H), 3.64 (dd, *J* = 10.7, 5.9 Hz, 1H), 3.61 (dd, *J* = 10.1, 3.3 Hz, 1H), 2.86 (s, 3H), 2.78 (app t, *J* = 10.5 Hz,

1H), 2.18 (s, 3H), 2.13–2.06 (m, 3H), 1.44–1.40 (m, 2H), 1.34–1.28 (m, 2H), 0.94 (t, $J = 7.3$ Hz, 3H).

HRMS (ESI+, m/z): $[M+2H]^{2+}$ calc'd for $C_{23}H_{36}N_8O_5S$, 269.1337; found 269.1328.



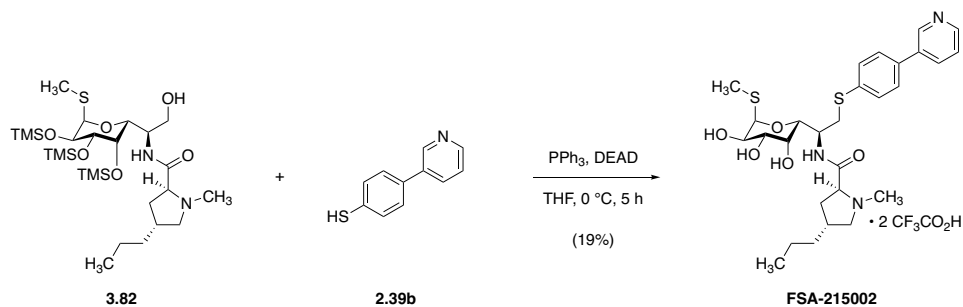
Synthetic lincosamide FSA-215077.

A solution of azide **FSA-215003** (14 mg, 33 μmol , 1 equiv) in methanol (330 μL) was treated sequentially with acetic acid (19 μL , 330 μmol , 10 equiv) and platinum(IV) oxide (7.5 mg, 33 μmol , 1.0 equiv). The headspace was flushed with hydrogen gas, and the dark gray heterogeneous mixture was stirred at 23 $^\circ\text{C}$ under 1 atm of hydrogen for 1 h, whereupon LCMS analysis indicated that no starting material remained. The reaction mixture was diluted with methanol (500 μL), and activated charcoal was added in order to adsorb the platinum-black particles; the mixture was stirred 5 min to ensure complete adsorption. The black suspension was then filtered through a Celite pad, and the filter cake was rinsed with fresh methanol ($2 \times 1 \text{ mL}$). The filtrate was concentrated, and the residue thus obtained was purified by preparative HPLC-MS on a Waters SunFire Prep C_{18} column (5 μm , $250 \times 19 \text{ mm}$; eluting with 0.1% trifluoroacetic acid–water, grading to 0.1% trifluoroacetic acid–30% acetonitrile–water over 40 min, with a flow rate of 15 mL/min; monitored by UV absorbance at 210 nm and ESI+ selected ion monitoring [$m/z = 392$]; $R_t = 16.9 \text{ min}$) to provide diamine analog **FSA-215077** $\cdot 2 \text{CF}_3\text{CO}_2\text{H}$ as a white solid (3.7 mg, 18%).

$^1\text{H NMR}$ (500 MHz, CD_3OD) δ 5.33 (d, $J = 5.6 \text{ Hz}$, 1H), 4.42 (app td, $J = 8.0, 5.0 \text{ Hz}$, 1H), 4.31 (d, $J = 7.9 \text{ Hz}$, 1H), 4.21 (dd, $J = 10.3, 6.2 \text{ Hz}$, 1H), 4.10 (dd, $J = 10.1, 5.6 \text{ Hz}$, 1H), 3.88 (3.2, 1.3 Hz, 1H), 3.76 (dd, $J = 11.0, 6.7 \text{ Hz}$, 1H), 3.59 (dd, $J = 10.1, 3.3 \text{ Hz}$, 1H), 3.41 (dd,

$J = 13.1, 5.0$ Hz, 1H), 3.17 (dd, $J = 13.1, 8.2$ Hz, 1H), 2.95 (s, 3H), 2.90 (app t, $J = 10.8$ Hz, 1H), 2.40–2.31 (m, 2H), 2.26–2.20 (m, 1H), 2.10 (s, 3H), 1.51–1.46 (m, 2H), 1.40–1.34 (m, 2H), 0.96 (t, $J = 7.2$ Hz, 3H).

HRMS (ESI+, m/z): $[M+H]^+$ calc'd for $C_{17}H_{33}N_3O_5S$, 392.2214; found 392.2224.

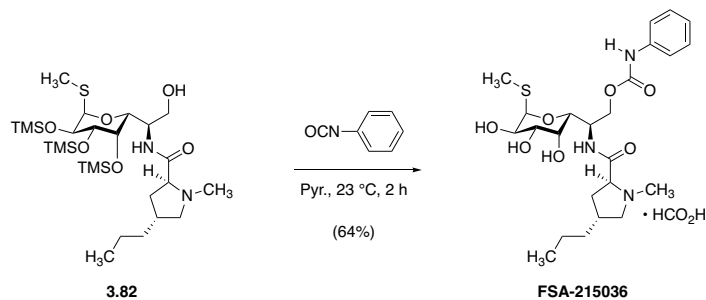


Synthetic lincosamide FSA-215002.

In a 1-mL glass vial, 2,3,4-tris-*O*-trimethylsilyl-8-norlincomycin (**3.82**, 20 mg, 33 μmol , 1 equiv) and triphenylphosphine (17 mg, 66 μmol , 2.0 equiv) were dissolved in tetrahydrofuran (660 μL), and the resulting solution was chilled to 0 $^\circ\text{C}$. With constant stirring, diethyl azodicarboxylate solution (40% w/w in toluene, 30 μL , 66 μmol , 2.0 equiv) was added dropwise, and the mixture was stirred at 0 $^\circ\text{C}$ for 5 min, during which time the original orange color of the azodicarboxylate reagent faded to afford a colorless reaction mixture. 4-(Pyridin-3-yl)benzenethiol (**S2.39b**, 15 mg, 82 μmol , 2.5 equiv) was added next, resulting in a flash of yellow-orange color that then disappeared. Progress was monitored by LCMS, and after 5 h, the reaction was judged to be complete. The mixture was concentrated to dryness under a stream of nitrogen, and the residue was then re-dissolved in 50% v/v methanol–1N aqueous hydrogen chloride solution (800 μL). After 30 min of stirring at 23 $^\circ\text{C}$, LCMS analysis showed that global desilylation was complete, and the mixture was passed through a 0.2- μm PTFE filter. The filtrate was concentrated, and the crude residue was subjected to preparative HPLC on a Waters SunFire Prep C₁₈ column (5 μm , 250 \times 19 mm; eluting with 0.1% trifluoroacetic acid–water, grading to 0.1% trifluoroacetic acid–40% acetonitrile–water over 40 min, with a flow rate of 15 mL/min; monitored by UV absorbance at 254 nm; $R_t = 27.8$ min) to provide arenesulfide analog **FSA-215002** \cdot 2 CF₃CO₂H as a white solid (4.8 mg, 19%).

^1H NMR (600 MHz, CD_3OD) δ 9.09 (s, 1H), 8.75 (d, $J = 4.9$ Hz, 1H), 8.70 (d, $J = 8.2$ Hz, 1H), 8.00 (dd, $J = 8.2, 5.4$ Hz, 1H), 7.75 (d, $J = 8.5$ Hz, 2H), 7.54 (d, $J = 8.5$ Hz, 2H), 5.33 (d, $J = 5.6$ Hz, 1H), 4.50 (app td, $J = 9.0, 3.4$ Hz, 1H), 4.24 (dd, $J = 8.8, 1.3$ Hz, 1H), 4.16 (dd, $J = 9.8, 6.3$ Hz, 1H), 4.11 (dd, $J = 10.1, 5.6$ Hz, 1H), 3.90 (dd, $J = 3.4, 1.2$ Hz, 1H), 3.74 (dd, $J = 11.1, 6.8$ Hz, 1H), 3.70 (dd, $J = 14.0, 3.5$ Hz, 1H), 3.60 (dd, $J = 10.1, 3.3$ Hz, 1H), 3.14 (dd, $J = 14.0, 9.2$ Hz, 1H), 2.92 (s, 3H), 2.86 (app t, $J = 11.1$ Hz, 1H), 2.34–2.26 (m, 1H), 2.22–2.15 (m, 2H), 2.11 (s, 3H), 1.46–1.39 (m, 2H), 1.33–1.28 (m, 2H), 0.90 (t, $J = 7.3$ Hz, 3H).

HRMS (ESI+, m/z): $[\text{M}+2\text{H}]^{2+}$ calc'd for $\text{C}_{28}\text{H}_{39}\text{N}_3\text{O}_5\text{S}_2$, 281.6238; found 281.6238.



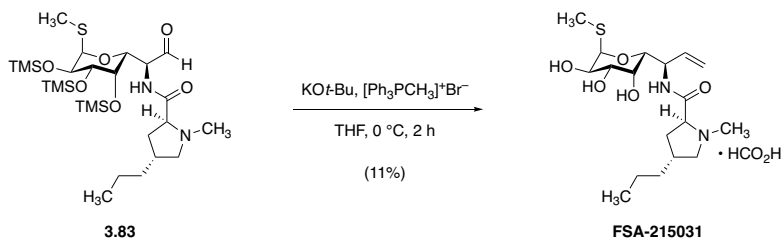
Synthetic lincosamide FSA-215036.

A 1-mL glass vial was charged with a magnetic stir bar, 2,3,4-tris-*O*-trimethylsilyl-8-norlincomycin (**3.82**, 10 mg, 16 μ mol, 1 equiv), pyridine (82 μ L), and phenyl isocyanate (3.6 μ L, 33 μ mol, 2.0 equiv). The vial was sealed with a PTFE-lined screw cap, and the reaction mixture was stirred at 23 °C for 2 h, at which point TLC analysis (8% methanol–dichloromethane, PAA) showed that all the starting material had been consumed. Excess phenyl isocyanate was quenched with the addition of methanol (1 drop), and the mixture was then concentrated to dryness. The residue was then re-dissolved in 50% v/v methanol–1N aqueous hydrogen chloride solution (500 μ L), after 30 min, LCMS analysis showed that global desilylation was complete. The product solution was passed through a 0.2- μ m PTFE filter, the filtrate was concentrated, and the crude residue was purified by preparative HPLC on a on a Waters SunFire Prep C₁₈ column (5 μ m, 250 \times 19 mm; eluting with 0.1% formic acid–5% acetonitrile–water, grading to 0.1% formic acid–50% acetonitrile–water over 40 min, with a flow rate of 15 mL/min; monitored by UV absorbance at 254 nm; R_t = 21.8 min) to provide phenyl carbamate analog **FSA-215036** • HCO₂H as a white solid (5.8 mg, 64%).

¹H NMR (600 MHz, CD₃OD) δ 8.38 (s, 1H), 7.43 (d, J = 8.0 Hz, 2H), 7.28–7.25 (m, 2H), 7.02 (tt, J = 7.4, 1.0 Hz, 1H), 5.31 (d, J = 5.6 Hz, 1H), 4.48 (app dt, J = 9.6, 5.1 Hz, 1H), 4.41–4.38

(m, 2H), 4.25 (dd, $J = 9.2, 1.2$ Hz, 1H), 4.12 (dd, $J = 10.1, 5.6$ Hz, 1H), 3.85 (dd, $J = 3.4, 1.2$ Hz, 1H), 3.61 (dd, $J = 10.1, 3.3$ Hz, 1H), 3.52–3.50 (m, 1H), 3.44 (dd, $J = 9.9, 6.5$ Hz, 1H), 2.60 (s, 3H), 2.41 (app t, $J = 10.3$ Hz, 1H), 2.21–2.15 (m, 1H), 2.11–2.09 (m, 1H), 2.08 (s, 3H), 1.95 (app dt, $J = 13.0, 9.9$ Hz, 1H), 1.34–1.21 (m, 4H), 0.87 (t, $J = 7.2$ Hz, 3H).

HRMS (ESI+, m/z): $[M+H]^+$ calc'd for $C_{24}H_{37}N_3O_7S$, 512.2425; found 512.2444.



Synthetic lincosamide FSA-215031.

An oven-dried 4-mL glass vial was charged with a magnetic stir bar, methyltriphenylphosponium bromide (16 mg, 46 μ mol, 1.4 equiv), and tetrahydrofuran (330 μ L). The vial was sealed with a silicone septum-lined screw cap, and the mixture was chilled to 0 °C before potassium *tert*-butoxide solution (1.0 M in tetrahydrofuran, 40 μ L, 40 μ mol, 1.2 equiv) was added. Upon treatment with alkoxide base, the heterogeneous mixture immediately attained a vibrant, highlighter-yellow color. This mixture was stirred at 0 °C for 30 min before a solution of aldehyde **3.83** (theoretically 20 mg, 33 μ mol, 1 equiv) in tetrahydrofuran (330 μ L) was added by cannula, causing the yellow color to disappear. After 5 min of stirring at 0 °C, TLC analysis (7% methanol–dichloromethane, PAA) revealed that no starting material remained, and excess Wittig reagent was quenched with the addition of acetone (150 μ L). The product mixture was diluted with hexanes (15 mL), dried over sodium sulfate, filtered, and concentrated to give a white film that was re-dissolved in 50% v/v methanol–1N aqueous hydrogen chloride solution (1.5 mL). This mixture was stirred at 23 °C for 1 h, at which point LCMS analysis indicated that global desilylation was complete. The mixture was passed through a 0.2- μ m PTFE filter, the filtrate was concentrated, and the crude residue was purified by preparative HPLC-MS on a Waters SunFire Prep C₁₈ column (5 μ m, 250 \times 19 mm; eluting with 0.1% formic acid–water, grading to 0.1% formic acid–35% acetonitrile–water over 40 min, with a flow rate of 15 mL/min; monitored by

UV absorbance at 210 nm and ESI+ selected ion monitoring [$m/z = 389$]; $R_t = 18.9$ min) to provide vinyl analog **FSA-215031** • HCO₂H as a white solid (1.5 mg, 11%, 2 steps).

¹H NMR (600 MHz, CD₃OD) δ 8.37 (s, 1H), 6.01 (ddd, $J = 17.3, 10.5, 5.5$ Hz, 1H), 5.28 (d, $J = 5.6$ Hz, 1H), 5.23 (app dt, $J = 17.3, 1.5$ Hz, 1H), 5.21 (app dt, $J = 10.4, 1.4$ Hz, 1H), 4.71 (app ddt, $J = 8.5, 5.5, 1.6$ Hz, 1H), 4.11 (dd, $J = 10.1, 5.7$ Hz, 1H), 4.09 (dd, $J = 8.2, 0.8$ Hz, 1H), 3.88 (dd, $J = 3.5, 1.3$ Hz, 1H), 3.59 (dd, $J = 10.1, 3.3$ Hz, 1H), 3.44–3.41 (m, 1H), 2.59 (s, 3H), 2.38 (app t, $J = 10.0$ Hz, 1H), 2.30–2.23 (m, 1H), 2.08 (ddd, $J = 13.5, 8.3, 5.4$ Hz, 1H), 2.04 (s, 3H), 2.01–1.95 (m, 1H), 1.42–1.32 (m, 4H), 0.94 (t, $J = 7.1$ Hz, 3H).

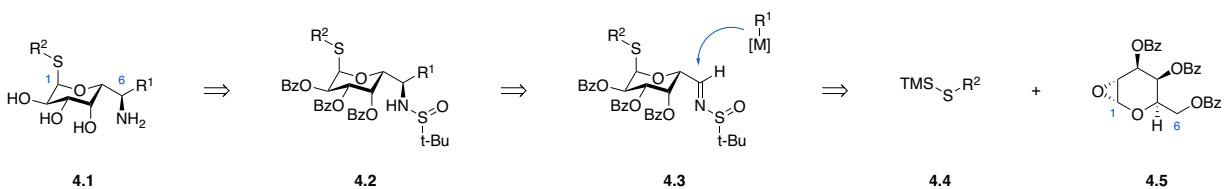
HRMS (ESI+, m/z): [M+H]⁺ calc'd for C₁₈H₃₂N₂O₅S, 389.2105; found 389.2111.

Page intentionally left blank

Chapter 4. A sulfinimine-based route to methylthiolincosamine variants

Introduction

In the fourth year of the lincosamide project, I developed a second-generation synthesis of the northern-half component of the class, motivated by the desire to more expediently test those hypotheses that had emerged in the course of my earlier work on this subunit. Specifically, SAR emerging through my prior route to MTL and its derivatives implicated conformational control as a critical design consideration, suggesting that *S*-glycosidic analogs bearing rigidified C6 appendages might represent the most promising path forward. The nitroaldol-based route was not ideally suited to put these plans into action, however, as it was relatively lengthy and unexpectedly unaccommodating toward changes to the nucleophile in the key nitroaldol coupling; thus, this technology did not practically enable exploration of diverse substitution at C6, the new focus of our efforts. Accordingly, in designing a second retrosynthesis of our targeted MTL analogs, I sought to identify a means by which to install C6 substituents at a late stage, ideally forging the C6–C7 bond with robust and predictable stereoselectivity.



Scheme 4.1. A revised retrosynthesis of northern-half variants bearing modifications to C1 and C6.

What emerged from this planning was a route not dissimilar to the one reported by Dondoni (and adopted by Vicuron), wherein a galactopyranoside C6-nitron (**1.42**) underwent coupling with Grignard nucleophiles to forge the acyclic portion of the lincosamides' northern half (Scheme 1.6). However, whereas the Vicuron scheme relied on subsequent anomeric-group interconversions to introduce C1 substituents, I aimed instead to employ glycosylation conditions

analogous to those I had developed in my previous route, and elected strategically to install the C1 substituent prior to C6–C7 bond formation (Scheme 4.1). In order to expand the scope of compatible nucleophiles, to improve the predictability of the stereochemical outcome of this pivotal coupling, and to facilitate more expedient deprotection of fully assembled glycosides, I opted to target a C6-sulfinimino electrophilic intermediate (**4.3**). Such an intermediate, it was hoped, would provide access to a host of C6 modifications extending far beyond the scope of those accessible through the earlier nitron route, leveraging the rich literature on diastereoselective nucleophilic additions to sulfinimine electrophiles famously pioneered by Professor Jonathan Ellman.¹⁵⁶

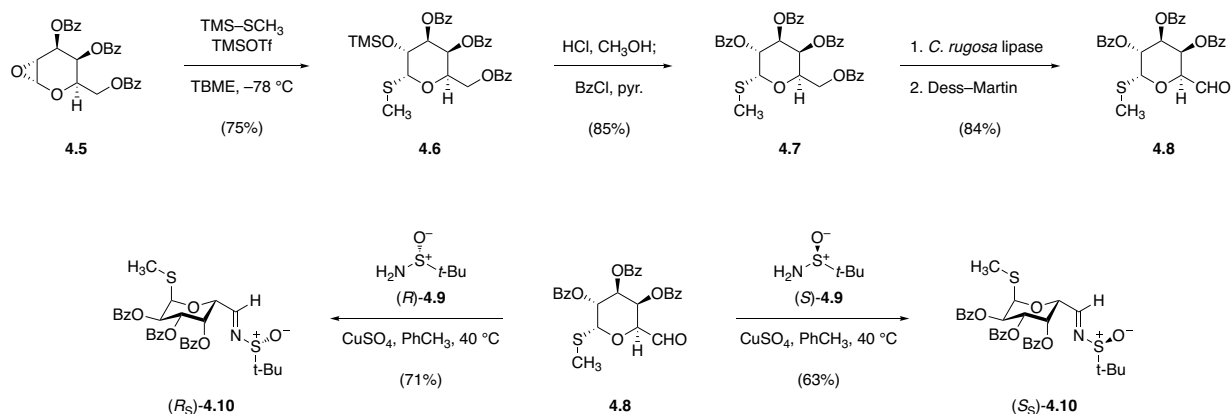
Synthesis of 6-modified propylhygramides by a sulfinimine-based route

Owing in part to the simplicity of this revised scheme, a route to both *R*_S- and *S*_S-sulfinimino electrophiles **4.10** was realized with minimal experimentation (Scheme 4.2). According to published and readily scaled protocols, tri-*O*-benzoyl-D-galactal was first epoxidized using dimethyldioxirane generated *in situ* within a heterogeneous reaction mixture containing acetone and Oxone monopersulfate compound.¹⁵⁷ The resulting “disarmed” Brigl’s anhydride, **4.5**, underwent diastereoselective *cis*- α -thioglycoside formation under the action of trimethylsilyl trifluoromethanesulfonate in *tert*-butyl methyl ether, and a protecting-group swap at C2 then provided tetrabenzoate **4.7**. The C6-benzoyl group within this intermediate could be hydrolyzed selectively using lipase from *Candida rugosa* according to a procedure described by Esmurziev,

¹⁵⁶ Ellman, J. A.; Owens, T. D.; Tang, T. P. *Acc. Chem. Res.* **2002**, *35*, 984–995.

¹⁵⁷ Wagschal, S.; Guilbaud, J.; Rabet, P.; Farina, V.; Lemaire, S. *J. Org. Chem.* **2015**, *80*, 9328–9335.

Sundby, and Hoff;¹⁵⁸ and oxidation of the resulting alcohol provided aldehyde **4.8** in good yield. Finally, this aldehyde was converted to its *N-tert*-butanesulfinyl aldimine derivatives (*R*_S)- and (*S*_S)-**4.10** using anhydrous copper(II) sulfate as Lewis-acid catalyst and water scavenger.¹⁵⁹



Scheme 4.2. Synthesis of *N-tert*-butanesulfinylaldimine building blocks.

These sulfinimine intermediates were remarkably general in regard to the scope of nucleophiles with which they could be coupled. The first such pairing involved simple Grignard addition of 2-(1,3-dioxan-2-yl)ethylmagnesium bromide to the *R*_S epimer, which proceeded in good yield to provide **4.11** as a single diastereomer after column chromatography (Scheme 4.3).¹⁶⁰ Notably, no debenzoylation was observed under these conditions – this chemoselectivity would prove general across a host of nucleophile classes, with the exception of some organolithiums, which were simply too nucleophilic to exhibit similar discrimination (*vide infra*). Using conditions originally developed by Ellman and Brinner,¹⁶¹ the γ -dioxanylsulfinamide **4.11** was converted to

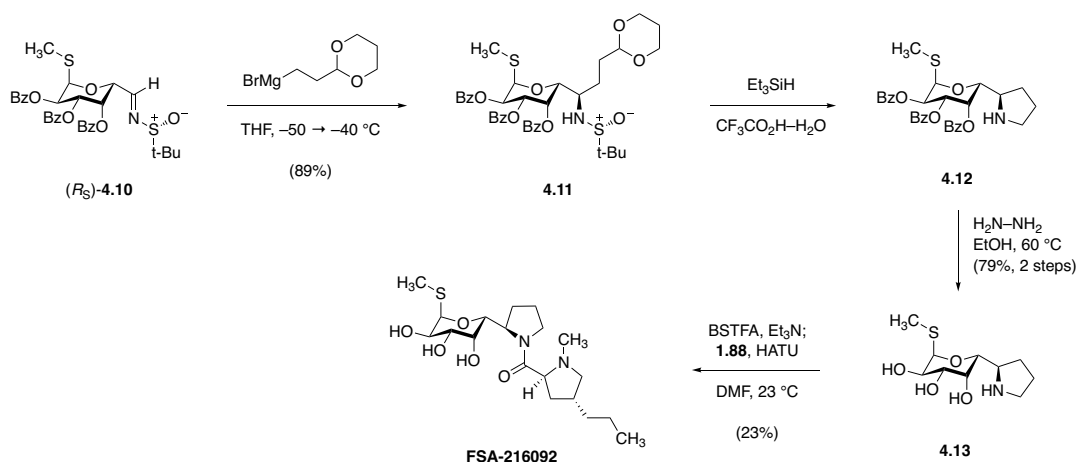
¹⁵⁸ Esmurziev, A.; Sundby, E.; Hoff, B. H. *Eur. J. Org. Chem.* **2009**, 1592–1597.

¹⁵⁹ Liu, G.; Cogan, D. A.; Owens, T. D.; Tang, T. P.; Ellman, J. A. *J. Org. Chem.* **1999**, *64*, 1278–1284.

¹⁶⁰ In all cases shown, C6 stereochemistry was assigned by analogy to published protocols for sulfinimine addition, and has not been corroborated independently by X-ray crystallography or other means.

¹⁶¹ Brinner, K. M.; Ellman, J. A. *Org. Biomol. Chem.* **2005**, *3*, 2109–2113.

the corresponding pyrrolidine under ionic-reduction conditions (triethylsilane, trifluoroacetic acid–water, 23 °C, 24 h) in excellent yield. Hydrazinolysis of the benzoyl protecting groups provided **4.12**,¹⁶² which was elaborated to the tricyclic lincomycin analog **FSA-216092** in the usual fashion. By design, this analog contained a conformationally restricted C6 substituent, which was calculated to roughly overlap with the 1-chloroethyl group of clindamycin.



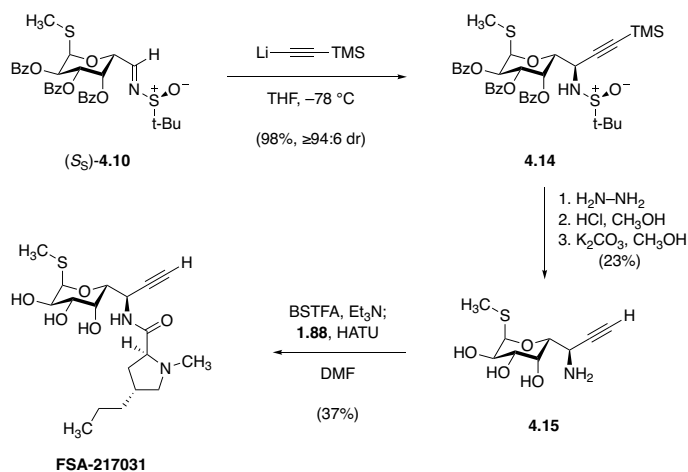
Scheme 4.3. Synthesis of a conformationally constrained, tricyclic analog.

Installation of a nonrotatable alkynyl appendage to C6 was achieved in a similar fashion (Scheme 4.4). Lithiation of ethynyltrimethylsilane, followed by introduction of **(S)**-**4.10** as a solution in tetrahydrofuran provided the propargylic sulfonamide **4.14** in excellent yield and diastereoselectivity. The diastereochemical outcome of this coupling, arising through a putative closed transition state, was assigned by analogy to reported alkynyllithium addition procedures upon which this transformation was based,¹⁶³ with the caveat that a greater proportion of ethereal solvent (tetrahydrofuran, whose coordinating activity can favor open-transition-state pathways¹⁵⁶)

¹⁶² The *N*-benzoyl triol arising by base-promoted acyl-group migration was a major by-product in this hydrazinolysis transformation. In subsequent examples, debenzoylation was performed before amine desulfinylation, so as to preempt this troublesome side-reaction.

¹⁶³ (a) Ding, C.-H.; Chen, D.-D.; Luo, Z.-B.; Dai, L.-X.; Hou, X.-L. *Synlett* **2006**, 1272–1274. (b) Wang, D.; Nugent, W. A. *J. Org. Chem.* **2007**, *72*, 7307–7312.

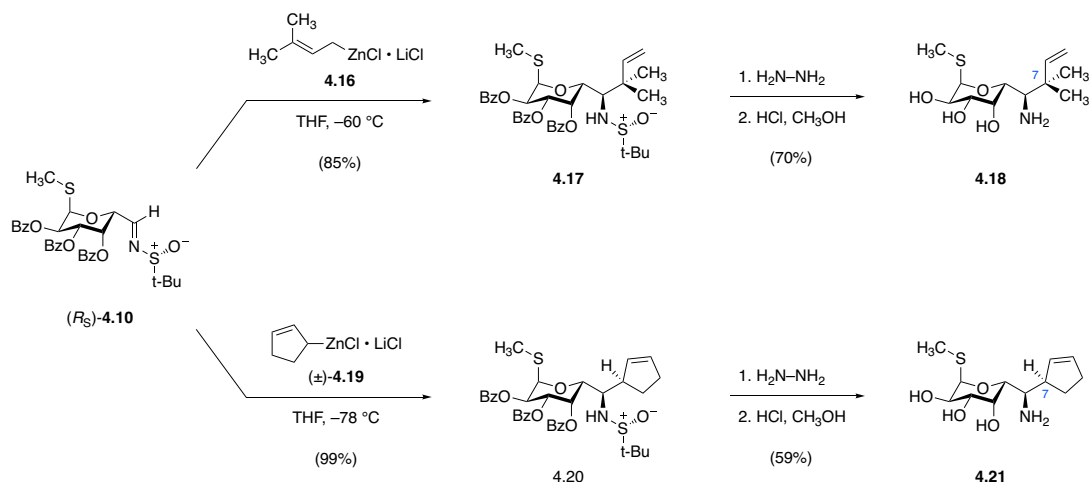
was required in order to guarantee the solubility of the sulfinimine starting material. Sequential hydrazinolysis of **4.14**, acid-promoted desulfinylation, and alkyne deprotection then provided **4.15**, which I advanced to propylhygramide candidate **FSA-217031** by established means.



Scheme 4.4. Synthesis of 6-alkynyl analog **FSA-217031**.

Another important class of nucleophiles that underwent successful coupling were allylzinc reagents, whose ease of preparation, broad functional group compatibility, and stereospecific engagement of sulfinimine electrophiles rendered them particularly valuable in the campaign to explore C6 substitution (Scheme 4.5). For instance, prenylzinc reagent **4.16** underwent efficient coupling with (*R*_S)-**4.10** to provide, after deprotection, MTL variant **4.17**, featuring a quaternary center at C7. Racemic cyclopentenylzinc reagent (\pm)-**4.19** likewise underwent quantitative, rapid ($-78\text{ }^\circ\text{C}$, 10 min), doubly diastereoselective coupling¹⁶⁴ to provide **4.21** bearing a stereochemically differentiated olefin for subsequent functionalization if so desired.

¹⁶⁴ Reddy, L. R.; Hu, B.; Prashad, M.; Prasad, K. *Org. Lett.* **2008**, *10*, 3109–3112.

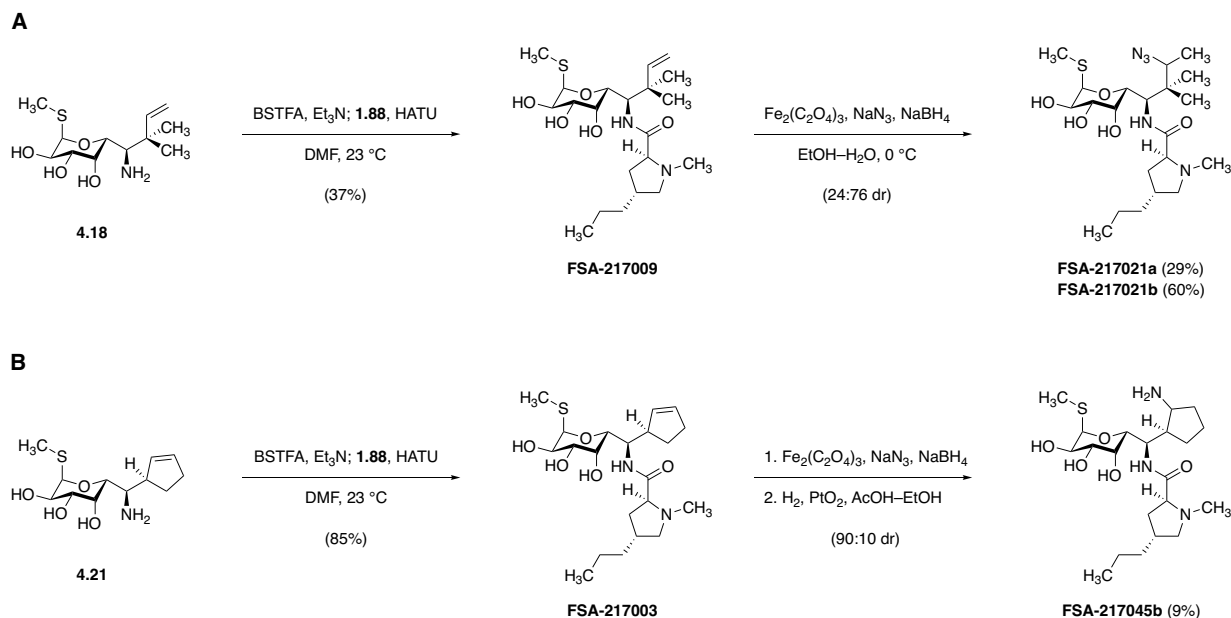


Scheme 4.5. Diastereoselective coupling of allylzinc reagents with sulfinimine (R_S)-**4.10**.

While aminosugars such as **4.18** and **4.21** possessed alkene groups with potential utility for late-stage diversification, the task of selectively functionalizing these olefins in the presence of sulfide, alcohol, and amino groups presented a formidable challenge. Conditions for radical-Markovnikov olefin hydrofunctionalization developed by Professor Dale Boger and co-workers provided an excellent solution, permitting late-stage, site-selective manipulation of lincosamide analogs **FSA-217009** and **FSA-217003** as illustrated in Scheme 4.6. Iron(III)/sodium borohydride-promoted radical hydroazidation¹⁶⁵ proceeded smoothly for both of these substrates, providing diastereomeric mixtures that could be readily separated (e.g., **FSA-217021a/b**, stereochemistry not assigned), or subjected directly to hydrogenation to provide the corresponding amines. As might be expected, the diastereoselectivity of this reaction was dependent upon the steric environment of the nascent asymmetric center – cyclopentenyl analog **FSA-217003** provided a 90:10 mixture of epimeric products (LCMS analysis), which following hydrogenation permitted

¹⁶⁵ Leggans, E. K.; Barker, T. J.; Duncan, K. K.; Boger, D. L. *Org. Lett.* **2012**, *14*, 1428–1431.

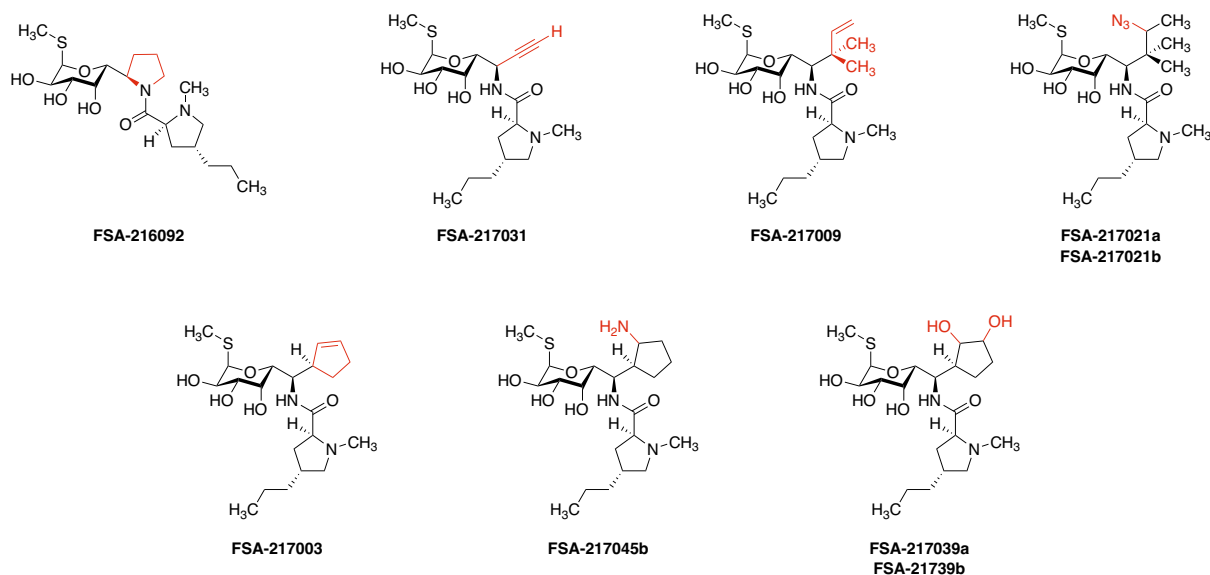
the isolation only of the major epimeric cyclopentylamine **FSA-217045b** (stereochemistry not assigned).



Scheme 4.6. Synthesis and late-stage diversification of propylhygramine analogs bearing olefin functional groups.

The antimicrobial activities of propylhygramine analogs prepared by this sulfinimine-based route are tabulated in Figure 4.1. While no analogs surpassed clindamycin in activity, particularly against Gram-negative strains, some important lessons emerged from this series. Consistent with X-ray evidence implicating the lincosamides' amide N–H hydrogen atom in the recognition of rRNA residue G2505 (Figure 1.5) for example, **FSA-216092**, which lacks this hydrogen-bond donor, displayed no antimicrobial activity. Unexpectedly, alkyne analog **FSA-217031** demonstrated poor activity as well, perhaps owing to a diminished barrier to rotation about the C5–C6 bond attributable to the minimal steric demands exacted by the C6-alkynyl appendage. The bulkier reverse-prenylated analog **FSA-217009** by contrast demonstrated some of the best activity of the lot, surpassed only by its major hydroazidation product, **FSA-217021b**. Cyclopentenyl analog **FSA-217003** displayed modest activity, while its polar derivatives **FSA-**

217045b and *cis*-diols **FSA-217039a/b** (prepared by osmylative dihydroxylation) featured little to no activity. Together these results tentatively supported the hypothesis that conformational restraint within the exocyclic portion of the lincosamides' northern hemisphere could be used to design active, fully synthetic analogs bearing alternatives to clindamycin's native 6-(1-chloroethyl) group.



	Species	Description	Clinda	216092	217031	217009	217021a	217021b	217003	217045b	217039a	217039b
Gram +	<i>S. aureus</i>	ATCC 29213	0.25	>64	64	0.25	4	0.25	1	>64	>64	4
	<i>S. aureus</i>	MP-549; USA 300; MsrA	0.125	>64	32	0.25	4	0.25	1	>64	>64	8
	<i>S. pneumoniae</i>	ATCC 49619	0.125	>64	4	0.5	2	0.125	0.5	32	8	1
	<i>S. pyogenes</i>	ATCC 19615	0.06	>64	8	0.125	2	0.125	0.5	>64	8	0.5
	<i>E. faecalis</i>	ATCC 29212	16	>64	64	64	>64	64	64	>64	>64	>64
Gram -	<i>K. pneumoniae</i>	ATCC 10031	8	>64	>64	>64	>64	>64	>64	>64	>64	>64
	<i>E. coli</i>	ATCC 25922	>64	>64	>64	>64	>64	>64	>64	>64	>64	>64
	<i>E. coli</i>	MP-9 ΔTolC	8	>64	>64	>64	>64	32	>64	>64	>64	>64
	<i>E. coli</i>	LptD mutant	2	>64	>64	32	>64	8	>64	>64	>64	>64
	<i>H. influenzae</i>	ATCC 49247	16	>64	>64	64	>64	32	>64	>64	>64	>64

Figure 4.1. Minimum inhibitory concentrations ($\mu\text{g/mL}$) of propylhygramide analogs bearing modifications to C6.

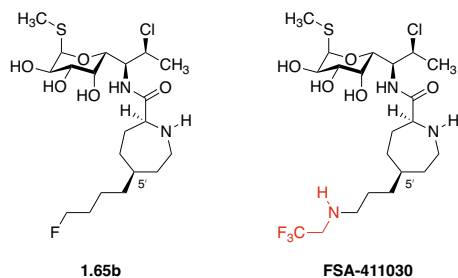
Design and synthesis of C6-modified azepanamides by the same strategy

With these results in hand, I sought to investigate the influence of azepane southern halves in combination with C6-modified aminosugars. Around this time, my teammate Ioana Moga had discovered a (trifluoroethylamino)propyl 5' substituent within the azepane scaffold that imparted

modest activity against Gram-negative species, comparable to those activities observed for Vicuron's 5'-fluorobutyl candidate **1.65b** (Figure 4.2). Importantly, this scaffold featured an amino group with attenuated basicity (calculated $pK_a' = 3.7-5.6$), a structural element that our group had identified as a key driver of Gram-negative activity across a wide range of ribosome-targeting structural classes. This empirical observation was reinforced when an early biophysical study led by Dr. Sunil David of the Wellcome Trust Research Laboratory came to our attention – in it, David and co-workers had found that diamines with intercationic distances of $\geq 11 \text{ \AA}$ reliably display affinity for the lipid A component of the Gram-negative outer membrane.¹⁶⁶ Reasoning that lipid A binding and subsequent self-promoted uptake¹⁶⁷ of rationally designed polyamines might offer an actionable path toward the discovery of broad-spectrum lincosamides, I sought to apply this newly developed route to C6 derivatives toward the evaluation of this hypothesis.

¹⁶⁶ David, S. A.; Mathan, V. I.; Balaram, P. *J. Endotoxin Res.* **1995**, *2*, 325–336.

¹⁶⁷ (a) Hancock, R. E.; Bell, A. *Eur. J. Clin. Microbiol. Infect. Dis.* **1988**, *7*, 713–720. (b) Farmer, S.; Li, Z. S.; Hancock, R. E. *J. Antimicrob. Chemother.* **1992**, *29*, 27–33.



	Species	Description	Clinda	1.65b	411030
Gram +	<i>S. aureus</i>	ATCC 29213	0.25	≤0.06	0.25
	<i>S. aureus</i>	BAA 977; iErmA	0.25	≤0.06	0.25
	<i>S. aureus</i>	MP-549; USA 300; MsrA	0.125	≤0.06	0.25
	<i>S. aureus</i>	Micromyx USA 300	0.25	≤0.06	NT
	<i>S. aureus</i>	MMX 3035; cErmA	>64	64	>64
	<i>S. pneumoniae</i>	ATCC 49619	0.125	≤0.06	≤0.06
	<i>S. pneumoniae</i>	MMX 3028; cErmB	>64	8	64
	<i>S. pneumoniae</i>	MMX 3031; cMefA	0.06	≤0.06	1
	<i>S. pyogenes</i>	ATCC 19615	0.06	≤0.06	≤0.06
	<i>S. pyogenes</i>	MMX 946; cErmB	>64	4	64
	<i>E. faecalis</i>	ATCC 29212	16	≤0.06	4
	<i>E. faecalis</i>	MMX 847; cErmB	>64	64	>64
	<i>C. difficile</i>	BAA 1805	8	≤0.06	NT
	<i>C. difficile</i>	ATCC 700057	8	NT	1
Gram -	<i>B. fragilis</i>	ATCC 25285	0.5	0.25	NT
	<i>K. pneumoniae</i>	ATCC 10031	8	0.5	4
	<i>E. coli</i>	ATCC 25922	>64	4	64
	<i>E. coli</i>	MP-9 ΔToIC	8	0.25	4
	<i>E. coli</i>	LptD mutant	2	4	64
	<i>P. aeruginosa</i>	ATCC 27853	>64	>64	NT
	<i>H. influenzae</i>	ATCC 49247	16	0.25	16
	<i>A. baumannii</i>	ATCC 19606	64	NT	>64

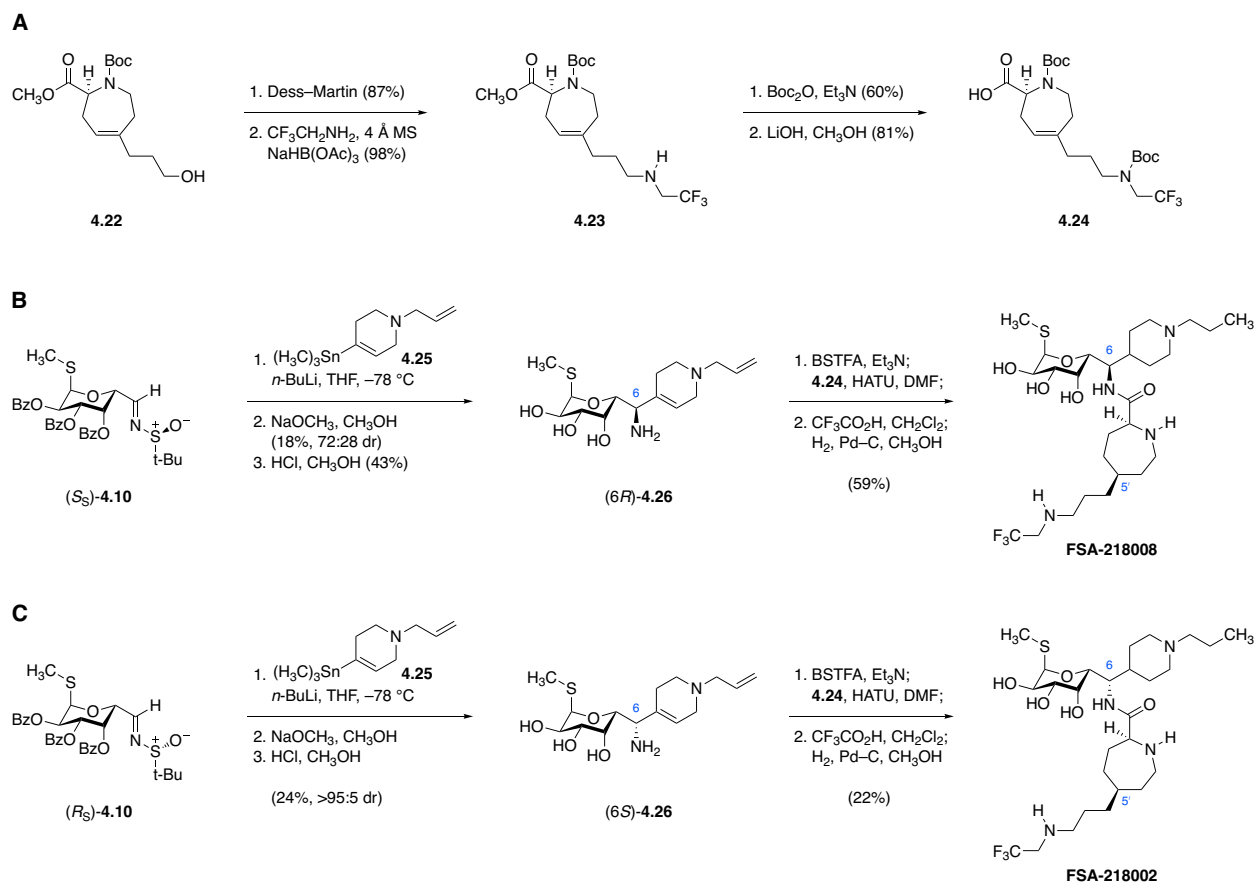
Figure 4.2. Comparison of minimum inhibitory concentrations ($\mu\text{g/mL}$) of 5'-substituted azepanamides displaying activity against Gram-negative species.

Toward this end, I targeted a C6-piperidin-4-yl analog, **FSA-218008**, designed based on its calculated inter-amine (trifluoroethylamine to piperidine) distance of ~ 12 Å and conformationally constrained northern-half architecture. The southern-half component was synthesized through straightforward manipulation of 5'-hydroxypropyl azepine **4.22**, first described by Vicuron,⁶⁸ through a sequence involving Dess–Martin oxidation, reductive amination, Boc protection, and saponification (Scheme 4.7A). The desired northern-half component was likewise prepared from (*S*)-**4.10** and vinyl stannane **4.25**¹⁶⁸ by a sequence closely mirroring those used to prepare the

¹⁶⁸ This vinyl stannane was generously provided by Dr. Md. Ataur Rahman, who prepared it from 1-allyl-4-ketopiperidine by application of a known enolization–triflation–stannylation sequence. See: Sünemann, H. W.; Banwell, M. G.; de Meijere, A. *Eur. J. Org. Chem.* **2007**, 3879–3893.

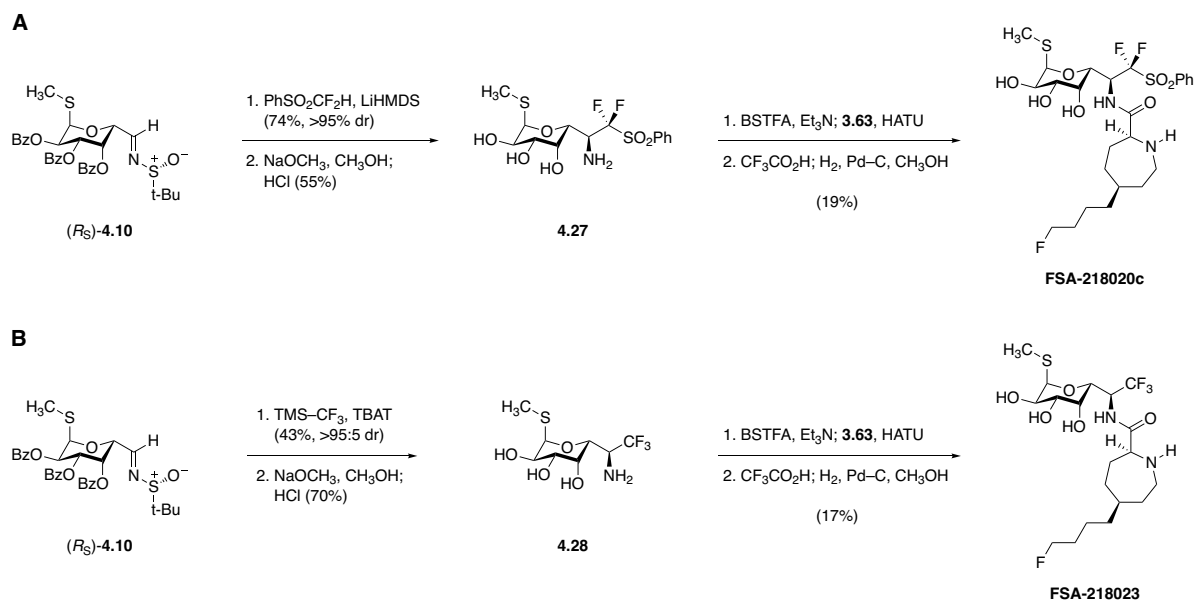
MTL analogs described above (Scheme 4.7B). In the key step, tin–lithium exchange provided a vinyl lithium species that underwent diastereoselective (but not chemoselective) addition to the tri-*O*-benzoyl sulfinimine electrophile; as a result, an excess of nucleophile was required, and a mixture of debenzoylated sulfinamide products was obtained after aqueous workup. In order to resolve this mixture, it was first subjected to conditions for global debenzoylation (catalytic sodium methoxide, methanol, 23 °C);¹⁶⁹ the resulting mixture of C6 epimers (72:28, favoring the desired 6*R* diastereomer) was then separated by flash-column chromatography to provide diastereomerically pure intermediate in 18% yield. Acid-promoted desulfinylation provided diamino triol (6*R*)-**4.26**, suitable for coupling with **4.24**. Boc removal and hydrogenation finally provided the target analog **FSA-218008** in 59% yield.

¹⁶⁹ Basic methanolysis was found to be preferable to hydrazinolysis for reasons of safety and practicality – the catalytic base used in this transformation could be quenched easily by an excess of hydrogen chloride, permitting tandem debenzoylation–desulfinylation in a single flask, without the need for intermediate evaporative workup.



Scheme 4.7. Synthesis of C6-piperidin-4-yl azepanamide analogs featuring 5'-(trifluoroethylamino)propyl substitution.

As I was unable to definitively establish the stereochemical outcome of organolithium–sulfonamide coupling $(S_S)\text{-4.10} + \mathbf{4.25} \rightarrow (6R)\text{-4.26}$, I synthesized the 6-*epi* congener of **FSA-218008** as well, so as to ensure the target analog was successfully prepared (Scheme 4.7C). In this case, $(R_S)\text{-4.10}$ was coupled under identical conditions, this time providing MTL derivative $(6S)\text{-4.26}$ in >90% diastereomeric excess, signaling that this particular pairing represented the matched case. Through straightforward application of coupling, deprotection, and hydrogenation conditions as before, **FSA-218002** was produced.



Scheme 4.8. Synthesis of 7-fluorinated azepanamide analogs.

The early finding by Upjohn scientists that 7-halo substitution positively influences Gram-negative activity (Figure 1.10) prompted me to investigate 7-fluoro derivatives as well. Difluoromethyl phenyl sulfone underwent smooth, diastereoselective addition to *(R_S)-4.10* following deprotonation with lithium hexamethyldisilazide, for example,¹⁷⁰ providing 7,7-difluoro compound **FSA-218020c** after coupling with 5'-fluorobutyl azepine **3.63**, deprotection, and hydrogenation (Scheme 4.8A). Originally, it was planned that this compound could undergo reductive desulfonylation with sodium–mercury amalgam or magnesium in methanol to provide the corresponding C6-difluoromethyl lincosamide, however this transformation was not attempted. The C6-trifluoromethyl analog **FSA-218023** was prepared as well, using tetrabutylammonium difluorotriphenylsilicate (TBAT) to promote *in situ* formation of trifluoromethyl anion from Ruppert's reagent (Scheme 4.8B).¹⁷¹ Notably, both 7-fluorinated

¹⁷⁰ (a) Li, Y.; Hu, J. *Angew. Chem. Int. Ed.* **2005**, *44*, 5882–5886. (b) Liu, J.; Li, Y.; Hu, J. *J. Org. Chem.* **2007**, *72*, 3119–3121.

¹⁷¹ Prakash, G. K. S.; Mandal, M.; Olah, G. A. *Org. Lett.* **2001**, *3*, 2847–2850.

aminosugars **4.27** and **4.28** underwent exceptionally slow and inefficient amide coupling under standard conditions, doubtless owing to their diminished nucleophilicity.

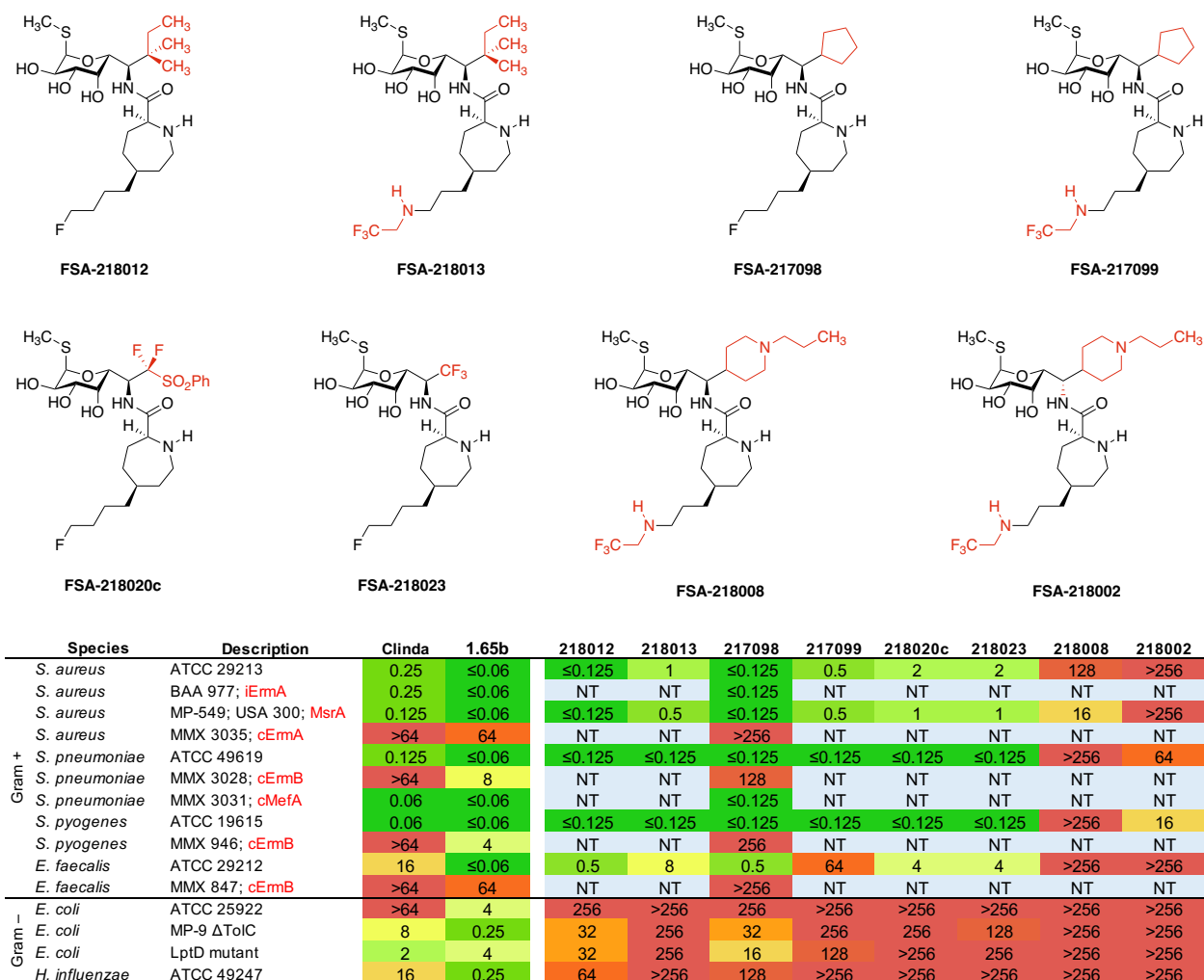


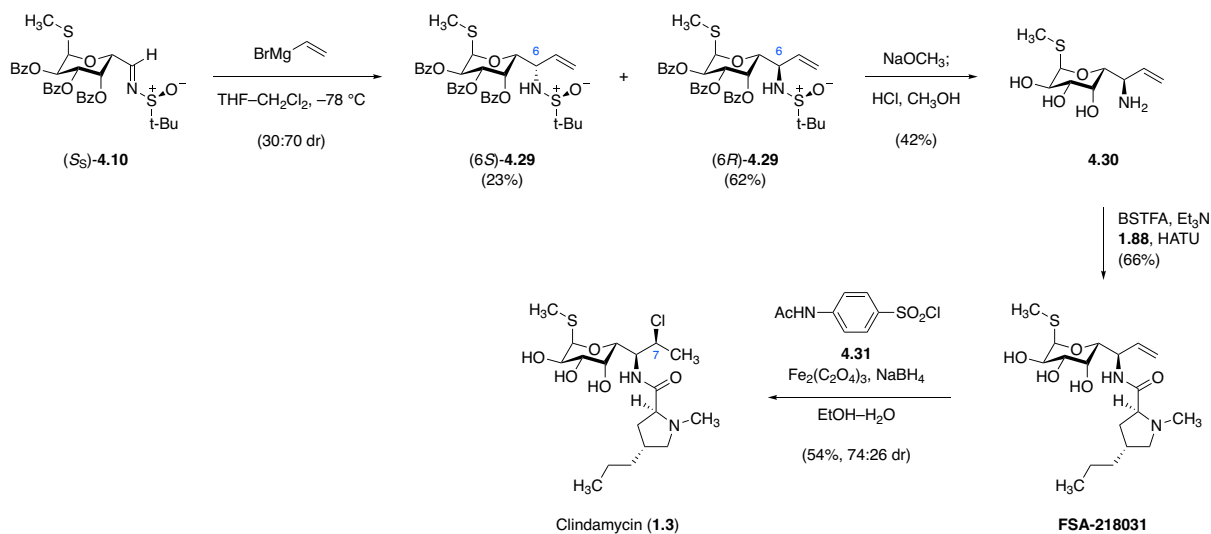
Figure 4.3. Minimum inhibitory concentrations ($\mu\text{g/mL}$) of azepanamides bearing C6 modification.

Figure 4.3 lists the *in vitro* antimicrobial activities of azepanamides bearing C6 modifications introduced by the sulfinimine platform. Unfortunately, neither the designed triamine **FSA-218008** nor the 7-fluorinated analogs **FSA-218020c** and **FSA-218023** demonstrated any appreciable Gram-negative activity; the former in fact were inactive even against lincosamide-susceptible Gram-positive strains. Fluorobutyl and (trifluoroethylamino)propyl azepanamides

bearing C6 *tert*-pentyl and cyclopentyl decoration performed better, although even in the case of **FSA-217098**, activity against MLS_B and Gram-negative pathogens was substantially diminished with respect to its C6-(1-chloroethyl) counterpart, **1.65b**.

Synthesis of clindamycin by radical hydrochlorination of a 6-vinyl lincosamide precursor

Since in the course of this work no C6 substituent had yet been found to outperform the chloroethyl group native to clindamycin and related analogs, I aimed to identify a means by which to install this important appendage using the sulfinimine route described above. Such a technology, it was hoped, would open the door to more expedient exploration of C1 modifications than the earlier nitroaldol route had allowed, and thus would offer a concise, unified approach to MTL variants bearing targeted modifications to either (or both) of these strategic positions. Conditions for radical-Markovnikov hydrofunctionalization, which earlier had empowered the synthesis of **FSA-217021a/b** and **FSA-217045b** from olefinic precursors, presented an appealing path forward – in Boger’s report, the authors described the feasibility of radical hydrochlorination through the use of a suitable chlorine-radical trap, such as *N*-acetylsulfanilyl chloride (**4.31**). Accordingly, I envisioned that hydrochlorination of a C6-vinyl lincosamide precursor might afford the desired 6-(1-chloroethyl) motif with similar ease, efficiency, and regioselectivity as I had observed in the case of late-stage hydroazidation.



Scheme 4.9. A concise synthesis of clindamycin enabled by late-stage Markovnikov hydrochlorination of an olefinic precursor.

As a proof of concept, I successfully synthesized clindamycin in 4 steps from key building block (S_S) -**4.10** (Scheme 4.9). Addition of vinylmagnesium bromide proceeded with modest diastereoselectivity to provide the desired epimer $(6R)$ -**4.29** in 63% yield after chromatographic isolation.¹⁷² Global deprotection was then performed in a one-pot optimized procedure (catalytic sodium methoxide in methanol, followed by hydrochloric acid, 23 °C) to provide 6-vinyl MTL derivative **4.30**, which in turn was coupled with *trans*-4-propyl-L-hygic acid (**1.88**) to produce **FSA-215031**, chemically identical to the sample prepared by Wittig olefination of 8-norlincomycin derivative **3.83** (Figure 3.8). In the key step, addition of sodium borohydride to a degassed, ice-cold solution of **FSA-215031**, iron(III) oxalate, and *N*-acetylsulfanyl chloride (**4.31**) in an ethanol–water mixture provided clindamycin (**1.3**) and its 7-*epi* congener as a 74:26 mixture, isolated together in 54% yield. While improvements in yield and diastereoselectivity are likely achievable through modulation of temperature, solvent, radical trap structure, and reagent

¹⁷² While the commercially available solution of this Grignard reagent in tetrahydrofuran was used here, freshly prepared vinylmagnesium bromide in diethyl ether is known to provide improved diastereoselectivities in similar reactions. See: Lee, A.; Ellman, J. A. *Org. Lett.* **2001**, *3*, 3707–3709.

stoichiometry; this may be unnecessary, as the concision and functional-group compatibility of this route is arguably preferable to schemes relying on more traditional Vilsmeier or Appel approaches to the 6-(1-chloroethyl) group.

Summary and conclusion

In the final months of my graduate work, I developed a concise, scalable, and flexible synthetic route to methylthiolincosamine derivatives, relying on *N*-*tert*-butanesulfinimines **4.10** as key intermediates. The value of this approach is evident in the range of nucleophilic species that successfully engage these sulfinimines, and in the expediency with which the resulting adducts are converted to C6-modified aminosugars suitable for coupling to various southern-half scaffolds. This route enabled the preparation of lincosamide analogs bearing quaternization and fluorination of the C7 position, as well as the synthesis of rationally designed polyamines bearing C6-piperidin-4-yl decoration. From this work emerged the discovery that radical-based methods for olefin hydrofunctionalization can provide expedient access to active lincosamides, exemplified by the synthesis of clindamycin in four steps from sulfinimine (*S*_s)-**4.10**.

Broadly speaking, our original aims to develop a synthetic platform for the discovery of new lincosamides have been achieved, and our chemical approaches to this underexploited class continue to evolve alongside our understanding of the structural basis for these antibiotics' activity. Based on the findings I have presented here, we expect that further refinement of those promising scaffolds we have uncovered, together with efforts to unlock yet more chemical space within the class, will continue to drive advances in the antimicrobial activities, spectra of action, PK/PD, and safety profiles of next-generation lincosamide candidates. It is our hope, then, that this platform for lincosamide discovery will offer further evidence of the enabling potential of fully synthetic approaches to address the challenges of contemporary infectious disease.

Experimental section

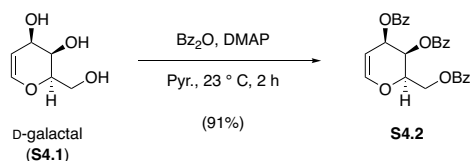
General Experimental Procedures. All reactions were performed in oven- or flame-dried round-bottomed or modified Schlenk flasks fitted with rubber septa under a positive pressure of argon (dried by passage through a column of Drierite calcium sulfate desiccant), unless otherwise noted. Air- and moisture-sensitive liquids and solutions were transferred via syringe or stainless-steel cannula. When necessary (so noted), solutions were deoxygenated by three cycles of freezing (liquid nitrogen), evacuation, and thawing under static vacuum. Organic solutions were concentrated by rotary evaporation (house vacuum, ~60 Torr) at 23–30 °C. Flash-column chromatography was performed as described by Still and co-workers,¹⁰⁵ employing silica gel (60-Å pore size, 230–400 mesh, Agela Technologies, Chicago, IL; or RediSep silica cartridges, Teledyne Isco, Lincoln, NE). Analytical thin-layer chromatography (TLC) was performed using glass plates pre-coated with silica gel (0.25 mm, 60-Å pore size, 230–400 mesh, Merck KGA) impregnated with a fluorescent indicator (254 nm). In special cases (so noted), analytical TLC was performed with aminopropyl-modified silica gel (NH₂ silica gel, 60-Å pore size, Wako Chemicals USA) impregnated with a fluorescent indicator (254 nm). TLC plates were visualized by exposure to ultraviolet light (UV) and/or exposure to iodine vapor (I₂), basic aqueous potassium permanganate solution (KMnO₄), acidic ethanolic *para*-anisaldehyde solution (PAA), acidic aqueous ceric ammonium molybdate solution (CAM), or ethanolic solution of phosphomolybdic acid (PMA) followed by brief heating on a hot plate as needed (~200 °C, ≤15 s).¹⁰⁶ In some cases, reaction monitoring was carried out by analytical liquid chromatography–mass spectrometry (LCMS), or by flow-injection analysis–high-resolution mass spectrometry (FIA-HRMS).

Materials. Commercial reagents and solvents were used as received, unless mentioned otherwise. Dichloromethane, diethyl ether, tetrahydrofuran, 1,4-dioxane, *N,N*-dimethylformamide, toluene, and benzene were purified by passage through Al₂O₃ under argon, according to the method of Pangborn and co-workers.¹⁰⁷ D-Galactal was purchased from Toronto Research Chemicals, Inc. (North York, ON, Canada). Oxone monopersulfate compound, Dess–Martin periodinane, trifluoroacetic acid, HATU, and di-*tert*-butyl dicarbonate were purchased from Oakwood Products, Inc. (Estill, SC, USA). 1-Chloro-3-methyl-2-butene (prenyl chloride) and ethynyltrimethylsilane were purchased from Alfa Aesar (Haverhill, MA, USA). *Trans*-4-*n*-propyl-L-hygric acid hydrochloride (**1.88**) was prepared according to Herr and Slomp.^{9c} 5'-(3-Hydroxypropyl)azepine ester **4.22** and 5'-fluorobutyl azepine acid **3.63** were prepared according to Lewis and co-workers.⁶⁸ All other chemicals and reagents were purchased from Sigma-Aldrich Corporation (Natick, MA, USA).

Instrumentation. Proton nuclear magnetic resonance (¹H NMR) spectra and carbon nuclear magnetic resonance (¹³C NMR) spectra were recorded on Varian Mercury 400 (400 MHz/100 MHz), Varian Inova 500 (500 MHz/125 MHz), or Varian Inova 600 (600 MHz/150 MHz) NMR spectrometers at 23 °C. Proton chemical shifts are expressed in parts per million (ppm, δ scale) and are referenced to residual protium in the NMR solvent (CHCl₃, δ 7.26; CHD₃OD, δ 3.31; C₆H₅D, δ 7.16). Carbon chemical shifts are expressed as parts per million (ppm, δ scale) and are referenced to the carbon resonance of the NMR solvent (CDCl₃, δ 77.2; CD₃OD, δ 49.0; C₆D₆, δ 128.1). Data are reported as follows: Chemical shift, multiplicity (s = singlet, d = doublet, t = triplet, q = quartet, qn = quintet, dd = doublet of doublets, td = triplet of doublets, ABq = AB quartet, m = multiplet, br = broad, app = apparent), integration, and coupling constant (*J*) in Hertz

(Hz). Infrared transmittance (IR) spectra were obtained using a Bruker ALPHA FTIR spectrophotometer referenced to a polystyrene standard. Data are represented as follows: Frequency of absorption (cm^{-1}), and intensity (s = strong, m = medium, br = broad). Melting points were determined using a Thomas Scientific capillary melting point apparatus. High-resolution mass spectrometry (including FIA-HRMS reaction monitoring) was performed at the Harvard University Mass Spectrometry Facility using a Bruker micrOTOF-QII mass spectrometer. X-ray crystallographic analysis was performed at the Harvard University X-Ray Crystallographic Laboratory by Dr. Shao-Liang Zheng. High-performance liquid chromatography–mass spectrometry (LCMS) was performed using an Agilent Technologies 1260-series analytical HPLC system in tandem with an Agilent Technologies 6120 Quadrupole mass spectrometer; a Zorbax Eclipse Plus reverse-phase C_{18} column (2.1×50 mm, $1.8 \mu\text{m}$ pore size, 600 bar rating; Agilent Technologies, Santa Clara, CA) was employed as stationary phase. LCMS samples were eluted at a flow rate of $650 \mu\text{L}/\text{min}$, beginning with 5% acetonitrile–water containing 0.1% formic acid, grading linearly to 100% acetonitrile containing 0.1% formic acid over 3 minutes, followed by 100% acetonitrile containing 0.1% formic acid for 2 minutes (5 minutes total run time).

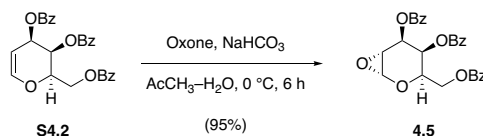
For clarity, intermediates that have not been assigned numbers in the preceding text are numbered sequentially in the following section, beginning with **S4.1**.



Tri-*O*-benzoyl-D-galactal (S4.2).

In a 500-mL round-bottomed flask, D-galactal (**S4.1**, 4.40 g, 30.1 mmol, 1 equiv) was dissolved in pyridine (44.0 mL). To this solution was added benzoic anhydride (52.8 g, 233 mmol, 7.75 equiv), followed by 4-dimethylaminopyridine (368 mg, 3.01 mmol, 0.10 equiv). Upon addition of benzoic anhydride, the solution became cold (ca. 5 °C). The mixture was stirred at ambient temperature, and after 2 h, TLC analysis (20% ethyl acetate–hexanes, UV+KMnO₄) showed the reaction was complete. Excess benzoic anhydride was quenched with the dropwise addition of *N,N*-dimethylethylenediamine (18.1 mL, 166 mmol, 5.50 equiv), and the mixture was stirred at 23 °C for 10 min to ensure complete reaction. The mixture was then diluted with ethyl acetate (500 mL), and the diluted mixture was washed repeatedly with 1N aqueous hydrogen chloride solution (150 mL each), until the aqueous washes were acidic (pH ≤ 0). The organic solution was then washed with water (150 mL), saturated aqueous sodium chloride solution (150 mL), and saturated aqueous sodium chloride solution (150 mL). The washed organic product solution was then dried over sodium sulfate, the dried solution was filtered, and the filtrate was concentrated to provide tri-*O*-benzoyl-D-galactal (**S4.2**) as a foaming white solid (12.6 g, 91%) suitable for use in the subsequent epoxidation reaction without further purification. The corresponding ¹H NMR, ¹³C NMR, and HRMS spectral data were identical to those reported for tri-*O*-benzoyl-D-galactal.¹⁷³

¹⁷³ Chen, H.; Xian, T.; Zhang, W.; Si, W.; Luo, X.; Zhang, B.; Zhang, M.; Wang, Z.; Zhang, J. *Carbohydr. Res.* **2016**, *431*, 42–46.



Brigl's anhydride 4.5.

To a solution of glycal **S4.2** (12.6 g, 27.5 mmol, 1 equiv) in dichloromethane (139 mL) was added acetone (30.3 mL, 412 mmol, 15.0 equiv) and saturated aqueous sodium bicarbonate solution (278 mL). The resulting biphasic mixture was chilled to 0 °C before a solution of Oxone monopersulfate compound (50.7 g) in water (194 mL) was added dropwise. Rapid stirring (>700 rpm) was maintained at 0 °C throughout the course of the reaction to ensure vigorous mixing of the two phases. After 6 h, TLC analysis (30% ethyl acetate–hexanes, UV+PAA) showed complete consumption of the starting material, and the mixture was transferred to a separatory funnel, where the layers were separated. The aqueous phase was extracted with dichloromethane (2 × 100 mL), and the combined organic phases were then washed sequentially with saturated aqueous sodium bicarbonate solution (200 mL) and water (200 mL). The washed organic solution was dried over sodium sulfate, the dried solution was filtered, and the filtrate was concentrated to afford epoxide **4.5** as a white, foaming solid (12.4 g, 95%). This material was used without further purification.

$R_f = 0.39$ (NH₂ silica gel,¹⁷⁴ 30% ethyl acetate–hexanes, UV+PAA).

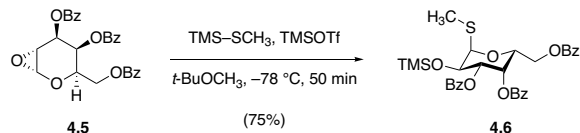
¹H NMR (500 MHz, C₆D₆) δ 8.10–8.08 (m, 2H), 8.07–8.05 (m, 2H), 7.97–7.95 (m, 2H), 7.14–7.08 (m, 2H), 7.06–6.99 (m, 5H), 6.93 (app t, $J = 7.8$ Hz, 2H), 5.69 (d, $J = 4.1$ Hz, 1H), 5.43 (d, $J = 0.9$ Hz, 1H), 4.85 (d, $J = 2.2$ Hz, 1H), 4.56 (dd, $J = 11.4, 6.8$ Hz, 1H), 4.28 (dd, $J = 11.5, 5.8$ Hz, 1H), 4.03 (app t, $J = 6.3$ Hz, 1H), 2.74 (dd, $J = 2.3, 1.5$ Hz, 1H).

¹⁷⁴ Note: The acid-sensitive product is unstable toward chromatography using standard silica gel.

^{13}C NMR (126 MHz, C_6D_6) δ 165.8, 165.6, 165.0, 133.4 (2 \times C), 133.1, 130.1 (2 \times C), 130.0, 128.7 (2 \times C), 128.6, 77.1, 68.0, 67.7, 63.1, 62.9, 50.3.

IR (neat, cm^{-1}): 1724 (s), 1451 (m), 1267 (s), 1247 (s), 1094 (s), 766 (s), 496 (s).

HRMS (ESI+, m/z): $[\text{M}+\text{H}]^+$ calc'd for $\text{C}_{27}\text{H}_{22}\text{O}_8$, 475.1387; found 475.1408.



Thioglycoside 4.6.

A 200-mL round-bottomed flask fitted with a stir bar and charged with 3.00 g of powdered, activated 4Å molecular sieves was flame-dried. Once cooled, the flask was then charged with epoxide **4.5** (3.00 g, 6.32 mmol, 1 equiv) and anhydrous *tert*-butyl methyl ether (63.2 mL). The resulting suspension was chilled to $-78\text{ }^\circ\text{C}$, whereupon (methylthio)trimethylsilane (2.69 mL, 19.0 mmol, 3.00 equiv) was added. Trimethylsilyl trifluoromethanesulfonate (1.14 mL, 6.32 mmol, 1.00 equiv) was added dropwise next, and stirring was continued at $-78\text{ }^\circ\text{C}$. After 50 min, TLC analysis (NH_2 silica gel, 30% ethyl acetate–hexanes, UV+CAM) showed disappearance of both starting material and of a polar spot believed to arise by quenching of unreacted oxocarbenium intermediate during TLC spotting. A 5% v/v triethylamine–dichloromethane solution (88.2 mL, 31.6 mmol triethylamine, 5.00 equiv) was added before the reaction mixture was warmed to $23\text{ }^\circ\text{C}$. Celite (3.00 g) was added to the warmed mixture (to facilitate filtration), and the mixture was filtered through a pad of Celite. The filtrate was washed with saturated aqueous sodium bicarbonate solution (100 mL), and the aqueous layer was extracted with dichloromethane (2×50 mL). The combined organic layers were washed with water (100 mL), dried over sodium sulfate, and filtered to obtain a white foaming solid residue. This crude product was purified by flash-column chromatography (120 g silica gel; eluting with hexanes initially, grading to 25% ethyl acetate–hexanes) to furnish α -methylthioglycoside product as a foaming white solid (2.82 g, 75%).

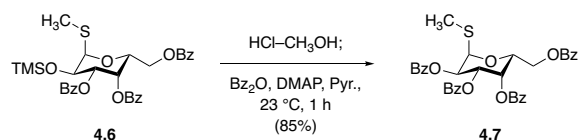
$R_f = 0.62$ (40% ethyl acetate–hexanes, UV+PAA).

^1H NMR (600 MHz, CDCl_3) δ 8.07 (dd, $J = 8.4, 1.5$ Hz, 2H), 8.02 (dd, $J = 8.4, 1.4$ Hz, 2H), 7.84 (dd, $J = 8.4, 1.4$ Hz, 2H), 7.61 (td, $J = 7.4, 1.3$ Hz, 1H), 7.53 (td, $J = 7.4, 1.4$ Hz, 1H), 7.49–7.45 (m, 3H), 7.40 (app t, $J = 7.8$ Hz, 2H), 7.29 (app t, $J = 7.9$ Hz, 2H), 5.97 (dd, $J = 3.6, 1.3$ Hz, 1H), 5.59 (dd, $J = 9.9, 3.5$ Hz, 1H), 5.49 (d, $J = 5.6$ Hz, 1H), 4.92 (ddd, $J = 7.1, 5.2, 1.3$ Hz, 1H), 4.66 (dd, $J = 9.9, 5.5$ Hz, 1H), 4.63 (dd, $J = 11.5, 7.5$ Hz, 1H), 4.41 (dd, $J = 11.5, 5.2$ Hz, 1H), 2.10 (s, 3H), 0.08 (s, 9H).

^{13}C NMR (126 MHz, CDCl_3) δ 166.0, 165.4 ($2 \times \text{C}$), 133.5, 133.2, 133.0, 129.8, 129.6 ($3 \times \text{C}$), 129.5, 129.4, 128.6, 128.4, 128.2, 86.8, 71.7, 69.3, 67.8, 67.1, 62.8, 12.0, 0.0.

FTIR (neat, cm^{-1}): 1720 (s), 1451 (m), 1249 (s), 1094 (s), 840 (s), 765 (s).

HRMS (ESI+, m/z): $[\text{M}+\text{H}]^+$ calc'd for $\text{C}_{31}\text{H}_{34}\text{O}_8\text{SSi}$, 595.1816; found 595.1820.



Tetra-*O*-benzoyl thiogalactoside **4.7**.

To a stirred solution of trimethylsilyl ether **4.6** (6.15 g, 10.3 mmol, 1 equiv) in methanol (103 mL) were added 2 drops of 1N aqueous hydrogen chloride solution at 23 °C. Within 10 minutes, TLC analysis (60% ethyl acetate–hexanes, UV) demonstrated complete consumption of starting material, with concomitant formation of desilylated intermediate ($R_f = 0.56$, 40% ethyl acetate–hexanes, UV+PAA). The stir bar was removed from the flask, and the reaction mixture was concentrated *in vacuo*; in order to remove residual methanol, the residue was then re-dissolved in toluene (100 mL) and this solution was re-concentrated. To this dried residue were then added pyridine (25.8 mL), benzoic anhydride (2.80 g, 12.4 mmol, 1.20 equiv), and 4-(dimethylamino)pyridine (126 mg, 1.03 mmol, 0.100 equiv) sequentially. After 1 h of stirring at 23 °C, TLC analysis (40% ethyl acetate–hexanes, UV+PAA) showed complete consumption of the intermediate alcohol, and excess benzoic anhydride was quenched with the dropwise addition of *N,N*-dimethylethylenediamine (563 μL , 5.15 mmol, 0.500 equiv). Following this quench, the mixture was incubated at 23 °C for 10 min before toluene (100 mL) was added and the mixture concentrated *in vacuo* (to remove excess pyridine). The residue was dissolved in ethyl acetate (250 mL), and the organic solution was washed sequentially with 1N aqueous hydrogen chloride solution (3×100 mL), water (100 mL), saturated aqueous sodium bicarbonate solution (100 mL), and saturated aqueous sodium chloride solution (100 mL). The washed organic solution was then dried over sodium sulfate, filtered, and concentrated to provide a white foaming solid. This residue was purified by flash-column chromatography (330 g silica gel; eluting with hexanes initially,

grading to 30% ethyl acetate–hexanes) to furnish tetra-*O*-benzoyl galactoside product (5.48 g, 85%) as a brilliant white, foaming solid.

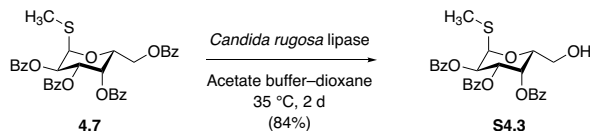
$R_f = 0.56$ (40% ethyl acetate–hexanes, UV+PAA).

$^1\text{H NMR}$ (600 MHz, CDCl_3) δ 8.12 (dd, $J = 8.4, 1.3$ Hz, 2H), 8.04 (dd, $J = 8.4, 1.3$ Hz, 2H), 8.00 (dd, $J = 8.4, 1.3$ Hz, 2H), 7.81 (dd, $J = 8.4, 1.3$ Hz, 2H), 7.63 (ddt, $J = 8.8, 7.1, 1.3$ Hz, 1H), 7.56 (ddt, $J = 8.8, 7.1, 1.3$ Hz, 1H), 7.53–7.49 (m, 3H), 7.45–7.41 (m, 3H), 7.39 (ddt, $J = 7.4, 6.2, 1.1$ Hz, 2H), 7.27–7.24 (m, 2H), 6.07 (app q, $J = 1.4$ Hz, 1H), 5.95–5.92 (m, 3H), 5.01 (ddd, $J = 6.9, 5.4, 1.3$ Hz, 1H), 4.65 (dd, $J = 11.6, 7.4$ Hz, 1H), 4.48 (dd, $J = 11.6, 5.4$ Hz, 1H), 2.13 (s, 3H).

$^{13}\text{C NMR}$ (126 MHz, CDCl_3) δ 166.1, 165.8, 165.6, 165.5, 133.7, 133.6, 133.3, 130.1, 130.0, 129.8 ($2 \times \text{C}$), 129.6, 129.2, 129.1, 129.0, 128.8, 128.6, 128.5, 128.4, 83.7, 69.2, 69.1 ($2 \times \text{C}$), 67.3, 62.8, 12.5.

FTIR (neat, cm^{-1}): 1721 (s), 1451 (m), 1262 (s), 1105 (s), 1069 (s), 708 (s).

HRMS (ESI+, m/z): $[\text{M}+\text{H}]^+$ calc'd for $\text{C}_{35}\text{H}_{30}\text{O}_9\text{S}$, 627.1683; found 627.1688.



Alcohol S4.3.

Sodium acetate buffer was prepared by dissolving acetic acid (5.71 mL, 0.100 mol) in water (450 mL) to which a small quantity of aqueous bromocresol green solution had been added as pH indicator. Aqueous sodium hydroxide (1N) solution was then added until pH 4.5–5.0 was achieved (indicated by aquamarine color and corroborated by testing with a pH strip).

In a 1-L round-bottomed flask fitted with a large magnetic stir bar, tetra-*O*-benzoyl galactoside **4.7** (5.48 g, 8.74 mmol, 1 equiv) was dissolved in 1,4-dioxane (131 mL). To this solution was added freshly prepared acetate buffer (306 mL), followed by *Candida rugosa* lipase (11.0 g, type VII, ≥ 700 unit/mg, Aldrich). After the headspace of the vessel was flushed with argon, rapid stirring (900 rpm) was initiated, and the heterogeneous mixture was heated to 35 °C in a pre-heated oil bath. After 2 d, TLC analysis (40% ethyl acetate–hexanes, UV+PAA) showed complete consumption of starting material. The mixture was filtered through a Celite pad, and the filter cake was rinsed with ethyl acetate (500 mL). The filtrate was separated, and the organic phase was washed with saturated aqueous sodium bicarbonate solution (100 mL), water (100 mL), and saturated aqueous sodium chloride solution (100 mL). The washed solution was then dried over sodium sulfate, filtered, and concentrated to give a foaming syrup. This crude residue was purified by flash-column chromatography (220 g silica gel; eluting with 10% ethyl acetate–hexanes initially, grading to 40% ethyl acetate–hexanes) to provide the product (3.82 g, 84%) as a white foaming solid.

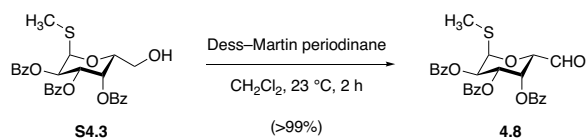
$R_f = 0.34$ (40% ethyl acetate–hexanes, UV+PAA).

$^1\text{H NMR}$ (500 MHz, CDCl_3) δ 8.11 (d, $J = 8.3$ Hz, 2H), 7.99 (d, $J = 8.3$ Hz, 2H), 7.81 (d, $J = 8.3$ Hz, 2H), 7.64 (t, $J = 7.5$ Hz, 1H), 7.55–7.49 (m, 3H), 7.45–7.38 (m, 3H), 5.94–5.86 (m, 4H), 4.69 (app t, $J = 6.7$ Hz, 1H), 3.78 (app dt, $J = 13.0, 6.8$ Hz, 1H), 3.68 (app dt, $J = 12.4, 6.6$ Hz, 1H), 2.40 (t, $J = 6.9$ Hz, 1H), 2.13 (s, 3H).

$^{13}\text{C NMR}$ (126 MHz, CDCl_3) δ 166.5, 165.8, 165.4, 133.8, 133.6, 133.3, 130.0 (2 \times C), 129.7, 128.7, 128.5, 128.3, 83.6, 69.8, 69.6, 69.3, 69.2, 61.0, 12.6.

IR (neat, cm^{-1}): 1720 (s), 1451 (m), 1257 (s), 1093 (s), 1067 (s), 1025 (s), 706 (s).

HRMS (ESI+, m/z): $[\text{M}+\text{H}]^+$ calc'd for $\text{C}_{28}\text{H}_{26}\text{O}_8\text{S}$, 523.1421; found 523.1421.



Aldehyde 4.8.

To a solution of alcohol **S4.3** (3.80 g, 7.27 mmol, 1 equiv) in dichloromethane (48.5 mL) was added Dess–Martin periodinane (4.63 g, 10.9 mmol, 1.50 equiv) at 23 °C. After 2 h, TLC analysis (60% ethyl acetate–hexanes, UV+PAA) showed complete consumption of starting material. Consequently, and with constant stirring throughout, the mixture was diluted with diethyl ether (200 mL); the diluted mixture was then treated with saturated aqueous sodium bicarbonate solution (75 mL), followed by aqueous sodium thiosulfate solution (50 wt%, 75 mL). The mixture was stirred at 23 °C for 1 h, at which time both the organic and aqueous phases had become clear. These layers were separated, and the aqueous phase was extracted with diethyl ether (3 × 30 mL). The combined organic extracts were washed with fresh saturated aqueous sodium bicarbonate solution (75 mL), then with saturated aqueous sodium chloride solution (75 mL). The washed organic solution was dried over sodium sulfate, filtered, and concentrated to provide the product as a white solid (4.00 g, 106%). This material was sufficiently pure for use in subsequent sulfinimine condensations without further purification.

For characterization purposes, a small portion of crude product (~30 mg) was purified by flash-column chromatography (4 g silica gel, eluting with hexanes initially, grading to 80% ethyl acetate–hexanes) to furnish an analytically pure sample.

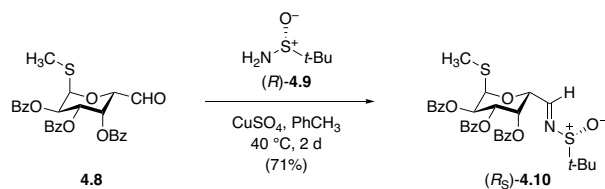
$R_f = 0.31\text{--}0.59$ (60% ethyl acetate–hexanes, UV+PAA).

^1H NMR (400 MHz, CDCl_3) δ 9.67 (d, $J = 0.6$ Hz, 1H), 8.01–7.97 (m, 4H), 7.81–7.79 (m, 2H), 7.62–7.58 (m, 1H), 7.56–7.51 (m, 1H), 7.48–7.44 (m, 3H), 7.40 (t, $J = 7.9$ Hz, 2H), 7.27 (t, $J = 7.9$ Hz, 2H), 6.30 (dd, $J = 3.0, 1.7$ Hz, 1H), 6.02 (d, $J = 5.0$ Hz, 1H), 5.90–5.82 (m, 2H), 5.11 (d, $J = 1.6$ Hz, 1H), 2.17 (s, 3H).

^{13}C NMR (100 MHz, CDCl_3) δ 196.1, 165.7, 165.5, 165.2, 133.8 ($2 \times \text{C}$), 133.5, 130.1, 129.9, 129.0, 128.9, 128.7 ($2 \times \text{C}$), 128.4, 84.5, 74.4, 68.7 ($2 \times \text{C}$), 68.5, 13.2. Two phenyl carbons are not observed: Both are believed to coincide with other adjacent resonances (likely δ 130.1 and δ 128.7).

FTIR (neat, cm^{-1}): 2923 (w), 1721 (s), 1451 (m), 1259 (s), 1246 (s), 1092 (s), 1068 (s), 908 (m), 706 (s).

HRMS (ESI+, m/z): $[\text{M}+\text{H}]^+$ calc'd for $\text{C}_{28}\text{H}_{24}\text{O}_8\text{S}$, 521.1265; found 521.1288.



***tert*-Butanesulfinaldimine (*R_S*)-4.10.**

In a flame-dried 10–20 mL glass microwave vial fitted with a magnetic stir bar, aldehyde **4.8** (1.00 g, 1.92 mmol, 1 equiv), (*R*)-(+)-2-methyl-2-propanesulfinamide (*[R]*-**4.9**, 466 mg, 3.84 mmol, 2.00 equiv), and anhydrous cupric sulfate (460 mg, 2.88 mmol, 1.50 equiv) were combined. To this mixture was added toluene (6.40 mL); the vial was then sealed, and the mixture was heated to 40 °C in a pre-heated oil bath. After stirring for 2 d, TLC analysis (60% ethyl acetate–hexanes, UV+PAA) showed complete consumption of aldehyde starting material, as well as disappearance of a polar spot ($R_f = 0.28$, UV-active, staining brown with PAA) believed to represent hemiaminal intermediate. The mixture was filtered through a pad of Celite to remove insoluble salts, and the filter cake was rinsed with dichloromethane (3×15 mL). The filtrate was concentrated to provide a lime green-colored oily residue, which was purified by flash-column chromatography (30 g silica gel; eluting with 10% ethyl acetate–hexanes initially, grading to 50% ethyl acetate–hexanes) to provide (*R_S*)-sulfinimine product as a white solid (845 mg, 71%).

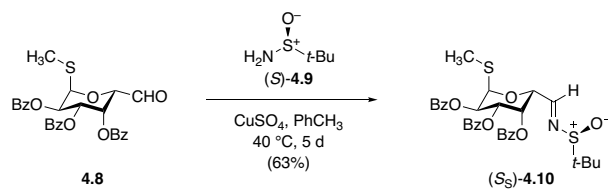
$R_f = 0.60$ (60% ethyl acetate–hexanes, UV+PAA).

^1H NMR (600 MHz, CDCl_3) δ 8.06 (d, $J = 2.2$ Hz, 1H), 7.98 (dd, $J = 8.3, 1.3$ Hz, 2H), 7.97 (dd, $J = 8.4, 1.3$ Hz, 2H), 7.79 (dd, $J = 8.4, 1.3$ Hz, 2H), 7.59 (tt, $J = 7.8, 1.3$ Hz, 1H), 7.52 (tt, $J = 7.8, 1.3$ Hz, 1H), 7.46–7.42 (m, 3H), 7.40–7.37 (m, 2H), 7.26–7.24 (m, 2H), 6.32 (dd, $J = 3.2, 1.5$ Hz, 1H), 6.01 (d, $J = 5.4$ Hz, 1H), 5.89 (dd, $J = 10.6, 5.4$ Hz, 1H), 5.85 (dd, $J = 10.6, 3.2$ Hz, 1H), 5.49 (app t, $J = 1.9$ Hz, 1H), 2.15 (s, 3H), 0.98 (s, 9H).

^{13}C NMR (126 MHz, CDCl_3) δ 165.7, 165.5, 165.4, 164.8, 133.7 (2 \times C), 133., 130.0 (2 \times C),
129.8, 129.2, 129.1, 129.0, 128.7, 128.6, 128.4, 84.5, 71.3, 69.5, 69.2, 68.7, 57.2, 22.2,
13.0.

FTIR (neat, cm^{-1}): 1724 (s), 1451 (m), 1259 (s), 1246 (s), 1088 (s), 1067 (s), 704 (s).

HRMS (ESI+, m/z): $[\text{M}+\text{H}]^+$ calc'd for $\text{C}_{32}\text{H}_{33}\text{NO}_8\text{S}_2$, 624.1720; 624.1743.



***tert*-Butanesulfinaldimine (*S_S*)-4.10.**

In a flame-dried 10–20 mL glass microwave vial fitted with a magnetic stir bar, aldehyde **29** (750 mg, 1.44 mmol, 1 equiv), (*S*)-(-)-2-methyl-2-propanesulfinamide ([*S*]-**4.9**, 349 mg, 2.88 mmol, 2.00 equiv), and anhydrous cupric sulfate (345 mg, 2.16 mmol, 1.50 equiv) were combined. To this mixture was added toluene (4.80 mL); the vial was then sealed, and the mixture was heated to $40\text{ }^\circ\text{C}$ in a pre-heated oil bath. After stirring for 5 d, TLC analysis (60% ethyl acetate–hexanes, UV+PAA) showed complete consumption of aldehyde starting material, as well as disappearance of a polar spot ($R_f \sim 0.25$, UV-active, staining brown with PAA) believed to represent hemiaminal intermediate. The mixture was filtered through a pad of Celite to remove insoluble salts, and the filter cake was rinsed with dichloromethane ($3 \times 10\text{ mL}$). The filtrate was concentrated to provide a yellow moss-green oil that was subjected to flash column chromatography (40 g silica gel; eluting with 10% ethyl acetate–hexanes initially, grading to 50% ethyl acetate–hexanes) to give (*S_S*)-sulfinimine product as a white solid (563 mg, 63%).

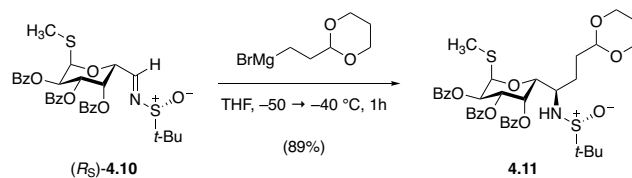
$R_f = 0.54$ (50% ethyl acetate–hexanes, UV+PAA)

$^1\text{H NMR}$ (500 MHz, CDCl_3) δ 8.05 (d, $J = 2.2\text{ Hz}$, 1H), 8.00–7.97 (m, 4H), 7.82–7.79 (m, 2H), 7.59 (tt, $J = 7.1, 1.3\text{ Hz}$, 1H), 7.52 (tt, $J = 7.1, 1.3\text{ Hz}$, 1H), 7.47–7.42 (m, 3H), 7.40–7.37 (m, 2H), 7.27–7.24 (m, 2H), 6.29 (dd, $J = 2.8, 1.5\text{ Hz}$, 1H), 6.00 (d, $J = 4.5\text{ Hz}$, 1H), 5.91–5.86 (m, 2H), 5.43 (app t, $J = 1.9\text{ Hz}$, 1H), 2.16 (s, 3H), 1.13 (s, 9H).

^{13}C NMR (126 MHz, CDCl_3) δ 165.7, 165.6, 165.3, 163.8, 133.7, 133.5, 133.4, 130.0, 129.9, 129.8, 129.2, 129.0 (2 \times C), 128.6 (2 \times C), 128.4, 84.5, 70.9, 69.2, 69.0, 68.8, 57.4, 22.4, 13.0.

FTIR (neat, cm^{-1}): 1724 (s), 1451 (m), 1277 (s), 1247 (s), 1088 (s), 1068 (s), 706 (s).

HRMS (ESI+, m/z): $[\text{M}+\text{H}]^+$ calc'd for $\text{C}_{32}\text{H}_{33}\text{NO}_8\text{S}_2$, 624.1720; found 624.1731.



Dioxolane 4.11.

In a 2–5 mL microwave vial, sulfinimine (R_S) -**4.10** (100 mg, 160 μmol , 1 equiv) was dried by azeotropic removal of benzene. The dried starting material was then dissolved in tetrahydrofuran (802 μL), and the resulting solution was chilled to $-50 \text{ }^\circ\text{C}$ in an acetone bath. With constant stirring throughout, a solution of (1,3-dioxan-2-ylethyl)magnesium bromide (0.5 M, 481 μL , 240 μmol , 1.50 equiv) was added dropwise, and the temperature of the cooling bath was allowed to warm to $-40 \text{ }^\circ\text{C}$ gradually over approximately 15 min. After 1 h of stirring at that temperature, TLC analysis (60% ethyl acetate–hexanes, UV) showed full consumption of starting material. Excess Grignard reagent was quenched with the addition of saturated aqueous ammonium chloride solution (1 mL), and the mixture was warmed to $23 \text{ }^\circ\text{C}$. The warmed mixture then diluted with additional saturated aqueous ammonium chloride solution (5 mL), and the diluted mixture was extracted with ethyl acetate ($3 \times 6 \text{ mL}$). The combined organic extracts were washed with saturated aqueous sodium chloride solution (5 mL), and the washed organic solution was dried over sodium sulfate. The dried solution was filtered, and the filtrate was concentrated to provide crude sulfinamide as a colorless film that produced a foaming white solid upon re-concentration from hexanes. This crude residue was purified by flash-column chromatography (12 g silica gel; eluting with 50% ethyl acetate–hexanes initially; grading to 90% ethyl acetate–hexanes) to afford pure sulfinamide product as a white solid (105 mg, 89%).

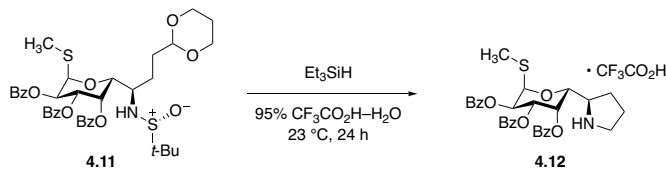
$R_f = 0.25$ (60% ethyl acetate–hexanes, UV+PMA).

^1H NMR (500 MHz, CDCl_3) δ 8.09 (dd, $J = 8.3, 1.3$ Hz, 2H), 7.97 (dd, $J = 8.4, 1.3$ Hz, 2H), 7.76 (dd, $J = 8.4, 1.3$ Hz, 2H), 7.62 (tt, $J = 7.1, 1.3$ Hz, 1H), 7.53–7.47 (m, 3H), 7.42 (tt, $J = 7.7, 1.3$, 1H), 7.39–7.36 (m, 2H), 7.24–7.21 (m, 2H), 6.08 (dd, $J = 3.3, 1.1$ Hz, 1H), 5.90 (d, $J = 5.6$ Hz, 1H), 5.83 (dd, $J = 10.6, 5.6$ Hz, 1H), 5.77 (dd, $J = 10.6, 3.2$ Hz, 1H), 4.75 (d, $J = 7.5$ Hz, 1H), 4.49 (t, $J = 4.4$ Hz, 1H), 3.98–3.93 (m, 2H), 3.92 (d, $J = 5.6$ Hz, 1H), 3.68–3.57 (m, 3H), 2.15 (s, 3H), 2.09–2.03 (m, 1H), 1.94–1.86 (m, 1H) 1.85–1.74 (m, 3H), 1.23–1.20 (m, 1H), 1.18 (s, 9H).

^{13}C NMR (126 MHz, CDCl_3) δ 165.8, 165.6, 165.5, 133.7, 133.6, 133.2, 130.1, 130.0, 129.8, 129.4, 129.2, 129.1, 128.8, 128.6, 128.3, 102.1, 84.4, 70.4, 69.6, 69.1, 69.0, 66.9 (2 \times C), 56.3, 55.4, 31.0, 26.2, 25.8, 22.7, 13.2.

FTIR (neat, cm^{-1}): 2959 (w), 2855 (w), 1725 (s), 1452 (m), 1280 (s), 1261 (s), 1093 (s), 1068 (s), 711 (s).

HRMS (ESI+, m/z): $[\text{M}+\text{H}]^+$ calc'd for $\text{C}_{38}\text{H}_{45}\text{NO}_{10}\text{S}_2$, 740.2558; found 740.2556.



Pyrrolidine 4.12.

In a 4-mL glass scintillation vial in open air, sulfinamide **4.11** (39 mg, 53 μmol , 1 equiv) was dissolved in 95% v/v trifluoroacetic acid–water. The vial was sealed with a PTFE-lined screw-cap, and the resulting solution was stirred at 23 $^\circ\text{C}$ for 30 min in order for desulfinylative cyclization to occur. The vessel was then opened, triethylsilane (84 μL , 530 μmol , 10 equiv) was then added, the vial was re-sealed, and the mixture was stirred for 22 h at 23 $^\circ\text{C}$. Finally, the reaction mixture was concentrated to dryness in vacuo to provide crude amine **4.12** \cdot $\text{CF}_3\text{CO}_2\text{H}$ (>95%, $^1\text{H NMR}$), which was used without purification in the subsequent hydrazinolysis step.

For characterization purposes, a small quantity (ca. 10 mg) of crude residue was purified by HPLC-MS on a Waters SunFire Prep C_{18} column (5 μm , 250 \times 19 mm; eluting with 0.1% trifluoroacetic acid–10% acetonitrile–water initially, grading to 0.1% trifluoroacetic acid–acetonitrile over 30 min, with a flow rate of 15 mL/min; monitored by UV absorbance at 254 nm and ESI+ selected ion monitoring [$m/z = 562$]; $R_t = 20.0$ min) to afford **4.12** \cdot $\text{CF}_3\text{CO}_2\text{H}$ as a white solid.

$^1\text{H NMR}$ (500 MHz, CDCl_3) δ 9.73 (br, 1H), 9.42 (br, 1H), 7.99 (dd, $J = 4.3, 1.2$ Hz, 2H), 7.97 (dd, $J = 4.4, 1.3$ Hz, 2H), 7.73 (dd, $J = 8.4, 1.3$ Hz, 2H), 7.60 (tt, $J = 7.5, 1.3$ Hz, 1H), 7.52 (tt, $J = 7.1, 1.3$ Hz, 1H), 7.47–7.37 (m, 5H), 7.24–7.20 (m, 2H), 6.03 (d, $J = 3.0$ Hz, 1H), 5.86 (d, $J = 5.6$ Hz, 1H), 5.82 (dd, $J = 10.6, 5.6$ Hz, 1H), 5.74 (dd, $J = 10.6, 3.2$ Hz, 1H),

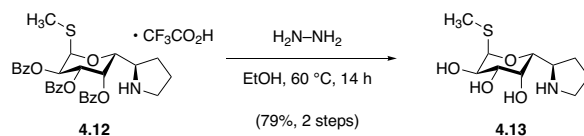
4.99 (d, $J = 8.2$ Hz, 1H), 3.88 (br, 1H), 3.40 (br, 1H), 2.28–2.21 (m, 1H), 2.15 (s, 3H),
2.10–2.03 (m, 2H), 1.98–1.90 (m, 2H).

^{13}C NMR (126 MHz, CDCl_3) δ 166.2, 165.9, 165.3, 134.0, 133.7, 133.4, 130.1 (2 \times C), 129.7,
129.1, 129.0, 128.8, 128.7, 128.6, 128.4, 85.1, 69.4, 69.0, 68.6, 68.5, 58.3, 46.4, 28.5, 24.0,
13.4. Trifluoroacetate carbons were not resolved due to ^{19}F coupling.

^{19}F NMR (471 Hz, CDCl_3) δ -75.8 (s, 3F).

FTIR (neat, cm^{-1}): 2960 (w), 1728 (s), 1673 (m), 1452 (m), 1279 (s), 1261 (s), 1122 (s), 709 (s).

HRMS (ESI+, m/z): $[\text{M}+\text{H}]^+$ calc'd for $\text{C}_{31}\text{H}_{31}\text{NO}_7\text{S}$, 562.1894; found 562.1891.



Aminotriol 4.13.

In an 8-mL glass scintillation vial, triester **4.12** • CF₃CO₂H (theoretically 53 μmol, crude product of reductive cyclization) was dissolved in ethanol (960 μL). Hydrazine (anhydrous, 96 μL) was added, the reaction vial was capped with a PTFE-lined screw-cap, and the mixture was heated to 60 °C with stirring in a pre-heated oil bath. After 15 h, LCMS analysis showed the reaction was complete, and the reaction mixture was consequently diluted with toluene. The diluted mixture was concentrated under a stream of argon, and residual hydrazine was removed by repeated concentration from 50% v/v toluene–methanol. The white solid residue thus obtained was purified by flash-column chromatography (4.0 g silica gel; eluting with 2% ammonium hydroxide–5% methanol–dichloromethane initially, grading to 5% ammonium hydroxide–10% methanol–dichloromethane) to provide aminotriol product (10.5 mg, 79%, 2 steps) as a white solid.

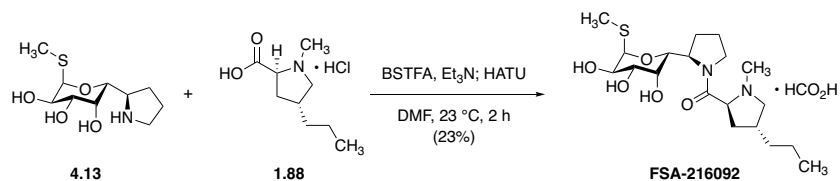
R_f = 0.23 (10% methanol–5% ammonium hydroxide–dichloromethane, PAA).

¹H NMR (500 MHz, CD₃OD) δ 5.27 (d, *J* = 5.6 Hz, 1H), 4.10 (dd, *J* = 10.1, 5.6 Hz, 1H), 4.01 (dd, *J* = 3.3, 1.0 Hz, 1H), 3.95 (dd, *J* = 7.5, 0.9 Hz, 1H), 3.59 (dd, *J* = 10.1, 3.3 Hz, 1H), 3.44 (app q, *J* = 7.7 Hz, 1H), 3.02–2.91 (m, 2H), 2.07 (s, 3H), 2.07–2.01 (m, 1H), 1.90–1.77 (m, 2H), 1.62 (app dq, *J* = 12.7, 8.4 Hz, 1H).

¹³C NMR (126 MHz, CD₃OD) δ 89.3, 73.5, 72.1, 70.9, 69.6, 59.5, 47.0, 29.9, 25.9, 12.9.

FTIR (neat, cm⁻¹): 3316 (br), 2919 (m), 1411 (m), 1079 (s), 1056 (s).

HRMS (ESI+, *m/z*): [M+H]⁺ calc'd for C₁₀H₁₉NO₄S, 250.1108; found 250.1118.



Synthetic lincosamide FSA-216092.

In a flame-dried, 0.5–2 mL conical microwave vial, aminotriol **4.13** (10.0 mg, 40.0 μmol, 1.00 equiv) was dissolved in anhydrous *N,N*-dimethylformamide (201 μL). The resulting solution was chilled to 0 °C, whereupon triethylamine (25.2 μL, 180 μmol, 4.50 equiv) and *N,O*-bis(trimethylsilyl)trifluoroacetamide (16.1 μL, 60.0 μmol, 1.50 equiv) were added. The mixture was allowed to warm to 23 °C with stirring over the course of 1 h, at which point *trans*-4-*n*-propyl-L-hygric acid hydrochloride (**1.88**, 10.8 mg, 52.0 μmmol, 1.30 equiv) was added, followed by HATU (22.9 mg, 60.0 μmol, 1.50 equiv). The dull sand-brown cloudy mixture adopted a vibrant canary-yellow color upon addition of HATU. The mixture was stirred at 23 °C for 2 h, at which point LCMS analysis indicated full consumption of aminotriol and its (oligo)trimethylsilylated congeners. The mixture was diluted with ethyl acetate (15 mL), and the diluted solution was washed sequentially with saturated aqueous sodium bicarbonate solution (7 mL), water (7 mL), and saturated aqueous sodium chloride solution (7 mL). The washed organic solution was then dried over sodium sulfate, the dried solution was filtered, and the filtrate was concentrated. The colorless residue was then re-dissolved in 4 mL of 50% v/v methanol–1N aqueous hydrochloric acid, and the resulting solution was incubated at 23 °C for 30 min to effect global desilylation. The mixture was then passed through a 0.2-μm PTFE syringe filter, the filtrate was concentrated, and the residue was purified by preparative HPLC-MS on a Waters SunFire Prep C₁₈ column (5 μm, 250 × 19 mm; eluting with 0.1% formic acid–5% acetonitrile–water, grading to 0.1% formic acid–30% acetonitrile–water over 40 min, with a flow rate of 15 mL/min; monitored by UV absorbance

at 210 nm and ESI+ selected ion monitoring [$m/z = 403$]; $R_t = 19.0$ min; mixed fractions containing tetramethylurea [ESI+ $m/z = 117$] were discarded) to afford pyrrolidinamide analog **FSA-216092**

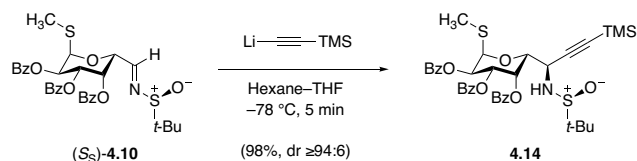
• HCO₂H (4.2 mg, 23%) as a white solid.

¹H NMR (500 MHz, CD₃OD) δ 8.28 (br s, 1H), 5.29 (d, $J = 5.5$ Hz, 1H), 4.43 (dd, $J = 10.3, 6.7$ Hz, 1H), 4.35 (app t, $J = 7.5$ Hz, 1H), 4.11–4.08 (m, 2H), 3.78 (d, $J = 3.2$ Hz, 1H), 3.75 (dd, $J = 10.6, 6.6$ Hz, 1H), 3.63 (ddd, $J = 10.9, 8.8, 2.9$ Hz, 1H), 3.58 (ddd, $J = 10.2, 3.5, 1.4$ Hz, 1H), 3.44 (app q, $J = 8.5$ Hz, 1H), 2.89 (s, 3H), 2.87 (app t, $J = 11.2$ Hz, 1H), 2.44–2.37 (m, 1H), 2.35–2.27 (m, 2H), 2.24–2.17 (m, 1H), 2.10–1.92 (m, 3H), 2.06 (s, 3H), 1.52–1.48 (m, 2H), 1.44–1.32 (m, 2H), 0.96 (t, $J = 7.2$ Hz, 3H).

¹³C NMR (126 MHz, CD₃OD) δ 168.8, 166.8, 89.5, 71.8, 71.1, 70.9, 69.5, 69.0, 62.0, 59.9, 47.8, 40.6, 38.0, 35.8, 35.0, 27.6, 24.5, 22.1, 14.3, 13.2.

FTIR (neat, cm⁻¹): 3358 (br), 2923 (m), 1638 (s), 1595 (s), 1458 (m), 1346 (m), 1201 (m), 1062 (m).

HRMS (ESI+, m/z): [M+H]⁺ calc'd for C₁₉H₃₄N₂O₅S, 403.2261; found 403.2280.



Propargylic sulfinamide **4.14**.

In a 25-mL round-bottomed flask, ethynyltrimethylsilane (51.7 μL , 369 μmol , 2.30 equiv) was dissolved in hexanes (2.92 mL). This solution was chilled to $-78\text{ }^\circ\text{C}$ before it was treated with the dropwise addition of freshly titrated *n*-butyllithium solution (2.30 M in hexane, 160 μL , 369 μmol , 2.30 equiv). The resulting mixture was stirred at $-78\text{ }^\circ\text{C}$ for 15 min, then warmed to $0\text{ }^\circ\text{C}$ for 15 min to ensure complete deprotonation. The lithium acetylide solution was then chilled again to $-78\text{ }^\circ\text{C}$ before a solution of sulfinimine (*S_S*)-**4.10** (100 mg, 160 μmol , 1 equiv) in tetrahydrofuran (1.29 μL) was added dropwise by cannula. After 5 min, FIA-HRMS analysis¹⁷⁵ showed complete consumption of sulfinimine starting material, and excess lithium acetylide was quenched with the addition of saturated aqueous ammonium chloride solution (5 mL). The resulting mixture was extracted with ethyl acetate ($3 \times 10\text{ mL}$), the combined organic extracts were dried over sodium sulfate, the dried solution was filtered, and the filtrate was concentrated to provide an orange-colored oil. ¹H-NMR analysis indicated that the propargyl sulfonamide product was sufficiently pure for use in subsequent deprotection operations without further purification (113 mg, 98%, dr \geq 94:6).

$R_f = 0.38$ (40% ethyl acetate–hexanes, UV+PAA).

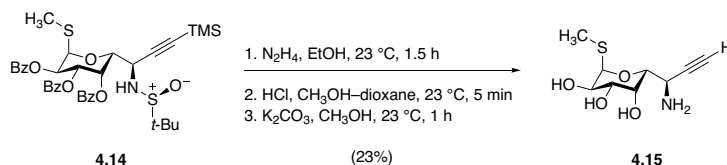
¹⁷⁵ Despite extensive experimentation, TLC conditions could not be identified to adequately distinguish starting material from product for purposes of reaction monitoring.

^1H NMR (600 MHz, CDCl_3) δ 8.08 (dd, $J = 8.3, 1.3$ Hz, 2H), 7.97 (dd, $J = 8.4, 1.4$ Hz, 2H), 7.76 (dd, $J = 8.4, 1.4$ Hz, 2H), 7.65–7.62 (m, 1H), 7.53–7.49 (m, 3H), 7.42 (tt, $J = 7.4, 1.3$ Hz, 1H), 7.40–7.37 (m, 2H), 7.25–7.22 (m, 2H), 6.01 (dd, $J = 3.1, 1.0$ Hz, 1H), 5.94 (d, $J = 5.6$ Hz, 1H), 5.87 (dd, $J = 10.6, 3.1$ Hz, 1H), 5.83 (dd, $J = 10.6, 5.5$ Hz, 1H), 4.70 (d, $J = 10.0$ Hz, 1H), 4.28 (dd, $J = 9.9, 6.7$ Hz, 1H), 4.00 (d, $J = 6.8$ Hz, 1H), 2.21 (s, 3H), 1.23 (s, 9H), 0.15 (s, 9H).

^{13}C NMR (126 MHz, CDCl_3) δ 166.1, 165.8, 165.3, 133.9, 133.6, 133.3, 130.1 ($2 \times \text{C}$), 129.8, 129.3, 129.1 ($2 \times \text{C}$), 128.9, 128.6, 128.4, 102.7, 91.2, 83.8, 71.5, 69.3, 68.9, 56.8, 48.6, 29.9, 22.8, 12.5, -0.1 .

FTIR (neat, cm^{-1}): 2923 (m), 1729 (s), 1452 (m), 1282 (s), 1260 (s), 1091 (s), 1069 (s), 844 (s), 710 (s).

HRMS (ESI+, m/z): $[\text{M}+\text{H}]^+$ calc'd for $\text{C}_{37}\text{H}_{43}\text{NO}_8\text{S}_2\text{Si}$, 722.2272; found 722.2300.



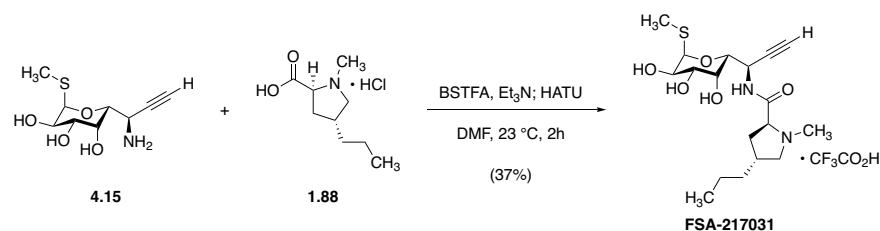
Aminotriol 4.15.

In a conical 0.5–2 mL glass microwave vial, sulfinamide **4.14** (38 mg, 53 μmol , 1 equiv) was dissolved in ethanol (200 proof, 48 μL). Anhydrous hydrazine (48 μL) was added, and after stirring at 23 $^\circ\text{C}$ for 1.5 h, FIA-HRMS showed debenzoylation was complete. The mixture was diluted with toluene (1 mL), and the diluted solution was concentrated *in vacuo*. The dried residue was then dissolved in anhydrous methanol (130 μL) before hydrogen chloride solution (4 M in 1,4-dioxane, 130 μL) was added. Upon acidification of the reaction mixture, a thick white precipitate formed immediately, and within 5 min, LCMS analysis showed removal of the *tert*-butanesulfinyl group was complete. The mixture was diluted with toluene (1 mL) and was concentrated *in vacuo*; in order to remove residual hydrogen chloride, the residue was re-concentrated twice more from 25% methanol–toluene. The dried residue was then dissolved in methanol (1.0 mL), and the solution was treated with Amberlyst A26 resin (hydroxide form, 200 mg) and potassium carbonate (2.0 mg). After 1 h of stirring at 23 $^\circ\text{C}$, LCMS analysis showed that removal of the trimethylsilyl group was complete, and the mixture was filtered through a Celite pad in order to remove insoluble salts and the ion-exchange beads. The filtrate was concentrated *in vacuo* to give a light yellow, oily residue that was purified by flash-column chromatography (4.0 g silica gel; eluting with 0.5% ammonium hydroxide–5% methanol–dichloromethane initially, grading to 2% ammonium hydroxide–2% methanol–dichloromethane) to provide pure aminotriol product (2.9 mg, 23%) as a white solid.

$R_f = 0.26$ (2% ammonium hydroxide–18% methanol–dichloromethane, PAA).

$^1\text{H NMR}$ (600 MHz, CD_3OD) δ 5.31 (d, $J = 5.6$ Hz, 1H), 4.16 (dd, $J = 3.3, 1.2$ Hz, 1H), 4.11 (dd, $J = 10.1, 5.6$ Hz, 1H), 4.09 (dd, $J = 7.9, 1.1$ Hz, 1H), 3.97 (dd, $J = 7.9, 2.3$ Hz, 1H), 3.63 (dd, $J = 10.0, 3.4$ Hz, 1H), 2.80 (d, $J = 2.3$ Hz, 1H), 2.10 (s, 3H).

MS (ESI+, m/z): $[\text{M}+\text{H}]^+$ calc'd for $\text{C}_9\text{H}_{15}\text{NO}_4\text{S}$, 234.1; found 234.1.



Synthetic lincosamide FSA-217031.

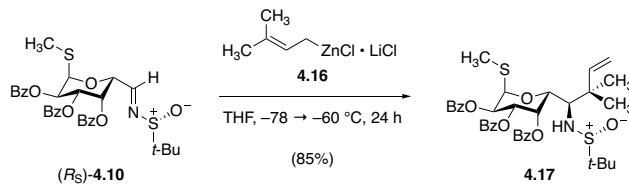
In a 4-mL glass vial fitted with a magnetic stir bar and silicone septum screw-cap, aminotriol **4.15** (2.9 mg, 12 μ mol, 1 equiv) was dissolved in *N,N*-dimethylformamide (124 μ L). To this solution were added triethylamine (7.8 μ L, 56 μ mol, 4.5 equiv) and *N,O*-bis(trimethylsilyl)trifluoroacetamide (5.0 μ L, 19 μ mol, 1.50 equiv); and the resulting solution was stirred at 23 °C for 1 h to ensure complete *O*-silylation. To this reaction mixture were then added *trans*-4-*n*-propyl-L-hygric acid hydrochloride (**1.88**, 3.1 mg, 15 μ mol, 1.2 equiv) and HATU (6.1 mg, 16 μ mol, 1.3 equiv). Upon addition of HATU, the reaction mixture attained a canary yellow color. After stirring this mixture at 23 °C for 2 h, LCMS analysis showed complete consumption of aminotriol starting material and its (oligo)trimethylsilylated congeners. Excess HATU and activated prolyl intermediate were quenched with the addition of 1N aqueous hydrogen chloride solution (400 μ L) and methanol (400 μ L). The mixture was stirred at 23 °C for 10 min, whereupon LCMS analysis showed complete desilylation of (oligo)trimethylsilylated product derivatives. The mixture was concentrated to dryness under a stream of nitrogen, and the residue was purified by preparative HPLC-MS on a Waters SunFire Prep C₁₈ column (5 μ m, 250 \times 19 mm; eluting with 0.1% trifluoroacetic acid–15% acetonitrile–water, grading to 0.1% trifluoroacetic acid–50% acetonitrile–water over 40 min, with a flow rate of 15 mL/min; monitored by UV absorbance at 210 nm and ESI+ selected ion monitoring [*m/z* = 387]; *R_t* = 11.7 min) to provide **FSA-217031** • 2 CF₃CO₂H as a white solid (2.3 mg, 37%).

^1H NMR (500 MHz, CD_3OD) δ 5.32 (d, $J = 5.7$ Hz, 1H), 5.01 (app dt, $J = 9.3, 1.8$ Hz, 1H), 4.27 (d, $J = 9.3$ Hz, 1H), 4.16 (dd, $J = 9.6, 7.1$ Hz, 1H), 4.11 (dd, $J = 10.0, 5.6$ Hz, 1H), 3.91 (app dt, $J = 3.1, 1.4$ Hz, 1H), 3.77 (dd, $J = 10.9, 6.9$ Hz, 1H), 3.61 (ddd, $J = 10.1, 3.3, 1.4$ Hz, 1H), 2.93 (s, 3H), 2.89 (app t, $J = 11.1$ Hz, 1H), 2.80 (dd, $J = 2.5, 1.5$ Hz, 1H), 2.41–2.33 (m, 1H), 2.25–2.18 (m, 2H), 2.12 (s, 3H), 1.51–1.45 (m, 2H), 1.42–1.33 (m, 2H), 0.96 (t, $J = 7.3$ Hz, 3H).

^{13}C NMR (126 MHz, CD_3OD) δ 168.3, 88.8, 82.0, 73.5, 72.0, 69.6, 69.5, 69.4, 62.3, 43.2, 41.0, 37.9, 36.1, 35.8, 22.1, 14.2, 12.5. One carbon is not observed, which is believed to be due to coincidence with another resonance.

FTIR (neat, cm^{-1}): 3269 (br), 1669 (s), 1201 (s), 1135 (s), 1083 (s), 721 (m).

HRMS (ESI+, m/z): $[\text{M}+\text{H}]^+$ calc'd for $\text{C}_{18}\text{H}_{30}\text{N}_2\text{O}_5\text{S}$, 387.1948; found 387.1967.



Reverse-prenyl compound 4.17.

Prenylzinc chloride–lithium chloride complex solution was prepared according to the method reported by Sämman and Knochel.¹⁷⁶ In a 100-mL round-bottomed flask, lithium chloride (892 mg, 21.0 mmol) was flame-dried. Once the apparatus had cooled, activated zinc powder (2.50 g, 38.2 mmol) was added, followed by tetrahydrofuran (19.1 mL). The mixture was stirred at 23 °C for 10 min to ensure complete saturation of the solution with lithium chloride; then 1,2-dibromoethane (33 μL, 382 μmol) and trimethylsilyl chloride (122 μL, 956 μmol) were added. The resulting mixture was stirred at 23 °C for 10 min before a solution of prenyl chloride (2.16 mL, 19.1 mmol) in tetrahydrofuran (19.1 mL) was added dropwise via cannula over a period of approximately 5 min. Zinc insertion was monitored by aliquot NMR: After 2.5 h, a small aliquot of the reaction mixture (~100 μL) was diluted with chloroform-*d* (~300 μL), and this mixture was filtered through a cotton plug to remove insoluble zinc solids. ¹H-NMR analysis of this mixture revealed complete consumption of prenyl chloride, signaling completion of the reaction. Stirring was discontinued, and the suspension was allowed to settle for 1 h. The supernatant was then transferred via cannula to an oven-dried Schlenk bomb flask for storage. Titration of this reagent solution against iodine¹⁵¹ indicated a reagent concentration of 0.40 M (theoretical titer = 0.50 M, 80% yield).

¹⁷⁶ Sämman, C.; Knochel, P. *Synthesis* **2013**, 45, 1870–1876.

An oven-dried 25-mL round-bottomed flask was charged with a stir bar and freshly titrated prenylzinc chloride–lithium chloride reagent solution (2.4 mL, 0.40 M in tetrahydrofuran, 960 μmol , 3.0 equiv). This mixture was then chilled to $-78\text{ }^{\circ}\text{C}$ before a solution of sulfinimine (*R*_S)-**4.10** (200 mg, 320 μmol , 1 equiv) in tetrahydrofuran (1.0 mL) was added by cannula. After 3 h of stirring at $-78\text{ }^{\circ}\text{C}$, the mixture was warmed to $-60\text{ }^{\circ}\text{C}$. The mixture was stirred at $-60\text{ }^{\circ}\text{C}$ for 24 h, whereupon TLC analysis (60% ethyl acetate–hexanes, UV+PAA) demonstrated complete consumption of starting material. The mixture was diluted with ethyl acetate (10 mL), and excess prenylzinc reagent was quenched with the addition of saturated aqueous ammonium chloride solution (20 mL). The resulting biphasic mixture, once warmed to $23\text{ }^{\circ}\text{C}$, was separated; and the aqueous layer was extracted with ethyl acetate ($3 \times 20\text{ mL}$). The combined organic extracts were then dried over sodium sulfate, filtered, and concentrated to provide a solid white residue. This crude product was purified by flash-column chromatography (24 g silica gel; eluting with 10% ethyl acetate–hexanes initially, grading to 50% ethyl acetate–hexanes) to provide sulfinamide product as a white foaming solid (190 mg, 85%).

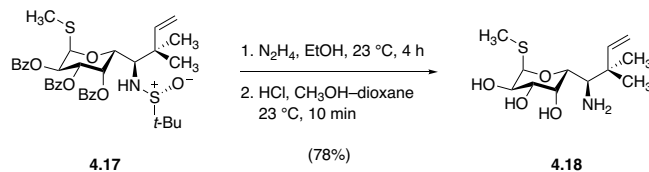
$R_f = 0.49$ (60% ethyl acetate–hexanes, UV+PAA).

$^1\text{H NMR}$ (600 MHz, CDCl_3) δ 8.11 (dd, $J = 8.3, 1.3\text{ Hz}$, 2H), 7.94 (dd, $J = 8.3, 1.4\text{ Hz}$, 2H), 7.71 (dd, $J = 8.4, 1.3\text{ Hz}$, 2H), 7.63–7.60 (m, 1H), 7.50–7.46 (m, 3H), 7.39 (tt, $J = 7.5, 1.3\text{ Hz}$, 1H), 7.35–7.33 (m, 2H), 7.21–7.18 (m, 2H), 6.17 (d, $J = 2.9\text{ Hz}$, 1H), 5.96 (d, $J = 5.9\text{ Hz}$, 1H), 5.92 (dd, $J = 17.4, 10.7\text{ Hz}$, 1H), 5.84 (dd, $J = 10.7, 5.8\text{ Hz}$, 1H), 5.64 (dd, $J = 10.7, 3.2\text{ Hz}$, 1H), 5.13 (dd, $J = 12.5, 1.0\text{ Hz}$, 1H), 5.11 (dd, $J = 5.8, 1.0\text{ Hz}$, 1H), 4.84 (d, $J = 5.1\text{ Hz}$, 1H), 3.99 (d, $J = 6.6\text{ Hz}$, 1H), 3.45 (dd, $J = 6.6, 5.0\text{ Hz}$, 1H), 2.18 (s, 3H), 1.18 (s, 3H), 1.10 (s, 3H), 1.08 (s, 9H).

^{13}C NMR (126 MHz, CDCl_3) δ 165.4 (2 \times C), 165.0, 143.7, 133.8, 133.4, 133.1, 130.1, 129.9, 129.7, 129.2, 129.1 (2 \times C), 128.8, 128.5, 128.2, 113.7, 84.7, 70.1, 70.0, 68.4, 67.5, 66.5, 57.0, 41.2, 26.4, 24.6, 23.2, 13.5.

FTIR (neat, cm^{-1}): 1725 (s), 1451 (m), 1277 (s), 1247 (s), 1065 (s), 908 (m), 705 (s).

HRMS (ESI+, m/z): $[\text{M}+\text{H}]^+$ calc'd for $\text{C}_{37}\text{H}_{43}\text{NO}_8\text{S}_2$, 694.2503; found 694.2530.



Aminotriol 4.18.

In a 2–5 mL glass microwave vial, sulfinamide **4.17** (189 mg, 272 μmol , 1 equiv) was dissolved in ethanol (2.48 mL). Anhydrous hydrazine (248 μL) was then added, and the mixture was stirred at 23 $^\circ\text{C}$. After 4 h, FIA-HRMS analysis of the reaction mixture showed debenzoylation was complete; the mixture was diluted with toluene (2 mL), and volatiles were then removed *in vacuo* to give a white solid. This residue was re-dissolved in anhydrous methanol (680 μL) before hydrogen chloride solution (4.0 M in 1,4-dioxane, 680 μL) was added at 23 $^\circ\text{C}$ (upon acidification, the colorless methanolic solution became an opaque white suspension). After 10 min, removal of the *tert*-butanesulfonyl group was confirmed by LCMS analysis. The reaction mixture was diluted with toluene (1.5 mL), and the mixture was concentrated *in vacuo*. The resulting residue was then re-dissolved in methanol (15 mL), the resulting solution was treated with Amberlyst A26 resin (hydroxide form, 2.0 g), and the mixture was stirred at 23 $^\circ\text{C}$ for 1 h prior to filtration to remove the ion-exchange beads. The filtrate was concentrated to provide crude aminotriol product in free-base form, contaminated with benzoylhydrazine by-product. This mixture was separated by flash-column chromatography (12 g silica gel; eluting with 0.2% ammonium hydroxide–2% methanol–dichloromethane initially; grading to 1% ammonium hydroxide–10% methanol–dichloromethane) to provide pure aminotriol product as a white solid (58.9 mg, 78%).

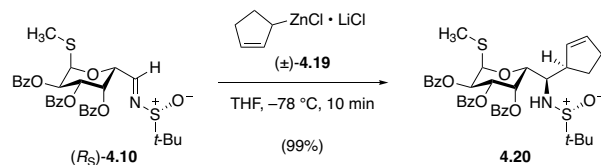
$R_f = 0.29$ (2% ammonium hydroxide–20% methanol–dichloromethane, PAA).

^1H NMR (500 MHz, CD_3OD) δ 5.96 (dd, $J = 17.4, 10.9$ Hz, 1H), 5.22 (d, $J = 5.6$ Hz, 1H), 5.08 (dd, $J = 9.1, 1.4$ Hz, 1H), 5.05 (app q, $J = 1.4$ Hz, 1H), 4.11–4.08 (m, 2H), 4.05 (dd, $J = 3.3, 1.3$ Hz, 1H), 3.48 (dd, $J = 10.2, 3.2$ Hz, 1H), 2.90 (d, $J = 6.0$ Hz, 1H), 2.14 (s, 3H), 1.13 (s, 3H), 1.12 (s, 3H).

^{13}C NMR (126 MHz, CD_3OD) δ 147.1, 112.8, 90.7, 72.3, 72.0, 71.9, 69.5, 60.9, 41.3, 25.8, 23.5, 14.7.

FTIR (neat, cm^{-1}): 3272 (br), 2966 (m), 1444 (m), 1114 (m), 1070 (s), 1041 (s), 859 (m).

HRMS (ESI+, m/z): $[\text{M}+\text{H}]^+$ calc'd for $\text{C}_{12}\text{H}_{23}\text{NO}_4\text{S}$, 278.1421; found 278.1434.



Cyclopentenyl compound 4.20.

A solution of sulfinimine (*R_S*)-**4.10** (150 mg, 240 μmol, 1 equiv) in tetrahydrofuran (1.00 μL) was chilled to -78 °C. With constant stirring, a freshly titrated¹⁵¹ solution of 2-cyclopentenylzinc chloride–lithium chloride complex¹⁷⁷ (0.35 M in tetrahydrofuran, 2.06 mL, 721 μmol, 3.0 equiv) was added dropwise over 3 min. After 10 min of stirring at -78 °C, TLC analysis (60% ethyl acetate–hexanes, UV) indicated that the starting material was fully consumed, and the reaction was quenched by the addition of saturated aqueous ammonium chloride solution (7 mL). The mixture was warmed to 23 °C and was extracted with ethyl acetate (3×10 mL). The combined organic extracts were then washed with saturated aqueous sodium chloride solution (10 mL), and the washed organic solution was dried over sodium sulfate. The dried solution was filtered, and the filtrate was concentrated to give a colorless film. This crude residue was purified by flash-column chromatography (12 g silica gel; eluting with 10% ethyl acetate–hexanes initially; grading to 50% ethyl acetate–hexanes) to provide cyclopentenylated product (165 mg, 99%) as a brilliant white solid.

$R_f = 0.38$ (50% ethyl acetate–hexanes, UV+KMnO₄).

¹H NMR (600 MHz, CDCl₃) δ 8.11 (d, $J = 8.1$ Hz, 2H), 7.97 (d, $J = 8.2$ Hz, 2H), 7.76 (d, $J = 8.2$ Hz, 2H), 7.62 (app t, $J = 7.4$ Hz, 1H), 7.50 (app t, $J = 7.5$ Hz, 3H), 7.40 (app t, $J = 7.8$ Hz,

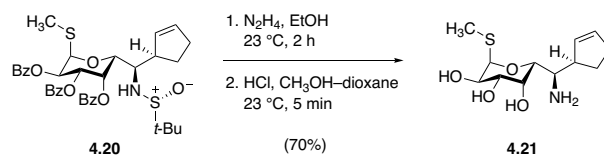
¹⁷⁷ Ren, H.; Dunet, G.; Mayer, P.; Knochel, P. *J. Am. Chem. Soc.* **2007**, *129*, 5376–5377.

1H), 7.37 (app t, $J = 7.6$ Hz, 2H), 7.22 (app t, $J = 7.6$ Hz, 2H), 6.25 (d, $J = 2.6$ Hz, 1H), 5.93 (d, $J = 5.3$ Hz, 1H), 5.89–5.87 (m, 1H), 5.83–4.77 (m, 3H), 4.78 (d, $J = 6.3$ Hz, 1H), 3.58 (d, $J = 8.2$ Hz, 1H), 3.53–3.50 (m, 1H), 3.33 (br, 1H), 2.38–2.27 (m, 2H), 2.17 (s, 3H), 2.03 (app dtd, $J = 13.4, 9.1, 4.4$ Hz, 1H), 1.64 (app ddt, $J = 13.1, 9.7, 6.5$ Hz, 1H), 1.14 (s, 9H).

^{13}C NMR (126 MHz, CDCl_3) δ 165.8, 165.4, 165.3, 134.2, 133.6, 133.5, 133.1, 130.2, 130.0 (2 \times C), 129.8, 129.5, 129.3, 129.1, 128.8, 128.7, 128.5 (2 \times C), 128.2, 84.9, 71.1, 69.8, 69.7, 69.1, 60.2, 56.8, 47.6, 32.5, 27.1, 22.8, 13.7.

FTIR (neat, cm^{-1}): 2957 (w), 1724 (s), 1451 (m), 1278 (s), 1258 (s), 1066 (s), 908 (m), 705 (s).

HRMS (ESI+, m/z): $[\text{M}+\text{H}]^+$ calc'd for $\text{C}_{37}\text{H}_{41}\text{NO}_8\text{S}_2$, 692.2346; found 692.2371.



Aminotriol 4.21.

In a 2–5 mL glass microwave vial, sulfinamide **4.20** (165 mg, 238 μmol , 1 equiv) was dissolved in ethanol (200 proof, 2.17 mL). To this solution was then added anhydrous hydrazine (217 μL) at 23 $^\circ\text{C}$; after 2 h of stirring, FIA-HRMS analysis of the reaction mixture indicated that debenzoylation was complete. The mixture was diluted with toluene (2 mL), and the diluted mixture was concentrated *in vacuo*. The dried residue was then dissolved in anhydrous methanol (595 μL), and the resulting solution was treated with hydrogen chloride solution (4 M in 1,4-dioxane) at 23 $^\circ\text{C}$. Upon acidification, a white precipitate formed immediately. Within 5 min, LCMS analysis of the reaction mixture revealed that removal of the *tert*-butanesulfinyl group was complete. The mixture was diluted with toluene (2 mL), and the diluted mixture was concentrated *in vacuo*; in order to remove residual hydrogen chloride, the residue was re-concentrated twice more from 25% v/v methanol–toluene. The dried, off-white powder thus obtained was then treated with Amberlyst A26 resin (hydroxide form, 1.00 g) and methanol (10 mL). After stirring this mixture for 1 h, the ion-exchange beads were filtered off, and the filtrate was concentrated to afford crude product in its free-base form, contaminated with benzoylhydrazine by-product. These components were separated by flash-column chromatography (5.0 g silica gel; eluting with 0.5% ammonium hydroxide–5% methanol–dichloromethane initially, grading to 2% ammonium hydroxide–20% methanol–dichloromethane) to provide pure aminotriol product as a white solid (46 mg, 70%).

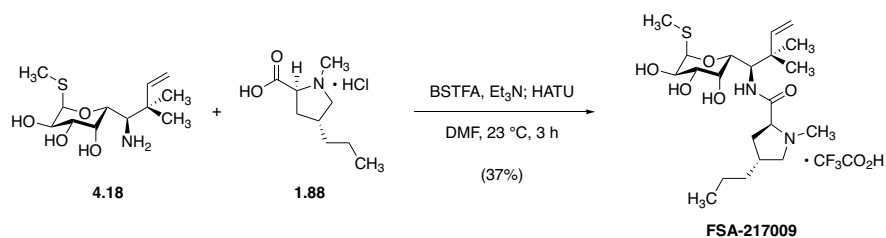
$R_f = 0.23$ (2% ammonium hydroxide–20% methanol–dichloromethane, PAA).

^1H NMR (500 MHz, CD_3OD) δ 5.90 (app dq, $J = 4.6, 2.3$ Hz, 1H), 5.74 (app dq, $J = 6.1, 2.2$ Hz, 1H), 5.28 (d, $J = 5.6$ Hz, 1H), 4.10 (dd, $J = 10.2, 5.7$ Hz, 1H), 4.09 (dd, $J = 3.4, 1.1$ Hz, 1H), 3.96 (dd, $J = 8.2, 1.3$ Hz, 1H), 3.58 (dd, $J = 10.1, 3.3$ Hz, 1H), 3.17 (app dddq, $J = 9.2, 7.0, 4.8, 2.4$ Hz, 1H), 3.01 (dd, $J = 8.3, 4.3$ Hz, 1H), 2.47–2.39 (m, 1H), 2.36–2.28 (app dddq, $J = 16.4, 9.1, 6.9, 2.4$ Hz), 2.06 (s, 3H), 2.06–2.02 (m, 1H), 1.72–1.68 (m, 1H).

^{13}C NMR (126 MHz, CD_3OD) δ 134.6, 130.6, 89.6, 73.1, 72.4, 70.4, 69.7, 55.2, 48.1, 33.3, 27.8, 13.3.

FTIR (neat, cm^{-1}): 3288 (br), 2915 (m), 1422 (w), 1095 (m), 1051 (s).

HRMS (ESI+, m/z): $[\text{M}+\text{H}]^+$ calc'd for $\text{C}_{12}\text{H}_{21}\text{NO}_4\text{S}$, 276.1264; found 276.1263.



Synthetic lincosamide FSA-217009.

In a conical, 0.5–2 mL microwave vial, aminotriol **4.18** (27 mg, 97 μ mol, 1 equiv) was dried by azeotropic removal of benzene. The dried material was dissolved in *N,N*-dimethylformamide (490 μ L), and to this solution were added triethylamine (61 μ L, 440 μ mol, 4.5 equiv) and *N,O*-bis(trimethylsilyl)trifluoroacetamide (39 μ L, 150 μ mol, 1.5 equiv) at 23 °C. The solution was stirred at 23 °C for 1 h to ensure complete *O*-silylation. *Trans*-4-*n*-propyl-L-hygric acid hydrochloride (**1.88**, 26 mg, 130 μ mol, 1.3 equiv) and HATU (56 mg, 150 μ mol, 1.5 equiv) were then added sequentially, and the resulting canary-yellow solution was stirred at 23 °C for 3 h, at which point LCMS analysis demonstrated full consumption of aminotriol starting material and its (oligo)trimethylsilylated congeners. The mixture was diluted with ethyl acetate (25 mL), and the diluted mixture was washed sequentially with saturated aqueous sodium bicarbonate solution (10 mL) and saturated aqueous sodium chloride solution (10 mL). The washed organic solution was dried over sodium sulfate, the dried solution was filtered, and the filtrate was concentrated to give a colorless residue. This residue was re-dissolved in 1:1 methanol–1N aqueous hydrogen chloride solution; this solution was incubated at 23 °C for 1 h to ensure complete desilylation of the coupling product mixture, and was then concentrated to afford a dull yellow oily residue. This crude residue was purified by HPLC-MS on a Waters SunFire Prep C₁₈ column (5 μ m, 250 \times 19 mm; eluting with 0.1% trifluoroacetic acid–2.5% acetonitrile–water, grading to 0.1% trifluoroacetic acid–50% acetonitrile–water over 40 min, with a flow rate of 15 mL/min;

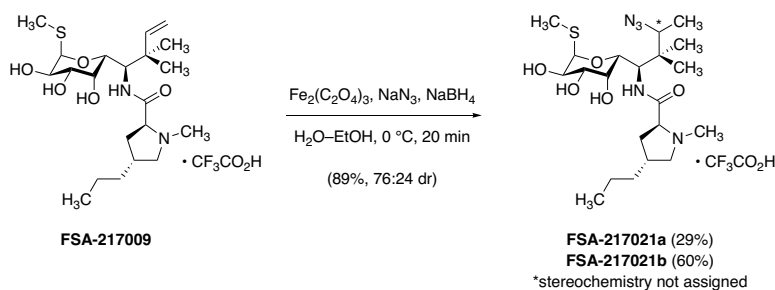
monitored by UV absorbance at 210 nm and ESI+ selected ion monitoring [$m/z = 431$]; $R_t = 31.7$ min) to afford reverse-prenyl analog **FSA-217009** • $\text{CF}_3\text{CO}_2\text{H}$ as a white solid (19 mg, 37%).

^1H NMR (500 MHz, CD_3OD) δ 8.27 (d, $J = 8.9$ Hz, 1H), 5.99 (dd, $J = 17.5, 10.8$ Hz, 1H), 5.20 (d, $J = 5.7$ Hz, 1H), 5.02 (d, $J = 17.6$ Hz, 1H), 4.97 (d, $J = 10.8$ Hz, 1H), 4.29–4.23 (m, 2H), 4.13 (app t, $J = 8.1$ Hz, 1H), 4.05 (dd, $J = 10.3, 5.7$ Hz, 1H), 3.86 (d, $J = 3.2$ Hz, 1H), 3.76 (dd, $J = 11.1, 6.8$ Hz, 1H), 3.46 (dd, $J = 10.3, 3.2$ Hz, 1H), 2.93 (s, 3H), 2.86 (app t, $J = 11.0$ Hz, 1H), 2.38–2.28 (m, 1H), 2.22–2.18 (m, 2H), 2.18 (s, 3H), 1.52–1.43 (m, 2H), 1.40–1.31 (m, 2H), 1.13 (s, 3H), 1.12 (s, 3H), 0.95 (t, $J = 7.3$ Hz, 3H).

^{13}C NMR (126 MHz, CD_3OD) δ 168.5, 146.8, 112.0, 91.2, 72.3, 71.5, 71.3, 69.8, 69.3, 62.1, 57.6, 42.0, 41.0, 38.0, 36.4, 35.8, 25.6, 23.9, 22.1, 15.2, 14.2.

FTIR (neat, cm^{-1}): 3361 (br), 2966 (m), 1671 (s), 1467 (m), 1202 (s), 1181 (s), 1135 (s).

HRMS (ESI+, m/z): $[\text{M}+\text{H}]^+$ calc'd for $\text{C}_{21}\text{H}_{38}\text{N}_2\text{O}_5\text{S}$, 431.2574; found 431.2594.



Synthetic lincosamides FSA-217021a and FSA-217021b.

To begin, a 0.050 M stock solution of ferric oxalate was prepared by stirring ferric oxalate hexahydrate (100 mg) in 4.1 mL water until completely dissolved (ca. 24 h). An aliquot of this solution (920 μL , 46 μmol , 5.0 equiv) was then transferred to an 8-mL glass vial fitted with a stir bar and a silicone septum screw-cap, and this solution was chilled to 0 $^\circ\text{C}$ before nitrogen gas was bubbled through it for 5 min to remove any residual dioxygen. An aqueous solution of sodium azide (73 μL , 1.0 M, 73 μmol , 8.0 equiv) was then added, causing the lemon-lime solution to turn a deep sunset orange. Ethanol (190 proof, 460 μL) was added next to the ice-cold solution, followed by an ethanolic solution of **FSA-217009** \cdot $\text{CF}_3\text{CO}_2\text{H}$ (5.0 mg, 9.2 μmol , 1 equiv). Finally, under a stream of nitrogen gas (to help exclude oxygen) sodium borohydride (2.8 mg, 73 μmol , 8.0 equiv) was added in two portions over 5 min with rapid stirring (CAUTION: Addition of sodium borohydride to water causes rapid hydrogen gas evolution – the vial should be ventilated to avoid overpressurization). After 20 min of stirring at 0 $^\circ\text{C}$, LCMS analysis showed complete consumption of starting material. The reaction mixture was quenched with the addition of aqueous ammonia solution (28% w/w, 400 μL), and the mixture was extracted exhaustively with 10% v/v methanol–dichloromethane (5 \times 10 mL). The combined extracts were dried over sodium sulfate, filtered, and concentrated to afford a colorless residue that was subjected to preparative HPLC-MS on a Waters SunFire Prep C_{18} column (5 μm , 250 \times 19 mm; eluting with 0.1% trifluoroacetic acid–15% acetonitrile–water, grading to 0.1% trifluoroacetic acid–50% acetonitrile–water over 40

min, with a flow rate of 15 mL/min; monitored by UV absorbance at 210 nm and ESI+ selected ion monitoring [$m/z = 474$]; dr = 76:24; **FSA-217021a** $R_t = 26.3$ min; **FSA-217021b** $R_t = 26.7$ min) to provide **FSA-217021a** • CF₃CO₂H (1.4 mg, 29%) and **FSA-217021b** • CF₃CO₂H (3.0 mg, 60%) as white solids.

FSA-217021a • CF₃CO₂H

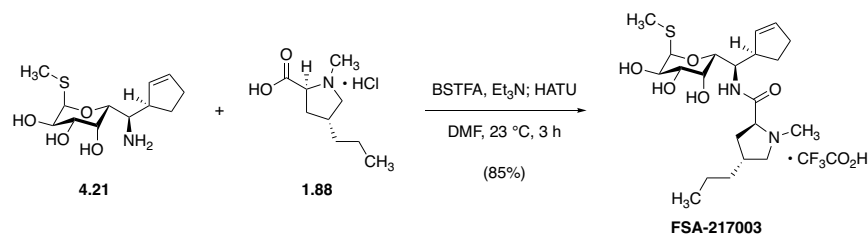
¹H NMR (600 MHz, CD₃OD) δ 5.24 (d, $J = 5.7$ Hz, 1H), 4.54 (d, $J = 8.2$ Hz, 1H), 4.31 (d, $J = 8.2$ Hz, 1H), 4.10 (dd, $J = 9.9, 7.5$ Hz, 1H), 4.07 (dd, $J = 5.6, 4.7$ Hz, 1H), 3.92 (q, $J = 6.7$ Hz, 1H), 3.85 (d, $J = 3.2$ Hz, 1H), 3.77 (dd, $J = 11.2, 7.0$ Hz, 1H), 3.49 (dd, $J = 10.3, 3.3$ Hz, 1H), 2.94 (s, 3H), 2.88 (app t, $J = 10.9$ Hz, 1H), 2.40–2.35 (m, 1H), 2.24–2.20 (m, 2H), 2.20 (s, 3H), 1.52–1.48 (m, 2H), 1.43–1.31 (m, 2H), 1.28 (d, $J = 6.7$ Hz, 3H), 1.00 (s, 3H), 0.96 (t, $J = 7.3$ Hz, 3H), 0.88 (s, 3H).

HRMS (ESI+, m/z): [M+H]⁺ calc'd for C₂₁H₃₉N₅O₅S, 474.2745; found 474.2763.

FSA-2017021b • CF₃CO₂H:

¹H NMR (600 MHz, CD₃OD) δ 5.24 (d, $J = 5.7$ Hz, 1H), 4.44 (d, $J = 9.4$ Hz, 1H), 4.28 (d, $J = 9.4$ Hz, 1H), 4.14 (app t, $J = 7.9$ Hz, 1H), 4.06 (dd, $J = 10.3, 5.7$ Hz, 1H), 3.91 (q, $J = 6.7$ Hz, 1H), 3.80 (d, $J = 2.7$ Hz, 1H), 3.77 (dd, $J = 11.1, 7.0$ Hz, 1H), 3.46 (dd, $J = 10.4, 3.2$ Hz, 1H), 2.94 (s, 3H), 2.88 (app t, $J = 11.0$ Hz, 1H), 2.40–2.32 (m, 1H), 2.25–2.22 (m, 5H), 1.52–1.47 (m, 2H), 1.41–1.33 (m, 2H), 1.31 (d, $J = 6.6$ Hz, 3H), 1.02 (s, 3H), 0.97–0.94 (m, 6H).

HRMS (ESI+, m/z): [M+H]⁺ calc'd for C₂₁H₃₉N₅O₅S, 474.2745; found 474.2762.



Synthetic lincosamide FSA-217003.

In a conical, 0.5–2 mL microwave vial, aminotriol **4.21** (20 mg, 73 μ mol, 1 equiv) was dried by azeotropic removal of benzene. The dried material was dissolved in *N,N*-dimethylformamide (360 μ L), and to this solution were added triethylamine (46 μ L, 330 μ mol, 4.5 equiv) and *N,O*-bis(trimethylsilyl)trifluoroacetamide (29 μ L, 110 μ mol, 1.5 equiv) at 23 °C. The solution was stirred at 23 °C for 1 h to ensure complete *O*-silylation. *Trans*-4-*n*-propyl-L-hygric acid hydrochloride (**1.88**, 18 mg, 87 μ mol, 1.2 equiv) and HATU (36 mg, 94 μ mol, 1.3 equiv) were then added sequentially, and the resulting canary-yellow solution was stirred at 23 °C for 3 h, at which point LCMS analysis demonstrated full consumption of aminotriol starting material and its (oligo)trimethylsilylated congeners. The mixture was diluted with ethyl acetate (25 mL), and the diluted mixture was washed with saturated aqueous sodium chloride solution–saturated aqueous sodium bicarbonate solution (1:1, 10 mL). The washed organic solution was dried over sodium sulfate, the dried solution was filtered, and the filtrate was concentrated to give a colorless residue. This residue was re-dissolved in 1:1 methanol–1N aqueous hydrogen chloride solution (5 mL); this solution was incubated at 23 °C for 1 h to ensure complete desilylation of the coupling product mixture, and was then concentrated to afford a dull yellow oily residue. This residue was then re-dissolved in methanol (5 mL) and was treated with Amberlyst A26 resin (500 mg, hydroxide form). The heterogeneous mixture was stirred at 23 °C for 30 minutes, at which point the ion-exchange beads were removed by filtration, and the filtrate was concentrated to afford

crude product in its free-base form as a colorless oil. This residue was purified by flash-column chromatography (3.0 g silica gel; eluting with 0.1% ammonium hydroxide–1% methanol–dichloromethane initially; grading to 1% ammonium hydroxide–10% methanol–dichloromethane) to obtain **FSA-217003** as an off-white foaming solid (27 mg, 85%).

The crude residue obtained after desilylation with methanolic hydrogen chloride could also be purified by HPLC-MS on a Waters SunFire Prep C₁₈ column (5 μm, 250 × 19 mm; eluting with 0.1% trifluoroacetic acid–2.5% acetonitrile–water, grading to 0.1% trifluoroacetic acid–40% acetonitrile–water over 40 min, with a flow rate of 15 mL/min; monitored by UV absorbance at 210 nm and ESI+ selected ion monitoring [*m/z* = 429]; *R_t* = 35.7 min) to afford **FSA-217003** • CF₃CO₂H as a white solid. It was in this form that the material was evaluated in *in vitro* susceptibility assays.

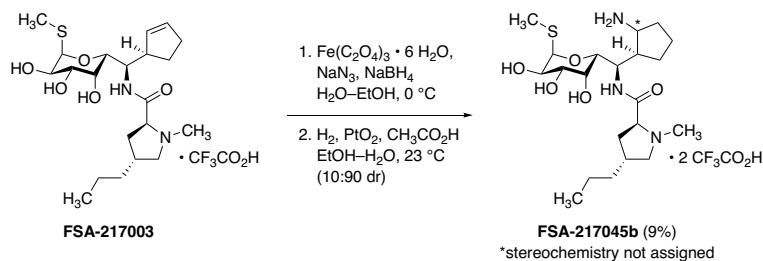
R_f = 0.34 (free base, 1% ammonium hydroxide–9% methanol–dichloromethane, PAA).

¹H NMR (hydrotrifluoroacetate salt, 500 MHz, CD₃OD) δ 5.95 (dd, *J* = 5.7, 2.4 Hz, 1H), 5.71 (dd, *J* = 5.8, 2.2 Hz, 1H), 5.30 (d, *J* = 5.7 Hz, 1H), 4.37 (dd, *J* = 10.0, 3.6 Hz, 1H), 4.17–4.14 (m, 2H), 4.11 (dd, *J* = 10.2, 5.7 Hz, 1H), 3.81 (d, *J* = 3.1 Hz, 1H), 3.77 (dd, *J* = 11.1, 6.9 Hz, 1H), 3.55 (dd, *J* = 10.2, 3.3 Hz, 1H), 3.30–3.27 (m, 1H), 2.93 (s, 3H), 2.87 (app t, *J* = 11.0 Hz, 1H), 2.36–2.28 (m, 3H), 2.21–2.12 (m, 2H), 2.10 (s, 3H), 2.08–2.02 (m, 1H), 1.59–1.32 (m, 5H), 0.95 (t, *J* = 7.2 Hz, 3H).

¹³C NMR (hydrotrifluoroacetate salt, 126 MHz, CD₃OD) δ 169.4, 135.4, 129.8, 90.1, 72.3, 71.4, 70.1, 69.6 (2 × C), 62.2, 53.2, 47.3, 41.1, 38.0, 36.8, 35.7, 33.4, 27.4, 22.1, 14.2, 13.6.

FTIR (neat, cm⁻¹): 3277 (br), 2928 (m), 1666 (s), 1555 (m), 1199 (s), 1176 (s), 1130 (s), 799 (s), 719 (s).

HRMS (ESI+, m/z): $[M+H]^+$ calc'd for $C_{21}H_{36}N_2O_5S$, 429.2422; found 429.2418.



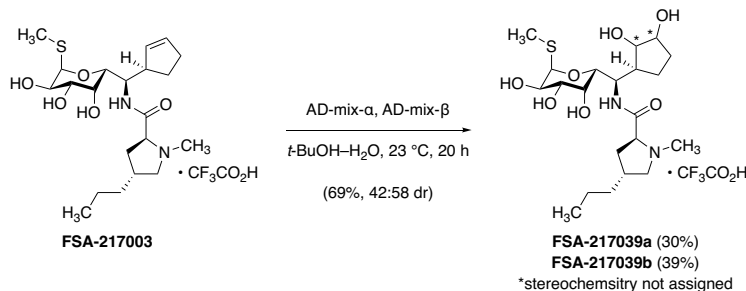
Synthetic lincosamide FSA-217045b.

To begin, a 0.050 M stock solution of ferric oxalate was prepared by stirring ferric oxalate hexahydrate (200 mg) in 8.2 mL water until completely dissolved (ca. 24 h). An aliquot of this solution (4.20 mL, 0.210 mmol, 5.00 equiv) was transferred to a 10–20 mL glass microwave vial fitted with a stir bar and a rubber septum, and this solution was chilled to $0\text{ }^\circ\text{C}$ before nitrogen gas was bubbled through it for 5 min to remove any residual dioxygen. An aqueous solution of sodium azide (1.00 M, 336 μL , 0.336 mmol, 8.00 equiv) was then added, causing the lemon-lime solution to turn a deep sunset orange. Ethanol (190 proof, 2.10 mL) was added next to the ice-cold solution, followed by an ethanolic solution of **FSA-217003** \cdot $\text{CF}_3\text{CO}_2\text{H}$ (18.0 mg, 42.0 μmol , 1 equiv). Finally, under a stream of nitrogen gas (to help exclude oxygen), sodium borohydride (12.7 mg, 0.336 mmol, 8.00 equiv) was added in two portions over 5 min with rapid stirring (CAUTION: Addition of sodium borohydride to water causes rapid hydrogen gas evolution – the vial should be ventilated to avoid overpressurization). After 20 min of stirring at $0\text{ }^\circ\text{C}$, LCMS analysis of the reaction mixture showed that no starting material remained. The reaction was quenched with the addition of aqueous ammonia solution (28 w/w, 2.0 mL), and the mixture was extracted exhaustively with 10% v/v methanol–dichloromethane ($4 \times 10\text{ mL}$). The organic extracts were dried over sodium sulfate, filtered, and concentrated to provide a colorless residue that was then re-dissolved in 50% v/v ethanol–water (840 μL) and transferred to a 4-mL glass vial fitted with a stir bar and silicone septum screw cap. Acetic acid (60.1 μL , 1.05 mmol, 25.0 equiv) and

platinum(IV) oxide (30 mg, 132 μmol , 3.15 equiv) were added to this solution, the vial was sealed, and the mixture was stirred rapidly under 1 atm of hydrogen gas at 23 $^{\circ}\text{C}$. After 2.5 h, LCMS analysis indicated that no azide intermediate remained, and activated charcoal (300 mg) was added in order to adsorb platinum black particles. The mixture was stirred at 23 $^{\circ}\text{C}$ for 5 min to ensure complete adsorption before the black suspension was filtered through a Celite pad. The filter cake was rinsed with methanol ($2 \times 2 \text{ mL}$), and the filtrate was concentrated to give a colorless residue that was subjected to preparative HPLC-MS on a Waters SunFire Prep C_{18} column (5 μm , $250 \times 19 \text{ mm}$; eluting with 0.1% trifluoroacetic acid–2.5% acetonitrile–water initially, grading to 0.1% trifluoroacetic acid–35 acetonitrile–water over 40 min, with a flow rate of 15 mL/min; monitored by UV-210 nm and ESI+ selected ion monitoring [$m/z = 223.5$]; dr = 10:90; major diastereomer $R_t = 20.8 \text{ min}$) to provide the major diastereomer **FSA-217045b** $\cdot 2 \text{ CF}_3\text{CO}_2\text{H}$ as a white solid (2.49 mg, 9%).

$^1\text{H NMR}$ (500 MHz, CD_3OD) δ 5.33 (d, $J = 5.7 \text{ Hz}$, 1H), 4.50 (app t, $J = 4.8 \text{ Hz}$, 1H), 4.31 (d, $J = 5.3 \text{ Hz}$, 1H), 4.17 (dd, $J = 9.9, 7.2 \text{ Hz}$, 1H), 4.13 (dd, $J = 10.1, 5.7 \text{ Hz}$, 1H), 3.96 (d, $J = 3.1 \text{ Hz}$, 1H), 3.76 (dd, $J = 11.2, 7.0 \text{ Hz}$, 1H), 3.73–3.70 (m, 1H), 3.53 (dd, $J = 10.1, 3.1 \text{ Hz}$, 1H), 2.92 (s, 3H), 2.91 (app t, $J = 10.9 \text{ Hz}$, 1H), 2.65 (app dq, $J = 12.9, 4.1 \text{ Hz}$, 1H), 2.39 (app hept, $J = 7.3 \text{ Hz}$, 1H), 2.29–2.23 (m, 1H), 2.20–2.14 (m, 1H), 2.17 (s, 3H), 2.11–2.07 (m, 1H), 1.99–1.94 (m, 1H), 1.79–1.69 (m, 3H), 1.53–1.45 (m, 3H), 1.37 (tq, $J = 13.5, 6.1 \text{ Hz}$, 2H), 0.95 (t, $J = 7.3 \text{ Hz}$, 3H).

HRMS (ESI+, m/z): [$\text{M}+\text{H}$] $^+$ calc'd for $\text{C}_{21}\text{H}_{39}\text{N}_3\text{O}_5\text{S}$, 446.2683; found 446.2693.



Synthetic lincosamides FSA-217039a and FSA-217039b.

In a 1-mL glass vial fitted with a magnetic stir bar and PTFE-lined screw cap, cyclopentene analog **FSA-217003** • CF₃CO₂H (5.0 mg, 9.2 μmol, 1 equiv) was dissolved in 50% v/v *tert*-butanol–water. To this solution were then added AD-mix-α (15 mg) and AD-mix-β (15 mg) at 23 °C, and the vial was sealed. After 20 h of stirring at 23 °C, LCMS analysis indicated that the reaction was complete (≥60% conversion of starting material). The reaction mixture was diluted with methanol (2 mL), causing a yellow precipitate to form, and this suspension was passed through a 0.2-μm PTFE filter. The filtrate was concentrated and the crude residue was purified by preparative HPLC on a Waters SunFire Prep C₁₈ column (5 μm, 250 × 19 mm; eluting with 0.1% trifluoroacetic acid–2.5% acetonitrile–water initially, grading to 0.1% trifluoroacetic acid–40% acetonitrile–water over 40 min; monitored by UV-210 nm and ESI+ selected ion monitoring [*m/z* = 463]; dr = 42:58; **FSA-217039a** *R_t* = 18.2 min, **FSA-217039b** *R_t* = 19.9 min) to provide diastereomeric cyclopentenediol analogs **FSA-217039a** • CF₃CO₂H (1.6 mg, 30%) and **FSA-217039b** • CF₃CO₂H (2.1 mg, 39%) as white solids.

FSA-217039a • CF₃CO₂H:

¹H NMR (600 MHz, CD₃OD) δ 5.26 (d, *J* = 5.6 Hz, 1H), 4.27 (app t, *J* = 7.9 Hz, 1H), 4.23 (dd, *J* = 7.5, 1.3 Hz, 1H), 4.15 (dd, *J* = 10.1, 5.5 Hz, 1H), 4.07 (dd, *J* = 10.2, 5.6 Hz, 1H), 3.95

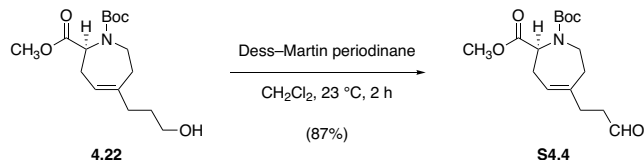
(dd, $J = 3.4, 1.3$ Hz, 1H), 3.90 (app q, $J = 4.8$ Hz, 1H), 3.77 (dd, $J = 7.6, 5.0$ Hz, 1H), 3.78–3.74 (m, 1H), 3.57 (dd, $J = 10.2, 3.3$ Hz, 1H), 2.94 (s, 3H), 2.86 (app t, $J = 10.8$ Hz, 1H), 2.41–2.34 (m, 2H), 2.22–2.17 (m, 2H), 2.11 (s, 3H), 2.01–1.96 (m, 1H), 1.98 (app dtd, $J = 14.3, 9.0, 5.4$ Hz, 1H), 1.84 (app ddt, $J = 14.4, 10.4, 5.3$ Hz, 1H), 1.64 (dddd, $J = 13.3, 8.8, 7.0, 4.3$ Hz, 1H), 1.49–1.46 (m, 2H), 1.40–1.34 (m, 2H), 0.95 (t, $J = 7.3$ Hz, 3H).

HRMS (ESI+, m/z): $[M+H]^+$ calc'd for $C_{21}H_{38}N_2O_7S$, 463.2472; found 463.2490.

FSA-217039b • CF_3CO_2H :

1H NMR (600 MHz, CD_3OD) δ 5.27 (d, $J = 5.7$ Hz, 1H), 4.31–4.25 (m, 3H), 4.10 (dd, $J = 10.2, 5.6$ Hz, 1H), 4.06–4.01 (m, 2H), 3.89 (d, $J = 3.3$ Hz, 1H), 3.79 (dd, $J = 11.2, 6.9$ Hz, 1H), 3.55 (dd, $J = 10.2, 3.3$ Hz, 1H), 2.95 (s, 3H), 2.87 (app t, $J = 10.9$ Hz, 1H), 2.38–2.22 (m, 4H), 2.12 (s, 3H), 1.94–1.90 (m, 1H), 1.71–1.62 (m, 3H), 1.51–1.47 (m, 2H), 1.41–1.34 (m, 2H), 0.96 (t, $J = 7.3$ Hz, 3H).

HRMS (ESI+, m/z): $[M+H]^+$ calc'd for $C_{21}H_{38}N_2O_7S$, 463.2472; found 463.2486.



Aldehyde S4.4.

To a solution of alcohol **4.22** (230 mg, 734 μmol , 1 equiv)⁶⁸ in dichloromethane (7.34 mL) was added Dess–Martin periodinane (374 mg, 881 μmol , 1.20 equiv) in one portion at 23 °C. The resulting white suspension was stirred for 2 h, at which point TLC analysis (80% ethyl acetate–hexanes, PAA) showed that no starting material remained. The mixture was treated with saturated aqueous sodium bicarbonate solution (5.0 mL), and the resulting biphasic mixture was stirred rapidly (1000 rpm) for 2 min before aqueous sodium thiosulfate solution (50% w/w, 5.0 mL) was added as well. After 15 min, stirring was discontinued, and the layers were separated. The aqueous phase was extracted with fresh dichloromethane (2×10 mL), and the combined organic extracts were dried over sodium sulfate. The dried solution was filtered, and the filtrate was concentrated to provide the product as a colorless oil (198 mg, 87%).

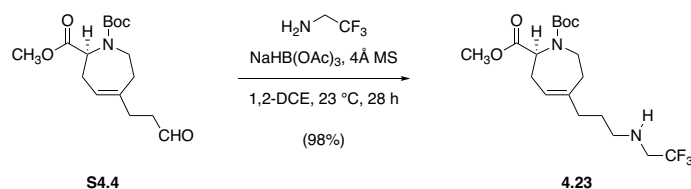
$R_f = 0.58$ (80% ethyl acetate–hexanes, KMnO_4).

^1H NMR (60:40 mixture of rotamers, asterisk [*] denotes minor rotameric peaks that could be resolved, 500 MHz, CDCl_3) δ 9.61 (app t, $J = 1.7$ Hz, 1H),* 9.60 (app t, $J = 1.7$ Hz, 1H), 5.30 (app t, $J = 6.2$ Hz, 1H),* 5.27 (app t, $J = 6.3$ Hz, 1H), 4.56 (dd, $J = 10.5, 4.3$ Hz, 1H),* 4.37 (dd, $J = 9.7, 4.0$ Hz, 1H), 3.73–3.61 (m, 2H), 3.57 (s, 3H),* 3.56 (s, 3H), 3.48 (ddd, $J = 14.6, 8.8, 5.2$ Hz, 1H),* 2.56–2.49 (m, 1H), 2.41–2.33 (m, 3H), 2.28–2.09 (m, 4H), 1.34 (s, 9H),* 1.28 (s, 9H).

^{13}C NMR (60:40 mixture of rotamers, asterisk [*] denotes minor rotameric peaks that could be resolved, 126 MHz, CDCl_3) δ 201.7, 201.6,* 172.9, 172.6,* 155.4,* 154.8, 140.8, 140.4,* 119.4,* 119.0, 80.0, 79.9,* 60.1, 58.8,* 51.8,* 51.7, 42.0,* 41.9, 40.6,* 39.7, 34.4, 34.3,* 31.0,* 30.9, 28.2,* 28.1, 27.0,* 26.9.

IR (neat, cm^{-1}): 2974 (w), 1747 (m), 1724 (m), 1686 (s), 1400 (s), 1160 (s).

HRMS (ESI+, m/z): $[\text{M}+\text{H}]^+$ calc'd for $\text{C}_{16}\text{H}_{25}\text{NO}_5$, 312.1805; found 312.1801.



Trifluoroethylamine derivative **4.23**.

In a 100-mL round-bottomed flask, aldehyde **S4.4** (198 mg, 636 μmol , 1 equiv) was dried by azeotropic removal of benzene. To the dried starting material were then added anhydrous 1,2-dichloroethane (12.7 mL); powdered, activated 4 \AA molecular sieves (200 mg); and 2,2,2-trifluoroethan-1-amine (100 μL , 1.27 mmol, 2.00 equiv). The resulting suspension was stirred at 23 $^\circ\text{C}$ for 10 min before sodium triacetoxyborohydride (80.0 mg, 377 μmol , 0.593 equiv) was added. After stirring at 23 $^\circ\text{C}$ for 24 h, acetic acid (182 μL , 3.18 mmol, 5.00 equiv) and additional sodium triacetoxyborohydride (190 mg, 896 μmol , 1.41 equiv) were added. After 4 hours, TLC analysis (80% ethyl acetate–hexanes, PAA) showed that no starting material remained. Excess reductant was quenched with the dropwise addition of saturated aqueous sodium bicarbonate solution (10 mL). The resulting biphasic mixture was stirred for 10 min at 23 $^\circ\text{C}$ before stirring was discontinued and the layers were separated. The aqueous phase was extracted with dichloromethane (3 \times 7 mL), the combined organic extracts were dried over sodium sulfate, the dried solution was filtered, and the filtrate was concentrated to provide analytically pure product as a colorless oil (245 mg, 98%).

$R_f = 0.53$ (60% ethyl acetate–hexanes, KMnO_4).

$^1\text{H NMR}$ (60:40 mixture of rotamers, asterisk [*] denotes minor rotameric peaks that could be resolved, 500 MHz, CDCl_3) δ 5.39 (app t, $J = 6.5$ Hz, 1H),* 5.35 (app t, $J = 6.5$ Hz, 1H), 4.69 (dd, $J = 10.6, 4.3$ Hz, 1H),* 4.49 (dd, $J = 9.9, 4.0$ Hz, 1H), 3.85–3.71 (m, 2H), 3.68

(s, 3H), 3.57 (ddd, $J = 14.6, 8.1, 6.1$ Hz, 1H),* 3.14 (q, $J = 9.5$ Hz, 2H), 2.66–2.41 (m, 4H),
2.36–2.25 (m, 2H), 1.95 (t, $J = 7.6$ Hz, 2H), 1.57–1.50 (m, 2H), 1.44 (s, 9H),* 1.39 (s, 9H).

^{13}C NMR (126 MHz, CDCl_3) δ 173.3, 173.0,* 155.7,* 155.1, 142.4, 141.9,* 125.7 (q, $J = 279.9$
Hz), 119.1,* 118.6, 80.3, 80.2,* 60.6, 59.1,* 52.1,* 52.0, 50.6 (q, $J = 31.0$ Hz), 49.0,* 49.0,
41.0,* 40.2, 36.6,* 36.5, 34.4, 34.3,* 28.5,* 28.5, 28.4, 27.5, 27.3.

$^{19}\text{F}\{^1\text{H}\}$ NMR (471 MHz, CDCl_3) δ -71.74 (s, 3F).

IR (neat, cm^{-1}): 2976 (w), 1747 (m), 1690 (s), 1402 (m), 1269 (m), 1158 (s).

HRMS (ESI+, m/z): $[\text{M}+\text{H}]^+$ calc'd for $\text{C}_{18}\text{H}_{29}\text{F}_3\text{N}_2\text{O}_4$, 395.2152; found 395.2145.



Azepine S4.5.

In a 20-mL glass vial, amine **4.23** (245 mg, 621 μmol , 1 equiv) was dissolved in dichloromethane (2.07 mL). Di-*tert*-butyl dicarbonate (159 μL , 683 μmol , 1.10 equiv) and triethylamine (113 μL , 807 μmol , 1.30 equiv) were then added sequentially. The vial was sealed, and the mixture was stirred at 23 $^\circ\text{C}$ for 18 h, at which point LCMS analysis showed that no starting material remained. Excess acylation reagent was quenched with the dropwise addition of 50% v/v saturated aqueous ammonium chloride solution–water (4.0 mL). The resulting mixture was stirred at 23 $^\circ\text{C}$ for 10 min before the layers were separated. The aqueous layer was extracted with ethyl acetate (3 \times 4 mL), and the organic solutions were combined. The resulting product solution was then washed sequentially with 5-mL portions of water and saturated aqueous sodium chloride solution. The washed organic solution was dried over sodium sulfate, filtered, and concentrated. The residue thus obtained was purified by flash-column chromatography (12 g silica gel, eluting with hexanes initially, grading to 20% ethyl acetate–hexanes) to provide the product as a colorless oil (183 mg, 60%).

$R_f = 0.56$ (40% ethyl acetate–hexanes, KMnO_4).

^1H NMR (60:40 mixture of azepane *N*-Boc rotamers, asterisk [*] denotes minor rotameric peaks that could be resolved, 500 MHz, CDCl_3) δ 5.34 (app t, $J = 6.2$ Hz, 1H),* 5.31 (app t, $J = 6.1$ Hz, 1H), 4.64 (dd, $J = 10.5, 4.3$ Hz, 1H),* 4.44 (dd, $J = 9.8, 4.0$ Hz, 1H), 3.80–3.68 (m, 4H), 3.62 (s, 3H), 3.53 (app dt, $J = 14.6, 7.0$ Hz, 1H),* 3.17 (br app s, 2H), 2.62–2.55 (m,

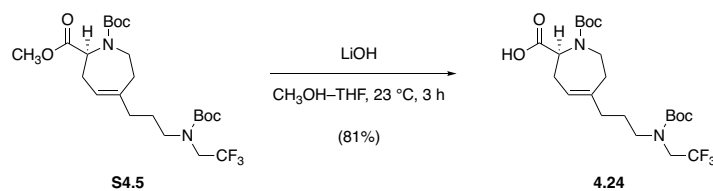
1H), 2.43–2.37 (m, 1h), 2.32–2.20 (m, 2H), 1.84 (t, $J = 7.7$ Hz, 2H), 1.60–1.52 (m, 2H), 1.40 (s, 18H), 1.34 (s, 18H).*

^{13}C NMR (60:40 mixture of azepane *N*-Boc rotamers, asterisk [*] denotes minor rotameric peaks that could be resolved, 126 MHz, CDCl_3) δ 173.1, 172.8,* 155.6,* 155.0, 142.0, 141.6,* 124.7 (q, $J = 283.4$ Hz), 119.2,* 118.6, 80.8, 80.1, 80.0,* 60.4, 59.0,* 51.9,* 51.8, 48.1 (br), 40.9,* 40.1, 36.3, 36.2,* 34.4, 34.3,* 28.4,* 28.3, 28.2 (br), 27.4,* 27.3, 26.2 (br).

$^{19}\text{F}\{^1\text{H}\}$ NMR (471 MHz, CDCl_3) δ -70.80 (s, 3F).

IR (neat, cm^{-1}): 2977 (w), 1691 (m), 1410 (m), 1367 (m), 1147 (s), 730 (m).

HRMS (ESI+, m/z): $[\text{M}+\text{H}]^+$ calc'd for $\text{C}_{23}\text{H}_{37}\text{F}_3\text{N}_2\text{O}_6$, 495.2676; found 495.2666.



Carboxylic acid 4.24.

At 23 °C, a solution of methyl ester **S4.5** (183 mg, 370 μmol, 1 equiv) in 50% v/v methanol–tetrahydrofuran (1.85 mL) was treated with aqueous lithium hydroxide solution (1.00 M, 555 μL, 555 μmol, 1.50 equiv). After 3 h, TLC analysis (40% ethyl acetate–hexanes, KMnO₄) showed that no starting material remained, and the mixture was transferred to a separatory funnel containing distilled water (15 mL). Saturated aqueous sodium chloride solution (5 mL) was then added in order to prevent emulsification, and the aqueous product mixture was washed with 50% v/v ethyl acetate–hexanes. The washed aqueous solution was then transferred to a clean round-bottomed flask, where it was chilled to 0 °C with stirring. Once cooled, the mixture was acidified with the dropwise addition of aqueous hydrogen chloride solution (1.0 N) until pH = 2 was achieved. The acidified aqueous mixture was then extracted with ethyl acetate (4 × 15 mL), and the combined extracts were dried over sodium sulfate. The dried organic solution was filtered, and the filtrate was concentrated to give analytically pure product as a foaming white solid (144 mg, 81%).

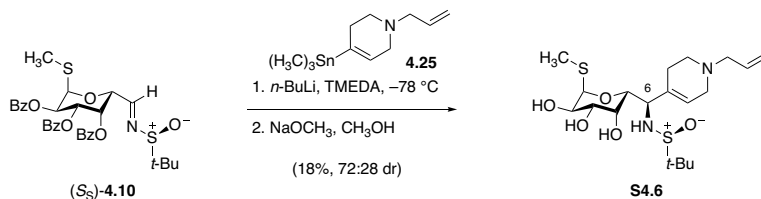
¹H NMR (60:40 mixture of azepane *N*-Boc rotamers, asterisk [*] denotes minor rotameric peaks that could be resolved, 500 MHz, CDCl₃) δ 11.49 (br s, 1H), 5.39 (app t, *J* = 6.0 Hz, 1H),* 5.36 (app t, *J* = 6.0 Hz, 1H), 4.66 (dd, *J* = 11.0, 4.3 Hz, 1H),* 4.49 (dd, *J* = 9.7, 4.0 Hz, 1H), 3.85–3.70 (m, 4H), 3.56 (app dt, *J* = 14.7, 7.2 Hz, 1H),* 3.29–3.13 (m, 2H), 2.72–

2.62 (m, 1H), 2.54–2.42 (m, 1H), 2.39–2.20 (m, 2H), 1.88 (t, $J = 7.6$ Hz, 2H), 1.59 (p, $J = 8.1$, 7.7 Hz, 2H), 1.43 (s, 18H), 1.38 (s, 18H).*

^{13}C NMR (complex rotameric mixture, asterisk [*] denotes minor rotameric peaks that could be resolved, 126 MHz, CDCl_3) δ 178.3,* 177.9, 177.1, 177.0,* 156.2, 155.6,* 144.1, 154.8,* 141.9, 124.8 (q, $J = 279.9$ Hz),* 124.6 (q, $J = 281.9$ Hz), 119.0, 118.7, 118.5,* 81.1,* 80.7, 60.3, 59.2,* 48.2 (br), 47.6, 40.9,* 40.1, 36.3, 36.1,* 34.4, 34.3,* 28.5,* 28.3, 28.2,* 27.1, 27.0,* 26.5,* 26.2, 26.0,* 25.7.

$^{19}\text{F}\{^1\text{H}\}$ NMR (376 MHz, CDCl_3) δ -70.70 (s, 3F).

HRMS (ESI+, m/z): $[\text{M}+\text{H}]^+$ calc'd for $\text{C}_{22}\text{H}_{35}\text{F}_3\text{N}_2\text{O}_6$, 479.2374; found 479.2374.



Dehydropiperidine S4.6.

In a 25-mL round-bottomed flask fitted with a stir bar, vinyl stannane **4.25** (183 mg, 641 μmol , 4.00 equiv) was dissolved in tetrahydrofuran (3.00 mL). The resulting solution was chilled to -78°C before *n*-butyllithium solution (2.40 M in hexanes, 267 μL , 641 μmol , 4.00 equiv) was added dropwise. The resulting mixture was stirred at -78°C for 30 min before *N,N,N',N'*-tetramethylethylenediamine (242 μL , 1.60 mmol, 10.0 equiv) was added. After stirring the reaction mixture for an additional 30 min at -78°C , a solution of sulfinimine (*S_S*)-**4.10** (100 mg, 0.160 mmol, 1 equiv) in tetrahydrofuran (500 μL) was added dropwise by syringe. Within 5 min, TLC analysis (60% ethyl acetate–hexanes, UV+CAM) indicated that no sulfinimine starting material remained, and the mixture was neutralized with the addition of acetic acid (184 μL , 3.21 mmol, 20.0 equiv). The mixture was warmed to ambient temperature before it was transferred to a separatory funnel containing ethyl acetate (10 mL) and saturated aqueous sodium bicarbonate solution (20 mL). The layers were shaken, then separated; the aqueous layer was extracted with 10% v/v methanol–dichloromethane (5×10 mL). The combined organic extracts were dried over sodium sulfate, filtered and concentrated to provide a crude mixture of (oligo)debenzoylated dehydropiperidine adducts.

This crude residue was dissolved in anhydrous methanol (2.91 mL), and the resulting solution was treated with methanolic sodium methoxide solution (0.5 M, 290 μL) at 23°C . After 40 min of stirring, LCMS analysis indicated that debenzoylation was complete. The mixture was neutralized with the addition of acetic acid (~ 18 μL) until $\text{pH} = 7$ was achieved. The mixture was

then concentrated to dryness to provide a mahogany-colored, solid residue. LCMS analysis of this crude residue revealed that a 72:28 diastereomeric mixture of dehydropiperidine adducts was present. Purification by flash-column chromatography (6.0 g silica gel, eluting with dichloromethane initially, grading to 0.85% ammonium hydroxide–8.5% methanol–dichloromethane) provided the product as a light brown solid (12.3 mg, 18%).

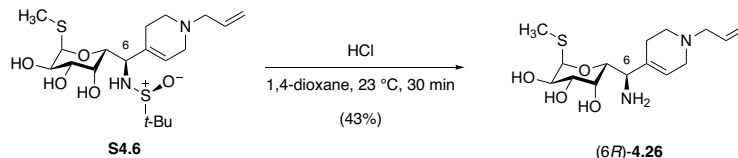
$R_f = 0.31$ (2% ammonium hydroxide–20% methanol–dichloromethane, PAA).

$^1\text{H NMR}$ (600 MHz, CD_3OD) δ 5.95–5.93 (m, 1H), 5.92 (ddt, $J = 17.0, 10.2, 6.8$ Hz, 1H), 5.36 (d, $J = 5.7$ Hz, 1H), 5.27 (app dq, $J = 17.2, 1.5$ Hz, 1H), 5.22 (ddd, $J = 10.2, 2.0, 1.0$ Hz, 1H), 4.23 (d, $J = 9.2$ Hz, 1H), 4.15 (d, $J = 9.3, 1.1$ Hz, 1H), 4.11 (dd, $J = 10.1, 5.6$ Hz, 1H), 3.85 (dd, $J = 3.3, 1.1$ Hz, 1H), 3.57 (dd, $J = 10.1, 3.3$ Hz, 1H), 3.17–3.12 (m, 3H), 3.02 (app dq, $J = 17.0, 2.9$ Hz, 1H), 2.77 (app dt, $J = 10.8, 5.1$ Hz, 1H), 2.51 (ddd, $J = 11.8, 7.8, 4.5$ Hz, 1H), 2.26 (br d, $J = 17.7$ Hz, 1H), 2.14–2.11 (m, 1H), 2.11 (s, 3H), 1.22 (s, 9H).

$^{13}\text{C NMR}$ (126 MHz, CD_3OD) δ 135.2, 132.6, 129.0, 119.5, 89.2, 72.2, 72.0, 70.1, 69.5, 62.0, 60.1, 56.4, 53.3, 50.3, 25.4, 22.9, 13.1.

IR (neat, cm^{-1}): 3377 (br), 2917 (m), 1363 (w), 1052 (s), 997 (m).

HRMS (ESI+, m/z): $[\text{M}+\text{H}]^+$ calc'd for $\text{C}_{19}\text{H}_{34}\text{N}_2\text{O}_5\text{S}_2$, 435.1982; found 435.1976.



Diaminotriol (**6R**)-4.26.

To a solution of **S4.6** (12 mg, 28 μmol , 1 equiv) in methanol (140 μL) was added a solution of hydrogen chloride in 1,4-dioxane (4M, 140 μL) at 23 $^{\circ}\text{C}$. After 25 min, LCMS analysis indicated that no starting material remained. Consequently, the mixture was diluted with toluene (1 mL), and the diluted solution was concentrated to dryness in vacuo. The residue was re-dissolved in methanol (2 mL), and Amberlyst A26 ion-exchange resin (hydroxide form, 500 mg) was added. The resulting suspension was stirred at 23 $^{\circ}\text{C}$ for 30 min before the ion-exchange beads were removed by filtration. The filtrate was concentrated to provide crude product in its free-base form; this material was purified by flash-column chromatography (4.0 g silica gel, eluting with 0.2% ammonium hydroxide–2% methanol–dichloromethane initially, grading to 2% ammonium hydroxide–20% methanol–dichloromethane) to provide the product as a sand-brown solid (3.9 mg, 43%).

$R_f = 0.30$ (3% ammonium hydroxide–30% methanol–dichloromethane, PAA).

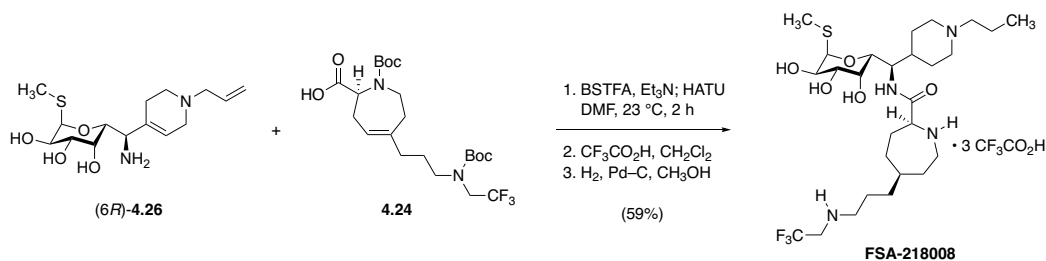
$^1\text{H NMR}$ (600 MHz, CD_3OD) δ 5.91 (ddt, $J = 17.0, 10.2, 6.7$ Hz, 1H), 5.79 (td, $J = 3.4, 1.5$ Hz, 1H), 5.31 (d, $J = 5.7$ Hz, 1H), 5.36 (app dq, $J = 17.1, 1.6$ Hz, 1H), 5.21 (ddt, $J = 10.2, 1.9, 1.0$ Hz, 1H), 4.10 (dd, $J = 10.1, 5.6$ Hz, 1H), 4.08 (dd, $J = 7.5, 1.2$ Hz, 1H), 3.87 (dd, 3.3, 1.2 Hz, 1H), 3.72 (d, $J = 7.5$ Hz, 1H), 3.55 (dd, $J = 10.1, 3.2$ Hz, 1H), 3.12 (dt, $J = 6.8, 1.3$ Hz, 1H), 3.07 (app dq, $J = 16.8, 2.8$ Hz, 1H), 3.00 (app dq, $J = 16.7, 2.9$ Hz, 1H), 2.70

(app dt, $J = 11.3, 5.5$ Hz, 1H), 2.60 (ddd, $J = 11.7, 7.0, 4.8$ Hz, 1H), 2.35 (br d, $J = 17.2$ Hz, 1H), 2.16 (dtt, $J = 17.2, 5.2, 2.4$ Hz, 1H), 2.10 (s, 3H).

^{13}C NMR (126 MHz, CD_3OD) δ 136.0, 135.2, 124.6, 119.4, 89.6, 72.6, 72.2, 71.4, 69.5, 62.0, 57.9, 53.2, 50.5, 26.5, 13.4.

IR (neat, cm^{-1}): 3369 (br), 2917 (m), 1095 (s), 1053 (s), 993 (m).

HRMS (ESI+, m/z): $[\text{M}+\text{H}]^+$ calc'd for $\text{C}_{15}\text{H}_{26}\text{N}_2\text{O}_4\text{S}$, 331.1686; found 331.1685.



Synthetic lincosamide FSA-218008.

In a 4-mL glass microwave vial fitted with a magnetic stir bar, diaminotriol **(6R)-4.26** (3.9 mg, 12 μ mol, 1 equiv) was dissolved in *N,N*-dimethylformamide (120 μ L). To this solution were then added triethylamine (7.4 μ L, 53 μ mol, 4.5 equiv) and *N,O*-bis(trimethylsilyl)trifluoroacetamide (4.8 μ L, 18 μ mol, 1.5 equiv) at 23 °C. After stirring 1 h to ensure complete *O*-silylation, a solution of azepine acid **4.24** (7.4 mg, 15 μ mol, 1.3 equiv) in *N,N*-dimethylformamide (100 μ L) was added by micropipette, followed by HATU (6.7 mg, 18 μ mol, 1.5 equiv). After 2 h, LCMS analysis demonstrated complete consumption of aminotriol starting material and its (oligo)trimethylsilylated congeners. The mixture was diluted with ethyl acetate (20 mL), and the diluted mixture was washed with 50% v/v saturated aqueous sodium bicarbonate solution–saturated aqueous sodium chloride solution (7 mL), then with saturated aqueous sodium chloride solution (7 mL). The washed organic solution was dried over sodium sulfate, filtered, and concentrated to provide crude, (oligo)trimethylsilylated coupling product

This material was dissolved in 33% v/v trifluoroacetic acid–dichloromethane (600 μ L), and the resulting solution was stirred at 23 °C for 30 min, until LCMS analysis indicated that global desilylation and *N*-Boc deprotection were complete. The mixture was diluted with toluene (1 mL) before it was concentrated to dryness in vacuo. Methanol (1 mL) was then added, followed by palladium on carbon (10% w/w, 25 mg). Hydrogen gas was bubbled through the resulting black suspension for 2 min before bubbling was discontinued; the mixture was then rapidly stirred (700

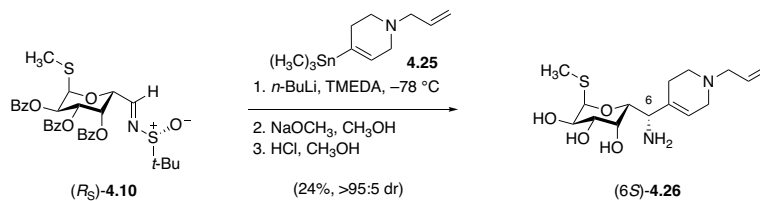
rpm) under 1 atm of hydrogen gas (supplied by a balloon) at 23 °C for 2 d. After this time, LCMS analysis indicated that hydrogenation was complete, and the mixture was filtered through a pad of Celite in order to remove the heterogeneous catalyst. The filter cake was rinsed with methanol (3 × 1 mL) and the filtrate was concentrated to provide a colorless film. This material was purified by preparative HPLC-MS on a Waters SunFire prep C₁₈ column (5 μL, 250 × 19 mm; eluting with 0.1% trifluoroacetic acid–5% acetonitrile–water initially, grading to 0.1% trifluoroacetic acid–30% acetonitrile–water over 40 min, with a flow rate of 15 mL/min; monitored by UV absorbance at 210 nm and ESI+ selected ion monitoring [*m/z* = 599]; R_t = 12.6 min) to provide **FSA-218008** • 3 CF₃CO₂H as a white solid (6.7 mg, 59%).

¹H NMR (600 MHz, CD₃OD) δ 5.24 (d, *J* = 5.6 Hz, 1H), 4.26 (t, *J* = 5.6 Hz, 1H), 4.18 (dd, *J* = 6.1, 1.4 Hz, 1H), 4.08–4.06 (m, 2H), 4.01 (q, *J* = 9.0 Hz, 1H), 3.88 (dd, *J* = 3.3, 1.3 Hz, 1H), 3.59–3.56 (m, 3H), 3.44 (ddd, *J* = 13.9, 5.8, 2.1 Hz, 1H), 3.15–3.11 (m, 3H), 3.02 (t, *J* = 8.3 Hz, 2H), 2.93 (td, *J* = 13.0, 2.9 Hz, 2H), 2.24–2.14 (m, 2H), 2.13 (s, 3H), 2.03–1.94 (m, 4H), 1.86 (td, *J* = 9.4, 4.4 Hz, 1H), 1.79–1.59 (m, 9H), 1.43 (dtd, *J* = 12.9, 8.9, 3.5 Hz, 1H), 1.39–1.35 (m, 2H), 1.01 (t, *J* = 7.4 Hz, 3H).

¹⁹F NMR (376 MHz, CD₃OD) δ –70.15 (t, *J* = 9.0 Hz, 3F), –77.19 (s, 9F).

IR (neat, cm⁻¹): 1671 (s), 1436 (w), 1201 (s), 1134 (s).

HRMS (ESI+, *m/z*): [M+H]⁺ calc'd for C₂₇H₄₉F₃N₄O₅S, 599.3449; found 599.3436.



Diaminotriol (6S)-4.26.

In a 25-mL round-bottomed flask fitted with a stir bar, vinyl stannane **4.25** (183 mg, 641 μmol , 4.00 equiv) was dissolved in tetrahydrofuran (3.00 mL). The resulting solution was chilled to $-78\text{ }^\circ\text{C}$ before *n*-butyllithium solution (2.40 M in hexanes, 267 μL , 641 μmol , 4.00 equiv) was added dropwise. The resulting mixture was stirred at $-78\text{ }^\circ\text{C}$ for 30 min before *N,N,N',N'*-tetramethylethylenediamine (242 μL , 1.60 mmol, 10.0 equiv) was added. After stirring the reaction mixture for an additional 30 min at $-78\text{ }^\circ\text{C}$, a solution of sulfinimine (*R_S*)-**4.10** (100 mg, 0.160 mmol, 1 equiv) in tetrahydrofuran (500 μL) was added dropwise by syringe. Within 5 min, TLC analysis (60% ethyl acetate–hexanes, UV+CAM) indicated that no sulfinimine starting material remained, and the mixture was neutralized with the addition of acetic acid (184 μL , 3.21 mmol, 20.0 equiv). The mixture was warmed to ambient temperature before it was transferred to a separatory funnel containing ethyl acetate (10 mL) and saturated aqueous sodium bicarbonate solution (20 mL). The layers were shaken, then separated; the aqueous layer was extracted with 10% v/v methanol–dichloromethane ($5 \times 10\text{ mL}$). The combined organic extracts were dried over sodium sulfate, filtered and concentrated to provide a crude mixture of (oligo)debenzoylated dehydropiperidine adducts.

This crude residue was dissolved in anhydrous methanol (2.91 mL), and the resulting solution was treated with methanolic sodium methoxide solution (0.5 M, 290 μL) at $23\text{ }^\circ\text{C}$. After 40 min of stirring, LCMS analysis indicated that debenzoylation was complete. The mixture was neutralized with the addition of acetic acid ($\sim 18\text{ } \mu\text{L}$) until $\text{pH} = 7$ was achieved. The mixture was

then concentrated to dryness to provide a mahogany-colored, solid residue. LCMS analysis of this crude residue revealed the presence of only a single diastereomeric product.

Finally, this material was transferred to a 4-mL glass vial fitted with a magnetic stir bar, where it was dissolved in methanol (480 μ L). A solution of hydrogen chloride in 1,4-dioxane (4M, 480 μ L) was added at 23 $^{\circ}$ C, and the resulting mixture was stirred at 23 $^{\circ}$ C for 30 min. After this time, LCMS analysis indicated that desulfinylation was complete, and the mixture was diluted with toluene (2 mL). The diluted mixture was concentrated in vacuo, the dried residue was re-dissolved in methanol (10 mL), and the crude product solution was treated with Amberlyst A26 ion-exchange resin (hydroxide form, 2.0 g). The suspension was stirred at 23 $^{\circ}$ C for 30 min before the ion-exchange beads were removed by filtration. The filtrate was concentrated to afford crude product in its free-base form, which was purified by flash column chromatography (4.0 g silica gel, eluting with 1% ammonium hydroxide–10% methanol–dichloromethane initially, grading to 10% ammonium hydroxide–40% methanol–dichloromethane) to provide the product as a white solid (13 mg, 24%, 3 steps).

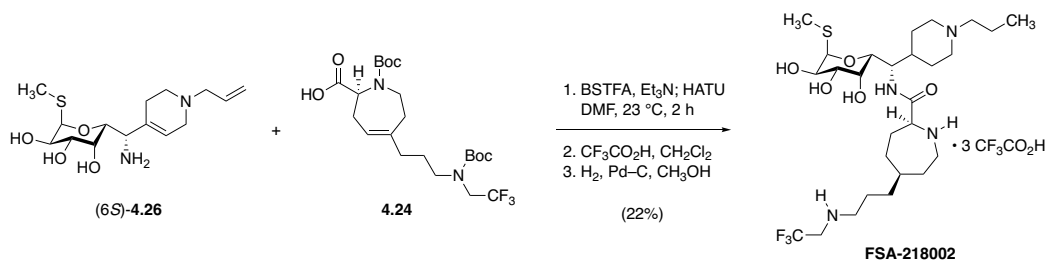
R_f = 0.41 (10% ammonium hydroxide–40% methanol–dichloromethane, PAA).

^1H NMR (600 MHz, CD_3OD) δ 5.90 (ddt, J = 16.9, 10.1, 6.7 Hz, 1H), 5.69 (t, J = 3.4 Hz, 1H), 5.25 (app dq, J = 17.2, 1.5 Hz, 1H), 5.22–5.19 (m, 2H), 4.09 (dd, J = 10.1, 5.6 Hz, 1H), 4.03 (d, J = 3.4 Hz, 1H), 4.01 (d, J = 8.5 Hz, 1H), 3.60 (d, J = 8.1 Hz, 1H), 3.56 (dd, J = 10.2, 3.3 Hz, 1H), 3.10 (dt, J = 6.7, 1.3 Hz, 1H), 3.05 (app dq, J = 16.6, 3.2 Hz, 1H), 2.98 (app dq, J = 16.4, 2.9 Hz, 1H), 2.70 (app dt, J = 11.2, 5.5 Hz, 1H), 2.56 (ddd, J = 11.6, 7.1, 4.9 Hz, 1H), 2.33–2.27 (m, 1H), 2.19–2.14 (m, 1H), 2.05 (s, 3H).

^{13}C NMR (126 MHz, CD_3OD) δ 138.1, 135.4, 122.4, 119.2, 89.6, 72.8, 72.3, 70.3, 69.7, 62.0, 57.1, 53.3, 50.7, 26.7, 13.5.

IR (neat, cm^{-1}): 3355 (br), 2916 (m), 1094 (s), 1081 (s), 1055 (s), 993 (m).

HRMS (ESI+, m/z): $[\text{M}+\text{H}]^+$ calc'd for $\text{C}_{15}\text{H}_{26}\text{N}_2\text{O}_4\text{S}$, 331.1686; found 331.1684.



Synthetic lincosamide FSA-218002.

In a 4-mL vial fitted with a silicone septum screw cap, diaminotriol (6*S*)-**4.26** (12.5 mg, 37.8 μmol , 1 equiv) was dissolved in *N,N*-dimethylformamide (189 μL). To this solution were then added triethylamine (23.7 μL , 170 μmol , 4.50 equiv) and *N,O*-bis(trimethylsilyl)trifluoroacetamide (15.2 μL , 56.8 μmol , 1.50 equiv) at 23 °C. The resulting solution was stirred for 1 h to ensure complete *O*-silylation. Next, a solution of azepane acid **4.24** (23.6 mg, 49.2 μmol , 1.30 equiv) in *N,N*-dimethylformamide (100 μL) was added by micropipette, followed by HATU (21.6 mg, 57.8 μmol , 1.50 equiv), which was added in one portion. Consumption of diaminotriol starting material and its (oligo)trimethylsilylated congeners was monitored by LCMS, and after 1.5 h, the reaction was judged to be complete. The reaction mixture was diluted with ethyl acetate (20 mL), and the diluted solution was washed first with 50% v/v saturated aqueous sodium bicarbonate solution–saturated aqueous sodium chloride solution (10 mL), followed by saturated sodium chloride solution (10 mL). The washed organic phase was then dried over sodium sulfate, filtered, and concentrated to give a light brown oil.

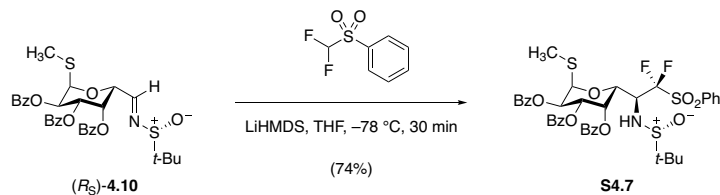
In an 8-mL glass vial, this crude residue was dissolved in 33% v/v trifluoroacetic acid–dichloromethane (3.0 mL), and the resulting solution was stirred at 23 °C for 30 min, at which point LCMS analysis indicated that global desilylation and Boc removal were complete. Toluene (5 mL) was added, and the diluted mixture was concentrated to dryness in vacuo. The dried residue was then re-dissolved in methanol (1.0 mL), and palladium on carbon (10% w/w, 50 mg) was

added. Hydrogen gas was bubbled through the resulting black suspension for 2 min before bubbling was discontinued; the reaction mixture was stirred rapidly (700 rpm) under 1 atm of hydrogen gas (supplied by a balloon) overnight. After this time, LCMS analysis indicated that hydrogenation was complete, and the mixture was filtered through a pad of Celite in order to remove the heterogeneous catalyst. The filter cake was rinsed with fresh portions of methanol (3 × 2 mL), and the filtrate was concentrated. The residue obtained was finally purified by preparative HPLC-MS on a Waters SunFire prep C₁₈ column (5 μm, 250 × 19 mm; eluting with 0.1% trifluoroacetic acid–0.5% acetonitrile–water initially; grading to 0.1% trifluoroacetic acid–30% acetonitrile–water over 40 min, with a flow rate of 15 mL/min; monitored by UV absorbance at 210 nm and ESI+ selected ion monitoring [*m/z* = 599]) to provide **FSA-218002 • 3 CF₃CO₂H** as a white solid (7.85 mg, 22%, 2 steps).

¹H NMR (600 MHz, CD₃OD) δ 5.26 (d, *J* = 5.8 Hz, 1H), 4.39 (dd, *J* = 10.2, 3.3 Hz, 1H), 4.13 (dd, *J* = 10.1, 1.2 Hz, 1H), 4.08 (dd, *J* = 10.3, 5.7 Hz, 1H), 4.04–3.99 (m, 3H), 3.80 (dd, *J* = 3.4, 1.1 Hz, 1H), 3.66 (br d, *J* = 12.5 Hz, 1H), 3.57 (br d, *J* = 12.1 Hz, 1H), 3.50 (dd, *J* = 10.3, 3.3 Hz, 1H), 3.45 (ddd, *J* = 14.0, 5.8, 2.4 Hz, 1H), 3.16–3.11 (m, 3H), 3.03–2.93 (m, 4H), 2.27–2.17 (m, 2H), 2.15–2.09 (m, 1H), 2.13 (s, 3H), 2.05–1.95 (m, 2H), 1.94–1.86 (m, 2H), 1.78–1.58 (m, 8H), 1.44 (app dtd, *J* = 12.9, 8.9, 3.8 Hz, 1H), 1.40–1.36 (m, 2H), 0.99 (t, *J* = 7.4 Hz, 1H).

¹⁹F {¹H} NMR (471 MHz, CD₃OD) δ –70.10 (3F), –77.14 (9F).

HRMS (ESI+, *m/z*): [M+2H]²⁺ calc'd for C₂₇H₄₉F₃N₄O₅S, 299.1682; found 299.1688.



Difluoro compound S4.7.

In a 0.5–2 mL conical glass microwave vial, sulfinimine (R_S)-4.10 (30.7 mg, 49.2 μmol , 1.05 equiv) and difluoromethyl phenyl sulfone (9.00 mg, 46.9 μmol , 1 equiv) were dissolved in tetrahydrofuran (234 μL). The resulting solution was chilled to $-78\text{ }^\circ\text{C}$ before a freshly prepared solution of lithium hexamethyldisilazide (1.00 M in tetrahydrofuran, 51.5 μL , 51.5 μmol , 1.10 equiv) was added, causing a vibrant yellow color to evolve. Consumption of sulfinimine starting material was monitored by TLC (40% ethyl acetate–hexanes, UV+PAA), and after 30 min, it appeared that the reaction had stalled, signaling completion. The mixture was neutralized with the dropwise addition of saturated aqueous ammonium chloride solution (1 mL). Ethyl acetate (3 mL) was then added, and the mixture was allowed to warm to $23\text{ }^\circ\text{C}$. The biphasic mixture was transferred to a separatory funnel containing saturated aqueous sodium chloride solution (5 mL) and ethyl acetate (10 mL); the layers were shaken, then separated. The aqueous layer was extracted with fresh portions of ethyl acetate ($2 \times 5\text{ mL}$), and the combined extracts were dried over sodium sulfate. The dried product solution was then filtered, and the filtrate was concentrated. The colorless residue obtained in this fashion was purified by flash-column chromatography (4 g silica gel, eluting with hexanes initially, grading to 50% ethyl acetate–hexanes) to provide the product as a brilliant white solid (28.4 mg, 74%).

$R_f = 0.40$ (60% ethyl acetate–hexanes, UV+PAA).

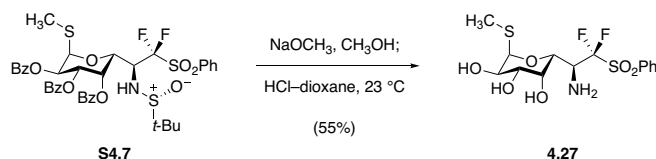
^1H NMR (600 MHz, CDCl_3) δ 8.12 (dd, $J = 8.3, 1.4$ Hz, 2H), 8.01 (d, $J = 7.6$ Hz, 2H), 7.97 (dd, $J = 8.2, 1.0$ Hz, 2H), 7.78–7.74 (m, 3H), 7.64–7.61 (m, 3H), 7.51–49 (m, 3H), 7.41 (tt, $J = 7.4, 1.3$ Hz, 1H), 7.37 (t, $J = 7.8$ Hz, 2H), 7.22 (t, $J = 7.8$ Hz, 1H), 6.37 (app s, 1H), 6.04 (d, $J = 5.3$ Hz, 1H), 5.88 (dd, $J = 10.7, 5.3$ Hz, 1H), 5.84 (dd, $J = 10.7, 3.0$ Hz, 1H), 5.44 (d, $J = 5.4$ Hz, 1H), 4.67 (app ddt, $J = 19.1, 9.5, 6.5$ Hz, 1H), 4.20 (d, $J = 6.9$ Hz, 1H), 2.22 (s, 3H), 1.02 (s, 9H).

^{13}C NMR (126 MHz, CDCl_3) δ 165.5, 165.2, 164.7, 135.8, 133.9, 133.6, 133.2, 132.7, 130.9, 130.1 ($2 \times \text{C}$), 129.8, 129.5, 129.2, 129.1, 129.0, 128.6, 128.3, 121.0 (t, $J = 122.2$ Hz), 84.8, 69.8 (app d, $J = 2.6$ Hz), 69.3, 68.4, 64.2 (app d, $J = 5.3$ Hz), 59.1 (t, $J = 19.3$ Hz), 57.4, 22.5, 13.2.

^{19}F NMR (376 MHz, CDCl_3) δ -99.54 (dd, $J = 241.3, 9.7$ Hz, 1F), -109.29 (dd, $J = 241.2, 19.1$ Hz, 1F).

IR (neat, cm^{-1}): 1728 (s), 1451 (m), 1279 (s), 1246 (s), 1090 (s), 1067 (s), 709 (s).

HRMS (ESI+, m/z): $[\text{M}+\text{H}]^+$ calc'd for $\text{C}_{39}\text{H}_{39}\text{F}_2\text{NO}_{10}\text{S}_3$, 816.1777; found 816.1761.



Aminotriol 4.27.

In a 2–5 mL glass microwave vial fitted with a magnetic stir bar, sulfinamide **S4.7** (28 mg, 34 μmol , 1 equiv) was dissolved in anhydrous methanol (620 μL). To this solution was then added a methanolic solution of sodium methoxide (0.5 M, 62 μL) at 23 $^\circ\text{C}$; after 30 min, LCMS analysis of the reaction mixture indicated that global debenzoylation was complete. A solution of hydrogen chloride in 1,4-dioxane (4M, 600 μL) was then added in order to acidify the mixture. After stirring for an additional 30 min, LCMS indicated that the *tert*-butanesulfonyl group had been cleaved as well. The mixture was diluted with toluene (1 mL) before it was concentrated to dryness in vacuo. Prior to purification, the crude residue containing aminotriol hydrochloride salt was converted to the corresponding free base by re-dissolving it in methanol (2 mL) and treating the resulting solution with Amberlyst A26 resin (hydroxide form, 300 mg). After stirring the mixture for 30 min at 23 $^\circ\text{C}$, the ion-exchange beads were removed by filtration, and the filtrate was concentrated. The residue was finally purified by flash-column chromatography (4 g silica gel, eluting with 0.1% ammonium hydroxide–1% methanol–dichloromethane initially, grading to 1% ammonium hydroxide–10% methanol–dichloromethane) to provide the product as a white solid (7.6 mg, 55%).

$R_f = 0.55$ (2% ammonium hydroxide–20% methanol–dichloromethane (UV+PAA)).

$^1\text{H NMR}$ (500 MHz, CD_3OD) δ 8.00 (d, $J = 8.0$ Hz, 2H), 7.84 (t, $J = 7.5$ Hz, 1H), 7.70 (t, $J = 7.6$ Hz, 2H), 5.23 (d, $J = 5.6$ Hz, 1H), 4.42 (d, $J = 8.2$ Hz, 1H), 4.17 (d, $J = 3.3$ Hz, 1H), 4.10

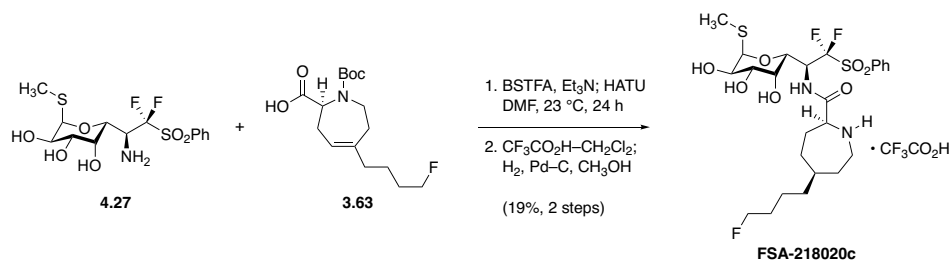
(dd, $J = 10.1, 5.6$ Hz, 1H), 3.98 (app dt, $J = 21.0, 7.6$ Hz, 1H), 3.58 (dd, $J = 10.2, 3.3$ Hz, 1H), 1.99 (s, 3H).

^{13}C NMR (126 MHz, CD_3OD) δ 136.6, 135.4, 131.7, 130.5, 89.5, 72.0, 70.4, 70.1, 69.5, 54.0 (t, $J = 17.6$ Hz), 13.0.

^{19}F NMR (471 MHz, CD_3OD) δ -102.25 (d, 233.5 Hz, 1F), -114.06 (dd, $J = 233.5, 4.4$ Hz, 1F).

IR (neat, cm^{-1}): 3372 (br), 1336 (s), 1162 (m), 1084 (s).

HRMS (ESI+, m/z): $[\text{M}+\text{H}]^+$ calc'd for $\text{C}_{14}\text{H}_{19}\text{F}_2\text{NO}_6\text{S}_2$, 400.0695; found 400.0697.



Synthetic lincosamide FSA-218020c.

In a 1-mL glass vial fitted with a magnetic stir bar, aminotriol **4.27** (7.0 mg, 18 μ mol, 1 equiv) was dissolved in *N,N*-dimethylformamide (180 μ L). Triethylamine (11 μ L, 79 mmol, 4.5 equiv) and *N,O*-bis(trimethylsilyl)trifluoroacetamide (7.1 μ L, 26 μ mol, 1.5 equiv) were then added sequentially, and the resulting solution was stirred at 23 °C for 1 h to ensure complete *O*-silylation. A solution of azepane acid **3.63** (7.2 mg, 23 μ mol, 1.3 equiv) in *N,N*-dimethylformamide (175 μ L) was introduced, followed by HATU (10 mg, 26 μ mol, 1.5 equiv), which was added in a single portion. Consumption of aminotriol starting material and its (oligo)trimethylsilylated congeners was monitored by LCMS – owing to the attenuated nucleophilicity of the β,β -difluoroamino group, coupling was observed to be sluggish. After 24 h of stirring at 23 °C, the reaction mixture was diluted with ethyl acetate (10 mL), and the diluted solution was washed sequentially with 5-mL portions of aqueous citric acid solution (10% w/v), saturated aqueous sodium bicarbonate solution, and saturated aqueous sodium chloride solution. The washed organic layer was then dried over sodium sulfate, filtered, and concentrated to give a colorless residue.

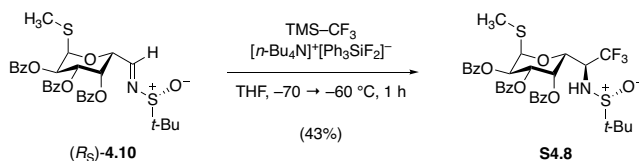
This residue was transferred to a 4-mL glass vial fitted with a magnetic stir bar, where it was dissolved in 33% v/v trifluoroacetic acid–dichloromethane (900 μ L). The resulting solution was stirred at 23 °C for 30 min, at which point LCMS analysis indicated that Boc removal was complete. The mixture was diluted with toluene (1.0 mL), and the diluted mixture was concentrated to dryness in vacuo. The dried residue was then re-dissolved in methanol (1.0 mL),

and palladium on carbon (10% w/w, 30 mg) was added. Hydrogen gas was bubbled through this mixture for 2 min before bubbling was discontinued; the mixture was then stirred under hydrogen gas (1 atm, supplied by a balloon) at 23 °C for 24 h, at which point LCMS analysis indicated that hydrogenation was complete. The mixture was filtered through a pad of Celite in order to remove the heterogeneous catalyst, and the filter cake was rinsed with fresh portions of methanol (3 × 1 mL). The filtrate was concentrated, and the crude residue was purified by preparative HPLC-MS on a Waters SunFire prep C₁₈ column (5 μm, 250 × 19 mm; eluting with 0.1% trifluoroacetic acid–15% acetonitrile–water initially, grading to 0.1% trifluoroacetic acid–70% acetonitrile–water over 40 min, with a flow rate of 15 mL/min; monitored by UV absorbance at 254 nm and by ESI+ selected ion monitoring [*m/z* = 599]; R_t = 26.1 min) to provide **FSA-218020c** • CF₃CO₂H as a white solid (2.4 mg, 19%, 2 steps).

¹H NMR (500 MHz, CD₃OD) δ 7.99 (d, *J* = 7.6 Hz, 2H), 7.88 (t, *J* = 7.5 Hz, 1H), 7.72 (t, *J* = 7.8 Hz, 2H), 5.36 (app dt, *J* = 18.6, 8.1 Hz, 1H), 5.24 (d, *J* = 5.7 Hz, 1H), 4.66 (d, *J* = 8.6 Hz, 1H), 4.41 (dt, *J* = 47.5, 6.0 Hz, 2H), 4.09 (d, *J* = 5.4 Hz, 1H), 4.07 (dd, *J* = 5.5, 3.5 Hz, 1H), 3.90 (d, *J* = 3.3 Hz, 1H), 3.56 (dd, *J* = 10.2, 3.3 Hz, 1H), 3.45 (ddd, *J* = 14.0, 5.7, 2.0 Hz, 1H), 3.15 (app t, *J* = 12.1 Hz, 1H), 2.34–2.21 (m, 2H), 2.04–2.00 (m, 1H), 2.00 (s, 3H), 1.94–1.88 (m, 1H), 1.72–1.57 (m, 4H), 1.50–1.41 (m, 3H), 1.37–1.33 (m, 1H).

IR (neat, cm⁻¹): 3356 (br), 1672 (s), 1449 (w), 1345 (w), 1203 (m), 1131 (m).

HRMS (ESI+, *m/z*): [M+H]⁺ calc'd for C₂₅H₃₇F₃N₂O₇S₂, 599.2067; found 599.2071.



Trifluoromethyl compound S4.8.

In a 0.5–2 mL conical glass microwave vial, sulfinimine (*R_S*)-**4.10** (32 mg, 51 μmol, 1 equiv) and tetra-*n*-butylammonium difluorotriphenylsilicate (TBAT, 9.5 mg, 56 μmol, 1.1 equiv) were suspended in tetrahydrofuran (510 μL; TBAT does not freely dissolve). The white suspension was chilled to $-70 \text{ }^\circ\text{C}$ before trifluoromethyltrimethylsilane (10 μL, 67 μmol, 1.3 equiv) was added. The suspension was allowed to warm to $-60 \text{ }^\circ\text{C}$ and stirring was maintained at that temperature until the mixture had clarified to form a peach-colored homogeneous solution (1 h), signaling that the reaction was complete. The mixture was neutralized with the addition of saturated aqueous ammonium chloride solution (1 mL), ethyl acetate (2 mL) was added, and the biphasic mixture was allowed to warm to $23 \text{ }^\circ\text{C}$. The mixture was then transferred to a separatory funnel containing additional saturated aqueous ammonium chloride solution (5 mL) and ethyl acetate (5 mL); the layers were shaken, then separated. The aqueous layer was extracted with fresh portions of ethyl acetate ($3 \times 2 \text{ mL}$), and the combined organic extracts were washed with saturated aqueous sodium chloride solution (5 mL). The washed solution was then dried over sodium sulfate, filtered, and concentrated to provide a colorless oil. ^1H - and ^{19}F -NMR analysis (CDCl_3) of this crude residue revealed a roughly 50:50 mixture of recovered sulfinimine starting material and a single diastereomeric β,β,β -trifluoro sulfonamide product. After flash-column chromatography (4 g silica gel, eluting with 20% diethyl ether–hexanes initially, grading to 80% diethyl ether–hexanes), pure product (15 mg, 43%) was obtained.

$R_f = 0.20$ (70% diethyl ether–hexanes, UV+PAA).

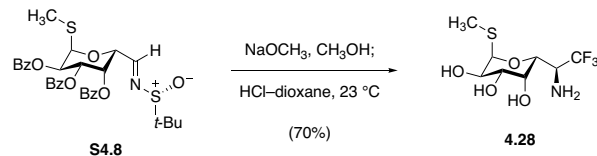
^1H NMR (500 MHz, CDCl_3) δ 8.08 (dd, $J = 8.4, 1.4$ Hz, 2H), 7.96 (dd, $J = 8.3, 1.4$ Hz, 2H), 7.75 (dd, $J = 8.5, 1.5$ Hz, 2H), 7.63 (tt, $J = 7.4, 1.4$ Hz, 1H), 7.53–7.48 (m, 3H), 7.43 (tt, $J = 7.4, 1.3$ Hz, 1H), 7.38 (t, $J = 7.8$ Hz, 2H), 7.24 (t, $J = 7.9$ Hz, 2H), 6.13 (dd, $J = 3.3, 1.1$ Hz, 1H), 5.98 (d, $J = 5.7$ Hz, 1H), 5.84 (dd, $J = 10.8, 5.7$ Hz, 1H), 5.76 (dd, $J = 10.8, 3.2$ Hz, 1H), 5.05 (dd, $J = 7.0, 1.2$ Hz, 1H), 4.14 (app dp, $J = 14.5, 7.2$ Hz, 1H), 3.97 (d, $J = 6.5$ Hz, 1H), 2.18 (s, 3H), 1.10 (s, 9H).

^{13}C NMR (126 MHz, CDCl_3) δ 165.6, 165.5, 164.6, 133.9, 133.7, 133.3, 130.1 (2 \times C), 129.9, 129.1 (2 \times C), 129.0, 128.9, 128.6, 128.3, 85.1, 69.3, 68.7, 68.3, 65.7, 58.9 (q, $J = 30.1$ Hz), 57.3, 22.4, 13.3. The trifluoromethyl carbon signal was not resolved due to coupling to adjacent ^{19}F nuclei.

^{19}F $\{^1\text{H}\}$ NMR (471 MHz, CDCl_3) δ -71.58 (s, 3F).

IR (neat, cm^{-1}): 1727 (s), 1258 (s), 1089 (s), 1067 (s), 1025 (m), 907 (m), 704.

HRMS (ESI+, m/z): $[\text{M}+\text{H}]^+$ calc'd for $\text{C}_{33}\text{H}_{34}\text{F}_3\text{NO}_8\text{S}_2$, 694.1751; found 694.1752.



Aminotriol 4.28.

In a 4-mL glass vial fitted with a stir bar, sulfinamide **S4.8** (15 mg, 22 μ mol, 1 equiv) was dissolved in anhydrous methanol (390 μ L). To this solution was then added methanolic sodium methoxide solution (0.5 M, 39 μ L) at 23 $^{\circ}$ C; after 30 min of stirring, LCMS analysis indicated that global debenzoylation was complete. The mixture was consequently treated with a solution of hydrogen chloride in 1,4-dioxane (4 M, 400 μ L), and after 30 additional minutes, LCMS analysis showed that cleavage of the *tert*-butanesulfinyl group was complete. Toluene (1 mL) was added, and the diluted mixture was concentrated to dryness in vacuo. The residue was then re-dissolved in methanol (2 mL), and Amberlyst A26 resin (hydroxide form, 100 mg) was added with stirring. After 30 min, the ion-exchange beads were removed by filtration, and the filtrate was concentrated to provide crude product in free-base form. This residue was subjected to flash-column chromatography (4 g silica gel, eluting with 0.4% ammonium hydroxide–4% methanol–dichloromethane initially, grading to 2% ammonium hydroxide–20% methanol–dichloromethane) to provide the product as a white solid (4.2 mg, 70%).

$R_f = 0.27$ (2% ammonium hydroxide–20% methanol–dichloromethane, PAA).

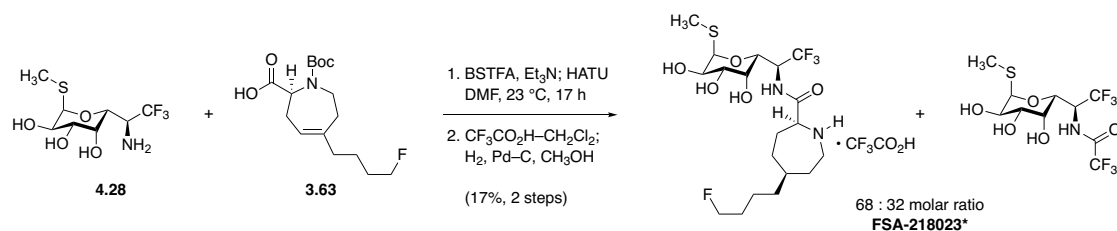
$^1\text{H NMR}$ (500 MHz, CD_3OD) δ 5.27 (d, $J = 5.7$ Hz, 1H), 4.26 (dd, $J = 9.1, 1.3$ Hz, 1H), 4.12 (dd, $J = 3.4, 1.3$ Hz, 1H), 4.10 (dd, $J = 10.2, 5.7$ Hz, 1H), 3.60 (dd, $J = 10.2, 3.3$ Hz, 1H), 3.55 (dq, $J = 9.1, 8.7$ Hz, 1H), 2.06 (s, 3H).

^{13}C NMR (126 MHz, CD_3OD) δ 89.4, 72.0, 70.3, 70.0, 69.5, 54.6 (q, $J = 28.1$ Hz), 12.7. The trifluoromethyl carbon signal was not resolved due to coupling to adjacent ^{19}F nuclei.

$^{19}\text{F}\{^1\text{H}\}$ NMR (471 MHz, CD_3OD) δ -75.01 (s, 3F).

IR (neat, cm^{-1}): 3360 (br), 2924 (w), 1262 (m), 1164 (s), 1119 (s), 1108 (s), 1058 (s), 983 (w).

HRMS (ESI+, m/z): $[\text{M}+\text{H}]^+$ calc'd for $\text{C}_8\text{H}_{14}\text{F}_3\text{NO}_4\text{S}$, 278.0668; found 278.0669.



Synthetic lincosamide FSA-218023.

In a 1-mL glass vial fitted with a magnetic stir bar, aminotriol **4.28** (4.2 mg, 15 μ mol, 1 equiv) was dissolved in *N,N*-dimethylformamide (150 μ L). To this solution were then added triethylamine (9.5 μ L, 68 μ mol, 4.5 equiv) and *N,O*-bis(trimethylsilyl)trifluoroacetamide (6.1 μ L, 23 μ mol, 1.5 equiv) at 23 °C. The resulting solution was stirred for 1 h to ensure complete *O*-silylation. A solution of azepane acid **3.63** (6.2 mg, 20 μ mol, 1.3 equiv) in *N,N*-dimethylformamide (50 μ L) was then added by micropipette, followed by HATU (8.6 mg, 23 μ mol, 1.5 equiv), which was added in a single portion. Consumption of aminotriol starting material and its (oligo)trimethylsilylated congeners was monitored by LCMS, and, owing to the low nucleophilicity of the β,β,β -trifluoro-substituted amino group, conversion was slow. After stirring for 17 h at 23 °C, the mixture was diluted with ethyl acetate (20 mL), and the diluted solution was washed sequentially with 5-mL portions of aqueous citric acid solution (10% w/v), water, saturated aqueous sodium bicarbonate solution, and saturated aqueous sodium chloride solution. The washed organic layer was then dried over sodium sulfate, filtered, and concentrated to give crude, (oligo)trimethylsilylated coupling product as a light-yellow oil.

This residue was transferred to a 2–5 mL glass microwave vial. A magnetic stir bar was added to the vial, and the residue was dissolved in 33% v/v trifluoroacetic acid–dichloromethane (600 μ L). The mixture was stirred at 23 °C for 30 min, at which point LCMS analysis indicated that global desilylation and Boc removal were complete. The mixture was diluted with toluene (1

mL), and the diluted solution was concentrated to dryness in vacuo. The dried residue was then re-dissolved in methanol (1.0 mL), and palladium on carbon (10% w/w, 25 mg) was added. Hydrogen gas was bubbled through this black reaction suspension for 2 min before bubbling was discontinued; the mixture was then stirred rapidly (700 rpm) under 1 atm of hydrogen gas (supplied by a balloon). After 24 h, LCMS analysis indicated that hydrogenation was complete, and the mixture was filtered through a pad of Celite in order to remove the heterogeneous catalyst. The filter cake was rinsed with fresh methanol (3×1 mL), and the filtrate was concentrated. The crude residue was finally subjected to preparative HPLC-MS on a Waters SunFire prep C₁₈ column (5 μ m, 250 \times 19 mm; eluting with 0.1% trifluoroacetic acid–10% acetonitrile–water initially, grading to 0.1% trifluoroacetic acid–60% acetonitrile–water over 40 min, with a flow rate of 15 mL/min; monitored by UV absorbance at 210 nm and ESI+ selected ion monitoring [$m/z = 477$]; $R_t = 23.3$ min) to provide **FSA-218023** as a mixture of the desired lincosamide hydrotrifluoroacetate salt and undesired *N*-trifluoroacetyl aminosugar by-product in a 68:32 molar ratio (77:23 weight ratio). The mass of this mixture was 2.0 mg, corresponding to 17% overall yield.

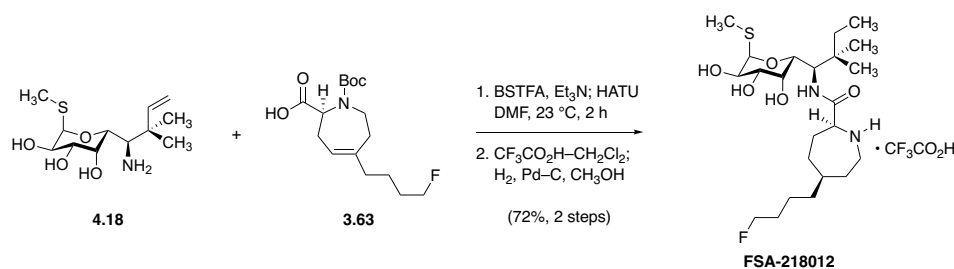
Desired lincosamide hydrotrifluoroacetate salt:

¹H NMR (500 MHz, CD₃OD) δ 5.31 (d, $J = 5.7$ Hz, 1H), 5.01–4.93 (m, 1H), 4.53 (dd, $J = 9.8, 1.4$ Hz, 1H), 4.42 (dt, $J = 47.5, 6.0$ Hz, 2H), 4.10 (dd, $J = 10.2, 5.7$ Hz, 1H), 4.06 (dd, $J = 7.0, 4.4$ Hz, 1H), 3.84 (d, $J = 3.3$ Hz, 1H), 3.58 (dd, $J = 10.2, 3.3$ Hz, 1H), 3.45 (ddd, $J = 13.5, 5.6, 1.9$ Hz, 1H), 3.13 (app t, $J = 12.5$ Hz, 1H), 2.21–2.11 (m, 2H), 2.07 (s, 3H), 2.01 (br dd, $J = 13.9, 5.7$ Hz, 1H), 1.95–1.90 (m, 1H), 1.72–1.53 (m, 4H), 1.47–1.31 (m, 5H).

¹⁹F NMR (471 MHz, CD₃OD) δ –72.99 (s, 1F), –77.16 (s, 3F).

FTIR (neat, cm⁻¹): 3337 (br), 1672 (s), 1188 (s), 1142 (s).

HRMS (ESI+, m/z): $[M+H]^+$ calc'd for $C_{19}H_{32}F_4N_2O_5S$, 278.0668; found 278.0669.



Synthetic lincosamide FSA-218012.

In a 1-mL glass vial fitted with a magnetic stir bar, aminotriol **4.18** (10.5 mg, 37.9 μmol , 1 equiv) was dissolved in *N,N*-dimethylformamide (189 μL). Triethylamine (23.7 μL , 170 mmol, 4.50 equiv) and *N,O*-bis(trimethylsilyl)trifluoroacetamide (15.2 μL , 56.9 μmol , 1.50 equiv) were then added sequentially, and the resulting solution was stirred at 23 $^\circ\text{C}$ for 1 h to ensure complete *O*-silylation. A solution of azepane acid **3.63** (15.5 mg, 49.3 μmol , 1.30 equiv) in *N,N*-dimethylformamide (150 μL) was introduced, followed by HATU (21.6 mg, 56.8 μmol , 1.50 equiv), which was added in a single portion. Upon addition of HATU, the reaction mixture attained a vibrant tennis ball yellow color. After 2 h of stirring at 23 $^\circ\text{C}$, LCMS analysis of the reaction mixture showed that aminotriol starting material and its (oligo)trimethylsilylated congeners were fully consumed; the reaction mixture was consequently diluted with ethyl acetate (12 mL), and the diluted solution was washed sequentially with 7-mL portions of aqueous citric acid solution (10% w/v), saturated aqueous sodium bicarbonate solution, and saturated aqueous sodium chloride solution. The washed organic layer was then dried over sodium sulfate, filtered, and concentrated to give a light rose-colored residue.

This residue was transferred to a 4-mL glass vial fitted with a magnetic stir bar, where it was dissolved in 33% v/v trifluoroacetic acid–dichloromethane (600 μL). The resulting solution was stirred at 23 $^\circ\text{C}$ for 30 min, at which point LCMS analysis indicated that Boc removal was complete. The mixture was diluted with toluene (1.0 mL), and the diluted mixture was

concentrated to dryness in vacuo. The dried residue was then re-dissolved in methanol (1.0 mL), and palladium on carbon (10% w/w, 30 mg) was added. Hydrogen gas was bubbled through this mixture for 2 min before bubbling was discontinued; the mixture was then stirred under hydrogen gas (1 atm, supplied by a balloon) at 23 °C for 18 h, at which point LCMS analysis indicated that hydrogenation was complete. The mixture was filtered through a pad of Celite in order to remove the heterogeneous catalyst, and the filter cake was rinsed with fresh portions of methanol (3 × 1 mL). The filtrate was concentrated, and the crude residue was purified by preparative HPLC-MS on a Waters SunFire prep C₁₈ column (5 μm, 250 × 19 mm; eluting with 0.1% trifluoroacetic acid–10% acetonitrile–water initially, grading to 0.1% trifluoroacetic acid–50% acetonitrile–water over 40 min, with a flow rate of 15 mL/min; monitored by UV absorbance at 210 nm and by ESI+ selected ion monitoring [*m/z* = 479]; R_t = 30.0 min) to provide **FSA-218012** • CF₃CO₂H as a white solid (16.1 mg, 72%, 2 steps).

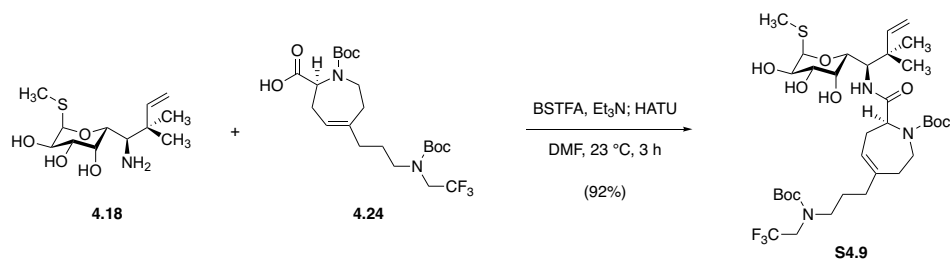
¹H NMR (600 MHz, CD₃OD) δ 5.22 (d, *J* = 5.7 Hz, 1H), 4.42 (dt, *J* = 47.5, 6.0 Hz, 2H), 4.23 (d, *J* = 8.9 Hz, 1H), 4.20 (d, *J* = 8.8 Hz, 1H), 4.09 (dd, *J* = 6.8, 4.5 Hz, 1H), 4.05 (dd, *J* = 10.4, 5.7 Hz, 1H), 3.88 (d, *J* = 3.3 Hz, 1H), 3.48–3.43 (m, 2H), 3.14 (app t, *J* = 12.1 Hz, 1H), 2.25–2.19 (m, 1H), 2.19 (s, 3H), 2.15–2.09 (m, 1H), 2.05–2.00 (m, 1H), 1.94–1.88 (m, 1H), 1.72–1.56 (m, 4H), 1.50–1.32 (m, 7H), 1.01 (s, 3H), 0.97 (s, 3H), 0.88 (t, *J* = 7.4 Hz, 3H).

¹³C NMR (126 MHz, CD₃OD) δ 170.8, 91.4, 84.7 (d, *J* = 163.8 Hz), 72.2, 71.8, 71.4, 69.4, 60.6, 56.1, 45.7, 38.8, 38.3, 37.4, 33.8, 33.2, 31.6 (d, *J* = 19.7 Hz), 30.6, 28.9, 24.8, 24.6, 23.8 (d, *J* = 5.1 Hz), 15.3, 8.5.

¹⁹F NMR (471 MHz, CD₃OD) δ –77.15 (s, 3F), –220.28 (tt, *J* = 14.4, 5.8 Hz, 1F).

IR (neat, cm⁻¹): 3368 (br), 2937 (w), 1659 (s), 1473 (m), 1202 (s), 1137 (s).

HRMS (ESI+, m/z): $[M+H]^+$ calc'd for $C_{23}H_{43}FN_2O_5S$, 479.2949; found 479.2962.



Protected lincosamide S4.9.

In a 4-mL glass vial, aminotriol **4.18** (37.9 mg, 137 μ mol, 1 equiv) was dissolved in *N,N*-dimethylformamide (683 μ L). Triethylamine (86.0 μ L, 615 μ mol, 4.50 equiv) and *N,O*-bis(trimethylsilyl)trifluoroacetamide (55.0 μ L, 205 μ mol, 1.50 equiv) were then added sequentially at 23 °C, and the colorless solution was stirred for 1 h to ensure complete *O*-silylation. Next, a solution of azepane acid **4.24** (85.0 mg, 178 μ mol, 1.30 equiv) in *N,N*-dimethylformamide (500 μ L) was added by micropipette, followed by HATU (77.9 mg, 205 μ mol, 1.50 equiv), which was added in a single portion. Following HATU addition, the reaction mixture attained a vibrant tennis ball yellow color. After 3 h, LCMS analysis showed complete consumption of aminotriol starting material and its (oligo)trimethylsilylated congeners; the mixture was consequently diluted with ethyl acetate (30 mL), and the diluted solution washed sequentially with 10-mL portions of aqueous citric acid solution (10% w/v), saturated aqueous sodium bicarbonate solution, and saturated aqueous sodium chloride solution. The organic layer was then dried over sodium sulfate, filtered, and concentrated to give a colorless residue. In order to desilylate the coupled product, this residue was then re-dissolved in 50% v/v acetic acid–methanol (4.0 mL) and the resulting solution was heated to 40 °C overnight. The mixture was then diluted with toluene (5.0 mL), and the diluted mixture was concentrated to dryness. Residual acetic acid was removed by repeated concentration from 50% v/v ethanol–toluene. The crude, desilylated product was purified by flash-

column chromatography (12 g silica gel, eluting with dichloromethane initially, grading to 5% methanol–dichloromethane) to furnish product as a white solid (91.8 mg, 91%).

$R_f = 0.55$ (10% methanol–dichloromethane, PAA).

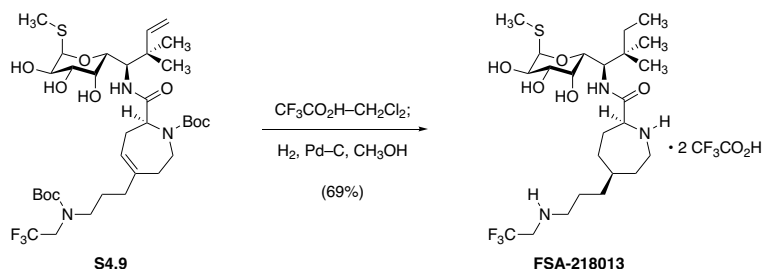
^1H NMR (55:45 rotameric mixture, asterisk [*] denotes minor rotameric signals that could be resolved, 600 MHz, CD_3OD) δ 6.04 (dd, $J = 17.5, 10.7$ Hz, 1H),* 5.99 (dd, $J = 17.5, 10.8$ Hz, 1H),* 5.51–5.49 (m, 1H), 5.21 (d, $J = 5.6$ Hz, 1H), 5.19 (d, $J = 5.6$ Hz, 1H),* 5.09–4.98 (m, 2H), 4.49–4.47 (m, 1H), 4.21 (m, 1H), 4.49–4.47 (m, 1H), 4.21–4.19 (m, 1H), 4.08–4.03 (m, 1H), 3.93 (q, $J = 9.0$ Hz, 2F), 3.88–3.83 (m, 1H), 3.71–3.65 (m, 1H), 3.51–3.47 (m, 1H), 3.29–3.22 (m, 2H), 2.73–2.68 (m, 1H), 2.53–2.33 (m, 3H), 2.12 (s, 3H), 2.08 (s, 3H),* 1.95–1.93 (m, 2H), 1.71–1.64 (m, 2H), 1.48 (s, 18H), 1.46 (s, 18H),* 1.14 (s, 3H),* 1.12 (s, 3H), 1.10 (s, 3H),* 1.07 (s, 3H).

^{13}C NMR (55:45 rotameric mixture, asterisk [*] denotes minor rotameric signals that could be resolved, 126 MHz, CD_3OD) δ 175.3,* 174.9, 157.6,* 157.1, 146.2, 145.7,* 142.2, 142.1,* 120.3, 120.1,* 112.6,* 112.2, 90.3, 89.7,* 82.1, 81.7,* 71.9, 71.8,* 71.5,* 71.3, 70.8, 69.7,* 69.4, 69.4,* 63.7,* 62.9, 60.1,* 58.6, 41.8, 41.7, 41.7,* 41.2 (br), 37.1 (br), 35.3 (br), 34.5, 28.9,* 28.7, 28.7,* 28.6,* 28.4, 28.3, 27.8 (br), 27.0 (br), 26.0, 25.8,* 25.5,* 25.5.

$^{19}\text{F}\{^1\text{H}\}$ NMR (471 MHz, CD_3OD) δ –72.20 (s, 3F).

IR (neat, cm^{-1}): 3401 (br), 2974 (w), 1702 (s), 1410 (s), 1151 (s), 1096 (m).

HRMS (ESI+, m/z): $[\text{M}+\text{H}]^+$ calc'd for $\text{C}_{34}\text{H}_{56}\text{F}_3\text{N}_3\text{O}_9\text{S}$, 740.3762; found 740.3757.



Synthetic lincosamide FSA-218013.

In a 4-mL glass vial fitted with a stir bar, azepine **S4.9** (9.5 mg, 13 μmol , 1 equiv) was dissolved in 33% v/v trifluoroacetic acid–dichloromethane (900 μL). The resulting solution was stirred at 23 $^{\circ}\text{C}$ for 30 min, whereupon LCMS analysis showed that global Boc deprotection was complete. Toluene (1.0 mL) was added, and the mixture was concentrated to dryness in vacuo. The dried residue was then re-dissolved in methanol (700 μL), and palladium on carbon (10% w/w, 25 mg) was added. Hydrogen gas was bubbled through the mixture for 2 min, then bubbling was discontinued, and the reaction mixture was stirred rapidly (600 rpm) under an atmosphere of hydrogen gas (supplied by a balloon) at 23 $^{\circ}\text{C}$. After 2 h, LCMS analysis indicated that hydrogenation was complete, and the mixture was filtered through a pad of Celite in order to remove the heterogeneous catalyst. The filter cake was rinsed with fresh methanol (3×1 mL), and the filtrate was concentrated. This crude residue was purified by preparative HPLC-MS on a Waters SunFire Prep C₁₈ column (5 μm , 250 \times 19 mm; eluting with 0.1% trifluoroacetic acid–5% acetonitrile–water initially, grading to 0.1% trifluoroacetic acid–40% acetonitrile–water over 40 min, with a flow rate of 15 mL/min; monitored by UV absorbance at 210 nm and by ESI+ selected ion monitoring [$m/z = 544$]) to afford **FSA-218013** • 2 CF₃CO₂H as a white solid (6.8 mg, 69%).

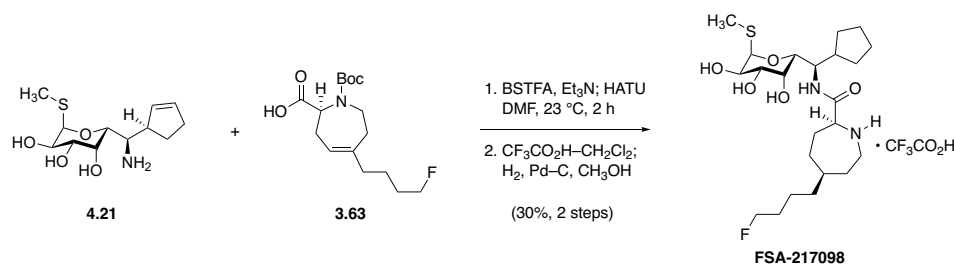
¹H NMR (500 MHz, CD₃OD) δ 5.21 (d, $J = 5.7$ Hz, 1H), 4.24 (d, $J = 9.0$ Hz, 1H), 4.21 (d, $J = 8.8$ Hz, 1H), 4.10 (br s, 1), 4.07–3.99 (m, 3H), 3.86 (app s, 1H), 3.48–3.43 (m, 2H), 3.19–3.11

(m, 3H), 2.26–2.10 (m, 2H), 2.18 (s, 3H), 2.05 (br d, $J = 14.7$ Hz, 1H), 1.95–1.91 (m, 1H), 1.79–1.73 (m, 2H), 1.70–1.56 (m, 2H), 1.52–1.35 (m, 5H), 1.01 (s, 3H), 0.97 (s, 3H), 0.88 (t, $J = 7.4$ Hz, 3H).

$^{19}\text{F}\{^1\text{H}\}$ NMR (471 MHz, CD_3OD) δ -70.12 (s, 3F), -77.16 (s, 6F).

IR (neat, cm^{-1}): 3370 (br), 1671 (s), 1201 (s), 1184 (s), 1137 (s).

HRMS (ESI+, m/z): $[\text{M}+\text{H}]^+$ calc'd for $\text{C}_{24}\text{H}_{44}\text{F}_3\text{N}_3\text{O}_5\text{S}$, 544.3027; found 544.3018.



Synthetic lincosamide FSA-217098.

In a 1-mL glass vial fitted with a magnetic stir bar, aminotriol **4.21** (5.0 mg, 18 μmol, 1 equiv) was dissolved in *N,N*-dimethylformamide (180 μL). To this solution were then added triethylamine (11 μL, 82 μmol, 4.5 equiv) and *N,O*-bis(trimethylsilyl)trifluoroacetamide (7.3 μL, 27 μmol, 1.5 equiv) sequentially at 23 °C. The mixture was stirred at ambient temperature for 1 h to ensure complete *O*-silylation before a solution of azepane acid **3.63** (7.4 mg, 24 μmol, 1.3 equiv) in *N,N*-dimethylformamide (200 μL) was added. Finally, HATU (10 mg, 27 μmol, 1.5 equiv) was added in one portion at 23 °C, causing the reaction mixture to attain a tennis ball yellow color. After 2 h, LCMS analysis of the reaction mixture demonstrated that aminotriol starting material and its (oligo)trimethylsilylated congeners were fully consumed. The mixture was diluted with ethyl acetate (15 mL), and the diluted mixture was washed sequentially with 5-mL portions of aqueous citric acid solution (10% w/v), saturated aqueous sodium chloride solution, and saturated aqueous sodium chloride solution. The organic solution was then dried over sodium sulfate, filtered, and concentrated to give a colorless residue.

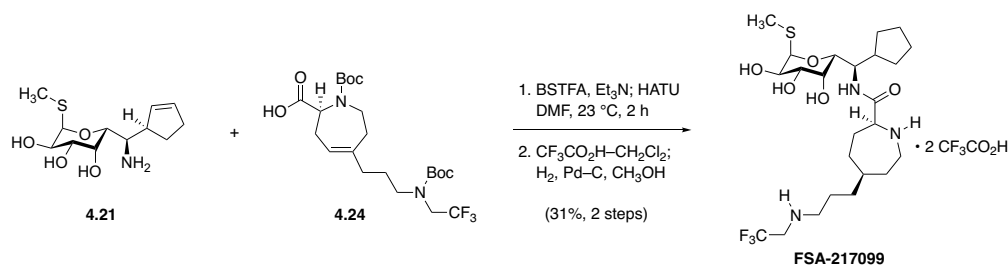
This crude residue was re-dissolved in 33% v/v trifluoroacetic acid–dichloromethane (600 mL), and after 30 min of stirring at 23 °C, LCMS analysis indicated that global Boc deprotection was complete. The mixture was diluted with toluene (1 mL), and the diluted mixture was concentrated to dryness. The residue was then re-dissolved in methanol (300 μL), and to this solution was added palladium on carbon (10% w/w, 20 mg). Hydrogen gas was bubbled through

this black suspension for 2 min before bubbling was discontinued, and the mixture was stirred rapidly (700 rpm) under 1 atm of hydrogen gas (supplied by a balloon). After 1 d, LCMS indicated that hydrogenation was incomplete; additional palladium on carbon (10% w/w, 20 mg) was added. The reaction mixture was stirred for 1 d further under an atmosphere of hydrogen gas before LCMS indicated that hydrogenation was complete. The mixture was filtered through a pad of Celite in order to remove the heterogeneous catalyst, and the filter cake was rinsed with fresh portions of methanol (3×1 mL). The filtrate was concentrated, and the residue was purified by preparative HPLC-MS on a Waters SunFire prep C₁₈ column (5 μ m, 250 \times 19 mm; eluting with 0.1% trifluoroacetic acid–water initially, grading to 0.1% trifluoroacetic acid–40% acetonitrile–water over 40 min, with a flow rate of 15 mL/min; monitored by UV absorbance at 210 nm and ESI+ selected ion monitoring [$m/z = 477$]; $R_t = 39.2$ min) to provide **FSA-217098** • CF₃CO₂H as a white solid (3.2 mg, 30%, 2 steps).

¹H NMR (500 MHz, CD₃OD) δ 5.26 (d, $J = 5.7$ Hz, 1H), 4.42 (dt, $J = 47.6, 6.0$ Hz, 2H), 4.28 (dd, $J = 8.8, 5.8$ Hz, 1H), 4.09–4.06 (m, 3H), 3.88 (d, $J = 3.4$ Hz, 1H), 3.54 (dd, $J = 10.2, 3.3$ Hz, 1H), 3.44 (ddd, $J = 13.9, 6.0, 2.2$ Hz, 1H), 3.13 (app t, $J = 12.3$ Hz, 1H), 2.34–2.26 (m, 1H), 2.23–2.12 (m, 2H), 2.10 (s, 3H), 2.04–2.00 (m, 1H), 1.95–1.89 (m, 1H), 1.79–1.54 (m, 10H), 1.47–1.29 (m, 6H), 1.29–1.21 (m, 1H).

¹⁹F NMR (471 MHz, CD₃OD) δ –77.06 (s, 3F), –220.35 (tt, $J = 14.3, 5.6$ Hz, 1F).

HRMS (ESI+, m/z): [$M+H$]⁺ calc'd for C₂₃H₄₁FN₂O₅S, 477.2793; found 477.2791.



Synthetic lincosamide FSA-217099.

In a 1-mL glass vial fitted with a magnetic stir bar, aminotriol **4.21** (5.0 mg, 18 μ mol, 1 equiv) was dissolved in *N,N*-dimethylformamide (180 μ L). To this solution were then added triethylamine (11 μ L, 82 μ mol, 4.5 equiv) and *N,O*-bis(trimethylsilyl)trifluoroacetamide (7.3 μ L, 27 μ mol, 1.5 equiv) sequentially at 23 °C. The mixture was stirred at ambient temperature for 1 h to ensure complete *O*-silylation before a solution of azepane acid **4.24** (11 mg, 24 μ mol, 1.3 equiv) in *N,N*-dimethylformamide (200 μ L) was added. Finally, HATU (10 mg, 27 μ mol, 1.5 equiv) was added in one portion at 23 °C, causing the reaction mixture to attain a tennis ball yellow color. After 2 h, LCMS analysis of the reaction mixture demonstrated that aminotriol starting material and its (oligo)trimethylsilylated congeners were fully consumed. The mixture was diluted with ethyl acetate (15 mL), and the diluted mixture was washed sequentially with 5-mL portions of aqueous citric acid solution (10% w/v), saturated aqueous sodium chloride solution, and saturated aqueous sodium chloride solution. The organic solution was then dried over sodium sulfate, filtered, and concentrated to give a colorless residue.

This crude residue was re-dissolved in 33% v/v trifluoroacetic acid–dichloromethane (600 mL), and after 30 min of stirring at 23 °C, LCMS analysis indicated that global Boc deprotection was complete. The mixture was diluted with toluene (1 mL), and the diluted mixture was concentrated to dryness. The residue was then re-dissolved in methanol (300 μ L), and to this solution was added palladium on carbon (10% w/w, 20 mg). Hydrogen gas was bubbled through

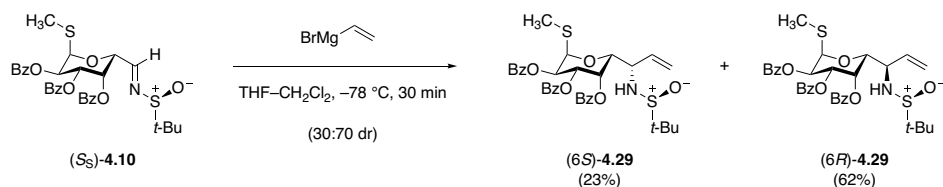
this black suspension for 2 min before bubbling was discontinued, and the mixture was stirred rapidly (700 rpm) under 1 atm of hydrogen gas (supplied by a balloon). After 1 d, LCMS indicated that hydrogenation complete. The mixture was filtered through a pad of Celite in order to remove the heterogeneous catalyst, and the filter cake was rinsed with fresh portions of methanol (3×1 mL). The filtrate was concentrated, and the residue was purified by preparative HPLC-MS on a Waters SunFire prep C₁₈ column (5 μ m, 250 \times 19 mm; eluting with 0.1% trifluoroacetic acid–2.5% acetonitrile–water initially, grading to 0.1% trifluoroacetic acid–50% acetonitrile–water over 40 min, with a flow rate of 15 mL/min; monitored by UV absorbance at 210 nm and ESI+ selected ion monitoring [$m/z = 271.5$]; $R_t = 25.3$ min) to provide **FSA-217099** • 2 CF₃CO₂H as a white solid (4.4 mg, 31%, 2 steps).

¹H NMR (500 MHz, CD₃OD) δ 5.25 (d, $J = 5.6$ Hz, 1H), 4.28 (dd, $J = 8.8, 5.7$ Hz, 1H), 4.11–4.05 (m, 3H), 4.01 (q, $J = 9.0$ Hz, 2H), 3.88 (dd, $J = 3.5, 1.1$ Hz, 1H), 3.54 (dd, $J = 10.2, 3.3$ Hz, 1H), 3.45 (ddd, $J = 13.8, 5.9, 2.1$ Hz, 1H), 3.19–3.11 (m, 3H), 2.34–2.27 (m, 1H), 2.23–2.12 (m, 2H), 2.10 (s, 3H), 2.06–2.01 (m, 1H), 1.95–1.89 (m, 1H), 1.79–1.53 (m, 10H), 1.43–1.32 (m, 4H), 1.28–1.20 (m, 1H).

¹⁹F {¹H} NMR (471 MHz, CD₃OD) δ –70.13 (3F), –77.18 (6F).

IR (neat, cm⁻¹): 3373 (br), 1669 (s), 1427 (w), 1201 (s), 1183 (s), 1137 (s).

HRMS (ESI+, m/z): [$M+H$]⁺ calc'd for C₂₄H₄₂F₃N₃O₅S, 542.2870; found 542.2867.



Allylic sulfonamides (6*S*)-4.29 and (6*R*)-4.29.

A solution of sulfonimine (*S_S*)-4.10 (100. mg, 160. μmol, 1 equiv) in dichloromethane (1.60 mL) was chilled to $-78\text{ }^\circ\text{C}$ before a solution of vinylmagnesium bromide in tetrahydrofuran (0.60 M, 800 μL, 480 μmol, 3.0 equiv) was added dropwise. After stirring for 30 min at $-78\text{ }^\circ\text{C}$, TLC analysis (60% ethyl acetate–hexanes, UV+PAA) indicated that no sulfonimine starting material remained. Unreacted Grignard reagent was destroyed with the dropwise addition of saturated aqueous ammonium chloride solution (5 mL), and the resulting mixture was warmed to $23\text{ }^\circ\text{C}$ before it was transferred to a separatory funnel containing water (1 mL) and saturated aqueous sodium chloride solution (5 mL). This mixture was extracted with dichloromethane ($3 \times 10\text{ mL}$), the combined organic extracts were dried over sodium sulfate, the dried solution was filtered, and the filtrate was concentrated to furnish a colorless film. $^1\text{H-NMR}$ analysis (CDCl_3) of this crude residue revealed a 71:29 mixture of diastereomeric products. Separation of this mixture by flash-column chromatography (12 g silica gel, eluting with 15% ethyl acetate–hexanes initially, grading to 60% ethyl acetate–hexanes) provided, in order of elution from the column, (6*S*)-4.29 (24.4 mg, 23%) and (6*R*)-4.29 (65.1 mg, 62%), both as white amorphous solids.

(6*R*)-4.29:

$R_f = 0.29$ (60% ethyl acetate–hexanes, UV+ KMnO_4).

$^1\text{H NMR}$ (500 MHz, CDCl_3) δ 8.07 (dd, $J = 8.4, 1.3\text{ Hz}$, 2H), 7.96 (dd, $J = 8.4, 1.4\text{ Hz}$, 2H), 7.78 (dd, $J = 8.4, 1.3\text{ Hz}$, 2H), 7.63 (tt, $J = 7.5, 1.3\text{ Hz}$, 1H), 7.53–7.49 (m, 3H), 7.43 (tt, $J = 7.5,$

1.2 Hz, 1H), 7.38 (t, $J = 7.8$ Hz, 2H), 7.25 (t, $J = 7.8$ Hz, 2H), 6.12–6.05 (m, 2H), 5.89–5.88 (m, 1H), 5.83–5.78 (m, 2H), 5.43 (app dt, $J = 17.2, 1.0$ Hz, 1H), 5.29 (10.5, 1.0 Hz, 1H), 4.51 (dd, $J = 9.1, 1.1$ Hz, 1H), 4.06 (app td, $J = 8.7, 6.7$ Hz, 1H), 3.66 (d, $J = 8.5$ Hz, 1H), 2.11 (s, 3H), 1.21 (s, 9H).

^{13}C NMR (126 MHz, CDCl_3) δ 165.8, 165.7, 165.5, 136.1, 133.7, 133.6, 133.3, 130.0 (2 \times C), 129.9, 129.4, 129.3, 129.1, 128.8, 128.6, 128.4, 118.8, 84.5, 71.5, 69.6, 69.2, 68.9, 58.0, 56.7, 22.9, 13.1.

IR (neat, cm^{-1}): 1729 (s), 1452 (w), 1282 (s), 1261 (s), 1094 (m), 1069 (s), 686 (s).

HRMS (ESI+, m/z): $[\text{M}+\text{H}]^+$ calc'd for $\text{C}_{34}\text{H}_{37}\text{NO}_8\text{S}_2$, 652.2033; found 652.2031.

(6S)-4.29:

$R_f = 0.38$ (60% ethyl acetate–hexanes, UV+ KMnO_4).

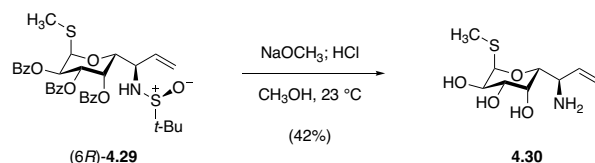
^1H NMR (500 MHz, CDCl_3) δ 8.04 (dd, $J = 8.3, 1.3$ Hz, 2H), 7.96 (dd, $J = 8.4, 1.3$ Hz, 2H), 7.77 (dd, $J = 8.4, 1.3$ Hz, 2H), 7.63 (tt, $J = 7.1, 1.3$ Hz, 1H), 7.53–7.47 (m, 3H), 7.44 (tt, $J = 7.8, 1.3$ Hz, 1H), 7.38 (dd, $J = 8.3, 7.4$ Hz, 2H), 7.25 (dd, $J = 8.3, 7.6$ Hz, 2H), 4.93 (d, $J = 4.8$ Hz, 1H), 5.88 (dd, $J = 3.2, 1.2$ Hz, 1H), 5.82–5.76 (m, 2H), 5.62 (ddd, $J = 17.1, 10.3, 8.7$ Hz, 1H), 5.37 (d, $J = 10.4$ Hz, 1H), 5.24 (dt, $J = 17.2, 0.9$ Hz, 1H), 4.48 (dd, $J = 9.6, 1.4$ Hz, 1H), 4.22 (td, $J = 9.1, 1.7$ Hz, 1H), 3.92 (d, $J = 1.8$ Hz, 1H), 2.16 (s, 3H), 1.22 (s, 9H).

^{13}C NMR (126 MHz, CDCl_3) δ 165.7, 165.6, 165.3, 133.8, 133.7, 133.3, 132.4, 130.1, 129.9, 129.2, 129.1, 128.9, 128.6, 128.4, 123.6, 84.2, 71.5, 69.4, 68.9, 68.4, 57.1, 55.5, 22.8, 13.0.

Only 10 phenyl carbon resonances are observed; the 2 missing signals are believed to coincide with observed resonances (δ 130.1, 129.2).

IR (neat, cm^{-1}): 1729 (s), 1452 (w), 1282 (s), 1262 (s), 1106 (m), 1069 (s), 711 (m).

HRMS (ESI+, m/z): $[M+H]^+$ calc'd for $C_{34}H_{37}NO_8S_2$, 652.2033; found 652.2037.



Aminotriol 4.30.

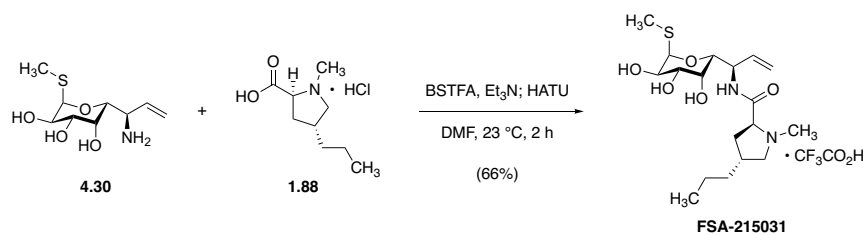
In a 4-mL glass vial fitted with a magnetic stir bar, sulfinamide (6*R*)-**4.29** (19 mg, 29 μmol , 1 equiv) was dissolved in anhydrous methanol (530 μL). To this solution was then added a methanolic solution of sodium methoxide (0.5 M, 53 μL) at 23 $^\circ\text{C}$. After 30 min of stirring at ambient temperature, LCMS analysis indicated that global debenzoylation was complete, and a solution of hydrogen chloride in 1,4-dioxane (4 M, 500 μL) was added next. After an additional 30 min, LCMS analysis indicated that the *tert*-butanesulfinyl group had been completely removed. The mixture was diluted with toluene (1 mL), and the diluted mixture was concentrated in vacuo. The residue was re-dissolved in methanol (1 mL), and the solution was treated with Amberlyst A26 ion-exchange resin (hydroxide form, 100 mg). The mixture was stirred at 23 $^\circ\text{C}$ for 30 min before the resin was filtered off; the filtrate was concentrated to provide crude product in free-base form. This residue was finally purified by flash-column chromatography (4 g silica gel, eluting with 0.5% ammonium hydroxide–5% methanol–dichloromethane initially, grading to 2% ammonium hydroxide–20% methanol–dichloromethane) to furnish the product as a white solid (2.9 mg, 42%).

$R_f = 0.24$ (2% ammonium hydroxide–20% methanol–dichloromethane, PAA).

$^1\text{H NMR}$ (500 MHz, CD_3OD) δ 5.98 (ddd, $J = 17.2, 10.3, 6.7$ Hz, 1H), 5.36–5.24 (m, 3H), 4.11 (dd, $J = 10.2, 5.6$ Hz, 1H), 4.05 (br s, 1H), 3.94 (d, $J = 7.6$ Hz, 1H), 3.74 (app t, $J = 6.5$ Hz, 1H), 3.60 (dd, $J = 10.2, 3.0$ Hz, 1H), 2.04 (s, 3H).

IR (neat, cm^{-1}): 3342 (br), 1581 (m), 1080 (s), 1054 (s).

HRMS (ESI+, m/z): $[\text{M}+\text{H}]^+$ calc'd for $\text{C}_9\text{H}_{17}\text{NO}_4\text{S}$, 236.1; found 236.2.

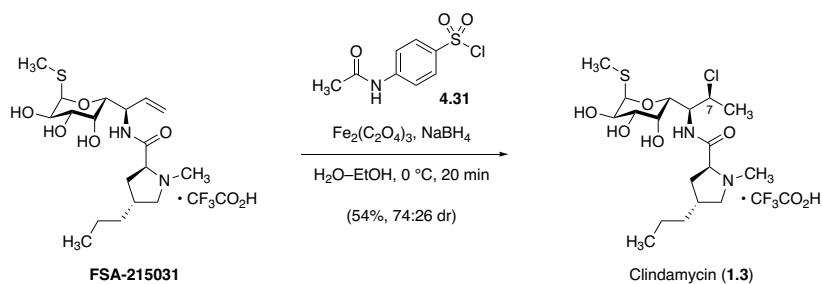


Synthetic lincosamide FSA-215031.

In a 1-mL glass vial fitted with a magnetic stir bar, aminotriol **4.30** (2.9 mg, 12 μmol, 1 equiv) was dissolved in *N,N*-dimethylformamide (120 μL). To this solution were then added triethylamine (7.7 μL, 55 μmol, 4.5 equiv) and *N,O*-bis(trimethylsilyl)trifluoroacetamide (5.0 μL, 18 μmol, 1.5 equiv) at 23 °C. The solution was stirred at 23 °C for 1 h in order to ensure complete *O*-silylation before *trans*-4-*n*-propyl-L-hygric acid hydrochloride (**1.88**, 3.3 mg, 16 μmol, 1.3 equiv) and HATU (7.0 mg, 18 μmol, 1.5 equiv) were added sequentially. Upon addition of HATU, the colorless mixture changed to a dull tennis-ball yellow. After 2 h, LCMS analysis of the reaction mixture demonstrated complete consumption of the aminotriol starting material and its (oligo)trimethylsilylated congeners; the mixture was diluted with 50% v/v acetic acid–methanol (2 mL), and the resulting solution was heated to 35 °C overnight in order to effect global desilylation of the coupling product. The mixture was then concentrated to dryness in vacuo, and the crude residue was purified by preparative HPLC-MS on a Waters SunFire prep C₁₈ column (5 μm, 250 × 19 mm; eluting with 0.1% trifluoroacetic acid–5% acetonitrile–water initially, grading to 0.1% trifluoroacetic acid–40% acetonitrile–water over 40 min, with a flow rate of 15 mL/min; monitored by UV absorbance at 210 nm and ESI+ selected ion monitoring [*m/z* = 389]; *R*_t = 29.0 min) to furnish **FSA-215031** • CF₃CO₂H as a white solid (4.1 mg, 66%).

¹H NMR (hydrotrifluoroacetate salt, 500 MHz, CD₃OD) δ 6.00 (ddd, *J* = 17.5, 10.2, 5.6 Hz, 1H), 5.29 (d, *J* = 5.6 Hz, 1H), 5.23–5.19 (m, 2H), 4.77 (ddt, *J* = 8.8, 5.7, 1.6 Hz, 1H), 4.18 (dd, *J* = 9.7, 6.8 Hz, 1H), 4.12–4.09 (m, 2H), 3.90 (dd, *J* = 3.4, 1.2 Hz, 1H), 3.77 (dd, *J* = 11.1, 6.8 Hz, 1H), 3.59 (dd, *J* = 10.1, 3.3 Hz, 1H), 2.94 (s, 3H), 2.83 (app t, *J* = 11.0 Hz, 1H), 2.37 (app p, *J* = 7.8 Hz, 1H), 2.29–2.20 (m, 2H), 2.04 (s, 3H), 1.52–1.47 (m, 2H), 1.42–1.32 (m, 2H), 0.96 (t, *J* = 7.3 Hz, 3H).

The hydroformate salt, **FSA-215031** • HCO₂H, was characterized as well. Refer to the Experimental Section of Chapter 3 for details.



Synthesis of clindamycin (1.3) by radical hydrochlorination.

In a 12×100 mm glass test tube fitted with a magnetic stir bar, an aqueous solution of iron(III) oxalate (0.050 M, 400 μL , 0.020 mmol, 5.0 equiv) was chilled to $0\text{ }^\circ\text{C}$. Argon was bubbled through this solution for 10 min in order to sparge it of dissolved oxygen gas. A suspension of *N*-acetylsulfanyl chloride (**4.31**, 4.7 mg, 0.020 mmol, 5.0 equiv) in ethanol (190 proof, 200 μL) was added by micropipette, followed by a solution of **FSA-215031** \cdot $\text{CF}_3\text{CO}_2\text{H}$ (2.0 mg, 4.0 mmol, 1 equiv) in ethanol (190 proof, 200 μL). Sodium borohydride (0.96 mg, 0.025 mmol, 6.4 equiv) was finally added at $0\text{ }^\circ\text{C}$ under a blanket of argon gas, causing rapid gas evolution. The mixture gradually changed color from a light-yellow solution to the color of orange juice. After 20 min, LCMS analysis indicated that the reaction was complete; the mixture was treated with ammonium hydroxide solution (200 μL), and the resulting suspension was extracted with 10% v/v methanol–dichloromethane (4×2 mL). The combined organic extracts were dried over sodium sulfate, filtered, and concentrated to provide a colorless film, which was purified by preparative HPLC–MS on a Waters SunFire prep C_{18} column (5 μm , 19×250 mm; eluting with 0.1% trifluoroacetic acid–5% acetonitrile–water initially, grading to 0.1% trifluoroacetic acid–40% acetonitrile–water over 40 min, with a flow rate of 15 mL/min; monitored by UV absorbance at 210 nm and ESI+ selected ion monitoring [$m/z = 425$]; $R_t = 29.0$ min) to provide clindamycin hydrotrifluoroacetate (**1.3** \cdot $\text{CF}_3\text{CO}_2\text{H}$) and 7-epi-clindamycin hydrotrifluoroacetate as a 74:26 mixture (1.2 mg, 54%).

The ^1H NMR spectrum of the major diastereomer was identical to that of an authentic sample of clindamycin hydrotrifluoroacetate.

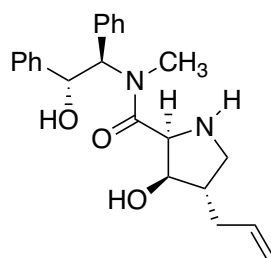
Page intentionally left blank

Appendix A. Catalog of X-ray crystal structures

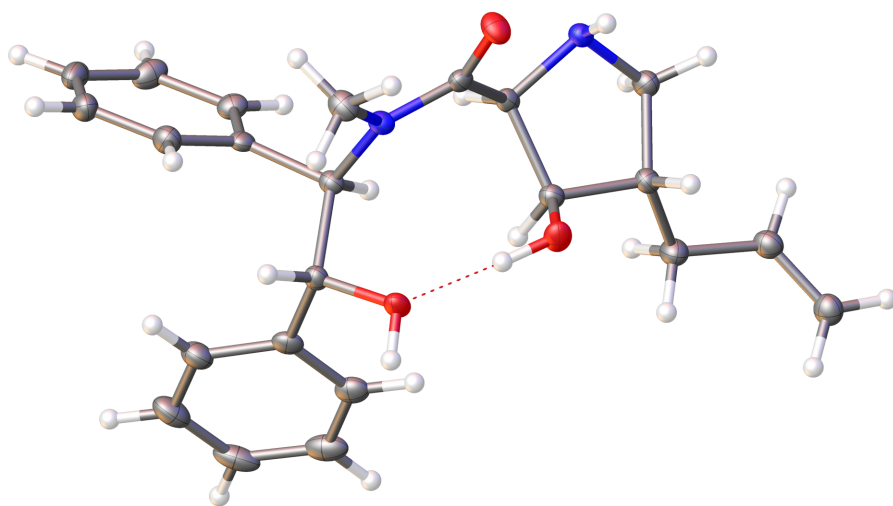
X-ray Crystallographic Laboratory Structure Report

Dr. Shao-Liang Zheng, Harvard University

January 10, 2014



2.9



X-Ray Crystallography: A crystal mounted on a diffractometer was collected data at 100 K. The intensities of the reflections were collected by means of a Bruker APEX II DUO CCD diffractometer (Cu $\text{K}\alpha$ radiation, $\lambda=1.54178$ Å), and equipped with an Oxford Cryosystems nitrogen flow apparatus. The collection method involved 1.0° scans in ω at 30° , 55° , 80° and 115° in 2θ . Data integration down to 0.84 Å resolution was carried out using SAINT V7.46 A with reflection spot size optimization. Absorption corrections were made with the program SADABS.¹⁷⁸ The structure was solved by the direct methods procedure and refined by least-squares methods again F^2 using SHELXS-97 and SHELXL-97¹⁷⁹ with OLEX 2 interface.¹⁸⁰ Non-hydrogen atoms were refined anisotropically, and hydrogen atoms were allowed to ride on the respective atoms. Crystal data as well as details of data collection and refinement are summarized in Table B.1, geometric parameters are shown in B.2, and hydrogen-bond parameters are listed in Table B.3. The Ortep plots produced with SHELXL-97 program, and the other drawings were produced with Accelrys DS Visualizer 2.0.¹⁸¹

Table A1. Experimental details

	mml-042-np-d2
Crystal data	
Chemical formula	C ₂₃ H ₂₈ N ₂ O ₃
M_r	380.47
Crystal system, space group	Orthorhombic, $P2_12_12_1$
Temperature (K)	100
a, b, c (Å)	7.7089 (1), 13.4375 (2), 19.3877 (3)
V (Å ³)	2008.34 (5)

¹⁷⁸ Bruker AXS APEX II, Bruker AXS, Madison, Wisconsin, 2009.

¹⁷⁹ Sheldrick, G. M. *Acta Cryst.* **2008**, *A64*, 112–122.

¹⁸⁰ Dolomanov, O. V.; Bourhis, L. J.; Gildea, R. J.; Howard, J. A. K.; Puschmann, H. *J. Appl. Cryst.* **2009**, *42*, 339–341.

¹⁸¹ Accelrys DS Visualizer v2.0.1, Accelrys Software, Inc., 2007.

Table A1 (Continued)

Z	4
Radiation type	Cu $K\alpha$
μ (mm ⁻¹)	0.67
Crystal size (mm)	0.16 × 0.12 × 0.10
Data collection	
Diffractometer	Bruker D8 goniometer with CCD area detector diffractometer
Absorption correction	Multi-scan <i>SADABS</i>
T_{\min} , T_{\max}	0.901, 0.936
No. of measured, independent and observed [$I > 2\sigma(I)$] reflections	49871, 3482, 3417
R_{int}	0.030
$(\sin \theta/\lambda)_{\text{max}}$ (Å ⁻¹)	0.595
Refinement	
$R[F^2 > 2\sigma(F^2)]$, $wR(F^2)$, S	0.024, 0.060, 1.06
No. of reflections	3482
No. of parameters	266
H-atom treatment	H atoms treated by a mixture of independent and constrained refinement
$\Delta\rho_{\text{max}}$, $\Delta\rho_{\text{min}}$ (e Å ⁻³)	0.12, -0.18
Absolute structure	Flack H D (1983), Acta Cryst. A39, 876-881
Absolute structure parameter	-0.02 (14)

Computer programs: *APEX2* v2009.3.0 (Bruker-AXS, 2009), *SAINT* 7.46A (Bruker-AXS, 2009), *SHELXS97* (Sheldrick, 2008), *SHELXL97* (Sheldrick, 2008), Bruker *SHELXTL* (Sheldrick, 2008).

Table A2. Geometric parameters (Å, °)

C1—O1	1.2260 (14)	C11—C12	1.3813 (19)
C1—N2	1.3625 (15)	C11—H11	0.9500
C1—C2	1.5236 (15)	C12—C13	1.3877 (19)
C2—N1	1.4731 (15)	C12—H12	0.9500
C2—C3	1.5682 (15)	C13—C14	1.3909 (17)

Table A2 (Continued)

C2—H2	1.0000	C13—H13	0.9500
C3—O2	1.4154 (14)	C14—C15	1.3932 (17)
C3—C4	1.5338 (16)	C14—H14	0.9500
C3—H3	1.0000	C15—C16	1.5243 (15)
C4—C5	1.5311 (17)	C16—N2	1.4740 (14)
C4—C6	1.5312 (16)	C16—C17	1.5600 (15)
C4—H4	1.0000	C16—H16	1.0000
C5—N1	1.4763 (15)	C17—O3	1.4145 (14)
C5—H5A	0.9900	C17—C18	1.5233 (16)
C5—H5B	0.9900	C17—H17	1.0000
C6—C7	1.4951 (17)	C18—C23	1.3909 (18)
C6—H6A	0.9900	C18—C19	1.3920 (17)
C6—H6B	0.9900	C19—C20	1.3911 (19)
C7—C8	1.3182 (18)	C19—H19	0.9500
C7—H7	0.9500	C20—C21	1.383 (2)
C8—H8A	0.9500	C20—H20	0.9500
C8—H8B	0.9500	C21—C22	1.391 (2)
C9—N2	1.4582 (15)	C21—H21	0.9500
C9—H9A	0.9800	C22—C23	1.3889 (18)
C9—H9B	0.9800	C22—H22	0.9500
C9—H9C	0.9800	C23—H23	0.9500
C10—C11	1.3874 (17)	N1—H1	0.884 (15)
C10—C15	1.3960 (17)	O2—H2A	0.92 (2)
C10—H10	0.9500	O3—H3A	0.87 (2)
O1—C1—N2	121.27 (11)	C11—C12—C13	119.16 (12)
O1—C1—C2	119.09 (10)	C11—C12—H12	120.4
N2—C1—C2	119.61 (10)	C13—C12—H12	120.4
N1—C2—C1	109.98 (9)	C12—C13—C14	120.48 (12)
N1—C2—C3	106.62 (9)	C12—C13—H13	119.8
C1—C2—C3	112.18 (9)	C14—C13—H13	119.8
N1—C2—H2	109.3	C13—C14—C15	120.68 (11)
C1—C2—H2	109.3	C13—C14—H14	119.7
C3—C2—H2	109.3	C15—C14—H14	119.7
O2—C3—C4	108.64 (9)	C14—C15—C10	118.19 (11)

Table A2 (Continued)

O2—C3—C2	113.45 (9)	C14—C15—C16	119.78 (10)
C4—C3—C2	104.76 (9)	C10—C15—C16	122.00 (10)
O2—C3—H3	109.9	N2—C16—C15	112.01 (9)
C4—C3—H3	109.9	N2—C16—C17	112.18 (9)
C2—C3—H3	109.9	C15—C16—C17	110.30 (9)
C5—C4—C6	115.23 (10)	N2—C16—H16	107.4
C5—C4—C3	104.31 (9)	C15—C16—H16	107.4
C6—C4—C3	111.65 (9)	C17—C16—H16	107.4
C5—C4—H4	108.5	O3—C17—C18	112.19 (9)
C6—C4—H4	108.5	O3—C17—C16	108.01 (9)
C3—C4—H4	108.5	C18—C17—C16	109.51 (9)
N1—C5—C4	105.85 (9)	O3—C17—H17	109.0
N1—C5—H5A	110.6	C18—C17—H17	109.0
C4—C5—H5A	110.6	C16—C17—H17	109.0
N1—C5—H5B	110.6	C23—C18—C19	118.79 (11)
C4—C5—H5B	110.6	C23—C18—C17	120.98 (10)
H5A—C5—H5B	108.7	C19—C18—C17	120.23 (11)
C7—C6—C4	114.93 (10)	C20—C19—C18	120.49 (12)
C7—C6—H6A	108.5	C20—C19—H19	119.8
C4—C6—H6A	108.5	C18—C19—H19	119.8
C7—C6—H6B	108.5	C21—C20—C19	120.39 (13)
C4—C6—H6B	108.5	C21—C20—H20	119.8
H6A—C6—H6B	107.5	C19—C20—H20	119.8
C8—C7—C6	125.35 (12)	C20—C21—C22	119.48 (12)
C8—C7—H7	117.3	C20—C21—H21	120.3
C6—C7—H7	117.3	C22—C21—H21	120.3
C7—C8—H8A	120.0	C23—C22—C21	120.07 (13)
C7—C8—H8B	120.0	C23—C22—H22	120.0
H8A—C8—H8B	120.0	C21—C22—H22	120.0
N2—C9—H9A	109.5	C22—C23—C18	120.74 (13)
N2—C9—H9B	109.5	C22—C23—H23	119.6
H9A—C9—H9B	109.5	C18—C23—H23	119.6
N2—C9—H9C	109.5	C2—N1—C5	104.43 (9)
H9A—C9—H9C	109.5	C2—N1—H1	107.9 (10)
H9B—C9—H9C	109.5	C5—N1—H1	109.2 (9)

Table A2 (Continued)

C11—C10—C15	120.87 (12)	C1—N2—C9	116.70 (9)
C11—C10—H10	119.6	C1—N2—C16	125.23 (10)
C15—C10—H10	119.6	C9—N2—C16	118.06 (9)
C12—C11—C10	120.54 (12)	C3—O2—H2A	107.2 (12)
C12—C11—H11	119.7	C17—O3—H3A	108.3 (12)
C10—C11—H11	119.7		
O1—C1—C2—N1	-12.59 (14)	C10—C15—C16—C17	49.10 (14)
N2—C1—C2—N1	169.04 (9)	N2—C16—C17—O3	-42.50 (12)
O1—C1—C2—C3	105.89 (11)	C15—C16—C17—O3	-168.11 (9)
N2—C1—C2—C3	-72.48 (13)	N2—C16—C17—C18	-164.95 (9)
N1—C2—C3—O2	106.65 (10)	C15—C16—C17—C18	69.43 (12)
C1—C2—C3—O2	-13.79 (13)	O3—C17—C18—C23	149.86 (11)
N1—C2—C3—C4	-11.68 (11)	C16—C17—C18—C23	-90.21 (12)
C1—C2—C3—C4	-132.13 (9)	O3—C17—C18—C19	-30.94 (14)
O2—C3—C4—C5	-132.86 (10)	C16—C17—C18—C19	88.98 (13)
C2—C3—C4—C5	-11.31 (11)	C23—C18—C19—C20	0.77 (18)
O2—C3—C4—C6	102.07 (11)	C17—C18—C19—C20	-178.44 (11)
C2—C3—C4—C6	-136.38 (9)	C18—C19—C20—C21	1.10 (19)
C6—C4—C5—N1	153.54 (10)	C19—C20—C21—C22	-1.9 (2)
C3—C4—C5—N1	30.78 (11)	C20—C21—C22—C23	0.8 (2)
C5—C4—C6—C7	64.17 (14)	C21—C22—C23—C18	1.1 (2)
C3—C4—C6—C7	-177.07 (10)	C19—C18—C23—C22	-1.85 (19)
C4—C6—C7—C8	126.50 (13)	C17—C18—C23—C22	177.35 (11)
C15—C10—C11—C12	0.1 (2)	C1—C2—N1—C5	152.76 (9)
C10—C11—C12—C13	-2.0 (2)	C3—C2—N1—C5	30.91 (11)
C11—C12—C13—C14	1.77 (19)	C4—C5—N1—C2	-38.66 (11)
C12—C13—C14—C15	0.44 (19)	O1—C1—N2—C9	-2.66 (16)
C13—C14—C15—C10	-2.35 (17)	C2—C1—N2—C9	175.68 (10)
C13—C14—C15—C16	175.80 (11)	O1—C1—N2—C16	176.23 (10)
C11—C10—C15—C14	2.11 (18)	C2—C1—N2—C16	-5.44 (16)
C11—C10—C15—C16	-176.00 (11)	C15—C16—N2—C1	-112.52 (12)
C14—C15—C16—N2	105.32 (12)	C17—C16—N2—C1	122.81 (11)
C10—C15—C16—N2	-76.60 (14)	C15—C16—N2—C9	66.35 (13)
C14—C15—C16—C17	-128.97 (11)	C17—C16—N2—C9	-58.32 (12)

Table A3. Hydrogen-bond parameters

$D-H\cdots A$	$D-H$ (Å)	$H\cdots A$ (Å)	$D\cdots A$ (Å)	$D-H\cdots A$ (°)
$N1-H1\cdots O2^i$	0.884 (15)	2.160 (15)	2.9550 (13)	149.3 (12)
$O2-H2A\cdots O3$	0.92 (2)	1.76 (2)	2.6785 (12)	174.6 (18)
$O3-H3A\cdots N1^{ii}$	0.87 (2)	1.83 (2)	2.6906 (13)	169.7 (17)

Symmetry code(s): (i) $x+1/2, -y+3/2, -z+1$; (ii) $x-1, y, z$.

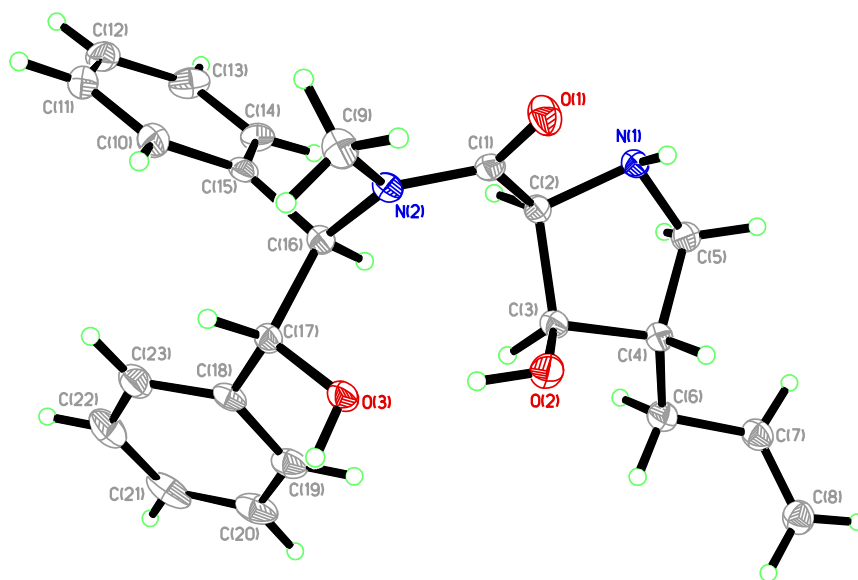


Figure A1. Perspective views showing 50% probability displacement.

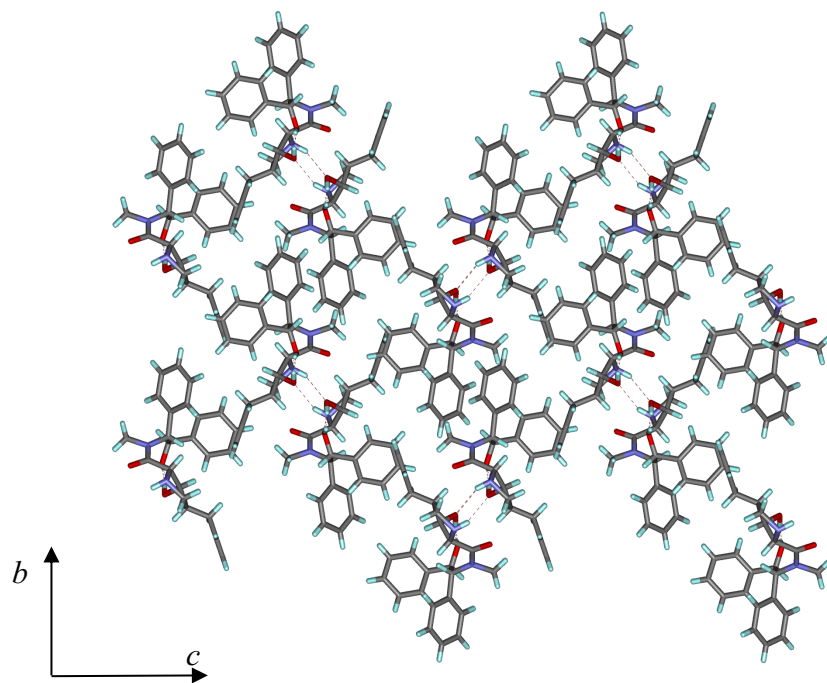
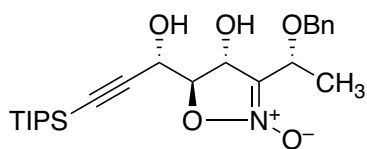


Figure A2. Three-dimensional supramolecular architecture viewed along the a -axis direction.

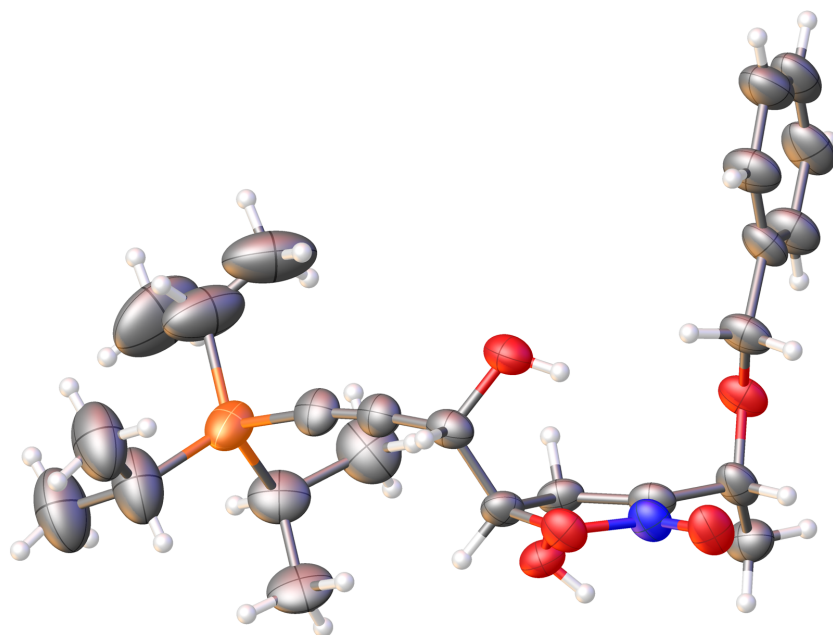
X-ray Crystallographic Laboratory Structure Report

Dr. Shao-Liang Zheng, Harvard University

October 13, 2015



3.36



X-Ray Crystallography: A crystal mounted on a diffractometer was collected data at 100 K. The intensities of the reflections were collected by means of a Bruker APEX II DUO CCD diffractometer (Cu $K\alpha$ radiation, $\lambda=1.54178$ Å), and equipped with an Oxford Cryosystems nitrogen flow apparatus. The collection method involved 1.0° scans in ω at -30°, -55°, -80°, 30°, 55°, 80° and 115° in 2θ . Data integration down to 0.84 Å resolution was carried out using SAINT V8.34 C with reflection spot size optimization. Absorption corrections were made with the program SADABS.¹⁸² The structure was solved by the Intrinsic Phasing methods and refined by least-squares methods again F^2 using SHELXT-2014 and SHELXL-2014¹⁸³ with OLEX 2 interface. Non-hydrogen atoms were refined anisotropically, and hydrogen atoms were allowed to ride on the respective atoms. Crystal data as well as details of data collection and refinement are summarized in Table B.4, geometric parameters are shown in Table B.5, and hydrogen-bond geometric parameters are listed in Table B.6. The Ortep plots produced with SHELXL-2014 program, and the other drawings were produced with Accelrys DS Visualizer 2.0.

Table A4. Experimental details

	mm8-002-np-d
Crystal data	
Chemical formula	C ₂₄ H ₃₇ NO ₅ Si
M_r	447.63
Crystal system, space group	Monoclinic, $P2_1$
Temperature (K)	100
a, b, c (Å)	11.7798 (16), 6.7133 (10), 19.712 (3)
β (°)	103.006 (7)
V (Å ³)	1518.8 (4)
Z	2
Radiation type	Cu $K\alpha$

¹⁸² Bruker AXS APEX3, Bruker AXS, Madison, Wisconsin, 2015.

¹⁸³ (a) Sheldrick, G. M. *Acta Cryst.* **2015**, *A71*, 3–8. Sheldrick, G. M. *Acta Cryst.* **2015**, *C21*, 3–8.

Table A4 (Continued)

μ (mm ⁻¹)	0.90
Crystal size (mm)	0.12 × 0.01 × 0.01
Data collection	
Diffractometer	Bruker D8 goniometer with CCD area detector diffractometer
Absorption correction	Multi-scan <i>SADABS</i>
T_{\min} , T_{\max}	0.683, 0.864
No. of measured, independent and observed [$I > 2\sigma(I)$] reflections	22195, 4853, 3617
R_{int}	0.109
$(\sin \theta/\lambda)_{\text{max}}$ (Å ⁻¹)	0.596
Refinement	
$R[F^2 > 2\sigma(F^2)]$, $wR(F^2)$, S	0.084, 0.231, 1.04
No. of reflections	4853
No. of parameters	314
No. of restraints	85
H-atom treatment	H-atom parameters constrained
$\Delta\rho_{\text{max}}$, $\Delta\rho_{\text{min}}$ (e Å ⁻³)	0.49, -0.26
Absolute structure	Flack x determined using 1118 quotients [(I+)-(I-)]/[(I+)+(I-)] (Parsons, Flack and Wagner, Acta Cryst. B69 (2013) 249-259).
Absolute structure parameter	0.05 (5)

Computer programs: *APEX3* v2015.5.2 (Bruker-AXS, 2015), *SAINT* 8.34C (Bruker-AXS, 2014), *SHELXT2014* (Sheldrick, 2015), *SHELXL2014* (Sheldrick, 2015), Bruker *SHELXTL* (Sheldrick, 2015).

Table A5. Geometric parameters (Å, °)

C1—C6	1.361 (10)	C20—H20A	0.9800
C1—C2	1.385 (10)	C20—H20B	0.9800
C1—H1	0.9500	C20—H20C	0.9800
C2—C3	1.374 (13)	C21—H21A	0.9800
C2—H2	0.9500	C21—H21B	0.9800

Table A5 (Continued)

C3—C4	1.392 (14)	C21—H21C	0.9800
C3—H3	0.9500	C22—C24	1.50 (2)
C4—C5	1.370 (10)	C22—C23	1.57 (2)
C4—H4	0.9500	C22—H22	1.0000
C5—C6	1.392 (11)	C23—H23A	0.9800
C5—H5	0.9500	C23—H23B	0.9800
C6—C7	1.506 (8)	C23—H23C	0.9800
C7—O1	1.430 (9)	C24—H24A	0.9800
C7—H7A	0.9900	C24—H24B	0.9800
C7—H7B	0.9900	C24—H24C	0.9800
C8—O1	1.416 (7)	C14A—C15A	1.248 (19)
C8—C10	1.495 (9)	C15A—Si1A	1.90 (2)
C8—C9	1.510 (10)	Si1A—C16A	1.82 (2)
C8—H8	1.0000	Si1A—C22A	1.94 (2)
C9—H9A	0.9800	Si1A—C19A	1.96 (3)
C9—H9B	0.9800	C16A—C18A	1.53 (3)
C9—H9C	0.9800	C16A—C17A	1.61 (3)
C10—N1	1.312 (8)	C16A—H16A	1.0000
C10—C11	1.504 (9)	C17A—H17D	0.9800
C11—O4	1.413 (8)	C17A—H17E	0.9800
C11—C12	1.555 (9)	C17A—H17F	0.9800
C11—H11	1.0000	C18A—H18D	0.9800
C12—O2	1.451 (7)	C18A—H18E	0.9800
C12—C13	1.510 (9)	C18A—H18F	0.9800
C12—H12	1.0000	C19A—C20A	1.36 (3)
C13—O5	1.422 (8)	C19A—C21A	1.47 (3)
C13—C14A	1.475 (9)	C19A—H19A	1.0000
C13—C14	1.475 (9)	C20A—H20D	0.9800
C13—H13	1.0000	C20A—H20E	0.9800
C13—H13A	1.0000	C20A—H20F	0.9800
C14—C15	1.199 (12)	C21A—H21D	0.9800
C15—Si1	1.851 (13)	C21A—H21E	0.9800
Si1—C16	1.854 (12)	C21A—H21F	0.9800
Si1—C19	1.881 (16)	C22A—C24A	1.49 (3)
Si1—C22	1.931 (17)	C22A—C23A	1.59 (3)

Table A5 (Continued)

C16—C18	1.560 (17)	C22A—H22A	1.0000
C16—C17	1.61 (2)	C23A—H23D	0.9800
C16—H16	1.0000	C23A—H23E	0.9800
C17—H17A	0.9800	C23A—H23F	0.9800
C17—H17B	0.9800	C24A—H24D	0.9800
C17—H17C	0.9800	C24A—H24E	0.9800
C18—H18A	0.9800	C24A—H24F	0.9800
C18—H18B	0.9800	N1—O3	1.261 (7)
C18—H18C	0.9800	N1—O2	1.424 (7)
C19—C20	1.36 (2)	O4—H4A	0.8400
C19—C21	1.50 (2)	O5—H5A	0.8400
C19—H19	1.0000		
C6—C1—C2	122.8 (8)	C19—C20—H20C	109.5
C6—C1—H1	118.6	H20A—C20—H20C	109.5
C2—C1—H1	118.6	H20B—C20—H20C	109.5
C3—C2—C1	117.8 (7)	C19—C21—H21A	109.5
C3—C2—H2	121.1	C19—C21—H21B	109.5
C1—C2—H2	121.1	H21A—C21—H21B	109.5
C2—C3—C4	121.5 (7)	C19—C21—H21C	109.5
C2—C3—H3	119.2	H21A—C21—H21C	109.5
C4—C3—H3	119.2	H21B—C21—H21C	109.5
C5—C4—C3	118.3 (9)	C24—C22—C23	111.7 (18)
C5—C4—H4	120.9	C24—C22—Si1	116.5 (14)
C3—C4—H4	120.9	C23—C22—Si1	106.8 (13)
C4—C5—C6	121.9 (8)	C24—C22—H22	107.1
C4—C5—H5	119.1	C23—C22—H22	107.1
C6—C5—H5	119.1	Si1—C22—H22	107.1
C1—C6—C5	117.7 (6)	C22—C23—H23A	109.5
C1—C6—C7	123.6 (7)	C22—C23—H23B	109.5
C5—C6—C7	118.6 (6)	H23A—C23—H23B	109.5
O1—C7—C6	108.4 (5)	C22—C23—H23C	109.5
O1—C7—H7A	110.0	H23A—C23—H23C	109.5
C6—C7—H7A	110.0	H23B—C23—H23C	109.5
O1—C7—H7B	110.0	C22—C24—H24A	109.5

Table A5 (Continued)

C6—C7—H7B	110.0	C22—C24—H24B	109.5
H7A—C7—H7B	108.4	H24A—C24—H24B	109.5
O1—C8—C10	111.2 (6)	C22—C24—H24C	109.5
O1—C8—C9	106.4 (5)	H24A—C24—H24C	109.5
C10—C8—C9	113.4 (6)	H24B—C24—H24C	109.5
O1—C8—H8	108.6	C15A—C14A—C13	170 (4)
C10—C8—H8	108.6	C14A—C15A—Si1A	172 (7)
C9—C8—H8	108.6	C16A—Si1A—C15A	110 (2)
C8—C9—H9A	109.5	C16A—Si1A—C22A	125.3 (15)
C8—C9—H9B	109.5	C15A—Si1A—C22A	109 (3)
H9A—C9—H9B	109.5	C16A—Si1A—C19A	112.3 (16)
C8—C9—H9C	109.5	C15A—Si1A—C19A	106 (3)
H9A—C9—H9C	109.5	C22A—Si1A—C19A	90.8 (17)
H9B—C9—H9C	109.5	C18A—C16A—C17A	115 (2)
N1—C10—C8	121.0 (6)	C18A—C16A—Si1A	102 (2)
N1—C10—C11	109.4 (5)	C17A—C16A—Si1A	113 (2)
C8—C10—C11	129.6 (5)	C18A—C16A—H16A	108.7
O4—C11—C10	113.5 (5)	C17A—C16A—H16A	108.7
O4—C11—C12	113.2 (5)	Si1A—C16A—H16A	108.7
C10—C11—C12	103.2 (5)	C16A—C17A—H17D	109.5
O4—C11—H11	108.9	C16A—C17A—H17E	109.5
C10—C11—H11	108.9	H17D—C17A—H17E	109.5
C12—C11—H11	108.9	C16A—C17A—H17F	109.5
O2—C12—C13	108.6 (5)	H17D—C17A—H17F	109.5
O2—C12—C11	105.6 (5)	H17E—C17A—H17F	109.5
C13—C12—C11	114.4 (5)	C16A—C18A—H18D	109.5
O2—C12—H12	109.3	C16A—C18A—H18E	109.5
C13—C12—H12	109.3	H18D—C18A—H18E	109.5
C11—C12—H12	109.3	C16A—C18A—H18F	109.5
O5—C13—C14A	111.8 (5)	H18D—C18A—H18F	109.5
O5—C13—C14	111.8 (5)	H18E—C18A—H18F	109.5
O5—C13—C12	109.5 (5)	C20A—C19A—C21A	111 (3)
C14A—C13—C12	108.9 (6)	C20A—C19A—Si1A	110 (3)
C14—C13—C12	108.9 (6)	C21A—C19A—Si1A	114 (3)
O5—C13—H13	108.9	C20A—C19A—H19A	106.9

Table A5 (Continued)

C14—C13—H13	108.9	C21A—C19A—H19A	106.9
C12—C13—H13	108.9	Si1A—C19A—H19A	106.9
O5—C13—H13A	108.9	C19A—C20A—H20D	109.5
C14A—C13—H13A	108.9	C19A—C20A—H20E	109.5
C12—C13—H13A	108.9	H20D—C20A—H20E	109.5
C15—C14—C13	173.3 (17)	C19A—C20A—H20F	109.5
C14—C15—Si1	168 (3)	H20D—C20A—H20F	109.5
C15—Si1—C16	104.6 (11)	H20E—C20A—H20F	109.5
C15—Si1—C19	108.3 (14)	C19A—C21A—H21D	109.5
C16—Si1—C19	111.1 (8)	C19A—C21A—H21E	109.5
C15—Si1—C22	103.5 (9)	H21D—C21A—H21E	109.5
C16—Si1—C22	111.5 (7)	C19A—C21A—H21F	109.5
C19—Si1—C22	116.8 (9)	H21D—C21A—H21F	109.5
C18—C16—C17	111.7 (13)	H21E—C21A—H21F	109.5
C18—C16—Si1	109.4 (8)	C24A—C22A—C23A	112 (3)
C17—C16—Si1	114.1 (12)	C24A—C22A—Si1A	114 (3)
C18—C16—H16	107.1	C23A—C22A—Si1A	104 (2)
C17—C16—H16	107.1	C24A—C22A—H22A	108.8
Si1—C16—H16	107.1	C23A—C22A—H22A	108.8
C16—C17—H17A	109.5	Si1A—C22A—H22A	108.8
C16—C17—H17B	109.5	C22A—C23A—H23D	109.5
H17A—C17—H17B	109.5	C22A—C23A—H23E	109.5
C16—C17—H17C	109.5	H23D—C23A—H23E	109.5
H17A—C17—H17C	109.5	C22A—C23A—H23F	109.5
H17B—C17—H17C	109.5	H23D—C23A—H23F	109.5
C16—C18—H18A	109.5	H23E—C23A—H23F	109.5
C16—C18—H18B	109.5	C22A—C24A—H24D	109.5
H18A—C18—H18B	109.5	C22A—C24A—H24E	109.5
C16—C18—H18C	109.5	H24D—C24A—H24E	109.5
H18A—C18—H18C	109.5	C22A—C24A—H24F	109.5
H18B—C18—H18C	109.5	H24D—C24A—H24F	109.5
C20—C19—C21	109.7 (19)	H24E—C24A—H24F	109.5
C20—C19—Si1	116.0 (15)	O3—N1—C10	131.2 (6)
C21—C19—Si1	111.6 (15)	O3—N1—O2	114.7 (4)
C20—C19—H19	106.3	C10—N1—O2	114.1 (5)

Table A5 (Continued)

C21—C19—H19	106.3	C8—O1—C7	113.6 (5)
Si1—C19—H19	106.3	N1—O2—C12	107.2 (4)
C19—C20—H20A	109.5	C11—O4—H4A	109.5
C19—C20—H20B	109.5	C13—O5—H5A	109.5
H20A—C20—H20B	109.5		
C6—C1—C2—C3	-0.4 (13)	C15—Si1—C16—C18	64.9 (15)
C1—C2—C3—C4	0.8 (13)	C19—Si1—C16—C18	-178.5 (10)
C2—C3—C4—C5	-0.5 (14)	C22—Si1—C16—C18	-46.4 (12)
C3—C4—C5—C6	0.0 (13)	C15—Si1—C16—C17	-61.1 (16)
C2—C1—C6—C5	-0.1 (12)	C19—Si1—C16—C17	55.5 (14)
C2—C1—C6—C7	179.2 (8)	C22—Si1—C16—C17	-172.4 (12)
C4—C5—C6—C1	0.3 (12)	C15—Si1—C19—C20	37 (2)
C4—C5—C6—C7	-179.0 (8)	C16—Si1—C19—C20	-77.8 (18)
C1—C6—C7—O1	-12.5 (9)	C22—Si1—C19—C20	152.8 (17)
C5—C6—C7—O1	166.8 (7)	C15—Si1—C19—C21	163.2 (17)
O1—C8—C10—N1	-114.6 (6)	C16—Si1—C19—C21	48.9 (19)
C9—C8—C10—N1	125.6 (7)	C22—Si1—C19—C21	-80.5 (18)
O1—C8—C10—C11	63.3 (9)	O5—C13—C14A—C15A	79 (28)
C9—C8—C10—C11	-56.4 (9)	C12—C13—C14A—C15A	-42 (28)
N1—C10—C11—O4	-117.9 (6)	C15A—Si1A—C16A—C18A	39 (4)
C8—C10—C11—O4	64.0 (8)	C22A—Si1A—C16A—C18A	-95 (3)
N1—C10—C11—C12	4.9 (7)	C19A—Si1A—C16A—C18A	157 (2)
C8—C10—C11—C12	-173.2 (6)	C15A—Si1A—C16A—C17A	163 (4)
O4—C11—C12—O2	116.0 (5)	C22A—Si1A—C16A—C17A	29 (3)
C10—C11—C12—O2	-7.1 (6)	C19A—Si1A—C16A—C17A	-79 (2)
O4—C11—C12—C13	-124.6 (6)	C8—C10—N1—O3	-0.7 (11)
C10—C11—C12—C13	112.3 (6)	C11—C10—N1—O3	-179.0 (6)
O2—C12—C13—O5	67.1 (6)	C8—C10—N1—O2	177.5 (5)
C11—C12—C13—O5	-50.6 (7)	C11—C10—N1—O2	-0.9 (7)
O2—C12—C13—C14A	-170.4 (5)	C10—C8—O1—C7	65.1 (7)
C11—C12—C13—C14A	71.9 (7)	C9—C8—O1—C7	-171.1 (6)
O2—C12—C13—C14	-170.4 (5)	C6—C7—O1—C8	172.2 (5)
C11—C12—C13—C14	71.9 (7)	O3—N1—O2—C12	174.4 (5)
C14—C15—Si1—C16	-15 (11)	C10—N1—O2—C12	-4.0 (7)

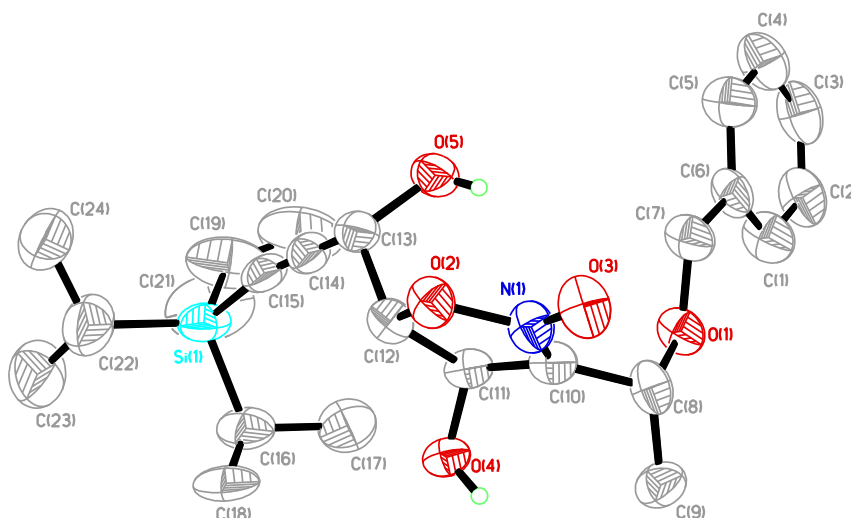
Table A5 (Continued)

C14—C15—Si1—C19	-134 (11)	C13—C12—O2—N1	-116.4 (5)
C14—C15—Si1—C22	102 (10)	C11—C12—O2—N1	6.8 (6)

Table A6. Hydrogen-bond parameters

$D-H\cdots A$	$D-H$ (Å)	$H\cdots A$ (Å)	$D\cdots A$ (Å)	$D-H\cdots A$ (°)
O4—H4A \cdots O3 ⁱ	0.84	2.43	2.727 (6)	101.5
O5—H5A \cdots O2	0.84	2.46	2.871 (6)	111.1

Symmetry code(s): (i) $-x+1, y-1/2, -z+1$.

**Figure A3.** Perspective views showing 50% probability displacement

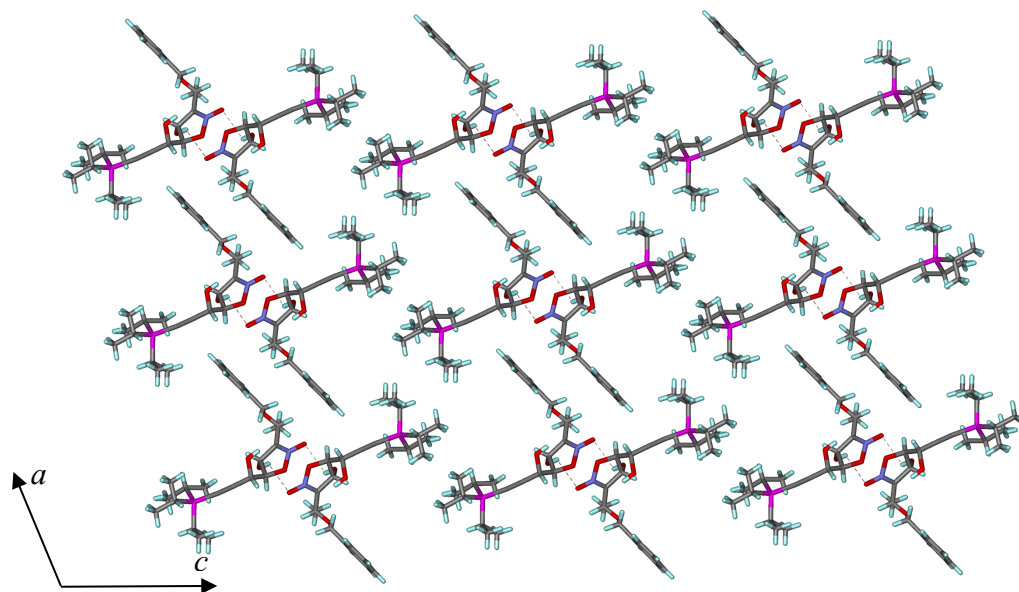
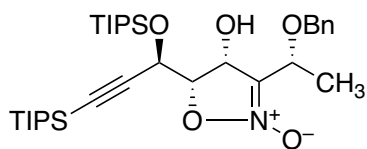


Figure A4. Three-dimensional supramolecular architecture viewed along the *b*-axis direction.

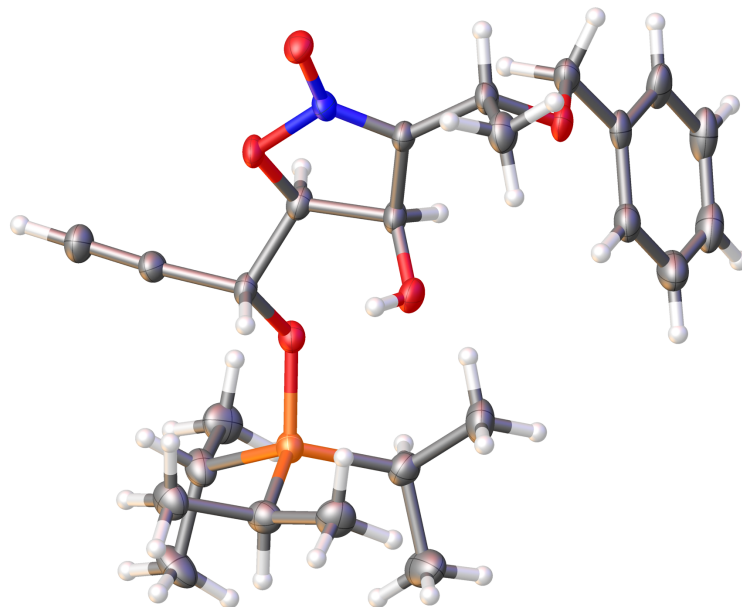
X-ray Crystallographic Laboratory Structure Report

Dr. Shao-Liang Zheng, Harvard University

December 10, 2015



3.44b



X-Ray Crystallography: A crystal mounted on a diffractometer was collected data at 100 K. The intensities of the reflections were collected by means of a Bruker APEX II DUO CCD diffractometer (Cu $K\alpha$ radiation, $\lambda=1.54178$ Å), and equipped with an Oxford Cryosystems nitrogen flow apparatus. The collection method involved 1.0° scans in ω at -30°, -55°, -80°, 30°, 55°, 80° and 115° in 2θ . Data integration down to 0.84 Å resolution was carried out using SAINT V8.34 C with reflection spot size optimization. Absorption corrections were made with the program SADABS (Bruker diffractometer, 2014). The structure was solved by the Intrinsic Phasing methods and refined by least-squares methods again F^2 using SHELXT-2014 and SHELXL-2014 with OLEX 2 interface. Non-hydrogen atoms were refined anisotropically, and hydrogen atoms were allowed to ride on the respective atoms. Crystal data as well as details of data collection and refinement are summarized in Table B.7, geometric parameters are shown in Table B.8 and hydrogen-bond parameters are listed in Table B.9. The Ortep plots produced with SHELXL-2014 program, and the other drawings were produced with Accelrys DS Visualizer 2.0.

Table A7. Experimental details

	mm8-092
Crystal data	
Chemical formula	C ₂₄ H ₃₇ NO ₅ Si
M_r	447.63
Crystal system, space group	Monoclinic, $P2_1$
Temperature (K)	100
a, b, c (Å)	10.4700 (7), 6.9042 (4), 17.1454 (10)
β (°)	92.914 (5)
V (Å ³)	1237.79 (13)
Z	2
Radiation type	Cu $K\alpha$
μ (mm ⁻¹)	1.11
Crystal size (mm)	0.16 × 0.08 × 0.01

Table A7 (Continued)

Data collection	
Diffractionmeter	Bruker D8 goniometer with CCD area detector diffractometer
Absorption correction	Multi-scan <i>SADABS</i>
T_{\min} , T_{\max}	0.688, 0.864
No. of measured, independent and observed [$I > 2\sigma(I)$] reflections	16287, 3956, 3393
R_{int}	0.081
$(\sin \theta/\lambda)_{\text{max}}$ (\AA^{-1})	0.596
Refinement	
$R[F^2 > 2\sigma(F^2)]$, $wR(F^2)$, S	0.055, 0.143, 1.10
No. of reflections	3956
No. of parameters	291
No. of restraints	1
H-atom treatment	H atoms treated by a mixture of independent and constrained refinement
$\Delta\rho_{\text{max}}$, $\Delta\rho_{\text{min}}$ (e \AA^{-3})	0.32, -0.41
Absolute structure	Flack x determined using 1252 quotients $[(I^+)-(I^-)]/[(I^+)+(I^-)]$ (Parsons, Flack and Wagner, Acta Cryst. B69 (2013) 249-259).
Absolute structure parameter	0.01 (5)

Computer programs: *APEX3* v2015.5.2 (Bruker-AXS, 2015), *SAINT* 8.34C (Bruker-AXS, 2014), *SHELXT2014* (Sheldrick, 2015), *SHELXL2014* (Sheldrick, 2015), Bruker *SHELXTL* (Sheldrick, 2015).

Table A8. Geometric parameters (\AA , $^\circ$)

C1—C2	1.184 (7)	C16—C17	1.534 (8)
C1—H1	0.9500	C16—C18	1.535 (7)
C2—C3	1.480 (7)	C16—Si1	1.885 (5)
C3—O1	1.419 (5)	C16—H16	1.0000
C3—C4	1.529 (6)	C17—H17A	0.9800
C3—H3	1.0000	C17—H17B	0.9800
C4—O4	1.454 (5)	C17—H17C	0.9800
C4—C5	1.537 (6)	C18—H18A	0.9800

Table A8 (Continued)

C4—H4	1.0000	C18—H18B	0.9800
C5—O2	1.410 (6)	C18—H18C	0.9800
C5—C6	1.495 (6)	C19—C21	1.538 (7)
C5—H5	1.0000	C19—C20	1.542 (7)
C6—N1	1.300 (6)	C19—Si1	1.882 (6)
C6—C7	1.505 (6)	C19—H19	1.0000
C7—O3	1.426 (6)	C20—H20A	0.9800
C7—C15	1.516 (7)	C20—H20B	0.9800
C7—H7	1.0000	C20—H20C	0.9800
C8—O3	1.435 (6)	C21—H21A	0.9800
C8—C9	1.508 (7)	C21—H21B	0.9800
C8—H8A	0.9900	C21—H21C	0.9800
C8—H8B	0.9900	C22—C23	1.525 (7)
C9—C10	1.379 (8)	C22—C24	1.532 (7)
C9—C14	1.392 (8)	C22—Si1	1.880 (5)
C10—C11	1.396 (7)	C22—H22	1.0000
C10—H10	0.9500	C23—H23A	0.9800
C11—C12	1.371 (9)	C23—H23B	0.9800
C11—H11	0.9500	C23—H23C	0.9800
C12—C13	1.385 (9)	C24—H24A	0.9800
C12—H12	0.9500	C24—H24B	0.9800
C13—C14	1.403 (8)	C24—H24C	0.9800
C13—H13	0.9500	N1—O5	1.259 (5)
C14—H14	0.9500	N1—O4	1.435 (4)
C15—H15A	0.9800	O1—Si1	1.672 (3)
C15—H15B	0.9800	O2—H2	0.84 (8)
C15—H15C	0.9800		
C2—C1—H1	180.0	C18—C16—H16	106.3
C1—C2—C3	176.0 (5)	Si1—C16—H16	106.3
O1—C3—C2	112.5 (3)	C16—C17—H17A	109.5
O1—C3—C4	105.6 (4)	C16—C17—H17B	109.5
C2—C3—C4	109.9 (4)	H17A—C17—H17B	109.5
O1—C3—H3	109.6	C16—C17—H17C	109.5
C2—C3—H3	109.6	H17A—C17—H17C	109.5

Table A8 (Continued)

C4—C3—H3	109.6	H17B—C17—H17C	109.5
O4—C4—C3	107.5 (4)	C16—C18—H18A	109.5
O4—C4—C5	105.5 (3)	C16—C18—H18B	109.5
C3—C4—C5	115.0 (4)	H18A—C18—H18B	109.5
O4—C4—H4	109.6	C16—C18—H18C	109.5
C3—C4—H4	109.6	H18A—C18—H18C	109.5
C5—C4—H4	109.6	H18B—C18—H18C	109.5
O2—C5—C6	110.1 (4)	C21—C19—C20	110.6 (4)
O2—C5—C4	117.0 (4)	C21—C19—Si1	116.6 (4)
C6—C5—C4	99.9 (4)	C20—C19—Si1	113.9 (4)
O2—C5—H5	109.8	C21—C19—H19	104.8
C6—C5—H5	109.8	C20—C19—H19	104.8
C4—C5—H5	109.8	Si1—C19—H19	104.8
N1—C6—C5	110.2 (4)	C19—C20—H20A	109.5
N1—C6—C7	121.0 (4)	C19—C20—H20B	109.5
C5—C6—C7	128.5 (4)	H20A—C20—H20B	109.5
O3—C7—C6	108.6 (4)	C19—C20—H20C	109.5
O3—C7—C15	107.1 (4)	H20A—C20—H20C	109.5
C6—C7—C15	112.0 (4)	H20B—C20—H20C	109.5
O3—C7—H7	109.7	C19—C21—H21A	109.5
C6—C7—H7	109.7	C19—C21—H21B	109.5
C15—C7—H7	109.7	H21A—C21—H21B	109.5
O3—C8—C9	109.9 (4)	C19—C21—H21C	109.5
O3—C8—H8A	109.7	H21A—C21—H21C	109.5
C9—C8—H8A	109.7	H21B—C21—H21C	109.5
O3—C8—H8B	109.7	C23—C22—C24	109.9 (4)
C9—C8—H8B	109.7	C23—C22—Si1	113.2 (4)
H8A—C8—H8B	108.2	C24—C22—Si1	113.9 (3)
C10—C9—C14	119.5 (5)	C23—C22—H22	106.4
C10—C9—C8	122.0 (5)	C24—C22—H22	106.4
C14—C9—C8	118.3 (5)	Si1—C22—H22	106.4
C9—C10—C11	120.4 (6)	C22—C23—H23A	109.5
C9—C10—H10	119.8	C22—C23—H23B	109.5
C11—C10—H10	119.8	H23A—C23—H23B	109.5
C12—C11—C10	120.3 (6)	C22—C23—H23C	109.5

Table A8 (Continued)

C12—C11—H11	119.9	H23A—C23—H23C	109.5
C10—C11—H11	119.9	H23B—C23—H23C	109.5
C11—C12—C13	120.1 (5)	C22—C24—H24A	109.5
C11—C12—H12	119.9	C22—C24—H24B	109.5
C13—C12—H12	119.9	H24A—C24—H24B	109.5
C12—C13—C14	119.8 (6)	C22—C24—H24C	109.5
C12—C13—H13	120.1	H24A—C24—H24C	109.5
C14—C13—H13	120.1	H24B—C24—H24C	109.5
C9—C14—C13	119.9 (6)	O5—N1—C6	132.6 (4)
C9—C14—H14	120.1	O5—N1—O4	114.4 (3)
C13—C14—H14	120.1	C6—N1—O4	112.9 (4)
C7—C15—H15A	109.5	C3—O1—Si1	127.9 (3)
C7—C15—H15B	109.5	C5—O2—H2	117 (6)
H15A—C15—H15B	109.5	C7—O3—C8	113.0 (4)
C7—C15—H15C	109.5	N1—O4—C4	104.0 (3)
H15A—C15—H15C	109.5	O1—Si1—C22	103.0 (2)
H15B—C15—H15C	109.5	O1—Si1—C19	114.1 (2)
C17—C16—C18	109.8 (4)	C22—Si1—C19	113.2 (2)
C17—C16—Si1	112.5 (3)	O1—Si1—C16	107.2 (2)
C18—C16—Si1	115.0 (4)	C22—Si1—C16	110.3 (2)
C17—C16—H16	106.3	C19—Si1—C16	108.7 (2)
O1—C3—C4—O4	179.1 (3)	C2—C3—O1—Si1	-84.3 (5)
C2—C3—C4—O4	57.6 (5)	C4—C3—O1—Si1	155.9 (3)
O1—C3—C4—C5	-63.8 (5)	C6—C7—O3—C8	73.1 (5)
C2—C3—C4—C5	174.7 (4)	C15—C7—O3—C8	-165.7 (4)
O4—C4—C5—O2	91.9 (5)	C9—C8—O3—C7	-156.6 (4)
C3—C4—C5—O2	-26.3 (6)	O5—N1—O4—C4	170.6 (4)
O4—C4—C5—C6	-26.8 (5)	C6—N1—O4—C4	-12.0 (5)
C3—C4—C5—C6	-145.0 (4)	C3—C4—O4—N1	147.5 (3)
O2—C5—C6—N1	-103.3 (5)	C5—C4—O4—N1	24.3 (5)
C4—C5—C6—N1	20.4 (5)	C3—O1—Si1—C22	-149.6 (3)
O2—C5—C6—C7	69.8 (6)	C3—O1—Si1—C19	-26.4 (4)
C4—C5—C6—C7	-166.5 (5)	C3—O1—Si1—C16	94.0 (4)
N1—C6—C7—O3	-162.7 (5)	C23—C22—Si1—O1	170.0 (4)

Table A8 (Continued)

C5—C6—C7—O3	24.8 (7)	C24—C22—Si1—O1	43.5 (4)
N1—C6—C7—C15	79.2 (6)	C23—C22—Si1—C19	46.3 (5)
C5—C6—C7—C15	-93.3 (6)	C24—C22—Si1—C19	-80.2 (4)
O3—C8—C9—C10	26.4 (6)	C23—C22—Si1—C16	-75.8 (5)
O3—C8—C9—C14	-158.1 (4)	C24—C22—Si1—C16	157.7 (4)
C14—C9—C10—C11	0.3 (7)	C21—C19—Si1—O1	-67.6 (4)
C8—C9—C10—C11	175.7 (5)	C20—C19—Si1—O1	63.1 (4)
C9—C10—C11—C12	-1.3 (8)	C21—C19—Si1—C22	49.8 (4)
C10—C11—C12—C13	1.4 (9)	C20—C19—Si1—C22	-179.5 (3)
C11—C12—C13—C14	-0.6 (8)	C21—C19—Si1—C16	172.8 (4)
C10—C9—C14—C13	0.5 (7)	C20—C19—Si1—C16	-56.5 (4)
C8—C9—C14—C13	-175.1 (5)	C17—C16—Si1—O1	64.1 (4)
C12—C13—C14—C9	-0.3 (8)	C18—C16—Si1—O1	-169.2 (4)
C5—C6—N1—O5	170.6 (5)	C17—C16—Si1—C22	-47.4 (5)
C7—C6—N1—O5	-3.1 (9)	C18—C16—Si1—C22	79.3 (5)
C5—C6—N1—O4	-6.2 (6)	C17—C16—Si1—C19	-172.1 (4)
C7—C6—N1—O4	-179.9 (4)	C18—C16—Si1—C19	-45.4 (5)

Table A9. Hydrogen-bond parameters

$D-H\cdots A$	$D-H$ (Å)	$H\cdots A$ (Å)	$D\cdots A$ (Å)	$D-H\cdots A$ (°)
O2—H2 \cdots O5 ⁱ	0.84 (8)	1.97 (8)	2.798 (5)	167 (8)

Symmetry code(s): (i) $-x+1, y-1/2, -z+1$.

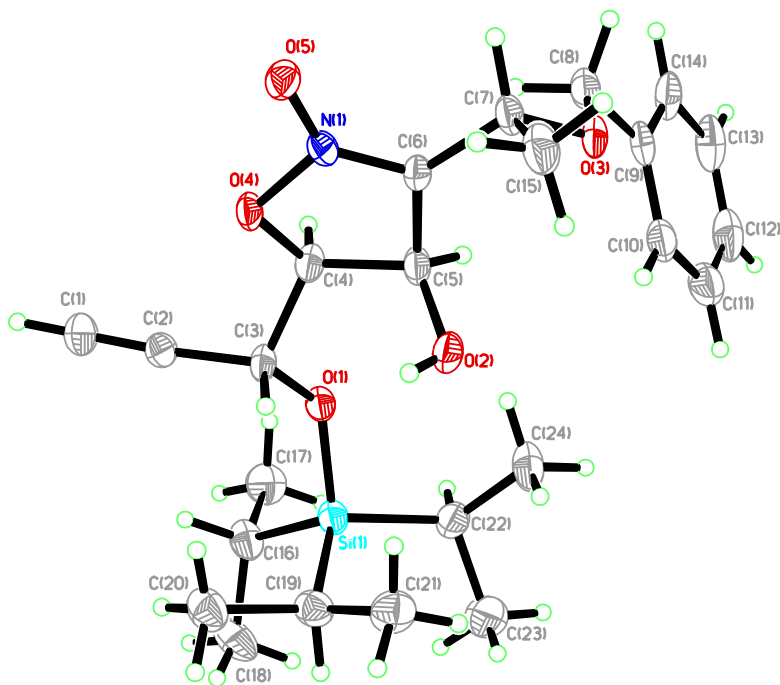


Figure A5. Perspective views showing 50% probability displacement

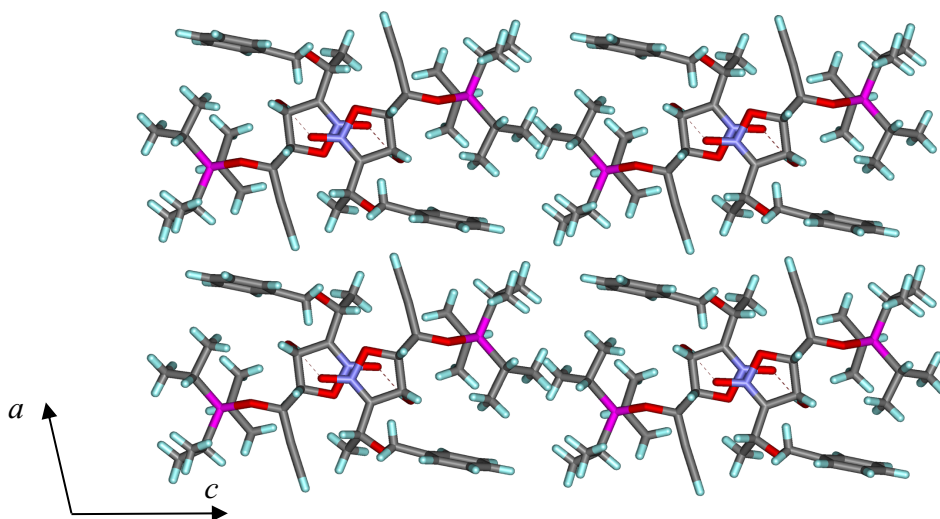
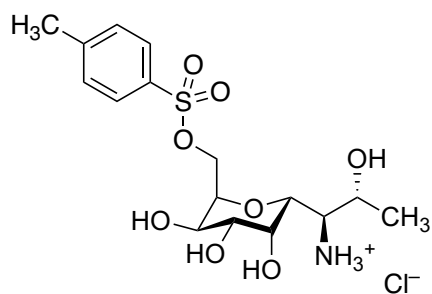


Figure A6. Three-dimensional supramolecular architecture viewed along the *b*-axis direction.

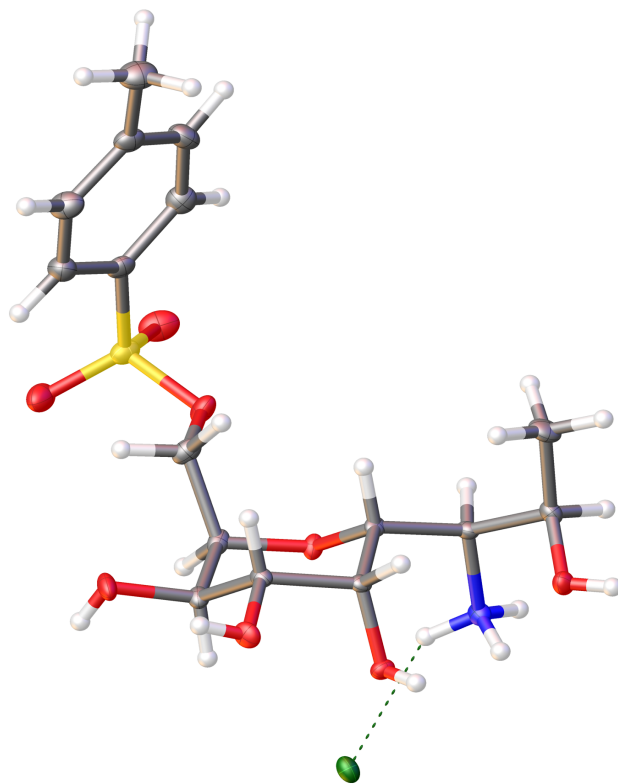
X-ray Crystallographic Laboratory Structure Report

Dr. Shao-Liang Zheng, Harvard University

December 10, 2015



3.60



X-Ray Crystallography: A crystal mounted on a diffractometer was collected data at 100 K. The intensities of the reflections were collected by means of a Bruker APEX II CCD diffractometer (MoK α radiation, $\lambda=0.71073$ Å), and equipped with an Oxford Cryosystems nitrogen flow apparatus. The collection method involved 0.5° scans in ω at 28° in 2θ . Data integration down to 0.78 Å resolution was carried out using SAINT V8.37A with reflection spot size optimization. Absorption corrections were made with the program SADABS.¹⁸⁴ The structure was solved by the Intrinsic Phasing methods and refined by least-squares methods again F^2 using SHELXT-2014 and SHELXL-2014 with OLEX 2 interface. Non-hydrogen atoms were refined anisotropically, and hydrogen atoms were allowed to ride on the respective atoms. Crystal data as well as details of data collection and refinement are summarized in Table B.10, geometric parameters are shown in Table B.11 and hydrogen-bond parameters are listed in Table B.12. The Ortep plots produced with SHELXL-2014 program, and the other drawings were produced with Accelrys DS Visualizer 2.0.

Table A10. Experimental details

	mm11-029-c
Crystal data	
Chemical formula	C ₁₆ H ₂₆ ClNO ₈ S
M_r	427.89
Crystal system, space group	Monoclinic, $P2_1$
Temperature (K)	100
a, b, c (Å)	6.0507 (3), 9.9307 (4), 16.3874 (7)
β (°)	97.2807 (15)
V (Å ³)	976.74 (8)
Z	2
Radiation type	Mo $K\alpha$
μ (mm ⁻¹)	0.35

¹⁸⁴ Bruker AXS APEX3, Bruker AXS, Madison, Wisconsin, 2016.

Table A10 (Continued)

Crystal size (mm)	0.20 × 0.12 × 0.06
Data collection	
Diffractometer	Bruker D8 goniometer with CCD area detector
Absorption correction	Multi-scan <i>SADABS</i>
T_{\min}, T_{\max}	0.806, 0.862
No. of measured, independent and observed [$I > 2\sigma(I)$] reflections	7929, 4202, 3942
R_{int}	0.020
$(\sin \theta/\lambda)_{\text{max}}$ (\AA^{-1})	0.641
Refinement	
$R[F^2 > 2\sigma(F^2)], wR(F^2), S$	0.032, 0.067, 1.08
No. of reflections	4202
No. of parameters	274
No. of restraints	1
H-atom treatment	H atoms treated by a mixture of independent and constrained refinement
$\Delta\rho_{\text{max}}, \Delta\rho_{\text{min}}$ (e \AA^{-3})	0.22, -0.29
Absolute structure	Flack x determined using 1719 quotients [(I+)-(I-)]/[(I+)+(I-)] (Parsons, Flack and Wagner, Acta Cryst. B69 (2013) 249-259).
Absolute structure parameter	-0.02 (2)

Computer programs: *APEX3* v2016.1-0 (Bruker-AXS, 2016), *SAINT* 8.37A (Bruker-AXS, 2016), *SHELXT2014* (Sheldrick, 2015), *SHELXL2014* (Sheldrick, 2015), Bruker *SHELXTL* (Sheldrick, 2015).

Table A11. Geometric parameters ($\text{\AA}, ^\circ$)

S1—O8	1.428 (2)	C4—C5	1.524 (4)
S1—O7	1.434 (2)	C4—H4A	1.0000
S1—O6	1.578 (2)	C5—C6	1.531 (4)
S1—C10	1.747 (3)	C5—H5A	1.0000
O1—C2	1.428 (3)	C6—C7	1.506 (4)
O1—H1	0.72 (4)	C6—H6	1.0000

Table A11 (Continued)

O2—C8	1.435 (3)	C7—C8	1.524 (4)
O2—C4	1.435 (3)	C7—H7	1.0000
O3—C5	1.432 (3)	C8—C9	1.525 (4)
O3—H3	0.74 (4)	C8—H8	1.0000
O4—C6	1.430 (3)	C9—H9A	0.9900
O4—H4	0.76 (4)	C9—H9B	0.9900
O5—C7	1.431 (3)	C10—C11	1.387 (4)
O5—H5	0.73 (4)	C10—C15	1.394 (4)
O6—C9	1.471 (3)	C11—C12	1.387 (4)
N1—C3	1.491 (4)	C11—H11	0.9500
N1—H1A	0.84 (4)	C12—C13	1.387 (5)
N1—H1B	0.91 (4)	C12—H12	0.9500
N1—H1C	0.90 (4)	C13—C14	1.391 (5)
C1—C2	1.513 (4)	C13—C16	1.505 (4)
C1—H1D	0.9800	C14—C15	1.383 (4)
C1—H1E	0.9800	C14—H14	0.9500
C1—H1F	0.9800	C15—H15	0.9500
C2—C3	1.525 (4)	C16—H16A	0.9800
C2—H2	1.0000	C16—H16B	0.9800
C3—C4	1.530 (4)	C16—H16C	0.9800
C3—H3A	1.0000		
O8—S1—O7	119.62 (15)	O4—C6—C7	110.6 (2)
O8—S1—O6	103.82 (12)	O4—C6—C5	107.8 (2)
O7—S1—O6	108.86 (12)	C7—C6—C5	111.2 (2)
O8—S1—C10	110.90 (14)	O4—C6—H6	109.1
O7—S1—C10	109.04 (15)	C7—C6—H6	109.1
O6—S1—C10	103.23 (12)	C5—C6—H6	109.1
C2—O1—H1	108 (3)	O5—C7—C6	108.3 (2)
C8—O2—C4	115.4 (2)	O5—C7—C8	111.0 (2)
C5—O3—H3	106 (3)	C6—C7—C8	111.7 (2)
C6—O4—H4	106 (3)	O5—C7—H7	108.6
C7—O5—H5	105 (3)	C6—C7—H7	108.6
C9—O6—S1	117.63 (16)	C8—C7—H7	108.6
C3—N1—H1A	110 (2)	O2—C8—C7	110.2 (2)

Table A11 (Continued)

C3—N1—H1B	112 (2)	O2—C8—C9	111.7 (2)
H1A—N1—H1B	106 (3)	C7—C8—C9	113.3 (2)
C3—N1—H1C	114 (2)	O2—C8—H8	107.1
H1A—N1—H1C	109 (3)	C7—C8—H8	107.1
H1B—N1—H1C	107 (3)	C9—C8—H8	107.1
C2—C1—H1D	109.5	O6—C9—C8	106.3 (2)
C2—C1—H1E	109.5	O6—C9—H9A	110.5
H1D—C1—H1E	109.5	C8—C9—H9A	110.5
C2—C1—H1F	109.5	O6—C9—H9B	110.5
H1D—C1—H1F	109.5	C8—C9—H9B	110.5
H1E—C1—H1F	109.5	H9A—C9—H9B	108.7
O1—C2—C1	111.3 (2)	C11—C10—C15	120.1 (3)
O1—C2—C3	107.6 (2)	C11—C10—S1	120.1 (2)
C1—C2—C3	113.5 (2)	C15—C10—S1	119.6 (2)
O1—C2—H2	108.1	C12—C11—C10	119.5 (3)
C1—C2—H2	108.1	C12—C11—H11	120.3
C3—C2—H2	108.1	C10—C11—H11	120.3
N1—C3—C2	108.6 (2)	C11—C12—C13	121.3 (3)
N1—C3—C4	109.8 (2)	C11—C12—H12	119.3
C2—C3—C4	117.2 (2)	C13—C12—H12	119.3
N1—C3—H3A	106.9	C12—C13—C14	118.2 (3)
C2—C3—H3A	106.9	C12—C13—C16	120.7 (3)
C4—C3—H3A	106.9	C14—C13—C16	121.1 (3)
O2—C4—C5	112.1 (2)	C15—C14—C13	121.5 (3)
O2—C4—C3	102.8 (2)	C15—C14—H14	119.3
C5—C4—C3	117.1 (2)	C13—C14—H14	119.3
O2—C4—H4A	108.1	C14—C15—C10	119.2 (3)
C5—C4—H4A	108.1	C14—C15—H15	120.4
C3—C4—H4A	108.1	C10—C15—H15	120.4
O3—C5—C4	110.1 (2)	C13—C16—H16A	109.5
O3—C5—C6	109.8 (2)	C13—C16—H16B	109.5
C4—C5—C6	108.0 (2)	H16A—C16—H16B	109.5
O3—C5—H5A	109.6	C13—C16—H16C	109.5
C4—C5—H5A	109.6	H16A—C16—H16C	109.5
C6—C5—H5A	109.6	H16B—C16—H16C	109.5

Table A11 (Continued)

O8—S1—O6—C9	-176.1 (2)	C4—O2—C8—C7	-54.4 (3)
O7—S1—O6—C9	-47.6 (2)	C4—O2—C8—C9	72.5 (3)
C10—S1—O6—C9	68.1 (2)	O5—C7—C8—O2	173.5 (2)
O1—C2—C3—N1	-53.8 (3)	C6—C7—C8—O2	52.5 (3)
C1—C2—C3—N1	-177.4 (2)	O5—C7—C8—C9	47.5 (3)
O1—C2—C3—C4	71.3 (3)	C6—C7—C8—C9	-73.5 (3)
C1—C2—C3—C4	-52.3 (3)	S1—O6—C9—C8	134.41 (19)
C8—O2—C4—C5	57.4 (3)	O2—C8—C9—O6	59.8 (3)
C8—O2—C4—C3	-175.9 (2)	C7—C8—C9—O6	-175.1 (2)
N1—C3—C4—O2	-55.1 (3)	O8—S1—C10—C11	156.8 (2)
C2—C3—C4—O2	-179.6 (2)	O7—S1—C10—C11	23.1 (3)
N1—C3—C4—C5	68.3 (3)	O6—S1—C10—C11	-92.5 (2)
C2—C3—C4—C5	-56.1 (3)	O8—S1—C10—C15	-27.4 (3)
O2—C4—C5—O3	64.8 (3)	O7—S1—C10—C15	-161.2 (2)
C3—C4—C5—O3	-53.7 (3)	O6—S1—C10—C15	83.2 (2)
O2—C4—C5—C6	-55.1 (3)	C15—C10—C11—C12	-2.8 (4)
C3—C4—C5—C6	-173.6 (2)	S1—C10—C11—C12	172.9 (2)
O3—C5—C6—O4	56.1 (3)	C10—C11—C12—C13	-0.2 (4)
C4—C5—C6—O4	176.1 (2)	C11—C12—C13—C14	3.9 (4)
O3—C5—C6—C7	-65.3 (3)	C11—C12—C13—C16	-175.8 (3)
C4—C5—C6—C7	54.7 (3)	C12—C13—C14—C15	-4.7 (4)
O4—C6—C7—O5	62.9 (3)	C16—C13—C14—C15	175.0 (3)
C5—C6—C7—O5	-177.4 (2)	C13—C14—C15—C10	1.7 (4)
O4—C6—C7—C8	-174.6 (2)	C11—C10—C15—C14	2.1 (4)
C5—C6—C7—C8	-54.8 (3)	S1—C10—C15—C14	-173.7 (2)

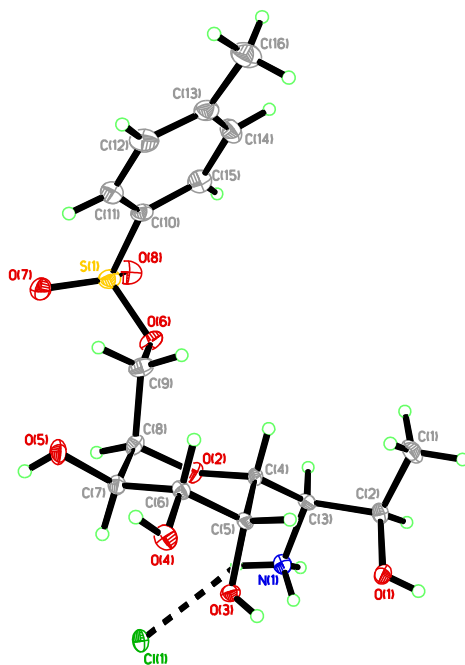
Table A12. Hydrogen-bond parameters

$D-H\cdots A$	$D-H$ (Å)	$H\cdots A$ (Å)	$D\cdots A$ (Å)	$D-H\cdots A$ (°)
O4—H4 \cdots O5	0.76 (4)	2.55 (4)	2.832 (3)	104 (4)
N1—H1B \cdots O1	0.91 (4)	2.31 (4)	2.737 (3)	108 (3)
N1—H1C \cdots O2	0.90 (4)	2.29 (4)	2.686 (3)	107 (3)
N1—H1B \cdots O3	0.91 (4)	2.43 (3)	2.789 (3)	104 (2)
O1—H1 \cdots Cl1 ⁱ	0.72 (4)	2.47 (4)	3.155 (2)	160 (4)
O3—H3 \cdots Cl1 ⁱⁱ	0.74 (4)	2.45 (4)	3.176 (2)	170 (5)

Table A12 (Continued)

O5—H5 \cdots C11 ⁱⁱⁱ	0.73 (4)	2.38 (4)	3.108 (3)	172 (4)
N1—H1A \cdots C11 ^{iv}	0.84 (4)	2.36 (4)	3.191 (3)	168 (3)
N1—H1B \cdots O4 ⁱ	0.91 (4)	2.23 (4)	2.847 (3)	125 (3)

Symmetry code(s): (i) $-x-1, y+1/2, -z$; (ii) $x-1, y, z$; (iii) $-x, y-1/2, -z$; (iv) $-x, y+1/2, -z$.

**Figure A7.** Perspective views showing 50% probability displacement

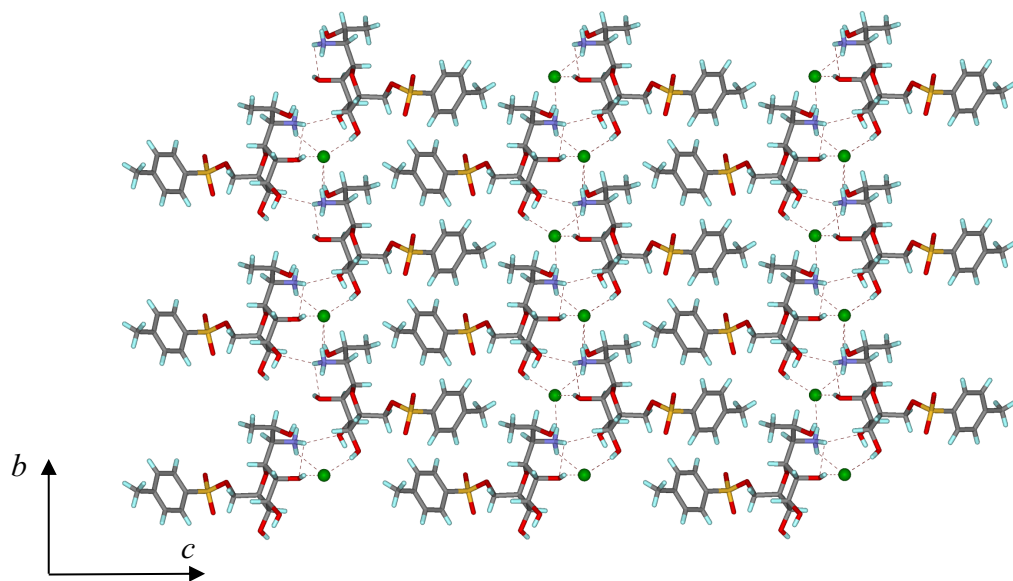


Figure A8. Three-dimensional supramolecular architecture viewed along the a -axis direction.

Appendix B. Catalog of synthetic lincosamide structures

According to Myers laboratory convention, antibiotic candidates are assigned FSA (fully synthetic antibiotic) numbers, permitting their identification according to the specific chemical experiment that generated them. The coding scheme used (as of May 2018) is depicted below:

FSA - 2 13 064

Chemist identifier — Notebook number — Page number

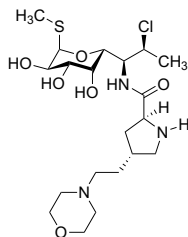
or

FSA - 2 4 035

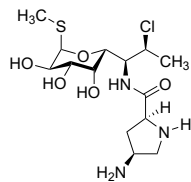
Chemist identifier — Notebook number — Page number

Identifier	Chemist
2	Matthew Mitcheltree
4	Ioana Moga
5	Katherine Silvestre
6	Jack Stevenson

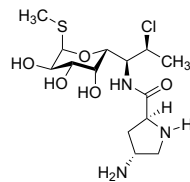
γ -Substituted prolinamides



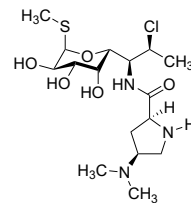
FSA-22095



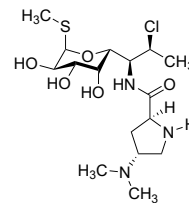
FSA-510026



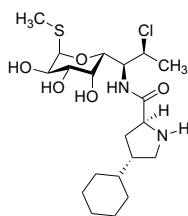
FSA-510027



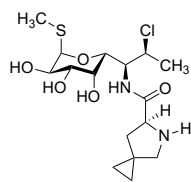
FSA-510031



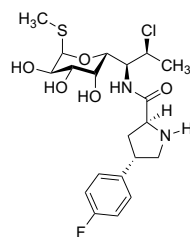
FSA-510032



FSA-412090

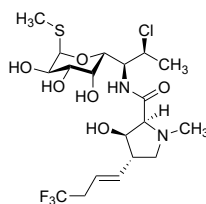


FSA-412092

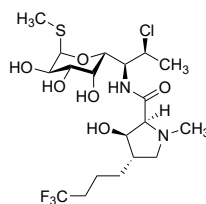


FSA-412094

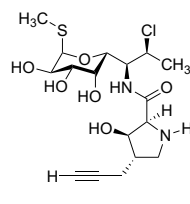
β -Hydroxy prolinamides



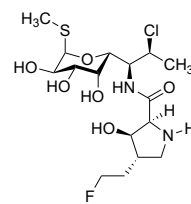
FSA-21194



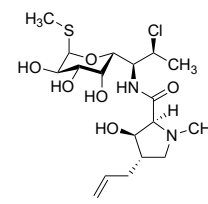
FSA-22018



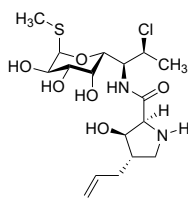
FSA-22035



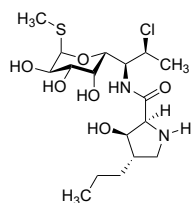
FSA-22093



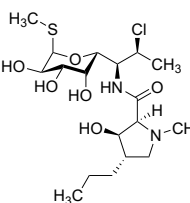
FSA-21134



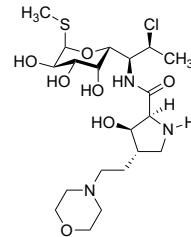
FSA-21141



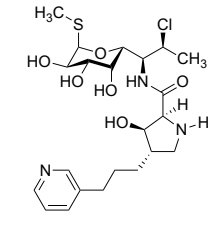
FSA-21147



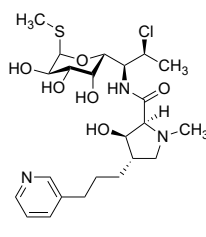
FSA-21193



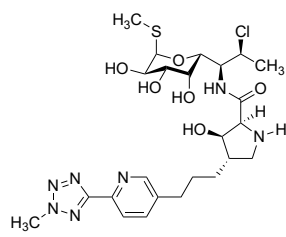
FSA-22097



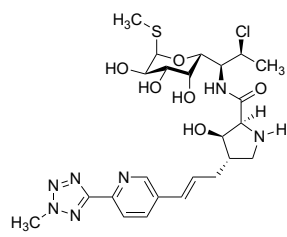
FSA-22099



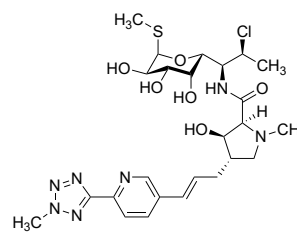
FSA-23003



FSA-23001

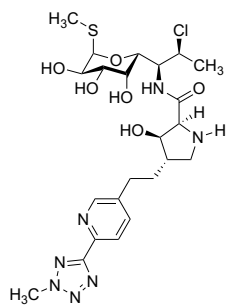


FSA-23022

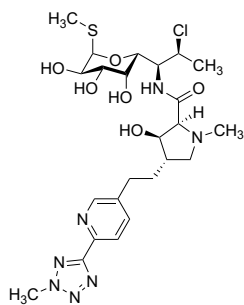


FSA-23023

β -Hydroxy prolinamides

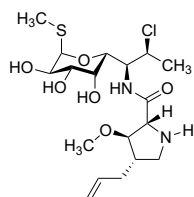


FSA-23010

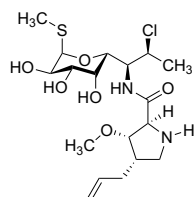


FSA-23011

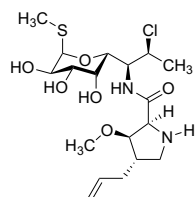
β -Alkoxy prolinamides



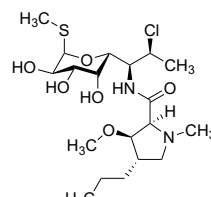
FSA-22090a



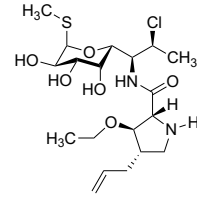
FSA-22090b



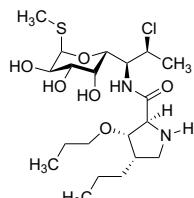
FSA-22090c



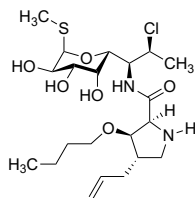
FSA-23005



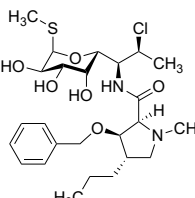
FSA-506006



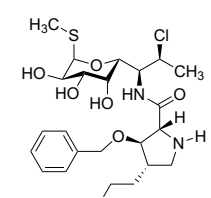
FSA-506015



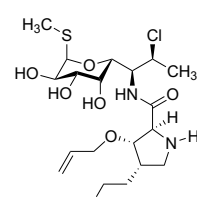
FSA-506046



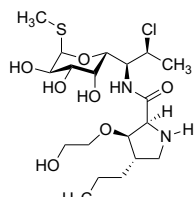
FSA-506008



FSA-506016

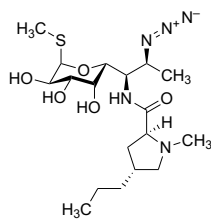


FSA-506007

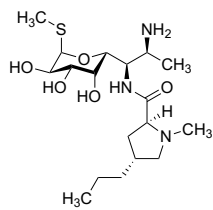


FSA-506044

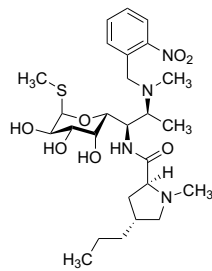
7-Deoxyaminolincomycin and derivatives



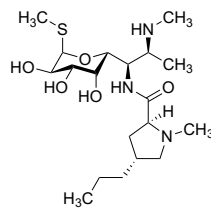
FSA-215038



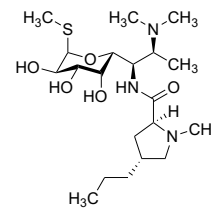
FSA-215049



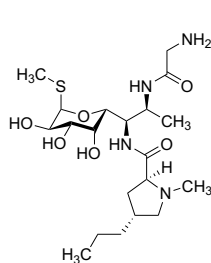
FSA-215081



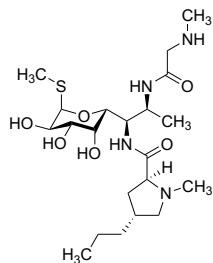
FSA-215082



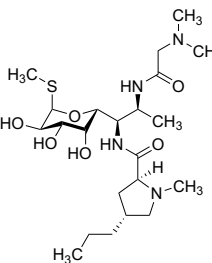
FSA-215070



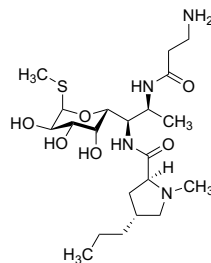
FSA-215071



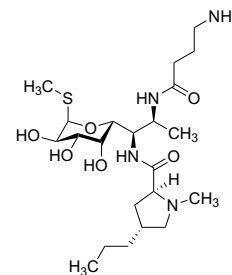
FSA-215078a



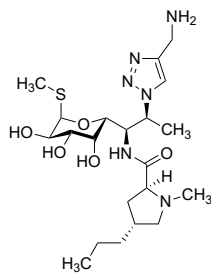
FSA-215078b



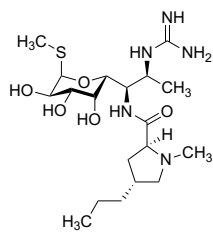
FSA-215054



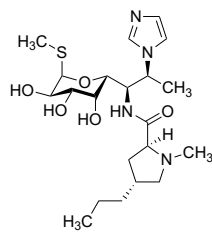
FSA-215052



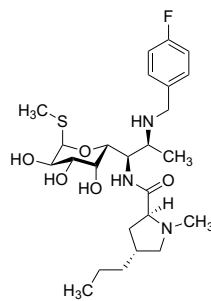
FSA-215072



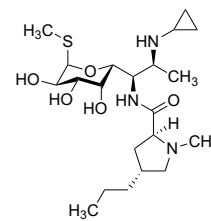
FSA-215059



FSA-215064

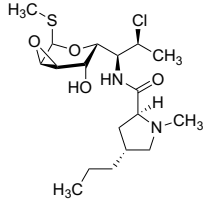


FSA-215025d

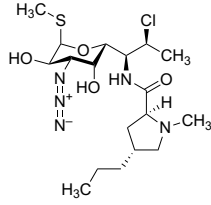


FSA-215028c

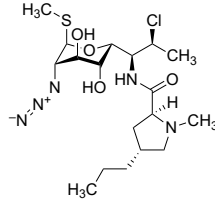
3-Modified clindamycin derivatives



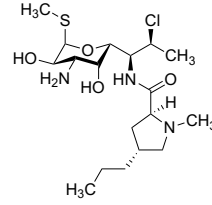
FSA-60127



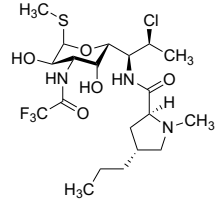
FSA-60132a



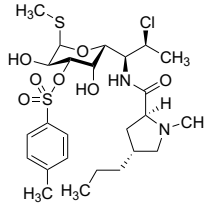
FSA-60132b



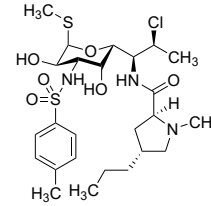
FSA-60131



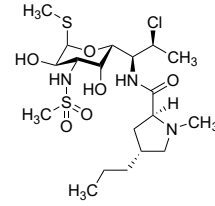
FSA-60142



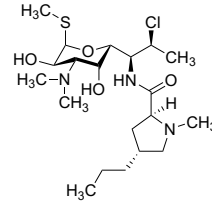
FSA-60144



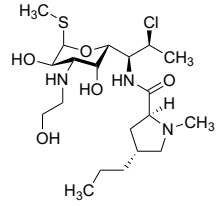
FSA-60145



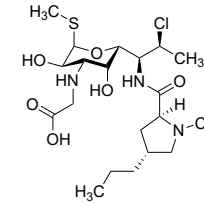
FSA-60149



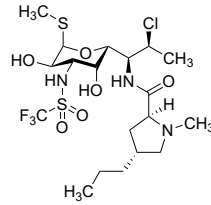
FSA-60134



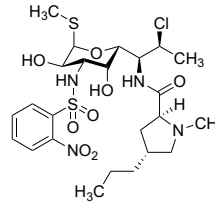
FSA-60159



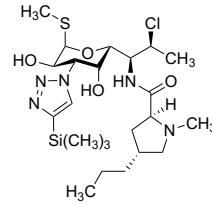
FSA-60160



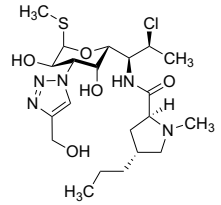
FSA-60151



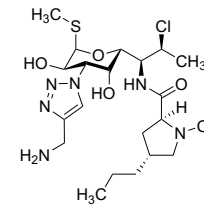
FSA-60154



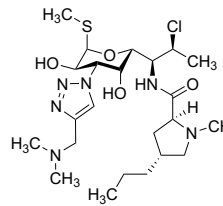
FSA-60146



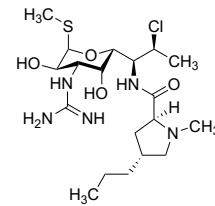
FSA-60147



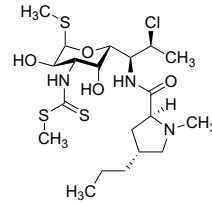
FSA-60165



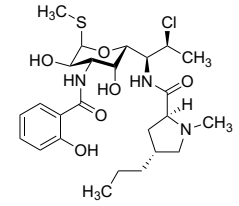
FSA-60169



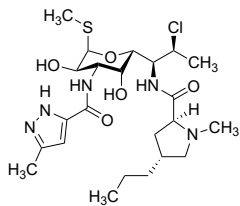
FSA-60167



FSA-60168

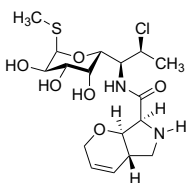


FSA-60156

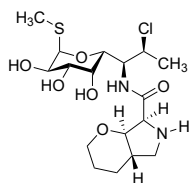


FSA-60157

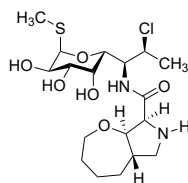
Bicyclic prolinamides



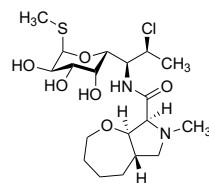
FSA-24039



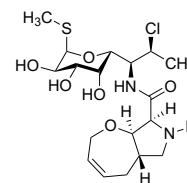
FSA-24041



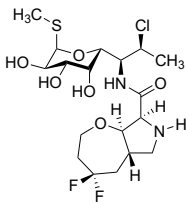
FSA-22091



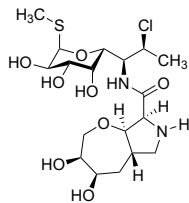
FSA-24040



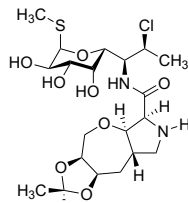
FSA-24035



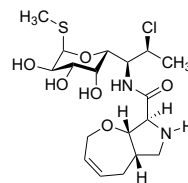
FSA-24036



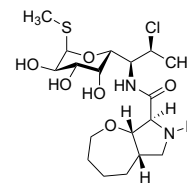
FSA-501076



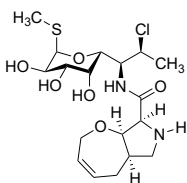
FSA-501099



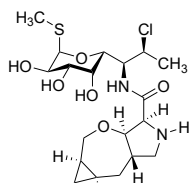
FSA-504059



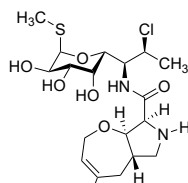
FSA-504062



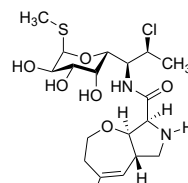
FSA-507051



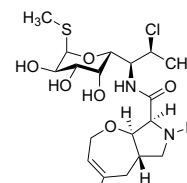
FSA-507007



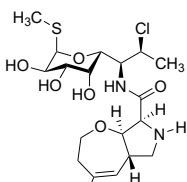
FSA-507041



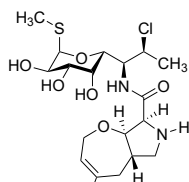
FSA-507031



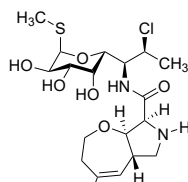
FSA-507056



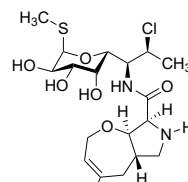
FSA-507052



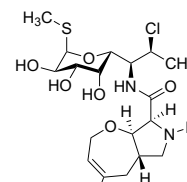
FSA-507057



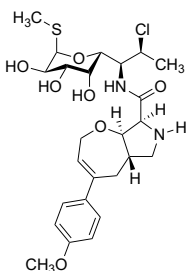
FSA-507053



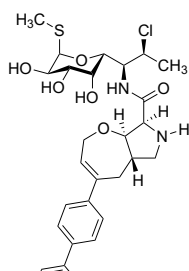
FSA-507060



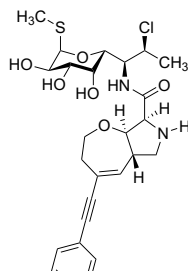
FSA-511019



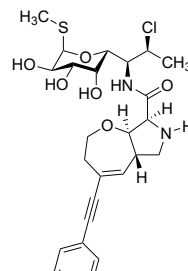
FSA-511020



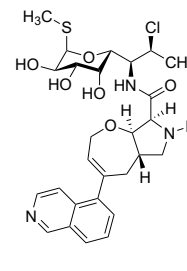
FSA-510001



FSA-510002

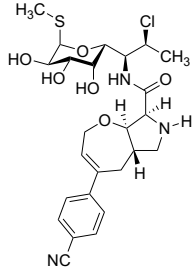


FSA-510003

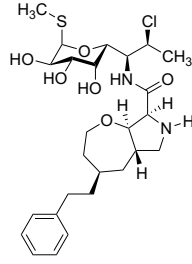


FSA-510006

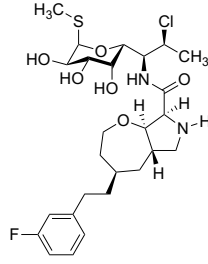
Bicyclic prolinamides



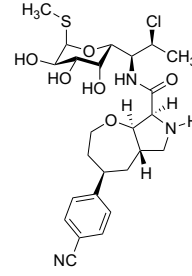
FSA-511033



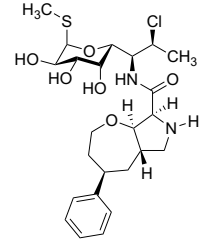
FSA-510021



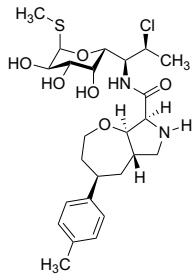
FSA-510022



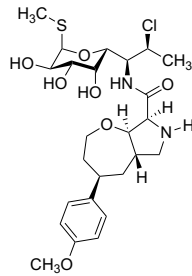
FSA-511046



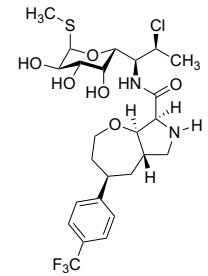
FSA-509018



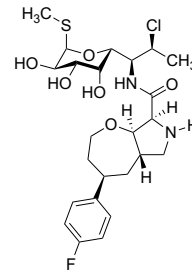
FSA-511044



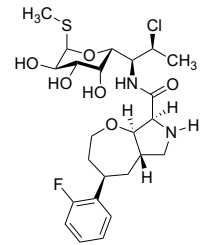
FSA-511045



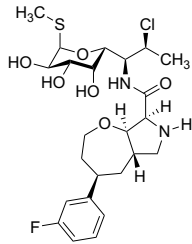
FSA-509019



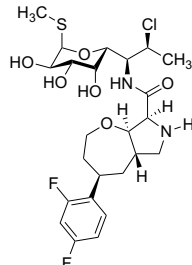
FSA-507061



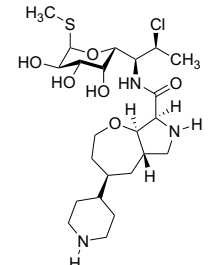
FSA-511100



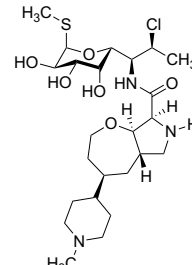
FSA-511077



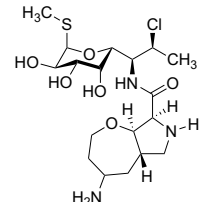
FSA-511078



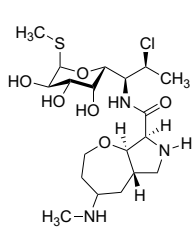
FSA-512011



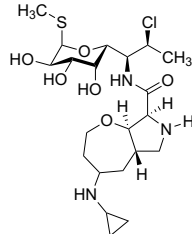
FSA-512012



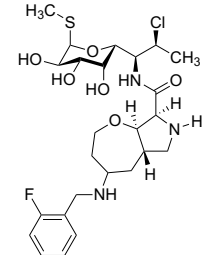
FSA-510012



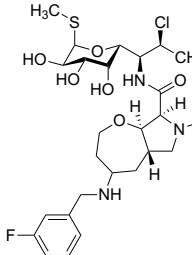
FSA-510065



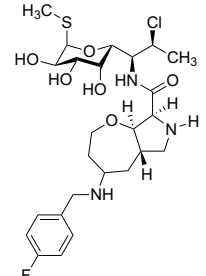
FSA-510011



FSA-510072

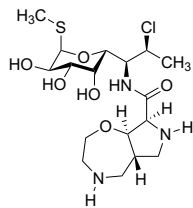


FSA-510073

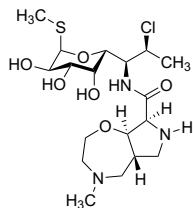


FSA-510074

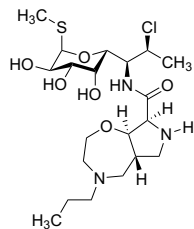
Oxazepanprolinamides



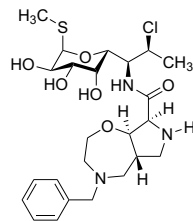
FSA-503001



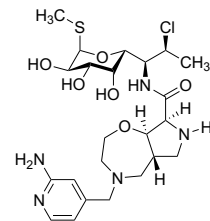
FSA-503002



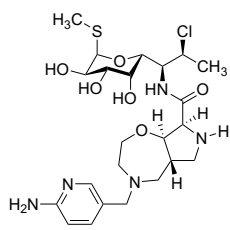
FSA-503003



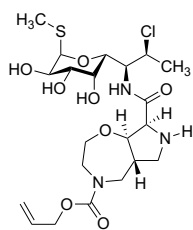
FSA-502002



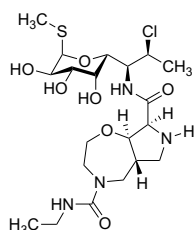
FSA-504049



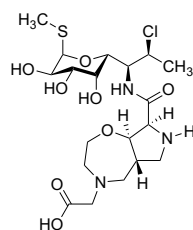
FSA-504050



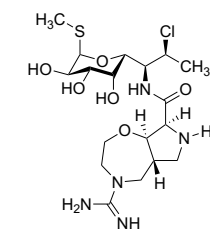
FSA-503073



FSA-503004

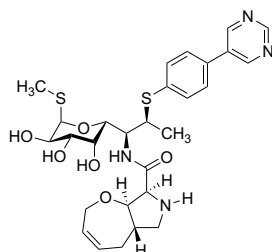


FSA-504057

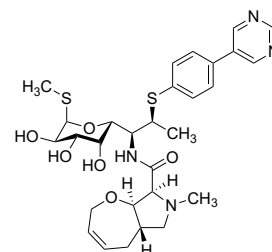


FSA-504063

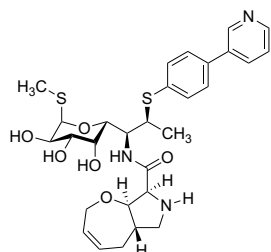
Oxepinprolinamides



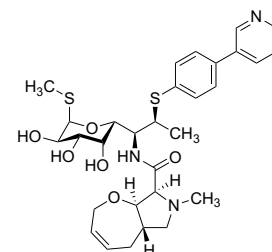
FSA-27049



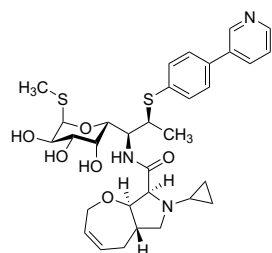
FSA-212034



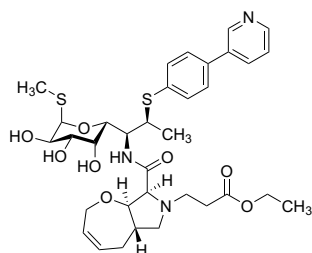
FSA-213061



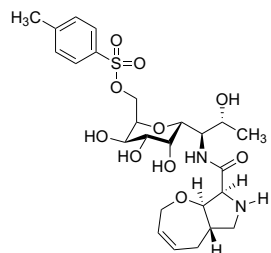
FSA-213064



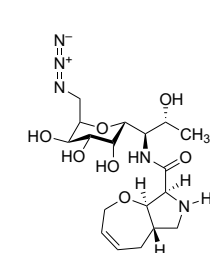
FSA-214009a



FSA-214009b

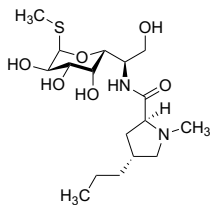


FSA-211030

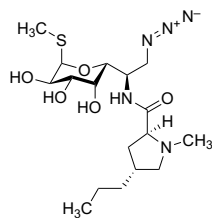


FSA-211064

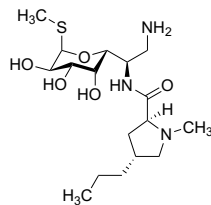
8-Norlincomycin and derivatives



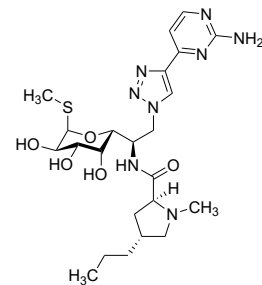
FSA-214043



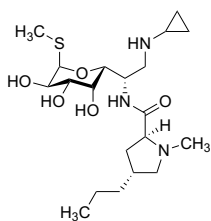
FSA-215003



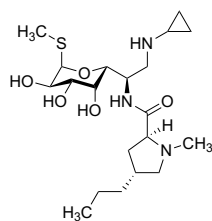
FSA-215077



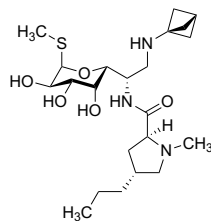
FSA-215011



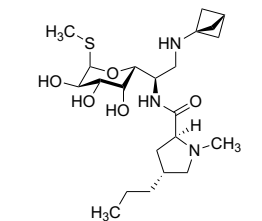
FSA-214082a



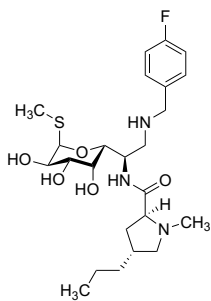
FSA-214082b



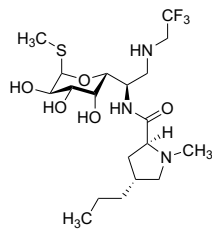
FSA-214083a



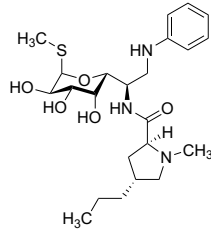
FSA-214083b



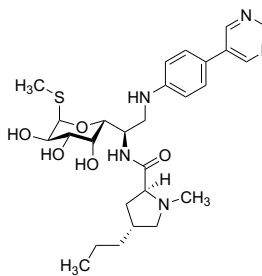
FSA-214084



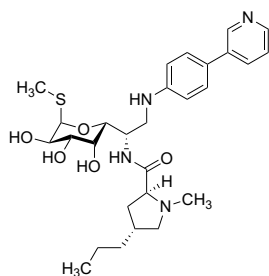
FSA-214099



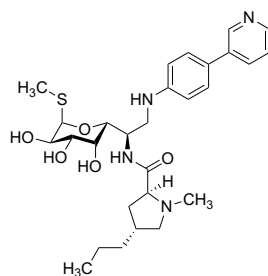
FSA-214088



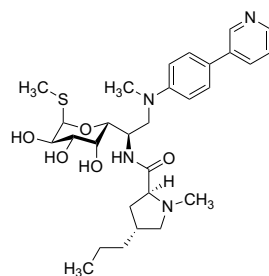
FSA-214080



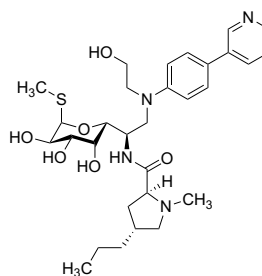
FSA-214074



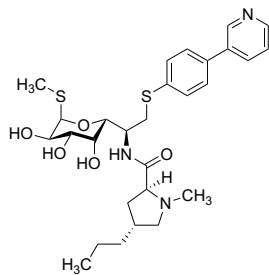
FSA-214087



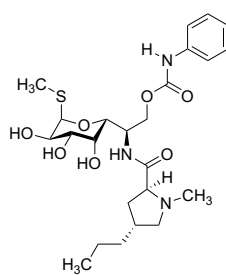
FSA-215009



FSA-215010

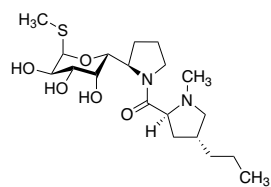


FSA-215002

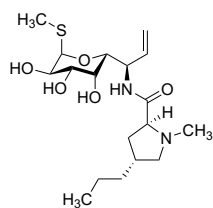


FSA-215036

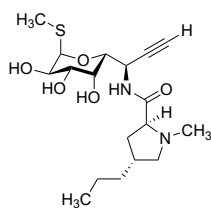
6-Modified propylhygramides



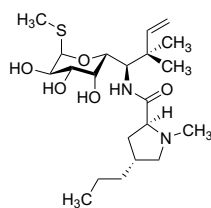
FSA-216092



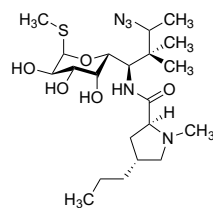
FSA-215031



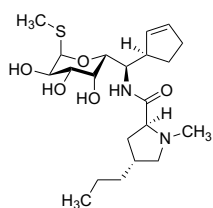
FSA-217031



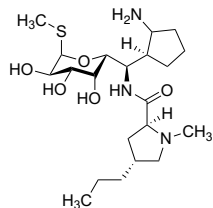
FSA-217009



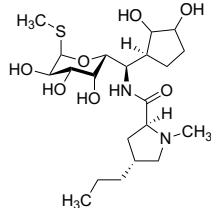
FSA-217021a/b



FSA-217003

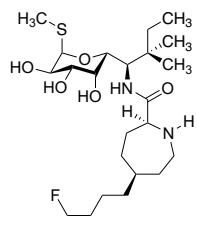


FSA-217045b

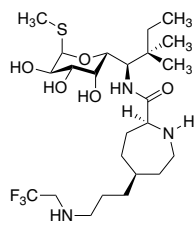


FSA-217039a/b

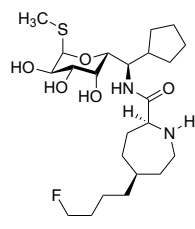
6-Modified azepanamides



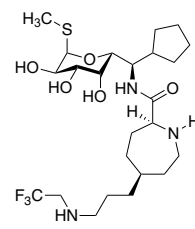
FSA-218012



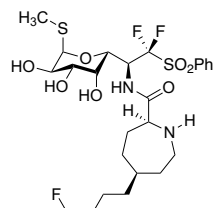
FSA-218013



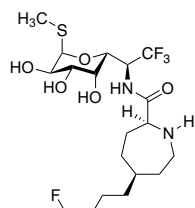
FSA-217098



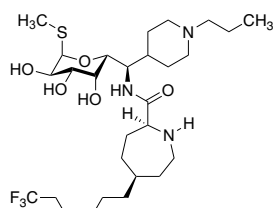
FSA-217099



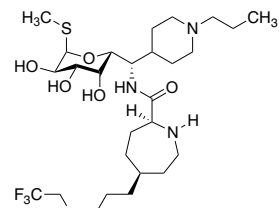
FSA-218020c



FSA-218023

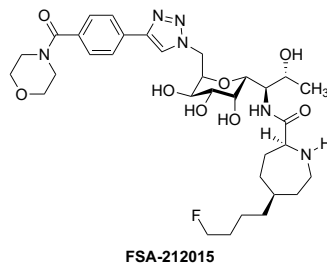
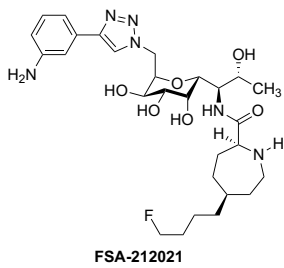
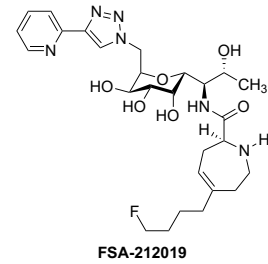
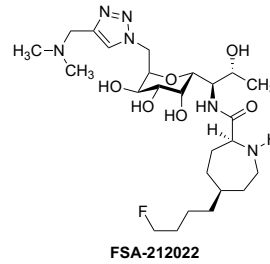
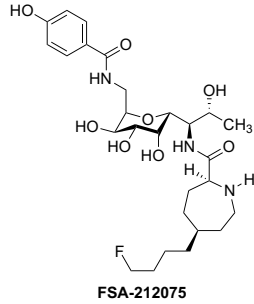
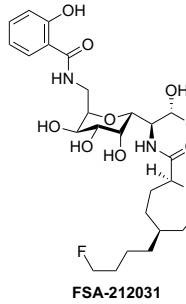
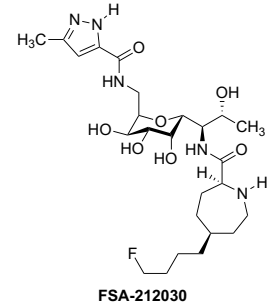
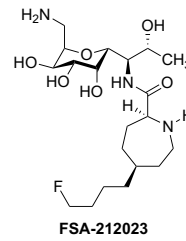
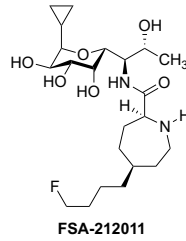
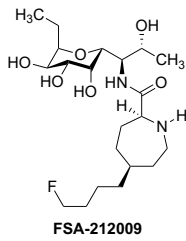


FSA-218008

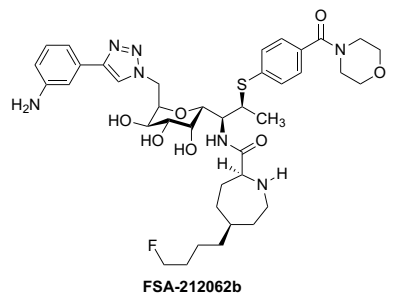
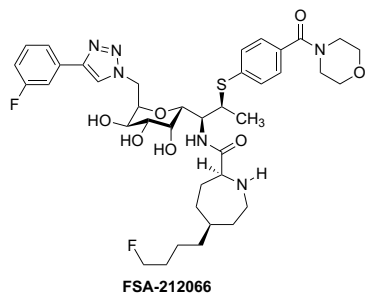
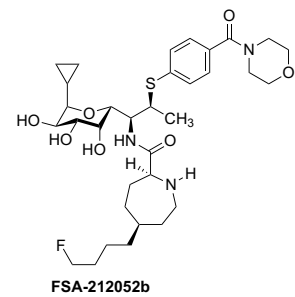
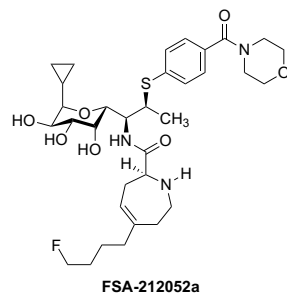
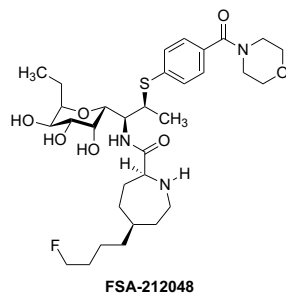
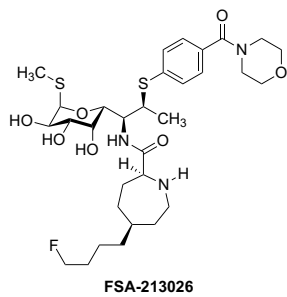


FSA-218002

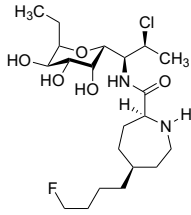
1-Modified 7-hydroxy azepanamides



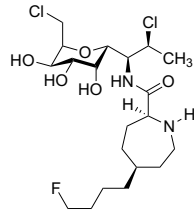
7-Arylthio azepanamides



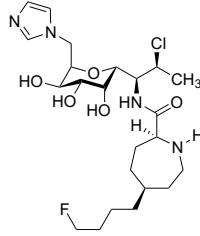
1-Modified 7-chloro azepanamides



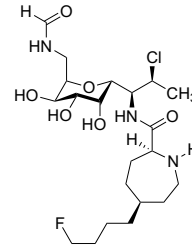
FSA-213008



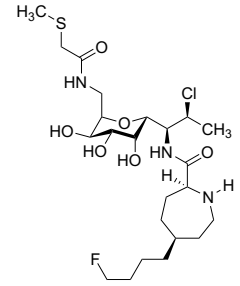
FSA-213038



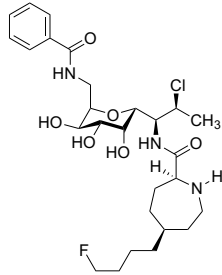
FSA-213040



FSA-213039c

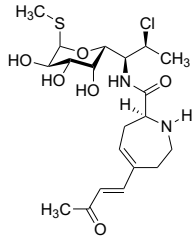


FSA-213039d

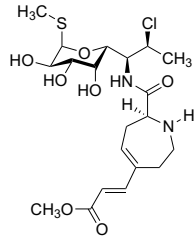


FSA-213037

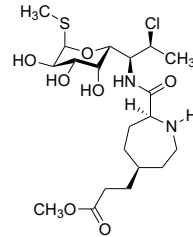
7-Chloro azepanamides



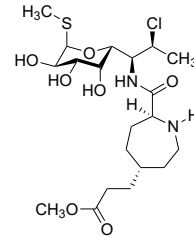
FSA-45064



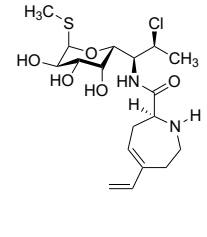
FSA-45066



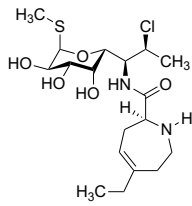
FSA-45068



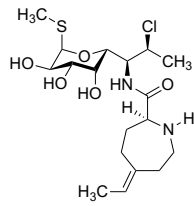
FSA-45068b



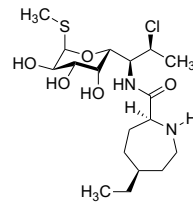
FSA-45030



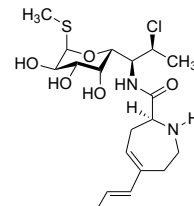
FSA-45031a



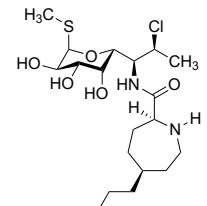
FSA-45031b



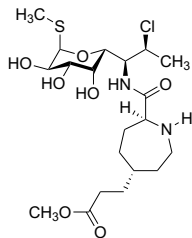
FSA-45062



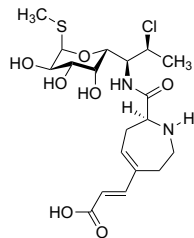
FSA-46027



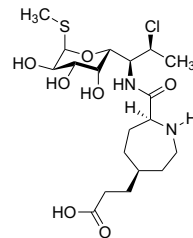
FSA-46029



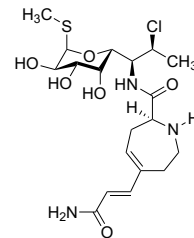
FSA-46029b



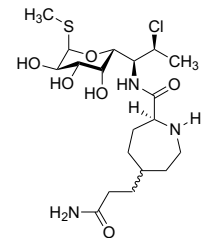
FSA-45070



FSA-45076

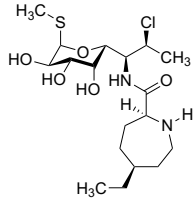


FSA-45090

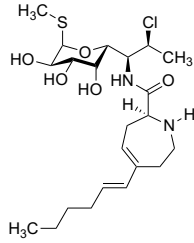


FSA-46001

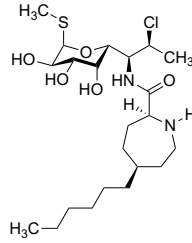
7-Chloro azepanamides



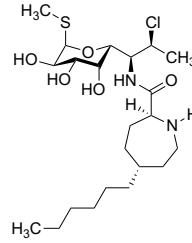
FSA-45062



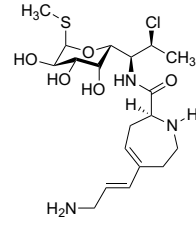
FSA-46033



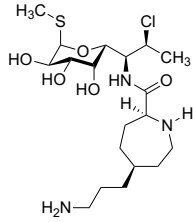
FSA-46036



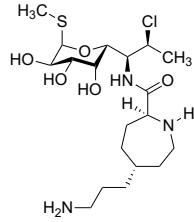
FSA-46036b



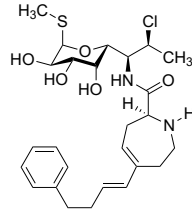
FSA-45086



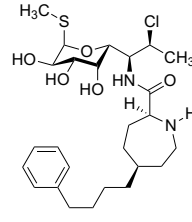
FSA-45098



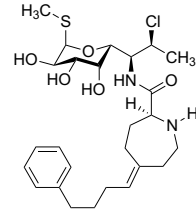
FSA-45098b



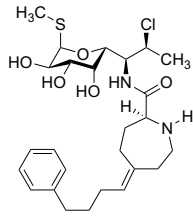
FSA-46044



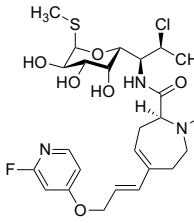
FSA-46049



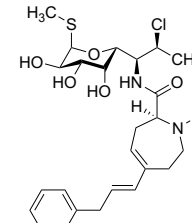
FSA-46049b



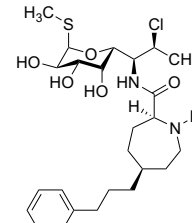
FSA-46049b



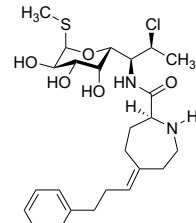
FSA-46053



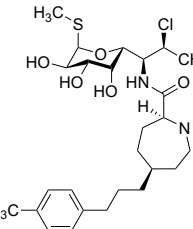
FSA-46057



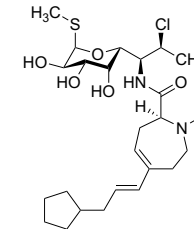
FSA-46069



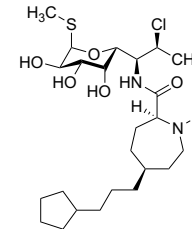
FSA-46069b



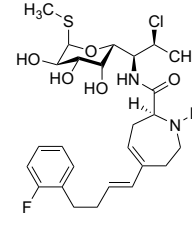
FSA-47004



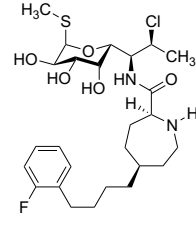
FSA-47039



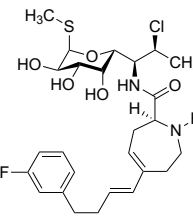
FSA-47041



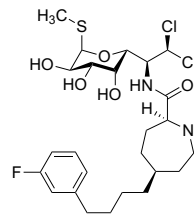
FSA-46082



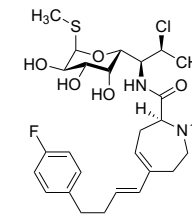
FSA-46085



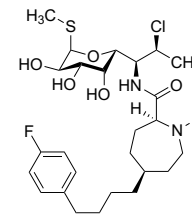
FSA-46084



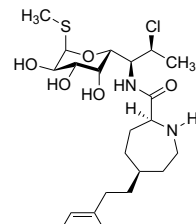
FSA-46090



FSA-46071

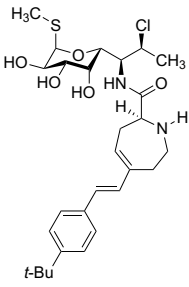


FSA-46073

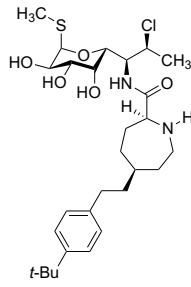


FSA-48046

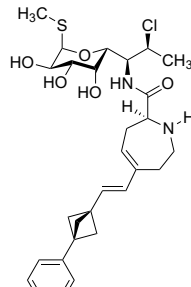
7-Chloro azepanamides



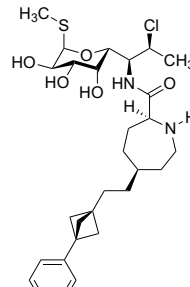
FSA-48098



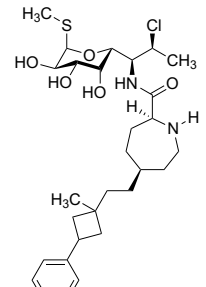
FSA-49002



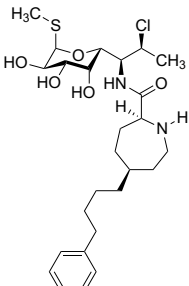
FSA-49023



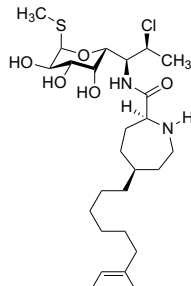
FSA-49025a



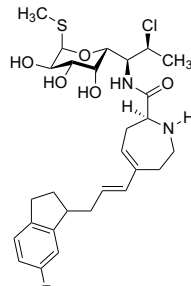
FSA-49025b



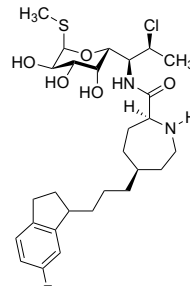
FSA-48072



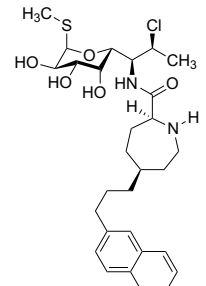
FSA-48058



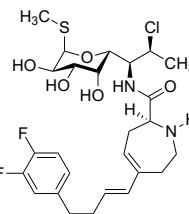
FSA-48099



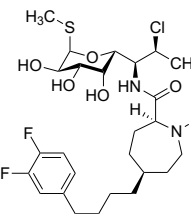
FSA-49001



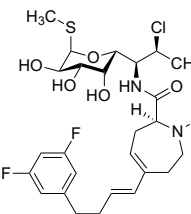
FSA-49006



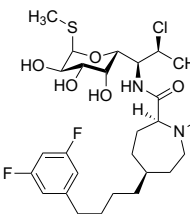
FSA-48060



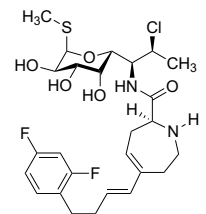
FSA-48067



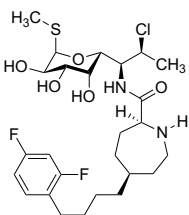
FSA-48056



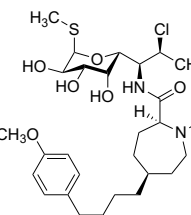
FSA-48065



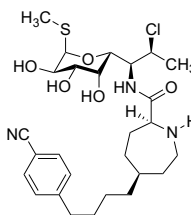
FSA-48086



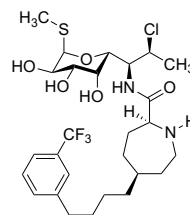
FSA-48087



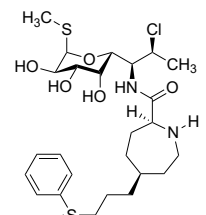
FSA-48023



FSA-48024

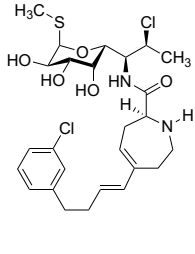


FSA-48070

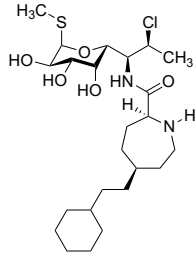


FSA-48039

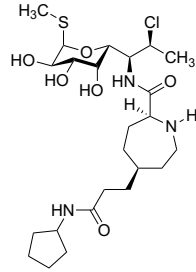
7-Chloro azepanamides



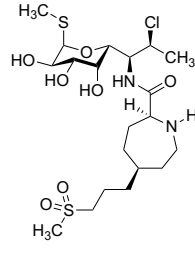
FSA-48079



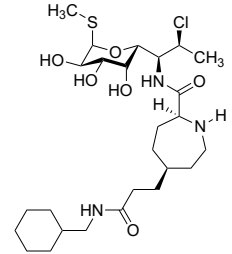
FSA-47078



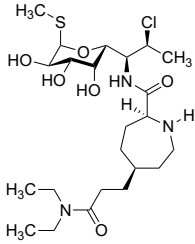
FSA-410034



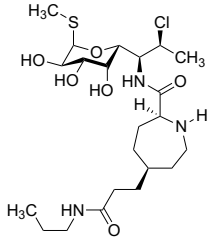
FAS-410041



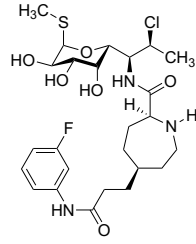
FSA-410052



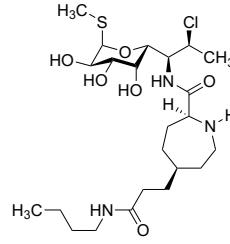
FSA-410061



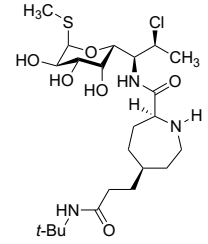
FSA-410001



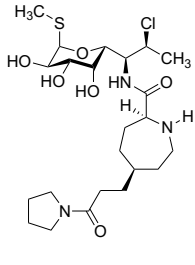
FSA-410033



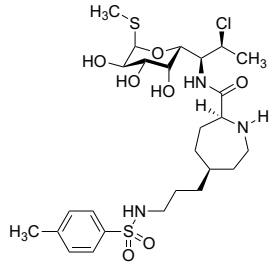
FSA-410037



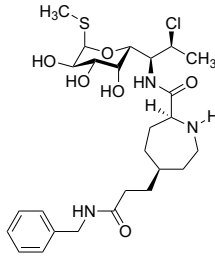
FSA-410049



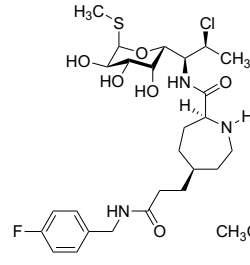
FSA-410060



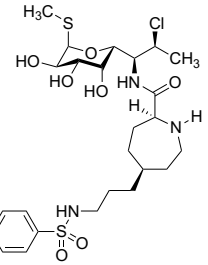
FSA-410082



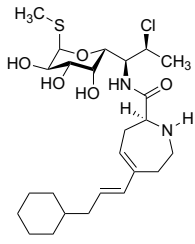
FSA-410090



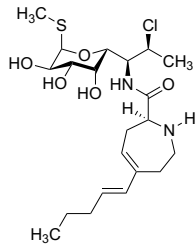
FSA-410095



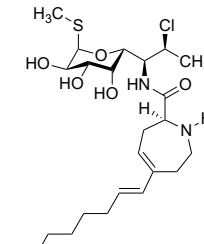
FSA-411015



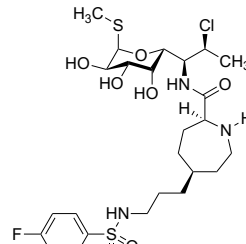
FSA-47042



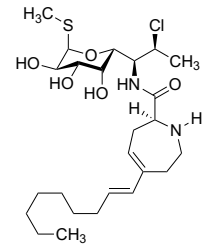
FSA-47063



FSA-47056

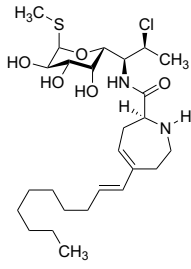


FSA-411004

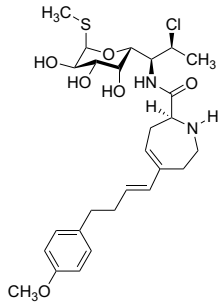


FSA-47095

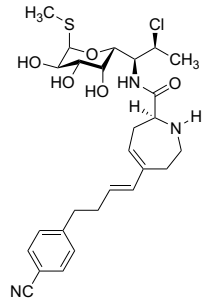
7-Chloro azepanamides



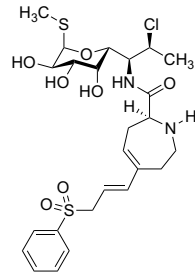
FSA-48013



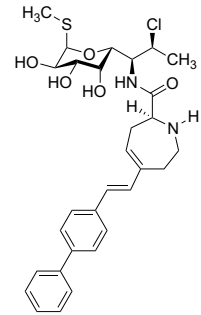
FSA-48020



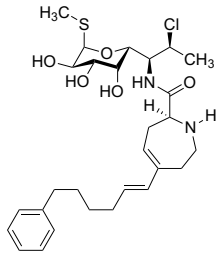
FSA-48021



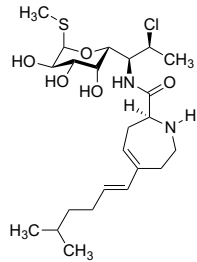
FSA-48036



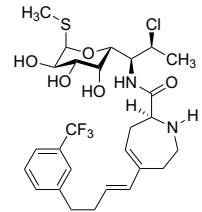
FSA-48043



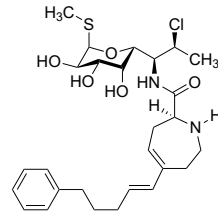
FSA-48052



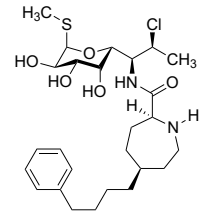
FSA-48053



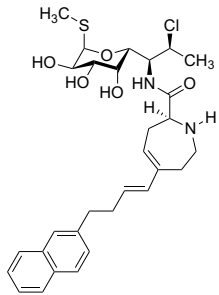
FSA-48066



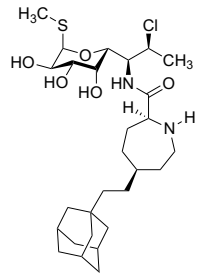
FSA-48069



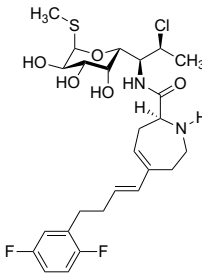
FSA-48083



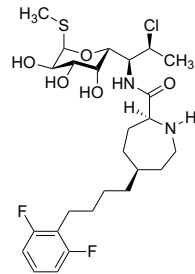
FSA-49005



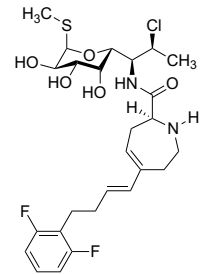
FSA-49036



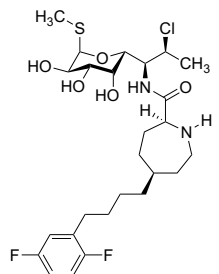
FSA-49050



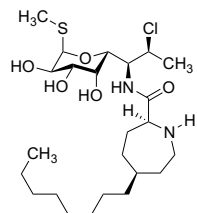
FSA-49060



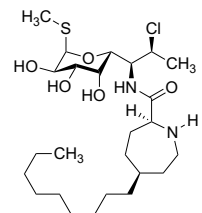
FSA-49057



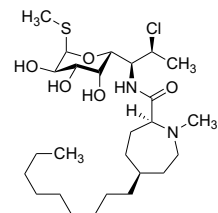
FSA-49053



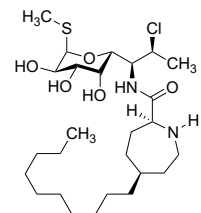
FSA-47090



FSA-48010

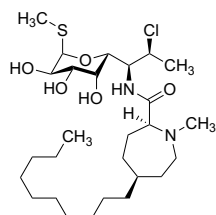


FSA-48016

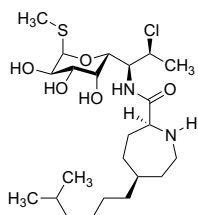


FSA-48014

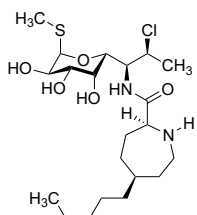
7-Chloro azepanamides



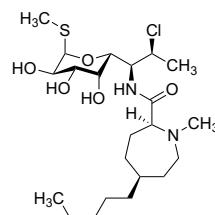
FSA-48027



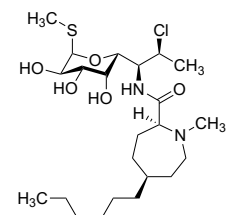
FSA-48063



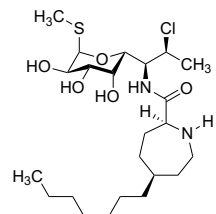
FSA-47068



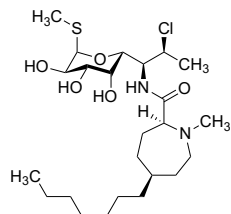
FSA-47077



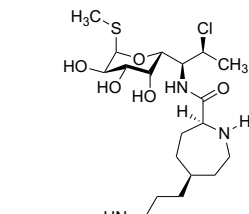
FSA-47091



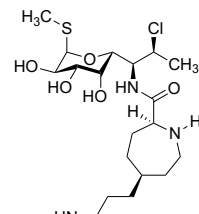
FSA-47060



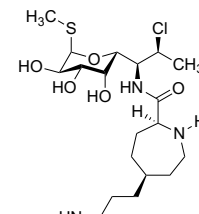
FSA-47072



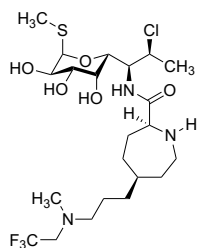
FSA-410097



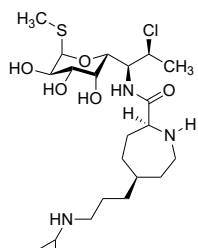
FSA-411019



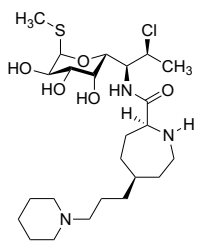
FSA-411030



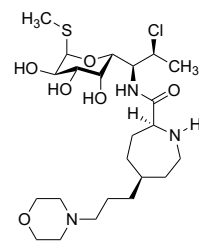
FSA-410055



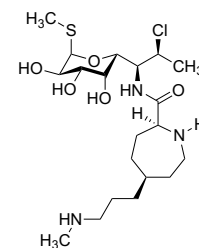
FSA-410056



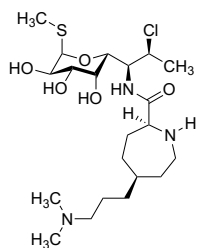
FSA-410057



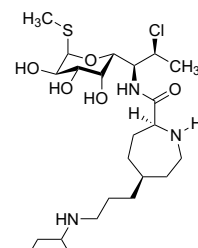
FSA-410058



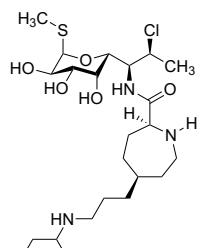
FSA-411081



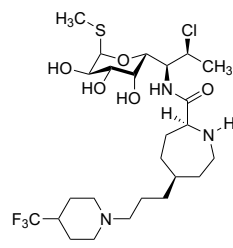
FSA-411082



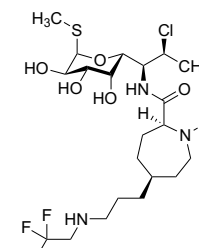
FSA-411085



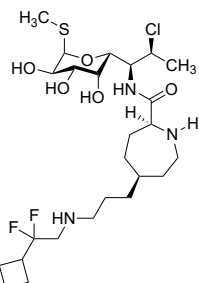
FSA-411089



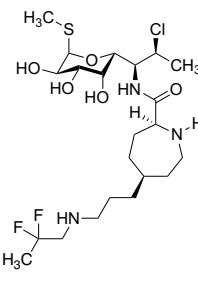
FSA-411090



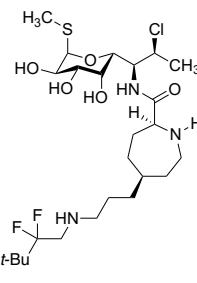
FSA-413005



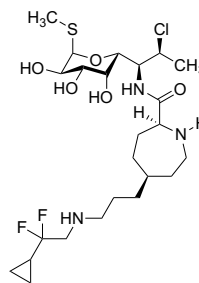
FSA-413006



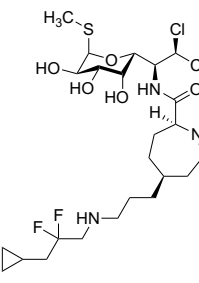
FSA-413007



FSA-413008

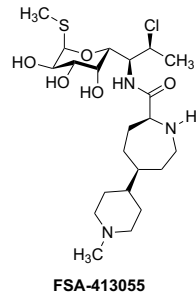
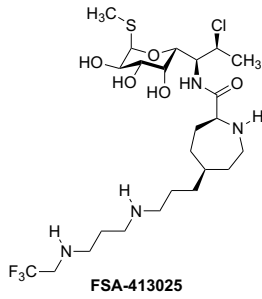


FSA-413010

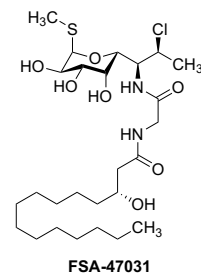
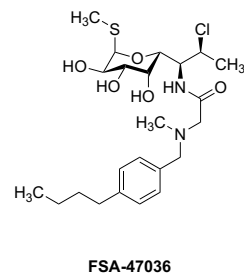
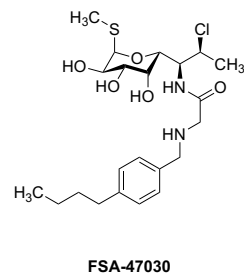
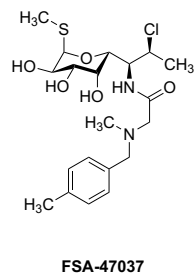
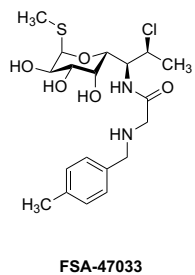
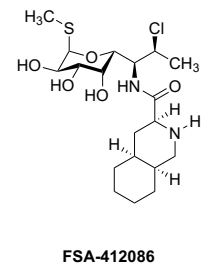
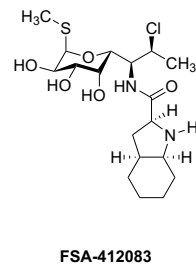
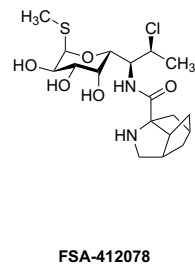
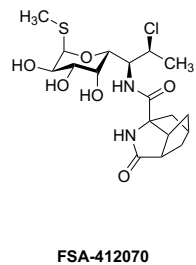
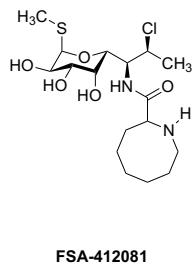
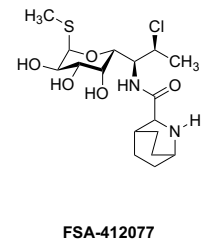
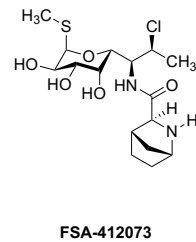
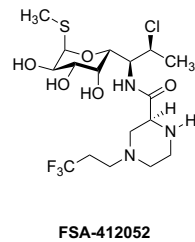
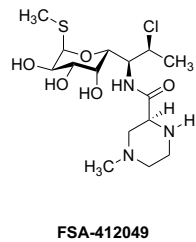
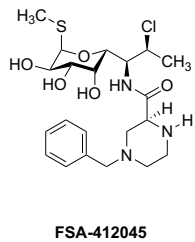
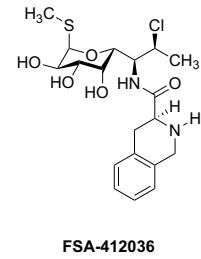
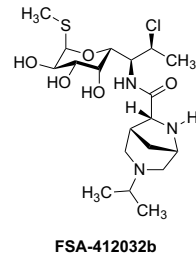
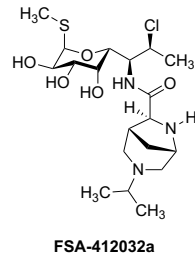
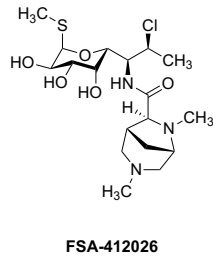
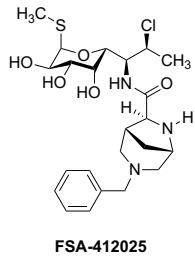


FSA-413028

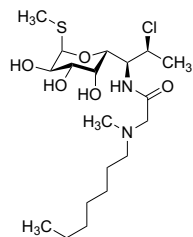
7-Chloro azepanamides



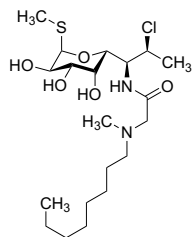
Miscellaneous southern halves



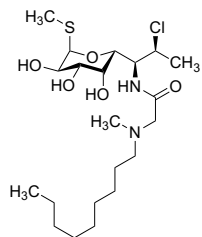
Miscellaneous southern halves



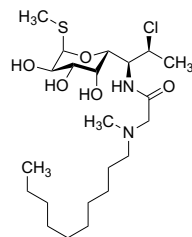
FSA-47005



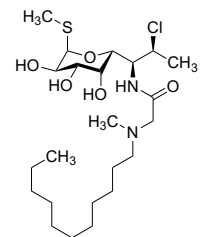
FSA-46099



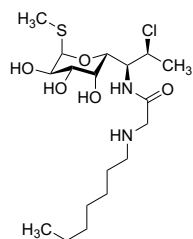
FSA-47006



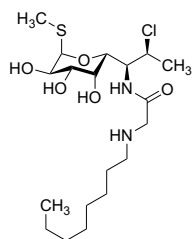
FSA-47007



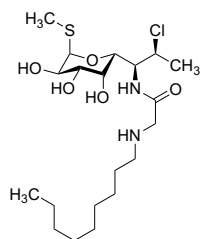
FSA-47008



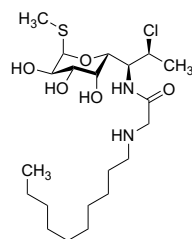
FSA-46093



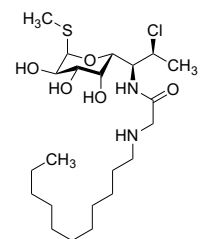
FSA-46087



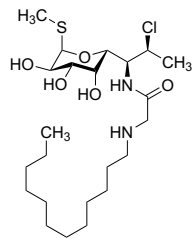
FSA-46094



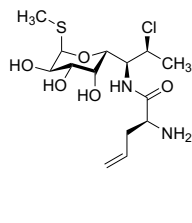
FSA-46095



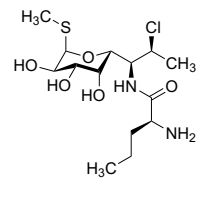
FSA-46096



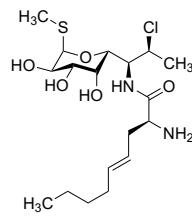
FSA-46097



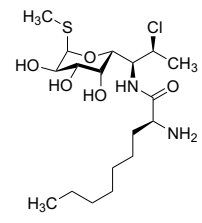
FSA-46078



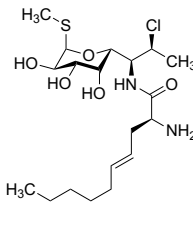
FSA-46089



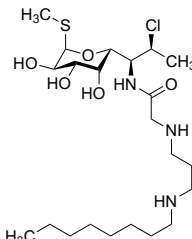
FSA-46088



FSA-46100



FSA-47035



FSA-47099

Appendix C. Minimum inhibitory concentrations of synthetic lincosamides

Table C1. Minimum inhibitory concentrations ($\mu\text{g/mL}$) of synthetic lincosamide antibiotics.

Species	Strain	22095	510026	510027	510031	510032	412090	412092	412094	21194	22018	22035	22083	21134	21141	21147	Clinda
S. aureus	ATCC 29213	>32	>64	>64	>64	>64	1	8	8	32	16	>32	16	8	4	16	0.25
	ATCC 49619	4	>64	>64	>64	>64	0.25	1	1	4	1	1	1	0.25	0.5	0.0625	0.125
	ATCC 19615	4	>64	>64	>64	>64	0.25	4	8	4	1	2	2	0.25	0.0625	<0.0313	0.125
	ATCC 29212	32	>64	>64	>64	>64	4	32	32	4	>32	2	16	>32	32	>32	0.06
	BAA 1805	NT	>64	>64	>64	>64	NT	NT	NT	NT	NT	NT	NT	NT	NT	NT	16
C. difficile	NT	NT	NT	NT	NT	NT	NT	NT	NT	NT	NT	NT	NT	NT	NT	NT	8
B. fragilis	ATCC 700057	NT	NT	NT	NT	NT	NT	NT	NT	NT	NT	NT	NT	NT	NT	NT	8
K. pneumoniae	ATCC 25285	NT	NT	NT	NT	NT	NT	NT	NT	NT	NT	NT	NT	NT	NT	NT	0.5
	ATCC 10031	>32	>64	>64	>64	>64	>64	>64	>64	>32	>32	>32	>32	>32	>32	>32	8
	ATCC 49619	>32	>64	>64	>64	>64	>64	>64	>64	>32	>32	>32	>32	>32	>32	>32	>64
	ATCC 25922	>32	NT	NT	NT	NT	NT	NT	NT	>32	>32	>32	>32	>32	>32	>32	>64
	ATCC 27853	>32	>64	>64	>64	>64	>64	>64	>64	>32	>32	>32	>32	>32	>32	>32	16
P. aeruginosa	ATCC 49247	>32	NT	NT	NT	NT	NT	NT	NT	>32	>32	>32	>32	>32	>32	>32	16
A. baumannii	ATCC 19606	>32	NT	NT	NT	NT	NT	NT	NT	>32	>32	>32	>32	>32	>32	>32	64
Species	Strain	21193	22097	22099	23003	23001	23022	23023	23010	23011	22090a	22090b	22090c	23005	506006	506015	Clinda
S. aureus	ATCC 29213	8	>32	>32	>32	>32	>32	>32	32	32	>32	>32	8	32	>32	>32	0.25
	ATCC 49619	0.5	>32	4	32	2	2	2	1	2	16	16	0.25	8	16	>32	0.125
	ATCC 19615	0.25	32	1	16	0.5	0.5	1	1	0.5	32	0.5	2	2	16	>32	0.06
	ATCC 29212	>32	>32	>32	>32	>32	>32	>32	>32	>32	>32	>32	>32	>32	>32	>32	16
	BAA 1805	NT	NT	NT	NT	NT	NT	NT	NT	NT	NT	NT	NT	NT	32	8	8
C. difficile	ATCC 700057	NT	NT	NT	NT	NT	NT	NT	NT	NT	NT	NT	NT	NT	NT	NT	8
B. fragilis	ATCC 25285	NT	NT	NT	NT	NT	NT	NT	NT	NT	NT	NT	NT	NT	NT	NT	0.5
K. pneumoniae	ATCC 10031	>32	>32	>32	>32	>32	>32	>32	>32	>32	>32	>32	>32	>32	>32	>32	8
	ATCC 49619	>32	>32	>32	>32	>32	>32	>32	>32	>32	>32	>32	>32	>32	>32	>32	>64
	ATCC 25922	>32	>32	>32	>32	>32	>32	>32	>32	>32	>32	>32	>32	>32	>32	>32	>64
	ATCC 27853	>32	>32	>32	>32	>32	>32	>32	>32	>32	>32	>32	>32	>32	>32	>32	>64
	ATCC 49247	>32	>32	>32	>32	>32	>32	>32	>32	>32	>32	>32	>32	>32	>32	>32	16
A. baumannii	ATCC 19606	>32	>32	>32	>32	>32	>32	>32	>32	>32	>32	>32	>32	>32	>32	>32	64
Species	Strain	506046	506008	506016	506007	506044	215038	215049	215081	215082	215070	215071	215078a	215054	215052	215072	Clinda
S. aureus	ATCC 29213	>32	>64	>32	>64	>64	0.25	64	4	64	64	>64	>64	>64	>64	>64	0.25
	ATCC 49619	>32	>64	>32	>64	>64	0.25	8	2	16	16	8	16	16	>64	>64	0.125
	ATCC 19615	>32	>64	>32	>64	64	0.125	16	1	32	32	16	8	64	32	8	0.06
	ATCC 29212	>32	>64	>32	>64	>64	32	>64	>64	>64	>64	>64	>64	>64	>64	>64	16
	BAA 1805	>32	64	>32	64	32	NT	>64	NT	>64	>64	>64	>64	NT	NT	NT	8
C. difficile	ATCC 700057	NT	NT	NT	NT	NT	NT	NT	NT	NT	NT	NT	NT	NT	NT	NT	8
B. fragilis	ATCC 25285	>32	64	>32	64	>64	NT	NT	NT	>64	NT	NT	>64	NT	NT	NT	0.5
K. pneumoniae	ATCC 10031	NT	NT	NT	NT	NT	>64	>64	>64	>64	>64	>64	>64	>64	>64	>64	8
	ATCC 49619	>32	>64	>32	>64	>64	>64	>64	>64	>64	>64	>64	>64	>64	>64	>64	>64
	ATCC 25922	>32	>64	>32	>64	>64	>64	>64	>64	>64	>64	>64	>64	>64	>64	>64	>64
	ATCC 27853	>32	>64	>32	>64	>64	NT	NT	NT	NT	NT	NT	NT	NT	NT	NT	16
	ATCC 49247	>32	16	>32	16	32	NT	>64	>64	>64	>64	>64	>64	NT	NT	NT	16
A. baumannii	ATCC 19606	NT	NT	NT	NT	NT	NT	NT	NT	NT	>64	>64	NT	NT	NT	>64	64

Table C1 (Continued). Minimum inhibitory concentrations ($\mu\text{g/mL}$) of synthetic lincosamide antibiotics.

Species	Strain	215059	215064	215025d	215028c	24039	24041	22091	24040	24035	24036	501076	501099	504059	504062	507051	Clinda
Gram +	<i>S. aureus</i>	32	64	4	64	1	0.5	0.125	<0.0313	0.12	0.25	>64	>64	2	2	16	0.25
	<i>S. pneumoniae</i>	8	16	2	16	0.0625	0.0625	<0.0313	<0.0313	<0.06	<0.06	64	8	0.25	0.25	1	0.125
	<i>S. pyogenes</i>	4	8	1	8	0.125	<0.0313	<0.0313	<0.0313	<0.0313	<0.0313	>64	16	0.125	0.125	0.5	0.06
	<i>E. faecalis</i>	>64	>64	>64	>64	32	32	>32	32	16	4	>64	>64	32	32	>32	16
Gram -	<i>C. difficile</i>	NT	NT	NT	NT	NT	NT	NT	NT	2	2	NT	NT	NT	NT	>32	8
	<i>C. difficile</i>	NT	NT	NT	NT	NT	NT	NT	NT	NT	NT	NT	NT	NT	NT	>32	8
	<i>B. fragilis</i>	NT	NT	NT	NT	NT	NT	NT	NT	8	4	NT	NT	NT	NT	32	0.5
	<i>K. pneumoniae</i>	>64	>64	>64	>64	>32	>32	8	8	>64	16	>64	>64	>64	>64	NT	8
Gram +	<i>E. coli</i>	>64	>64	>64	>64	>32	>32	32	>32	>64	>64	>64	>64	>64	>64	>32	>64
	<i>P. aeruginosa</i>	NT	NT	NT	NT	>32	>32	>32	>32	>64	>64	>64	>64	NT	NT	>32	>64
	<i>H. influenzae</i>	NT	NT	NT	NT	32	32	8	8	1	4	NT	NT	>64	>64	16	16
	<i>A. baumannii</i>	>64	>64	NT	NT	>32	>32	>32	>32	>32	>32	>64	>64	NT	NT	NT	64

Species	Strain	507007	507041	507031	507056	507052	507057	507053	507060	511019	511020	510001	510002	510003	510006	511033	Clinda
Gram +	<i>S. aureus</i>	0.25	0.5	>32	1	2	2	0.25	2	0.5	0.5	2	0.5	0.5	8	0.5	0.25
	<i>S. pneumoniae</i>	0.12	<0.03	32	0.25	0.25	0.0625	0.25	0.5	0.25	0.06	4	0.25	0.25	1	<0.06	0.125
	<i>S. pyogenes</i>	<0.06	0.06	32	0.25	0.25	0.12	<0.06	0.25	0.25	0.06	2	0.25	0.25	0.5	<0.06	0.06
	<i>E. faecalis</i>	16	2	>32	2	1	1	2	8	4	4	8	2	1	16	2	16
Gram -	<i>C. difficile</i>	4	0.5	>32	16	16	16	8	32	NT	NT	NT	NT	NT	NT	NT	8
	<i>C. difficile</i>	NT	NT	NT	NT	NT	NT	NT	NT	NT	NT	NT	NT	NT	NT	NT	8
	<i>B. fragilis</i>	32	2	>32	>32	>32	64	16	32	NT	NT	NT	NT	NT	NT	NT	0.5
	<i>K. pneumoniae</i>	>64	NT	NT	NT	NT	NT	NT	NT	>64	>64	>64	64	16	>64	64	8
Gram +	<i>E. coli</i>	>64	>32	>32	>32	>32	>64	>64	64	>64	>64	>64	>64	>64	>64	>64	>64
	<i>P. aeruginosa</i>	>64	>32	>32	>32	>32	>64	>64	>64	NT	NT	NT	NT	NT	NT	NT	>64
	<i>H. influenzae</i>	2	16	8	>32	>32	64	16	32	64	64	16	32	16	>64	64	16
	<i>A. baumannii</i>	>64	NT	NT	NT	NT	NT	NT	NT	NT	NT	>64	>64	>64	>64	NT	64

Species	Strain	510021	510022	511046	509018	511044	511045	509019	507061	511100	511077	511078	512011	512012	510012	510065	Clinda
Gram +	<i>S. aureus</i>	0.125	0.125	1	<0.06	0.25	0.5	<0.06	0.12	0.25	0.25	0.25	8	8	>64	>64	0.25
	<i>S. pneumoniae</i>	<0.06	<0.06	<0.06	<0.06	0.5	<0.06	<0.06	<0.06	0.125	<0.06	<0.06	1	1	>64	>64	0.125
	<i>S. pyogenes</i>	<0.06	<0.06	<0.06	<0.06	<0.06	<0.06	<0.06	<0.06	0.25	0.06	0.06	4	4	32	32	0.06
	<i>E. faecalis</i>	0.25	0.25	1	<0.06	2	1	1	1	<0.06	1	0.5	0.25	64	>64	>64	16
Gram -	<i>C. difficile</i>	NT	NT	NT	32	>64	NT	NT	8	NT	NT	NT	NT	NT	>64	>64	8
	<i>C. difficile</i>	NT	NT	NT	32	>64	NT	NT	8	NT	NT	NT	NT	NT	>64	>64	8
	<i>B. fragilis</i>	NT	NT	NT	NT	>64	NT	NT	64	NT	NT	NT	NT	NT	NT	NT	0.5
	<i>K. pneumoniae</i>	4	2	16	16	32	16	16	16	16	>64	8	8	NT	>64	>64	8
Gram +	<i>E. coli</i>	64	32	>64	64	>64	>64	>64	64	>64	>64	>64	>256	>256	>64	>64	>64
	<i>P. aeruginosa</i>	NT	NT	NT	NT	NT	NT	NT	>64	NT	NT	NT	NT	NT	NT	NT	>64
	<i>H. influenzae</i>	1	1	16	16	16	16	16	4	64	16	16	>256	>256	>64	>64	16
	<i>A. baumannii</i>	NT	NT	NT	>64	NT	NT	NT	64	NT	NT	NT	NT	NT	>64	>64	64

Table C1 (Continued). Minimum inhibitory concentrations ($\mu\text{g/mL}$) of synthetic lincosamide antibiotics.

Species	Strain	510011	510072	510073	510074	503001	503002	503003	502002	504049	504050	503073	503004	504057	504063	27049	Clinda
<i>S. aureus</i>	ATCC 29213	32	64	16	64	64	64	4	2	16	32	64	>64	>64	>64	1	0.25
<i>S. pneumoniae</i>	ATCC 49619	8	32	8	32	NT	NT	NT	0.25	NT	NT	NT	NT	NT	NT	≤ 0.06	0.125
<i>S. pyogenes</i>	ATCC 19615	2	8	2	8	NT	NT	NT	0.125	NT	NT	NT	NT	NT	NT	≤ 0.06	0.06
<i>E. faecalis</i>	ATCC 29212	>64	>64	>64	>64	NT	NT	NT	8	NT	NT	NT	NT	NT	NT	64	16
<i>C. difficile</i>	BAA 1805	NT	NT	NT	NT	NT	NT	NT	NT	NT	NT	NT	NT	NT	NT	1	8
<i>C. difficile</i>	ATCC 700057	NT	NT	NT	NT	NT	NT	NT	NT	NT	NT	NT	NT	NT	NT	NT	8
<i>B. fragilis</i>	ATCC 25285	NT	NT	NT	NT	NT	NT	NT	NT	NT	NT	NT	NT	NT	NT	NT	0.5
<i>K. pneumoniae</i>	ATCC 10031	>64	>64	>64	>64	>64	>64	>64	64	>64	>64	>64	>64	>64	>64	64	8
<i>E. coli</i>	ATCC 25922	>64	>64	>64	>64	>64	>64	>64	>64	>64	>64	>64	>64	>64	>64	>64	>64
<i>P. aeruginosa</i>	ATCC 27853	NT	NT	NT	NT	NT	NT	>64	>64	>64	>64	>64	>64	>64	>64	>64	>64
<i>H. influenzae</i>	ATCC 49247	>64	>64	>64	>64	NT	NT	NT	NT	NT	NT	NT	NT	NT	NT	32	16
<i>A. baumannii</i>	ATCC 19606	>64	NT	NT	NT	>64	>64	>64	>64	>64	>64	>64	>64	>64	>64	>64	64

Species	Strain	212034	213061	213064	214009a	214009b	211030	211064	214043	215003	215077	215011	214082a	214082b	214083a	214083b	Clinda
<i>S. aureus</i>	ATCC 29213	0.25	0.25	0.25	64	>64	>64	>64	32	8	>64	>64	>64	>64	>64	>64	0.25
<i>S. pneumoniae</i>	ATCC 49619	≤ 0.06	≤ 0.06	≤ 0.125	4	32	32	16	4	4	>64	27	>64	>64	>64	>64	0.125
<i>S. pyogenes</i>	ATCC 19615	≤ 0.06	≤ 0.06	≤ 0.125	4	8	1	4	8	2	>64	>64	>64	>64	>64	>64	0.06
<i>E. faecalis</i>	ATCC 29212	16	16	32	>64	>64	>64	>64	64	32	>64	>64	>64	>64	>64	>64	16
<i>C. difficile</i>	BAA 1805	0.5	NT	NT	NT	NT	>64	64	NT	NT	NT	NT	NT	NT	NT	NT	8
<i>C. difficile</i>	ATCC 700057	NT	4	NT	NT	NT	>64	64	NT	NT	NT	NT	NT	NT	NT	NT	8
<i>B. fragilis</i>	ATCC 25285	1	32	NT	NT	NT	>64	>64	NT	NT	NT	NT	NT	NT	NT	NT	0.5
<i>K. pneumoniae</i>	ATCC 10031	64	32	64	NT	NT	NT	NT	NT	NT	>64	>64	>64	>64	>64	>64	8
<i>E. coli</i>	ATCC 25922	>64	>64	>64	>64	>64	>64	>64	>64	>64	>64	>64	>64	>64	>64	>64	>64
<i>P. aeruginosa</i>	ATCC 27853	>64	NT	>64	NT	NT	>64	>64	NT	NT	NT	NT	NT	NT	NT	NT	>64
<i>H. influenzae</i>	ATCC 49247	4	32	2	NT	NT	>64	>64	NT	NT	>64	NT	NT	NT	NT	NT	16
<i>A. baumannii</i>	ATCC 19606	NT	>64	NT	NT	NT	NT	NT	NT	NT	NT	NT	NT	NT	NT	NT	64

Species	Strain	214084	214099	214088	214080	214074	214087	215009	215010	215002	215036	216092	215031	217031	217009	217021a	Clinda
<i>S. aureus</i>	ATCC 29213	>64	64	>64	>64	>64	32	64	>64	0.5	>64	>64	8	64	0.25	4	0.25
<i>S. pneumoniae</i>	ATCC 49619	>64	16	>64	>64	>64	8	64	64	0.25	16	>64	2	4	0.5	2	0.125
<i>S. pyogenes</i>	ATCC 19615	>64	8	>64	>64	64	8	32	64	≤ 0.06	64	>64	2	8	0.125	2	0.06
<i>E. faecalis</i>	ATCC 29212	>64	>64	>64	>64	>64	>64	>64	>64	32	>64	>64	32	64	64	>64	16
<i>C. difficile</i>	BAA 1805	NT	NT	NT	NT	NT	>64	NT	>64	32	>64	>64	NT	NT	NT	NT	8
<i>C. difficile</i>	ATCC 700057	NT	NT	NT	NT	NT	NT	NT	NT	NT	NT	NT	NT	NT	NT	NT	8
<i>B. fragilis</i>	ATCC 25285	NT	NT	NT	NT	NT	NT	NT	NT	NT	NT	NT	NT	NT	NT	NT	0.5
<i>K. pneumoniae</i>	ATCC 10031	NT	NT	NT	NT	NT	NT	NT	NT	NT	>64	>64	>64	>64	>64	>64	8
<i>E. coli</i>	ATCC 25922	>64	>64	>64	>64	>64	>64	>64	>64	>64	>64	>64	>64	>64	>64	>64	>64
<i>P. aeruginosa</i>	ATCC 27853	NT	NT	NT	NT	NT	NT	NT	NT	NT	NT	NT	NT	NT	NT	NT	>64
<i>H. influenzae</i>	ATCC 49247	NT	NT	NT	NT	NT	NT	NT	NT	NT	NT	>64	NT	>64	64	>64	16
<i>A. baumannii</i>	ATCC 19606	NT	NT	NT	NT	NT	NT	NT	NT	NT	NT	NT	NT	NT	NT	NT	64

Table C1 (Continued). Minimum inhibitory concentrations (µg/mL) of synthetic lincosamide antibiotics.

Species	Strain	217021b	217003	217045b	217039a	217039b	218012	218013	217098	217099	218020c	218023	218008	218002	212009	212011	Clinda	
+ Gram	<i>S. aureus</i>	ATCC 29213	0.25	1	>64	>64	1	1	≤ 0.125	0.5	2	2	128	>256	16	32	0.25	
	<i>S. pneumoniae</i>	ATCC 49619	0.125	0.5	>64	>64	≤ 0.125	≤ 0.125	≤ 0.125	≤ 0.125	≤ 0.125	≤ 0.125	>256	64	1	2	0.125	
	<i>S. pyogenes</i>	ATCC 19615	0.125	0.5	>64	>64	≤ 0.125	≤ 0.125	≤ 0.125	≤ 0.125	≤ 0.125	≤ 0.125	>256	16	0.25	0.5	0.06	
	<i>E. faecalis</i>	ATCC 29212	64	>64	>64	>64	0.5	8	0.5	64	4	4	>256	>256	16	32	16	
	<i>C. difficile</i>	BAA 1805	NT	NT	NT	NT	NT	NT	NT	NT	NT	NT	NT	NT	32	64	8	
+ Gram	<i>B. fragilis</i>	ATCC 700057	NT	NT	NT	NT	NT	NT	NT	NT	NT	NT	NT	NT	NT	NT	8	
	<i>K. pneumoniae</i>	ATCC 25285	NT	NT	NT	NT	NT	NT	NT	NT	NT	NT	NT	NT	NT	NT	0.5	
	<i>E. coli</i>	ATCC 10031	>64	>64	>64	>64	256	>256	>256	>256	>256	>256	>256	>256	>64	>64	8	
	<i>P. aeruginosa</i>	ATCC 25922	>64	>64	>64	>64	NT	NT	NT	NT	NT	NT	NT	NT	NT	NT	>64	
	<i>H. influenzae</i>	ATCC 27853	NT	NT	NT	NT	NT	NT	NT	NT	NT	NT	NT	NT	NT	NT	>64	
+ Gram	<i>H. influenzae</i>	ATCC 49247	32	>64	>64	>64	64	>256	128	>256	>256	>256	>256	>256	16	32	16	
	<i>A. baumannii</i>	ATCC 19606	NT	NT	NT	NT	NT	NT	NT	NT	NT	NT	NT	NT	NT	NT	64	
	<i>S. aureus</i>	ATCC 29213	>64	>64	>64	>64	>64	64	>64	8	2	32	8	32	≤ 0.06	16	0.25	
	<i>S. pneumoniae</i>	ATCC 49619	>64	32	16	32	64	64	>64	0.12	≤ 0.06	1	0.5	2	≤ 0.06	1	0.125	
	<i>S. pyogenes</i>	ATCC 19615	32	16	1	2	32	4	16	0.06	≤ 0.06	2	0.12	4	≤ 0.06	4	0.06	
+ Gram	<i>E. faecalis</i>	ATCC 29212	>64	>64	>64	>64	>64	>64	>64	4	2	>64	16	32	≤ 0.06	32	16	
	<i>C. difficile</i>	BAA 1805	>64	>64	>64	>64	>64	>64	1	1	0.5	NT	8	64	0.5	16	8	
	<i>C. difficile</i>	ATCC 700057	NT	NT	NT	NT	NT	NT	NT	NT	NT	NT	NT	NT	NT	NT	8	
	<i>B. fragilis</i>	ATCC 25285	64	>64	>64	>64	>64	>64	>32	>64	>64	NT	>64	>64	0.25	8	0.5	
	<i>K. pneumoniae</i>	ATCC 10031	NT	NT	NT	NT	NT	NT	NT	NT	NT	NT	NT	NT	NT	NT	8	
+ Gram	<i>E. coli</i>	ATCC 25922	>64	>64	>64	>64	>64	>64	>64	>64	>64	>64	>64	>64	32	>64	>64	
	<i>P. aeruginosa</i>	ATCC 27853	>64	>64	>64	>64	>64	>64	>64	>64	>64	NT	>64	>64	>64	>64	>64	
	<i>H. influenzae</i>	ATCC 49247	>64	>64	>64	>64	>64	>64	>32	>64	64	NT	64	>64	1	>64	16	
	<i>A. baumannii</i>	ATCC 19606	NT	NT	NT	NT	NT	NT	NT	NT	NT	NT	NT	NT	NT	NT	NT	64
	<i>S. aureus</i>	ATCC 29213	>64	>64	>64	>64	>64	0.25	>64	>64	64	0.25	0.12	>32	0.25	>64	>64	0.25
+ Gram	<i>S. pneumoniae</i>	ATCC 49619	8	8	2	0.5	NT	NT	NT	NT	NT	0.03	>32	≤ 0.06	32	32	0.125	
	<i>S. pyogenes</i>	ATCC 19615	4	8	2	1	NT	NT	NT	NT	NT	≤ 0.015	>32	≤ 0.06	32	32	0.06	
	<i>E. faecalis</i>	ATCC 29212	>64	>64	>64	64	NT	NT	NT	NT	NT	4	>32	>32	2	>64	16	
	<i>C. difficile</i>	BAA 1805	>64	64	32	NT	NT	NT	NT	NT	NT	2	>32	>32	1	>64	8	
	<i>C. difficile</i>	ATCC 700057	NT	NT	NT	NT	NT	NT	NT	NT	NT	NT	NT	NT	NT	NT	8	
+ Gram	<i>B. fragilis</i>	ATCC 25285	64	>64	64	NT	NT	NT	NT	NT	NT	0.12	>32	>32	64	>64	0.5	
	<i>K. pneumoniae</i>	ATCC 10031	NT	NT	NT	NT	NT	NT	NT	NT	NT	32	NT	NT	NT	NT	8	
	<i>E. coli</i>	ATCC 25922	>64	>64	>64	>64	>64	>64	>64	>64	>64	>64	>64	>64	>64	>64	8	
	<i>P. aeruginosa</i>	ATCC 27853	>64	>64	>64	>64	>64	>64	>64	>64	>64	NT	>64	>64	>64	>64	>64	
	<i>H. influenzae</i>	ATCC 49247	>64	>64	>64	>64	>64	>64	>64	>64	64	NT	64	>64	1	>64	16	
+ Gram	<i>H. influenzae</i>	ATCC 49247	>64	>64	>64	>64	>64	>64	>64	>32	>64	NT	64	>64	1	>64	16	
	<i>A. baumannii</i>	ATCC 19606	NT	NT	NT	NT	NT	NT	NT	NT	NT	NT	NT	NT	NT	NT	64	
	<i>S. aureus</i>	ATCC 29213	>64	>64	>64	>64	>64	0.25	>64	>64	64	0.25	0.12	>32	0.25	>64	>64	
	<i>S. pneumoniae</i>	ATCC 49619	8	8	2	0.5	NT	NT	NT	NT	NT	NT	0.03	>32	≤ 0.06	32	0.125	
	<i>S. pyogenes</i>	ATCC 19615	4	8	2	1	NT	NT	NT	NT	NT	≤ 0.015	>32	≤ 0.06	32	32	0.06	
+ Gram	<i>E. faecalis</i>	ATCC 29212	>64	>64	>64	64	NT	NT	NT	NT	NT	4	>32	>32	2	>64	16	
	<i>C. difficile</i>	BAA 1805	>64	64	32	NT	NT	NT	NT	NT	NT	2	>32	>32	1	>64	8	
	<i>C. difficile</i>	ATCC 700057	NT	NT	NT	NT	NT	NT	NT	NT	NT	NT	NT	NT	NT	NT	8	
	<i>B. fragilis</i>	ATCC 25285	64	>64	64	NT	NT	NT	NT	NT	NT	0.12	>32	>32	64	>64	0.5	
	<i>K. pneumoniae</i>	ATCC 10031	NT	NT	NT	NT	NT	NT	NT	NT	NT	32	NT	NT	NT	NT	8	
+ Gram	<i>E. coli</i>	ATCC 25922	>64	>64	>64	>64	>64	>64	>64	>64	>64	>64	>64	>64	>64	>64	>64	
	<i>P. aeruginosa</i>	ATCC 27853	>64	>64	>64	>64	>64	>64	>64	>64	>64	NT	>64	>64	>64	>64	>64	
	<i>H. influenzae</i>	ATCC 49247	>64	>64	>64	>64	>64	>64	>64	>64	>64	NT	>64	>64	>64	>64	>64	
	<i>H. influenzae</i>	ATCC 49247	>64	>64	>64	>64	>64	>64	>64	>64	>64	NT	>64	>64	>64	>64	>64	
	<i>A. baumannii</i>	ATCC 19606	NT	NT	NT	NT	NT	NT	NT	NT	NT	NT	NT	NT	NT	NT	NT	64

Table C1 (Continued). Minimum inhibitory concentrations (µg/mL) of synthetic lincosamide antibiotics.

Species	Strain	217003	217045b	217039a	217039b	218012	218013	217098	217099	218020c	218023	218008	218002	212009	212011	Clinda
		217021b	217003	217045b	217039a	217039b	218012	218013	217098	217099	218020c	218023	218008	218002	212009	
S. aureus	ATCC 29213	0.25	1	>64	>64	4	1	≤ 0.125	0.5	2	2	128	>256	16	32	0.25
	ATCC 49619	0.125	0.5	8	32	1	≤ 0.125	≤ 0.125	≤ 0.125	≤ 0.125	≤ 0.125	>256	64	1	2	0.125
	ATCC 19615	0.125	0.5	>64	8	0.5	≤ 0.125	≤ 0.125	≤ 0.125	≤ 0.125	≤ 0.125	>256	16	0.25	0.5	0.06
E. faecalis	ATCC 29212	64	>64	>64	>64	>64	8	0.5	64	4	4	>256	>256	16	32	16
	BAA 1805	NT	NT	NT	NT	NT	NT	NT	NT	NT	NT	NT	NT	32	64	8
C. difficile	ATCC 700057	NT	NT	NT	NT	NT	NT	NT	NT	NT	NT	NT	NT	NT	NT	8
	ATCC 25285	NT	NT	NT	NT	NT	NT	NT	NT	NT	NT	NT	NT	NT	NT	8
B. fragilis	ATCC 25285	NT	NT	NT	NT	NT	NT	NT	NT	NT	NT	NT	NT	NT	NT	0.5
	ATCC 10031	>64	>64	>64	>64	>64	>256	256	>256	>256	>256	>256	>256	>64	>64	8
K. pneumoniae	ATCC 10031	>64	>64	>64	>64	>64	>256	256	>256	>256	>256	>256	>256	>64	>64	>64
	ATCC 25922	NT	NT	NT	NT	NT	NT	NT	NT	NT	NT	NT	NT	>64	>64	>64
P. aeruginosa	ATCC 27853	NT	NT	NT	NT	NT	NT	NT	NT	NT	NT	NT	NT	>64	>64	>64
	ATCC 49247	32	>64	>64	>64	>64	64	128	>256	>256	>256	>256	>256	16	32	16
H. influenzae	ATCC 49247	NT	NT	NT	NT	NT	NT	NT	NT	NT	NT	NT	NT	NT	NT	16
	ATCC 19606	NT	NT	NT	NT	NT	NT	NT	NT	NT	NT	NT	NT	NT	NT	64

Species	Strain	212023	212030	212031	212075	212022	212019	212021	212015	213026	212048	212052a	212066	212062b	213008	213038	Clinda
		212023	212030	212031	212075	212022	212019	212021	212015	213026	212048	212052a	212066	212062b	213008	213038	
S. aureus	ATCC 29213	>64	>64	>64	>64	>64	>64	64	>64	8	2	32	8	32	≤ 0.06	16	0.25
	ATCC 49619	>64	32	16	32	64	>64	64	>64	0.12	≤ 0.06	1	0.5	2	≤ 0.06	1	0.125
	ATCC 19615	32	16	1	2	32	>64	4	16	0.06	≤ 0.06	2	0.12	4	≤ 0.06	4	0.06
E. faecalis	ATCC 29212	>64	>64	>64	>64	>64	>64	>64	>64	4	2	>64	16	32	≤ 0.06	32	16
	BAA 1805	>64	>64	>64	>64	>64	>64	>64	>64	1	0.5	NT	8	64	0.5	16	8
C. difficile	ATCC 700057	NT	NT	NT	NT	NT	NT	NT	NT	NT	NT	NT	NT	NT	NT	NT	8
	ATCC 25285	64	>64	>64	>64	>64	>64	>64	>64	>32	>64	NT	>64	>64	0.25	8	0.5
B. fragilis	ATCC 25285	NT	NT	NT	NT	NT	NT	NT	NT	NT	NT	NT	NT	NT	NT	NT	8
	ATCC 10031	NT	NT	NT	NT	NT	NT	NT	NT	NT	NT	NT	NT	NT	NT	NT	8
K. pneumoniae	ATCC 10031	NT	NT	NT	NT	NT	NT	NT	NT	NT	NT	NT	NT	NT	NT	NT	8
	ATCC 25922	>64	>64	>64	>64	>64	>64	>64	>64	>32	>64	NT	>64	>64	>64	>64	>64
P. aeruginosa	ATCC 27853	>64	>64	>64	>64	>64	>64	>64	>64	>32	>64	NT	>64	>64	>64	>64	>64
	ATCC 49247	>64	>64	>64	>64	>64	>64	>64	>64	>32	64	NT	>64	>64	>64	>64	16
H. influenzae	ATCC 49247	NT	NT	NT	NT	NT	NT	NT	NT	NT	NT	NT	NT	NT	NT	NT	16
	ATCC 19606	NT	NT	NT	NT	NT	NT	NT	NT	NT	NT	NT	NT	NT	NT	NT	64

Species	Strain	213040	213039c	213039d	213037	45064	45066	45068	45068b	45030	45031a	45031b	45062	46027	46029	46029b	Clinda
		213040	213039c	213039d	213037	45064	45066	45068	45068b	45030	45031a	45031b	45062	46027	46029	46029b	
S. aureus	ATCC 29213	>64	>64	>64	16	0.25	>64	0.25	>64	>64	64	0.25	0.12	>32	0.25	>64	0.25
	ATCC 49619	8	8	2	0.5	NT	NT	NT	NT	NT	NT	NT	0.03	>32	≤ 0.06	32	0.125
	ATCC 19615	4	8	2	1	NT	NT	NT	NT	NT	NT	NT	≤ 0.015	>32	≤ 0.06	32	0.06
E. faecalis	ATCC 29212	>64	>64	>64	64	NT	NT	NT	NT	NT	NT	NT	4	>32	2	>64	16
	BAA 1805	>64	64	32	NT	NT	NT	NT	NT	NT	NT	2	>32	1	>64	8	8
C. difficile	ATCC 700057	NT	NT	NT	NT	NT	NT	NT	NT	NT	NT	NT	NT	NT	NT	NT	8
	ATCC 25285	64	>64	64	NT	NT	NT	NT	NT	NT	NT	0.12	>32	>32	64	>64	0.5
B. fragilis	ATCC 25285	NT	NT	NT	NT	NT	NT	NT	NT	NT	NT	NT	NT	NT	NT	NT	8
	ATCC 10031	>64	>64	>64	>64	>64	>64	>64	>64	>64	>64	32	NT	NT	NT	NT	8
K. pneumoniae	ATCC 10031	>64	>64	>64	>64	>64	>64	>64	>64	>32	>64	NT	>64	>64	>64	>64	>64
	ATCC 25922	>64	>64	>64	>64	>64	>64	>64	>64	>32	>64	NT	>64	>64	>64	>64	>64
P. aeruginosa	ATCC 27853	>64	>64	>64	>64	>64	>64	>64	>64	>32	>64	NT	>64	>64	>64	>64	>64
	ATCC 49247	>64	>64	>64	>64	>64	>64	>64	>64	>32	64	NT	>64	>64	>64	>64	16
H. influenzae	ATCC 49247	>64	>64	>64	>64	>64	>64	>64	>64	>32	64	NT	>64	>64	>64	>64	16
	ATCC 19606	NT	NT	NT	NT	NT	NT	NT	NT	NT	NT	NT	NT	NT	NT	NT	64

Table C1 (Continued). Minimum inhibitory concentrations ($\mu\text{g/mL}$) of synthetic lincosamide antibiotics.

Species	Strain	48024	48070	48039	48079	47078	410034	410041	410052	410061	410037	410049	410060	410082	Clinda
<i>S. aureus</i>	ATCC 29213	<0.06	0.25	0.12	4	0.5	32	8	16	>32	32	64	32	2	0.25
<i>S. pneumoniae</i>	ATCC 49619	<0.06	<0.06	<0.06	4	0.12	4	1	1	16	2	16	4	<0.125	0.125
<i>S. pyogenes</i>	ATCC 19615	<0.06	0.06	<0.06	4	0.12	0.5	2	0.5	4	0.25	2	4	<0.125	0.06
<i>E. faecalis</i>	ATCC 29212	0.12	0.25	0.5	4	1	>64	32	>64	>64	>64	>64	>64	32	16
<i>C. difficile</i>	BAA 1805	<0.06	0.5	0.25	8	0.5	NT	NT	NT	NT	NT	NT	NT	NT	8
<i>C. difficile</i>	ATCC 700057	NT	NT	NT	NT	NT	NT	NT	NT	NT	NT	NT	NT	NT	8
<i>B. fragilis</i>	ATCC 25285	1	1	0.5	8	4	NT	NT	NT	NT	NT	NT	NT	NT	0.5
<i>K. pneumoniae</i>	ATCC 10031	NT	NT	NT	NT	NT	NT	NT	NT	NT	NT	NT	NT	NT	8
<i>E. coli</i>	ATCC 25922	32	16	>64	32	16	>64	>64	>64	>64	>64	>64	>64	>64	>64
<i>P. aeruginosa</i>	ATCC 27853	>64	>32	>64	>64	>32	>64	>64	>64	>64	>64	>64	>64	>64	>64
<i>H. influenzae</i>	ATCC 49247	4	4	4	16	8	NT	NT	NT	NT	NT	NT	NT	NT	16
<i>A. baumannii</i>	ATCC 19606	NT	NT	NT	NT	NT	NT	NT	NT	NT	NT	NT	NT	NT	64

Species	Strain	410090	410095	411015	47042	47063	47056	411004	47095	48013	48020	48036	48052	48053	Clinda
<i>S. aureus</i>	ATCC 29213	16	16	4	0.25	<0.06	0.125	4	2	2	4	>64	2	2	0.25
<i>S. pneumoniae</i>	ATCC 49619	2	2	0.125	<0.06	<0.06	<0.06	0.25	2	8	1	64	2	2	0.125
<i>S. pyogenes</i>	ATCC 19615	0.25	0.5	<0.06	<0.06	<0.06	<0.06	0.125	2	8	1	>64	2	2	0.06
<i>E. faecalis</i>	ATCC 29212	>64	>64	32	4	0.125	2	4	4	2	8	>64	4	16	16
<i>C. difficile</i>	BAA 1805	NT	NT	NT	NT	NT	NT	NT	NT	NT	NT	NT	NT	NT	8
<i>C. difficile</i>	ATCC 700057	NT	NT	NT	NT	NT	NT	NT	NT	NT	NT	NT	NT	NT	8
<i>B. fragilis</i>	ATCC 25285	NT	NT	NT	NT	NT	NT	NT	NT	NT	NT	NT	NT	NT	0.5
<i>K. pneumoniae</i>	ATCC 10031	NT	NT	16	NT	NT	NT	NT	NT	NT	NT	NT	NT	NT	8
<i>E. coli</i>	ATCC 25922	>64	>64	>64	64	32	64	>64	16	64	>64	>64	32	>64	>64
<i>P. aeruginosa</i>	ATCC 27853	>64	NT	NT	NT	NT	NT	NT	NT	NT	NT	NT	NT	NT	>64
<i>H. influenzae</i>	ATCC 49247	NT	NT	NT	NT	NT	NT	NT	NT	NT	NT	NT	NT	NT	16
<i>A. baumannii</i>	ATCC 19606	NT	NT	NT	NT	NT	NT	NT	NT	NT	NT	NT	NT	NT	64

Species	Strain	48066	48069	48083	49005	49036	49050	49060	49057	49053	47090	48010	48016	48014	48027	48063	Clinda
<i>S. aureus</i>	ATCC 29213	8	4	<0.06	4	4	2	0.25	4	0.125	0.25	0.25	0.5	0.5	1	0.12	0.25
<i>S. pneumoniae</i>	ATCC 49619	8	4	<0.06	8	8	2	<0.06	4	<0.06	<0.06	<0.06	0.5	0.5	2	0.12	0.125
<i>S. pyogenes</i>	ATCC 19615	16	4	<0.06	16	16	2	<0.06	4	<0.06	<0.06	<0.06	0.5	0.5	2	<0.06	0.06
<i>E. faecalis</i>	ATCC 29212	4	16	0.25	4	4	8	0.5	16	0.25	0.5	0.5	1	1	2	0.12	0.06
<i>C. difficile</i>	BAA 1805	NT	NT	NT	NT	NT	NT	NT	NT	NT	0.25	0.5	2	1	4	<0.06	16
<i>C. difficile</i>	ATCC 700057	NT	NT	NT	NT	NT	NT	NT	NT	NT	NT	NT	NT	NT	NT	NT	8
<i>B. fragilis</i>	ATCC 25285	NT	NT	NT	NT	NT	NT	NT	NT	NT	2	4	8	8	16	1	0.5
<i>K. pneumoniae</i>	ATCC 10031	NT	NT	NT	NT	NT	NT	NT	NT	NT	16	8	NT	NT	NT	NT	8
<i>E. coli</i>	ATCC 25922	32	64	8	>64	>64	>64	32	>64	8	16	8	>32	16	>32	16	>64
<i>P. aeruginosa</i>	ATCC 27853	NT	NT	NT	NT	NT	NT	NT	NT	NT	>64	>64	>32	>32	>32	>64	>64
<i>H. influenzae</i>	ATCC 49247	NT	NT	NT	NT	NT	NT	NT	NT	NT	4	2	>16	4	>32	2	16
<i>A. baumannii</i>	ATCC 19606	NT	NT	NT	NT	NT	NT	NT	NT	NT	NT	NT	NT	NT	NT	NT	64

Table C1 (Continued). Minimum inhibitory concentrations ($\mu\text{g/mL}$) of synthetic lincosamide antibiotics.

Species	Strain	47068	47077	47091	47060	47072	410097	411019	411030	410055	410056	410057	410058	411081	411082	411085	Clinda
<i>S. aureus</i>	ATCC 29213	<0.03	0.12	0.25	<0.06	0.25	8	4	0.25	0.5	8	8	4	8	4	8	0.25
<i>S. pneumoniae</i>	ATCC 49619	<0.03	<0.06	<0.03	<0.06	<0.06	2	0.5	<0.06	0.125	1	2	0.5	8	4	1	0.125
<i>S. pyogenes</i>	ATCC 19615	<0.03	<0.06	<0.03	<0.06	<0.06	0.5	0.25	<0.06	<0.06	0.5	0.5	0.25	8	4	0.5	0.06
<i>E. faecalis</i>	ATCC 29212	<0.03	<0.06	0.12	0.25	0.25	>64	>64	4	4	>64	>64	32	64	32	>64	16
<i>C. difficile</i>	BAA 1805	<0.03	0.25	0.12	<0.06	0.25	NT	NT	NT	NT	NT	NT	NT	>64	>64	NT	8
<i>C. difficile</i>	ATCC 700057	NT	NT	NT	NT	0.25	NT	NT	1	NT	NT	NT	NT	NT	NT	NT	8
<i>B. fragilis</i>	ATCC 25285	0.25	0.12	0.25	0.5	0.5	NT	NT	NT	NT	NT	NT	NT	NT	NT	NT	0.5
<i>K. pneumoniae</i>	ATCC 10031	NT	NT	NT	NT	NT	NT	NT	NT	NT	NT	NT	NT	NT	NT	NT	8
<i>E. coli</i>	ATCC 25922	8	64	>32	16	>64	>64	>64	64	>64	>64	>64	16	>64	16	>64	8
<i>P. aeruginosa</i>	ATCC 27853	>32	>64	>32	>64	>64	NT	NT	NT	NT	NT	NT	NT	NT	NT	NT	>64
<i>H. influenzae</i>	ATCC 49247	1	8	8	2	16	NT	NT	16	NT	NT	NT	NT	>64	>64	NT	16
<i>A. baumannii</i>	ATCC 19606	NT	NT	NT	NT	NT	NT	NT	>64	NT	NT	NT	NT	NT	NT	NT	64
<i>S. aureus</i>	ATCC 29213	16	1	0.5	0.5	0.5	1	0.5	0.5	16	128	>64	>64	>64	>64	4	0.25
<i>S. pneumoniae</i>	ATCC 49619	2	0.25	0.06	0.125	0.125	0.25	0.25	<0.06	4	16	>64	>64	>64	>64	1	0.125
<i>S. pyogenes</i>	ATCC 19615	2	0.25	<0.06	0.125	<0.06	0.25	0.125	<0.06	2	16	>64	>64	>64	>64	2	0.06
<i>E. faecalis</i>	ATCC 29212	>64	>64	16	32	16	>64	32	16	>64	>256	>64	>64	>64	32	32	16
<i>C. difficile</i>	BAA 1805	NT	NT	NT	NT	NT	NT	NT	NT	NT	NT	NT	NT	NT	NT	NT	8
<i>C. difficile</i>	ATCC 700057	NT	NT	NT	8	NT	NT	NT	NT	NT	NT	NT	NT	NT	NT	NT	8
<i>B. fragilis</i>	ATCC 25285	NT	NT	NT	64	NT	NT	NT	NT	NT	NT	NT	NT	NT	NT	NT	0.5
<i>K. pneumoniae</i>	ATCC 10031	64	32	2	2	4	4	4	>64	>64	NT	>64	>64	>64	>64	8	8
<i>E. coli</i>	ATCC 25922	>64	32	64	16	64	32	32	32	>64	>256	>64	>64	>64	>64	>64	>64
<i>P. aeruginosa</i>	ATCC 27853	NT	NT	>64	>64	>64	>64	NT	NT	NT	NT	NT	NT	NT	NT	NT	>64
<i>H. influenzae</i>	ATCC 49247	>64	8	32	32	8	64	16	32	32	>256	>64	>64	>64	>64	16	16
<i>A. baumannii</i>	ATCC 19606	NT	NT	>64	>64	>64	>64	NT	NT	NT	NT	NT	NT	NT	NT	NT	64
<i>S. aureus</i>	ATCC 29213	8	>64	16	>64	>64	>64	>64	>64	>64	0.25	4	>32	8	32	>64	0.25
<i>S. pneumoniae</i>	ATCC 49619	1	8	2	>64	64	>64	>64	16	>64	<0.06	2	>32	1	32	>64	0.125
<i>S. pyogenes</i>	ATCC 19615	2	32	2	>64	64	>64	>64	32	>64	<0.06	1	>32	1	32	>64	0.06
<i>E. faecalis</i>	ATCC 29212	>64	>64	>64	>64	>64	>64	>64	>64	>64	2	16	>32	16	32	>64	16
<i>C. difficile</i>	BAA 1805	NT	NT	>64	NT	NT	NT	NT	NT	NT	NT	4	>32	2	32	>64	8
<i>C. difficile</i>	ATCC 700057	NT	NT	NT	NT	NT	NT	NT	NT	NT	NT	NT	NT	NT	NT	NT	8
<i>B. fragilis</i>	ATCC 25285	NT	NT	NT	NT	NT	NT	NT	NT	NT	NT	1	8	2	32	>64	0.5
<i>K. pneumoniae</i>	ATCC 10031	>64	>64	>64	>64	>64	>64	>64	>64	>64	64	>64	>32	>64	>64	8	8
<i>E. coli</i>	ATCC 25922	>64	>64	>64	>64	>64	>64	>64	>64	>64	>64	>64	>32	>64	>64	>64	>64
<i>P. aeruginosa</i>	ATCC 27853	NT	NT	NT	NT	NT	NT	NT	NT	NT	NT	>64	>64	>64	>64	>64	>64
<i>H. influenzae</i>	ATCC 49247	>64	>64	>64	>64	>64	>64	>64	>64	>64	NT	>64	>64	>64	>64	>64	>64
<i>A. baumannii</i>	ATCC 19606	NT	NT	>64	>64	>64	>64	>64	>64	>64	>64	>64	>64	>64	>64	>64	16

Table C1 (Continued). Minimum inhibitory concentrations ($\mu\text{g/mL}$) of synthetic lincosamide antibiotics.

Species	Strain	47005	46099	47006	47007	47008	46093	46087	46094	46095	46096	46097	46078	46089	46088	46100	Clinda
<i>S. aureus</i>	ATCC 29213	32	64	32	16	4	>64	>64	>32	32	16	4	>64	>64	16	1	0.25
<i>S. pneumoniae</i>	ATCC 49619	>32	64	32	32	32	32	32	>32	32	16	16	64	32	16	0.25	0.125
<i>S. pyogenes</i>	ATCC 19615	32	32	32	32	32	16	16	32	32	16	16	64	16	4	0.25	0.06
<i>E. faecalis</i>	ATCC 29212	>32	64	32	16	4	64	64	>32	32	8	4	>64	>64	64	8	16
<i>C. difficile</i>	BAA 1805	32	32	>32	64	64	32	16	32	32	32	32	64	64	8	4	8
<i>C. difficile</i>	ATCC 700057	4	NT	8	32	NT	NT	NT	NT	NT	NT	NT	NT	NT	NT	NT	8
<i>B. fragilis</i>	ATCC 25285	NT	8	8	32	32	8	16	32	16	16	16	32	16	2	0.5	0.5
<i>K. pneumoniae</i>	ATCC 10031	NT	NT	NT	NT	NT	NT	NT	NT	NT	NT	NT	NT	NT	NT	NT	8
<i>E. coli</i>	ATCC 25922	>32	>64	>32	>64	>64	>64	>64	>32	>64	>64	>64	>64	>64	>64	>64	>64
<i>P. aeruginosa</i>	ATCC 27853	>32	>64	>32	>64	>64	>64	>64	>32	>64	>64	>64	>64	>64	>64	>64	>64
<i>H. influenzae</i>	ATCC 49247	>32	64	32	32	>64	>64	>64	>32	32	8	8	>64	>64	32	32	16
<i>A. baumannii</i>	ATCC 19606	NT	NT	NT	NT	NT	NT	NT	NT	NT	NT	NT	NT	NT	NT	NT	64

Species	Strain	47035	47099	Clinda
<i>S. aureus</i>	ATCC 29213	2	>64	0.25
<i>S. pneumoniae</i>	ATCC 49619	1	>64	0.125
<i>S. pyogenes</i>	ATCC 19615	0.5	>64	0.06
<i>E. faecalis</i>	ATCC 29212	8	>64	16
<i>C. difficile</i>	BAA 1805	2	>64	8
<i>C. difficile</i>	ATCC 700057	NT	NT	8
<i>B. fragilis</i>	ATCC 25285	1	>64	0.5
<i>K. pneumoniae</i>	ATCC 10031	NT	NT	8
<i>E. coli</i>	ATCC 25922	64	>64	>64
<i>P. aeruginosa</i>	ATCC 27853	>64	>64	>64
<i>H. influenzae</i>	ATCC 49247	16	>64	16
<i>A. baumannii</i>	ATCC 19606	NT	NT	64

Appendix D. Secondary *in vitro* profiling of FSA-213064

**Time-Kill, Post-Antibiotic Effect, and Post-Antibiotic Sub-MIC Effect Studies
of FSA-213064**

Dr. Amarnath Pisipati – October 25, 2017

Time Kill Studies:

Organism: *S. aureus* ATCC 29213 (Initial inoculum ~ 1×10^6 CFU/mL).

Antibiotics: Clindamycin and FSA-213064.

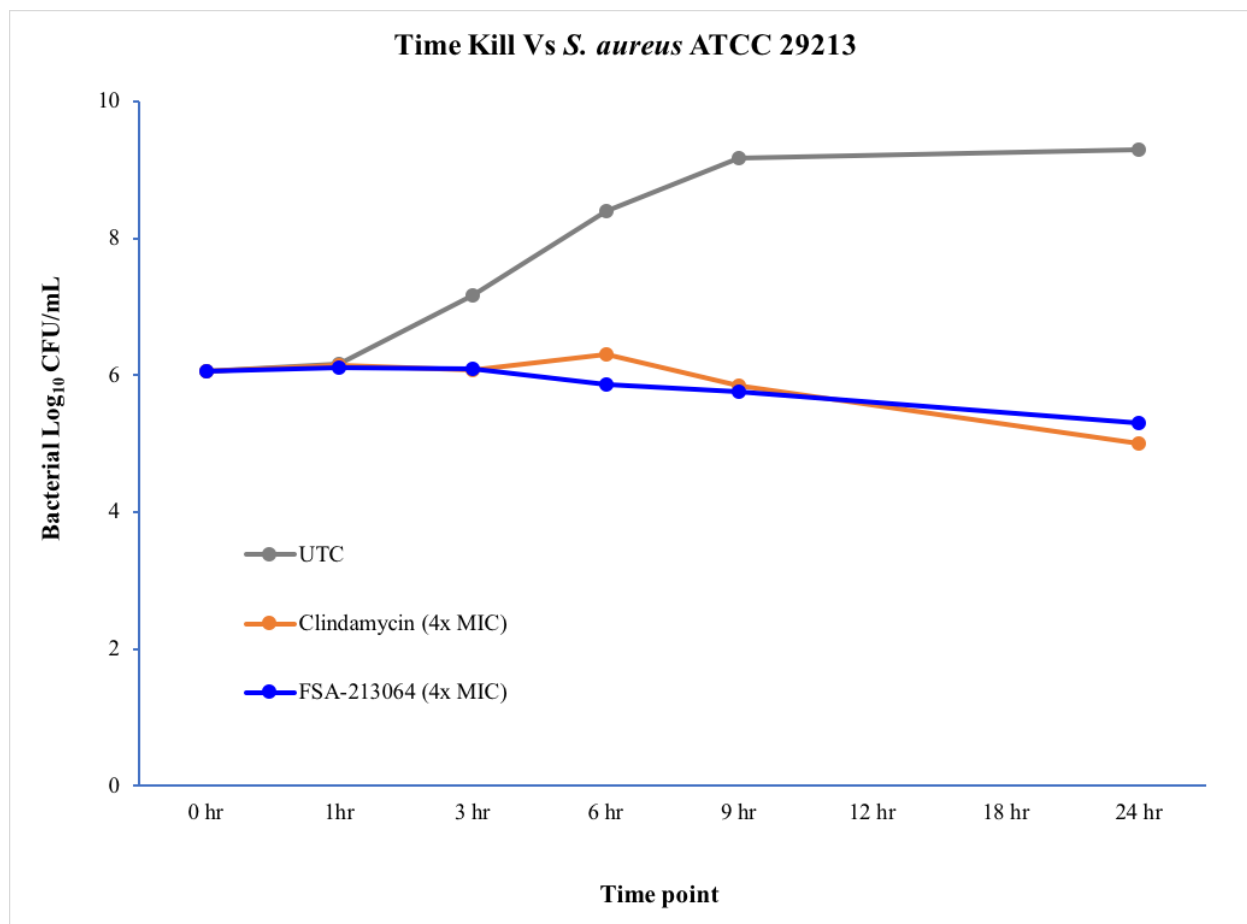
MIC against *S. aureus* ATCC 29213: Clindamycin, 0.125 $\mu\text{g/mL}$; FSA-213064, 0.25 $\mu\text{g/mL}$.

Antibiotic concentration: $4 \times \text{MIC}$.

Table D1.

Time Point	Bacterial log ₁₀ CFU/mL		
	UTC	Clindamycin (4 × MIC)	FSA-213064 (4 × MIC)
0 h	6.06	6.06	6.06
1 h	6.17	6.14	6.11
3 h	7.17	6.07	6.09
6 h	8.39	6.3	5.87
9 h	9.17	5.84	5.75
24 h	9.3	5	5.3

Figure D1.



Conclusion: Both compounds exhibited bacteriostatic effect for the duration of study.

Post Antibiotic Effect (PAE) Studies

Organism: *S. aureus* ATCC 29213 (Initial inoculum $\sim 1 \times 10^6$ CFU/mL).

Antibiotics: Clindamycin and FSA-213064.

MIC against *S. aureus* ATCC 29213: Clindamycin, 0.125 $\mu\text{g/mL}$; FSA-213064, 0.25 $\mu\text{g/mL}$.

Antibiotic concentration: $4 \times \text{MIC}$.

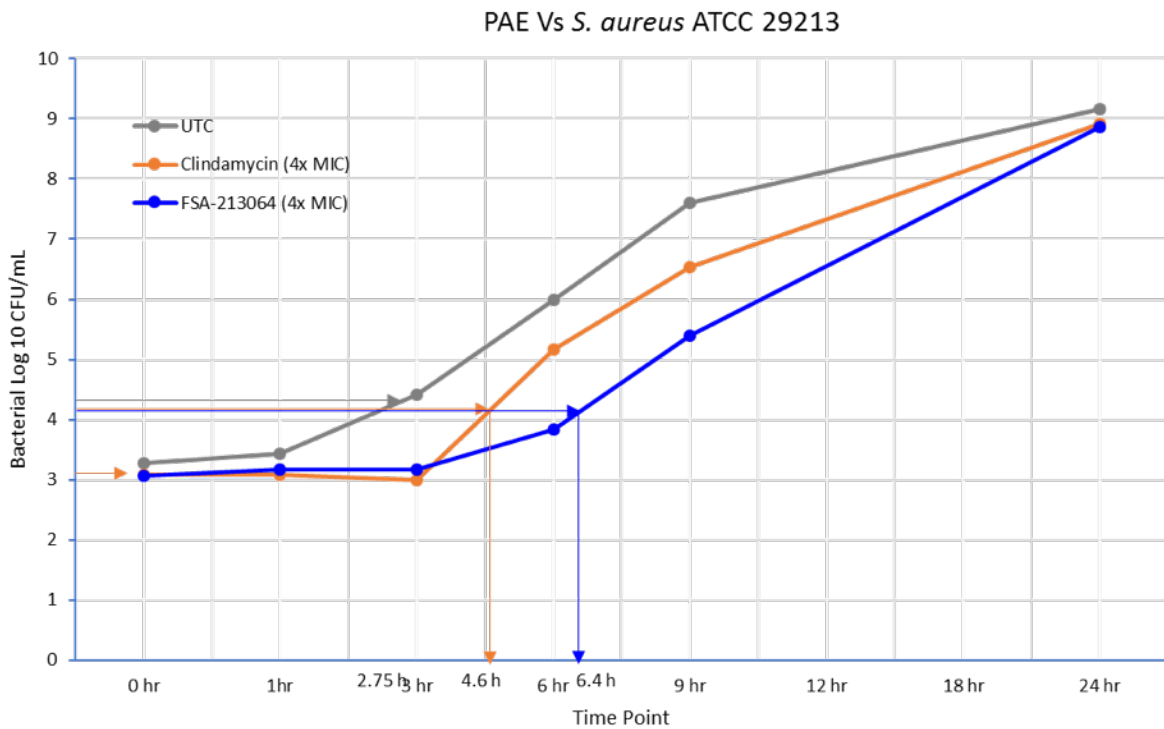
Procedure:

- Initial inoculum ($\sim 1 \times 10^6$ CFU/mL) is exposed to $4 \times \text{MIC}$ concentration of antibiotics for 1 hour.
- Inoculum diluted 1:1000 to remove antibiotic.
- One flask is left without adding antibiotic as untreated control (UTC).
- Counts determined from the diluted inoculum at 0 h, 1, 3, 6, 9 and 24 hours.
- Time taken by bacteria in untreated control (C) and treated samples (T) to grow $1 \log_{10}$ CFU/mL compared to 0 h count is determined.
- **PAE = T – C**

Table D2:

Time Point	Bacterial Log ₁₀ CFU/mL		
	UTC	Clindamycin (4 × MIC)	FSA-213064 (4 × MIC)
0 h	3.28	3.08	3.06
1 h	3.44	3.08	3.17
3 h	4.41	3	3.17
6 h	6	5.17	3.84
9 h	7.6	6.54	5.39
24 h	9.17	8.92	8.87

Figure D2:



Time taken by *S. aureus* ATCC 29213 in UTC to grow 1 log₁₀ CFU/mL (C) = 2.75 h

Time taken to grow 1 log₁₀ CFU/mL in Clindamycin, 4 × MIC treated flask (T) = 4.6 h

Time taken to grow 1 log₁₀ CFU/mL in FSA-213064, 4 × MIC treated flask (T) = 6.4 h

PAE of Clindamycin: T – C

$$= 4.6 \text{ h} - 2.75 \text{ h}$$

$$= \mathbf{1.85 \text{ h}}$$

PAE of FSA-213064: T – C

$$= 6.4 \text{ h} - 2.75 \text{ h}$$

$$= \mathbf{3.65 \text{ h}}$$

Conclusion:

FSA-213064 has exhibited a longer PAE compared to Clindamycin against *S. aureus* ATCC 29213 at 4 × MIC concentrations.

Post-Antibiotic Sub MIC Effect (PA-SME) study:

Organism: *S. aureus* ATCC 29213 (Initial inoculum $\sim 1 \times 10^6$ CFU/mL).

Antibiotics: Clindamycin and FSA-213064.

MIC against *S. aureus* ATCC 2921: Clindamycin, 0.125 μ g/mL; FSA-213064, 0.25 μ g/mL.

Procedure:

- Initial inoculum ($\sim 1 \times 10^6$ CFU/mL) is exposed to $4 \times$ MIC concentration of antibiotics for 1 hour
- Inoculum diluted 1:1000 to remove antibiotic
- The diluted inoculum containing media is substituted with $0.25 \times$ and $0.5 \times$ MIC concentrations of antibiotics in individual flasks respectively
- Counts determined from each flask at 0 h, 1, 3, 6, 9 and 24 hours.
- One flask is left without adding antibiotic as untreated control (UTC)
- Time taken by bacteria in untreated control (C) and treated samples (T) to grow 1 \log_{10} CFU/mL compared to 0 h count is determined.
- **PAE = T – C**

Time taken by *S. aureus* ATCC 29213 in Untreated Control to grow 1 \log_{10} CFU/mL (C) = 2.75 h

Time taken by bacteria to grow 1 \log_{10} CFU/mL in Clindamycin and FSA-213064 at $0.25 \times$ and $0.5 \times$ MICs:

S. aureus did not exhibit 1 \log_{10} CFU growth from start to 30 hours.

The bacterial counts were detectible with clindamycin at all time points, whereas with FSA-213064, bacterial counts were below the detection limit from 9th hour at $0.25 \times \text{MIC}$ and from 6th hour with $0.5 \times \text{MIC}$ concentrations.

(detection limit in our lab is 200 CFU/mL or 20 colonies per plate)

There was a complete bacteriostatic effect with Clindamycin at both the sub-MIC concentrations.

With Clindamycin:

There were a 0.65 and 0.22 log₁₀ CFU reductions with $0.25 \times \text{MIC}$ at 24th and 30th hour, respectively.

There were a 1.08 and 0.85 log₁₀ CFU reductions at $0.5 \times \text{MIC}$ by 24th and 30th hour respectively.

With FSA-213064:

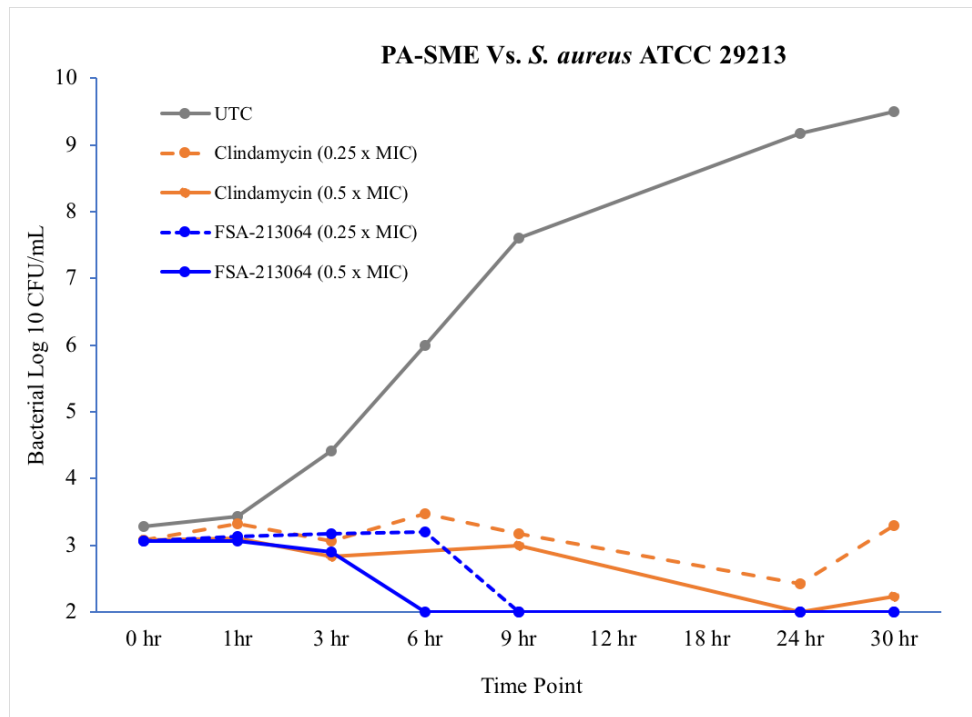
There were more than 1.0 log₁₀ CFU reductions from 9th hour and 6th hour onwards with $0.25 \times \text{MIC}$ and $0.5 \times \text{MIC}$ respectively. There was no regrowth observed even after 30th hour indicating a possible complete inhibition of growth.

Results are tabulated below.

Table D3:

Time Point	Bacterial Log ₁₀ CFU/mL				
	UTC	Clindamycin (0.25 × MIC)	Clindamycin (0.5 × MIC)	FSA-213064 (0.25 × MIC)	FSA-213064 (0.5 × MIC)
0 hr	3.28	3.08	3.08	3.06	3.06
1 hr	3.44	3.32	3.11	3.14	3.07
3 hr	4.41	3.07	2.84	3.17	2.9
6 hr	6	3.47	ND	3.2	2.0
9 hr	7.6	3.17	3.0	2.0	2.0
24 hr	9.17	2.43	2.0	2.0	2.0
30 hr	9.5	3.3	2.23	2.0	2.0

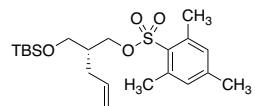
Figure D3:



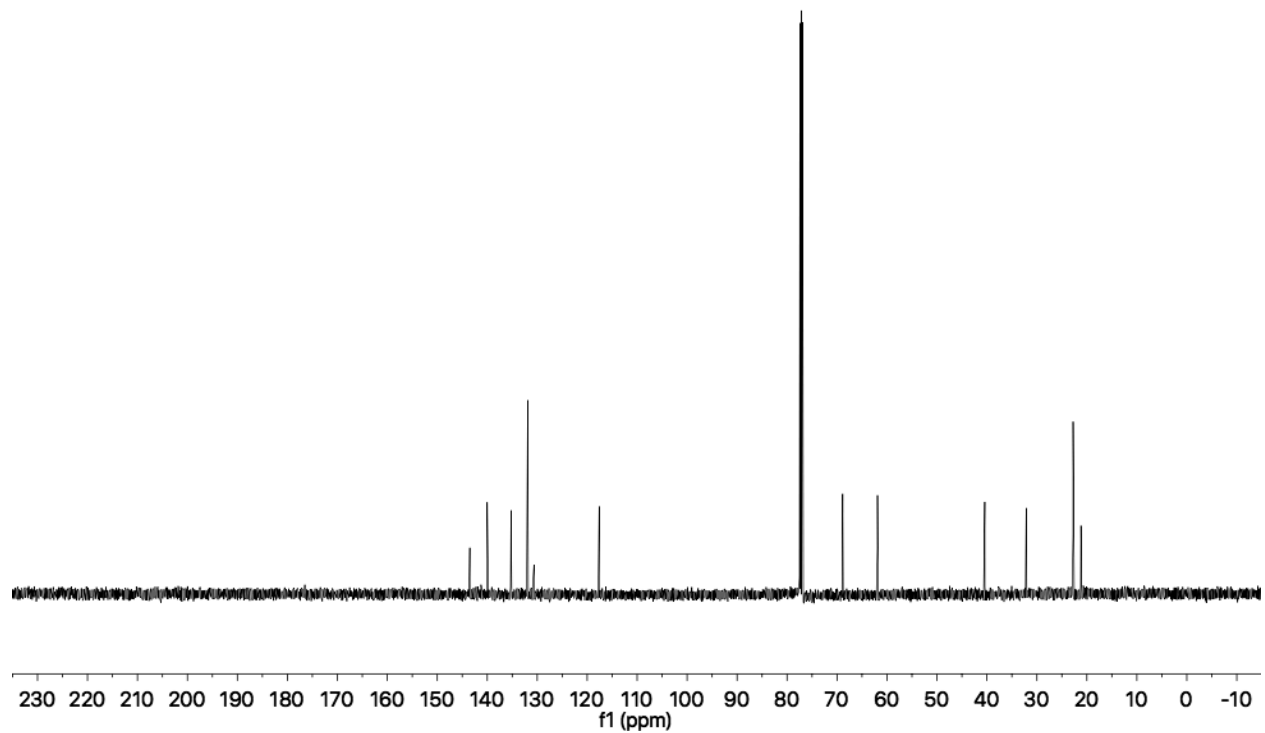
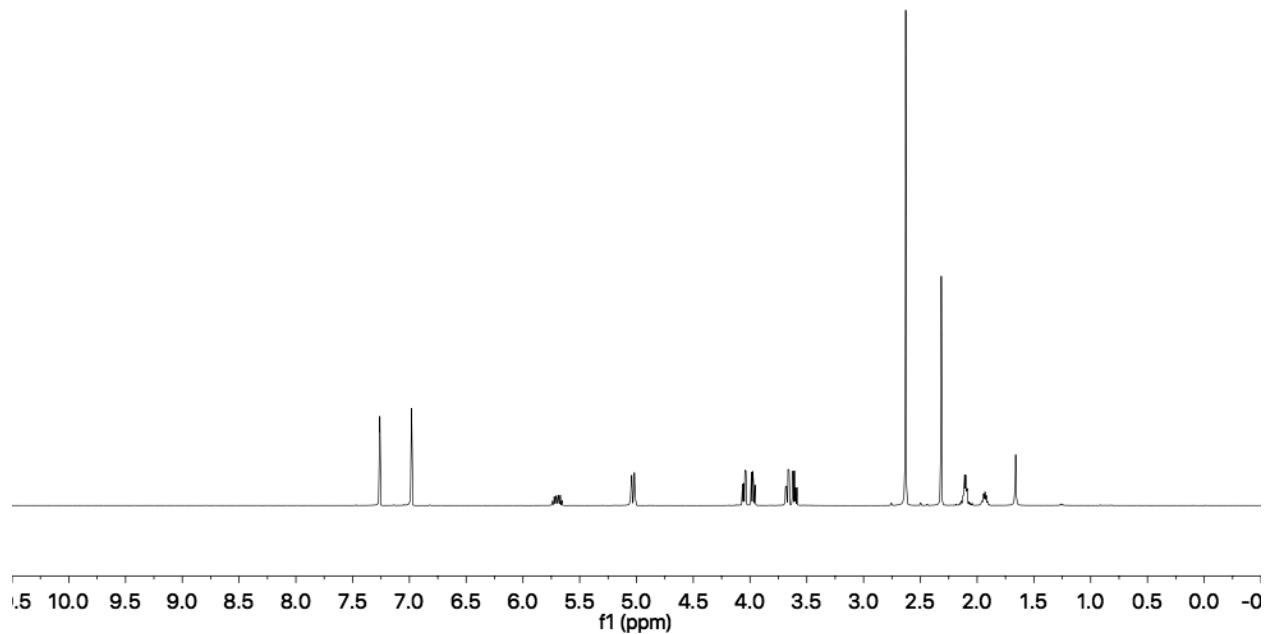
Conclusion:

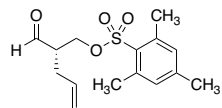
Clindamycin exhibited bacteriostatic effect at $0.25 \times \text{MIC}$ and $0.5 \times \text{MIC}$. There was a drop in \log_{10} CFUs below the detection limit at $0.5 \times \text{MIC}$ of clindamycin but the bacteria started to regrow by 30th hour onwards. Whereas FSA-213064 exhibited a complete elimination of bacteria (probable) from 9th and 6th hour at $0.25 \times$ and $0.5 \times \text{MIC}$ concentrations with no regrowth even at 30th hour. This indicates our compound to be superior compared to clindamycin against sensitive wild type *S. aureus* (ATCC 29213)

Appendix E. Catalog of spectra

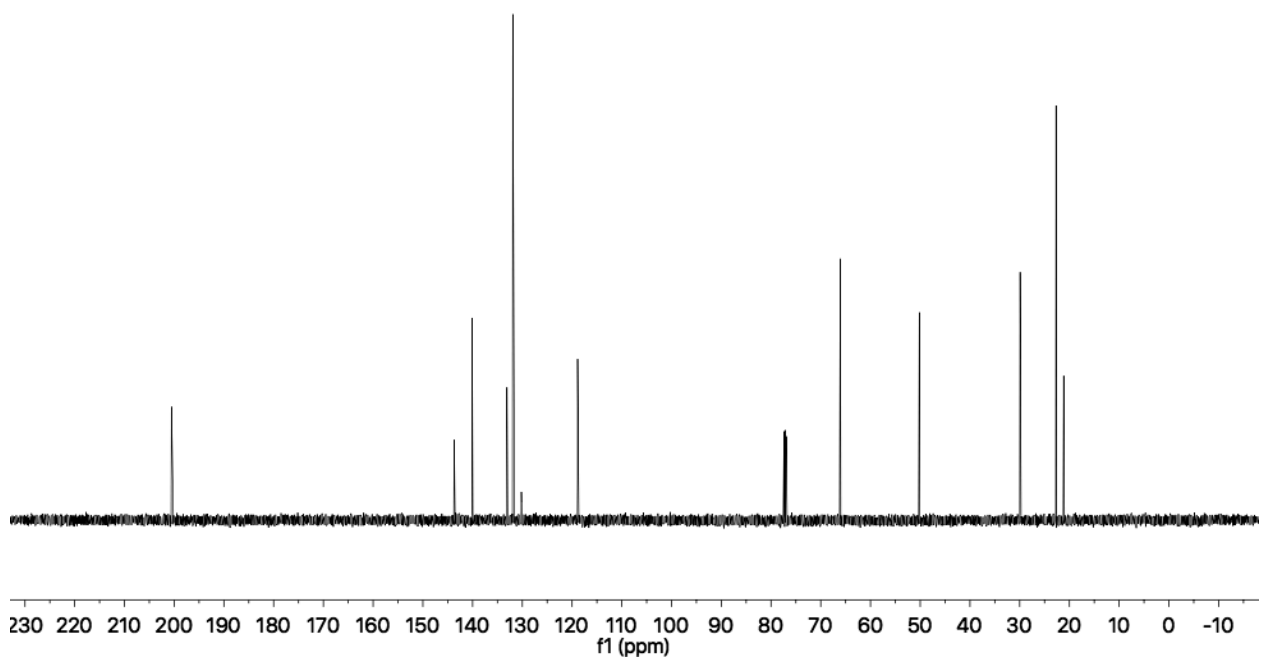
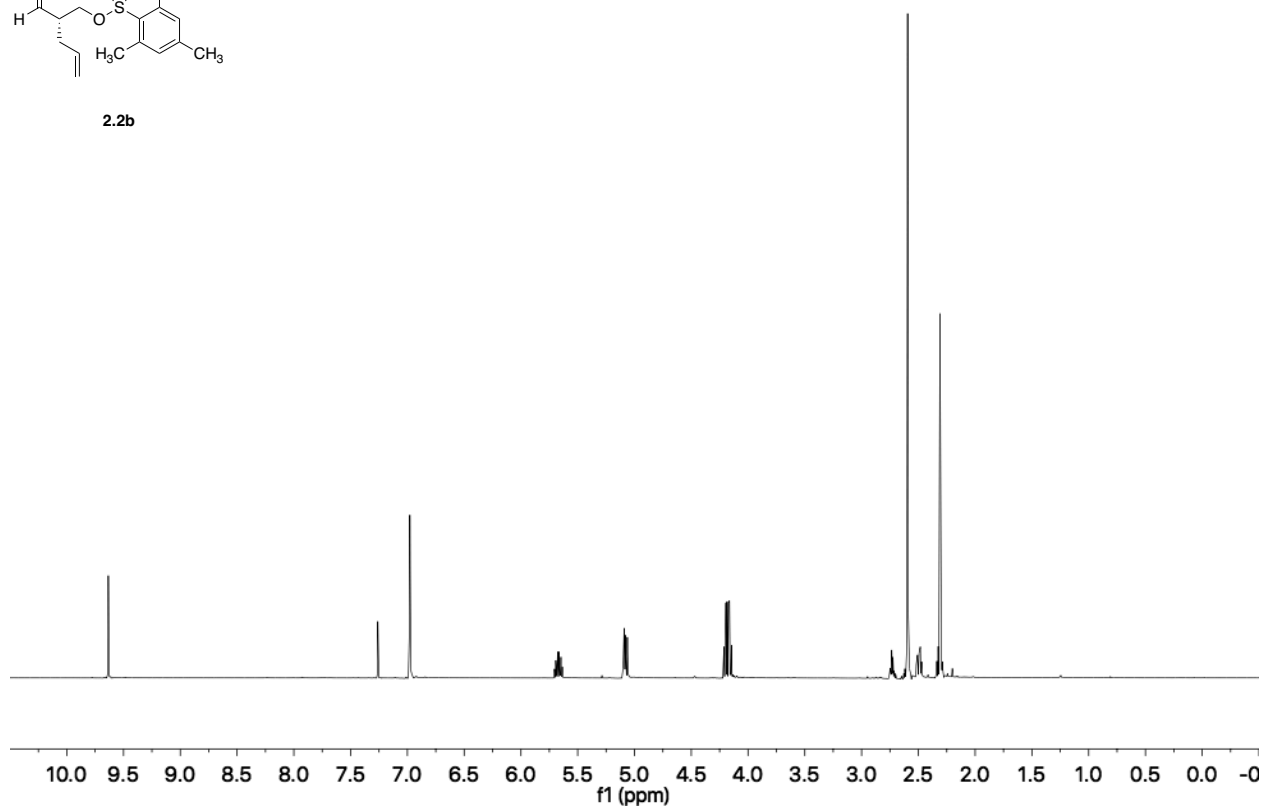


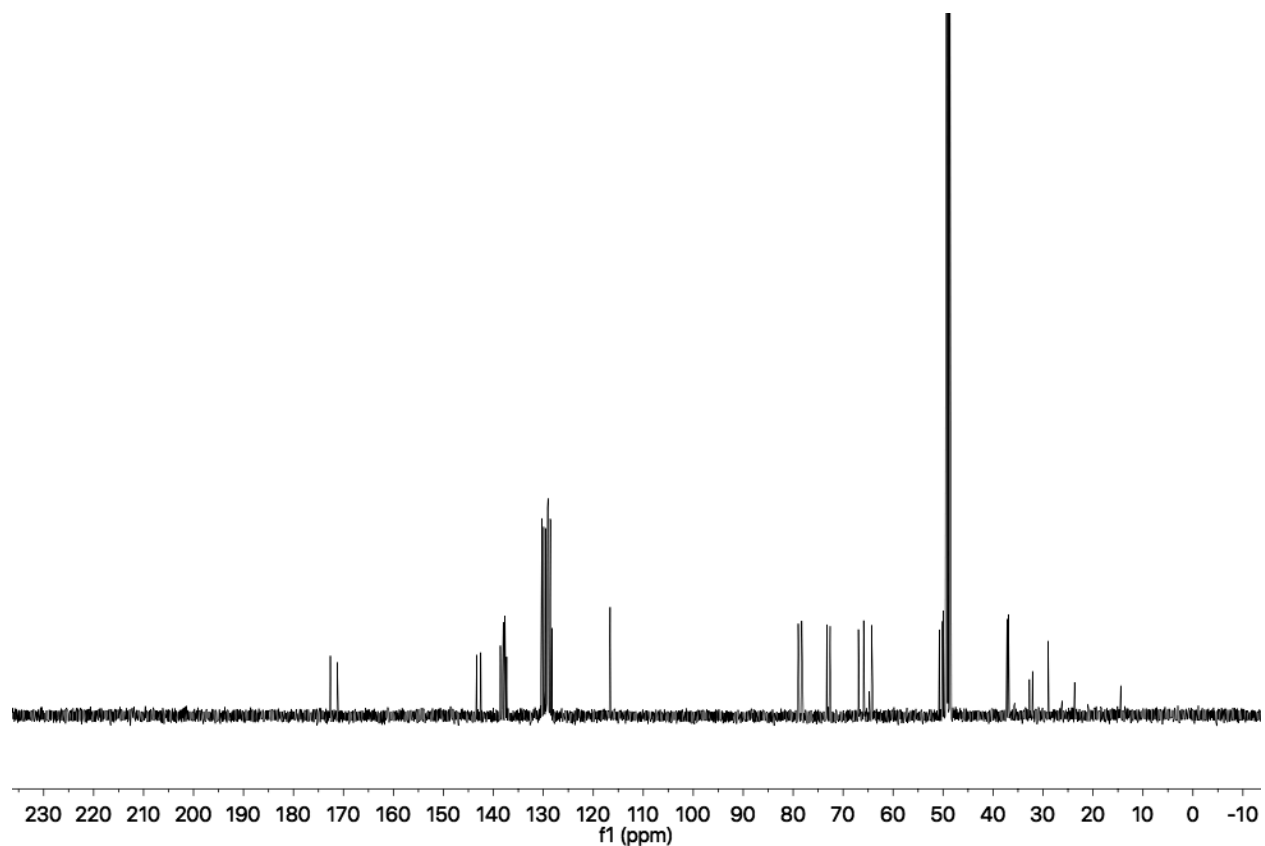
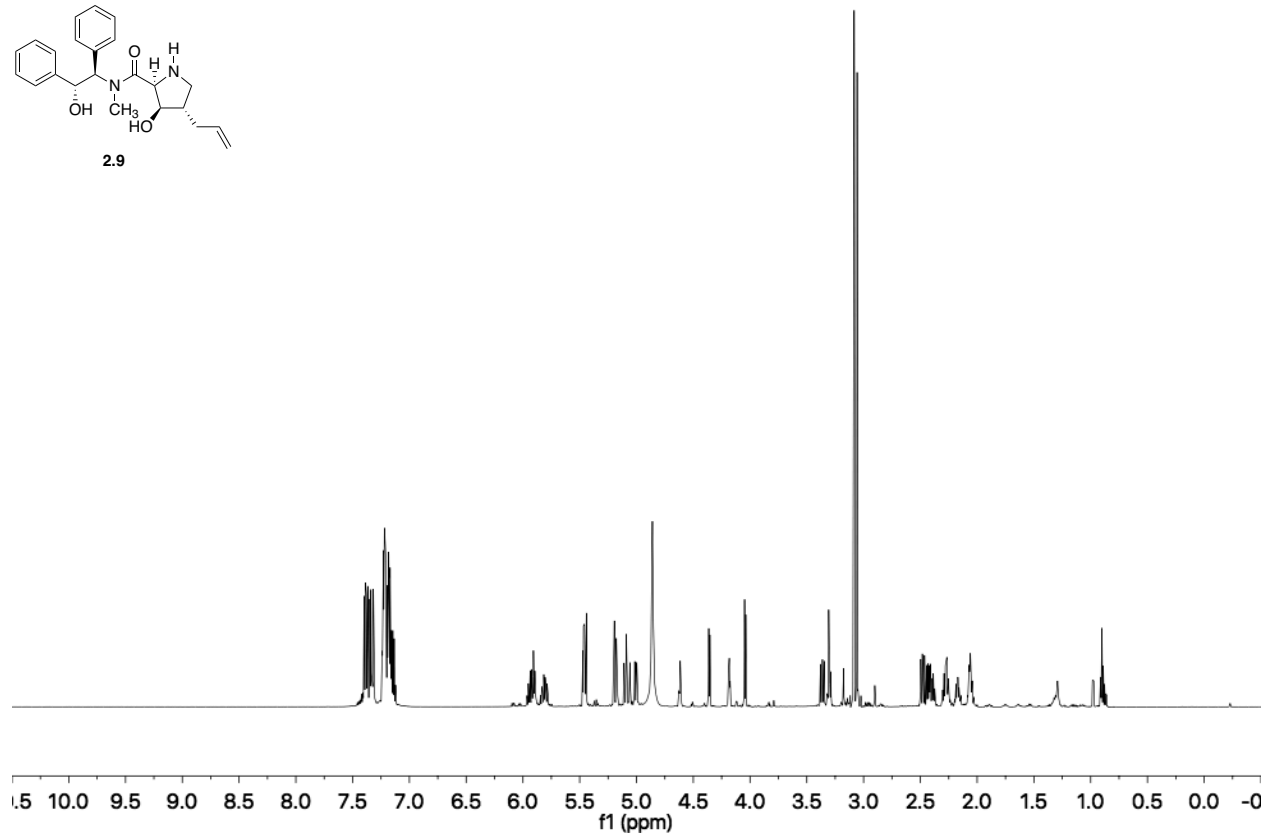
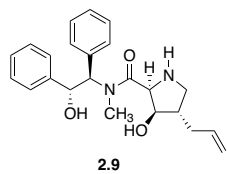
S2.2

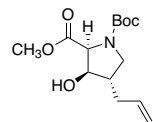




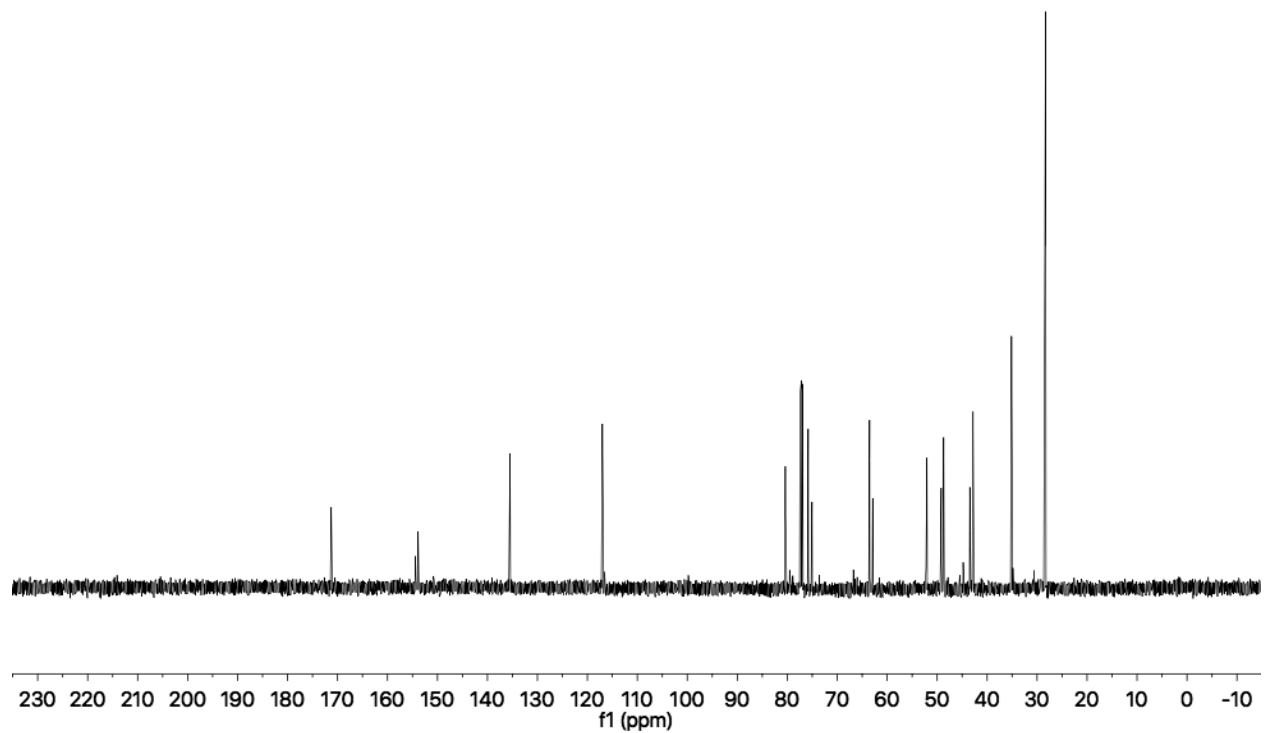
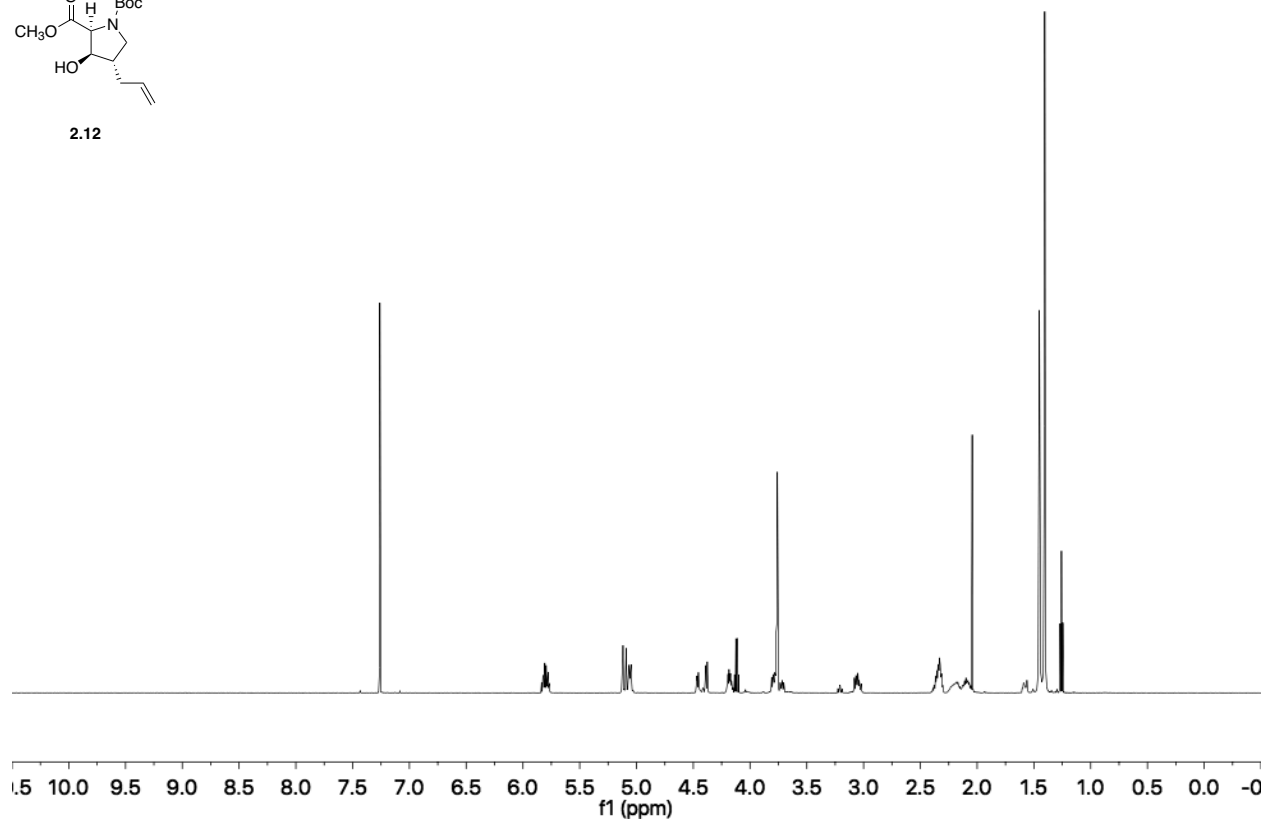
2.2b

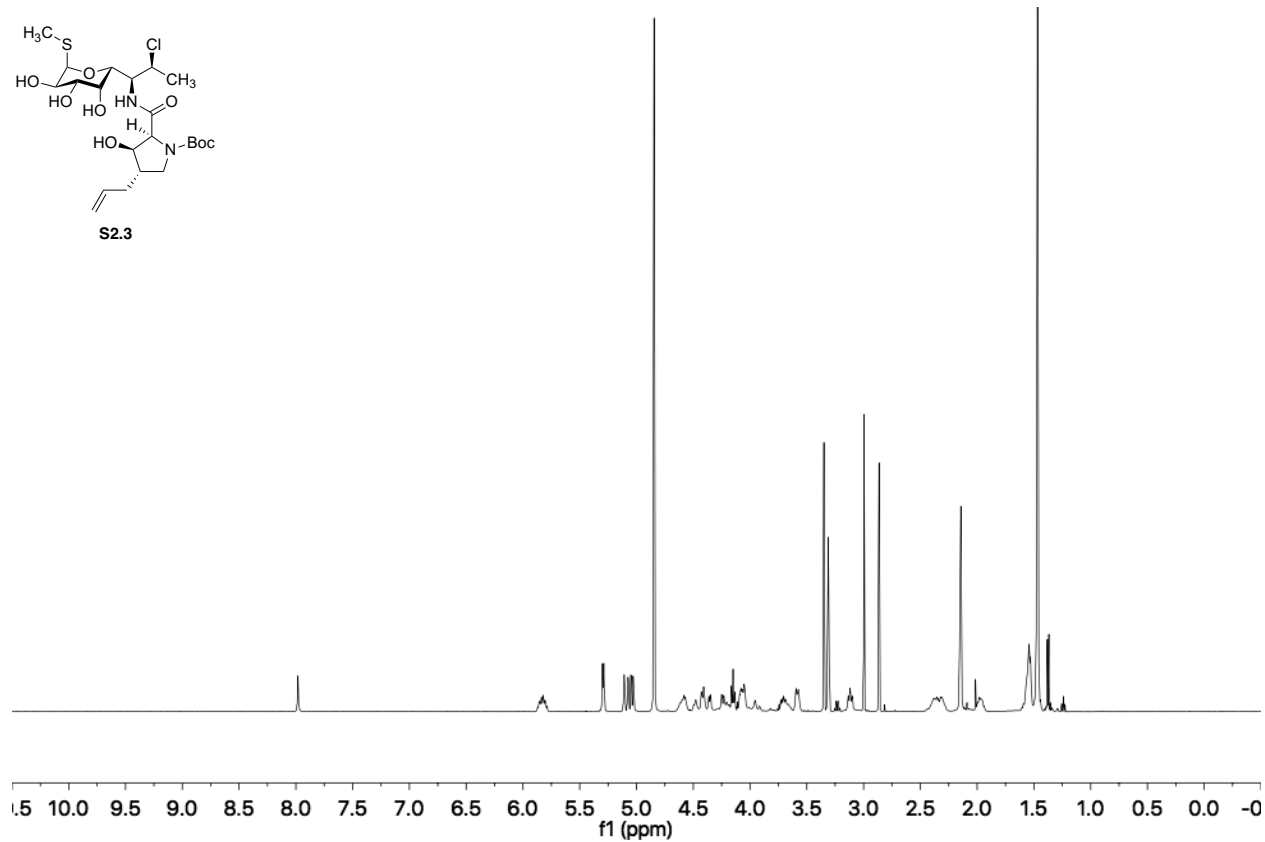
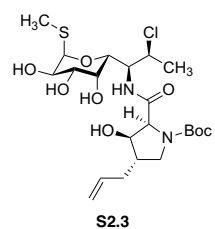
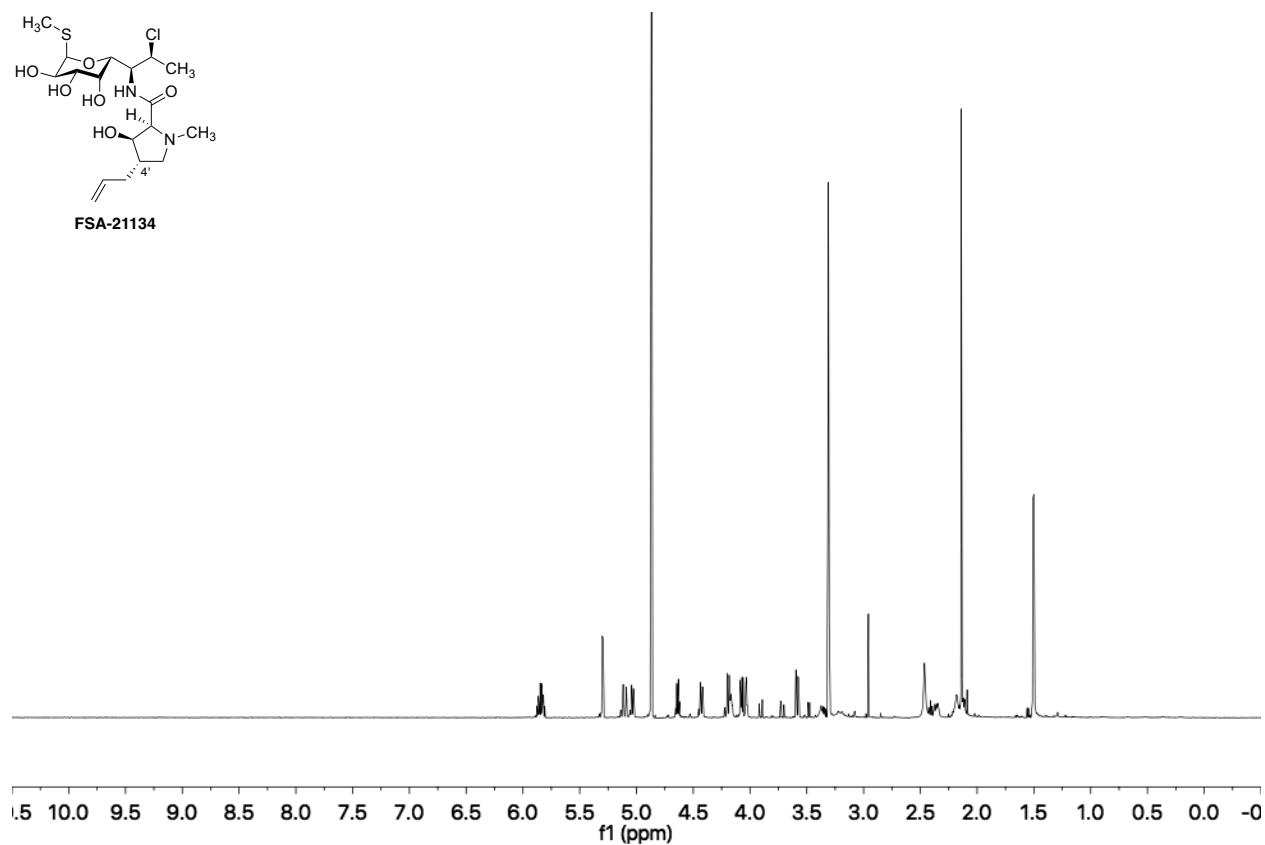
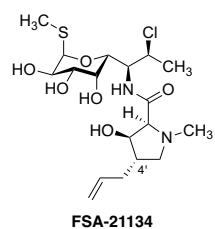


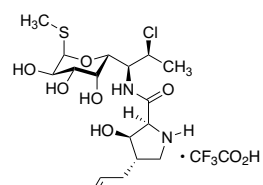




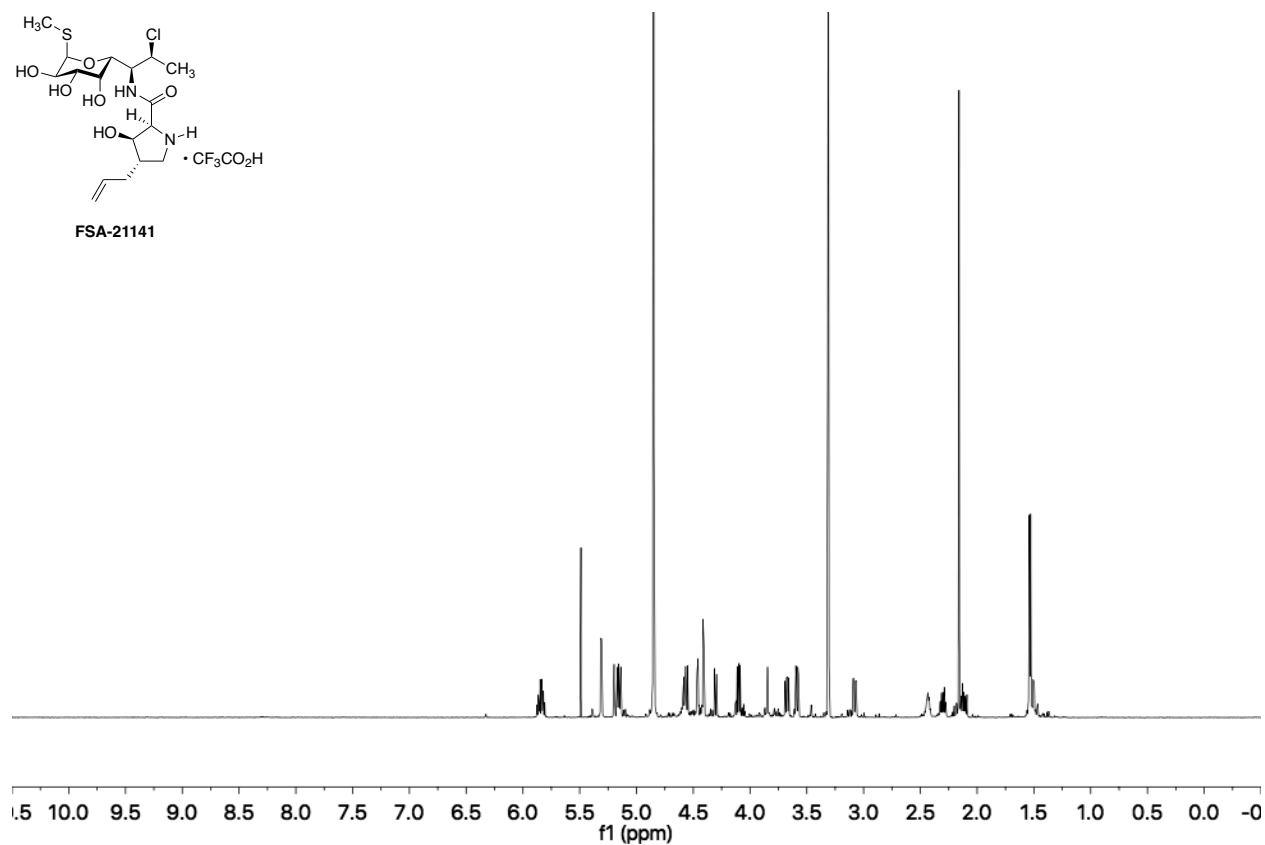
2.12

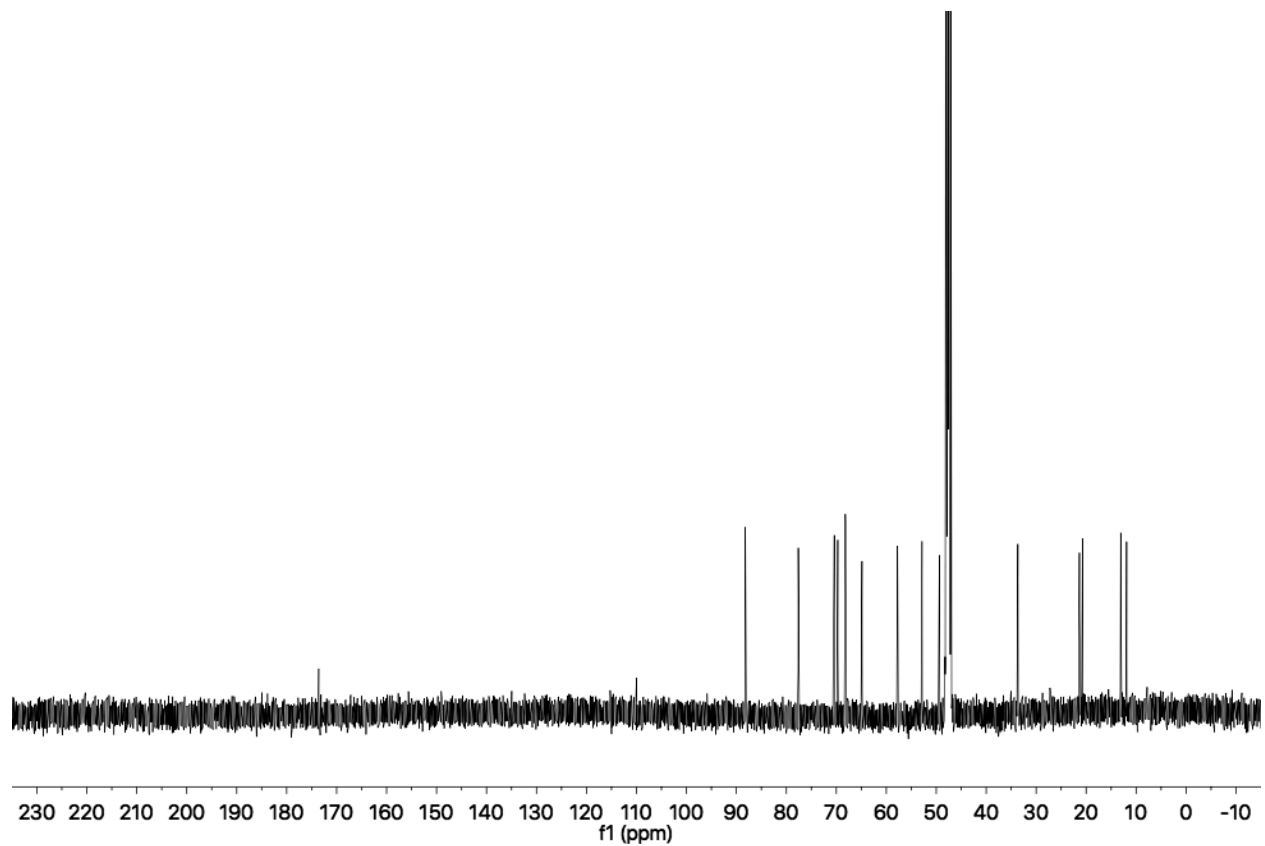
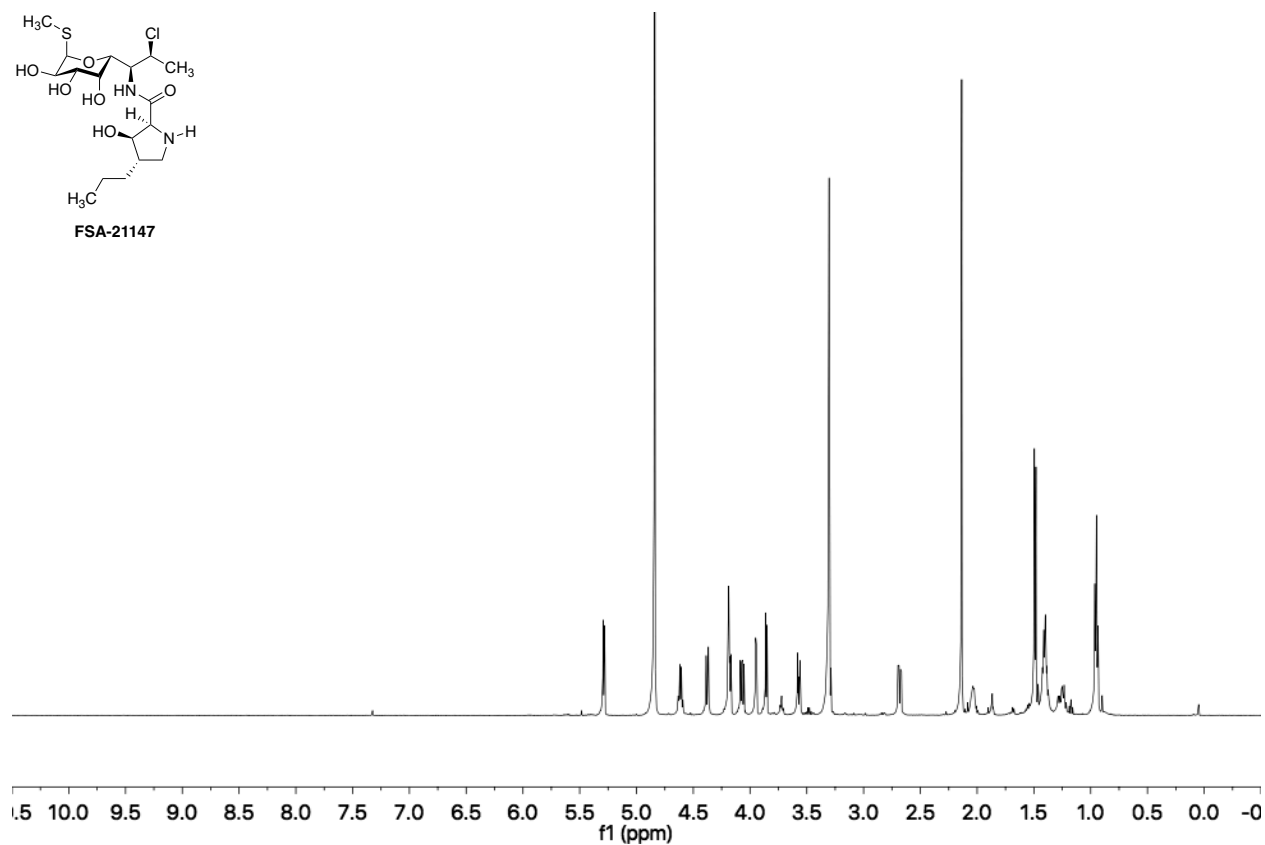
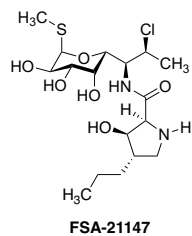


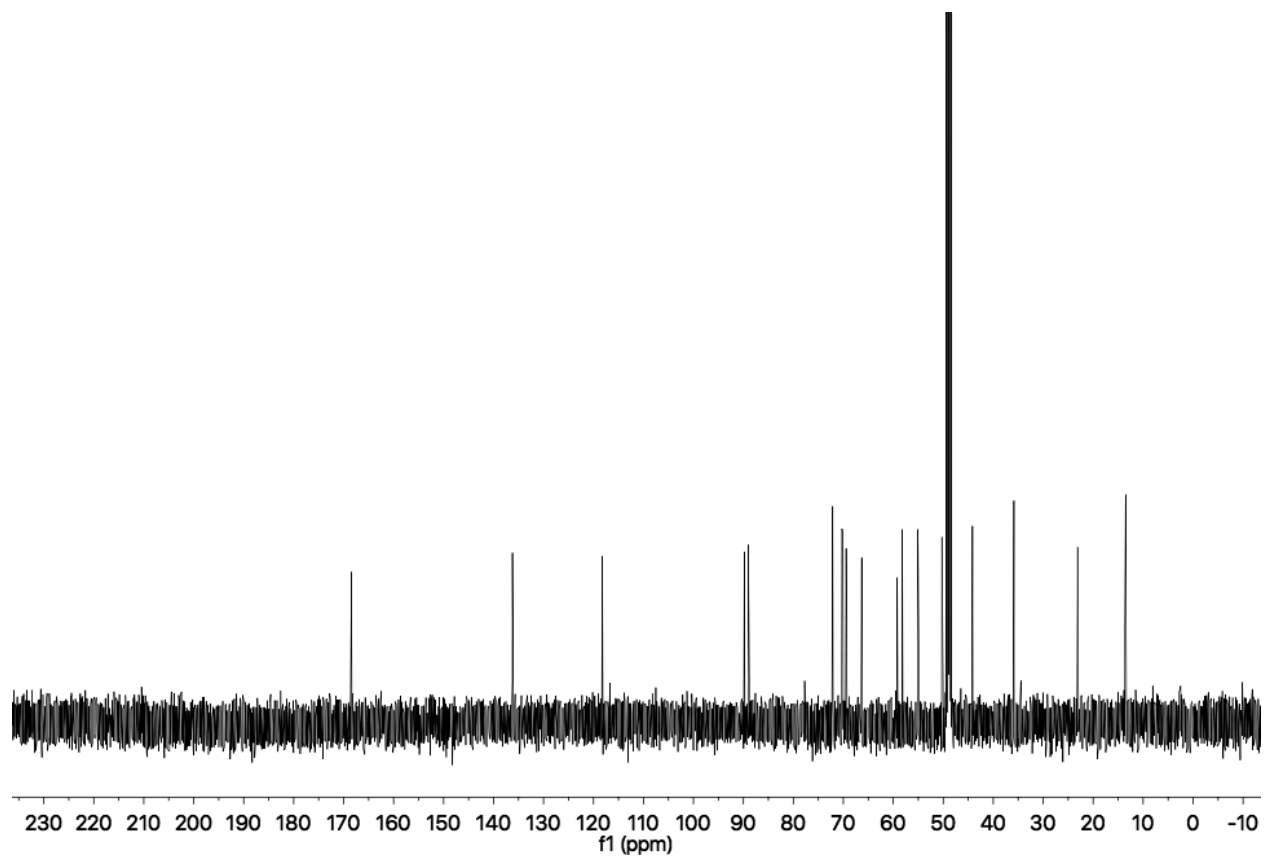
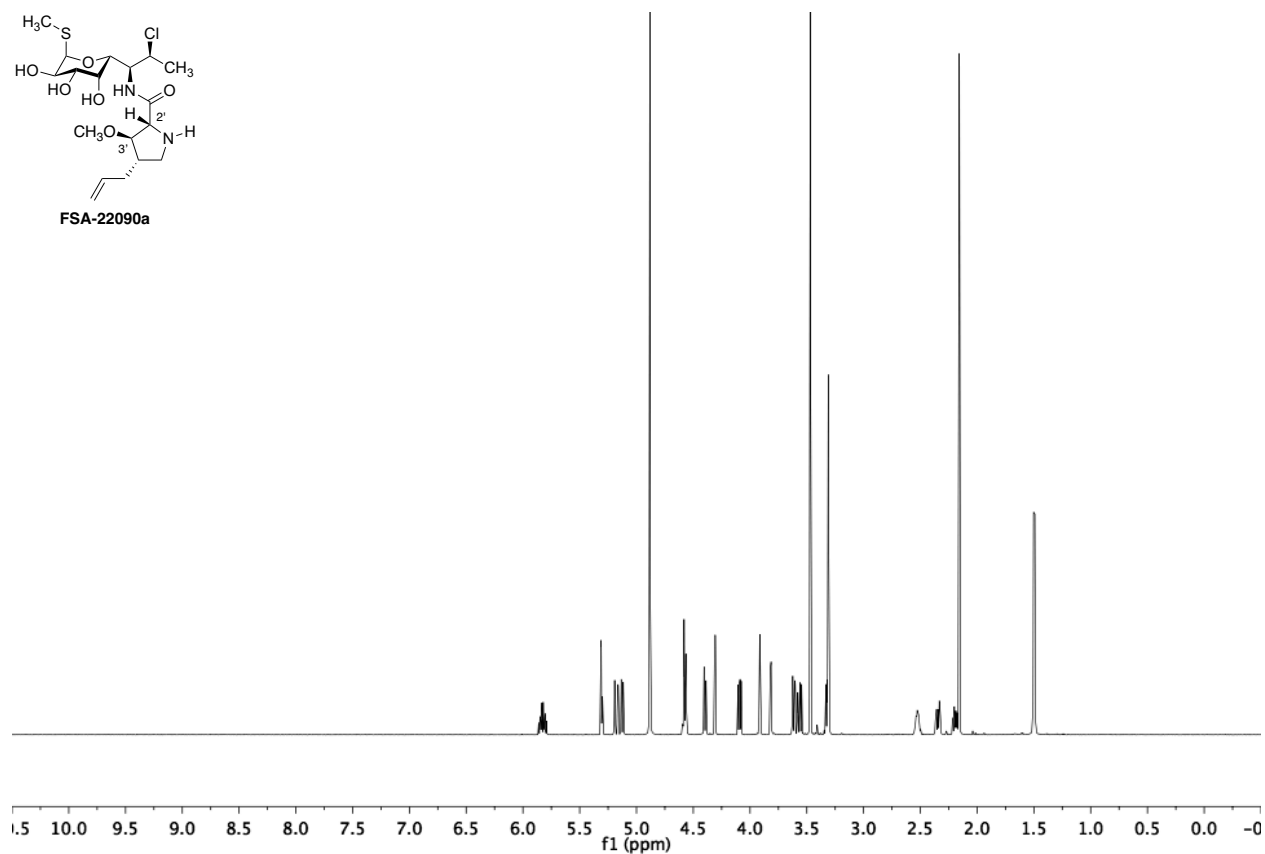
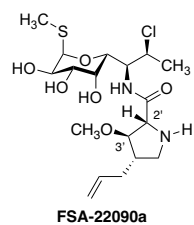


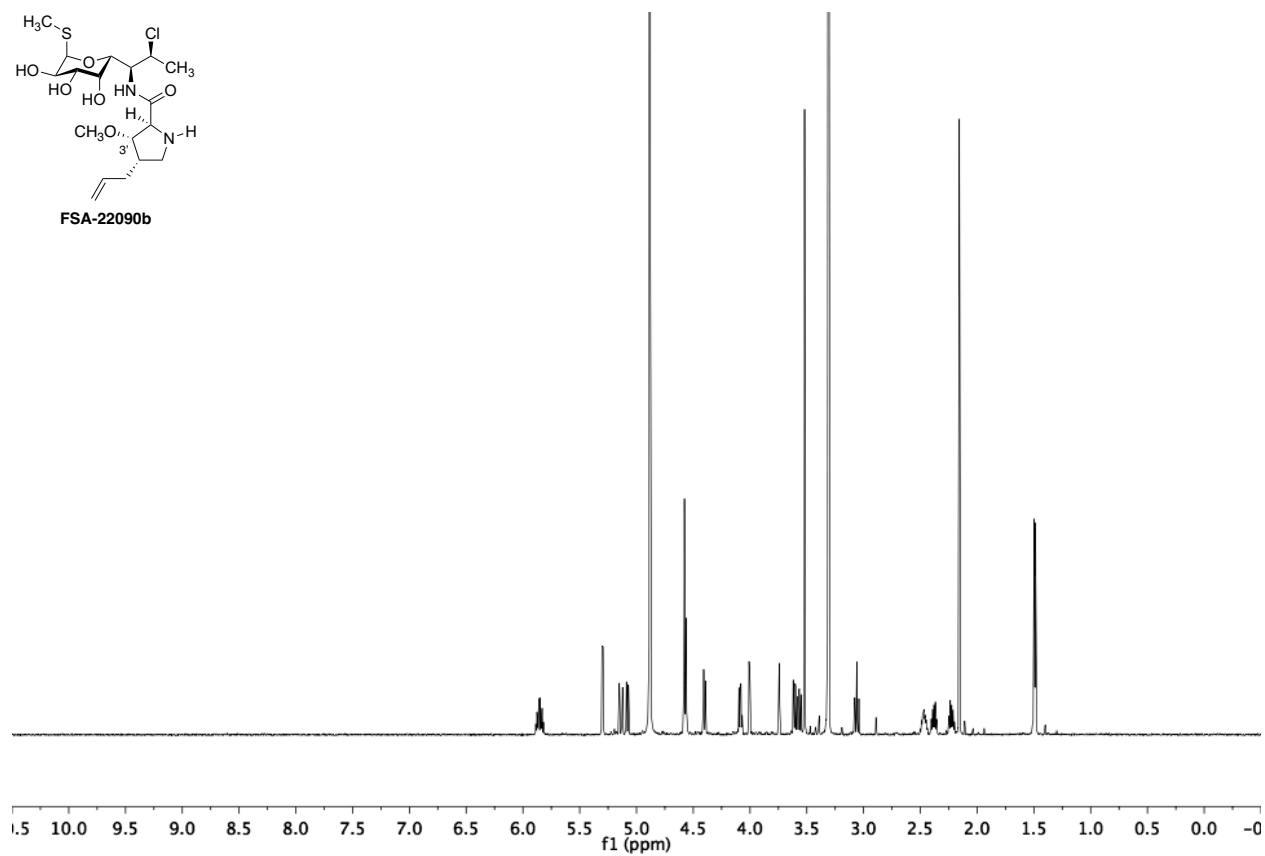
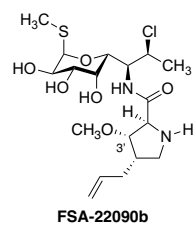


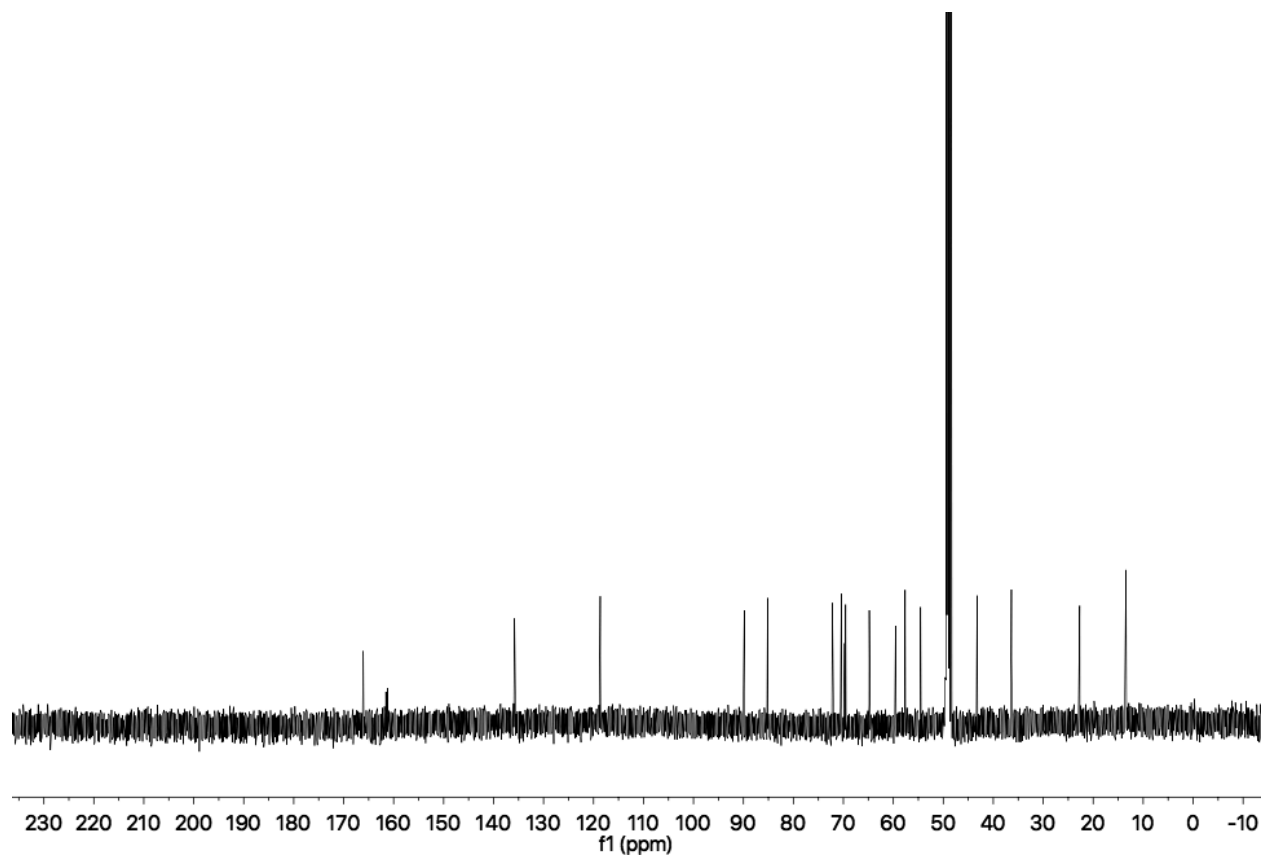
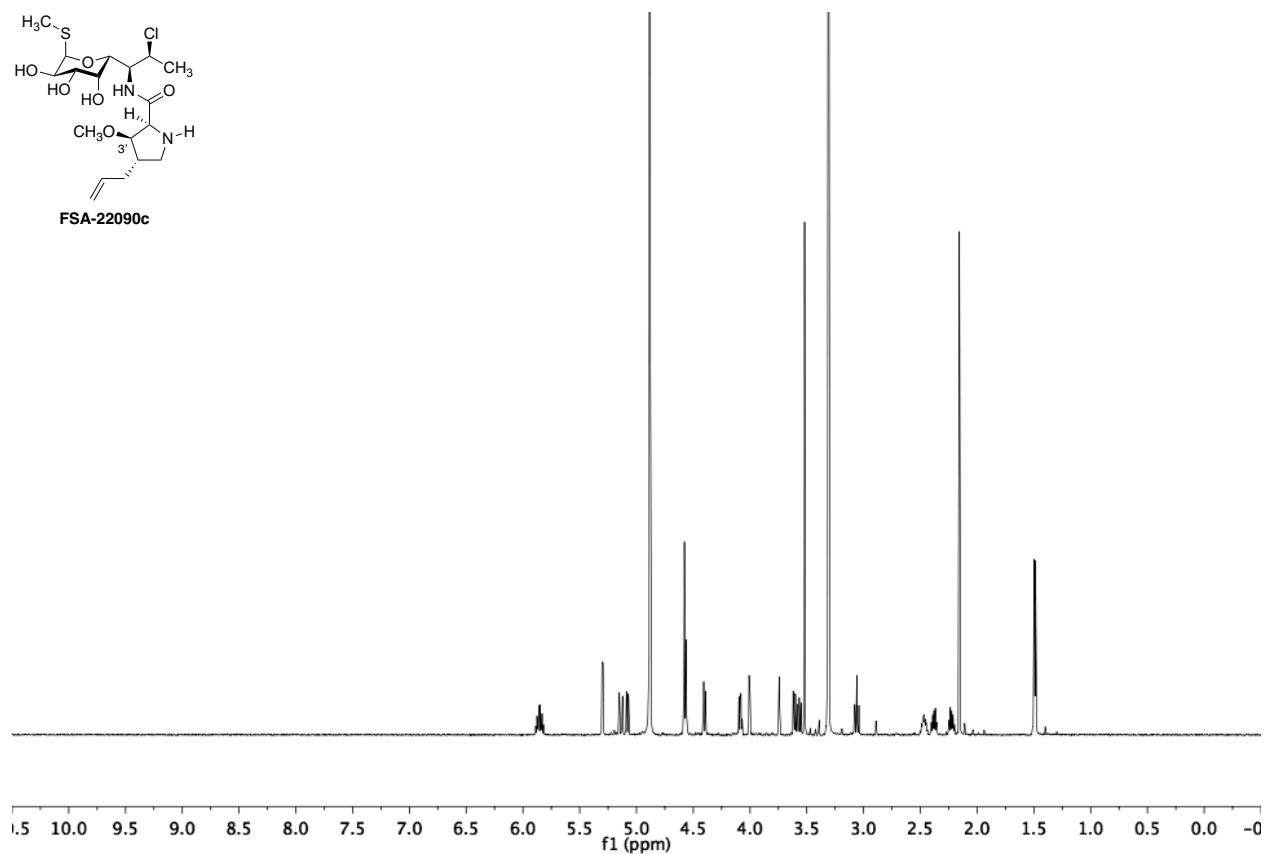
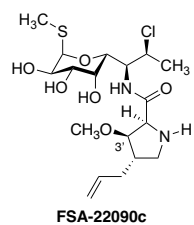
FSA-21141

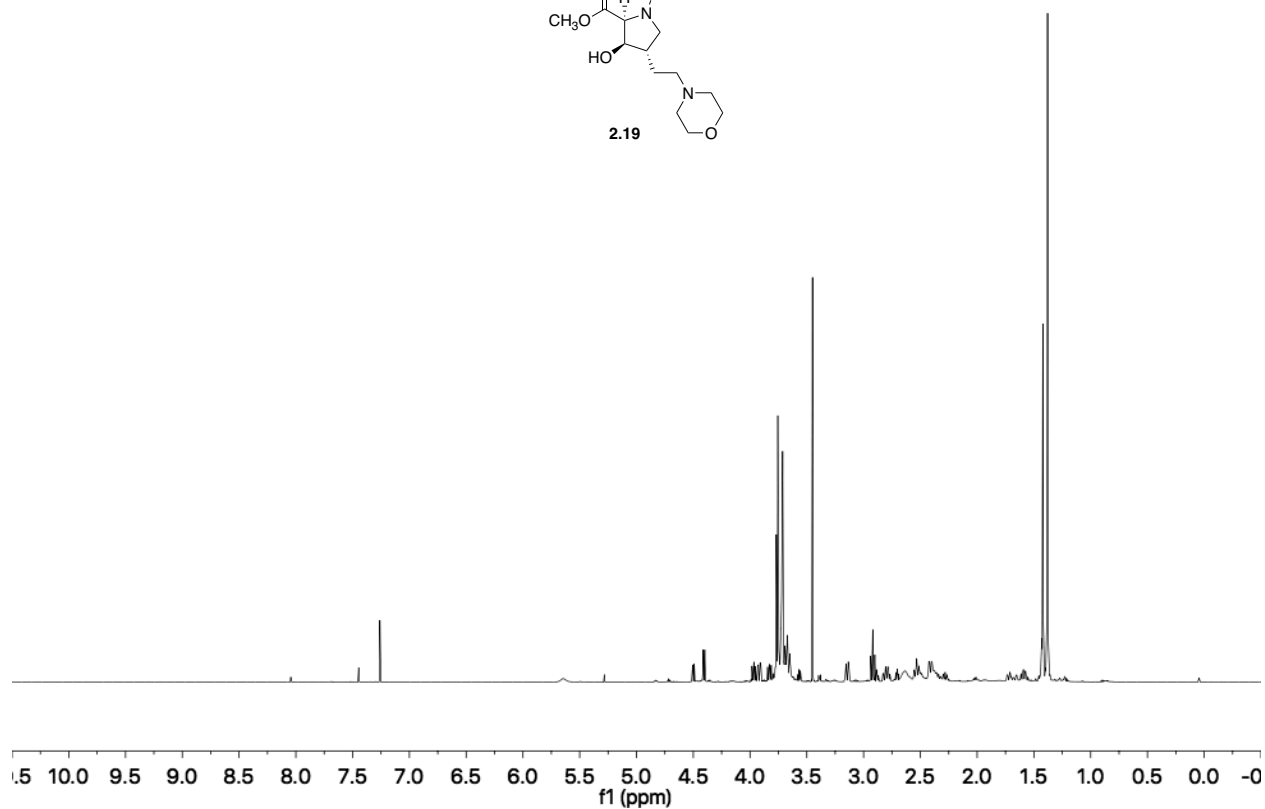
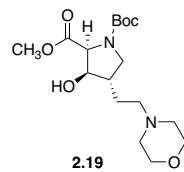


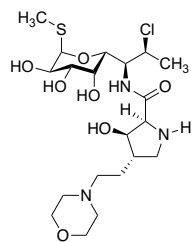




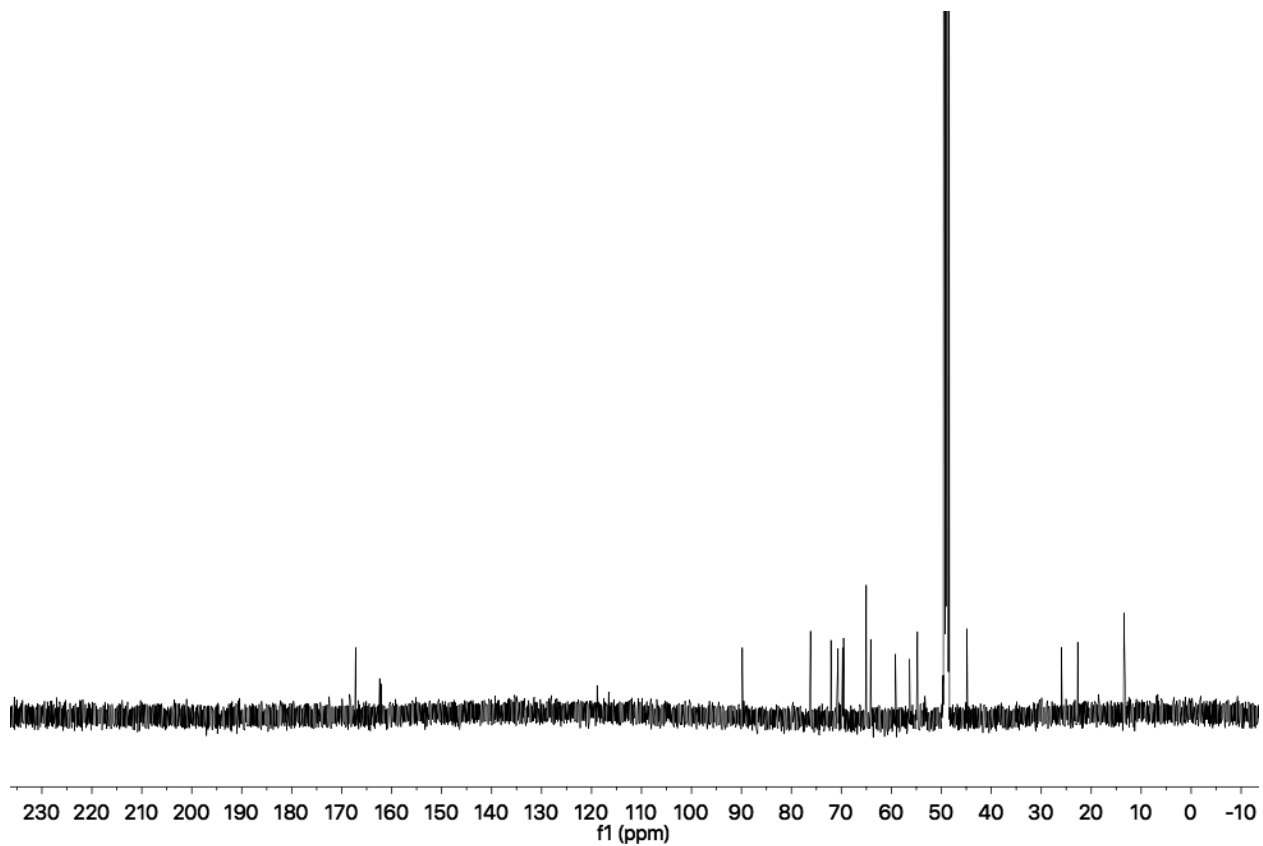
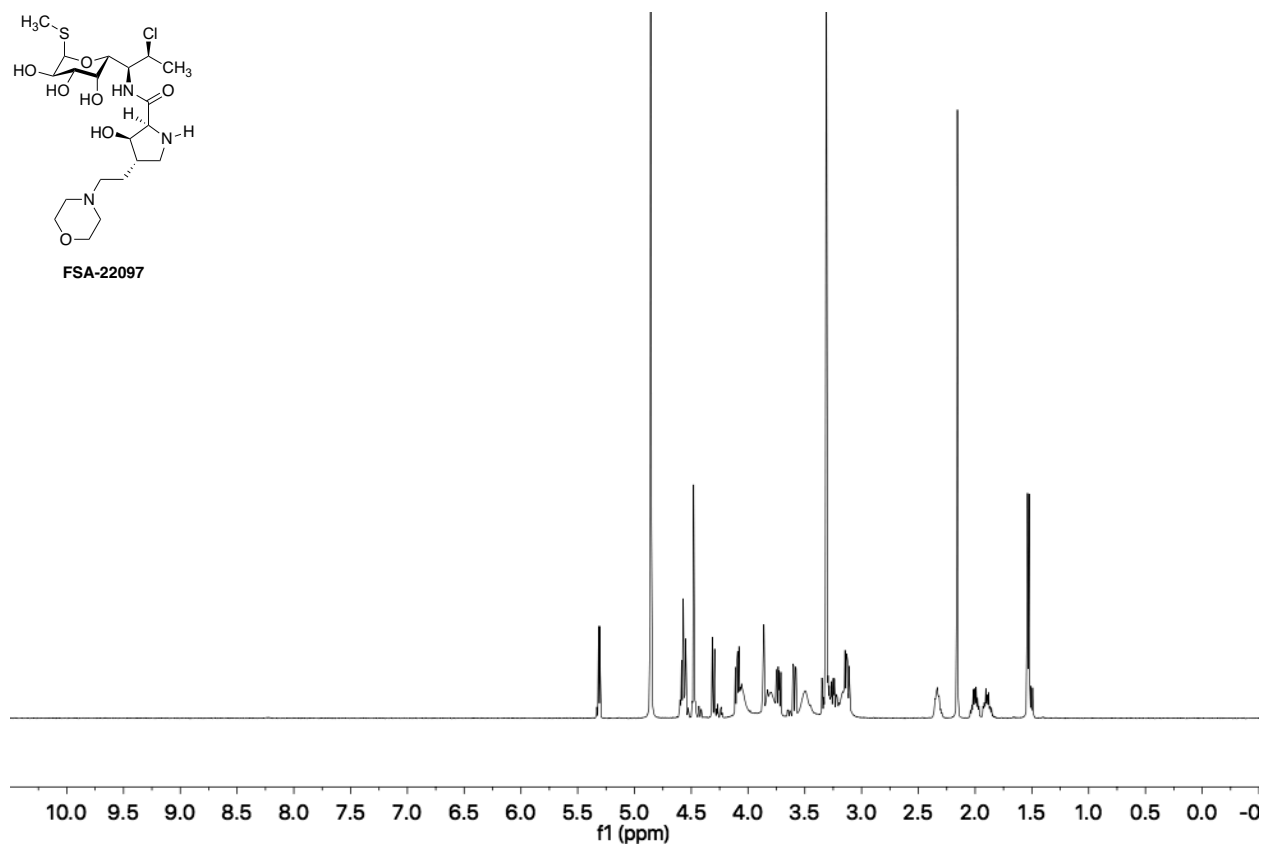


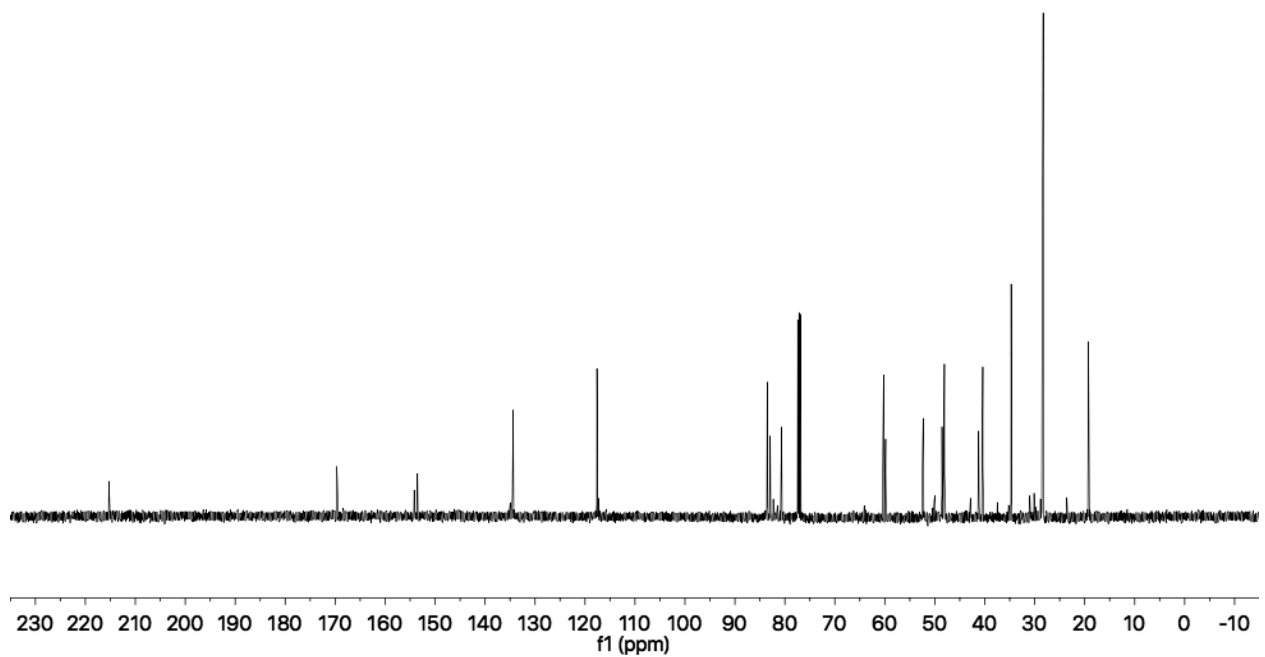
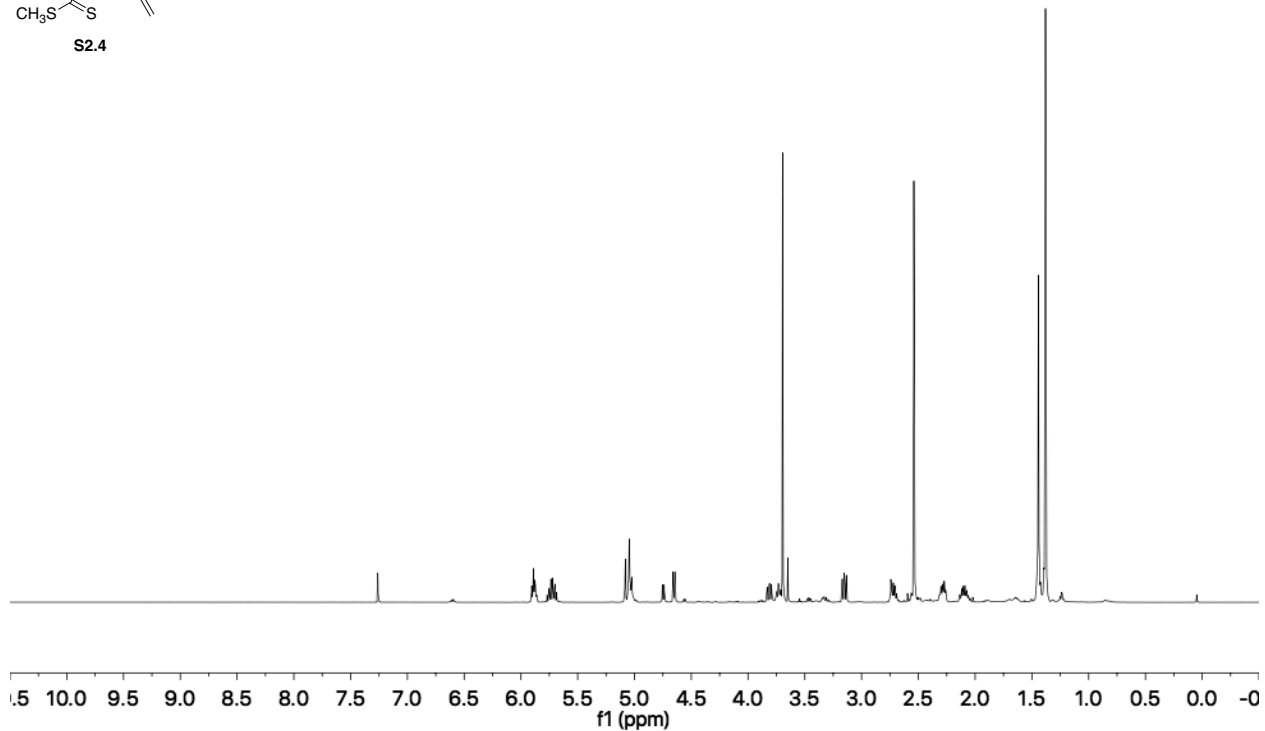
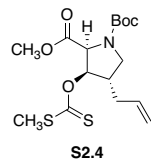


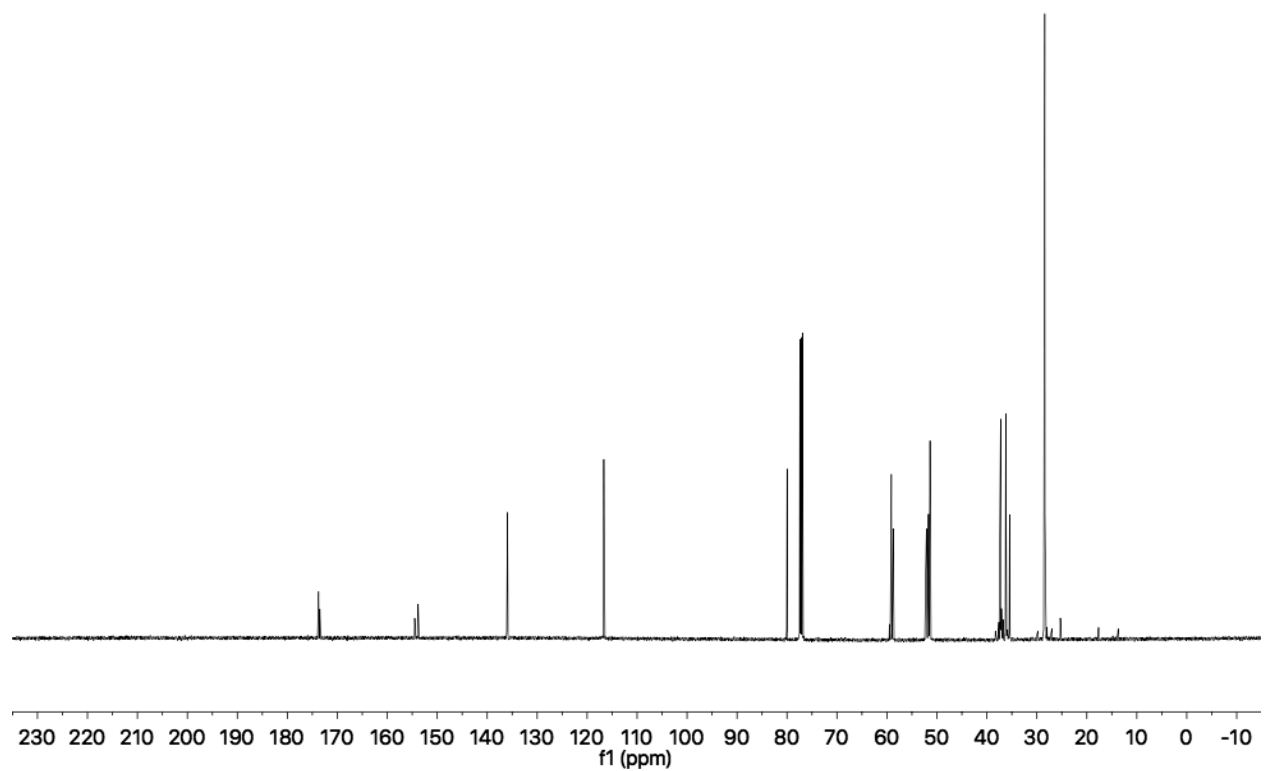
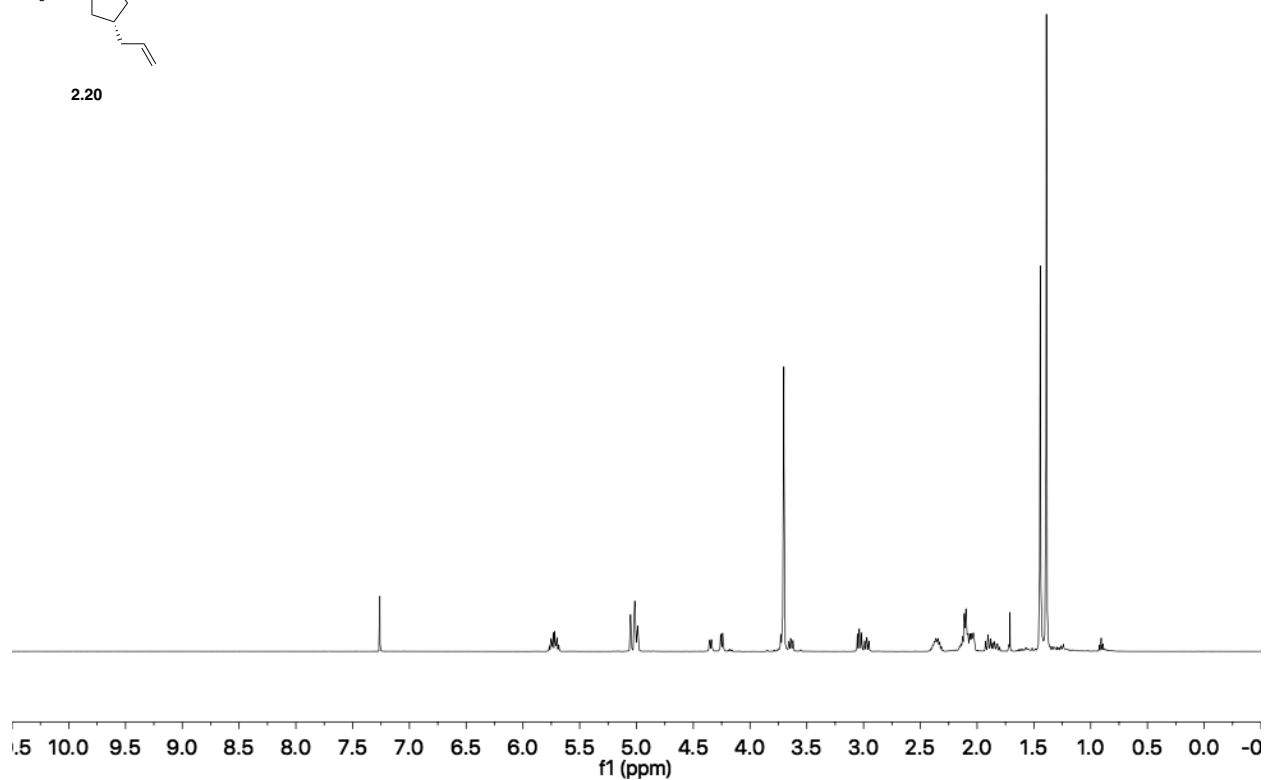
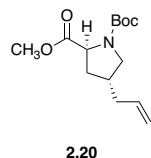


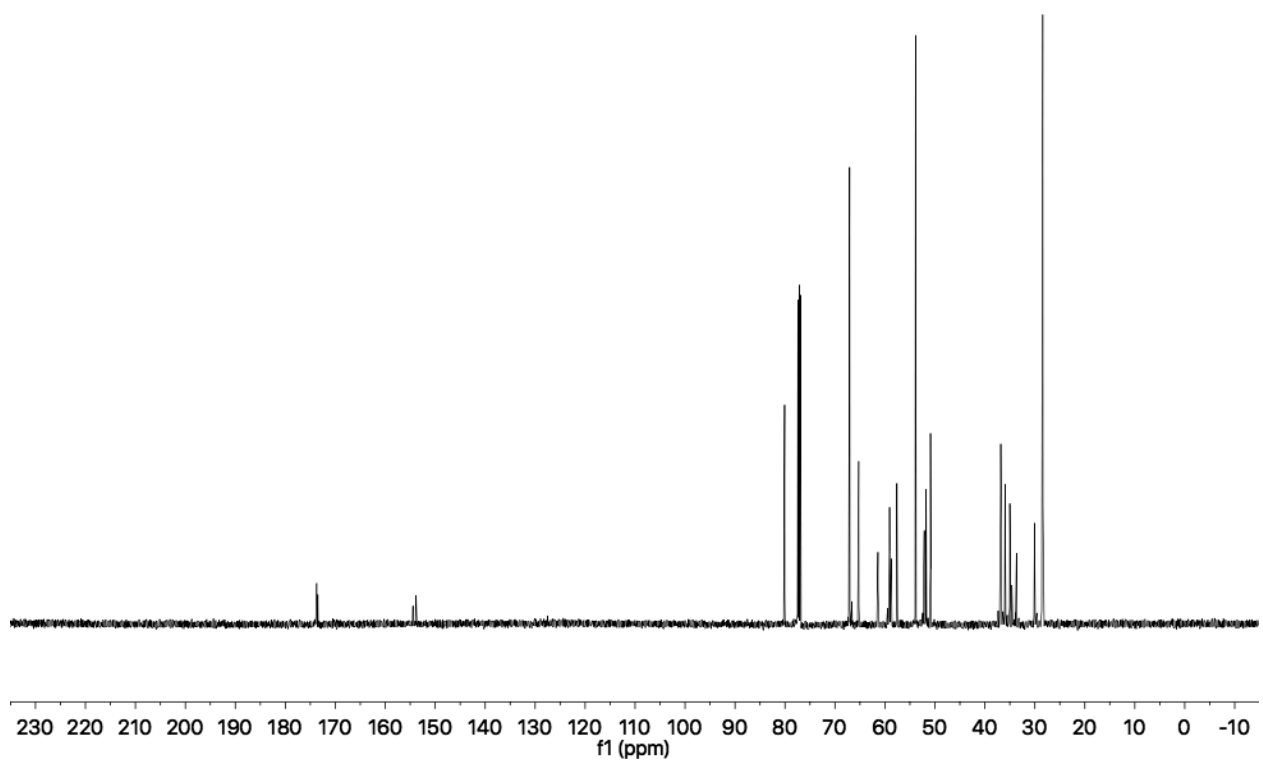
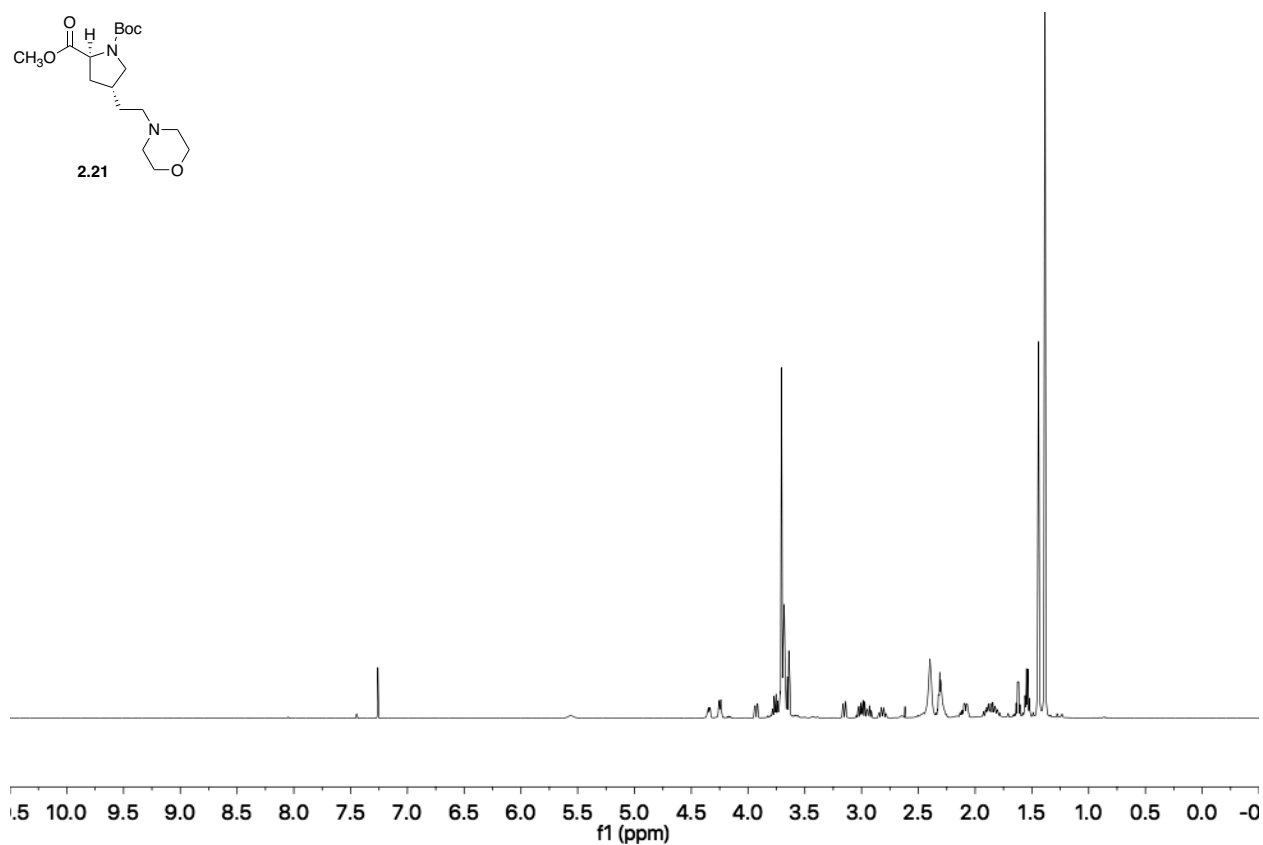
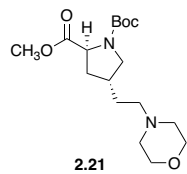


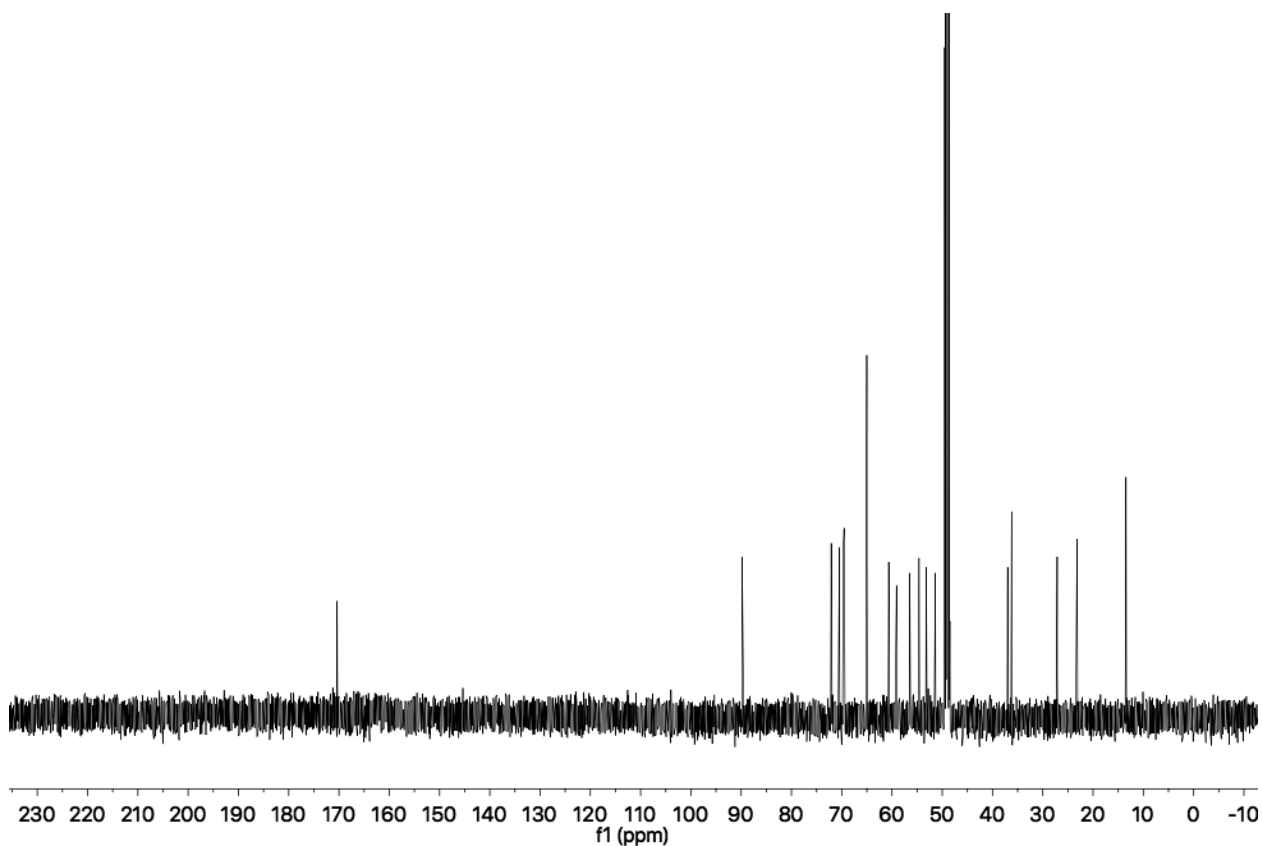
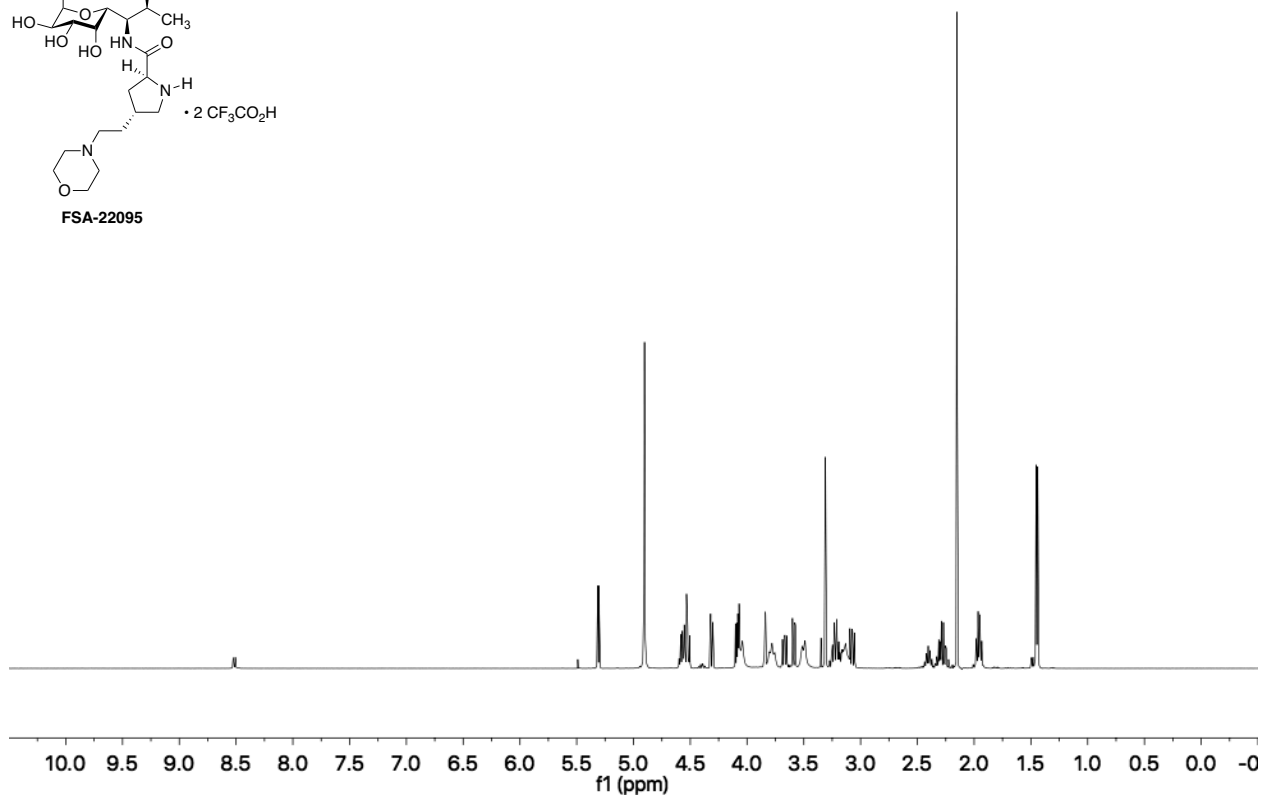
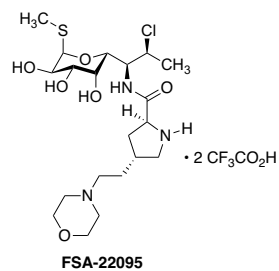
FSA-22097

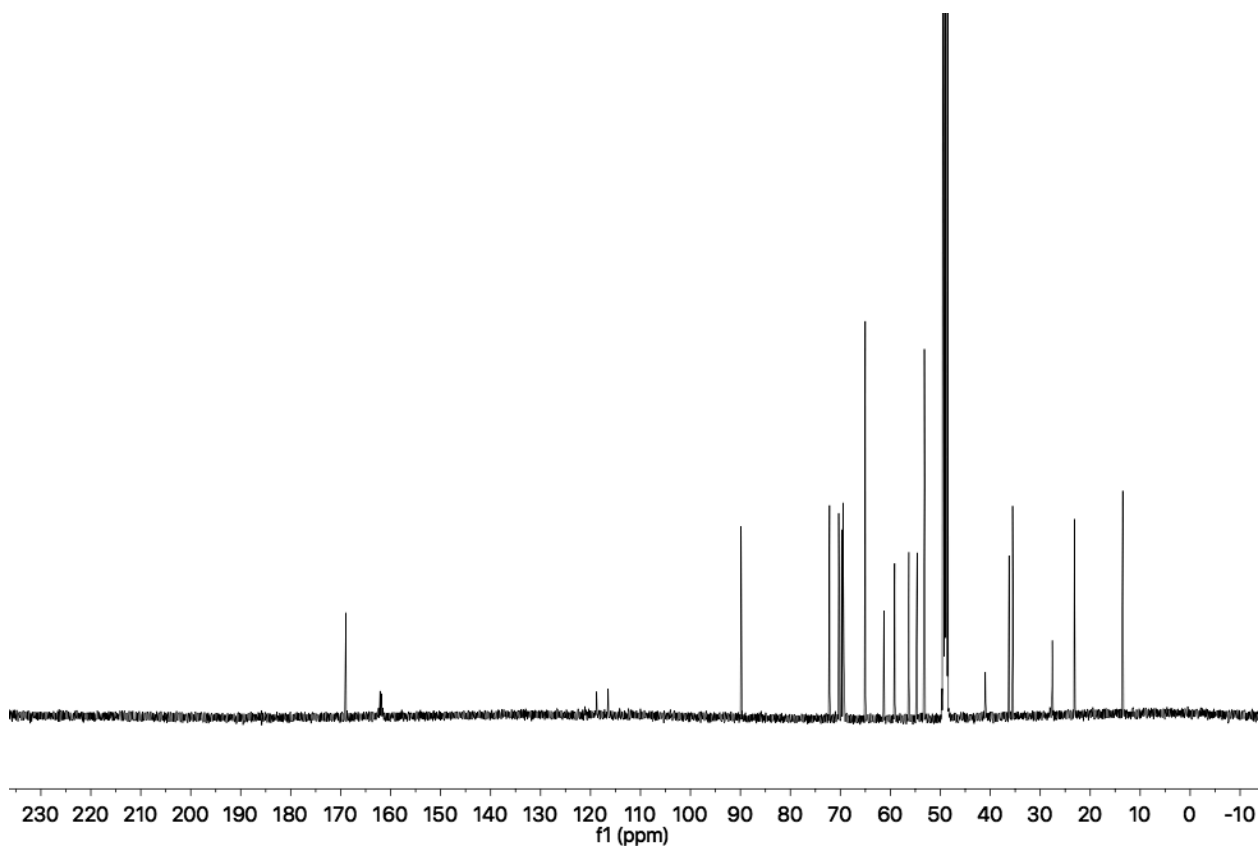
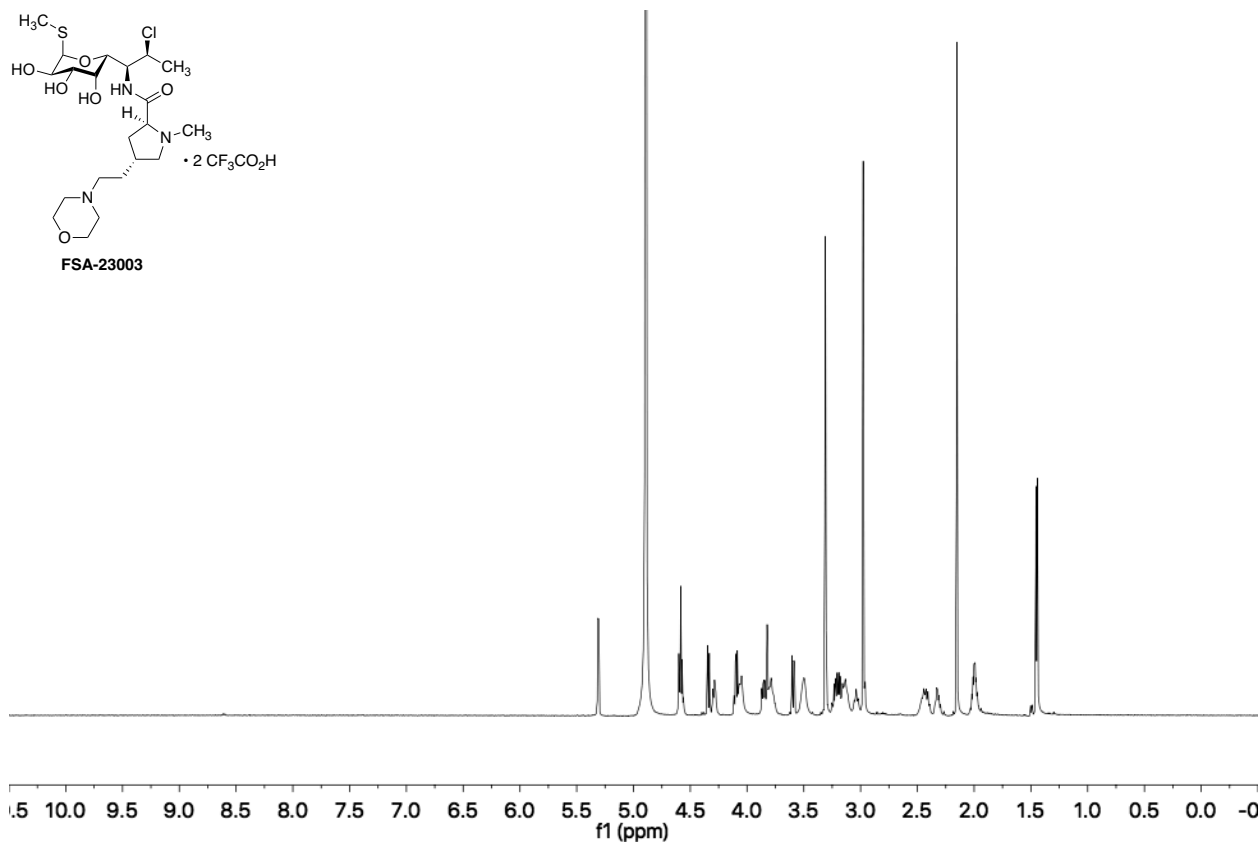
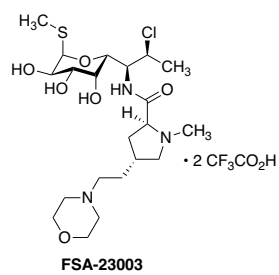


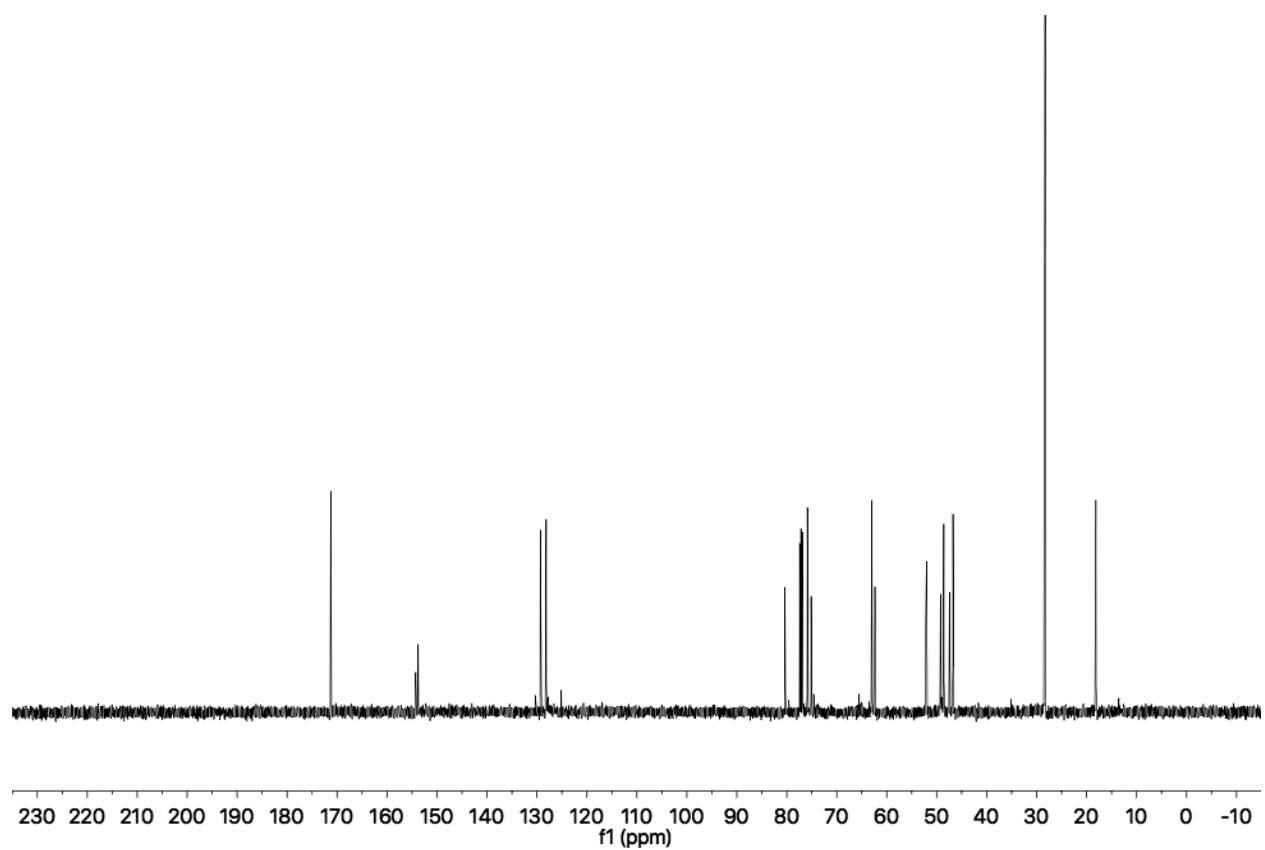
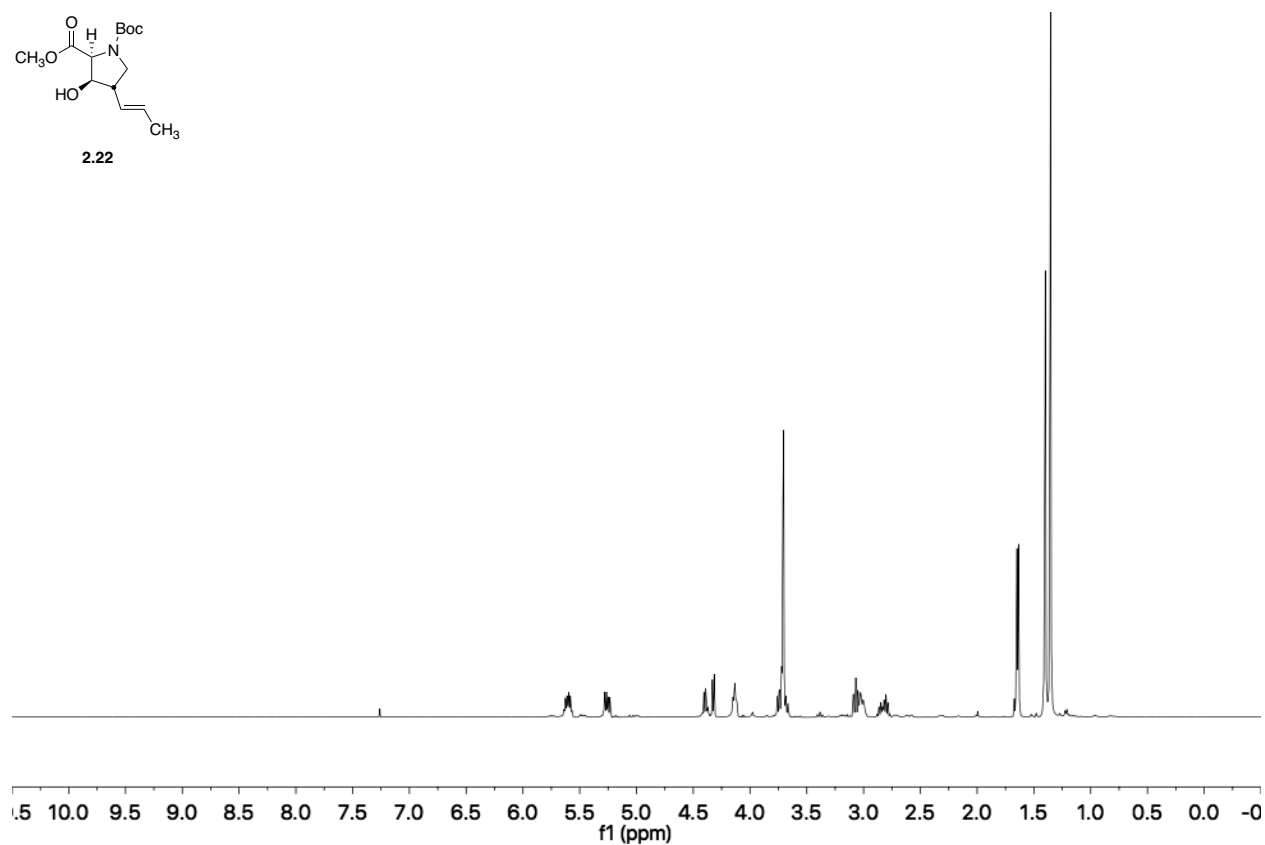
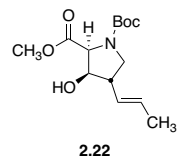


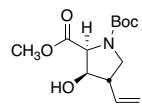




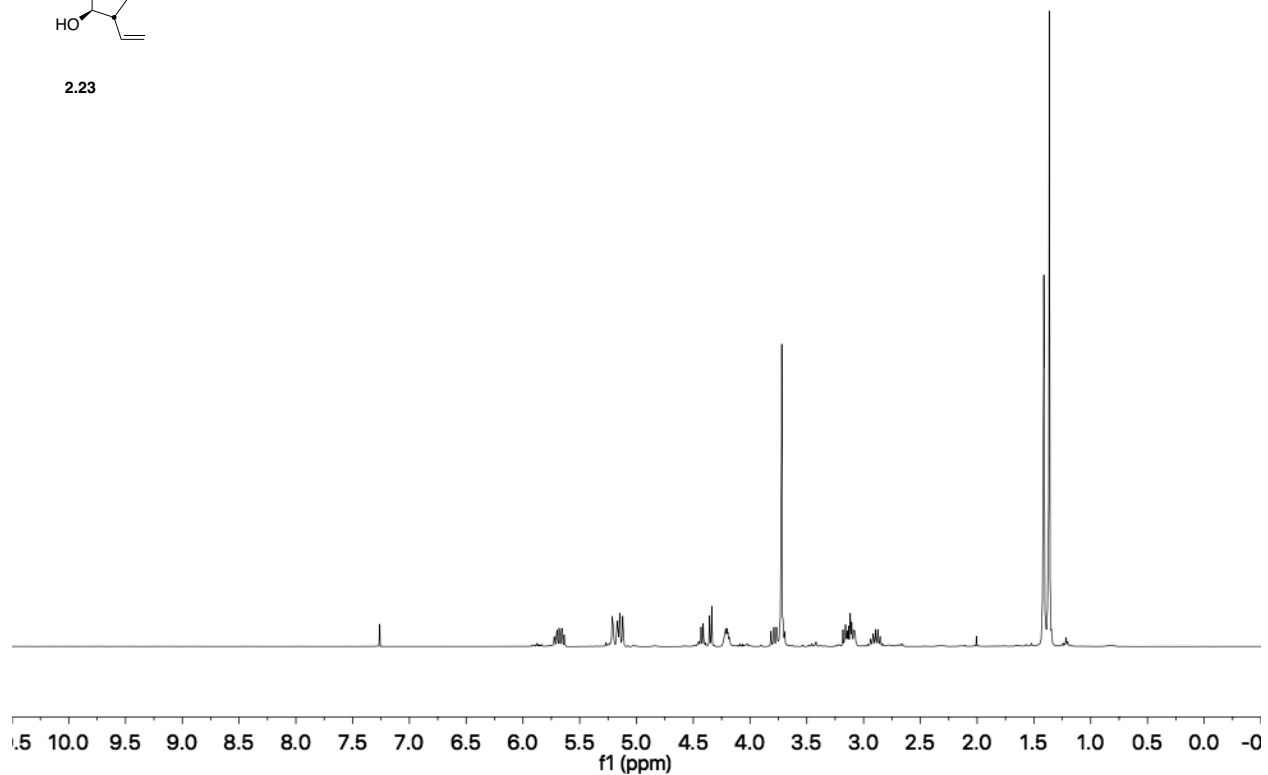


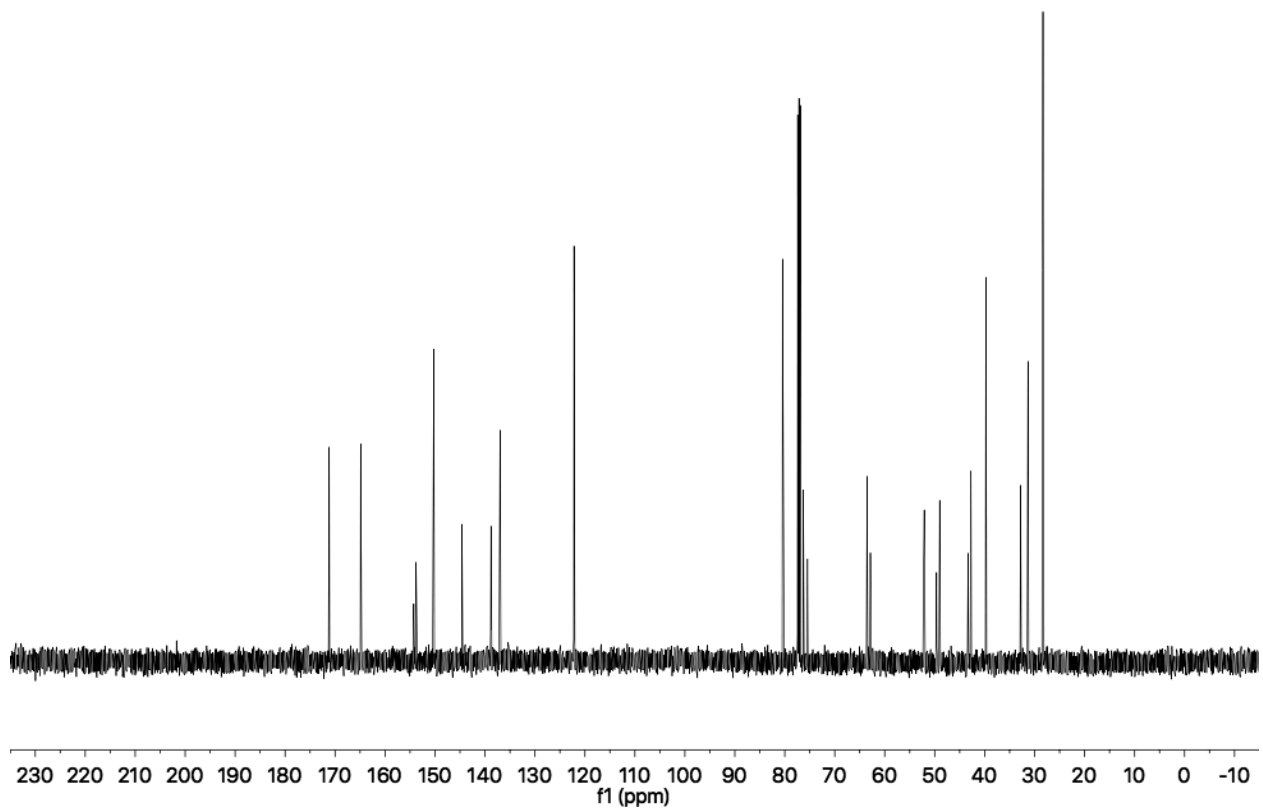
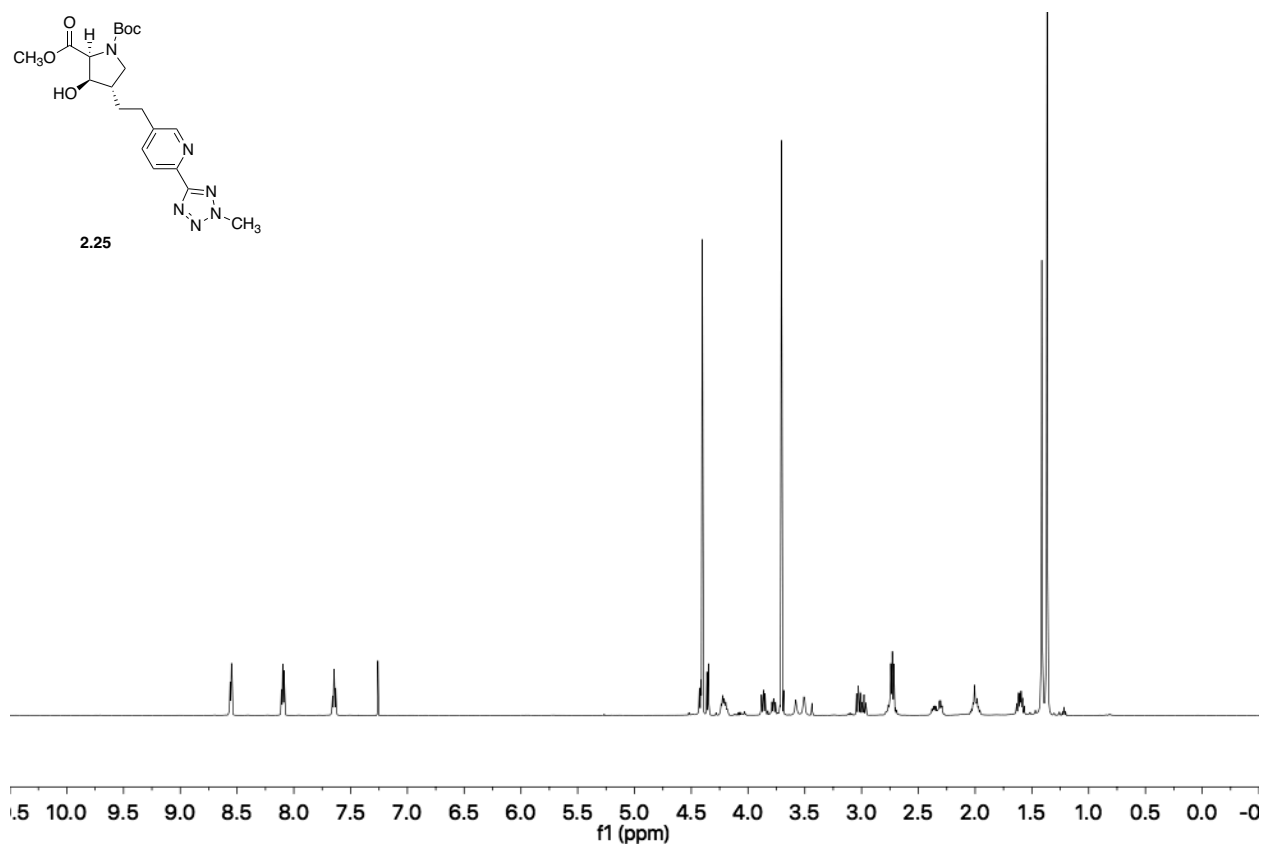
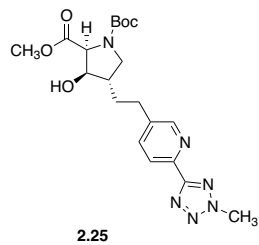


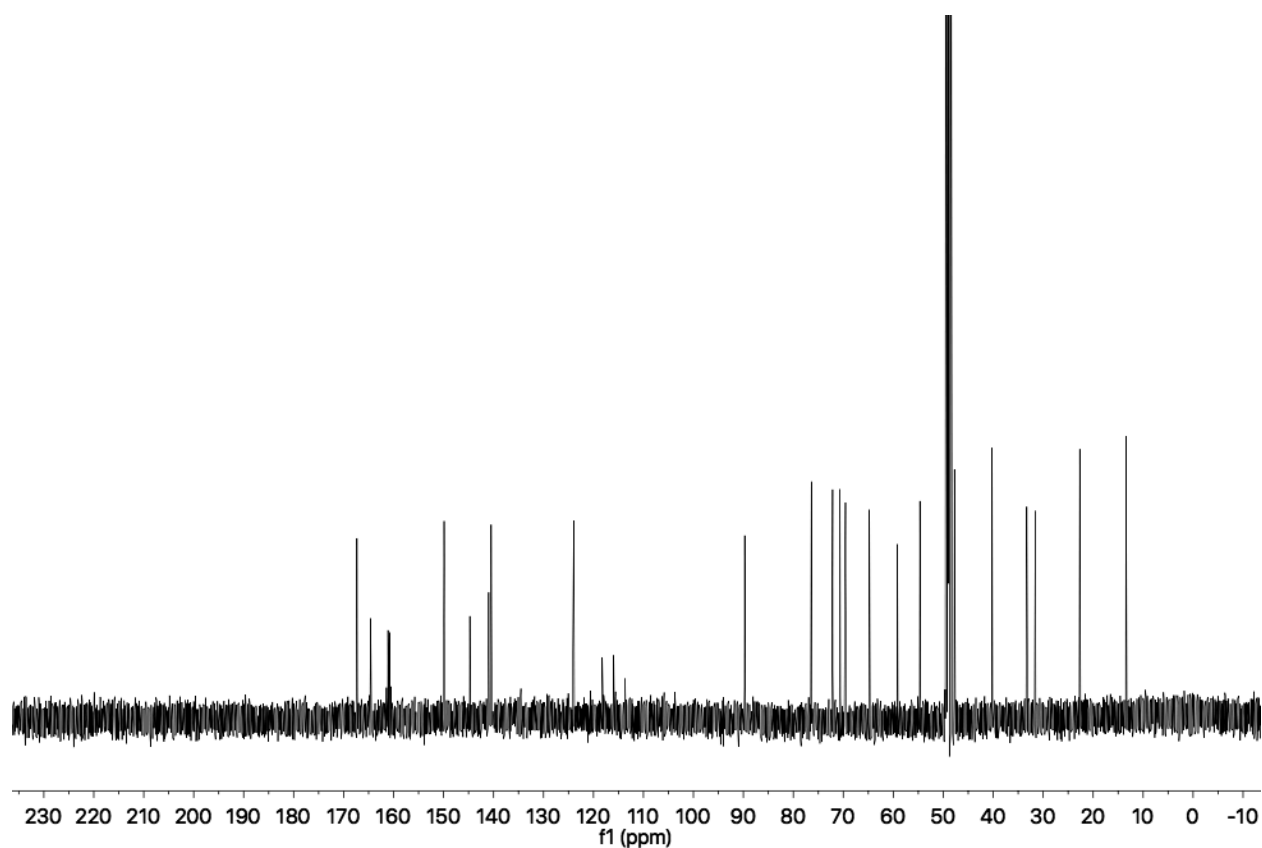
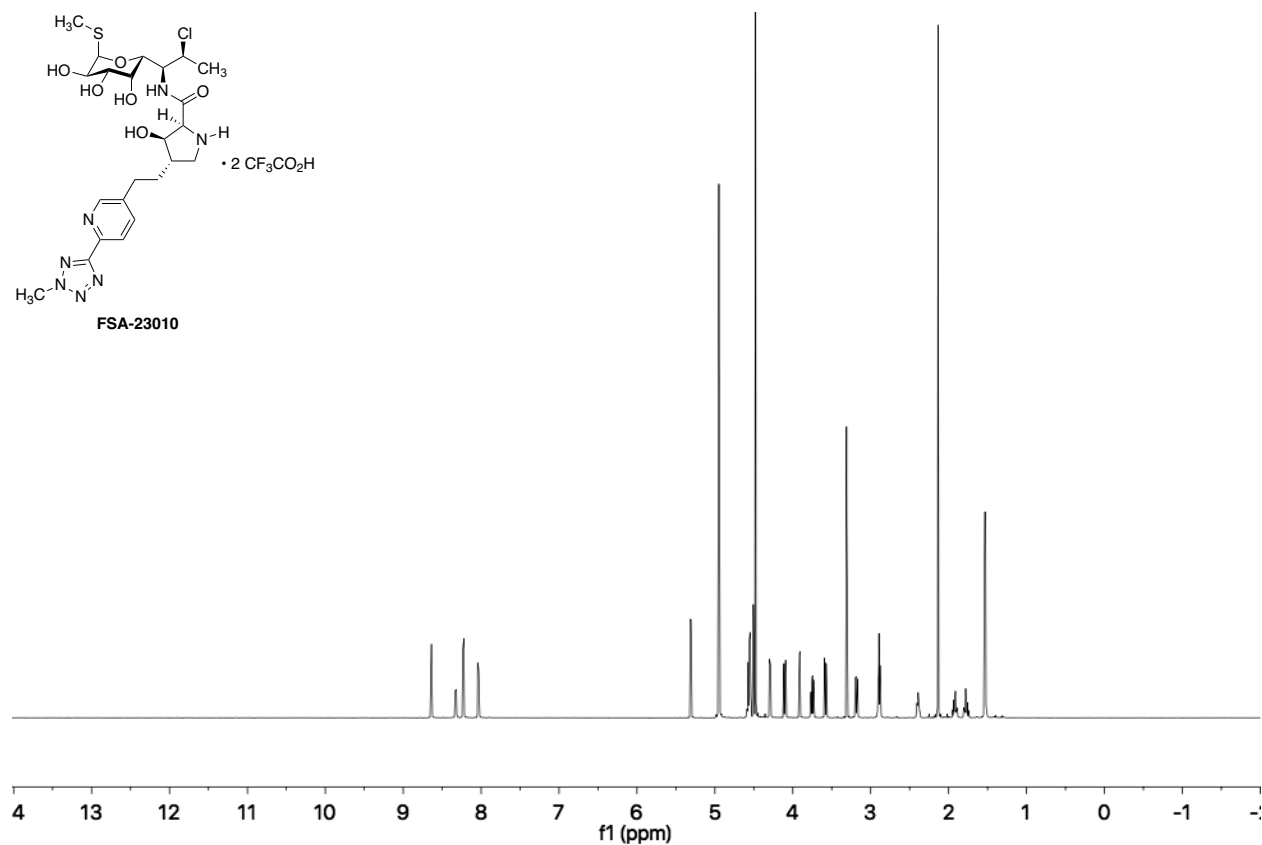
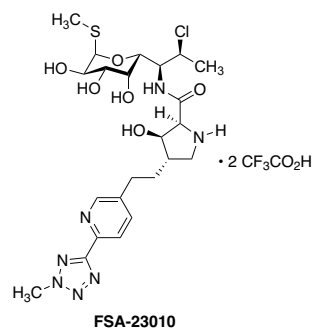


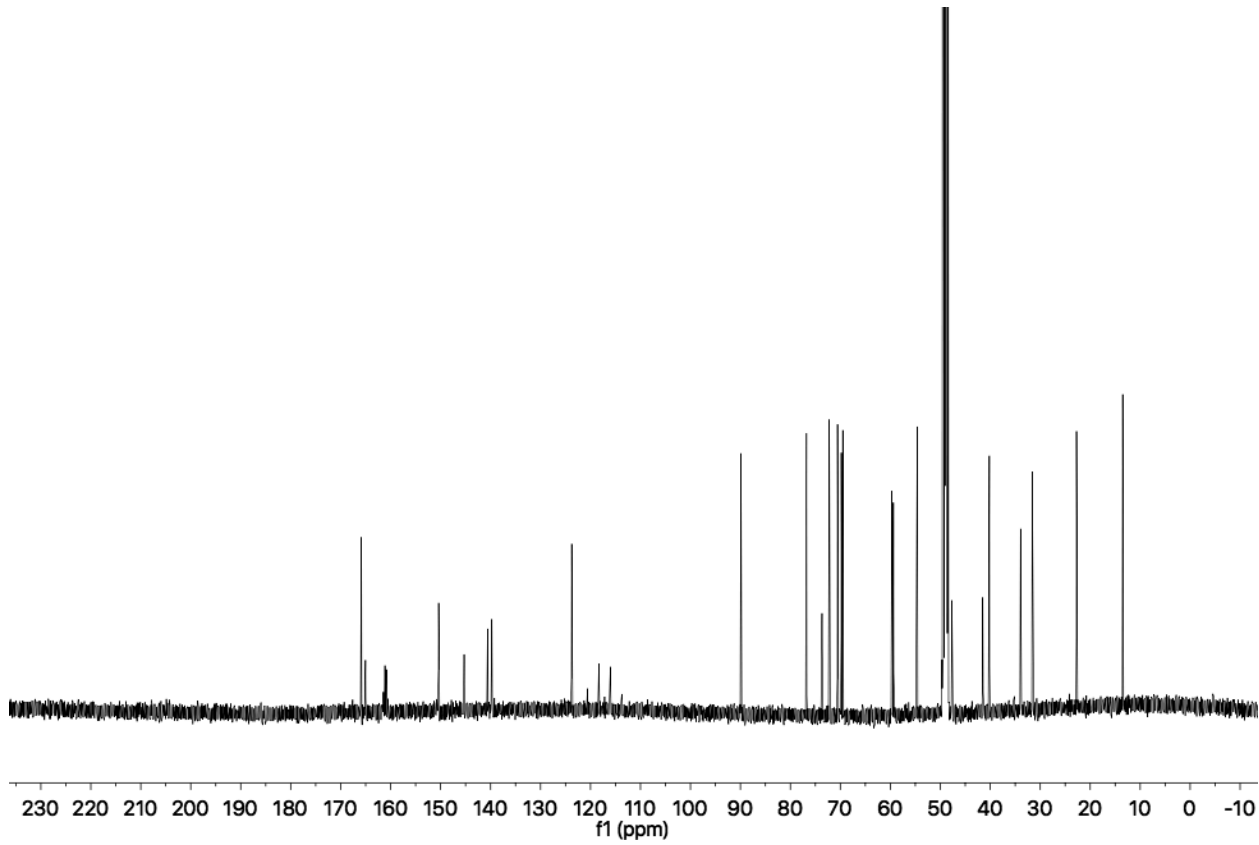
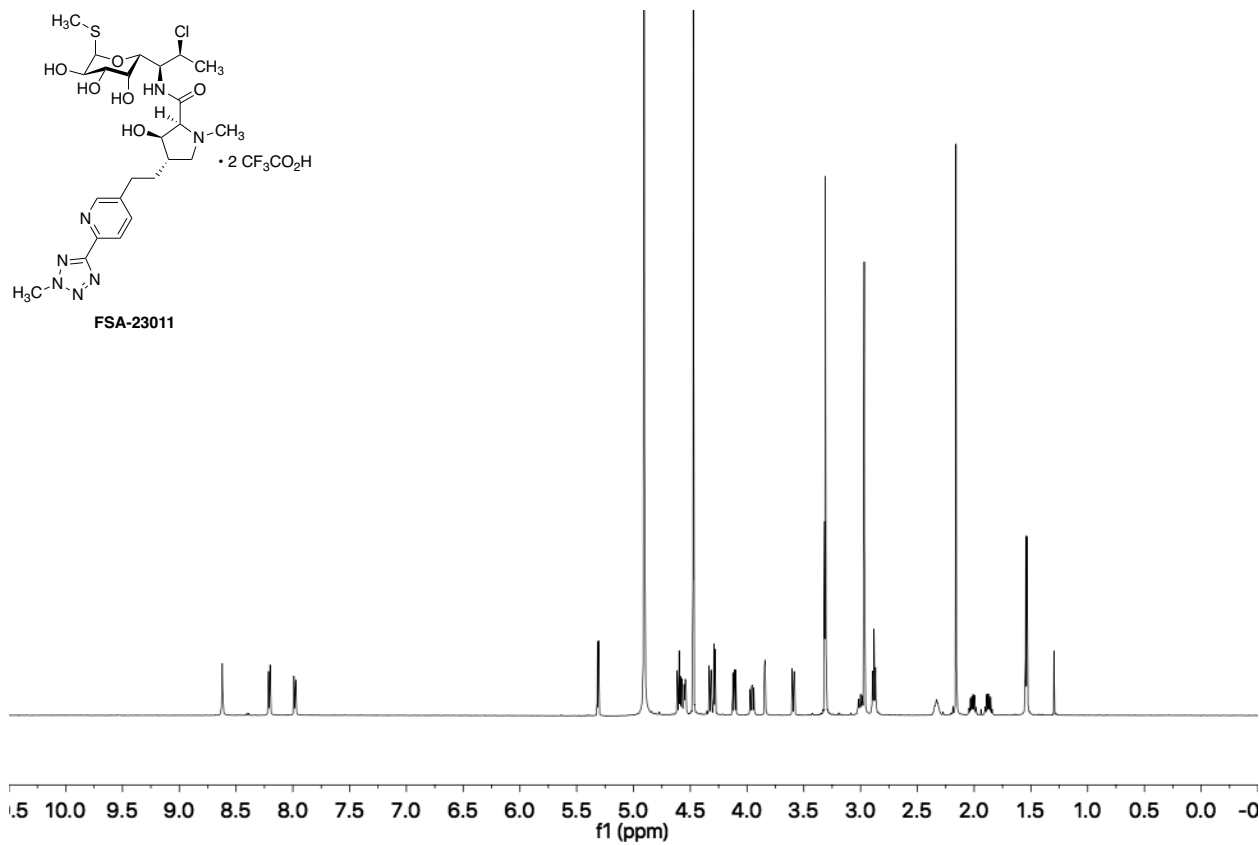
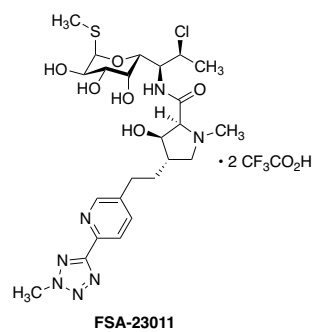


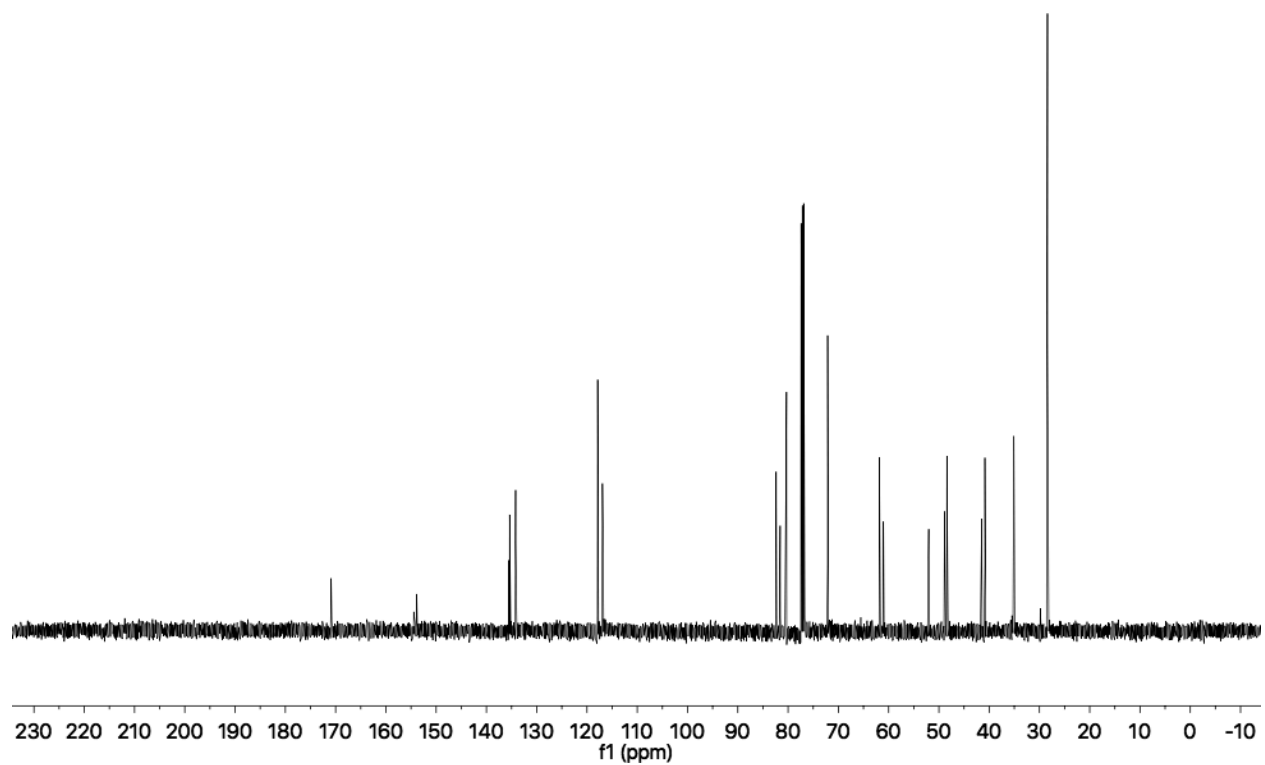
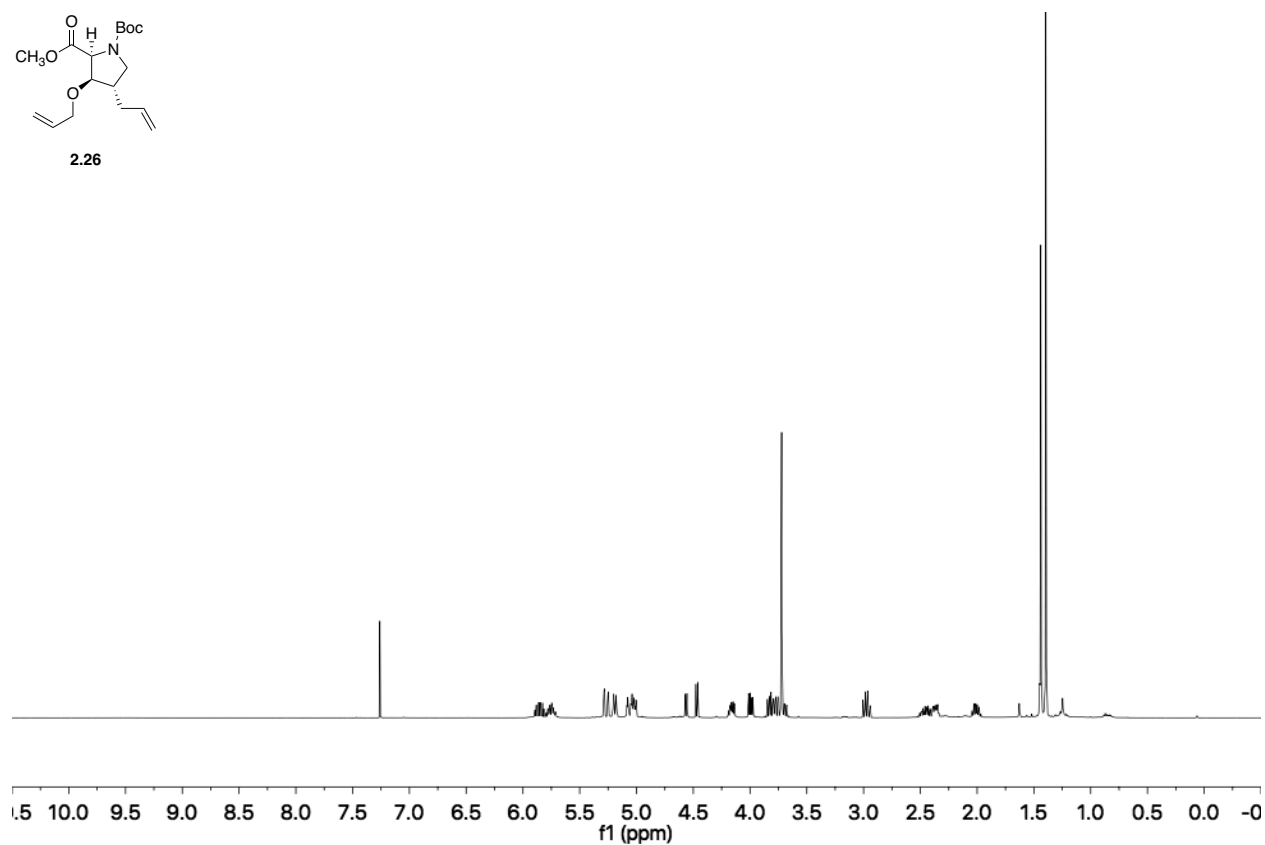
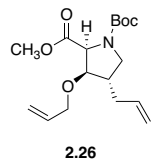
2.23

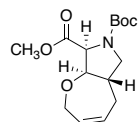




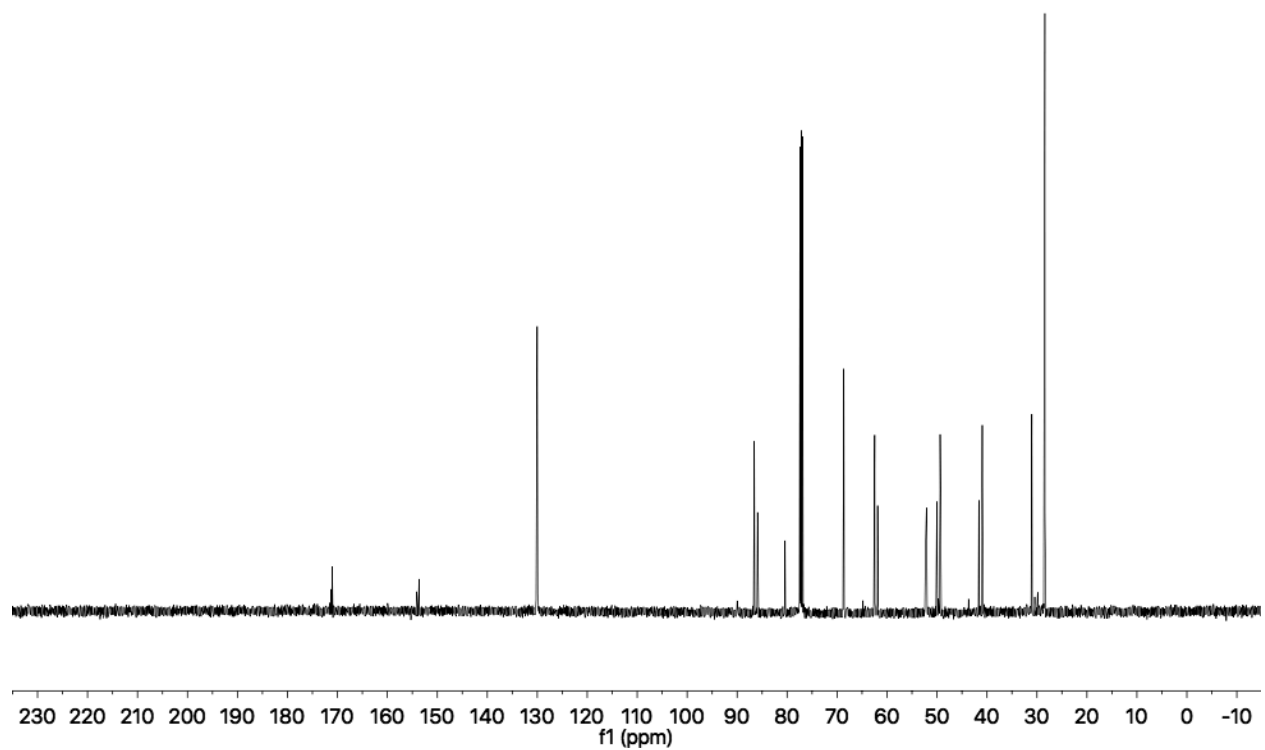
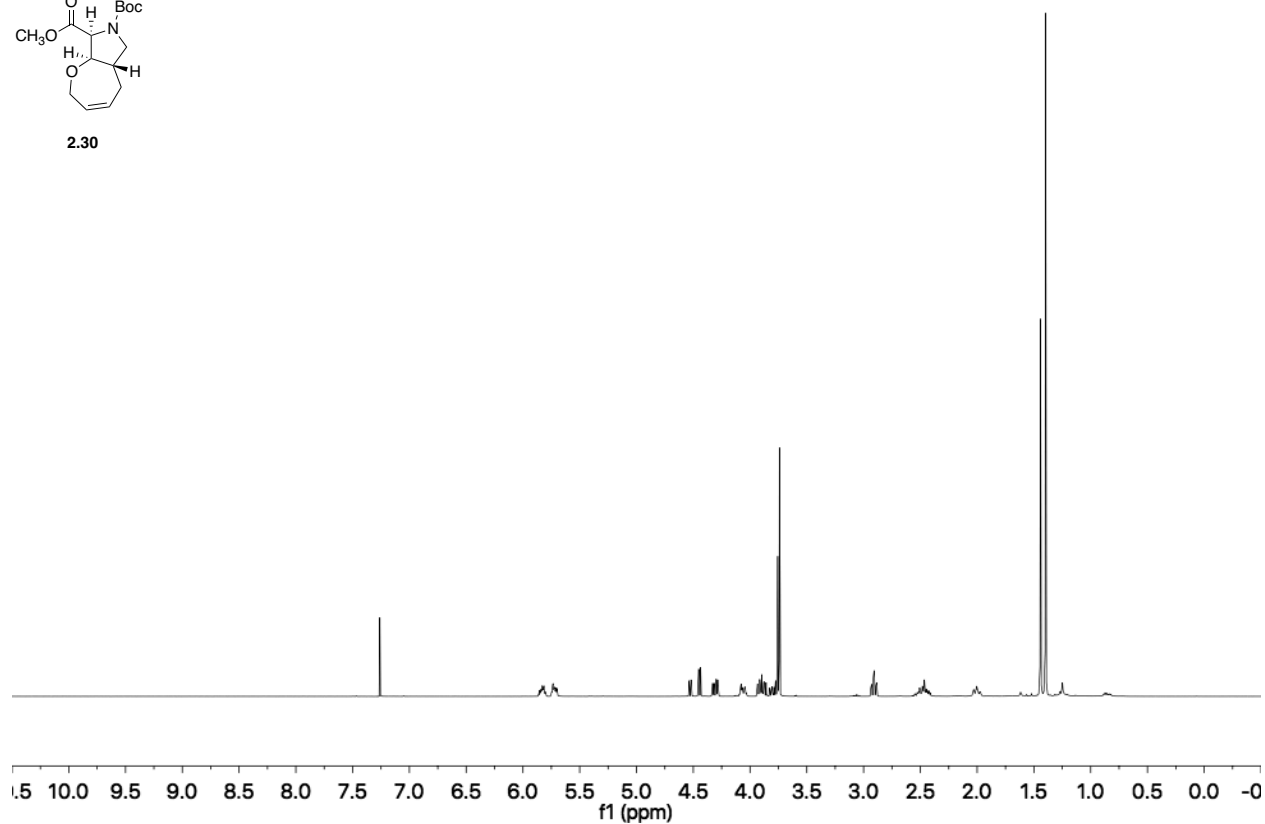


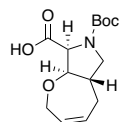




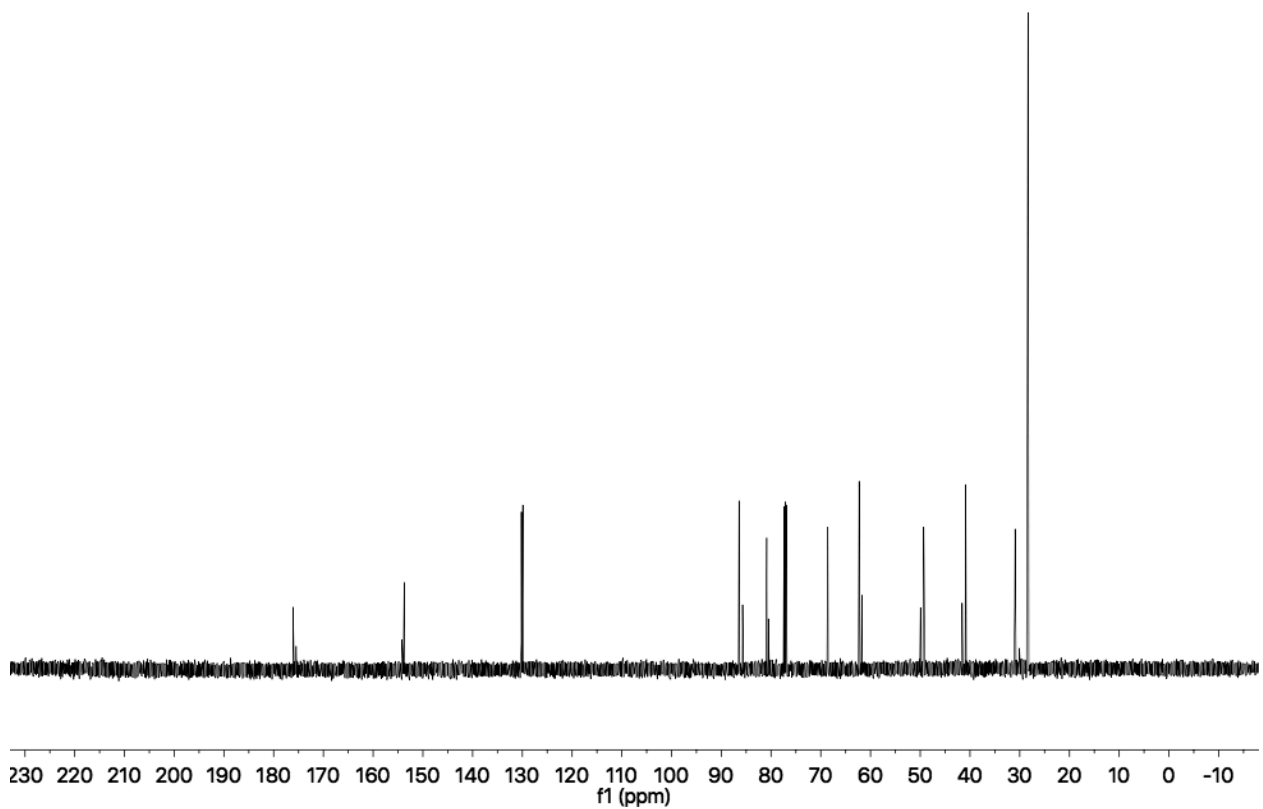
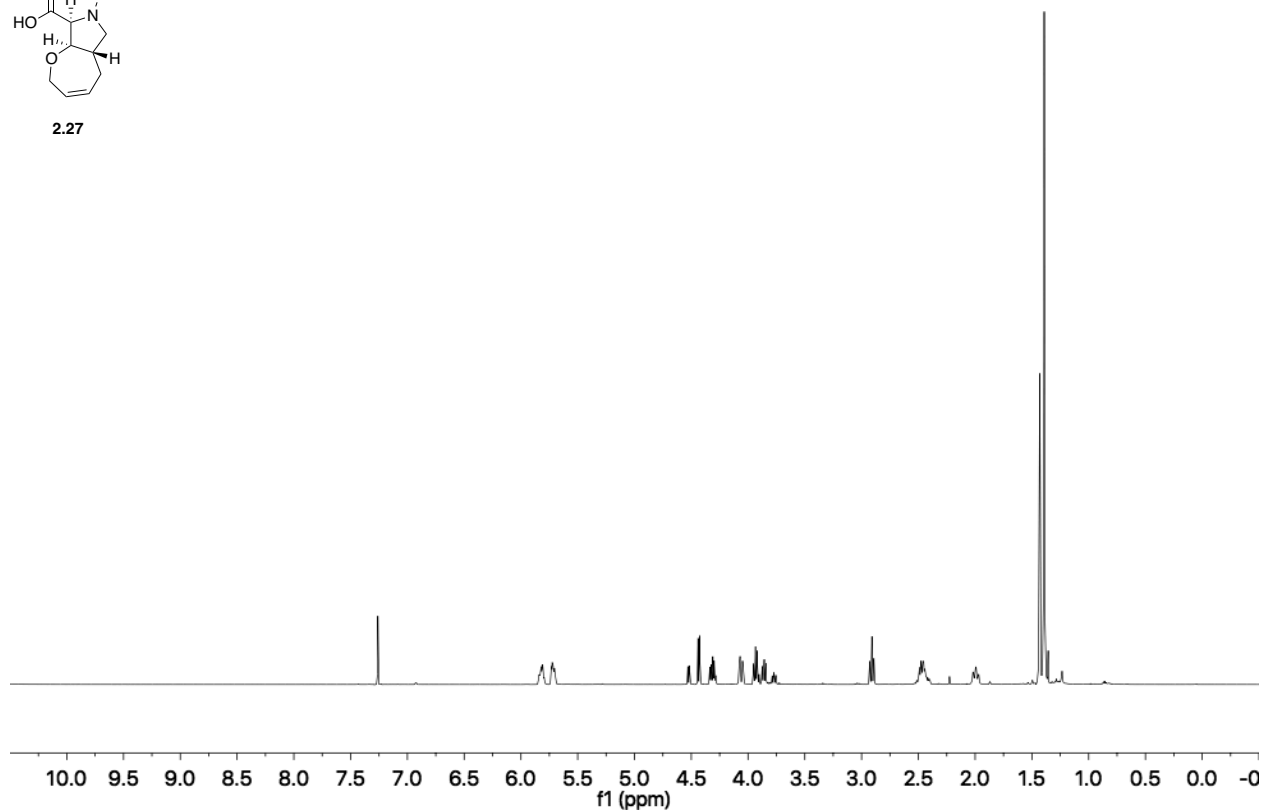


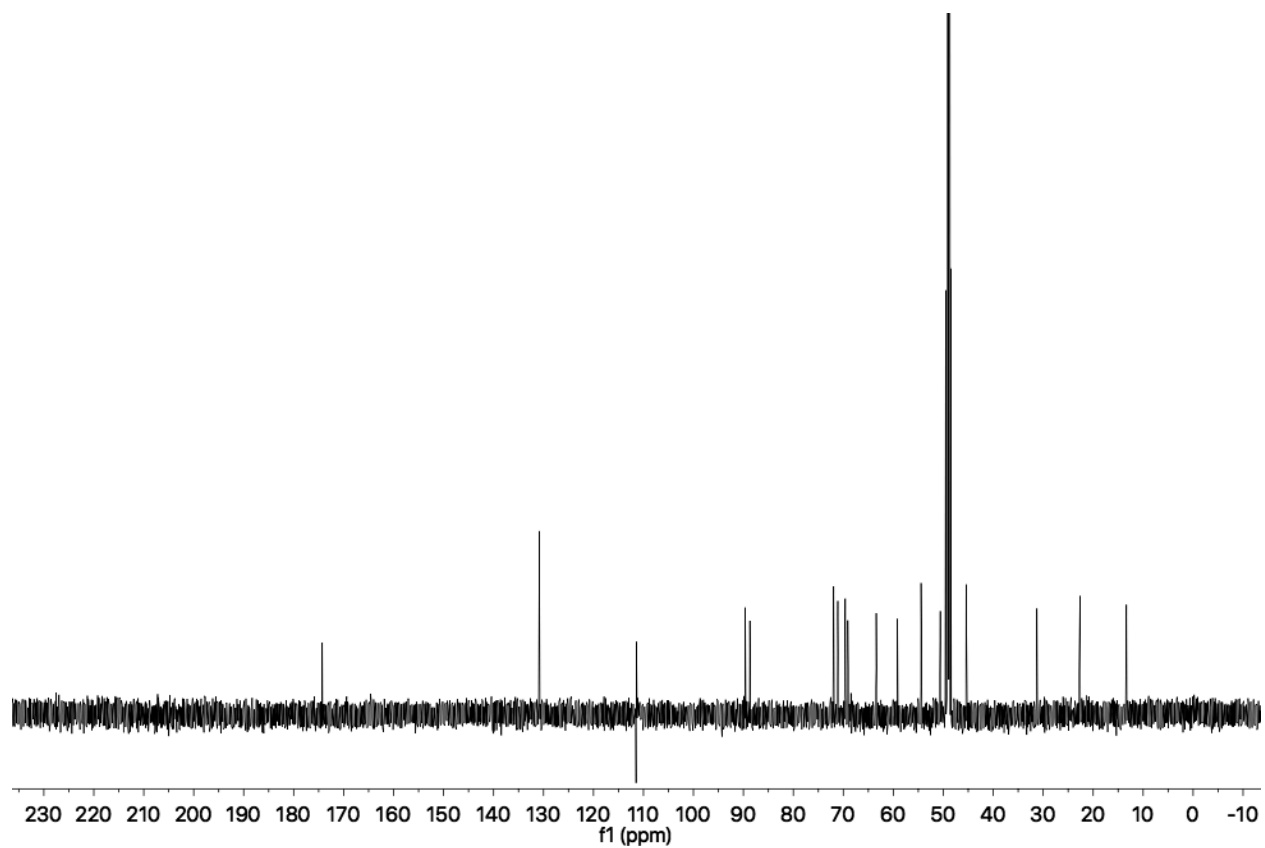
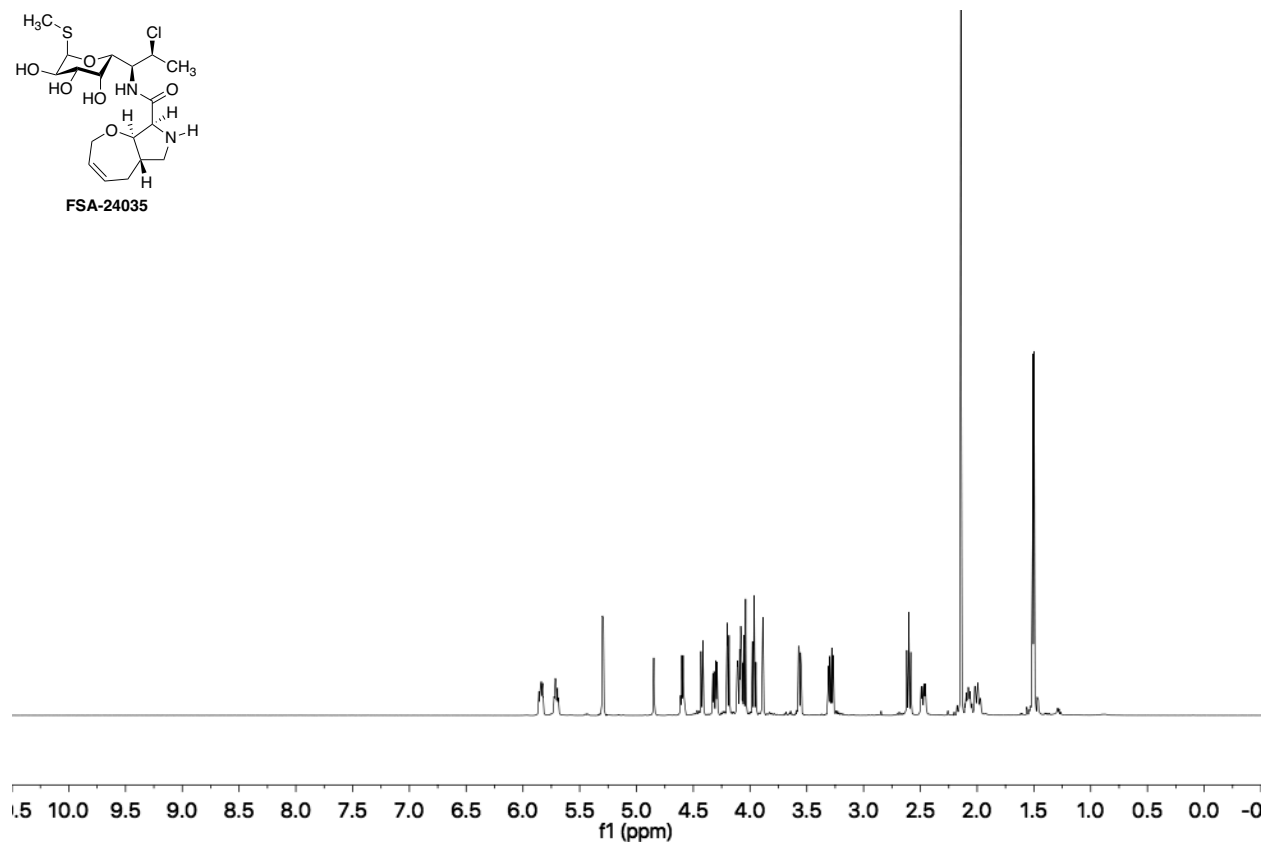
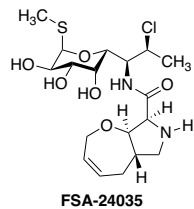
2.30

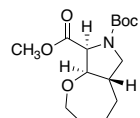




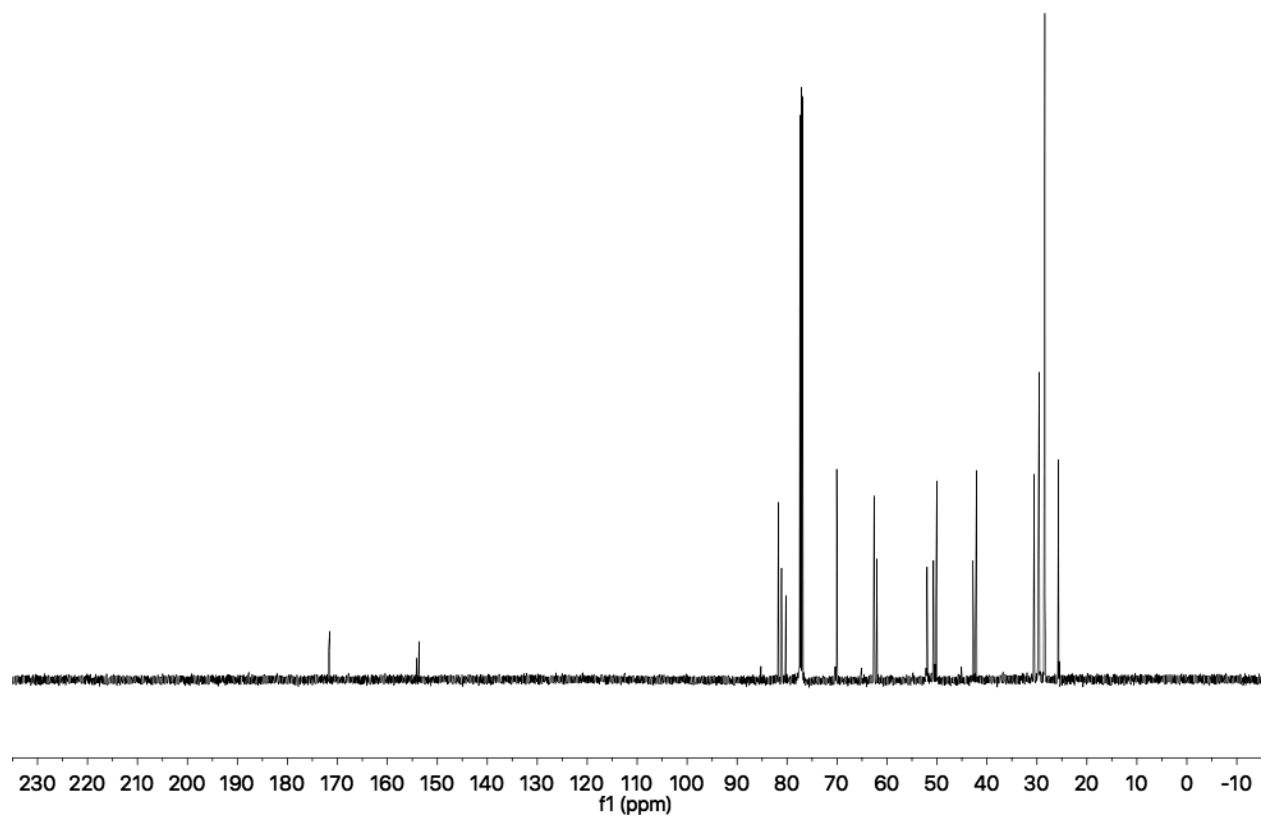
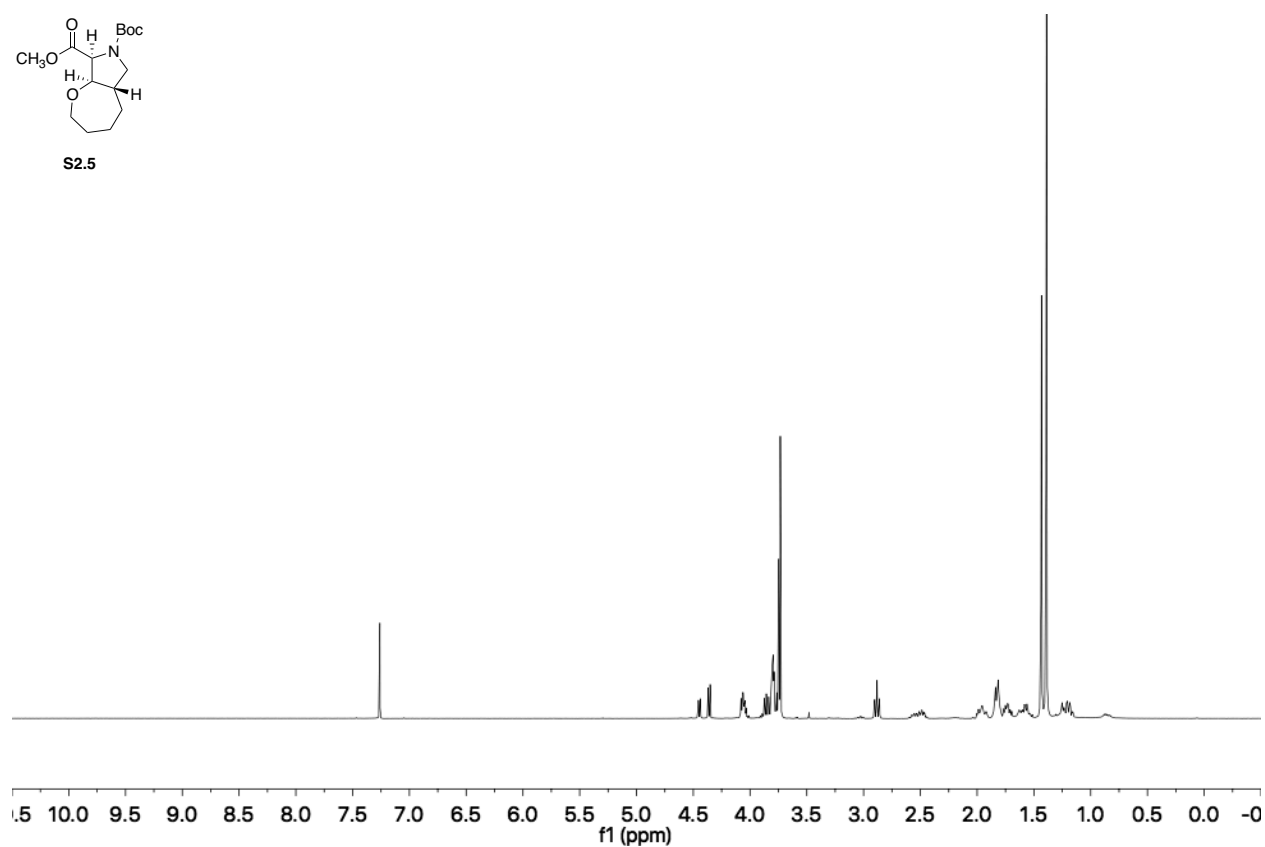
2.27

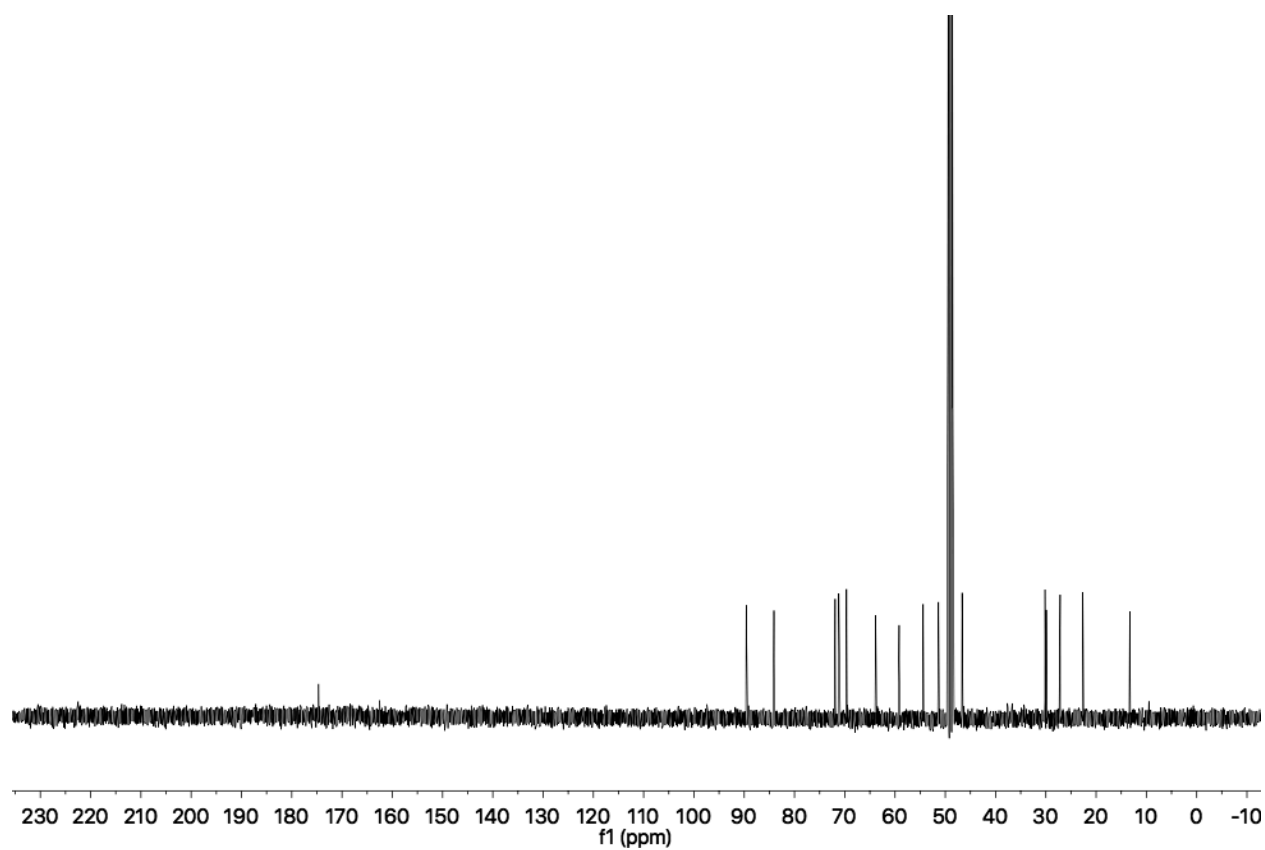
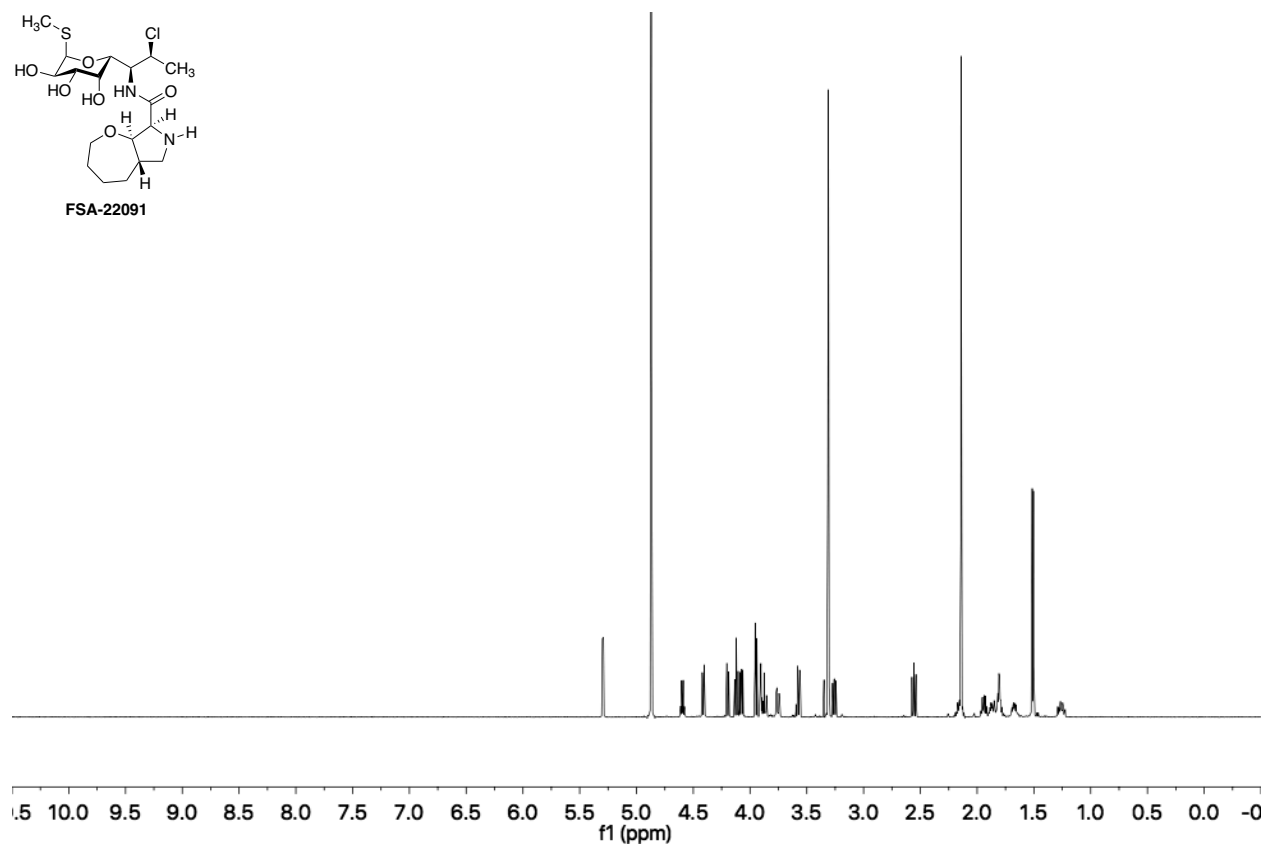
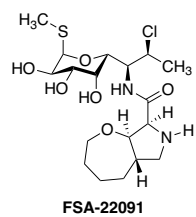


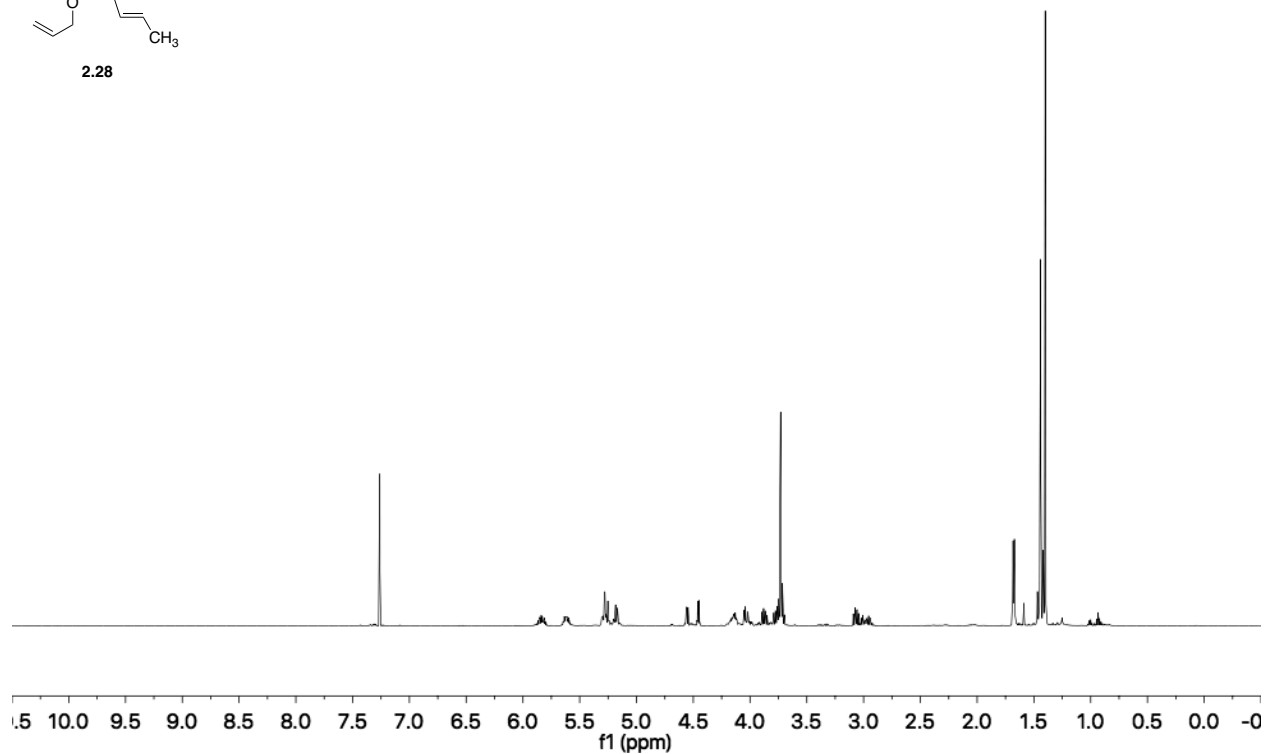
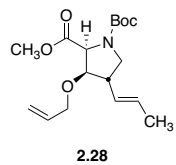


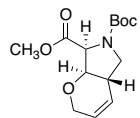


S2.5

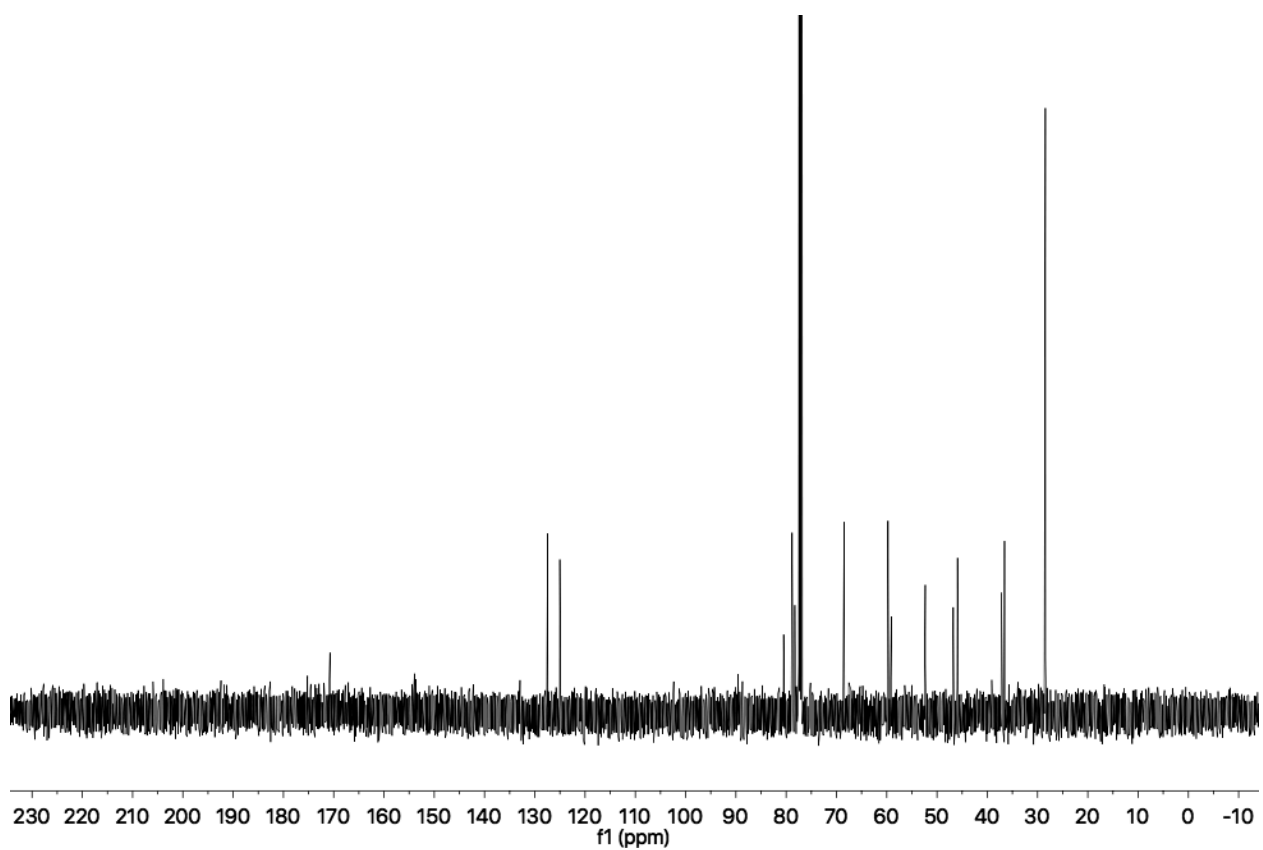
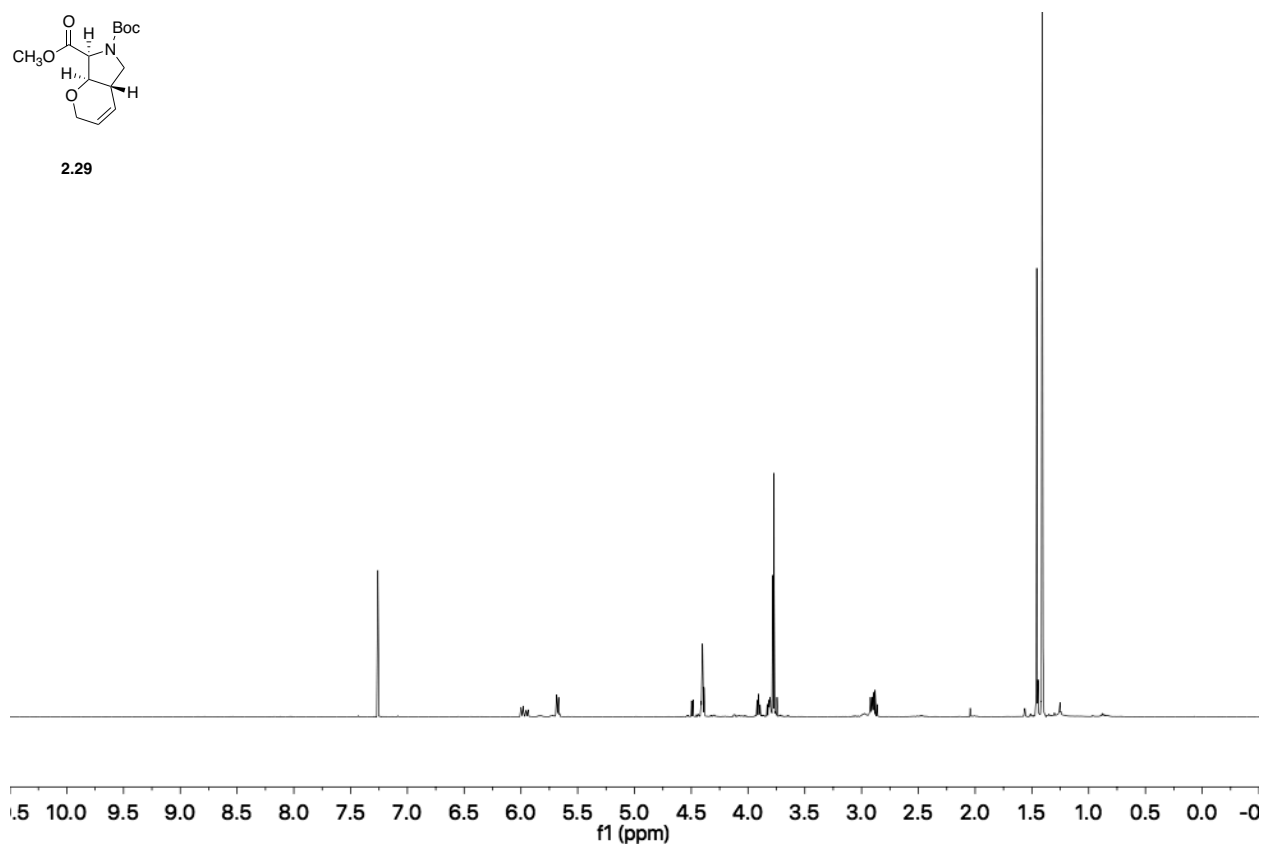


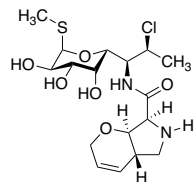




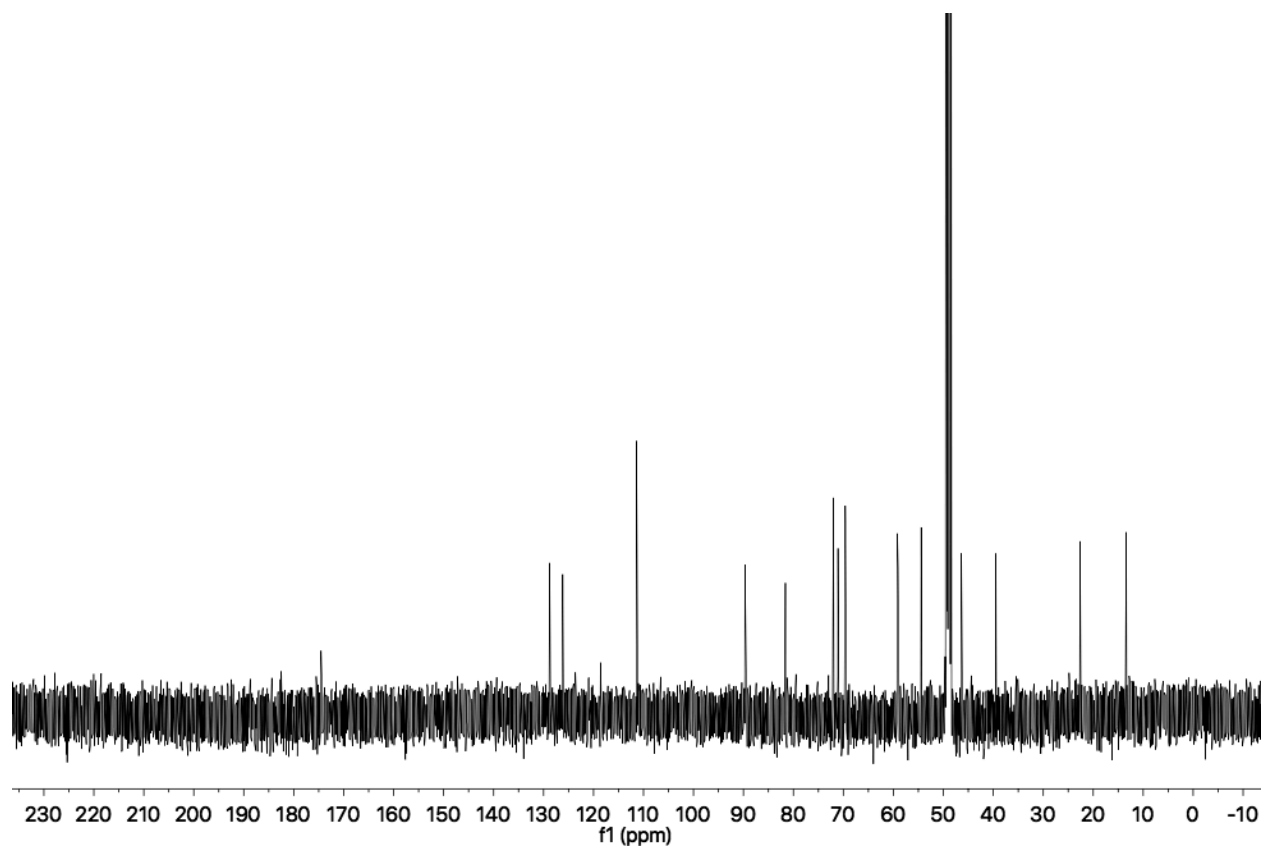
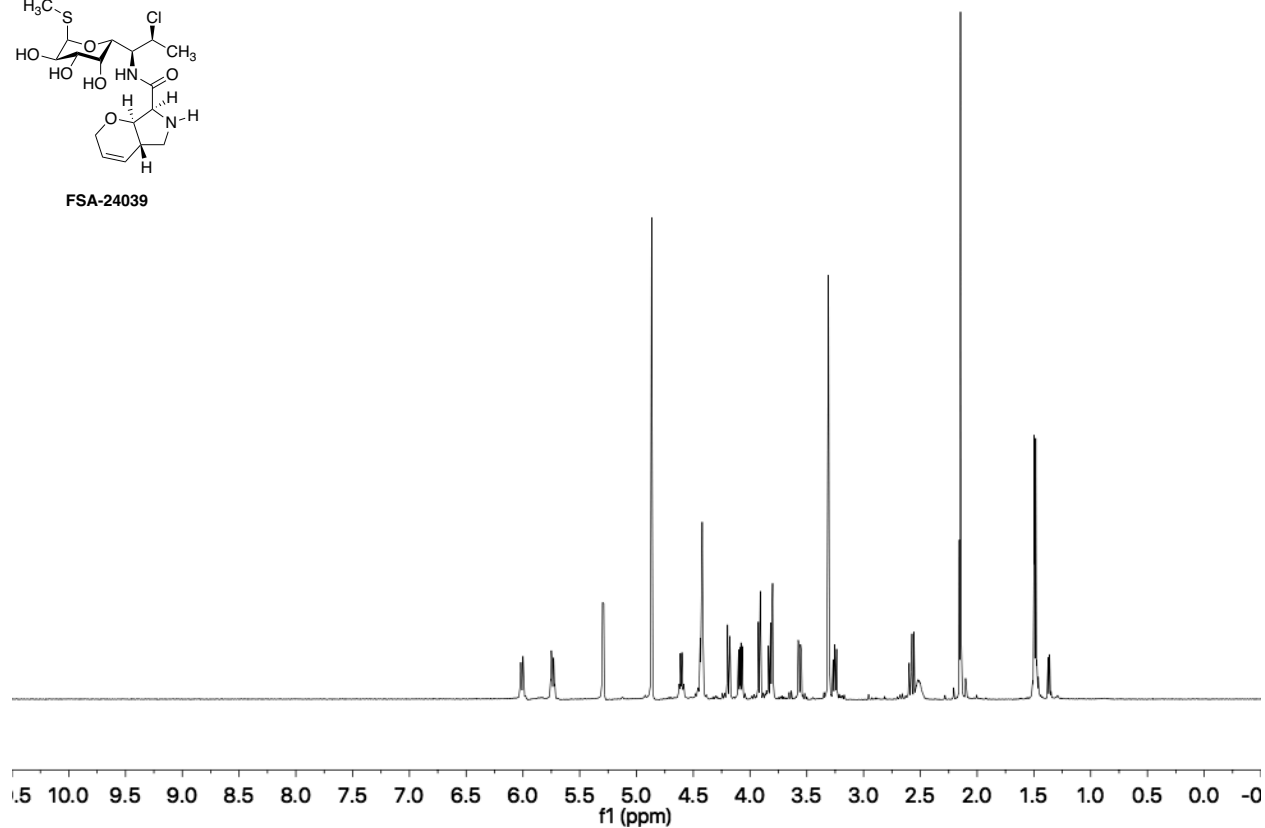


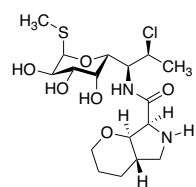
2.29



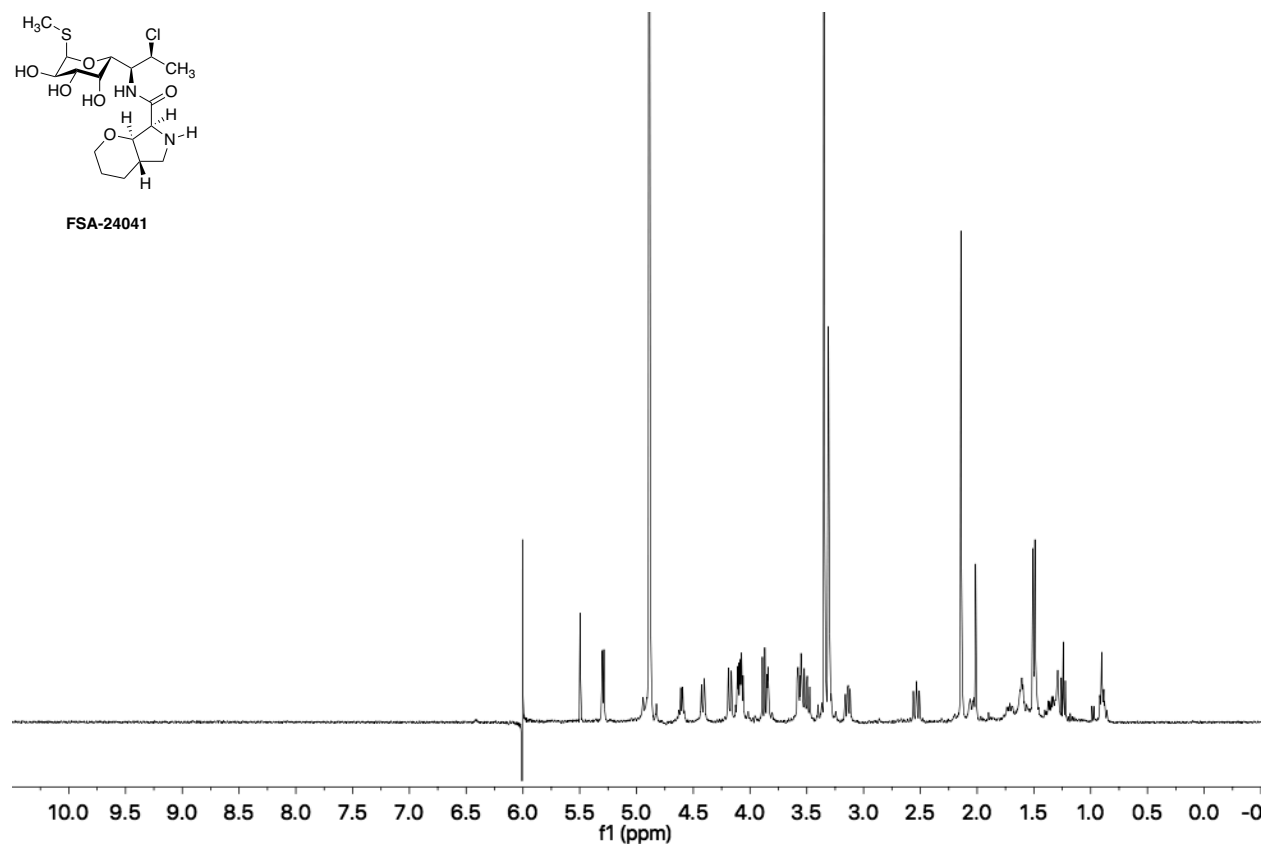


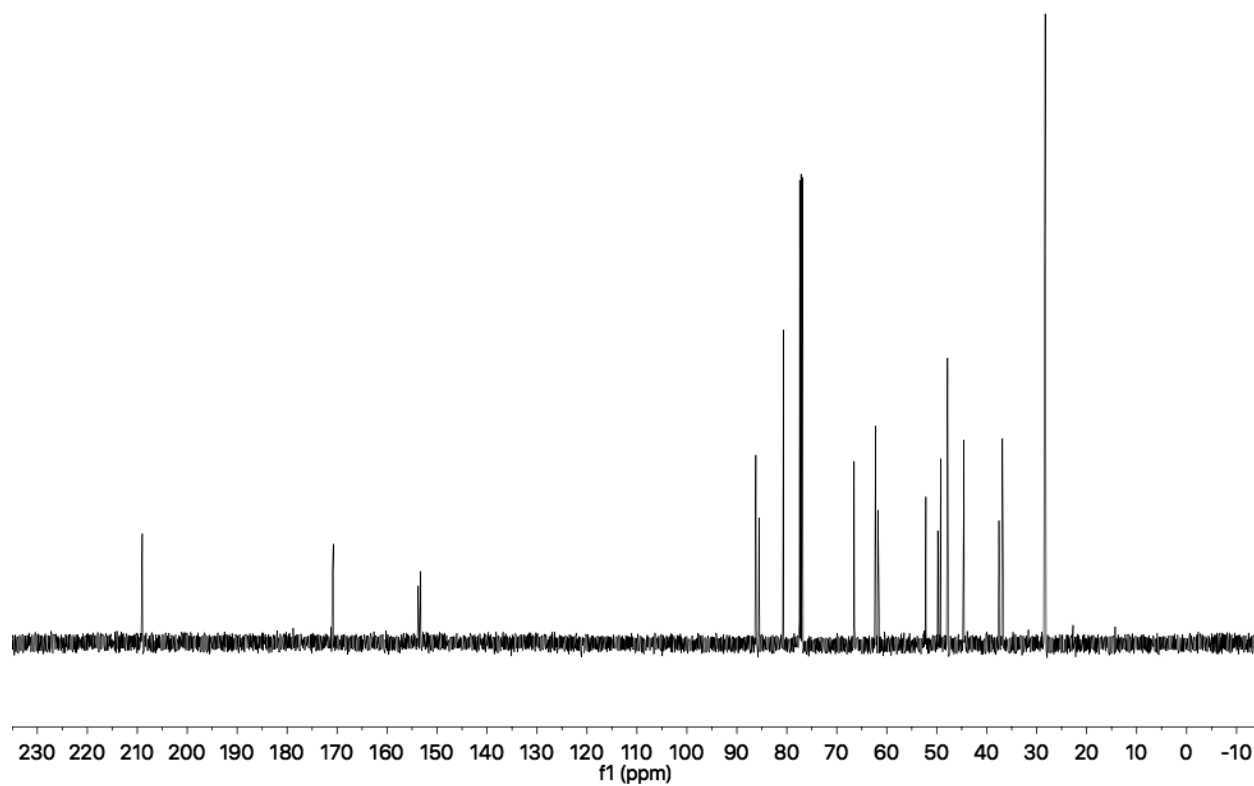
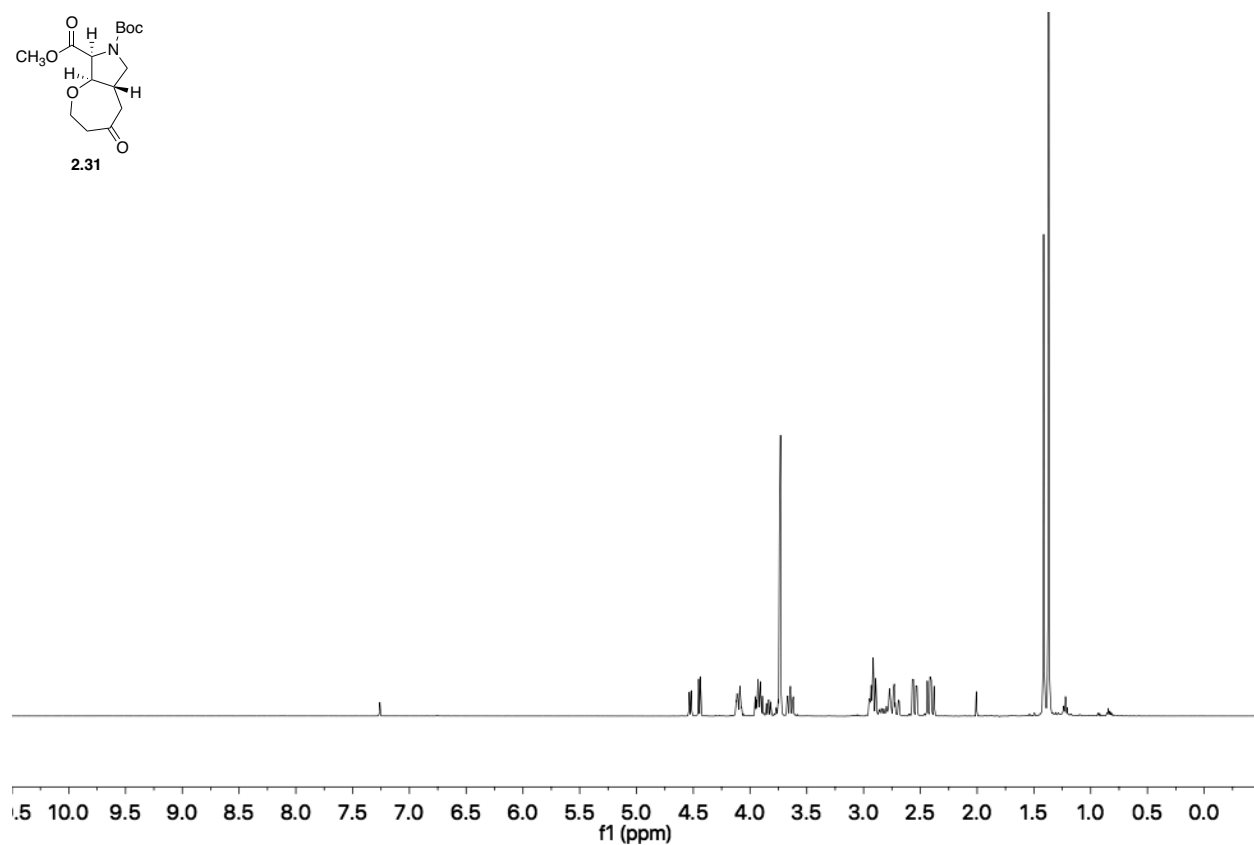
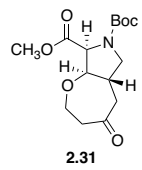
FSA-24039

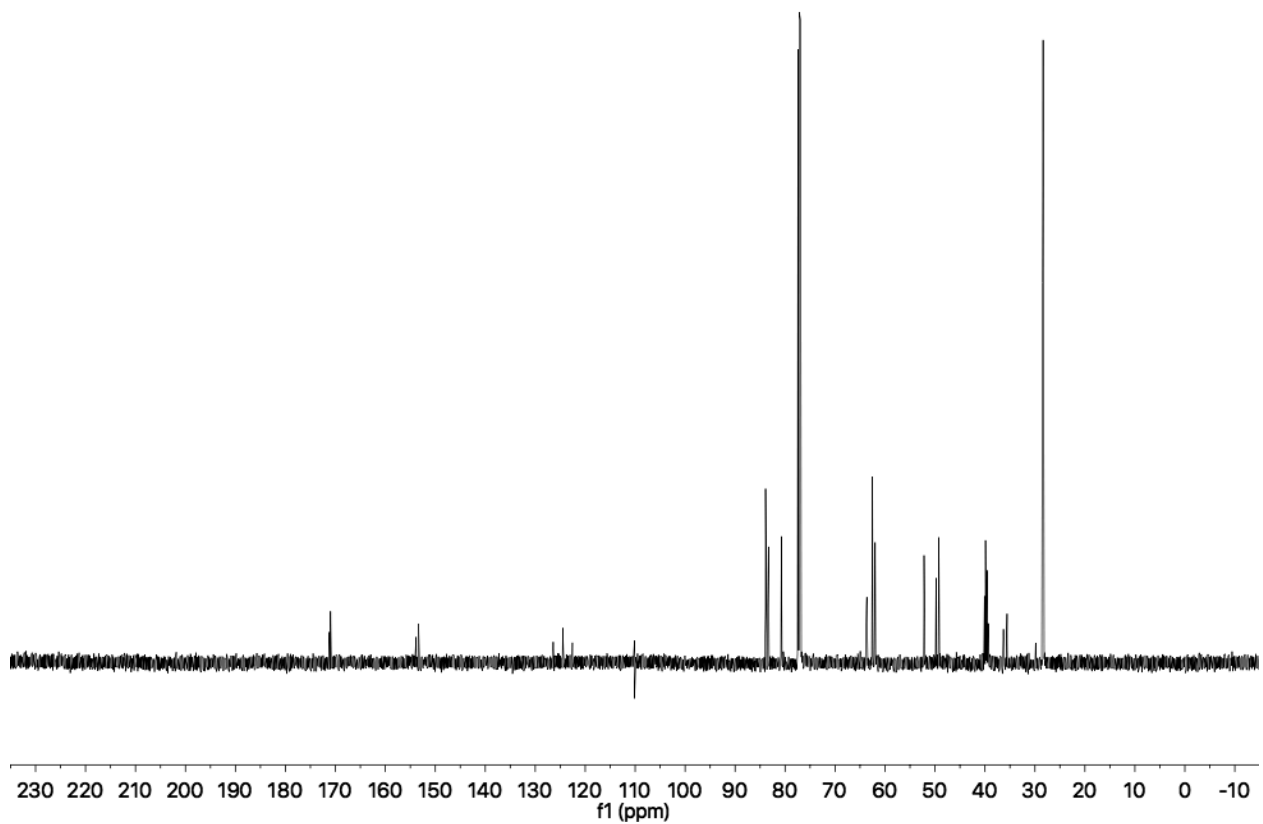
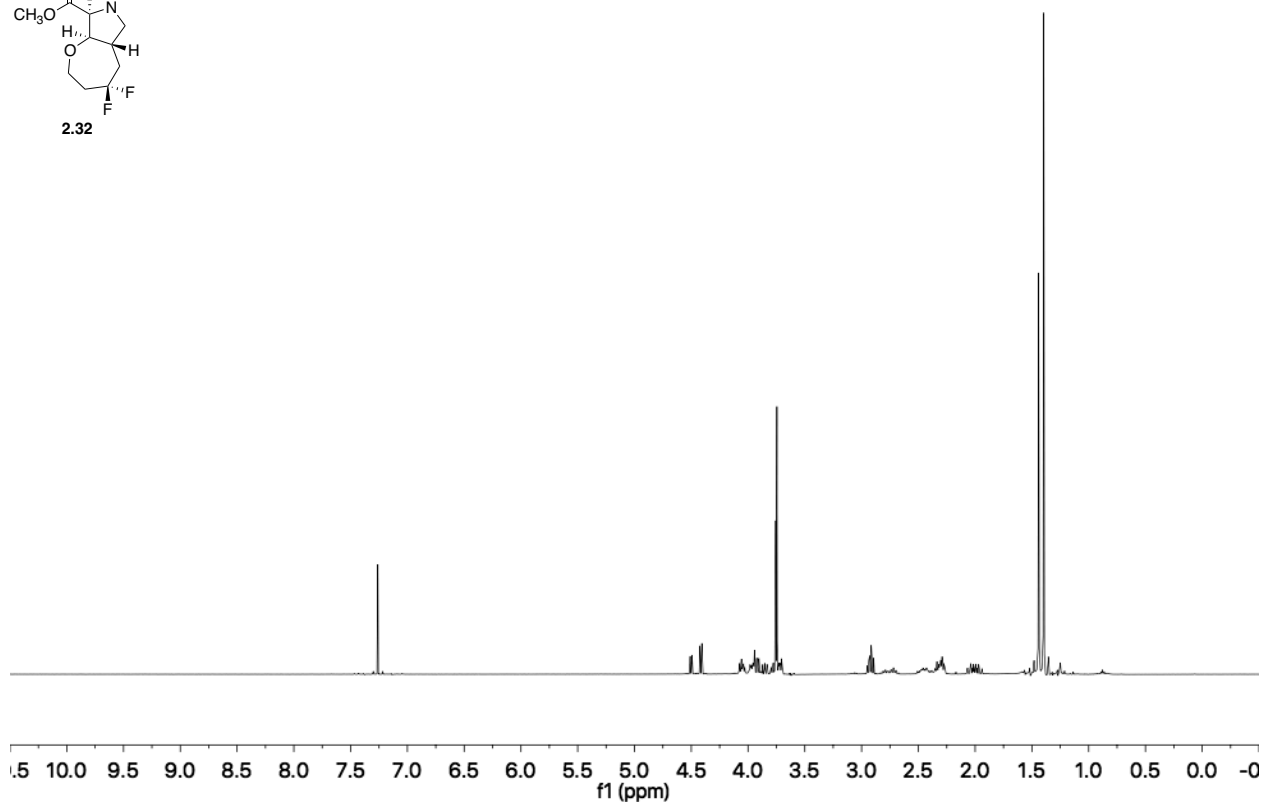
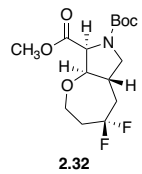


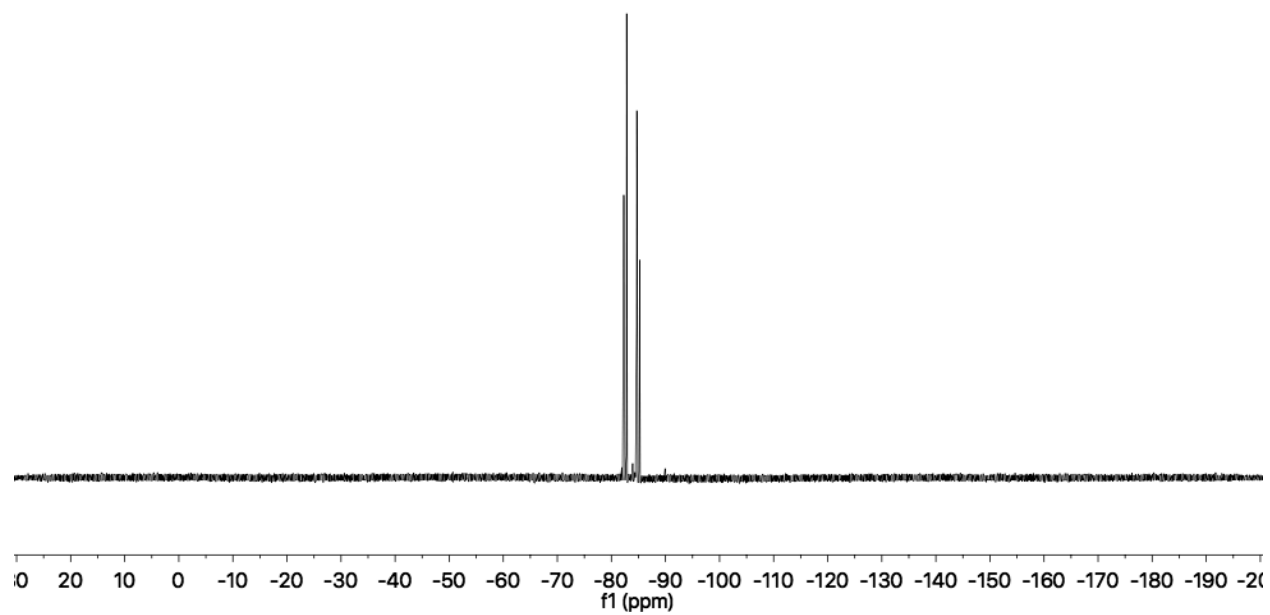


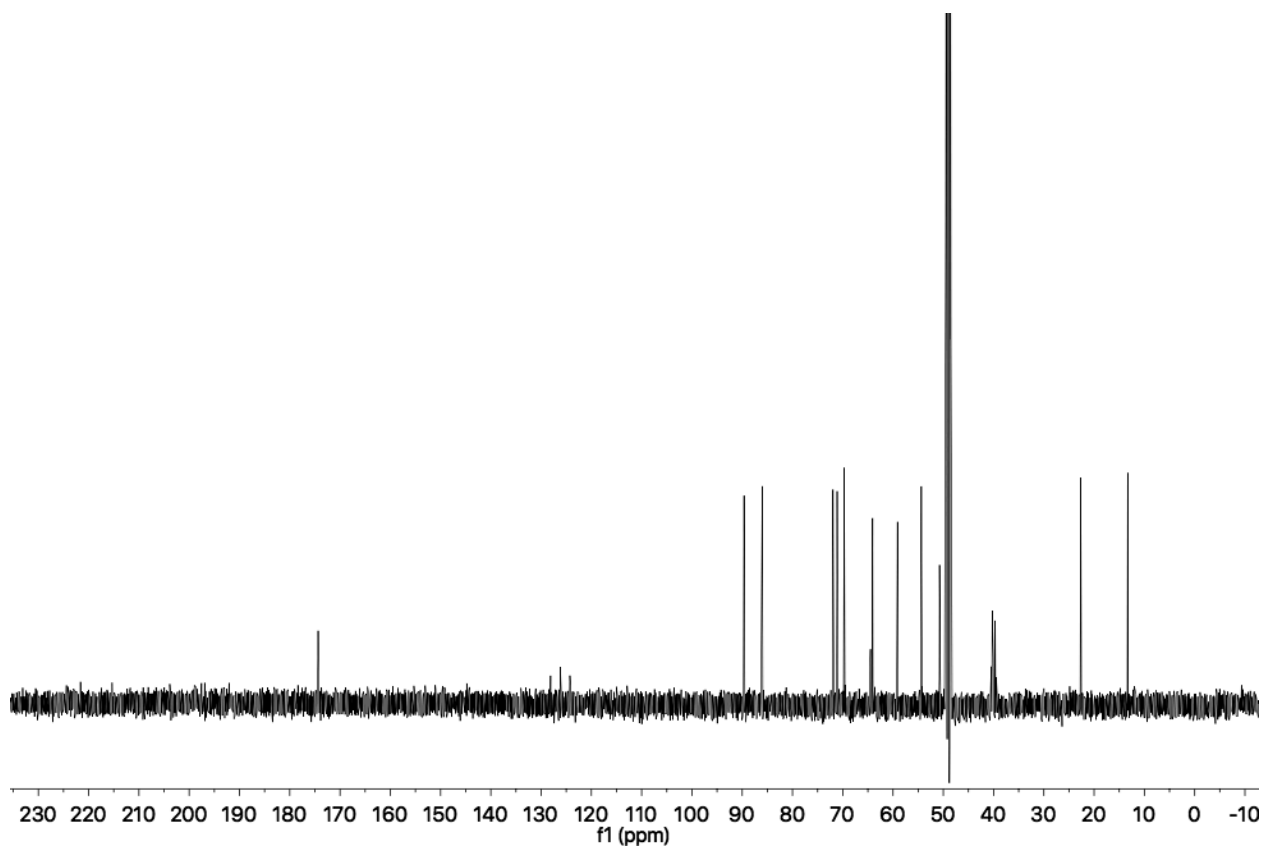
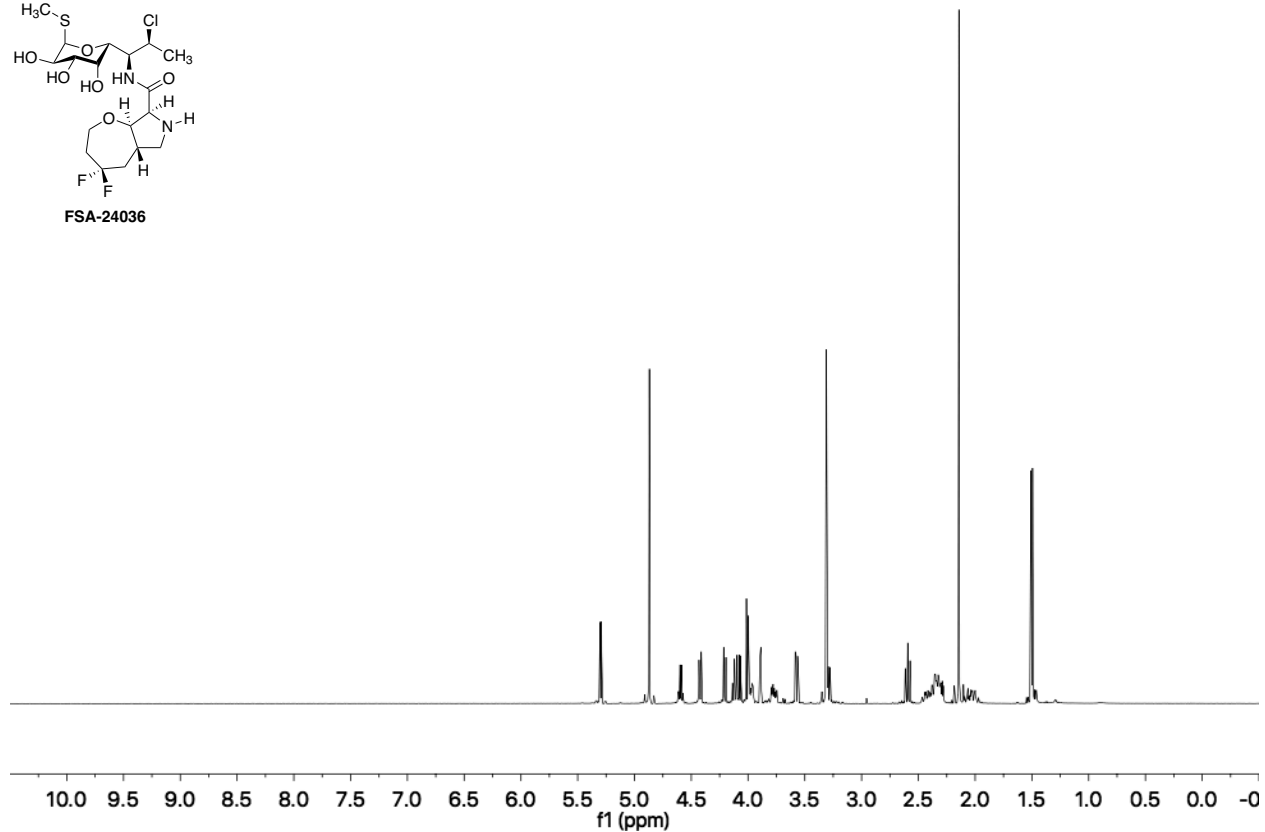
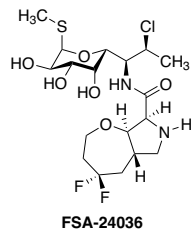
FSA-24041

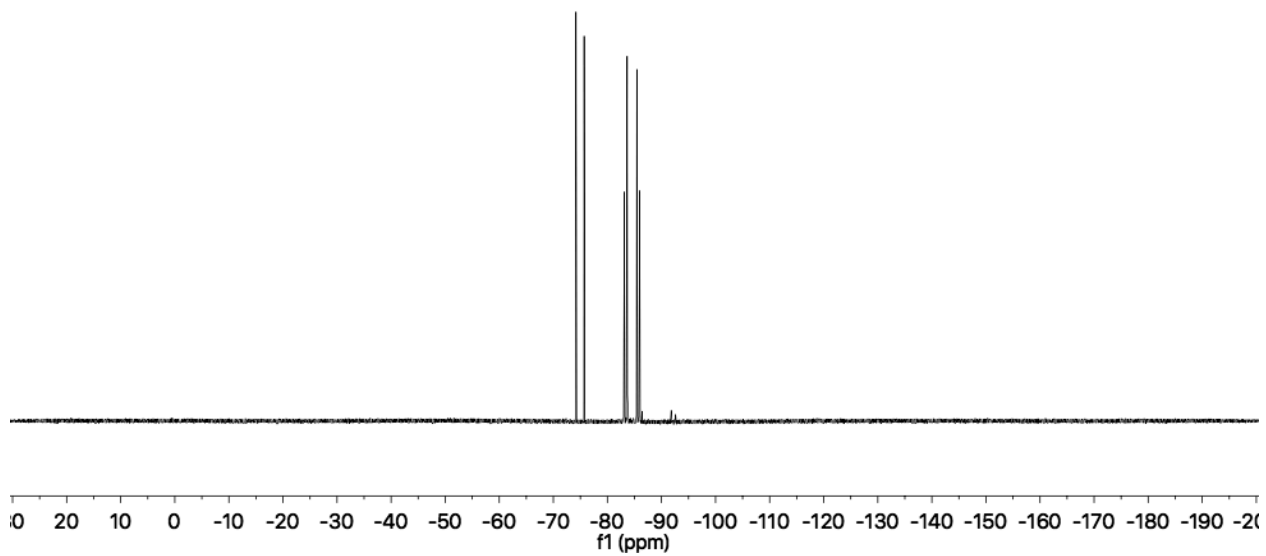


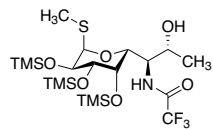




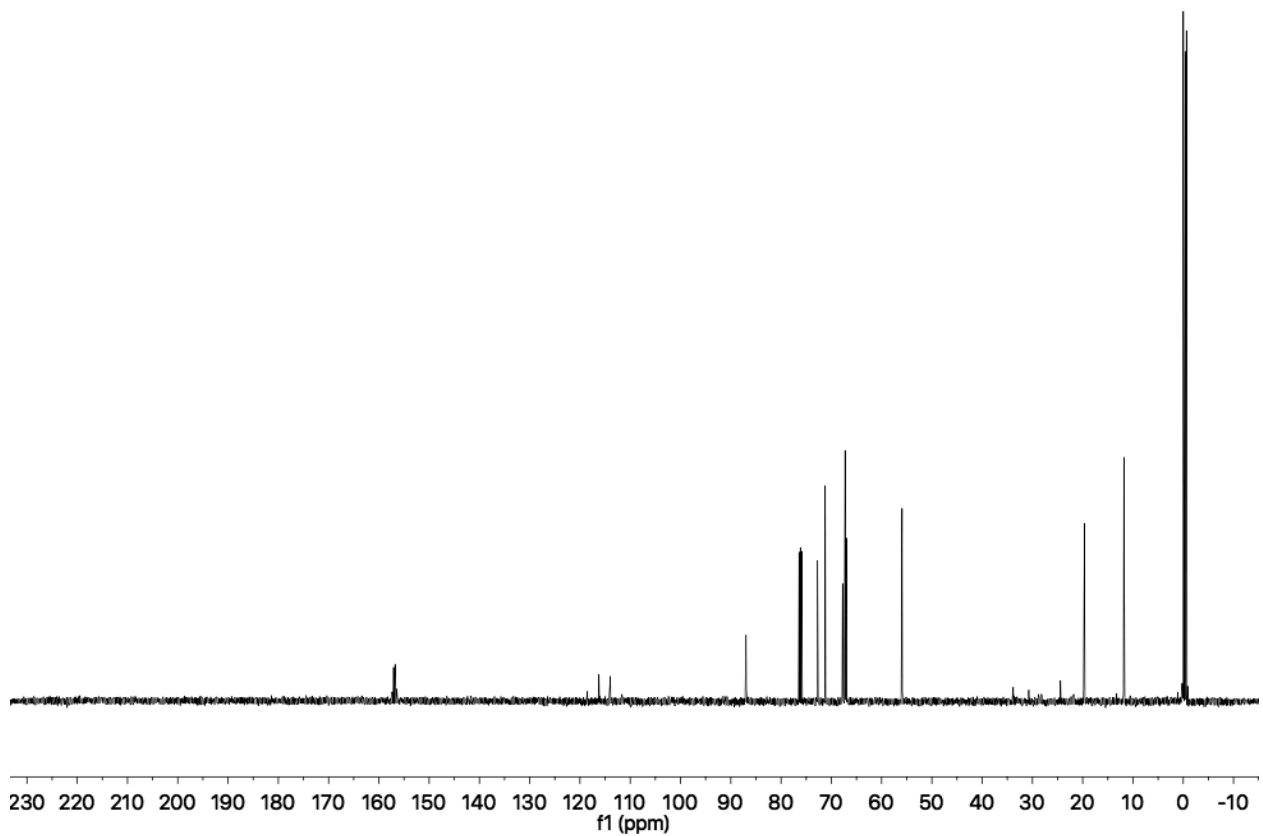
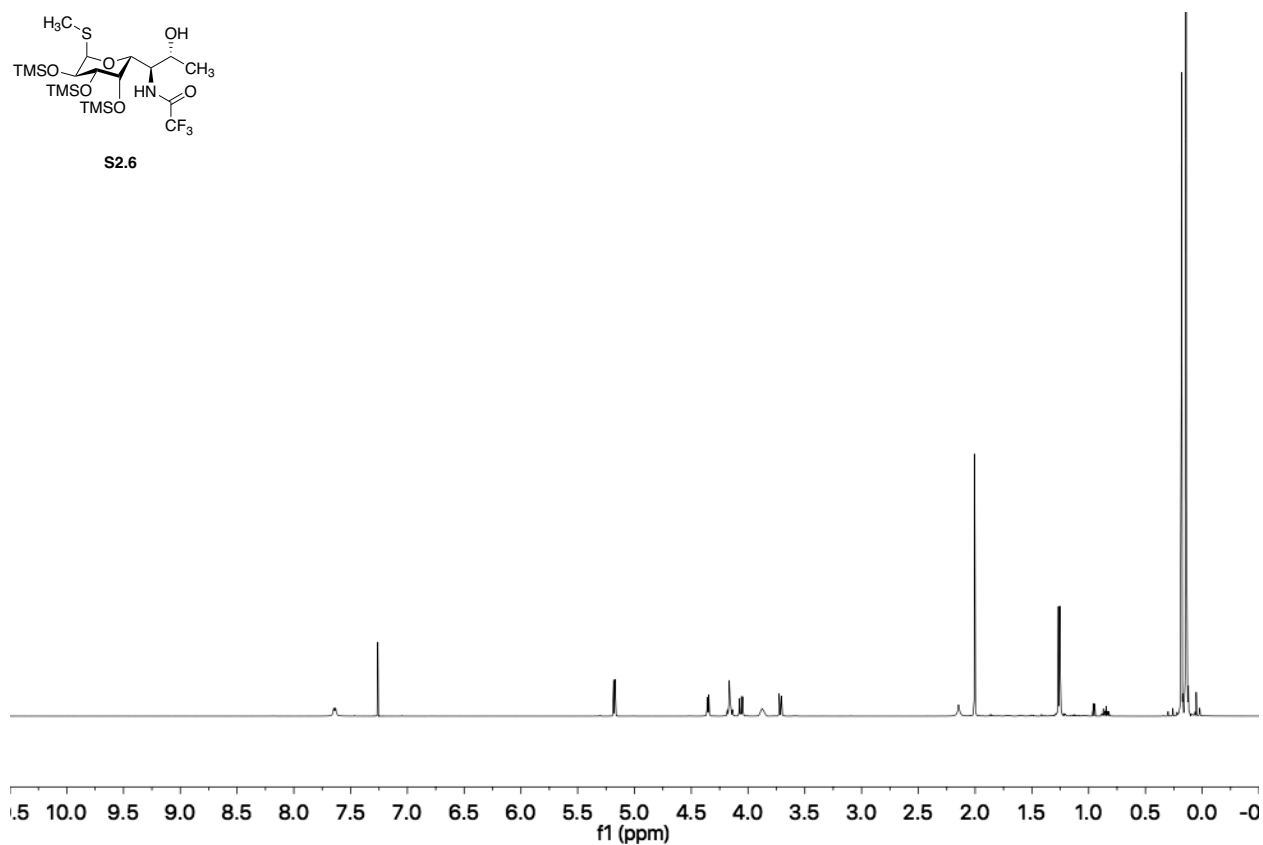


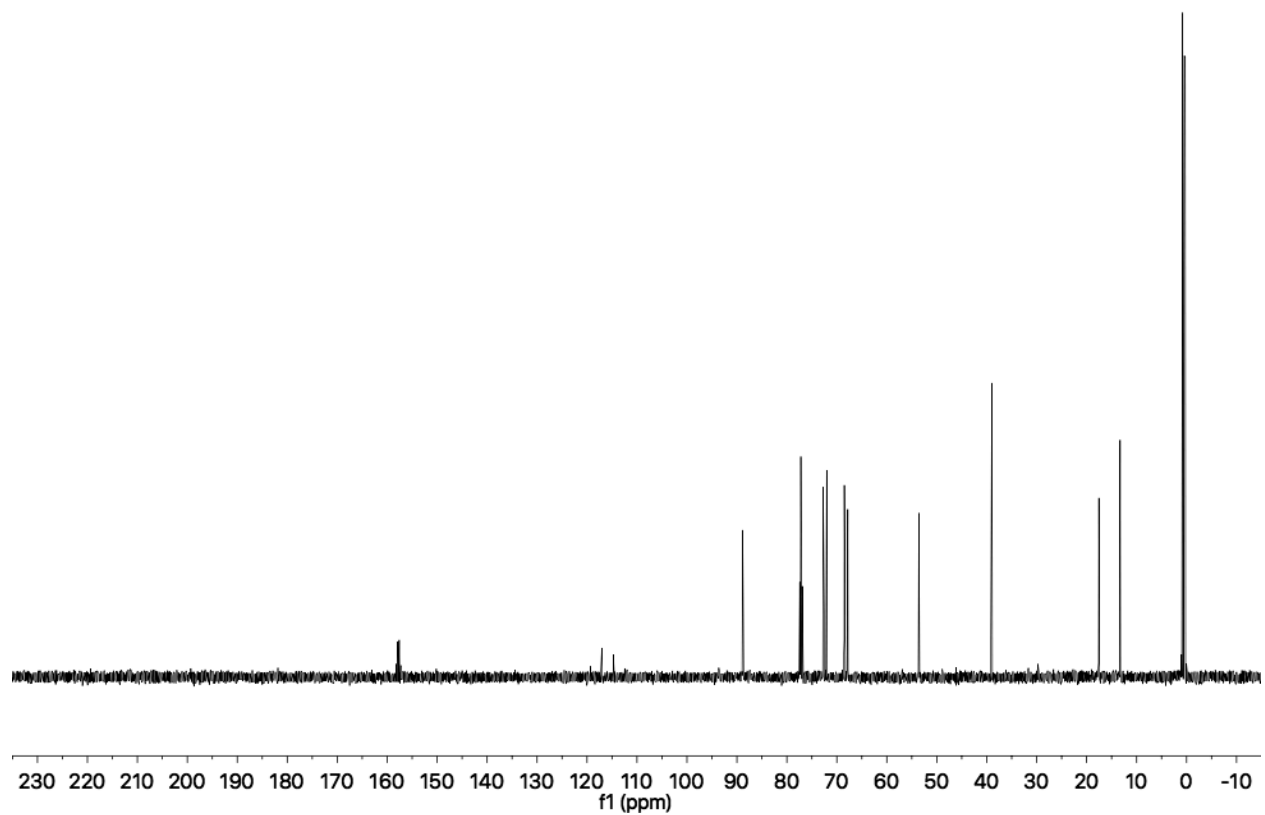
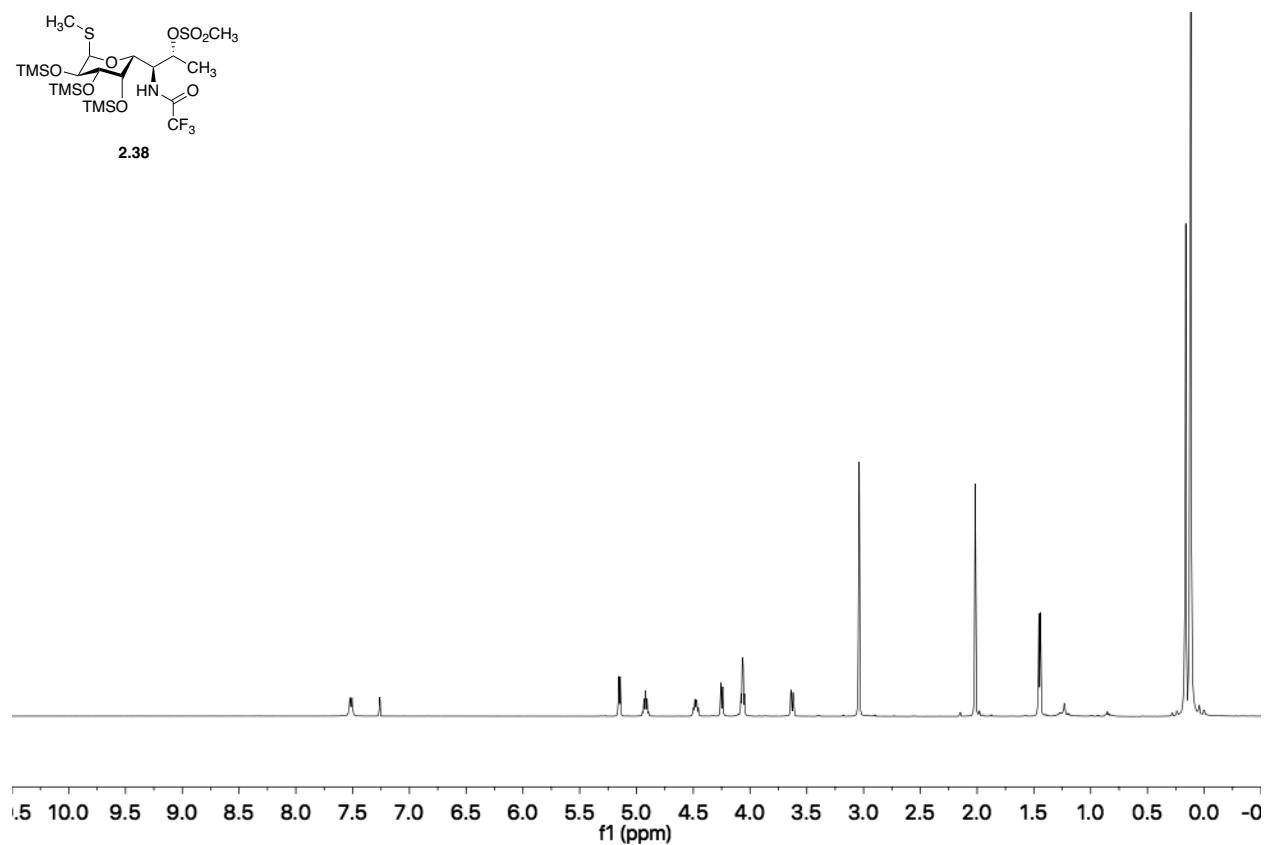
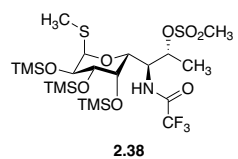


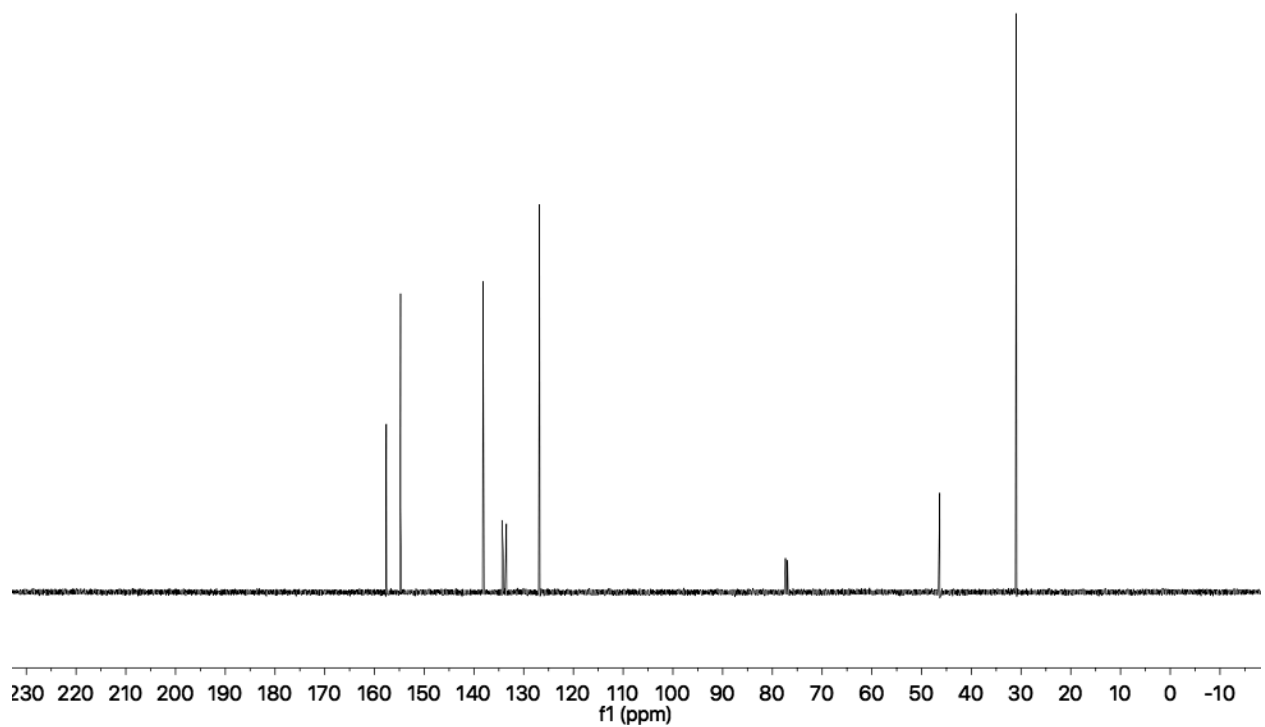
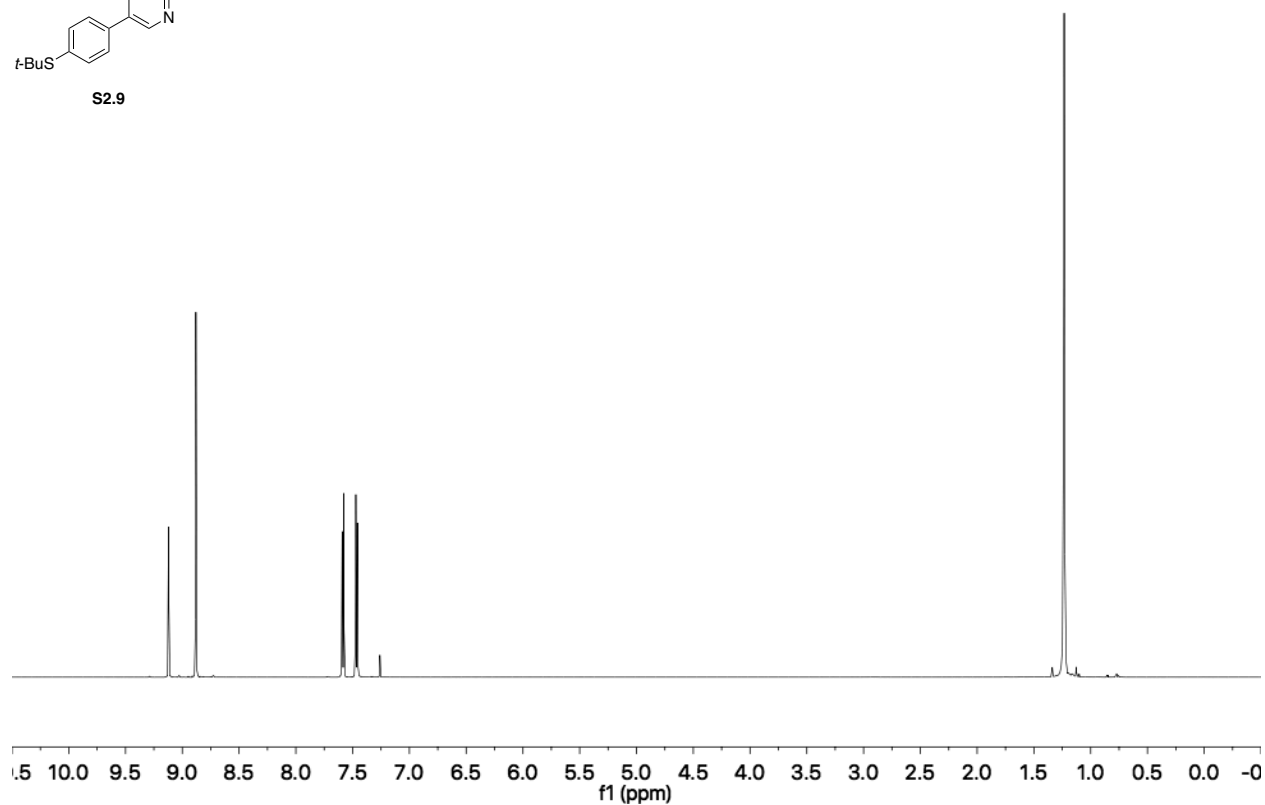
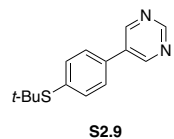


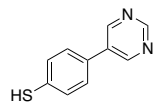


S2.6

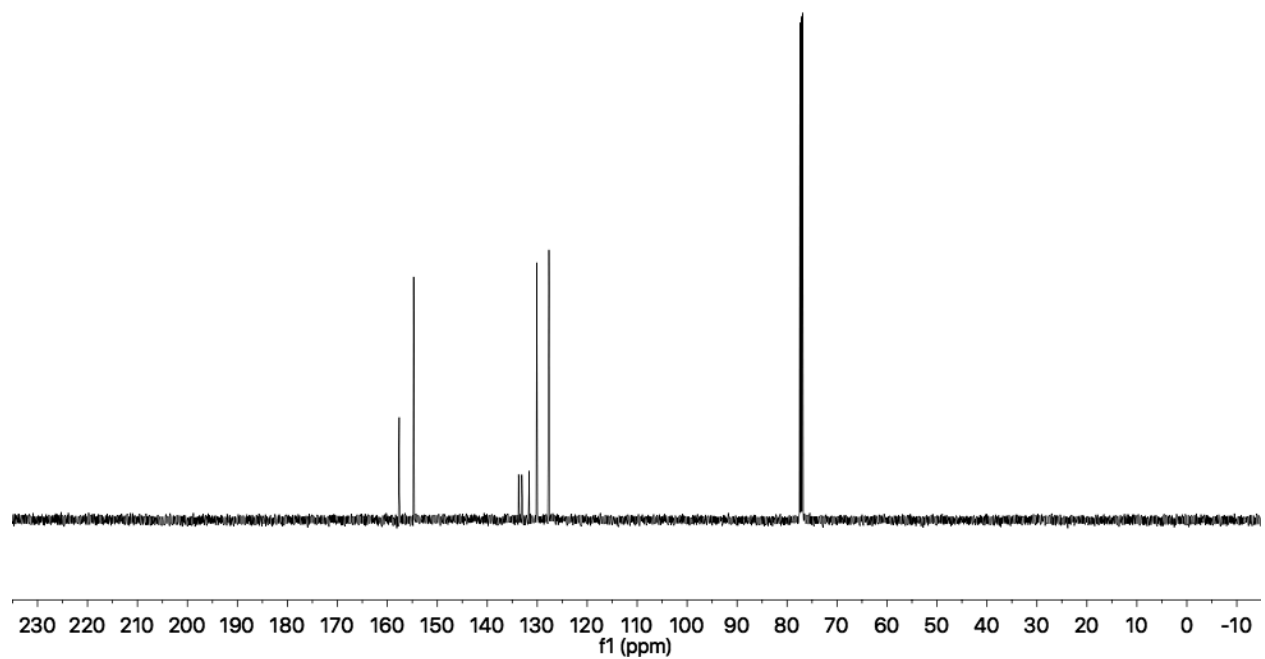
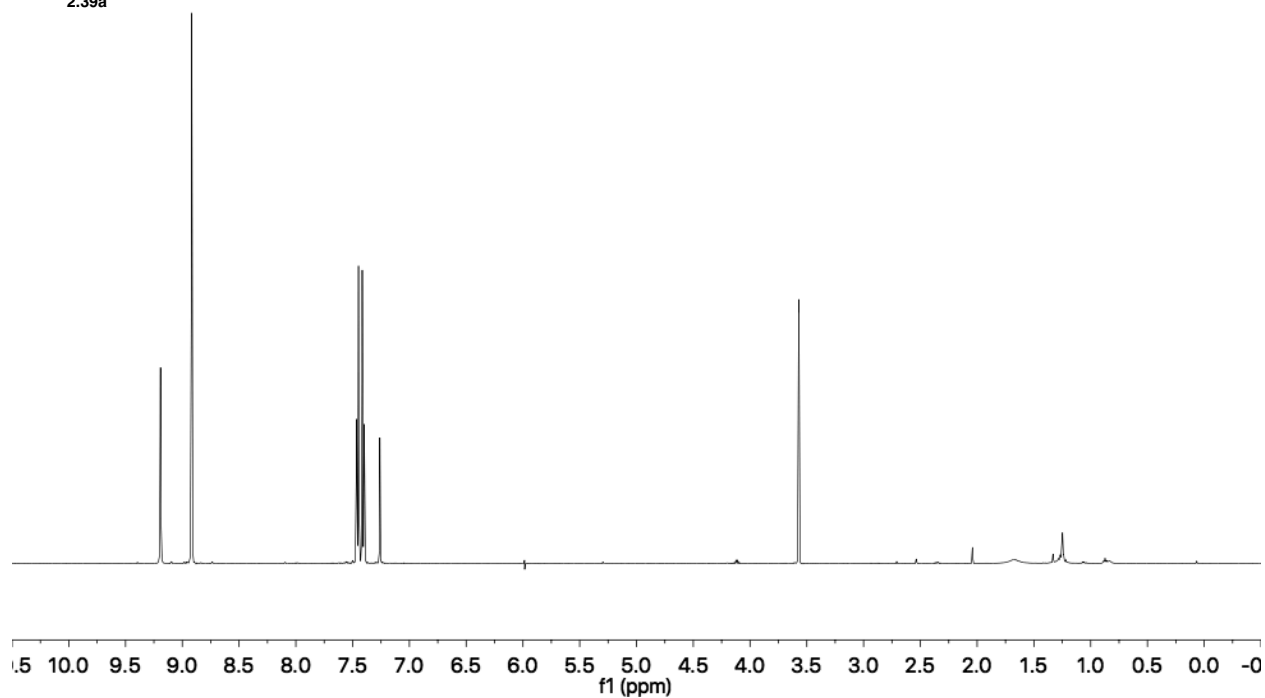


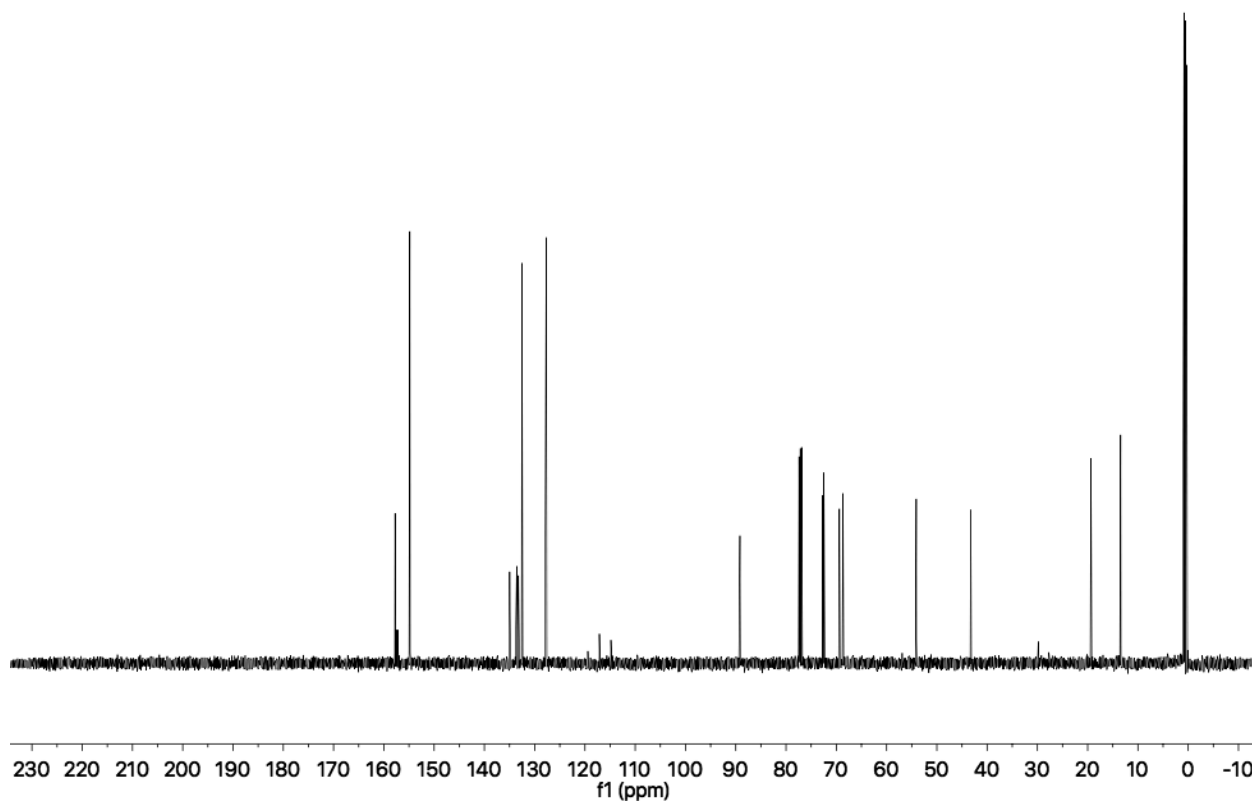
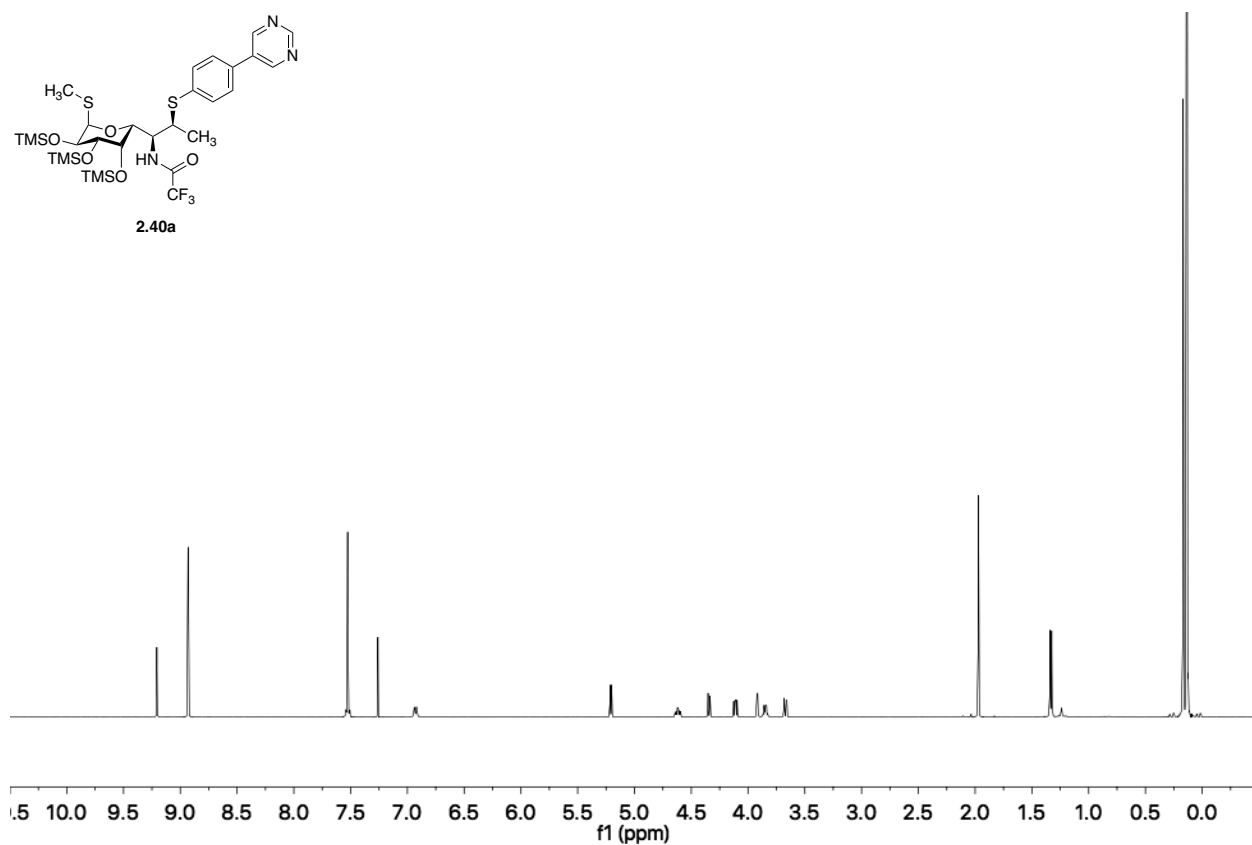
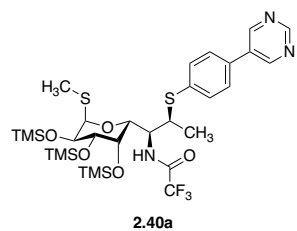


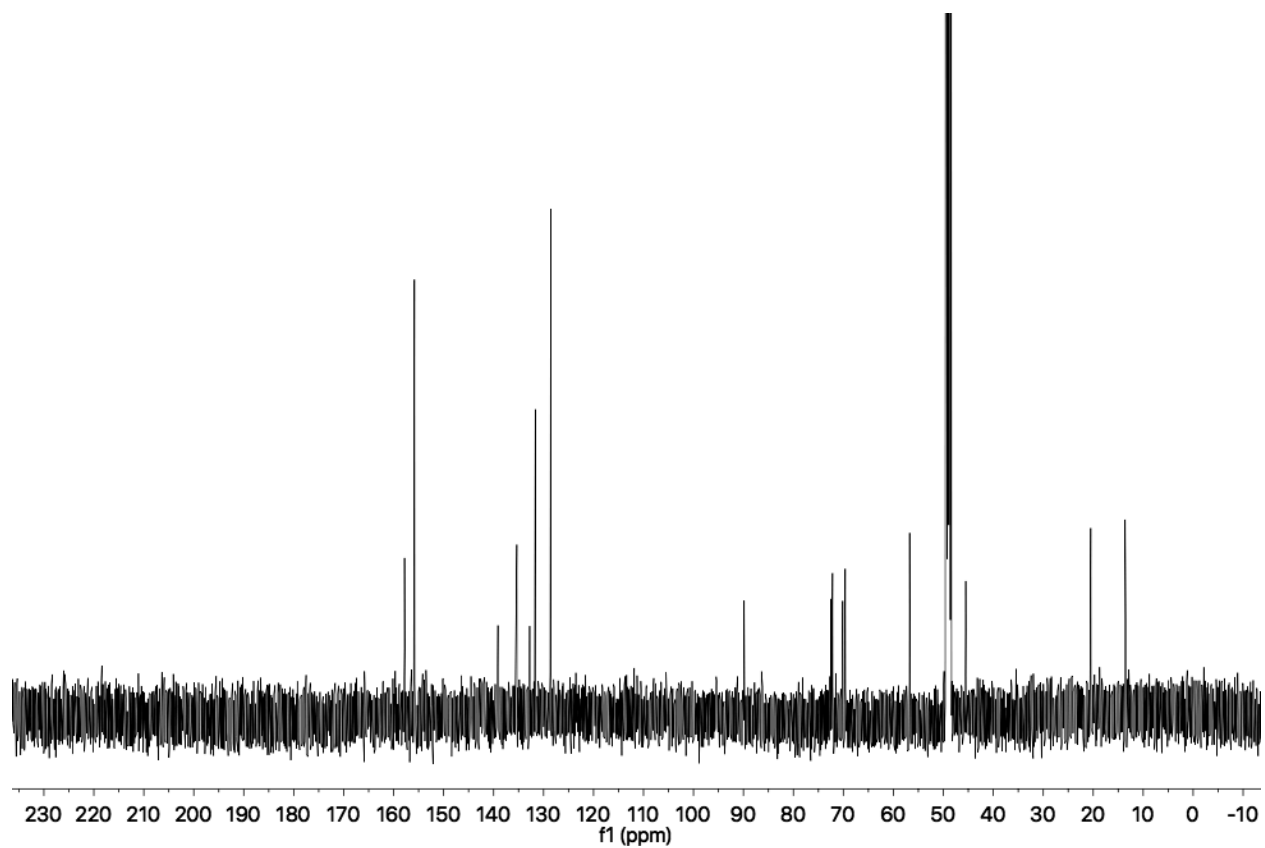
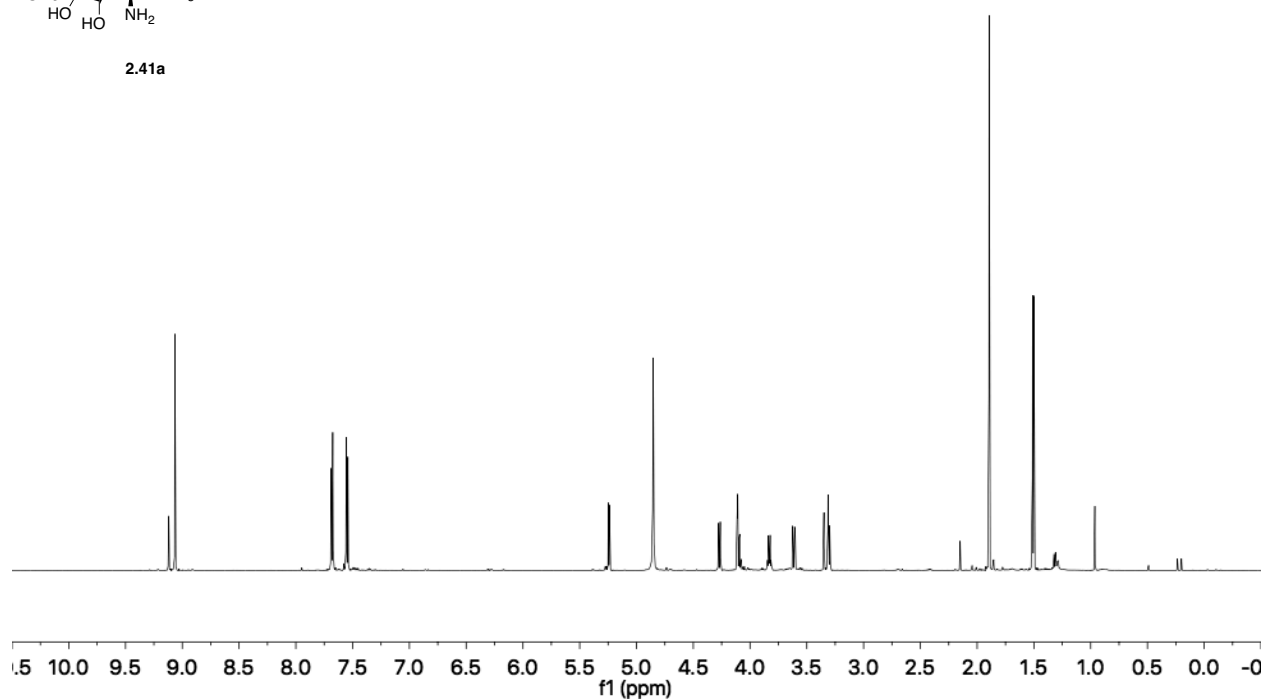
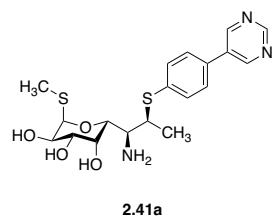


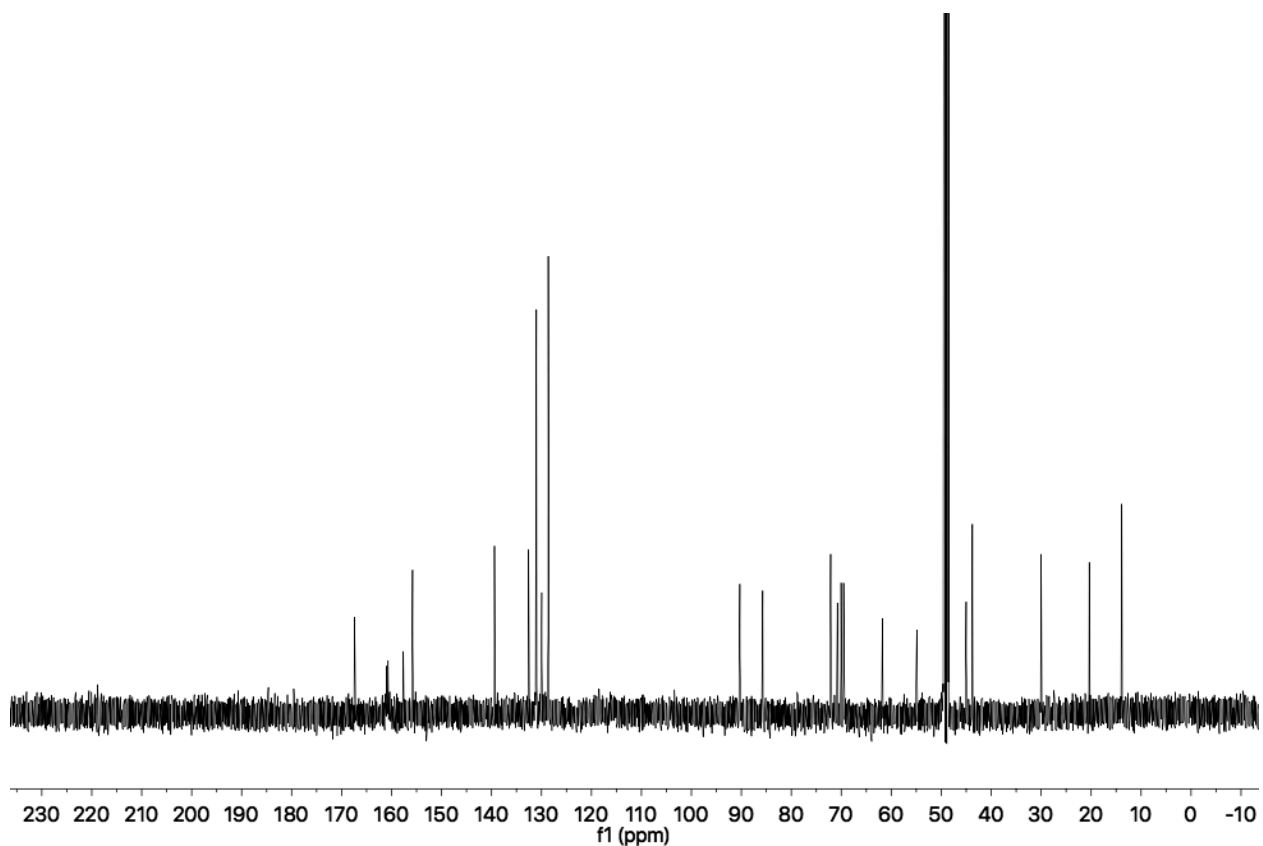
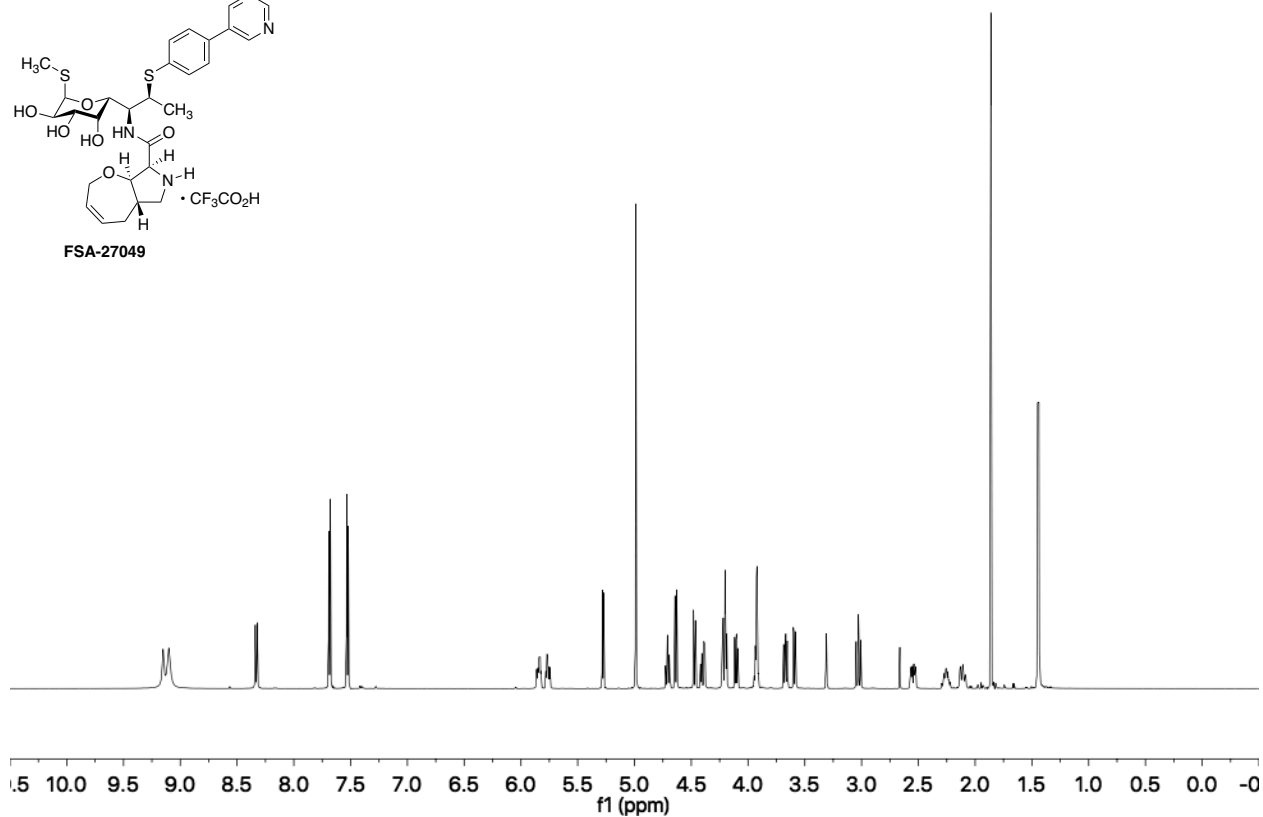
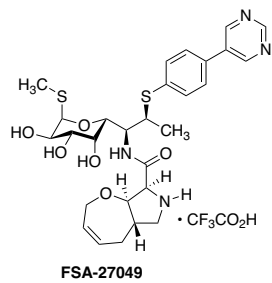


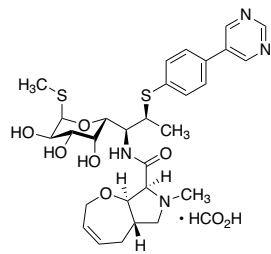
2.39a



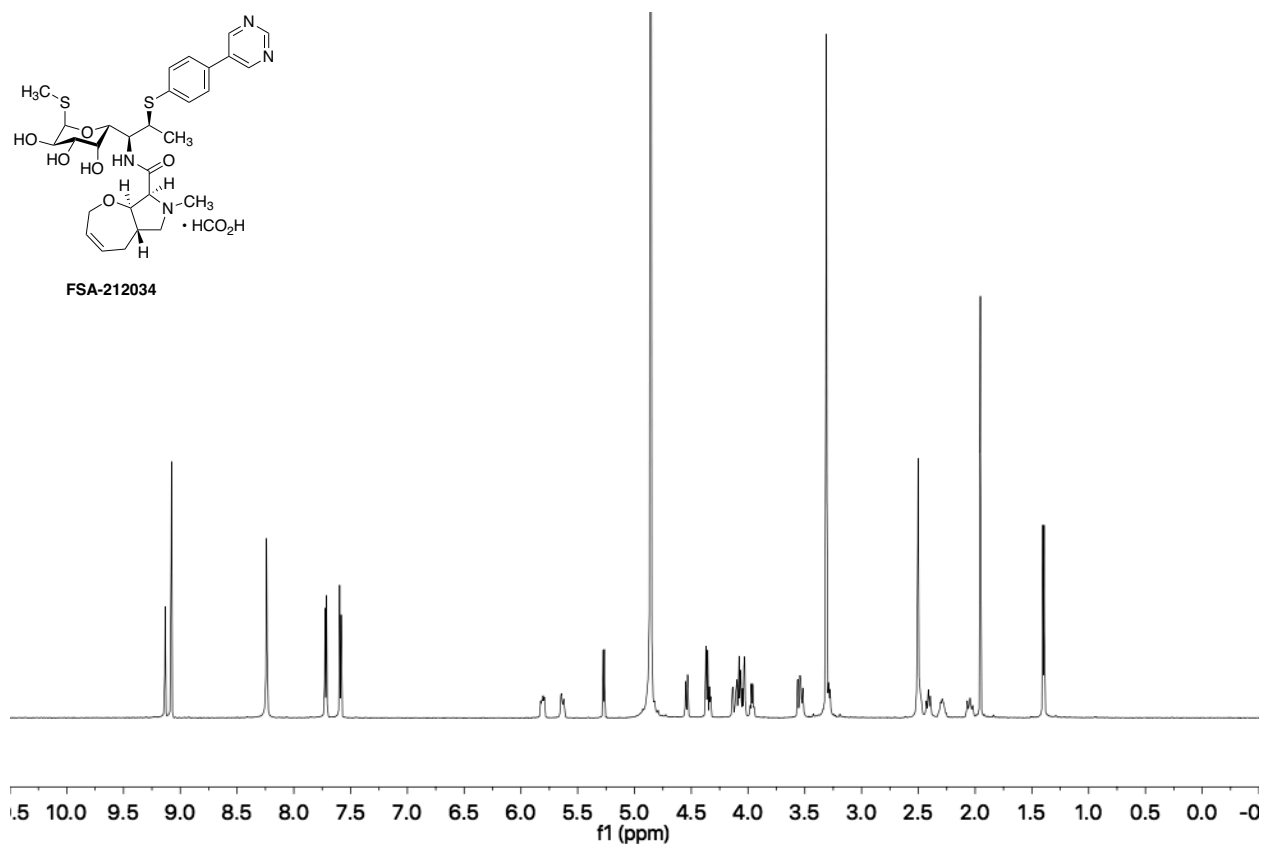


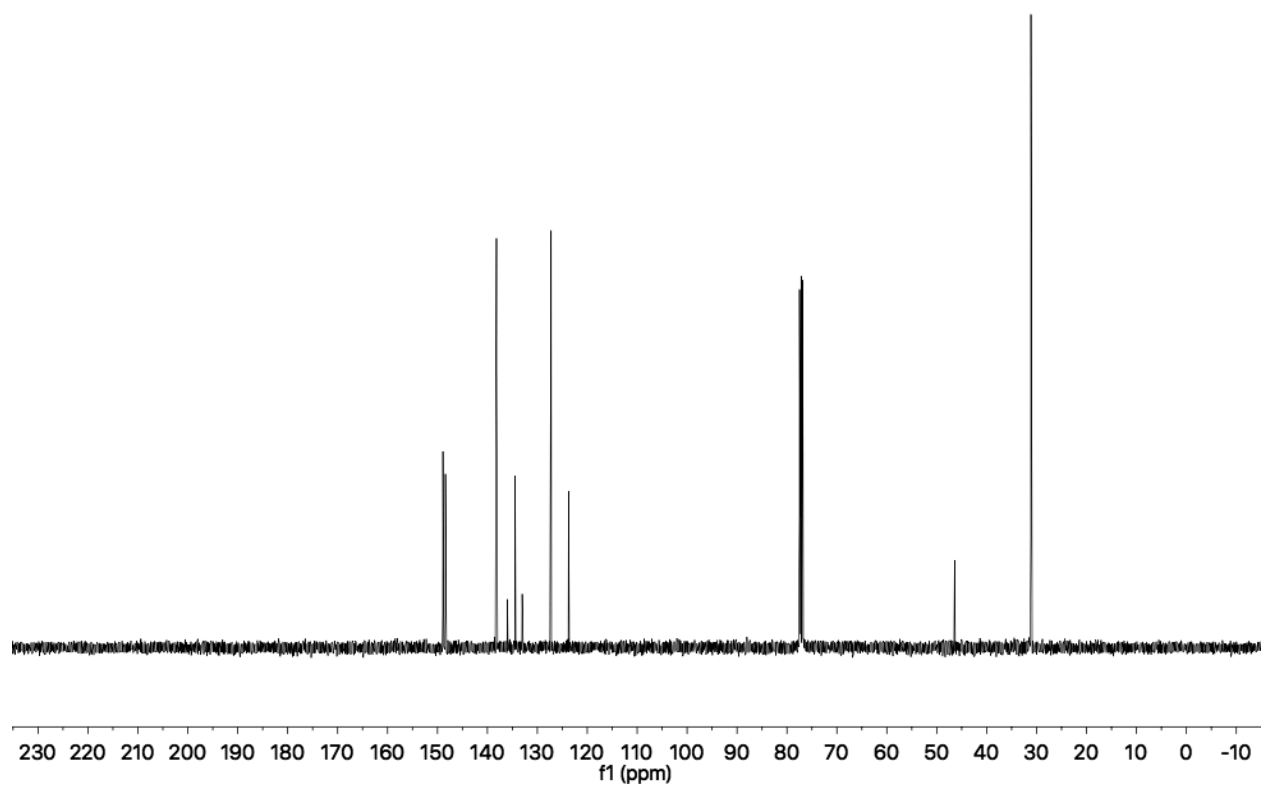
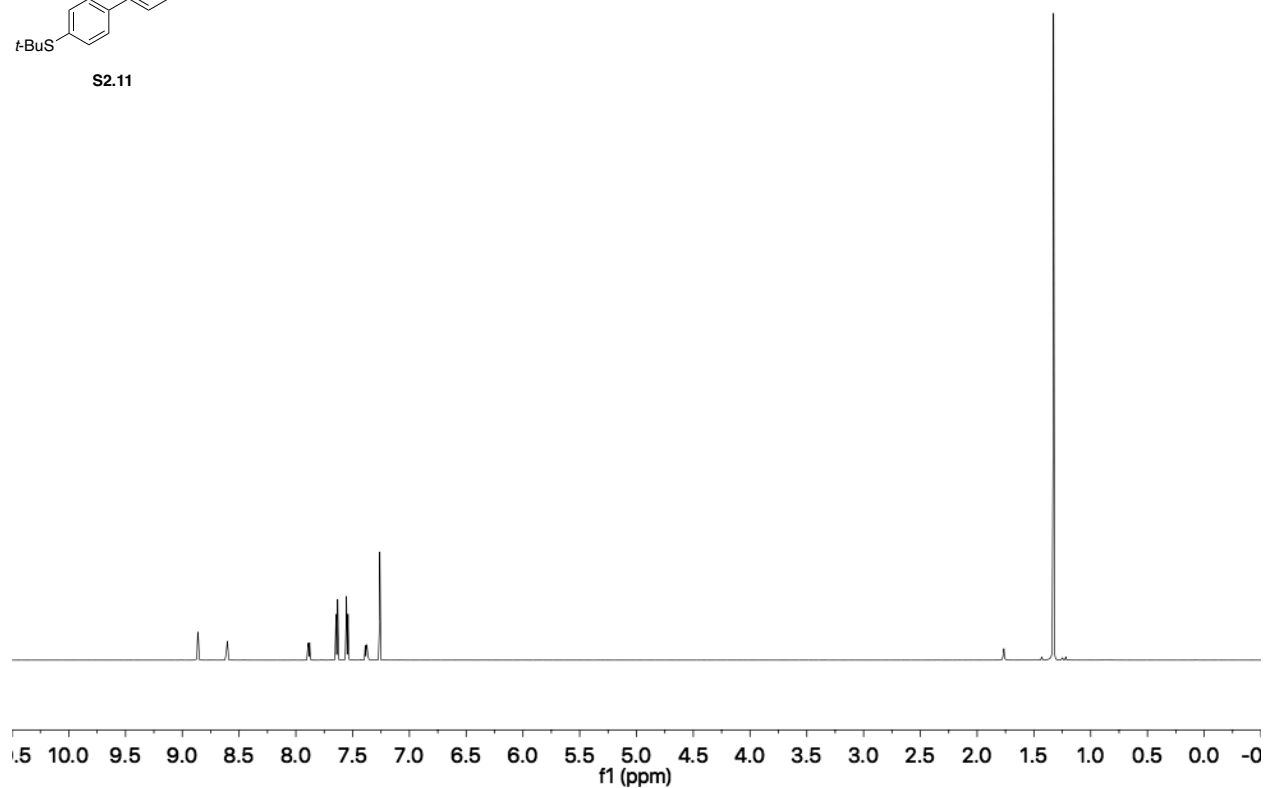
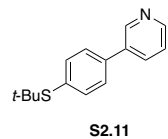


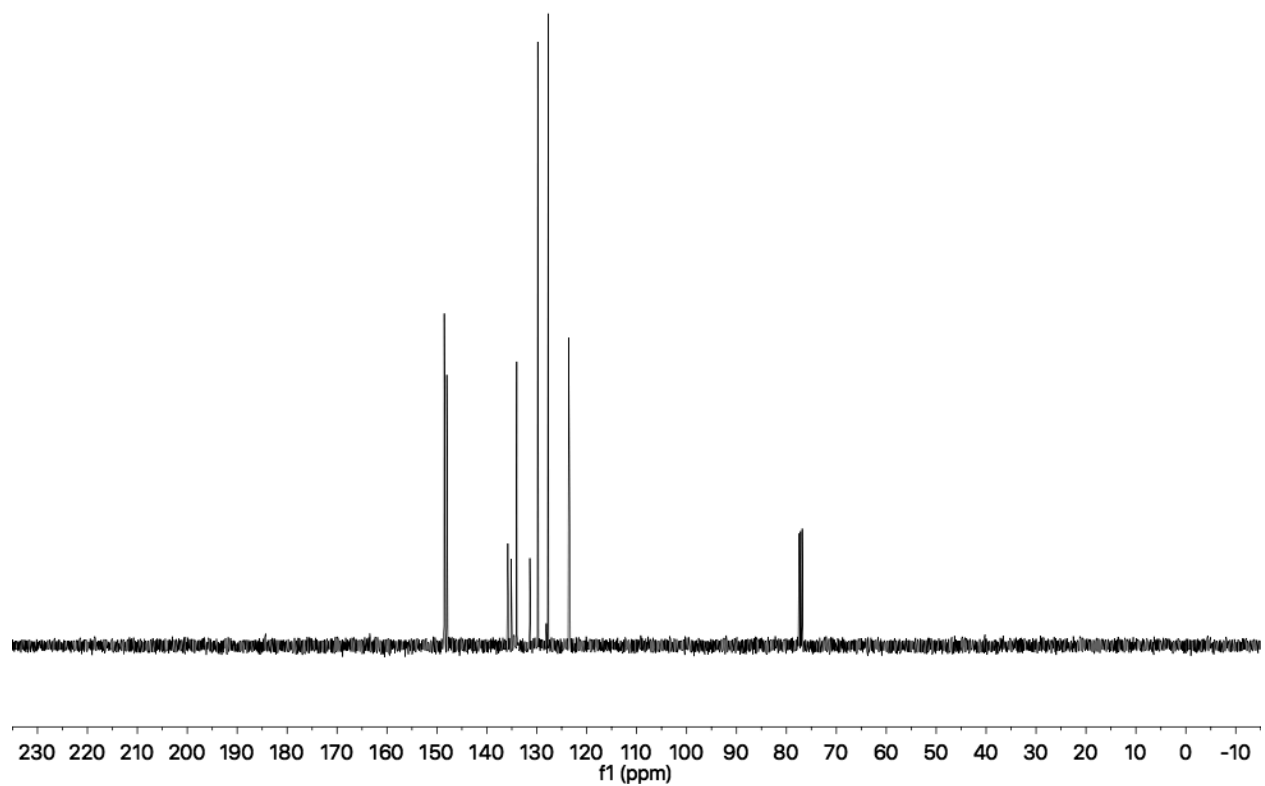
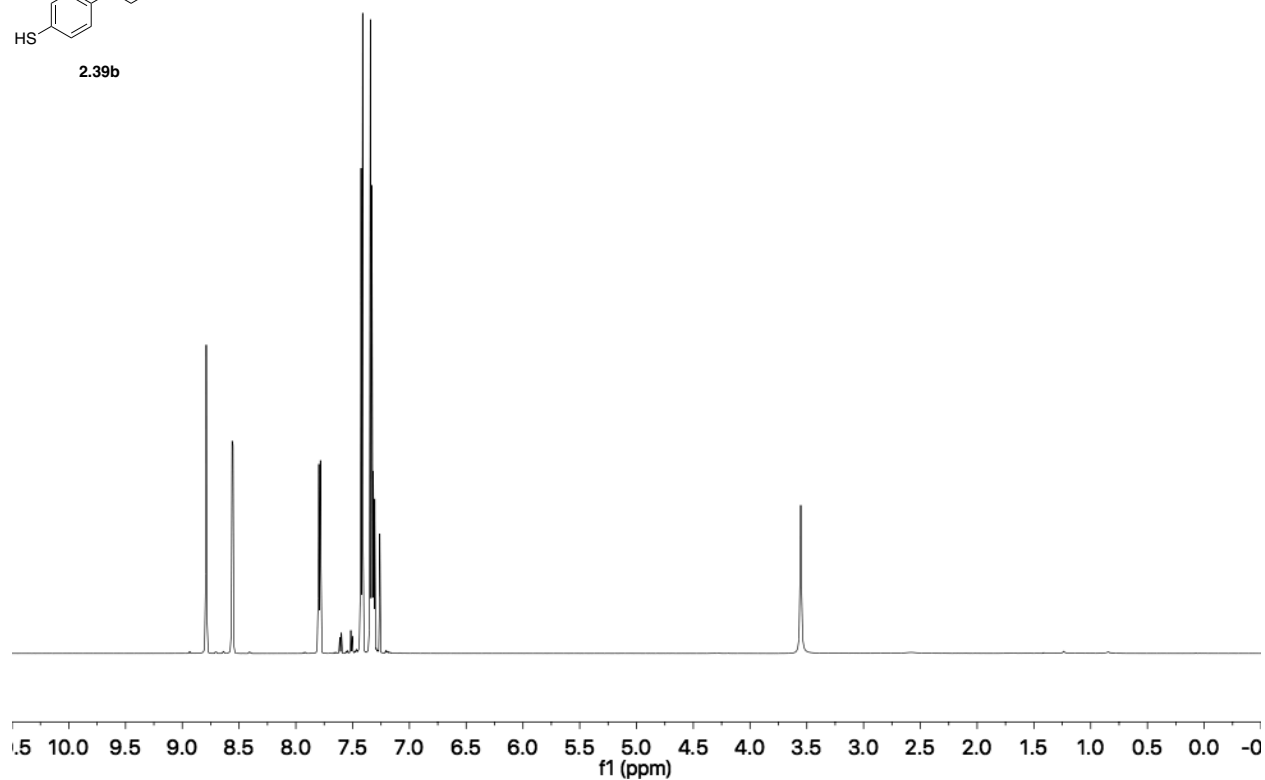
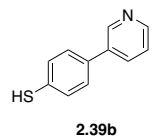


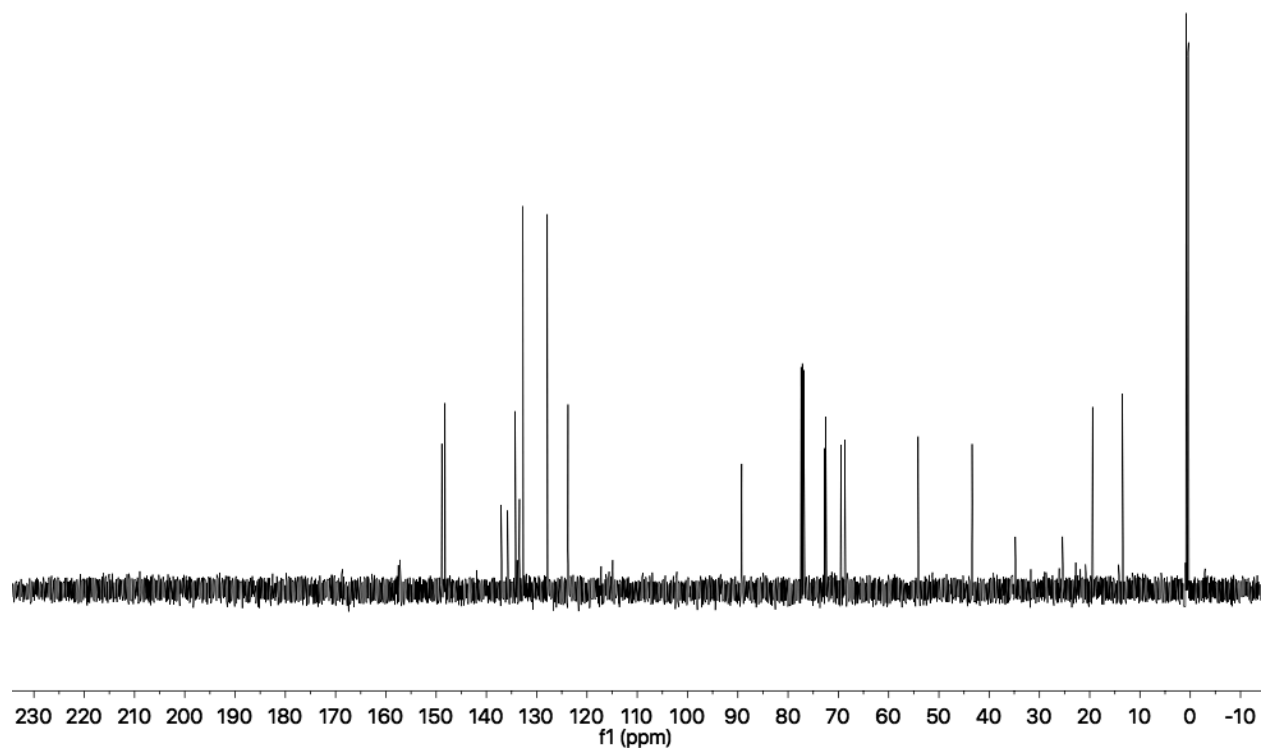
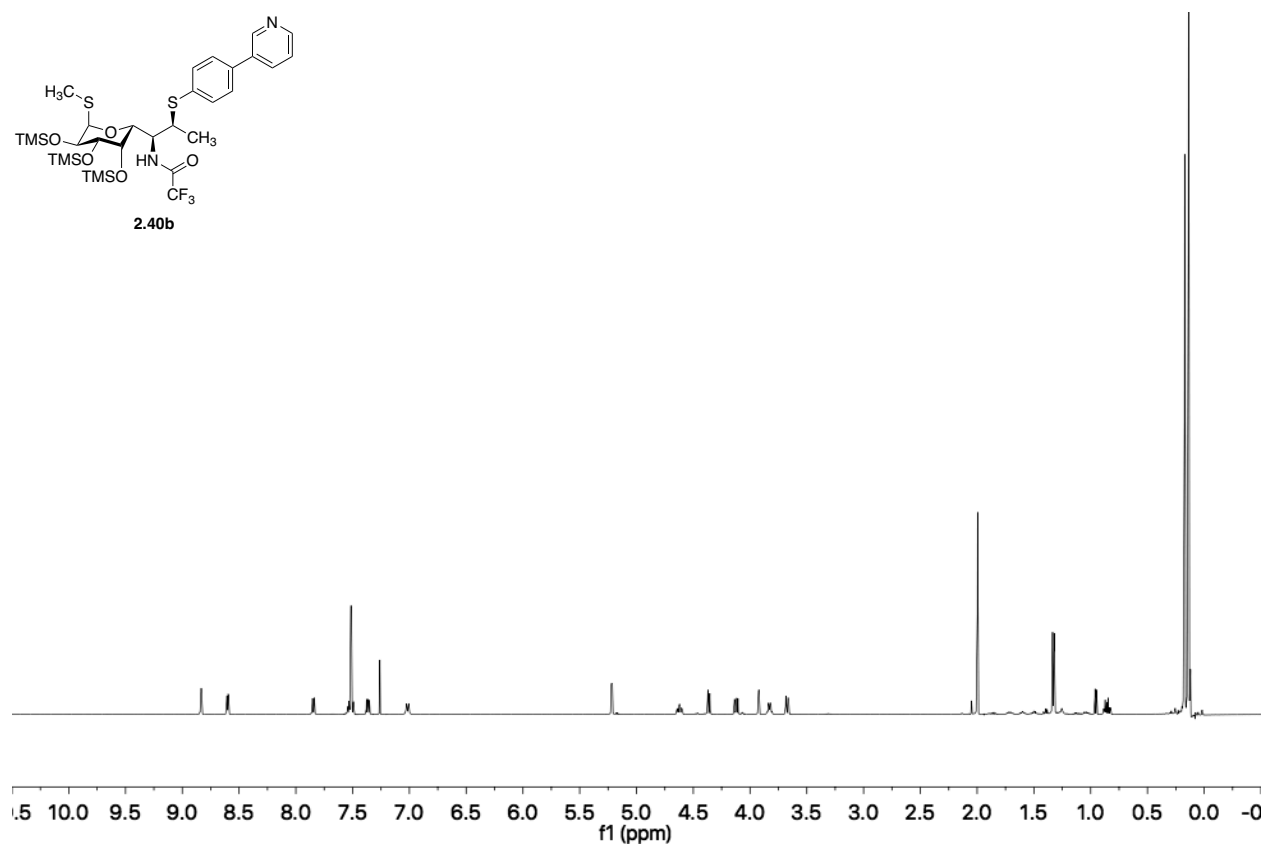
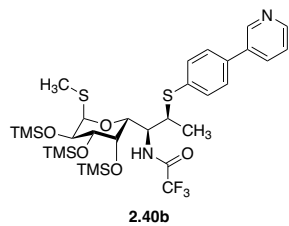


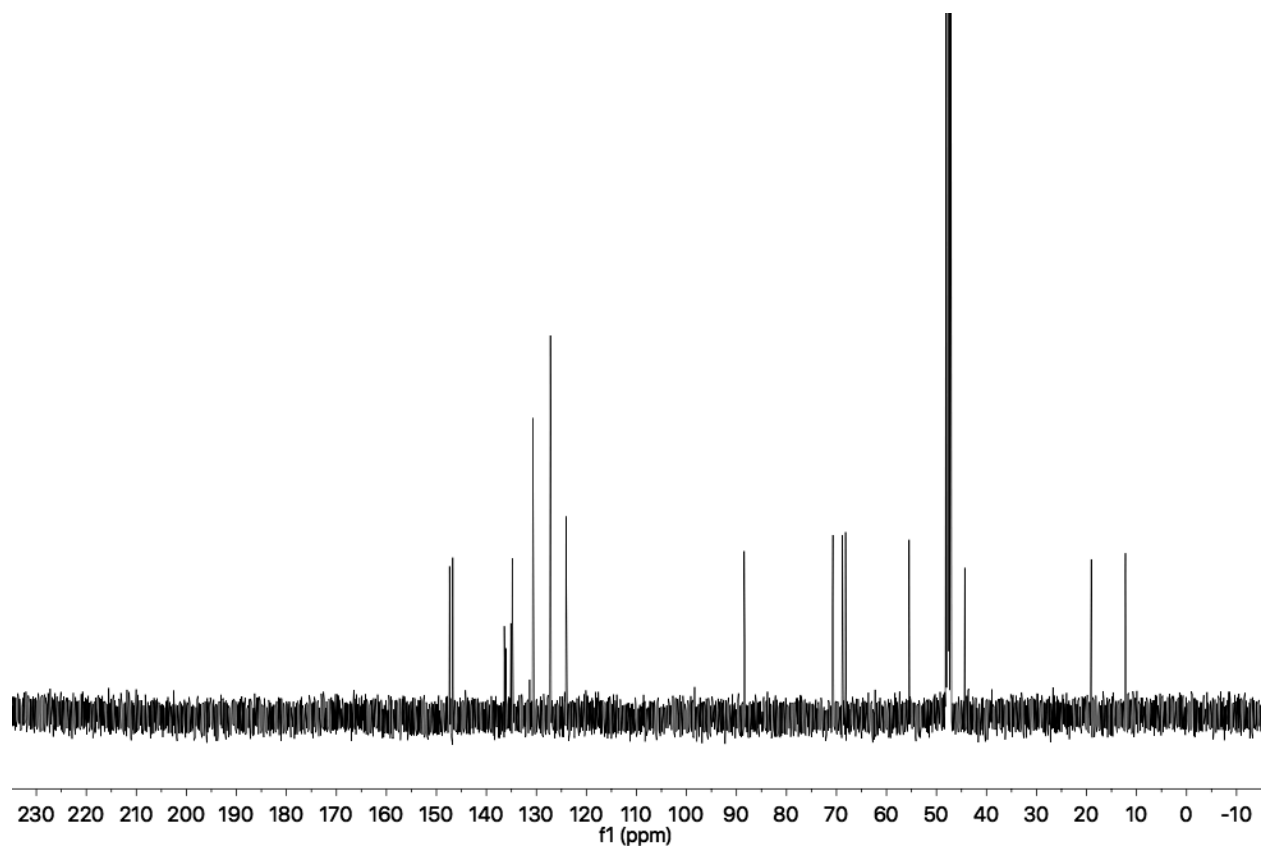
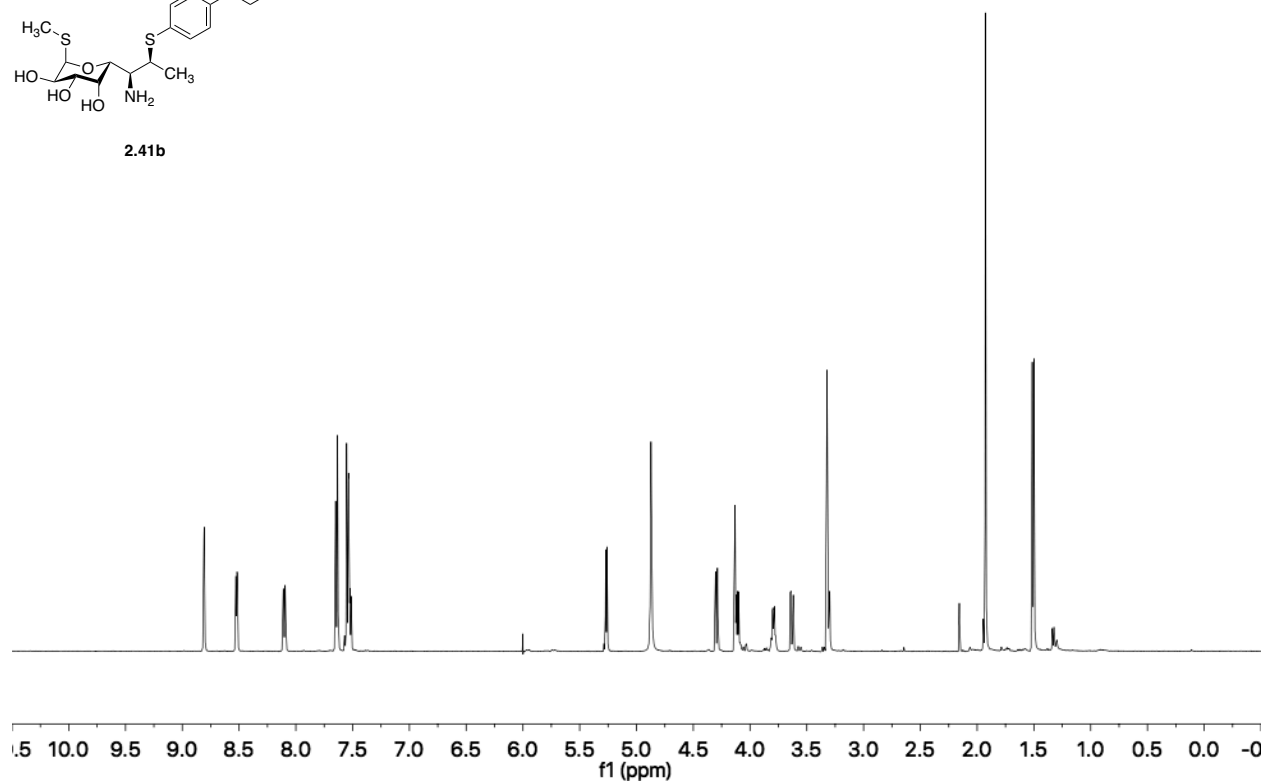
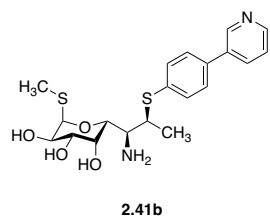
FSA-212034

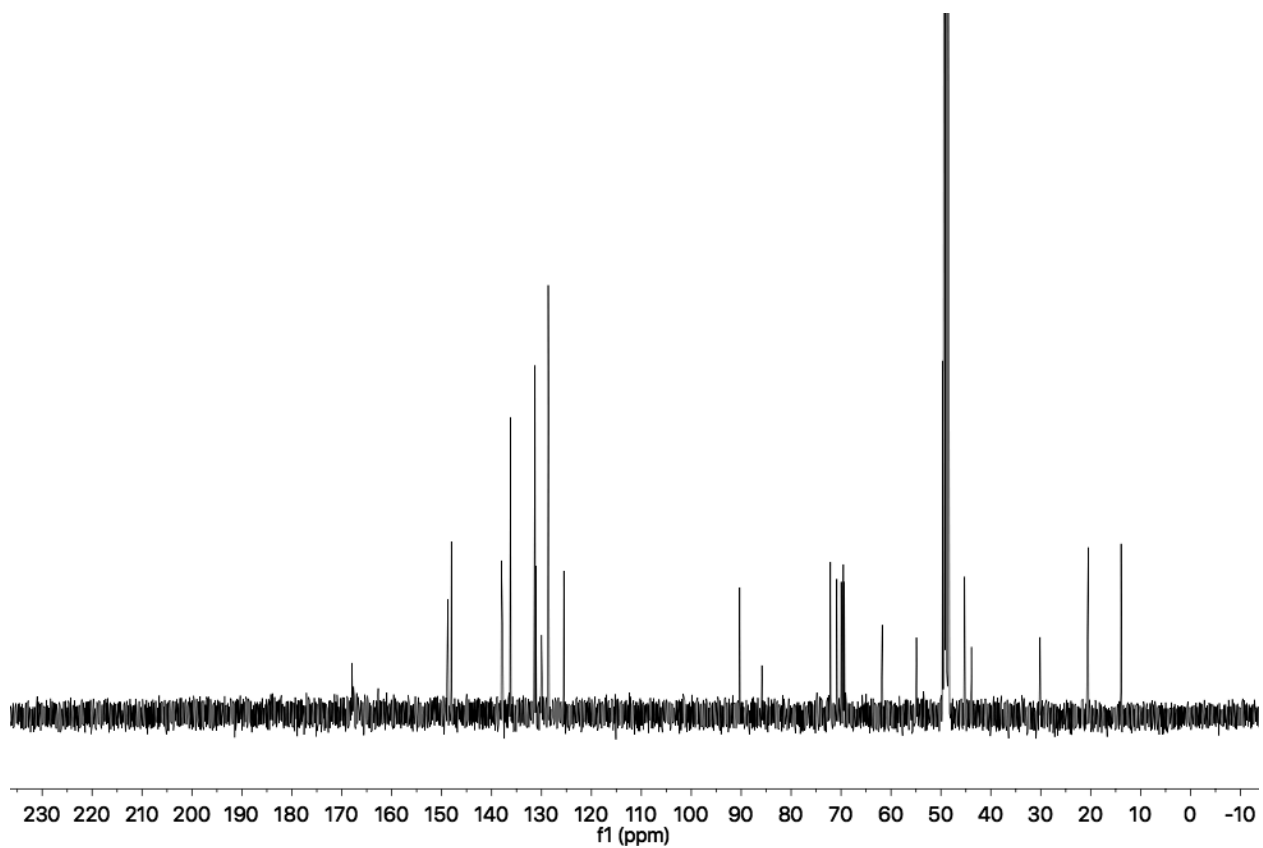
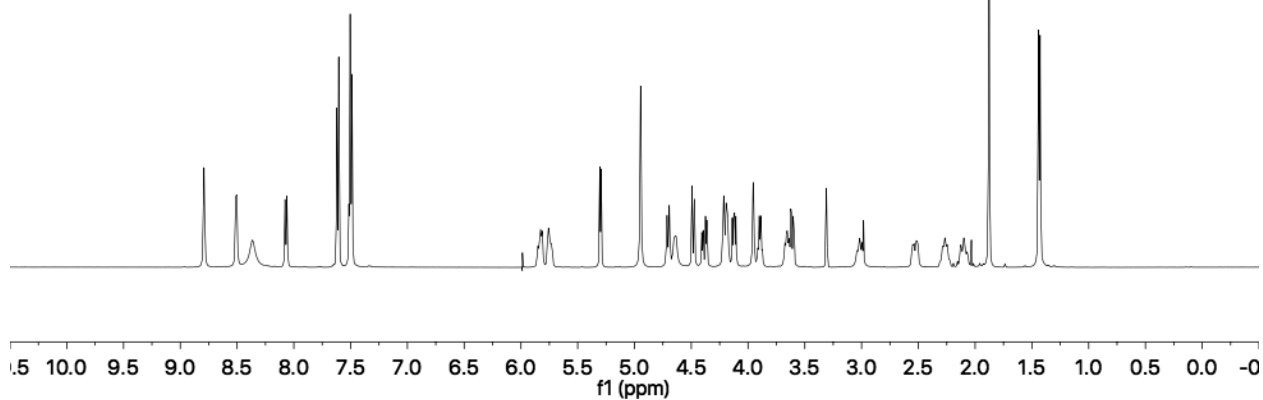
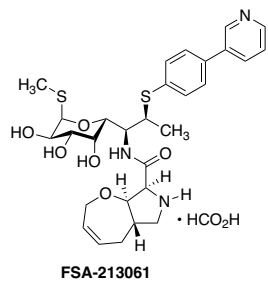


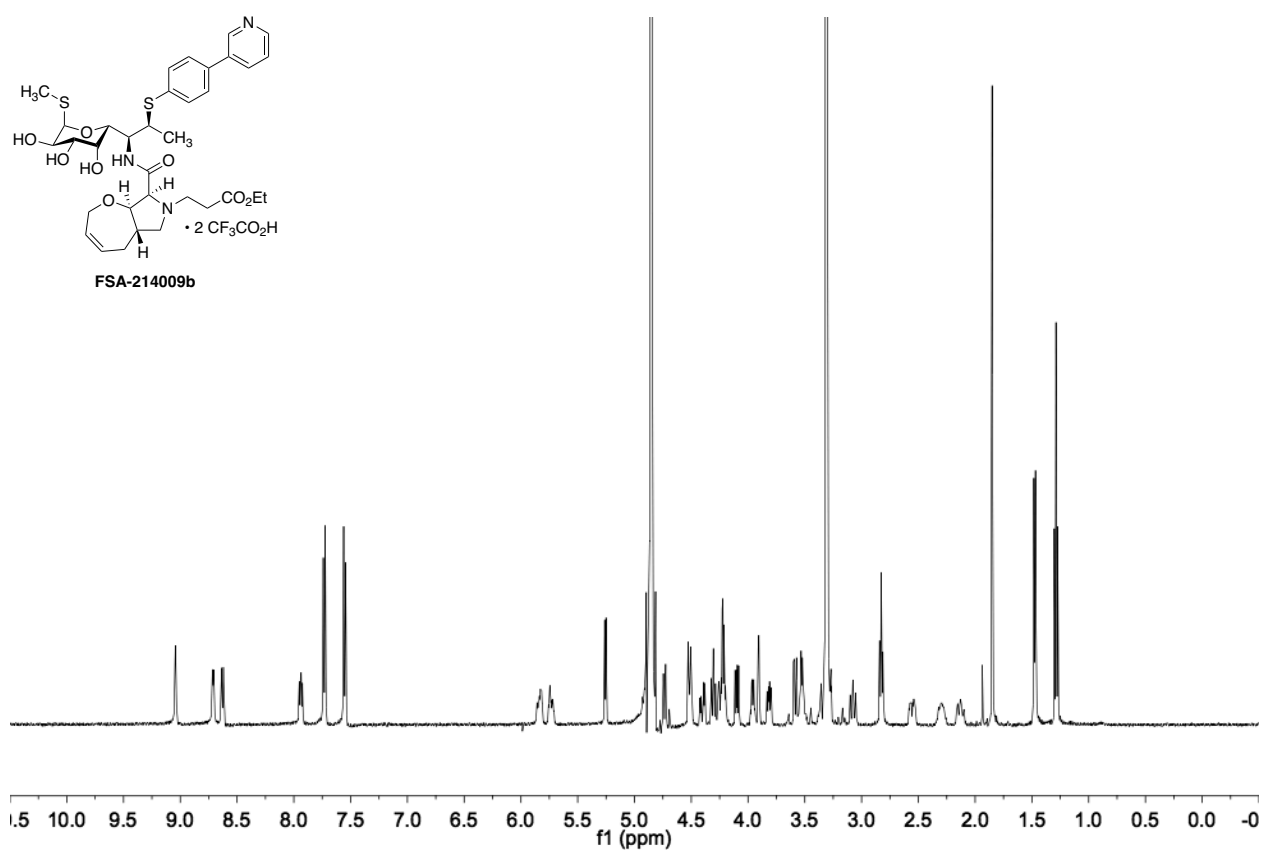
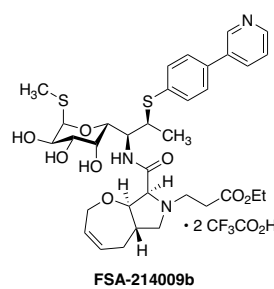
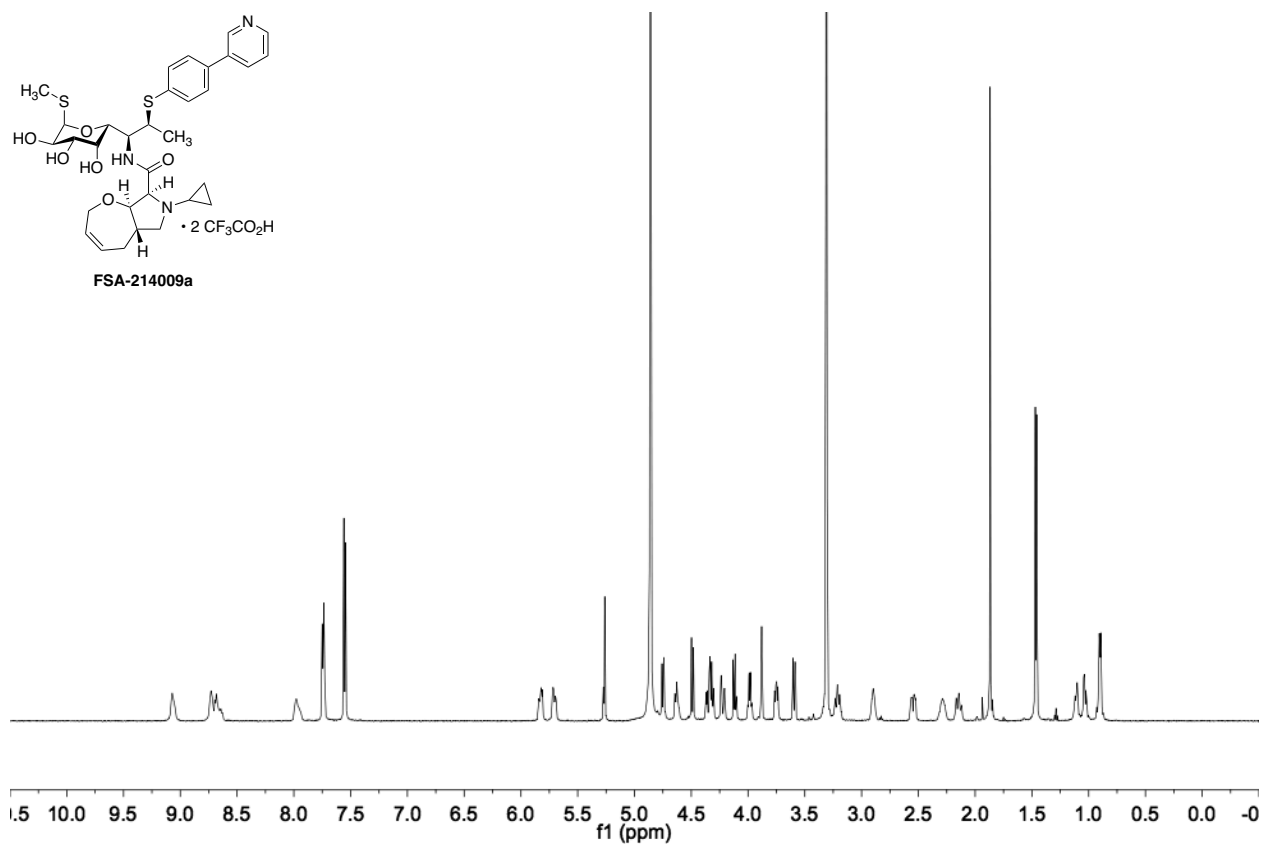
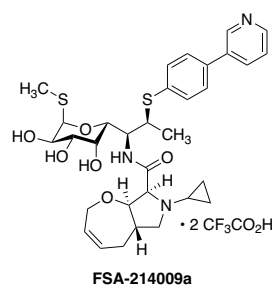


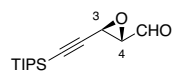




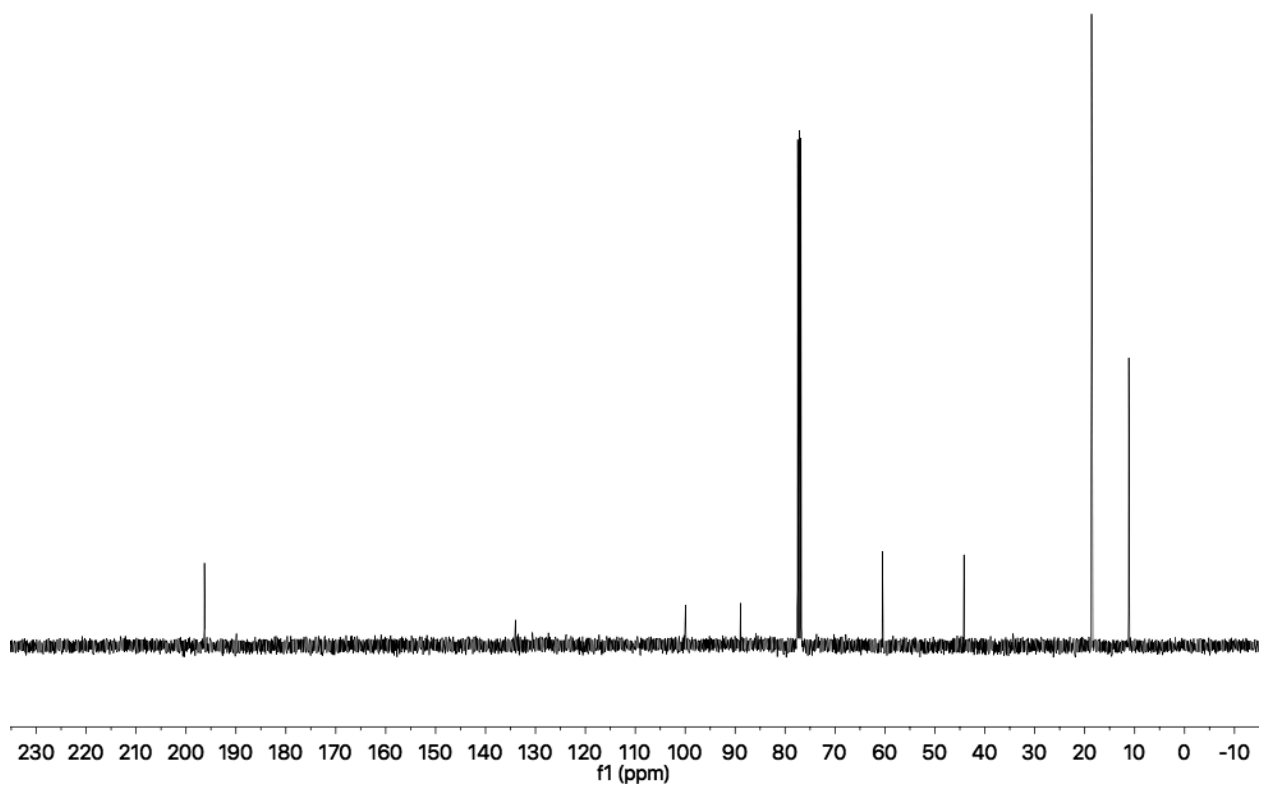
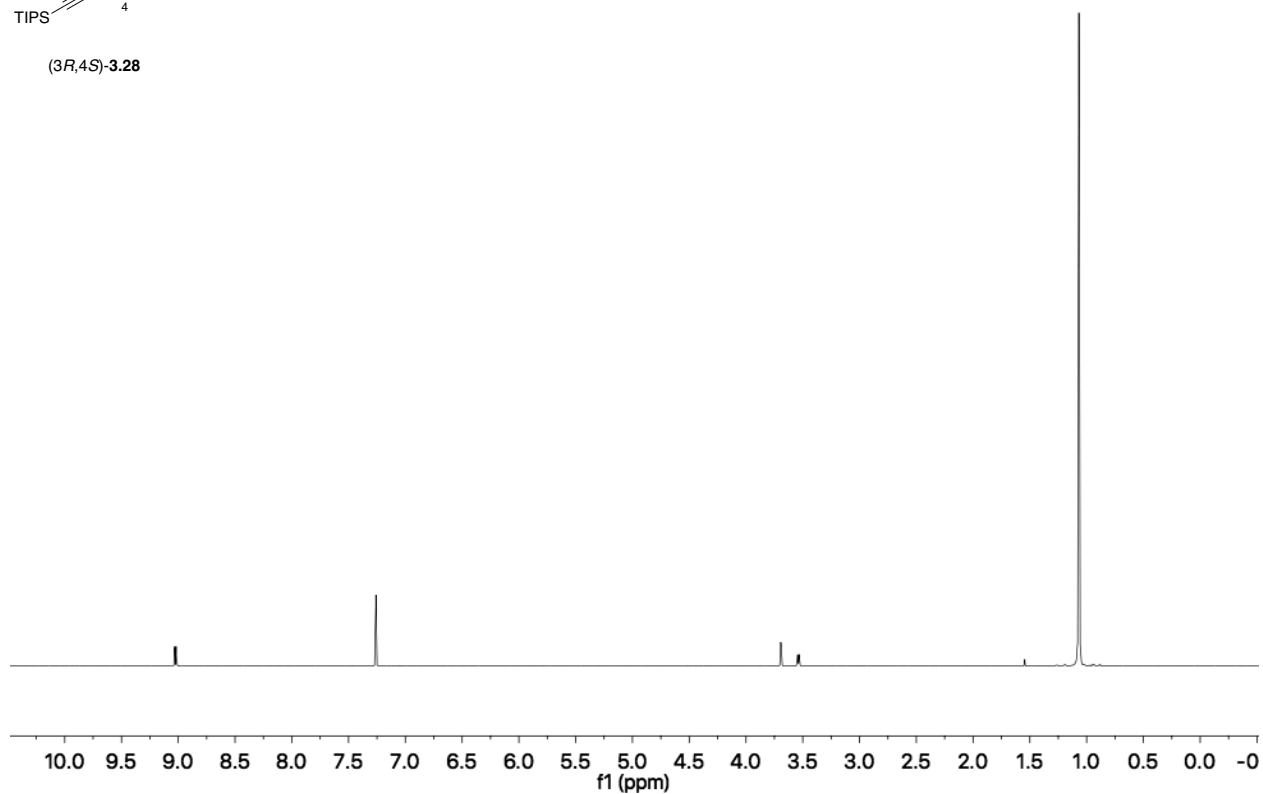


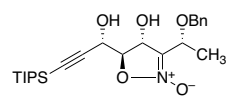




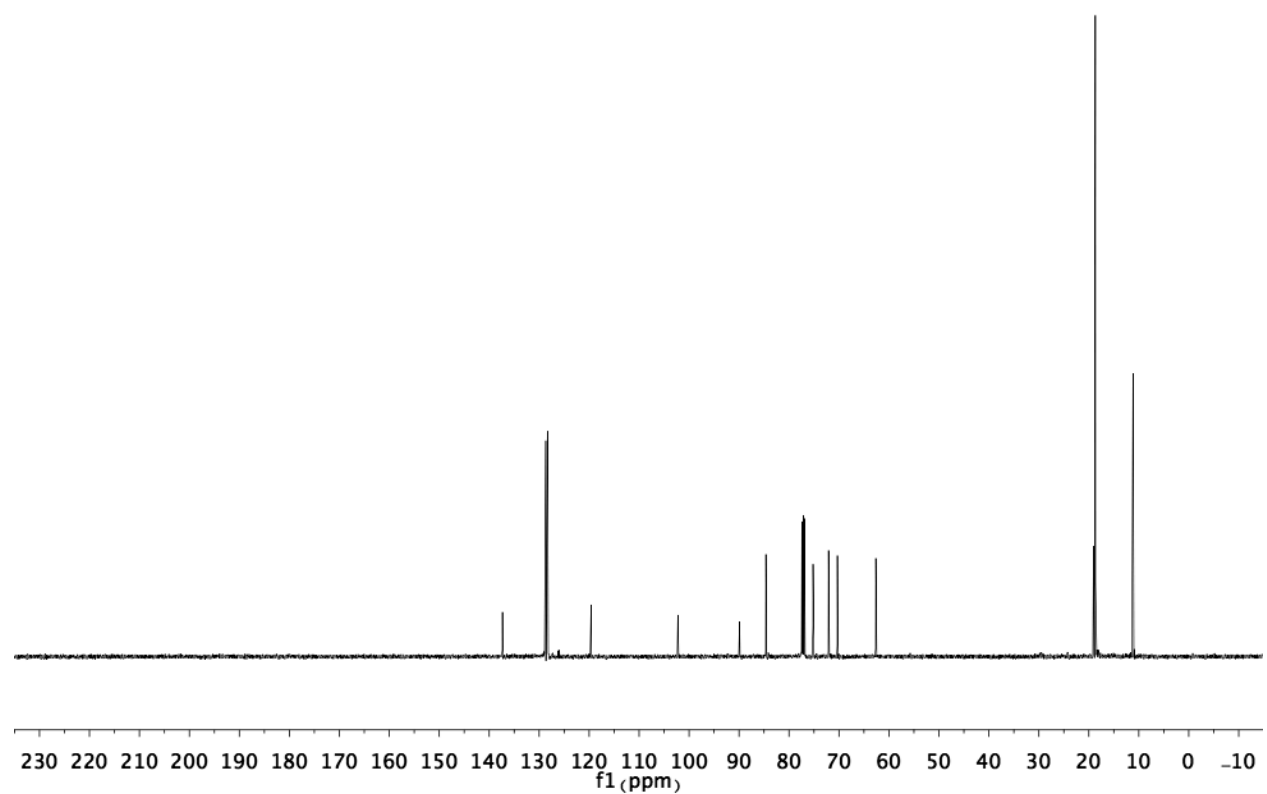
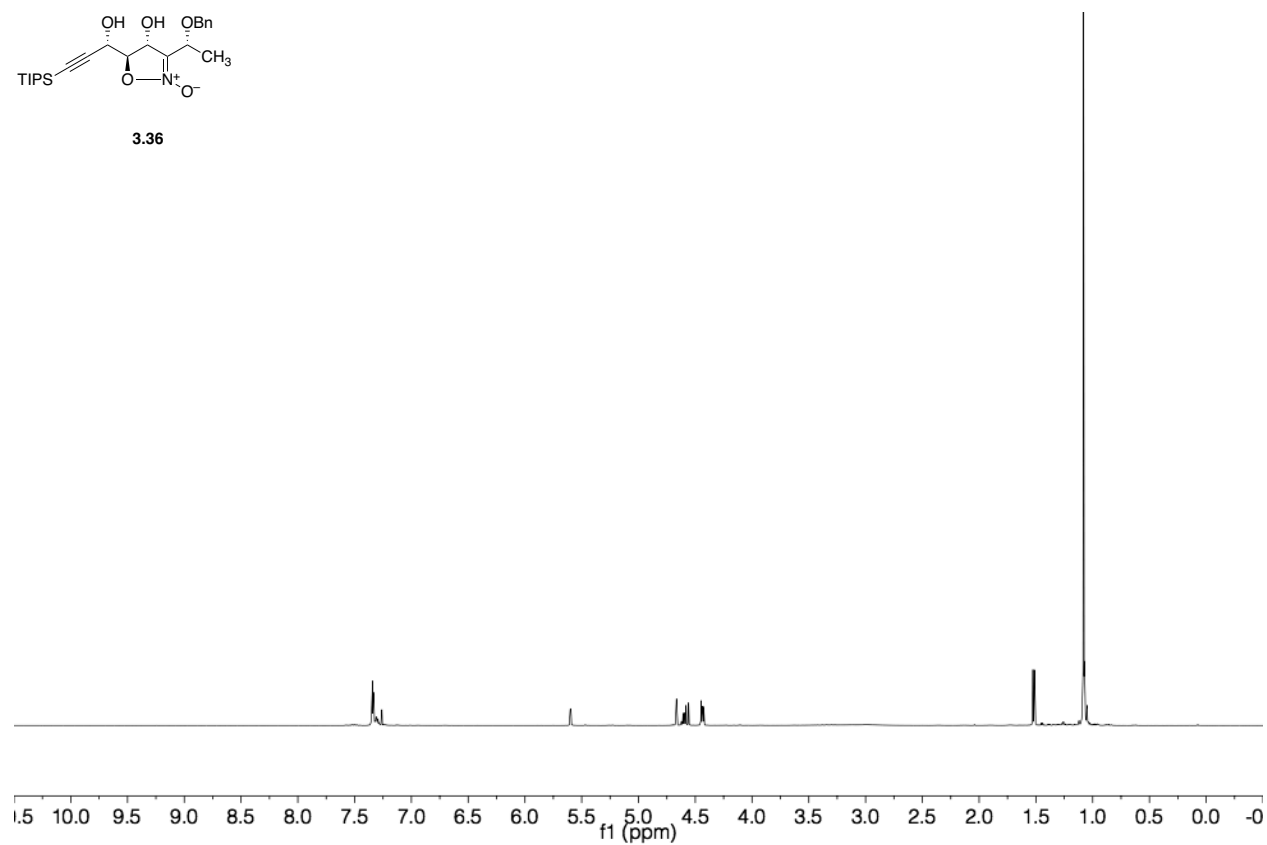


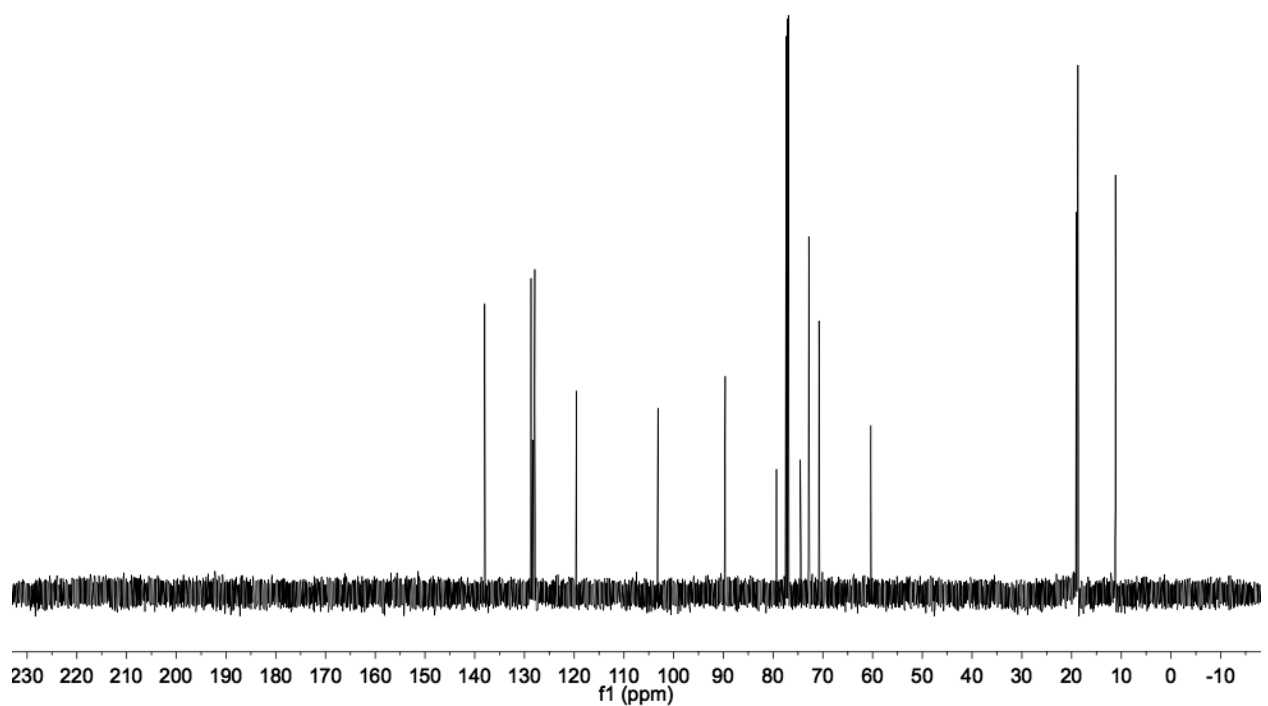
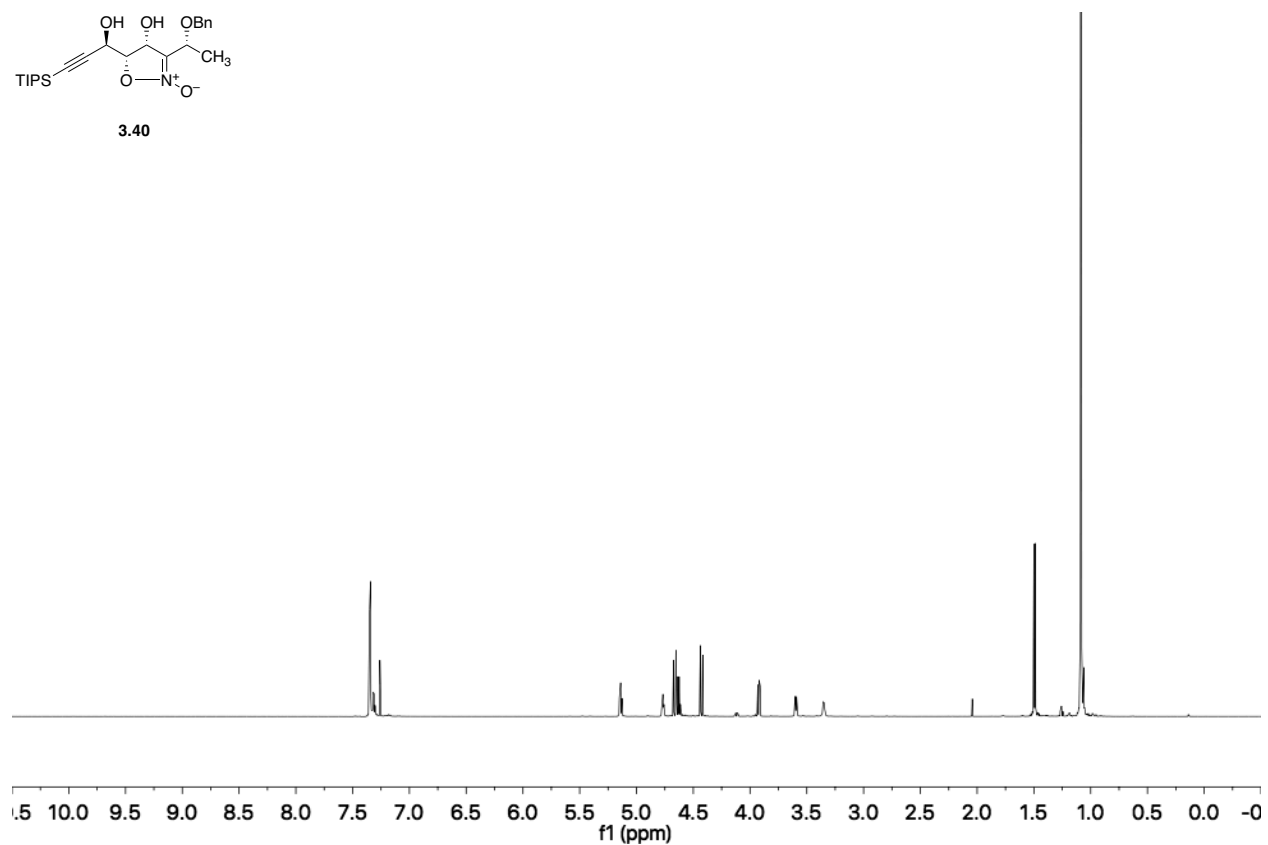
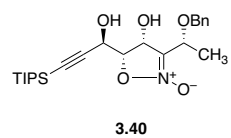
(3R,4S)-3.28

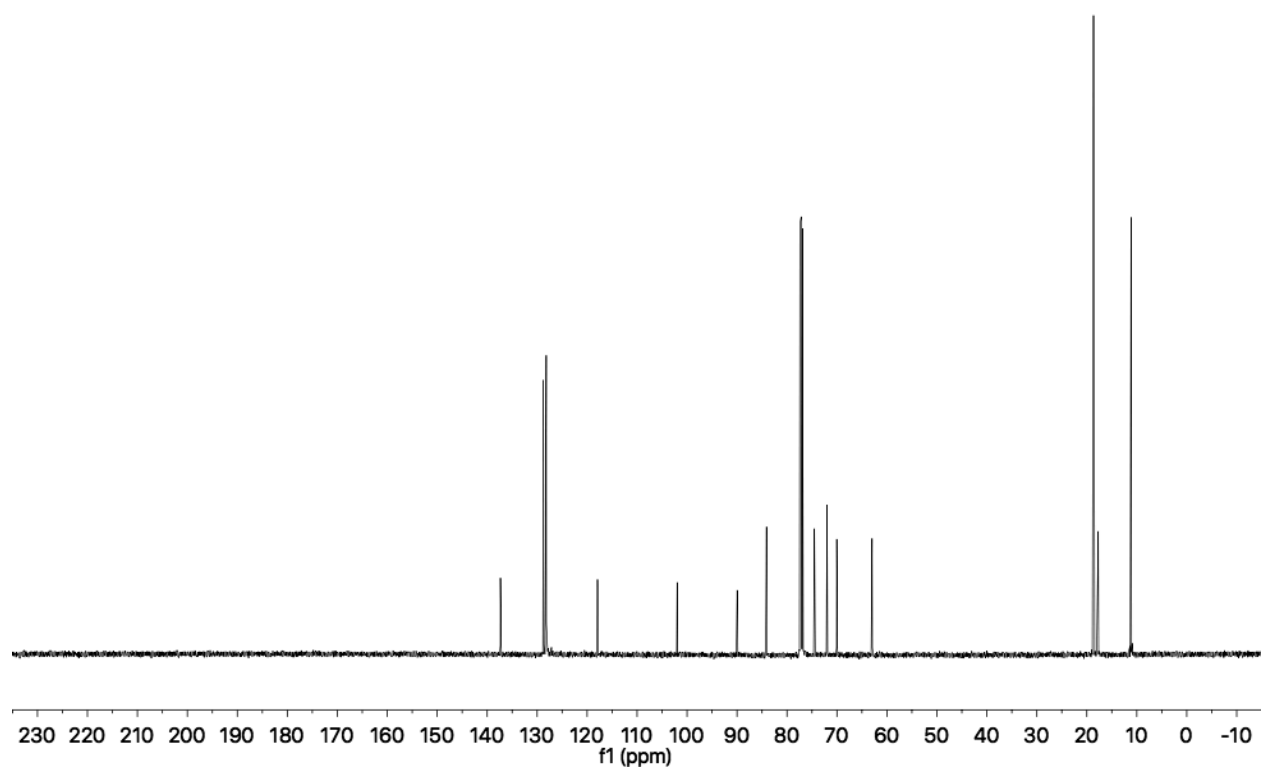
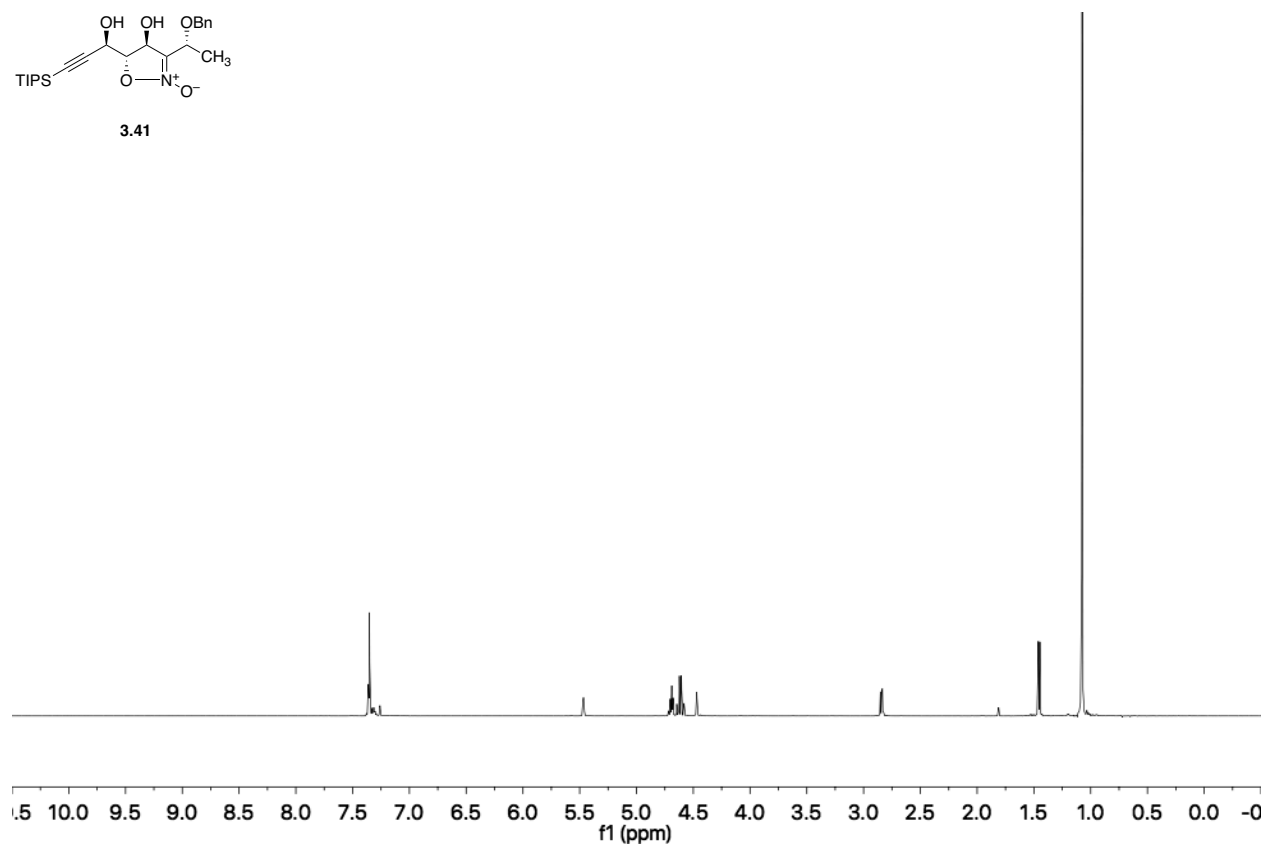
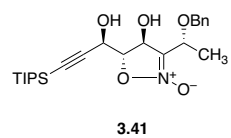


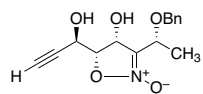


3.36

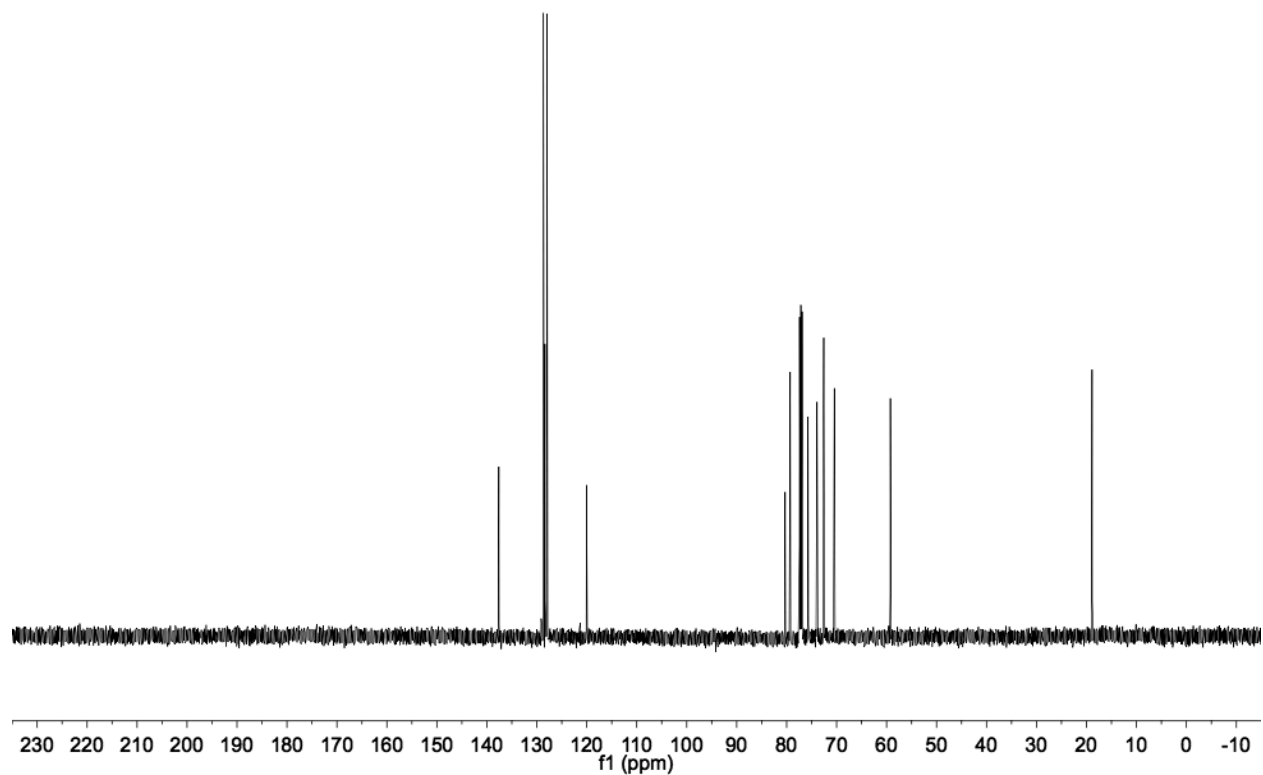
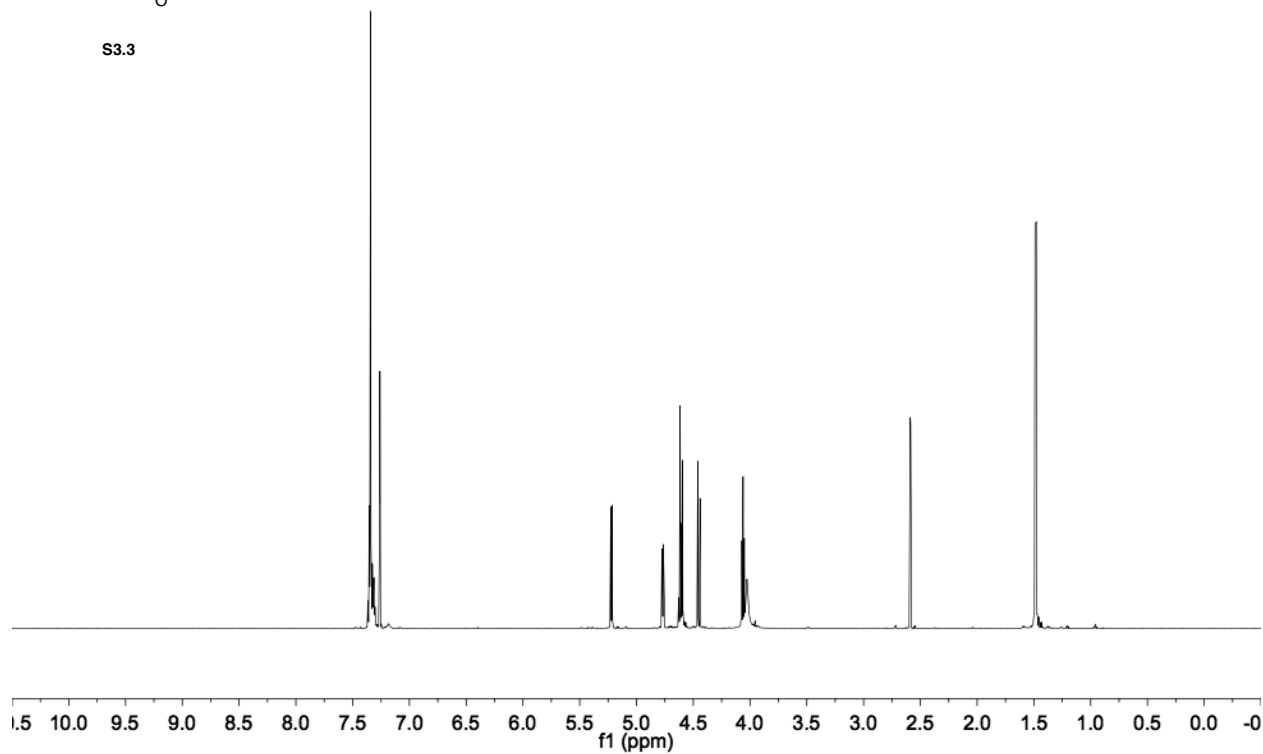


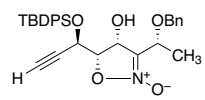




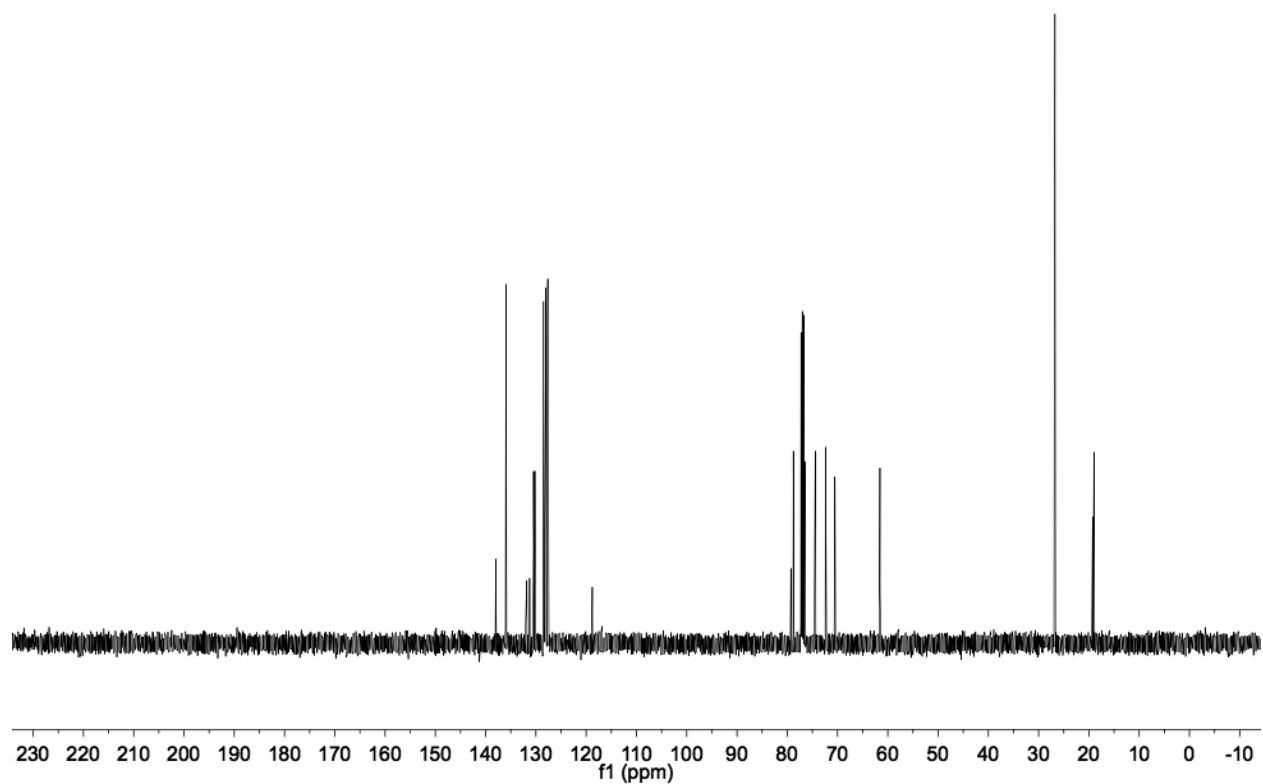
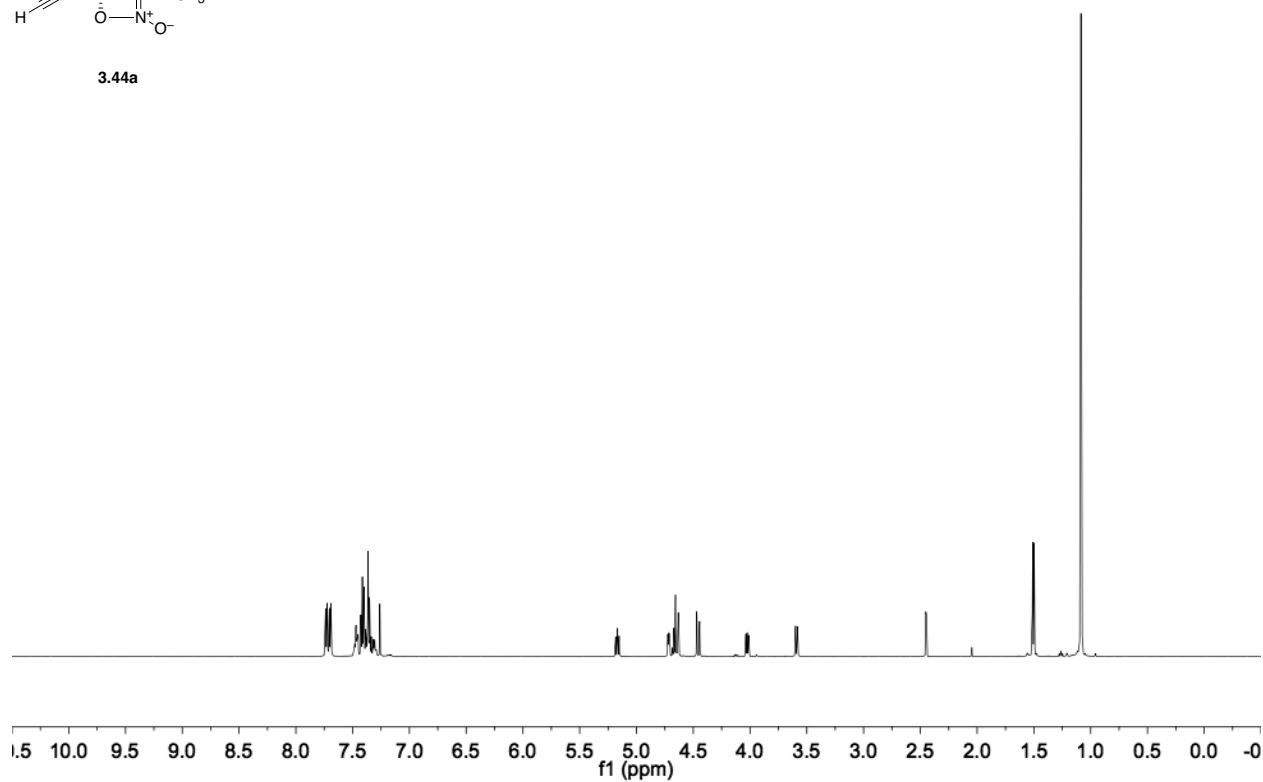


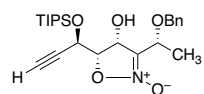
S3.3



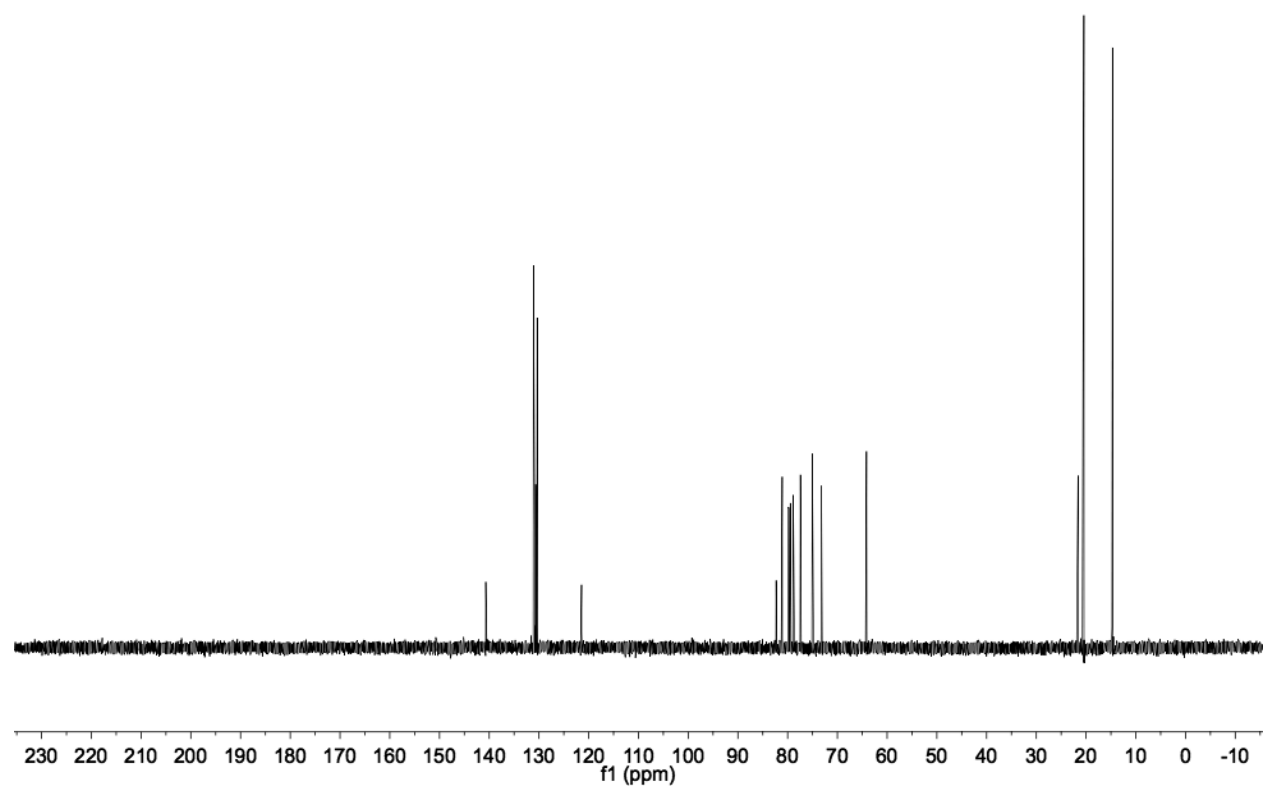
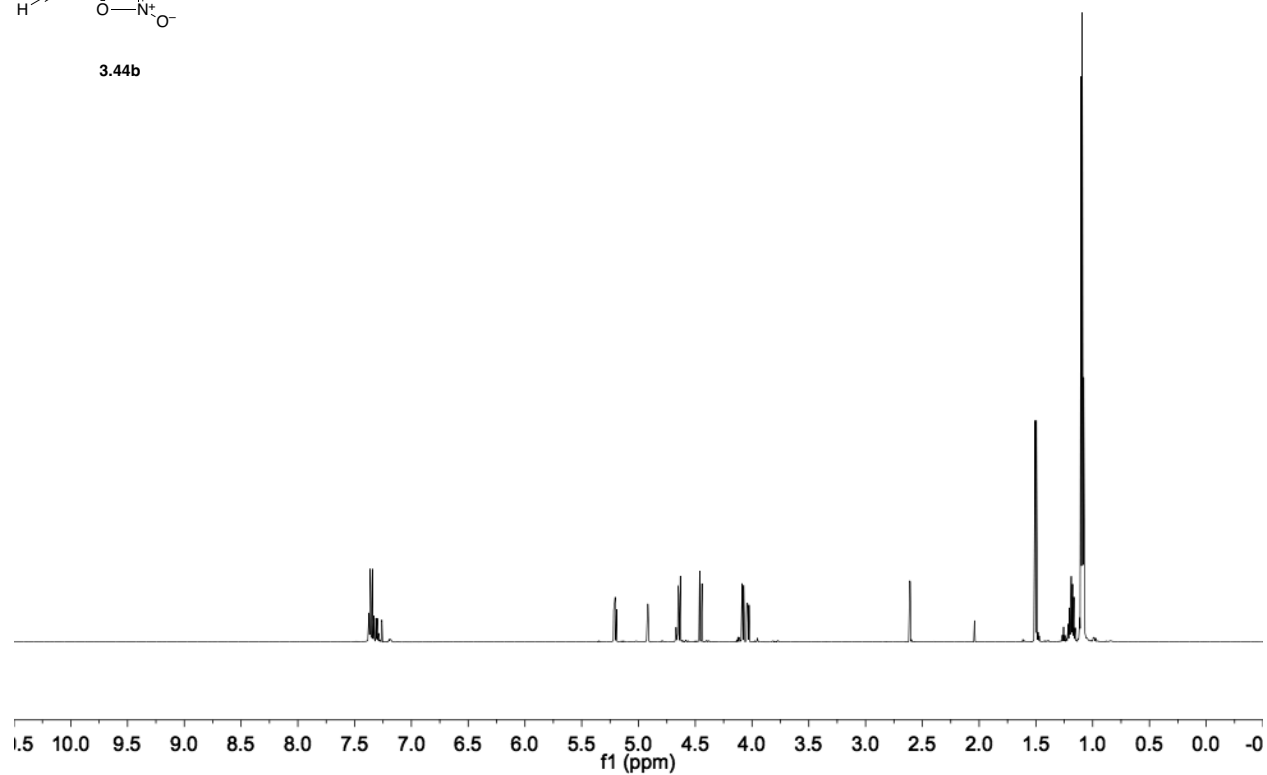


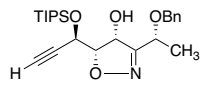
3.44a



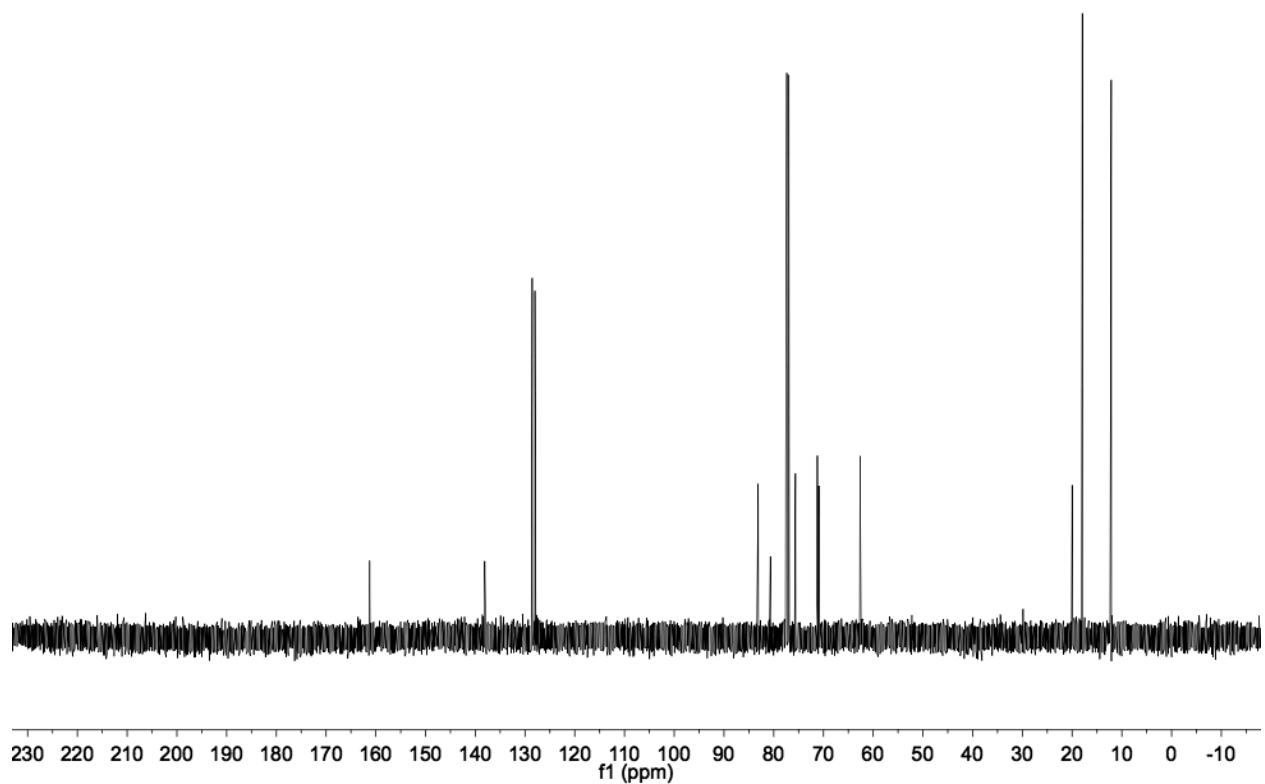
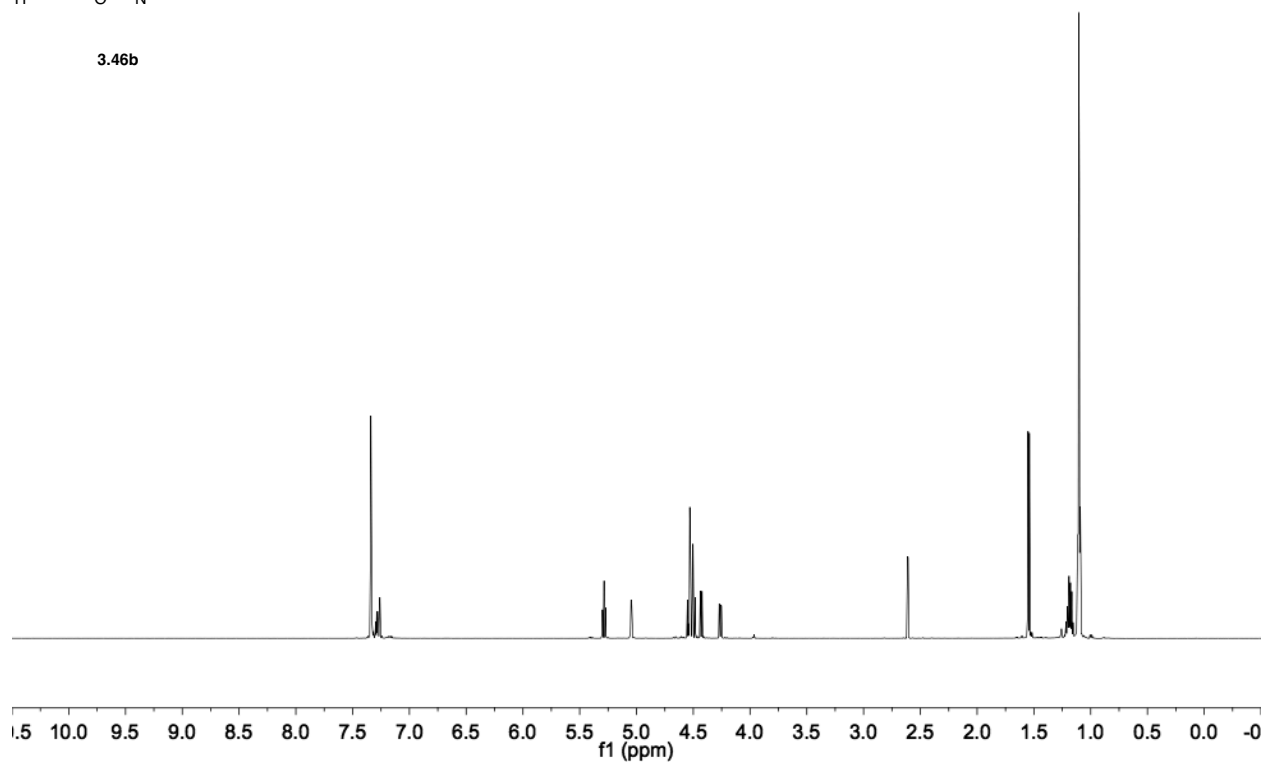


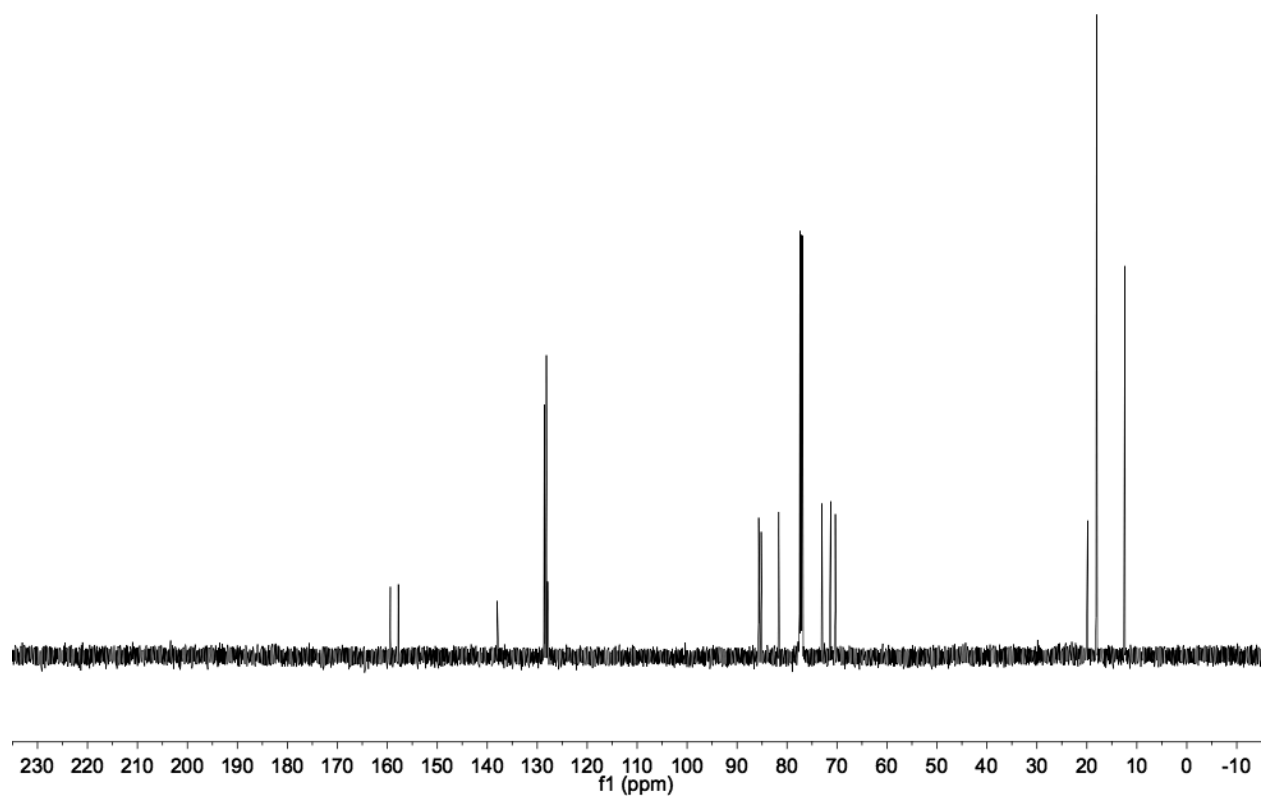
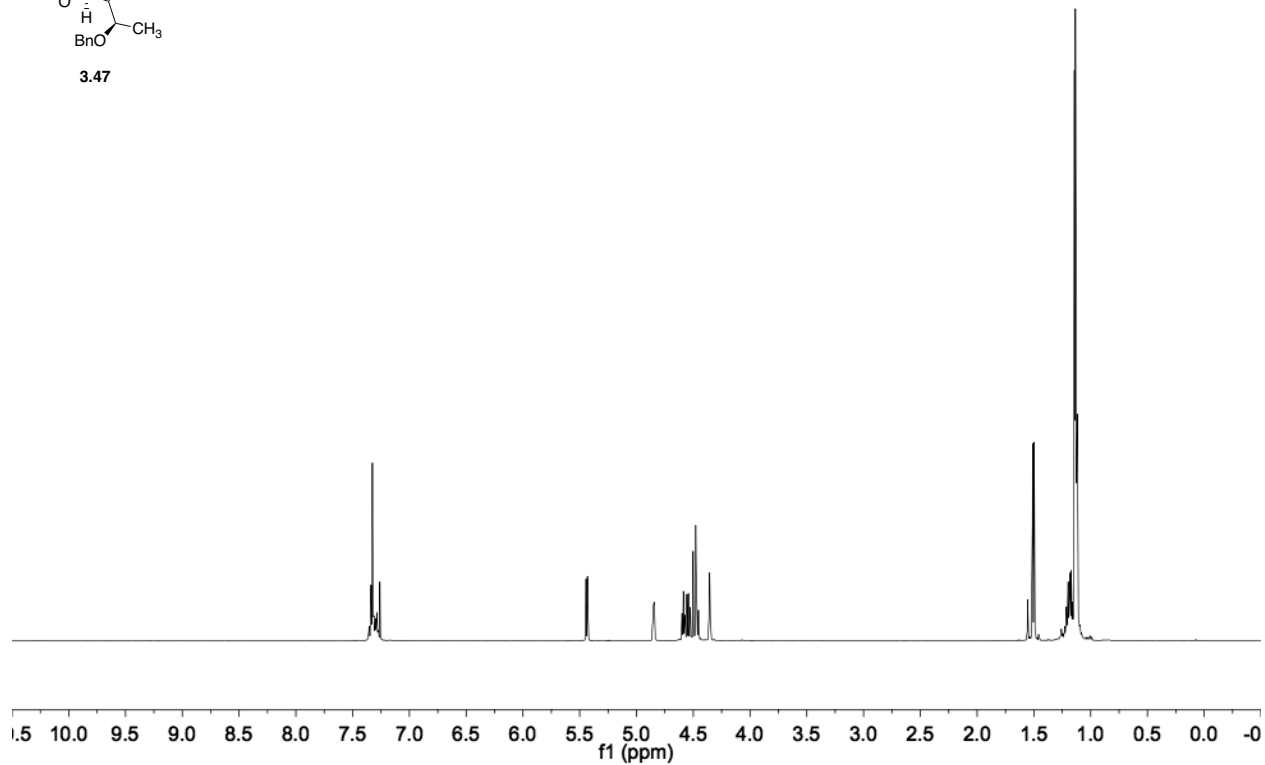
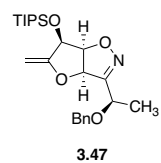
3.44b

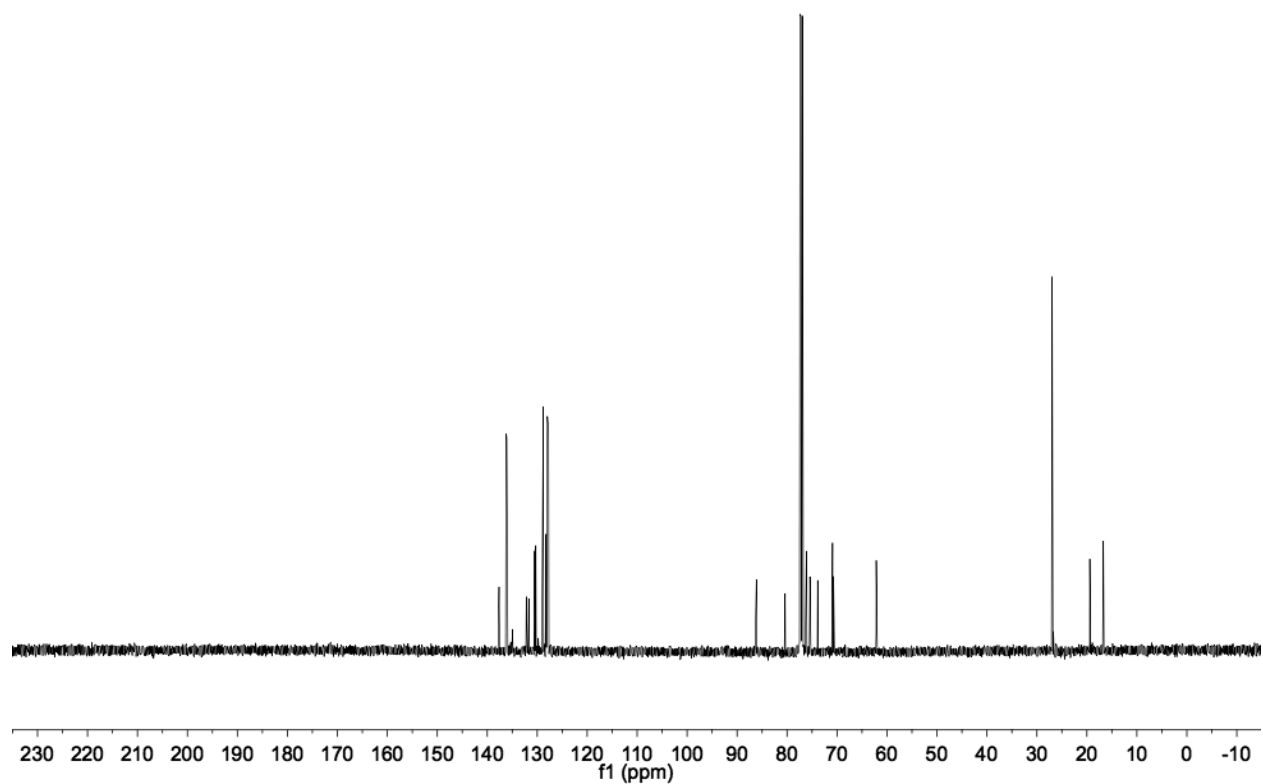
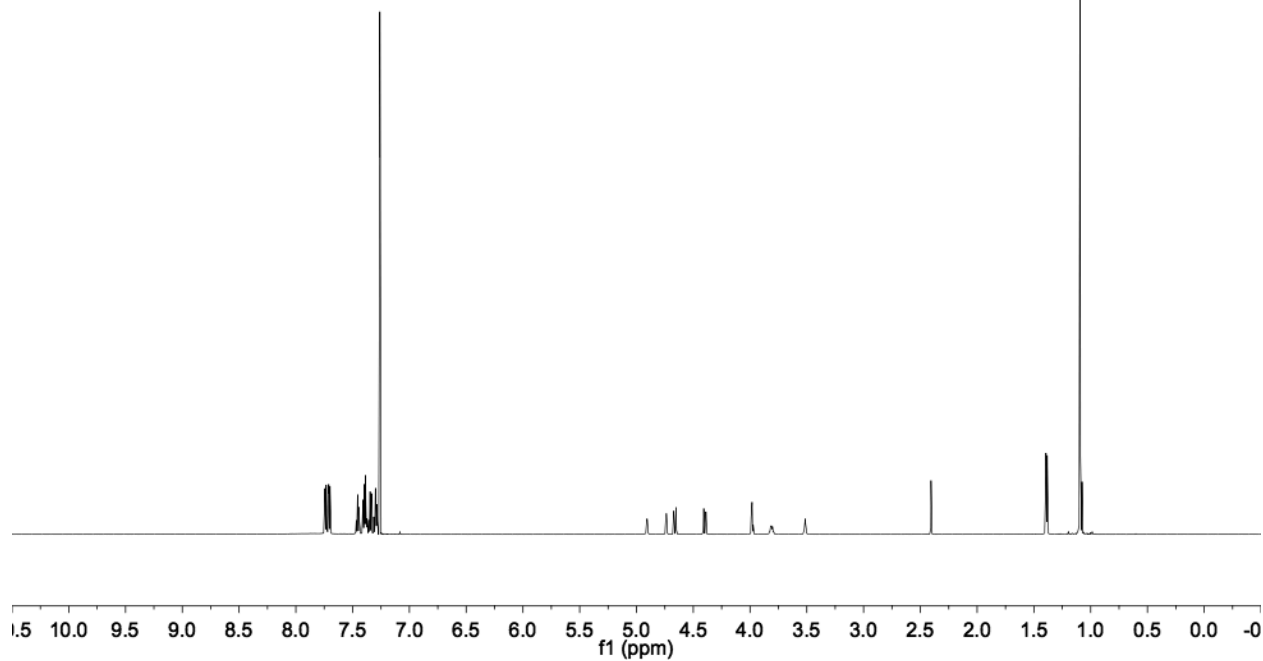
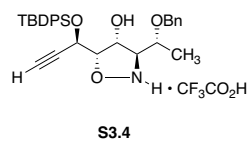


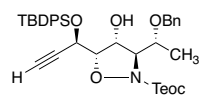


3.46b

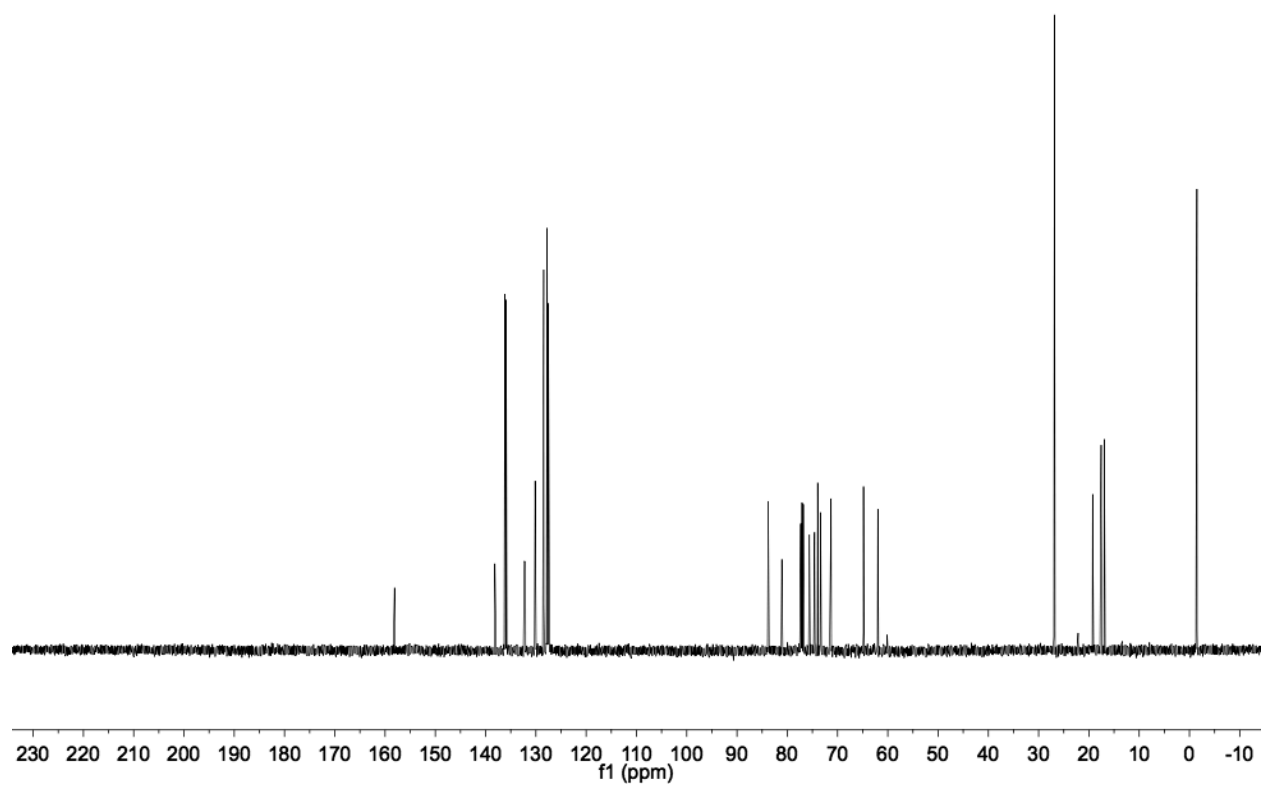
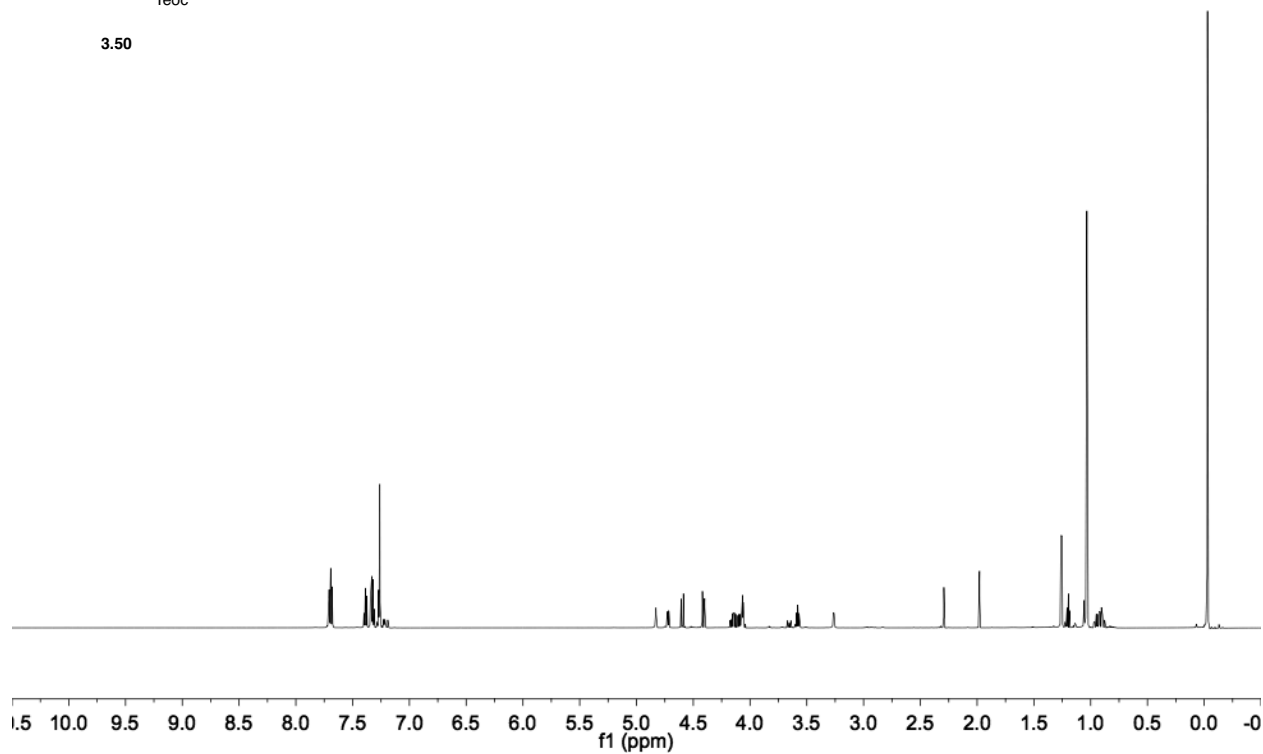


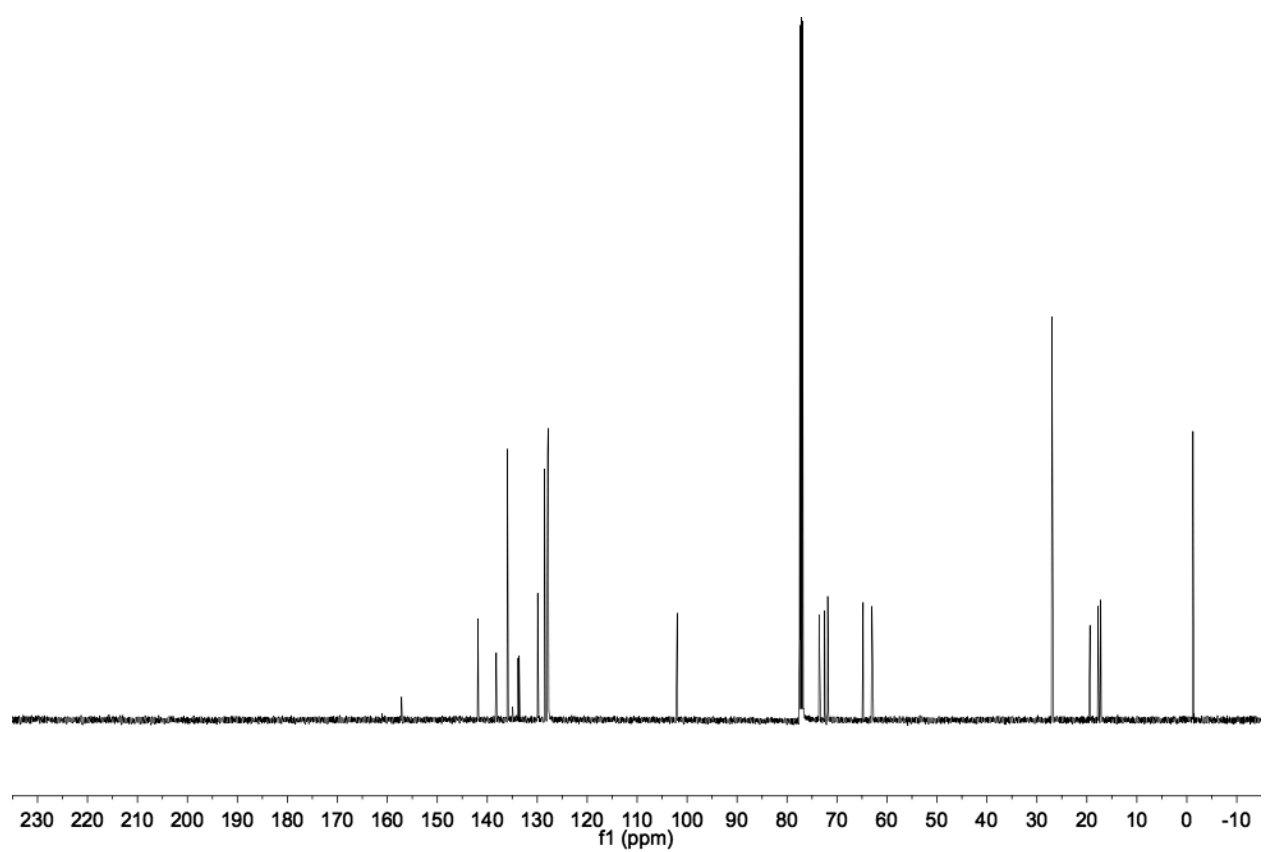
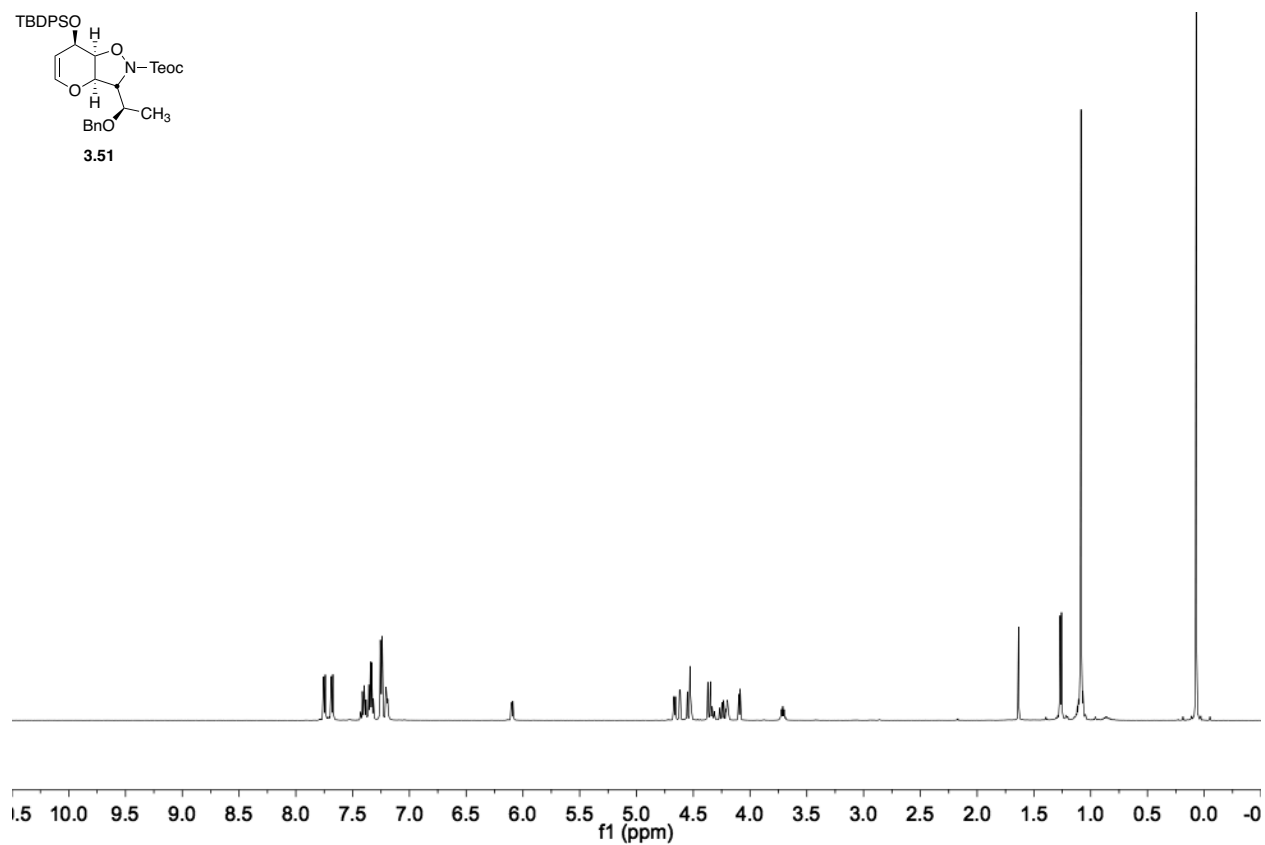
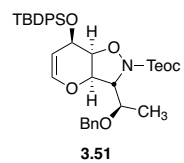


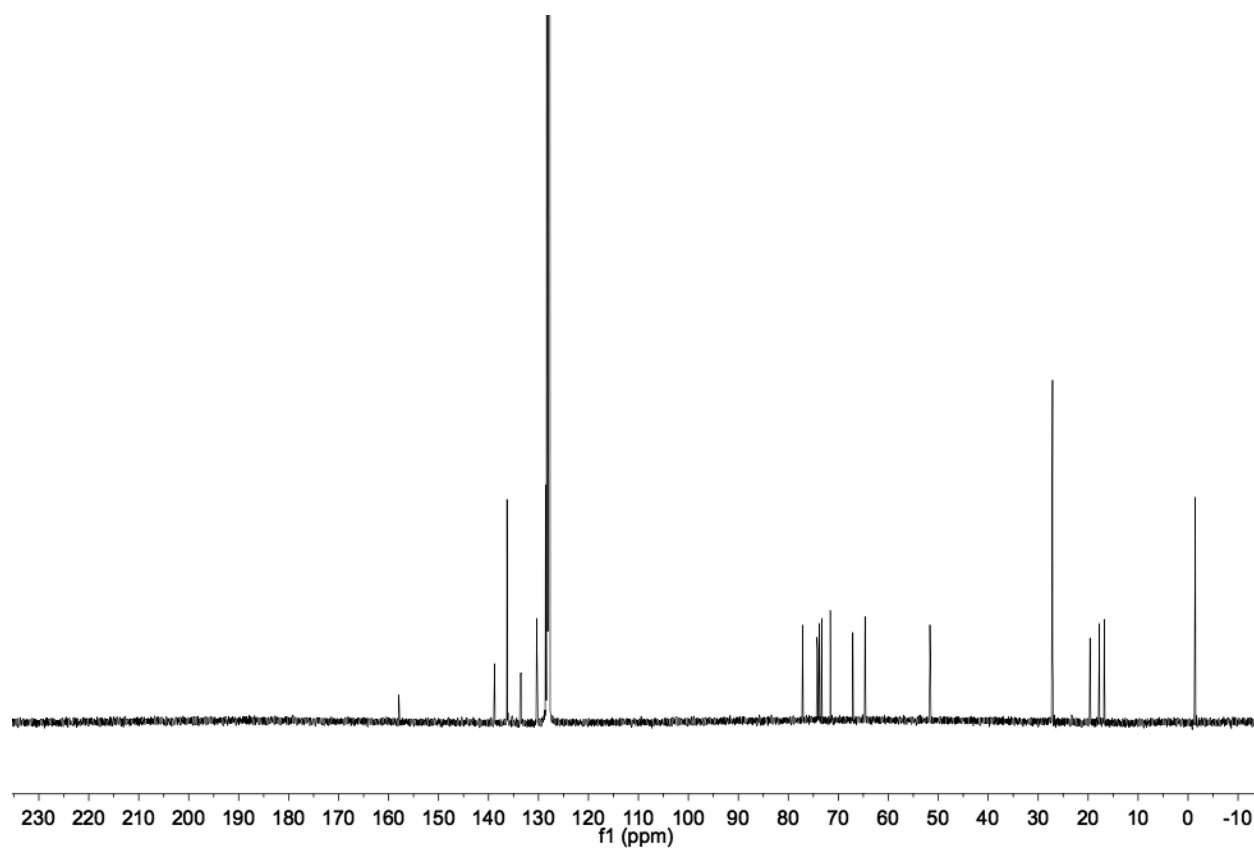
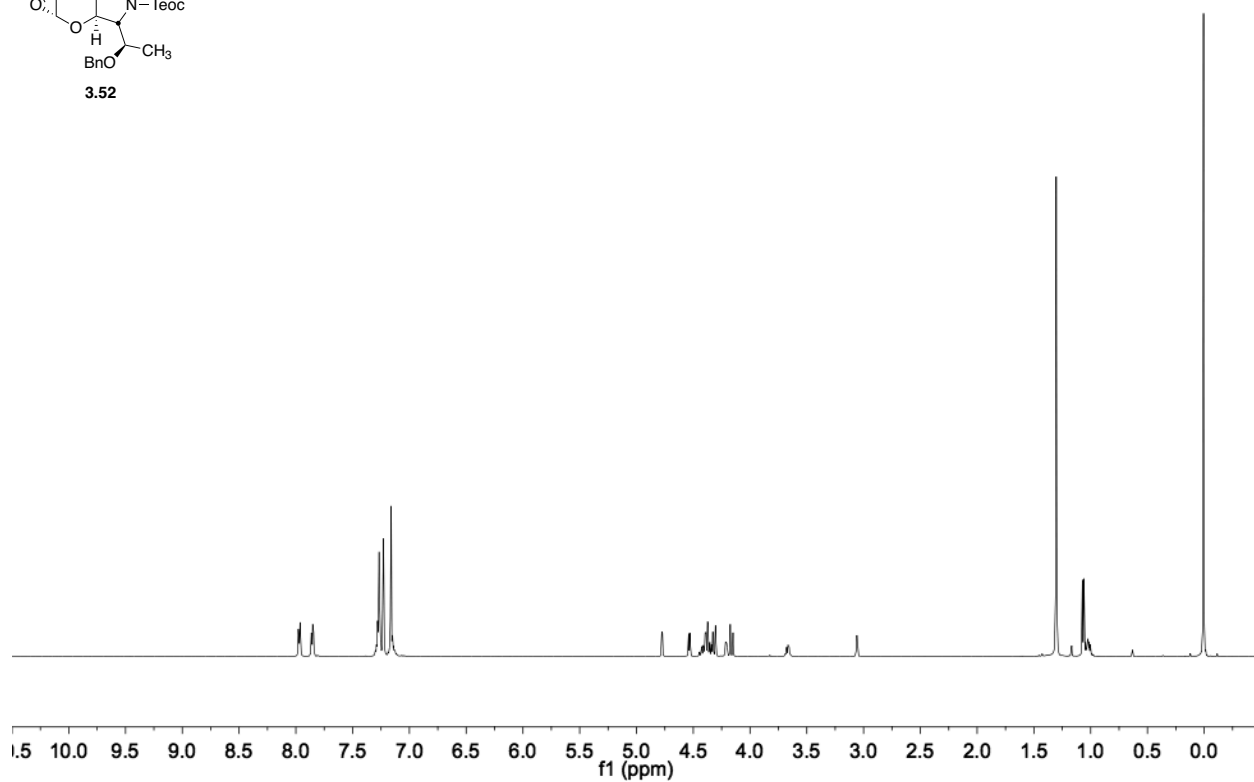
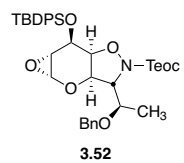


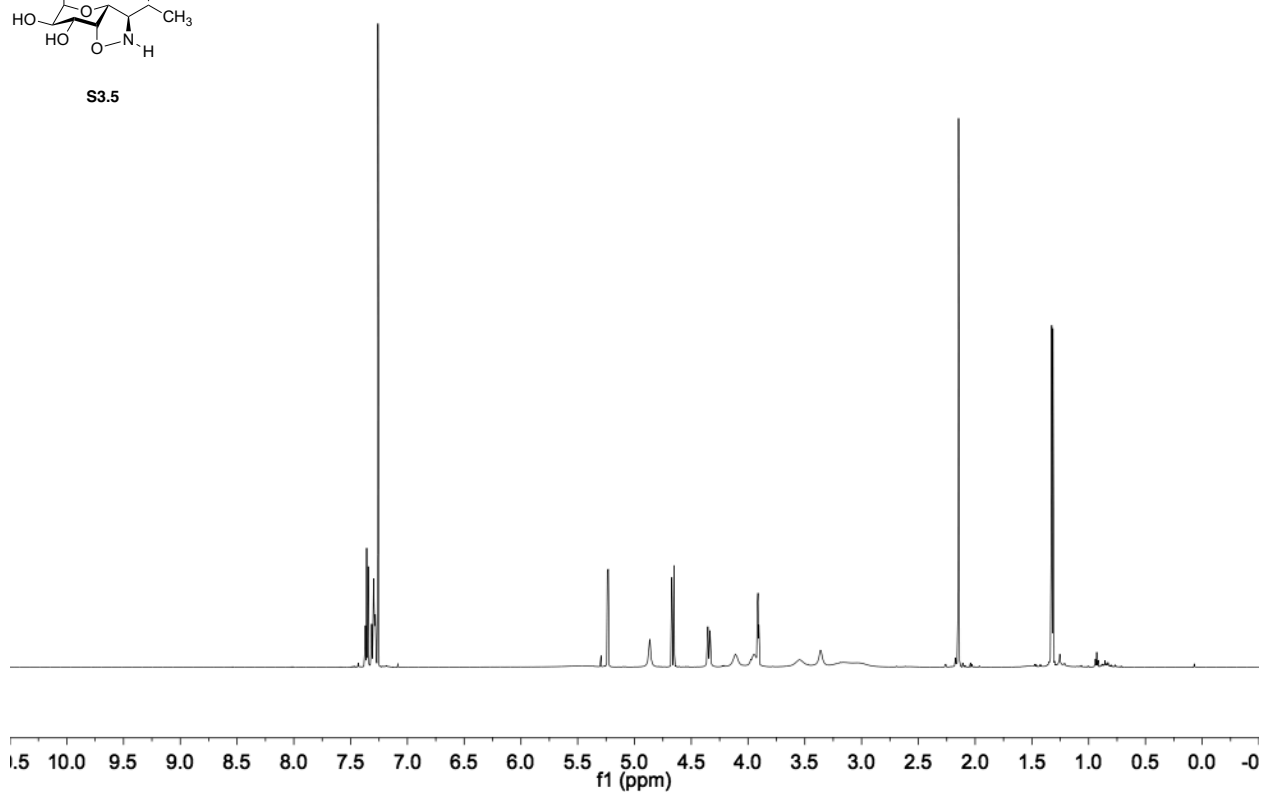
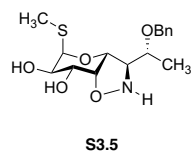
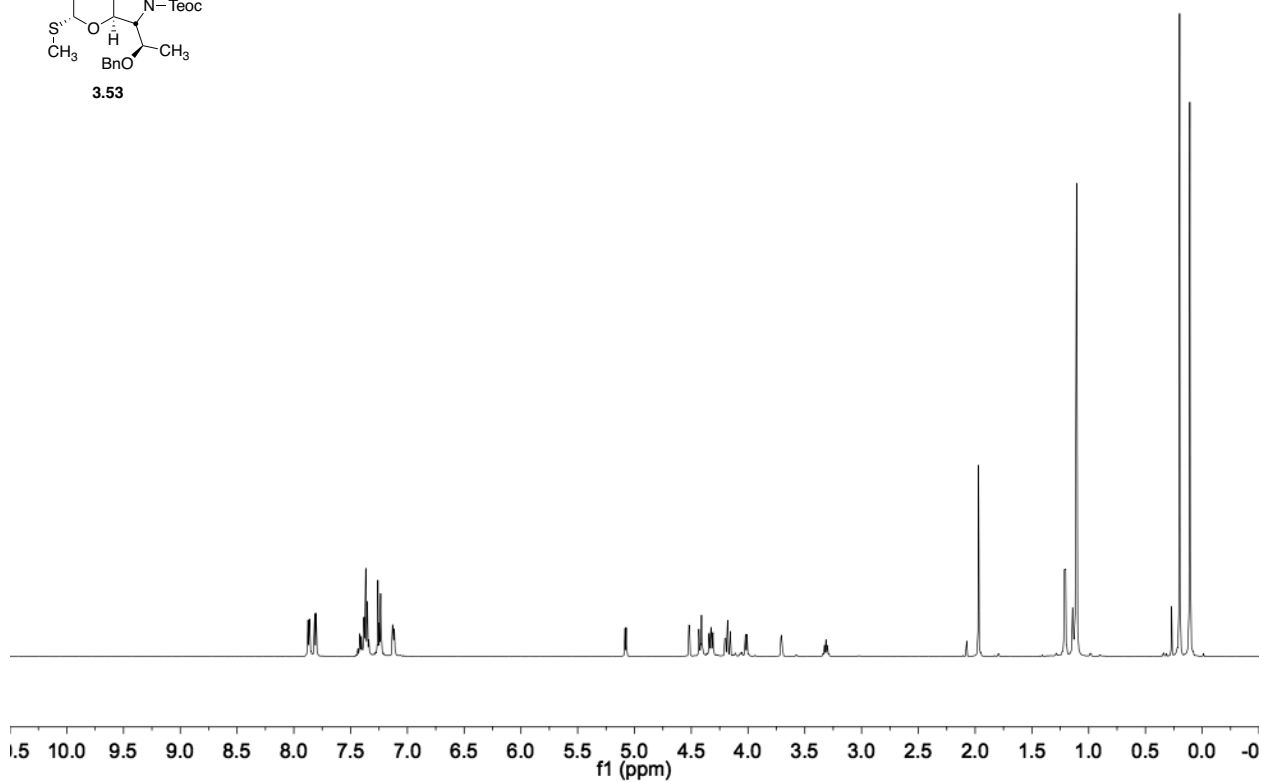
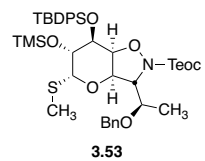


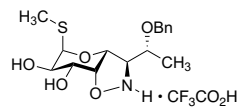
3.50



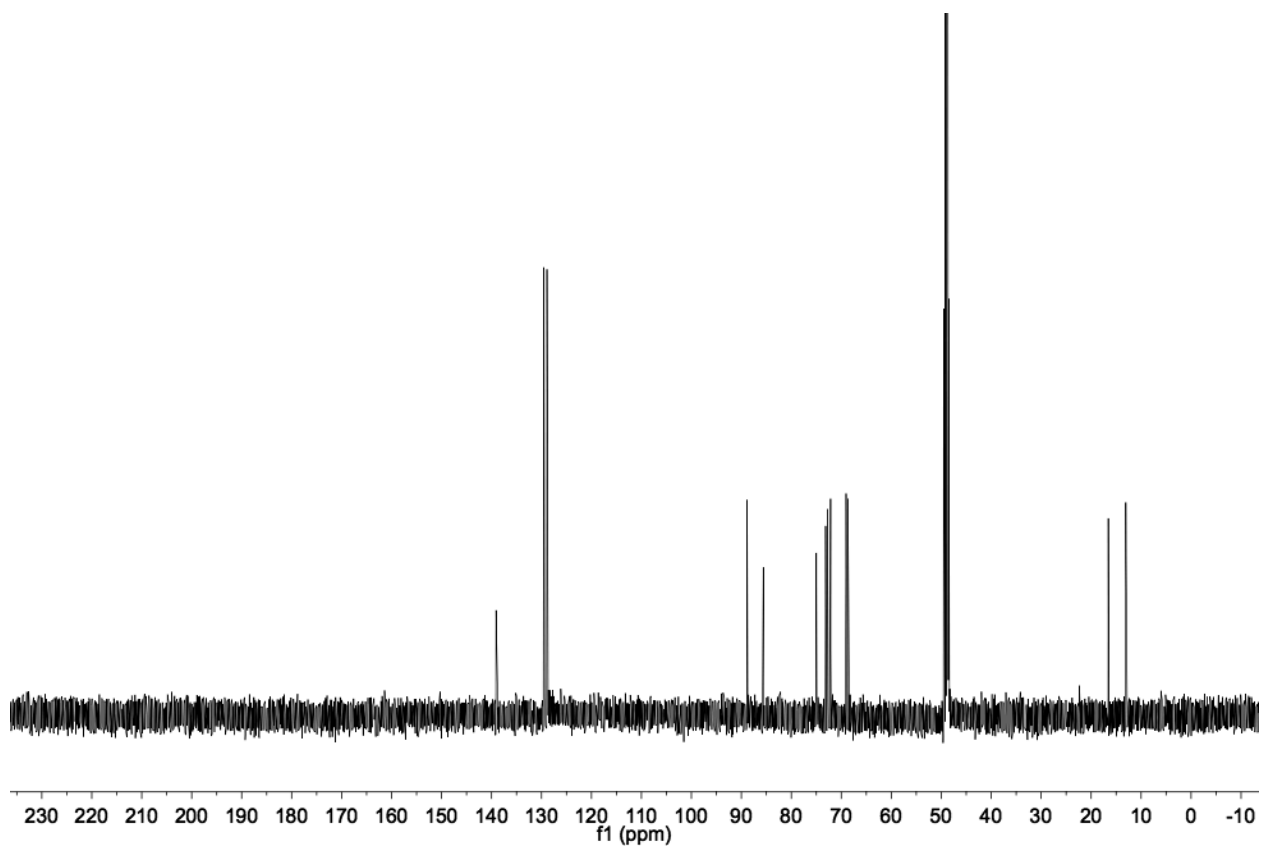
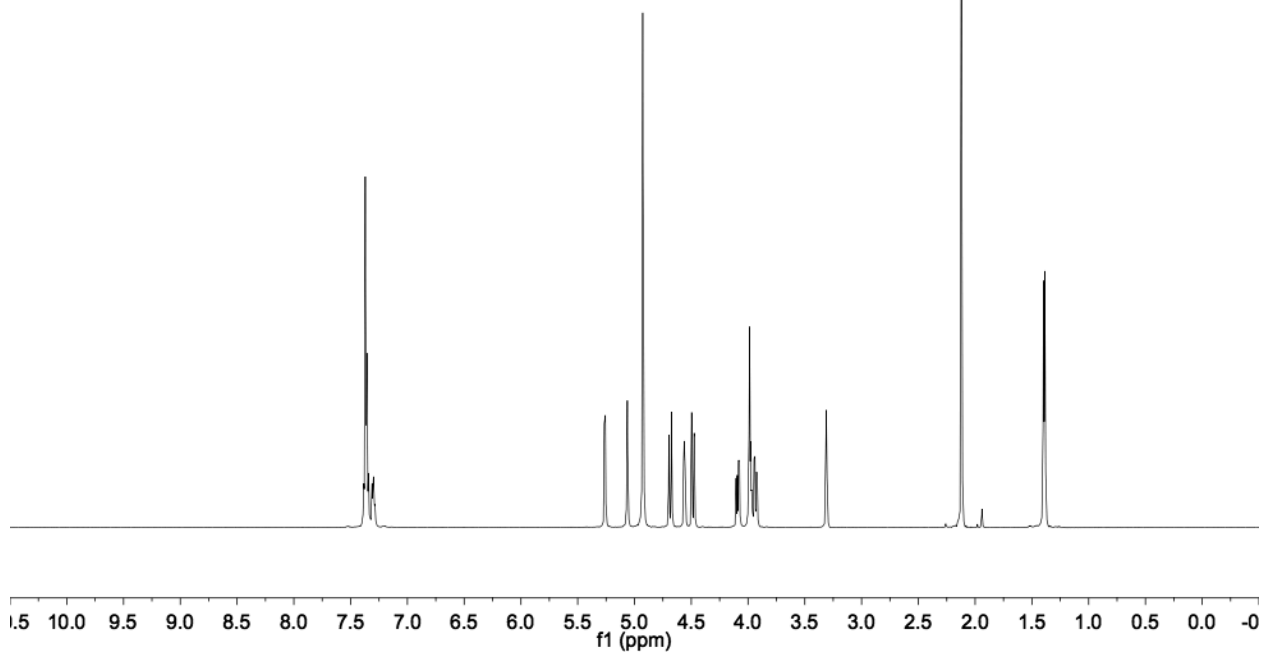


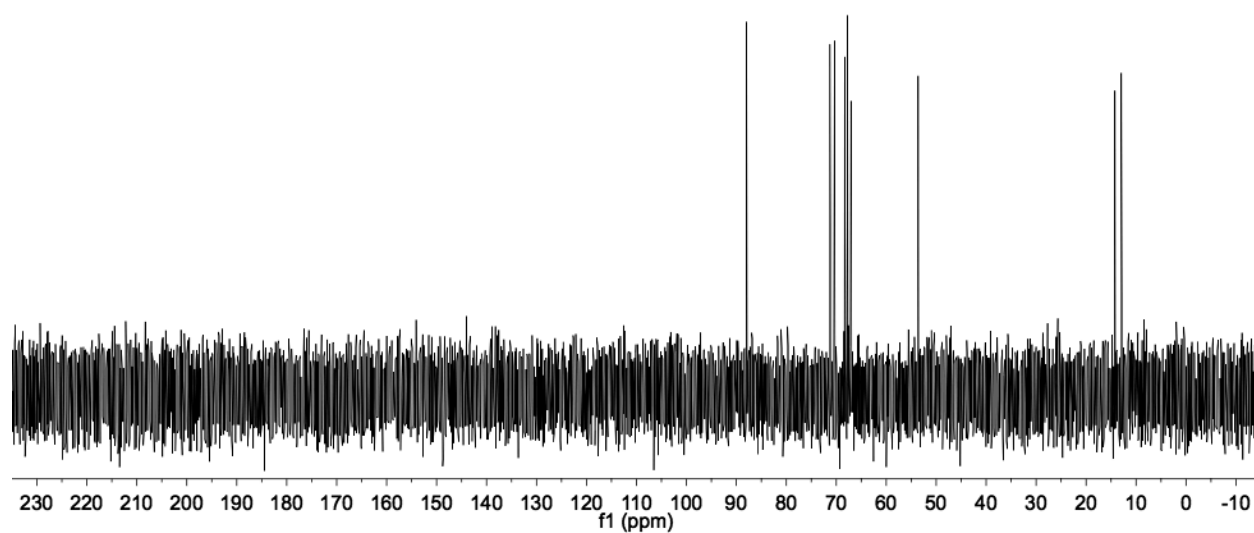
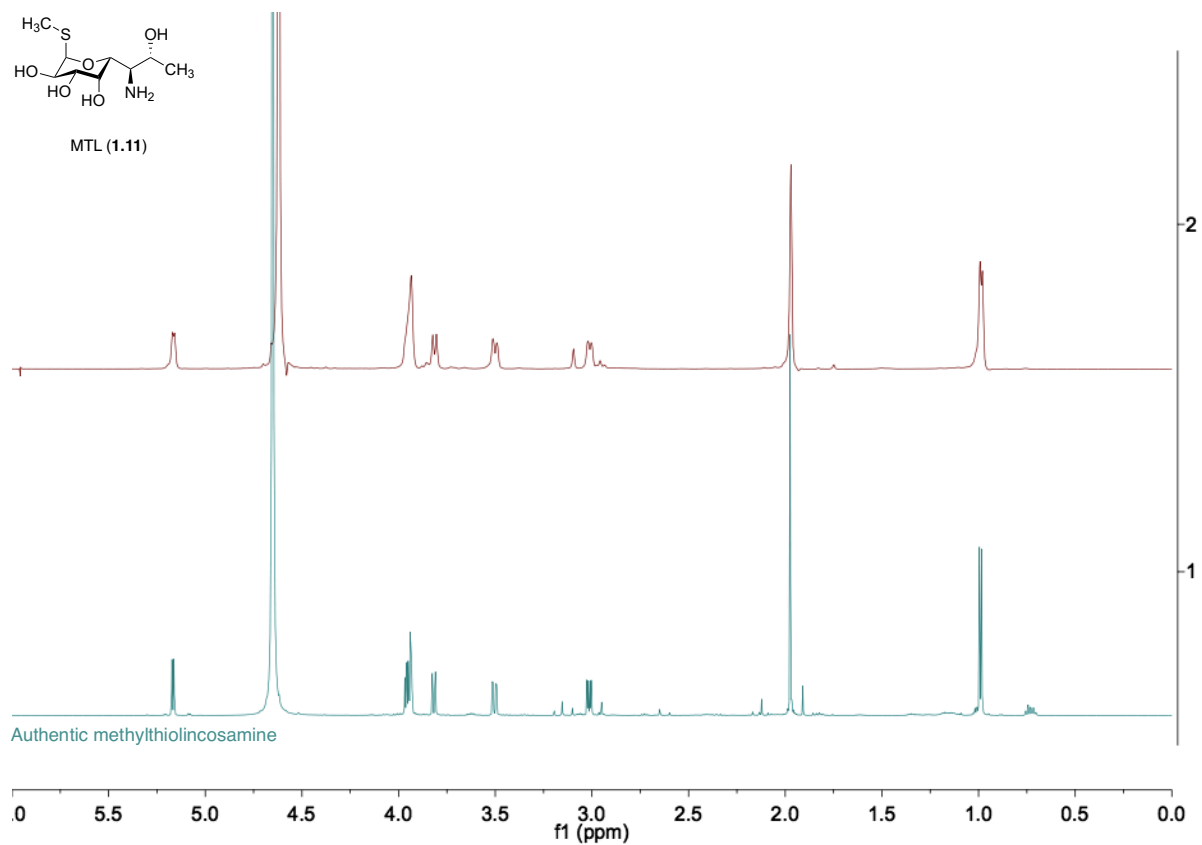
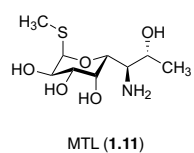


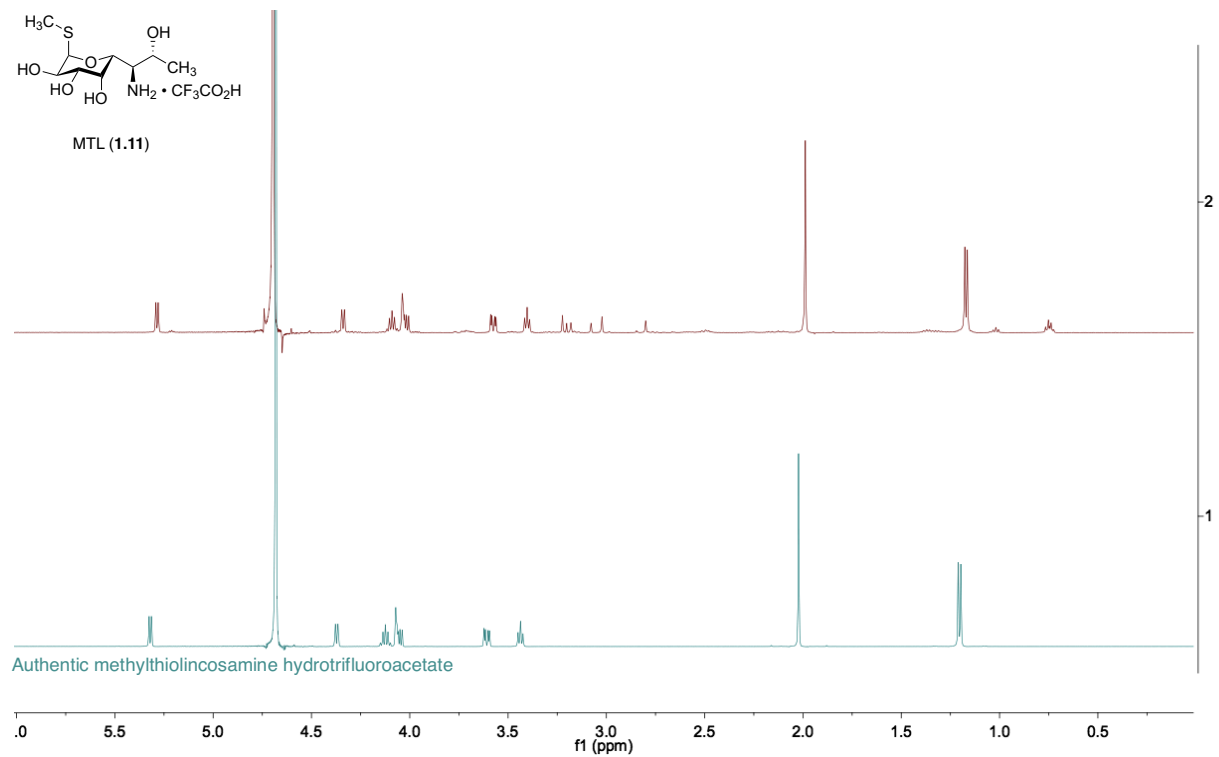
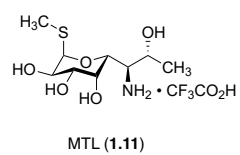


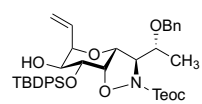


S3.5

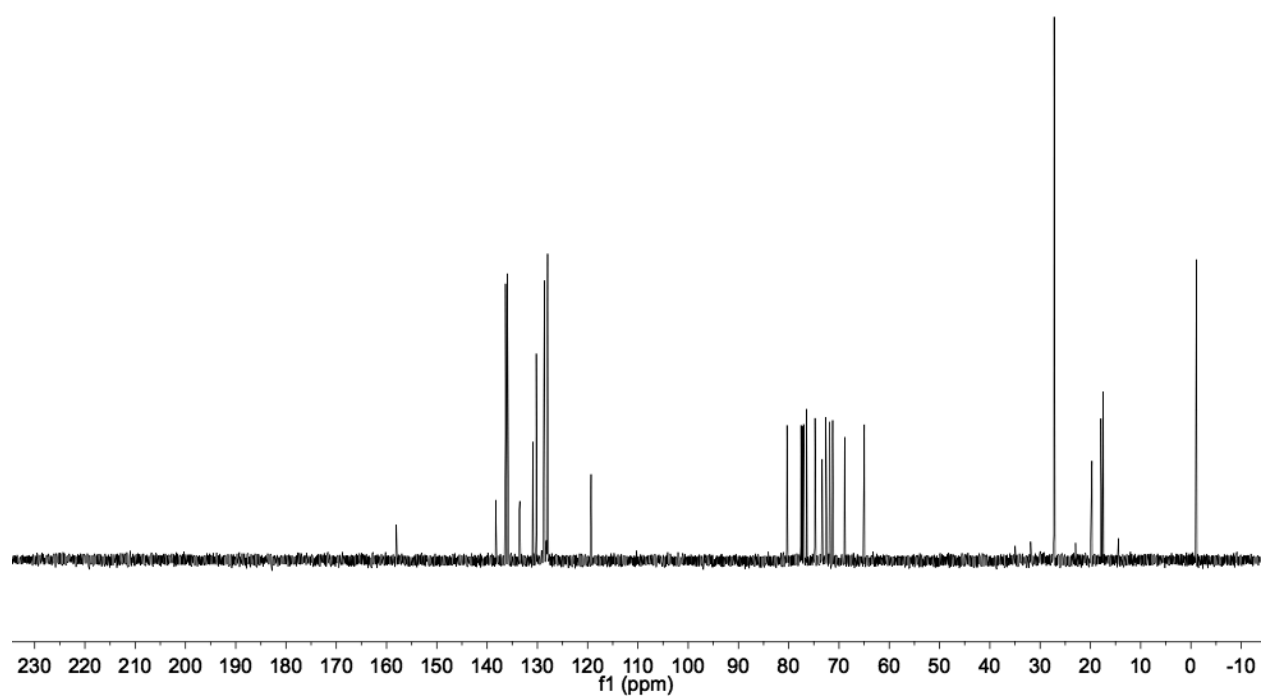
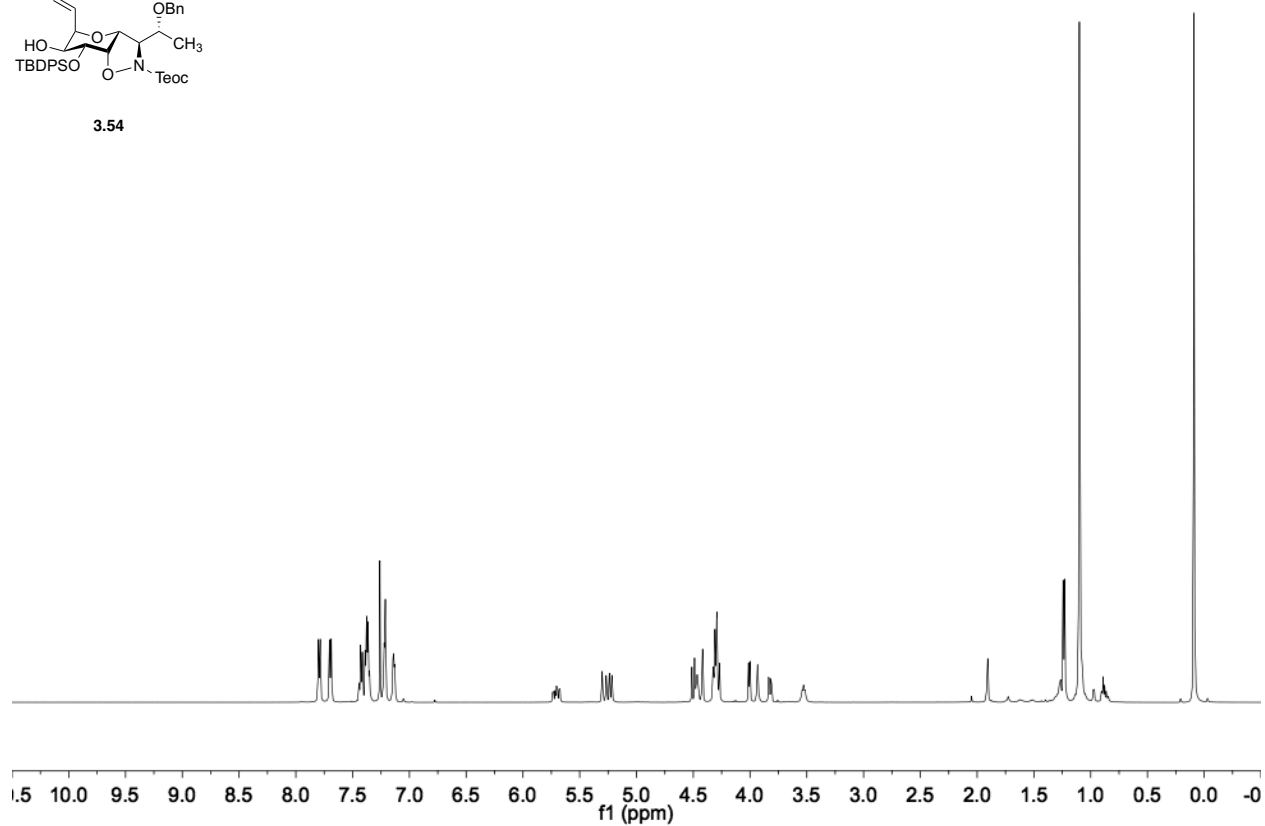


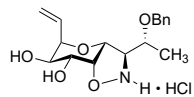




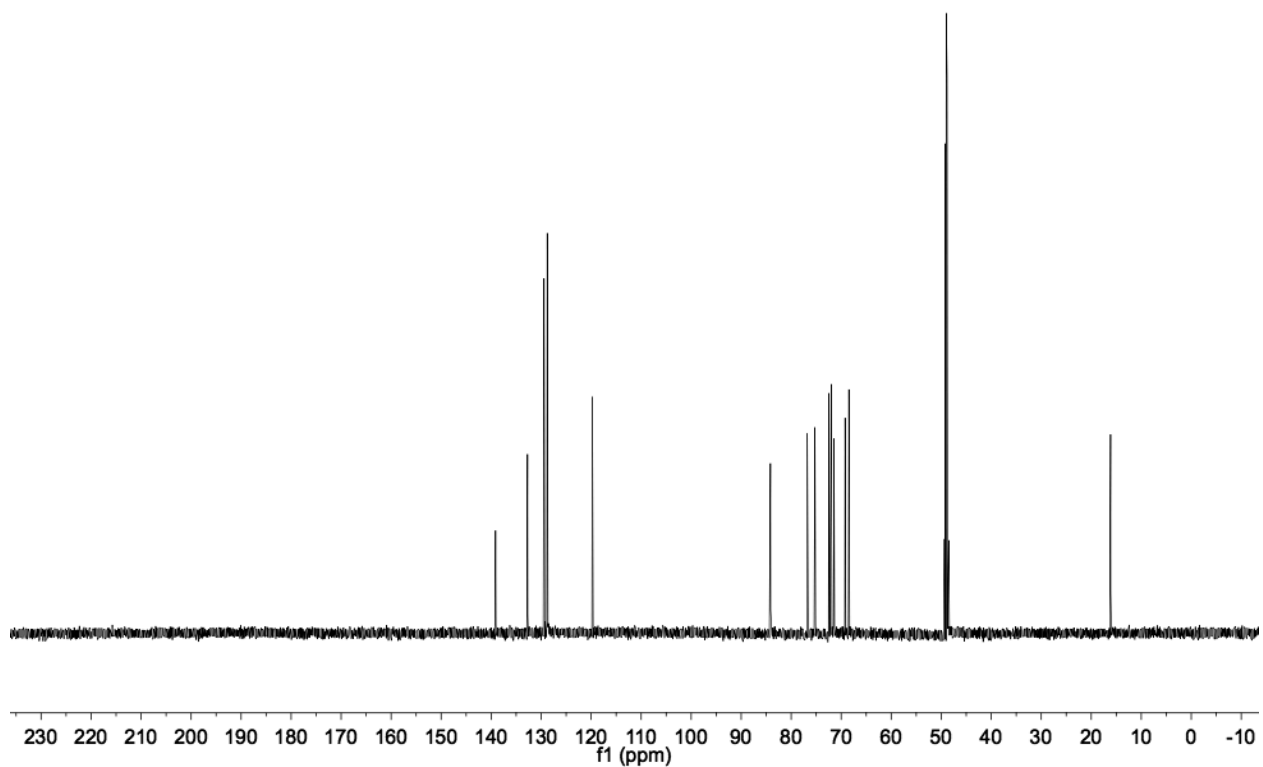
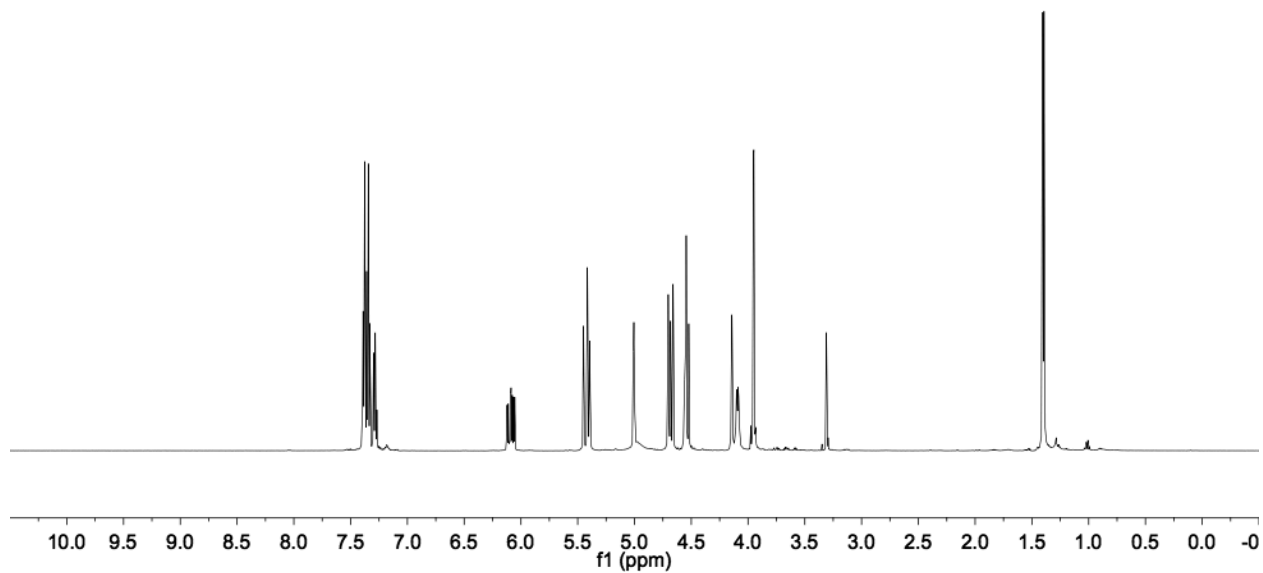


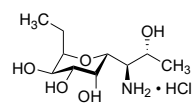
3.54



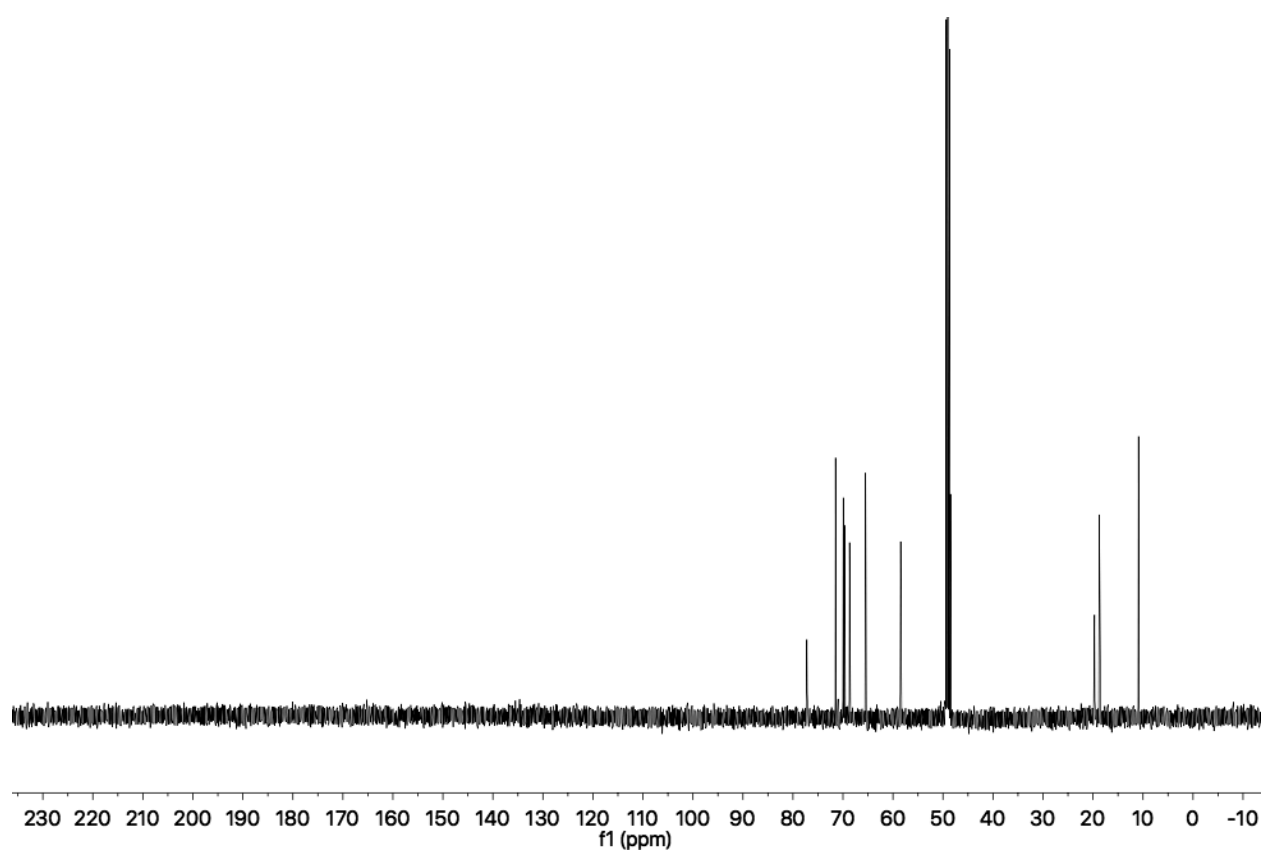
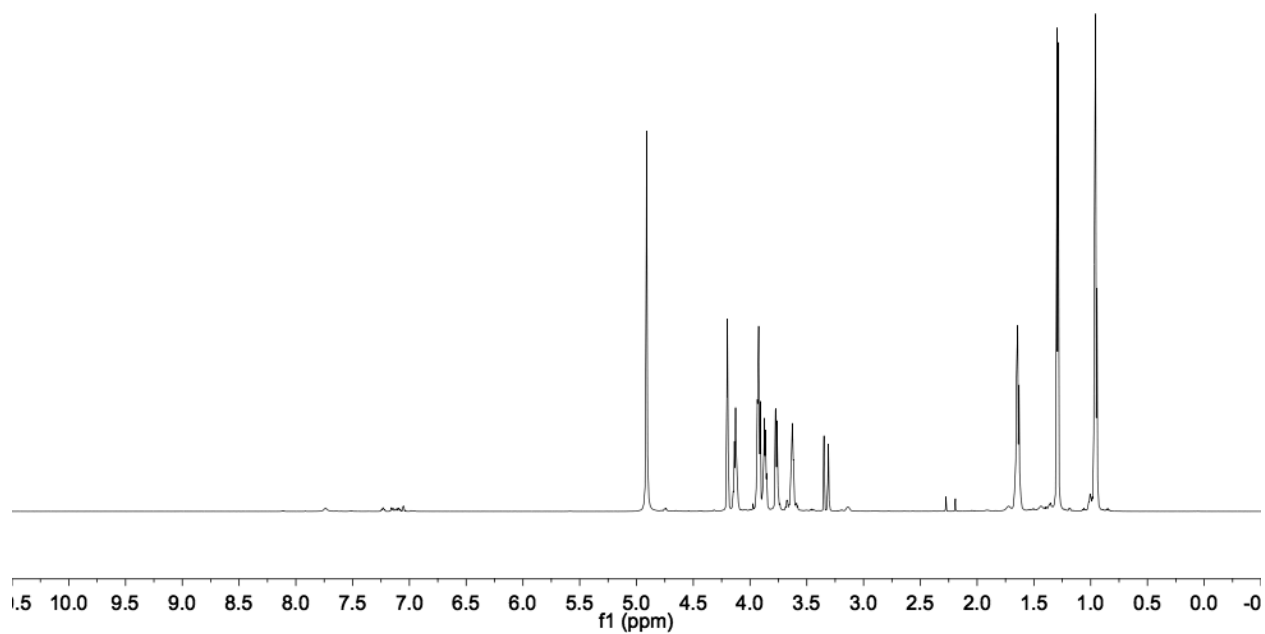


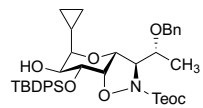
3.55



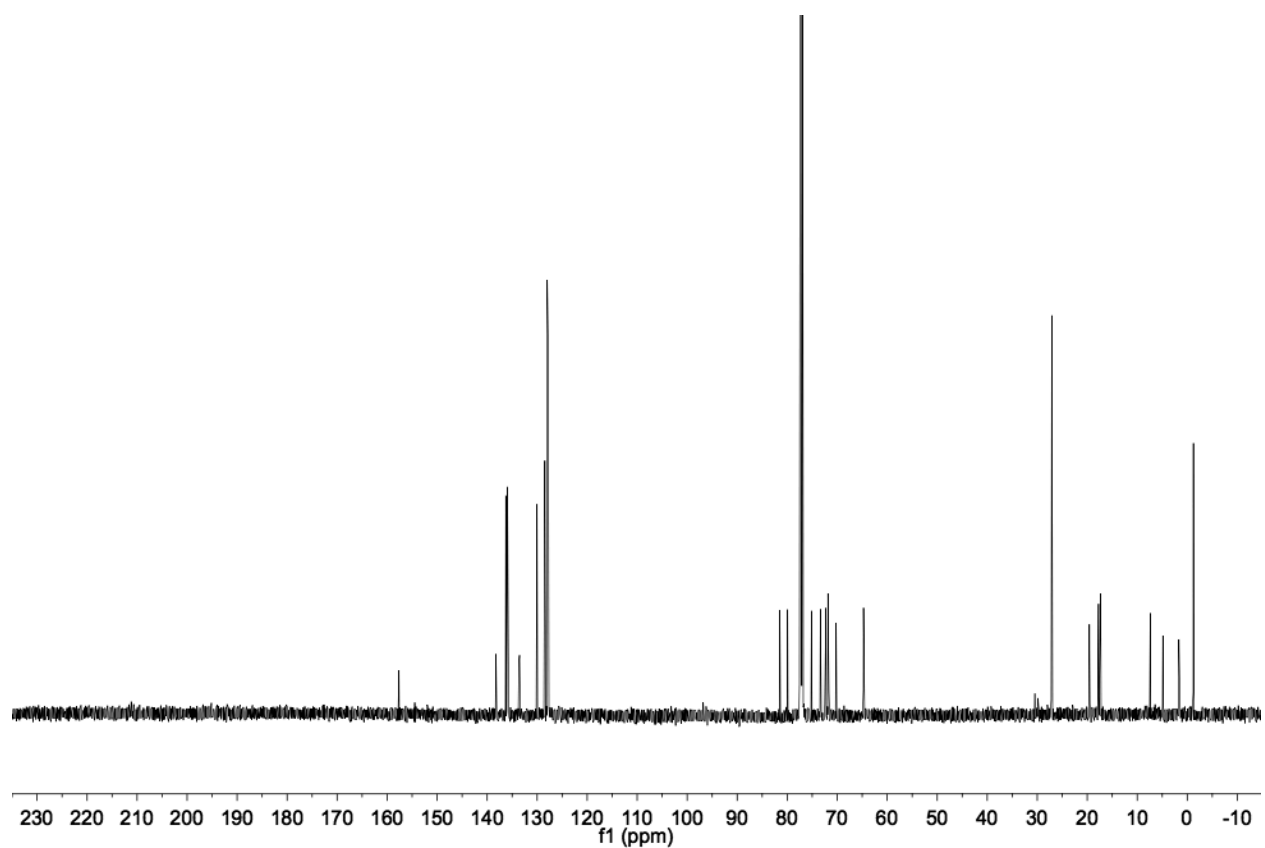
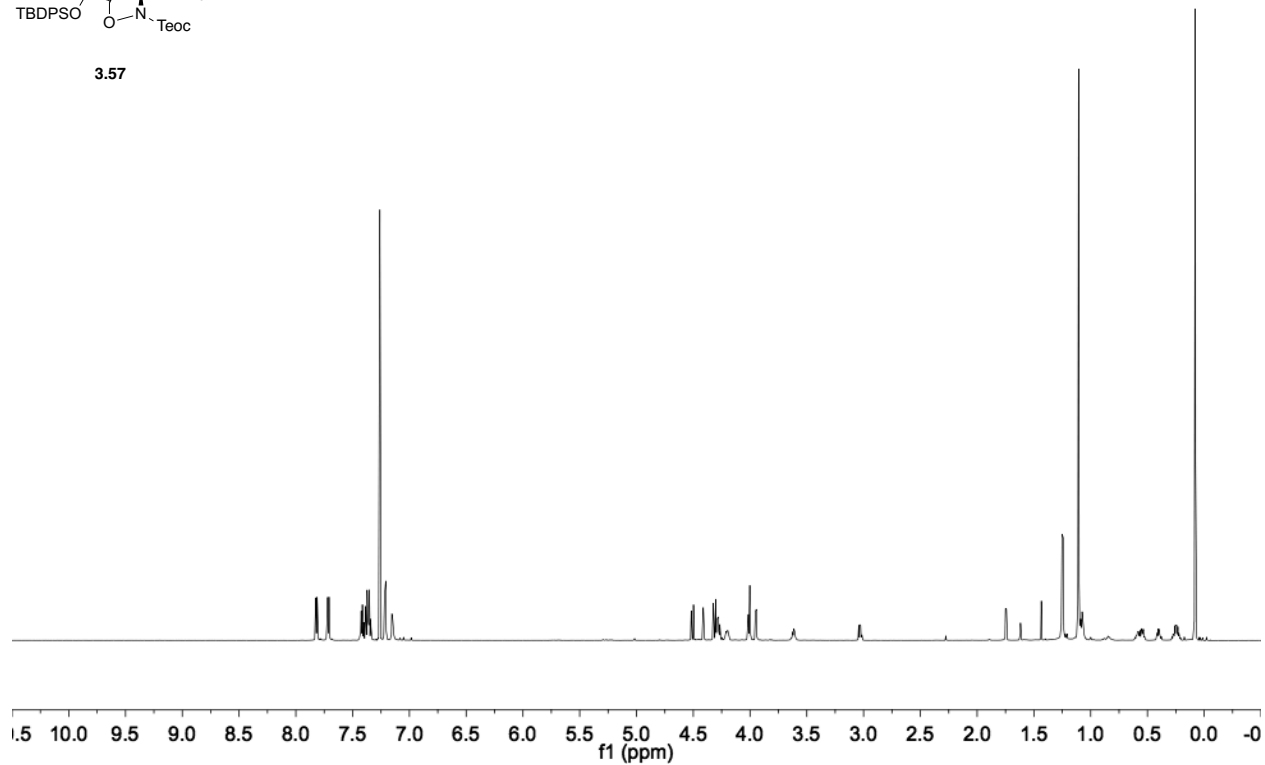


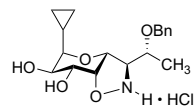
3.56



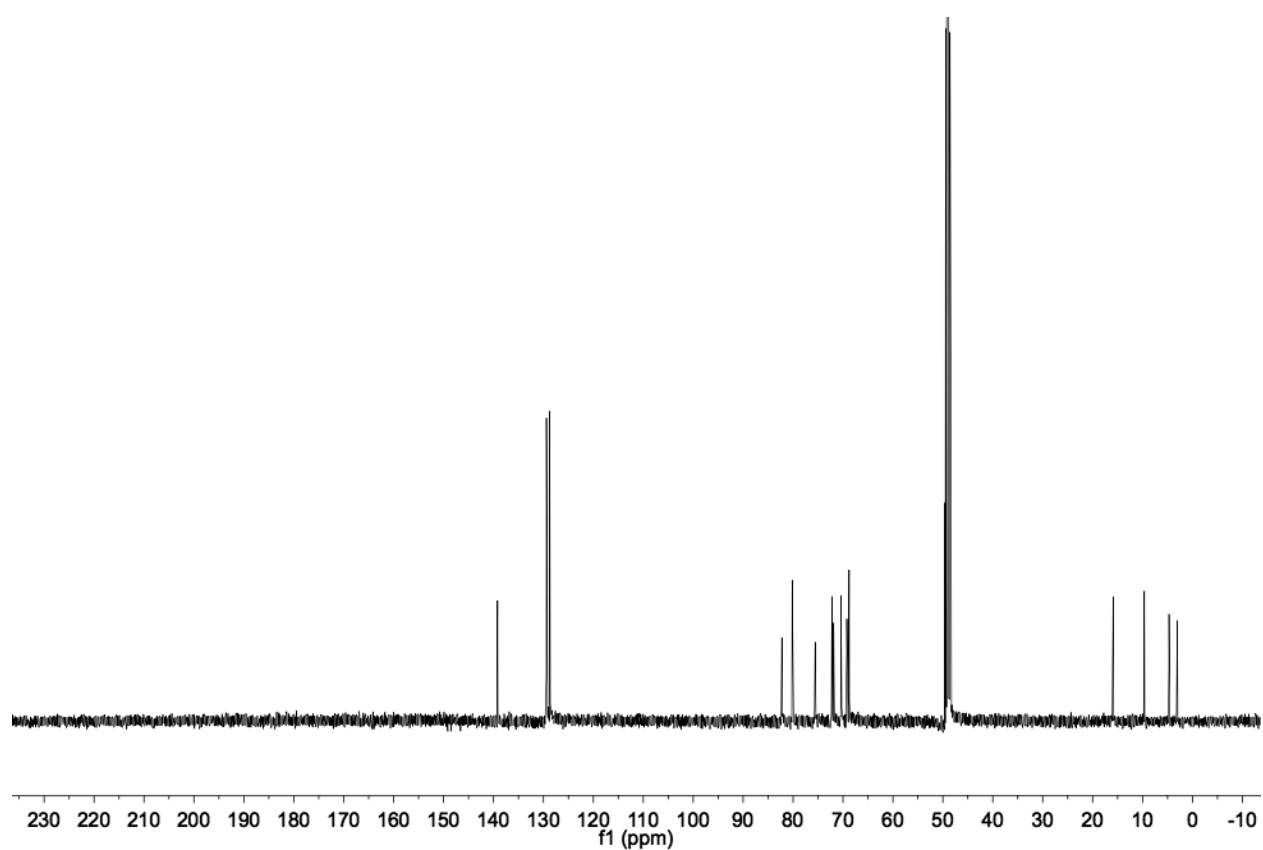
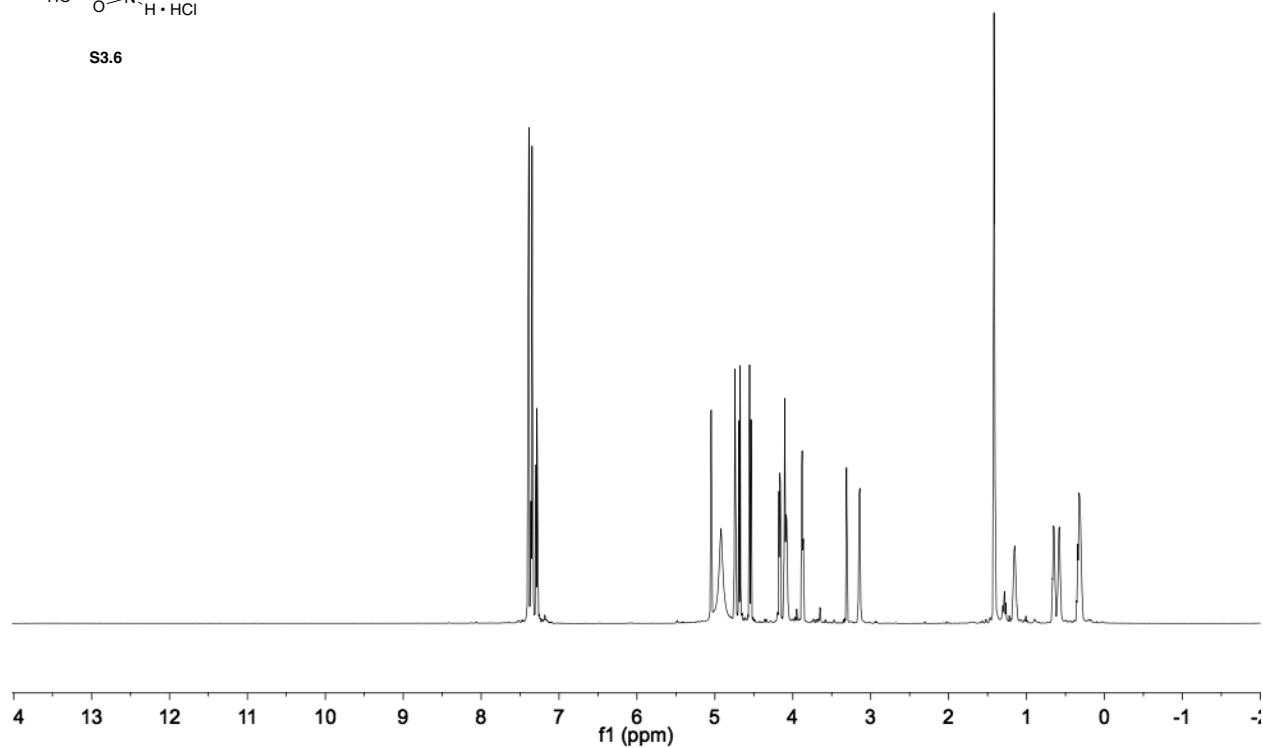


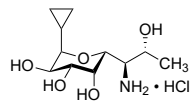
3.57



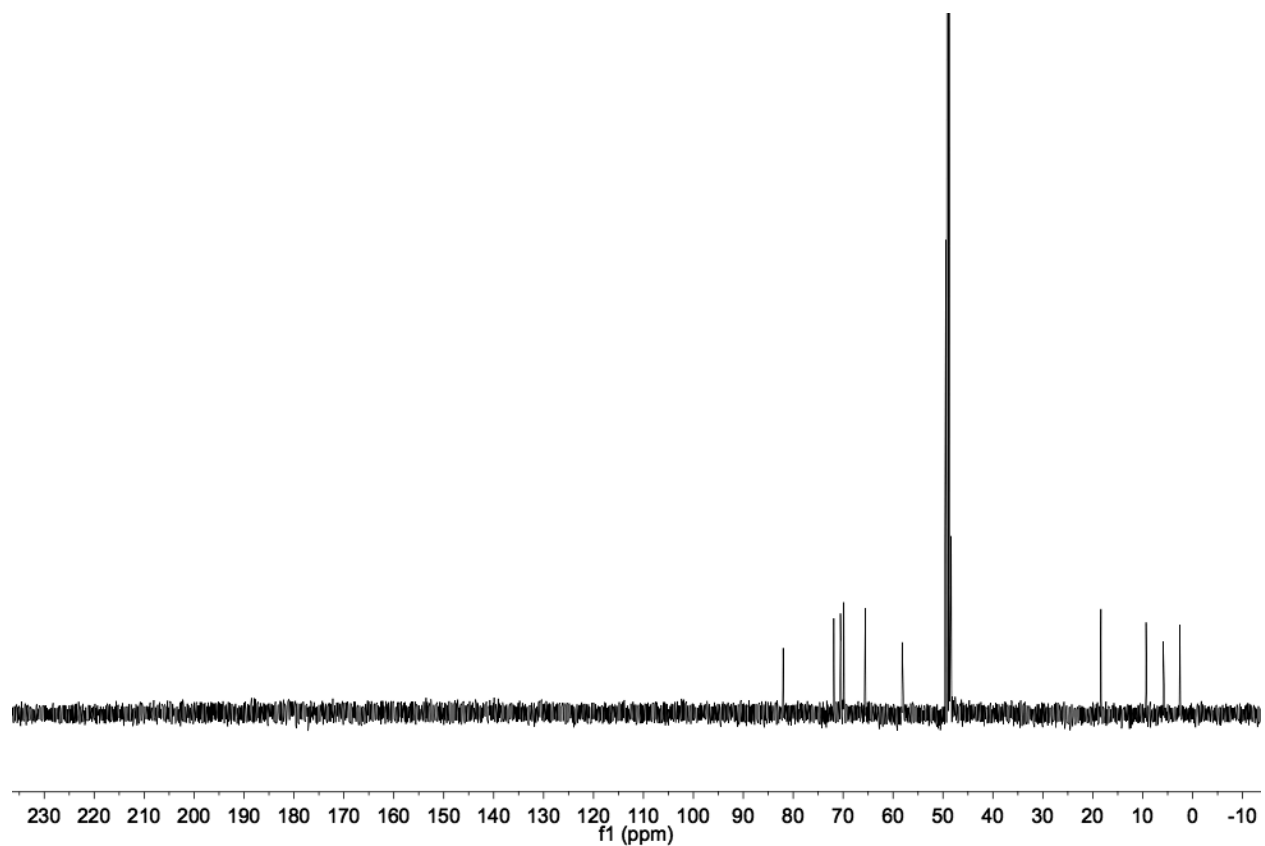
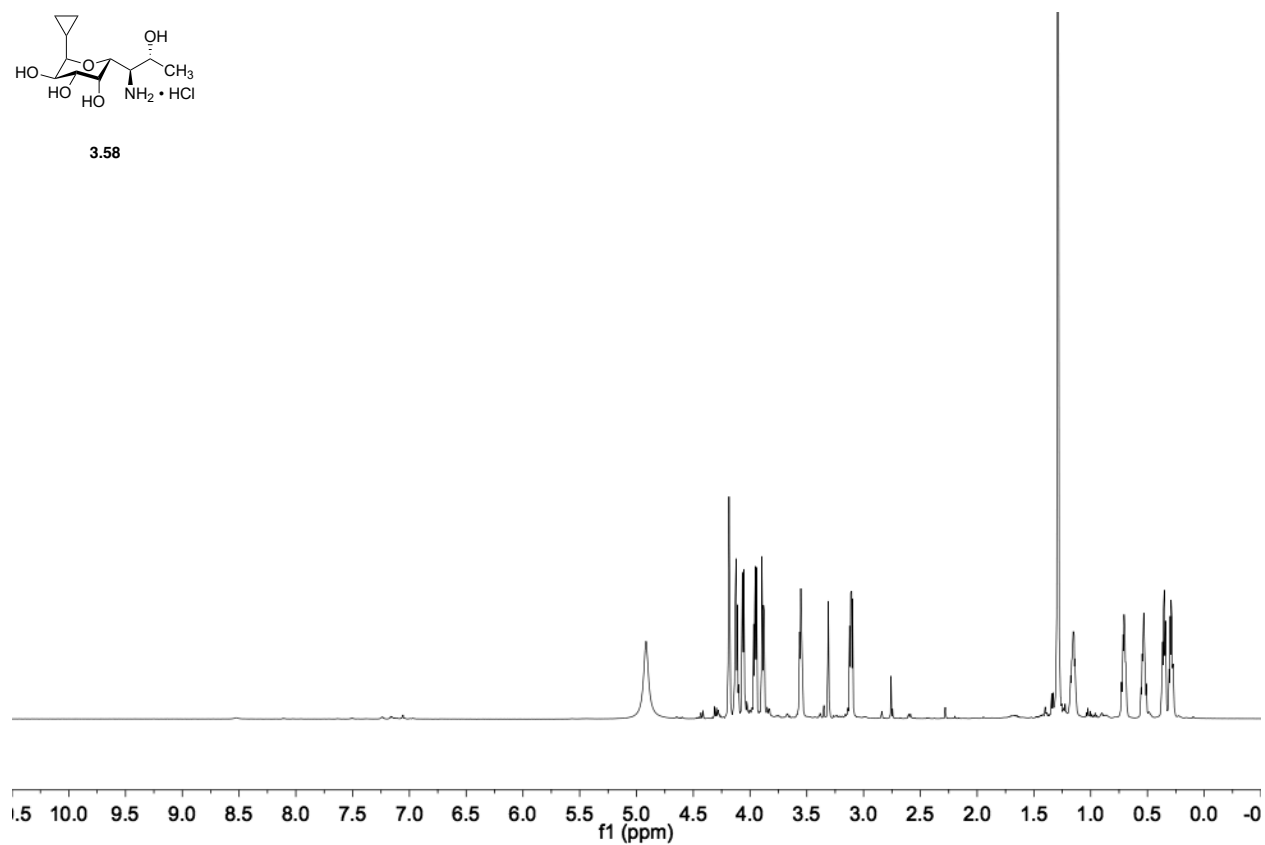


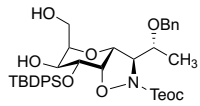
S3.6



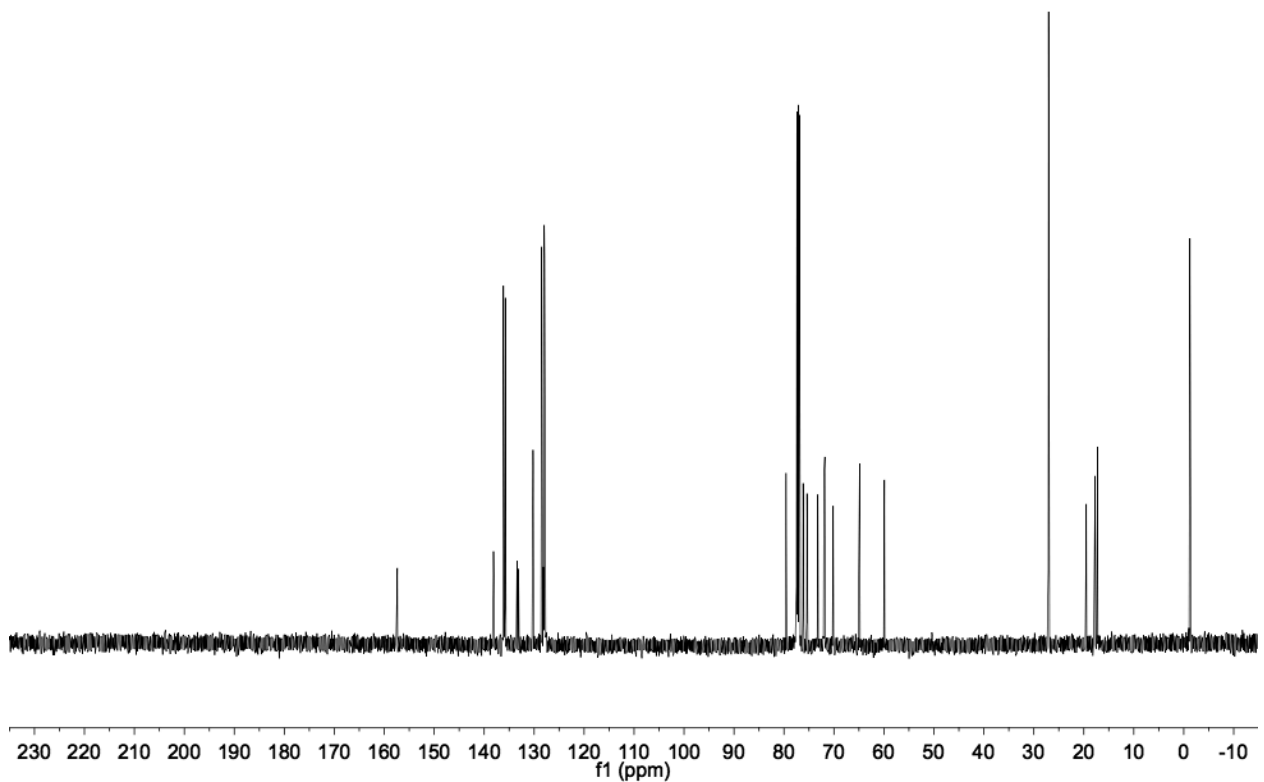
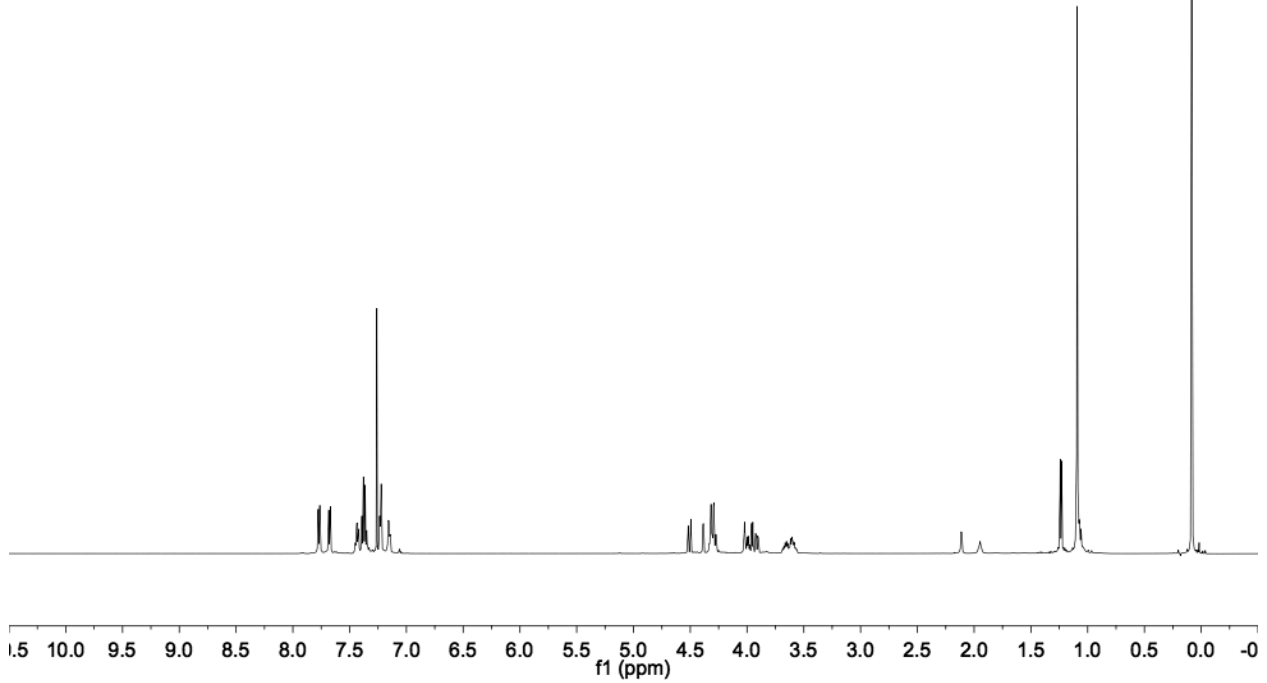


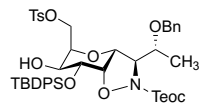
3.58



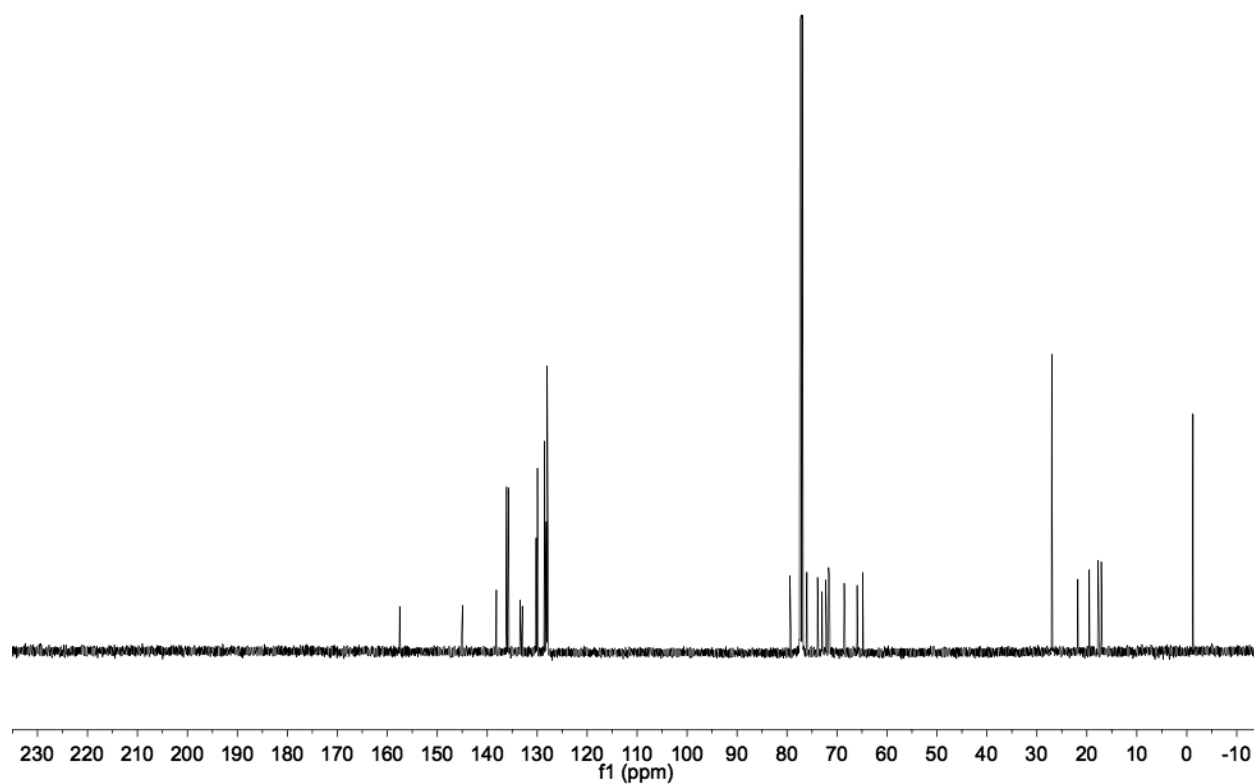
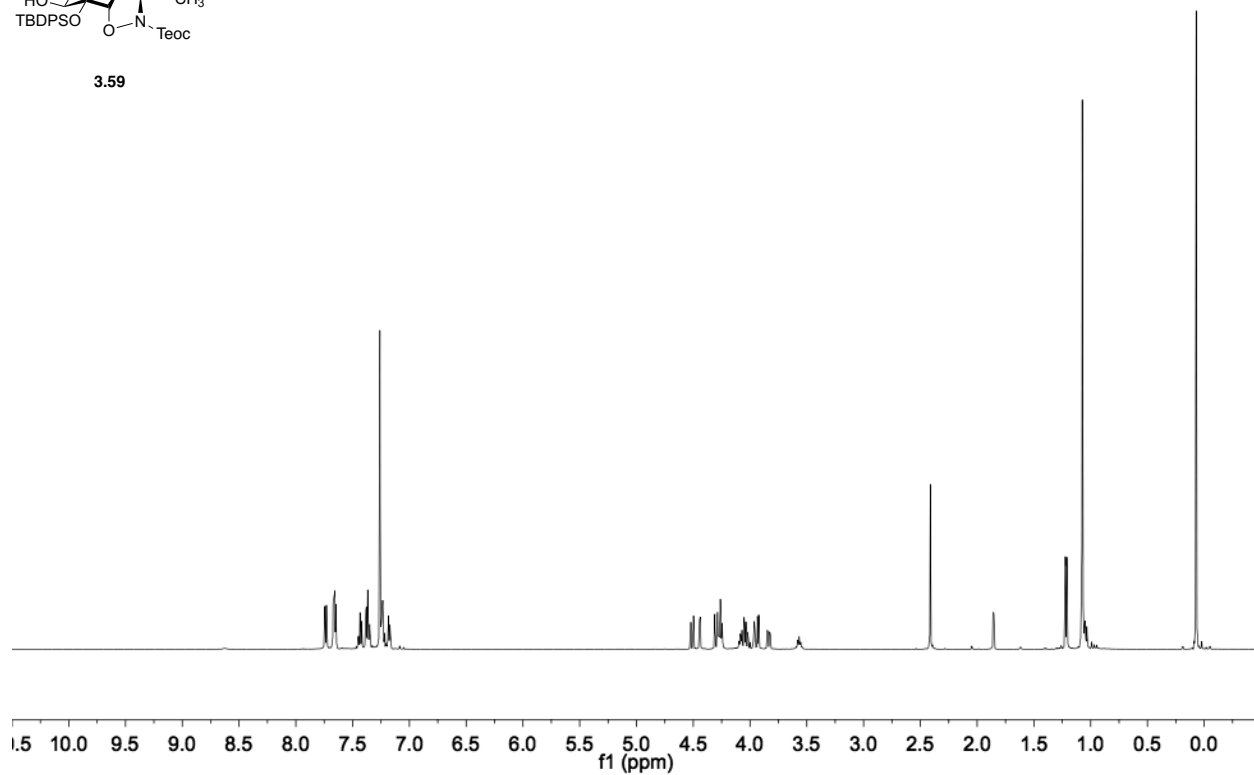


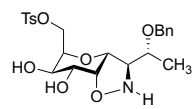
S3.7



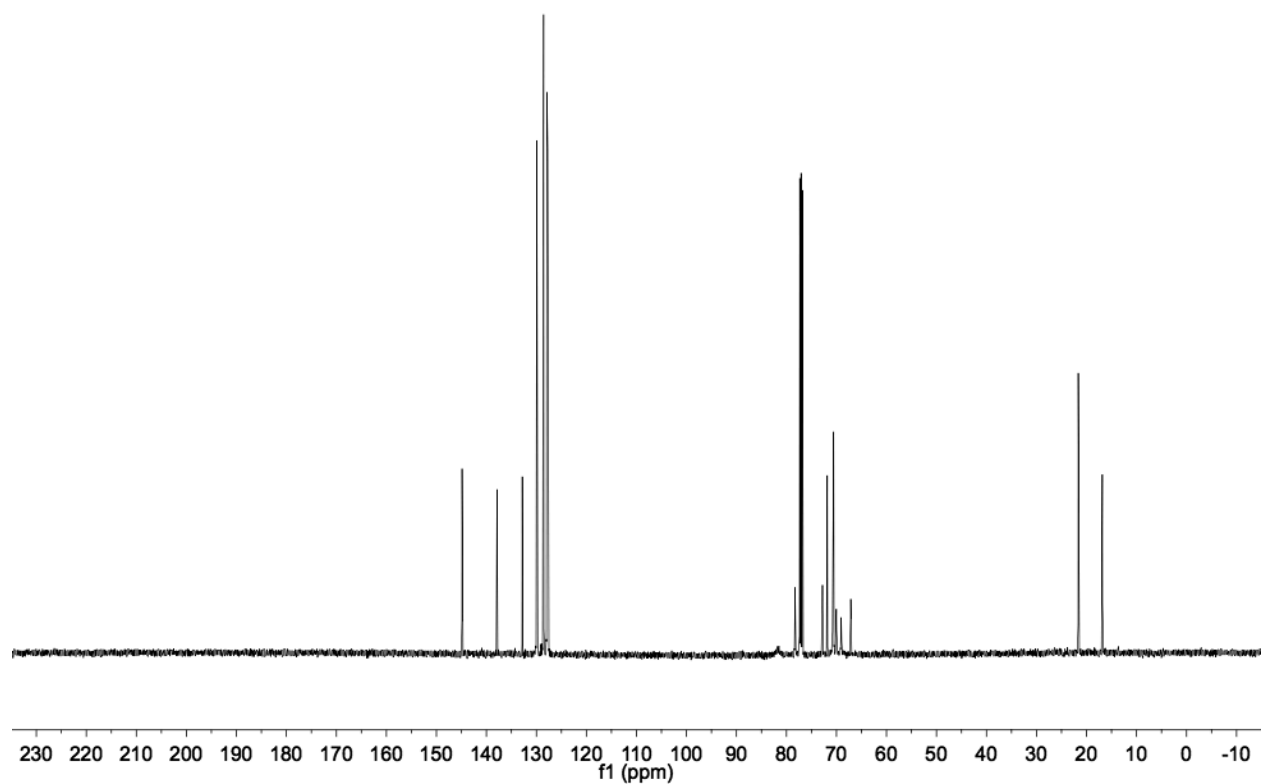
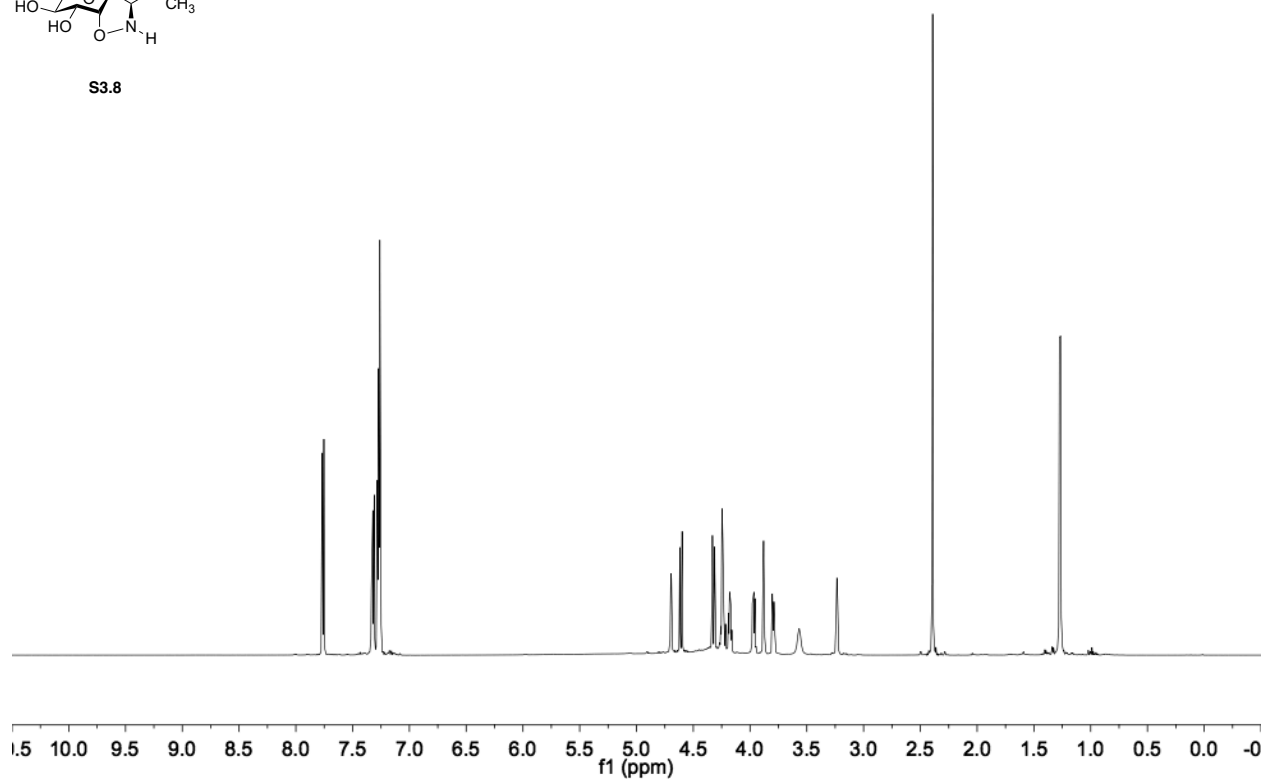


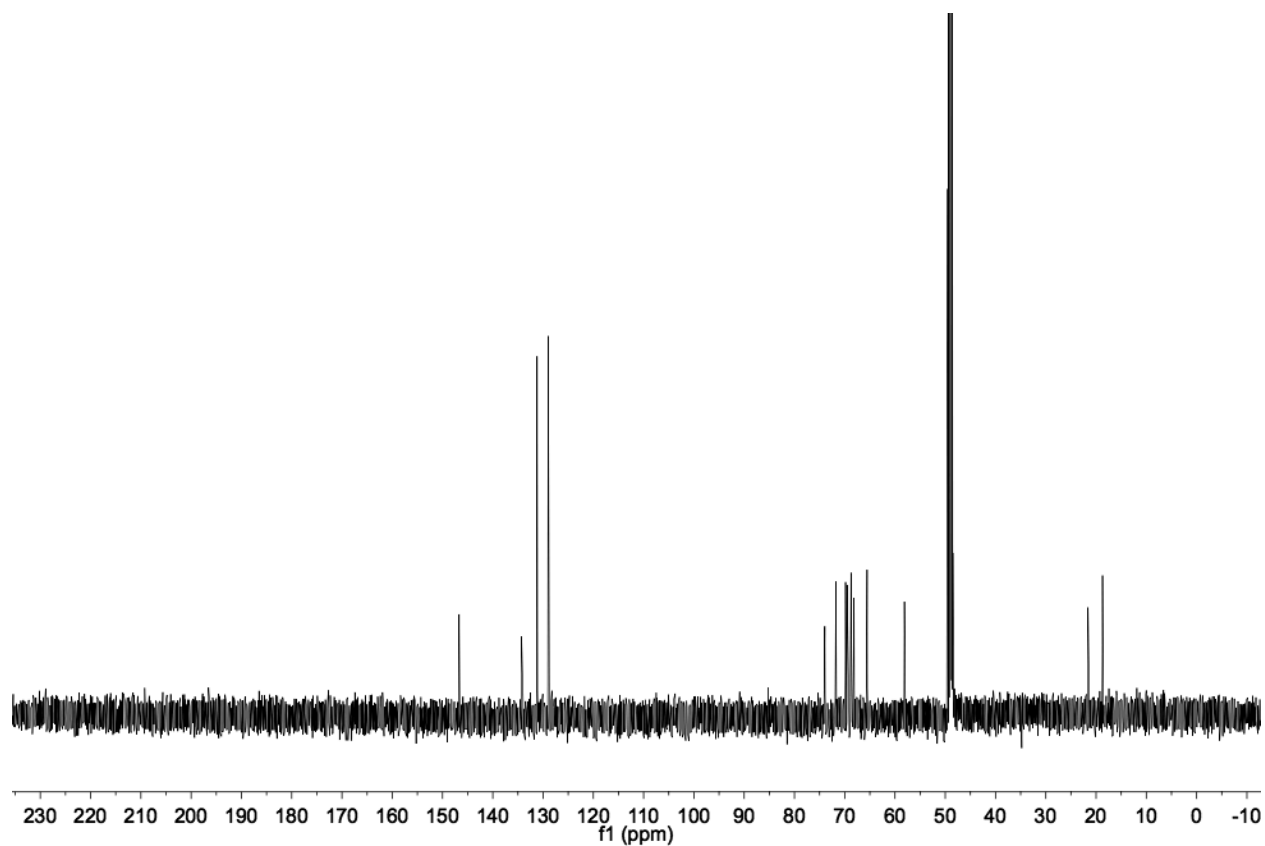
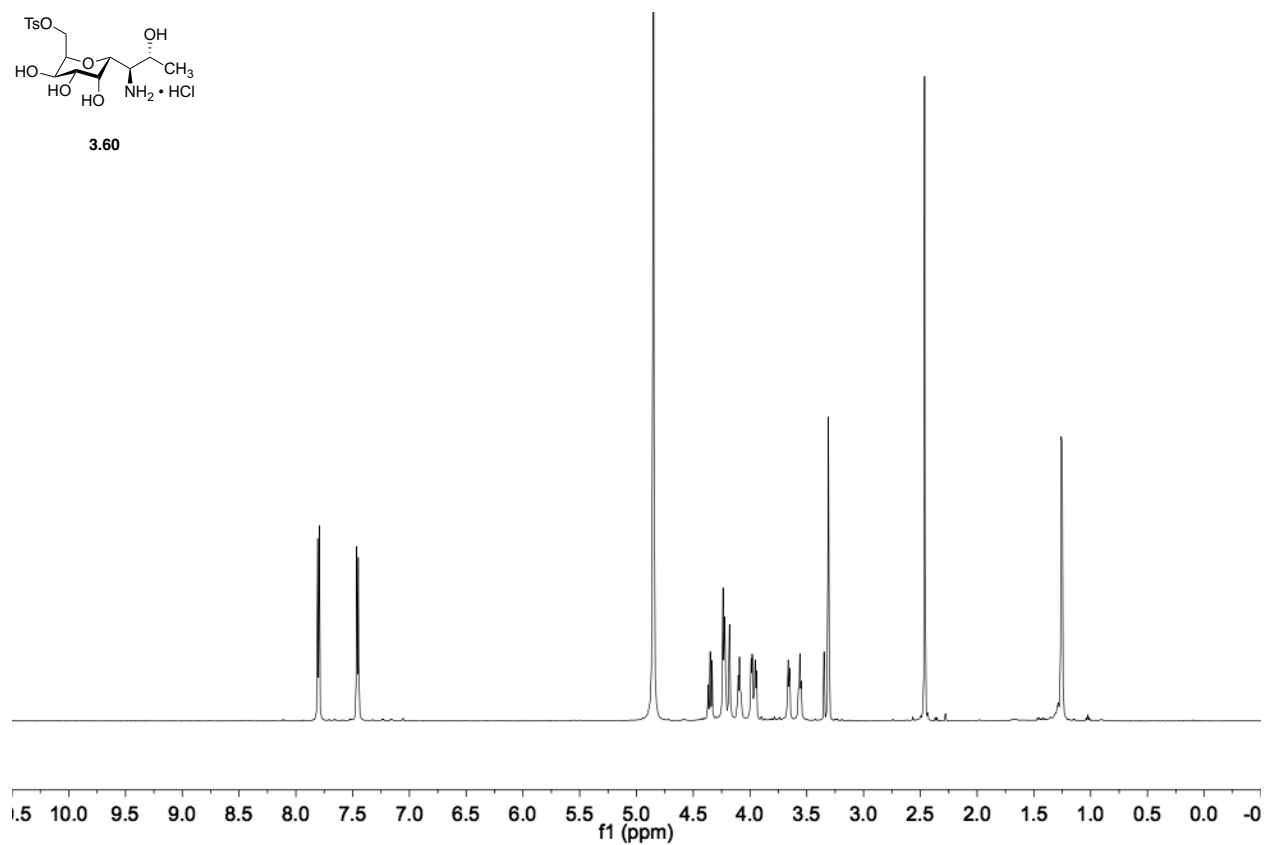
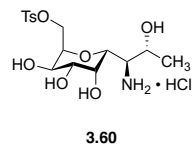
3.59

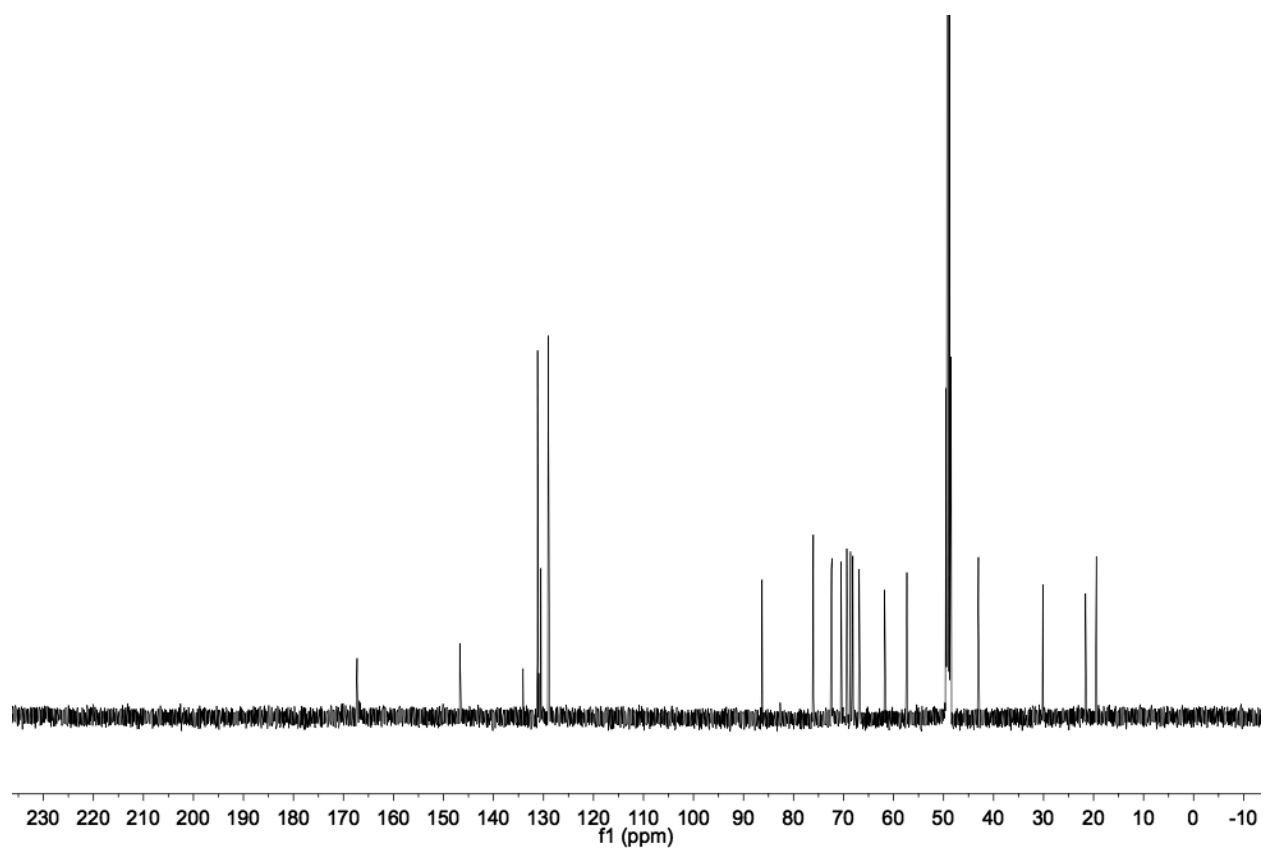
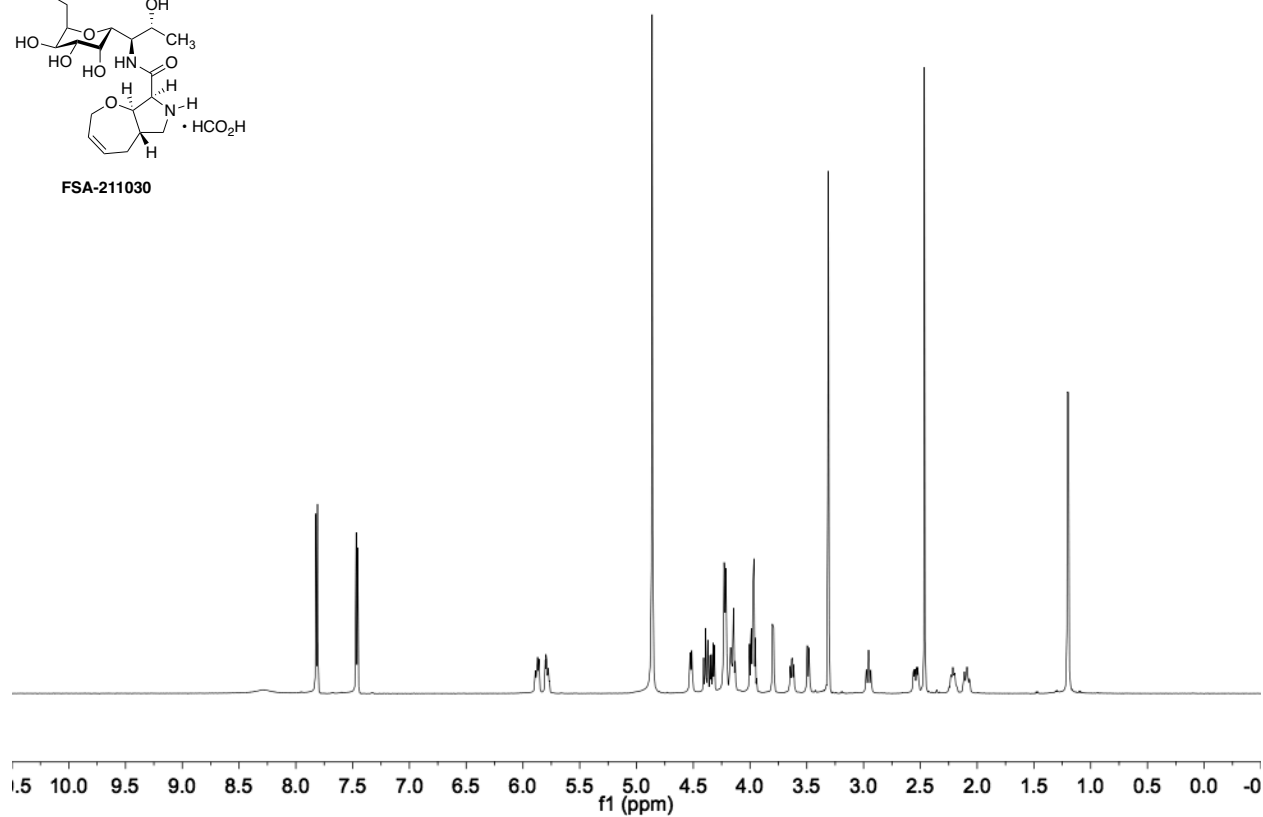
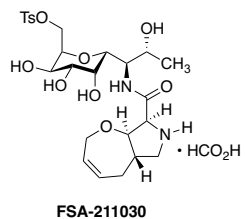


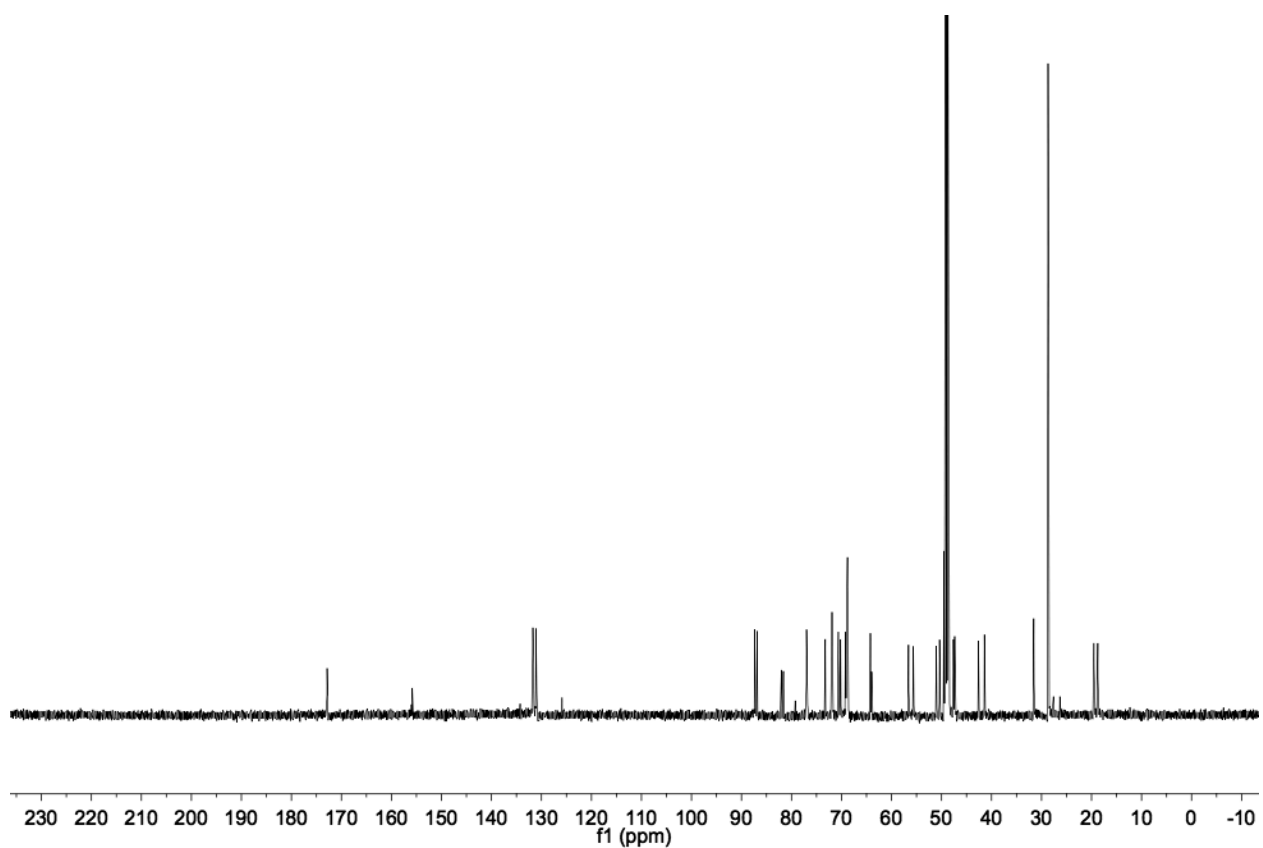
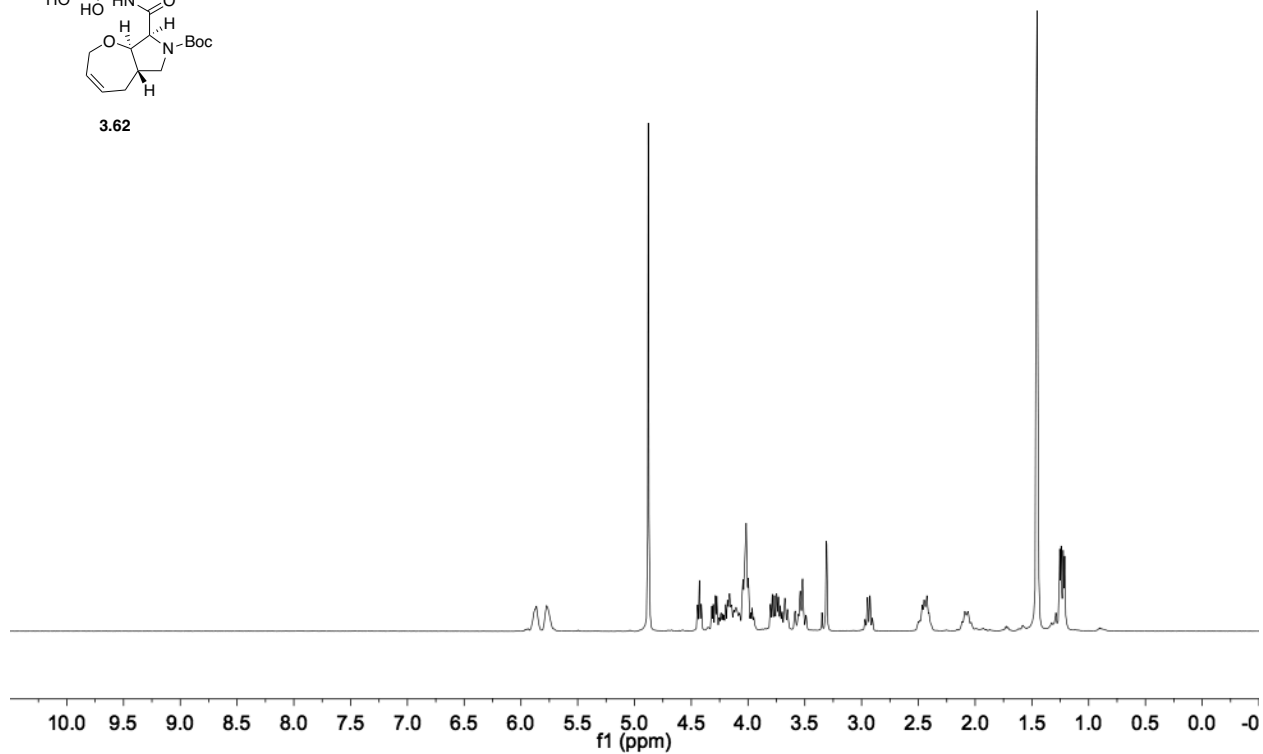
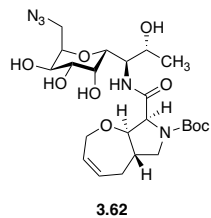


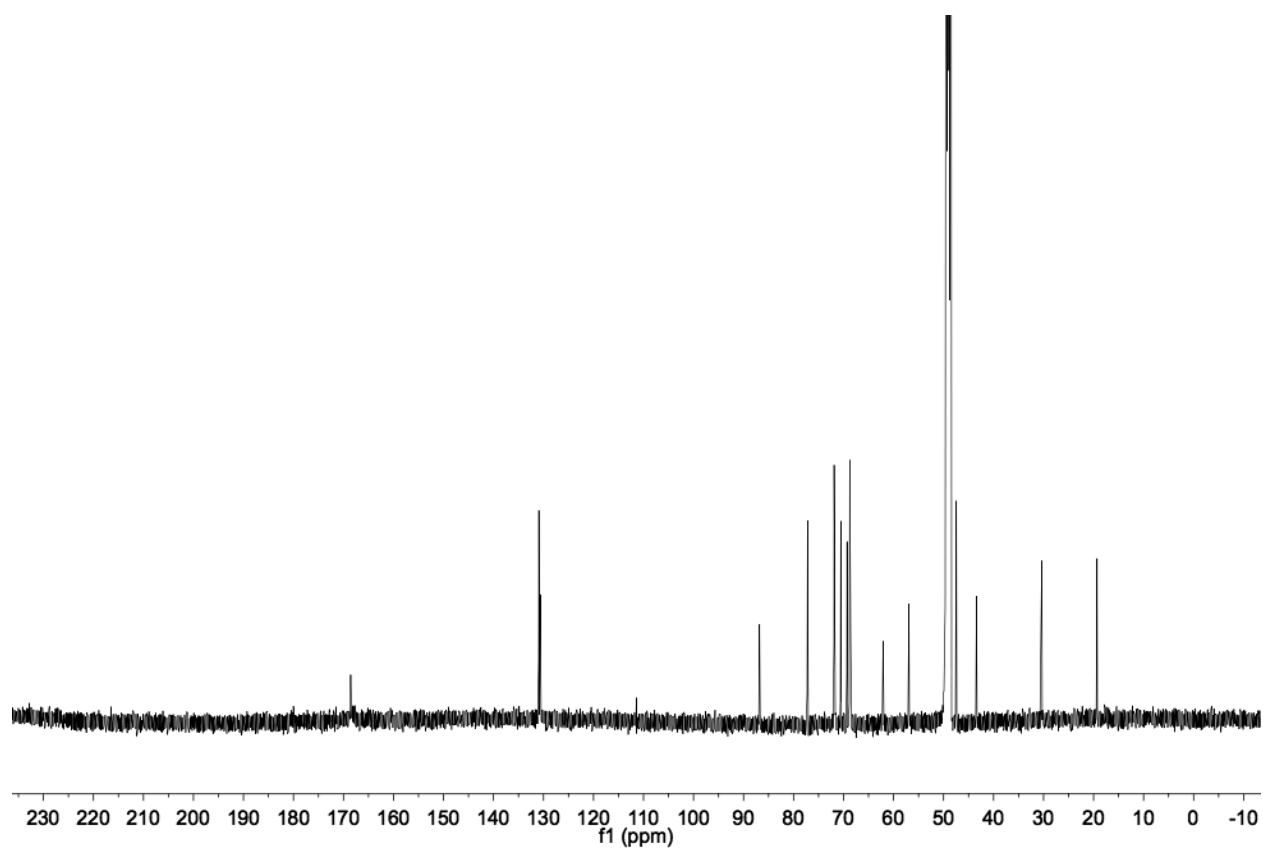
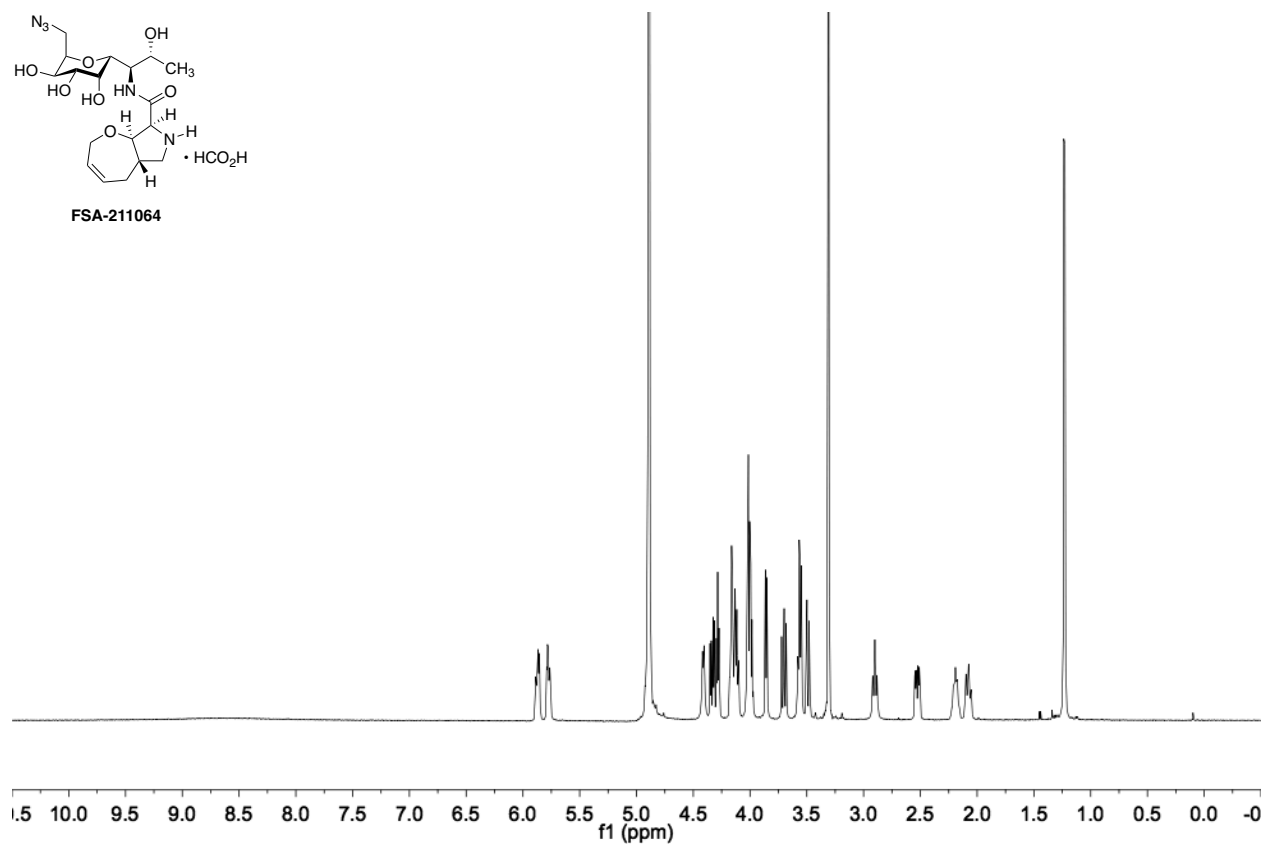
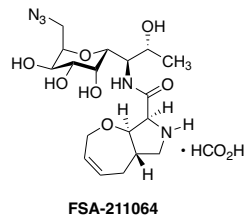
S3.8

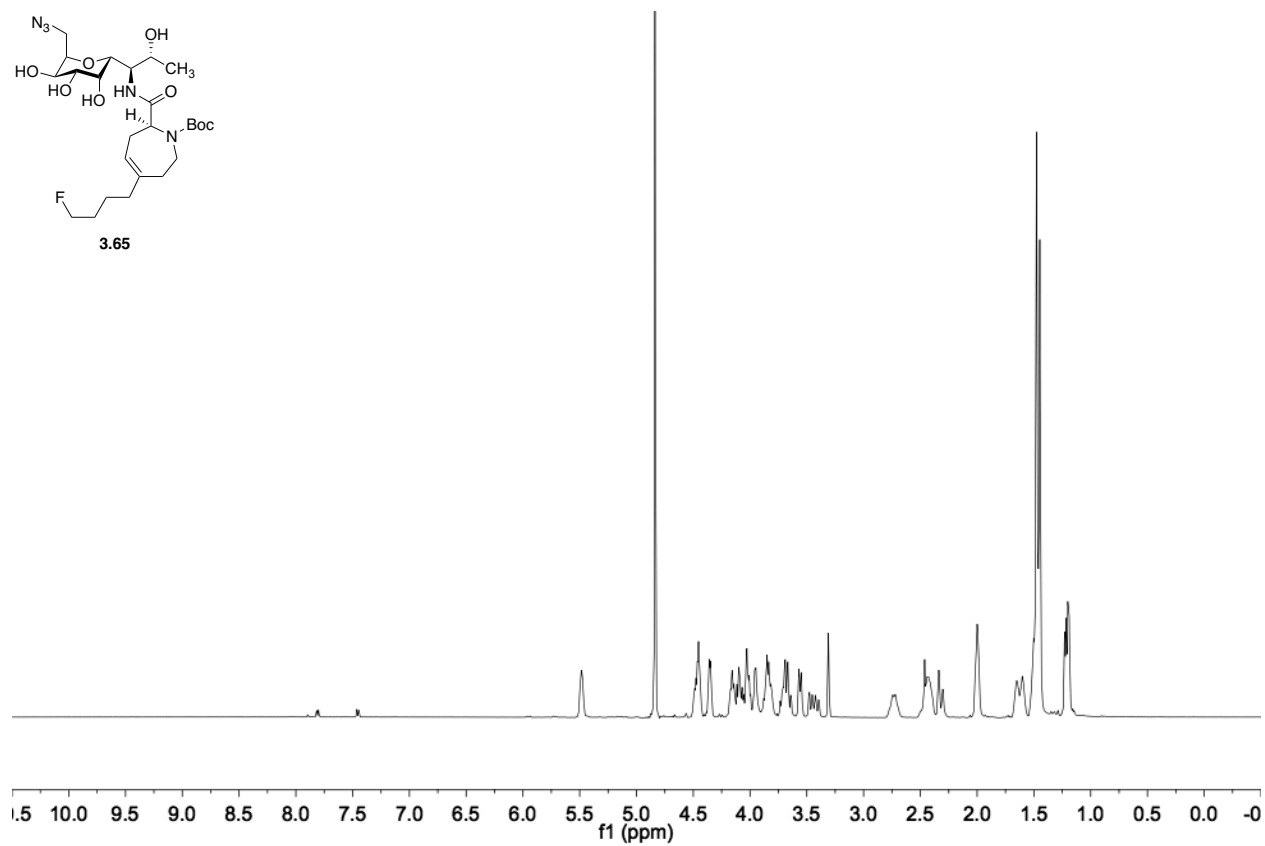
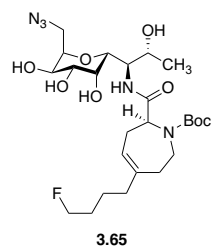
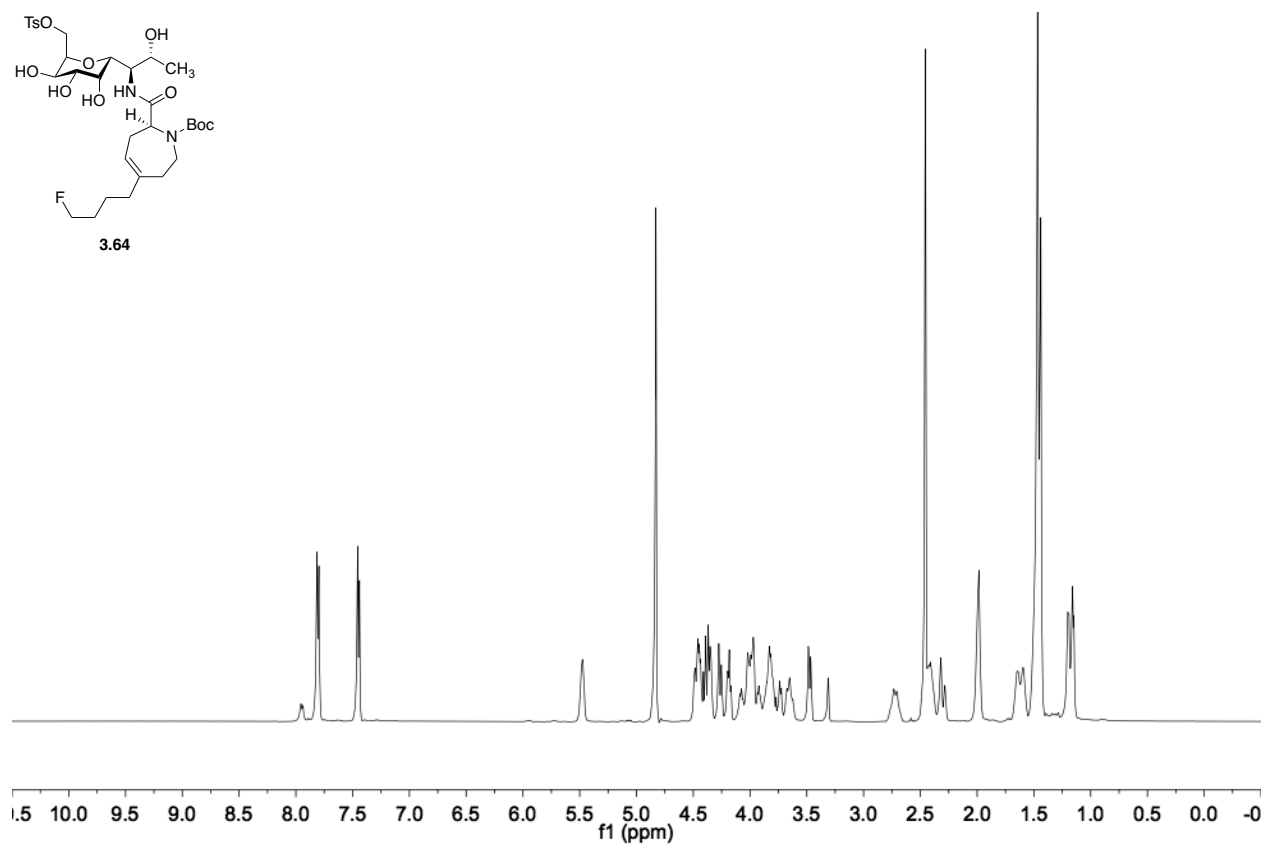
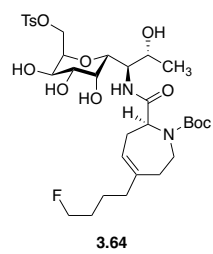


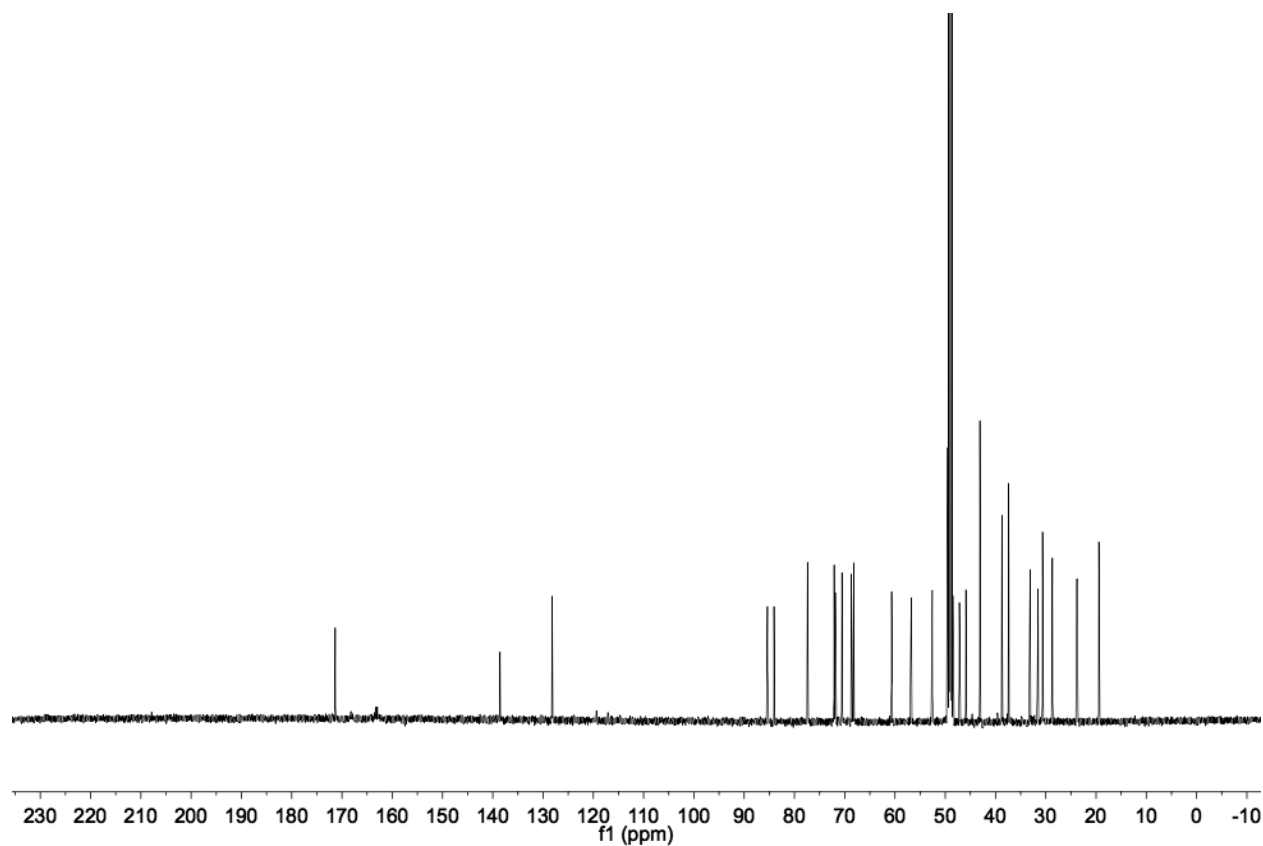
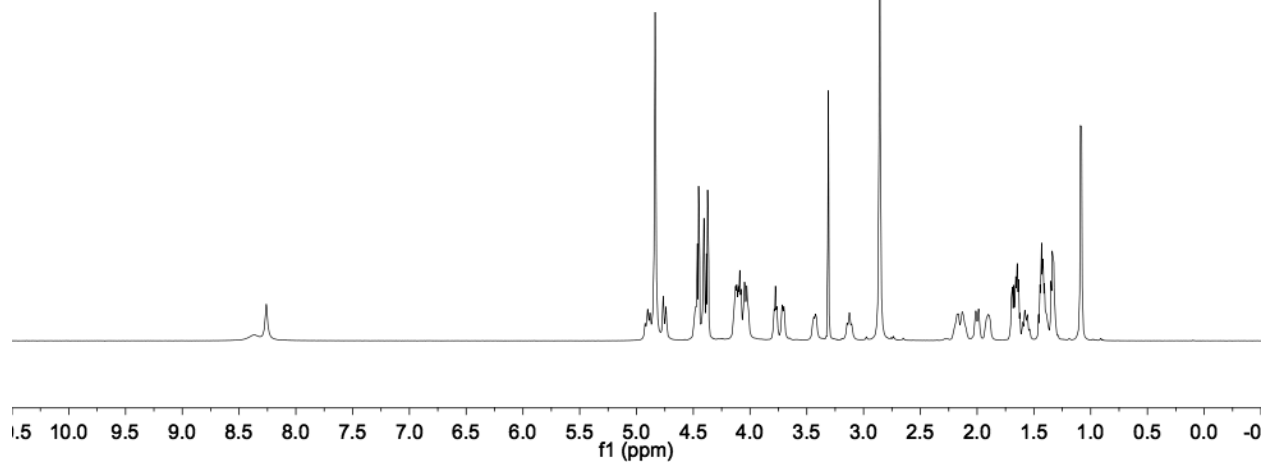
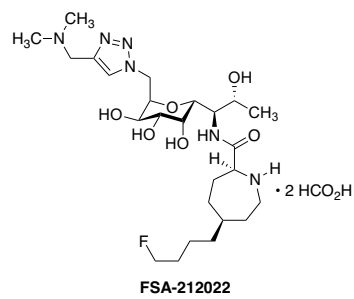


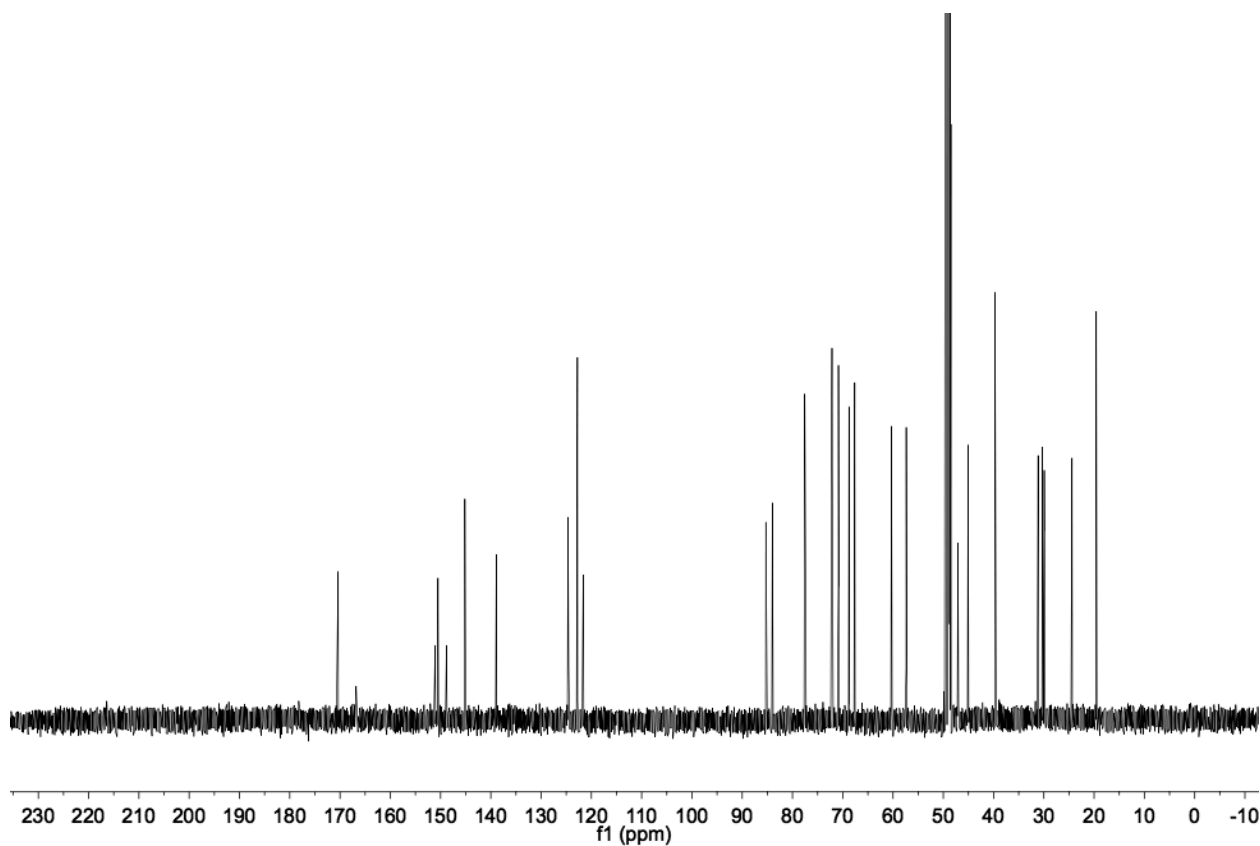
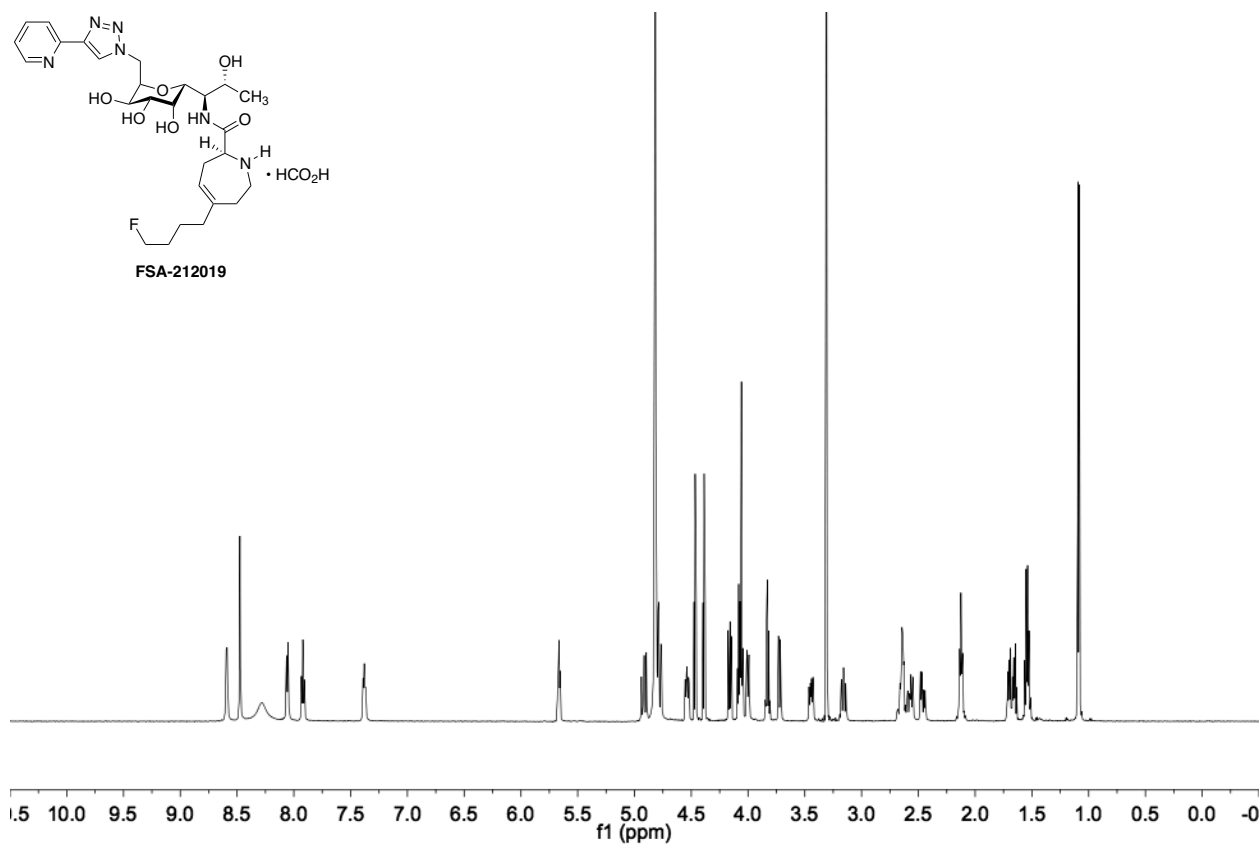
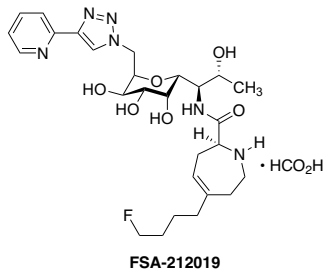


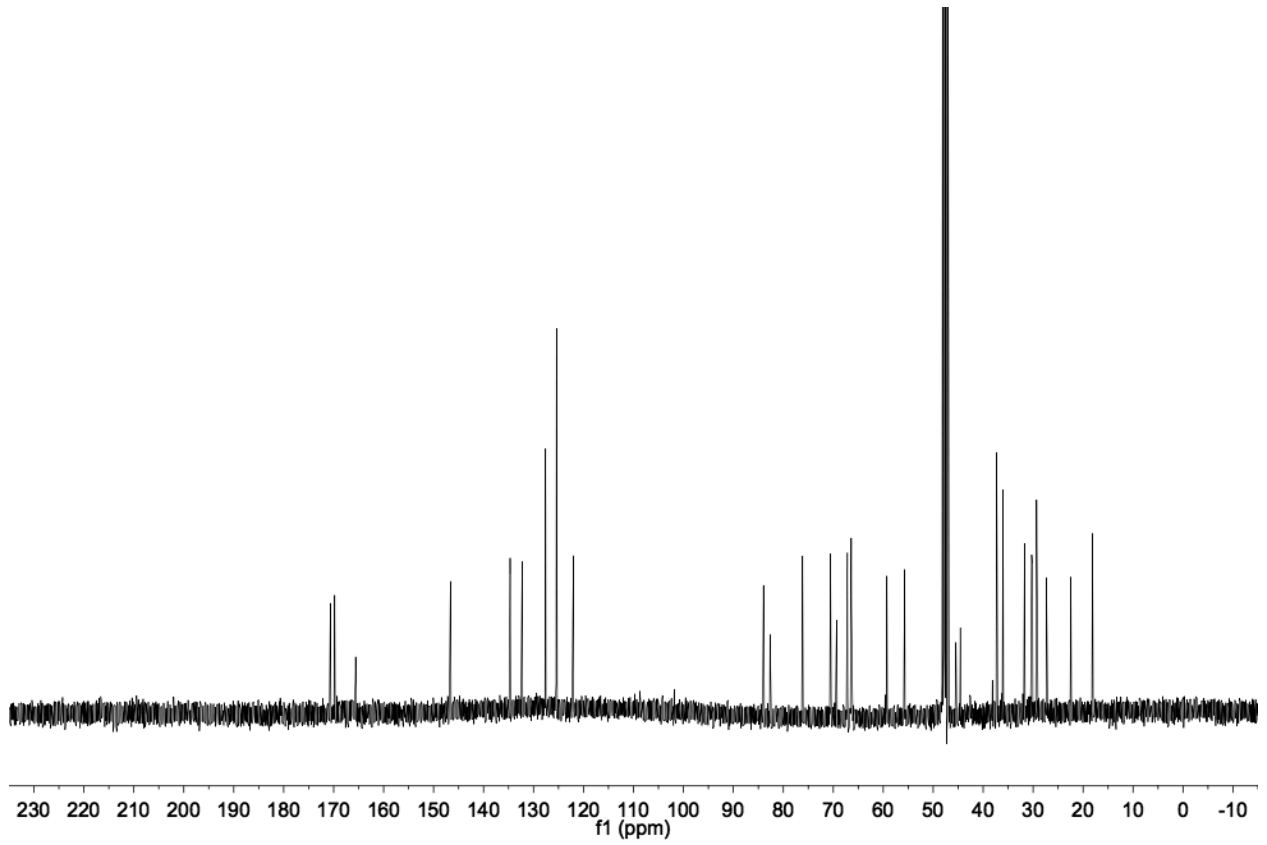
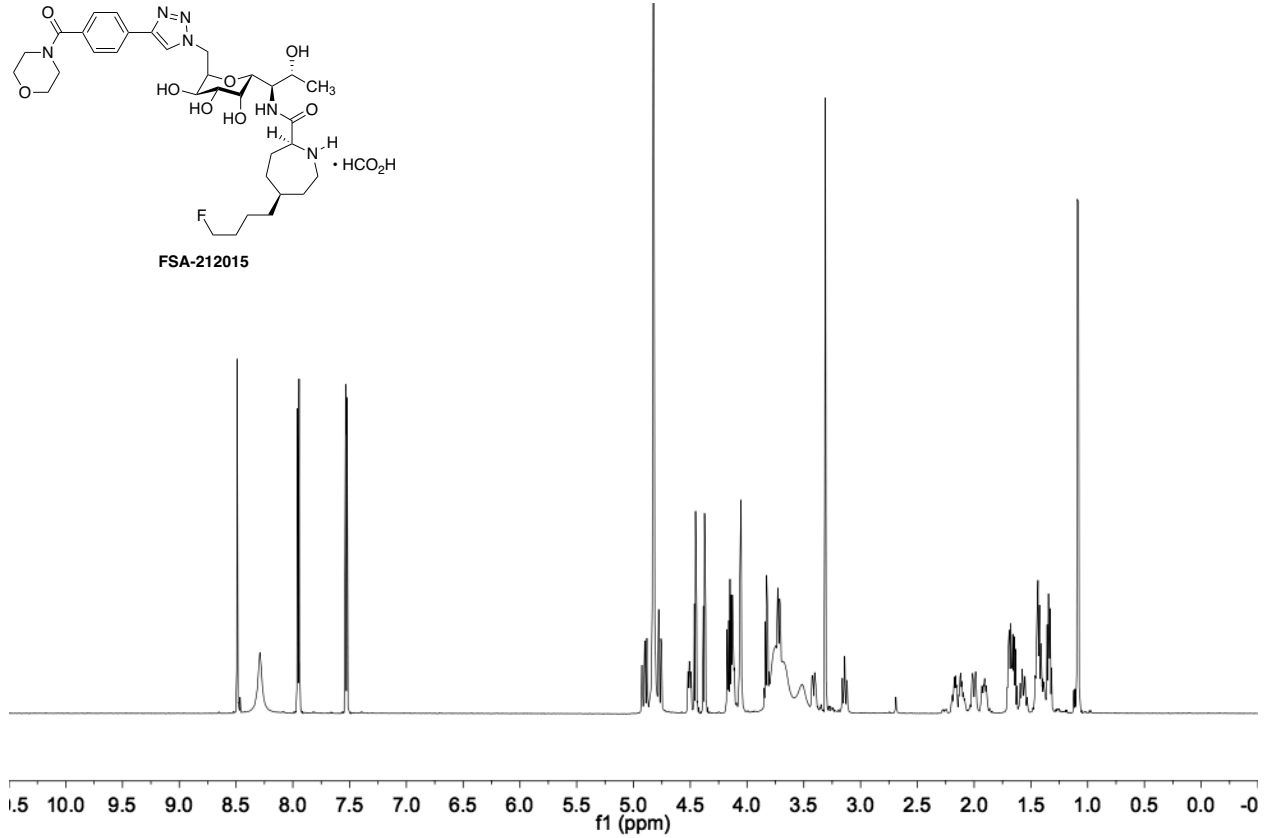
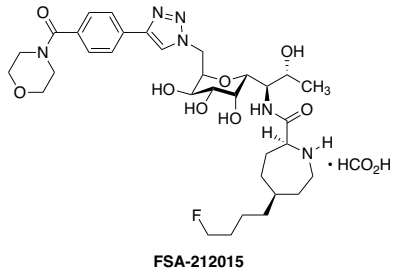


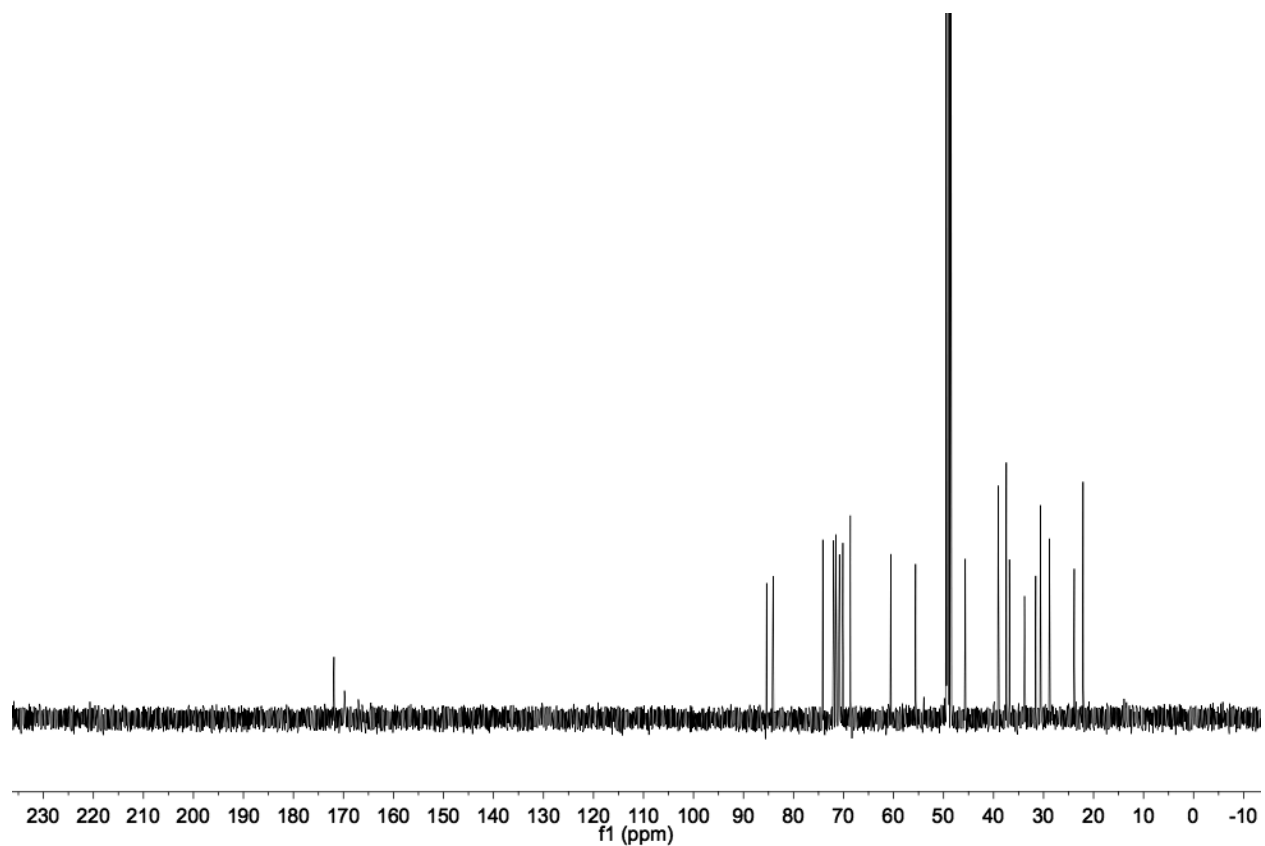
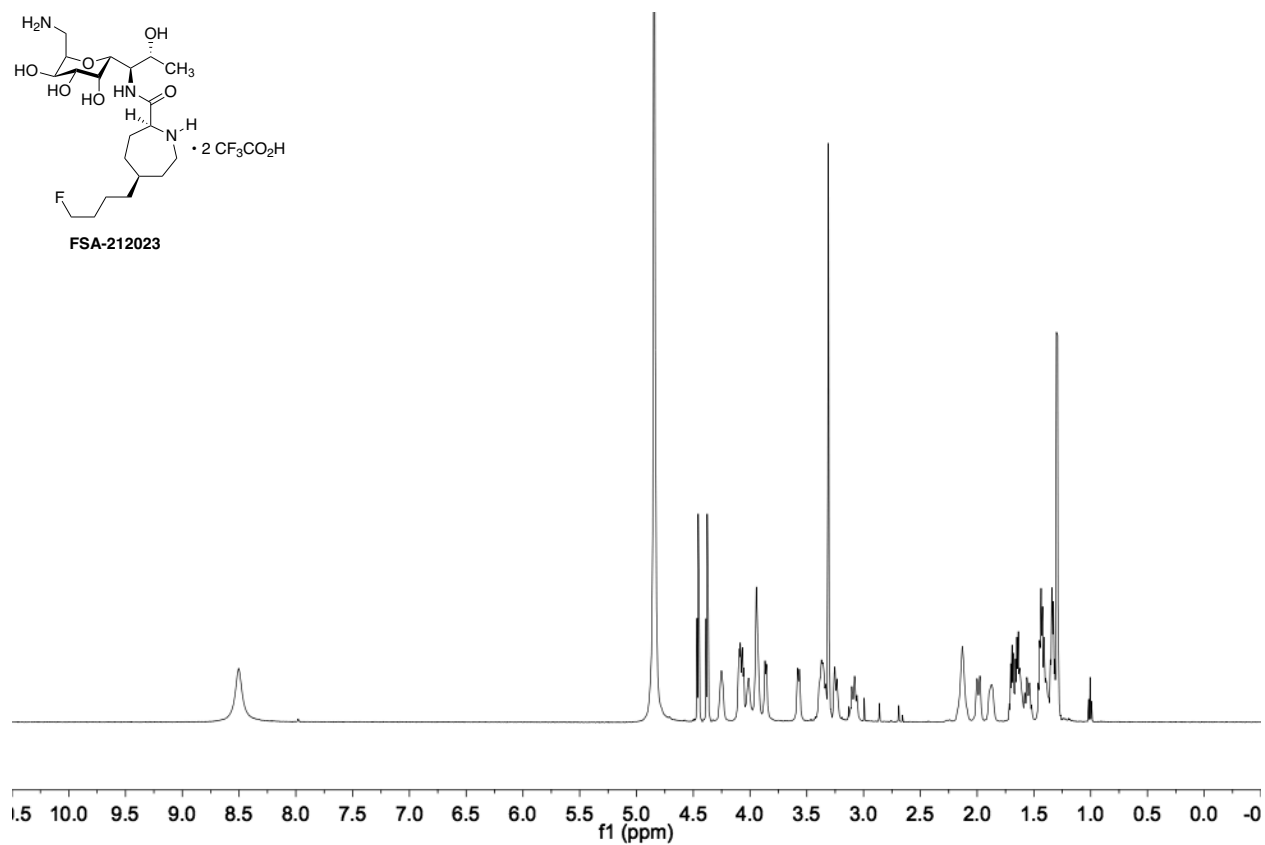
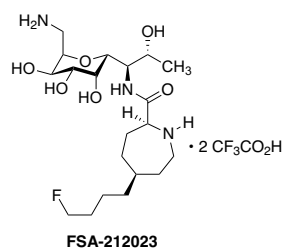


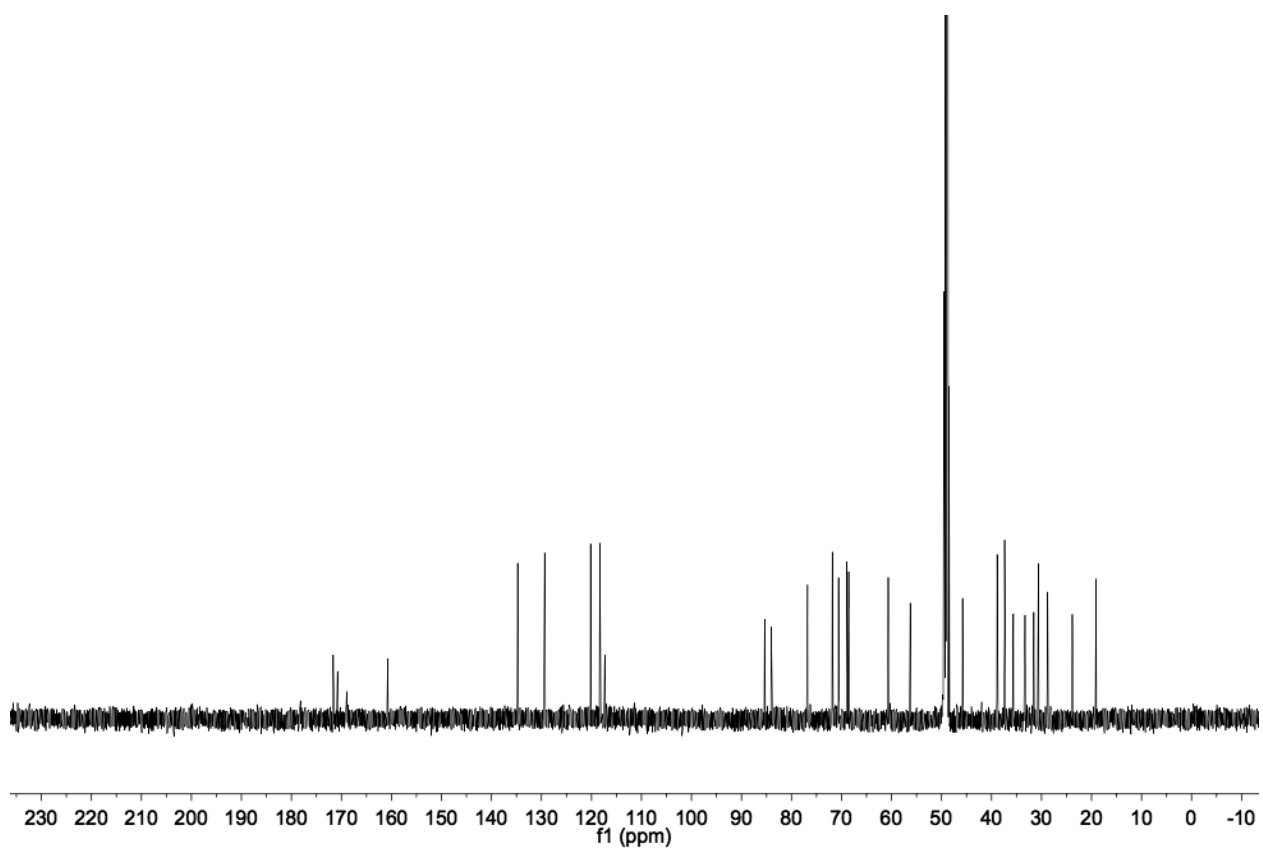
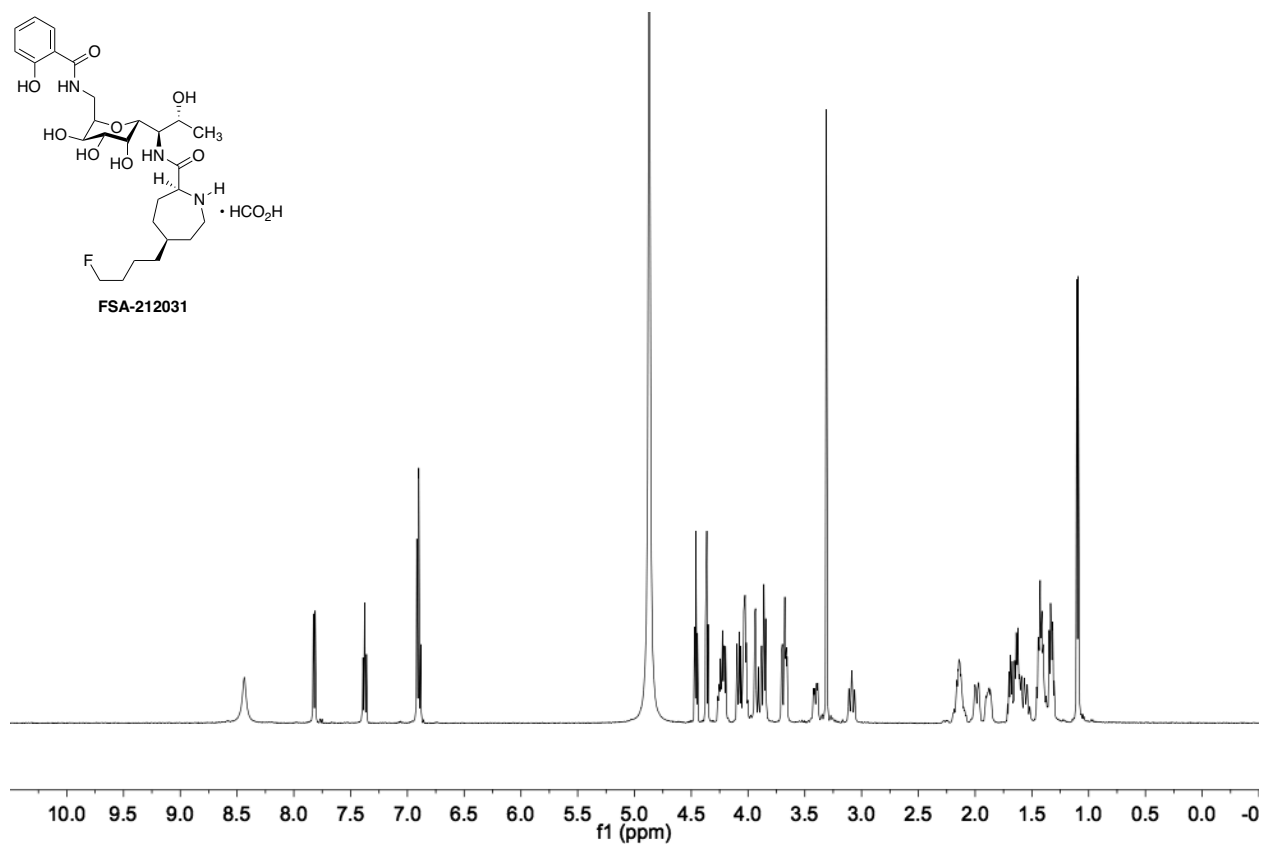
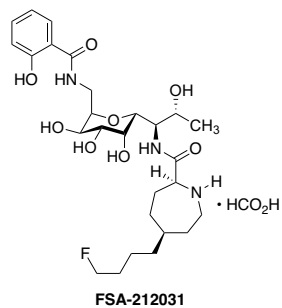


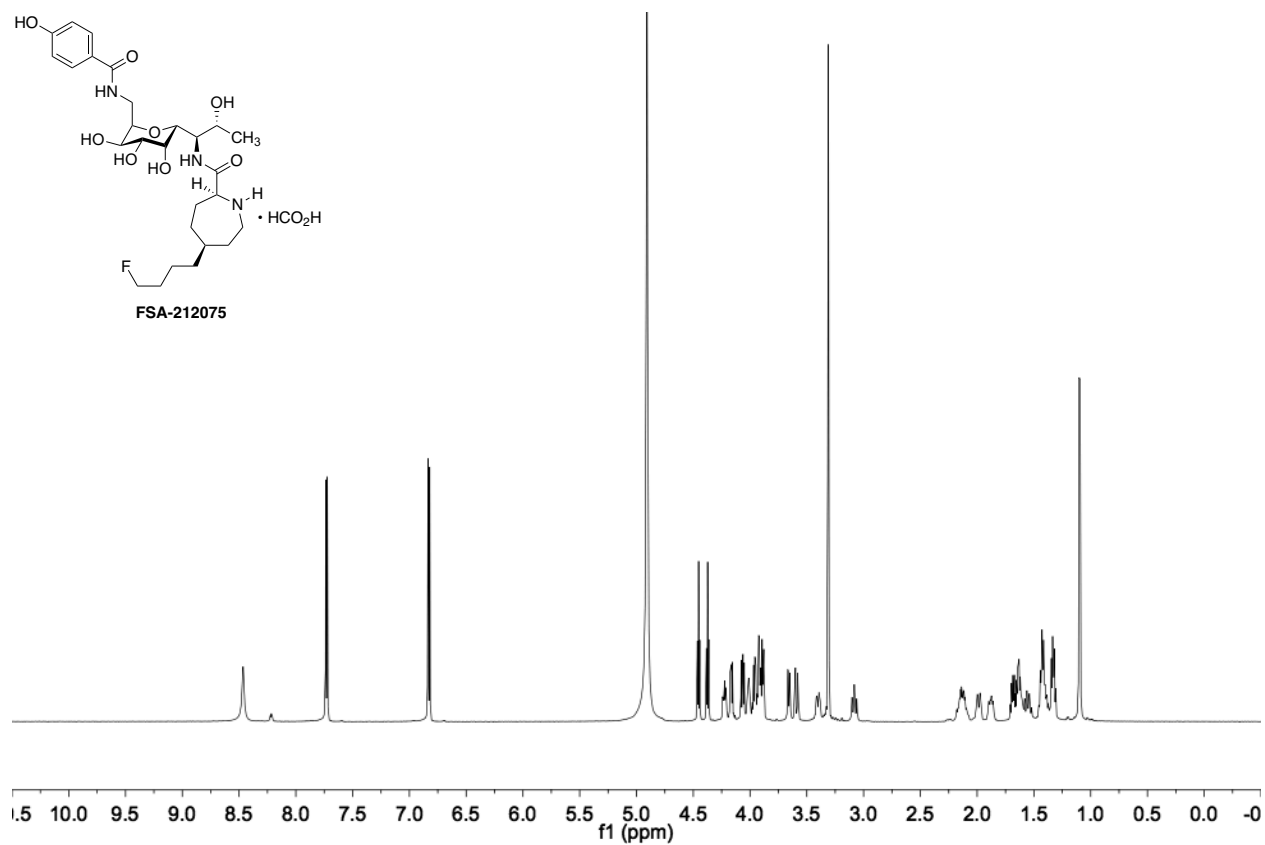
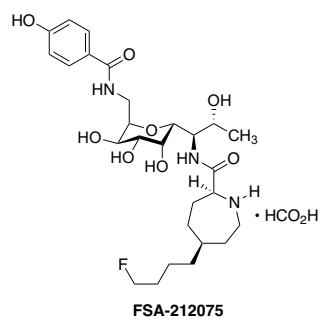


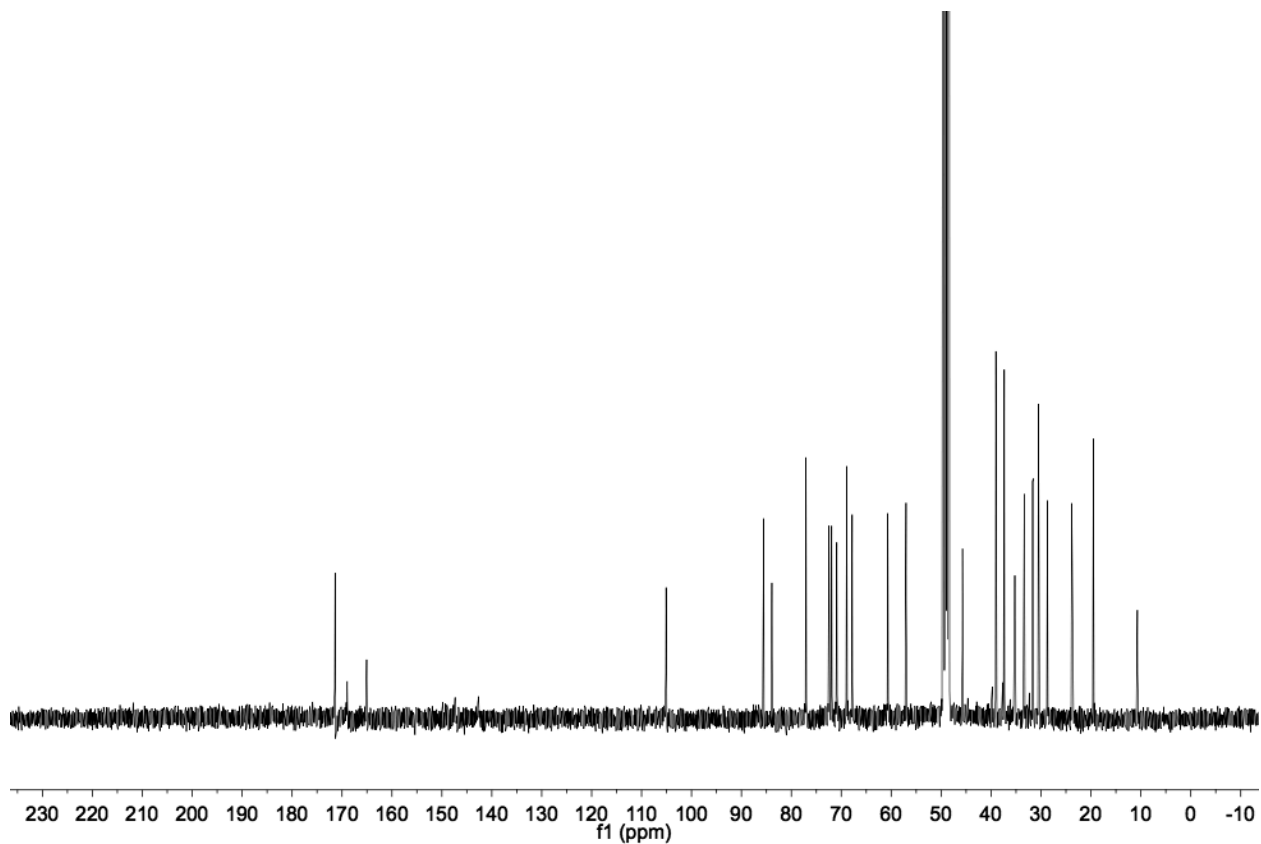
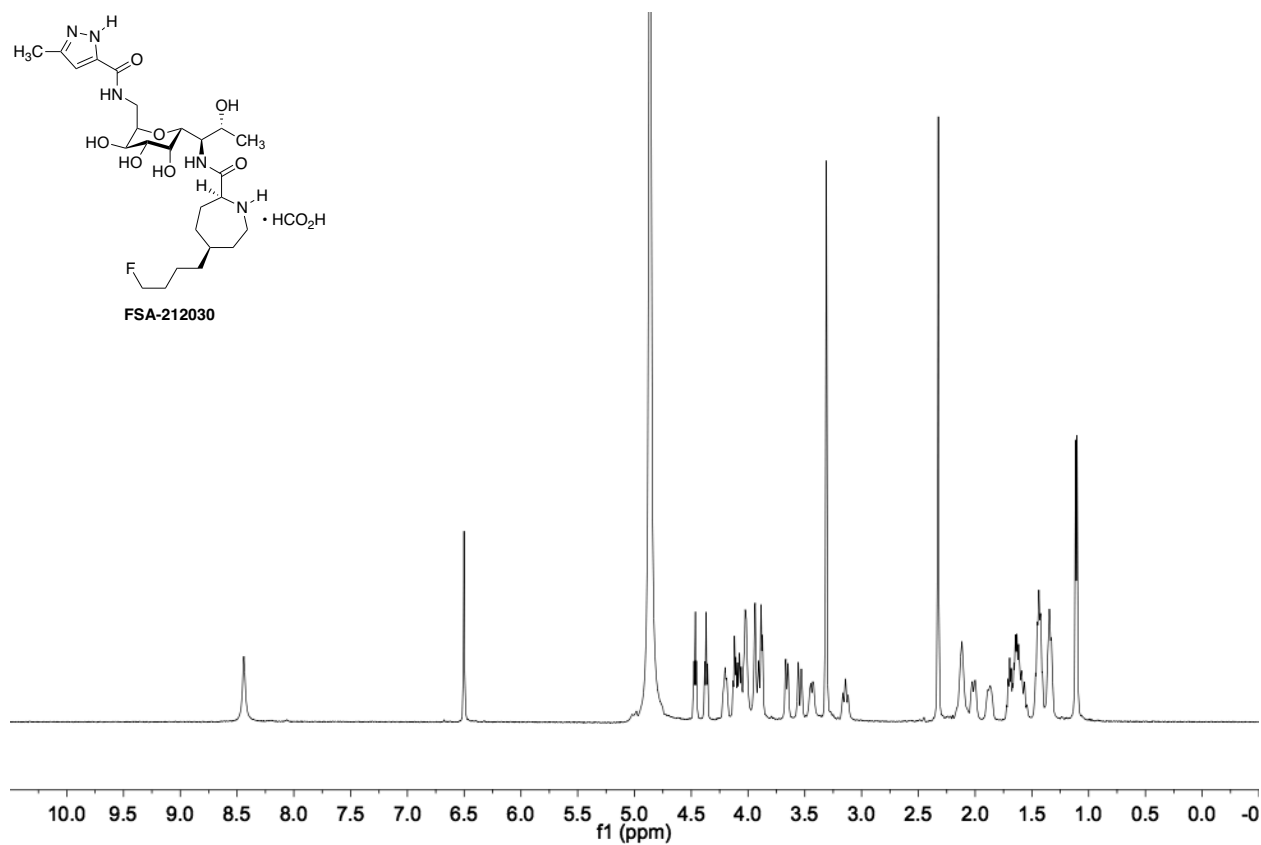
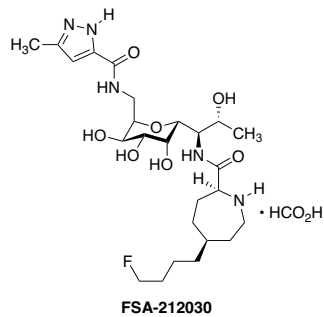


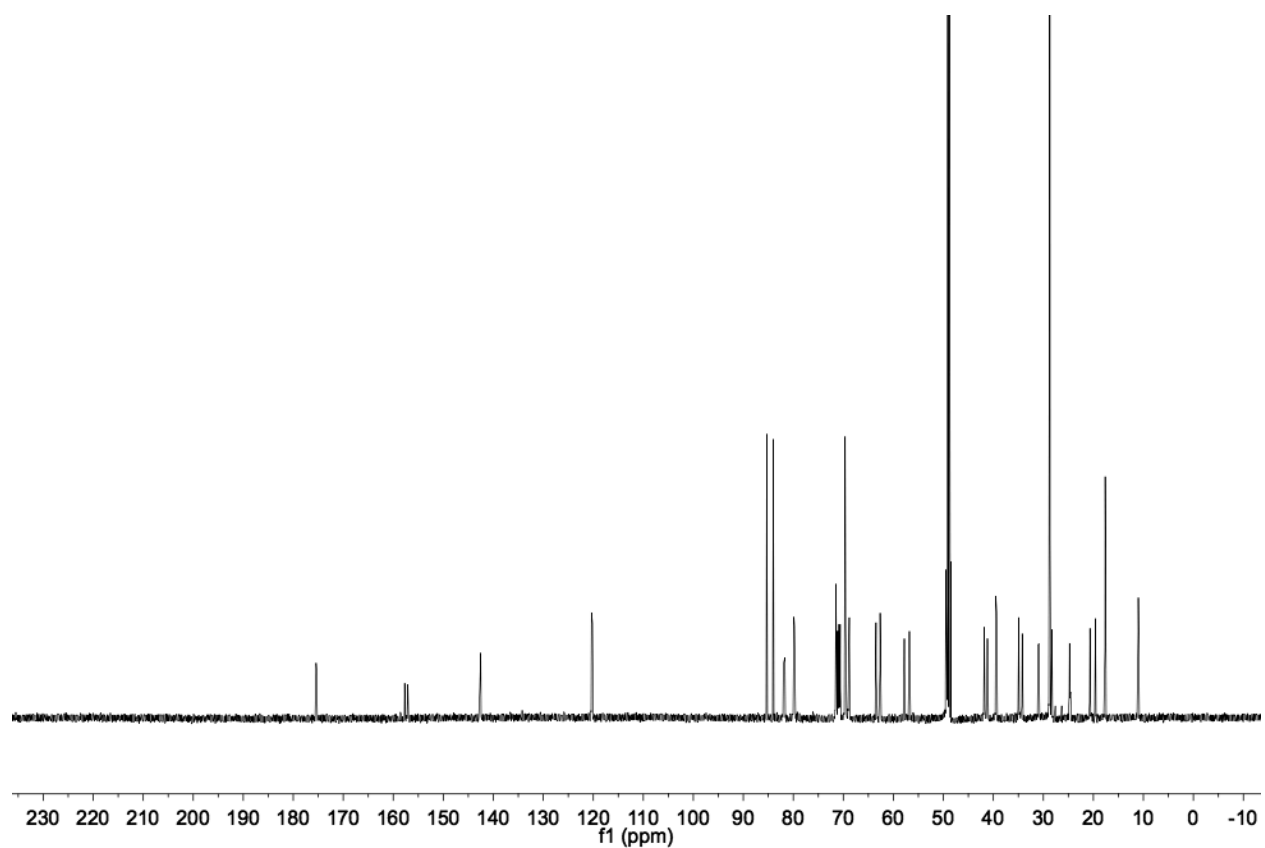
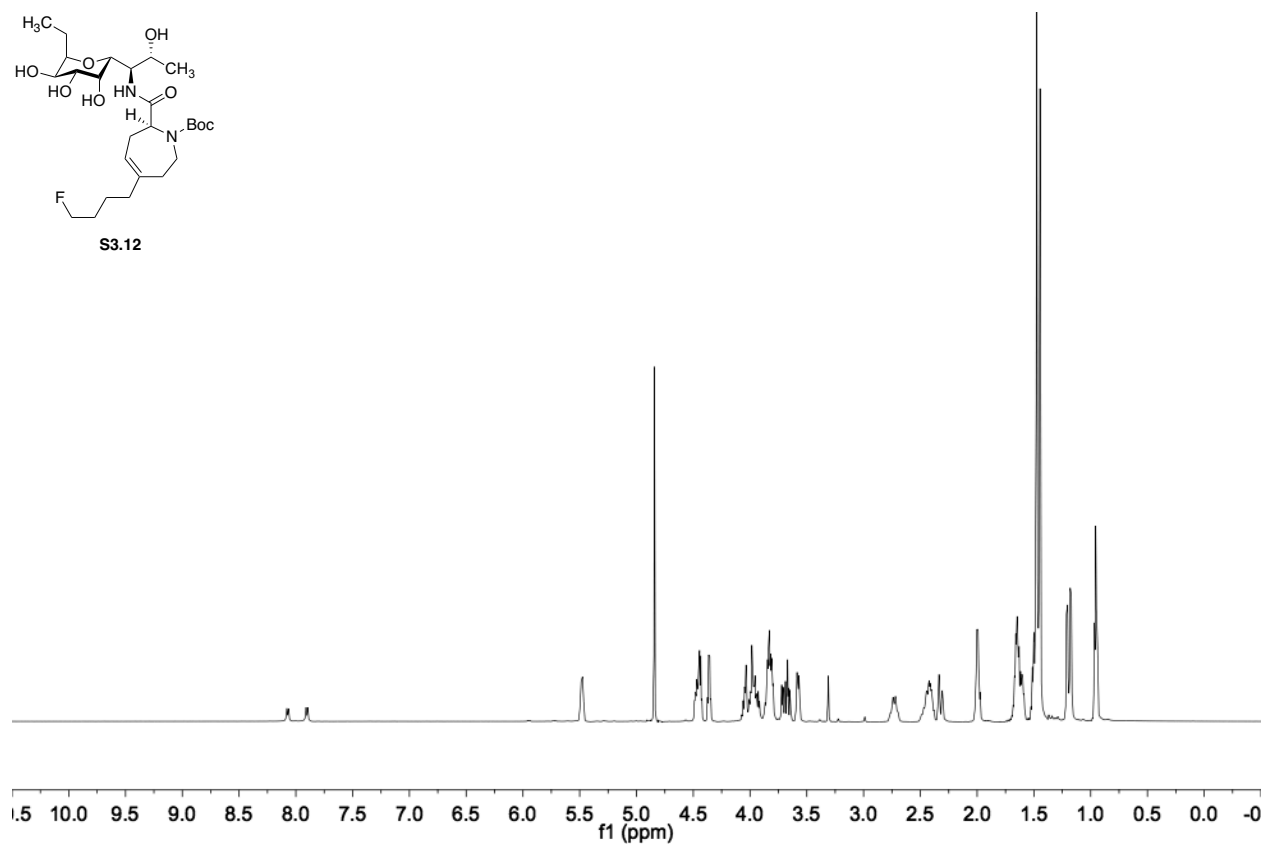
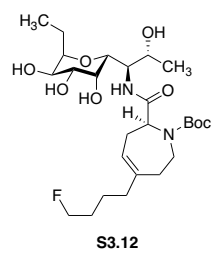


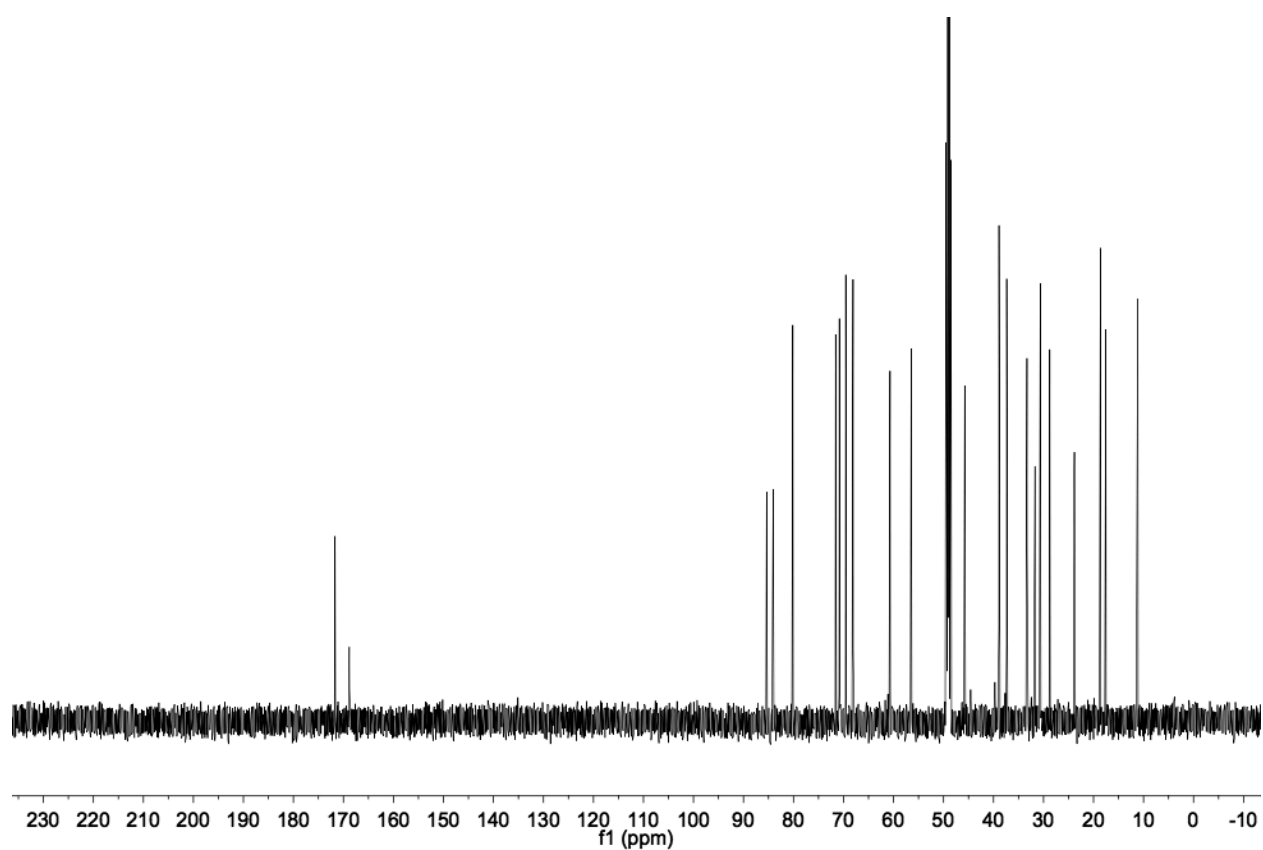
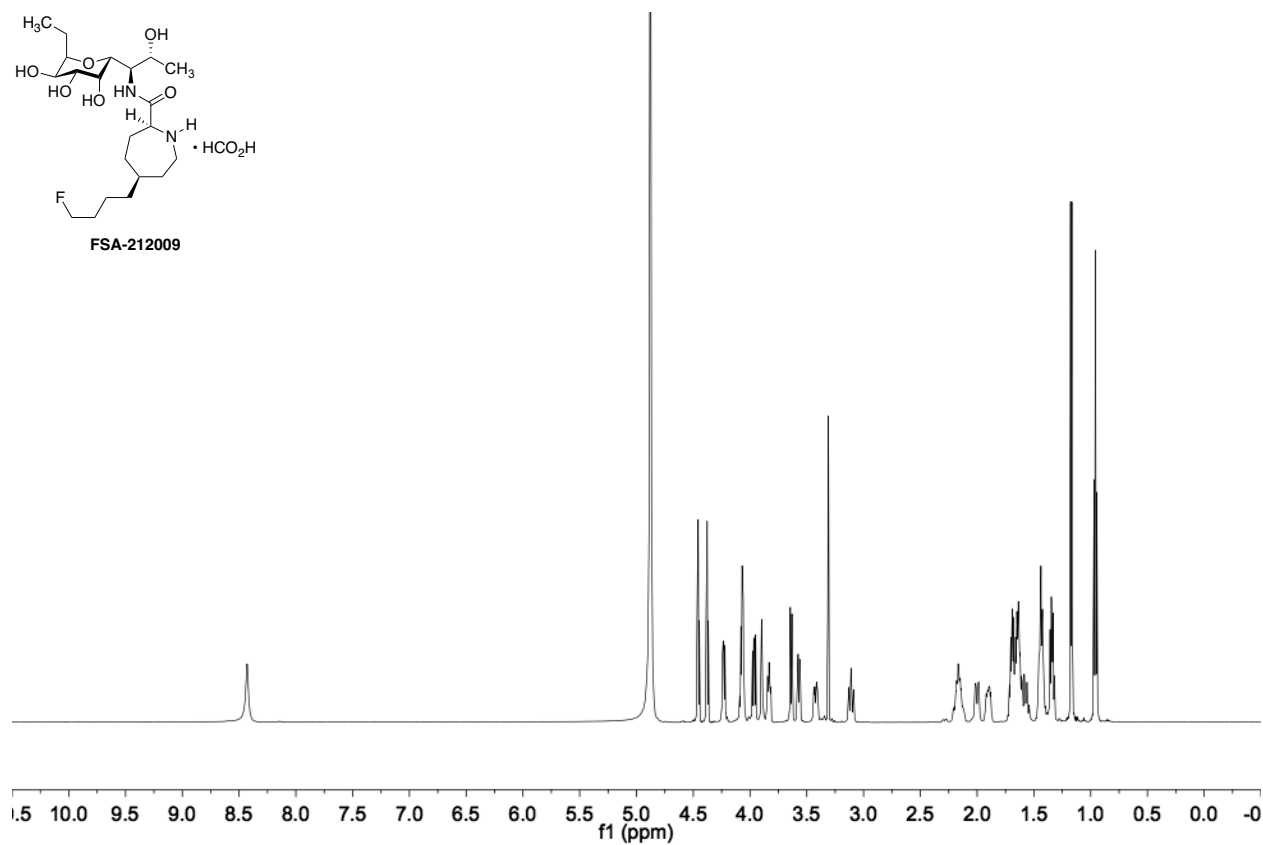
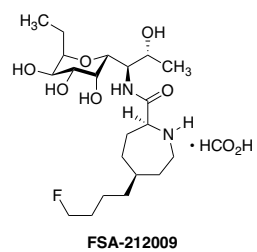


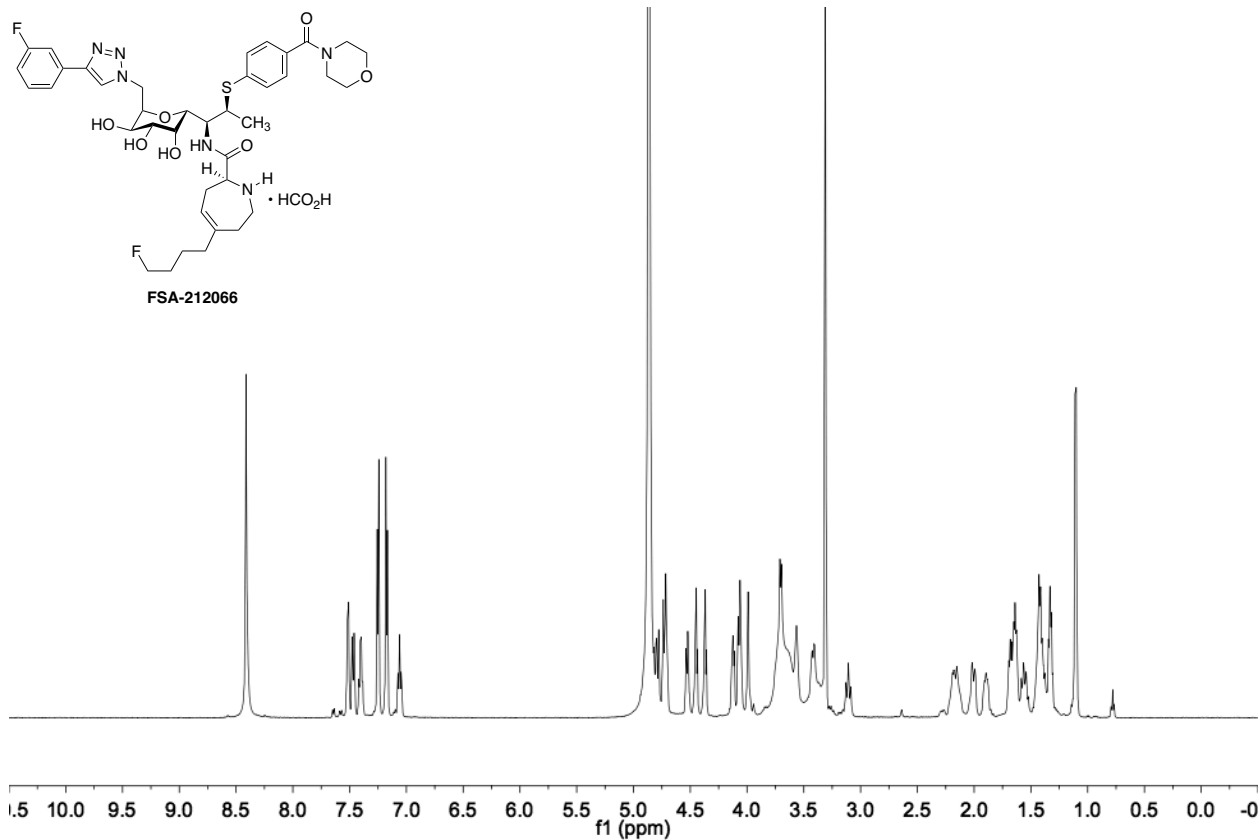
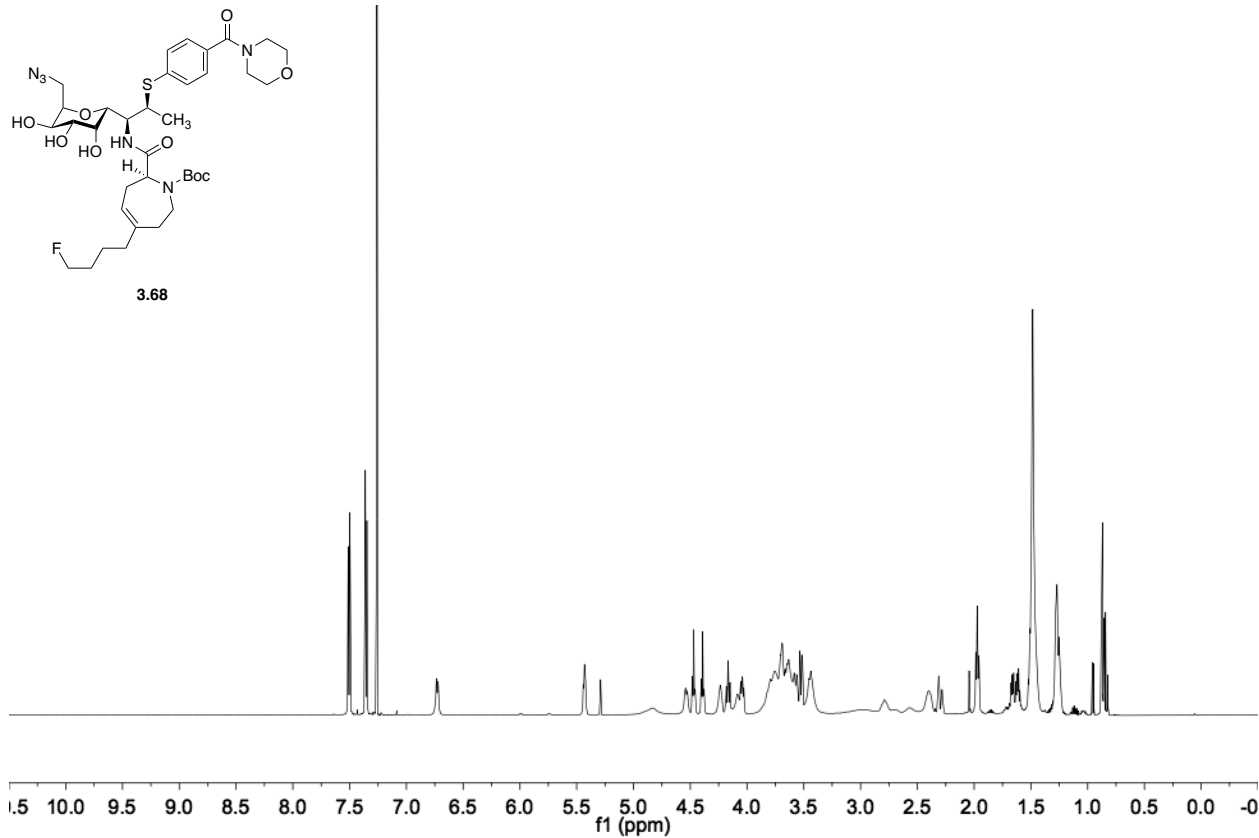


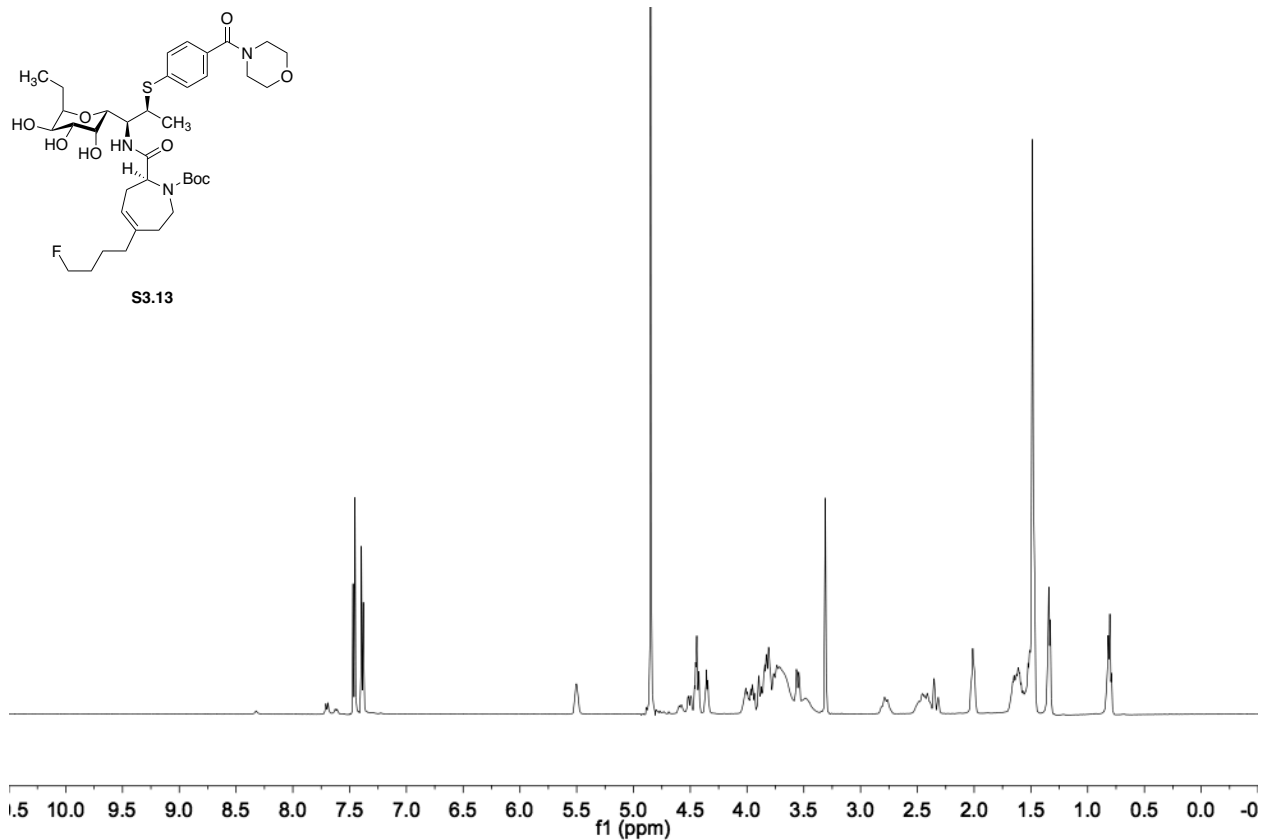
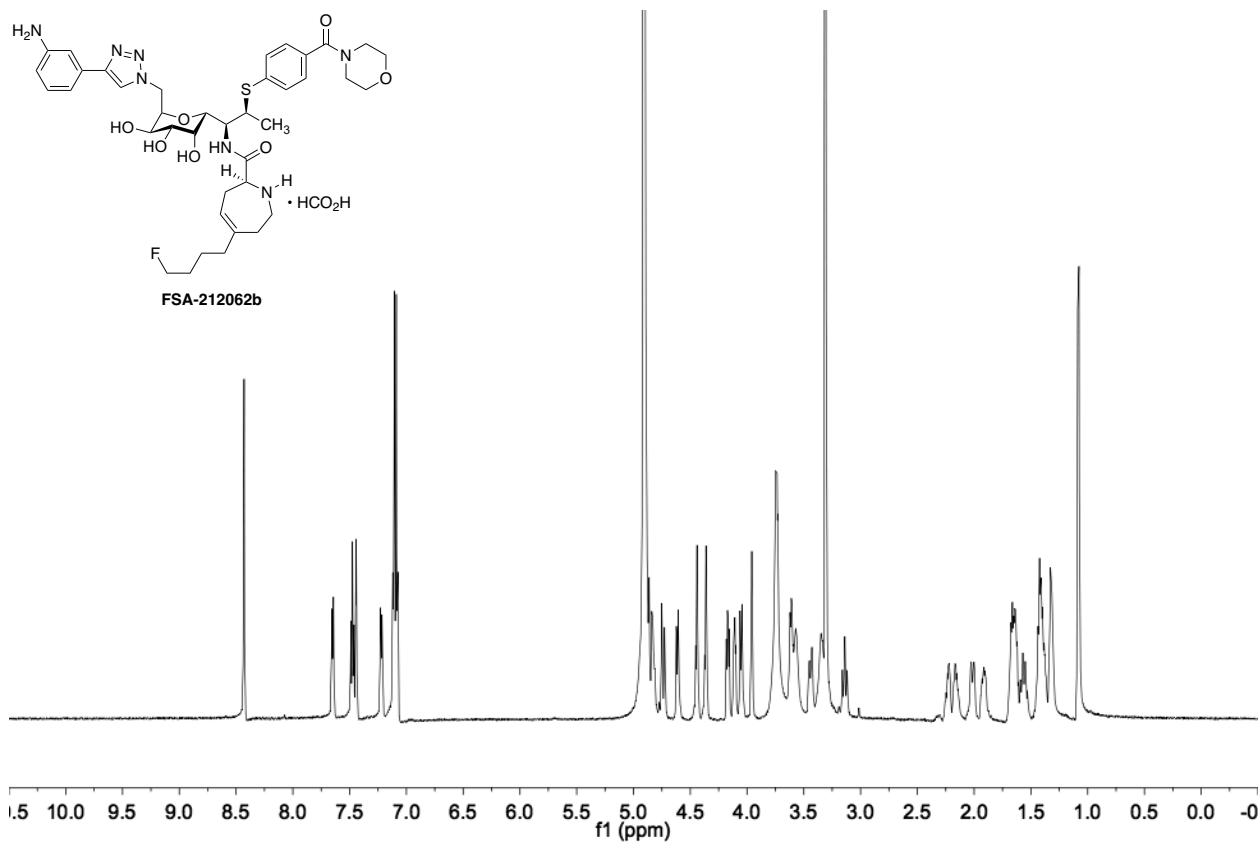


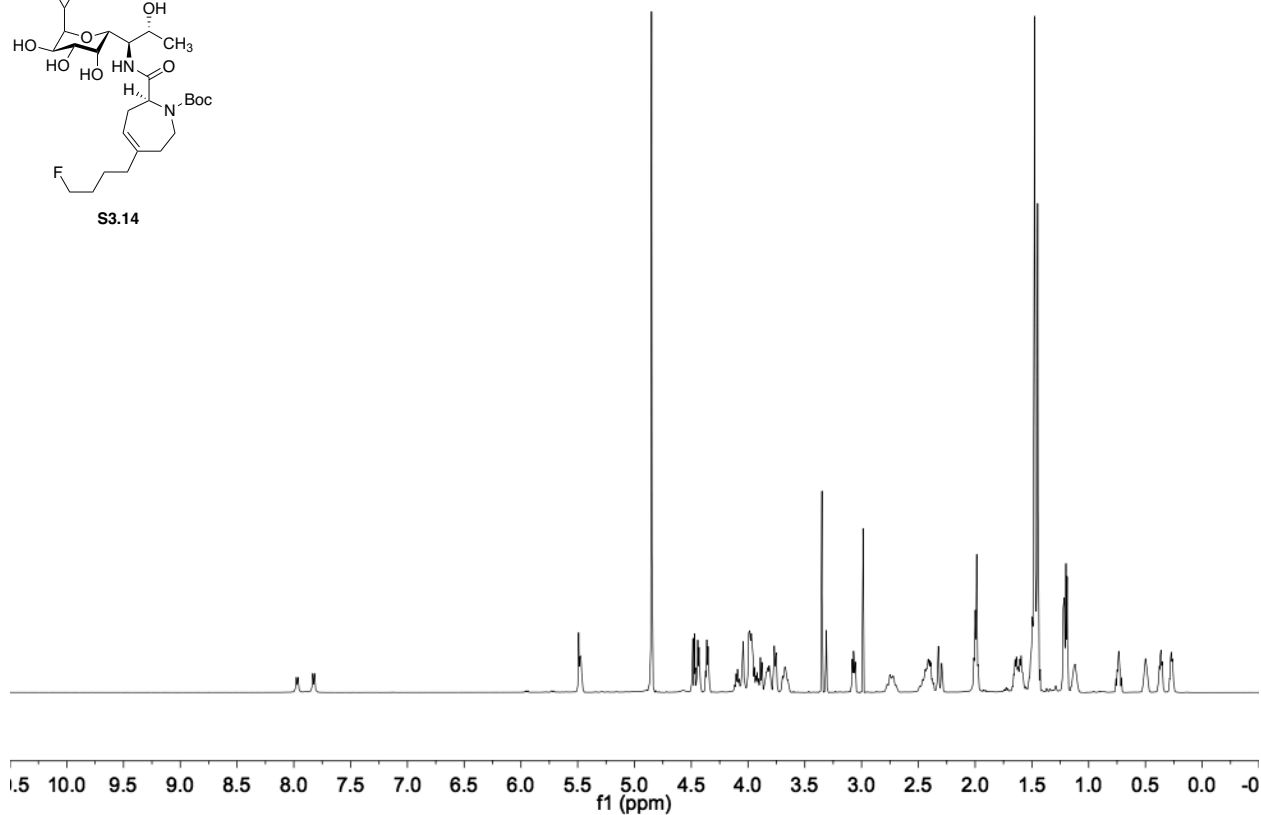
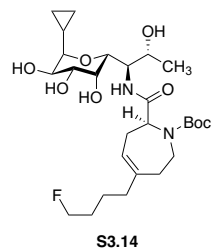
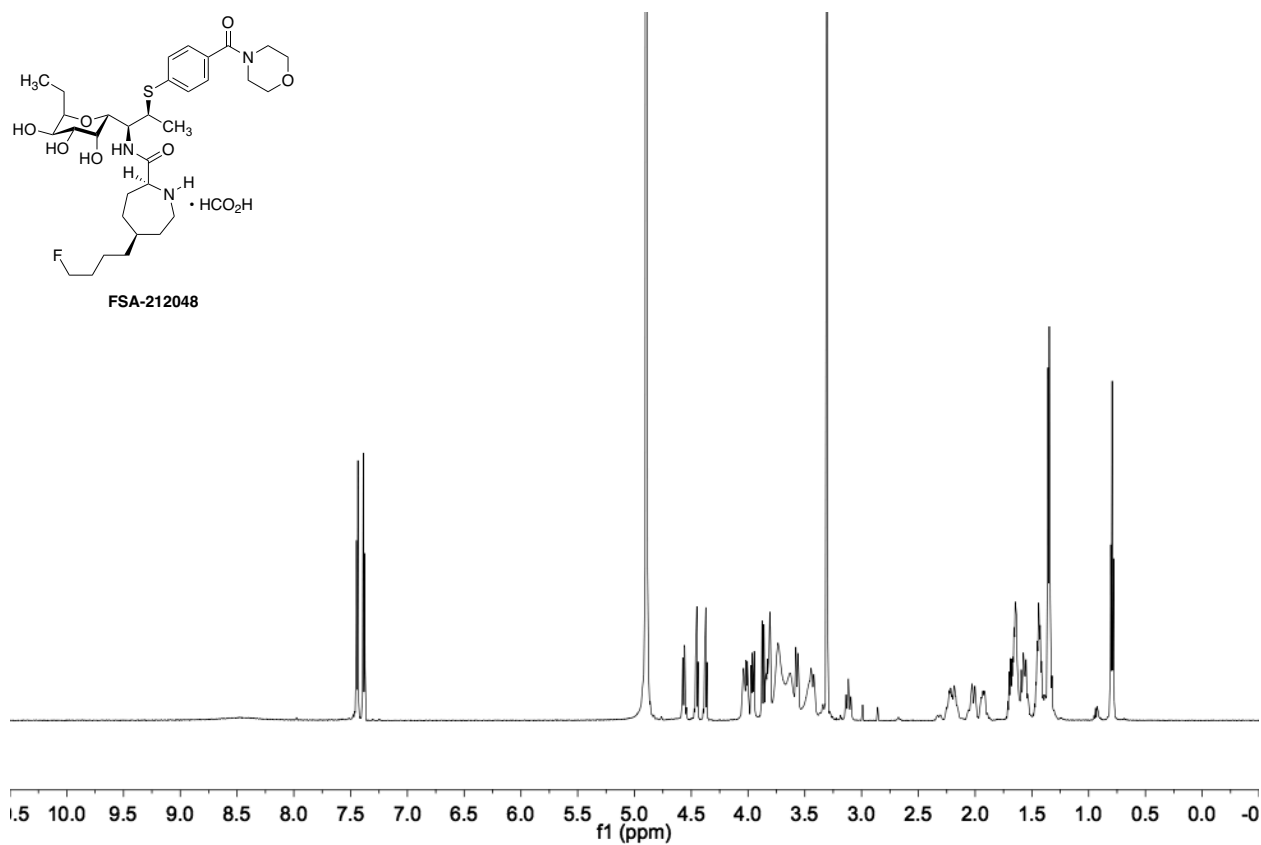
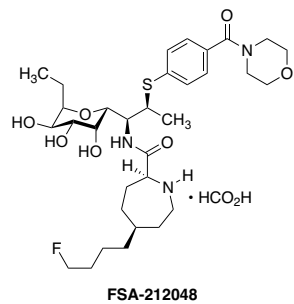


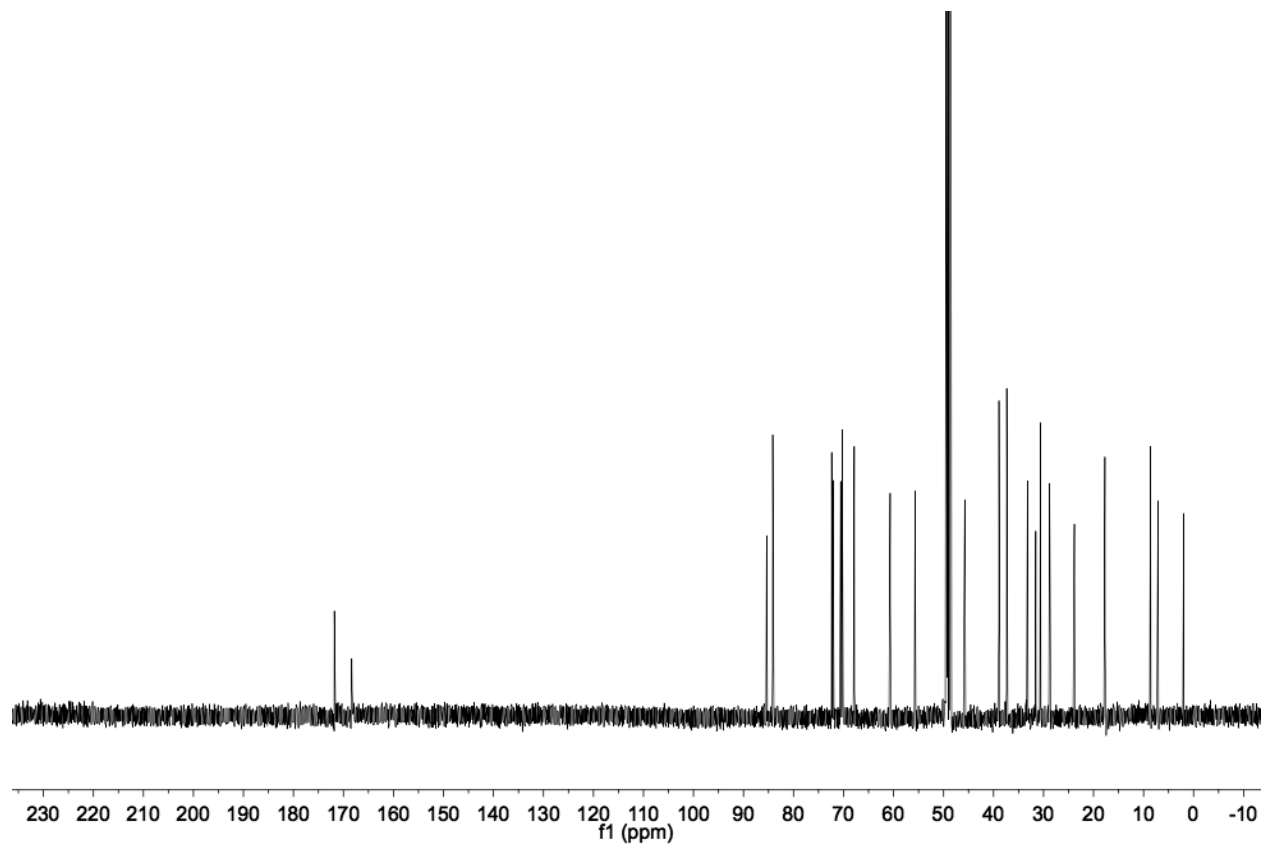
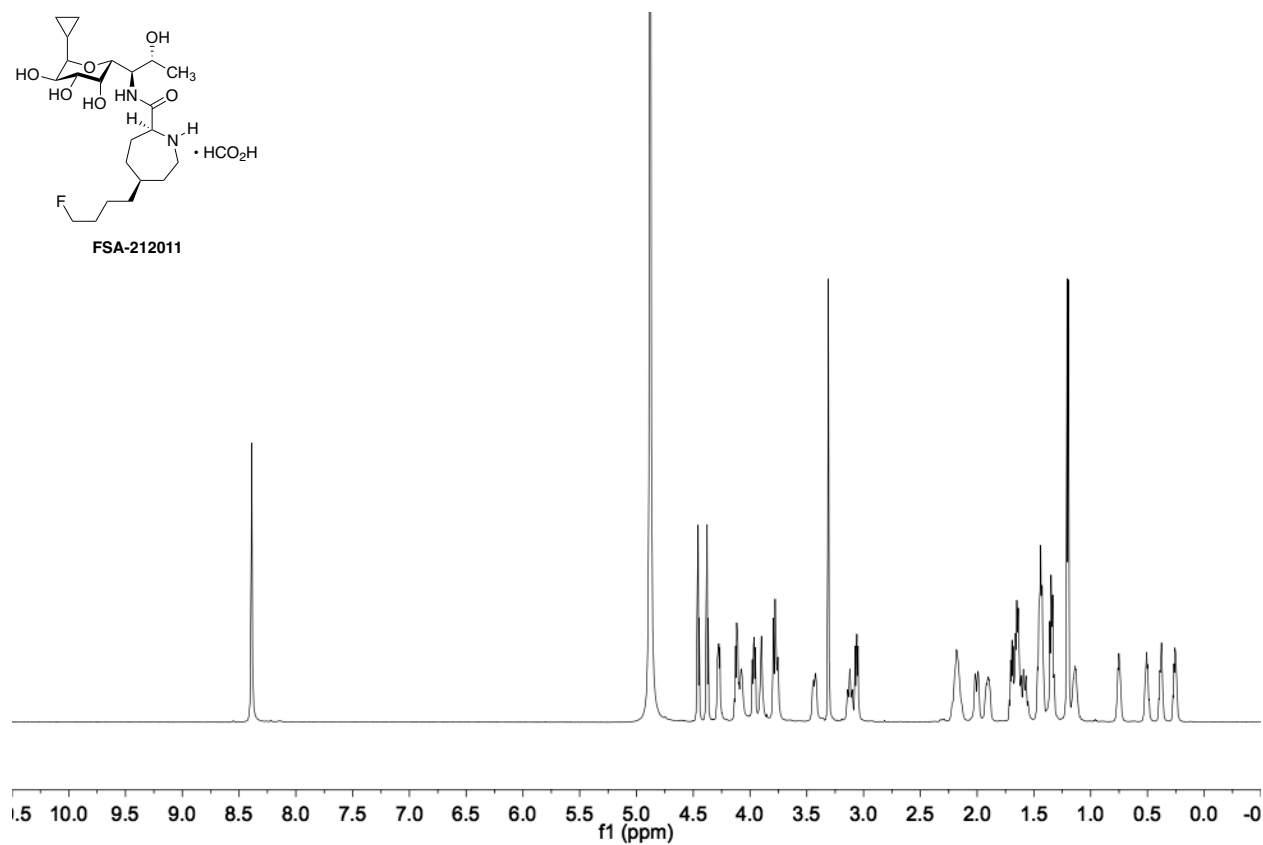
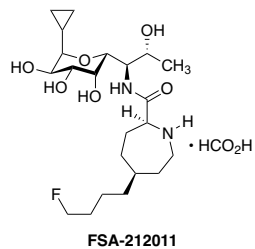


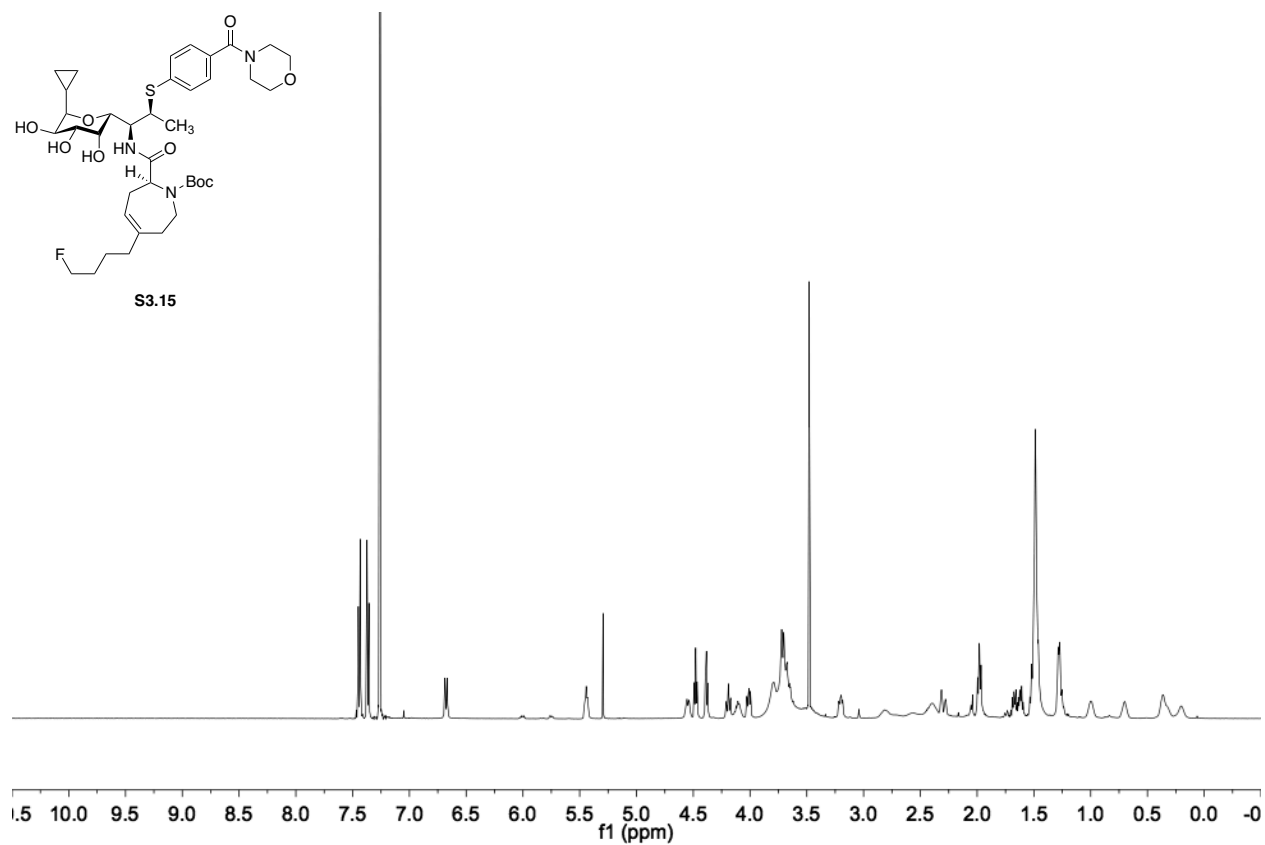
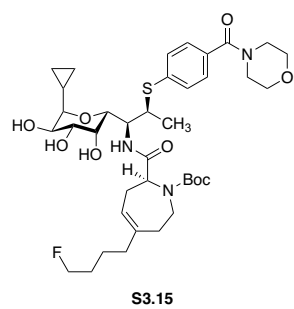


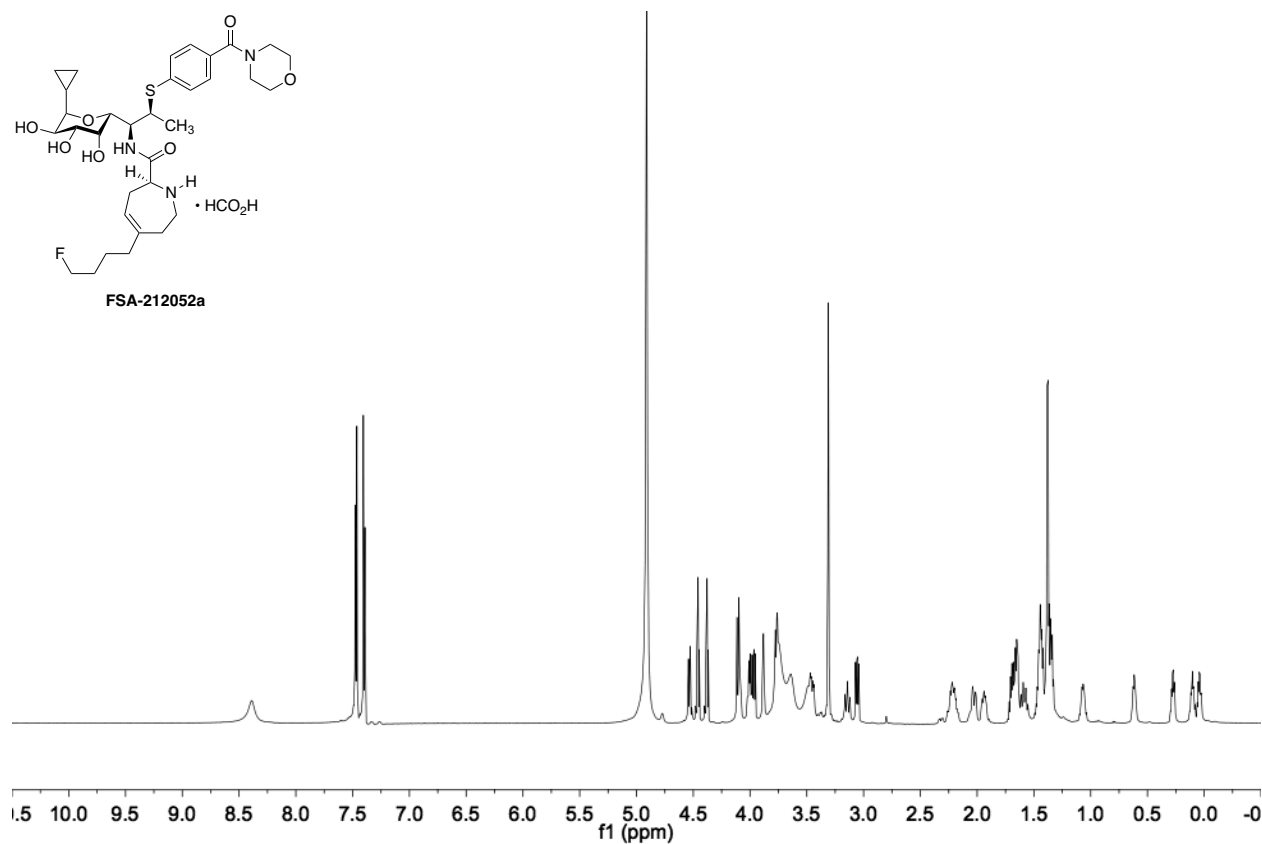
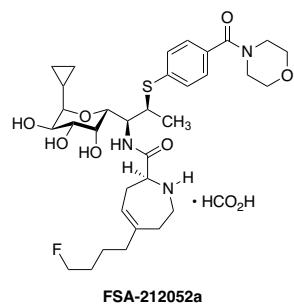
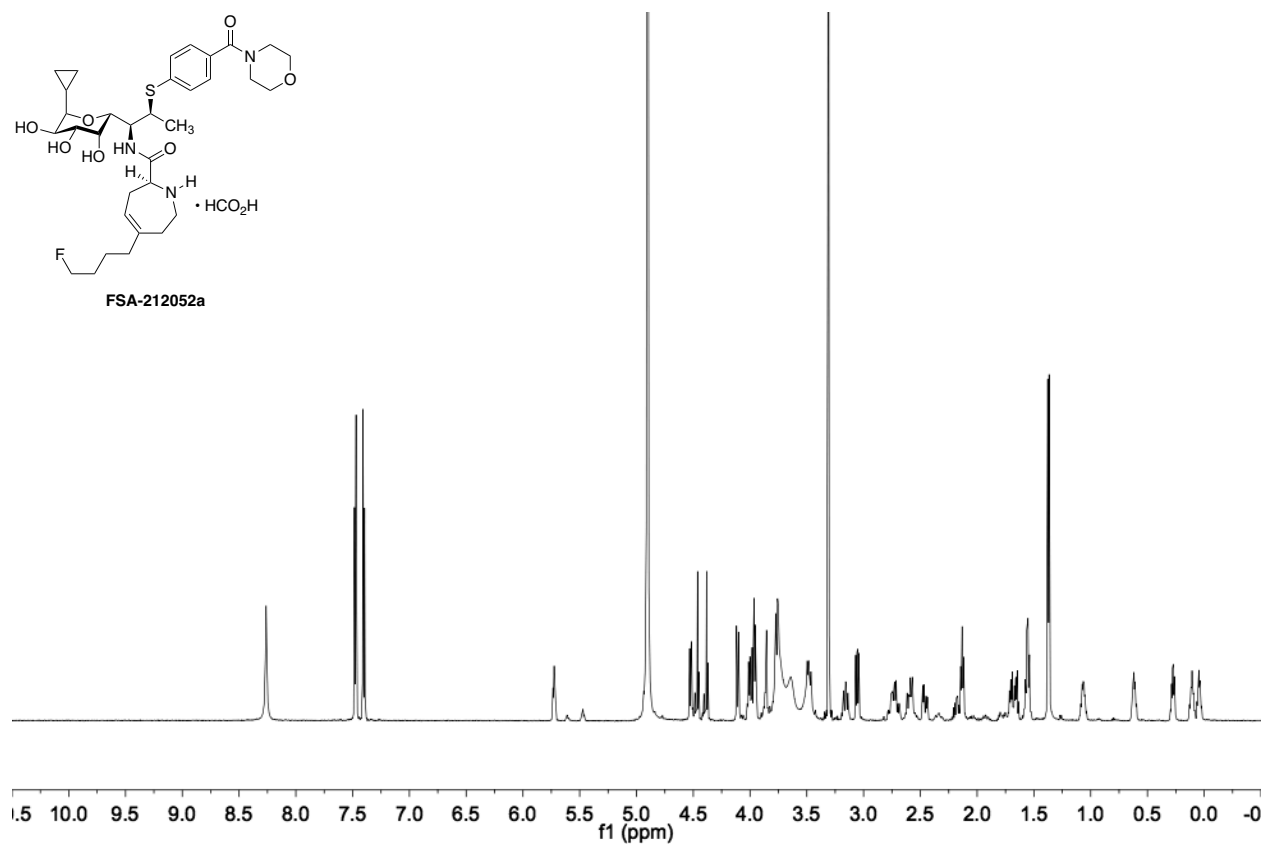
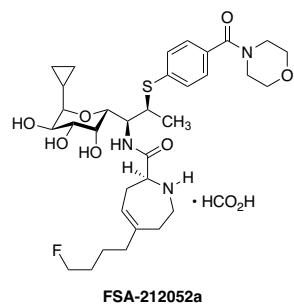


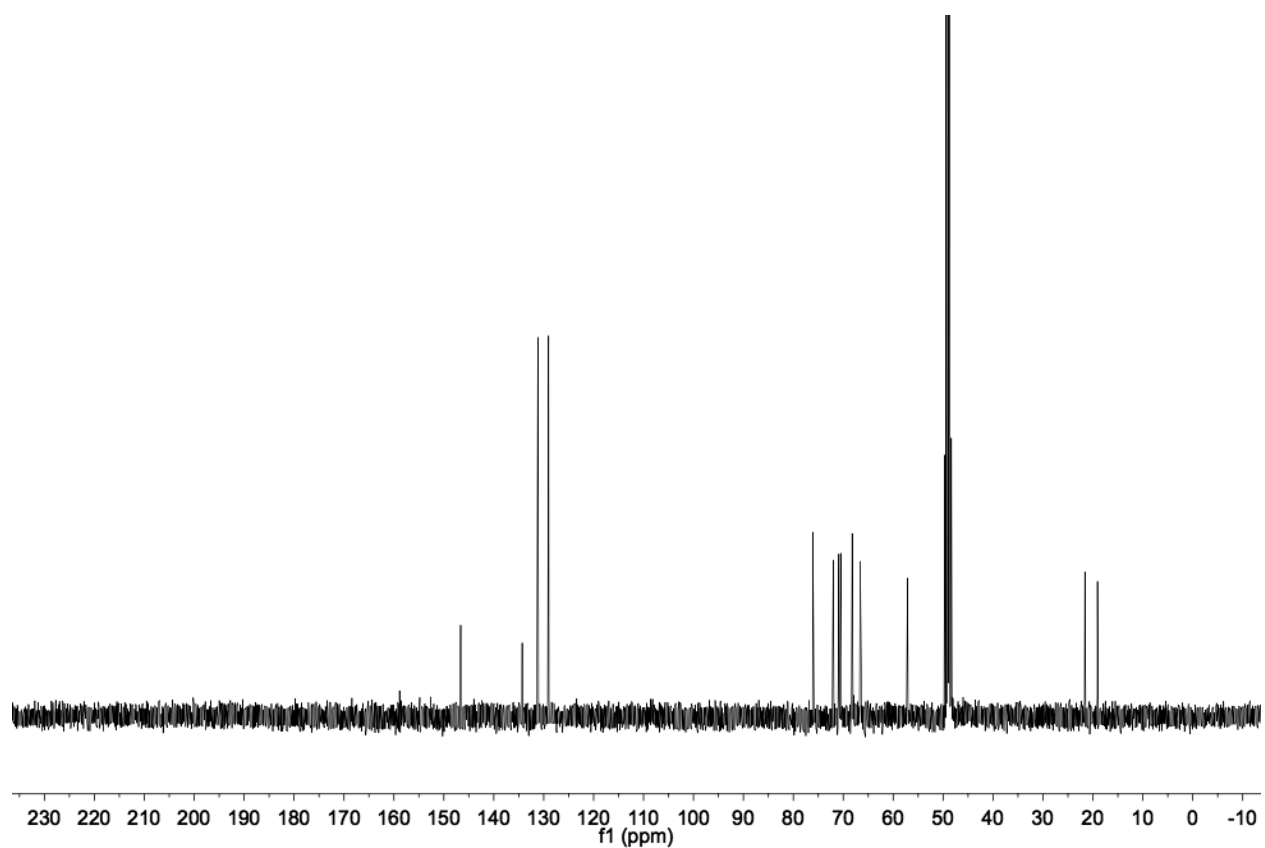
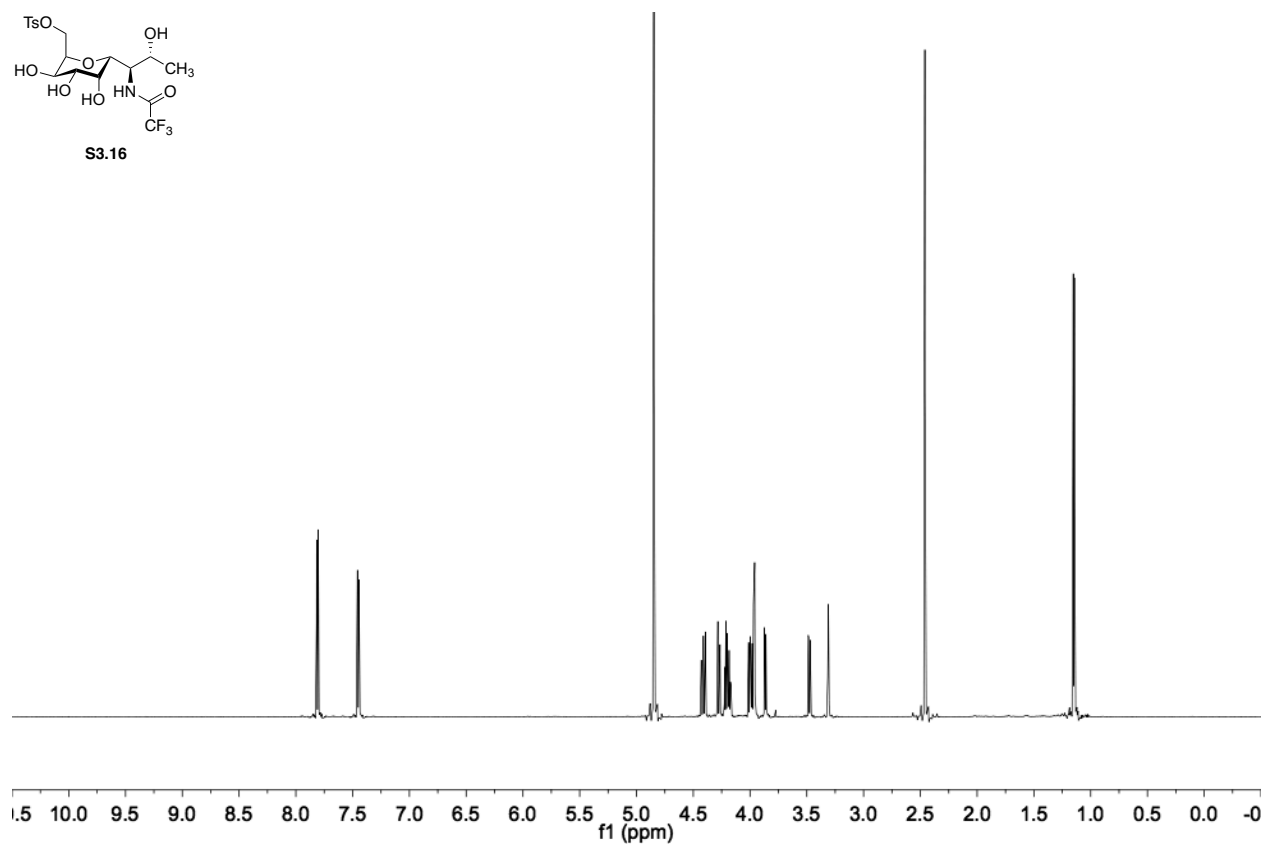
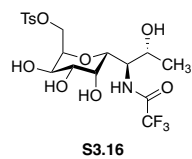


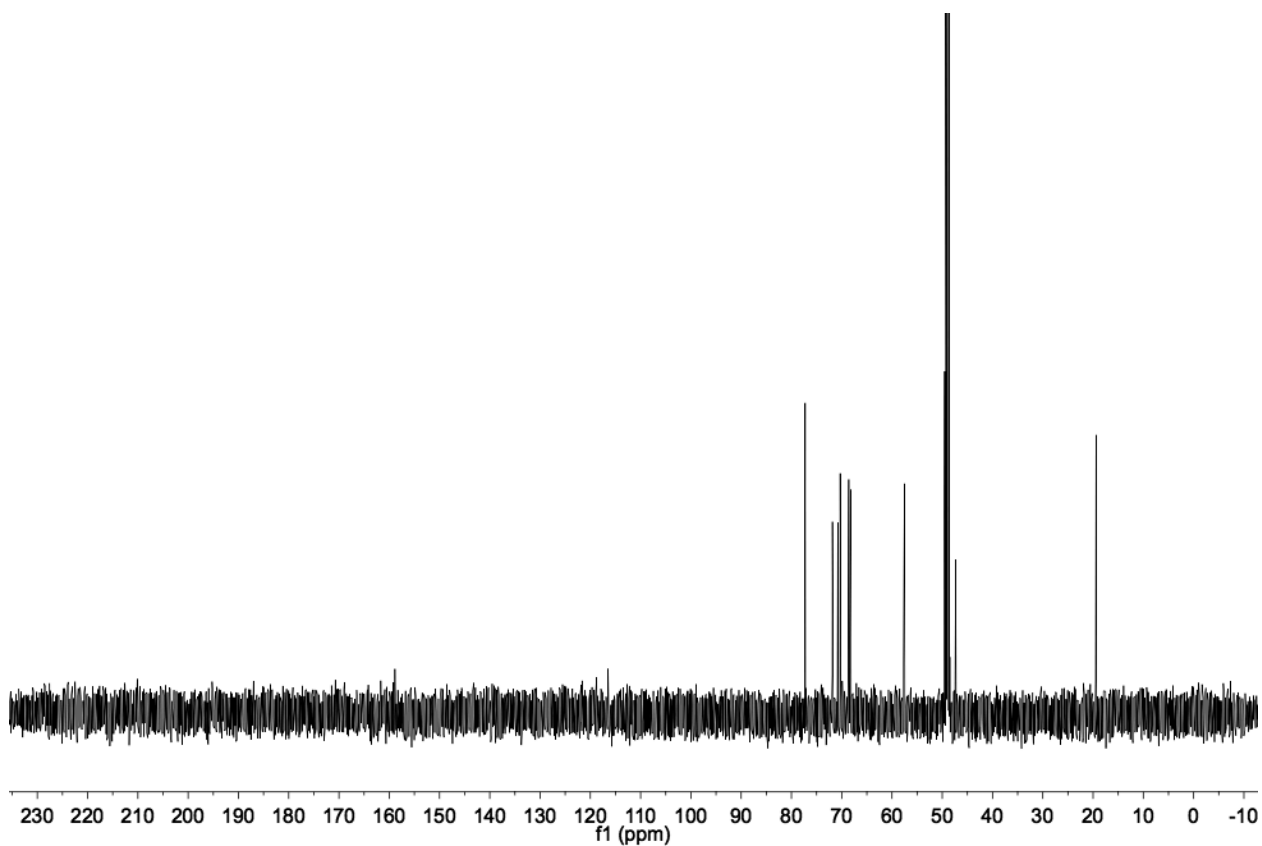
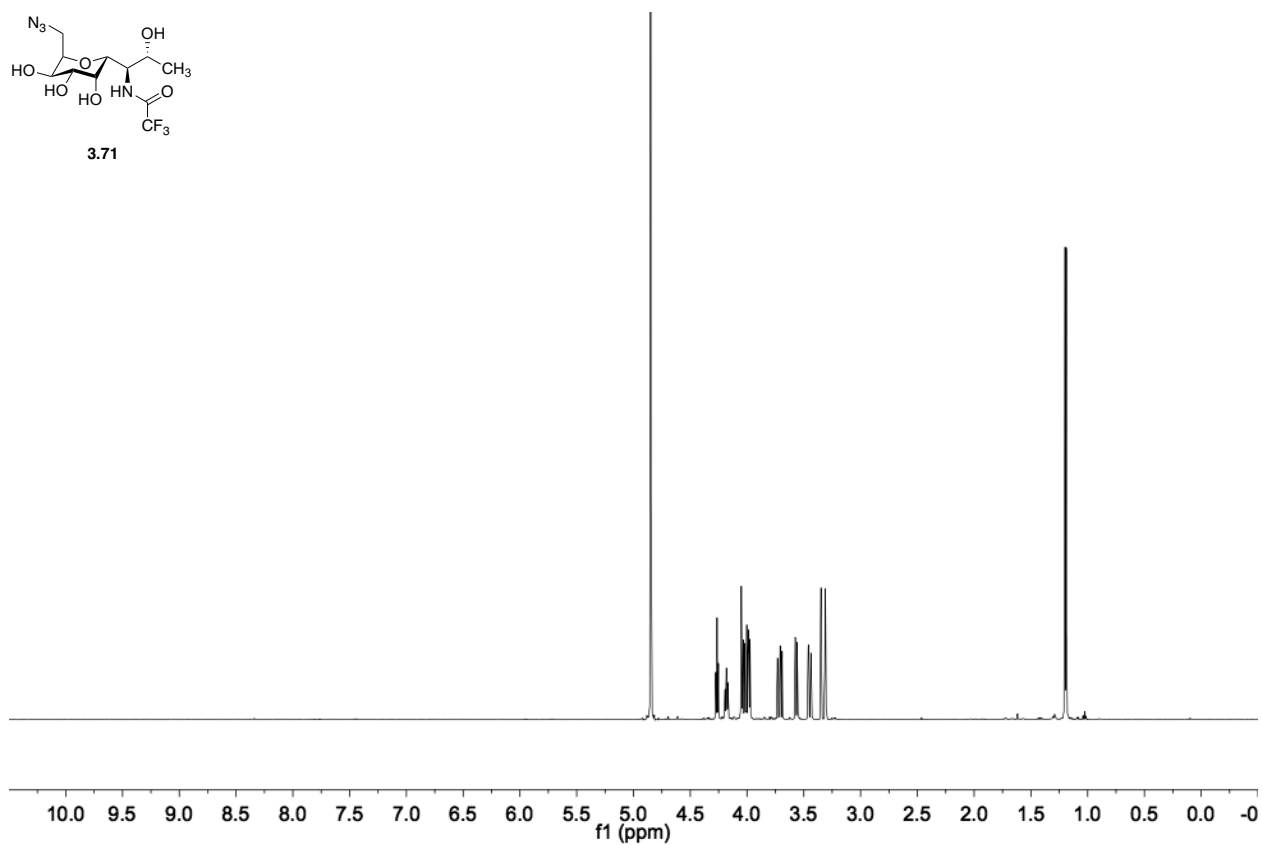
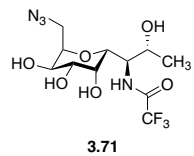


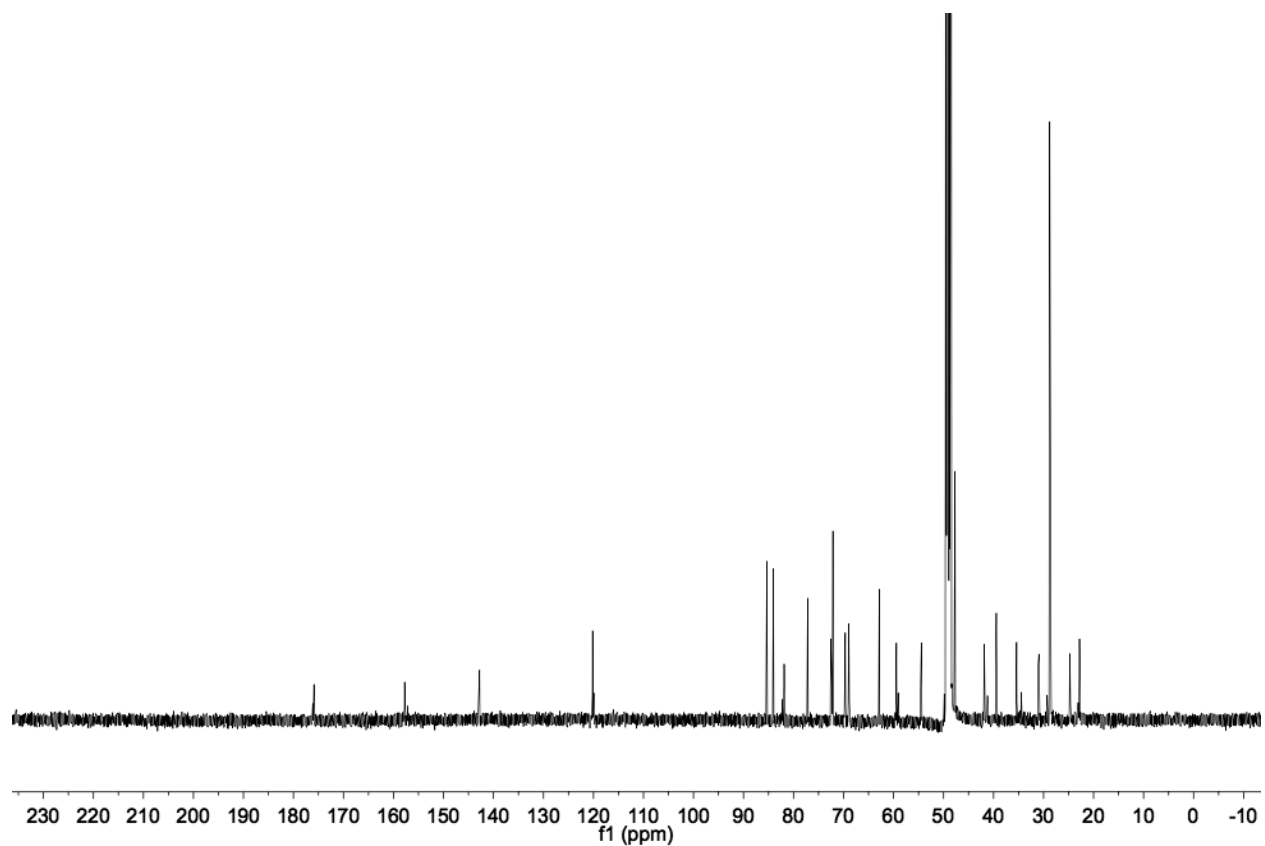
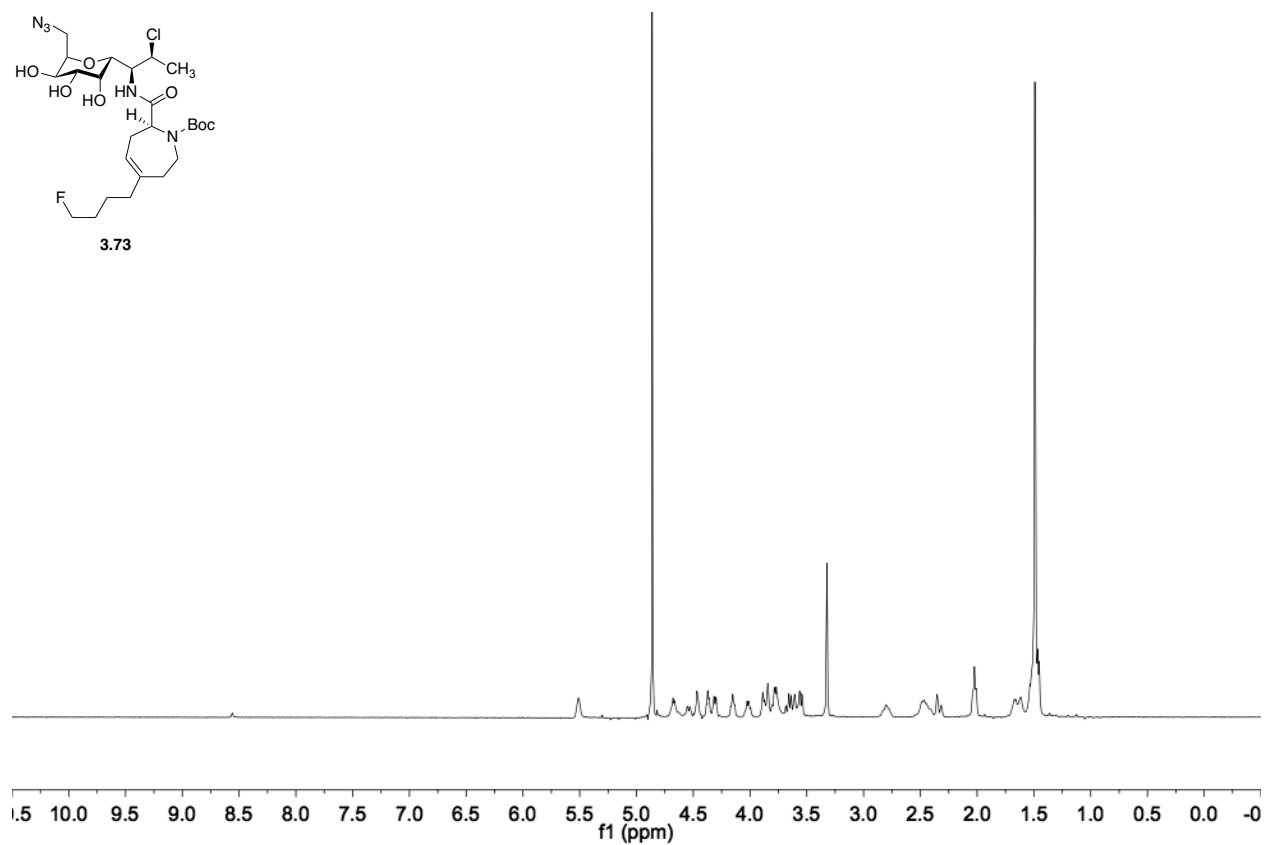
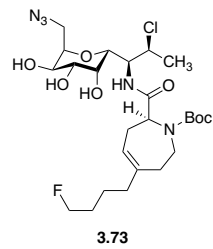


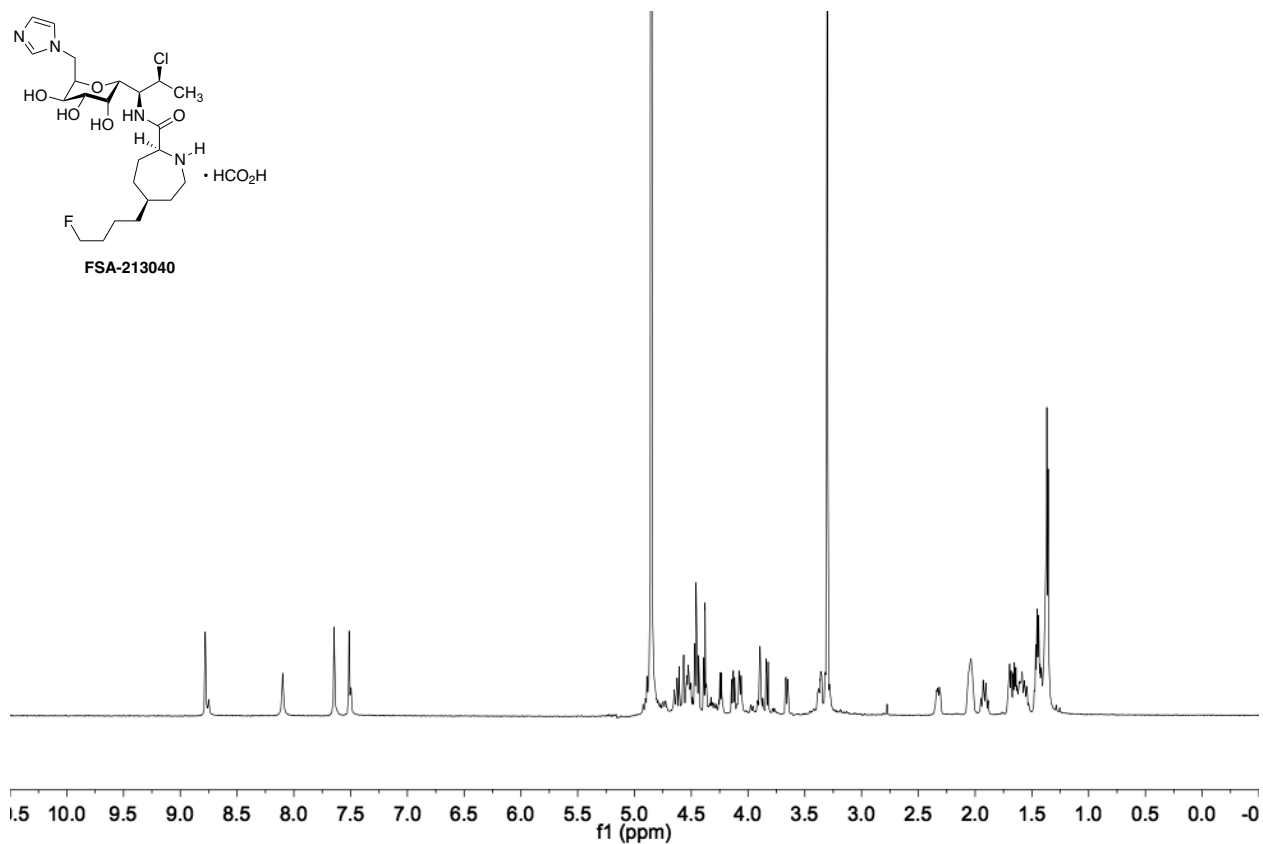
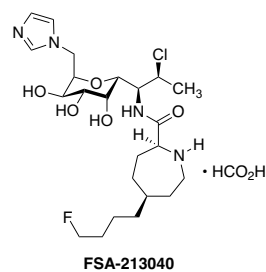
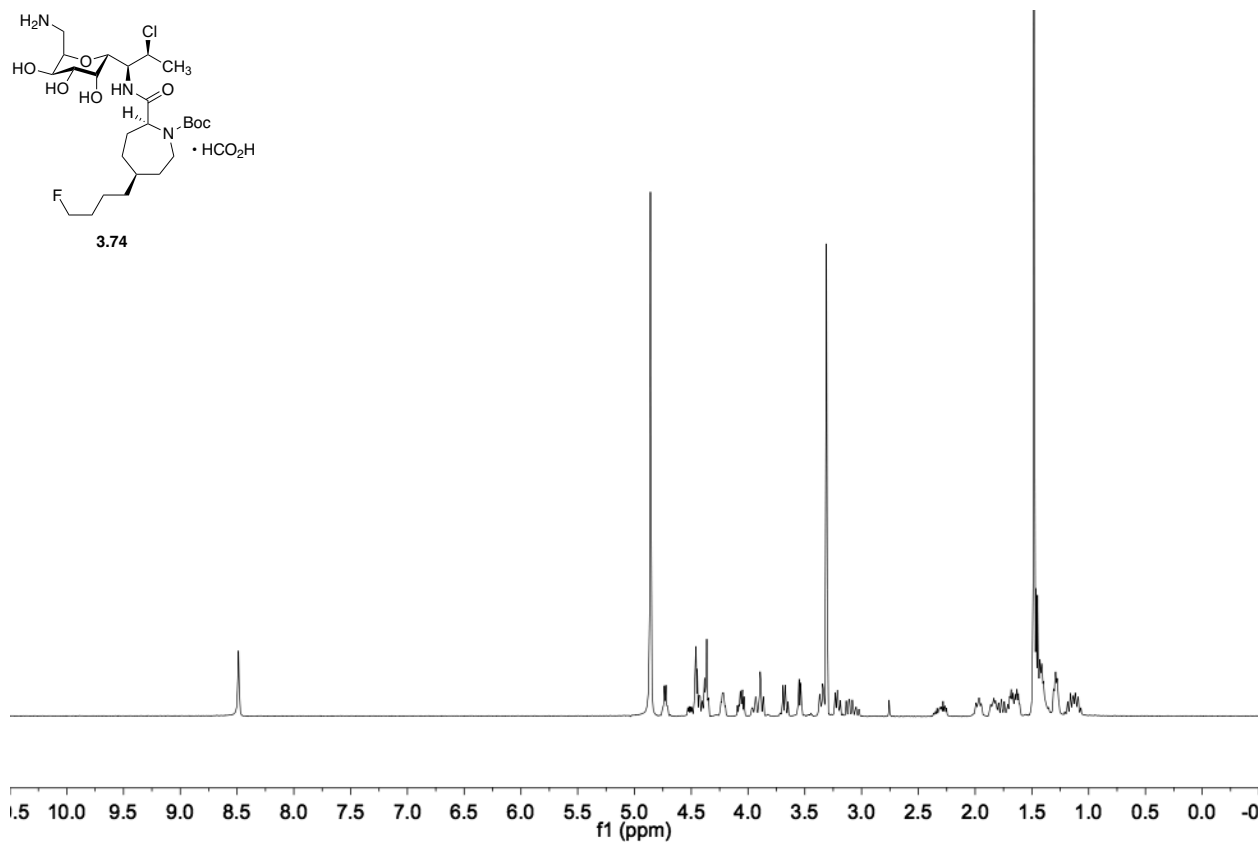
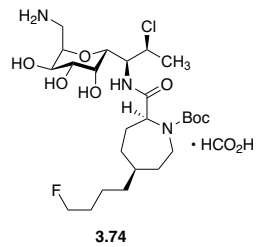


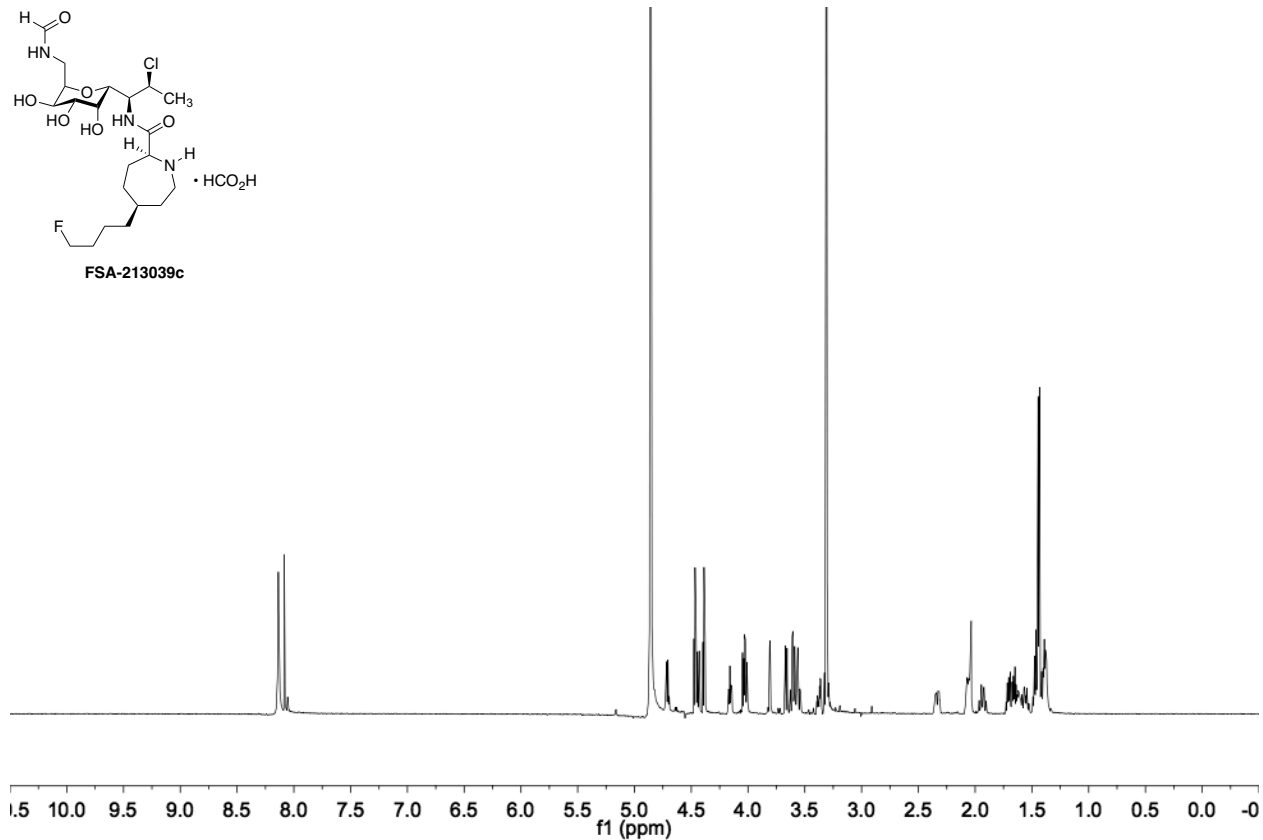
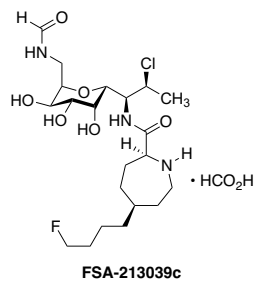
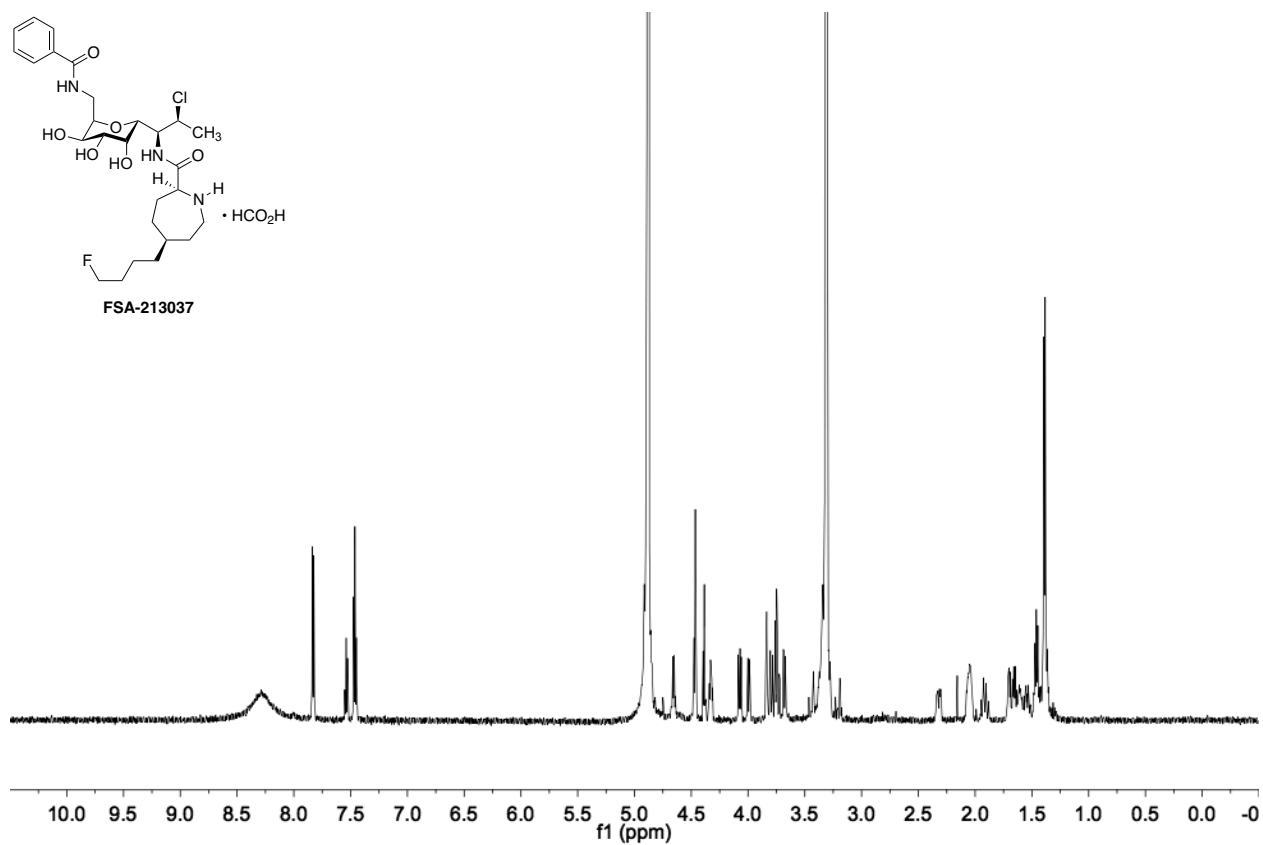
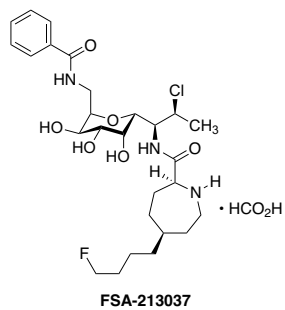


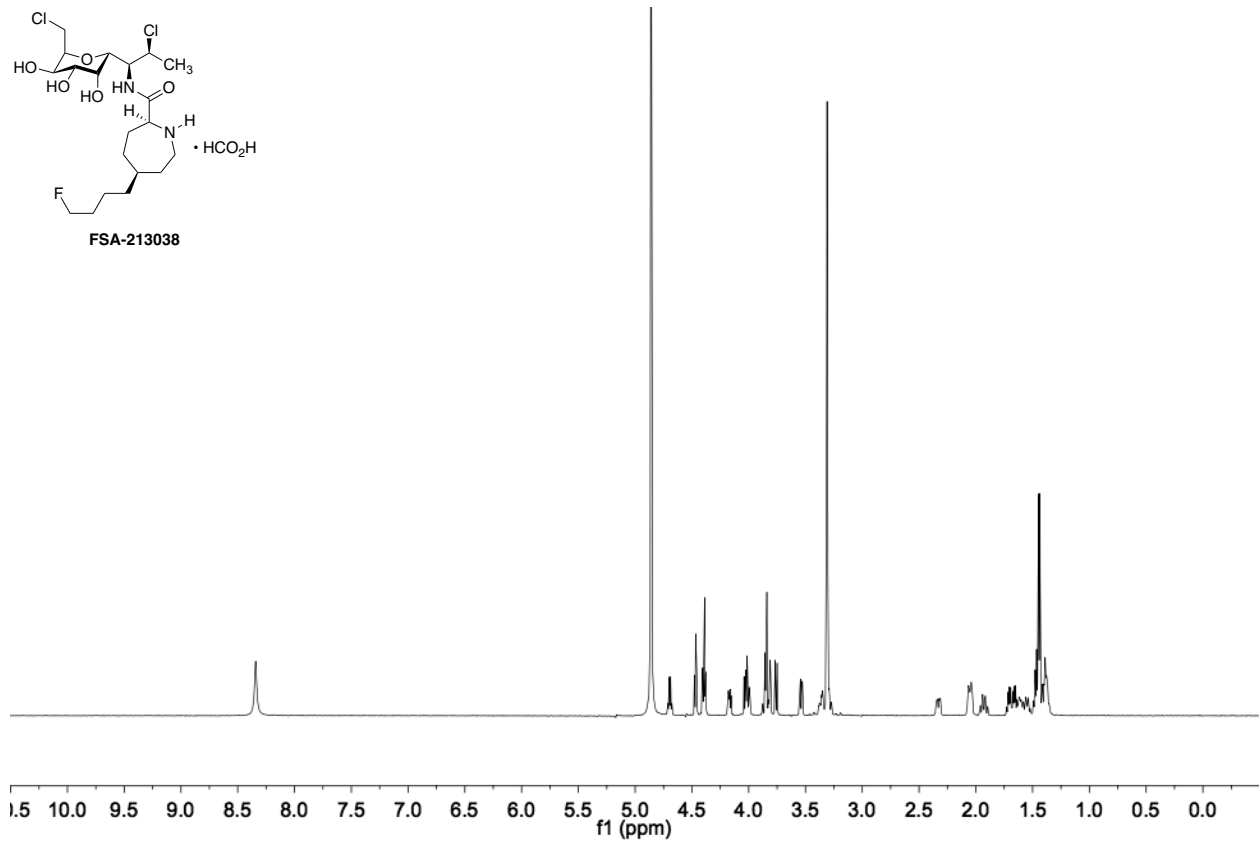
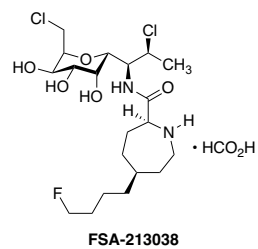
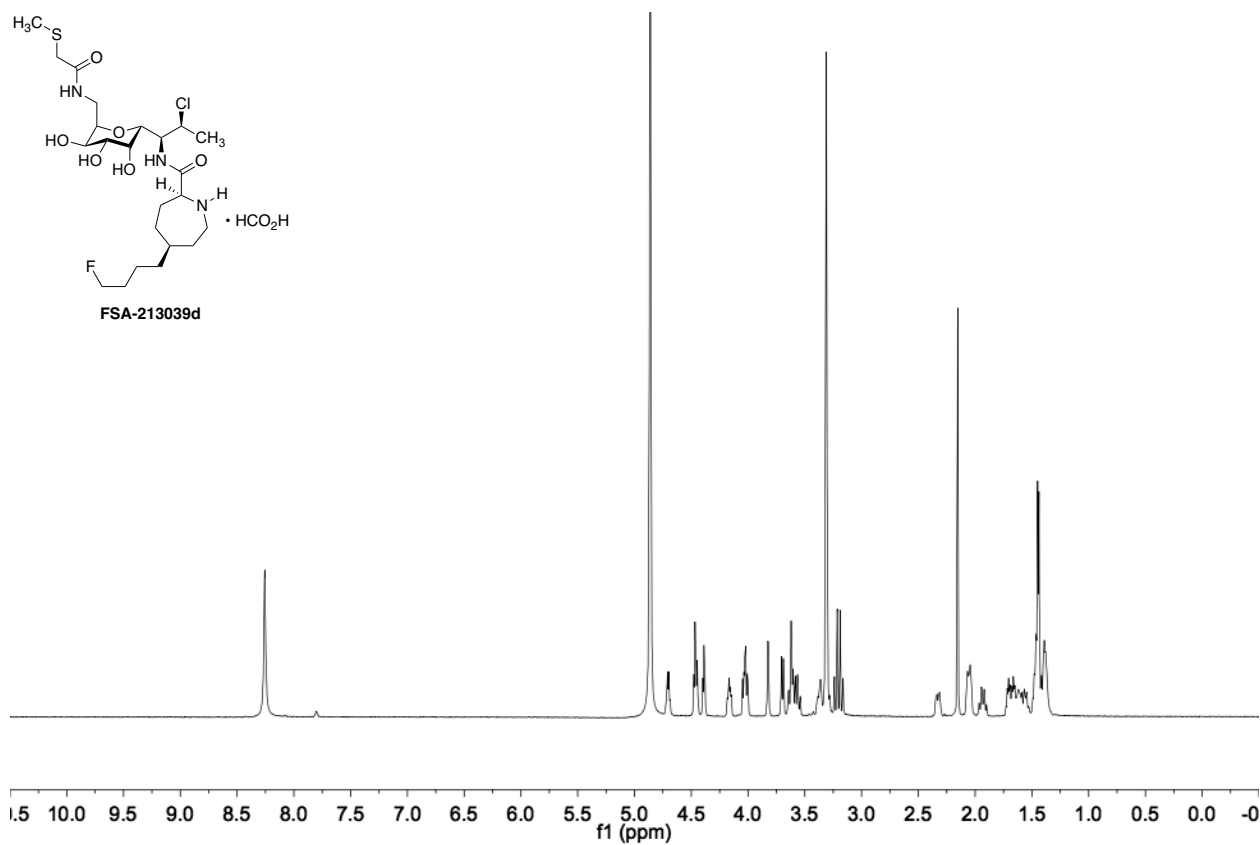
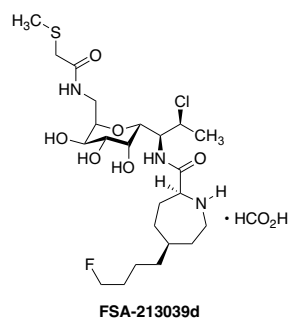


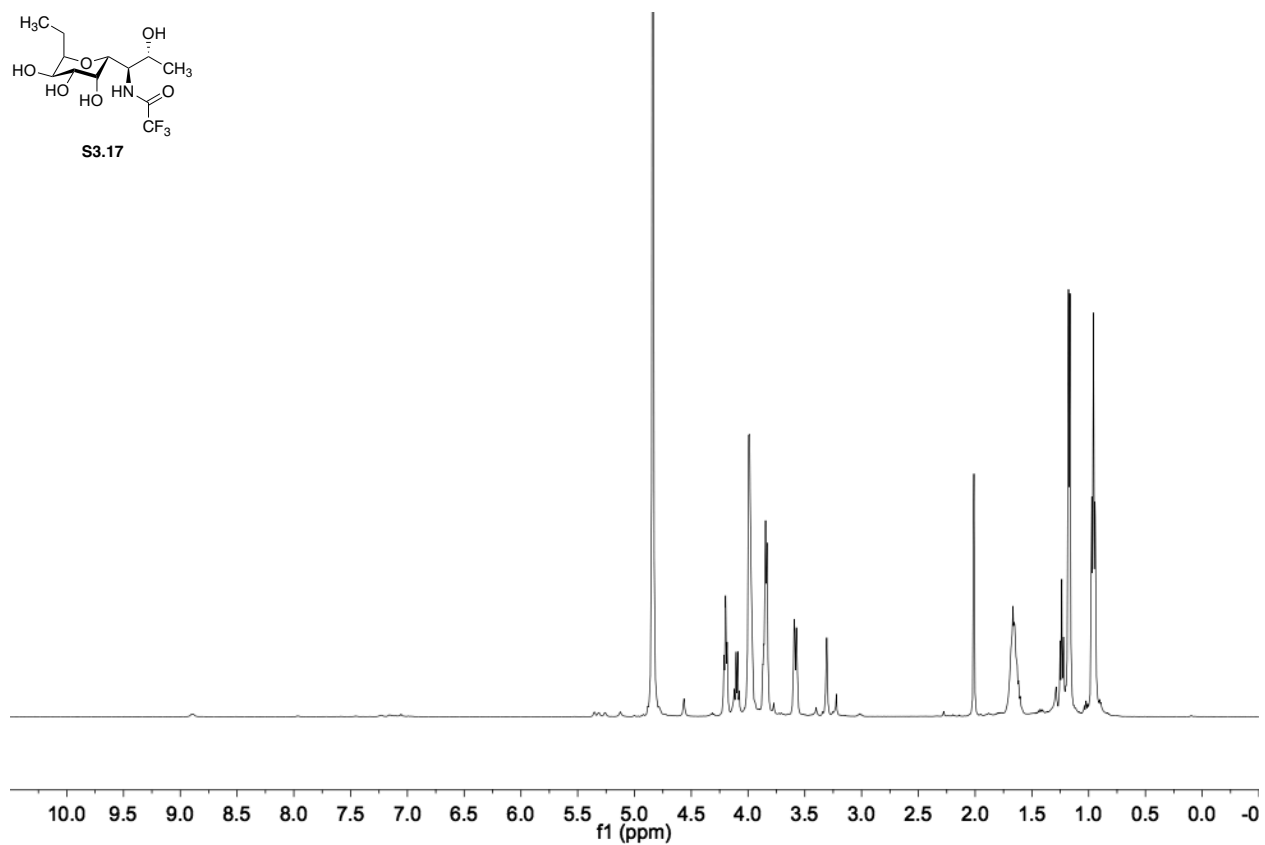
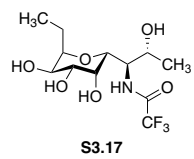


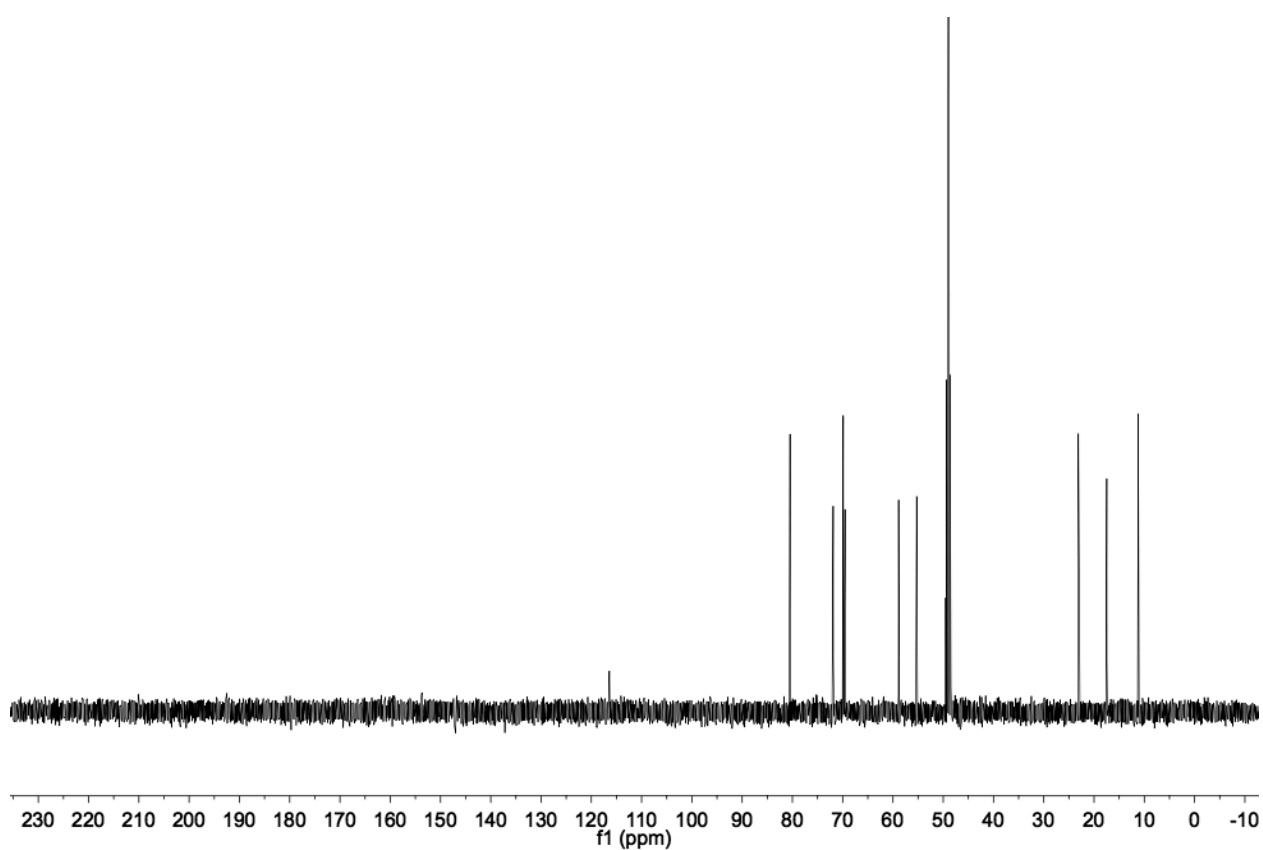
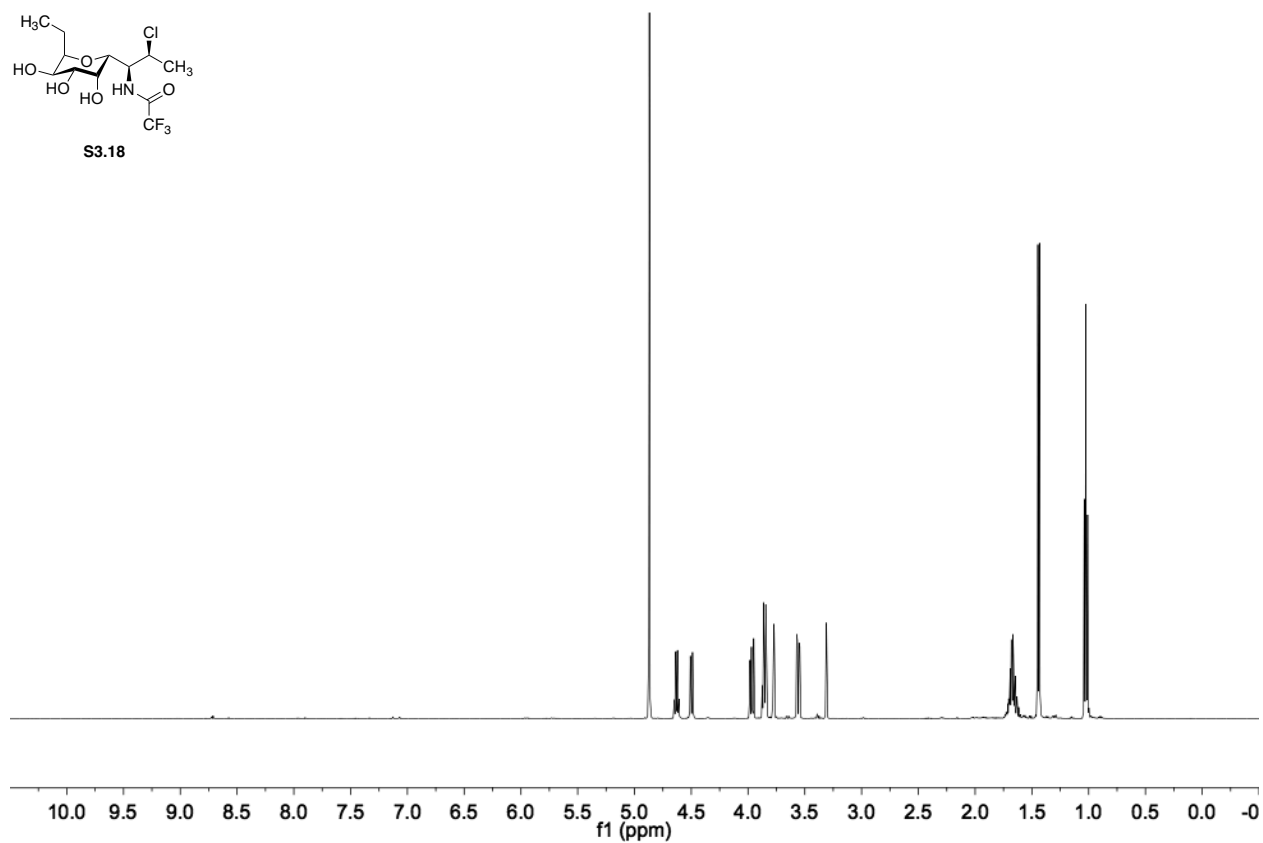
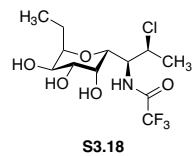


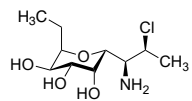




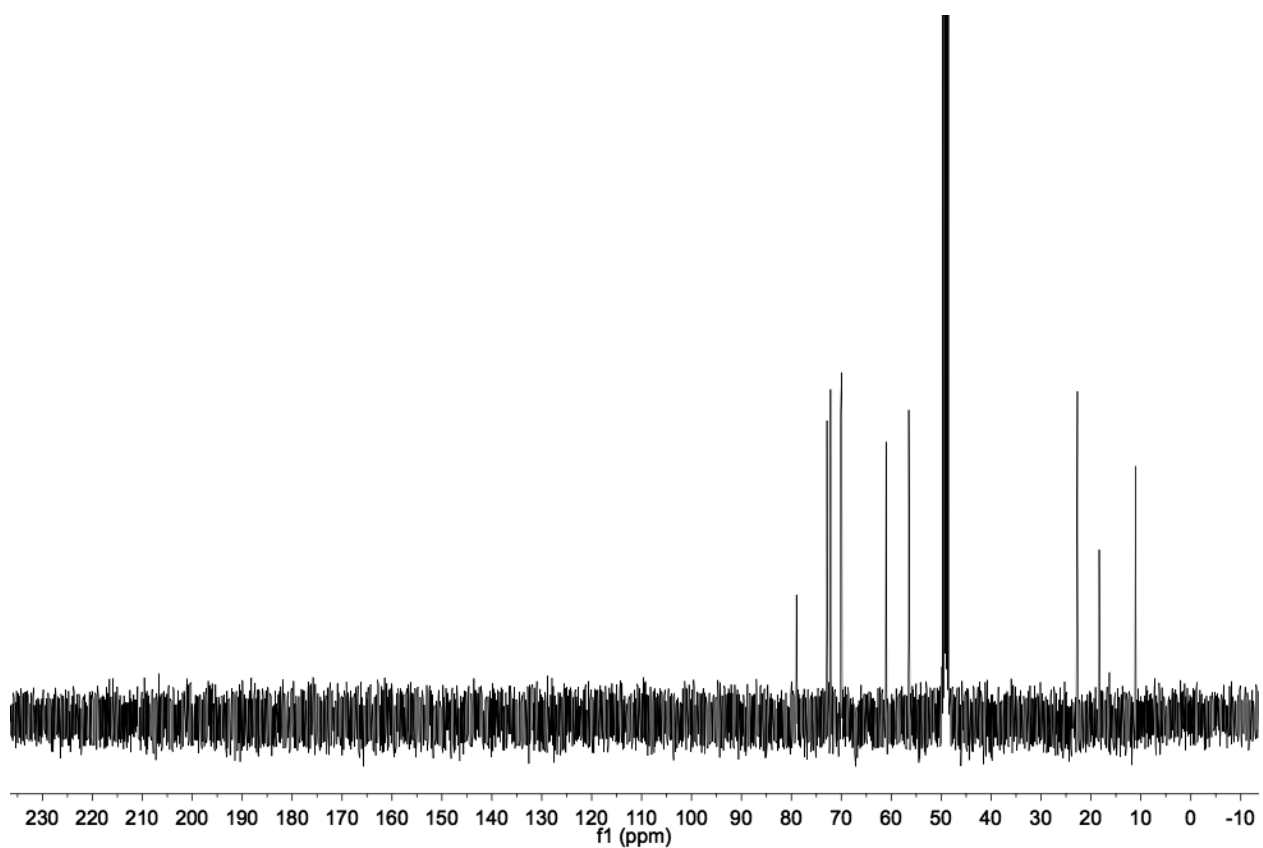
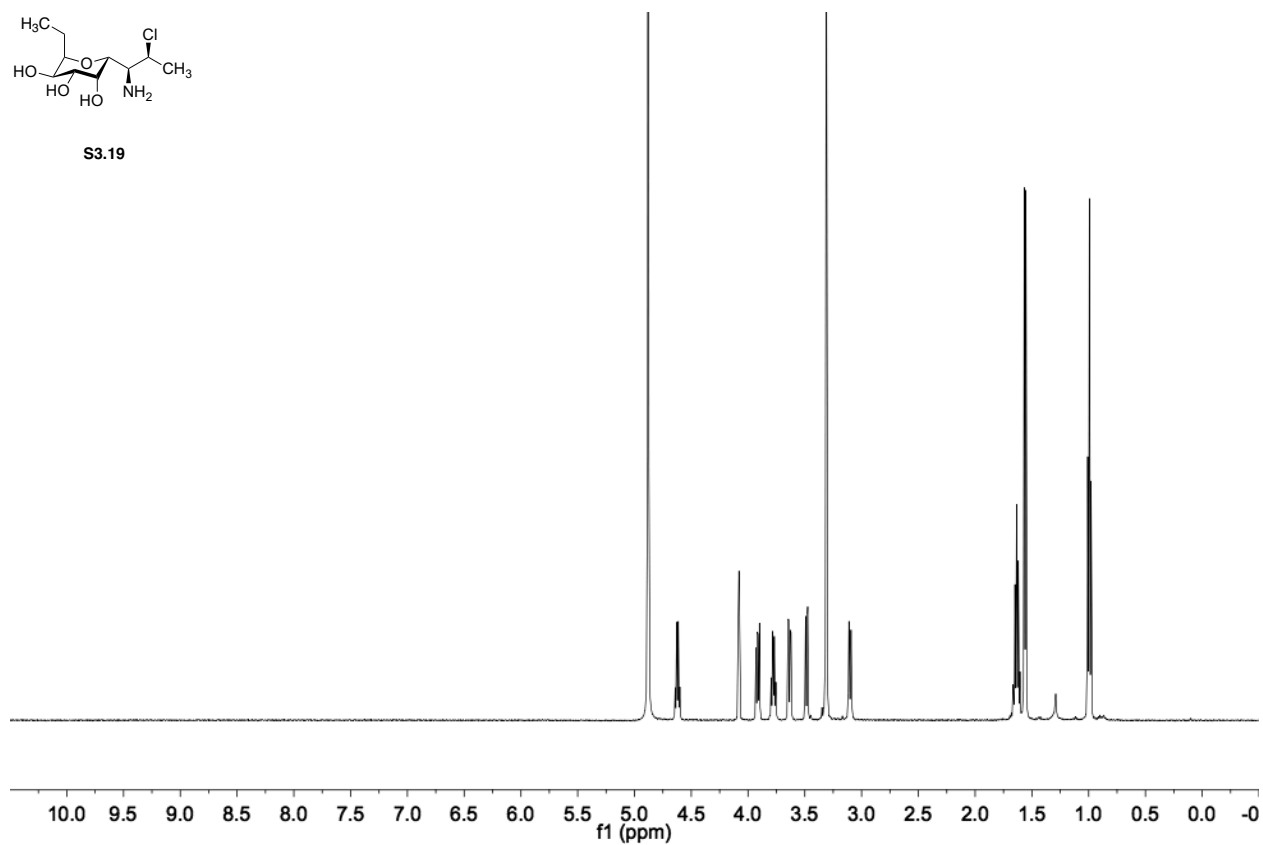


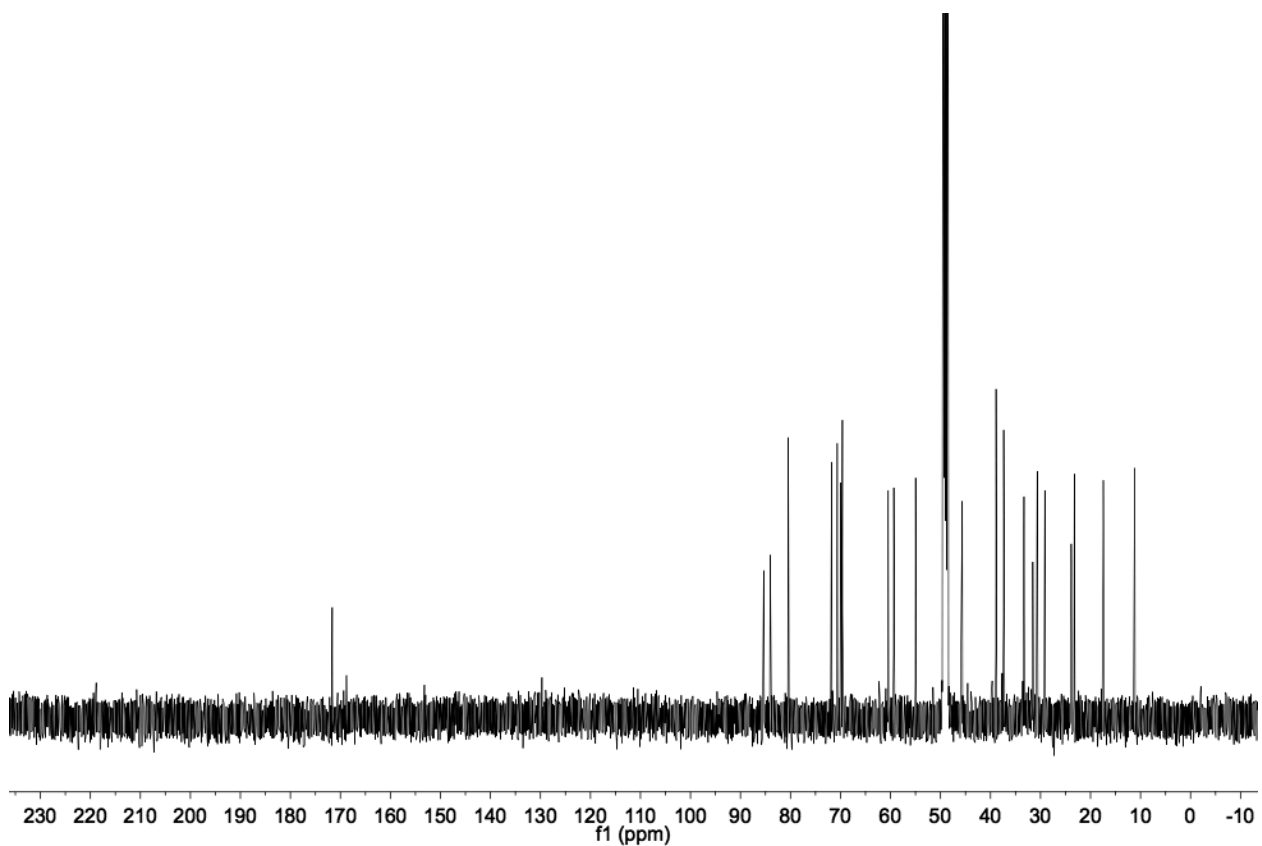
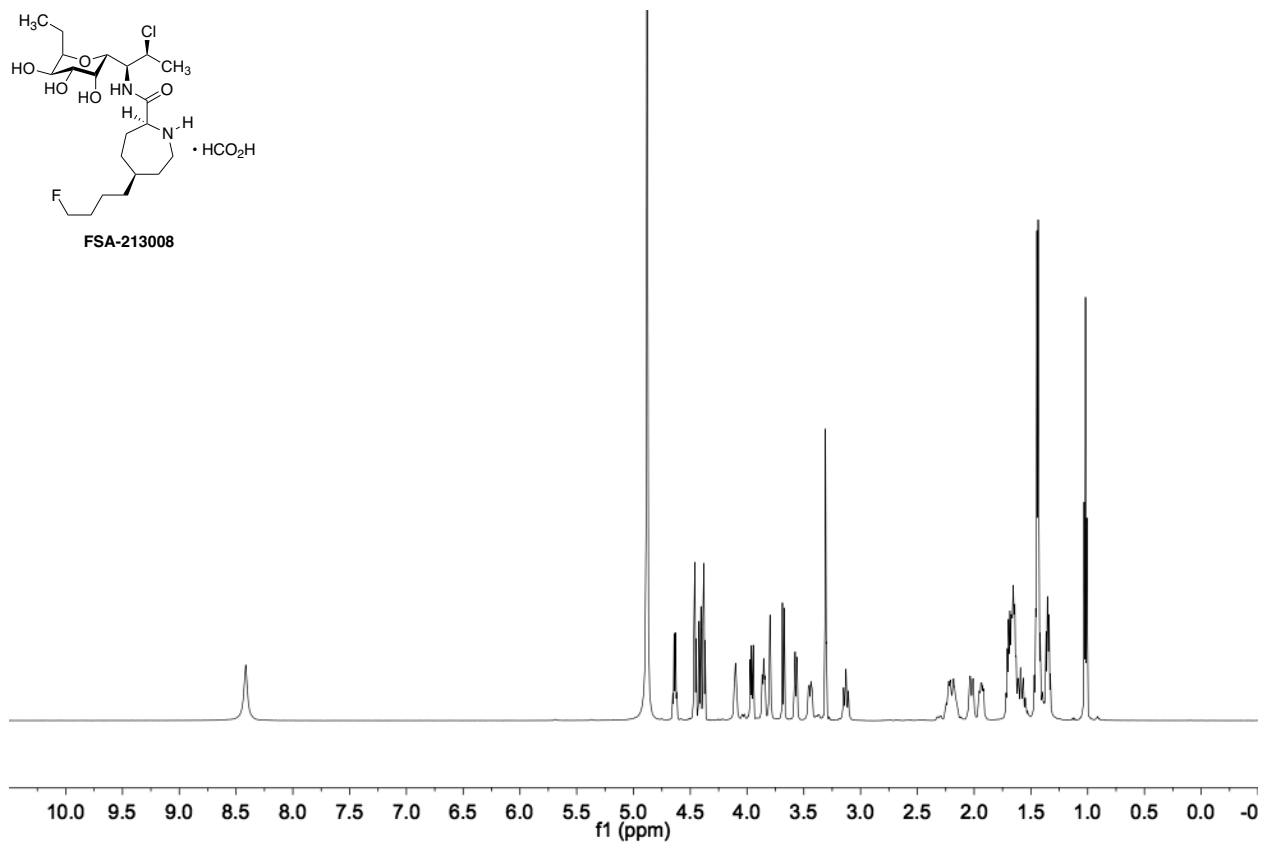
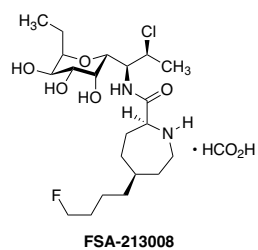


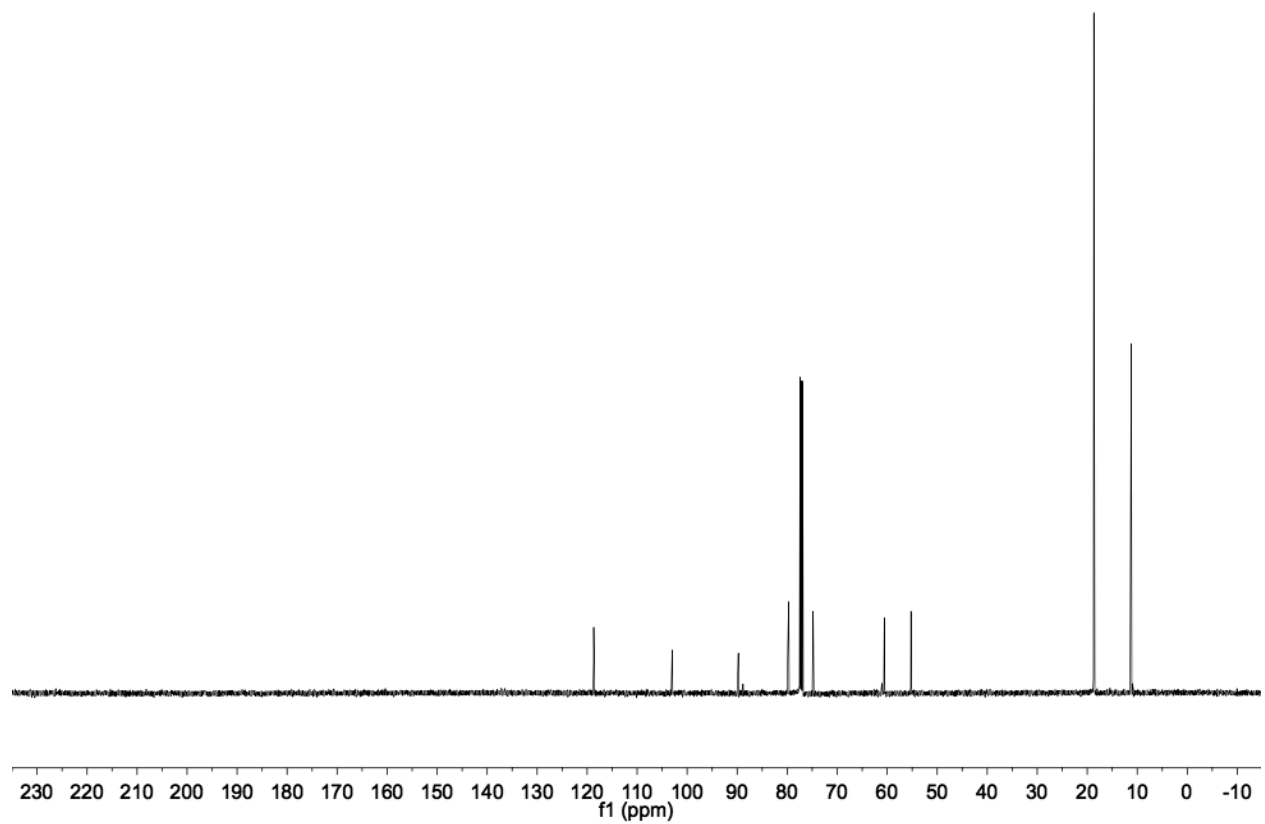
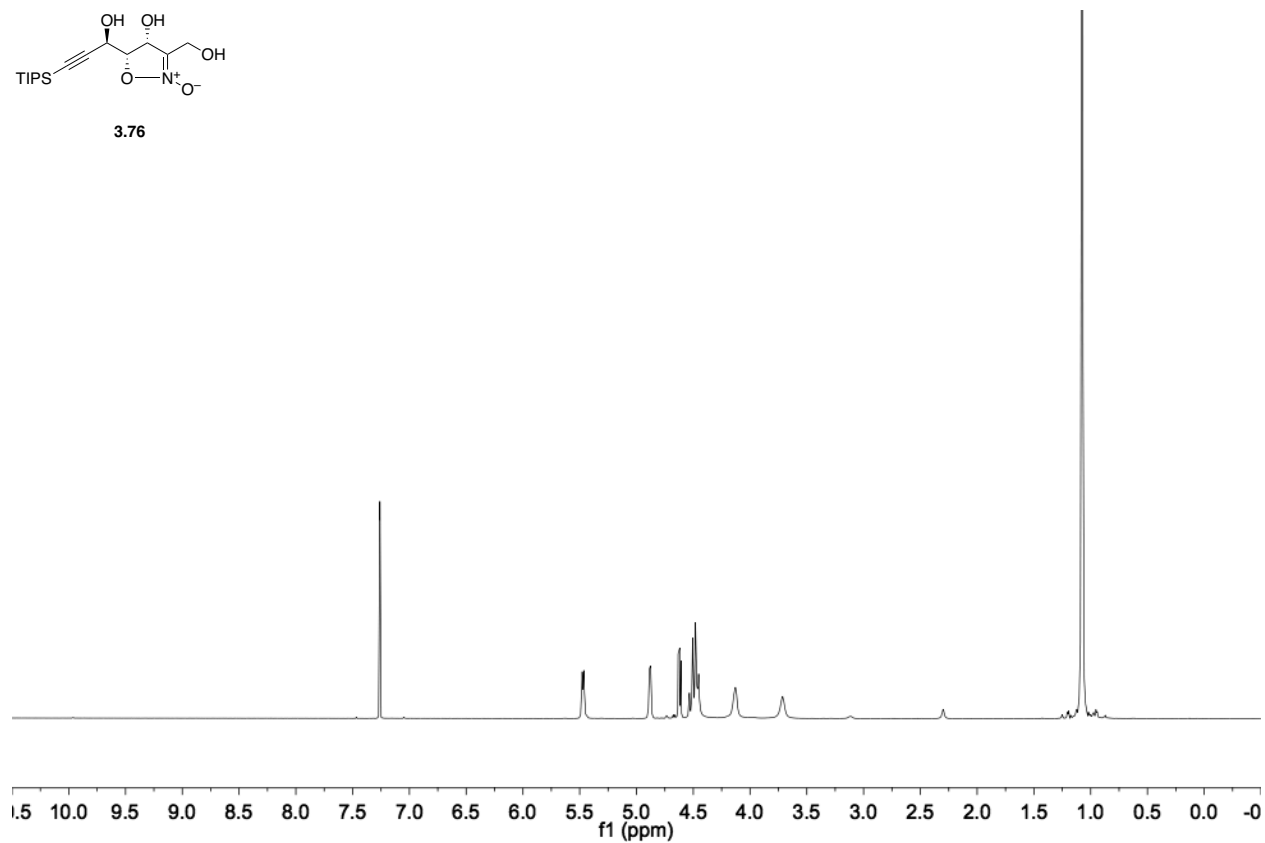
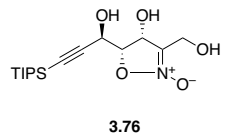


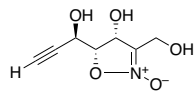


S3.19

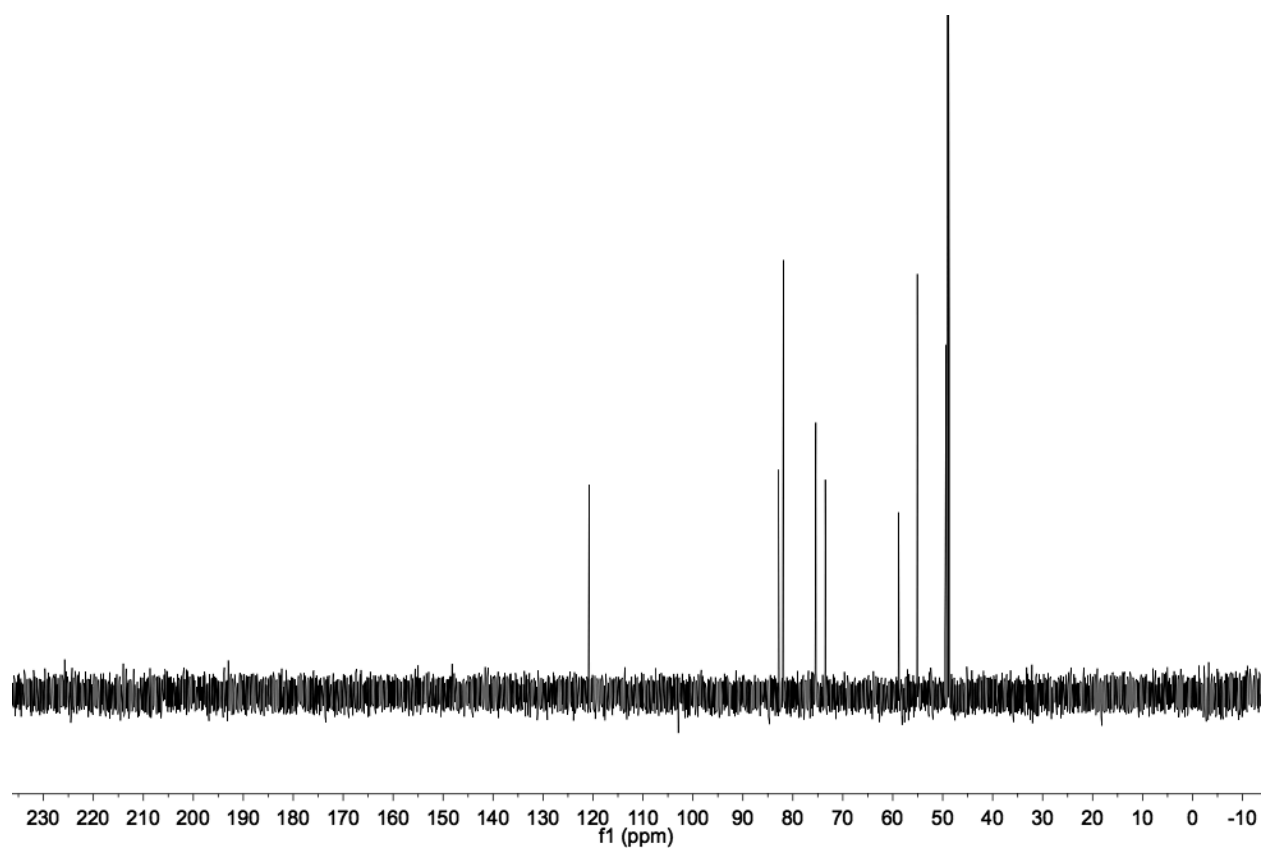
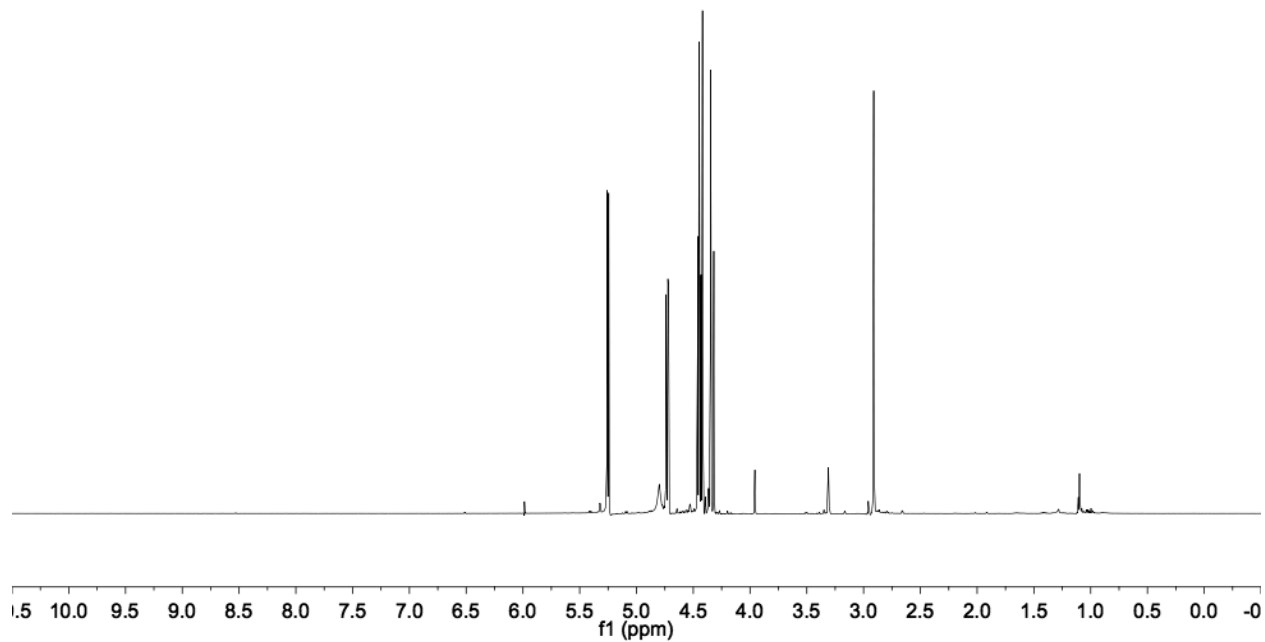


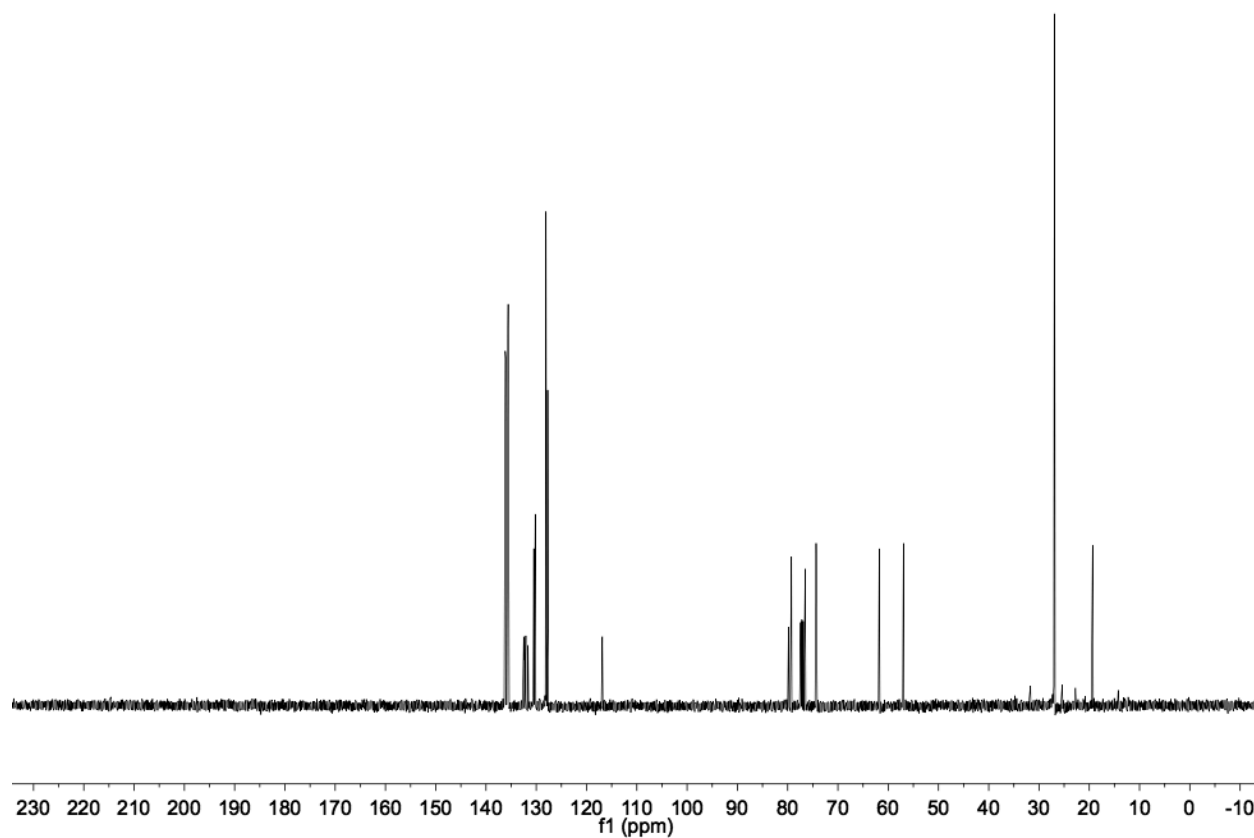
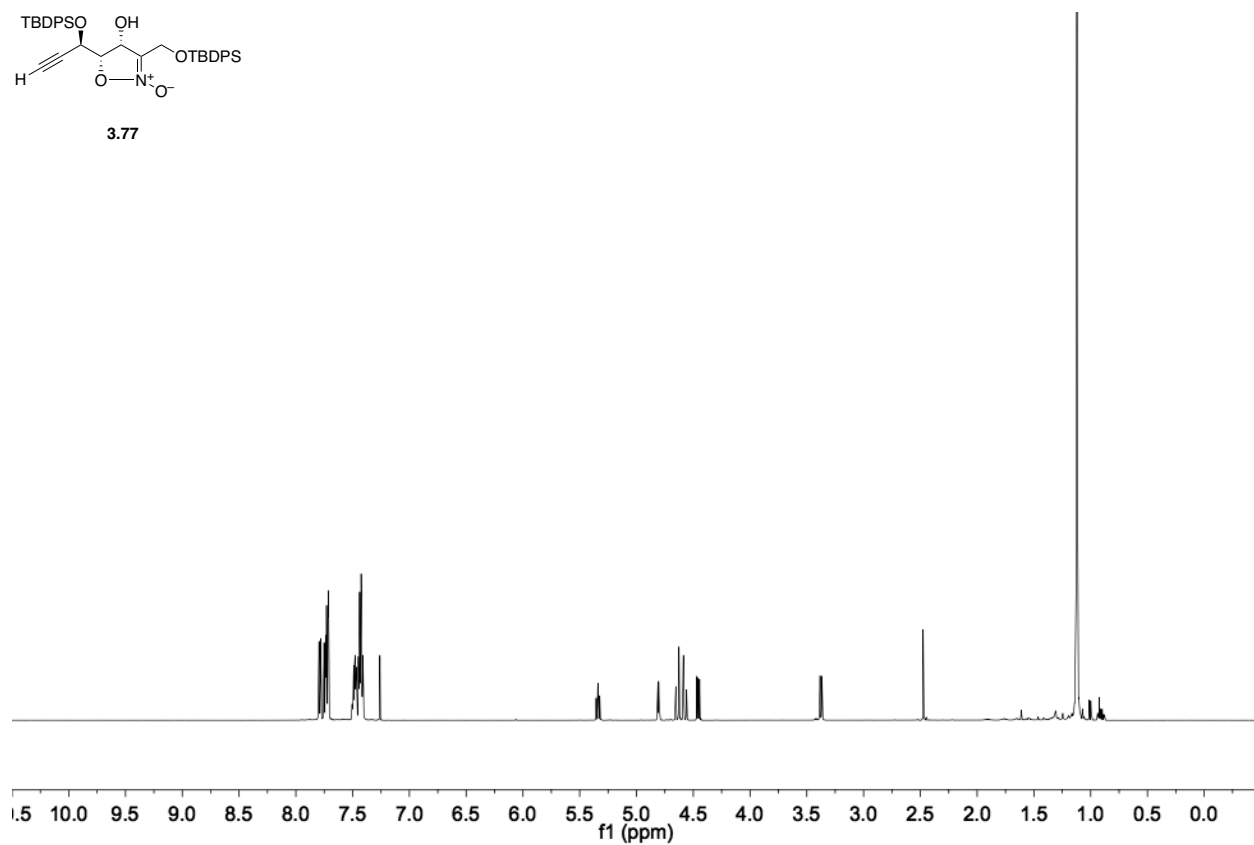
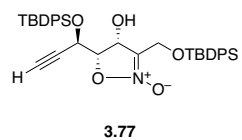


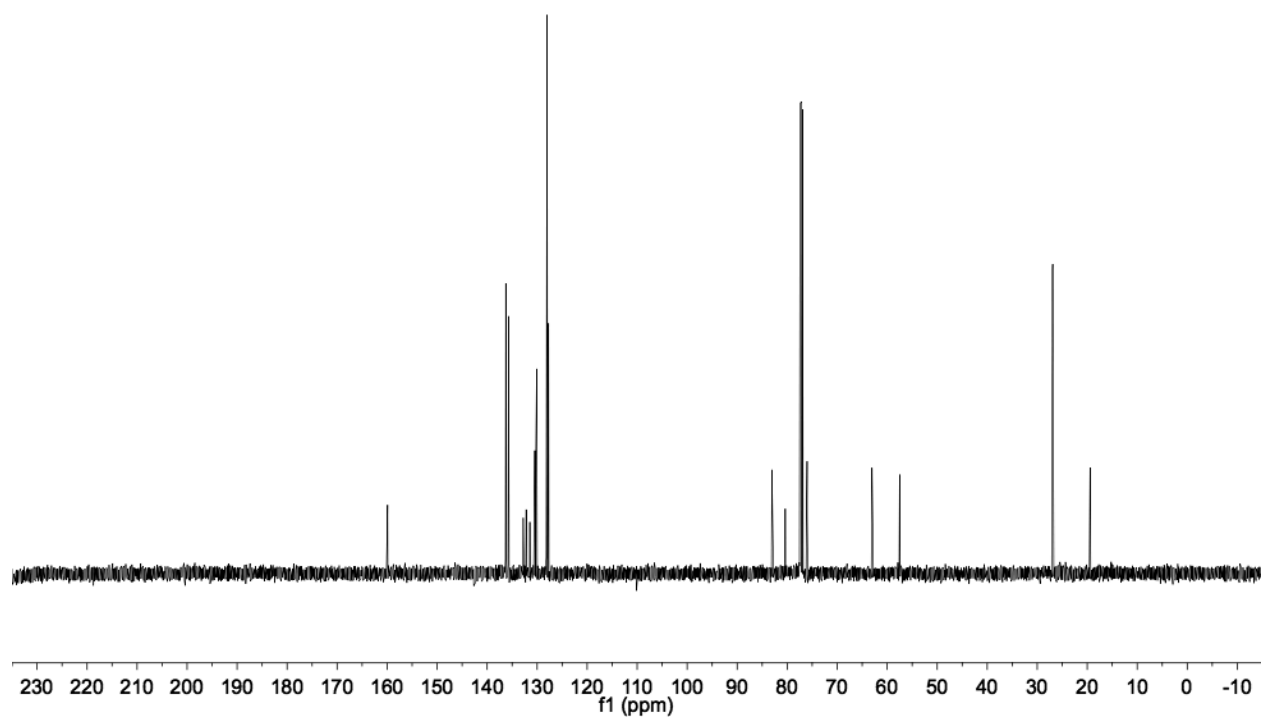
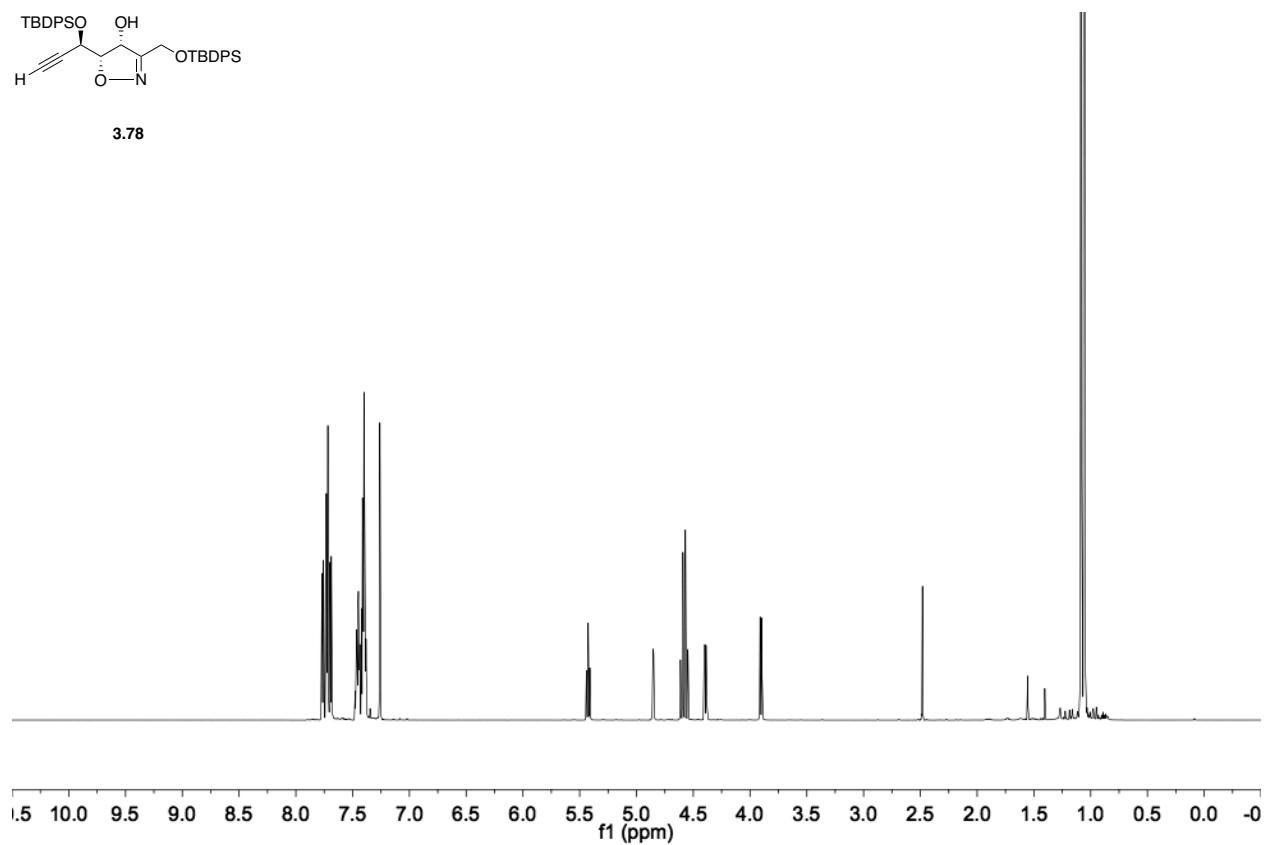
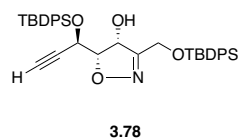


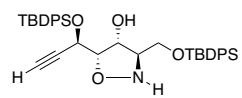


S3.20

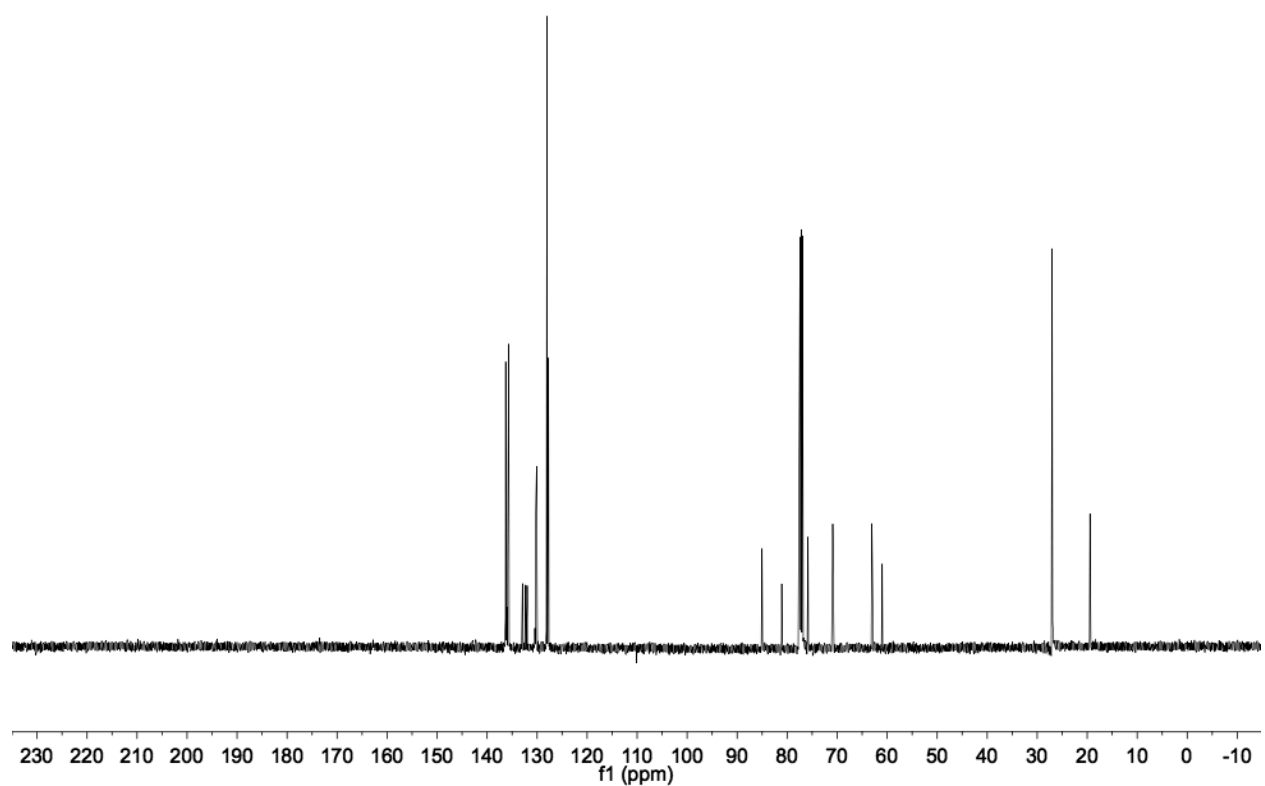
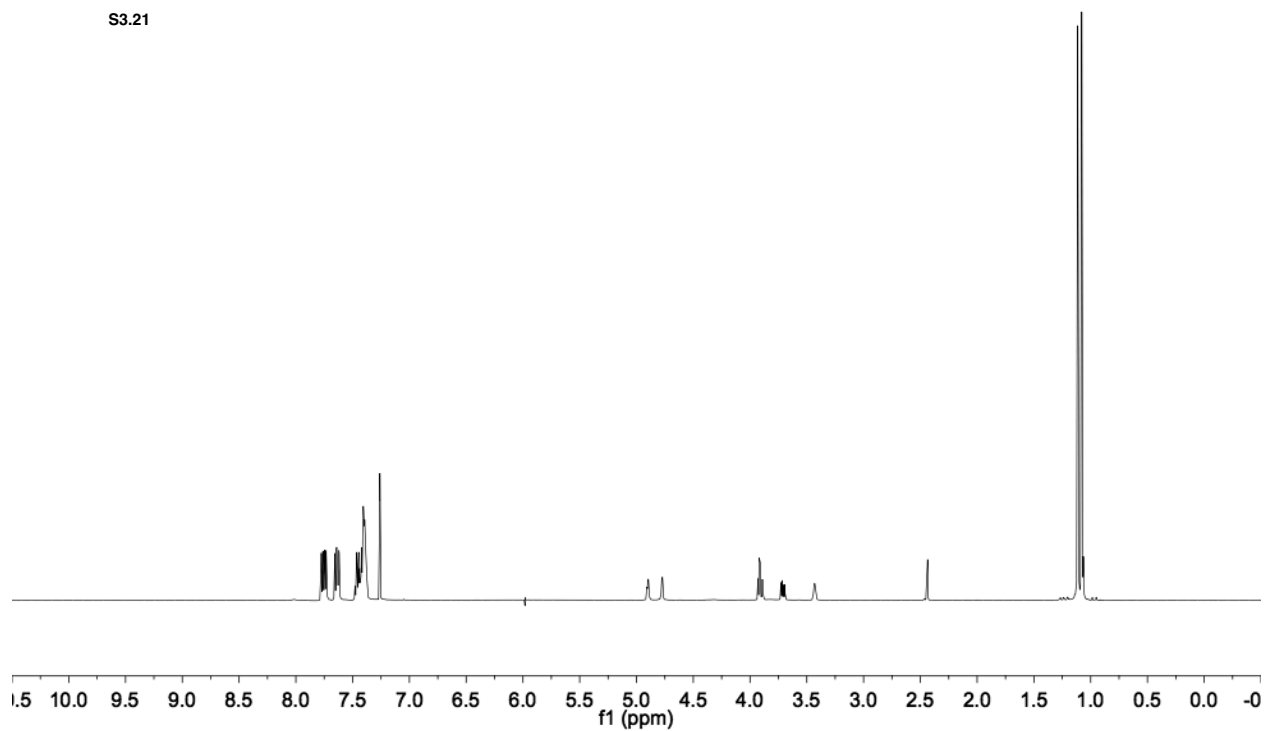


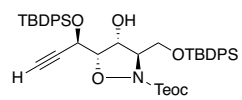




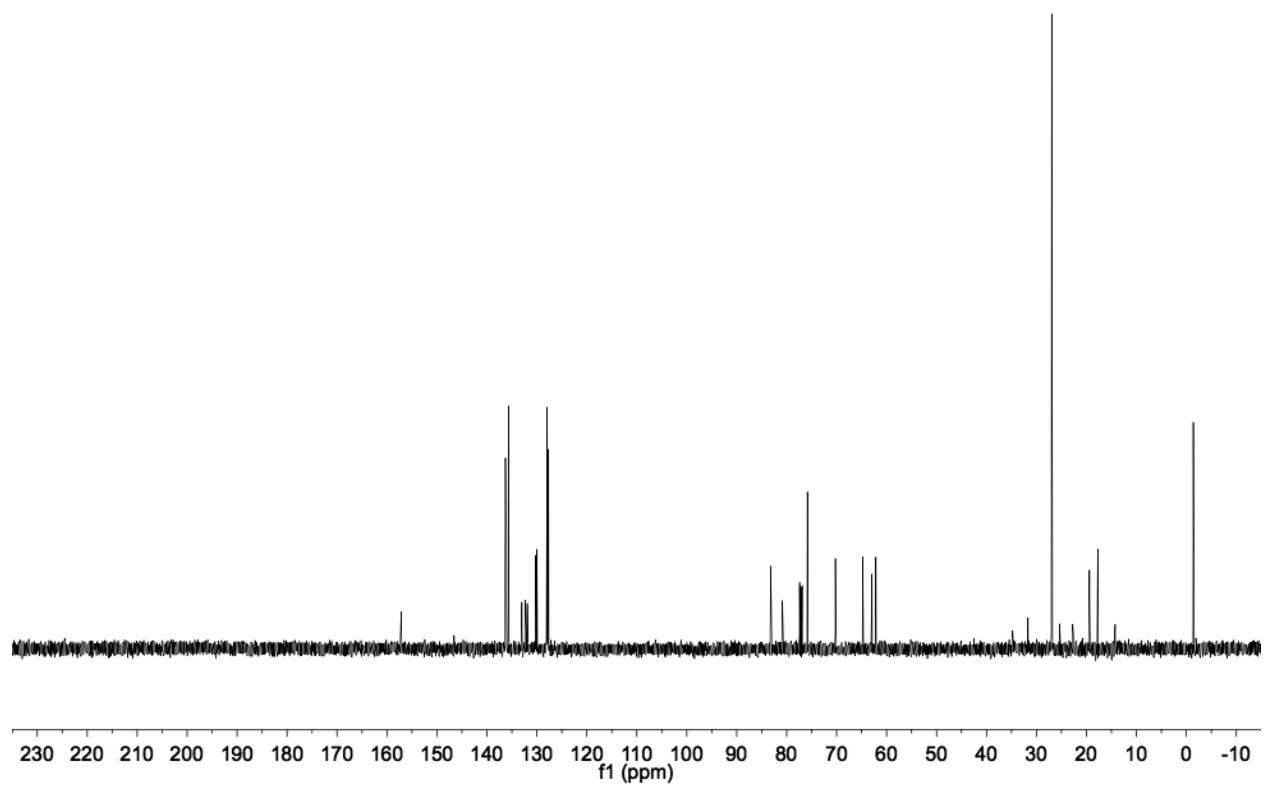
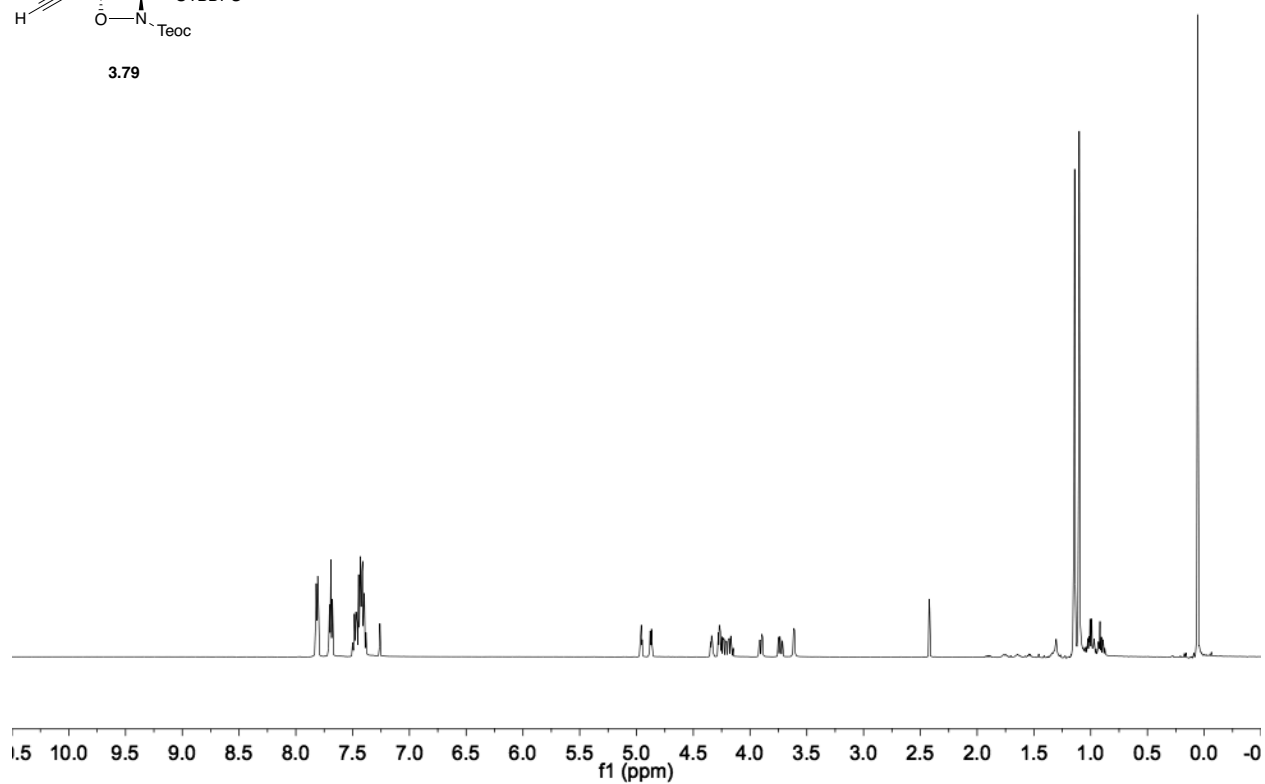


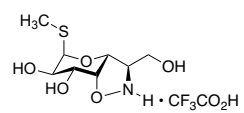
S3.21



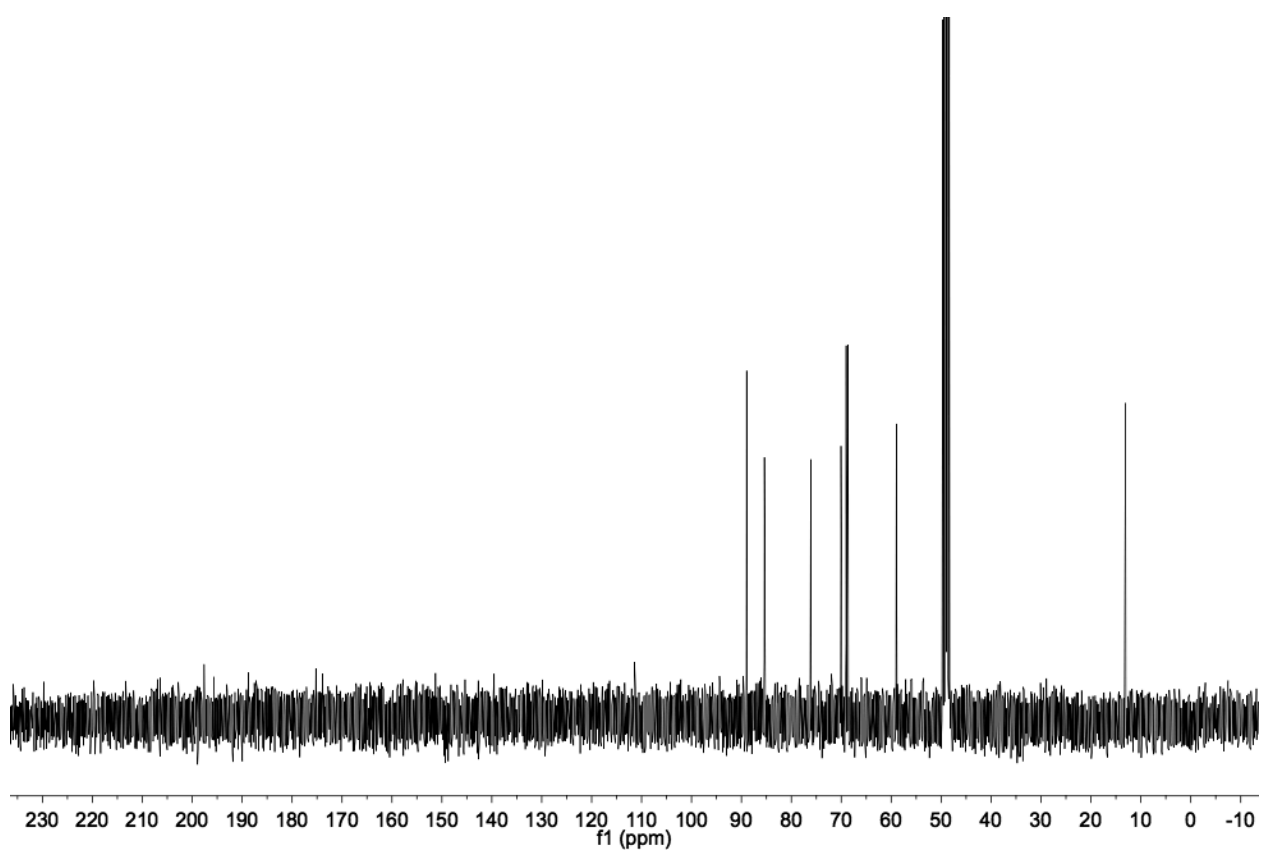
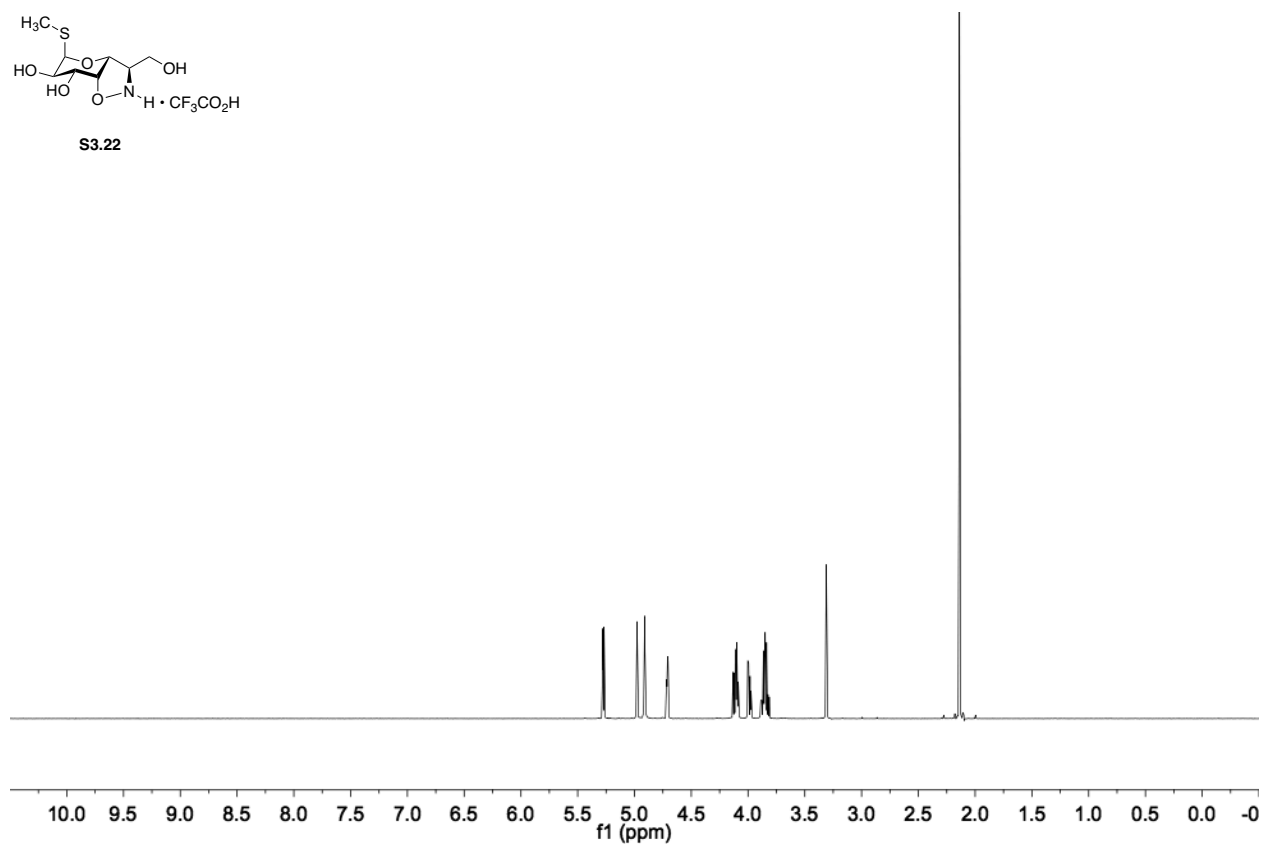


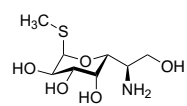
3.79



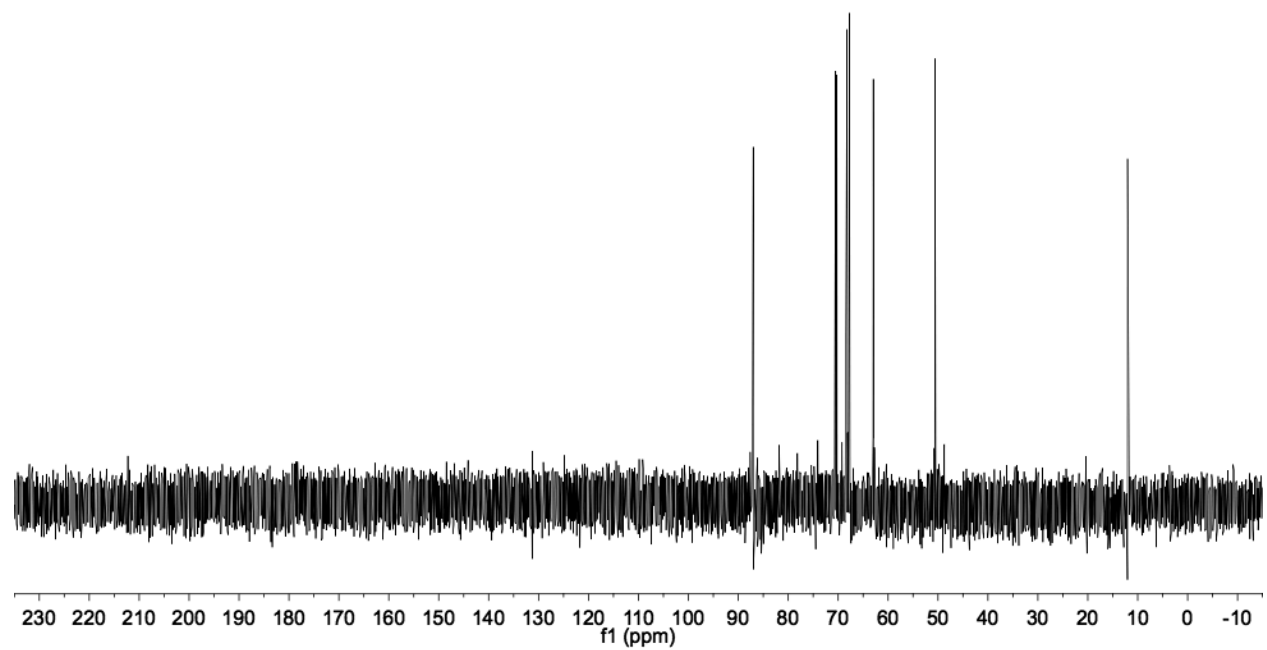
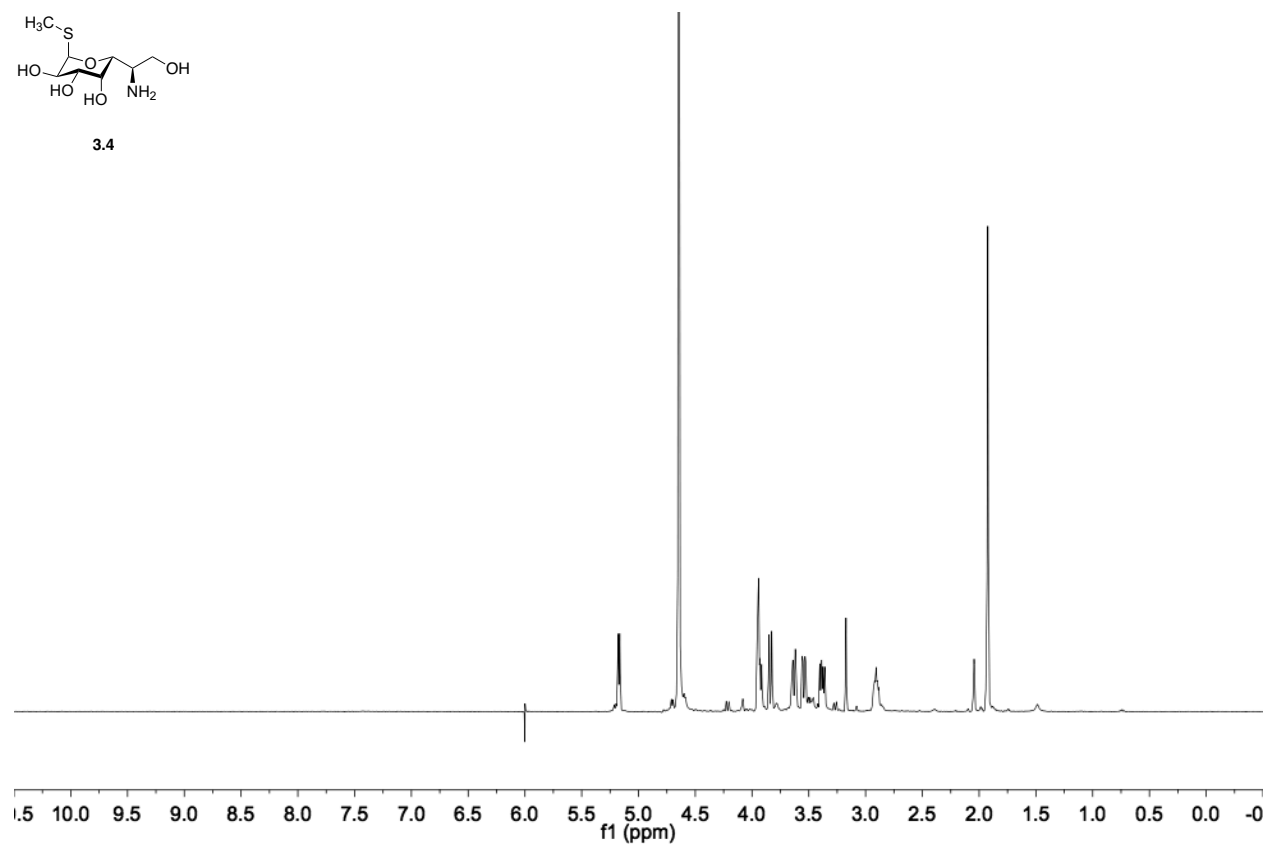


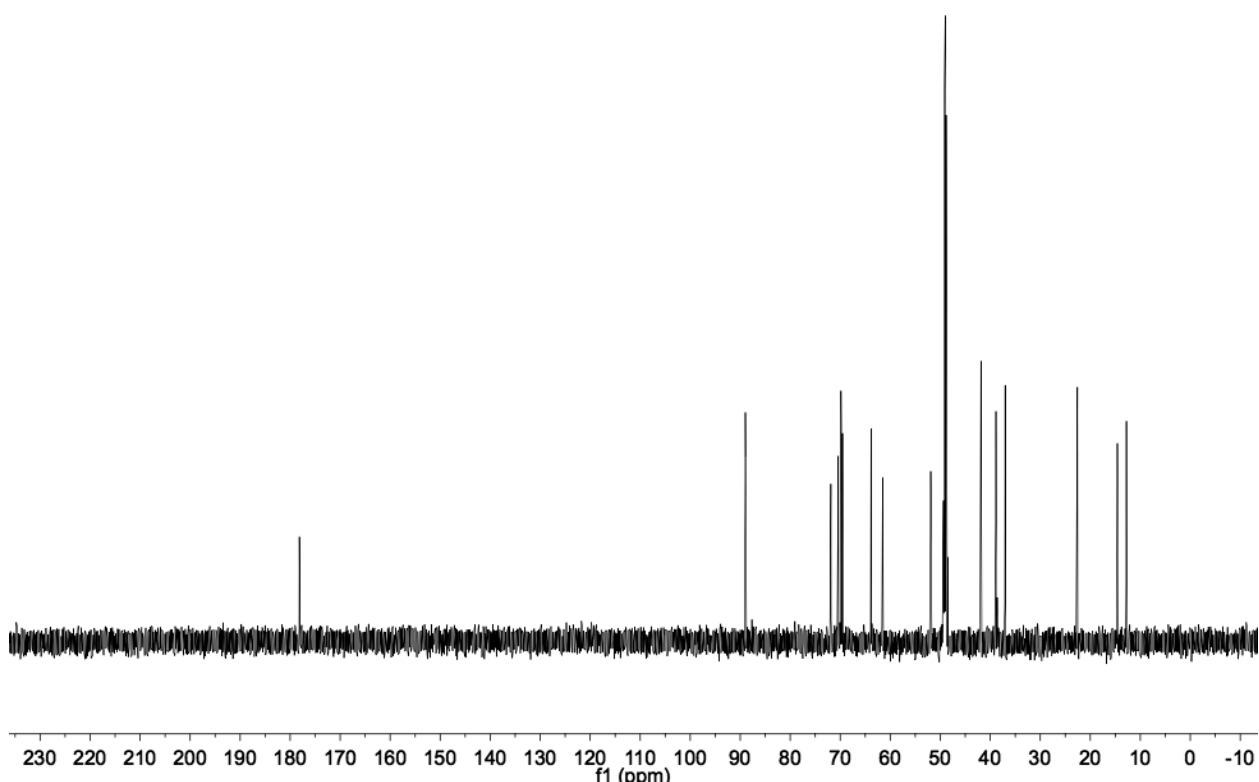
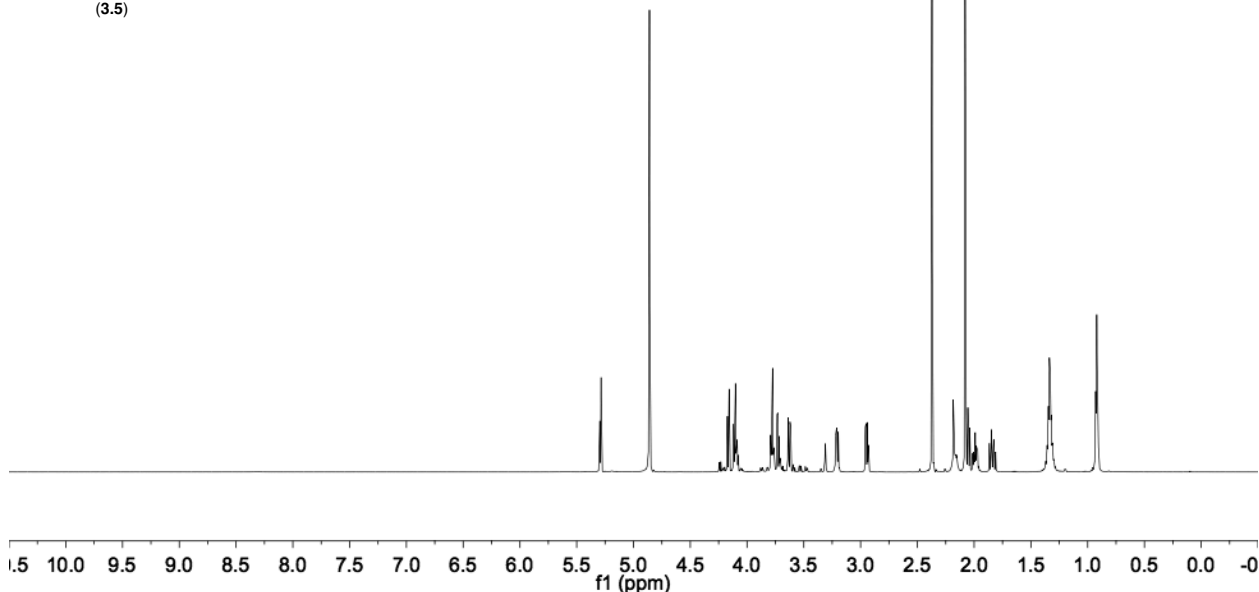
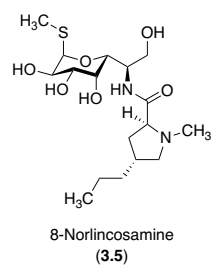
S3.22

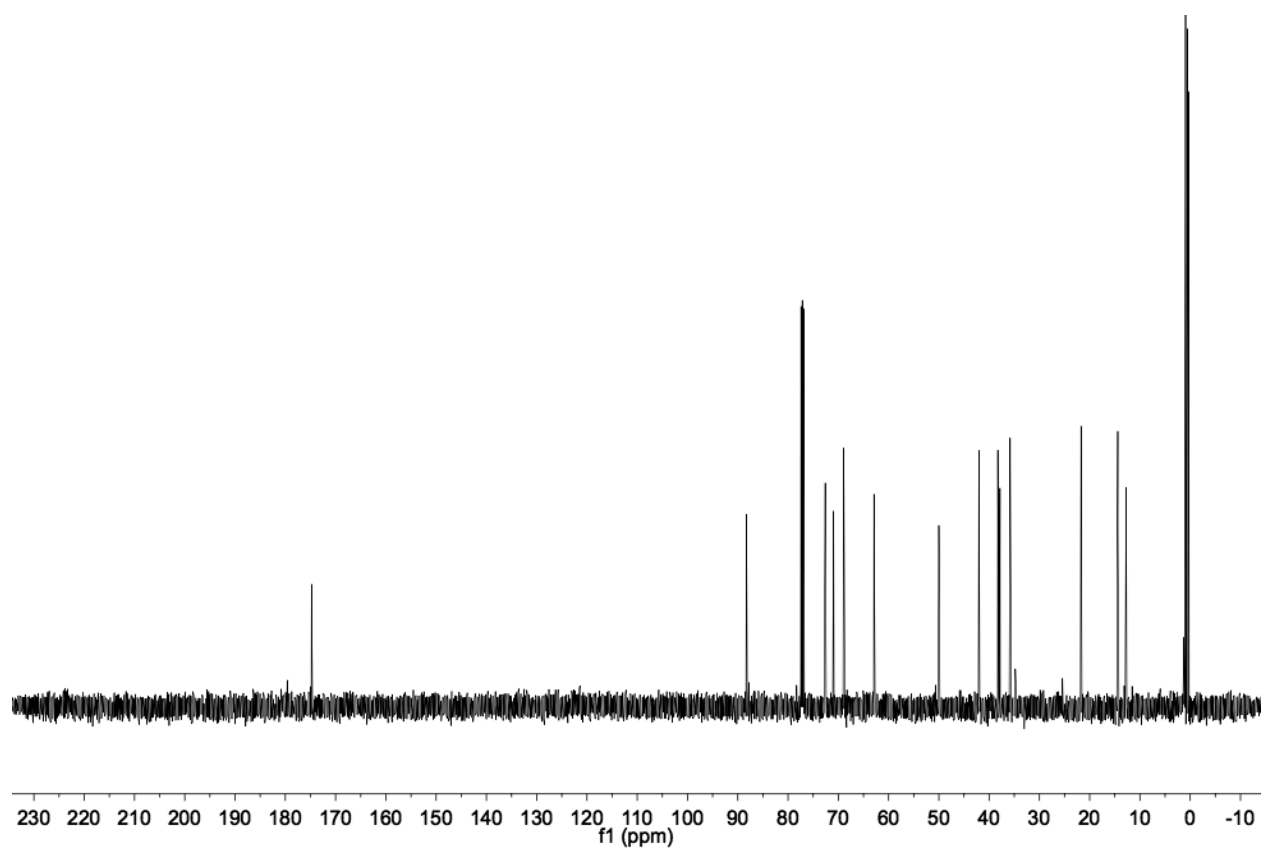
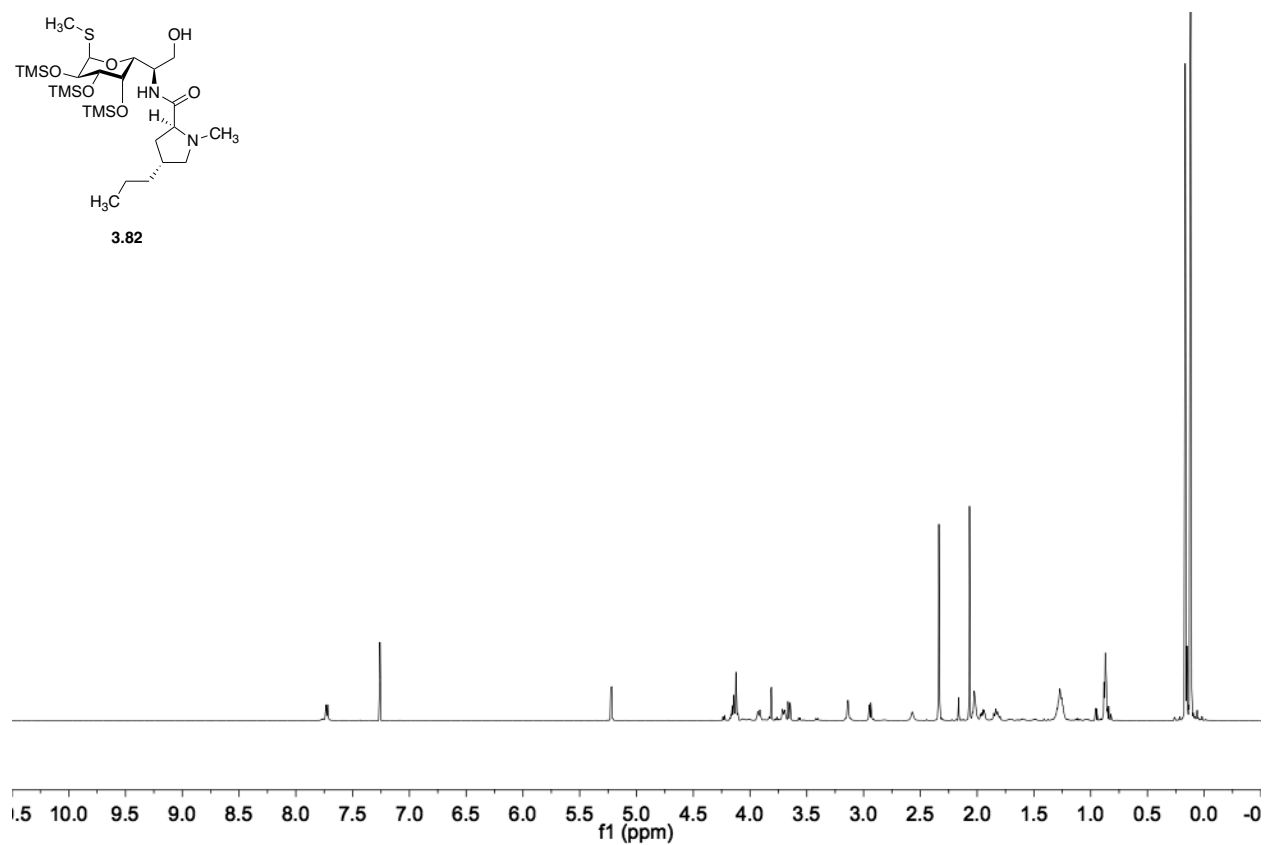
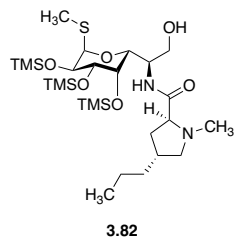


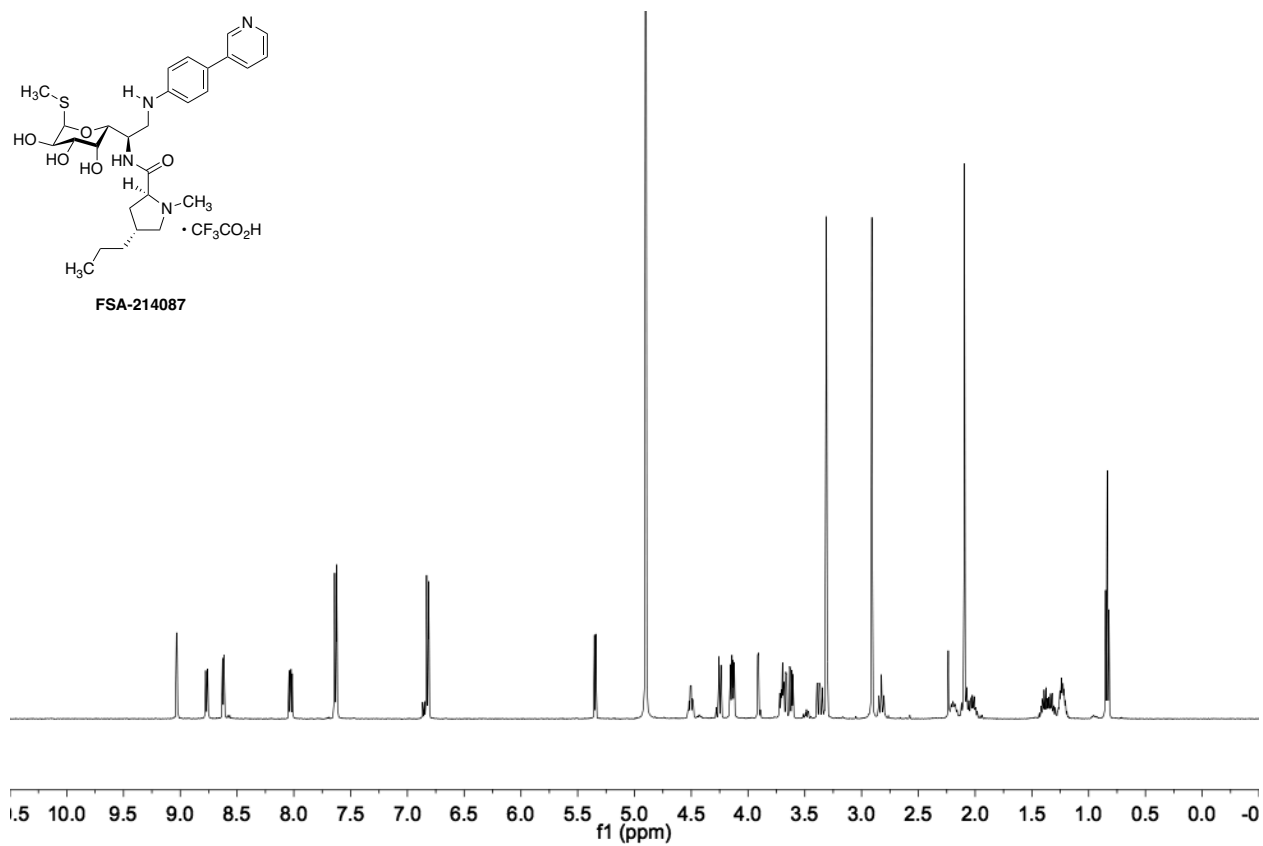
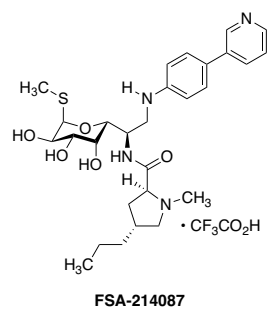
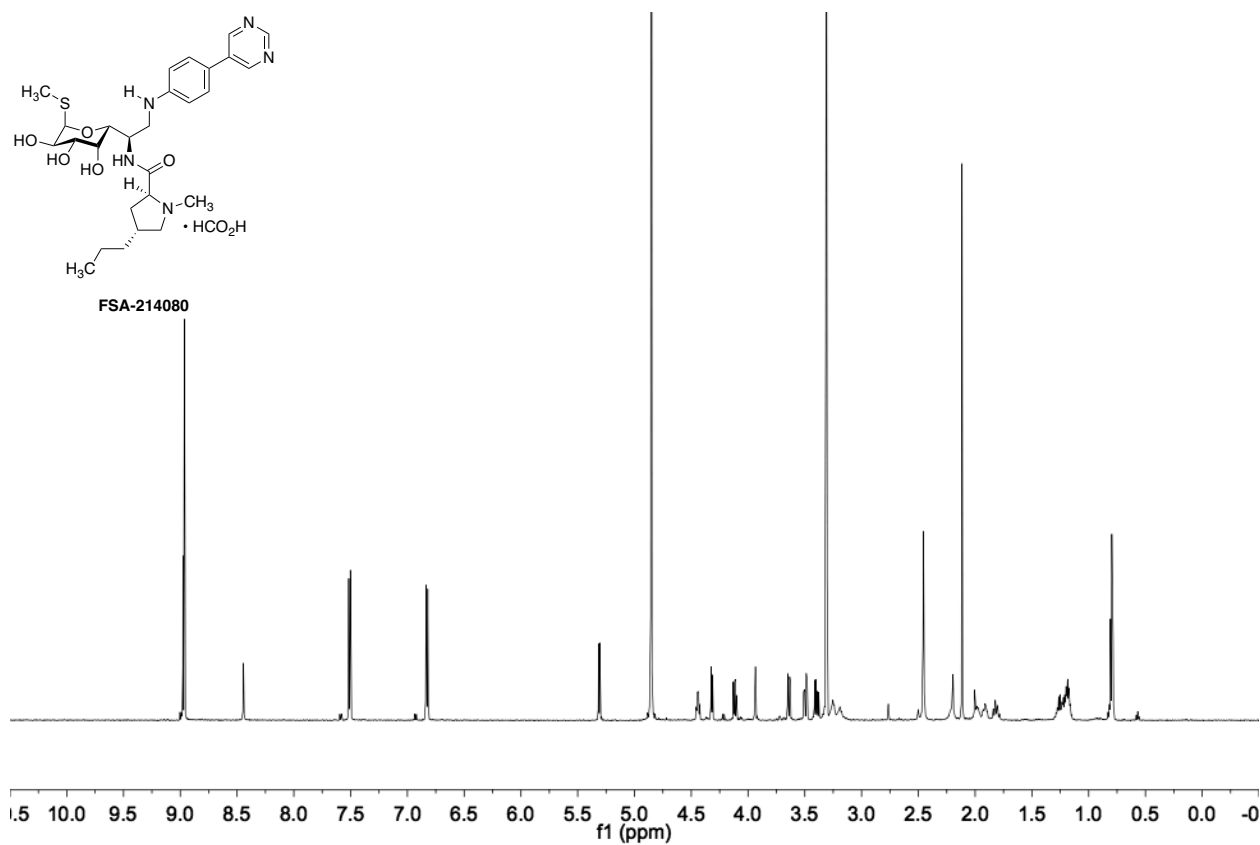
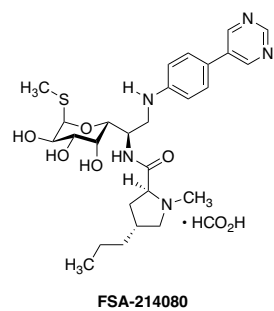


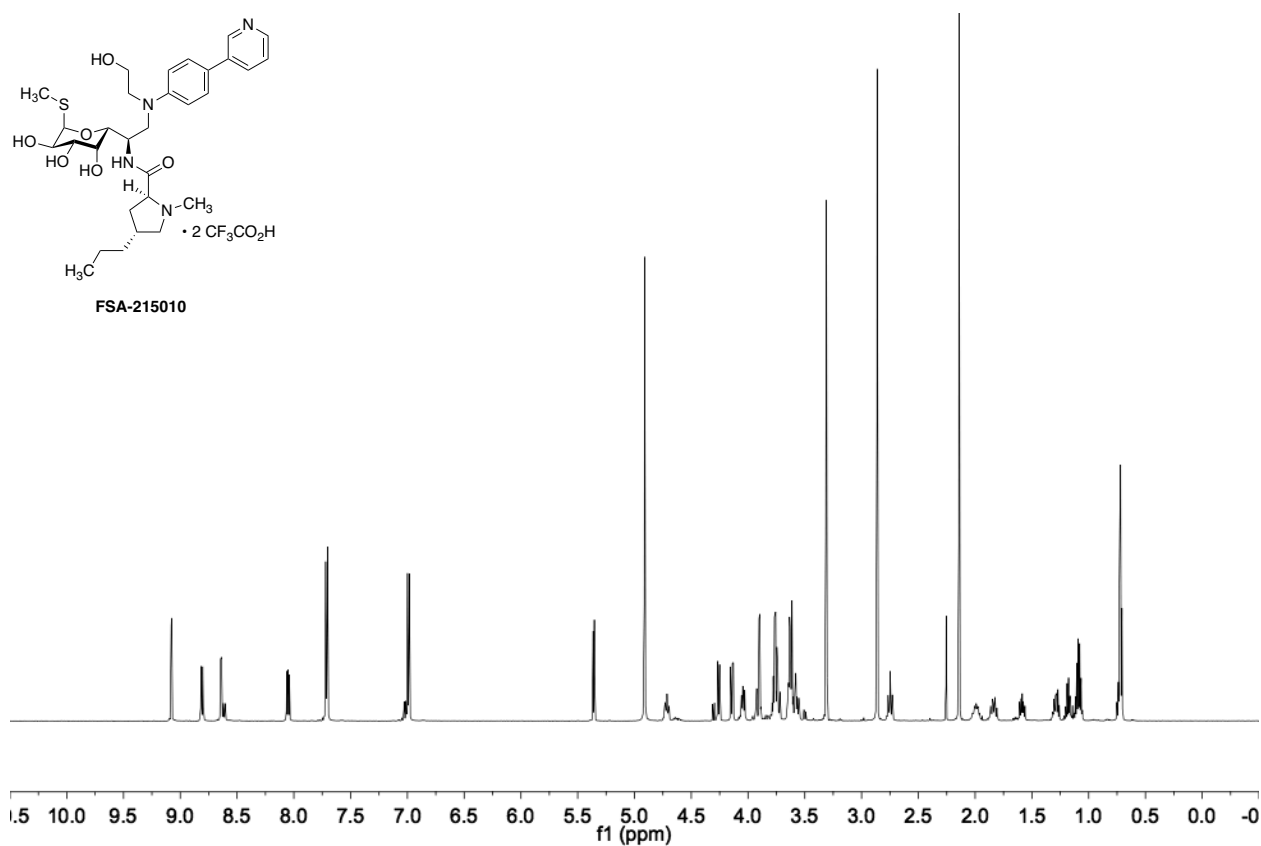
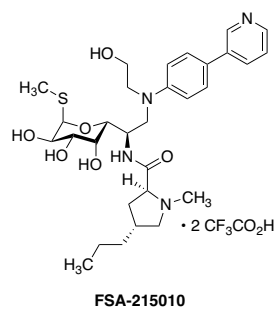
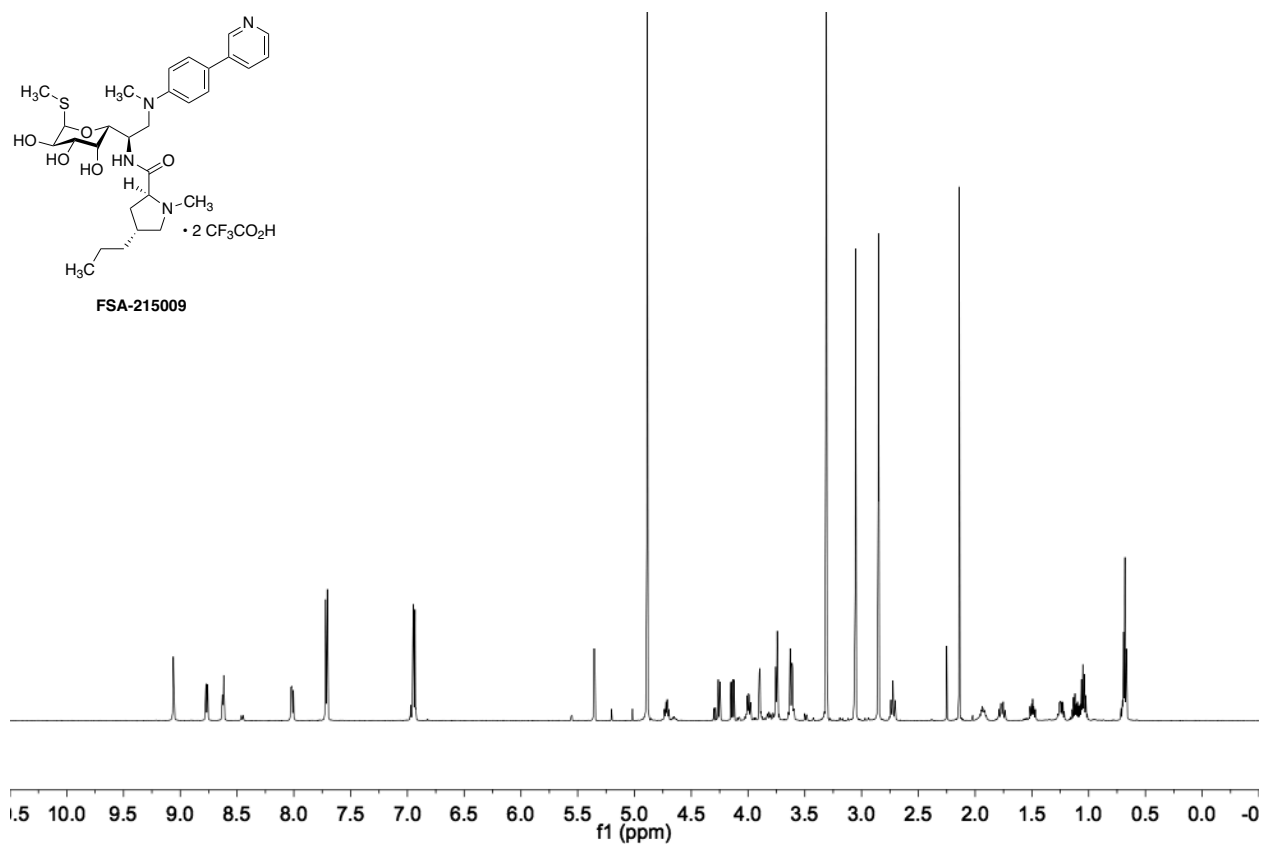
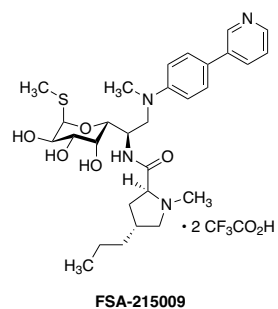
3.4

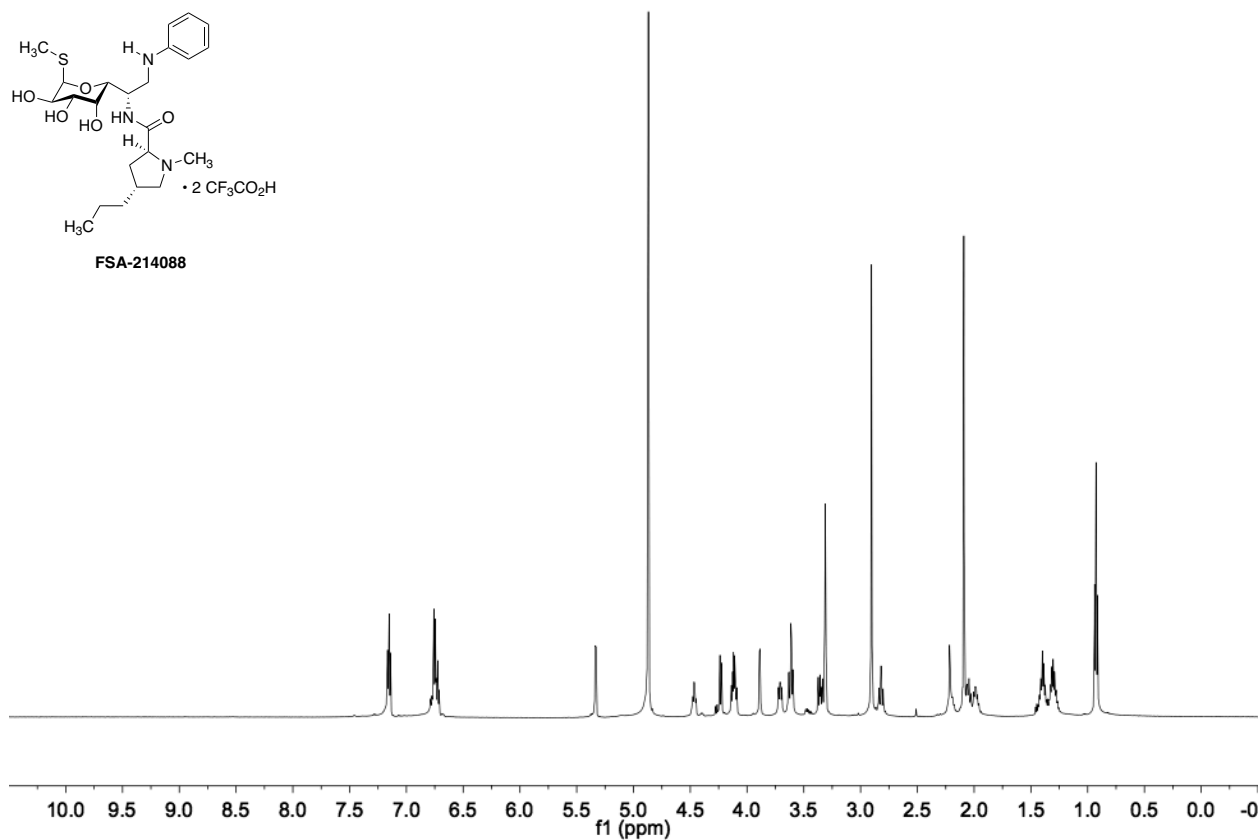
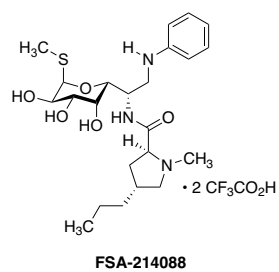
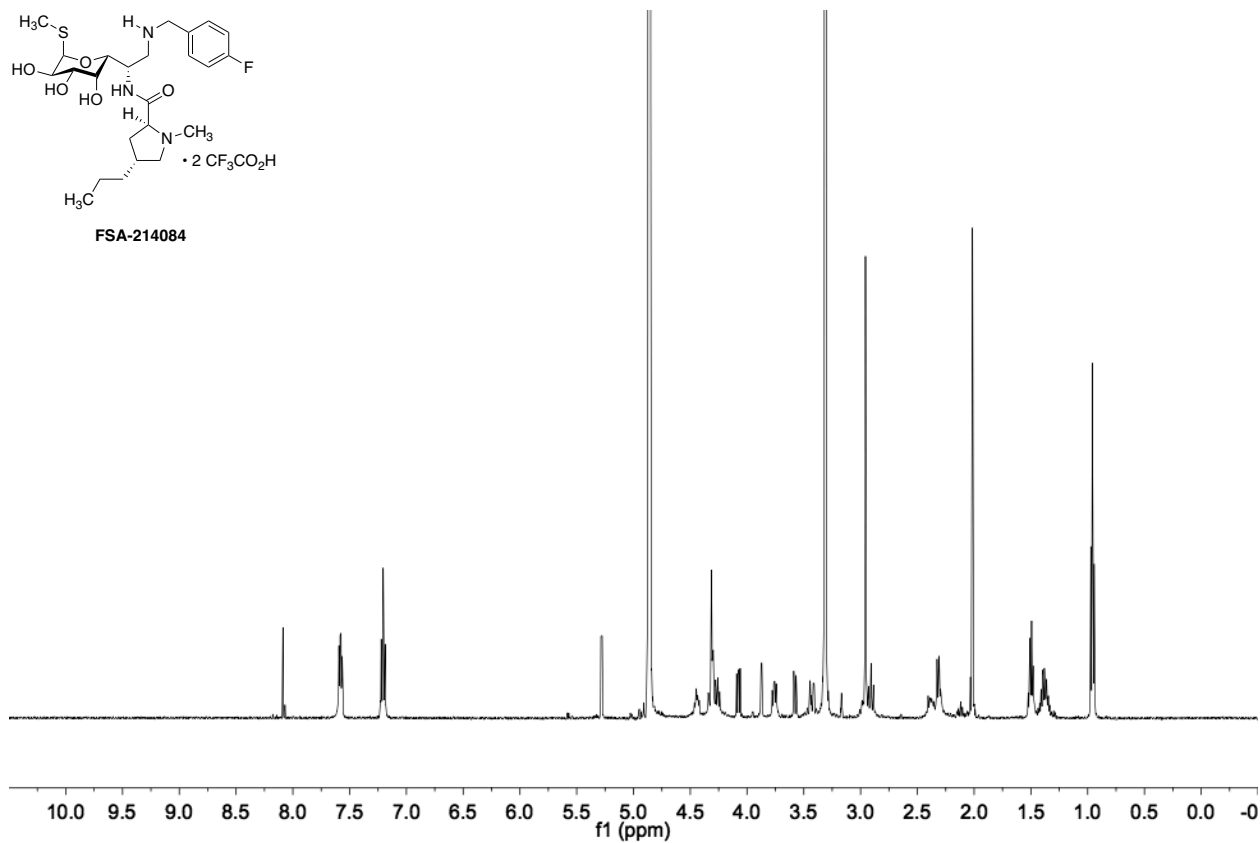
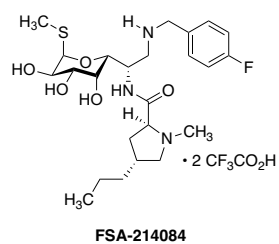


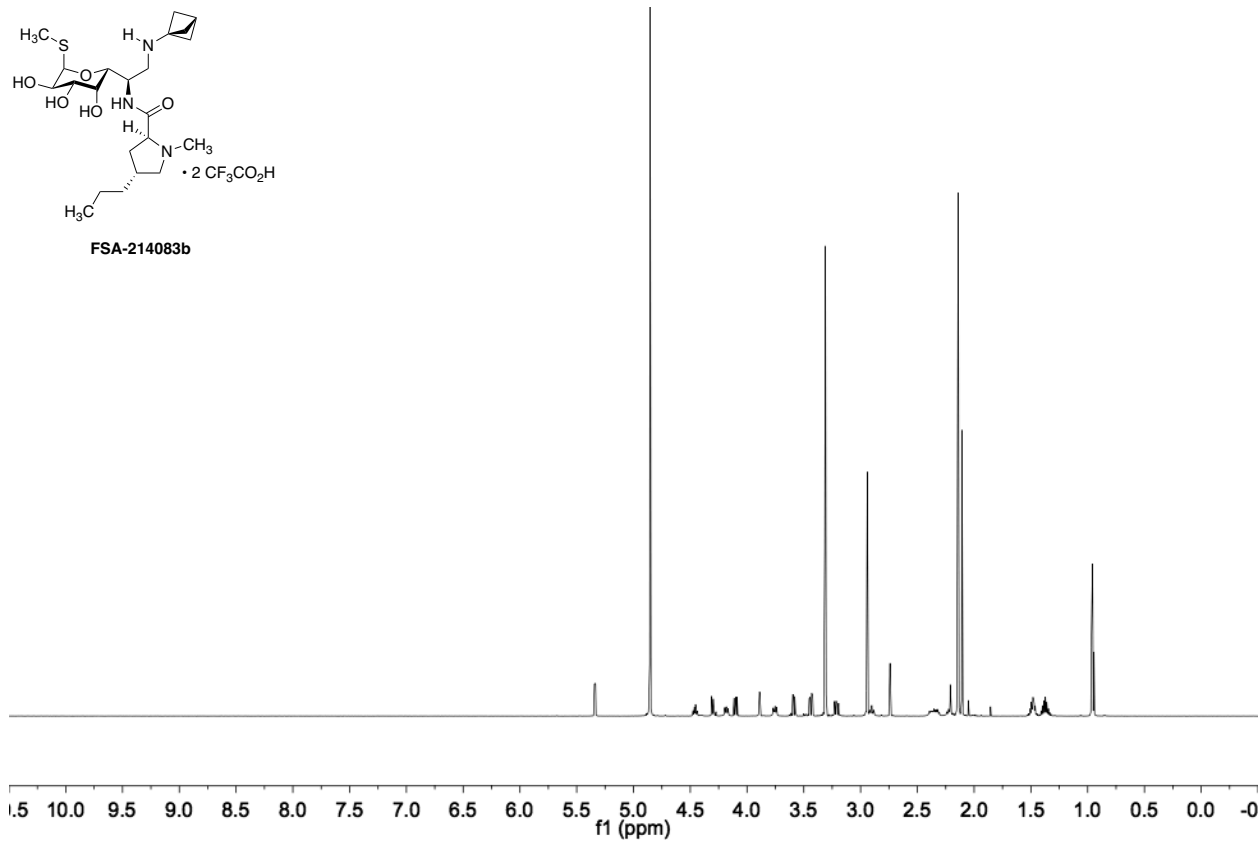
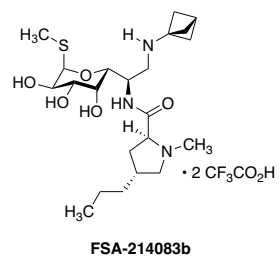
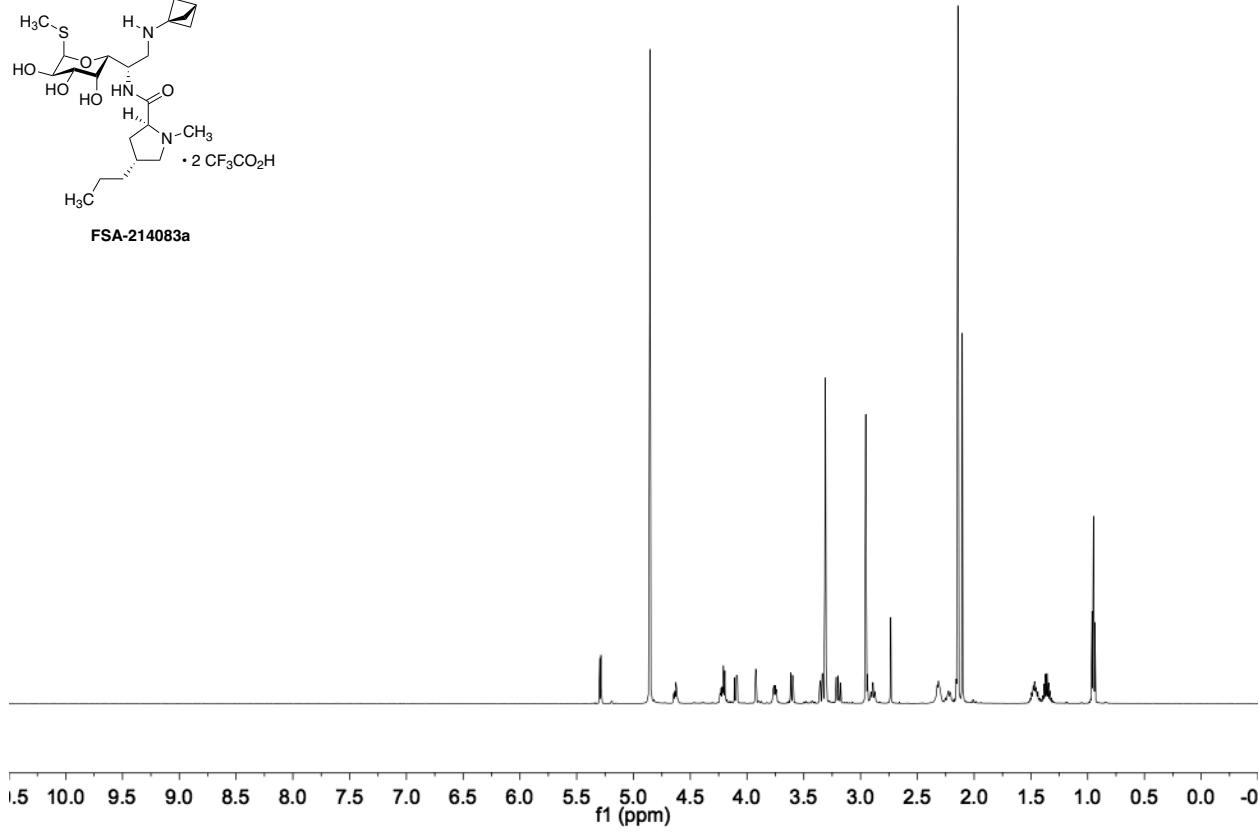
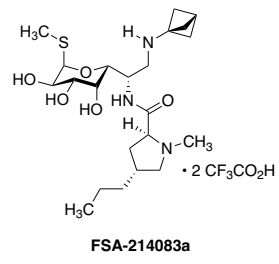


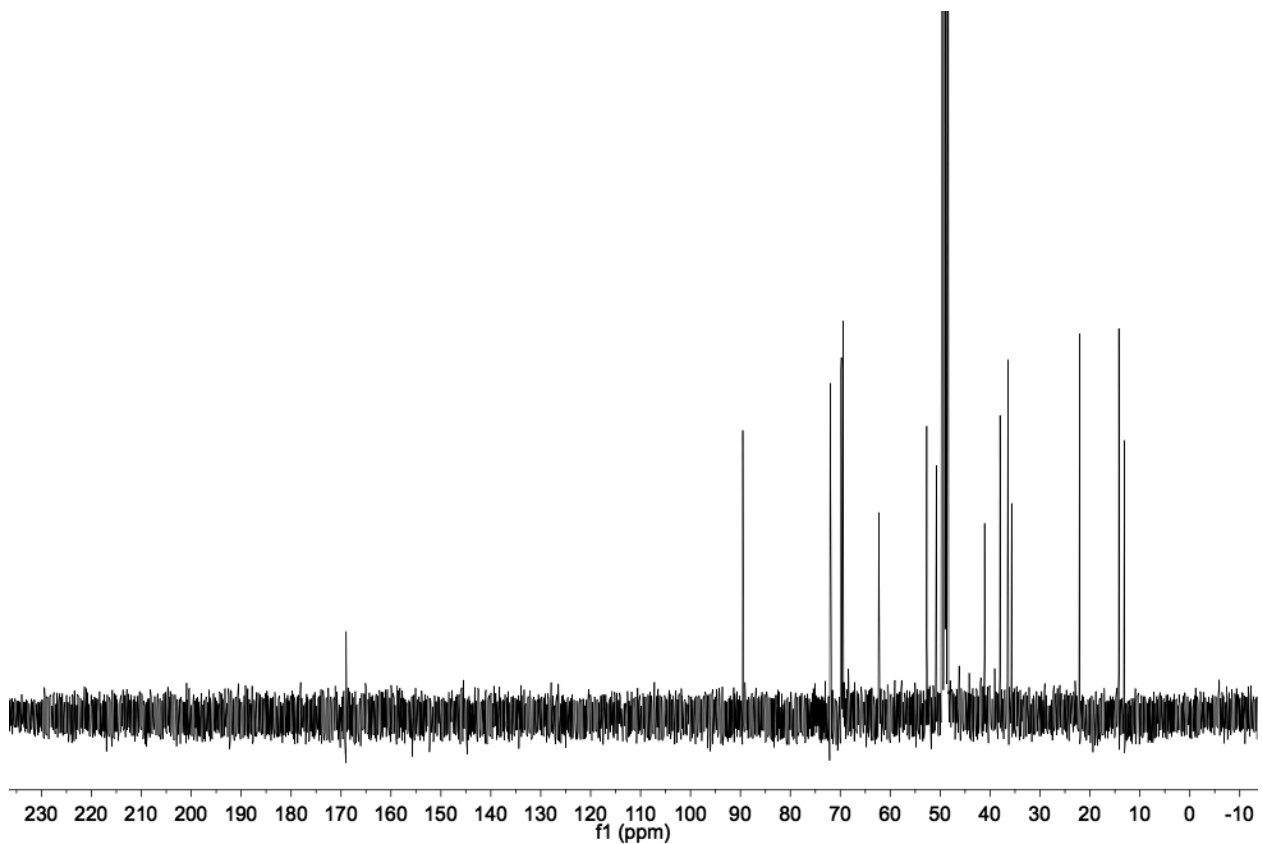
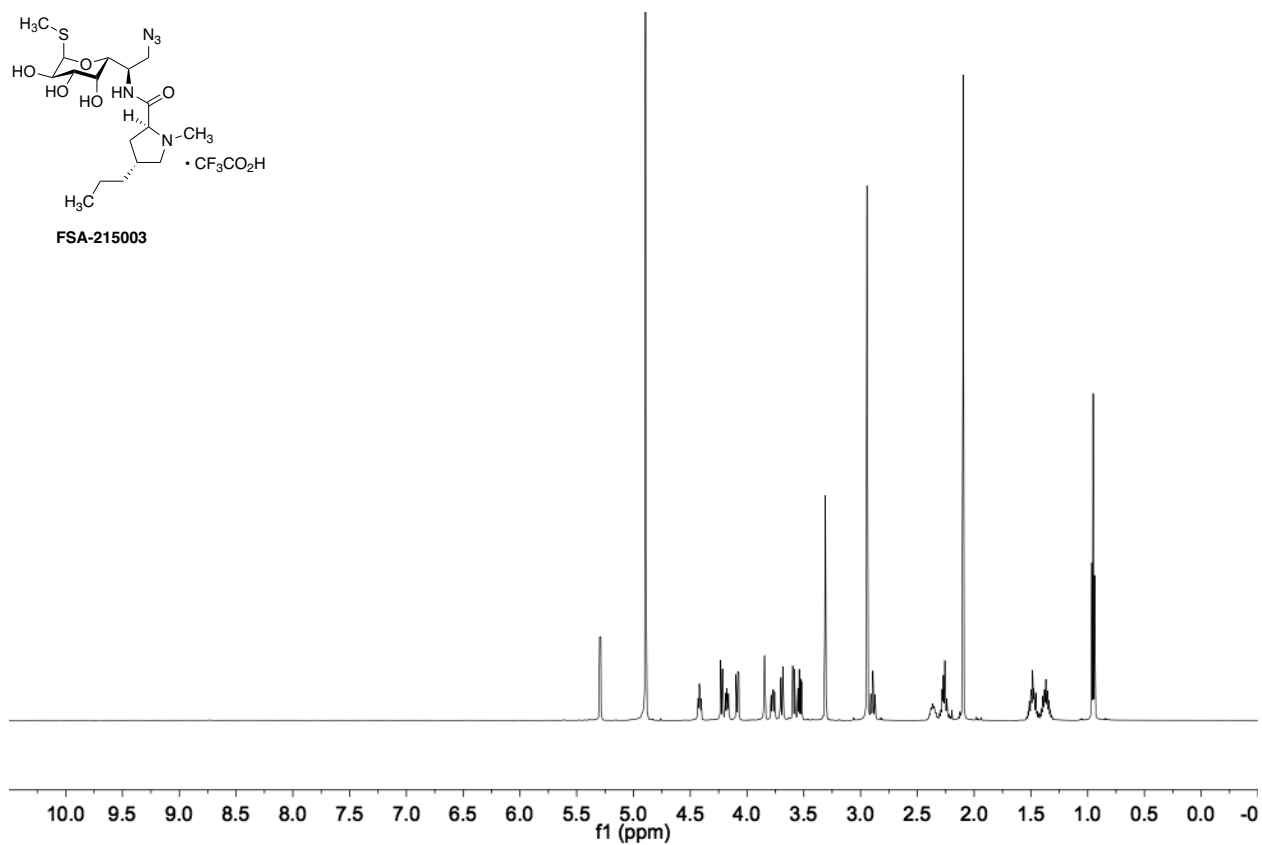
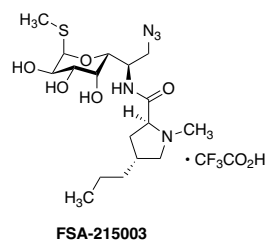


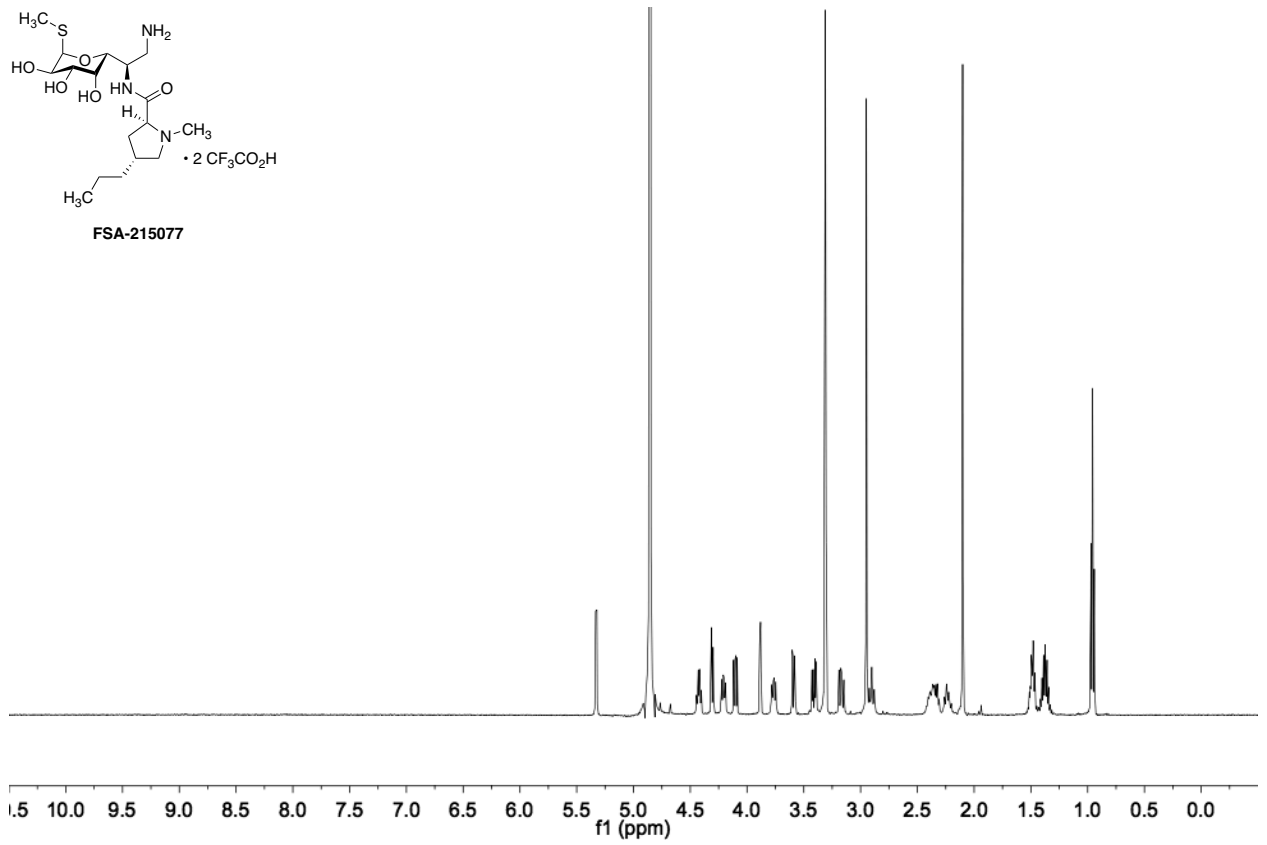
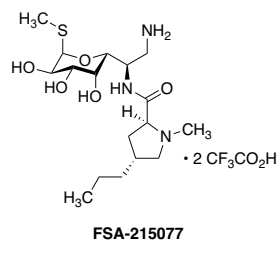
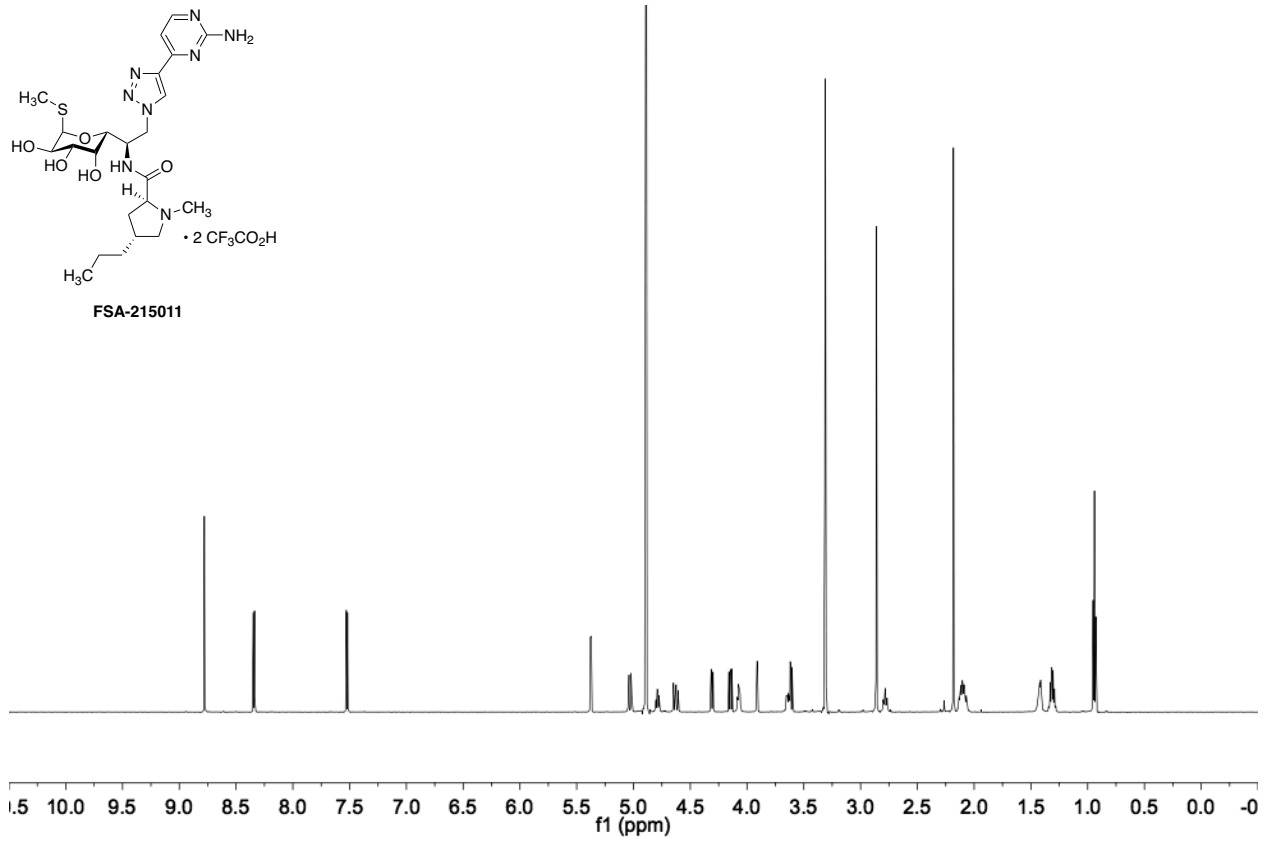
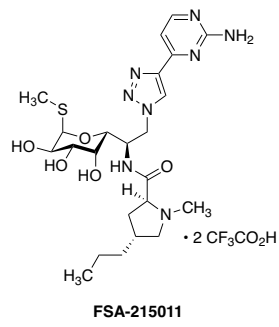


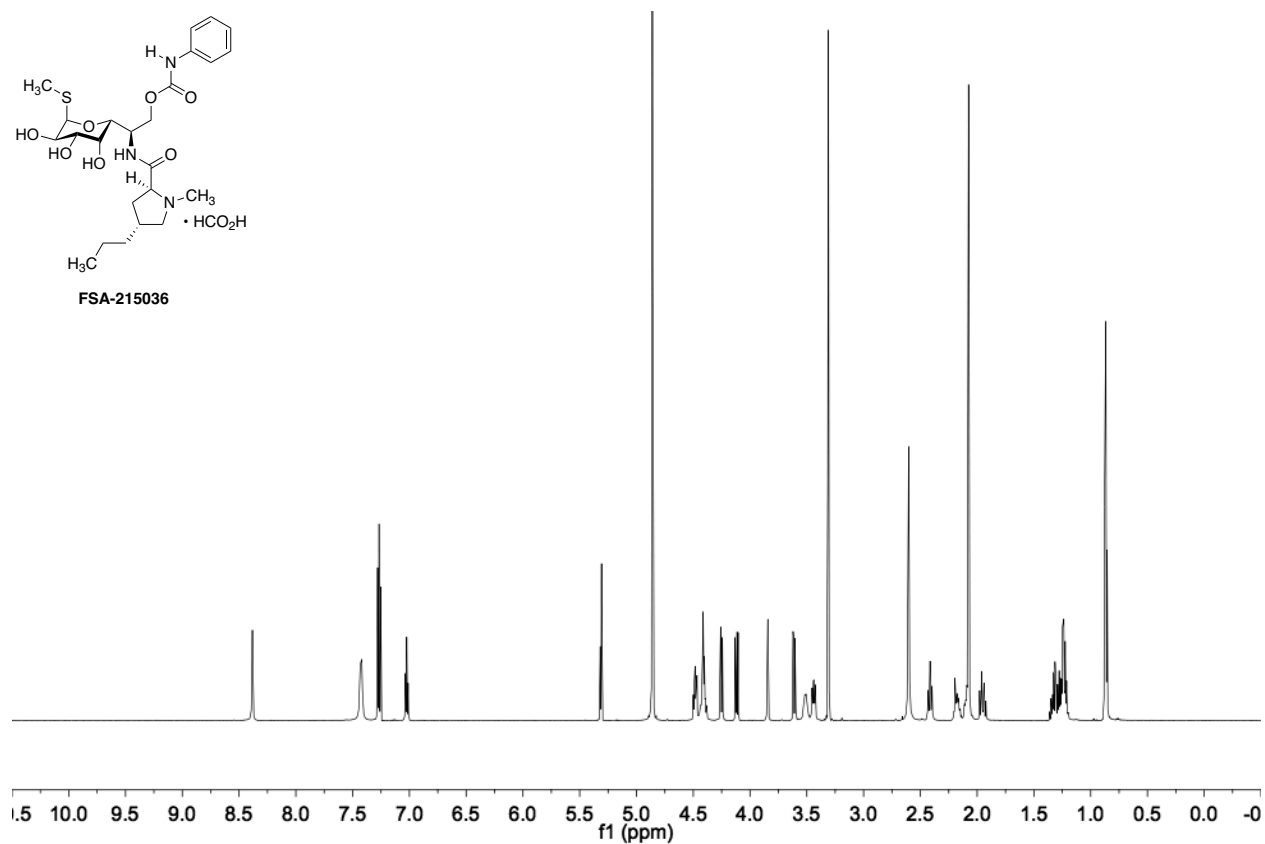
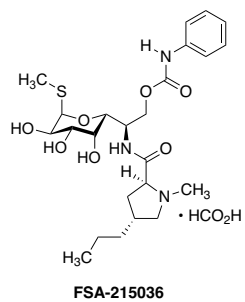
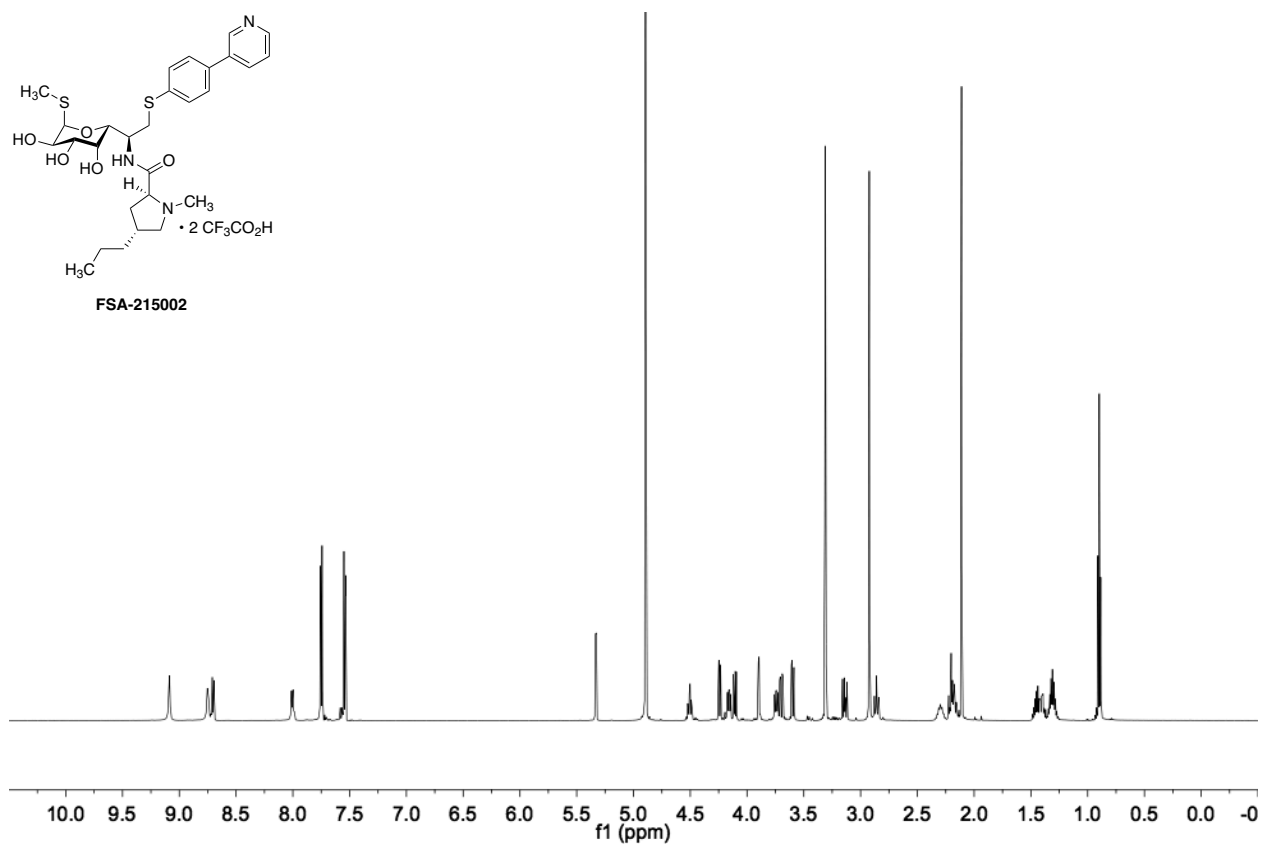
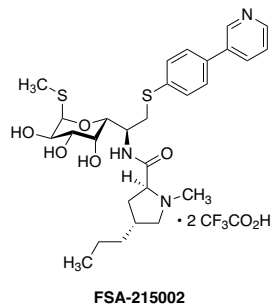


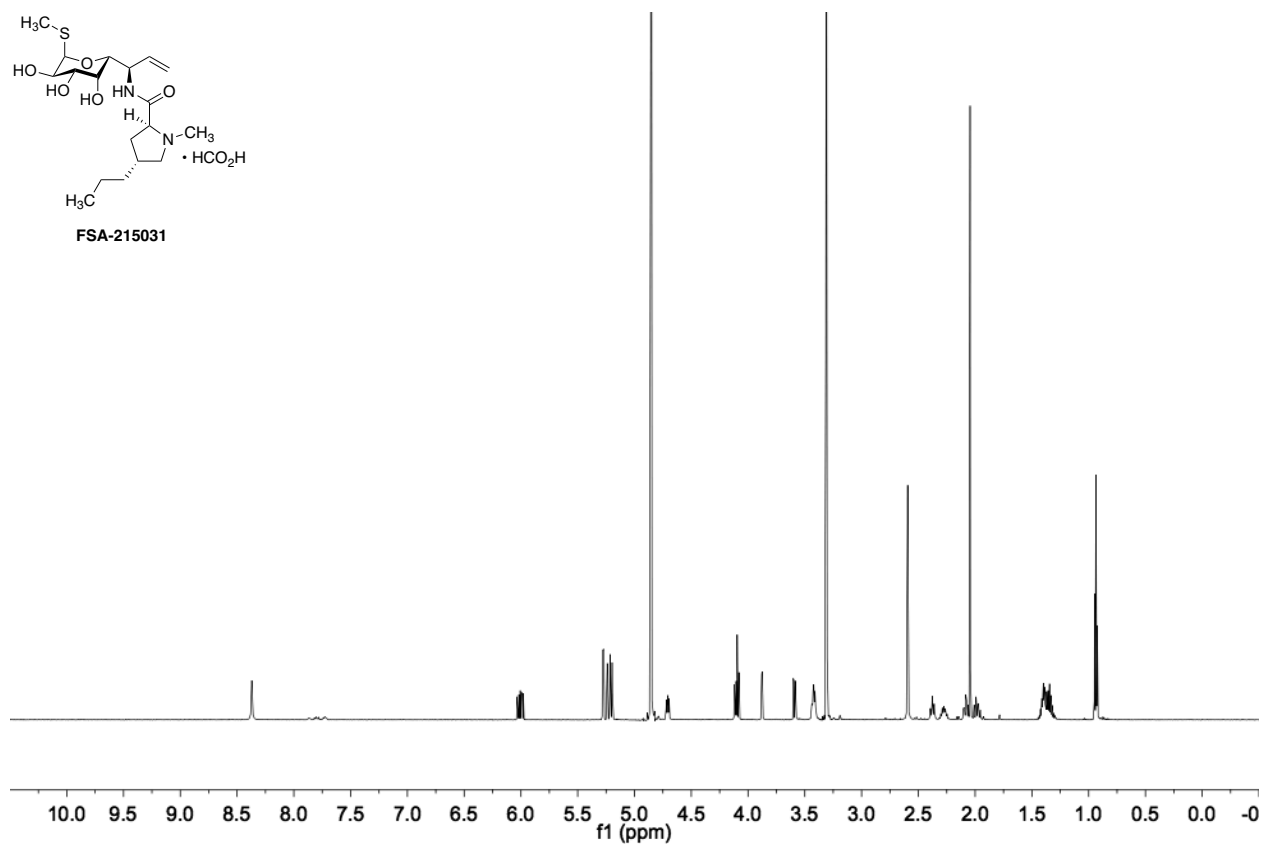
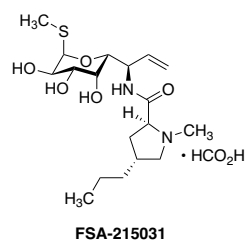


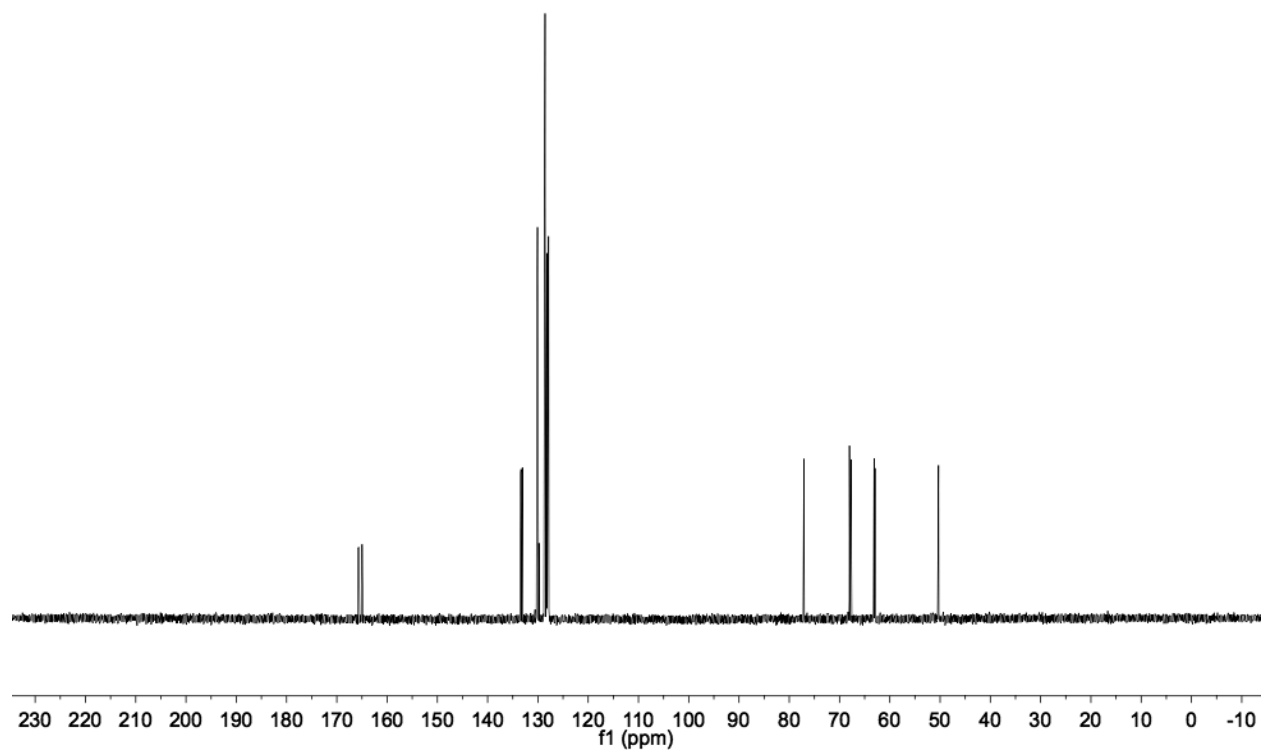
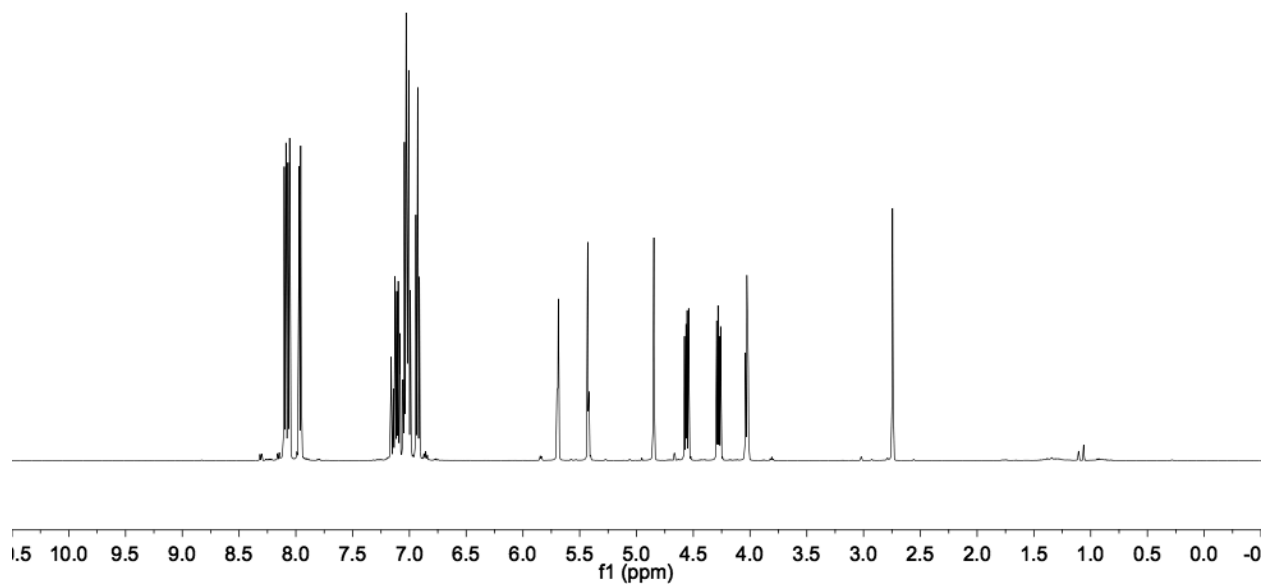
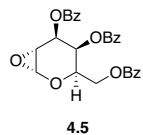


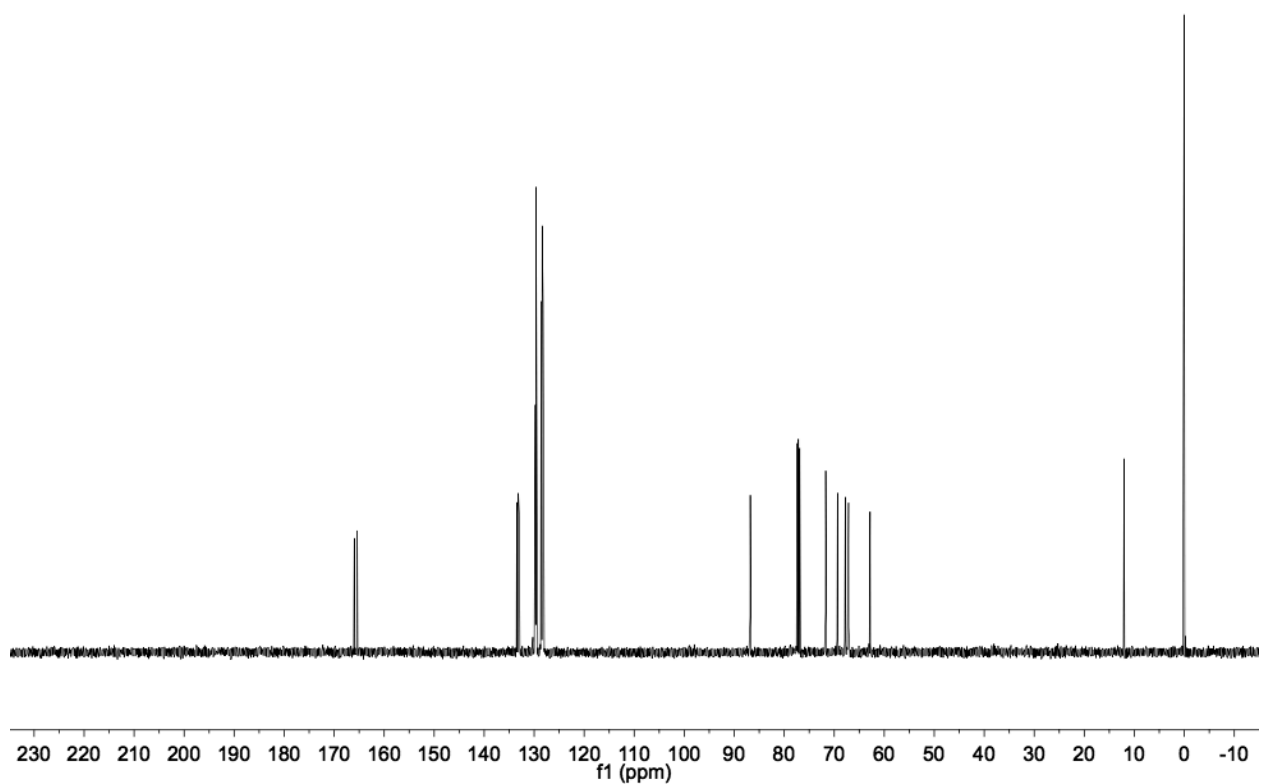
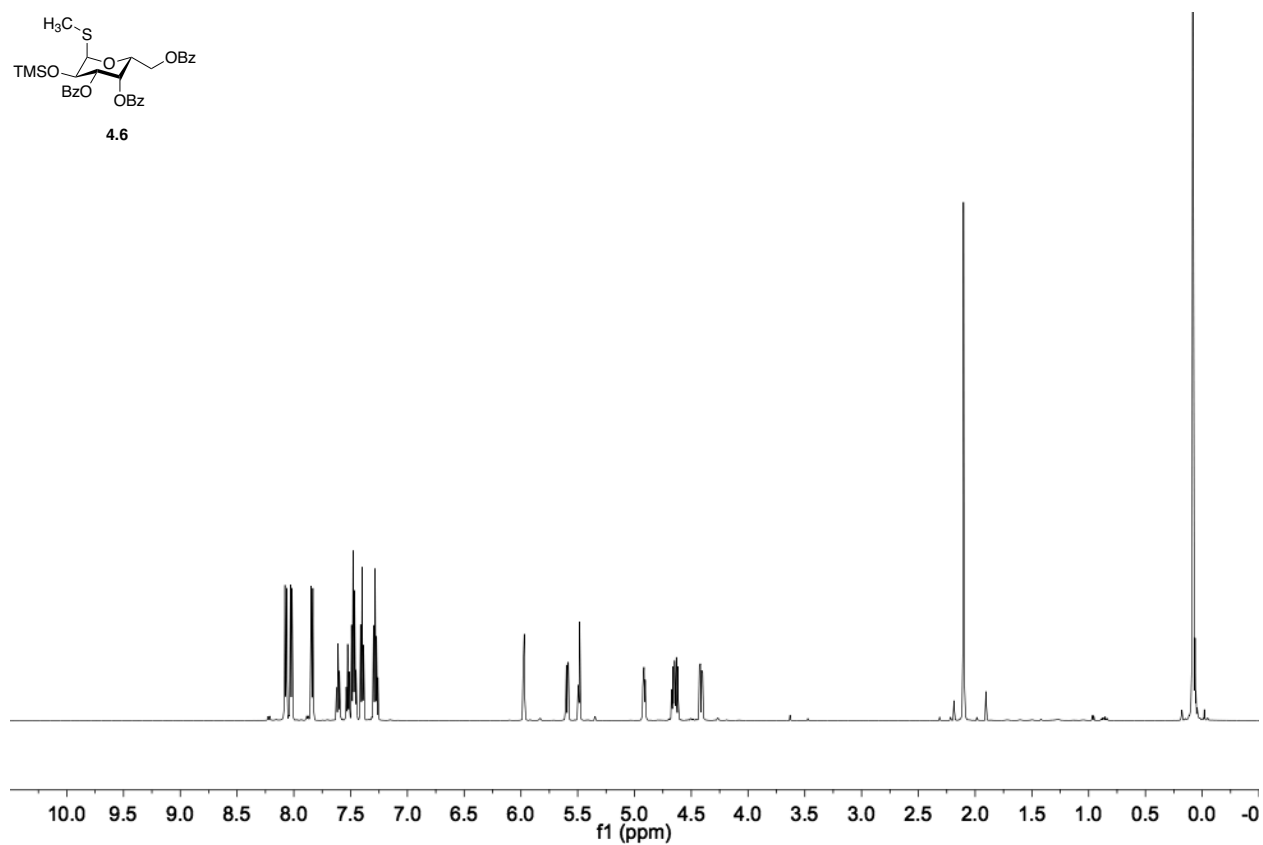
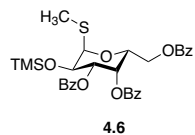


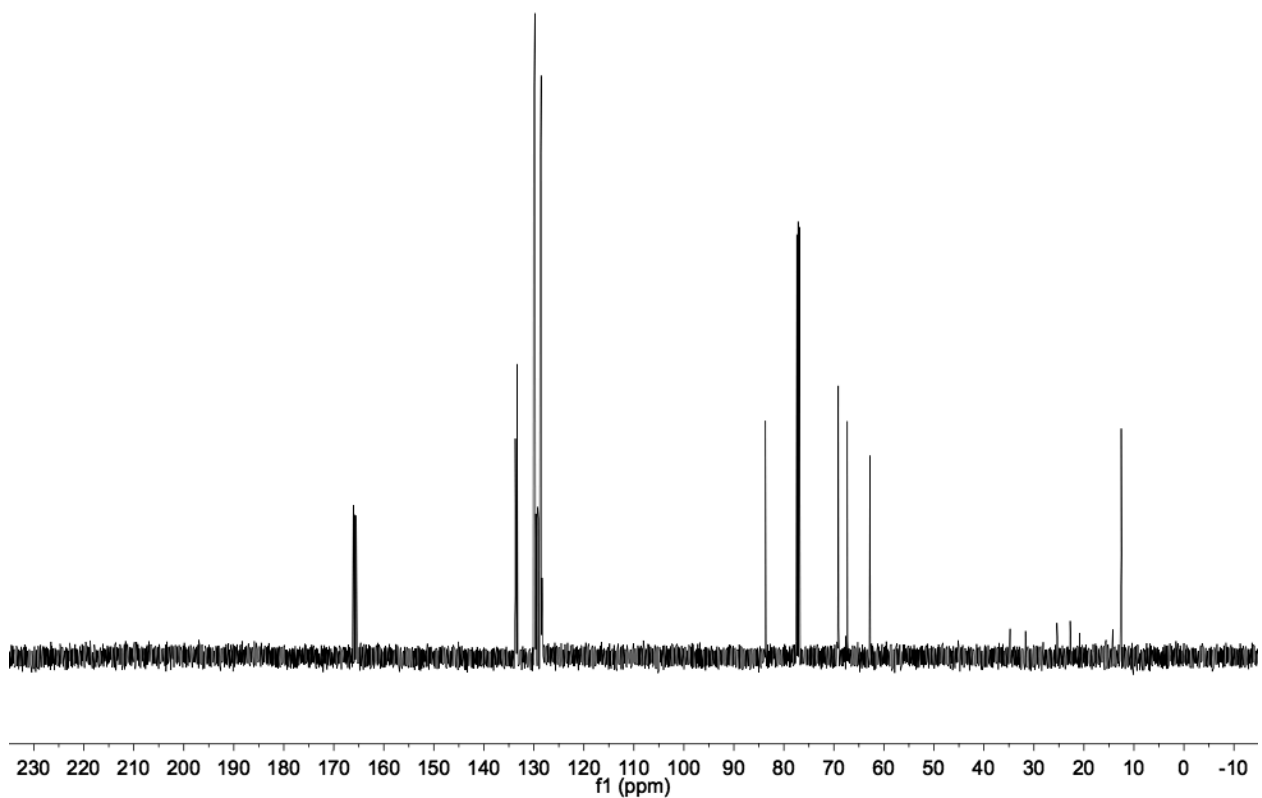
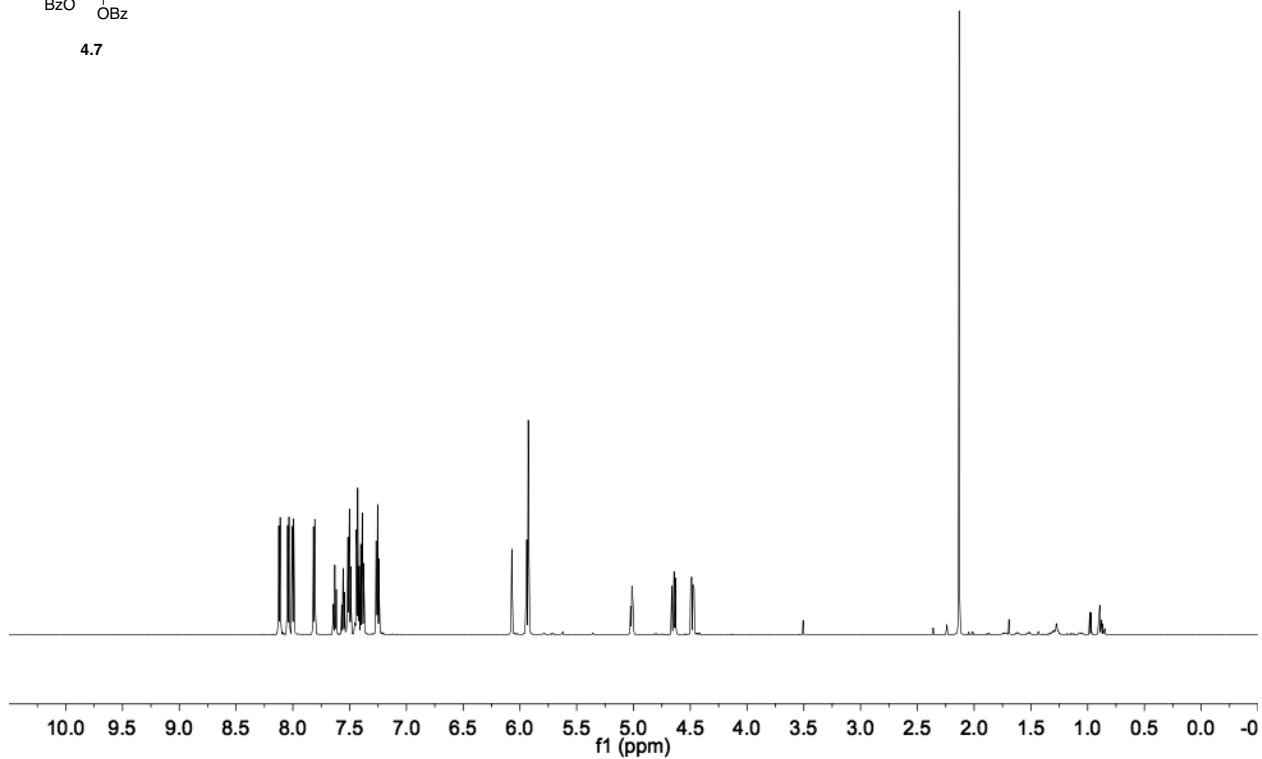
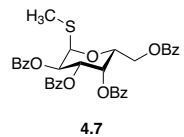


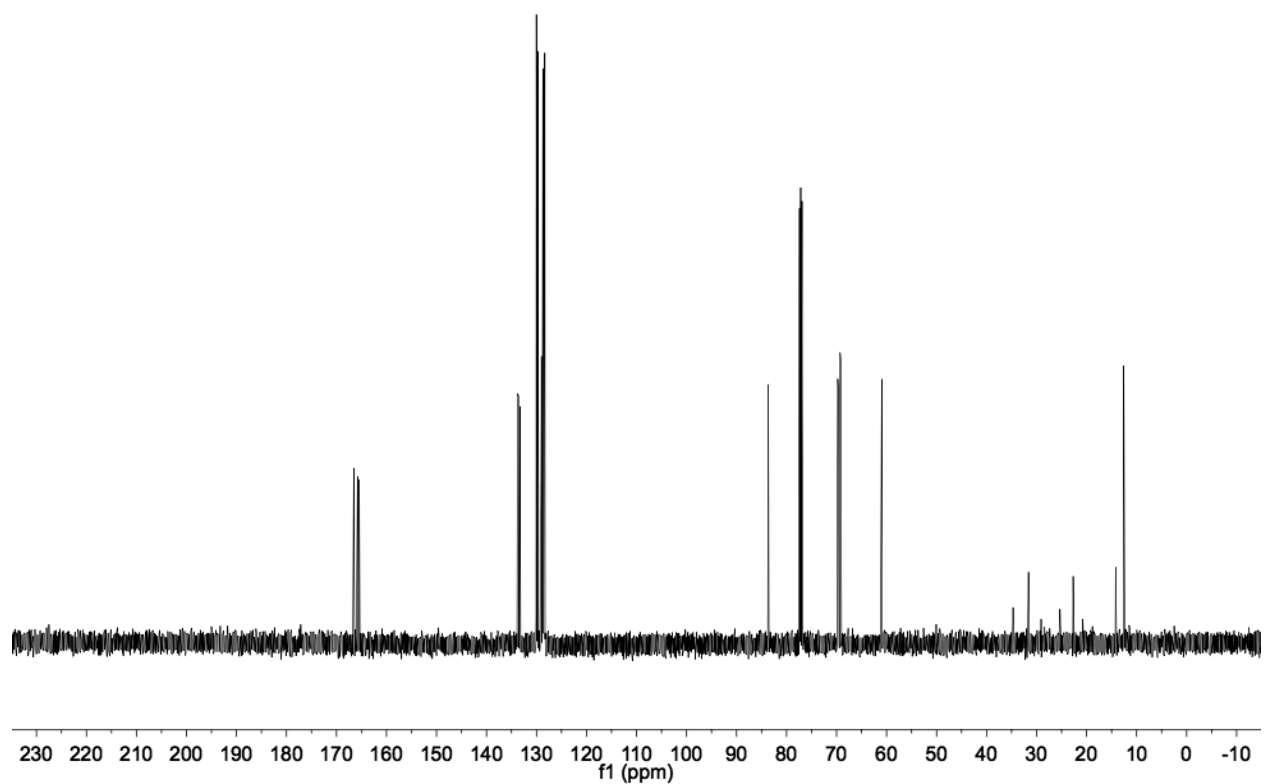
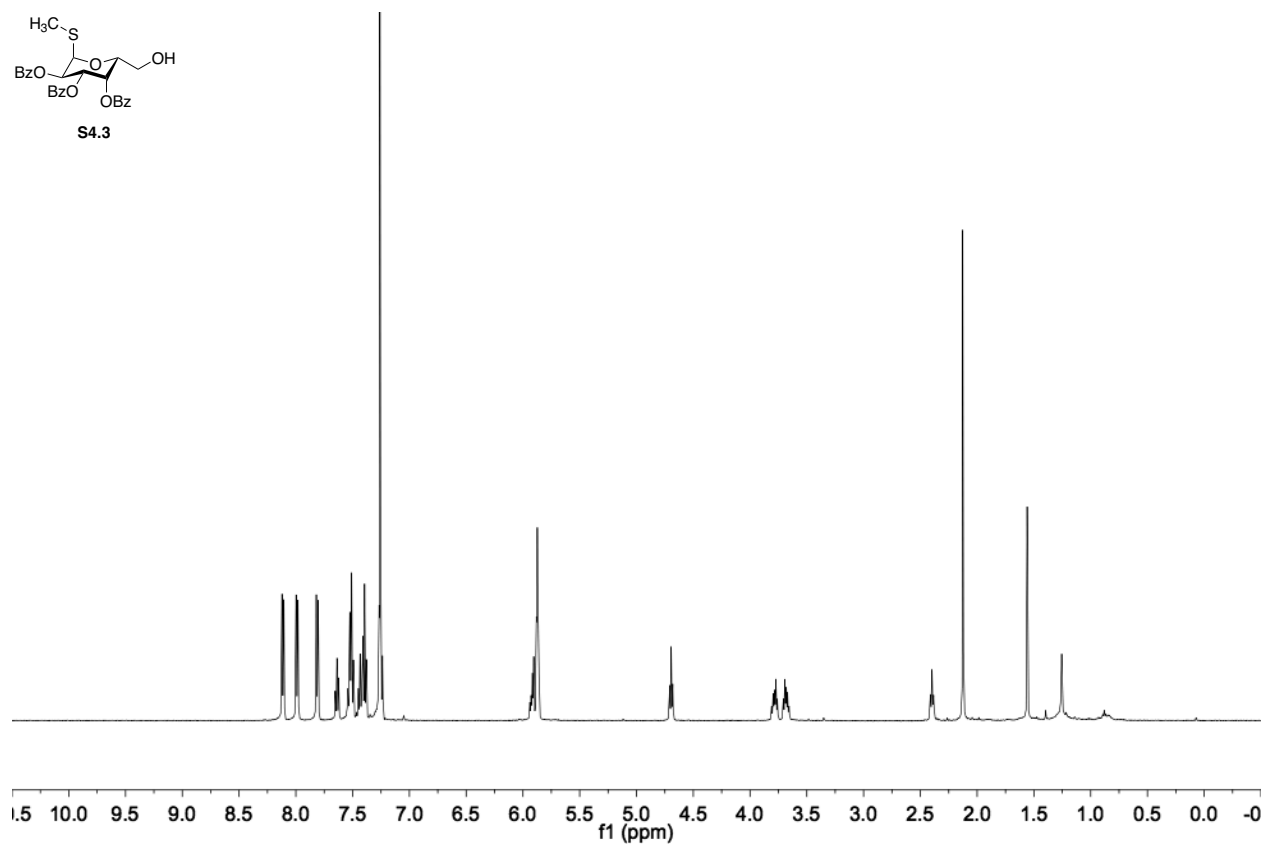
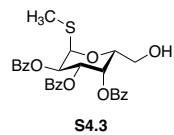


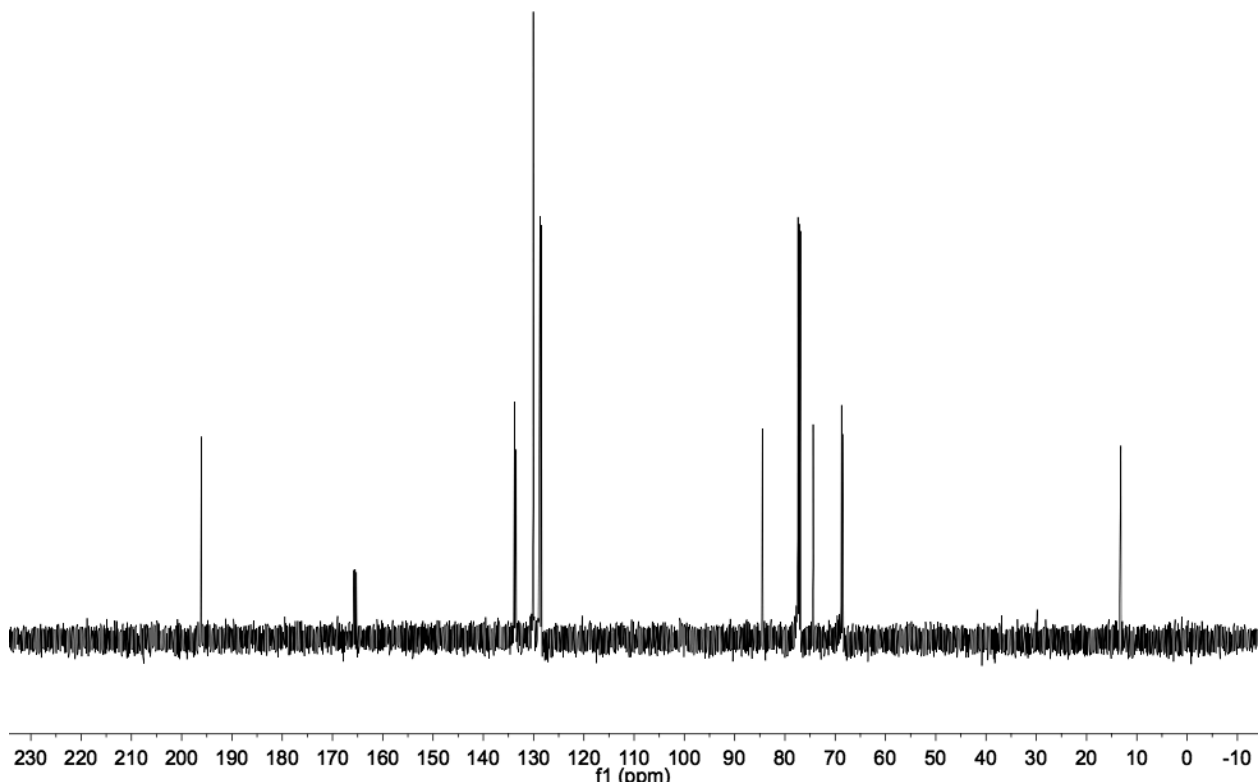
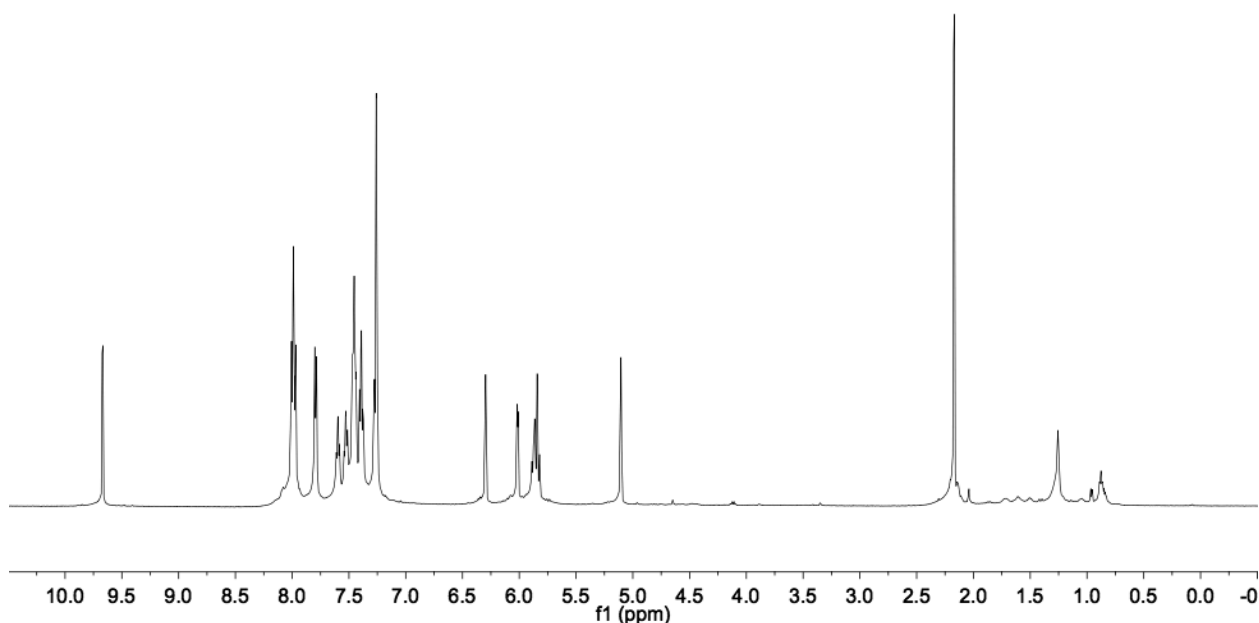
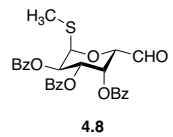


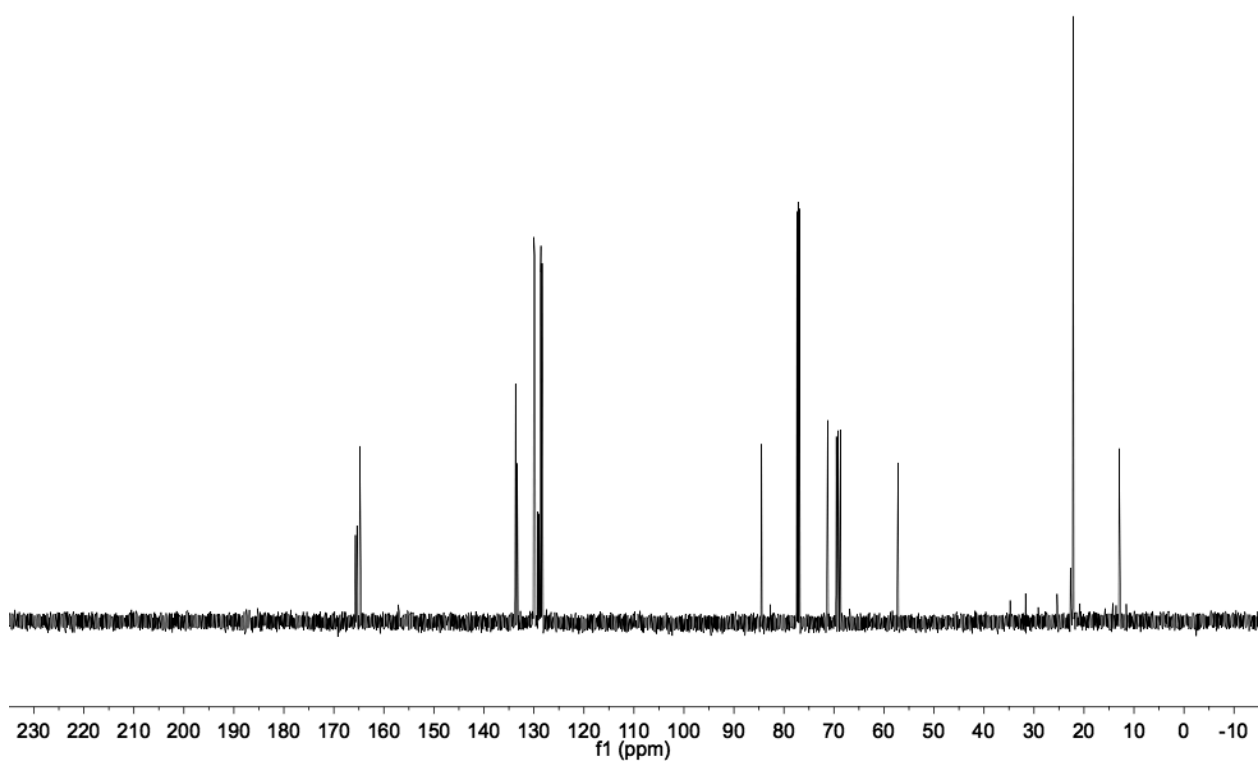
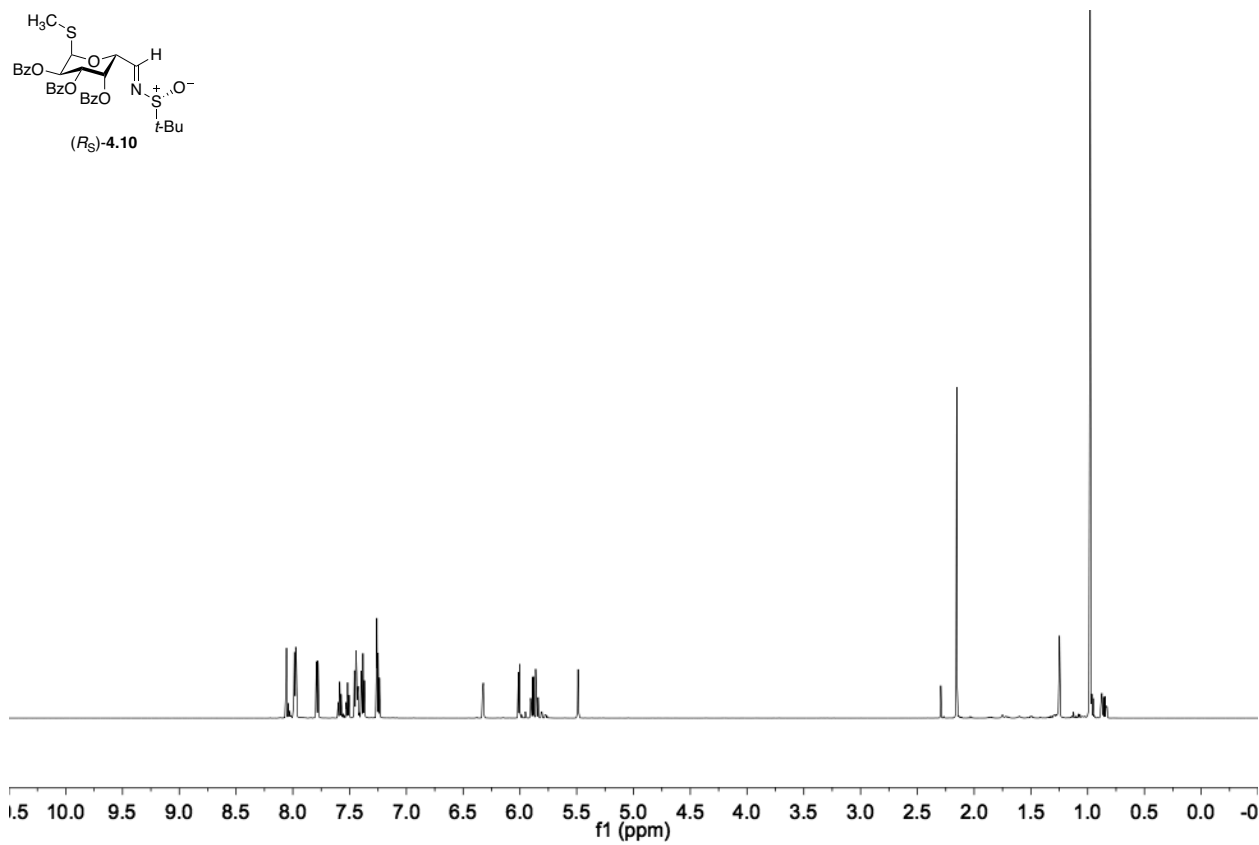
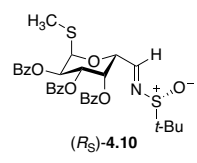


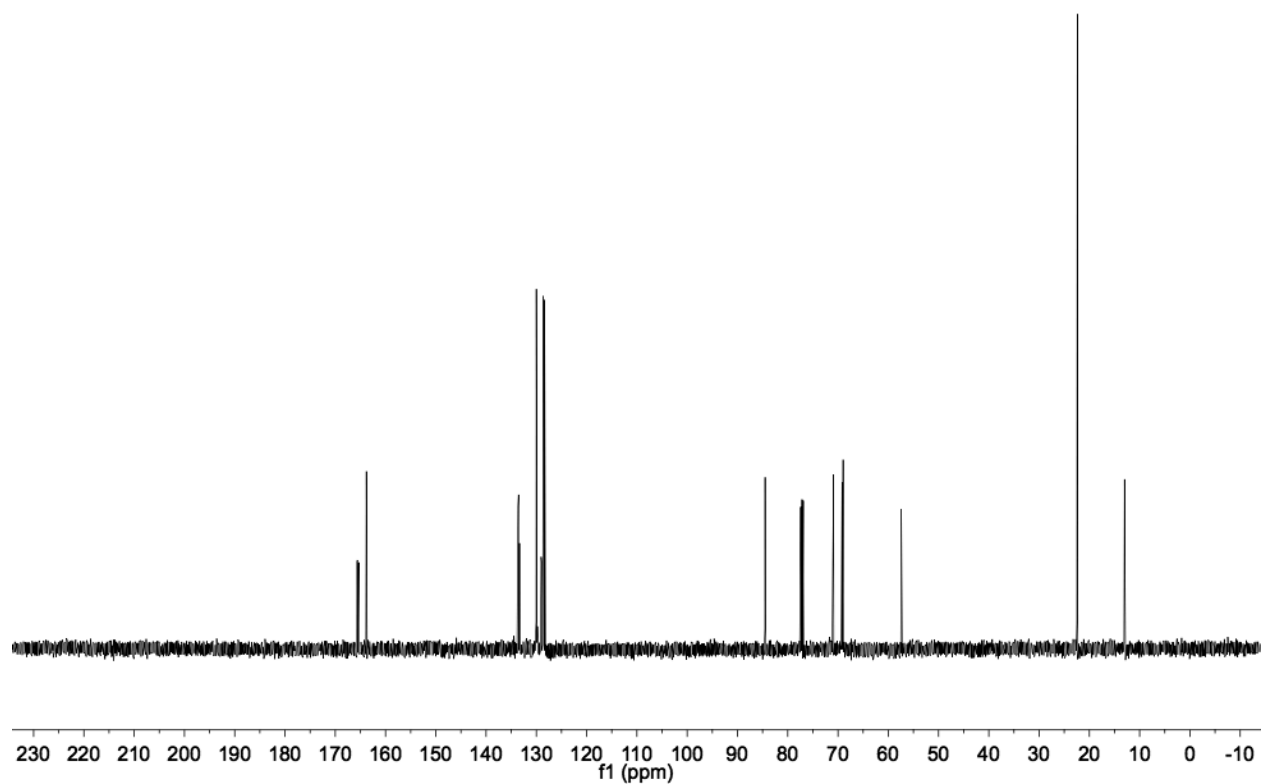
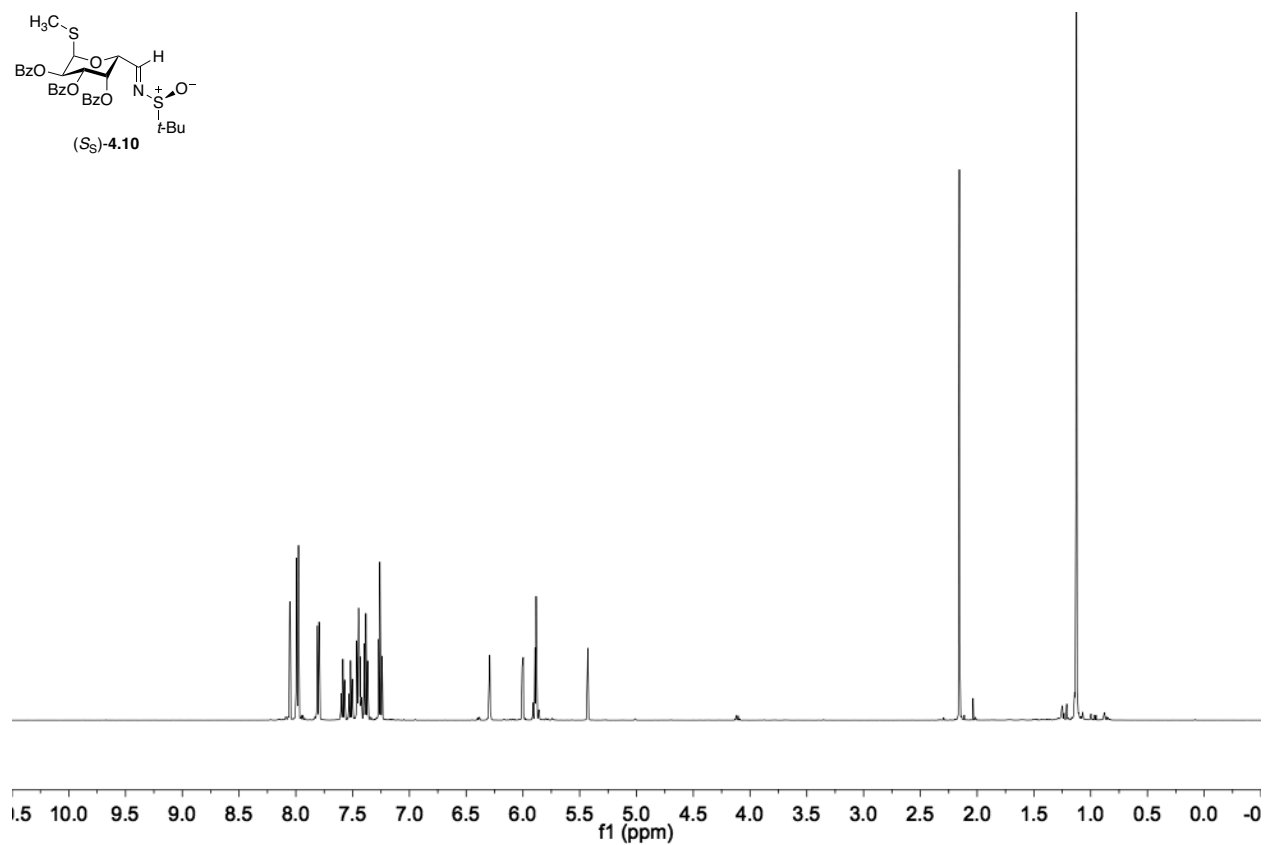
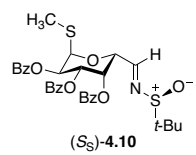


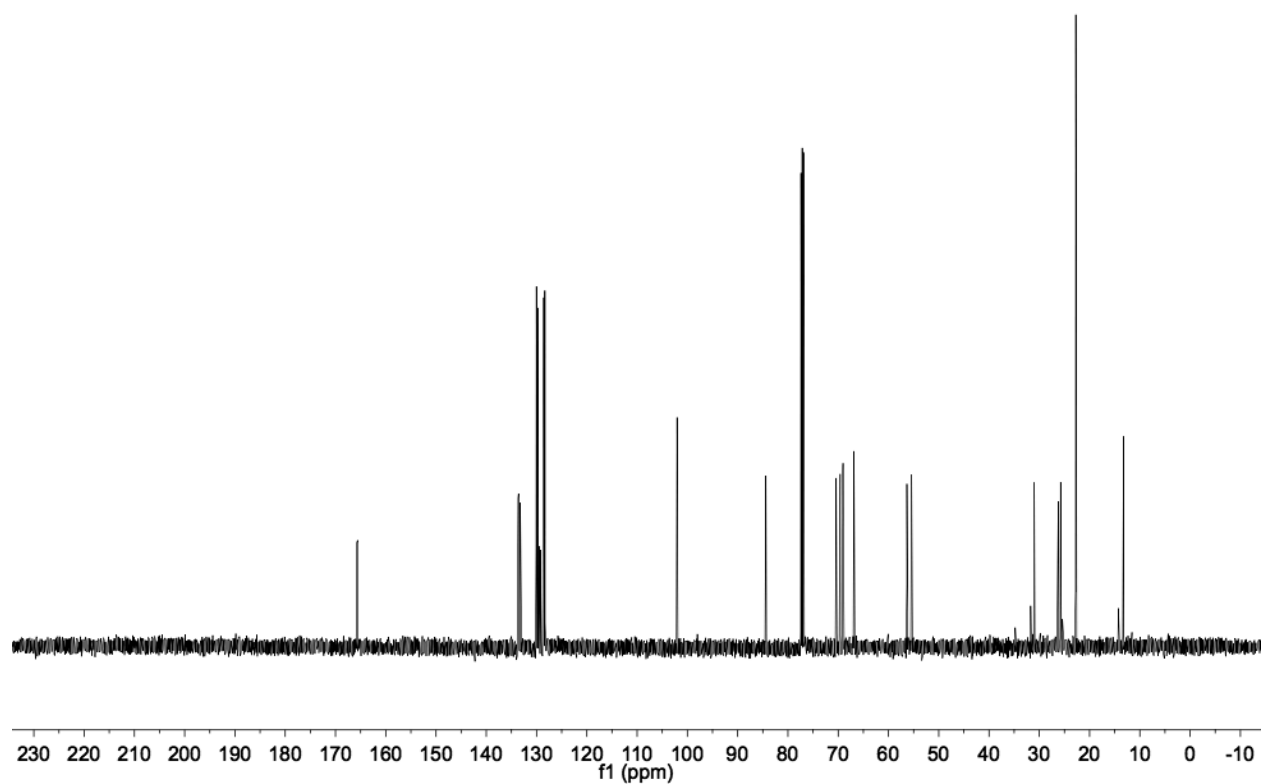
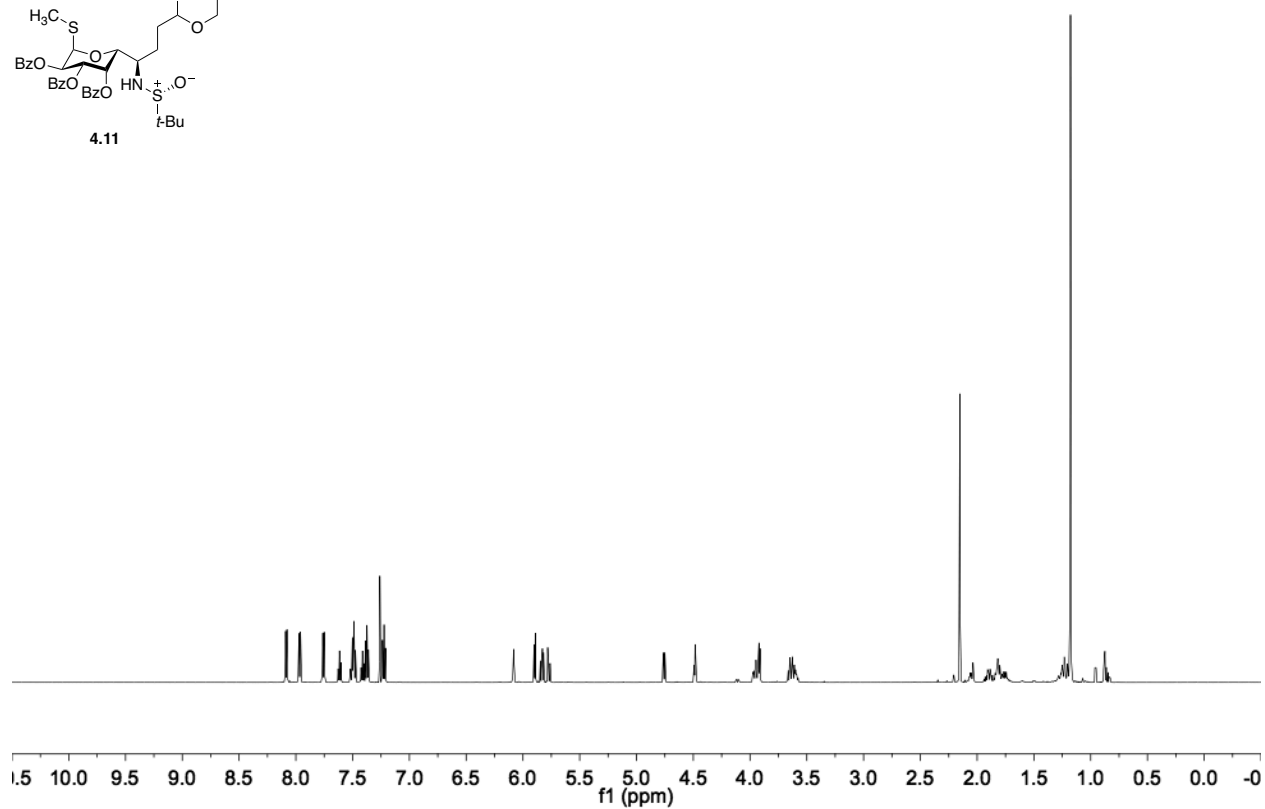
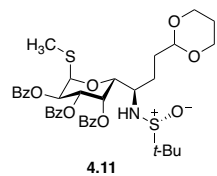


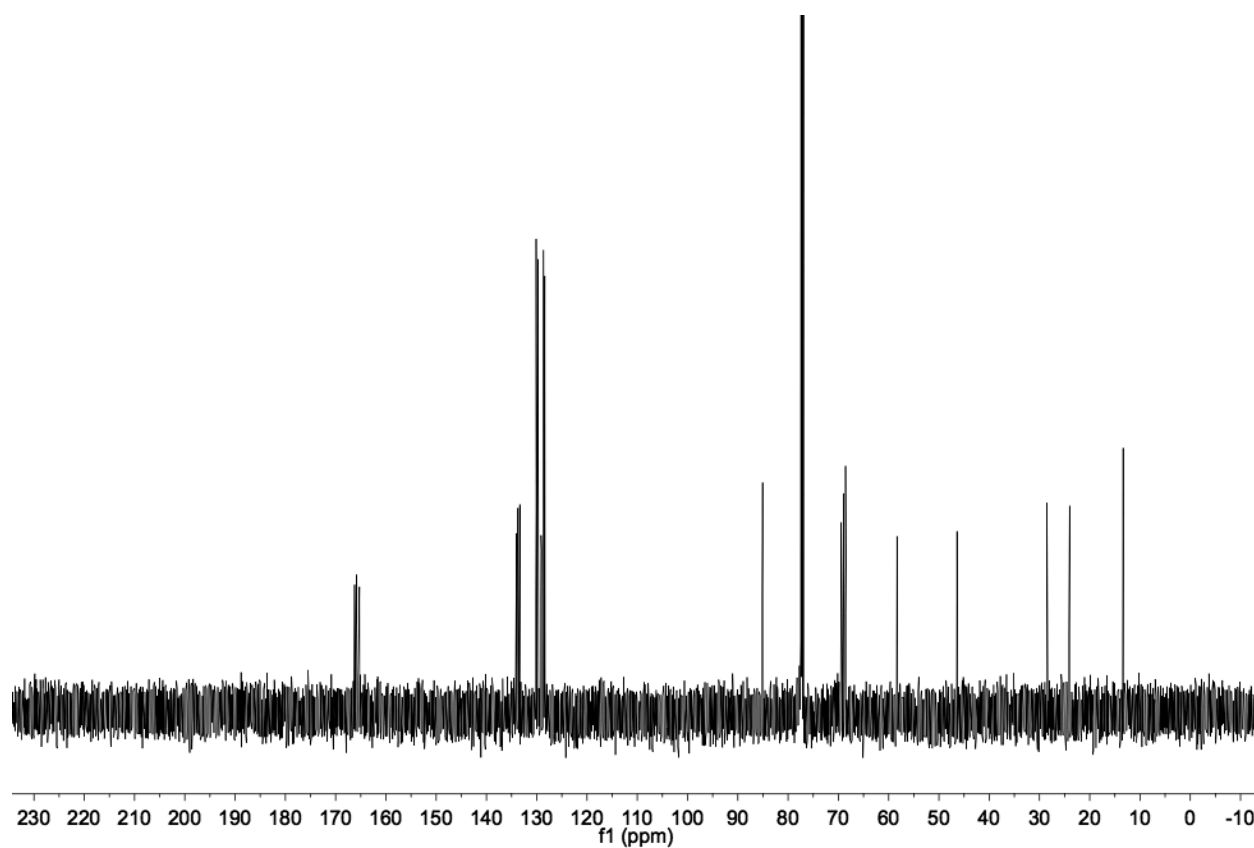
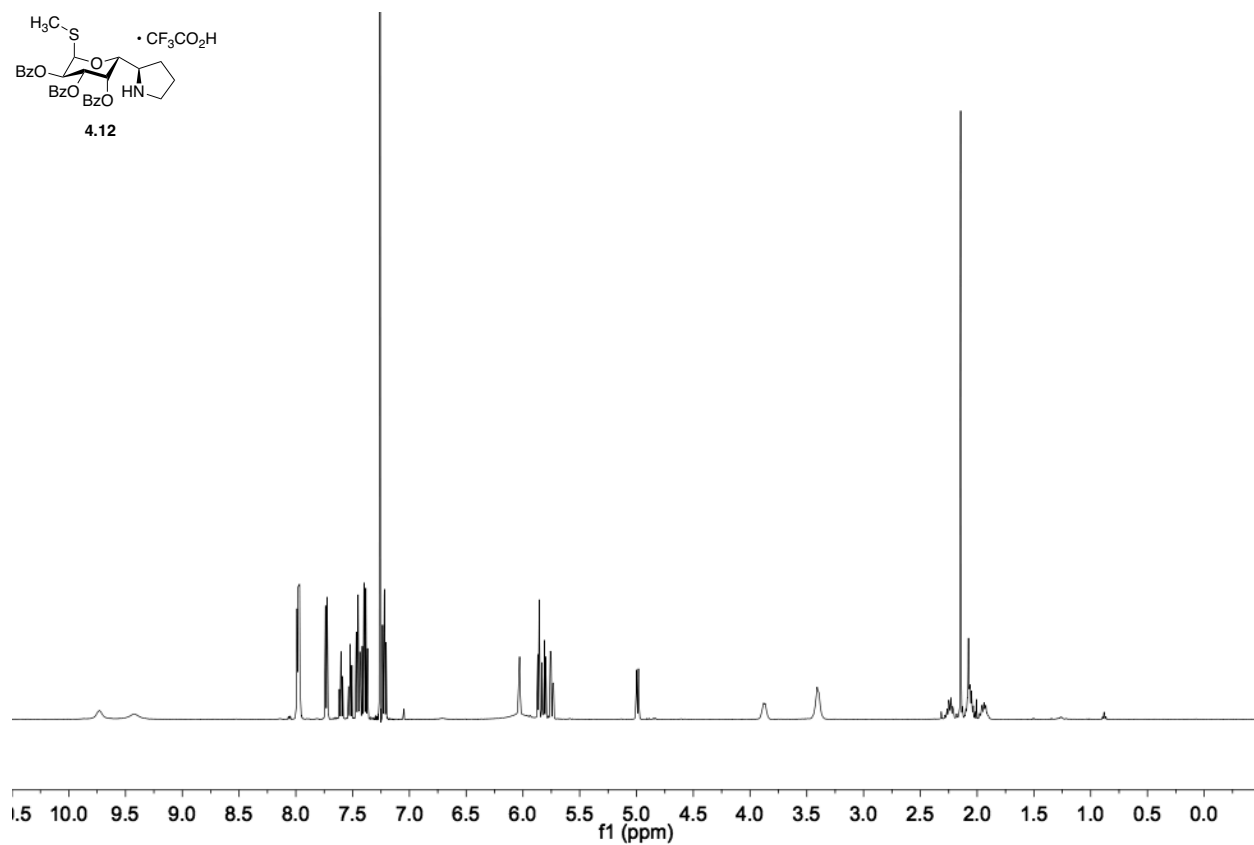
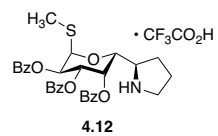


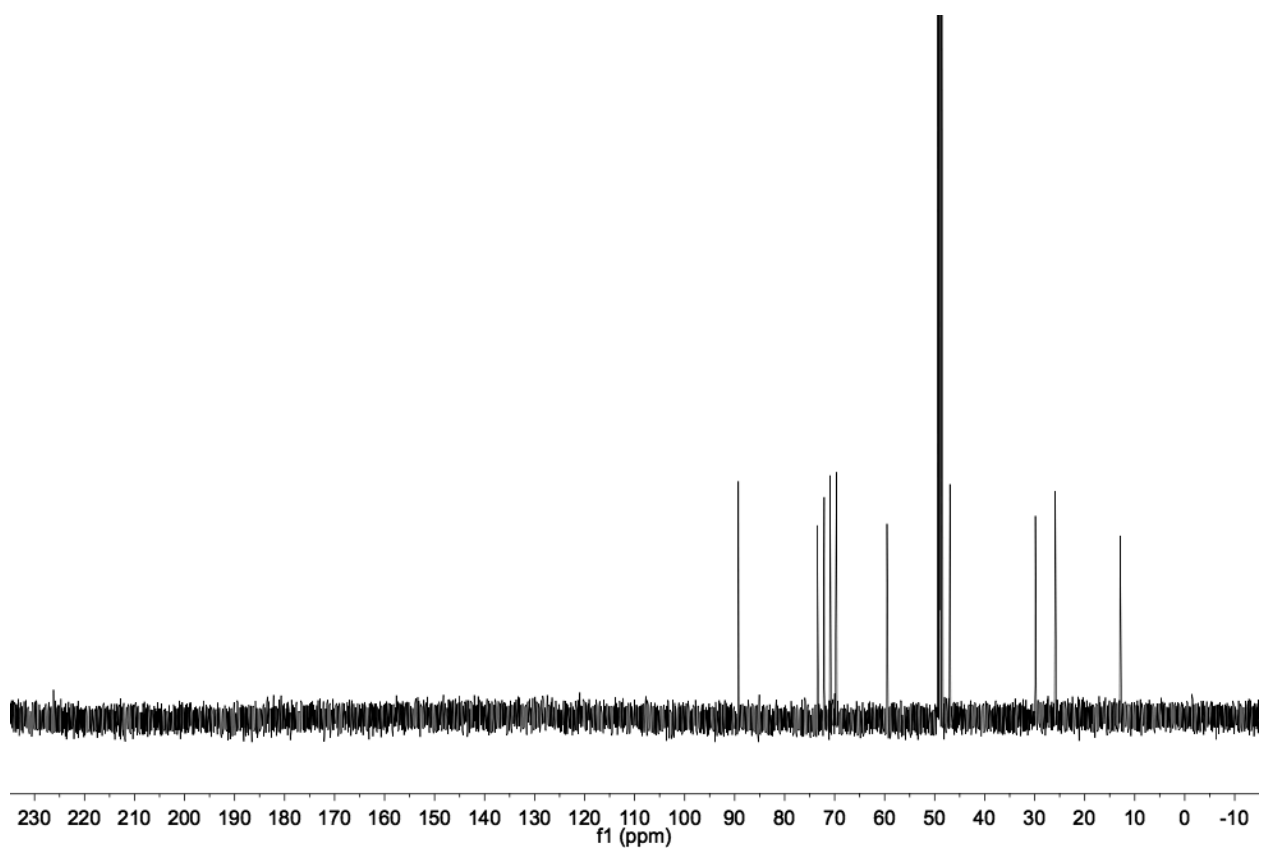
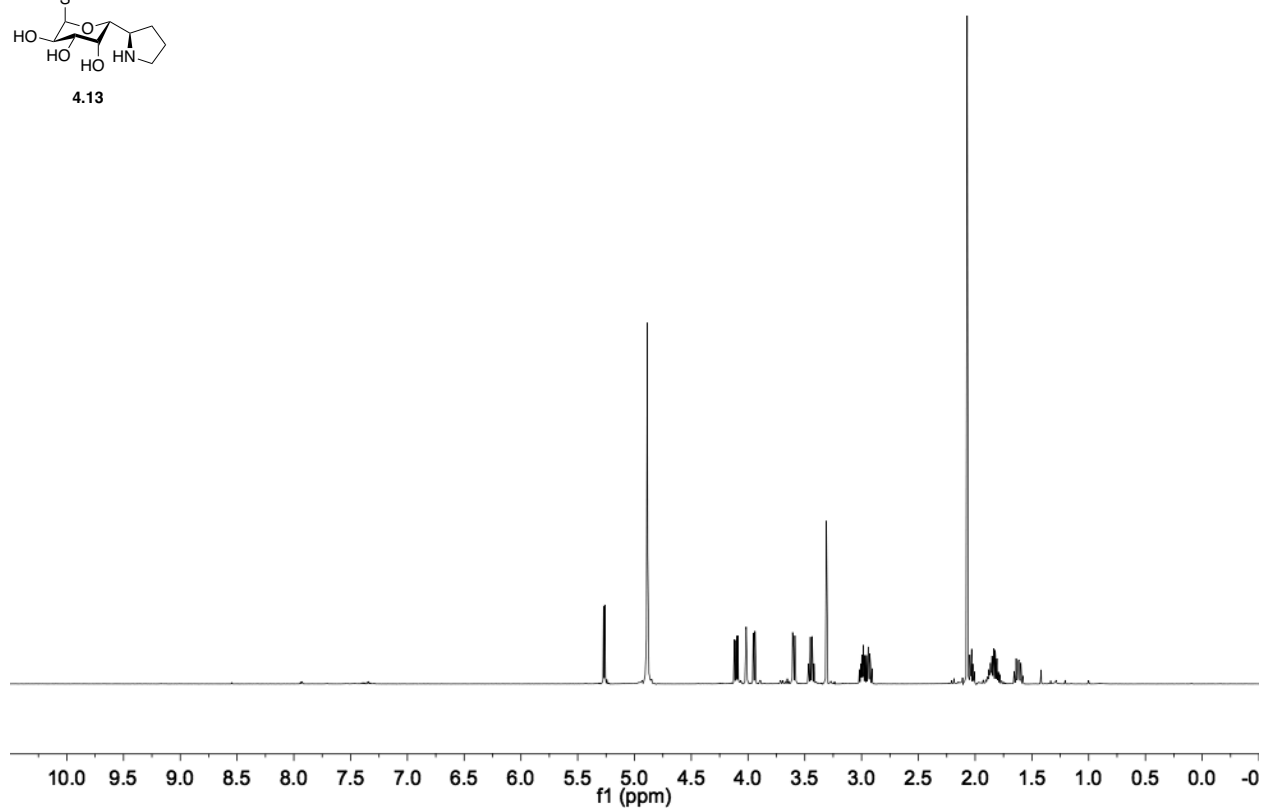
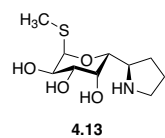


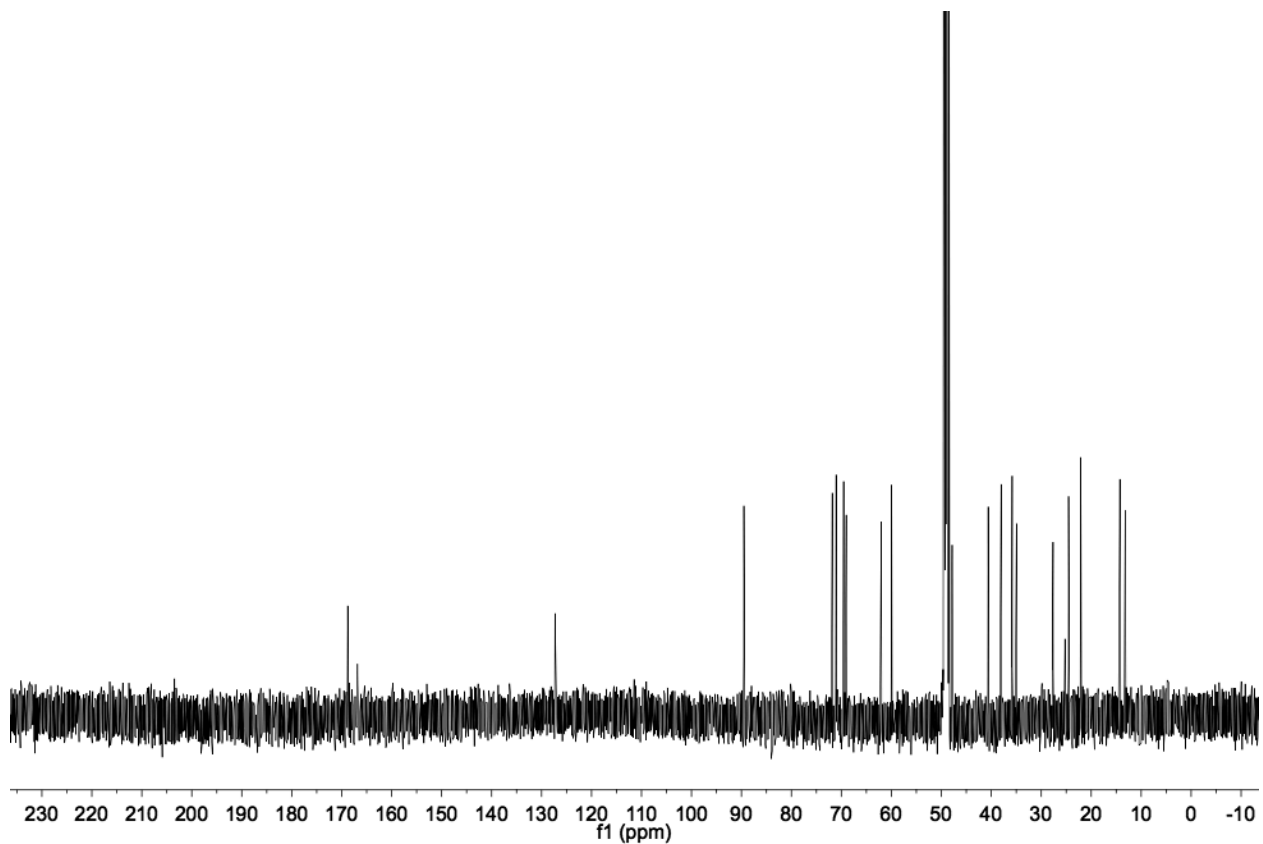
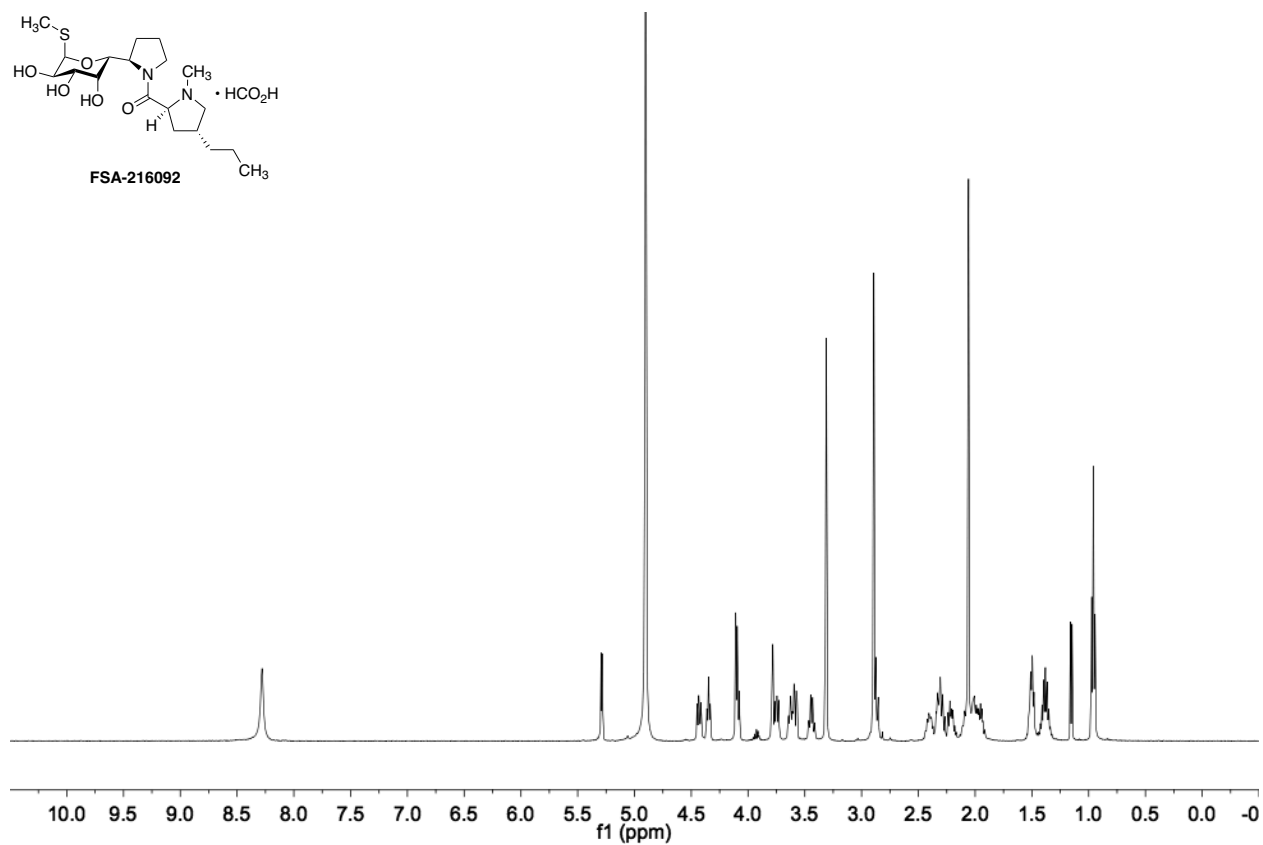
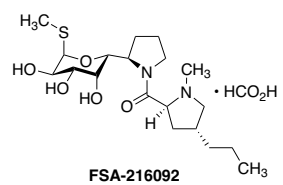


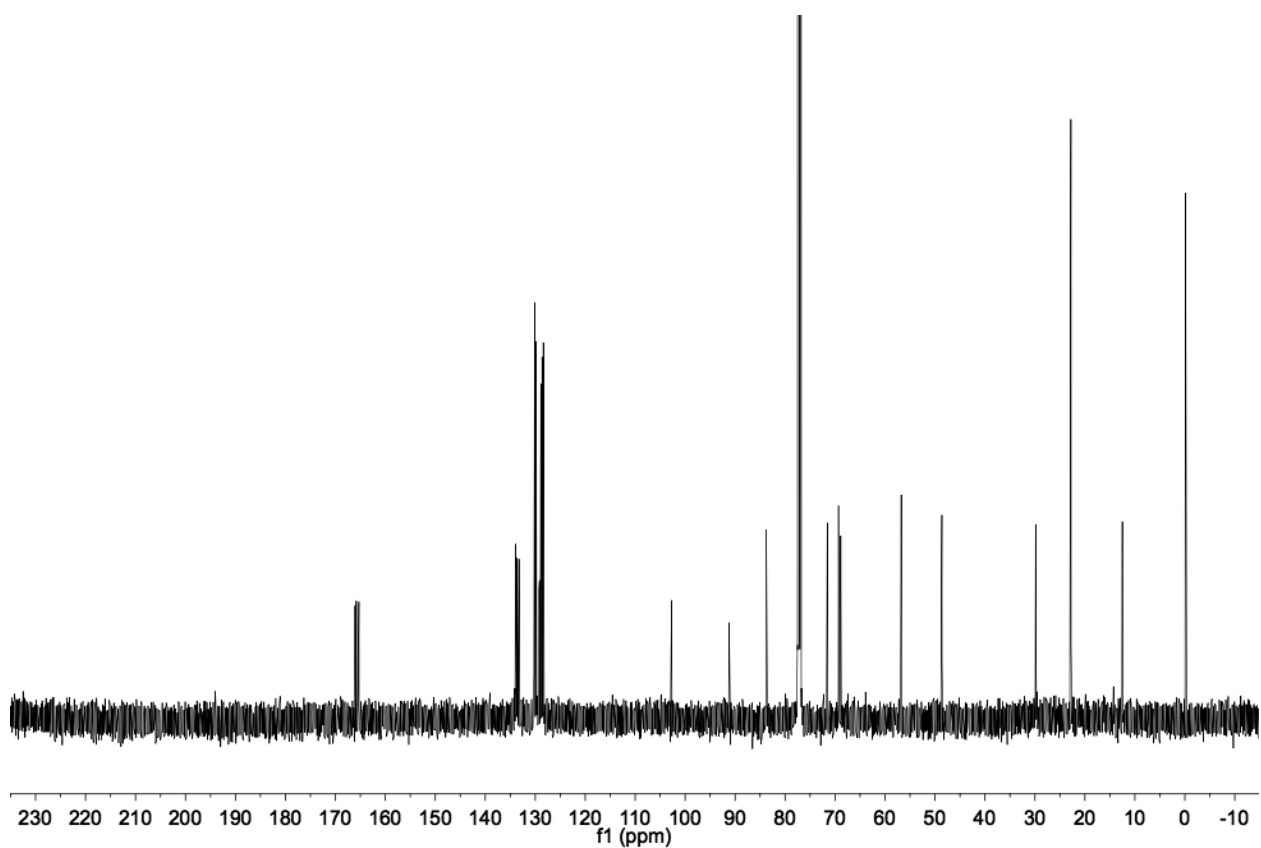
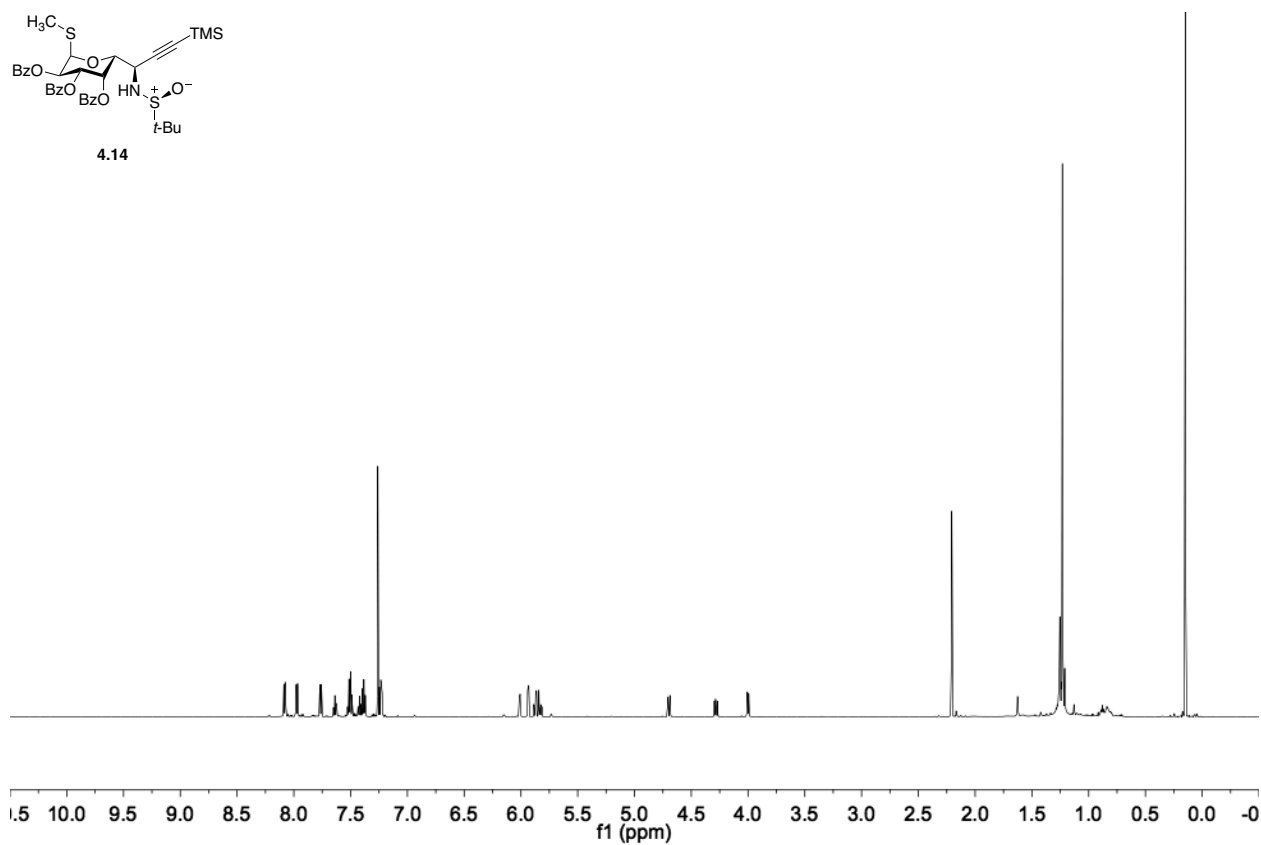
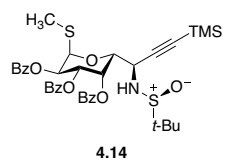


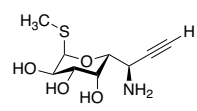




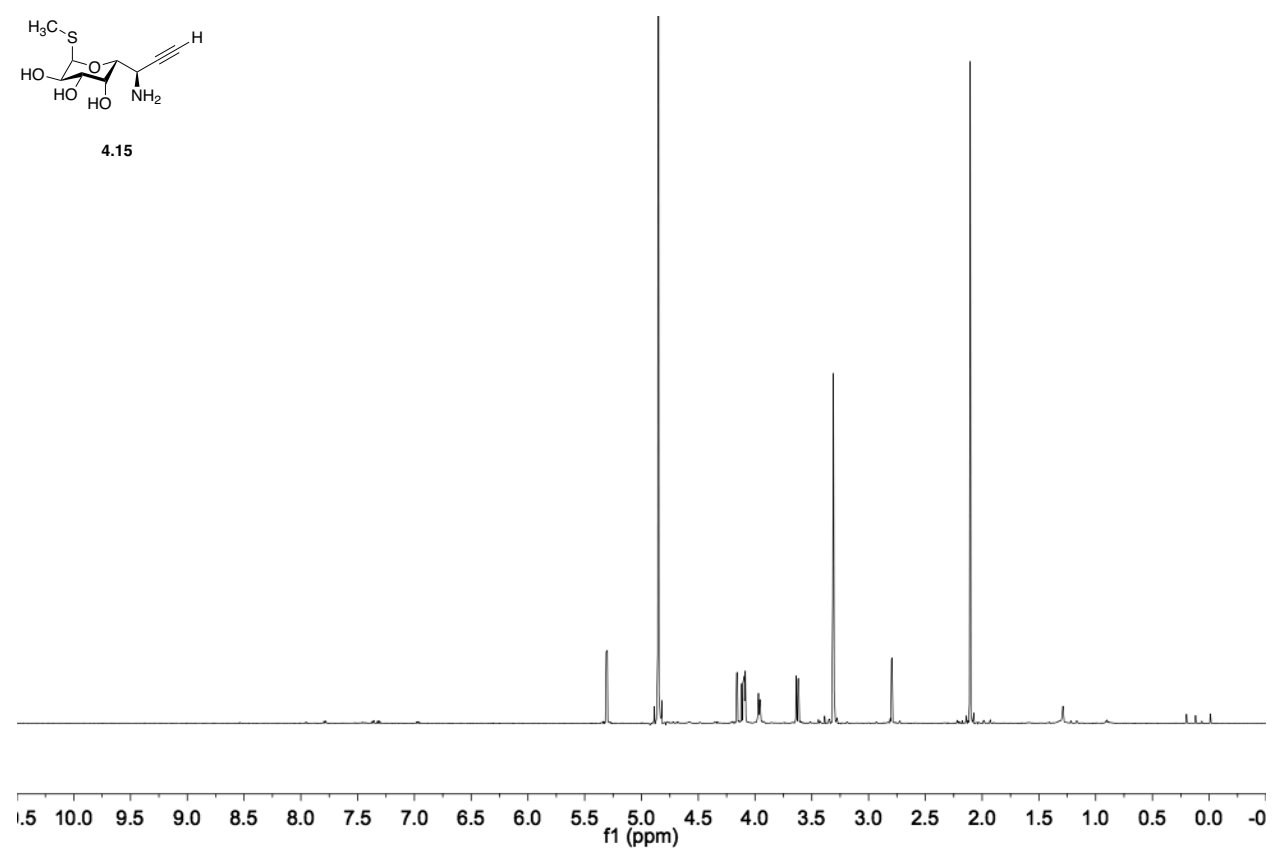


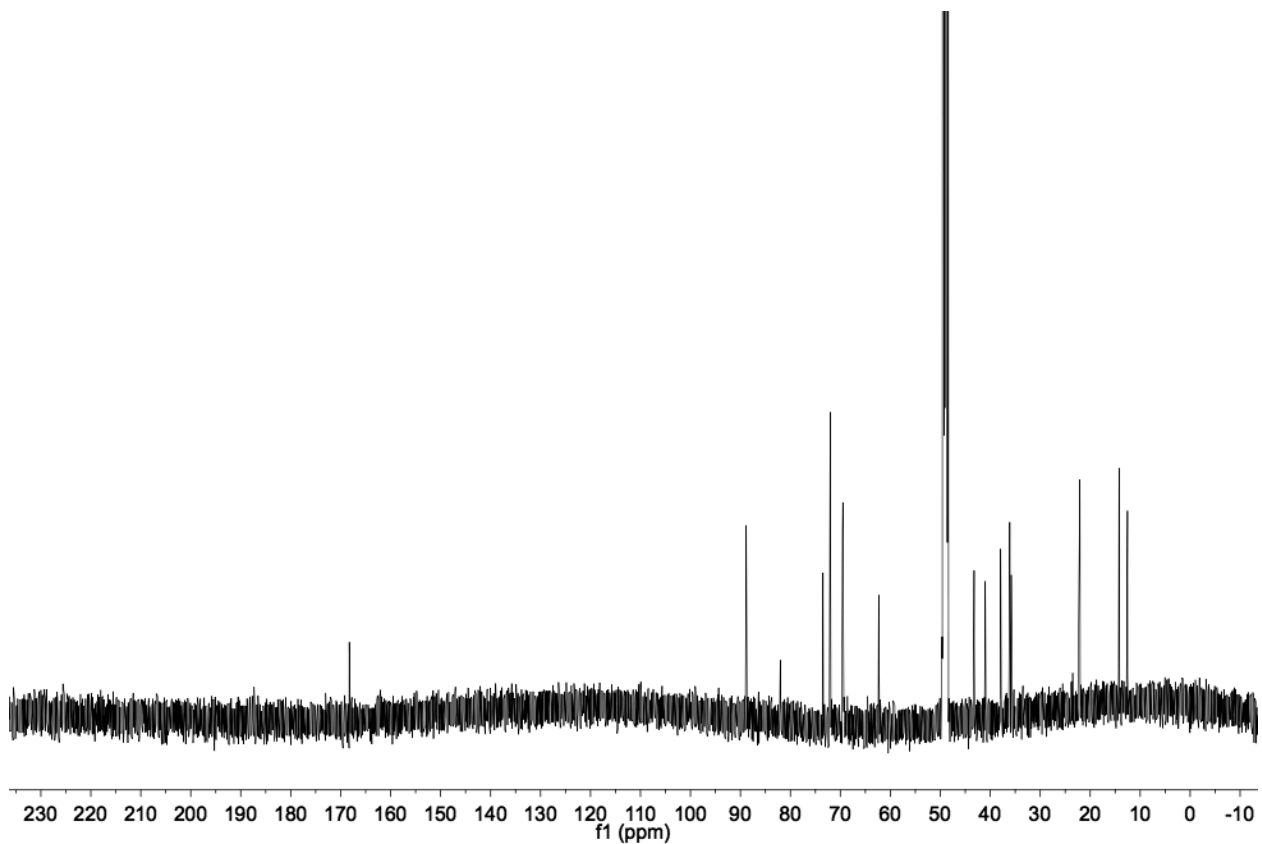
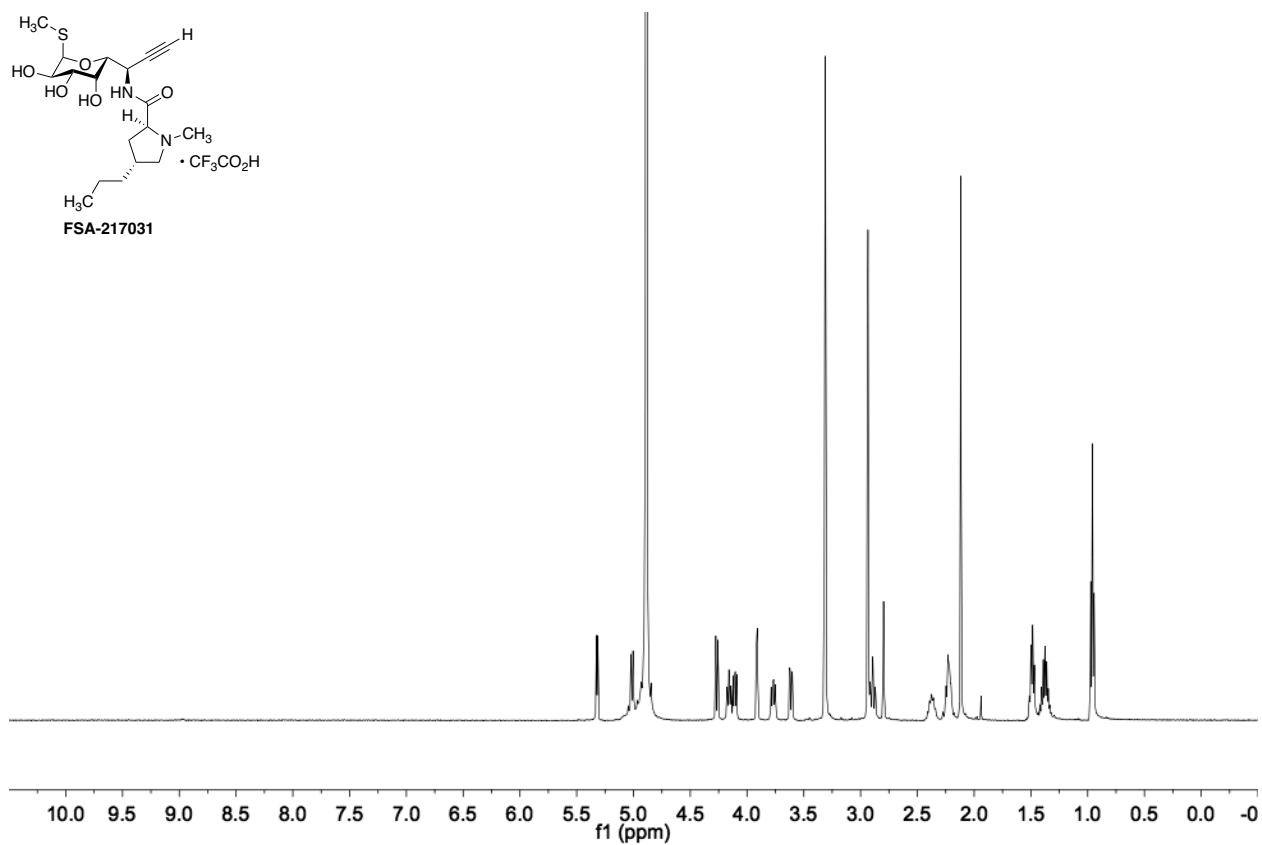
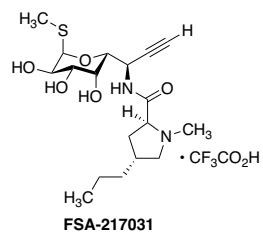


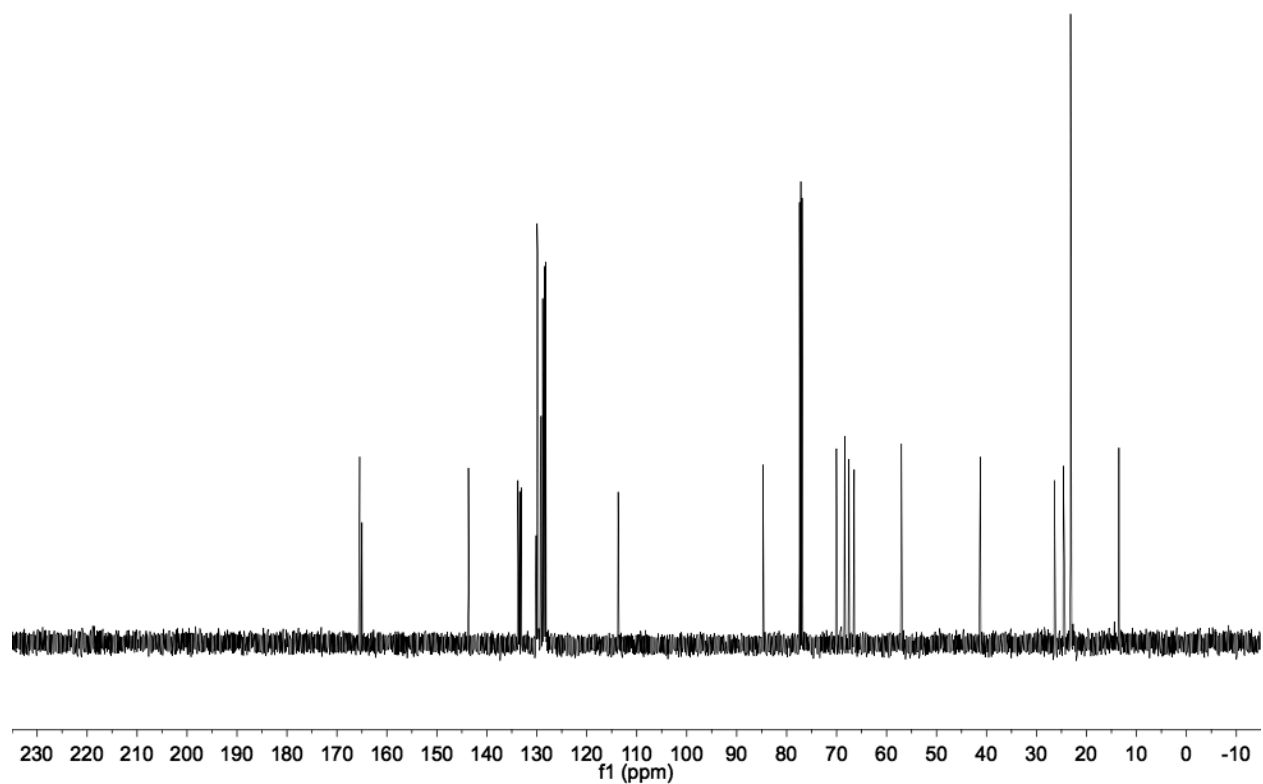
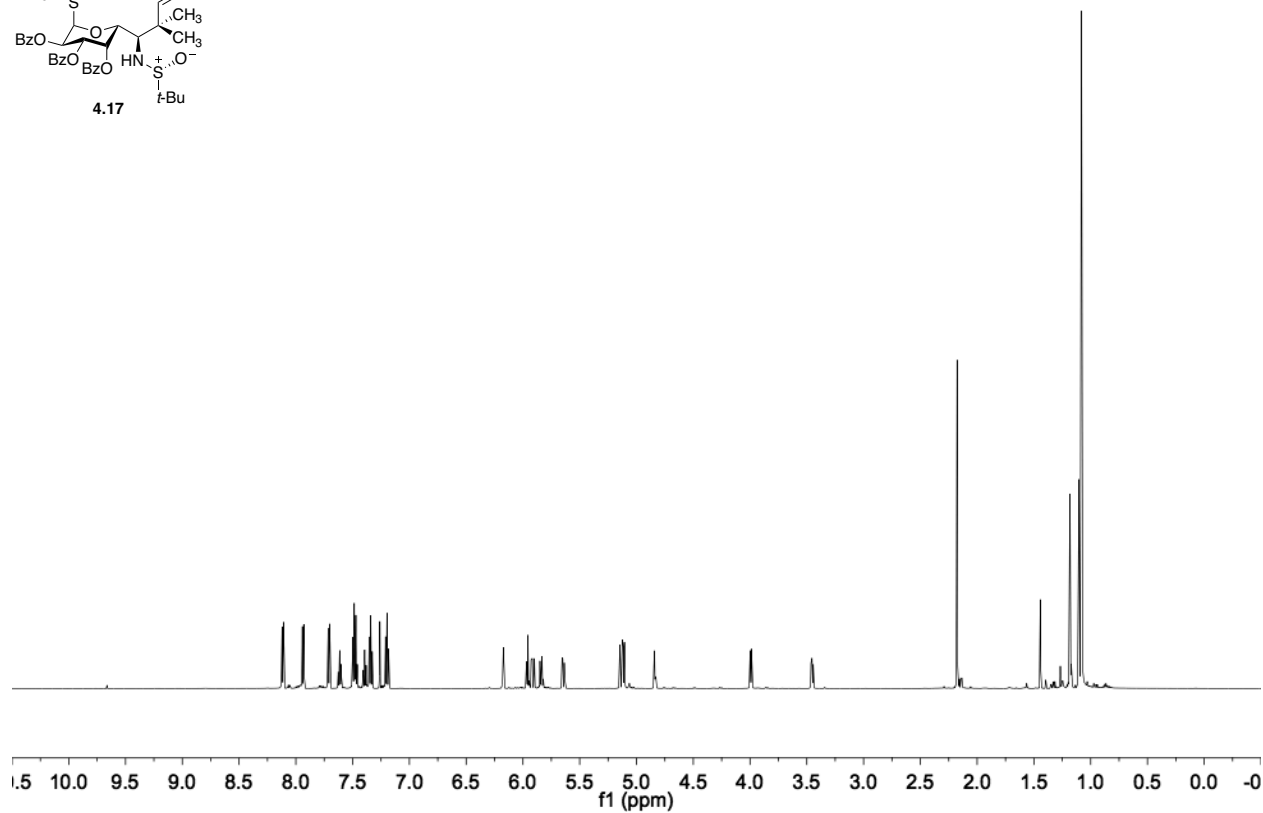
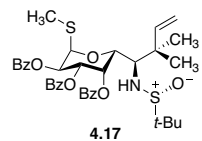


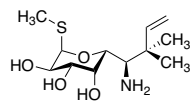


4.15

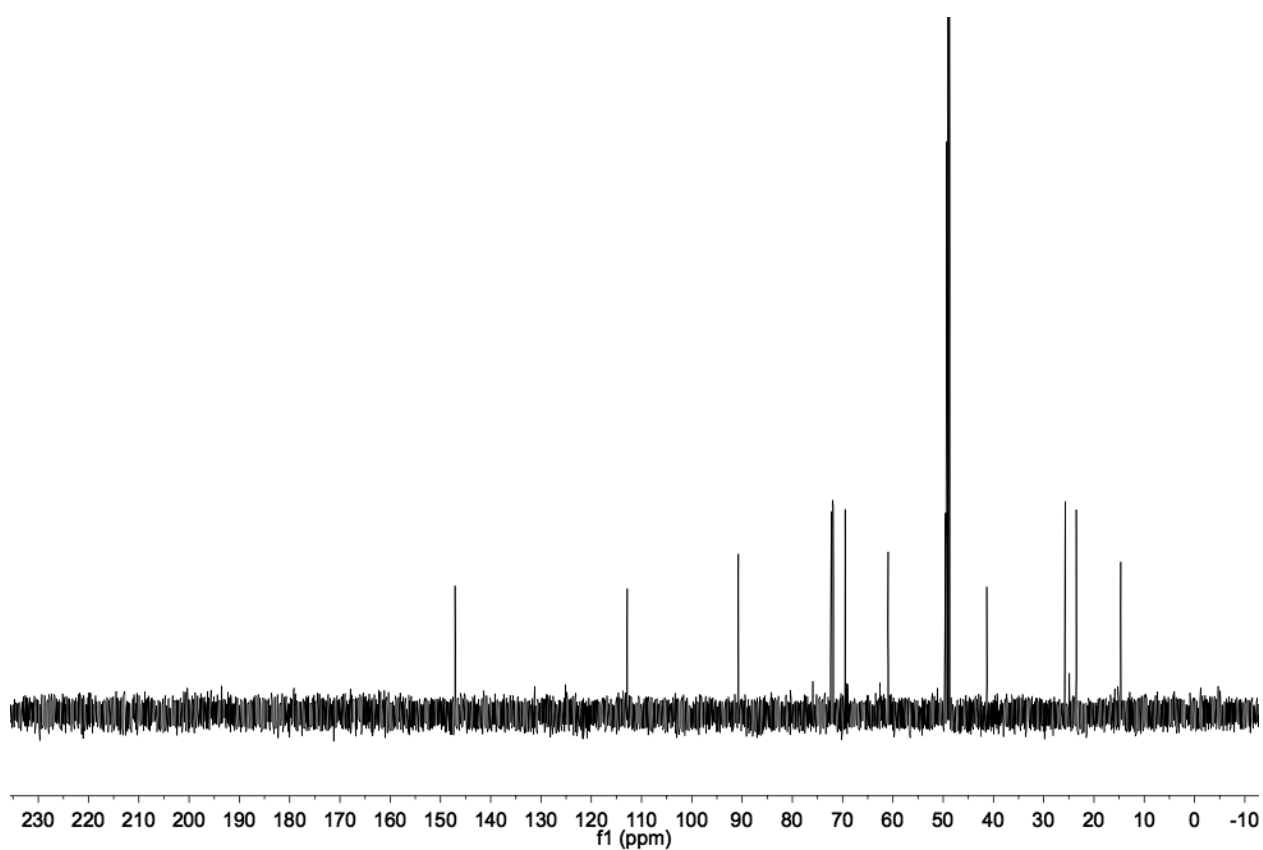
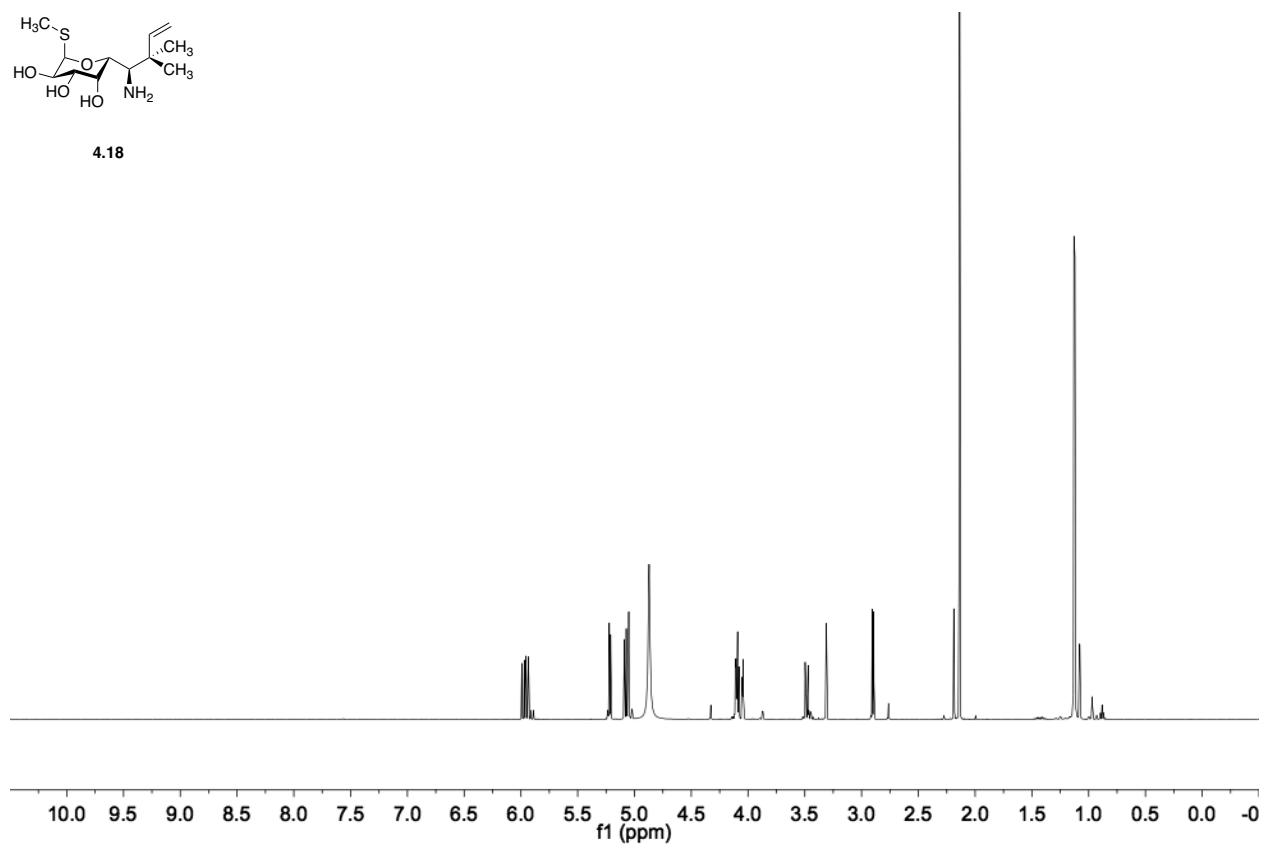


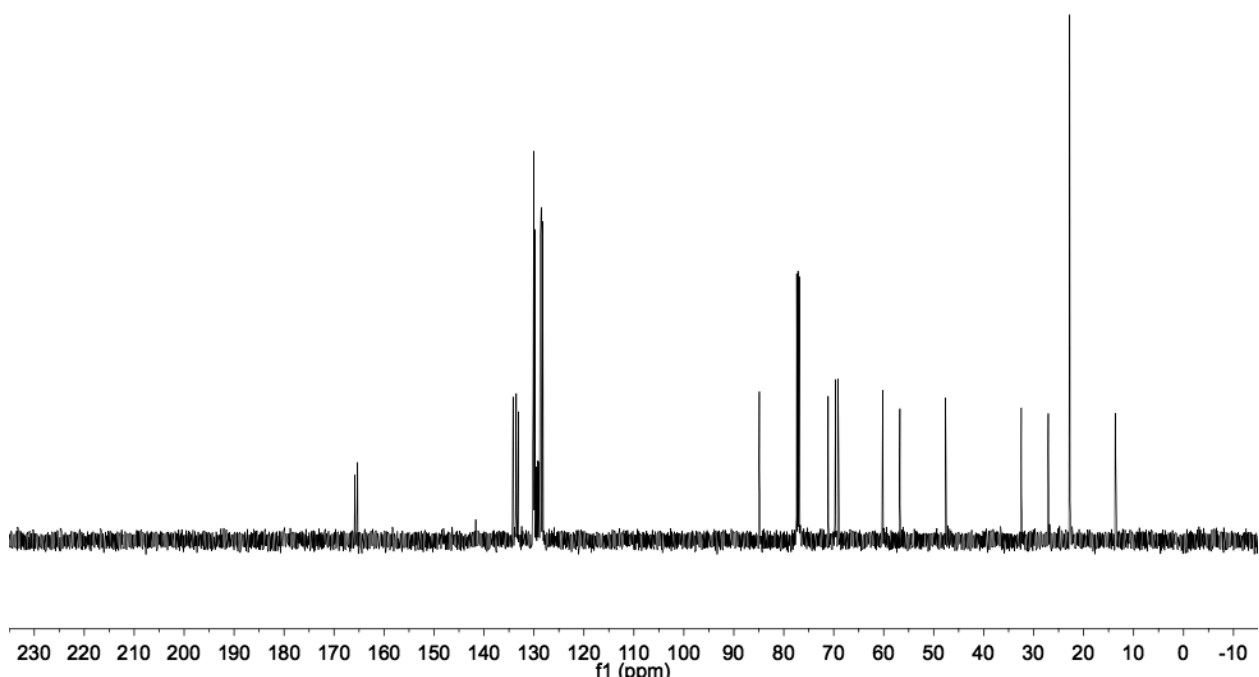
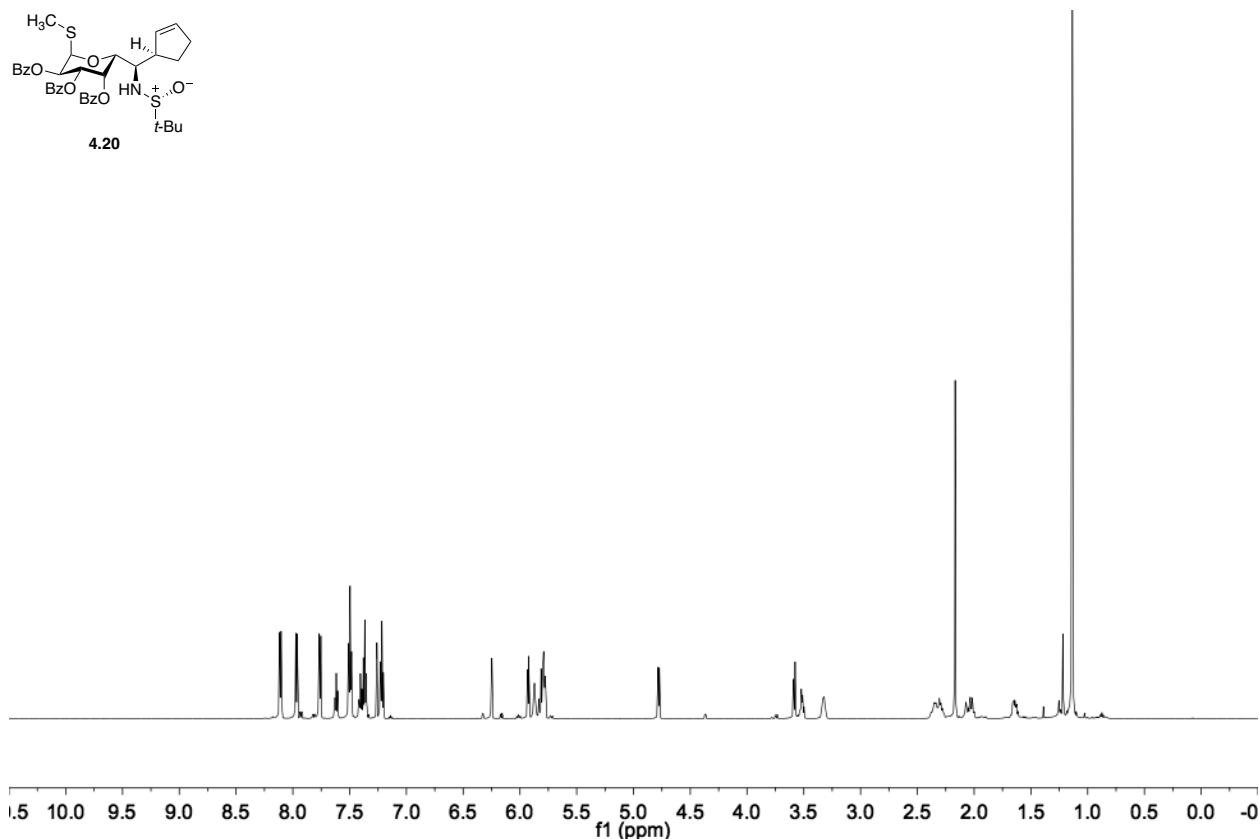
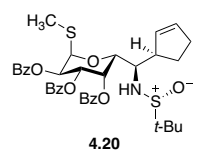


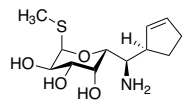




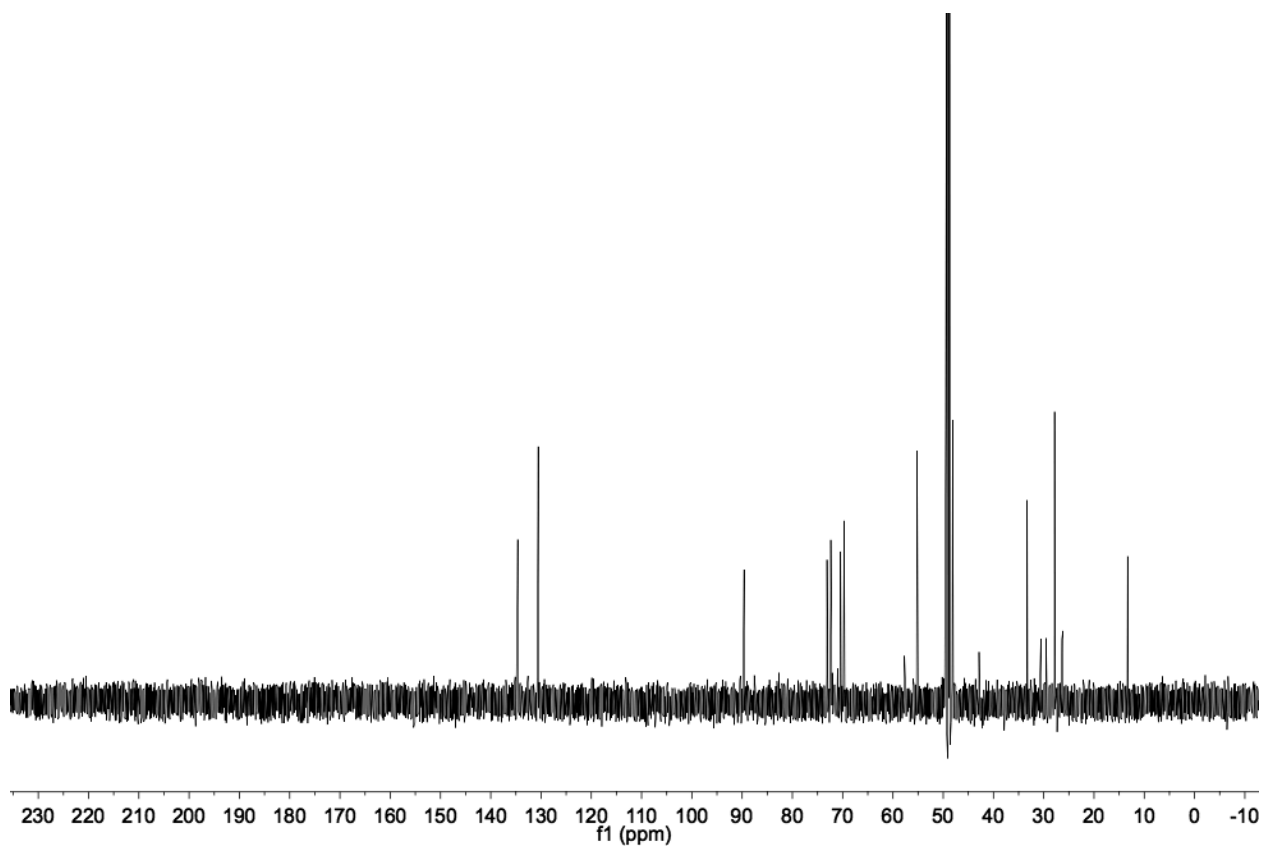
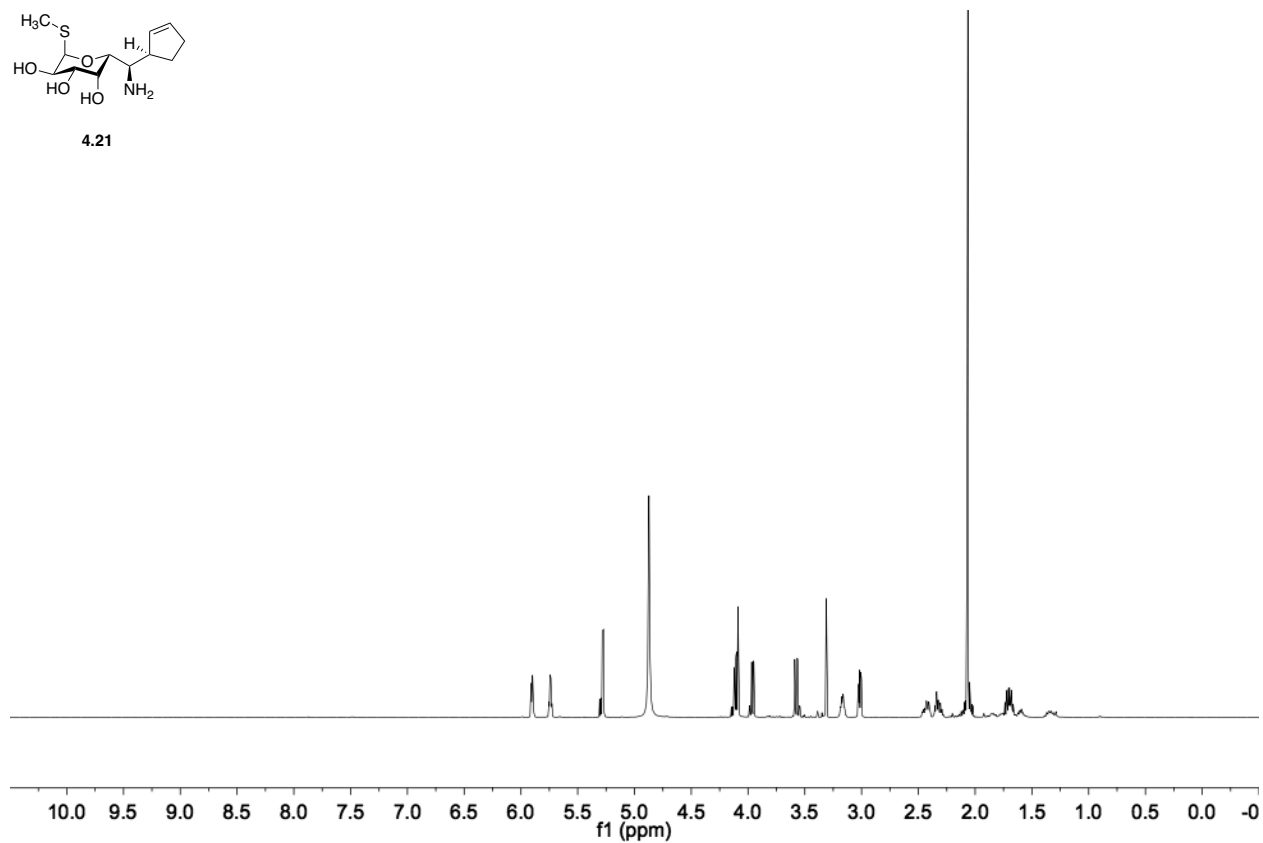
4.18

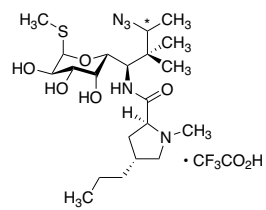






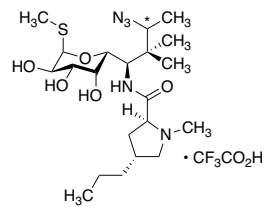
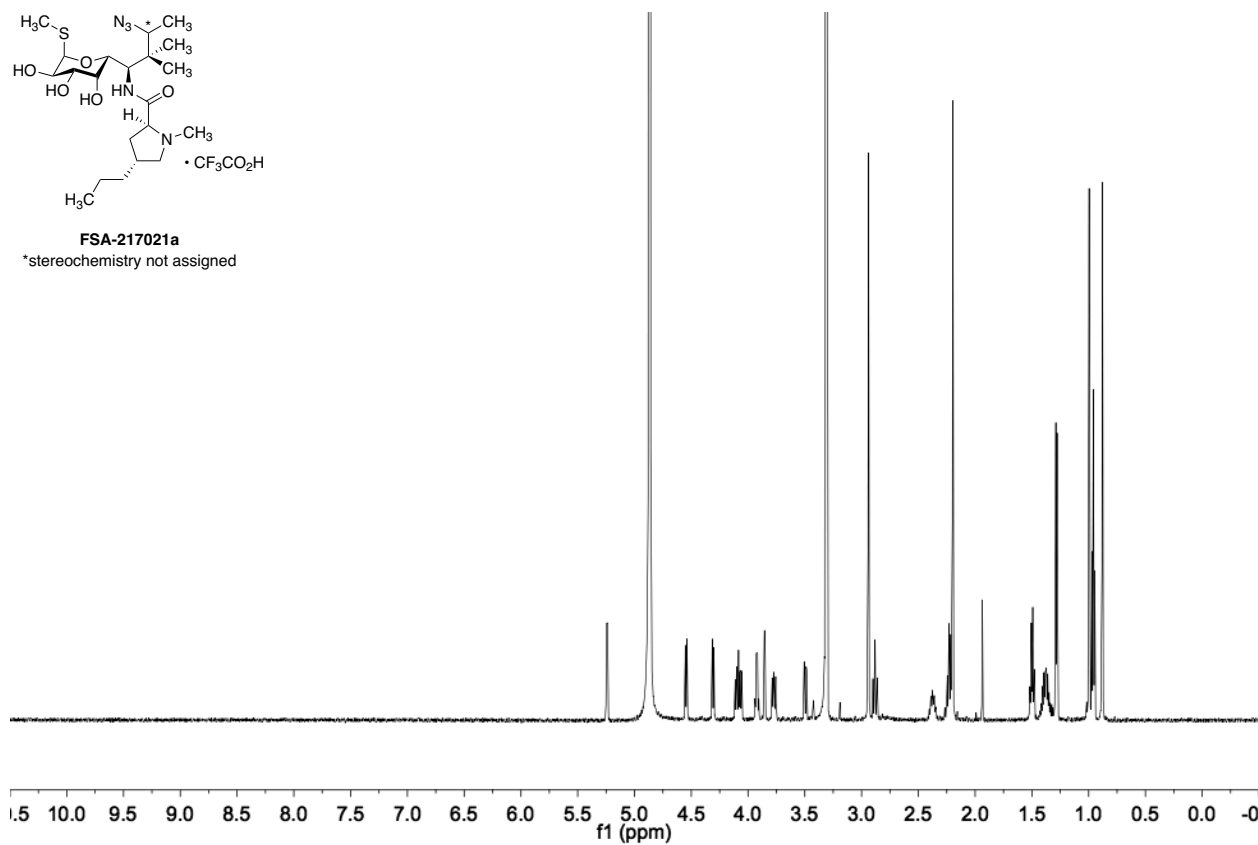
4.21





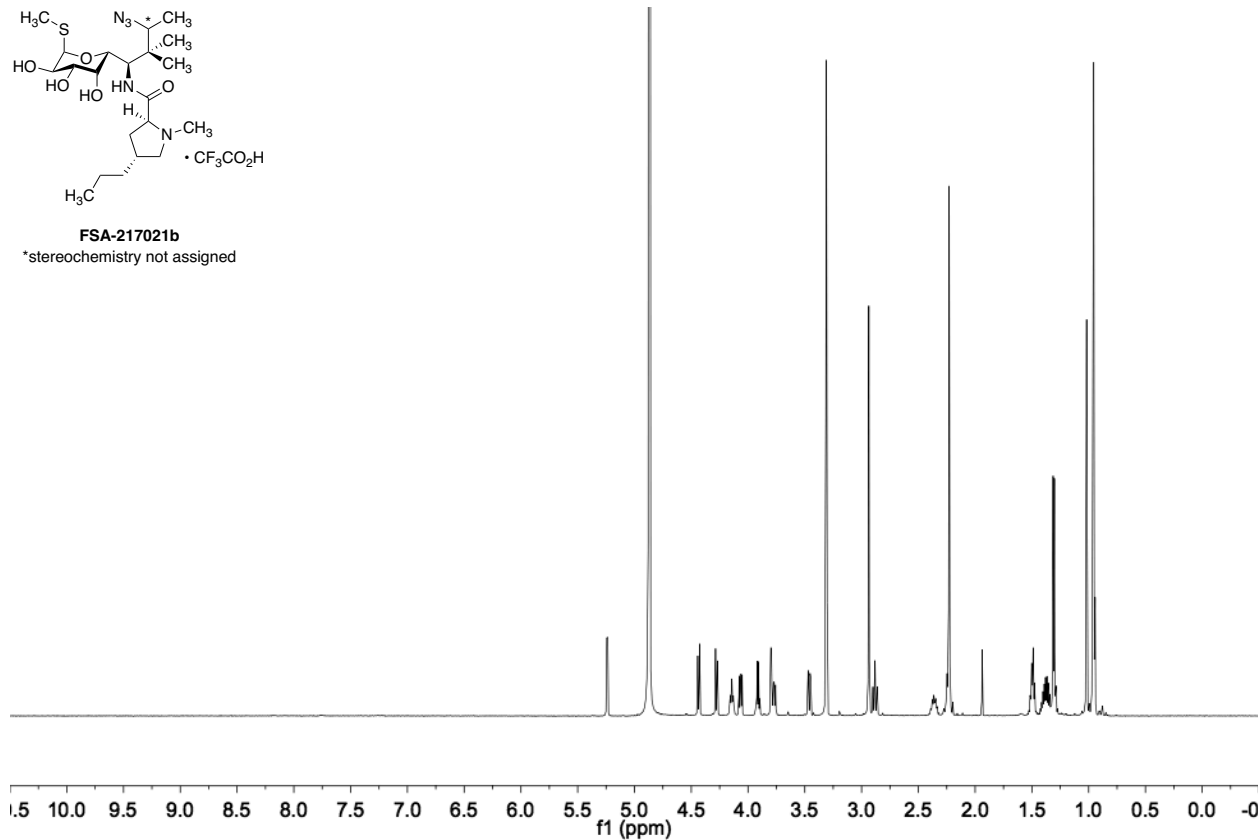
FSA-217021a

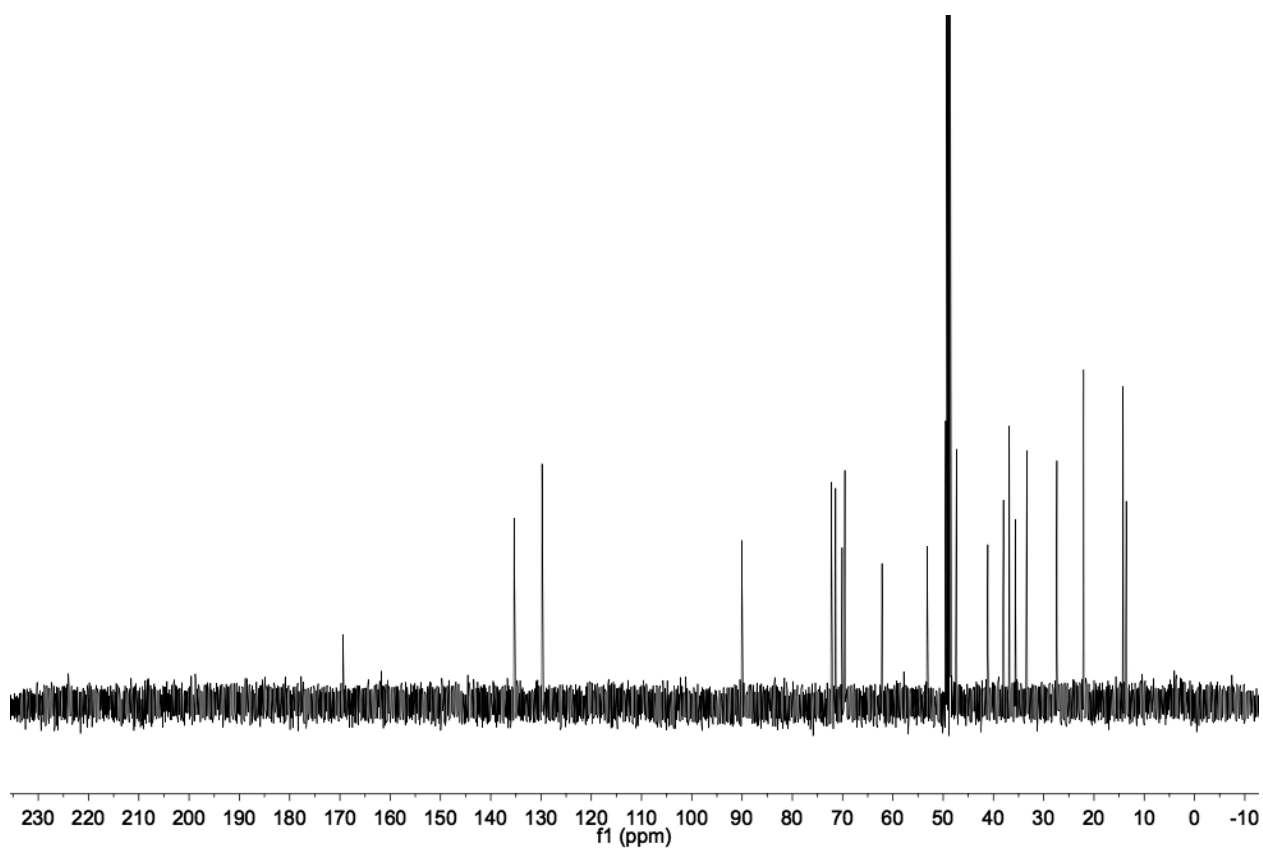
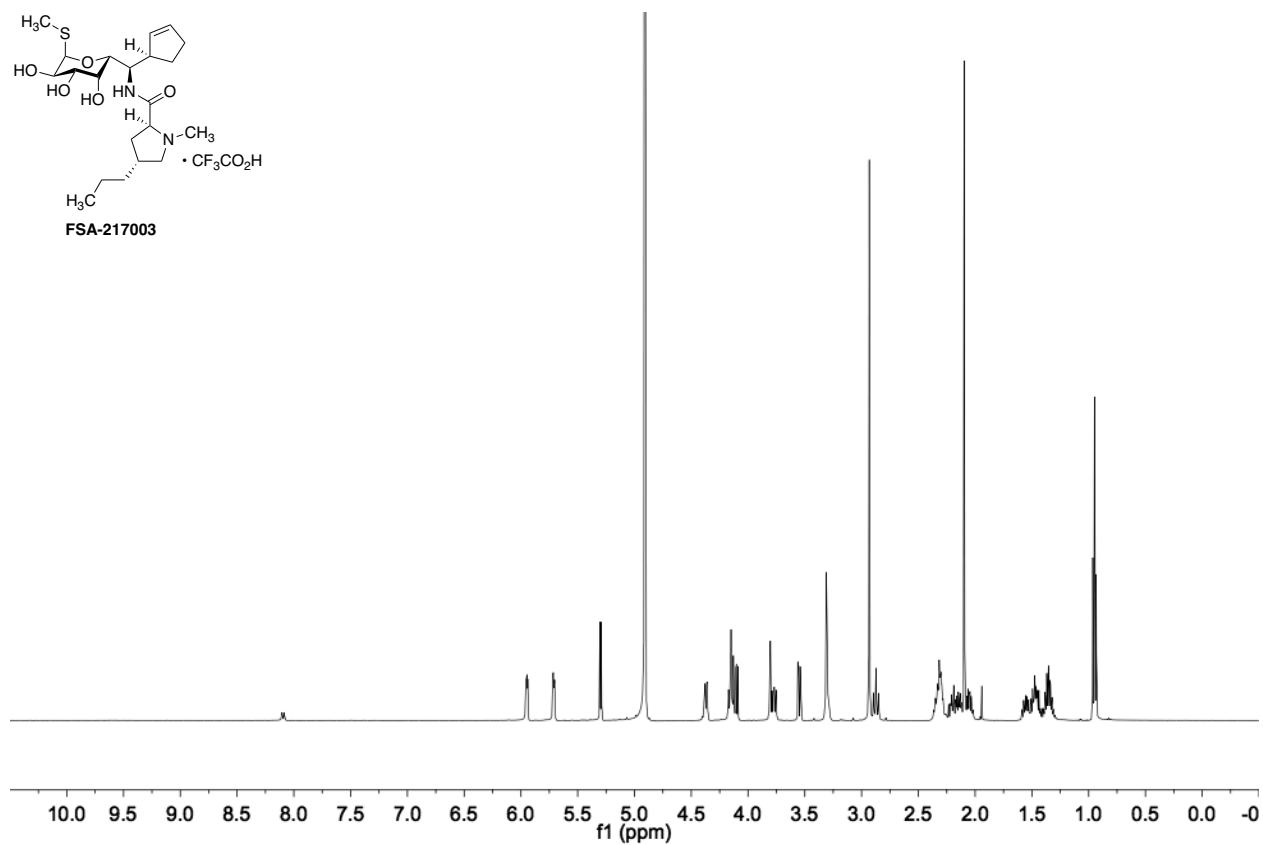
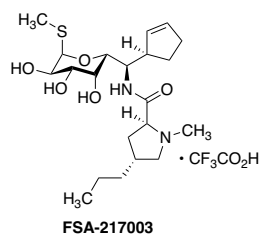
*stereochemistry not assigned

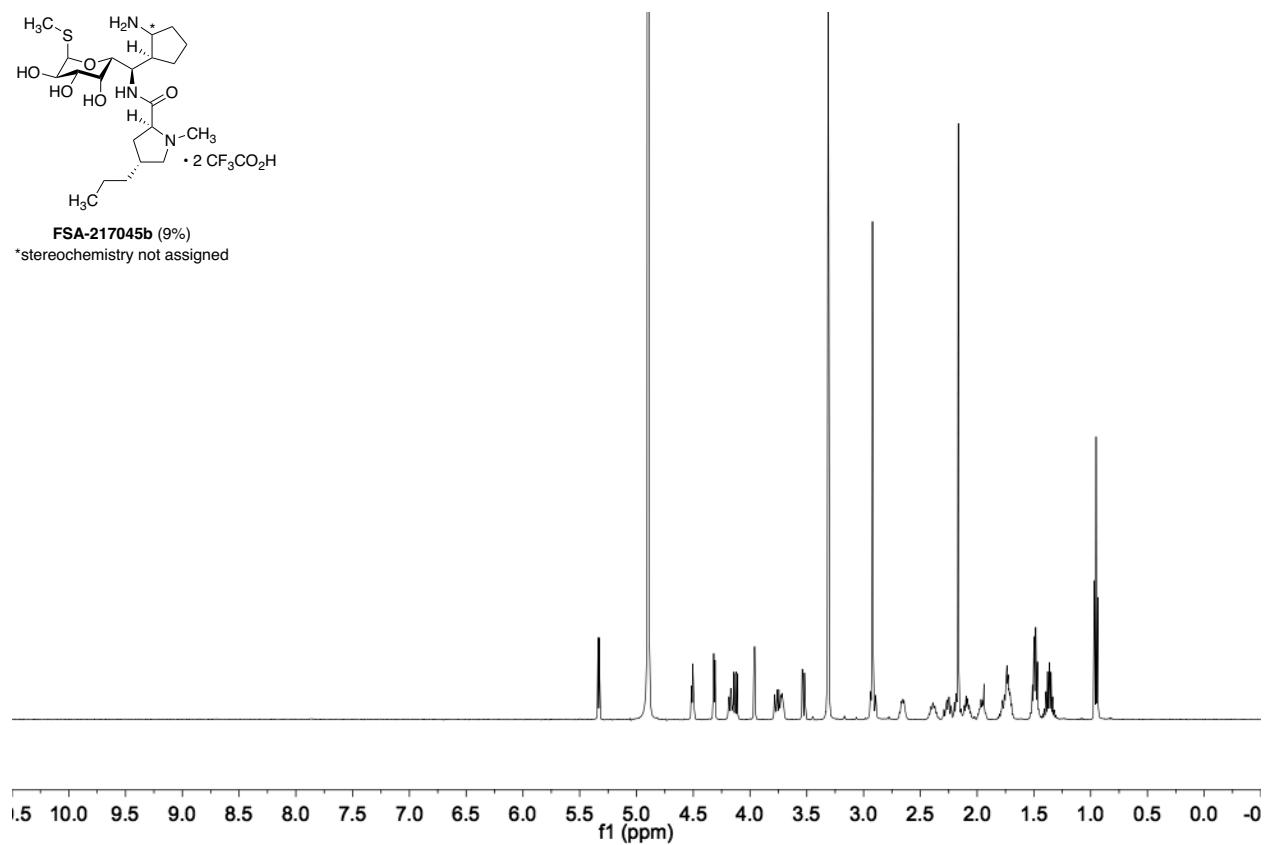
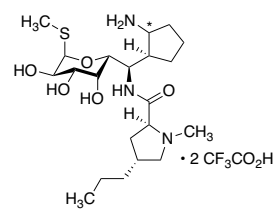


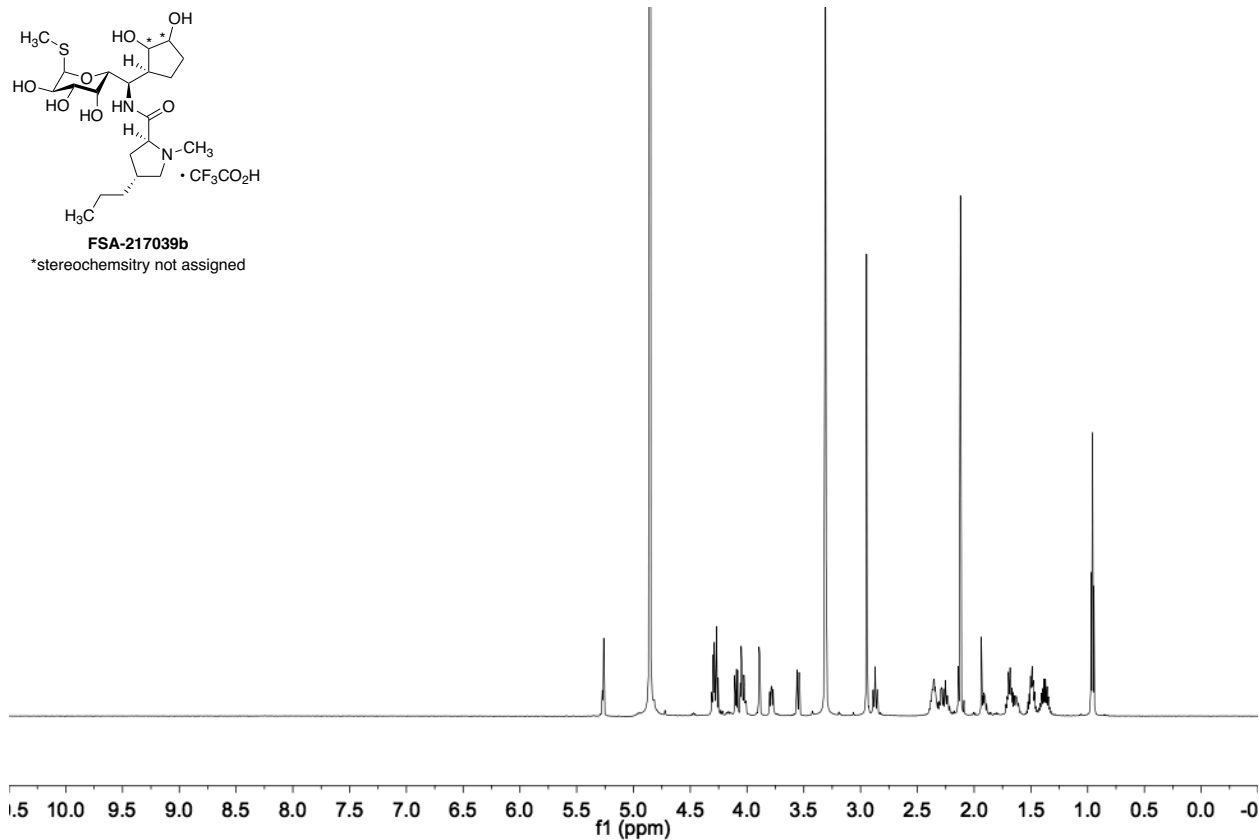
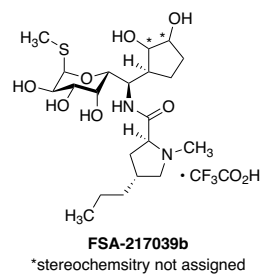
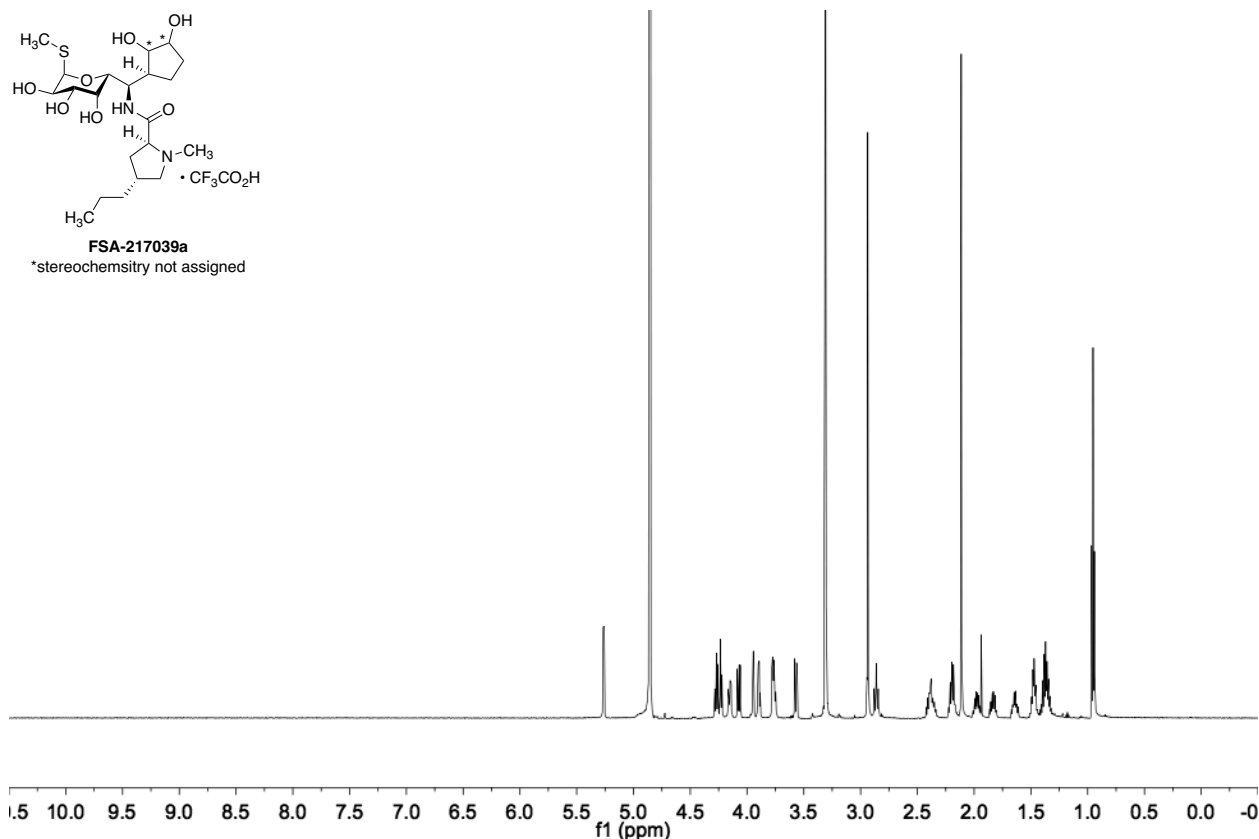
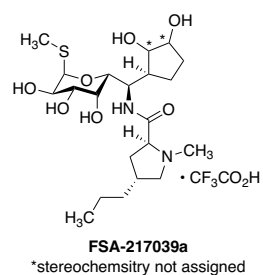
FSA-217021b

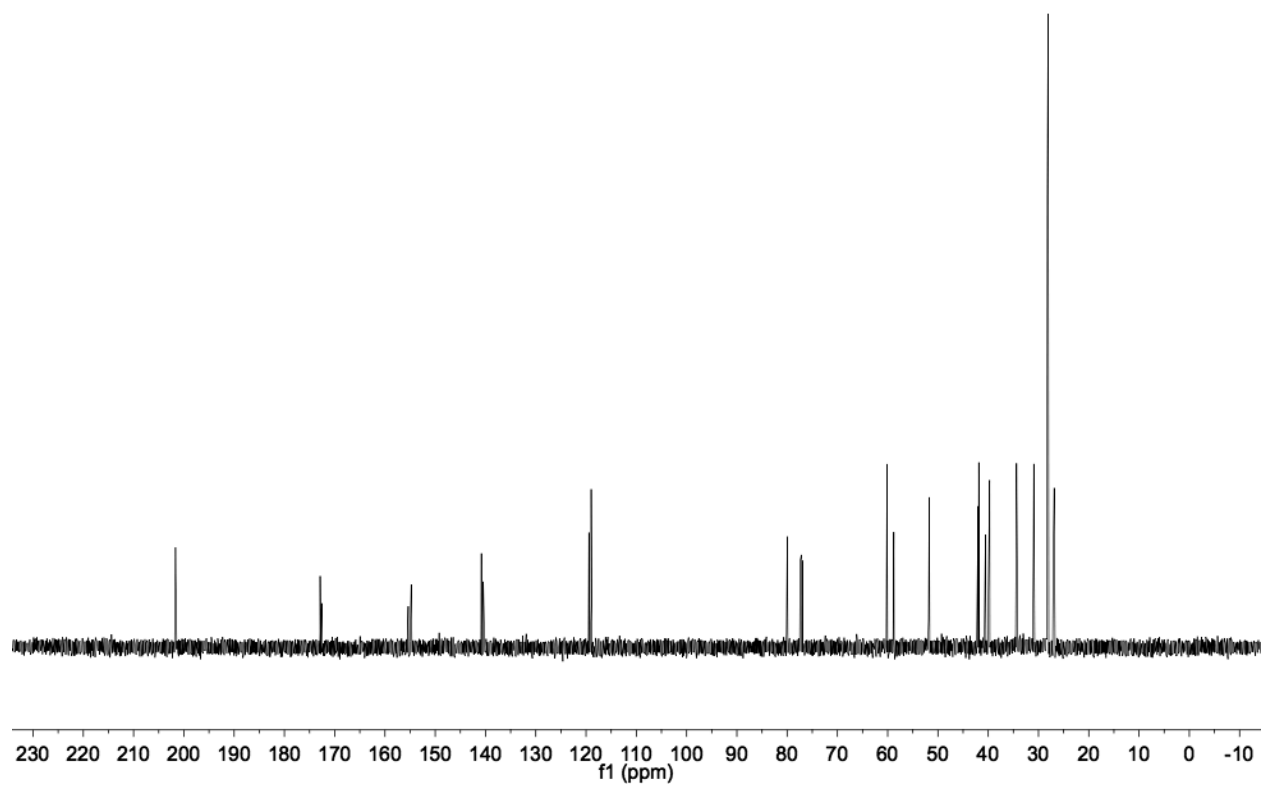
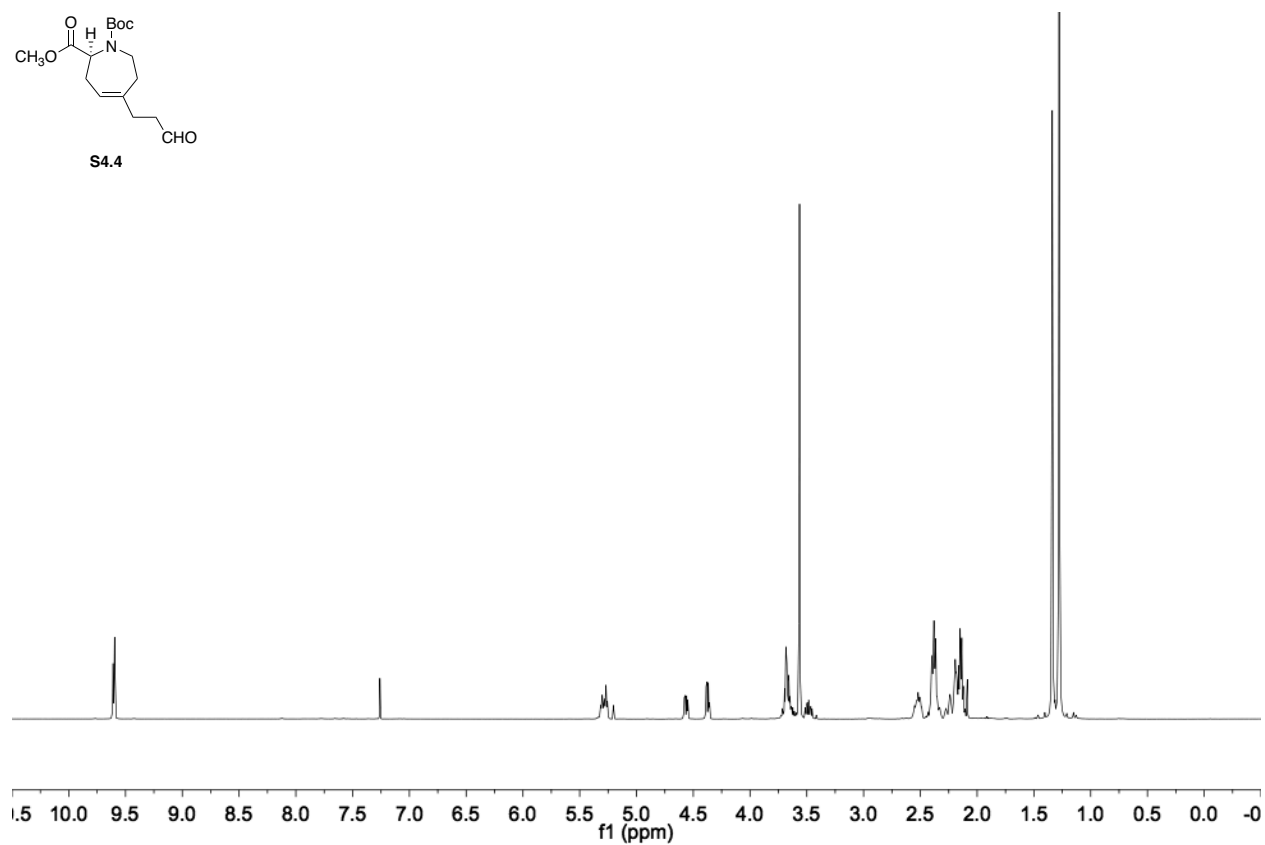
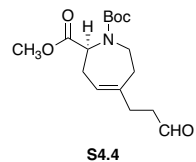
*stereochemistry not assigned

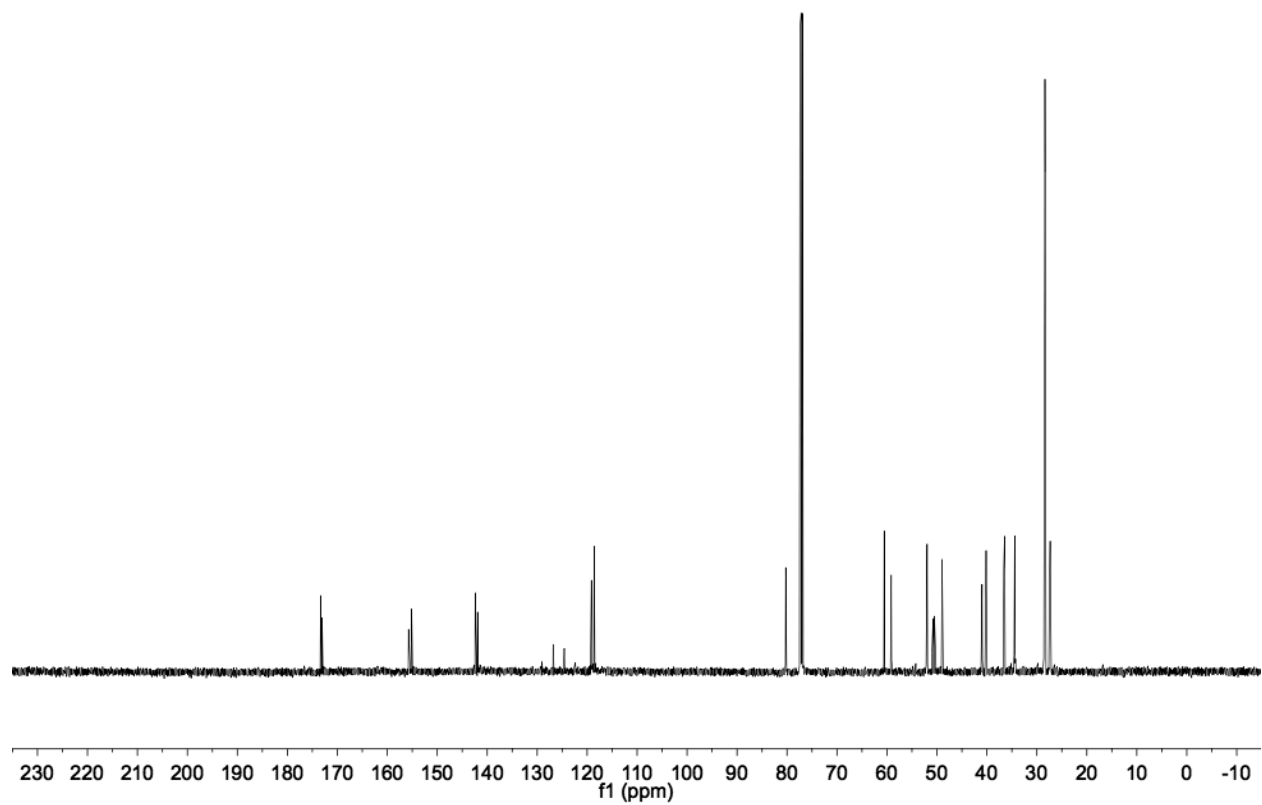
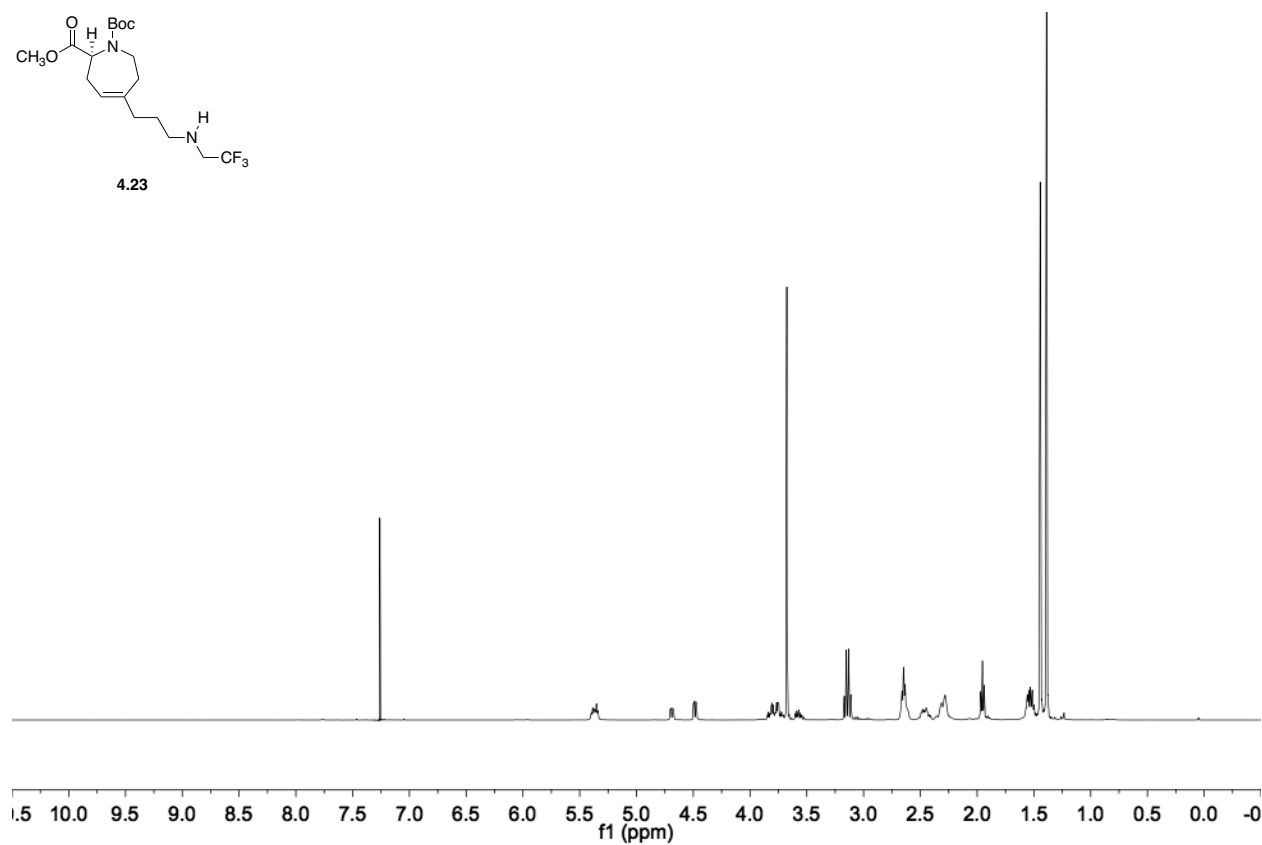
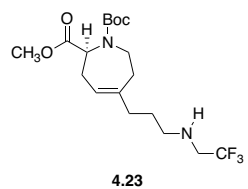


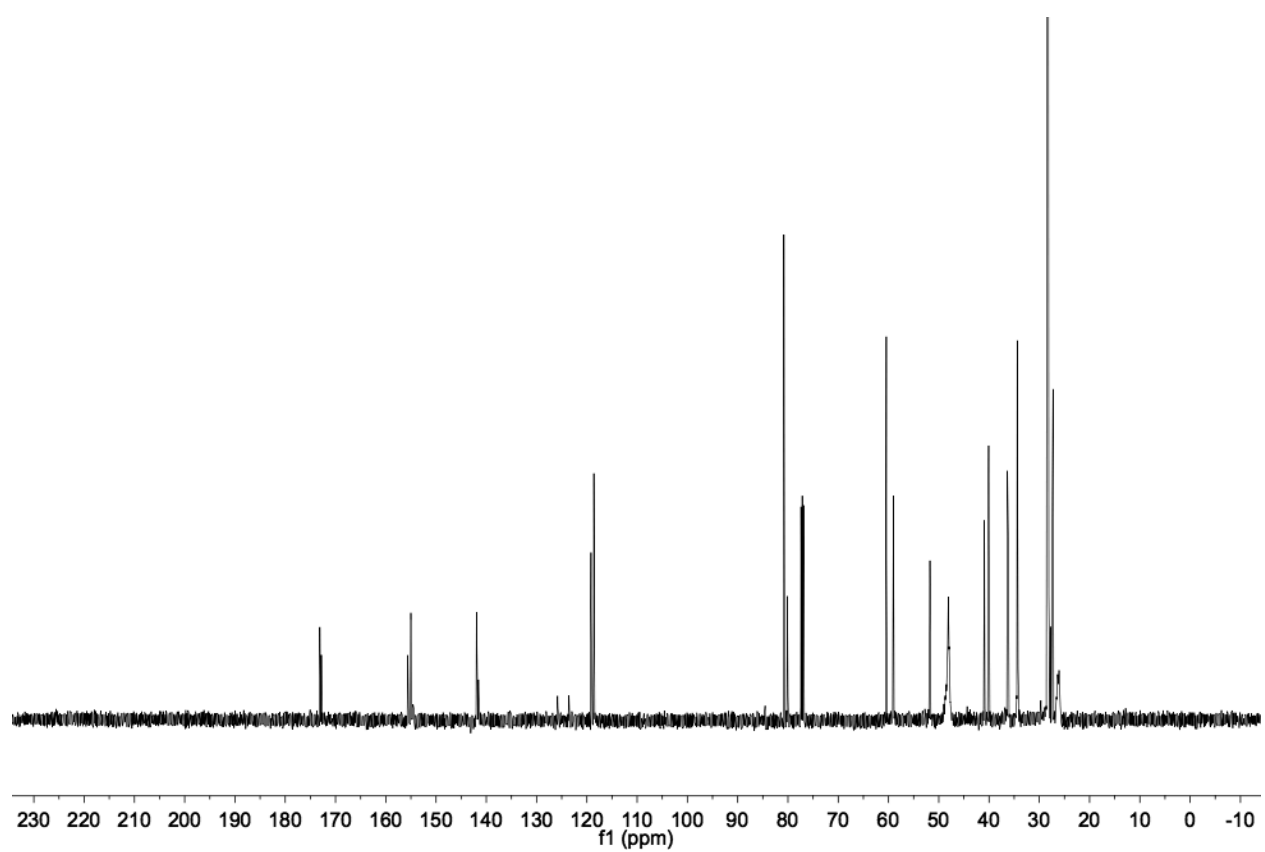
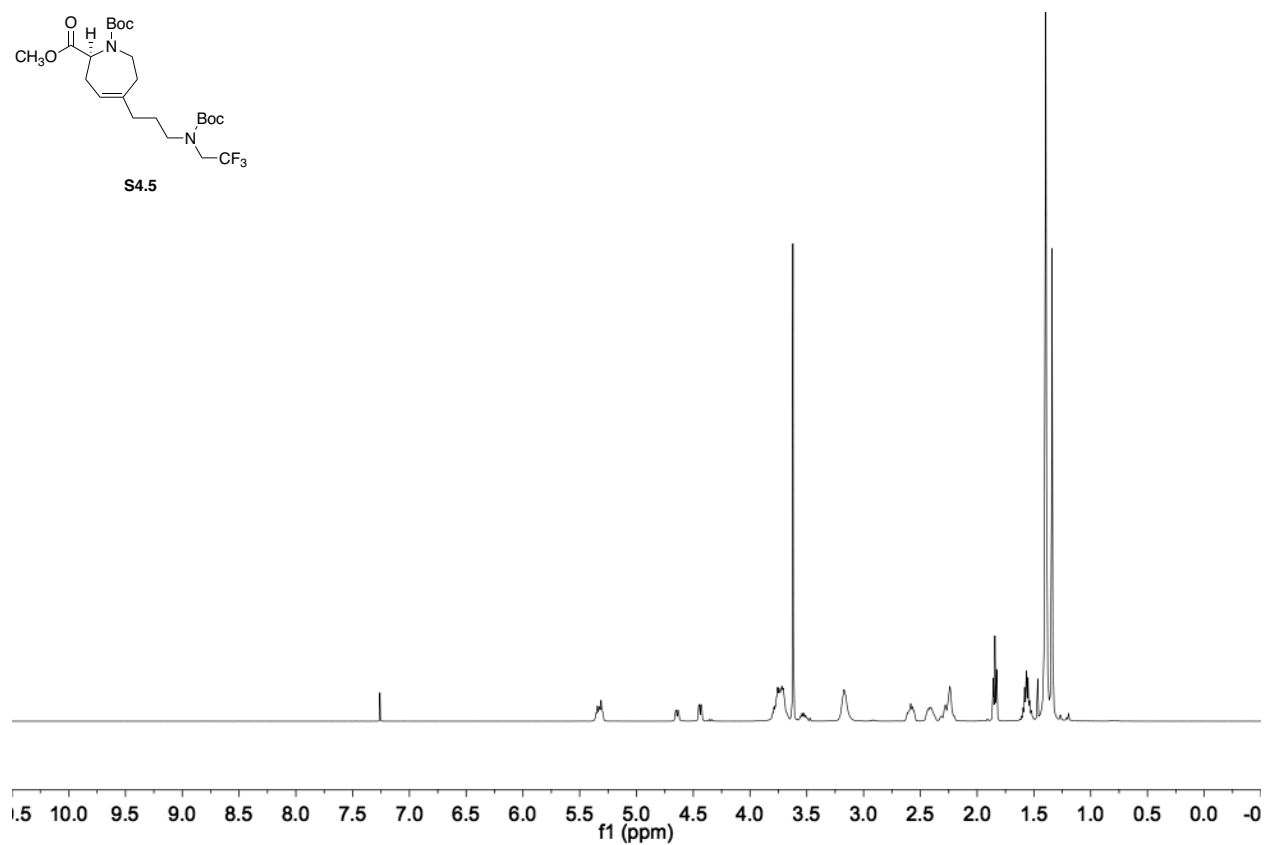
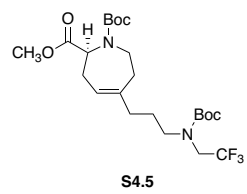


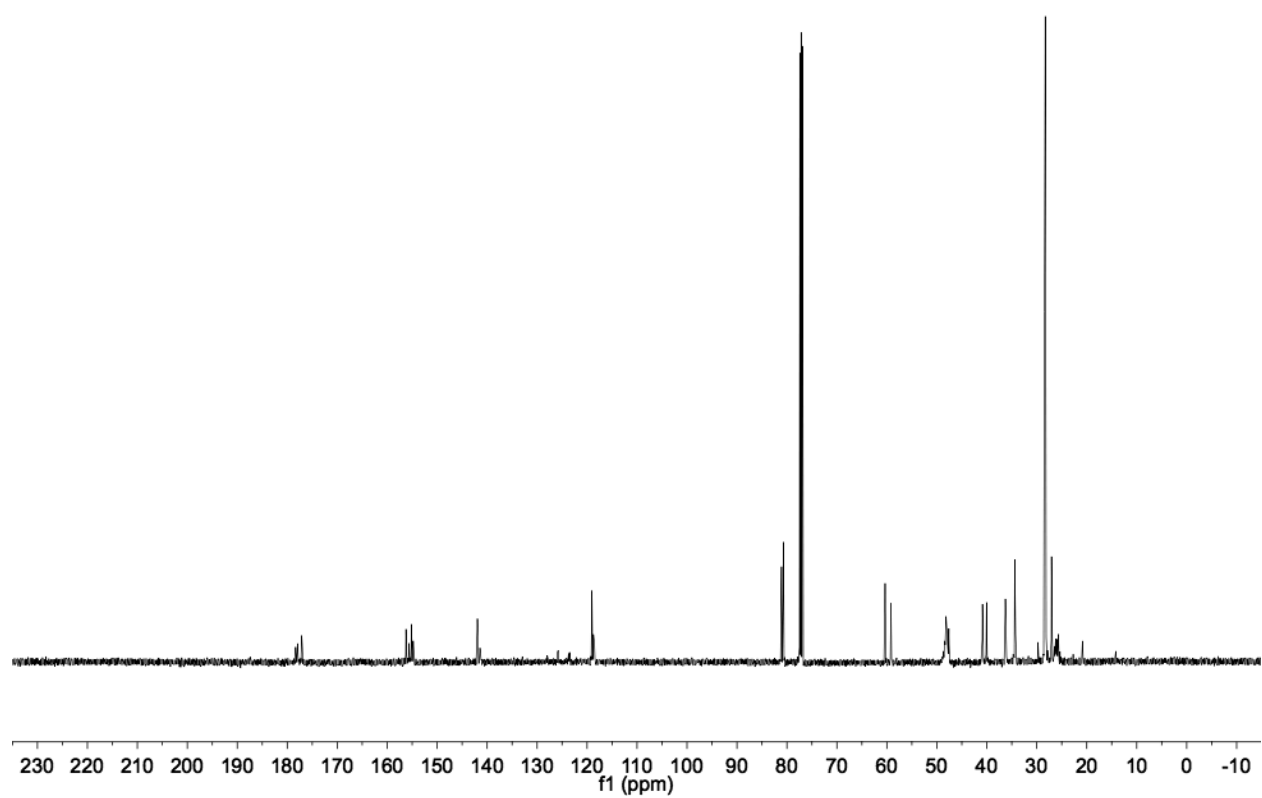
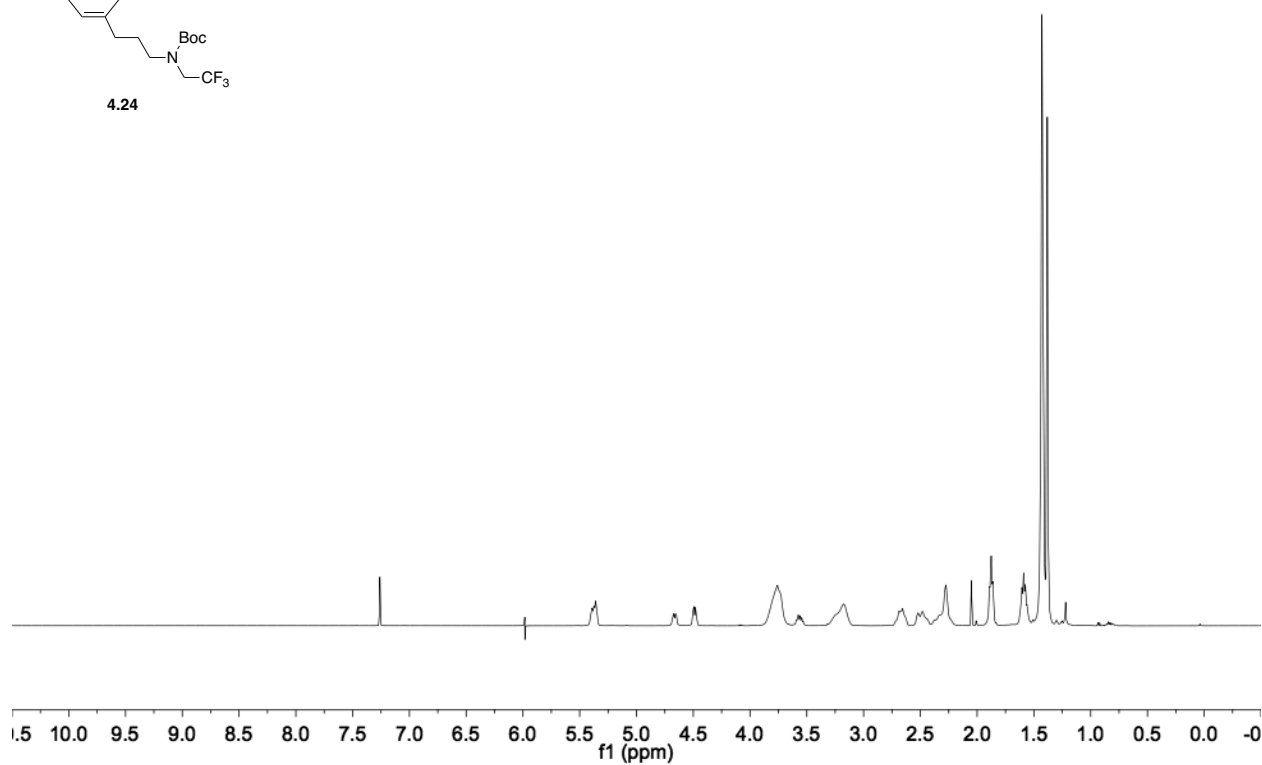
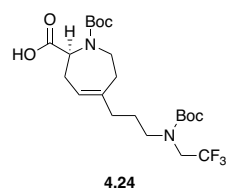


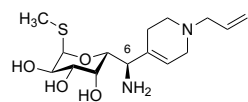




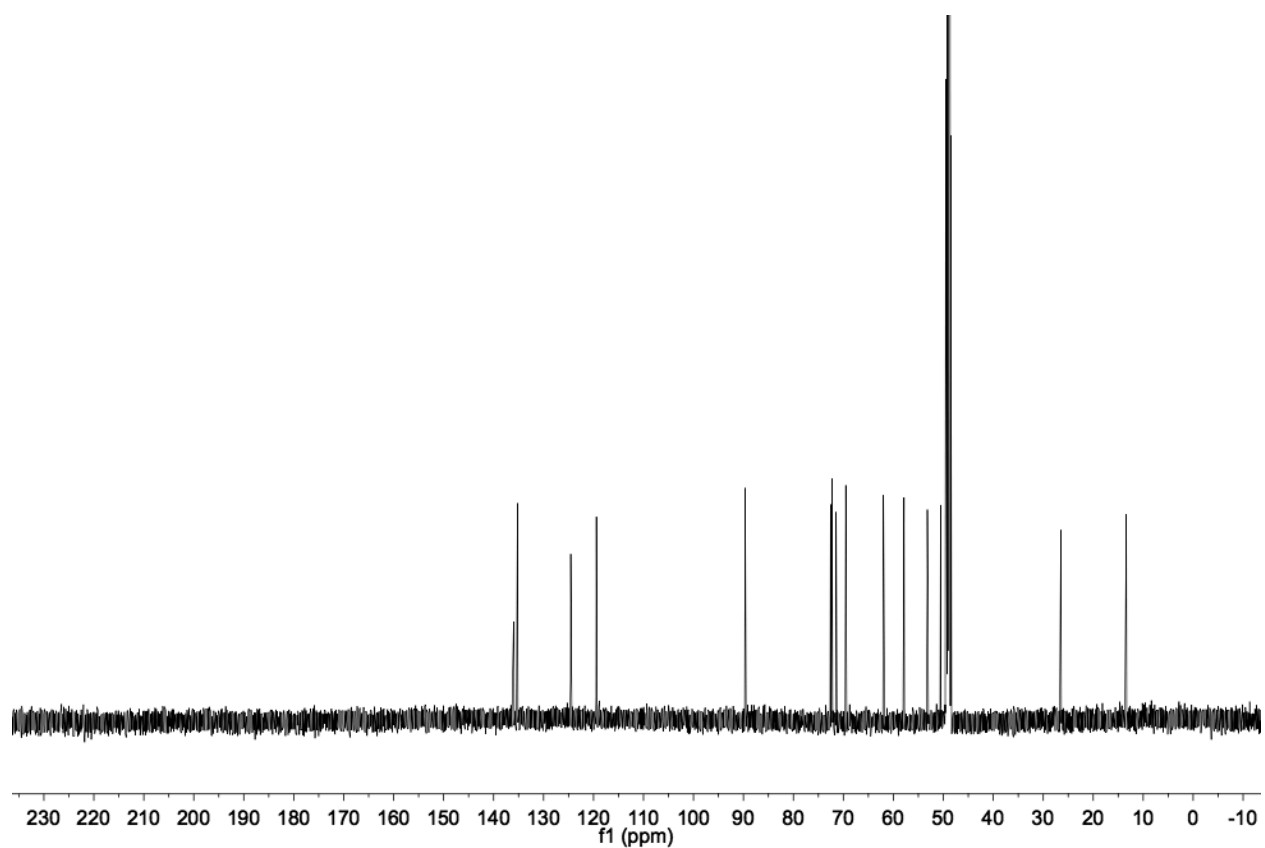
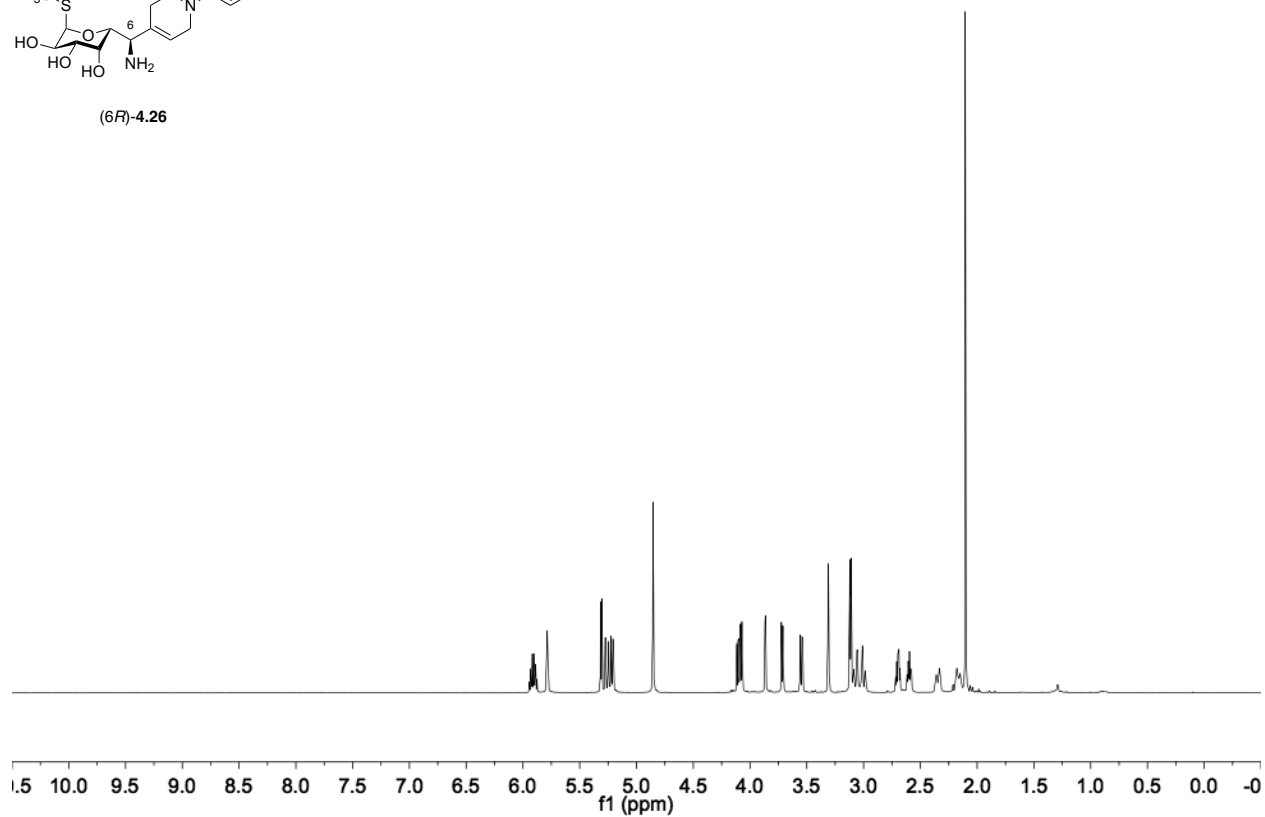


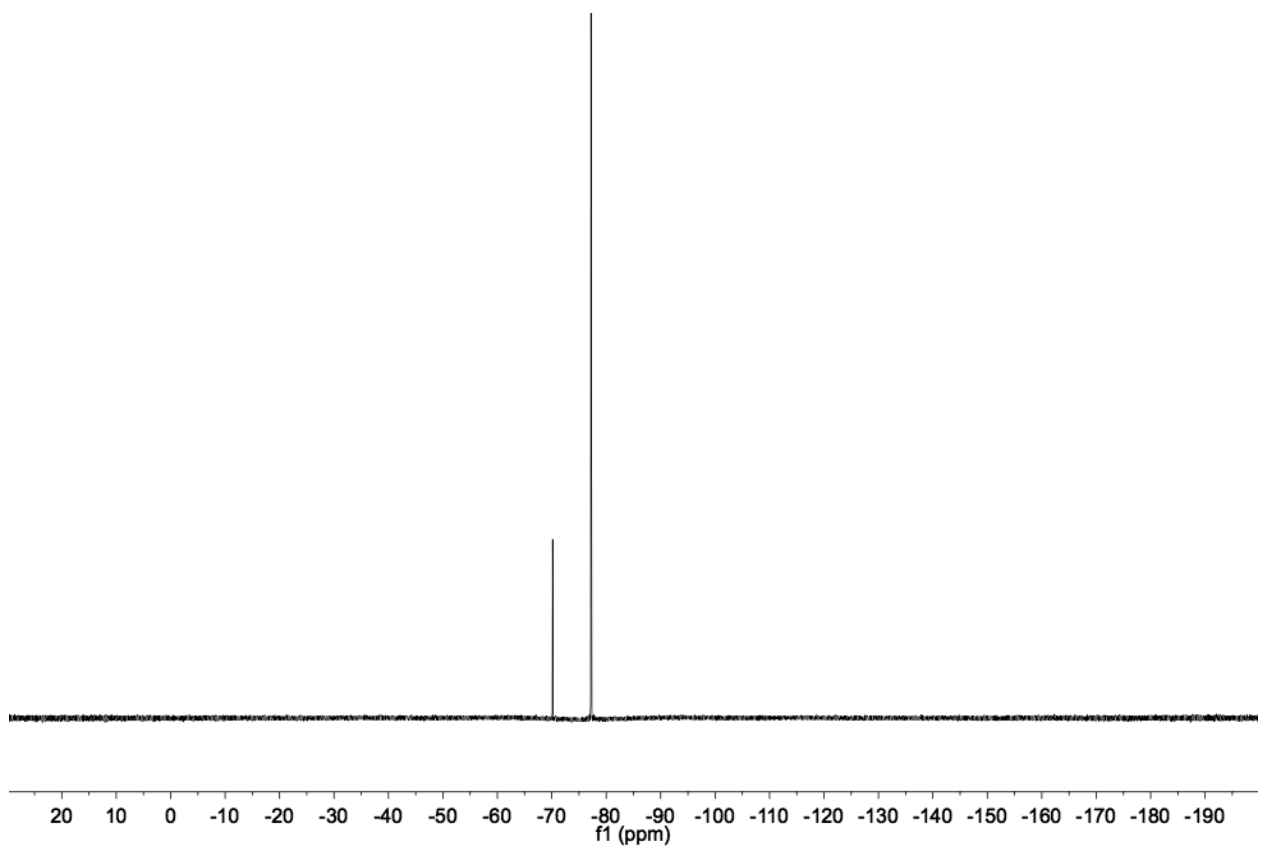
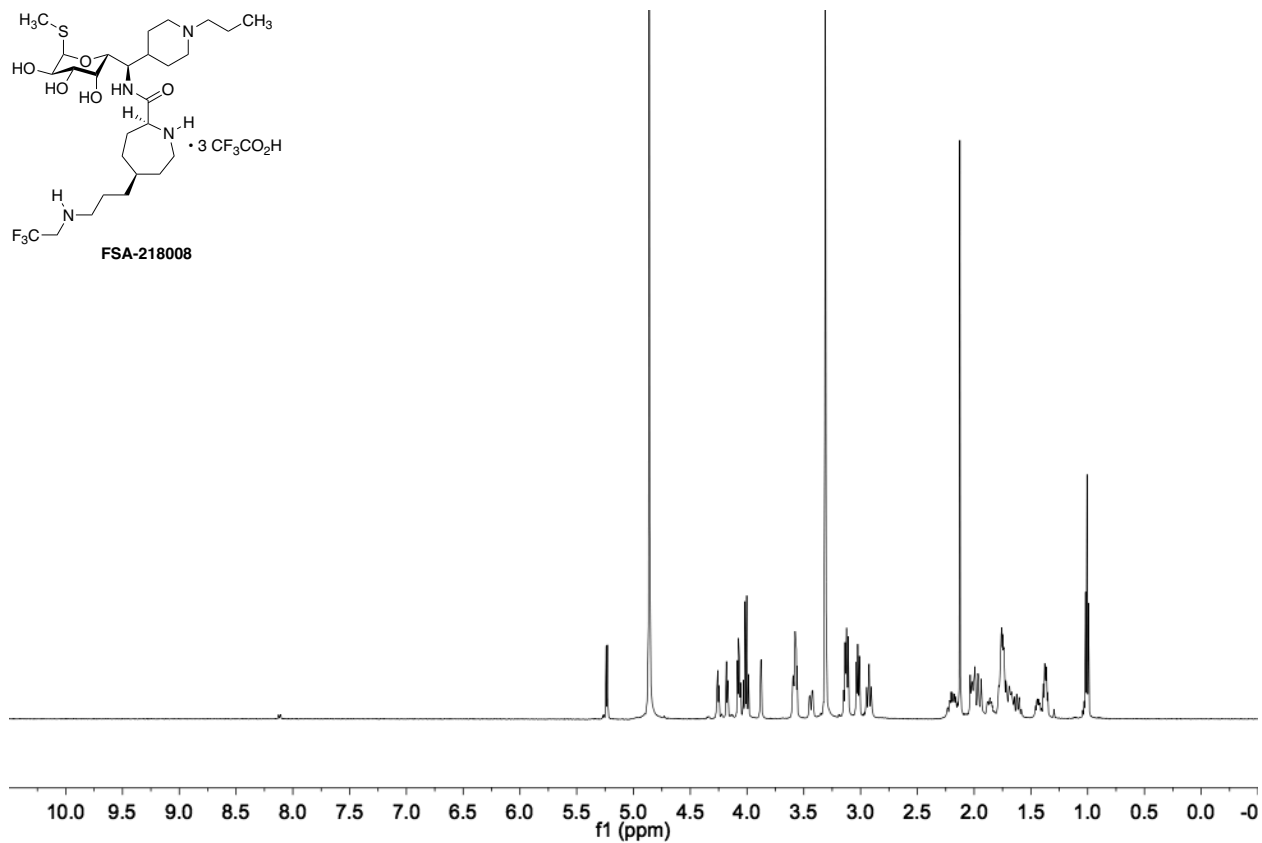
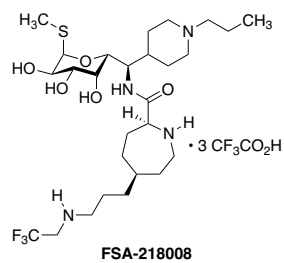


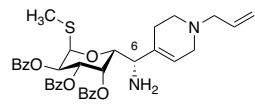




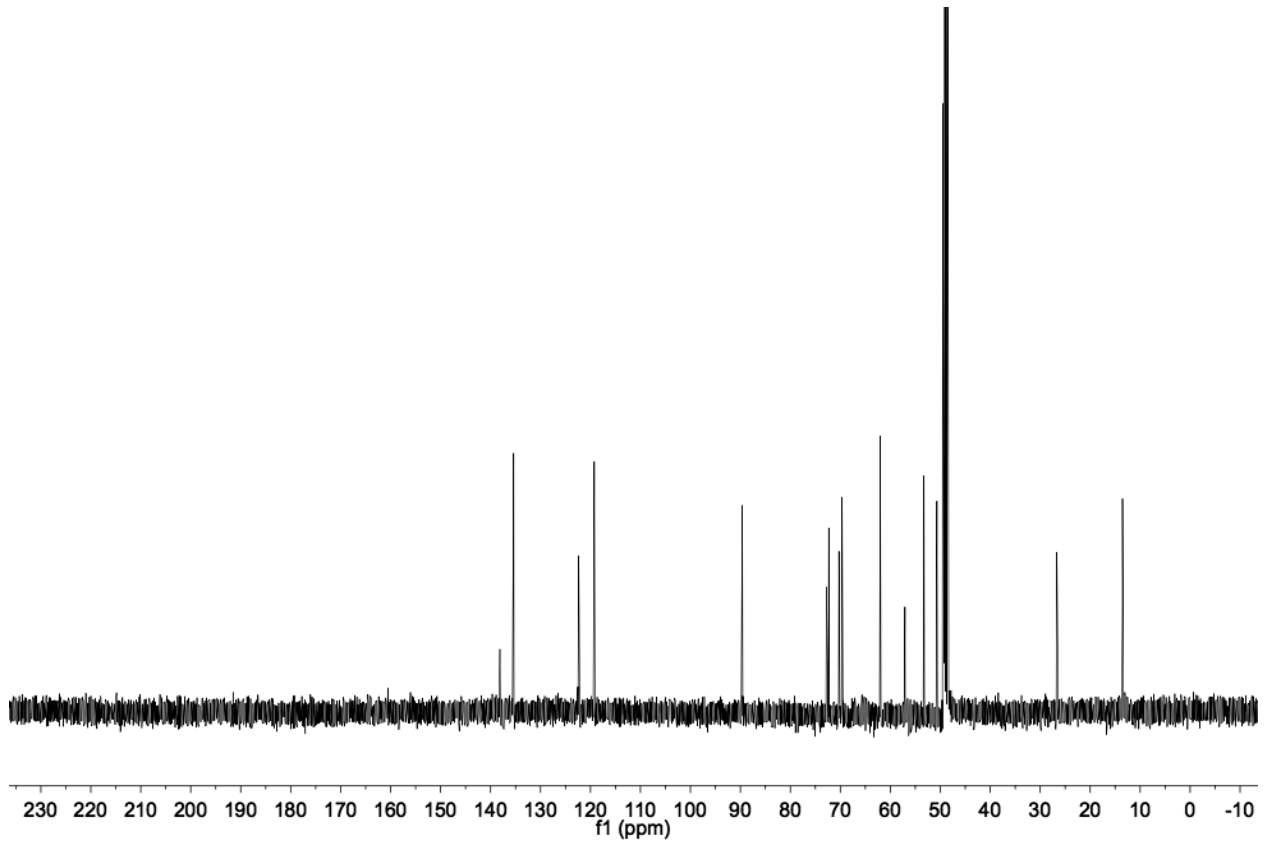
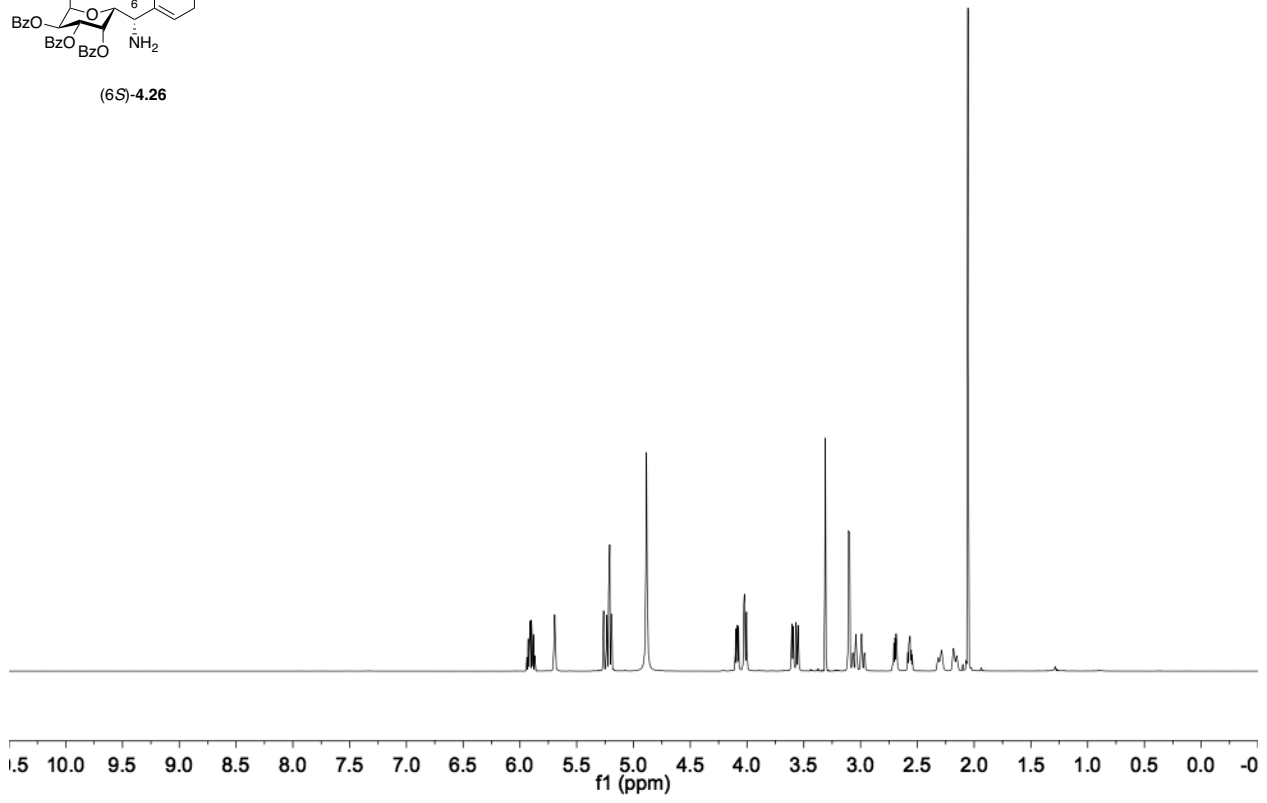
(6F)-4.26

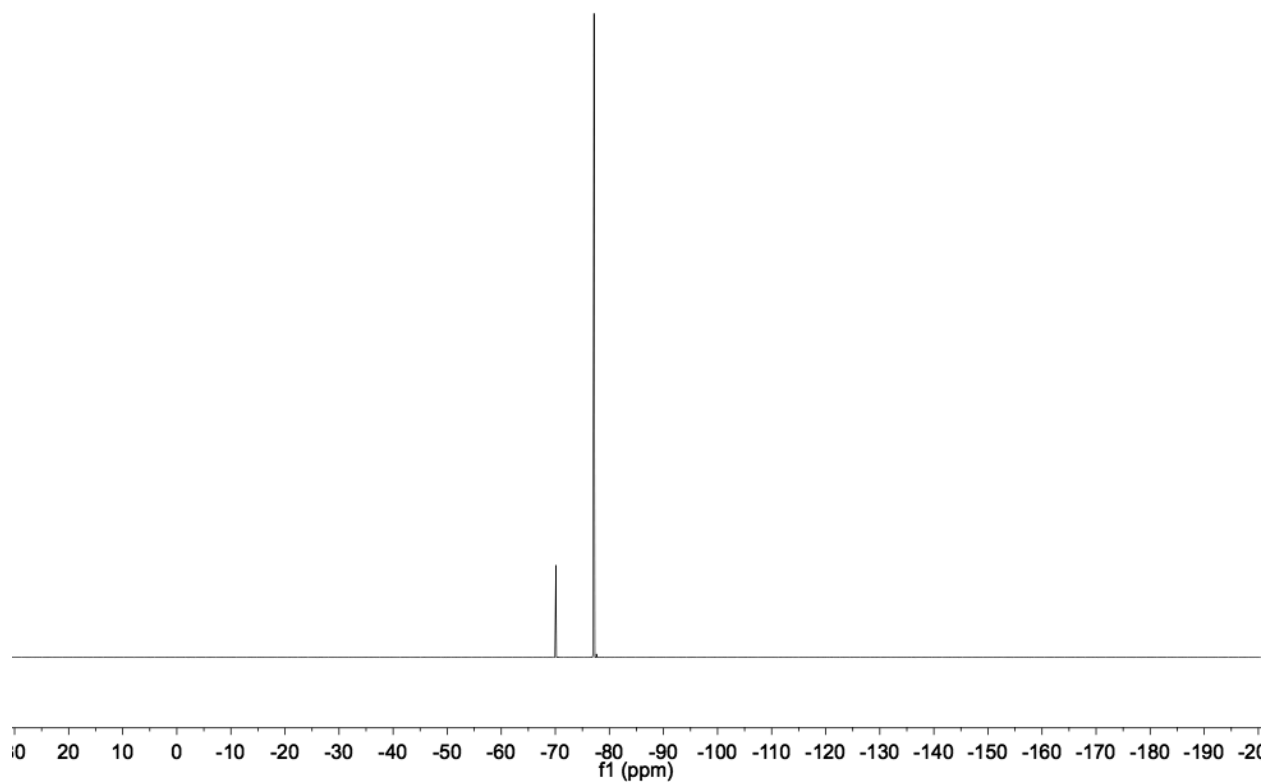
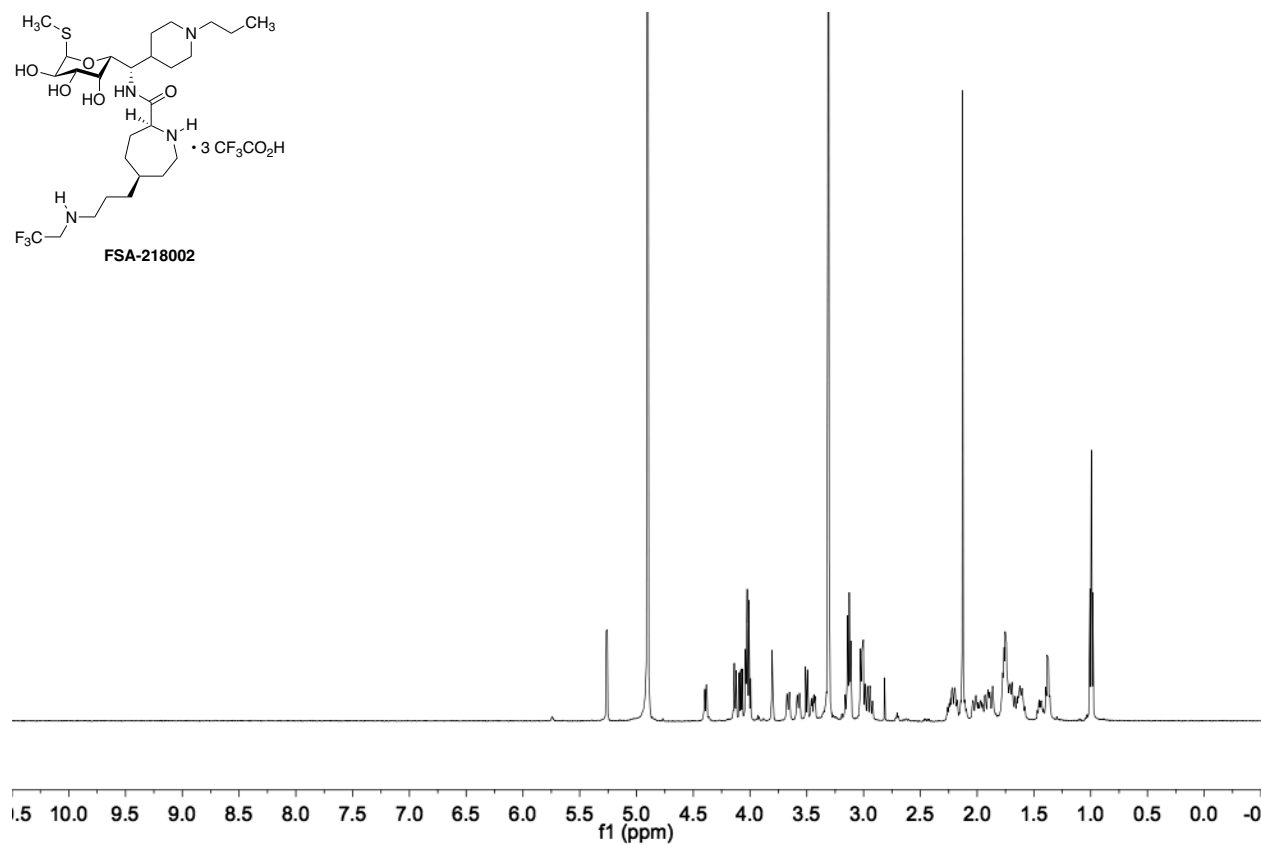
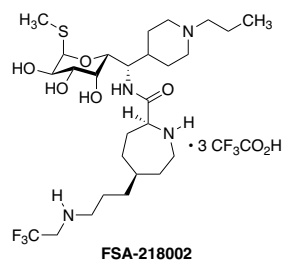


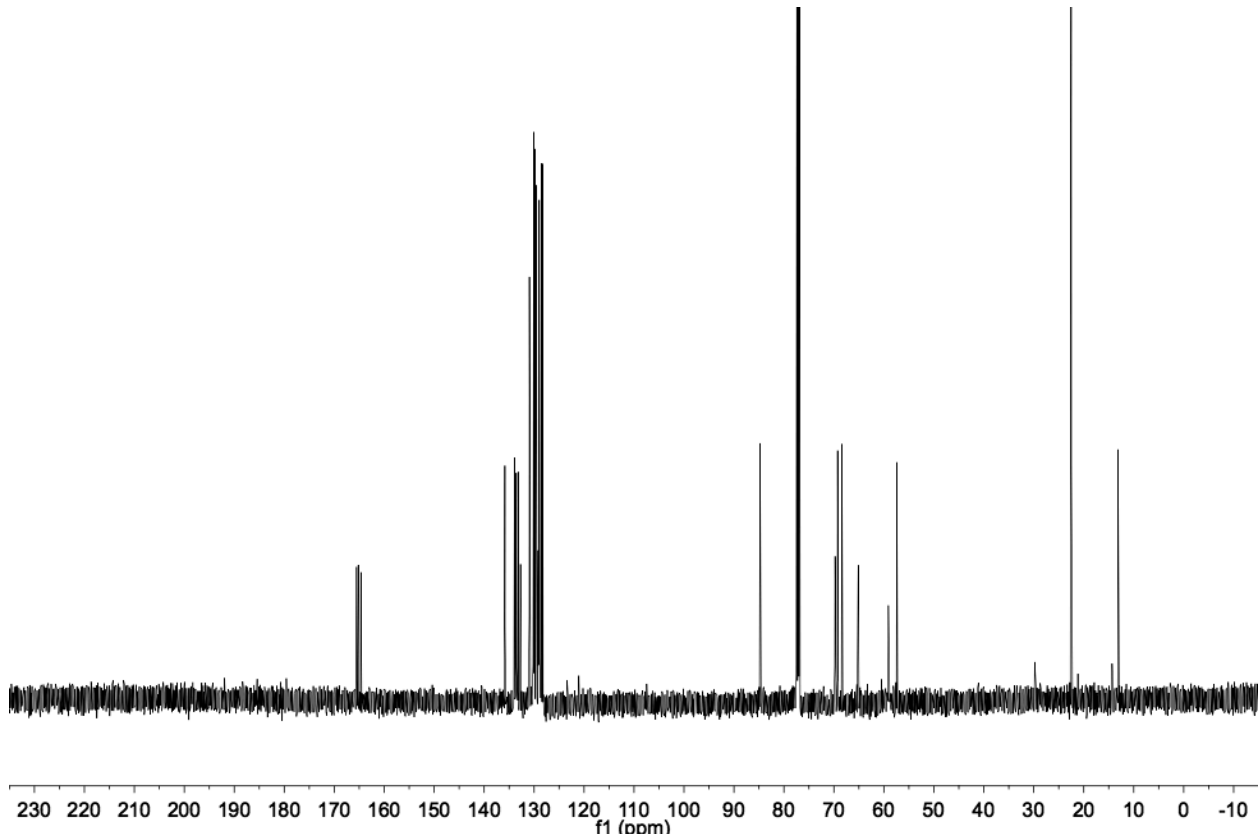
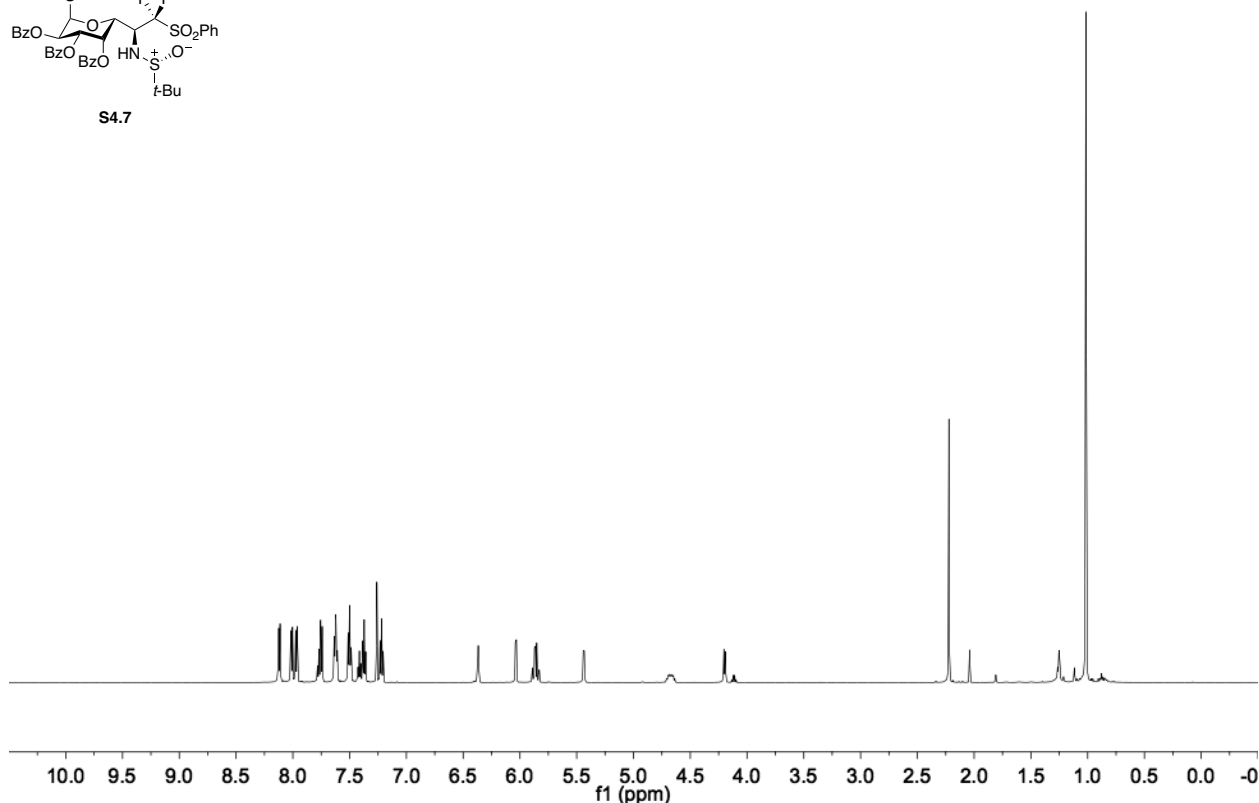
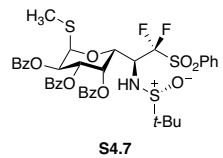


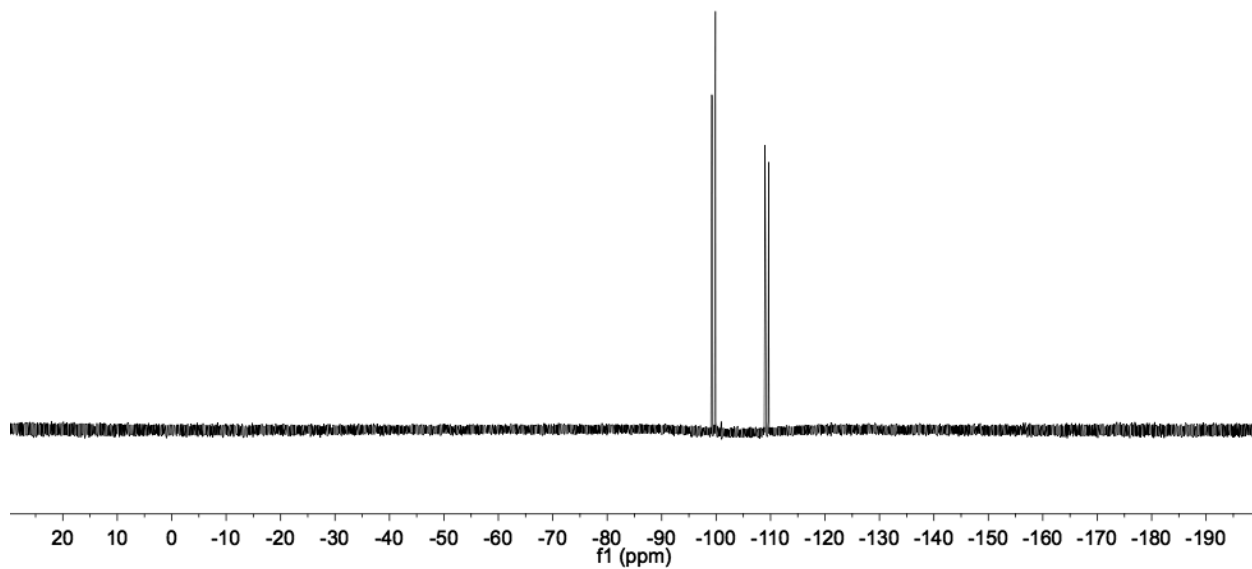


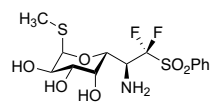
(6S)-4.26



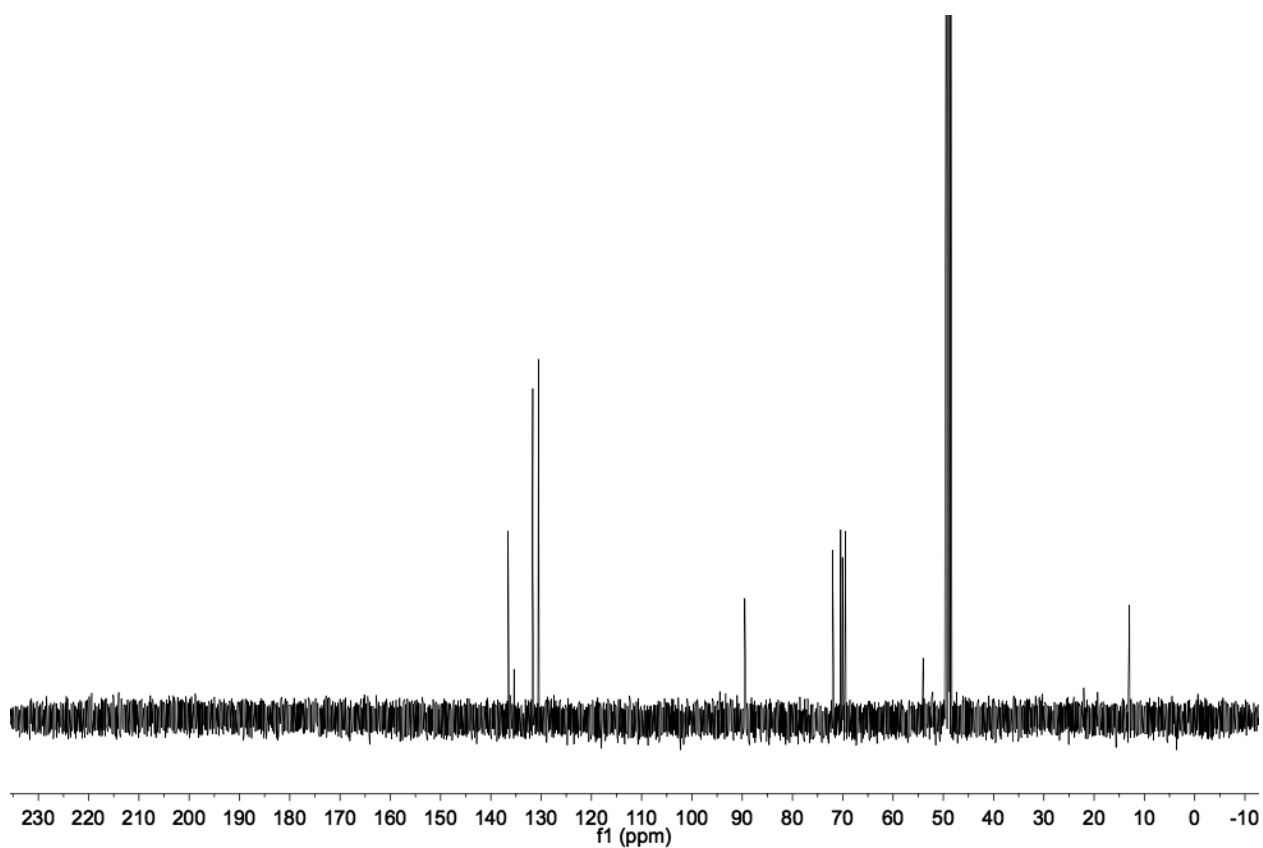
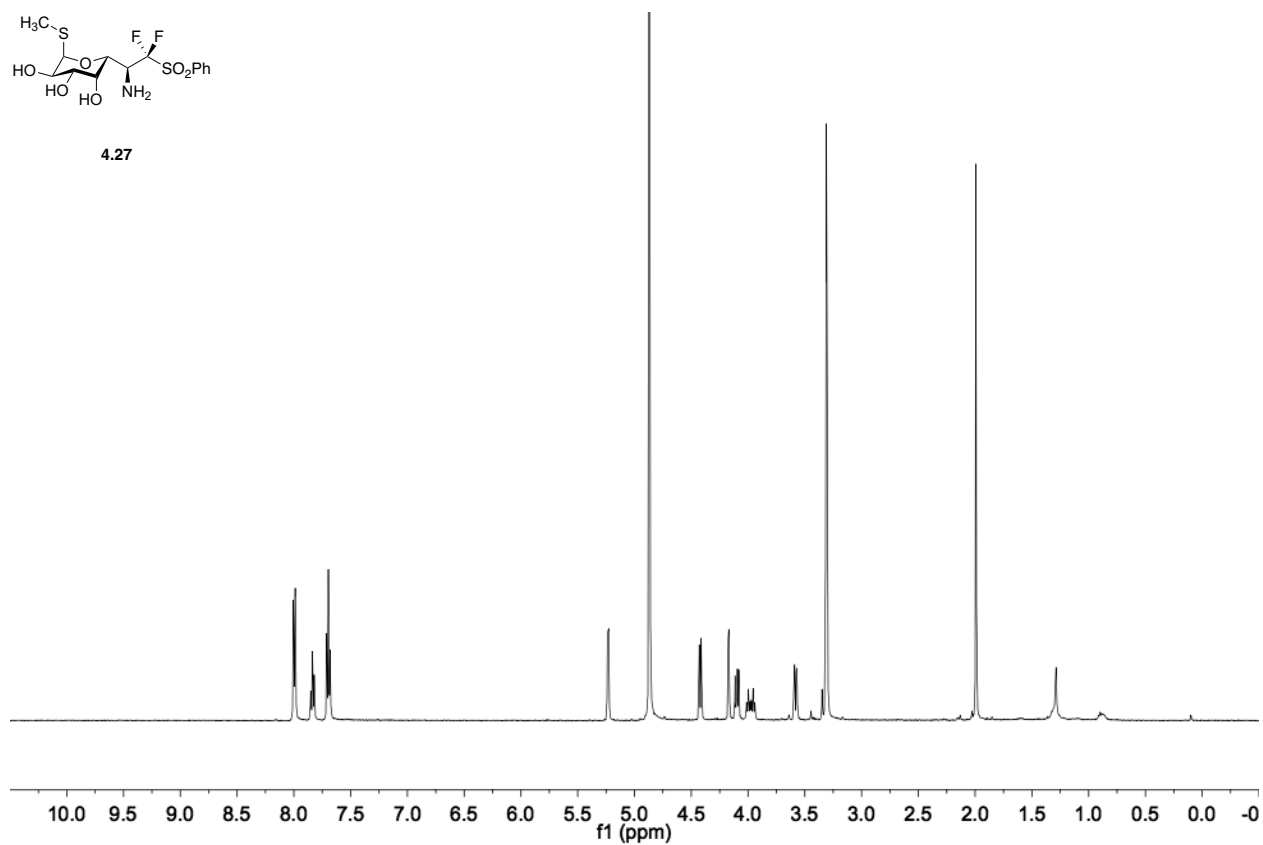


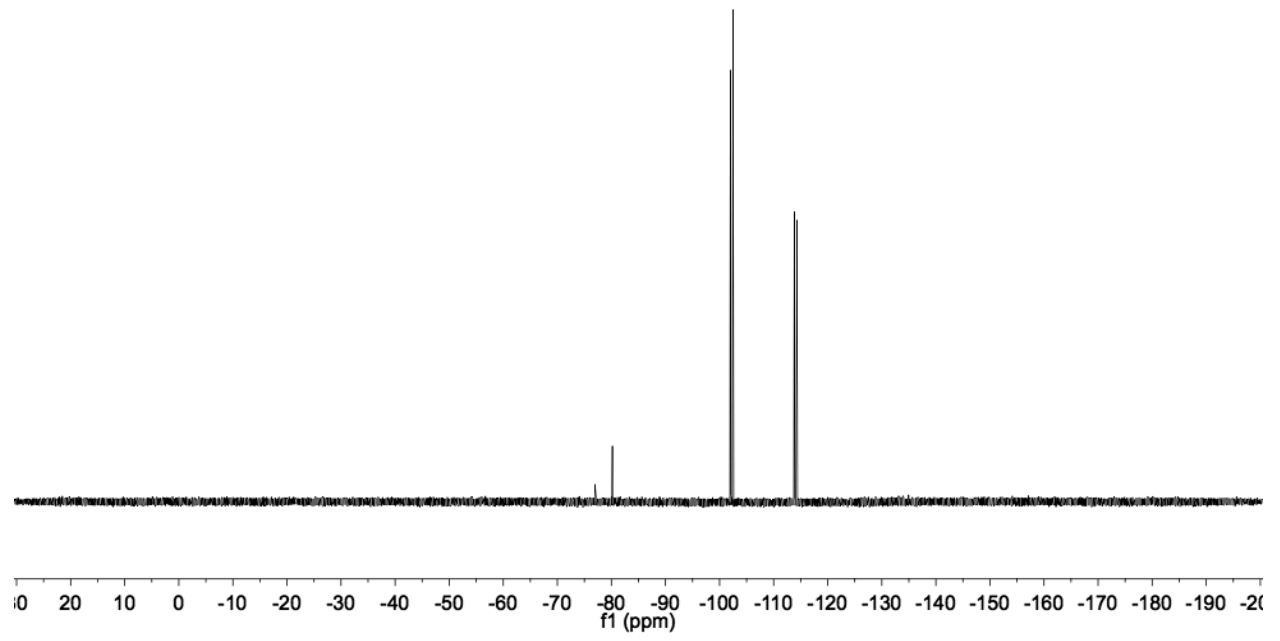


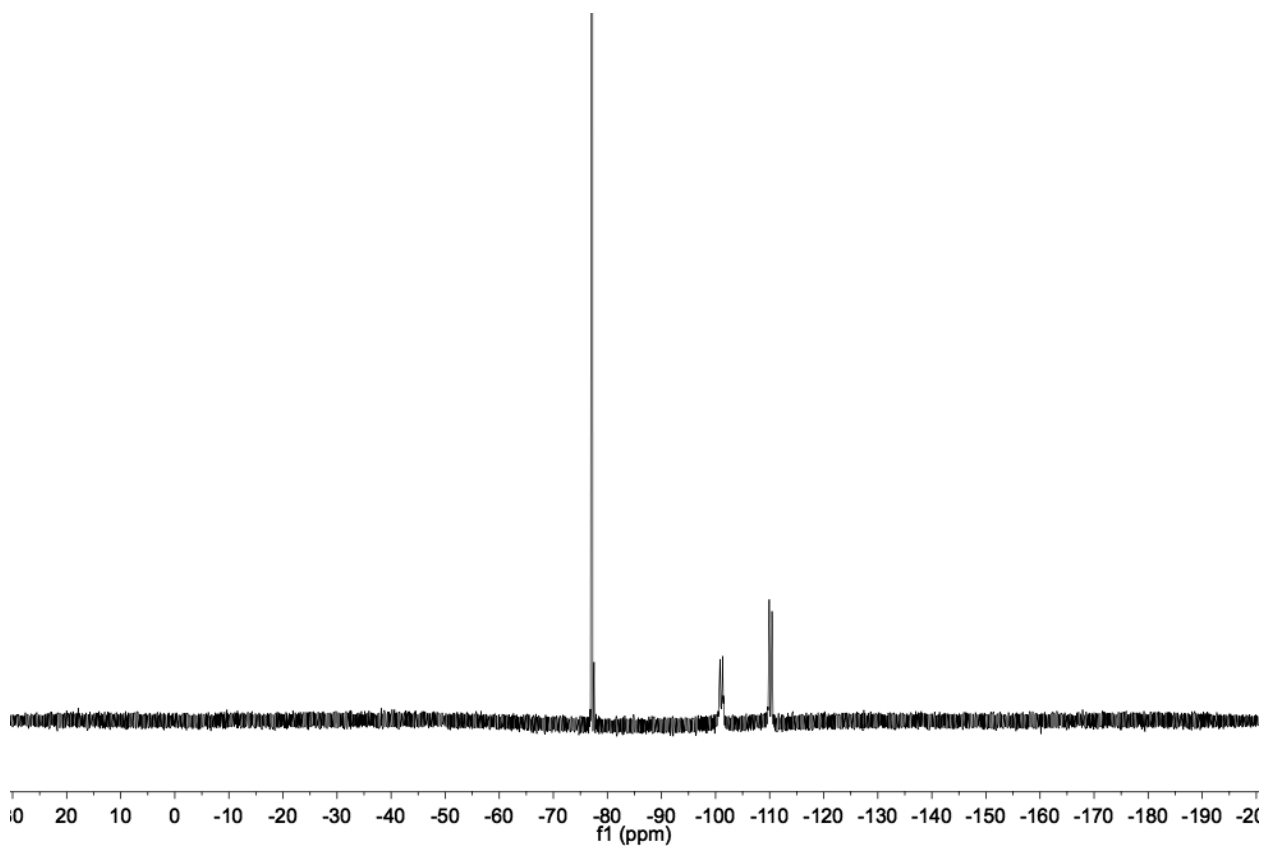
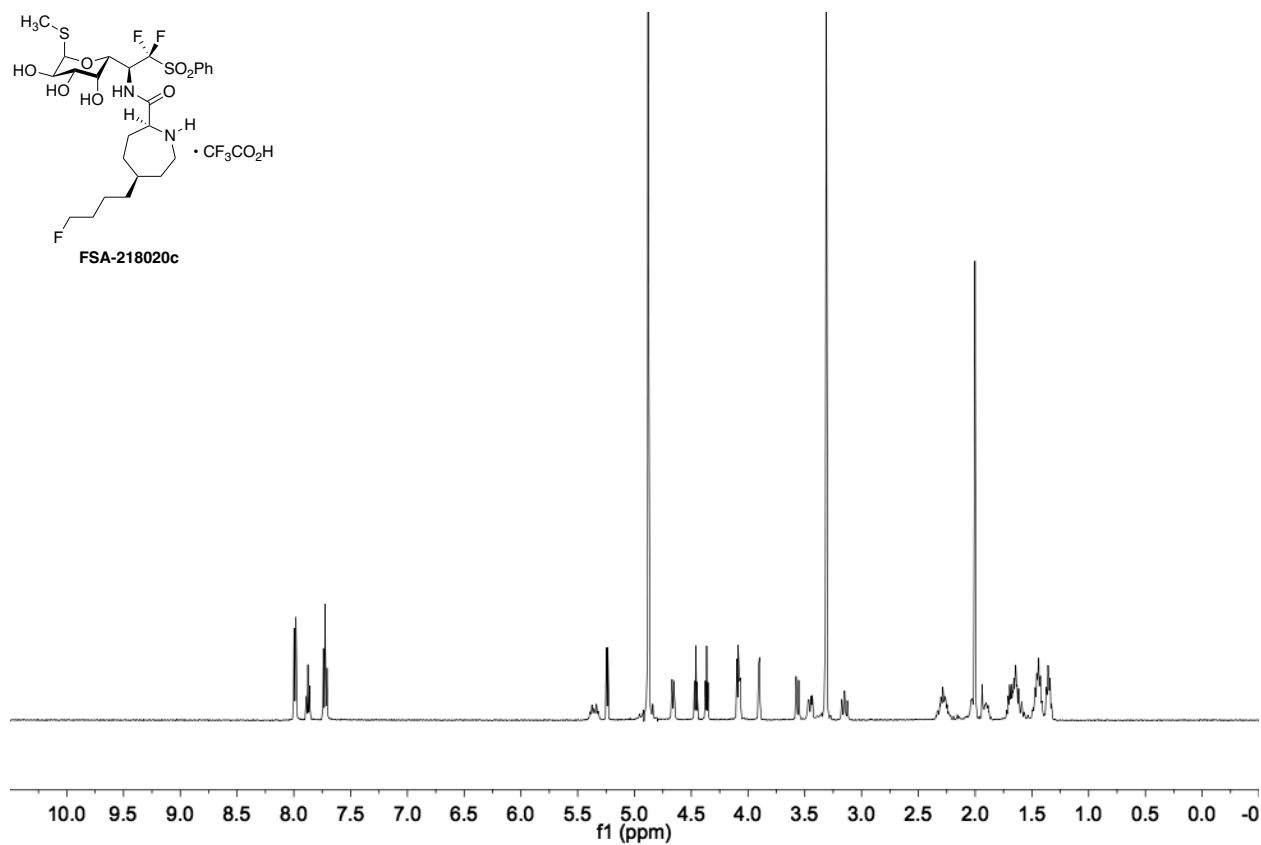
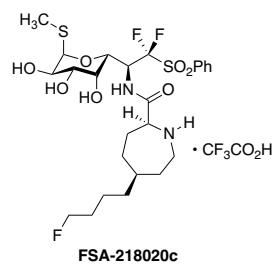


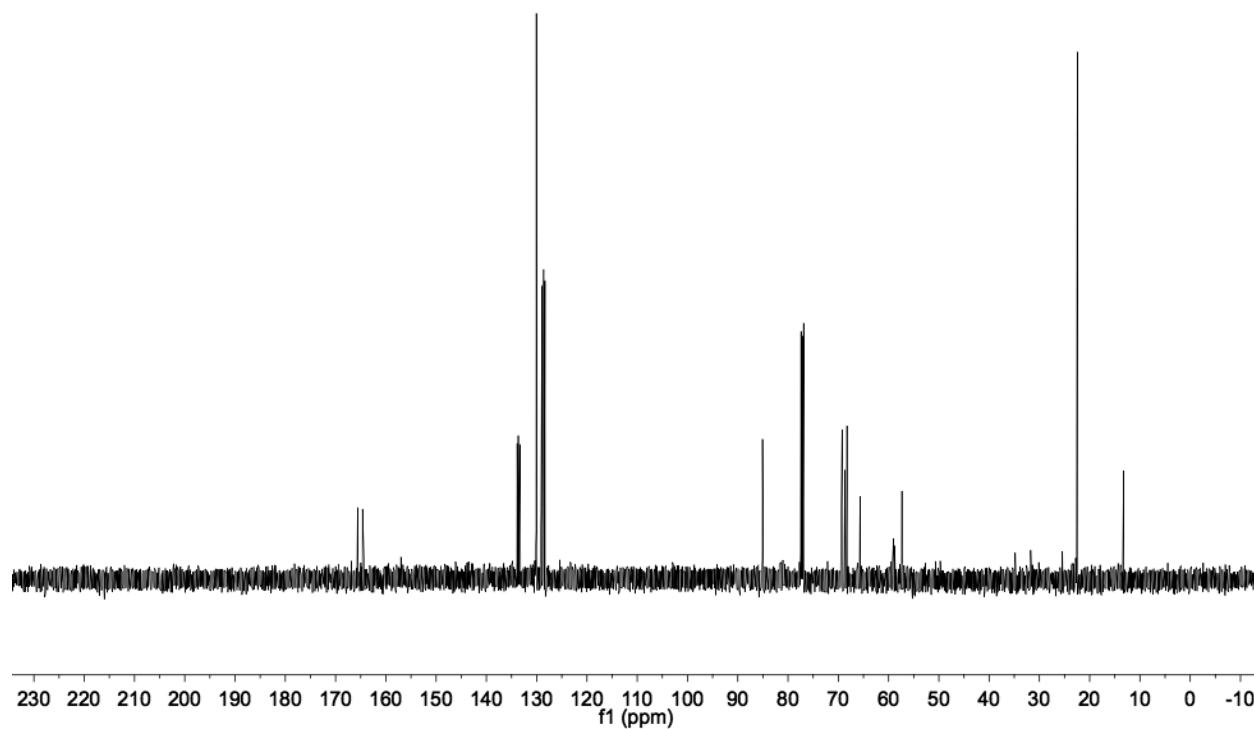
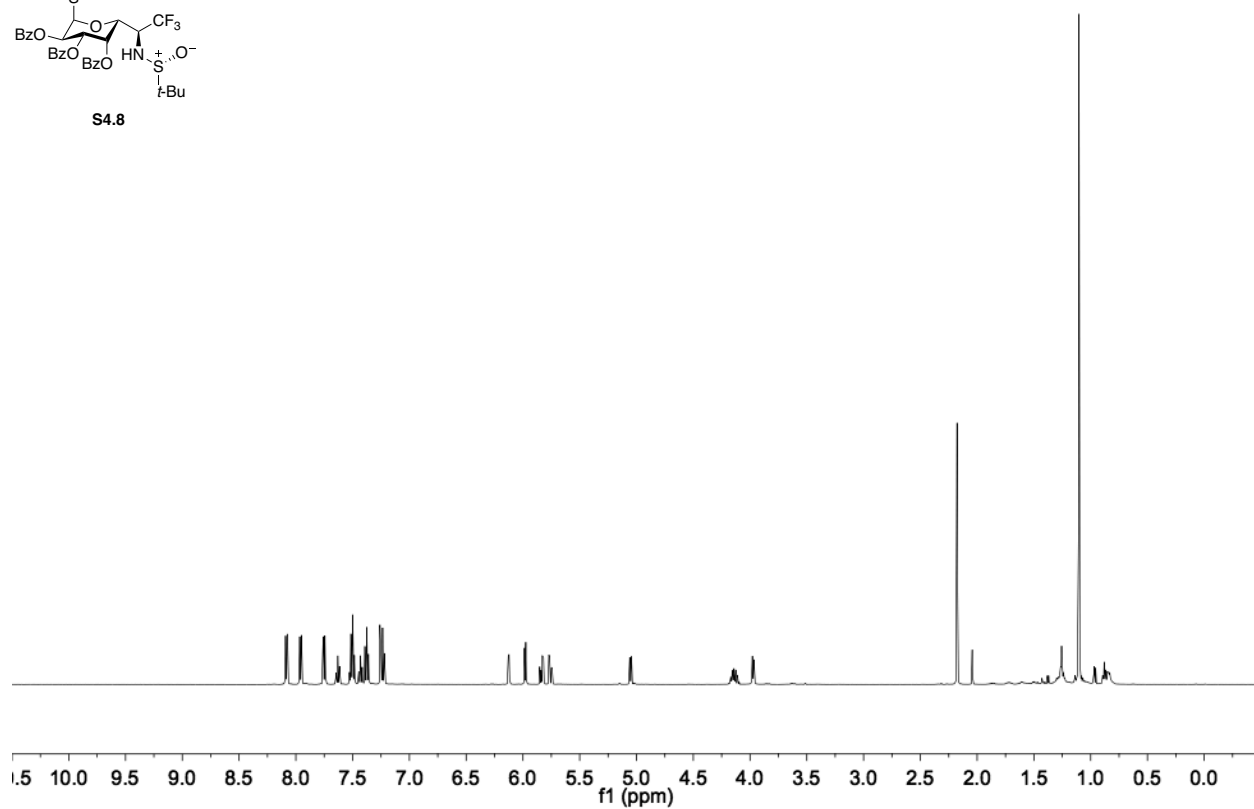
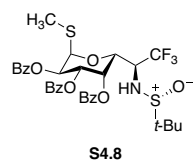


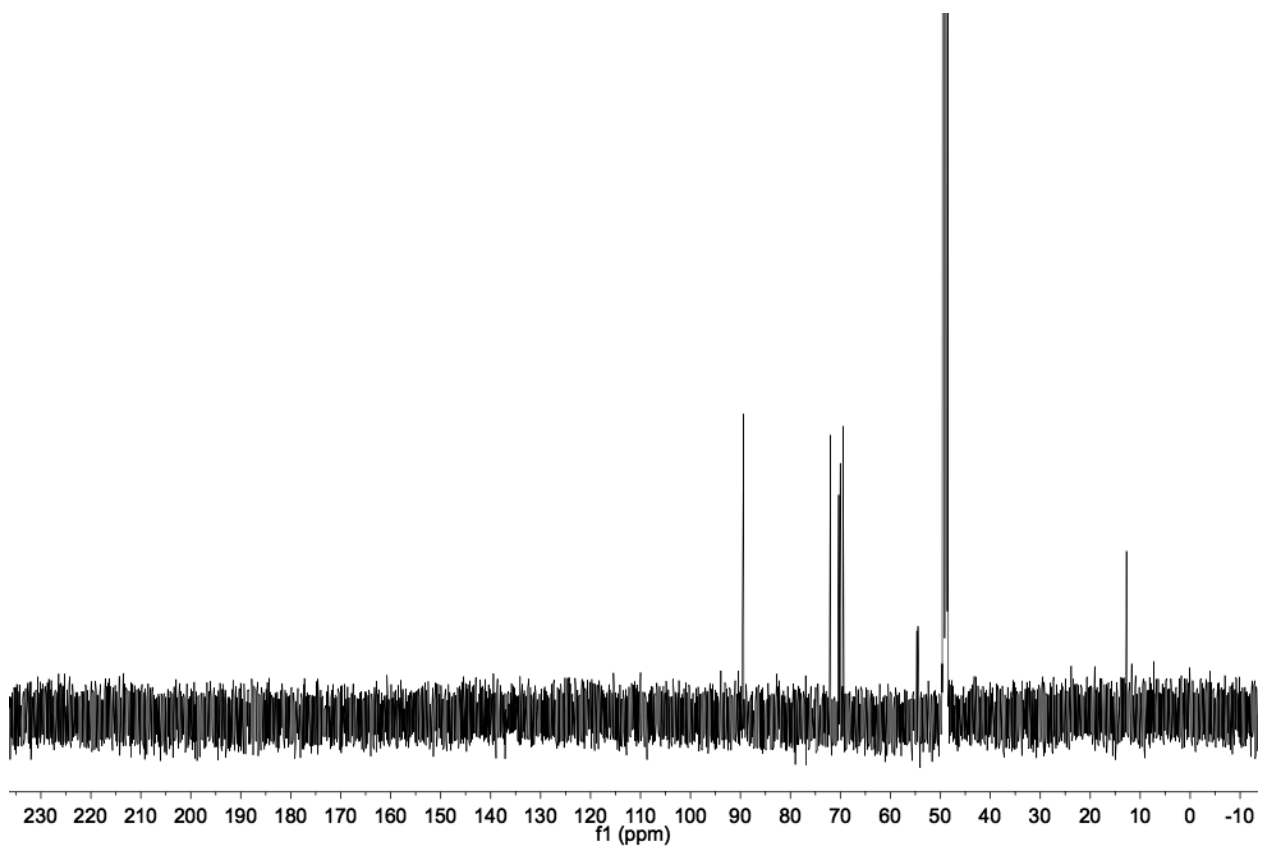
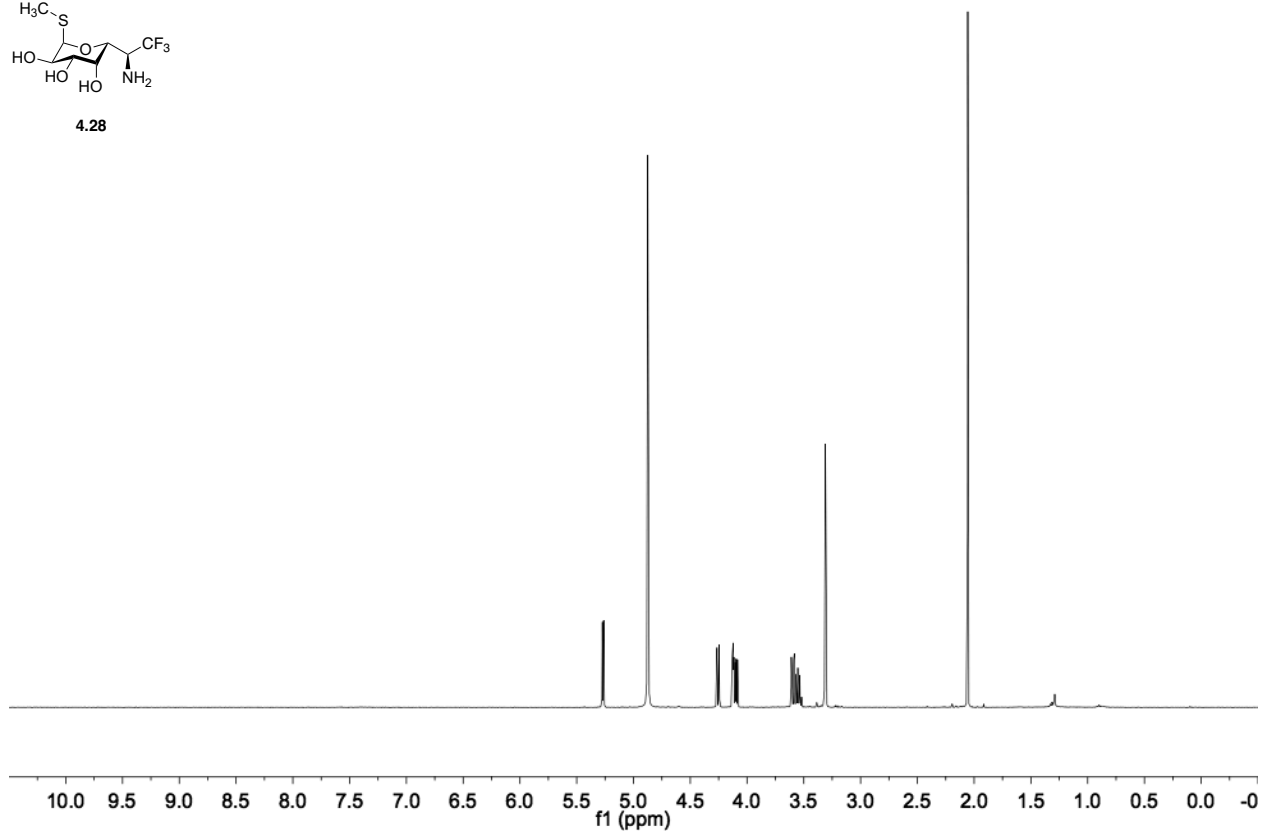
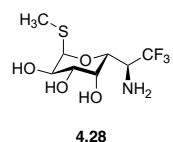
4.27

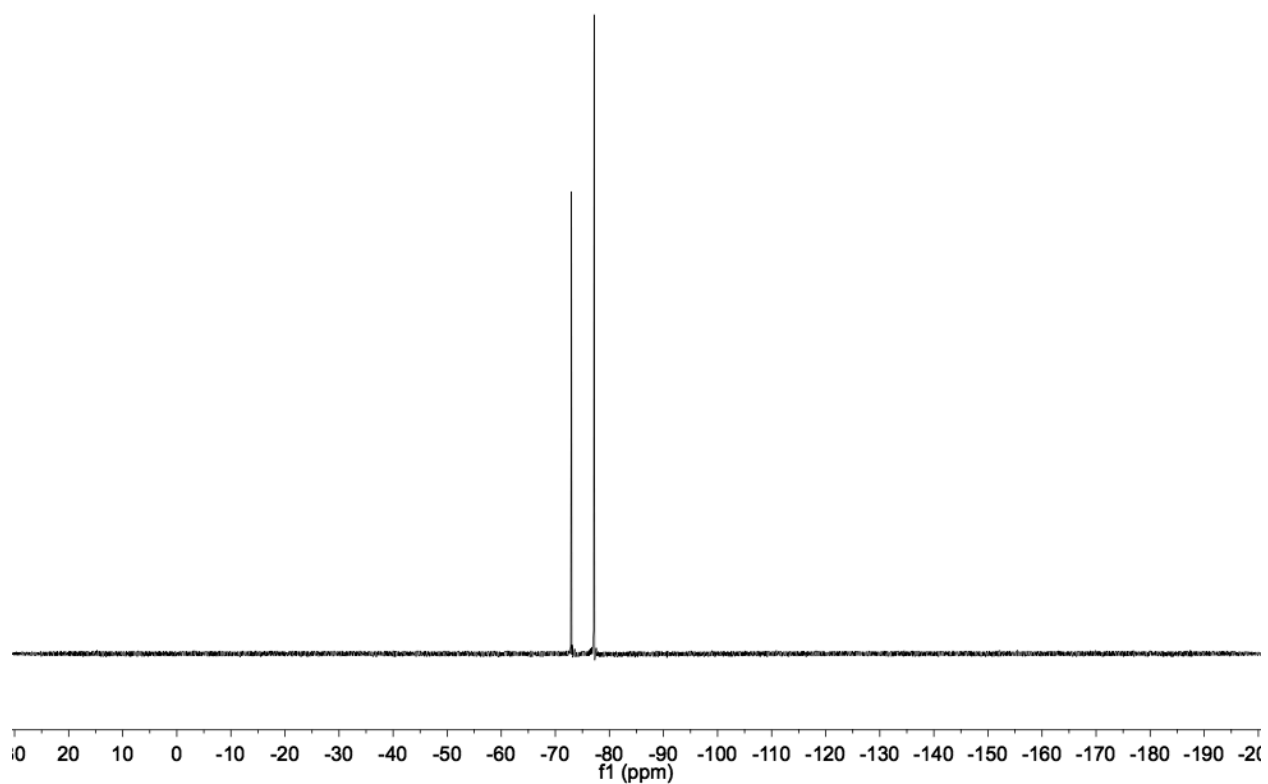
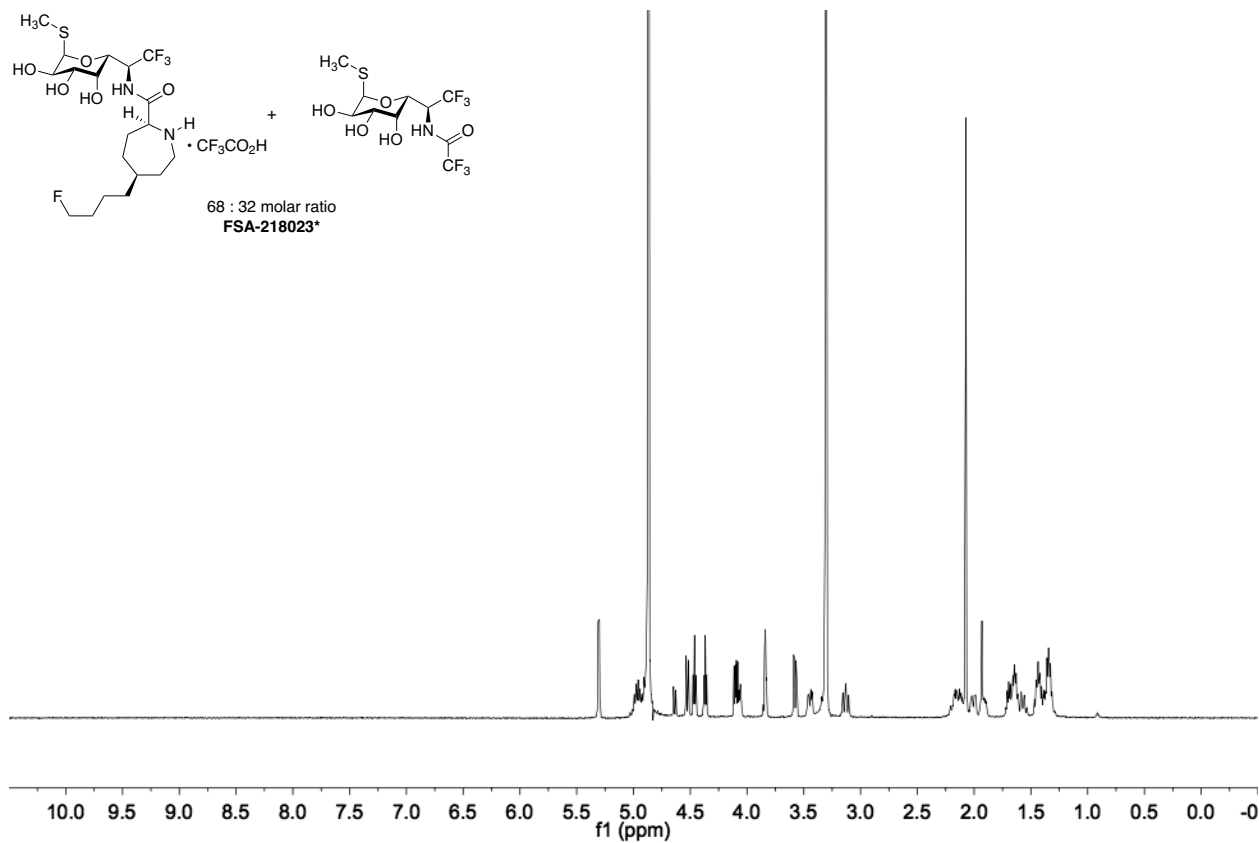


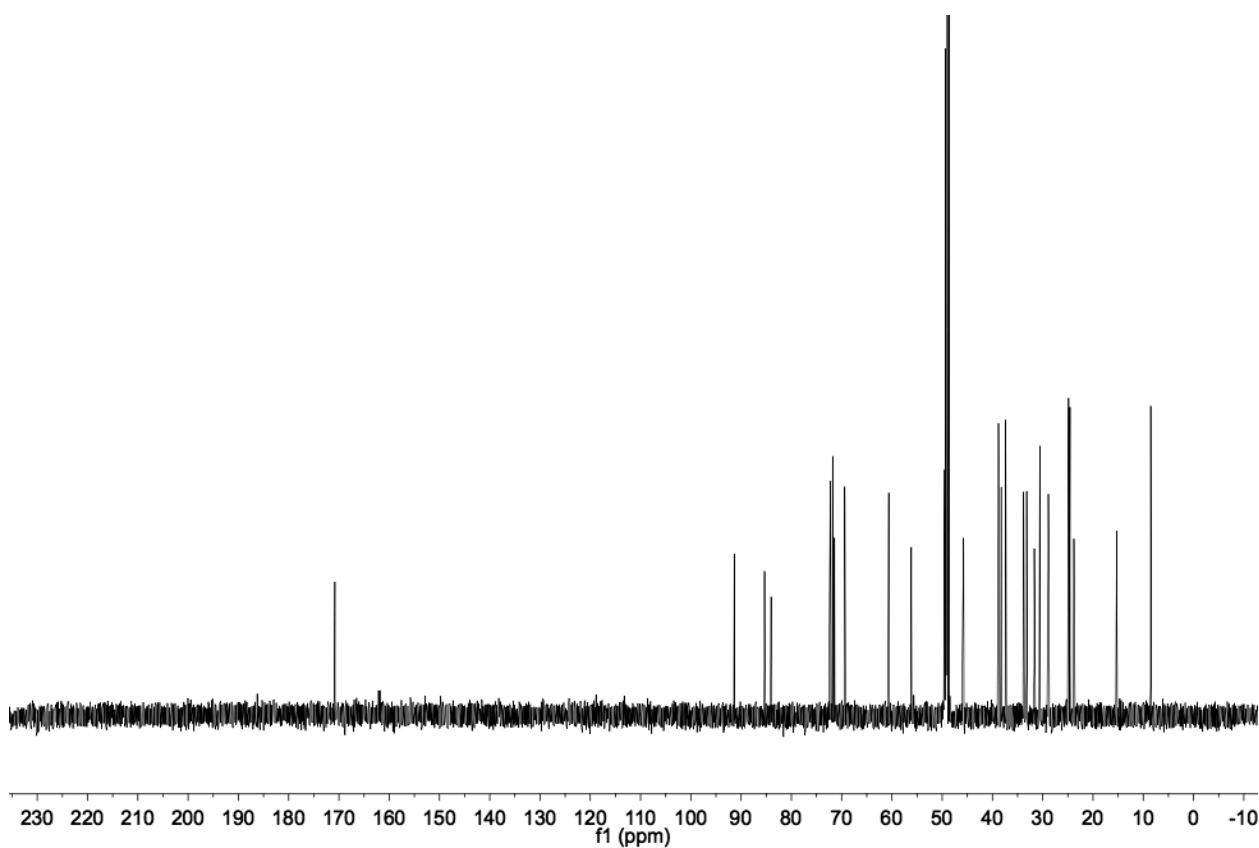
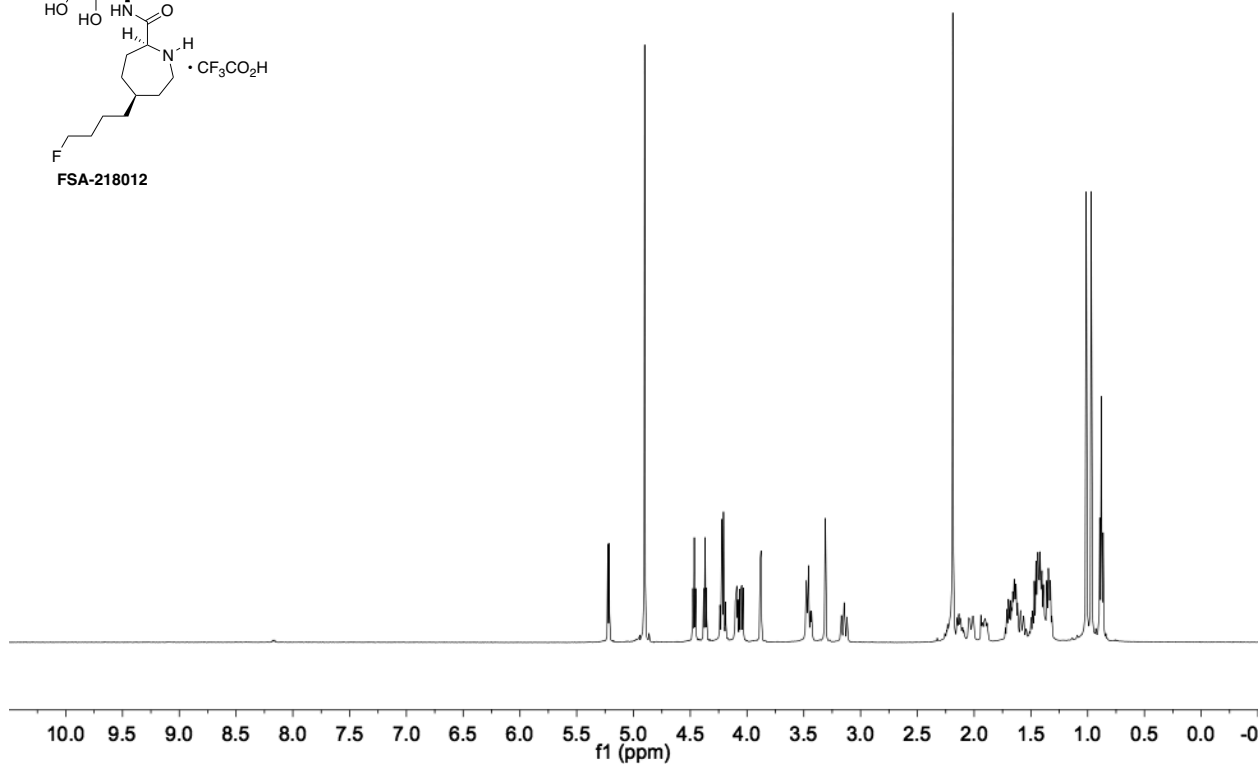
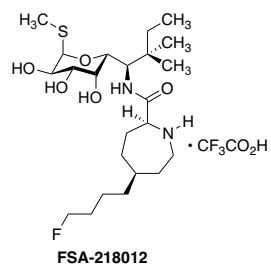


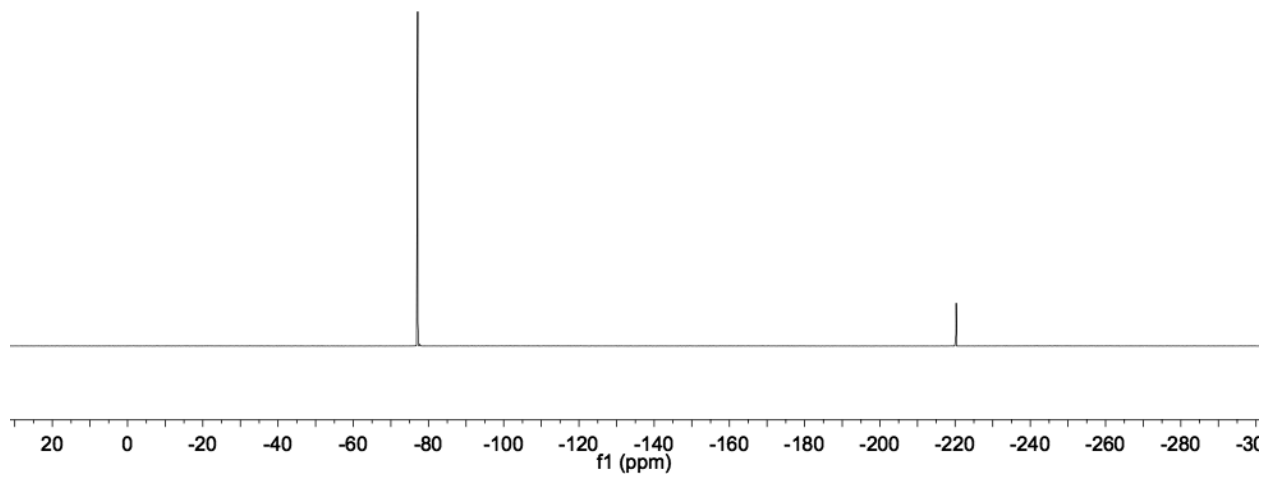


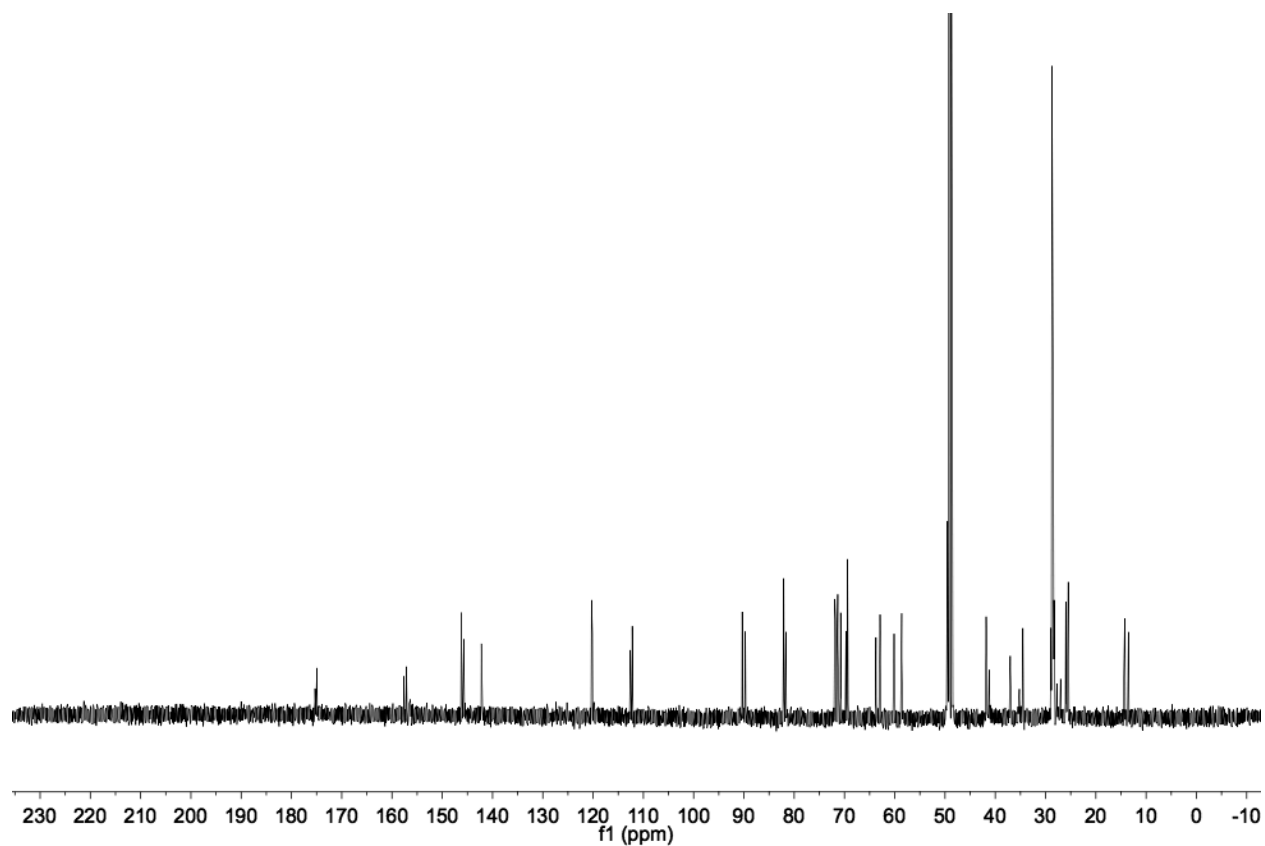
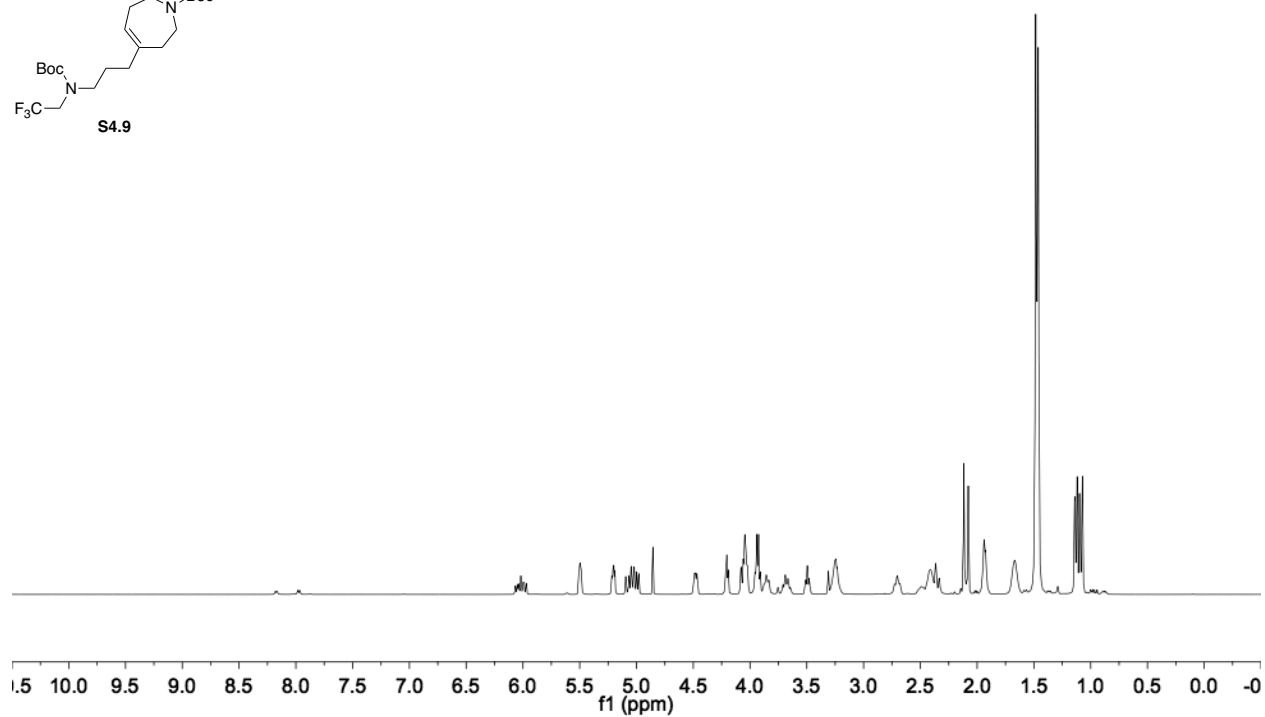
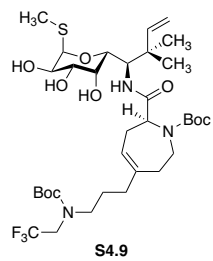


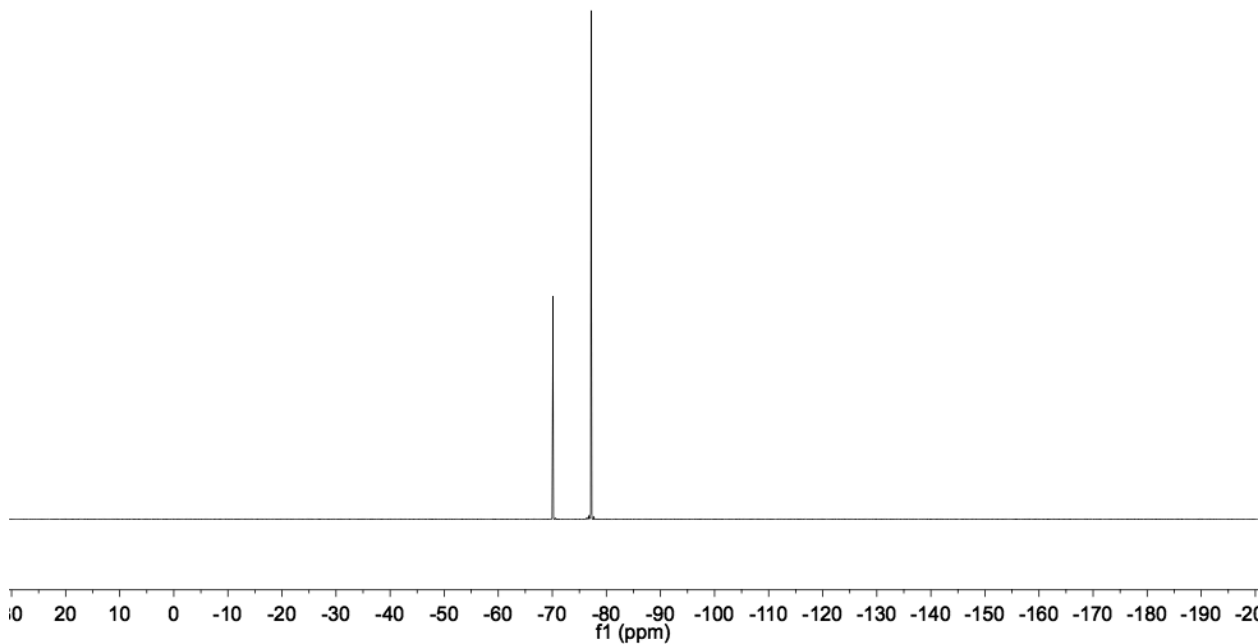
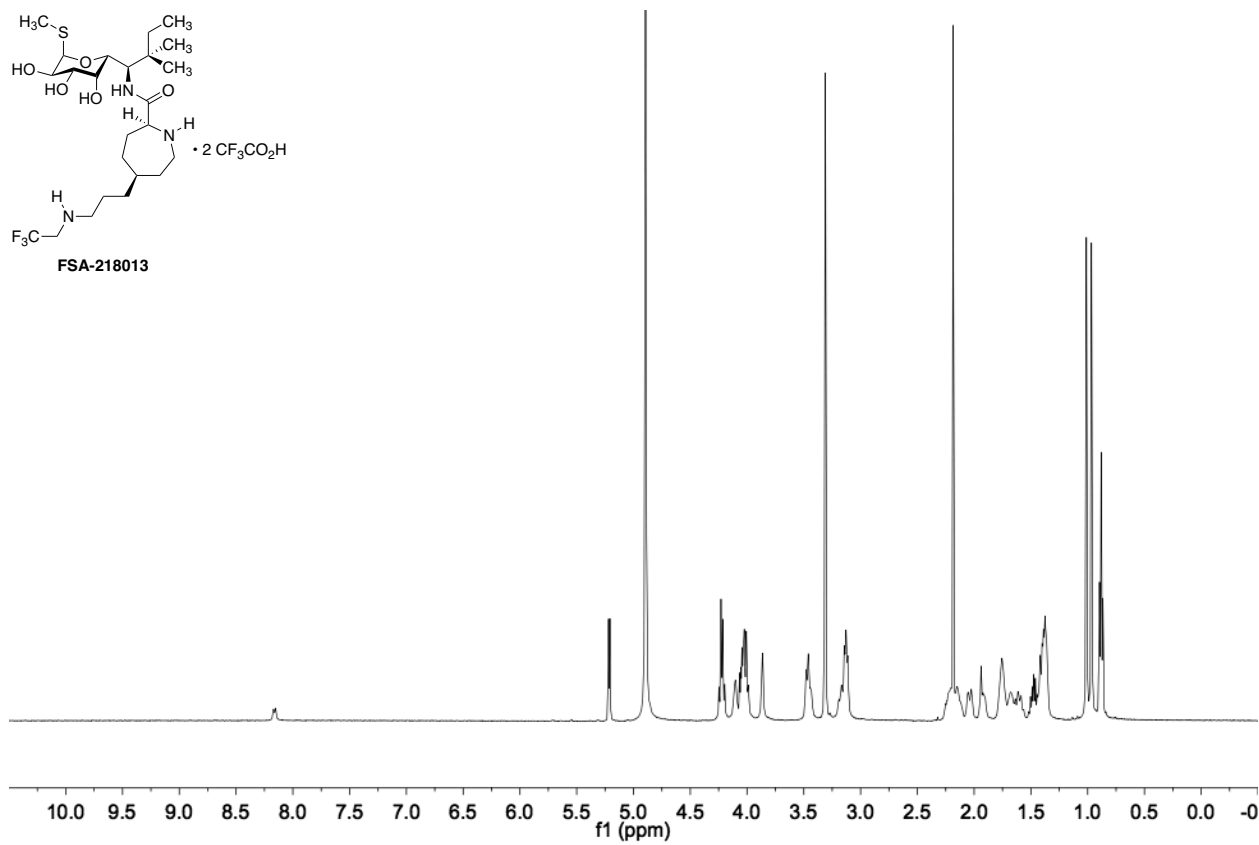
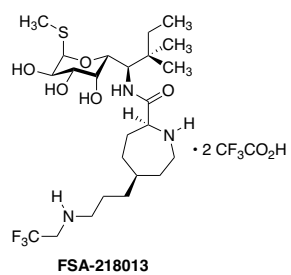


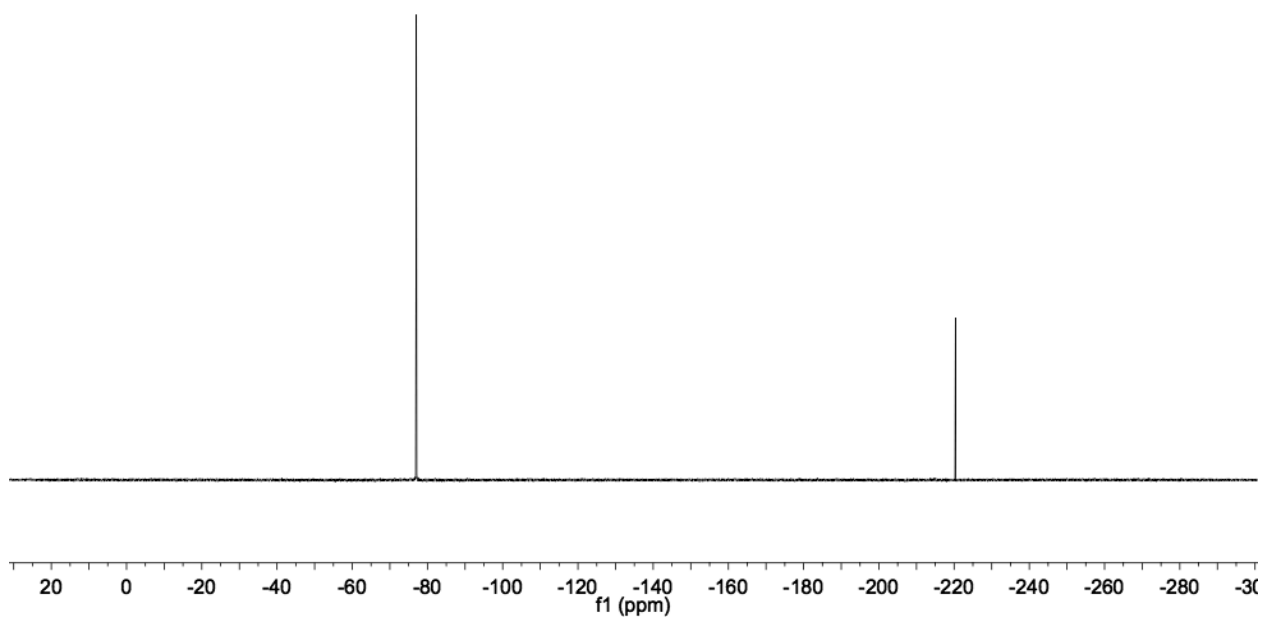
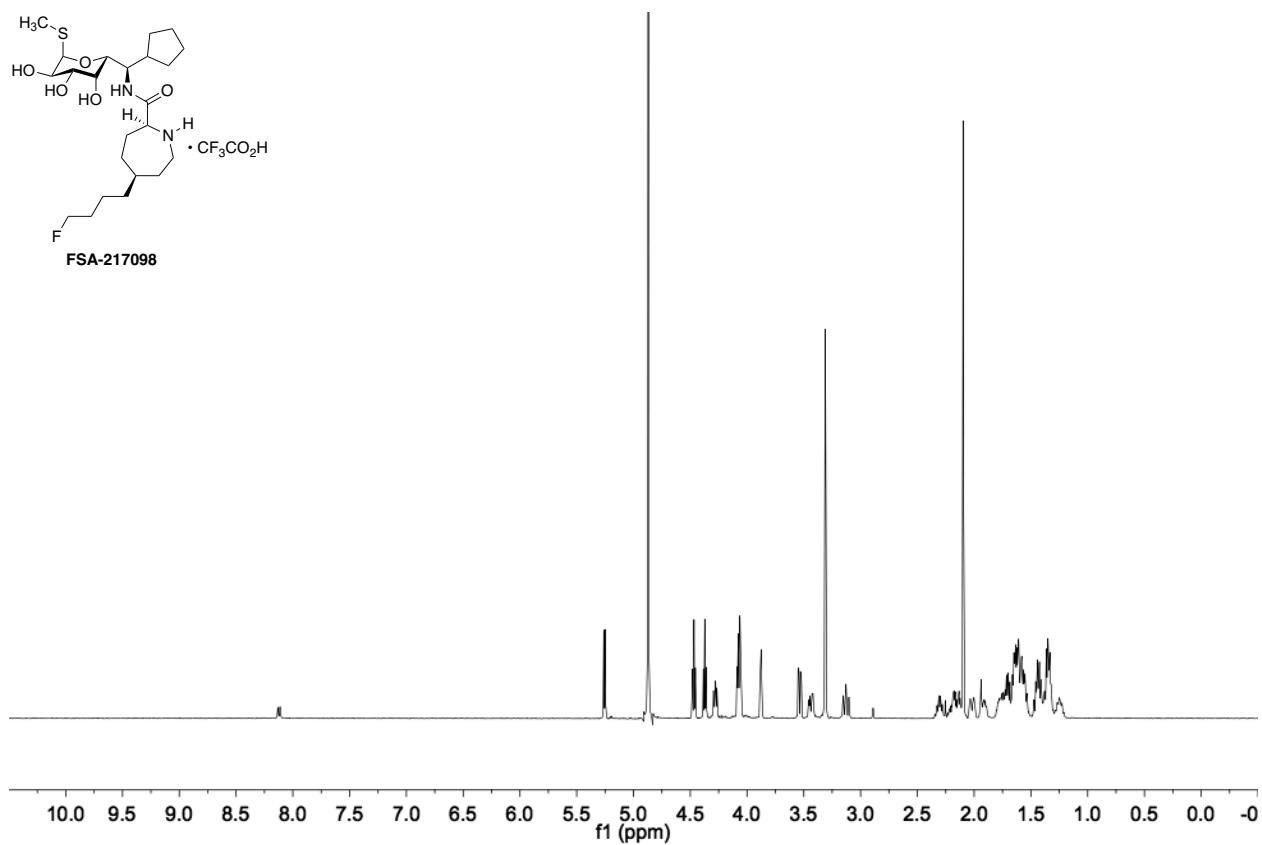
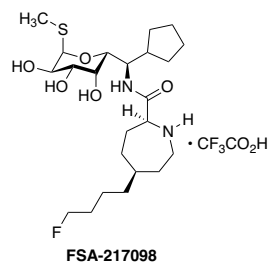


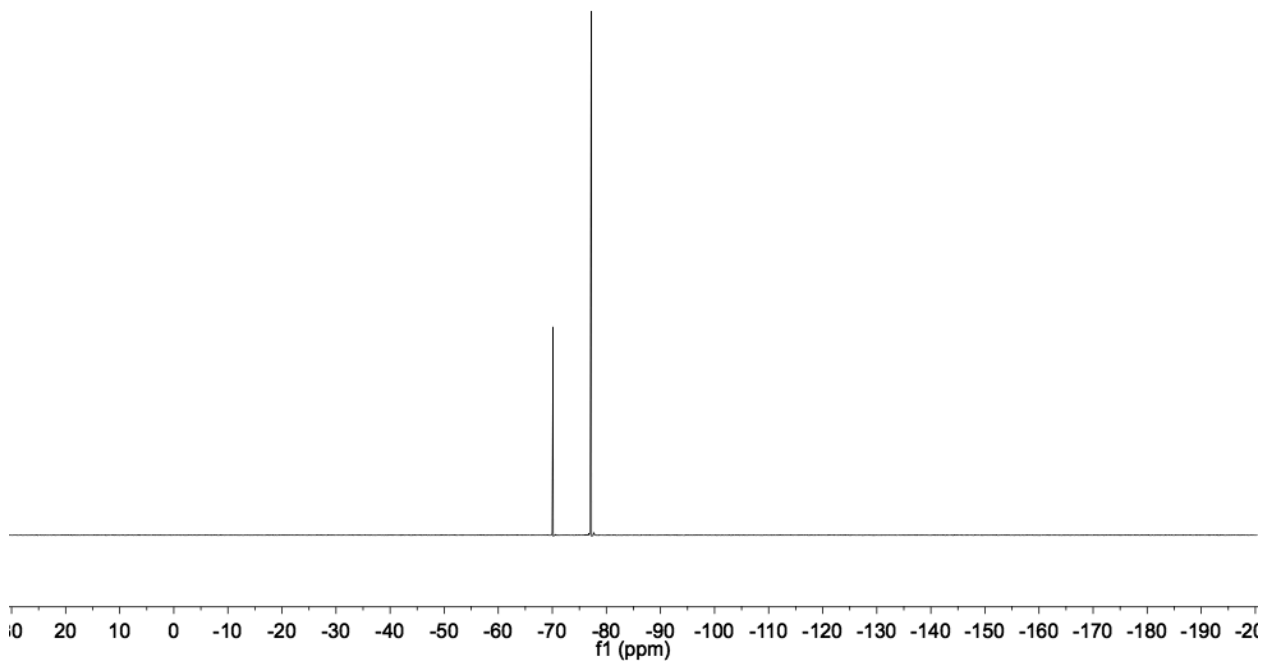
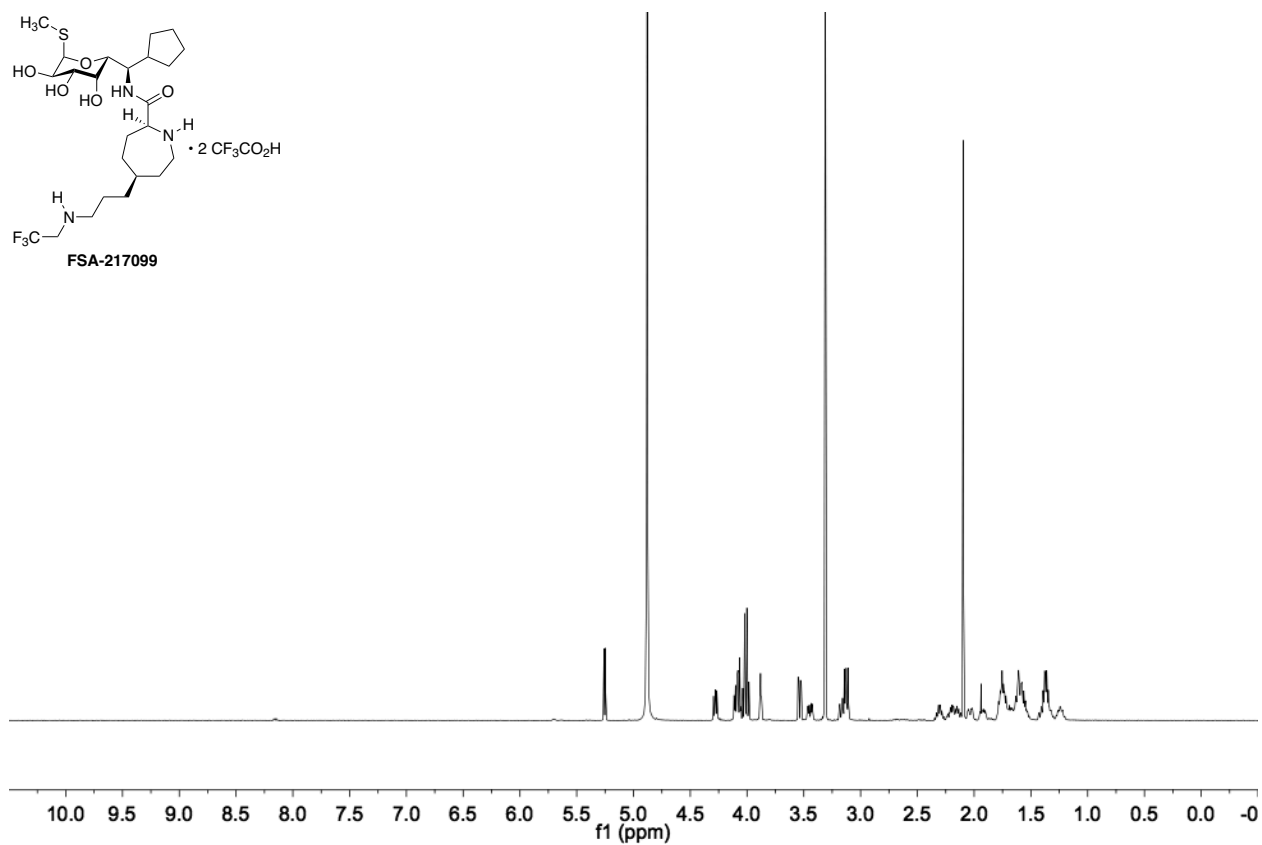
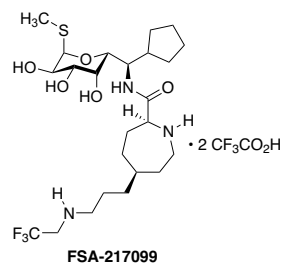


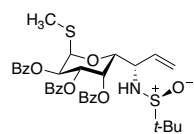




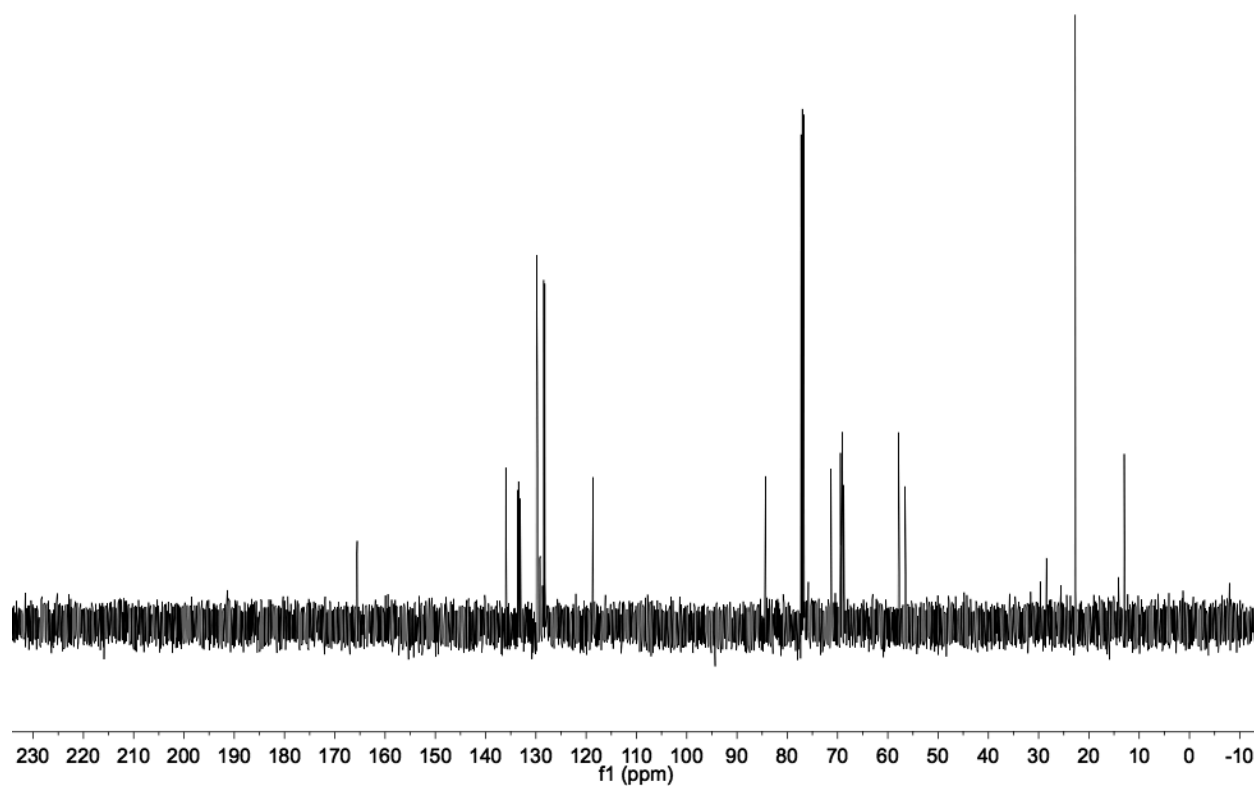
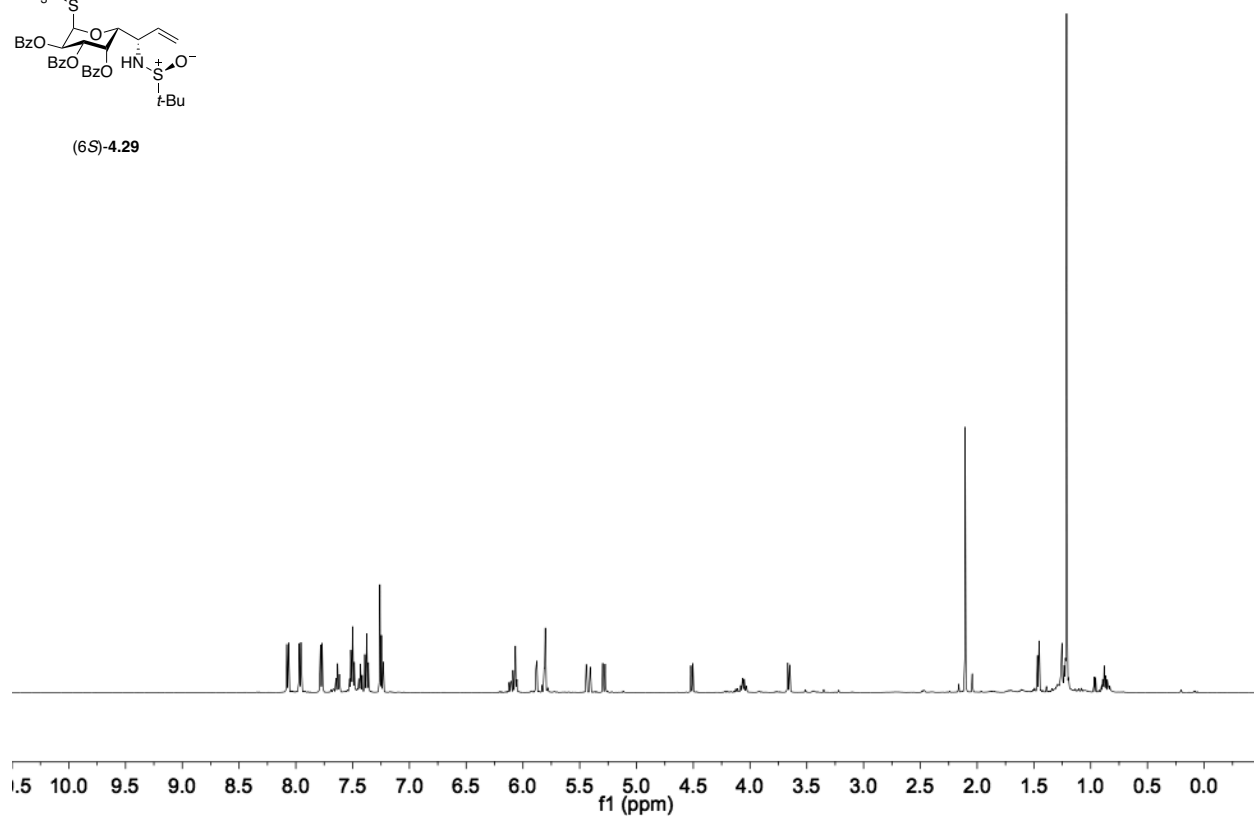


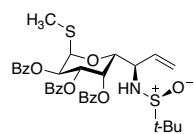




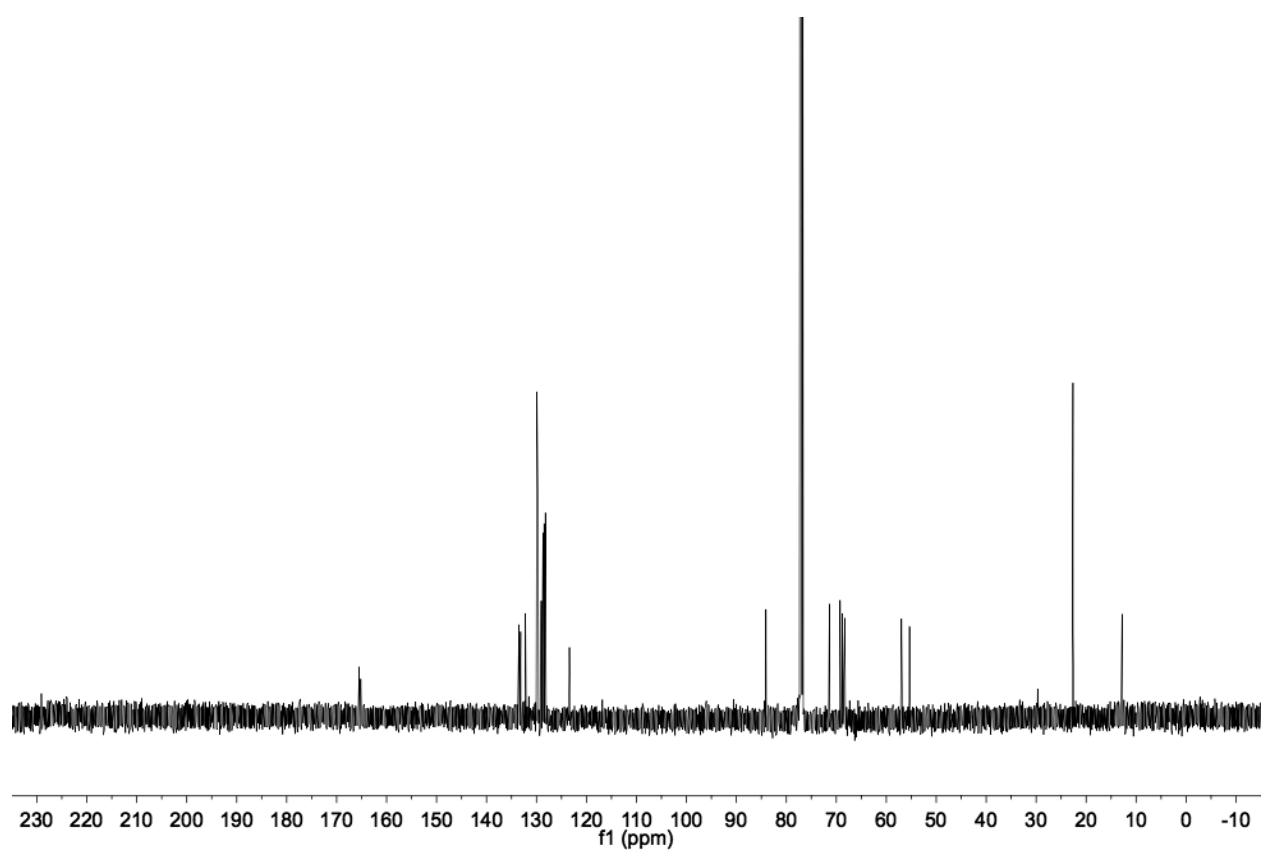
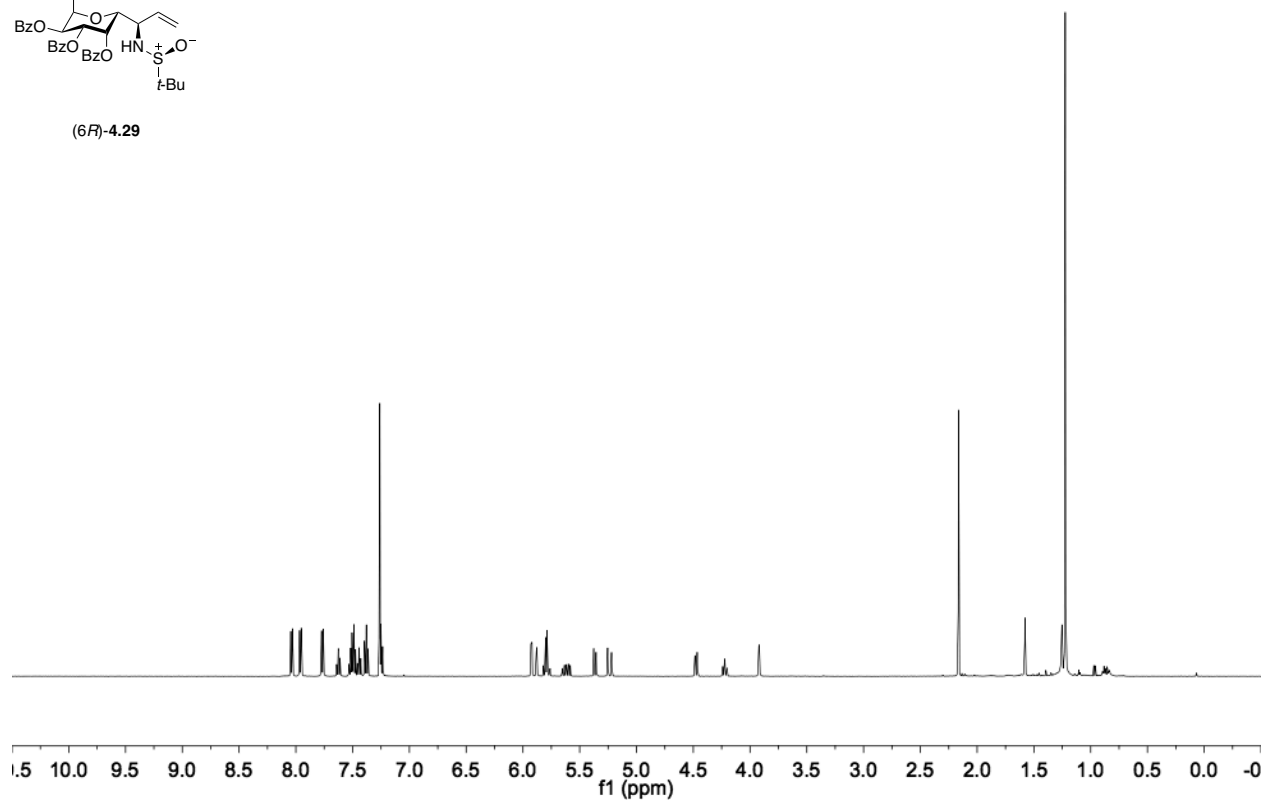


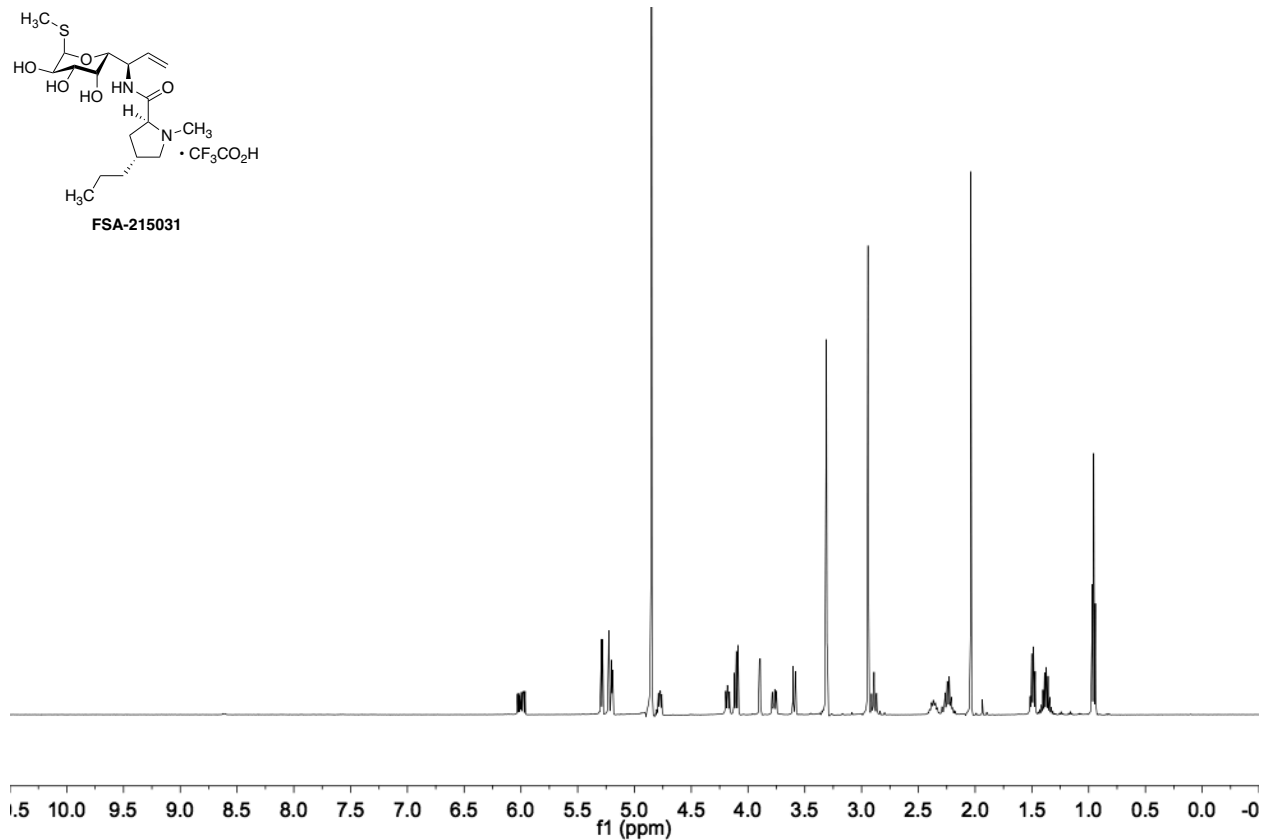
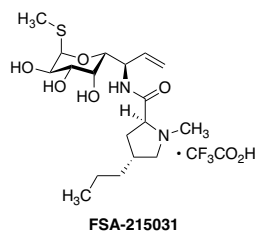
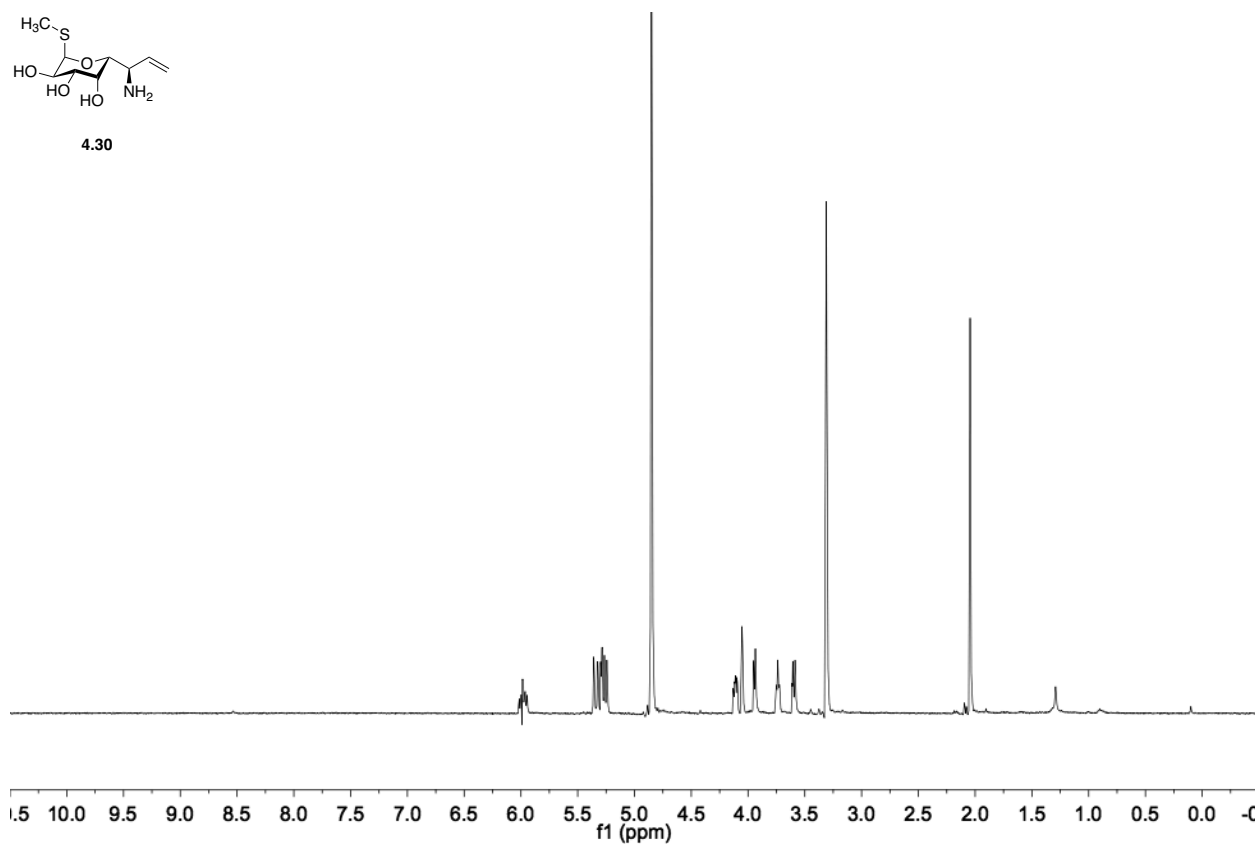
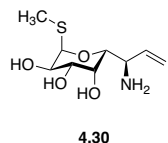
(6S)-4.29

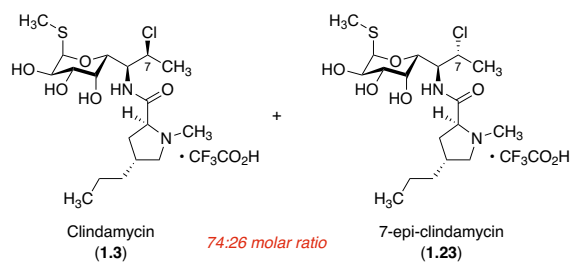




(6*R*)-4.29







Asterisks (*) denote 7-epi-clindamycin signals that could be resolved.

